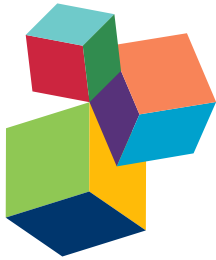


PLANT RESPONSES TO BIOTIC AND ABIOTIC STRESSES: LESSONS FROM CELL SIGNALING

EDITED BY: Sylvain Jeandroz and Olivier Lamotte

PUBLISHED IN: Frontiers in Plant Science and Frontiers in Physiology





frontiers

Frontiers Copyright Statement

© Copyright 2007-2017 Frontiers Media SA. All rights reserved.

All content included on this site, such as text, graphics, logos, button icons, images, video/audio clips, downloads, data compilations and software, is the property of or is licensed to Frontiers Media SA ("Frontiers") or its licensees and/or subcontractors. The copyright in the text of individual articles is the property of their respective authors, subject to a license granted to Frontiers.

The compilation of articles constituting this e-book, wherever published, as well as the compilation of all other content on this site, is the exclusive property of Frontiers. For the conditions for downloading and copying of e-books from Frontiers' website, please see the Terms for Website Use. If purchasing Frontiers e-books from other websites or sources, the conditions of the website concerned apply.

Images and graphics not forming part of user-contributed materials may not be downloaded or copied without permission.

Individual articles may be downloaded and reproduced in accordance with the principles of the CC-BY licence subject to any copyright or other notices. They may not be re-sold as an e-book.

As author or other contributor you grant a CC-BY licence to others to reproduce your articles, including any graphics and third-party materials supplied by you, in accordance with the Conditions for Website Use and subject to any copyright notices which you include in connection with your articles and materials.

All copyright, and all rights therein, are protected by national and international copyright laws.

The above represents a summary only. For the full conditions see the Conditions for Authors and the Conditions for Website Use.

ISSN 1664-8714

ISBN 978-2-88945-356-6

DOI 10.3389/978-2-88945-356-6

About Frontiers

Frontiers is more than just an open-access publisher of scholarly articles: it is a pioneering approach to the world of academia, radically improving the way scholarly research is managed. The grand vision of Frontiers is a world where all people have an equal opportunity to seek, share and generate knowledge. Frontiers provides immediate and permanent online open access to all its publications, but this alone is not enough to realize our grand goals.

Frontiers Journal Series

The Frontiers Journal Series is a multi-tier and interdisciplinary set of open-access, online journals, promising a paradigm shift from the current review, selection and dissemination processes in academic publishing. All Frontiers journals are driven by researchers for researchers; therefore, they constitute a service to the scholarly community. At the same time, the Frontiers Journal Series operates on a revolutionary invention, the tiered publishing system, initially addressing specific communities of scholars, and gradually climbing up to broader public understanding, thus serving the interests of the lay society, too.

Dedication to Quality

Each Frontiers article is a landmark of the highest quality, thanks to genuinely collaborative interactions between authors and review editors, who include some of the world's best academicians. Research must be certified by peers before entering a stream of knowledge that may eventually reach the public - and shape society; therefore, Frontiers only applies the most rigorous and unbiased reviews.

Frontiers revolutionizes research publishing by freely delivering the most outstanding research, evaluated with no bias from both the academic and social point of view.

By applying the most advanced information technologies, Frontiers is catapulting scholarly publishing into a new generation.

What are Frontiers Research Topics?

Frontiers Research Topics are very popular trademarks of the Frontiers Journals Series: they are collections of at least ten articles, all centered on a particular subject. With their unique mix of varied contributions from Original Research to Review Articles, Frontiers Research Topics unify the most influential researchers, the latest key findings and historical advances in a hot research area! Find out more on how to host your own Frontiers Research Topic or contribute to one as an author by contacting the Frontiers Editorial Office: researchtopics@frontiersin.org

PLANT RESPONSES TO BIOTIC AND ABIOTIC STRESSES: LESSONS FROM CELL SIGNALING

Topic Editors:

Sylvain Jeandroz, Agroécologie, AgroSup Dijon, Centre National de la Recherche Scientifique, Institut National de la Recherche Agronomique, Université Bourgogne Franche-Comté, Dijon, France

Olivier Lamotte, Agroécologie, AgroSup Dijon, Centre National de la Recherche Scientifique, Institut National de la Recherche Agronomique, Université Bourgogne Franche-Comté, Dijon, France



Young arabidopsis reporting his recent findings on cell signalling to his supervisor - Illustrated by Yuko Krzyzaniak.

Cover image : Carine Fournier.

Facing stressful conditions imposed by their environment and affecting their growth and their development throughout their life cycle, plants must be able to perceive, to process and to translate different stimuli into adaptive responses. Understanding the organism-coordinated responses involves a fine description of the mechanisms occurring at the cellular and molecular level. A major challenge is also to understand how the large diversity of molecules identified as signals, sensors or effectors could drive a cell to the appropriate plant response and to finally

cope with various environmental cues. In this Research Topic we aim to provide an overview of various signaling mechanisms or to present new molecular signals involved in stress response and to demonstrate how basic/fundamental research on cell signaling will help to understand stress responses at the whole plant level.

Citation: Jeandroz, S., Lamotte, O., eds. (2017). Plant Responses to Biotic and Abiotic Stresses: Lessons from Cell Signaling. Lausanne: Frontiers Media. doi: 10.3389/978-2-88945-356-6

Table of Contents

- 06 Editorial: Plant Responses to Biotic and Abiotic Stresses: Lessons from Cell Signaling**
Sylvain Jeandroz and Olivier Lamotte
- 09 Emerging roles of protein kinase CK2 in abscisic acid signaling**
Belmiro Vilela, Montserrat Pagès and Marta Riera
- 18 Dual Function of NAC072 in ABF3-Mediated ABA-Responsive Gene Regulation in Arabidopsis**
Xiaoyun Li, Xiaoling Li, Meijuan Li, Youcheng Yan, Xu Liu and Ling Li
- 27 Characterisation of Lipid Changes in Ethylene-Promoted Senescence and Its Retardation by Suppression of Phospholipase D δ in Arabidopsis Leaves**
Yanxia Jia and Weiqi Li
- 37 Transcriptomic Changes Drive Physiological Responses to Progressive Drought Stress and Rehydration in Tomato**
Paolo Iovieno, Paola Punzo, Gianpiero Guida, Carmela Mistretta, Michael J. Van Oosten, Roberta Nurcato, Hamed Bostan, Chiara Colantuono, Antonello Costa, Paolo Bagnaresi, Maria L. Chiusano, Rossella Albrizio, Pasquale Giorio, Giorgia Batelli and Stefania Grillo
- 51 Heterologous Expression of AtWRKY57 Confers Drought Tolerance in *Oryza sativa***
Yanjuan Jiang, Yuping Qiu, Yanru Hu and Diqu Yu
- 62 Soybean C2H2-Type Zinc Finger Protein GmZFP3 with Conserved QALGGH Motif Negatively Regulates Drought Responses in Transgenic Arabidopsis**
Dayong Zhang, Jinfeng Tong, Zhaolong Xu, Peipei Wei, Ling Xu, Qun Wan, Yihong Huang, Xiaolan He, Jiayin Yang, Hongbo Shao and Hongxiang Ma
- 71 Mutation of OsGIGANTEA Leads to Enhanced Tolerance to Polyethylene Glycol-Generated Osmotic Stress in Rice**
Shuai Li, Wenhao Yue, Min Wang, Wenmin Qiu, Lian Zhou and Huixia Shou
- 82 Salinity and High Temperature Tolerance in Mungbean [*Vigna radiata* (L.) Wilczek] from a Physiological Perspective**
Bindumadhava HanumanthaRao, Ramakrishnan M. Nair and Harsh Nayyar
- 102 Boron Toxicity Causes Multiple Effects on *Malus domestica* Pollen Tube Growth**
Kefeng Fang, Weiwei Zhang, Yu Xing, Qing Zhang, Liu Yang, Qingqin Cao and Ling Qin
- 114 Pronounced Phenotypic Changes in Transgenic Tobacco Plants Overexpressing Sucrose Synthase May Reveal a Novel Sugar Signaling Pathway**
Quynh Anh Nguyen, Sheng Luan, Seung G. Wi, Hanhong Bae, Dae-Seok Lee and Hyeun-Jong Bae
- 129 How Very-Long-Chain Fatty Acids Could Signal Stressful Conditions in Plants?**
Antoine De Bigault Du Granrut and Jean-Luc Casas
- 142 Carbon Monoxide as a Signaling Molecule in Plants**
Meng Wang and Weibiao Liao

- 150 Ammonium Inhibits Chromomethylase 3-Mediated Methylation of the Arabidopsis Nitrate Reductase Gene NIA2**
Joo Yong Kim, Ye Jin Kwon, Sung-Il Kim, Do Youn Kim, Jong Tae Song and Hak Soo Seo
- 160 Protein Phosphatase 2A in the Regulatory Network Underlying Biotic Stress Resistance in Plants**
Guido Durian, Moona Rahikainen, Sara Alegre, Mikael Brosché and Saijaliisa Kangasjärvi
- 177 Regulation of WRKY46 Transcription Factor Function by Mitogen-Activated Protein Kinases in Arabidopsis thaliana**
Arsheed H. Sheikh, Lennart Eschen-Lippold, Pascal Pecher, Wolfgang Hoehenwarter, Alok K. Sinha, Dierk Scheel and Justin Lee
- 192 Overexpression of Soybean Isoflavone Reductase (GmIFR) Enhances Resistance to Phytophthora sojae in Soybean**
Qun Cheng, Ninghui Li, Lidong Dong, Dayong Zhang, Sujie Fan, Liangyu Jiang, Xin Wang, Pengfei Xu and Shuzhen Zhang
- 203 The Novel Gene VpPR4-1 from Vitis pseudoreticulata Increases Powdery Mildew Resistance in Transgenic Vitis vinifera L.**
Lingmin Dai, Dan Wang, Xiaoqing Xie, Chaohong Zhang, Xiping Wang, Yan Xu, Yuejin Wang and Jianxia Zhang
- 215 Gene Expression Changes during the Gummosis Development of Peach Shoots in Response to Lasiodiplodia theobromae Infection Using RNA-Seq**
Lei Gao, Yuting Wang, Zhi Li, He Zhang, Junli Ye and Guohuai Li
- 227 RNA-Seq Analysis of Differential Gene Expression Responding to Different Rhizobium Strains in Soybean (Glycine max) Roots**
Songli Yuan, Rong Li, Shuilian Chen, Haifeng Chen, Chanjuan Zhang, Limiao Chen, Qingnan Hao, Zhihui Shan, Zhonglu Yang, Dezhen Qiu, Xiaojuan Zhang and Xinan Zhou
- 242 Calcium Sensors as Key Hubs in Plant Responses to Biotic and Abiotic Stresses**
Benoît Ranty, Didier Aldon, Valérie Cotelle, Jean-Philippe Galaud, Patrice Thuleau and Christian Mazars
- 249 Concurrent Drought Stress and Vascular Pathogen Infection Induce Common and Distinct Transcriptomic Responses in Chickpea**
Ranjita Sinha, Aarti Gupta and Muthappa Senthil-Kumar
- 267 Responses of In vitro-Grown Plantlets (*Vitis vinifera*) to Grapevine leafroll-Associated Virus-3 and PEG-Induced Drought Stress**
Zhen-Hua Cui, Wen-Lu Bi, Xin-Yi Hao, Yan Xu, Peng-Min Li, M. Andrew Walker and Qiao-Chun Wang
- 281 A Halotolerant Bacterium *Bacillus licheniformis* HSW-16 Augments Induced Systemic Tolerance to Salt Stress in Wheat Plant (*Triticum aestivum*)**
Rajnish P. Singh and Prabhat N. Jha



Editorial: Plant Responses to Biotic and Abiotic Stresses: Lessons from Cell Signaling

Sylvain Jeandroz and Olivier Lamotte*

Agroécologie, AgroSup Dijon, Centre National de la Recherche Scientifique, Institut National de la Recherche Agronomique, Université Bourgogne Franche-Comté, Dijon, France

Keywords: abiotic stress, biotic stress, signaling, plants, adaptation, physiological

Editorial on the Research Topic

Plant Responses to Biotic and Abiotic Stresses: Lessons from Cell Signaling

Facing stressful conditions imposed by their environment that could affect their growth and their development throughout their life cycle, plants must be able to perceive, to process, and to translate different stimuli into adaptive responses. Understanding the organism-coordinated responses involves fine description of the mechanisms occurring at the cellular and molecular level. These mechanisms involve numerous components that are organized into complex transduction pathways and networks, from signal perception to physiological responses. The major challenge of plant signaling is to understand how the large diversity of molecules identified as signals, sensors, or effectors could drive a cell to the appropriate plant response, to cope with various environmental challenges. The objective of this Research Topic is to give an overview of various signaling mechanisms or to present new molecular signals involved in stress response and to demonstrate how basic/fundamental research on cell signaling will help to understand stress responses at the whole plant level.

Under a changing climate, drought becomes one of the most critical abiotic stresses that severely reduces crop production. Molecular mechanisms involved in plant drought adaptation are addressed in several articles/contributions. Reversible protein phosphorylation, catalyzed by antagonistic activities of protein kinases and phosphatases, is a predominant molecular switch controlling the outcome of cell signaling after stress perception. Vilela et al. present an extensive review of the role of Casein Kinase 2 (CK2), an evolutionary conserved Ser/Thr protein kinase found in all eukaryotes, during abscisic acid (ABA) signaling and drought stress tolerance. For instance CK2 has a pivotal role in the regulation of ABA signaling through its action on *Zea mays* OST1/SnRK2.6 (Open Stomata 1/Sucrose Non Fermenting Kinase 2.6) a well-known Ser/Thr protein kinase involved in ABA signaling (Kulik et al., 2011). Furthermore, CK2-dependent phosphorylation enhances the stabilization and degradation of targeted proteins. CK2 is thought to be a housekeeping kinase which finely controls ABA signaling by mediating dynamic protein turnover. Another protein, this time involved in genome reprogramming during ABA signaling was identified by Li et al. They present new evidence showing interrelation between the transcription factor NAC072 and ABA responsive element binding factor ABF3, a positive regulator of ABA responsive gene expression. Interestingly, these two proteins could cooperate or act antagonistically, revealing a dual function of NAC072. ABA and other phytohormones could cooperate to orchestrate plant responses to stress. The research article of Jia and Li reports an example of this process known as hormone crosstalk in *Arabidopsis*, where ABA and ethylene accelerate senescence. The authors show that the suppression of phospholipase D (PLD) retards

OPEN ACCESS

Edited and reviewed by:

John Hancock,

University of the West of England,
United Kingdom

*Correspondence:

Olivier Lamotte

olivier.lamotte@inra.fr

Specialty section:

This article was submitted to

Plant Physiology,
a section of the journal
Frontiers in Plant Science

Received: 29 August 2017

Accepted: 28 September 2017

Published: 13 October 2017

Citation:

Jeandroz S and Lamotte O (2017)
Editorial: Plant Responses to Biotic
and Abiotic Stresses: Lessons from
Cell Signaling.

Front. Plant Sci. 8:1772.

doi: 10.3389/fpls.2017.01772

ethylene-promoted senescence (as previously reported for the ABA-promoted senescence) through an elusive mechanism resulting in the modification of plastidic lipid metabolism and maintenance of plasma membrane integrity. Lovieno et al. using a RNA sequencing approach, report on global transcriptomic changes associated with drought and rehydration in tomato. Transcriptomic analyses together with physiological measurements, quantification of metabolites and biometric parameters, yielded promising candidate genes and that could be used as specific physiological markers of plant drought response. Using a transgenic approach, two studies have functionally validated the role of two transcription factors during drought stress in rice and in soybean (*Glycine max*, Gm). Jiang et al. improved rice drought tolerance by overexpressing the *Arabidopsis thaliana* transcription factor WRKY57 (AtWRKY57) which was previously shown to enhanced drought resistance in *Arabidopsis* (Jiang et al., 2012). AtWRKY57 is a positive regulator of drought responses and appears to be a potential candidate gene for crop improvement but, as reported by the authors the effect on plant productivity should be analyzed to validate this strategy. However, Zhang et al. show that GmZFP3 (*Gl. max* Zinc Finger Protein 3) negatively regulates drought responses when overexpressed in *Arabidopsis*. GIGANTEA (GI), a plant specific nuclear protein, is a key component of flowering time regulation but is also known to be involved in a multitude of physiological responses. Finally, Li et al. report that mutation of *Oryza sativa* GI confers tolerance to osmotic stress and regulates transcript abundance of some gene encoding ABA-induced proteins. Tolerance to salinity and high temperature is also reviewed by HanumanthaRao et al. who presented an integrative view of mungbean responses from physiological, biochemical, and molecular aspects to agronomical perspectives and field management practices. Lastly, although Boron is considered as an essential micronutrients for plants, abnormal concentrations can be toxic and limit crop productivity. Fang et al. report that boron could alter calcium signaling and actin filament organization thus impacting on plant development (*Malus domestica* pollen tube growth). In addition to their essential function in plant primary metabolism, several molecules have now been considered as signal molecules. For instance, the signaling function of sugars has become the focus of numerous research efforts. Nguyen et al. using transgenic plants overexpressing sucrose synthase, reveal a novel sugar signaling pathway controlling pronounced phenotypic changes in tobacco. We can expect that future research will confirm the role of sugars throughout all stages of the plant's life cycle since sugar-signaling pathways could interact with other stimuli such as phytohormones or light (Smeekens, 2000). Lipids could also be considered at the interface of plant stress response and cellular primary metabolism. Levels of very long chain fatty acids (>18C, VLCFA) are known to be modified under stressful conditions. Based on preexisting data, De Bigault Du Grandrut and Cacas investigate through three scenarios, the concept that these VLCFA could also participate in stress signaling pathways. The authors proposed a model depicting the hypothetic role of VLCFA in a very informative and synthetic figure. Small molecule such as the diatomic gas carbon monoxide (CO), widely considered as detrimental, also

emerges as signaling molecule in plants. The review of Wang and Liao provides brief update on its role in growth, development and abiotic stress tolerance. CO has a positive effects on salt or heavy metal stresses in relation with other signaling molecules, such as phytohormones or NO and ROS. Last but not least, research conducted by Kim et al. reveals links between N metabolism and epigenetics (gene methylation). They report that ammonium treatment inhibits chromomethylase 3-mediated methylation of the gene encoding one of the two nitrate reductase isoform (Nia2) in *Arabidopsis*. These results bring new insights concerning the regulation of nitrate assimilation and its signaling properties and open interesting perspectives for the role of epigenetics in plant responses to stress.

Biotic stresses also cause major losses in crop productivity. Deciphering mechanisms involved in plant defense to pathogens will help to develop breeding and biotechnological strategies for crop protection. Durian et al. provide an overview of the Protein Phosphatase 2A (PP2A) functions, a crucial component that controls pathogenic responses in various plant species. The authors describe, in an exhaustive manner, the connections of these multifunctional enzymes with the signaling pathway that controls plant immunity, cell death and more globally primary and secondary metabolism. Using an elegant biochemical and targeted approach, Sheikh et al. reveal a post-translational regulation of AtWKY46 transcription factor by a MAPK3-dependent phosphorylation that mediates the stability of this transcription factor after PAMP elicitation in *Arabidopsis*. It is noteworthy that knowledge about plant molecular responses to biotic stress is obtained from model plants as well as from cultivated species. Thus, this topic reports the identification of regulators of plant immunity in different economically important crops. In soybean, Cheng et al. report the characterization of a novel member of the isoflavone reductase gene family, GmIFR, regulated by phytohormones (SA, ET, ABA) and involved in the resistance to the oomycete *Phytophthora sojae*. Using a quite similar functionally transgenic approach, Dai et al. have identified and characterized a new defense protein PR4-1 from a wild chinese grape *Vitis pseudoreticula*. When overexpressed in *Vitis vinifera*, it improved tolerance to powdery mildew. RNAseq methodology is now widely used to investigate gene expression in response to microbes in non-model species. Based on the analysis of the differentially expressed genes, Gao et al. propose a model illustrating the main molecular responses and gum polysaccharide formation in peach tree (*Prunus persica*) infected by *Lasiodiplodia theobromae*, the fungal agent of peach tree gummosis.

Yuan et al. compare by a RNAseq approach two symbiotic systems with notable different nodulation phenotypes in soybean roots. Many of the differentially expressed genes identified are related to plant immunity and could explain the different nodulation phenotypes. Their work highlights the delicate balance between beneficial and detrimental effects of microbes and, as written by the authors, it "sheds new light on the host legume control of nodulation specificity."

Crosstalk between abiotic and biotic stress responses are the last aspect developed in this topic. Comparative approaches can be interesting to test the hypotheses of common signaling

pathways and of physiological responses that are subject to pleiotropic gene action. In a mini-review article, Ranty et al. provide a broad perspective on the role of Ca^{2+} in plant responses to abiotic and biotic stress. The specific effects of this ubiquitous second messenger and the role of calcium sensor proteins are discussed. The authors put forward hypotheses to explain one crucial question of cell signaling: how are signals perceived and how do cells respond spatially and temporally to these signals to program a specific response at the organism level? More specifically, Sinha et al. have examined the transcriptome dynamics in chickpea plants exposed to a combination of water deficit stress and *Ralstonia solanacearum* infection and have identified a set of genes uniquely expressed in response to combined stress. Also comparing pathogenic and drought stress but focusing on the analysis of redox homeostasis and the role phytohormones, Cui et al. show that co-stress by virus and drought had much severer effects than single stress in *V. vinifera*. Finally, Singh and Jha have studied crosstalk between salt stress

and the bacteria *Bacillus licheniformis* HSW-16. They report biochemical and physiological characterization associated with bacteria-induced systemic tolerance to salt stress.

In conclusion, this Research Topic provides new results and reviews on the signaling pathways induced by abiotic and biotic environmental changes such as drought, high salinity, nutrient, pollutants, or microbial attacks. We think that the diversity of methodology, biological models, and physiological context used to decipher and understand these complex molecular mechanisms at the whole plant level will allow the development of sustainable practices and re-orientation of agricultural managements to improve stress tolerance in crops.

AUTHOR CONTRIBUTIONS

All authors listed have made a substantial, direct and intellectual contribution to the work, and approved it for publication.

REFERENCES

- Jiang, Y., Liang, G., and Yu, D. (2012). Activated expression of WRKY57 confers drought tolerance in *Arabidopsis*. *Mol. Plant* 5, 1375–1388. doi: 10.1093/mp/sss080
- Kulik, A., Wawer, I., Krzywinska, E., Bucholc, M., and Dobrowolska, G. (2011). SnRK2 Protein Kinases-key regulators of plant response to abiotic stresses. *OMICS* 15, 859–872. doi: 10.1089/omi.2011.0091
- Smeekens, S. (2000). Sugar-induced signal transduction in plants. *Annu. Rev. Plant Physiol. Plant Mol. Biol.* 51, 49–81. doi: 10.1146/annurev.arplant.51.1.49

Conflict of Interest Statement: The authors declare that the research was conducted in the absence of any commercial or financial relationships that could be construed as a potential conflict of interest.

Copyright © 2017 Jeandroz and Lamotte. This is an open-access article distributed under the terms of the Creative Commons Attribution License (CC BY). The use, distribution or reproduction in other forums is permitted, provided the original author(s) or licensor are credited and that the original publication in this journal is cited, in accordance with accepted academic practice. No use, distribution or reproduction is permitted which does not comply with these terms.



Emerging roles of protein kinase CK2 in abscisic acid signaling

Belmiro Vilela, Montserrat Pagès and Marta Riera*

Centre for Research in Agricultural Genomics (CRAG), CSIC-IRTA-UAB-UB Consortium, Campus UAB, Barcelona, Spain

The phytohormone abscisic acid (ABA) regulates many aspects of plant growth and development as well as responses to multiple stresses. Post-translational modifications such as phosphorylation or ubiquitination have pivotal roles in the regulation of ABA signaling. In addition to the positive regulator sucrose non-fermenting-1 related protein kinase 2 (SnRK2), the relevance of the role of other protein kinases, such as CK2, has been recently highlighted. We have recently established that CK2 phosphorylates the maize ortholog of open stomata 1 OST1, ZmOST1, suggesting a role of CK2 phosphorylation in the control of ZmOST1 protein degradation (Vilela et al., 2015). CK2 is a pleiotropic enzyme involved in multiple developmental and stress-responsive pathways. This review summarizes recent advances that taken together suggest a prominent role of protein kinase CK2 in ABA signaling and related processes.

OPEN ACCESS

Edited by:

Sylvain Jeandroz,
Agrosup Dijon, France

Reviewed by:

Ingo Dreyer,
Universidad de Talca, Chile
Stephane Bourque,
Institut national de la recherche agronomique, France

*Correspondence:

Marta Riera
marta.riera@cragenomica.es

Specialty section:

This article was submitted to
Plant Physiology,
a section of the journal
Frontiers in Plant Science

Received: 22 September 2015

Accepted: 22 October 2015

Published: 03 November 2015

Citation:

Vilela B, Pagès M and Riera M (2015)
Emerging roles of protein kinase CK2
in abscisic acid signaling.
Front. Plant Sci. 6:966.
doi: 10.3389/fpls.2015.00966

Keywords: protein kinase CK2, ABA signaling, proteasome degradation, circadian clock, post-translational modifications

INTRODUCTION

The phytohormone abscisic acid (ABA) plays a central role in plant development and responses to abiotic stress (Leung and Giraudat, 1998; Finkelstein et al., 2002). Water stress conditions induce the accumulation of ABA levels in guard cells and this increase promotes the closing of stomata in order to reduce transpiration and water loss (Schroeder et al., 2001). The molecular mechanism of ABA action is now well-established in *Arabidopsis* (Cutler et al., 2010; Kim et al., 2010; Klingler et al., 2010; Raghavendra et al., 2010; Umezawa et al., 2010; Zhang et al., 2015). ABA triggers downstream responses by binding to the cytosolic receptors pyrabactin resistance/pyrabactin-like/regulatory component of ABA receptor (PYR/PYL/RCAR), which then sequester the negative regulators clade A type 2C protein phosphatases (PP2C), allowing the activation of Group III Sucrose non-fermenting-1 related protein kinases 2 (SnRK2; Ma et al., 2009; Park et al., 2009). These three protein types are necessary and sufficient to mediate an ABA triggered model signaling cascade *in vitro* (Fujii et al., 2009). Recent advances engineering ABA receptors using agrochemicals open new possibilities for crop improvement (Park et al., 2015).

Reversible protein phosphorylation is therefore a key protein modification involved in ABA signaling and it allows for the rapid regulation of protein function. In addition to the central role of Group III SnRK2s, multiple kinases have been implicated in ABA signaling. Calcium-dependent protein kinases (CDPKs) function as calcium sensors and are hub regulators of Ca^{2+} -mediated immune and stress responses (Mori et al., 2006; Boudsocq and Sheen, 2013). CBL-interacting protein kinases (CIPKs), another family of kinases involved in calcium signaling, regulate potassium transport processes in roots and in stomatal guard cells (Cheong et al., 2007). Moreover, mitogen activated protein kinases (MAPKs) are induced by ABA to elicit a stress response (Danquah et al., 2015).

There is growing amount of data linking protein kinase CK2 to ABA signaling and abiotic stress responses, as shown in this review. CK2 is an evolutionary conserved Ser/Thr kinase found in all eukaryotes. The CK2 holoenzyme is a heterotetramer composed by two types of subunits, two catalytic (CK2 α) and two regulatory (CK2 β ; Litchfield, 2003). Unlike animals, in plants both kinds of subunits are encoded by multigenic families (Velez-Bermudez et al., 2011). Plant CK2 is a pleiotropic enzyme involved in relevant processes such as plant growth and development, light-regulated gene expression, circadian rhythm, hormone responses, cell-cycle regulation, flowering time, DNA repair or responses to biotic and abiotic stress, among others (Riera et al., 2013; Mulekar and Huq, 2014).

ROLE OF PROTEIN KINASE CK2 IN ABA SIGNALING

Since CK2 is essential for plant viability and the depletion of CK2 α is lethal, as previously demonstrated in yeast (Padmanabha et al., 1990), plant genetic approaches involving CK2 have been difficult. The first *Arabidopsis* CK2 α antisense plants produced confirmed the role of CK2 in light-regulated gene expression and plant growth (Lee et al., 1999). In recent years, several transgenic lines for CK2 α have been generated. An inducible dominant-negative for CK2 α plants evidenced that CK2 control chloroplast development, cotyledon expansion, root and shoot growth, as well as altered cell division, cell expansion and auxin transport (Moreno-Romero et al., 2008; Marqués-Bueno et al., 2011). *Arabidopsis* mutated for all three nuclear CK2 α subunits ($\alpha_1\alpha_2\alpha_3$) or doubly mutated in all possible combinations, show a significant decrease of CK2 activity, and a clear phenotype of late flowering. This indicates that CK2 α subunits influence the circadian clock period of oscillation (Lu et al., 2011). Moreover, CK2 α knockout lines display altered developmental and stress responsive pathways with a marked hyposensitivity to ABA and high salt when tested by the criteria of seed germination and cotyledon greening (Mulekar et al., 2012).

Chloroplastic isoforms of CK2 α (cpCK2 α) have been identified in most higher plants (Turkeri et al., 2012; Vélez-Bermúdez et al., 2015). Different phosphoproteomic approaches in *Arabidopsis* demonstrate the prominent role of cpCK2 for phosphorylation in these organelles (Reiland et al., 2009; Schonberg et al., 2014). ABA affects the transcription of most chloroplastic genes (Yamburenko et al., 2013, 2015). Mutation of chloroplastic isoform CKA4 in *Arabidopsis* gives a phenotype of reduced sensitivity to ABA during seed germination and seedling growth, and increased stomatal aperture and leaf water loss (Wang et al., 2014). These effects were attributed to the downregulation of ABA-responsive genes, including OST1, a representative SnRK2 kinase central to ABA signaling. The same work suggests that CK2 is involved in retrograde signaling from chloroplast to nucleus, since the expression levels of the transcription factor *ABI4*, directly involved in retrograde and ABA signaling, were reduced in the *cka4* mutant under ABA treatment (León et al., 2012). Recent work analyzing CK2A4 RNAi lines in the CK2 α triple mutant background confirmed the importance of this gene in the regulation of ABA response, lateral root formation and flowering

time, in a process that could be regulated by retrograde signaling (Mulekar and Huq, 2015).

Even though more than 300 substrates have been described for mammalian CK2 (Meggio and Pinna, 2003; Bian et al., 2013), the confirmed number of CK2 plant substrates is lower, around 50, as shown in Table 1. Among these substrates, CK2 phosphorylation of maize LEA protein RAB17 has been one of more extensively characterized examples (Plana et al., 1991). LEA proteins/RAB/dehydrins accumulate during embryogenesis and their protein level correlates with increased levels of ABA and acquisition of desiccation tolerance (Galau et al., 1986; Ingram and Bartels, 1996). Previous work performed in our group established that CK2 phosphorylation regulates the intracellular dynamics and subcellular localization of maize RAB17. The phosphodeficient mutant form of RAB17, when overexpressed in transgenic *Arabidopsis*, leads to a failure of seed germination arrest in osmotic stress conditions (Plana et al., 1991; Riera et al., 2004). The homologs of Rab17 in tomato (TAS14) and in *Arabidopsis* (ERD14) are also phosphorylated by CK2 (Godoy et al., 1994; Alsheikh et al., 2003). Other dehydrins as TsDHN1, 2 from *Thellungiella salsuginea* can stabilize the cytoskeleton under stress conditions, in a process that may involve CK2 phosphorylation (Rahman et al., 2011). Recently, ZmLEA5C that enhances tolerance to osmotic and low temperature stresses in transgenic tobacco and yeast has been also described as a CK2 substrate (Liu et al., 2014). Different types of transcription factors are also CK2 substrates, some of them involved in ABA response, as EmBP-2 and ZmBZ-1. These two b-ZIP transcription factors are phosphorylated by CK2 and this modification alters their DNA binding capacity (Nieva et al., 2005). Also OREB1, a rice ABRE binding factor is phosphorylated by multiple kinases such as SnRK2 and CK2 (Hong et al., 2011). These factors bind to ABRE (ABA Responsive Elements) in the nucleus and activate the transcription of ABA-inducible genes, suggesting that CK2 regulation of RAB proteins could involve not only direct phosphorylation but also altered gene expression.

We have recently established the maize ortholog of open stomata 1 OST1 (also known as SnRK2.6 or SnRK2E) as a phosphorylation target of CK2 (Vilela et al., 2015). CK2 phosphorylates ZmOST1 at a cluster of serines in the ABA box with implications on protein levels, kinase activity, and response to abiotic stimuli. Transgenic *Arabidopsis* plants overexpressing ZmOST1 mutagenized at CK2 phosphorylation sites are more resistant to drought and are hypersensitive to ABA at the level of stomata.

ABA SIGNALING AND PROTEASOME DEGRADATION

In addition to phosphorylation, other post-translational modifications such as ubiquitination, and sumoylation play significant roles in regulating ABA signaling (Lyzenga and Stone, 2012). Ubiquitination of the PYR/PYL/RCAR ABA receptors causes their degradation in the absence of ABA (Irigoyen et al., 2014). DDB1-ASSOCIATED1 (DDA1), a protein part of the CULLIN4-RING E3 ubiquitin ligase, binds to PYR8, PYL4 and PYL9 and facilitates their proteasomal degradation, negatively

TABLE 1 | List of plant CK2 substrates.

Name	Type	Species	Role	References
Light-signal transduction pathway and circadian clock				
AT-1	DNA binding factor	Pea	Binds to ATI-box elements in light regulated promoters	Datta and Cashmore (1989)
ATBP-1	DNA binding factor	Pea	Binds to ATI-box elements in light regulated promoters	Tjaden and Coruzzi (1994)
GBF1	bZIP TF	<i>Arabidopsis</i>	Binds to G-box elements in light regulated promoters	Klimczak et al. (1995)
Opaque2	bZIP TF	Maize	Circadian clock regulated	Ciceri et al. (1997)
CCA1	Myb-related TF	<i>Arabidopsis</i>	Circadian clock regulator	Sugano et al. (1998)
LHY, OsLHY	Myb-related TF	<i>Arabidopsis</i> , Rice	Circadian clock regulator	Sugano et al. (1998); Ogiso et al. (2010)
HY5	bZIP TF	<i>Arabidopsis</i>	Promotes photomorphogenesis	Hardtke et al. (2000)
HFR1	bHLH TF	<i>Arabidopsis</i>	Promotes photomorphogenesis	Park et al. (2008)
PIF1	Phytochrome interacting factor	<i>Arabidopsis</i>	Represses photomorphogenesis	Bu et al. (2011)
Abiotic and biotic stress				
ZmSnRK2/ZmOST1	Protein kinase	Maize	ABA signaling	Vilela et al. (2015)
Rabi7, ZmLEA5cERD14, TAS-14	LEA proteins	Maize, <i>Arabidopsis</i> , tomato, wheat	Stress responsive proteins	Plana et al. (1991); Liu et al. (2014); Alsheikh et al. (2003); Godoy et al. (1994)
TsDHNI,2	Dehydrins	<i>Thellungiella salsuginea</i>	Stress responsive proteins	Rahman et al. (2011)
EmBP-2/ZmBZ-I	bZIP TF	Maize	Activates transcription of the abscisic acid-inducible gene rab28	Nieva et al. (2005)
TGA2	bZIP TF	<i>Arabidopsis</i>	Binds to promoter of salicilic-induced genes	Kang and Klessig (2005)
OREB1	ABRE binding factor	Rice	Binds to ABRE (ABA responsive Elements)	Hong et al. (2011)
p23	co-chaperone protein	<i>Arabidopsis</i>	Plant response to Salicilic acid	Tosoni et al. (2011)
PCS	phytochelatin synthase	<i>Arabidopsis</i>	Synthesis of heavy metal-binding peptides	Wang et al., 2009
Chromatin associated and nuclear proteins				
lamin-like protein	lamina matrix protein	Pea	Nuclear stability, chromatin organization	Li and Roux (1992)
MFP1	coil-coil protein	Tomato <i>Allium cepa</i>	Structural roles in nuclear matrix and chloroplast	Meier et al. (1996); Samaniego et al. (2006)
NopA64/nopA61	nucleolin-like phosphoproteins	<i>Allium cepa</i>	Located in nucleolus	de Cárcer et al. (1997)
P-proteins	Ribosomal proteins	Maize	Complex with 60S ribosomal subunits	Bailey-Serres et al. (1997)
DNA helicase I	DNA helicase I	Pea	DNA transcription	Tuteja et al. (2001)
DNA topoisomerase I	DNA topoisomerase I	Pea	DNA transcription	Tuteja et al. (2003)
HMGB proteins	High mobility group B proteins	Maize, <i>Arabidopsis</i>	Chromatin associated proteins	Stemmer et al. (2002)
SSRP1	structure-specific recognition protein	Maize	Chromatin associated proteins	Krohn et al. (2003)
eIF2ab/3c/4b/5	elongation initiation factors	<i>Arabidopsis</i> , maize, wheat	Translation initiation	Dennis and Browning (2009)
Histone deacetylase 2B	Histone deacetylase	<i>Arabidopsis</i>	Chromatin remodeling enzyme	Dennis and Browning (2009)
Chloroplast machinery				
Chloroplast RNPs/28RNP/p34/RNP29,33	Ribonucleoproteins	Spinach, <i>Arabidopsis</i>	RNA binding proteins involved in chloroplast RNA processing and stabilization	Kanekatsu et al. (1993, 1995); Lisitsky and Schuster (1995); Reiland et al. (2009)
CP29	photosystem II subunit	Maize	Light harvesting complex import	Testi et al. (1996)
TOC159	preprotein receptor	<i>Arabidopsis</i>	Nuclear-encoded chloroplast preproteins from the cytosol	Agne et al. (2010)
SIG1/SIG6	plastid sigma factors	<i>Arabidopsis</i>	Gene-regulatory proteins for promoter binding and transcription initiation	Schweer et al. (2010)
Alb3	Thylakoid membrane protein	<i>Arabidopsis</i>	Thylakoid biogenesis	Schonberg et al. (2014)
Other				
CFOCF1-ATPase	Chloroplast ATP synthase (b subunit)	Spinach	ATP synthesis	Kanekatsu et al. (1998)
C2	subunit of the 20S proteasome	Rice	Protein degradation of ubiquitinated proteins	Umeda et al. (1997)
gp100/gp96	Glycyrrhizin (GL)-Binding Protein (gp100)	Soybean	Lipoxygenase that catalyzes the oxygenation of unsaturated fatty acids	Ohtsuki et al. (1994, 1995)
β-Conglycinin α Subunit	β-Conglycinin α Subunit	Soybean	storage protein	Ralet et al. (1999)
calreticulin	Calreticulin	Spinach	Ca ²⁺ binding protein	Baldan et al. (1996)
apyrase	apyrase	Pea	ATP hydrolysis	Hsieh et al. (2000)

regulating ABA responses. Conversely, ABA protects PYL8 from destabilization by limiting its polyubiquitination by a process that is still unknown. ABA also reduces PYL8 expression after 3 h of treatment in a process that would facilitate a faster receptor turnover, after the signal is attenuated (Irigoyen et al., 2014). In addition, the turnover of PYL4 and PYR1 in the proximity of the plasma membrane is regulated by the interaction with a single subunit RING-type E3 ubiquitin ligase, RSL1 (Bueso et al., 2014).

Several transcription factors involved in ABA signaling as ABI3, ABI5, ABFs ABI4, and ATHB6 can also be regulated by proteasome degradation. The B3-domain transcription factor ABSCISIC ACID-INSENSITIVE 3 (ABI3), a central regulator in ABA signaling, is an unstable protein that is polyubiquitinated by an ABI3-interacting protein (AIP2), which contains a RING motif. AIP2 negatively regulates ABA signaling by targeting ABI3 for post-translational destruction (Zhang et al., 2005). During vegetative growth, ABA induces AIP2 expression, tightly regulating ABI3 turnover while promoting its accumulation during seed maturation. Another example is ABSCISIC ACID INSENSITIVE 5 (ABI5), a member of the basic leucine zipper (bZIP) transcription factor, that plays an important role in controlling ABA dependent postgerminative growth arrest as well as late phases of seed maturation (Finkelstein and Lynch, 2000; Lopez-Molina et al., 2001). The abundance of ABI5 is tightly controlled by the ubiquitin-26S proteasome system. KEEPONGOING (KEG), a RING3-type E3 ubiquitin ligase, negatively regulates ABA signaling by promoting ABI5 ubiquitination and subsequent degradation by the 26S proteasome (Liu and Stone, 2010). This process occurs in the cytosol when ABA is absent (Liu and Stone, 2013). In the nucleus, ABI5 stability is regulated by another negative regulator of ABA, a E3 ubiquitin ligase assembled with ABA-hypersensitive DCAF1 (ABD1; Seo et al., 2014). In addition to ubiquitination, sumoylation of ABI5 is thought to maintain a degradation-resistant inactive pool of ABI5 in the absence of ABA (Miura et al., 2009). An additional class of ABI5-interacting proteins, the AFPs, has also been reported to alter ABI5 stability (Lopez-Molina et al., 2003). Another group of positive effectors in ABA responses regulated by proteasome degradation is the ABA Binding Factor/ABA-Responsive Element Binding Proteins (ABF/AREB) subfamily of bZIP-type transcription factors. ABF1 and ABF3 have similar functions to ABI5 in regulating seed germination and post-germinative growth (Finkelstein et al., 2005). ABF1 and ABF3 are ubiquitylation substrates of KEG and the abundance of both proteins is affected by ABA and the ubiquitin pathway (Chen et al., 2013). The stabilization of ABF1 and ABF3 by ABA is thought to be achieved by phosphorylation by SnRK2 kinases, which in turn promotes the binding of 14-3-3 proteins (Sirichandra et al., 2010). ABSCISIC ACID INSENSITIVE 4 (ABI4), a member of the DREB subfamily A-3 of ERF/AP2 transcription factors, is required for proper ABA signaling during seed development and germination (Gregorio et al., 2014). Like ABI3 and ABI5, ABI4 is subject to a stringent post-transcriptional regulation that targets the protein to degradation and prevents it from accumulating to high levels. However, unlike ABI3 and ABI5, ABI4 is not stabilized in the presence of ABA (Finkelstein et al., 2011). Finally, the

HD-Zip transcription factor ATHB6 physically interacts with the PP2C phosphatase ABI1 and it has been described as a negative regulator of the ABA signal pathway (Himmelbach et al., 2002). Moreover, ABA negatively regulates ATHB6 protein turnover (Lechner et al., 2011).

Proteosomal degradation in response to ABA is regulated by phosphorylation/dephosphorylation mechanisms (Figure 1A). For instance, ABA promotes the self ubiquitination and degradation of KEG after phosphorylation, a process that could be regulated by the SnRK2 kinases belonging to the core ABA signaling complex (Antoni et al., 2011). Another kinase, Calcineurin B-like Interacting Protein Kinase 26 (CIPK26) interacts with the ABA signaling components ABI1, ABI2, and ABI5. CIPK26 influences the sensitivity of germinating seeds to the inhibitory effects of ABA and is also targeted by KEG for proteasomal degradation (Lyzenga et al., 2013).

Our recent work points toward a role of protein kinase CK2 in control of ZmOST1 protein degradation (Vilela et al., 2015). CK2 phosphorylation enhances ZmOST1 interaction with PP2C phosphatases, probably causing a sustained “off” state of kinase activity, and also primes SnRK2 for protein degradation through the 26S proteasome pathway. Thus, CK2 seems to act in dampening the ABA signal output through its action on ZmOST1 while at the same time inducing ZmOST1 transcription (Figure 1A). This type of regulation would be particularly effective in the absence of ABA, with the silencing of SnRK2 output and the preparation of the new state of ABA response.

OTHER IMPLICATIONS OF CK2 ACTION IN ABA SIGNALING

One particularly important process in the regulation of plant-water relationship is the incorporation of circadian responses in the output of the ABA signal. In fact, the regulation of circadian rhythms to anticipate daily and seasonal environmental cycles allows the plant to optimally incorporate external conditions into internal processes. Stomata, for instance, are able to anticipate the dawn and dusk signals, and are more responsive to ABA in the afternoon, coinciding with the timing of (Ca^{2+}) peak oscillations (Seo and Mas, 2015).

Circadian rhythms are autoregulatory, endogenous rhythms with a period of approximately 24 h. In *Arabidopsis*, the core circadian clock is made up of genes that interact through a series of transcriptional and post-transcriptional feedback loops to create rhythmic gene expression (Seo et al., 2012; Bendix et al., 2015). Briefly, the core circadian clock consists of a negative feedback loop between the two homologous MYB-like transcription factors CIRCADIAN CLOCK ASSOCIATED 1 (CCA1) and LATE ELONGATED HYPOCOTYL (LHY) on one hand and TIMING OF CAB EXPRESSION1 (TOC1) on the other (Fogelmark and Troein, 2014).

TOC1 and ABA work antagonistically to achieve the optimal response to water status. ABA treatment induces TOC1 expression and, in a feedback loop, TOC1 attenuates ABA signaling and negatively regulates the expression of ABA signaling genes. TOC1 mis-expressing plants have defects in ABA-dependent stomata closure and altered tolerance to drought stress

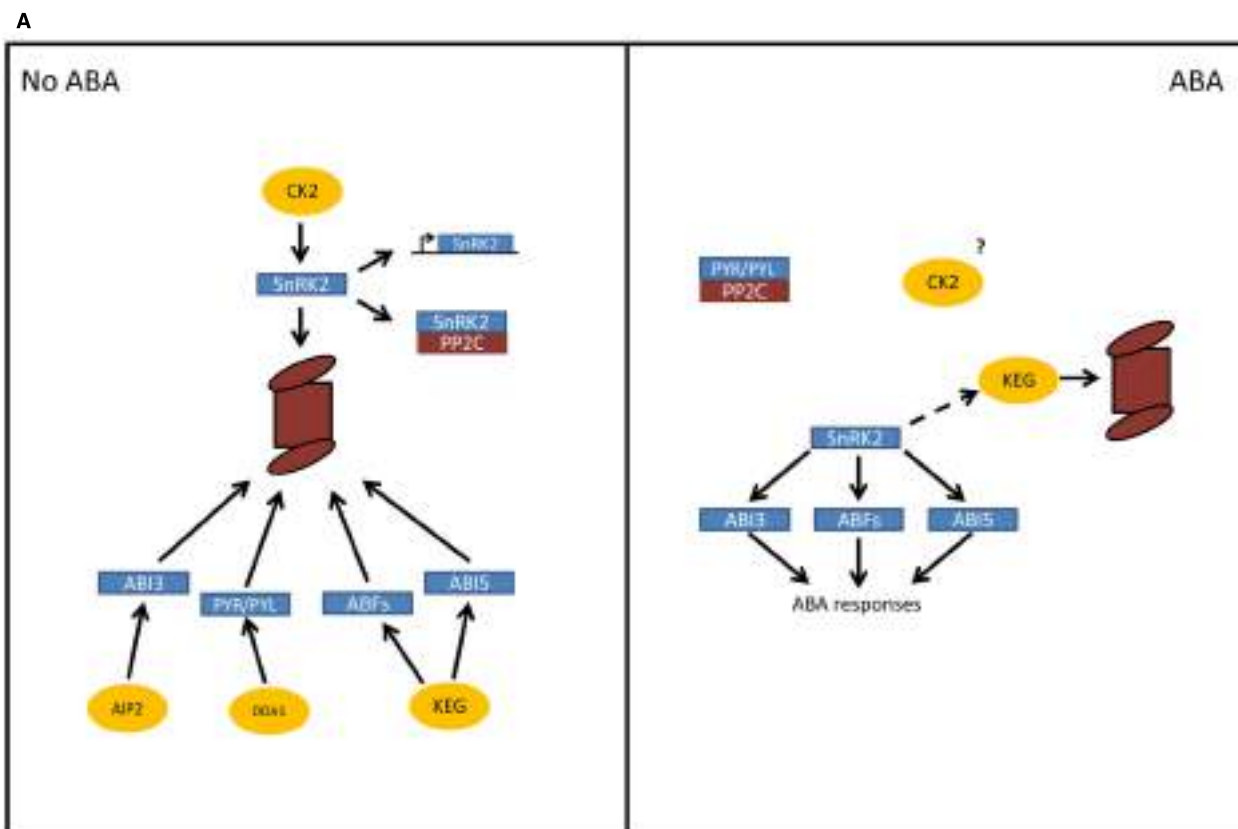
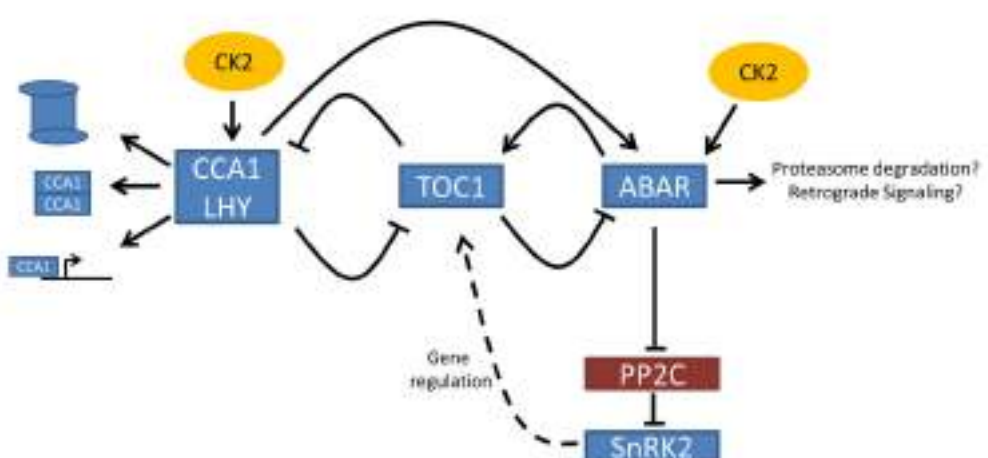
**B**

FIGURE 1 | (A) Regulation of ABA signaling by the control of protein turnover. In the absence of ABA, major regulators of the hormone such as the PYR/PYL/RCAR receptors, the SnRK2 kinases, and several transcription factors (ABI3, ABI5, ABF1, ABF3) are degraded by the proteasome, and/or inactivated. In this way the output of the ABA signal is thoroughly dampened in the absence of the hormone. When ABA levels rise, these major regulators are protected from degradation through the inactivation or degradation of the negative regulators such as KEG. CK2 is known to mediate the stabilization and destabilization of proteins in other systems and is a likely candidate to also have a role as a housekeeping kinase controlling protein turnover in ABA signaling. **(B)** Integration of the plant circadian clock on ABA signaling. The core circadian clock consists of a negative feedback loop between the CCA1 and LHY on one hand and TOC1 on the other. ABA treatment induces TOC1 expression and, in another feedback loop, TOC1 attenuates ABA signaling and negatively regulates the expression of ABA signaling genes like ABAR, known to interact with the ABA central signaling complex. CCA1 and LHY act synergistic to ABA and antagonistic to TOC1 expression. CCA1 and LHY are phosphorylated by CK2 targeting them for degradation, promoting CCA1 dimerization, CCA1-DNA complex formation, and interaction with the promoters of downstream genes. ABAR is also a substrate of CK2 and, even though the effects of this activity are still unknown, they could include protein turnover and altered gene expression by retrograde signaling from the chloroplast.

(Legnaioli et al., 2009). Consequently, CCA1 and LHY should be synergistic to ABA and antagonistic to TOC1 expression (Pokhilko et al., 2013). Interestingly, one of the ABA genes negatively regulated by TOC1 is the magnesium quelatase subunit H (ABAR/CHLH/GUN5). ABAR is involved in retrograde signaling and positively regulates guard cell signaling in response to ABA. It has been recently demonstrated that ABAR and OST1 can interact *in vitro*, but that ABAR phosphorylation is independent of OST1 since it apparently acts upstream of the PP2C-SnRK2 complex (Liang et al., 2015). It should be noted that ABAR has been suggested as a potential substrate of cpCK2 (Reiland et al., 2009; Schonberg et al., 2014) but additional experiments are required to elucidate the effect of CK2 activity on this protein.

The phosphorylation of clock proteins plays a critical role in generating proper circadian rhythms (Lu et al., 2011). Overexpression of CK2 regulatory subunits (CKB3 or CKB4) in *Arabidopsis* displays increased CK2 activity, a reduction of the subjective day length inducing alterations in clock-regulated gene expression, hypocotyl elongation, and flowering time (Sugano et al., 1999; Perales et al., 2006). CCA1 and LHY are phosphorylated by CK2 and this phosphorylation is required for the normal functioning of the CCA1 protein (Daniel et al., 2004). CK2 is involved in the temporal regulation of CCA1 protein activity, targeting it for degradation, promoting CCA1 dimerization, CCA1-DNA complex formation, and interaction with the promoters of downstream genes, such as TOC1 (Kusakina and Dodd, 2012).

Thus, increasing levels of ABA lead to an increase in TOC1 levels, resulting in the repression of the ABA signal through the down-regulation of ABAR/CHLH/GUN5 and CCA1 by TOC1. Concomitantly, CK2 activity would regulate the level of CCA1 repression through its controlled degradation, and regulation of protein and DNA interaction, in a process analogous to the SnRK2 repression explained earlier (**Figure 1B**).

CONCLUDING REMARKS

Our understanding of ABA signaling has expanded exponentially in recent years. Two seminal works on a family of soluble proteins that are able to bind ABA made possible the construction of a functional model for ABA signal transduction (Ma et al., 2009; Park et al., 2009). These ABA receptors (PYR/PYL/RCAR), together with SnRK2 kinases and PP2C phosphatases constitute the central core of ABA signaling.

The central core of ABA signaling controls a fast cellular response to ABA that ranges from activation of ion transports to a large transcription reprogramming. Nevertheless, there is

REFERENCES

- Agne, B., Andres, C., Montandon, C., Christ, B., Ertan, A., Jung, F., et al. (2010). The acidic a-domain of *Arabidopsis* toc159 occurs as a hyperphosphorylated protein. *Plant Physiol.* 153, 1016–1030. doi: 10.1104/pp.110.158048
- Alsheikh, M. K., Heyen, B. J., and Randall, S. K. (2003). Ion binding properties of the dehydrin ERD14 are dependent upon phosphorylation. *J. Biol. Chem.* 278, 40882–40889. doi: 10.1074/jbc.M307151200
- Antoni, R., Rodriguez, L., Gonzalez-Guzman, M., Pizzio, G. A., and Rodriguez, P. L. (2011). News on ABA transport, protein degradation, and ABFs/WRKYs

growing evidence that, following the initial response to ABA, the persistence of the signal results in a secondary response that leads to stress adaptation. ABA signaling is also capable of incorporating several other processes, such as circadian rhythms, in their output.

Protein phosphorylation and dephosphorylation play a central role in ABA signaling and promote the activation, deactivation, sequestration and degradation of a wide range of protein regulators. In addition to protein phosphorylation, regulation of protein stability by the 26S proteasome is an important mechanism for ABA signaling.

ABA signaling appears to undergo dynamic changes in the steady state of some of its major components (**Figure 1**). In the absence of the hormone, the PYR/PYL/RCAR receptors, the SnRK2 kinases, and several transcription factors that elicit ABA response are degraded by the proteasome, and/or inactivated. This results in an effective dampening of the ABA signal. Conversely, ABA has a protecting effect on the protein turnover of these components and their activation. At the same time, ABA transcriptionally regulates the future changes in the ABA signal.

CK2 mediated stabilization and destabilization of proteins represents a known evolutionarily conserved mechanism. Phosphorylation by CK2 enhances the polyubiquitination of target proteins, signaling to or protecting from proteasomal degradation. For instance, CK2 phosphorylation regulates photomorphogenesis stabilizing HY5 and HR1 and promoting degradation of PIF1 (Hardtke et al., 2000; Park et al., 2008; Bu et al., 2011). In addition, CK2 does not appear to be under major transcriptional regulation and the holoenzyme activity appears to always be in an “on” state. These characteristics make CK2 a housekeeping kinase that can modify protein functions and protein turnover in a dynamic way. In the context of ABA signaling, CK2 is already known to promote SnRK2 degradation through the 26S proteasome and inactivation through the interaction with PP2C, and has been connected with ABAR phosphorylation. Exploring the effects of CK2 in the phosphorylation and ubiquitination of other ABA regulators should help to give a broader perspective on ABA signal, protein stability and integration of other processes in abiotic stress responses.

FUNDING

This work was supported by grant BIO2012-31860 (MICINN, Spain) to MP.

ACKNOWLEDGMENT

We thank Dr. D. Ludevid for critical reading of this manuscript.

- in ABA signaling. *Curr. Opin. Plant Biol.* 14, 547–553. doi: 10.1016/j.pbi.2011.06.004
- Bailey-Serres, J., Vangala, S., Szick, K., and Lee, C. H. (1997). Acidic phosphoprotein complex of the 60S ribosomal subunit of maize seedling roots. Components and changes in response to flooding. *Plant Physiol.* 114, 1293–1305. doi: 10.1104/pp.114.4.1293
- Baldan, B., Navazio, L., Friso, A., Mariani, P., and Meggio, F. (1996). Plant calreticulin is specifically and efficiently phosphorylated by protein kinase CK2. *Biochem. Biophys. Res. Commun.* 221, 498–502. doi: 10.1006/bbrc.1996.0625

- Bendix, C., Marshall, C. M., and Harmon, F. G. (2015). Circadian clock genes universally control key agricultural traits. *Mol. Plant* 8, 1135–1152. doi: 10.1016/j.molp.2015.03.003
- Bian, Y., Ye, M., Wang, C., Cheng, K., Song, C., Dong, M., et al. (2013). Global screening of CK2 kinase substrates by an integrated phosphoproteomics workflow. *Sci. Rep.* 3, 3460. doi: 10.1038/srep03460
- Boudsocq, M., and Sheen, J. (2013). CDPKs in immune and stress signaling. *Trends Plant Sci.* 18, 30–40. doi: 10.1016/j.tplants.2012.08.008
- Bueso, E., Rodriguez, L., Lorenzo-Orts, L., Gonzalez-Guzman, M., Sayas, E., Munoz-Bertomeu, J., et al. (2014). The single-subunit RING-type E3 ubiquitin ligase RSL1 targets PYL4 and PYR1 ABA receptors in plasma membrane to modulate abscisic acid signaling. *Plant J.* 80, 1057–1071. doi: 10.1111/tpj.12708
- Bu, Q., Zhu, L., Dennis, M. D., Yu, L., Lu, S. X., Person, M. D., et al. (2011). Phosphorylation by CK2 enhances the rapid light-induced degradation of phytochrome interacting factor 1 in *Arabidopsis*. *J. Biol. Chem.* 286, 12066–12074. doi: 10.1074/jbc.M110.186882
- Chen, Y. T., Liu, H., Stone, S., and Callis, J. (2013). ABA and the ubiquitin E3 ligase KEEP ON GOING affect proteolysis of the *Arabidopsis thaliana* transcription factors ABF1 and ABF3. *Plant J.* 75, 965–976. doi: 10.1111/tpj.12259
- Cheong, Y. H., Pandey, G. K., Grant, J. J., Batistic, O., Li, L., Kim, B. G., et al. (2007). Two calcineurin B-like calcium sensors, interacting with protein kinase CIPK23, regulate leaf transpiration and root potassium uptake in *Arabidopsis*. *Plant J.* 52, 223–239. doi: 10.1111/j.1365-313X.2007.03236.x
- Ciceri, P., Gianazza, E., Lazzari, B., Lippoli, G., Genga, A., Hoschek, G., et al. (1997). Phosphorylation of Opaque 2 changes diurnally and impacts its DNA binding activity. *Plant Cell* 9, 97–108. doi: 10.1105/tpc.9.1.97
- Cutler, S. R., Rodriguez, P. L., Finkelstein, R. R., and Abrams, S. R. (2010). Abscisic acid: emergence of a core signaling network. *Annu. Rev. Plant Biol.* 61, 651–679. doi: 10.1146/annurev-arplant-042809-112122
- Daniel, X., Sugano, S., and Tobin, E. M. (2004). CK2 phosphorylation of CCA1 is necessary for its circadian oscillator function in *Arabidopsis*. *Proc. Natl. Acad. Sci. U.S.A.* 101, 3292–3297. doi: 10.1073/pnas.0400163101
- Danquah, A., de Zelicourt, A., Boudsocq, M., Neubauer, J., Frei Dit Frey, N., Leonhardt, N., et al. (2015). Identification and characterization of an ABA-activated MAP kinase cascade in *Arabidopsis thaliana*. *Plant J.* 82, 232–244. doi: 10.1111/tpj.12808
- Datta, N., and Cashmore, A. R. (1989). Binding of a pea nuclear-protein to promoters of certain photoregulated genes is modulated by phosphorylation. *Plant Cell* 1, 1069–1077. doi: 10.1105/tpc.1.11.1069
- de Cácer, G., Cerdido, A., and Medina, F. J. (1997). NopA64, a novel nucleolar phosphoprotein from proliferating onion cells, sharing immunological determinants with mammalian nucleolin. *Planta* 201, 487–495. doi: 10.1007/s004250050093
- Dennis, M. D., and Browning, K. S. (2009). Differential phosphorylation of plant translation initiation factors by *Arabidopsis thaliana* CK2 holoenzymes. *J. Biol. Chem.* 284, 20602–20614. doi: 10.1074/jbc.M109.006692
- Finkelstein, R., Gampala, S. S., Lynch, T. J., Thomas, T. L., and Rock, C. D. (2005). Redundant and distinct functions of the ABA response loci ABA-INSENSITIVE(ABI)5 and ABRE-BINDING FACTOR (ABF)3. *Plant Mol. Biol.* 59, 253–267. doi: 10.1007/s11103-005-8767-2
- Finkelstein, R., Lynch, T., Reeves, W., Petitfrère, M., and Mostachetti, M. (2011). Accumulation of the transcription factor ABA-insensitive (ABI)4 is tightly regulated post-transcriptionally. *J. Exp. Bot.* 62, 3971–3979. doi: 10.1093/jxb/err093
- Finkelstein, R. R., Gampala, S. S. L., and Rock, C. D. (2002). Abscisic Acid Signaling in Seeds and Seedlings. *Plant Cell* 14, S15–S45.
- Finkelstein, R. R., and Lynch, T. J. (2000). The *Arabidopsis* abscisic acid response gene ABI5 encodes a basic leucine zipper transcription factor. *Plant Cell* 12, 599–609. doi: 10.1105/tpc.12.4.599
- Fogelmark, K., and Troein, C. (2014). Rethinking transcriptional activation in the *Arabidopsis* circadian clock. *PLoS Comput. Biol.* 10:e1003705. doi: 10.1371/journal.pcbi.1003705
- Fujii, H., Chinnusamy, V., Rodrigues, A., Rubio, S., Antoni, R., Park, S. Y., et al. (2009). *In vitro* reconstitution of an abscisic acid signalling pathway. *Nature* 462, 660–664. doi: 10.1038/nature08599
- Galau, G., Hughes, D. W., and Dure, L., and III. (1986). Abscisic acid induction of cloned cotton late embryogenesis-abundant (Lea) mRNAs. *Plant Mol. Biol.* 7, 155–170. doi: 10.1007/bf00021327
- Godoy, J., Lunar, R., Torres-Schumann, S., Moreno, J., Rodrigo, R., and Pintor-Toro, J. (1994). Expression, tissue distribution and subcellular localization of dehydrin TAS14 in salt-stressed tomato plants. *Plant Mol. Biol.* 26, 1921–1934. doi: 10.1007/BF00019503
- Gregorio, J., Hernandez-Bernal, A. F., Cordoba, E., and Leon, P. (2014). Characterization of evolutionarily conserved motifs involved in activity and regulation of the ABA-INSENSITIVE (ABI) 4 transcription factor. *Mol. Plant* 7, 422–436. doi: 10.1093/mp/sst132
- Hardtke, C. S., Gohda, K., Osterlund, M. T., Oyama, T., Okada, K., and Deng, X. W. (2000). HY5 stability and activity in *Arabidopsis* is regulated by phosphorylation in its COP1 binding domain. *EMBO J.* 19, 4997–5006. doi: 10.1093/emboj/19.18.4997
- Himmelman, A., Hoffmann, T., Leube, M., Höhener, B., and Grill, E. (2002). Homeodomain protein ATHB6 is a target of the protein phosphatase ABI1 and regulates hormone responses in *Arabidopsis*. *EMBO J.* 21, 3029–3038. doi: 10.1093/emboj/cdf316
- Hong, J. Y., Chae, M. J., Lee, I. S., Lee, Y. N., Nam, M. H., Kim, D. Y., et al. (2011). Phosphorylation-mediated regulation of a rice ABA responsive element binding factor. *Phytochemistry* 72, 27–36. doi: 10.1016/j.phytochem.2010.10.005
- Hsieh, H. L., Song, C. J., and Roux, S. J. (2000). Regulation of a recombinant pea nuclear apyrase by calmodulin and casein kinase II. *Biochim. Biophys. Acta* 1494, 248–255. doi: 10.1016/s0167-4781(00)00245-1
- Ingram, J., and Bartels, D. (1996). The molecular basis of dehydration tolerance in plants. *Annu. Rev. Plant Physiol. Plant Mol. Biol.* 47, 377–403. doi: 10.1146/annurev.arplant.47.1.377
- Irigoyen, M. L., Iniesto, E., Rodriguez, L., Puga, M. I., Yanagawa, Y., Pick, E., et al. (2014). Targeted degradation of abscisic acid receptors is mediated by the ubiquitin ligase substrate adaptor DDA1 in *Arabidopsis*. *Plant Cell* 26, 712–728. doi: 10.1105/tpc.113.122234
- Kanekatsu, M., Ezumi, A., Nakamura, T., and Ohtsuki, K. (1995). Chloroplast ribonucleoproteins (RNPs) as phosphate acceptors for casein kinase II: purification by ssDNA-cellulose column chromatography. *Plant Cell Physiol.* 36, 1649–1656
- Kanekatsu, M., Munakata, H., Furuzono, K., and Ohtsuki, K. (1993). Biochemical characterization of a 34 kDa ribonucleoprotein (p34) purified from the spinach chloroplast fraction as an effective phosphate acceptor for casein kinase II. *FEBS Lett.* 335, 176–180. doi: 10.1016/0014-5793(93)80724-9
- Kanekatsu, M., Saito, H., Motohashi, K., and Hisabori, T. (1998). The beta subunit of chloroplast ATP synthase (CF0CF1-ATPase) is phosphorylated by casein kinase II. *Biochem. Mol. Biol. Int.* 46, 99–105.
- Kang, H. G., and Klessig, D. F. (2005). Salicylic acid-inducible *Arabidopsis* CK2-like activity phosphorylates TGA2. *Plant Mol. Biol.* 57, 541–557. doi: 10.1007/s11103-005-0409-1
- Kim, T.-H., Böhmer, M., Hu, H., Nishimura, N., and Schroeder, J. I. (2010). Guard cell signal transduction network: advances in understanding abscisic acid, CO₂, and Ca²⁺ Signaling. *Annu. Rev. Plant Biol.* 61, 561–591. doi: 10.1146/annurev-arplant-042809-112226
- Klimczak, L. J., Collinge, M. A., Farini, D., Giuliano, G., Walker, J. C., and Cashmore, A. R. (1995). Reconstitution of *Arabidopsis* casein kinase II from recombinant subunits and phosphorylation of transcription factor GBF1. *Plant Cell* 7, 105–115. doi: 10.1105/tpc.7.1.105
- Klingler, J. P., Batelli, G., and Zhu, J. K. (2010). ABA receptors: the START of a new paradigm in phytohormone signalling. *J. Exp. Bot.* 61, 3199–3210. doi: 10.1093/jxb/erq151
- Krohn, N. M., Stemmer, C., Fojan, P., Grimm, R., and Grasser, K. D. (2003). Protein kinase CK2 phosphorylates the high mobility group domain protein SSRP1, inducing the recognition of UV-damaged DNA. *J. Biol. Chem.* 278, 12710–12715. doi: 10.1074/jbc.M300250200
- Kusakina, J., and Dodd, A. N. (2012). Phosphorylation in the plant circadian system. *Trends Plant Sci.* 17, 575–583. doi: 10.1016/j.tplants.2012.06.008
- Lechner, E., Leonhardt, N., Eisler, H., Parmentier, Y., Alioua, M., Jacquet, H., et al. (2011). MATH/BTB CRL3 receptors target the homeodomain-leucine zipper ATHB6 to modulate abscisic acid signaling. *Dev. Cell* 21, 1116–1128. doi: 10.1016/j.devcel.2011.10.018
- Lee, Y., Lloyd, A. M., and Roux, S. J. (1999). Antisense Expression of the CK2 alpha -Subunit Gene in *Arabidopsis*: effects on light-regulated gene expression and plant growth. *Plant Physiol.* 119, 989–1000. doi: 10.1104/pp.119.3.989

- Legnaioli, T., Cuevas, J., and Mas, P. (2009). TOC1 functions as a molecular switch connecting the circadian clock with plant responses to drought. *EMBO J.* 28, 3745–3757. doi: 10.1038/emboj.2009.297
- León, P., Gregorio, J., and Cordoba, E. (2012). ABI4 and its role in chloroplast retrograde communication. *Front. Plant Sci.* 3:304. doi: 10.3389/fpls.2012.00304
- Leung, J., and Giraudat, J. (1998). ABScisic Acid SIGNAL TRANSDUCTION. *Annu. Rev. Plant Physiol. Plant Mol. Biol.* 49, 199–222. doi: 10.1146/annurev.arplant.49.1.199
- Li, H., and Roux, S. J. (1992). Casein kinase II protein kinase is bound to laminin-matrix and phosphorylates lamin-like protein in isolated pea nuclei. *Proc. Natl. Acad. Sci. U.S.A.* 89, 8434–8438.
- Liang, S., Lu, K., Wu, Z., Jiang, S.-C., Yu, Y.-T., Bi, C., et al. (2015). A link between magnesium-chelatase H subunit and sucrose non-fermenting 1 (SNF1)-related protein kinase SnRK2.6/OST1 in *Arabidopsis* guard cell signalling in response to abscisic acid. *J. Exp. Bot.* 66, 6355–6369. doi: 10.1093/jxb/erv341
- Lisitsky, I., and Schuster, G. (1995). Phosphorylation of a chloroplast rna-binding protein-changes its affinity to rna. *Nucleic Acids Res.* 23, 2506–2511. doi: 10.1093/nar/23.13.2506
- Litchfield, D. W. (2003). Protein kinase CK2: structure, regulation and role in cellular decisions of life and death. *Biochem. J.* 369, 1–15. doi: 10.1042/bj20021469
- Liu, H., and Stone, S. L. (2010). Abscisic acid increases *Arabidopsis* ABI5 transcription factor levels by promoting KEG E3 ligase self-ubiquitination and proteasomal degradation. *Plant Cell* 22, 2630–2641. doi: 10.1105/tpc.110.076075
- Liu, H., and Stone, S. L. (2013). Cytoplasmic degradation of the *Arabidopsis* transcription factor abscisic acid insensitive 5 is mediated by the RING-type E3 ligase KEEP ON GOING. *J. Biol. Chem.* 288, 20267–20279. doi: 10.1074/jbc.M113.465369
- Liu, Y., Wang, L., Jiang, S., Pan, J., Cai, G., and Li, D. (2014). Group 5 LEA protein, ZmLEA5C, enhance tolerance to osmotic and low temperature stresses in transgenic tobacco and yeast. *Plant Physiol. Biochem.* 84, 22–31. doi: 10.1016/j.plaphy.2014.08.016
- Lopez-Molina, L., Mongrand, S., and Chua, N. H. (2001). A postgermination developmental arrest checkpoint is mediated by abscisic acid and requires the ABI5 transcription factor in *Arabidopsis*. *Proc. Natl. Acad. Sci. U.S.A.* 98, 4782–4787. doi: 10.1073/pnas.081594298
- Lopez-Molina, L., Mongrand, S., Kinoshita, N., and Chua, N. H. (2003). AFP is a novel negative regulator of ABA signaling that promotes ABI5 protein degradation. *Genes Dev.* 17, 410–418. doi: 10.1101/gad.1055803
- Lu, S. X., Liu, H., Knowles, S. M., Li, J., Ma, L., Tobin, E. M., et al. (2011). A role for protein kinase casein kinase2 alpha-subunits in the *Arabidopsis* circadian clock. *Plant Physiol.* 157, 1537–1545. doi: 10.1104/pp.111.179846
- Lyzenga, W. J., Liu, H., Schofield, A., Muise-Hennessey, A., and Stone, S. L. (2013). *Arabidopsis* CIPK26 interacts with KEG, components of the ABA signalling network and is degraded by the ubiquitin-proteasome system. *J. Exp. Bot.* 64, 2779–2791. doi: 10.1093/jxb/ert123
- Lyzenga, W. J., and Stone, S. L. (2012). Abiotic stress tolerance mediated by protein ubiquitination. *J. Exp. Bot.* 63, 599–616. doi: 10.1093/jxb/err310
- Marqués-Bueno, M. M., Moreno-Romero, J., Abas, L., De Michele, R., and Martínez, M. C. (2011). A dominant negative mutant of protein kinase CK2 exhibits altered auxin responses in *Arabidopsis*. *Plant J.* 67, 169–180. doi: 10.1111/j.1365-313X.2011.04585.x
- Ma, Y., Szostkiewicz, I., Korte, A., Moes, D., Yang, Y., Christmann, A., et al. (2009). Regulators of PP2C phosphatase activity function as abscisic acid sensors. *Science* 324, 1064–1068. doi: 10.1126/science.1172408
- Meggio, F., and Pinna, L. A. (2003). One-thousand-and-one substrates of protein kinase CK2? *FASEB J.* 17, 349–368. doi: 10.1096/fj.02-0473rev
- Meier, I., Phelan, T., Gruissem, W., Spiker, S., and Schneider, D. (1996). MFP1, a novel plant filament-like protein with affinity for matrix attachment region DNA. *Plant Cell* 8, 2105–2115. doi: 10.1105/tpc.8.11.2105
- Miura, K., Lee, J., Jin, J. B., Yoo, C. Y., Miura, T., and Hasegawa, P. M. (2009). Sumoylation of ABI5 by the *Arabidopsis* SUMO E3 ligase SIZ1 negatively regulates abscisic acid signaling. *Proc. Natl. Acad. Sci. U.S.A.* 106, 5418–5423. doi: 10.1073/pnas.0811088106
- Moreno-Romero, J., Espunya, M. C., Platara, M., Arino, J., and Martinez, M. C. (2008). A role for protein kinase CK2 in plant development: evidence obtained using a dominant-negative mutant. *Plant J.* 55, 118–130. doi: 10.1111/j.1365-313X.2008.03494.x
- Mori, I. C., Murata, Y., Yang, Y., Munemasa, S., Wang, Y. F., Andreoli, S., et al. (2006). CDPKs CPK6 and CPK3 function in ABA regulation of guard cell S-type anion- and Ca²⁺-permeable channels and stomatal closure. *PLoS Biol.* 4:e327. doi: 10.1371/journal.pbio.0040327
- Mulekar, J., Bu, Q., Chen, F., and Huq, E. (2012). Casein kinase II alpha subunits affect multiple developmental and stress-responsive pathways in *Arabidopsis*. *Plant J.* 69, 343–354. doi: 10.1111/j.1365-313X.2011.04794.x
- Mulekar, J. J., and Huq, E. (2014). Expanding roles of protein kinase CK2 in regulating plant growth and development. *J. Exp. Bot.* 65, 2883–2893. doi: 10.1093/jxb/ert401
- Mulekar, J. J., and Huq, E. (2015). *Arabidopsis* casein kinase 2 α4 subunit regulates various developmental pathways in a functionally overlapping manner. *Plant Sci.* 236, 295–303. doi: 10.1016/j.plantsci.2015.04.013
- Nieva, C., Busk, P., Domínguez-Puigjaner, E., Lumbrales, V., Testillano, P., Risueño, M.-C., et al. (2005). Isolation and functional characterisation of two new bZIP maize regulators of the ABA responsive gene rab28. *Plant Mol. Biol.* 58, 899–914. doi: 10.1007/s11103-005-8407-x
- Ogiso, E., Takahashi, Y., Sasaki, T., Yano, M., and Izawa, T. (2010). The role of casein kinase II in flowering time regulation has diversified during evolution. *Plant Physiol.* 152, 808–820. doi: 10.1104/pp.109.148908
- Ohtsuki, K., Nakamura, S., Shimoyama, Y., Shibata, D., Munakata, H., Yoshiki, Y., et al. (1995). A 96-kDa glycyrrhizin-binding protein (gp96) from soybeans acts as a substrate for case in kinase II, and is highly related to lipoxygenase3. *J. Biochem. (Tokio)* 118, 1145–1150.
- Ohtsuki, K., Ohishi, M., Karino, A., Kanekatsu, M., and Shamsa, F. (1994). Purification and characterization of 100-kDa Glycyrrhizin (GL)-Binding Protein (gp100) as an effective phosphate acceptor for CK-II and the effect of GL on the phosphorylation of gp100 by CK-II *in vitro*. *Biochem. Biophys. Res. Commun.* 198, 1090–1098. doi: 10.1006/bbrc.1994.1155
- Padmanabha, R., Chen-Wu, J., Hanna, D., and Glover, C. (1990). Isolation, sequencing, and disruption of the yeast CKA2 gene: casein kinase II is essential for viability in *Saccharomyces cerevisiae*. *Mol. Cell. Biol.* 10, 4089–4099. doi: 10.1128/MCB.10.8.4089
- Park, H. J., Ding, L., Dai, M., Lin, R., and Wang, H. (2008). Multisite phosphorylation of *Arabidopsis* HFR1 by casein kinase II and a plausible role in regulating its degradation rate. *J. Biol. Chem.* 283, 23264–23273. doi: 10.1074/jbc.M801720200
- Park, S. Y., Fung, P., Nishimura, N., Jensen, D. R., Fujii, H., Zhao, Y., et al. (2009). Abscisic acid inhibits type 2C protein phosphatases via the PYR/PYL family of START proteins. *Science* 324, 1068–1071. doi: 10.1126/science.1173041
- Park, S. Y., Peterson, F. C., Mosquera, A., Yao, J., Volkman, B. F., and Cutler, S. R. (2015). Agrochemical control of plant water use using engineered abscisic acid receptors. *Nature* 520, 545–548. doi: 10.1038/nature14123
- Perales, M., Portolés, S., and Más, P. (2006). The proteasome-dependent degradation of CKB4 is regulated by the *Arabidopsis* biological clock. *Plant J.* 46, 849–860. doi: 10.1111/j.1365-313X.2006.02744.x
- Plana, M., Itarte, E., Eritja, R., Goday, A., Pages, M., and Martinez, M. C. (1991). Phosphorylation of maize RAB-17 protein by casein kinase 2. *J. Biol. Chem.* 266, 22510–22514.
- Pokhilko, A., Mas, P., and Millar, A. J. (2013). Modelling the widespread effects of TOC1 signalling on the plant circadian clock and its outputs. *BMC Syst. Biol.* 7:23. doi: 10.1186/1752-0509-7-23
- Raghavendra, A. S., Gonuguntla, V. K., Christmann, A., and Grill, E. (2010). ABA perception and signalling. *Trends Plant Sci.* 15, 395–401. doi: 10.1016/j.tplants.2010.04.006
- Rahman, L. N., Smith, G. S. T., Bamm, V. V., Voyer-Grant, J. A. M., Moffatt, B. A., Dutcher, J. R., et al. (2011). Phosphorylation of *Thellungiella salsuginea* dehydrins TsDHN-1 and TsDHN-2 facilitates cation-induced conformational changes and actin assembly. *Biochemistry* 50, 9587–9604. doi: 10.1021/bi201205m
- Ralet, M.-C., Fouques, D., Leonil, J., Molle, D., and Meunier, J.-C. (1999). Soybean β-conglycinin α subunit is phosphorylated on two distinct series by protein kinase CK2. *J. Protein Chem.* 18, 315–323. doi: 10.1023/a:1021091413084
- Reiland, S., Messerli, G., Baerenfaller, K., Gerrits, B., Endler, A., Grossmann, J., et al. (2009). Large-scale *Arabidopsis* phosphoproteome profiling reveals novel chloroplast kinase substrates and phosphorylation networks. *Plant Physiol.* 150, 889–903. doi: 10.1104/pp.109.138677
- Riera, M., Figueras, M., Lopez, C., Goday, A., and Pages, M. (2004). Protein kinase CK2 modulates developmental functions of the abscisic acid responsive

- protein Rab17 from maize. *Proc. Natl. Acad. Sci. U.S.A.* 101, 9879–9884. doi: 10.1073/pnas.0306154101
- Riera, M., Vélez-Bermudez, I. C., Legnaioli, T., and Pagès, M. (2013). “Specific features of plant CK2,” in *Protein Kinase CK2*, ed. L. Pinna (Wiley-Blackwell), 267–279. doi: 10.1002/9781118482490.ch9
- Samaniego, R., Jeong, S. Y., de la Torre, C., Meier, I., and Moreno Diaz de la Espina, S. (2006). CK2 phosphorylation weakens 90 kDa MFPI association to the nuclear matrix in Allium cepa. *J. Exp. Bot.* 57, 113–124. doi: 10.1093/jxb/erj010
- Schonberg, A., Bergner, E., Helm, S., Agne, B., Dunschede, B., Schunemann, D., et al. (2014). The peptide microarray “ChloroPhos1.0” identifies new phosphorylation targets of plastid casein kinase II (pCKII) in *Arabidopsis thaliana*. *PLoS ONE* 9:e108344. doi: 10.1371/journal.pone.0108344
- Schroeder, J. I., Kwak, J. M., and Allen, G. J. (2001). Guard cell abscisic acid signalling and engineering drought hardiness in plants. *Nature* 410, 327–330. doi: 10.1038/35066500
- Schweer, J., Turkeri, H., Link, B., and Link, G. (2010). AtSIG6, a plastid sigma factor from *Arabidopsis*, reveals functional impact of cpCK2 phosphorylation. *Plant J.* 62, 192–202. doi: 10.1111/j.1365-313X.2010.04138.x
- Seo, K. I., Lee, J. H., Nezames, C. D., Zhong, S., Song, E., Byun, M. O., et al. (2014). ABD1 is an *Arabidopsis* DCAF substrate receptor for CUL4-DDB1-based E3 ligases that acts as a negative regulator of abscisic acid signaling. *Plant Cell* 26, 695–711. doi: 10.1105/tpc.113.119974
- Seo, P. J., and Mas, P. (2015). STRESSing the role of the plant circadian clock. *Trends Plant Sci.* 20, 230–237. doi: 10.1016/j.tplants.2015.01.001
- Seo, P. J., Park, M. J., Lim, M. H., Kim, S. G., Lee, M., Baldwin, I. T., et al. (2012). A self-regulatory circuit of CIRCADIAN CLOCK-ASSOCIATED1 underlies the circadian clock regulation of temperature responses in *Arabidopsis*. *Plant Cell* 24, 2427–2442. doi: 10.1105/tpc.112.098723
- Sirichandra, C., Davanture, M., Turk, B. E., Zivy, M., Valot, B., Leung, J., et al. (2010). The *Arabidopsis* ABA-activated kinase OST1 phosphorylates the bZIP transcription factor ABF3 and creates a 14-3-3 binding site involved in its turnover. *PLoS ONE* 5:e13935. doi: 10.1371/journal.pone.0013935
- Stemmer, C., Schwander, A., Bauw, G., Fojan, P., and Grasser, K. D. (2002). Protein kinase CK2 differentially phosphorylates maize chromosomal high mobility group B (HMGB) proteins modulating their stability and DNA interactions. *J. Biol. Chem.* 277, 1092–1098. doi: 10.1074/jbc.M109503200
- Sugano, S., Andronis, C., Green, R. M., Wang, Z. Y., and Tobin, E. M. (1998). Protein kinase CK2 interacts with and phosphorylates the *Arabidopsis* circadian clock-associated 1 protein. *Proc. Natl. Acad. Sci. U.S.A.* 95, 11020–11025.
- Sugano, S., Andronis, C., Ong, M. S., Green, R. M., and Tobin, E. M. (1999). The protein kinase CK2 is involved in regulation of circadian rhythms in *Arabidopsis*. *Proc. Natl. Acad. Sci. U.S.A.* 96, 12362–12366. doi: 10.1073/pnas.96.22.12362
- Testi, M. G., Croce, R., Laureto, P. P.-D., and Bassi, R. (1996). A CK2 site is reversibly phosphorylated in the photosystem II subunit CP29. *FEBS Lett.* 399, 245–250. doi: 10.1016/s0014-5793(96)01333-6
- Tjaden, G., and Coruzzi, G. (1994). A novel AT-rich DNA binding protein that combines an HMG-like DNA binding protein with a putative transcription domain. *Plant Cell* 6, 107–118. doi: 10.1105/tpc.6.1.107
- Tosoni, K., Costa, A., Sarno, S., D’Alessandro, S., Sparla, F., Pinna, L. A., et al. (2011). The p23 co-chaperone protein is a novel substrate of CK2 in *Arabidopsis*. *Mol. Cell. Biochem.* 356, 245–254. doi: 10.1007/s11010-011-0969-0
- Turkeri, H., Schweer, J., and Link, G. (2012). Phylogenetic and functional features of the plastid transcription kinase cpCK2 from *Arabidopsis* signify a role of cysteinyl SH-groups in regulatory phosphorylation of plastid sigma factors. *FEBS J.* 279, 395–409. doi: 10.1111/j.1742-4658.2011.08433.x
- Tuteja, N., Beven, A. F., Shaw, P. J., and Tuteja, R. (2001). A pea homologue of human DNA helicase I is localized within the dense fibrillar component of the nucleolus and stimulated by phosphorylation with CK2 and cdc2 protein kinases. *Plant J.* 25, 9–17. doi: 10.1111/j.1365-313X.2001.00918.x
- Tuteja, N., Reddy, M. K., Mudgil, Y., Yadav, B. S., Chandok, M. R., and Sopory, S. K. (2003). Pea DNA topoisomerase I is phosphorylated and stimulated by casein kinase 2 and protein kinase C. *Plant Physiol.* 132, 2108–2115. doi: 10.1104/pp.103.024273
- Umeda, M., Manabe, Y., and Uchimiya, H. (1997). Phosphorylation of the C2 subunit of the proteasome in rice (*Oryza sativa* L.). *FEBS Lett.* 403, 313–317. doi: 10.1016/s0014-5793(97)00073-2
- Umezawa, T., Nakashima, K., Miyakawa, T., Kuromori, T., Tanokura, M., Shinozaki, K., et al. (2010). Molecular basis of the core regulatory network in ABA responses: sensing, signaling and transport. *Plant Cell Physiol.* 51, 1821–1839. doi: 10.1093/pcp/pcq156
- Vélez-Bermúdez, I. C., Carretero-Paulet, L., Legnaioli, T., Ludevid, D., Pagès, M., and Riera, M. (2015). Novel CK2α and CK2β subunits in maize reveal functional diversification in subcellular localization and interaction capacity. *Plant Sci.* 235, 58–69. doi: 10.1016/j.plantsci.2015.03.005
- Vélez-Bermúdez, I., Irar, S., Carretero-Paulet, L., Pagès, M., and Riera, M. (2011). Specific characteristics of CK2 regulatory subunits in plants. *Mol. Cell. Biochem.* 356, 255–260. doi: 10.1007/s11010-011-0971-6
- Vilela, B., Najar, E., Lumbrieras, V., Leung, J., and Pages, M. (2015). Casein kinase 2 negatively regulates abscisic acid-activated SnRK2s in the core abscisic acid-signaling module. *Mol. Plant* 8, 709–721. doi: 10.1016/j.molp.2014.12.012
- Wang, H.-C., Wu, J.-S., Chia, J.-C., Yang, C.-C., Wu, Y.-J., and Juang, R.-H. (2009). Phytochelatin synthase is regulated by protein phosphorylation at a threonine residue near its catalytic site. *J. Agric. Food Chem.* 57, 7348–7355. doi: 10.1021/jf9020152
- Wang, Y., Chang, H., Hu, S., Lu, X., Yuan, C., Zhang, C., et al. (2014). Plastid casein kinase 2 knockout reduces abscisic acid (ABA) sensitivity, thermotolerance, and expression of ABA- and heat-stress-responsive nuclear genes. *J. Exp. Bot.* 65, 4159–4175. doi: 10.1093/jxb/eru190
- Yamburenko, M. V., Zubov, Y. O., and Börner, T. (2015). Abscisic acid affects transcription of chloroplast genes via protein phosphatase 2C-dependent activation of nuclear genes: repression by guanosine-3'-5'-bis(diphosphate) and activation by sigma factor 5. *Plant J.* 82, 1030–1041. doi: 10.1111/tpj.12876
- Yamburenko, M. V., Zubov, Y. O., Vanková, R., Kusnetsov, V. V., Kulæva, O. N., and Börner, T. (2013). Abscisic acid represses the transcription of chloroplast genes. *J. Exp. Bot.* 64, 4491–4502. doi: 10.1093/jxb/ert258
- Zhang, X., Garretson, V., and Chua, N. H. (2005). The AIP2 E3 ligase acts as a novel negative regulator of ABA signaling by promoting ABI3 degradation. *Genes Dev.* 19, 1532–1543. doi: 10.1101/gad.1318705
- Zhang, X. L., Jiang, L., Xin, Q., Liu, Y., Tan, J. X., and Chen, Z. Z. (2015). Structural basis and functions of abscisic acid receptors PYLs. *Front. Plant Sci.* 6:88. doi: 10.3389/fpls.2015.00088
- Conflict of Interest Statement:** The authors declare that the research was conducted in the absence of any commercial or financial relationships that could be construed as a potential conflict of interest.
- Copyright © 2015 Vilela, Pages and Riera. This is an open-access article distributed under the terms of the Creative Commons Attribution License (CC BY). The use, distribution or reproduction in other forums is permitted, provided the original author(s) or licensor are credited and that the original publication in this journal is cited, in accordance with accepted academic practice. No use, distribution or reproduction is permitted which does not comply with these terms.



Dual Function of NAC072 in ABF3-Mediated ABA-Responsive Gene Regulation in *Arabidopsis*

Xiaoyun Li^{1†}, Xiaoling Li^{1†}, Meijuan Li¹, Youcheng Yan¹, Xu Liu^{2*} and Ling Li^{1*}

¹ Guangdong Provincial Key Lab of Biotechnology for Plant Development, College of Life Sciences, South China Normal University, Guangzhou, China, ² Key Laboratory of South China Agricultural Plant Molecular Analysis and Genetic Improvement, South China Botanical Garden, Chinese Academy of Sciences, Guangzhou, China

OPEN ACCESS

Edited by:

Sylvain Jeandroz,
Agrosup Dijon, France

Reviewed by:

Frederik Börnke,
Leibniz Institute of Vegetable
and Ornamental Crops (LG), Germany

Yanhui Yin,
Iowa State University, USA

*Correspondence:

Xu Liu
liuxu@scbg.ac.cn
Ling Li
liling@scnu.edu.cn

[†]These authors have contributed
equally to this work.

Specialty section:

This article was submitted to
Plant Physiology,
a section of the journal
Frontiers in Plant Science

Received: 04 September 2015

Accepted: 07 July 2016

Published: 19 July 2016

Citation:

Li X, Li X, Li M, Yan Y, Liu X and Li L (2016) Dual Function of NAC072 in ABF3-Mediated ABA-Responsive Gene Regulation in *Arabidopsis*. *Front. Plant Sci.* 7:1075.
doi: 10.3389/fpls.2016.01075

The NAM, ATAF1/2, and CUC2 (NAC) domain proteins play various roles in plant growth and stress responses. *Arabidopsis* NAC transcription factor NAC072 has been reported as a transcriptional activator in Abscisic acid (ABA)-responsive gene expression. However, the exact function of NAC072 in ABA signaling is still elusive. In this study, we present evidence for the interrelation between NAC072 and ABA-responsive element binding factor 3 (ABF3) that act as a positive regulator of ABA-responsive gene expression in *Arabidopsis*. The transcript of NAC072 is up-regulated by ABF3 in ABA response, and NAC072 protein interacts with ABF3. Enhanced ABA sensitivity occurs in *nac072* mutant plants that overexpressed ABF3. However, overexpression of NAC072 weakened the ABA sensitivity in the *abf3* mutant plants, but instead of recovering the ABA sensitivity of *abf3*. NAC072 and ABF3 cooperate to regulate *RD29A* expression, but are antagonistic when regulating *RD29B* expression. Therefore, NAC072 displays a dual function in ABF3-mediated ABA-responsive gene regulation.

Keywords: dual function, NAC072, ABF3, abscisic acid, RD29A, RD29B

INTRODUCTION

Abscisic acid (ABA) is an important signaling molecule that enables plants to tolerate unfavorable environmental stresses such as drought, salt, cold, heat, and oxidation (Hauser et al., 2011). Core components that consist of ABA signaling have been identified, including ABA receptors PYRABACTIN RESISTANCE (PYR/PYL; Park et al., 2009), PROTEIN PHOSPHATASE 2C (PP2C; Ma et al., 2009), SNF1-RELATED PROTEIN KINASE 2 (SnRK2; Nakashima et al., 2009), downstream transcription factors (TFs) such as ABA INSENSITIVE 3/4/5 (ABI3/4/5), ion channels, and NADPH oxidases (Mustilli et al., 2002; Schweighofer et al., 2004). In *Arabidopsis*, the ABA-responsive element binding factor (ABF/AREB) members (ABF1, AREB1/ABF2, AREB2/ABF4, and ABF3) can bind the ABA-responsive element (ABRE) and function in ABA-dependent signaling pathway (Yoshida et al., 2010). Principally, ABF1 is in response to cold; overexpression of ABF2 confers tolerance to drought, salt, heat, and oxidative stress; ABF4 is mainly induced by drought, salt, and cold; and overexpression of ABF3 confers tolerance to drought, salt, cold, heat, and oxidative stresses. ABF3 has largely overlapping functions with other ABF/AREB members and ABI5, and mainly acts in ABA-mediated response during seedling development (Finkelstein et al., 2005; Abdeen et al., 2010).

The NAC (NAM, ATAF1/2, and CUC2) TFs contain a plant-specific highly conserved N-terminal domain and play various roles in plant development, senescence and the response to

environmental stress (Woo et al., 2004). The molecular function of NAC TFs in abiotic stress-responses has been examined in *Arabidopsis*. For example, ORESARA1 (ORE1/AtNAC2) positively regulates the salt stress response (Balazadeh et al., 2010); JUNGBRUNNEN1 (JUB1/NAC042) directly regulates dehydration responsive element binding protein 2A (DREB2A) and acts as a negative regulator of the salt stress response (Shahnejat-Bushehri et al., 2012); NAC016 promotes drought stress responses by repressing AREB1/ABF2 transcription (Sakuraba et al., 2015); and NAC096 directly interacts with ABF2 and ABF4 (but not with ABF3) to assist plant survival during dehydration and osmotic stress (Xu et al., 2013). These results suggest that NAC family members may serve as mediators through crosstalk with other stress regulators, such as the stress-responsive TFs.

NAC072/RD26, NAC019, and NAC055/AtNAC3 belong to the same clade of NAC domain genes and may have overlapping functions in the drought response (Hickman et al., 2013). Overexpression of these NAC TFs in plants enhances drought tolerance, indicating that they may act as positive regulators of the drought stress response (Fujita et al., 2004). Meanwhile, NAC019 and NAC055 are involved in jasmonic acid and/or ethylene signaling pathways, whereas NAC072 has been reported to be associated with the ABA-dependent stress response and to be strongly induced by ABA (Fujita et al., 2004; Tran et al., 2004). Double and triple mutants of these three homologous NAC genes have been obtained by crossing the single mutants with each other, and subsequent ABA response and downstream gene expression were analyzed with or without exogenous ABA treatments. Following exogenous ABA treatment, there was no significant difference in germination rate or root growth between the single mutants and the double mutants, although they were more ABA insensitive than the wild type (WT). The triple mutant of *nac019nac055nac072* was only slightly more sensitive to ABA or dehydration than the single mutants of *nac019*, *nac055*, and *nac072* or the double mutants of *nac019nac055*, *nac055nac072*, and *nac019nac072* (Lu et al., 2015). However, NAC072 plays a dominant role in the development of green cotyledons, and NAC055 coordinates with NAC072 during this process to regulate the expression of ABA-responsive downstream genes (Lu et al., 2015). These findings indicate that NAC072, NAC019, and NAC055 may act individually in different stress responses, and that NAC072 is mainly responsible for ABA response.

Several TFs or downstream genes targeted by NAC family members have been identified. As previously mentioned, NAC016 directly represses the expression of *AREB1* (Sakuraba et al., 2015), and NAC096 binds ABF2/AREB1 and ABF4 (Xu et al., 2013), suggesting that the NAC family are closely involved with ABF/AREB TFs during senescence or stress responses. Promoter fragments of the NAC072, NAC019, and NAC055 genes contain ABRE motifs, and was bound either ABF3 or ABF4 according to yeast one-hybrid assays (Hickman et al., 2013). This suggests that ABF/ABRE TFs may also regulate these NAC TFs. NAC072/RD26 has been reported to be involved in the ABA-mediated regulation of drought-responsive genes; however, the specific genetic effect of NAC072 in the ABA signaling pathway is still unknown. Whether physical interactions occur between

NAC072 and ABF/AREB TFs or other ABA-responsive signaling components, and subsequently involve in ABA response, remains unresolved.

Here, we show that the *NAC072* gene is upregulated by overexpression of ABF3. Loss of *NAC072* function results in ABA insensitivity, while loss of both *NAC072* and *ABF3* function further improve ABA insensitivity. Overexpression of *NAC072* enhances ABA sensitivity in WT plants, but does not recover the ABA sensitivity of the *abf3* mutant. This suggests that *NAC072* is positively involved in the ABA response and is dependent on ABF3. On the other hand, *nac072* mutants with overexpressed *ABF3* display greater ABA sensitivity than WT plants with overexpressed *ABF3*, indicating that *NAC072* is negatively involved in the ABF3-mediated ABA response. Furthermore, *NAC072* is regulated by ABF3, and *NAC072* interacted with ABF3. In response to ABA, *NAC072* cooperates with ABF3 to regulate *RD29A* expression, but acts antagonistically to ABF3 in the mediation of *RD29B* regulation. In summary, *NAC072* displays a dual function in ABF3-mediated ABA signaling.

MATERIALS AND METHODS

Plant Materials and ABA Application

The *Arabidopsis* seeds for *abf3* (SALK_17755), *nac072* (SALK_083756), *nac055* (SALK_014331), and *nac019* (SALK_096295) were obtained from the *Arabidopsis* Biological Resource Center (ABRC¹). The seeds for *nac072abf3*, *nac055/72*, *nac019/72*, and *nac055/072/019* (3P) were obtained by hybridization. All seeds were surface sterilized in 70% ethanol containing 0.5% Tween-100. The supernatant was discarded and the seeds were suspended in ethyl alcohol and then air dried on filter paper. The seeds were sown on 0.5x MS medium with 0.8% agar containing 2% sucrose. After 2 days stratification at 4°C, the seeds were germinated and grown in a climate chamber under a daily cycle of 16 h light and 8 h dark at 20 ± 2°C. To examine the effects of ABA on germination and the development of green cotyledons, surface sterilized seeds were sown on 0.5x MS medium with 0.8% agar containing various concentrations of ABA (0, 0.5, 1, or 2 μM). The root growth experiment was conducted at 3 days after germination, for which the seedlings were transferred to new 0.5x MS media with 0.8% agar containing 10, 30, or 50 μM ABA.

Plasmid Construction and *Arabidopsis* Transformation

The cDNAs encoding *ABF3* or *NAC072* were amplified and cloned into the modified *pCAMBIA1301* plasmids (*p35S:mCherry-6Myc* or *p35S:eGFP-3Flag*) to obtain *p35S:ABF3-mCherry-6Myc* or *p35S:NAC072-eGFP-3Flag*, respectively. The primers used to construct these plasmids are listed in Supplementary Table S1. The plasmids were transformed into *Arabidopsis* by the floral dip method using *Agrobacterium tumefaciens* strain GV3101 as previously reported (Li et al., 2013). Transgenic lines were screened using 0.5x MS medium containing 40 mg/L hygromycin (Sigma-Aldrich). The plasmids

¹<http://www.arabidopsis.org>

of *pRD29A:GUS* and *pRD29B:GUS* were provided by Hou XL Lab, south china botanical garden, CAS.

Yeast Two-Hybrid Assay

To analyze the interactions between NAC072-F, NAC072-N, NAC072-C, and ABF3, the full NAC072-F and sectionalized sequences encoding NAC072-N (1–167aa) and NAC072-C (168–297aa) were amplified and cloned into pGBKT7 or pGADT7 (Clontech), respectively. The sequence encoding full-length ABF3 was amplified and cloned into pGADT7 or pGBKT7. The primers used to construct these plasmids are listed in Supplementary Table S1. All yeast transformants were grown on SD/-Trp/-Leu or SD/-Trp/-Leu/-His/-Ade (Clontech) medium for the interaction test.

Expression Analysis

Two-week-old seedlings under control conditions or after various treatments were analyzed for gene expression using quantitative real time PCR analysis. Total RNA was extracted using a TRIzol Kit (TaKaRa), and a PrimeScriptTM RT reagent Kit (Perfect Real Time, TaKaRa) was used for reverse transcription. Real-time PCR was performed in an ABI 7500 system with the SYBR[®] Premix DimerEraserTM (Perfect Real Time, TaKaRa), each reaction consisted of 20 ng of cDNA, 0.1 μM primers and 10 μL 2x SYBR Premix ExTaq in a final volume of 20 μL. The reactive cycle used 95°C for 30 s, then 40 cycles at 95°C for 5 s and 60°C for 34 s. The gene expression quantity was calculated using the relative $2^{-\Delta\Delta CT}$ method as previously reported (Li et al., 2013). The relative expression level was normalized to that of ACT2 internal control. Primers used for gene expression analysis are listed in Supplementary Table S1. Assessment of NAC072 and ABF3 protein levels was carried out using western blot (WB) with Flag (F3165, Sigma) or c-Myc antibody (sc-40, Santa Cruz) as previously described (Sakuraba et al., 2015). The β-glucuronidase (GUS) activity of the RD29A and RD29B promoters was previously described (Woo et al., 2004). The presented data are the average of three technical replicates, and experiments were biologically repeated at least three times with similar results.

Transient Transactivation Assay

To create the *pRD29A:GUS* or *pRD29B:GUS* reporter constructs, a ~1200 bp region of the RD29A promoter or a ~600 bp region of the RD29B promoter was cloned into pGreen vectors that was kindly provided by Hou XL Lab. The effector constructs (*p35S:ABF3-mCherry-6Myc* or *p35S:NAC072-eGFP-3Flag*) were generated by amplifying the corresponding cDNAs and then cloning into pGreen-35S. The *p35S:luciferase* (LUC) plasmid was used as an internal control to evaluate protoplast transfection efficiency. *Arabidopsis* mesophyll protoplasts were prepared and subsequently transfected as previously described (Sheen, 2001), after which GUS and LUC activities were analyzed and calculated. For each experiment, the 2 μg plasmids of NAC072 or ABF3 were used for transfection in every group in same amount of protoplast. More than 80% transformation efficiency were confirmed by confocal microscopy using the difference fluorescent label protein (GFP for NAC072, mCherry for ABF3),

respectively. The protein expression level of NAC072 and ABF3 was confirmed using WB with Flag or c-Myc antibody. The presented data are the average of three technical replicates, and experiments were biologically repeated at least three times with similar results.

Bimolecular Fluorescence Complementation (BiFC) Assay

For analysis of interactions between ABF3 and NAC072, full-length cDNA of ABF3 and NAC072 were cloned into the *pGreen* binary vector containing C- or N-terminal fusions of EYFP, generated *p35S:ABF3-EYFP^C* and *p35S:NAC072-EYFP^N*. Then both of them cotransformed into *Arabidopsis* mesophyll protoplasts as previously described (Sheen, 2001). After darkness cultured for 24 h, the YFP fluorescence was determined using a confocal microscopy (Carl Zeiss LSM 710).

Statistical Analysis

In order to evaluate the differences in data of physiological phenotype, gene expression and GUS reporter assay, student *T*-test was used to assess these data. Statistics quantitative data were expressed as mean ± SD. Means were compared using one-way analysis of variance or the student's *t*-test with SPSS13.0. Significance was assigned at *P* < 0.05.

Accession Numbers

Sequence data from this article can be found in the *Arabidopsis* genome initiative database under the following accession numbers: NAC072 (AT4G27410), ABF3 (AT4G34000), ACT2 (AT3G18780), RD29A (AT5G52310), RD29B (AT5G52300), NAC055 (AT3G15500), and NAC019 (AT1G52890).

RESULTS

The Relationship between NAC072 and ABF3 in ABA Response and ABA-Inducible Gene Regulation

Previous researches (Fujita et al., 2004; Tran et al., 2004) and our own observations confirm that overexpression of NAC072 improves ABA sensitivity in *Arabidopsis*, whereas loss of NAC072 function in plants reduces ABA sensitivity (Supplementary Figure S1). This indicates that NAC072 is a positive regulator for ABA signaling. To examine the relationship between NAC072 and ABF3, the expression of NAC072 was first analyzed in the loss-of-function mutant of ABF3 (*abf3*). The NAC072 expression was dramatically reduced in *abf3* after ABA treatment, whereas the transcript level of ABF3 was not affected in the NAC072 deficient mutant *nac072* (Figure 1A). It suggests that the expression of NAC072 is mediated by ABF3 under ABA treatment. Meanwhile, RD29A and RD29B are rapidly induced by drought stress or ABA, and are thus considered to be stress-response marker genes (Msanne et al., 2011). Both RD29A and RD29B were highly upregulated by ABA treatment, while their expressions were dramatically reduced in *abf3nac072* mutants, although different expression patterns were observed

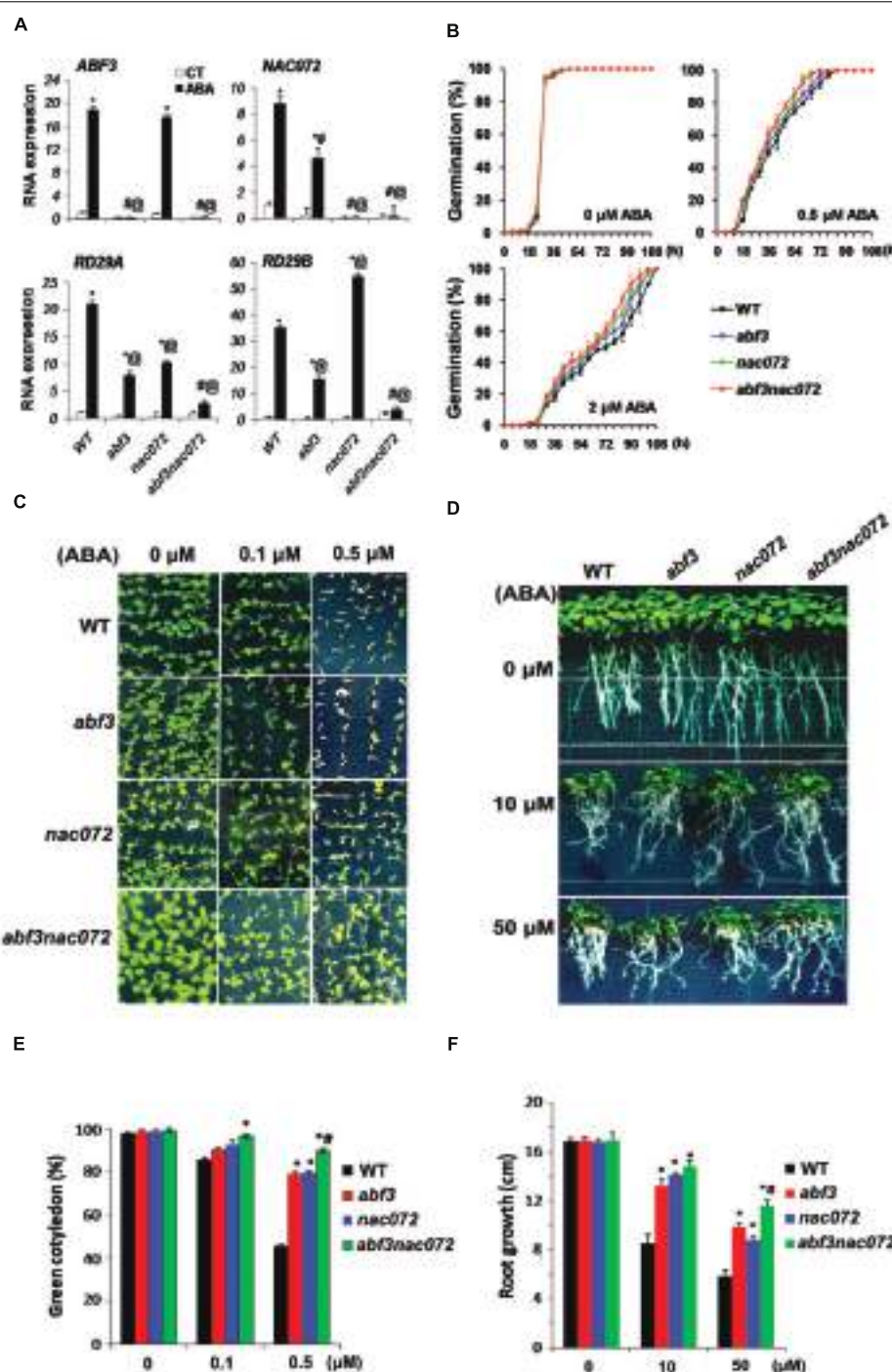


FIGURE 1 | The synergistic function of NAC072 in ABF3-mediated ABA response. (A) Gene expression of *ABF3*, *NAC072*, *RD29A*, and *RD29B* in mutant (*abf3*, *nac072*, and *abf3nac072*) and wild type (WT) plants in response to ABA. The seedlings were grown on 0.5x MS agar plates for 12 days and then sprayed either with water (CT) or 100 μ M ABA (ABA) and assayed after 2 h. Bars indicate standard deviation, $n = 3$. ** indicates a significant difference between CT and ABA treatments ($P < 0.05$). # indicates a significant difference between each mutant plants compared with WT plants under CT treatment ($P < 0.05$). @ indicates a significant difference between each mutants plants compared with WT plants under ABA treatment ($P < 0.05$). **(B)** Seed germination rate of mutant and WT in response to ABA. Germinations were recorded from 0 to 108 h after stratification on 0.5x MS agar plates containing 0, 0.5, or 2 μ M ABA. **(C)** Photographs of seedlings grown for 7 days after stratification on agar plates containing 0, 0.1, or 0.5 μ M ABA. **(D)** Photographs of seedlings grown for 20 days after transferral to control agar plates (0 μ M ABA) or plates containing 10 or 50 μ M ABA. **(E)** The statistical analysis of green cotyledons in **(C)**. Bars indicate standard deviation, $n = 30$. **(F)** The statistical analysis of axial root growth in **(D)**. Bars indicate standard deviation, $n = 10$. ** indicates a significant difference between *abf3* or *nac072* plants compared with WT plants under the same ABA treatment ($P < 0.05$). # indicates a significant difference between *abf3nac072* plants compared with *abf3* or *nac072* plants ($P < 0.05$).

in the single mutants. *RD29A* was repressed in *abf3* and *nac072* after ABA treatment; although *RD29B* was attenuated in *abf3* mutants, it increased notably in *nac072* after ABA treatment (**Figure 1A**). These suggest that NAC072 may cooperate with ABF3 in the regulation of *RD29A* gene expression, while acting antagonistically with ABF3 in the regulation of *RD29B* gene expression. Thus, NAC072 seems to play a dual role in ABA-inducible gene expression in combination with ABF3.

To examine this implication, ABA sensitivity was further assessed in *abf3*, *nac072*, and *abf3nac072* mutants by the physiological experiments on germination, the development of green cotyledons and axial root growth. During the germination process, no significant difference was observed between WT, *abf3*, *nac072*, and *abf3nac072* under 0, 0.5, or 2 μ M of ABA treatments (**Figure 1B**). However, remarkably, these mutants showed ABA insensitivity during the development of green cotyledons and axial root growth compared with the WT plants, especially the double mutant *abf3nac072* displayed the greatest ABA insensitivity (**Figures 1C–F**). All of the above results indicate that NAC072 partly cooperates with ABF3 in the ABA response during the development of green cotyledons and axial root growth, but not during the germination process. However, it seems contradictory that there is cooperation between NAC072 and ABF3 with respect to physiological function, yet there is antagonism between these TFs in the mediation of ABA-inducible expression of genes such as *RD29B*. Therefore, NAC072 may perform a dual function in ABF3-mediated gene regulation of the ABA response.

NAC072 Cooperates with and Partly Depends on ABF3 Involvement in ABA Signaling

Several NAC proteins interact with the ABF/AREB TFs involved in stress response signaling, including NAC016 and NAC096 (Xu et al., 2013; Sakuraba et al., 2015). Here, the interaction of NAC072 and ABF3 was demonstrated using the yeast two-hybrid system and BiFC assay. The results displayed that the full (NAC072-F) and N-terminal region of NAC072 (072-N) showed a stronger interaction with ABF3 in yeast (**Figure 2A**), and NAC072 and ABF3 also interact with each other in the nucleus (**Figure 2B**, Supplementary Figure S6). These data support the physical interactions between NAC072 protein and ABF3 TFs.

NAC072 was overexpressed under the control of the cauliflower mosaic virus 35S (35S) promoter in WT plants. *NAC072-OX/abf3* plants were obtained by crossing *NAC072-OX* transgenic line with the *abf3* mutant. For comparison, *ABF3-OX/072* plants were produced by crossing *ABF3-OX* with the *nac072* mutant. All homozygotes were determined by hygromycin resistance screening and tri-primer PCR after F2 generation segregation (data not shown). Accumulations of NAC072 or ABF3 in these plants were shown by western blot using antibodies against a Flag or c-Myc protein tag (**Figure 2C**). Thus, ABA sensitivities of these plants were examined during the development of green cotyledon and axial root growth. Overexpression of *NAC072* or *ABF3* (in the *NAC072-OX* or *ABF3-OX* plants) resulted in slight growth inhibition and

enhanced ABA sensitivity (**Figures 2C,D**; Supplementary Figures S1, S2 and S5). However, overexpression of *NAC072* in *abf3* (*NAC072-OX/abf3*) resulted in less ABA sensitivity than in *NAC072-OX* or WT plants, and *NAC072-OX/abf3* had less ABA sensitivity than *abf3* (**Figures 2C,D**; Supplementary Figures S3, S5, and S7). This suggests that NAC072 is partly dependent on ABF3 for the positive regulation in ABA response, and NAC072 had a negative role on ABA response. Furthermore, the *ABF3-OX/nac072* plants (where ABF3 was overexpressed in the *nac072*) showed further improved ABA sensitivity compared with *ABF3-OX* or WT plants (**Figures 2C–G**; Supplementary Figures S4, S5 and S7). These results indicate that NAC072 antagonizes ABF3 during the development of green cotyledon or axial root growth under ABA treatment. In addition, overexpression of ABF3 in *nac019nac072*, *nac055nac072*, or *nac055nac072nac019* resulted in the same degree of ABA sensitivity as the *ABF3-OX/nac072* plants, but they displayed higher ABA sensitivity than *ABF3-OX* plants (Supplementary Figure S5). These further suggest that NAC072 has a dual role in the ABA response.

NAC072 Antagonizes ABF3-Mediated ABA-Responsive Genes Regulation

To understand the crosstalk between NAC072 and ABF3 in ABA signaling, the regulations of NAC072 and ABF3 on *RD29A* and *RD29B* expression were further analyzed in different genotype combinations. Overexpression of *NAC072* or *ABF3* in WT plants (*NAC072-OX* or *ABF3-OX*) increased the transcription level of both *RD29A* and *RD29B*. In *NAC072-OX/abf3* plants, *RD29A* and *RD29B* expressions were enhanced under control conditions, but little change was observed after ABA treatment (**Figure 3A**). This suggests that, under ABA treatment, without ABF3, NAC072 cannot enhance the expression of *RD29A* or *RD29B*. That is NAC072 regulated the expression of *RD29A* and *RD29B* after ABA treatment need the ABF3 mediation. On the other hand, the loss of NAC072 function further contributed to ABF3-enhanced *RD29B* expression in *ABF3-OX/nac072* plants, but there was no obvious change in *RD29A* expression (**Figures 3A,B**). These findings add further confirmation that NAC072 is antagonistic to ABF3-mediated *RD29B* gene expression.

The expression regulation of *RD29A* and *RD29B* by ABF3 and/or NAC072 was further analyzed using GUS reporter systems. The 1200 bp region of the *RD29A* promoter and 600 bp region of the *RD29B* promoter were each fused with the GUS reporter gene. Either *NAC072* or *ABF3*, driven by the 35S promoter, was co-expressed with each GUS construct in protoplasts. The result showed the *RD29A* promoter fusion with the GUS gene was more strongly induced by *p35S::ABF3* together with *p35S::NAC072* than by *p35S::ABF3* or *p35S::NAC072* alone (**Figure 3C**), indicating that NAC072 cooperates with ABF3 to mediate the expression of the *RD29A* gene. A different regulation pattern was observed for *RD29B* expression. The single *p35S::ABF3* expression resulted in a stronger transactivation of *RD29B* compared with *p35S::NAC072* alone, or with *p35S::ABF3* and *p35S::NAC072* combined (**Figure 3C**). These results further indicate that NAC072 acts antagonistically with ABF3 in regulating the expression of *RD29B*. Taken together, NAC072

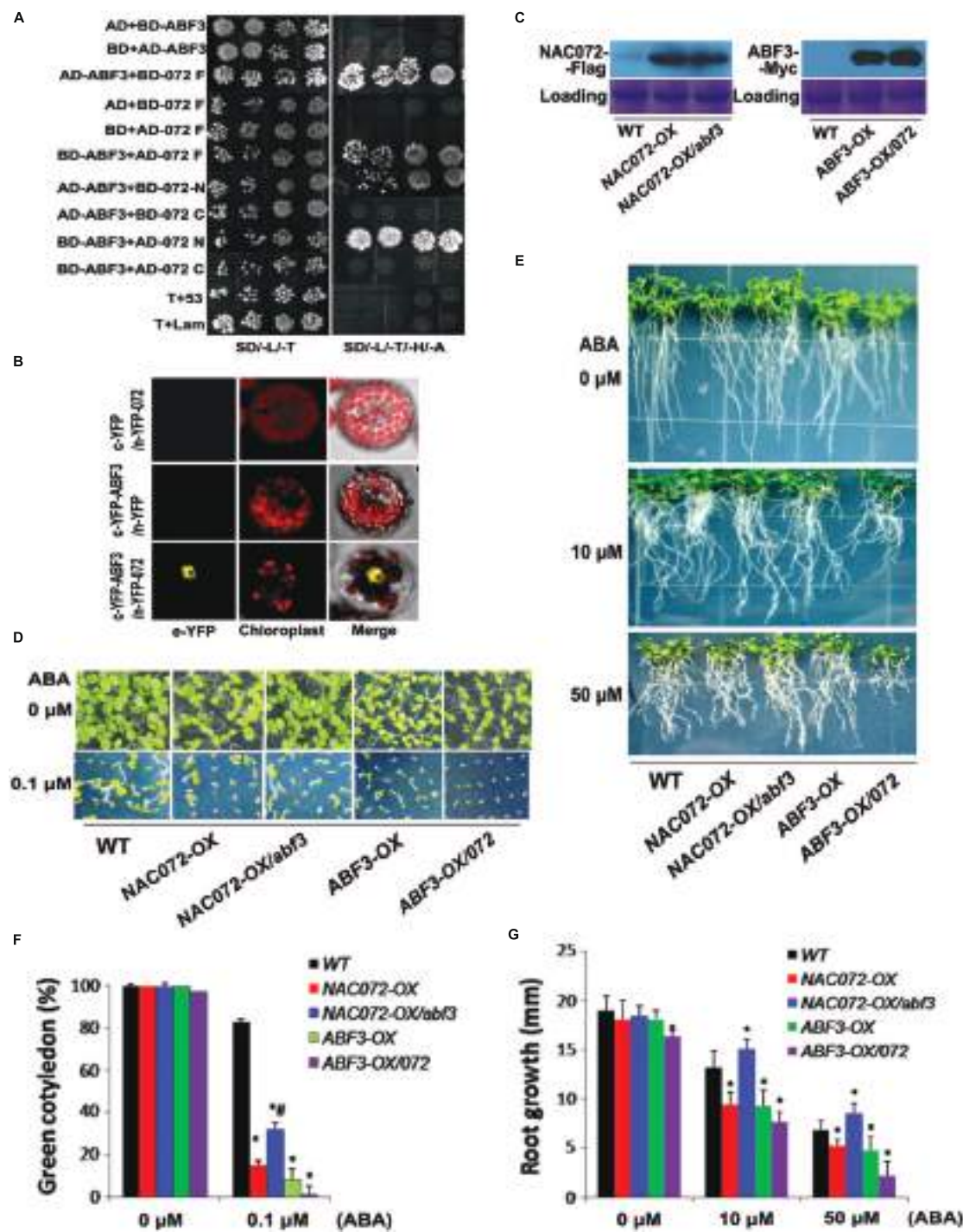


FIGURE 2 | The dual function of NAC072 in ABF3-mediated ABA response. (A) Interactions between ABF3 and both full length and sections (C- and N-terminal regions) of NAC072 were confirmed by yeast two-hybrid assay. The 072 F indicates NAC072 full length, 072 N or C indicates NAC072 N-terminal regions or C-terminal regions, respectively. T+53 and T+Lam were used as the negative controls. **(B)** Interactions of ABF3 and NAC072 were observed by BiFC assay. **(C)** NAC072 or ABF3 protein accumulation in the transgenic plants detected by western blot. **(D)** Photographs of seedlings recorded at 7 days after stratification on agar plates containing 0, or 1 μM ABA. **(E)** Photographs of seedlings recorded at 20 days after transferral to control agar plates (0 μM ABA) or plates containing 10 or 50 μM ABA. NAC072-OX or ABF3-OX indicates NAC072 or ABF3 overexpressed in WT under the control of the cauliflower mosaic virus (CaMV) 35S promoter, respectively. NAC072-OX/abf3 or ABF3-OX/072 indicates NAC072 or ABF3 overexpressed in abf3 or nac072, respectively. **(F)** The statistical analysis of green cotyledons in **(D)**. Bars indicate standard deviation, $n = 30$. **(G)** The statistical analysis of axial root growth in **(E)**. Bars indicate standard deviation, $n = 10$. ** indicates a significant difference between ABF3 or NAC072 transgenic plants compared with WT plants under the same ABA treatment ($P < 0.05$). # indicates a significant difference between NAC072-OX/abf3 compared with NAC072-OX plants or ABF3-OX/072 compared with ABF3-OX plants ($P < 0.05$).

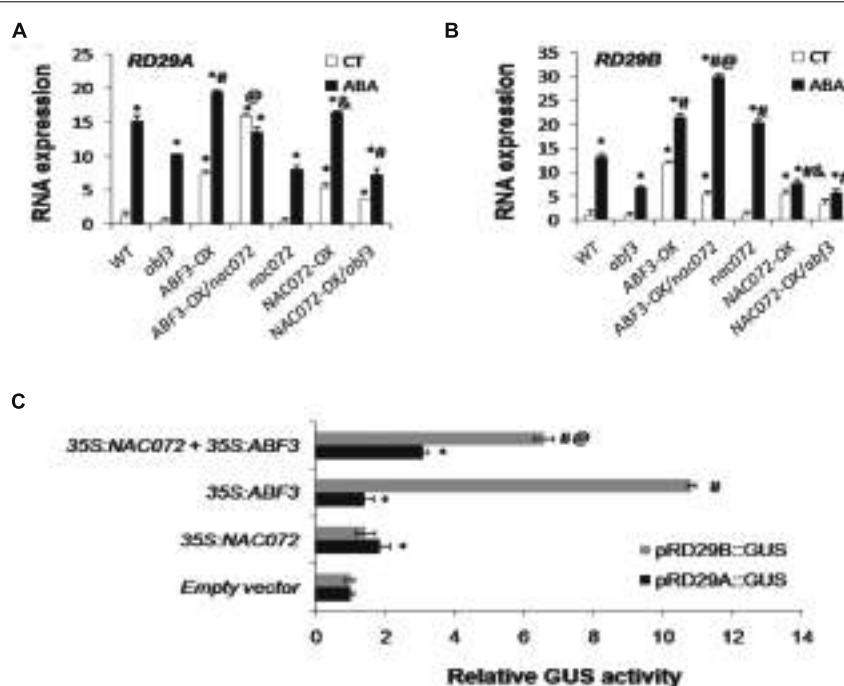


FIGURE 3 | NAC072 cooperates with or antagonizes ABF3-mediated ABA-responsive gene regulation. (A) Expression of *RD29A* in each mutant, transgenic line and WT plants under control treatment (CT) or 100 μ M ABA treatment (ABA) for 2 h. ** or # indicates a significant difference between *ABF3* or *NAC072* transgenic plants compared with WT or *abf3* and *nac072* plants under CT and ABA treatments, respectively ($P < 0.05$). @ indicates a significant difference between *ABF3-OX* and *ABF3-OX/nac072* plants ($P < 0.05$). & indicates a significant difference between *NAC072-OX* and *NAC072-OX/abf3* plants ($P < 0.05$). (B) *RD29B* in each mutant, transgenic and WT plants under CT or ABA treatment for 2 h. & indicates a significant difference between *NAC072-OX* and *nac072* mutants. (C) Transactivation of the *RD29A* or *RD29B* promoter-GUS fusion gene by *ABF3* and/or *NAC072* in *Arabidopsis* protoplasts. The reporter gene was transfected with each effector plasmid (35S:*ABF3* and/or 35S:*NAC072*) or the empty vector as a control groups. Co-transfection of the 35S driving *luciferase* (*LUC*) plasmid was used in each experiment to normalize transfection efficiency. Protoplasts were prepared from rosette leaves of 4-weeks-old WT. Bars indicate standard deviation, $n = 3$. ** or # indicates a significant difference between *ABF3* or *NAC072* groups compared with control groups ($P < 0.05$). @ indicates a significant difference between *ABF3* and *NAC072* compared with *ABF3* alone ($P < 0.05$).

may function as a cofactor, which not only cooperates with but also antagonizes *ABF3*-mediated regulation of the ABA response.

DISCUSSION

In our previous work, we obtained double and triple mutants of three *Arabidopsis* NAC homologous genes (*NAC019*, *NAC055*, and *NAC072*). ABA sensitivity analysis indicated that *NAC055* plays an important role during germination process, while *NAC072* partly inhibited the expression of *RD29B* and *RAB18*, both of which are widely described as ABA signaling marker genes as their expressions are always induced by dehydration or ABA (Tran et al., 2004; Lu et al., 2015). However, *NAC072* is reportedly involved in the ABA-dependent stress-signaling pathway and functions as a transcriptional activator in ABA-inducible gene expression (Fujita et al., 2004). These contradictory results prompted us to further explore the role of *NAC072* in ABA signaling.

ABF3 is the key downstream regulator of ABA signaling and is important for ABA-mediated main root growth. Reprogramming the drought response by changing the timing or strength of expression of some drought-responsive genes was observed in

plants with overexpressed *ABF3* (Finkelstein et al., 2005). ABA sensitivity in the *abf3* mutant was lower than that in the *abf2*, *abf4* mutants or WT during the development of cotyledon or main root growth (data not shown). Therefore, the *ABF3*-mediated ABA signaling pathway was chosen to illuminate the role of *NAC072* in the ABA response. Subsequently, we uncovered four key points as follows: (1) the transcription level of *NAC072* is partly regulated by *ABF3*; (2) *NAC072* interacts and cooperates with *ABF3* to regulate gene expression (including that of *RD29A*) in the ABA response; (3) *NAC072* partly depends on *ABF3* for its role in the ABA response during the development of cotyledon and main root growth; (4) *NAC072* antagonizes the action of *ABF3* to some extent in the regulation of *RD29B* expression.

Transcriptome data from plants overexpressing *ABF3* show that the expression of *NAC072/RD26* as well as *NAC019* and *NAC055/AtNAC3* is independent of *ABF3* (Abdeen et al., 2010). In accordance with these results, we detected *NAC072* expression in both *ABF3*-overexpressing plants and *abf3* mutants. However, either under control conditions or after ABA treatment, overexpression of *ABF3* increased the expression of *NAC072* (data not shown). Loss of *ABF3* function reduced *NAC072* transcript levels, but the expression of *NAC072* could still be

detected after ABA treatment (**Figure 1A**). Hence, the expression of NAC072 seems partly dependent on ABF3.

ABF3, AREB2, and AREB1 can form homo- or heterodimers and have redundant function (Yoshida et al., 2010). Some NAC proteins have been observed to interact with the AREB family. Typically, ANAC096 directly interacts with ABF2/AREB1 and AREB2/ABF4, and NAC016 interacts with ABF2/AREB1 (Xu et al., 2013; Sakuraba et al., 2015). The relationship between NACs and ABF3 is still unclear, but our yeast two-hybrid results show that the C- or N-terminal regions of NAC072 interact with ABF3 (**Figure 2A**). It seems likely, then, that the contradictory roles of NAC072 in ABA signaling might be resolved by an understanding of its relationship with ABF3. We assumed that NAC072 functions as a cofactor with ABF3 in the ABA signaling pathway. Accordingly, ABA sensitivity and ABA-inducible genes were analyzed in *abf3*, *nac072*, and *abf3nac072* mutants (**Figure 1**). The results indicate that NAC072 cooperates with ABF3 in mediation of *RD29A* expression, but antagonizes *RD29B* expression. It is well known that both *RD29A* and *RD29B* rapidly respond to various stresses and ABA treatment (Narusaka et al., 2003). In the present study, *RD29B* was directly and positively regulated by ABF3, while NAC072 may act as a repressor during this process. To further confirm this, NAC072 was overexpressed in WT and *abf3* mutant plants. The expression of *RD29B* was enhanced in NAC072-OX/WT and NAC072-OX/*abf3* plants under control conditions, but no change in expression occurred after ABA treatment. In contrast, overexpressed ABF3 rapidly increased *RD29B* transcription levels in control as well as ABA-treated plants. The combined loss of NAC072 function and ABF3 overexpression contributed to enhanced *RD29B* expression. Moreover, NAC072-OX/*abf3* plants were more ABA insensitive than WT or NAC072-OX/WT plants,

REFERENCES

- Abdeen, A., Schnell, J., and Miki, B. (2010). Transcriptome analysis reveals absence of unintended effects in drought-tolerant transgenic plants overexpressing the transcription factor ABF3. *BMC Genomics* 11:69. doi: 10.1186/1471-2164-11-69
- Balazadeh, S., Siddiqui, H., Allu, A. D., Matallana-Ramirez, L. P., Caldana, C., Mehrnia, M., et al. (2010). A gene regulatory network controlled by the NAC transcription factor ANAC092/AtNAC2/ORE1 during salt-promoted senescence. *Plant J.* 62, 250–264. doi: 10.1111/j.1365-313X.2010.04151.x
- Finkelstein, R., Gampala, S. S., Lynch, T. J., Thomas, T. L., and Rock, C. D. (2005). Redundant and distinct functions of the ABA response loci ABA-INSENSITIVE (ABI) 5 and ABRE-BINDING FACTOR (ABF) 3. *Plant Mol. Biol.* 59, 253–267. doi: 10.1007/s11103-005-8767-2
- Fujita, M., Fujita, Y., Maruyama, K., Seki, M., Hiratsu, K., Ohme-Takagi, M., et al. (2004). A dehydration-induced NAC protein, RD26, is involved in a novel ABA-dependent stress-signaling pathway. *Plant J.* 39, 863–876. doi: 10.1111/j.1365-313X.2004.02171.x
- Hauser, F., Waadt, R., and Schroeder, J. I. (2011). Evolution of abscisic acid synthesis and signaling mechanisms. *Curr. Biol.* 21, R346–R355. doi: 10.1016/j.cub.2011.03.015
- Hickman, R., Hill, C., Penfold, C. A., Breeze, E., Bowden, L., Moore, J. D., et al. (2013). A local regulatory network around three NAC transcription factors in stress responses and senescence in *Arabidopsis* leaves. *Plant J.* 75, 26–39. doi: 10.1111/tpj.12194
- Li, X. Y., Liu, X., Yao, Y., Li, Y. H., Liu, S., He, C. Y., et al. (2013). Overexpression of *Arachis hypogaea* AREB1 gene enhances drought tolerance by modulating ROS scavenging and maintaining endogenous ABA content. *Int. J. Mol. Sci.* 14, 12827–12842. doi: 10.3390/ijms140612827
- Lu, J. B., Li, X. Y., Liu, X., Li, X. L., Li, Y. H., and Li, L. (2015). Study on the response to applying ABA and expression changes of ABA induced relative genes in *Arabidopsis* mutants of three NAC homologous genes. *Life Sci. Res.* 19, 114–118.
- Ma, Y., Szostkiewicz, I., Korte, A., Moes, D., Yang, Y., Christmann, A., et al. (2009). Regulators of PP2C phosphatase activity function as abscisic acid sensors. *Science* 324, 1064–1068. doi: 10.1126/science.1172408
- Msanne, J., Lin, J., Stone, J. M., and Awada, T. (2011). Characterization of abiotic stress-responsive *Arabidopsis thaliana* RD29A and RD29B genes and evaluation of transgenes. *Planta* 234, 97–107. doi: 10.1007/s00425-011-1387-y
- Mustilli, A. C., Merlot, S., Vavasseur, A., Fenzi, F., and Giraudat, J. (2002). *Arabidopsis* OST1 protein kinase mediates the regulation of stomatal aperture by abscisic acid and acts upstream of reactive oxygen species production. *Plant Cell* 14, 3089–3099. doi: 10.1105/tpc.007906
- Nakashima, K., Fujita, Y., Kanamori, N., Katagiri, T., Umezawa, T., Kidokoro, S., et al. (2009). Three *Arabidopsis* SnRK2 protein kinases, SRK2D/SnRK2.2, SRK2E/SnRK2.6/OST1 and SRK2I/SnRK2.3, involved in ABA signaling are essential for the control of seed development and dormancy. *Plant Cell Physiol.* 50, 1345–1363. doi: 10.1093/pcp/pcp083
- Narusaka, Y., Nakashima, K., Shinwari, Z. K., Sakuma, Y., Furihata, T., Abe, H., et al. (2003). Interaction between two cis-acting elements, ABRE and DRE, in ABA-dependent expression of *Arabidopsis rd29A* gene in response to

whereas ABF3-OX/nac072 was more ABA sensitive than WT or ABF3-OX/WT plants. In addition, NAC072 collaborates with ABF3 to regulate *RD29A* expression. Thus, we hypothesize that NAC072 and ABF3 may act as a “push-pull” device. Under certain conditions, NAC072 cooperates with ABF3-mediated gene expression, thus providing a “push” stimulus, while under other conditions it acts antagonistically to ABF3, giving a “pull” effect. How the device works would depend on specific conditions, a detailed understanding of which requires further investigation.

AUTHOR CONTRIBUTIONS

XyL, XuL, and LL designed the research. XL, XIL, and YY performed research. XyL and XIL analyzed data. XyL and XuL wrote the article. The protein interaction experiments mainly performed for the revisions draft by XyL and ML.

ACKNOWLEDGMENTS

This work was supported by National Natural Science Foundation of China (31501167, 31471422), the Science and Technology Project of Guangdong Province (2015A030310457, S2012010009516).

SUPPLEMENTARY MATERIAL

The Supplementary Material for this article can be found online at: <http://journal.frontiersin.org/article/10.3389/fpls.2016.01075>

- dehydration and high-salinity stresses. *Plant J.* 34, 137–148. doi: 10.1046/j.1365-313X.2003.01708.x
- Park, S. Y., Fung, P., Nishimura, N., Jensen, D. R., Fujii, H., Zhao, Y., et al. (2009). Abscisic acid inhibits type 2C protein phosphatases via the PYR/PYL family of START proteins. *Science* 324, 1068–1071. doi: 10.1126/science.1173041
- Sakuraba, Y., Kim, Y. S., Han, S. H., Lee, B. D., and Paek, N. C. (2015). The *Arabidopsis* transcription factor NAC016 promotes drought stress responses by repressing AREB1 transcription through a trifurcate feed-forward regulatory loop involving NAP. *Plant Cell* 27, 1771–1787. doi: 10.1105/tpc.15.00222
- Schweighofer, A., Hirt, H., and Meskiene, I. (2004). Plant PP2C phosphatases: emerging functions in stress signaling. *Trends. Plant Sci.* 9, 236–243. doi: 10.1016/j.tplants.2004.03.007
- Shahnejat-Bushehri, S., Mueller-Roeber, B., and Balazadeh, S. (2012). *Arabidopsis* NAC transcription factor JUNGBRUNNEN1 affects thermomemory-associated genes and enhances heat stress tolerance in primed and unprimed conditions. *Plant Signal. Behav.* 7, 1518–1521. doi: 10.4161/psb.22092
- Sheen, J. (2001). Signal transduction in maize and *Arabidopsis* mesophyll protoplasts. *Plant Physiol.* 127, 1466–1475. doi: 10.1104/pp.010820
- Tran, L. S., Nakashima, K., Sakuma, Y., Simpson, S. D., Fujita, Y., Maruyama, K., et al. (2004). Isolation and functional analysis of *Arabidopsis* stress-inducible NAC transcription factors that bind to a drought-responsive cis-element in the early responsive to dehydration stress 1 promoter. *Plant Cell* 16, 2481–2498. doi: 10.1105/tpc.104.022699
- Woo, H. R., Kim, J. H., Nam, H. G., and Lim, P. O. (2004). The delayed leaf senescence mutants of *Arabidopsis*, ore1, ore3, and ore9 are tolerant to oxidative stress. *Plant Cell Physiol.* 45, 923–932. doi: 10.1093/pcp/pch110
- Xu, Z. Y., Kim, S. Y., Hyeon, D. Y., Kim, D. H., Dong, T., Park, Y., et al. (2013). The *Arabidopsis* NAC transcription factor ANAC096 cooperates with bZIP-type transcription factors in dehydration and osmotic stress responses. *Plant Cell* 25, 4708–4724. doi: 10.1105/tpc.113.119099
- Yoshida, T., Fujita, Y., Sayama, H., Kidokoro, S., Maruyama, K., Mizoi, J., et al. (2010). AREB1, AREB2, and ABF3 are master transcription factors that cooperatively regulate ABRE-dependent ABA signaling involved in drought stress tolerance and require ABA for full activation. *Plant J.* 61, 672–685. doi: 10.1111/j.1365-313X.2009.04092.x

Conflict of Interest Statement: The authors declare that the research was conducted in the absence of any commercial or financial relationships that could be construed as a potential conflict of interest.

Copyright © 2016 Li, Li, Li, Yan, Liu and Li. This is an open-access article distributed under the terms of the Creative Commons Attribution License (CC BY). The use, distribution or reproduction in other forums is permitted, provided the original author(s) or licensor are credited and that the original publication in this journal is cited, in accordance with accepted academic practice. No use, distribution or reproduction is permitted which does not comply with these terms.



Characterisation of Lipid Changes in Ethylene-Promoted Senescence and Its Retardation by Suppression of Phospholipase D δ in *Arabidopsis* Leaves

Yanxia Jia¹ and Weiqi Li^{1,2*}

¹ Germplasm Bank of Wild Species, Kunming Institute of Botany, Chinese Academy of Sciences, Kunming, China, ² Key Laboratory for Plant Diversity and Biogeography of East Asia, Kunming Institute of Botany, Chinese Academy of Sciences, Kunming, China

OPEN ACCESS

Edited by:

Olivier Lamotte,
Centre National de la Recherche
Scientifique, France

Reviewed by:

Maojin John Li,
University of Missouri-St. Louis, USA
Jean-luc Cacat,
AgroParisTech, France

*Correspondence:

Weiqili@mail.kib.ac.cn

Specialty section:

This article was submitted to
Plant Physiology,
a section of the journal
Frontiers in Plant Science

Received: 11 August 2015

Accepted: 09 November 2015

Published: 30 November 2015

Citation:

Jia Y and Li W (2015)

Characterisation of Lipid Changes
in Ethylene-Promoted Senescence
and Its Retardation by Suppression
of Phospholipase D δ in *Arabidopsis*

Leaves. *Front. Plant Sci.* 6:1045.

doi: 10.3389/fpls.2015.01045

Ethylene and abscisic acid (ABA) both accelerate senescence of detached *Arabidopsis* leaves. We previously showed that suppression of Phospholipase D δ (PLD δ) retarded ABA-promoted senescence. Here, we report that ethylene-promoted senescence is retarded in detached leaves lacking PLD δ . We further used lipidomics to comparatively profile the molecular species of membrane lipids between wild-type and PLD δ -knockout (PLD δ -KO) *Arabidopsis* during ethylene-promoted senescence. Lipid profiling revealed that ethylene caused a decrease in all lipids levels, except phosphatidic acid (PA), caused increases in the ratios of digalactosyl diglyceride/monogalactosyl diglyceride (MGDG) and phosphatidylcholine (PC)/phosphatidylethanolamine (PE), and caused degradation of plastidic lipids before that of extraplastidic lipids in wild-type plants. The accelerated degradation of plastidic lipids during ethylene-promoted senescence in wild-type plants was attenuated in PLD δ -KO plants. No obvious differences in substrate and product of PLD δ -catalyzed phospholipid hydrolysis were detected between wild-type and PLD δ -KO plants, which indicated that the retardation of ethylene-promoted senescence by suppressing PLD δ might not be related to the role of PLD δ in catalyzing phospholipid degradation. In contrast, higher plastidic lipid content, especially of MGDG, in PLD δ -KO plants was crucial for maintaining photosynthetic activity. The lower relative content of PA and higher PC/PE ratio in PLD δ -KO plants might contribute to maintaining cell membrane integrity. The integrity of the cell membrane in PLD δ -KO plants facilitated maintenance of the membrane function and of the proteins associated with the membrane. Taking these findings together, higher plastidic lipid content and the integrity of the cell membrane in PLD δ -KO plants might contribute to the retardation of ethylene-promoted senescence by the suppression of PLD δ .

Keywords: *Arabidopsis* leaf senescence, ethylene, lipidomics, membrane lipids, phospholipase D δ

INTRODUCTION

Leaf senescence, the final stage of leaf development, is a genetically regulated, highly ordered process by which plants mobilize and recycle nutrients from leaves to other plant parts, such as seeds, storage organs, or developing leaves and flowers (Lim et al., 2007). Chlorophyll degradation is the first visible symptom of senescence, and chloroplast membrane degradation, which parallels a loss in photosynthetic activity, was shown to occur before degradation of the membranes of other organelles (Woolhouse, 1984). Chloroplast membranes, especially the plastidic membrane, are believed to be highly vulnerable to heat-stress-associated damage (Woolhouse, 1984; Wanner et al., 1991), and the damage of these membranes is an event that occurs at an early stage during leaf senescence (Guo and Gan, 2005). The plastidic membrane consists mainly of four lipids: monogalactosyl diglyceride (MGDG), digalactosyl diglyceride (DGDG), phosphatidylglycerol (PG), and sulfoquinovosyl diacylglycerol (SQDG; Devaiah et al., 2006), with MGDG and DGDG comprising 70–80% of the plastidic lipid matrix associated with photosynthetic membranes. The cytosolic leaflet of the outer envelope membrane also contains a few phosphatidylcholine (PC; Devaiah et al., 2006).

Membranes of extraplastidic organelles mainly consist of phospholipids, and only a fraction of the extraplastidic membranes contain very small amount DGDG (Devaiah et al., 2006). The degradation of phospholipids is mediated by several enzyme cascades initiated by various phospholipases, including phospholipases A, C, and D. Phospholipase D (PLD) hydrolyzes phospholipids into phosphatidic acid (PA) and head group, and it has 12 members in *Arabidopsis* (Qin and Wang, 2002). The suppression of major PLD, PLD α 1, retards abscisic acid (ABA)- or ethylene-promoted senescence (Fan et al., 1997). Phospholipid D8 (PLD δ), one of most abundant PLDs, has several properties that distinguish it from other PLDs (Wang and Wang, 2001). PLD δ is activated by oleic acid and is tightly associated with the plasma membrane and microtubule (MT) cytoskeleton (Gardiner et al., 2001; Dhonukshe et al., 2003; Zhang et al., 2012). Analyses of PLD δ -altered *Arabidopsis* suggest that PLD δ positively regulates plant tolerance to stresses such as freezing (Li et al., 2004, 2008) and ultraviolet irradiation (Zhang et al., 2003). Our previous study found that the suppression of PLD δ retards ABA-promoted senescence through attenuating PA production (Jia et al., 2013). However, whether PLD δ functions in ethylene-promoted senescence is unknown so far.

Ethylene is considered to be a major hormonal regulator of senescence in most plant organs, including leaf, cotyledon, and petal (Grbic and Bleeker, 1995). It promotes senescence through the enhancement of various lipid catabolic processes (Baardseth and Vonelbe, 1989), and then the lipid metabolism enhances senescence through the regulation of ethylene production and/or action (Halevy et al., 1996). It is noted that the ethylene-mediated increase in membrane permeability in senescent *Tradescantia* correlated temporally with a reduction in the tissue levels of phospholipids (Suttle and Kende, 1980). The decline of phospholipid content is shown to result in the loss of membrane integrity and physical changes

in plant membrane lipids during senescence, which greatly increased the permeability of lipid bilayers (Wanner et al., 1991; Cheour et al., 1992). Given that PLD δ is one of major lipolytic enzymes, whether it has a role in the lipid changes during ethylene promoted senescence remains to be tested.

In the present study, we compared the ethylene-promoted leaf senescence between *Wassilewskija* (WS) ecotype and PLD δ -knockout mutant *Arabidopsis* and found that suppression of PLD δ retarded ethylene-promoted senescence. Profiling the changes of molecular lipid species by using electrospray ionization tandem mass spectrometry (ESI-MS/MS) in WS and PLD δ -KO detached leaves revealed how lipid changes and provided insight into the function of PLD δ in ethylene-promoted senescence.

MATERIALS AND METHODS

Plant Materials, Growth Conditions, and Hormone Treatments

A PLD δ -knockout mutant was previously isolated from *Arabidopsis* *Wassilewskija* ecotype (WS). The loss of PLD δ was confirmed by the absence of its transcript, protein and activity (Li et al., 2008).

Two *Arabidopsis* genotypes were grown in water in a controlled growth chamber at 23°C (day) and 19°C (night) and 60% relative humidity under a 12 h photoperiod, with fluorescent lighting at 120 $\mu\text{mol m}^{-2} \text{ sec}^{-1}$. Fully expanded leaves of the same age were collected from approximately 6-week-old plants of the two genotypes of *Arabidopsis*; the detached leaves were rinsed briefly with sterile water and placed with the adaxial side up in Petri dishes containing 50 μM ethephon (Sigma, C0143). We chose ethephon rather than ethylene for incubation of the detached leaves because it is easier to control, but has an identical effect on the detached leaves. The leaves were incubated at 23°C under a 12 h photoperiod and light at 120 $\mu\text{mol m}^{-2} \text{ sec}^{-1}$.

Measurements of Chlorophyll Content, Photosynthetic Activity and Cell Death

Chlorophyll was extracted incubation of leaves after incubation with ethephon in, 80% acetone. Chlorophyll content was determined spectrophotometrically at 663 and 646 nm as described previously (Craftsbrandner et al., 1984). Chlorophyll fluorescence was analyzed using an imaging chlorophyll fluorometer, MAXI-Imaging Pulse-Amplitude (PAM; Walz, Germany; Bonfig et al., 2006). The maximal quantum yield of photosystem II (PS II; F_v/F_m) photochemistry was measured after adaptation to complete darkness for 20 min.

Cell death, indicated by loss of plasma membrane integrity, was quantified spectrophotometrically by Evans blue staining of detached leaves, using a previously described method with minor modifications (Rea et al., 2004). Briefly, detached leaves were incubated with 0.1% (w/v) Evans blue for 2 h with shaking, and then washed extensively to remove unbound dye.

The leaves were ground into powder in liquid nitrogen. The tissue powder was incubated with 50% (v/v) methanol and 1% (w/v) SDS at 60°C for 30 min, and then centrifuged. For a control measurement of 100% cell death, the leaves were heated at 100°C for 5 min. Absorbance was measured at 600 nm.

Lipid Extraction and Analysis

The processes of lipid extraction, ESI-MS/MS analysis and quantification were performed in accordance with a protocol from Welti et al. (2002). Data processing was performed as previously described. The lipids in each class were quantified by comparison with two internal standards of the class. Five replicates of each treatment for each genotype were analyzed. The Q test was performed on the total amount of lipid in each head-group class, and data from discordant samples was removed (Devaiah et al., 2006).

Data Analysis

Statistical analysis was performed using Origin 7.0 (Origin Lab Corporation, Northampton, MA, USA). For all quantitative measurements in this study, five replicates from each sampling time were analyzed. The data were subjected to one-way ANOVA analysis (duncan's multiple range test) of variance with SPSS 16.0.

RESULTS

Suppression of PLD δ Retarded Ethylene-promoted Senescence

Leaves detached from WS plants started yellowing 1 day after treatment and turned almost completely yellow 5 days after incubation in 50 μ M ethephon under light. In contrast, most parts of the PLD δ -KO leaves were still green after the 5-day ethylene treatment, which indicated a much slower senescence process in the PLD δ -deficient leaves (Figure 1A, top). Consistent with the visible yellowing, the photochemical quantum efficiency of the photosystem II (PS II) reaction center (F_v/F_m) in ethylene-treated leaves was much lower in WS plants than in PLD δ -KO mutants (Figure 1A, bottom). Measurements of chlorophyll content showed that chlorophyll was lost more quickly from WS leaves, diminishing by 37% after 5 days, whereas PLD δ -KO mutant leaves lost just 20% of their chlorophyll content upon treatment with ethylene (Figure 1B, top). Data on cell viability showed that the rate of cell death was significantly higher in the WS leaves during the ethylene-promoted senescence process, as measured by Evans blue staining (Figure 1B, bottom). These results indicate that the suppression of PLD δ retarded, to some extent, ethylene-promoted senescence.

Large Changes in Lipid Profiles Occurred during Ethylene-promoted Senescence

Metabolism of membrane lipids is one of several biochemical manifestations of cellular senescence (Thompson et al., 1998).

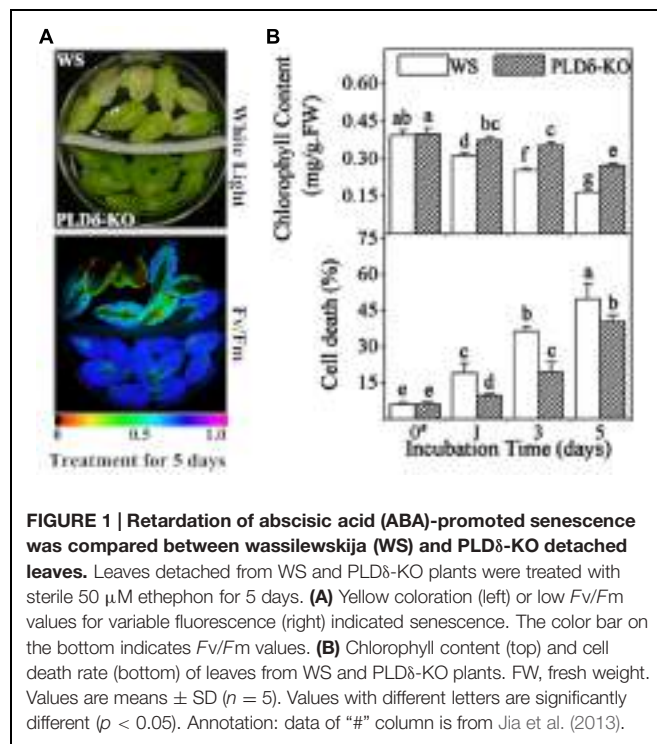


FIGURE 1 | Retardation of abscisic acid (ABA)-promoted senescence was compared between wassilewskija (WS) and PLD δ -KO detached leaves. Leaves detached from WS and PLD δ -KO plants were treated with sterile 50 μ M ethephon for 5 days. (A) Yellow coloration (left) or low F_v/F_m values for variable fluorescence (right) indicated senescence. The color bar on the bottom indicates F_v/F_m values. (B) Chlorophyll content (top) and cell death rate (bottom) of leaves from WS and PLD δ -KO plants. FW, fresh weight. Values are means \pm SD ($n = 5$). Values with different letters are significantly different ($p < 0.05$). Annotation: data of “#” column is from Jia et al. (2013).

Since the above results suggest that PLD δ is involved in ethylene-promoted senescence, combined with the participation of PLD δ in the metabolism of membrane lipids, we performed ESI-MS/MS analysis to determine whether the degradation of membrane lipids is affected by the suppression of PLD δ during ethylene-promoted senescence. ESI-MS/MS allowed the identification of alterations in >120 diverse polar glycerolipids, including six head-group classes of phospholipids [PC, phosphatidylethanolamine (PE), phosphatidylinositol (PI), phosphatidylserine (PS), PA, and PG] and two head-group classes of galactolipids (MGDG and DGDG; Table 1). Each molecular species was identified in terms of the total numbers of acyl carbon atoms and double bonds (Welti et al., 2002).

As an overview, most lipid species changed dramatically in terms of both their level (absolute value; Figure 2, left) and the composition (relative value; Figure 2, right) during ethylene-promoted senescence in the leaves of both genotypes of *Arabidopsis*. The levels of most lipids declined in both WS and PLD δ -KO leaves, although there were some differences in the profiles of membrane lipids between plants of the two genotypes during ethylene-promoted senescence (Figure 2). Clustering of the lipid contents of leaves in ethylene-promoted senescence suggested that the ethylene treatment was the main factor inducing the degradation of membrane lipids. The differences between WS and PLD δ -KO leaves subjected to ethylene treatment were greater than those between WS and PLD δ -KO leaves without such treatment (Figure 2). These results suggest that ethylene treatment affected lipid degradation, and that PLD δ

TABLE 1 | Total lipids in leaves of Wassilewskija (WS) and PLD δ -KO plants during ethylene-promoted senescence.

Lipids	Genotypes	Lipids/dry weight (nmol/mg)			RC (%)	
		Day 0 [#]	Day 3	Day 5	Day 3	Day 5
PG	WS	12.86 ± 1.89 ^a	10.82 ± 2.92 ^a	2.14 ± 0.72 ^c	—	-83.4
	PLD δ -KO	12.67 ± 4.97 ^a	6.73 ± 1.51 ^b	4.56 ± 1.76 ^b	-46.9	-64.0
PC	WS	16.73 ± 1.56 ^a	17.97 ± 6.90 ^a	9.25 ± 2.52 ^b	—	-44.7
	PLD δ -KO	15.21 ± 4.66 ^{ab}	13.82 ± 3.36 ^{ab}	10.93 ± 2.00 ^{ab}	—	—
PE	WS	9.86 ± 1.09 ^a	8.53 ± 3.27 ^{ab}	5.28 ± 1.85 ^{bc}	—	-46.5
	PLD δ -KO	9.17 ± 2.81 ^a	6.43 ± 1.67 ^{ab}	5.13 ± 1.43 ^c	—	-44.1
PI	WS	2.38 ± 0.56 ^{ab}	2.90 ± 0.80 ^a	1.62 ± 0.87 ^b	—	—
	PLD δ -KO	2.55 ± 0.52 ^{ab}	3.14 ± 1.00 ^a	2.05 ± 0.53 ^{ab}	—	—
PA	WS	0.07 ± 0.05 ^a	0.10 ± 0.01 ^a	0.07 ± 0.03 ^a	—	—
	PLD δ -KO	0.09 ± 0.06 ^a	0.09 ± 0.02 ^a	0.08 ± 0.02 ^a	—	—
PS	WS	0.35 ± 0.06 ^a	0.12 ± 0.11 ^b	0.33 ± 0.22 ^{ab}	-65.7	—
	PLD δ -KO	0.20 ± 0.06 ^{ab}	0.14 ± 0.07 ^b	0.36 ± 0.08 ^a	—	—
MGDG	WS	235.55 ± 17.65 ^a	175.83 ± 19.04 ^b	76.69 ± 16.18 ^d	-25.4	-67.4
	PLD δ -KO	217.78 ± 25.85 ^a	187.69 ± 43.08 ^b	103.67 ± 13.18 ^c	-13.8	-52.4
DGDG	WS	31.73 ± 4.78 ^a	25.22 ± 2.07 ^c	14.80 ± 1.25 ^e	-20.5	-53.4
	PLD δ -KO	31.85 ± 6.85 ^a	28.07 ± 1.83 ^b	16.43 ± 1.59 ^d	-11.9	-48.4
Total lipids/dry weight (nmol/mg)						
Total lipids	WS	302.20 ± 28.25 ^a	249.05 ± 8.51 ^b	94.53 ± 4.60 ^d	-17.6	-68.7
	PLD δ -KO	283.52 ± 38.85 ^a	252.81 ± 4.85 ^{ab}	139.84 ± 4.99 ^c	—	-50.7

The relative change (RC) in the levels of lipids from days 0 to 3 and 5 is the percentage value for the significant difference between the values at day 0 and days 3 and 5 over the value at day 0. Values in the same lipid molecular species with different letters are significantly different ($p < 0.05$). Values are means ± SD ($n = 5$). Annotation: data of “#” column is from Jia et al. (2013).

participated in this lipid degradation during ethylene-promoted senescence.

The Degradation of Plastidic Lipids Occurred before that of Extraplastidic Lipids during Ethylene-promoted Senescence

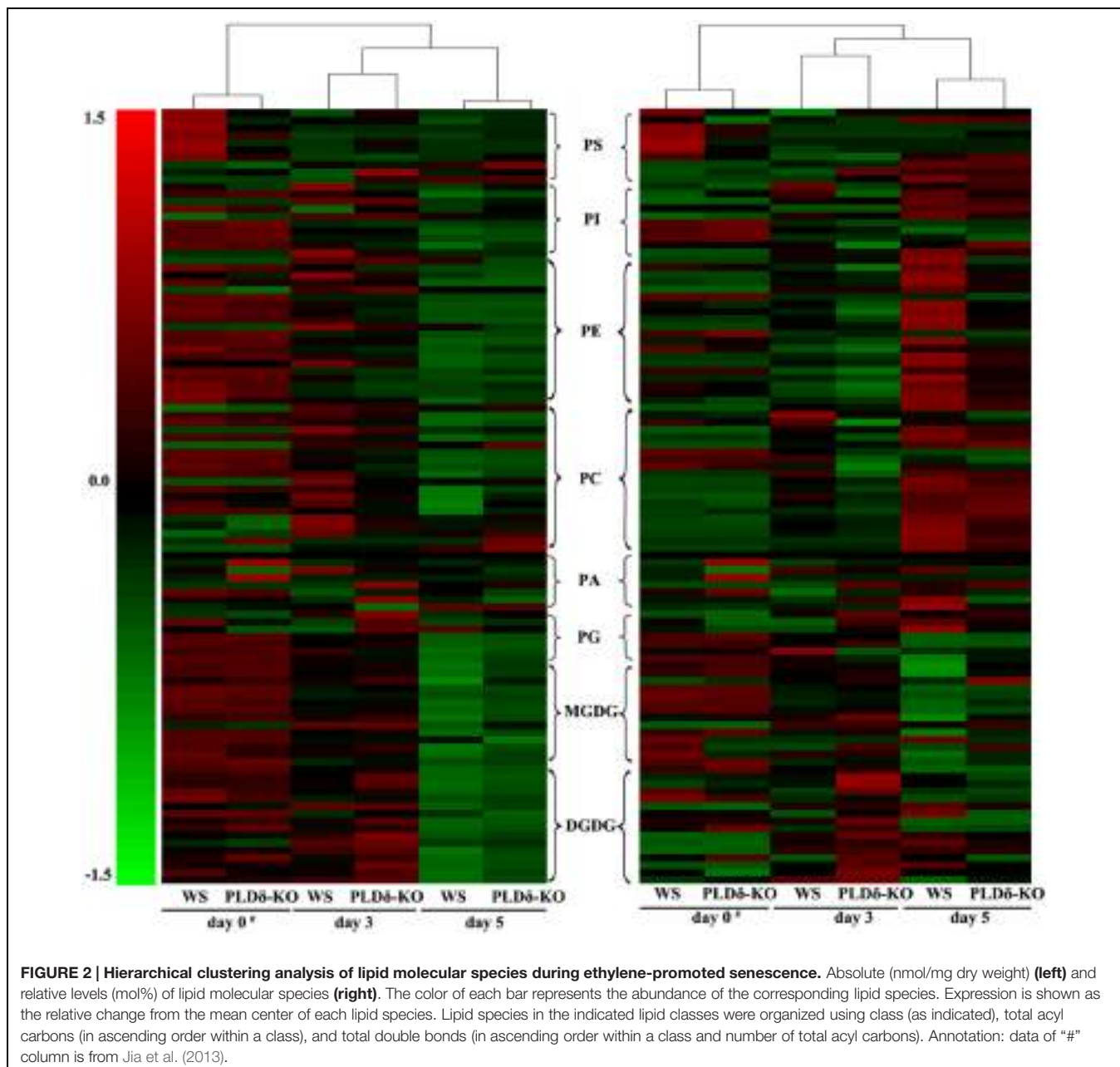
During ethylene-promoted senescence in WS leaves, the levels of leaf membrane lipids decreased significantly (Table 1). After ethylene treatment for 5 days, we found that the level of total lipids decreased by 68.7%, from 302.20 nmol/mg (non-senescent leaves, NS) to 94.53 nmol/mg (leaves treated with ethylene for 5 days). The levels of PG, PC, PE, DGDG, and MGDG all decreased significantly, but the abundances of PA, PI, and PS remained unchanged. As shown in Table 1, after ethylene-promoted senescence for 3 days, the levels of MGDG and DGDG, two main classes of plastidic lipid, decreased significantly compared with those in untreated leaves, whereas the levels of the main extraplastidic lipids (PC and PE) decreased significantly only after ethylene treatment for 5 days. These findings imply that plastidic lipids might be degraded before extraplastidic lipids.

To compare lipid degradation between plastidic and extraplastidic membranes further, the changes in the levels of molecular species of PG were analyzed. In *Arabidopsis*, PG includes four molecular species, namely, PG 34:1 (total carbon number:double bond number), 34:2, 34:3, and 34:4 (Welti et al.,

2002). PG 34:4, which contains a 16:1 acyl chain at the *sn*-2 position, is part of the plastidic membrane, whereas both PG 34:1 and 34:2 are extraplastidic lipids. Of the two molecules that correspond to PG 34:3, one contains a 16:1 acyl chain which is part of the plastidic membrane, whereas the other is extraplastidic (Marechal et al., 1997). During ethylene-promoted senescence in WS leaves, the level of PG 34:4 had decreased by 33.2% at day 3, whereas the levels of the other three PG molecular species, PG 34:3, 34:2, and 34:1, showed no significant decline after ethylene treatment for 3 days (Table 2). These results indicate that the degradation of plastidic membrane lipids occurred before that of extraplastidic lipids during ethylene-promoted senescence.

Suppression of PLD δ Attenuated the Decrease in Levels of Plastidic Lipids during Ethylene-promoted Senescence

During ethylene-promoted senescence, the amount of total lipids declined by 50.7% in PLD δ -KO plants (Table 1). Most of this decrease could be attributed to a decrease in plastidic lipids. For example, the level of MGDG in PLD δ -KO leaves decreased by 52.4% (from 217.78 to 103.67 nmol/mg), the level of DGDG decreased by 48.4% (from 31.85 to 16.43 nmol/mg), and the level of PG decreased by 64.0% (from 12.67 to 4.56 nmol/mg). The levels of both total lipids and the main plastidic lipids (MGDG, DGDG) were significantly higher in PLD δ -KO leaves than in WS leaves, whereas no differences in the levels of PC, PE, PI, PA,



and PS were detected between the plants with different genotypes (**Table 1**). Upon further analysis of the content of molecular species of each membrane lipid, we found that the contents of molecular species MGDG 34:2, 34:5, 34:6, and 36:6 as well as DGDG 36:6 in PLD δ -KO detached leaves were much higher than that in WS detached leaves (**Table 3**). Furthermore, the levels of the plastidic lipids PG 34:4 and 34:3 were higher in PLD δ -KO leaves than that in WS leaves. The extraplastidic lipids PG 34:2 and 34:1 in PLD δ -KO leaves showed no clear difference compared with those in WS leaves (**Table 2**). The lipids that are largely synthesized and localized in plastids, PG 34:4, MGDG, and DGDG, were previously shown to be the most abundant in leaves (Devaiah et al., 2006). Plastidic lipids have also been shown

to have a direct role in photosynthesis (Dormann and Benning, 2002). We also found that the main MGDG species 34:6 and 36:6 significantly decreased at day 3 of ethylene treatment, whereas the level of DGDG 34:6 increased obviously. These results indicated that these head group remodeling of galactolipids might contribute to maintenance of photosynthesis at early stage of leaf senescence. Combining these findings with our results, it is conceivable that the attenuated degradation of plastidic lipids might have contributed to higher photosynthetic activity in PLD δ -KO leaves during ethylene-promoted senescence, and the retardation of ethylene-promoted senescence by the suppression of PLD δ was a consequence of qualitative changes in plastidic lipids.

TABLE 2 | Levels of PG molecular species in leaves of WS and PLD δ -KO plants during ethylene-promoted senescence.

PG	Genotypes	Lipids/dry weight (ng/mg)			RC (%)	
		Day 0 [#]	Day 3	Day 5	Day 3	Day 5
34:1	WS	0.65 ± 0.19 ^a	0.37 ± 0.32 ^{ab}	0.05 ± 0.06 ^b		-91.7
	PLD δ -KO	0.69 ± 0.33 ^a	0.42 ± 0.49 ^{ab}	0.10 ± 0.14 ^b		-86.0
34:2	WS	0.98 ± 0.32 ^a	0.57 ± 0.36 ^a	0.18 ± 0.19 ^b		-81.4
	PLD δ -KO	0.93 ± 0.15 ^a	0.76 ± 0.41 ^a	0.24 ± 0.12 ^b		-74.3
34:3	WS	2.80 ± 0.17 ^a	2.69 ± 0.23 ^a	0.79 ± 0.27 ^c		-71.9
	PLD δ -KO	3.07 ± 0.47 ^a	2.97 ± 0.01 ^a	1.19 ± 0.13 ^b		-61.2
34:4	WS	8.18 ± 1.56 ^a	5.46 ± 1.37 ^b	1.35 ± 0.62 ^c	-33.3	-83.6
	PLD δ -KO	7.84 ± 1.67 ^a	4.66 ± 1.90 ^b	2.79 ± 1.20 ^b	-40.5	-64.4

The RC in lipids from day 0 to day 5 is the percentage value for the significant difference between the values at day 0 and day 3 and 5 over the value at day 0. Values in the same lipid molecular species with different letters are significantly different ($p < 0.05$). Values are means ± SD ($n = 5$). Annotation: data of “#” column is from Jia et al. (2013).

TABLE 3 | Levels of major lipid molecular species in leaves of WS and PLD δ -KO plants during ethylene-promoted senescence.

Galactolipids major lipids species	Genotypes	Lipids/dry weight (nmol/mg)			RC (%)	
		Day 0	Day 3	Day 5	Day 3	Day 5
DGDG 34:6	WS	2.51 ± 0.41 ^b	3.36 ± 0.54 ^a	1.53 ± 0.59 ^c	33.9	-39.0
	PLD δ -KO	2.26 ± 0.61 ^b	3.29 ± 0.59 ^a	1.85 ± 0.97 ^{b,c}	45.6	-
DGDG 34:5	WS	0.36 ± 0.07 ^a	0.13 ± 0.04 ^b	0.04 ± 0.02 ^c	-63.9	-88.9
	PLD δ -KO	0.29 ± 0.07 ^a	0.15 ± 0.03 ^b	0.07 ± 0.04 ^c	-48.3	-75.9
DGDG 34:3	WS	6.47 ± 1.10 ^a	5.67 ± 2.35 ^a	2.41 ± 1.07 ^b	-	-62.8
	PLD δ -KO	6.80 ± 1.14 ^a	7.75 ± 3.67 ^a	3.15 ± 1.42 ^b	-	-53.7
DGDG 34:2	WS	0.53 ± 0.05 ^a	0.44 ± 0.23 ^a	0.18 ± 0.07 ^b	-	-66.0
	PLD δ -KO	0.54 ± 0.16 ^a	0.65 ± 0.47 ^{ab}	0.22 ± 0.09 ^b	-	-59.3
DGDG 36:6	WS	19.98 ± 3.17 ^a	23.60 ± 8.68 ^a	10.87 ± 2.42 ^c	-	-45.6
	PLD δ -KO	20.26 ± 6.08 ^{ab}	25.52 ± 5.63 ^a	16.96 ± 5.05 ^b	-	-
DGDG 36:5	WS	0.63 ± 0.11 ^a	1.06 ± 0.50 ^a	0.56 ± 0.17 ^a	-	-
	PLD δ -KO	0.53 ± 0.17 ^a	1.14 ± 0.60 ^a	0.60 ± 0.21 ^a	-	-
MGDG 34:6	WS	218.94 ± 43.22 ^a	139.36 ± 46.31 ^b	68.55 ± 14.48 ^d	-36.4	-68.7
	PLD δ -KO	207.77 ± 52.62 ^a	161.64 ± 33.84 ^b	90.66 ± 11.24 ^c	-22.2	-56.4
MGDG 34:5	WS	7.89 ± 1.50 ^a	1.92 ± 0.86 ^c	0.26 ± 0.09 ^e	-75.7	-96.7
	PLD δ -KO	6.76 ± 2.15 ^a	2.51 ± 1.19 ^b	0.66 ± 0.05 ^d	-62.9	-90.2
MGDG 34:4	WS	2.91 ± 0.65 ^a	1.24 ± 0.48 ^b	0.22 ± 0.09 ^c	-57.4	-92.4
	PLD δ -KO	2.90 ± 0.87 ^a	1.49 ± 0.62 ^b	0.47 ± 0.27 ^c	-48.6	-83.8
MGDG 34:3	WS	1.69 ± 0.34 ^a	1.64 ± 0.71 ^a	0.62 ± 0.27 ^b	-	-63.3
	PLD δ -KO	1.86 ± 0.66 ^a	1.93 ± 0.80 ^a	1.36 ± 0.75 ^{ab}	-	-
MGDG 34:2	WS	0.33 ± 0.08 ^a	0.22 ± 0.09 ^a	0.54 ± 0.38 ^a	-	-
	PLD δ -KO	0.34 ± 0.11 ^a	0.25 ± 0.12 ^{ab}	0.13 ± 0.07 ^b	-	-61.8
MGDG 36:6	WS	22.74 ± 2.93 ^a	15.79 ± 5.58 ^{b,c}	5.48 ± 2.33 ^d	-30.6	-75.9
	PLD δ -KO	23.15 ± 6.14 ^a	17.90 ± 6.00 ^{ab}	9.30 ± 2.69 ^c	-	-59.8
MGDG 36:5	WS	0.68 ± 0.19 ^b	1.28 ± 0.51 ^a	0.43 ± 0.15 ^c	88.2	-36.8
	PLD δ -KO	0.60 ± 0.17 ^b	1.31 ± 0.48 ^a	0.77 ± 0.44 ^{abc}	118.3	-
MGDG 36:4	WS	0.42 ± 0.06 ^a	0.35 ± 0.15 ^a	0.11 ± 0.04 ^b	-	-73.8
	PLD δ -KO	0.44 ± 0.13 ^a	0.41 ± 0.18 ^a	0.20 ± 0.09 ^b	-	-54.6

The RC in the levels of lipids from days 0 to 3 and day 5 is the percentage value for the significant difference between the values at day 0 and days 3 and 5 over the value at day 0. Values in the same lipid molecular species with different letters are significantly different ($p < 0.05$). Values are means ± SD ($n = 5$).

Changes in the Composition of Lipid Classes during Ethylene-promoted Senescence

For the analysis of the relative contents of membrane lipids, for which the data are expressed as mol% lipids,

we found that the most important changes concerned the two galactolipids in WS plants after ethylene treatment for 5 days. The MGDG percentage decreased from 77.55% (NS) to 63.70% (leaves treated with ethylene for 5 days). In contrast, the DGDG percentage increased from 9.70% (NS) to 14.22% (leaves treated with ethylene for 5 days). The

PG percentage showed a slight decrease in WS plants. In addition, the relative percentages of the non-chloroplastic PE, PC, PI, and PS, which are mainly located in the membranes of non-photosynthetic organelles such as the plasma membrane, endoplasmic reticulum, and mitochondria (Singh and Privett, 1970), increased during senescence, in keeping with the preferential destruction of chloroplast membranes. The ratio of galactolipids/phospholipids decreased from 11.02 to 5.41, which represent a decrease of 50.9% (Table 4). This decrease might have resulted from the degradation of 67.4% of the MGDG, which initially constituted 77.6% of total lipids (Tables 1 and 4). The ratio of DGDG/MGDG increased in both WS and PLD δ -KO leaves during ethylene-promoted senescence. The relative content of MGDG was clearly higher in PLD δ -KO plants than in WS plants, whereas the relative content of DGDG in PLD δ -KO plants resembled that in WS plants, which resulted in the ratio of DGDG/MGDG in PLD δ -KO detached leaves being significantly lower than that in WS plants after ethylene treatment for 5 days, namely, 0.19 and 0.22, respectively (Table 4). The higher relative content of MGDG in PLD δ -KO leaves might have contributed to stabilizing the ultrastructure, fluidity and permeability of the chloroplast membrane, which resulted in higher photosynthetic activity.

The Lower Relative Content of PA and Higher Ratio of PC/PE Might Contribute to the Retardation of Ethylene-promoted Senescence in PLD δ -KO Plant Leaves

To investigate how PLD δ functions in ethylene-promoted senescence, we analyzed the changes in the absolute level and relative content of PA under ethylene treatment in the two genotypes plants leaves. During ethylene-promoted senescence, no significant changes were detected in absolute levels of PA in either WS or PLD δ -KO plants. Upon analysis of the relative content of membrane lipids, we found that the relative content of PA increased 3.5-fold (from 0.02 to 0.07%) in WS plants, but remained unchanged in PLD δ -KO plants, which resulted in the relative content of PA in WS being much higher than that in PLD δ -KO plants after ethylene treatment for 5 days, especially for the molecular species PA 34:3, 36:3, and 36:6 (Tables 1 and 3; Figure 3). PA is a non-bilayer lipid and a potent promoter of the formation of the hexagonal phase and destabilization of the plasma membrane. For further assessment of the cell membrane stabilization of *Arabidopsis* during ethylene-promoted senescence, we calculated the PC/PE ratio in this process. This ratio in WS plants increased from 1.61 (NS) to 2.11 (leaves treated with ethylene for 3 days), and then decreased to

TABLE 4 | Leaf membrane lipid composition in each head-group class and lipid ratio in WS and PLD δ -KO plants during ethylene-promoted senescence.

Lipid class	Genotype	Lipid (mol% of total lipid)		
		Day 0	Day 3	Day 5
PG	WS	3.92 ± 0.16 ^{ab}	3.12 ± 0.72 ^c	2.78 ± 0.28 ^c
	PLD δ -KO	4.23 ± 0.33 ^a	3.48 ± 0.82 ^{bcd}	3.15 ± 0.32 ^c
PI	WS	0.78 ± 0.11 ^c	1.13 ± 0.09 ^b	2.03 ± 0.46 ^a
	PLD δ -KO	0.82 ± 0.09 ^c	1.23 ± 0.35 ^{ab}	1.50 ± 0.38 ^a
PS	WS	0.11 ± 0.02 ^b	0.04 ± 0.02 ^c	0.38 ± 0.13 ^a
	PLD δ -KO	0.10 ± 0.05 ^b	0.21 ± 0.24 ^{abc}	0.26 ± 0.01 ^a
PA	WS	0.02 ± 0.01 ^b	0.04 ± 0.02 ^b	0.07 ± 0.02 ^a
	PLD δ -KO	0.03 ± 0.01 ^b	0.03 ± 0.01 ^b	0.03 ± 0.01 ^b
PC	WS	4.92 ± 0.55 ^{bcd}	7.30 ± 2.74 ^{ab}	9.72 ± 1.70 ^a
	PLD δ -KO	4.78 ± 0.42 ^c	5.37 ± 0.91 ^b	8.12 ± 1.79 ^a
PE	WS	3.04 ± 0.32 ^a	3.45 ± 0.23 ^a	4.27 ± 1.14 ^a
	PLD δ -KO	2.88 ± 0.26 ^a	2.68 ± 0.54 ^a	3.77 ± 1.10 ^a
MGDG	WS	77.55 ± 1.22 ^a	70.01 ± 1.86 ^c	63.70 ± 3.48 ^d
	PLD δ -KO	77.39 ± 1.66 ^a	72.87 ± 1.40 ^b	69.71 ± 3.18 ^{bc}
DGDG	WS	9.70 ± 0.54 ^b	13.86 ± 1.45 ^a	14.22 ± 1.67 ^a
	PLD δ -KO	10.08 ± 0.52 ^b	15.36 ± 2.11 ^a	13.41 ± 0.79 ^a
Lipid ratio				
PC/PE	WS	1.61 ± 0.07 ^c	2.11 ± 0.12 ^b	1.73 ± 0.14 ^c
	PLD δ -KO	1.66 ± 0.04 ^c	2.24 ± 0.37 ^{ab}	2.39 ± 0.18 ^a
DGDG/MGDG	WS	0.13 ± 0.01 ^c	0.20 ± 0.03 ^{ab}	0.22 ± 0.01 ^a
	PLD δ -KO	0.13 ± 0.01 ^c	0.21 ± 0.03 ^{ab}	0.19 ± 0.01 ^b
Galactolipids/Phospholipids	WS	11.02 ± 1.21 ^a	9.50 ± 0.71 ^b	5.41 ± 1.60 ^c
	PLD δ -KO	11.24 ± 0.94 ^a	9.41 ± 1.12 ^b	6.64 ± 1.24 ^c

Values in the same lipid molecular species with different letters are significantly different ($p < 0.05$). Values are means ± SD ($n = 5$).

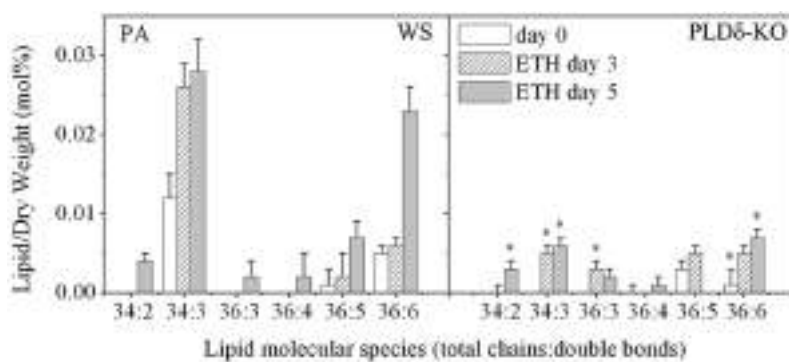


FIGURE 3 | Changes in the molecular species of PA in WS and PLD δ -KO plants during ethylene-promoted senescence. ** indicates that the value is significantly different from that of the WS under the same conditions ($p < 0.05$). Values are means \pm SD ($n = 4$ or 5).

the initial level of 1.73 (leaves treated with ethylene for 5 days). The PC/PE ratio in PLD δ -KO leaves increased constantly in the course of ethylene-promoted senescence, from 1.66 (NS) to 2.39 (leaves treated with ethylene for 5 days). In addition, the ratio of PC/PE in PLD δ -KO detached leaves was much higher than that in WS leaves after ethylene treatment for 5 days, namely, 2.39 and 1.73, respectively (Table 4). Our results indicate that the increase in the relative content of PA promoted destabilization of the plasma membrane; this may have led to the loss of membrane integrity and functions of membrane-associated proteins, thereby promoting senescence. Therefore, a reduction in the relative content of PA in PLD δ -KO leaves may have accounted for the higher ratio of PC/PE, which may have helped to maintain plasma membrane integrity and normal membrane protein function that eventually resulted in the retardation of ethylene-promoted senescence.

DISCUSSION

The senescence process takes place in a highly regulated manner and the cell constituents are dismantled via an ordered progression. Senescence affects both the plasma membrane and the intracellular membranes, which results in the loss of ionic and metabolite gradients that are essential for normal cell function (Fan et al., 1997; Thompson et al., 2000; He and Gan, 2002; Jia et al., 2013). With respect to organelle membranes, degradation occurs first at the plastidic membrane and last at the plasma membrane (Wanner et al., 1991). Many reports have indicated that ethylene accelerated the onset of membrane leakiness and phospholipid deterioration in leaves and petals (Suttle and Kende, 1980; Borochov et al., 1997). Our observations suggested that most membrane glycerolipids were degraded upon ethylene treatment, except for PS and PA, which were maintained unchanged, with the most extensive degradation occurring for MGDG, which plays a fundamental role in electron transfer between the antennae and cores of the photosystems (Siefermann-Harms et al., 1987; Table 1). With regard to the other plastidic lipids (DGDG and PG 34:4), ethylene treatment also caused noteworthy decreases in their

levels. We also verified that the degradation of extraplastidic lipids was later to plastidic lipids, and the degradation of plastidic lipids paralleled a loss in photosynthetic activity and chlorophyll degradation, which is the first visible symptom of senescence. By the time leaf yellowing could be seen, extraplastidic lipid degradation had occurred. For example, the level of the main plastidic lipid MGDG declined by 25.4% when the chlorophyll content decreased to 69.8% of its initial level; extraplastidic lipids decreased until as the chlorophyll content decreased to 40.1% of its initial level in WS leaves after ethylene treatment for 5 days (Tables 1–3 and Figure 1). Additionally, the degradation of lipids, in particular plastidic lipids, was accelerated during ABA-promoted senescence, and the degradation of plastidic lipids was earlier than extraplastidic lipids (Jia et al., 2013). Combined with the physiological observations, these results showed that degradation in levels of plastidic and extraplastidic lipids were correlated with the degree of leaf senescence during ABA- or ethylene-promoted senescence. One thing should be mentioned: given the drastic global lipid changes, the degradation of MGDG, PC, PE etc, we ignored the effects of PC in outer leaflet of chloroplast membranes and DGDG in the extraplastidic membranes on the concentration of plastidic lipids due to their small amount.

Both PC and DGDG have relatively large head groups, and tend to form a bilayer lipid phase. By contrast, PE and MGDG have small head groups involved in the formation of a non-bilayer lipid phase (Dormann and Benning, 2002; Welti et al., 2002). Adjustment of the molar PC/PE and DGDG/MGDG ratios is one of the most important approaches used by plants to respond to stress. The molar ratio of PC/PE tends to increase in plants under cold or hydration stress (Hazel and Williams, 1990; Welti et al., 2002). The DGDG/MGDG ratio increased significantly in salt-stressed jojoba leaves (Benraiss et al., 1993) and in *Duboisia* leaves with reference to aging and senescence (Mishra et al., 1998). Earlier studies revealed that ethylene can facilitate both chemical and physical changes in the membrane lipids of senescent tissues, which presumably lead to the loss of intracellular compartmentalisation (Suttle and Kende, 1980; Thompson et al., 1982). During ethylene-promoted senescence, the PC/PE ratio increased (at day 3) and then decreased to

its initial level (at day 5) in WS leaves, which indicated that the increase of the PC/PE ratio in early senescence stage might facilitate the maintenance of plasma membrane stability and function, and the decrease of the PC/PE ratio in late senescence stage might indicate cell membrane disintegration. Upon analysis of the relative contents of the two kinds of galactolipid, we found that the level of MGDG decreased, while that of DGDG increased, over the course of ethylene treatment, leading to an increase in the DGDG/MGDG ratio in both WS and PLD δ -KO plants (Table 4). This increase in the DGDG/MGDG ratio might help to maintain the chloroplast membrane in the bilayer conformation necessary for its biological functions, such as protein transport (Bruce, 1998) and photosystem activities, during leaf senescence (Dormann and Benning, 2002).

During senescence, the bulk of membrane phospholipids (i.e., PE, PC) were consumed by PLD, generating copious amounts of PA (Munnik, 2001; Munnik and Musgrave, 2001). PA can be further metabolized by PA phosphatase into diacylglycerol, a known activator of protein kinase C and a proposed enhancer of flower senescence (Borochov et al., 1997). PA was also shown to be a major intermediate during lipid metabolism, with both lipid degradation and lipid synthesis being regulated by the size of the PA pool (Li et al., 2009). PA is a non-bilayer lipid and a potent promoter of the formation of the hexagonal phase (Munnik, 2001). Suppression of PLD α 1 and PLD δ partly blocks the formation of PA, and thus reduces lipid degradation, which may prolong membrane integrity and eventually retard ABA-promoted senescence (Fan et al., 1997; Jia et al., 2013). In the present study, the retardation of the senescence in PLD δ -KO leaves during ethylene treatment was indicated by delayed leaf yellowing, a higher level of chlorophyll, greater photosynthetic activity and a lower rate of cell death compared with those in WS leaves. PLD δ cleaves major membrane phospholipids, such as PE, PC, and PG, into PA and a free head group (Dyer et al., 1994). However, no significant differences in the substrate and product of the two-step transphosphatidylation reaction were detected between WS and PLD δ -KO plants during ethylene-promoted senescence, which indicated that the retardation of senescence by the suppression of PLD δ might not

be related to the role of PLD δ in enzyme-catalyzed phospholipid hydrolysis.

Leaf senescence is accompanied by an early degradation of the cortical MT cytoskeleton in *Arabidopsis*, and the disruption of the MT network is affected by either repression or induction of microtubule-associated proteins (MAP; Keech et al., 2010). As a MAP in *Arabidopsis*, PLD δ acts as a bridge between the plasma membrane and MTs can thus convey external hormonal and environmental signal from plasma membrane to MT (Gardiner et al., 2001). It is possible that without PLD δ assistance, the signal of senescence through MT is blocked and therefore ethylene-promoted senescence is delayed in PLD δ -KO leaves.

CONCLUSION

In this study, we have shown that the suppression of PLD δ effectively retarded ethylene-promoted senescence, indicated by higher chlorophyll content and photosynthetic activity, and a lower cell death rate. The profiles of membrane lipids suggested that the suppression of PLD δ attenuates plastidic lipid (PG 34:4, MGDG and DGDG) metabolism, while having no direct effect on the degradation of extraplastidic lipids. No obvious increase in product and decrease in substrate of the PLD δ -catalyzed phospholipid hydrolysis were detected, which indicated that the retardation of ethylene-promoted senescence in PLD δ -KO plants might not be related to the direct role of PLD δ in catalyzing phospholipids, and higher plastidic lipid (PG 34:4, MGDG and DGDG) content and PC/PE ratio in PLD δ -KO plants might contribute to maintenance of membrane integrity and function, and then help to retard senescence.

ACKNOWLEDGMENTS

This research was supported by grants from the National Basic Research Program of China (31070262) and the Fund of the State Key Laboratory of Phytochemistry and Plant Resources in West China (O97C0211Z1).

REFERENCES

- Baardseth, P., and Vonelbe, J. H. (1989). Effect of ethylene, free fatty-acid, and some enzyme-systems on chlorophyll degradation. *J. Food Sci.* 54, 1361–1363. doi: 10.1111/j.1365-2621.1989.tb05993.x
- Benrais, L., Alpha, M. J., Bahl, J., Guillotsalomon, T., and Dubacq, J. P. (1993). Lipid and protein contents of jojoba leaves in relation to salt adaptation. *Plant Physiol. Biochem.* 31, 547–557.
- Bonfig, K., Schreiber, U., Gabler, A., Roitsch, T., and Berger, S. (2006). Infection with virulent and avirulent *P. syringae* strains differentially affects photosynthesis and sink metabolism in *Arabidopsis* leaves. *Planta* 225, 1–12. doi: 10.1007/s00425-006-0303-3
- Borochov, A., Spiegelstein, H., and Philosoph-Hadas, S. (1997). Ethylene and flower petal senescence: interrelationship with membrane lipid catabolism. *Physiol. Plant.* 100, 606–612. doi: 10.1034/j.1399-3054.1997.1000323.x
- Bruce, B. D. (1998). The role of lipids in plastid protein transport. *Plant Mol. Biol.* 38, 223–246. doi: 10.1023/A:1006094308805
- Cheour, F., Arul, J., Makhlouf, J., and Willemot, C. (1992). Delay of membrane lipid degradation by calcium treatment during cabbage leaf senescence. *Plant Physiol.* 100, 1656–1660. doi: 10.1104/pp.100.4.1656
- Craftsbrandner, S. J., Below, F. E., Harper, J. E., and Hageman, R. H. (1984). Effects of pod removal on metabolism and senescence of nodulating and nonnodulating soybean isolines. *Plant Physiol.* 75, 311–317.
- Devaiah, S. P., Roth, M. R., Baughman, E., Li, M., Tamura, P., Jeannotte, R., et al. (2006). Quantitative profiling of polar glycerolipid species from organs of wild-type *Arabidopsis* and a PHOSPHOLIPASE D α 1 knockout mutant. *Phytochemistry* 67, 1907–1924. doi: 10.1016/j.phytochem.2006.06.005
- Dhonukshe, P., Laxalt, A. M., Goedhart, J., Gadella, T. W., and Munnik, T. (2003). Phospholipase D activation correlates with microtubule reorganization in living plant cells. *Plant Cell* 15, 2666–2679.
- Dormann, P., and Benning, C. (2002). Galactolipids rule in seed plants. *Trends Plant Sci.* 7, 112–118. doi: 10.1016/S1360-1385(01)02216-6
- Dyer, J. H., Ryu, S. B., and Wang, X. (1994). Multiple forms of phospholipase D following germination and during leaf development of castor bean. *Plant Physiol.* 105, 715–724.

- Fan, L., Zheng, S., and Wang, X. (1997). Antisense suppression of phospholipase D alpha retards abscisic acid- and ethylene-promoted senescence of postharvest *Arabidopsis* leaves. *Plant Cell* 9, 2183–2196. doi: 10.2307/3871433
- Gardiner, J. C., Harper, J. D. I., Weerakoon, N. D., Collings, D. A., Ritchie, S., Gilroy, S., et al. (2001). A 90-kD phospholipase D from tobacco binds to microtubules and the plasma membrane. *Plant Cell* 13, 2143–2158. doi: 10.2307/3871433
- Grbic, V., and Bleeker, A. B. (1995). Ethylene regulates the timing of leaf senescence in *Arabidopsis*. *Plant J.* 8, 595–602. doi: 10.1046/j.1365-313X.1995.8040595.x
- Guo, Y., and Gan, S. (2005). Leaf senescence: signals, execution, and regulation. *Curr. Top. Dev. Biol.* 71, 83–112. doi: 10.1016/S0070-2153(05)71003-6
- Halevy, A. H., Porat, R., Spiegelstein, H., Borochoff, A., Botha, L., and Whitehead, C. S. (1996). Short-chain saturated fatty acids in the regulation of pollination-induced ethylene sensitivity of Phalaenopsis flowers. *Physiol. Plant.* 97, 469–474. doi: 10.1111/j.1399-3054.1996.tb00505.x
- Hazel, J. R., and Williams, E. E. (1990). The role of alterations in membrane lipid-composition in enabling physiological adaptation of organisms to their physical-environment. *Progr. Lipid Res.* 29, 167–227. doi: 10.1016/0163-7827(90)90002-3
- He, Y. H., and Gan, S. S. (2002). A gene encoding an acyl hydrolase is involved in leaf senescence in *Arabidopsis*. *Plant Cell* 14, 805–815. doi: 10.1105/tpc.010422
- Jia, Y., Tao, F., and Li, W. (2013). Lipid profiling demonstrates that suppressing *Arabidopsis* phospholipase D δ retards ABA-promoted leaf senescence by attenuating lipid degradation. *PLoS ONE* 8:e65687. doi: 10.1371/journal.pone.0065687
- Keech, O., Pesquet, E., Gutierrez, L., Ahad, A., Bellini, C., Smith, S. M., et al. (2010). Leaf Senescence is accompanied by an early disruption of the microtubule network in *Arabidopsis*. *Plant Physiol.* 154, 1710–1720. doi: 10.1104/pp.110.163402
- Li, M., Hong, Y., and Wang, X. (2009). Phospholipase D- and phosphatidic acid-mediated signaling in plants. *Biochim. Biophys. Acta* 1791, 927–935. doi: 10.1016/j.bbalip.2009.02.017
- Li, W., Li, M., Zhang, W., Welti, R., and Wang, X. (2004). The plasma membrane-bound phospholipase D delta enhances freezing tolerance in *Arabidopsis thaliana*. *Nat. Biotechnol.* 22, 427–433. doi: 10.1038/nbt949
- Li, W., Wang, R., Li, M., Li, L., Wang, C., Welti, R., et al. (2008). Differential degradation of extraplastidic and plastidic lipids during freezing and post-freezing recovery in *Arabidopsis thaliana*. *J. Biol. Chem.* 283, 461–468. doi: 10.1074/jbc.M706692200
- Lim, P. O., Kim, H. J., and Nam, H. G. (2007). Leaf senescence. *Annu. Rev. Plant Biol.* 58, 115–136. doi: 10.1146/annurev.arplant.57.032905.105316
- Marechal, E., Block, M. A., Dorne, A. J., and Joyard, J. (1997). Lipid synthesis and metabolism in the plastid envelope. *Physiol. Plant.* 100, 65–77. doi: 10.1034/j.1399-3054.1997.1000106.x
- Mishra, S., Shanker, S., and Sangwan, R. S. (1998). Lipid profile in relation to tropane alkaloid production and accumulation during leaf growth and senescence in *Duboisia myoporoides*. *Fitoterapia* 69, 65–72.
- Munnik, T. (2001). Phosphatidic acid: an emerging plant lipid second messenger. *Trends Plant Sci.* 6, 227–233. doi: 10.1016/S1360-1385(01)01918-5
- Munnik, T., and Musgrave, A. (2001). Phospholipid signaling in plants: holding On to Phospholipase D. *Sci. Signal.* 2001:pe42.
- Qin, C., and Wang, X. (2002). The *Arabidopsis* phospholipase D family. Characterization of a calcium-independent and phosphatidylcholine-selective PLD zeta 1 with distinct regulatory domains. *Plant physiol.* 128, 1057–1068.
- Rea, G., de Pinto, M. C., Tavazza, R., Biondi, S., Gobbi, V., Ferrante, P., et al. (2004). Ectopic expression of maize polyamine oxidase and pea copper amine oxidase in the cell wall of tobacco plants. *Plant Physiol.* 134, 1414–1426. doi: 10.1104/pp.103.03674
- Siefermann-Harms, D., Ninnemann, H., and Yamamoto, H. Y. (1987). Reassembly of solubilized chlorophyll-protein complexes in proteolipid particles — Comparison of monogalactosyldiacylglycerol and two phospholipids. *Biochim. Biophys. Acta Bioenerget.* 892, 303–313. doi: 10.1016/0005-2728(87)90234-9
- Singh, H., and Privett, O. S. (1970). Studies on the glycolipids and phospholipids of immature soybeans. *Lipids* 5, 692–697. doi: 10.1007/BF02531436
- Suttle, J. C., and Kende, H. (1980). Ethylene action and loss of membrane integrity during petal senescence in *Tradescantia*. *Plant Physiol.* 65, 1067–1072. doi: 10.1104/pp.65.6.1067
- Thompson, J., Taylor, C., and Wang, T. W. (2000). Altered membrane lipase expression delays leaf senescence. *Biochem. Soc. Trans.* 28, 775–777. doi: 10.1042/bst0280775
- Thompson, J. E., Froese, C. D., Madey, E., Smith, M. D., and Hong, Y. (1998). Lipid metabolism during plant senescence. *Prog. Lipid Res.* 37, 119–141. doi: 10.1016/S0163-7827(98)00006-X
- Thompson, J. E., Mayak, S., Shinitzky, M., and Halevy, A. H. (1982). Acceleration of membrane senescence in cut carnation flowers by treatment with ethylene. *Plant Physiol.* 69, 859–863. doi: 10.1104/pp.69.4.859
- Wang, C., and Wang, X. (2001). A novel phospholipase D of *Arabidopsis* that is activated by oleic acid and associated with the plasma membrane. *Plant Physiol.* 127, 1102–1112. doi: 10.1104/pp.010444
- Wanner, L., Keller, F., and Matile, P. (1991). Metabolism of radiolabeled galactolipids in senescent barley leaves. *Plant Sci.* 78, 199–206. doi: 10.1016/0168-9452(91)90199-I
- Welti, R., Li, W., Li, M., Sang, Y., Biesiada, H., Zhou, H. E., et al. (2002). Profiling membrane lipids in plant stress responses. Role of phospholipase D alpha in freezing-induced lipid changes in *Arabidopsis*. *J. Biol. Chem.* 277, 31994–32002.
- Woolhouse, H. W. (1984). The biochemistry and regulation of senescence in chloroplasts. *Can. J. Bot.* 62, 2934–2942. doi: 10.1139/b84-392
- Zhang, Q., Lin, F., Mao, T., Nie, J., Yan, M., Yuan, M., et al. (2012). Phosphatidic acid regulates microtubule organization by interacting with MAP65-1 in response to salt stress in *Arabidopsis*. *Plant Cell* 24, 4555–4576. doi: 10.1105/tpc.112.104182
- Zhang, W., Wang, C., Qin, C., Wood, T., Olafsdottir, G., Welti, R., et al. (2003). The oleate-stimulated phospholipase D, PLD δ , and phosphatidic acid decrease H2O2-induced cell death in *Arabidopsis*. *Plant Cell* 15, 2285–2295.

Conflict of Interest Statement: The authors declare that the research was conducted in the absence of any commercial or financial relationships that could be construed as a potential conflict of interest.

Copyright © 2015 Jia and Li. This is an open-access article distributed under the terms of the Creative Commons Attribution License (CC BY). The use, distribution or reproduction in other forums is permitted, provided the original author(s) or licensor are credited and that the original publication in this journal is cited, in accordance with accepted academic practice. No use, distribution or reproduction is permitted which does not comply with these terms.



Transcriptomic Changes Drive Physiological Responses to Progressive Drought Stress and Rehydration in Tomato

Paolo Iovieno¹, Paola Punzo¹, Gianpiero Guida², Carmela Mistretta², Michael J. Van Oosten³, Roberta Nurcato¹, Hamed Bostan³, Chiara Colantuono³, Antonello Costa¹, Paolo Bagnaresi⁴, Maria L. Chiusano³, Rossella Albrizio², Pasquale Giorio², Giorgia Batelli¹ and Stefania Grillo^{1*}

¹ National Research Council of Italy, Institute of Biosciences and Bioresources, Research Division Portici (CNR-IBBR) Portici, Italy, ² National Research Council of Italy, Institute for Agricultural and Forestry Systems in the Mediterranean (CNR-ISAFoM), Ercolano, Italy, ³ Department of Agriculture, University of Naples "Federico II," Portici, Italy, ⁴ CREA - Council for Agricultural Research and Economics, Genomics Research Centre, Fiorenzuola d'Arda, Italy

OPEN ACCESS

Edited by:

Olivier Lamotte,
CNRS UMR Agroécologie, France

Reviewed by:

Suleyman I. Allakhverdiev,
Russian Academy of Sciences, Russia
Giridara Kumar Surabhi,
Regional Plant Resource Centre, India

*Correspondence:

Stefania Grillo
grillo@unina.it

Specialty section:

This article was submitted to
Plant Physiology,
a section of the journal
Frontiers in Plant Science

Received: 16 December 2015

Accepted: 10 March 2016

Published: 31 March 2016

Citation:

Iovieno P, Punzo P, Guida G, Mistretta C, Van Oosten MJ, Nurcato R, Bostan H, Colantuono C, Costa A, Bagnaresi P, Chiusano ML, Albrizio R, Giorio P, Batelli G and Grillo S (2016) Transcriptomic Changes Drive Physiological Responses to Progressive Drought Stress and Rehydration in Tomato. *Front. Plant Sci.* 7:371.
doi: 10.3389/fpls.2016.00371

Tomato is a major crop in the Mediterranean basin, where the cultivation in the open field is often vulnerable to drought. In order to adapt and survive to naturally occurring cycles of drought stress and recovery, plants employ a coordinated array of physiological, biochemical, and molecular responses. Transcriptomic studies on tomato responses to drought and subsequent recovery are few in number. As the search for novel traits to improve the genetic tolerance to drought increases, a better understanding of these responses is required. To address this need we designed a study in which we induced two cycles of prolonged drought stress and a single recovery by rewetting in tomato. In order to dissect the complexity of plant responses to drought, we analyzed the physiological responses (stomatal conductance, CO₂ assimilation, and chlorophyll fluorescence), abscisic acid (ABA), and proline contents. In addition to the physiological and metabolite assays, we generated transcriptomes for multiple points during the stress and recovery cycles. Cluster analysis of differentially expressed genes (DEGs) between the conditions has revealed potential novel components in stress response. The observed reduction in leaf gas exchanges and efficiency of the photosystem PSII was concomitant with a general down-regulation of genes belonging to the photosynthesis, light harvesting, and photosystem I and II category induced by drought stress. Gene ontology (GO) categories such as cell proliferation and cell cycle were also significantly enriched in the down-regulated fraction of genes upon drought stress, which may contribute to explain the observed growth reduction. Several histone variants were also repressed during drought stress, indicating that chromatin associated processes are also affected by drought. As expected, ABA accumulated after prolonged water deficit, driving the observed enrichment of stress related GOs in the up-regulated gene fractions, which included transcripts putatively involved in stomatal movements. This transcriptomic study has yielded promising candidate genes that merit further functional studies to confirm

their involvement in drought tolerance and recovery. Together, our results contribute to a better understanding of the coordinated responses taking place under drought stress and recovery in adult plants of tomato.

Keywords: ABA, gene-expression cluster analysis, photosynthesis, proline, RNA sequencing, stomatal conductance, water stress

INTRODUCTION

Drought conditions historically constitute the abiotic stress with the biggest impact on crop yield and agricultural productivity (Boyer, 1982; Boyer et al., 2013). Predicted climate change threatens stable crop yields, will likely require changes in agricultural practices in response to altered rainfall patterns, and increased urban consumption. Multiple projections indicate that between 20 and 60 Mha of irrigated cropland may have to be reverted to rainfed management by the end of the century (Elliott et al., 2014). Formerly irrigated crops would become entirely dependent on rainfall and vulnerable to yield loss due to drought. This reduction is predicted to be severe in southern Spain and Italy, two major producers of tomatoes (Saadi et al., 2015). This increasing vulnerability to drought requires that we develop more resilient varieties capable of surviving drought conditions while maintaining yield (Mickelbart et al., 2015). Both traditional breeding and targeted genome editing for drought tolerance require a better understanding of drought responses mechanisms (Langridge and Reynolds, 2015), which include molecular mechanisms governing the timing of stomata closure, modulation of photosynthetic performances, accumulation of osmolytes, and growth retardation (Bosco De Oliveira et al., 2012). Stomata represent the first barrier plants employ to avoid dehydration, with the trade-off of a reduced CO₂ supply to the mesophyll. As water deficit intensifies, metabolic impairments impose further limitations to photosynthesis (Chaves et al., 2009). Along with plant responses to water deficit, understanding the recovery of photosynthesis upon rehydration is of paramount importance to understand water stress effects on photosynthesis (Flexas et al., 2004).

Impact of drought on gene expression has been intensely analyzed in numerous species such as *Arabidopsis* (Sakuraba et al., 2015), rice (Oono et al., 2014), maize (Kakumanu et al., 2012), sorghum (Dugas et al., 2011), and poplar (Barghini et al., 2015) by high-throughput transcriptomics.

A predominant role in driving drought-induced changes in gene expression is played by the hormone abscisic acid (ABA). The mechanisms of ABA perception and signal transduction are the subject of intense research and major breakthroughs have included the identification of a family of cellular receptors (Ma et al., 2009; Park et al., 2009). An increase in ABA changes the hydraulic regulation of stomata (Chaves et al., 2009), resulting in stomata closure under adverse hydraulic conditions by controlling guard cells behavior and decreasing water permeability within the leaf vascular tissue (Pantin et al., 2013). Tomato (*Solanum lycopersicum* L.) is one of the major horticultural crops and an important dietary source of vitamins A and C as well as carotenoids such as lycopene (Canene-Adams et al., 2005). Tomato is also considered a plant model

system for fleshy fruit development (Osorio et al., 2011) and interaction with pathogens (Andolfo and Ercolano, 2015), with several tools available, including the sequenced genome (Sato et al., 2012) and its large open source genomic repository (Suresh et al., 2014). Although tomato is cultivated worldwide, it is considered sensitive to stresses of biotic and abiotic nature (Rai et al., 2013; Kissoudis et al., 2015). Most modern tomato cultivars are sensitive to water deficit, which results in reduced seed development and germination, reduced vegetative growth, and impaired reproduction (Nuruddin et al., 2003; Bartels and Sunkar, 2005; Rai et al., 2013). Galmés et al. (2011) reported that Mediterranean drought-tolerant tomato showed higher intrinsic water use efficiency under water stress compared to a tomato accession originating from a humid habitat. Such results could be due to stress induced changes in anatomical development (Galmés et al., 2013) or the abundance and activity of aquaporins facilitating CO₂ transport through the mesophyll (Kaldenhoff, 2012).

The average water footprint per Kg of tomato is 215 liters, 30% of which is supplied by irrigation (Mekonnen and Hoekstra, 2011). Therefore, it is essential to develop drought tolerant, higher yielding varieties to cope with the increasing demand for tomato (Solankey et al., 2014). Only limited mapping research has been conducted on drought tolerance compared to other abiotic stresses in tomato (Foolad, 2007). Wild relatives, such as the drought tolerant *Solanum pennellii*, represent a valuable source of novel traits for genetic improvement. Gene expression studies in response to water stress have been carried out in leaves using microarray approaches identifying differentially expressed transcripts of genes involved in energy, plant hormones biosynthesis, and cation transporters and a number of transcription factors and signaling proteins (Gong et al., 2010; Sadder et al., 2014). However, studies that integrate the different levels of response to drought stress in tomato are under-represented.

The goal of our research was to identify in tomato the transcriptomic changes that control physiological adjustments under drought stress and recovery. In this study, we subjected plants to two drought treatments separated by a rehydration and recovery phase. We performed RNA sequencing on each of these stages to establish transcriptomes for drought and recovery. Each transcriptomic set is accompanied by physiological measurements (chlorophyll fluorescence, CO₂ assimilation, and stomatal conductance), quantification of key metabolites (proline and ABA), and biometric parameters. These measurements serve to define the conditions of drought and recovery and provide a snapshot of the physiological state in each condition. We performed genome-wide comparisons of transcriptomes using cluster analysis to identify stress-induced patterns of expression and integrated them with physiological responses.

MATERIALS AND METHODS

Plant Materials, Growth Conditions, and Stress Treatments

Seeds of cultivar M82 (accession LA3475) supplied by the Tomato Genetics Resource Center (TGRC, <http://tgrc.ucdavis.edu/>) were germinated in soil in a semi-controlled greenhouse. Air temperature (T_a , °C), humidity (RH, %), and solar radiation (R_s , W m⁻²) were acquired by a data logger (Spectrum Technologies, Plainfield, IL). The average air humidity and temperature were 58% and 22°C during the day and 86% and 18°C during night-time, while the cumulated daily global radiation during the day was 8.4 (±3.6) MJ/m² day.

When seedlings had developed two true leaves (25 days after sowing seeds), they were transplanted in pots, filled with soil (one plant per pot) and fertilized after 7 days with Nitrophoska gold (Compo Agricoltura, Cesano Maderno, Italy). Plants were well irrigated for 30 days prior to start the stress treatments. Then plants were equally divided into control and stress treatment, nine replicates per treatment, and arranged in a randomized block design.

Two cycles of water deficit were performed by water withholding until soil water content of stress pots was <1/3 of control pots, inducing a nearly complete closure of the stomata. This corresponded to 16 and 6 days of water withholding in the first and second cycle of drought, respectively. Between these two stress cycles, plants were well irrigated allowing a full recovery of soil water content and stomatal conductance. Control plants were well watered throughout the entire experimental period.

During the experiment, the soil water content (θ , m³/m³) was determined from dielectric measurements performed by a Time Domain Reflectometer (TDR100 Campbell Scientific Inc. Logan, UT) and applying the Topp's equation. The 14.2 cm trifilar probes were placed in 3 pots per treatment.

Leaf samples for molecular and biochemical analyses were collected at different time point of the experiment.

Gas Exchange and Modulated Chl a Fluorescence Emission

Net photosynthetic CO₂ assimilation rate (A, μmol m⁻² s⁻¹) and stomatal conductance to water vapor (g_s, mol m⁻² s⁻¹) were measured on a fully expanded, well-exposed top leaf on 5–6 plants per treatment between 10:00 a.m. and 1:00 p.m. Measurements were carried out using a portable open-system gas-exchange and modulated fluorometer analyser Li-6400XT (Li-Cor Biosciences, Lincoln, NE, USA), with CO₂ inside leaf chamber set to 400 μmol CO₂ mol⁻¹ air. An artificial light source LED with emission peaks centered at 635 nm in the red and at 465 nm in the blue provided a PPFD equal to 2000 μmol (photons) m⁻² s⁻¹ (90% red, 10% blue). The instrument was also used to measure the steady-state (F') and, upon a 0.8 s saturating light pulse emission, the maximum (F'_m) Chl a fluorescence emission of leaves under actinic light. The software of the instrument (Li-Cor, 2011) calculated the gas-exchange parameters on the basis of von Caemmerer and Farquhar (1981) model, and the effective quantum yield of PSII photochemistry in light-adapted leaves, Φ_{PSII} = (F'_m - F')/F'_m according to Genty et al. (1989).

Transient Chl a Fluorescence Emission

For fluorescence assays a continuous excitation Handy PEA fluorometer (Hansatech, Instruments Ltd., King's Lynn, Norfolk, England) was used. The excitation red light pulse for fluorescence induction (FI) was emitted by a (red) 650 nm light diode source, and applied for 1 s at the maximal available (sub-saturating) photosynthetic photon flux density (PPFD) of 3500 μmol (photon)/m² s. Leaves were dark adapted for 30 min by means of the equipped white leaf-clips, prior to the assessment of the basal fluorescence emission (F₀), and the peak fluorescence emission (F_p) reached during the fast polyphasic raise induced by the sub-saturating excitation light pulse. As F_p is a viable approximation of the maximum fluorescence emission (F_m) (Strasser et al., 2000; Giorio et al., 2011), the dark-adapted maximum quantum yield of PSII photochemistry was calculated by the instrument software as F_v/F_m = (F_m - F₀)/F_m according to Kitajima and Butler (1975).

Biomass Determinations

Plant leaf area (PLA, m²) was measured, at the end of the experiment, on excised leaves using a scanning planimeter (Li-3100, LiCor, Lincoln, NE, U.S.A.). The instrument is equipped with a fluorescent source and a solid state scanning camera to measure the area of leaves as they move through it. For dry weight measurements, leaves and stems were oven-dried at 70°C for 10 days until a stable weight was reached. Both leaf area and total dry weight were measured on three plants.

Isolation of RNA, cDNA Synthesis, and qRT-PCR

Total RNA was extracted from leaf tissues using 1 mL of TRIZOL Reagent (Life Technologies, Carlsbad, CA, USA) per 100 mg of pulverized tissue. The homogenized samples were incubated for 5 min at room temperature and 200 μL of chloroform was added per milliliter of TRIZOL reagent. After centrifugation at 12,000 g for 15 min at 4°C, the upper aqueous phase was removed and 500 μL of 100% isopropanol was added. The samples were incubated at room temperature for 10 min and centrifuged at 12,000 g for 10 min at 4°C. The supernatant was removed and the RNA pellet was washed with 1 mL of 75% ethanol and centrifuged at 7500 g for 5 min at 4°C. The pellet was air dried and dissolved in RNase-free water. RNA quantity was measured spectrophotometrically by NanoDrop ND-1000 Spectrophotometer (NanoDropTechnologies), and integrity was verified on a denaturing MOPS/formaldehyde gel. One microgram of DNase-treated total RNA was reverse transcribed using SuperScript II Reverse TranscriptaseTM and oligo (dT₂₀) (Life Technologies, Carlsbad, CA, USA) by incubation at 42°C for 50 min. The reaction was stopped by heat inactivation at 70°C. The complementary DNA was diluted 1:20 and 4.5 μL was used for each qRT-PCR reaction, performed with 6.25 μL of 1X Platinum SYBR Green qPCR SuperMix (Life Technologies, Carlsbad, CA, USA) and 1.75 μL of primer mix (4.28 μM). Primers used are listed in Supplementary Table S1. Preparation of reactions was automated using the Liquid Handler Robot Tecan Freedom Evo and ABI 7900 HT (Applied Biosystems, Foster City, CA, USA) and performed with ABI

7900 HT (Applied Biosystems, Foster City, CA, USA). Cycling conditions were 10 min at 95°C, followed by 40 cycles of 95°C for 15 s and 60°C for 1 min. Three biological replicates with three technical repetitions were tested. Quantification of gene expression was carried out using the $2^{-\Delta\Delta Ct}$ method (Livak and Schmittgen, 2001). Elongation Factor EF1- α was used as an endogenous reference gene (Nicot et al., 2005; Corrado et al., 2007) for the normalization of the expression levels of the target genes. RNA extracted from plants grown in control condition served as calibrator sample for relative quantification of gene expression.

Proline and ABA Content Measurements

Leaf samples were collected by excising the leaf at the petiole from three biological replicates. Two technical replicates were performed for each sample. Proline content was determined according to the method of Claussen (2005). Two hundred and fifty milligrams of finely ground leaf tissue were suspended in 1.5 mL of 3% sulfosalicylic acid and filtered through a layer of glass-fiber filter (Macherey-Nagel, Ø 55 mm, Germany). One milliliter of Glacial acetic acid and 1 mL ninhydrin reagent (2.5 g ninhydrin/100 mL of a 6:3:1 solution of glacial acetic acid, distilled water and 85% ortho-phosphoric acid, respectively) were added to 1 mL of the clear filtrate. The mixture was incubated for 1 h in a boiling water bath. The reaction was terminated at room temperature for 5 min. Readings were taken immediately at a wavelength of 546 nm. The proline concentration was determined by comparison with a standard curve.

For ABA measurements, 150 mg of fine powder were extracted in distilled, autoclaved water with constant shaking at 4°C overnight in the dark. The supernatant was collected after centrifugation (10,000 × g for 10 min) and diluted 50-fold with TBS buffer (50 mM TRIS, 1 mM MgCl₂, 150 mM NaCl, pH 7.8). Subsequently, ABA was analyzed by indirect enzyme-linked assay (ELISA) using the Phytodetek ABA test kit (Agdia, Elkhart, IN, USA) following the manufacturer's instructions. Color absorbance following reaction with substrate was read at 405 nm using a plate autoreader (1420 Multilabel Counter Victor³TM, PerkinElmer).

Statistical Analyses

The statistical significance of soil water content, gas-exchange and fluorescence parameters, ABA and proline contents between water treatments was evaluated through Student's *t*-test.

RNA Library Preparation and Library Sequencing

RNA pools of three biological replicates were used for all RNA-Seq experiments. The total RNA was DNase treated and purified using the RNeasy Plant Mini kit (Qiagen) following manufacturer's protocol (Qiagen, Valencia, CA, USA). RNA samples were analyzed quantitatively and qualitatively by NanoDrop ND-1000 Spectrophotometer (NanoDropTechnologies) and by Bioanalyzer (Agilent Technologies, Santa Clara, CA, USA).

cDNA libraries were prepared with 1 µg of starting total RNA and using the Illumina TruSeq RNA Sample Preparation Kit (Illumina, San Diego, CA), according to TruSeq protocol. Library size and integrity were determined using the Agilent Bioanalyzer 2100 (Santa Clara, CA). Each library was diluted to 2 nM and denatured. Eight pM of each library was loaded onto cBot (Illumina, San Diego CA) for cluster generation with cBot Paired End Cluster Generation Kit (Illumina, San Diego, CA) and sequenced using the Illumina HiSeq 1500 with 100 bp paired-end reads in triplicate obtaining ~14 million reads for replicate. The sequencing service was provided Genomix4life Ltd (<http://www.genomix4life.com>) at laboratory of Molecular Medicine and Genomics (University of Salerno, Italy).

RNA Sequencing Analysis

The cleaning of the raw sequences from the RNA sequencing data was made using the Trim Galore package (http://www.bioinformatics.babraham.ac.uk/projects/trim_galore/). In the first step, low-quality bases were trimmed from the 3' end of the reads. In the second step, Cutadapt (Martin, 2011) removed adapter sequences; the default settings for paired-end was used. The quality check of the remaining sequences was performed using FastQC (<http://www.bioinformatics.babraham.ac.uk/projects/fastqc/>). The (1) cleaned pairs, and (2) the high quality single reads obtained after the cleaning step, were used as input for the mapping to the tomato genome (version 2.40), independently. Bowtie version 2.1.0 (Langmead and Salzberg, 2012) and Tophat version 2.0.8 (Kim et al., 2013) were used for mapping. Paired and single reads, uniquely mapped, were counted, independently, per gene available from the iTAG annotation, version 2.3, using the HTSeq-count (<http://www-huber.embl.de/users/anders/HTSeq/>) version 0.5.4p1, in "union" default mode setting.

In order to define the set of expressed genes, raw read counts were normalized to RPKM (Reads per Kilobase per Million) and genes above the 1 RPKM cut-off were kept for the subsequent analyses. Differential expressed genes (DEGs) were found performing the negative binomial test implemented in the DESeq package (Anders and Huber, 2010) version 1.10.1, at a false discovery rate threshold (FDR) 0.01.

The k-means (MacQueen, 1967) cluster analyses were then performed on the log₂ of the gene expression level (size factor normalized implemented in DESeq Package (Anders and Huber, 2010) for DEGs detected in all the stages, using 20 cluster, a number defined by the Elbow method (Thorndike, 1953), i.e., minimizing the within group variance at different cut-offs. GO enrichments were estimated via the goseq Bioconductor package (Young et al., 2010) (FDR ≤ 0.05) on each detected cluster possessing similar expression profiles in all the stages. As goseq requires gene length data, median transcript length per gene was obtained by parsing with a custom R script cDNA fasta files, as obtained from Ensembl Plants repository. GO annotations for tomato genes were obtained via BLAST2GO (Conesa and Götz, 2008) against NR databases and default settings. Unless otherwise stated, further graphical outputs were obtained with R custom scripts.

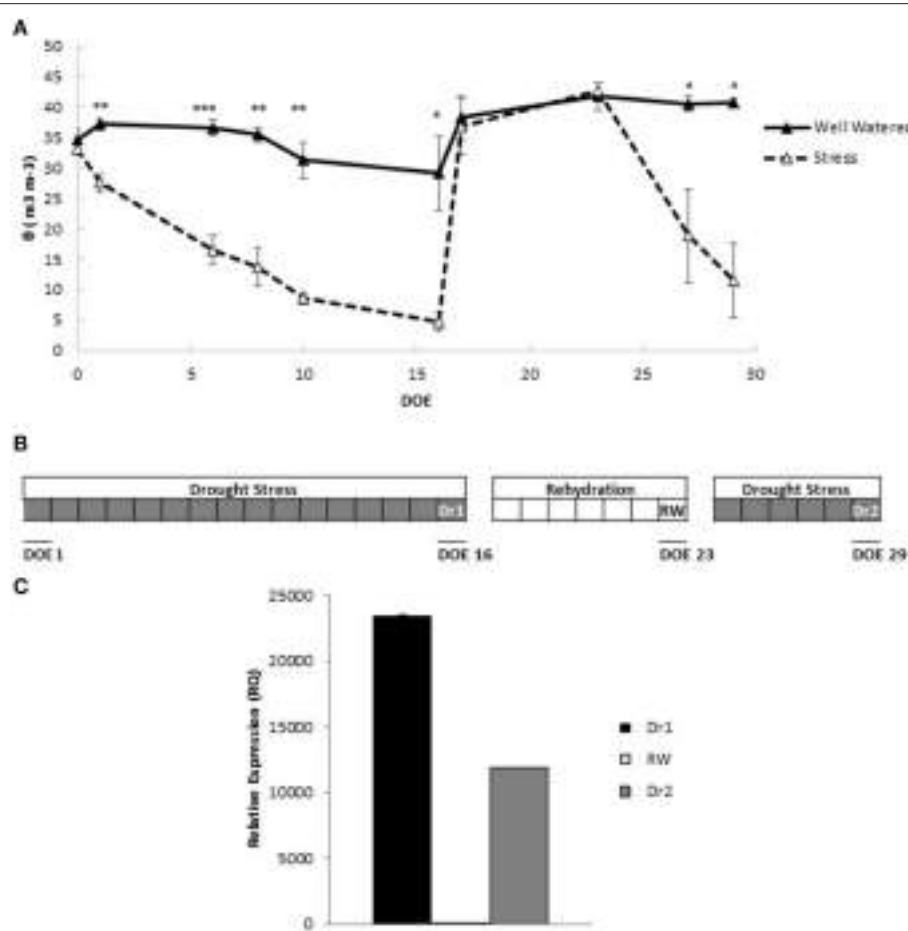


FIGURE 1 | Experimental outline. (A) Volumetric soil water content (θ) throughout the progression of the experiment. Values represent average measurements \pm SD of three replicates. Asterisks denote significant differences according to Student's *t*-test between well-watered and stressed pots. *, **, and *** indicate significantly different values in drought stress compared to well-watered pots at $p \leq 0.05$, $p \leq 0.01$, and $p \leq 0.001$, respectively. **(B)** Schematic representation of the experimental design highlighting the points Dr1 (16 d of irrigation withholding), RW (7 days of irrigation), and Dr2 (6 days of irrigation withhold). **(C)** Gene expression of *Solyc03g116390.2.1* in leaves after two cycles of drought stress (Dr1 and Dr2) and 1 week of rewatering (RW). RNA samples extracted from leaves of well-watered plants were used as controls. Gene expression analyses were conducted by qRT-PCR. DOE, days of experiment.

RESULTS

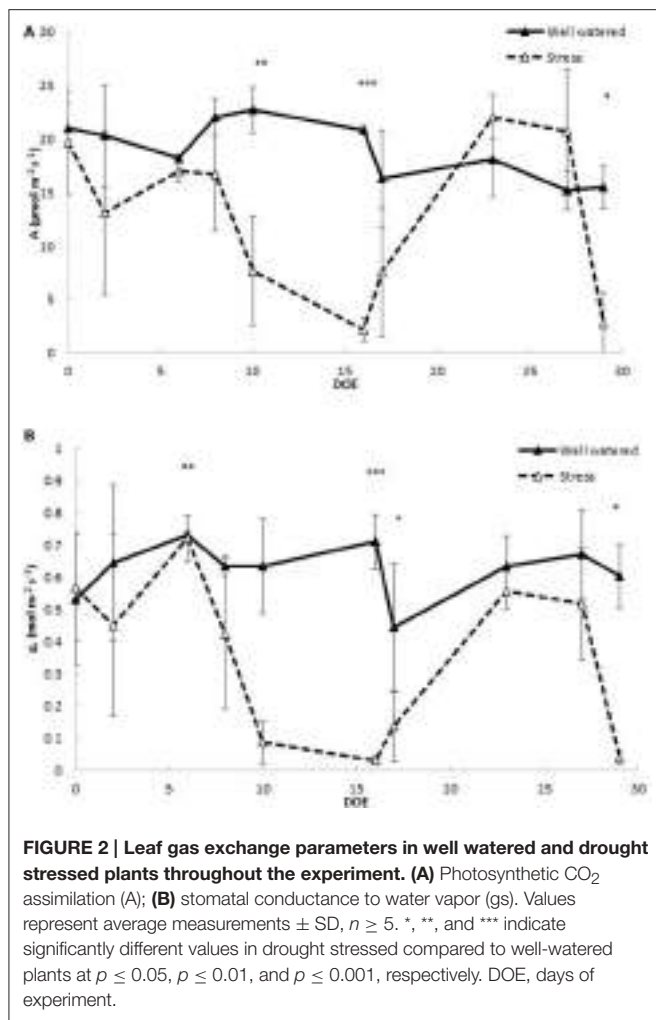
To gain a comprehensive understanding of mechanisms activated by dehydration and rehydration events, we subjected tomato plants to cycles of drought stress and rewatering. Soil water status was monitored throughout the experiment as a measure of the progression of drought stress, and recovery under rewatering. **Figure 1A** shows values of pots containing plants of the M82 genotype. When water was withheld, pots subjected to drought stress underwent a continuous decline in soil water content (θ), which was significantly lower compared to control pots starting 2 days from the beginning of water withholding (**Figure 1A**). Drought continued until θ was $\sim 22\%$ of the control pots. This was the maximum stress point (Dr1) for the 1st cycle of drought. Reinstatement of irrigation allowed an immediate full recovery of θ to control values, which were maintained until the end of rewatering (RW). A rapid decline in θ (**Figure 1A**) was observed when a second cycle of drought stress was imposed and

values similar to those of Dr1 were measured 6 days after the beginning of drought treatment (identified as Dr2). A graphic representation of the progression of the experiment is depicted in **Figure 1B**.

For a preliminary evaluation of the efficacy of the drought stress and rehydration cycles at the cellular level, gene expression of *Solyc03g116390.2.1*, encoding a late embryogenesis abundant protein previously shown to be inducible by drought stress (Gong et al., 2010), was measured at Dr1, RW and Dr2. As shown in **Figure 1C**, a fold increase in gene expression of at least 10,000 times was observed at Dr1 and Dr2 compared to unstressed control plants. At RW, expression levels in rehydrated plants were comparable to controls, indicating that a full recovery had occurred (**Figure 1C**).

Physiological Effects of Drought Stress

To assess the impact of drought stress and rehydration on the physiology of tomato, leaf gas exchange and photosystem



PSII efficiency were measured (Figure 2). Net CO_2 assimilation rate (Figure 2A) and stomatal conductance to water vapor (Figure 2B) decreased significantly in stressed plants after 10 days of withholding water. At Dr1 CO_2 assimilation (A) decreased to a minimum of $2.2 \mu\text{mol m}^{-2} \text{s}^{-1}$ in the stressed plants, 10% of the CO_2 assimilation rate measured in controls (Figure 2A). Similar patterns were observed for stomatal conductance (g_s), which in the stressed plants at Dr1 was as low as 0.030 , compared to $0.710 \text{ mol m}^{-2} \text{s}^{-1}$ found in the fully watered plants (Figure 2B). A moderate recovery of both A and g_s was observed 1 day after rewatering when soil water content was fully restored (Figure 1A). Both parameters rose to values comparable to those of the controls at RW. Under the second treatment CO_2 assimilation and stomatal conductance decreased more rapidly as compared to the previous stress cycle, reaching minimum average values of $4.0 \mu\text{mol m}^{-2} \text{s}^{-1}$ for A and $0.070 \text{ mol m}^{-2} \text{s}^{-1}$ for g_s at Dr2 (Figures 2A,B).

The effective quantum yield of PSII (ϕ_{PSII}) decreased in response to the first drought treatment from an average of 0.13 in the control plants to 0.10 in the stressed plants (Figure 3A). Upon rewatering these values recovered to levels similar to

controls. These values experienced even steeper declines during the 6 days of the second drought treatment (Figure 3A). The maximal quantum yield of the Photosystem II (PSII), measured in dark-adapted leaves, (F_v/F_m) remained stable throughout the experiment in the range of 0.81–0.83 in the control treatments while the values at Dr1 were lower, about 0.77 for F_v/F_m . Stressed plants partially recovered after 1 day of rewatering and completely recovered by RW (Figure 3B). Water stress reduced plant leaf area by 31% and dry matter accumulation by an average of 40% (Figures 4A,B).

Proline and ABA Content in Drought Stressed Tomato

Well known metabolic alterations induced by drought stress include leaf accumulation of the osmolyte proline (Claussen, 2005) and the hormone ABA (Sharp and LeNoble, 2002). We therefore measured proline and ABA content at several time points in our experiment by a spectrophotometer and ELISA assay, respectively (Figure 5). After 13 days of drought stress, there was a slight accumulation of proline in the stressed plants. Under more severe stress conditions (Dr1) the amount of proline in the stressed plants was about 10 fold higher than the control M82. Proline amount in the stressed plants decreased in response to rewatering. However, values were still higher than controls for both genotypes at RW. The accumulation of proline reached the highest observed values of 4.5 at Dr2 (Figure 5A).

Ten days of drought stress was not sufficient to elicit accumulation of leaf ABA as compared to the controls (Figure 5A). As the stress became more severe leaf ABA content was as high as 15,367 picomols/g fresh weight at Dr1. After rewatering, ABA levels decreased to values lower than those measured in the control plants at day 10 of experiment. At the end of second drought cycle (6 days of stress, Dr2), ABA content was 10 fold higher than that measured at RW, and about twice the 10-day stress values of first drought period (Figure 5B).

To investigate the correlation between proline and ABA accumulation and transcription of related biosynthetic genes we measured the gene expression of two rate-limiting steps in their biosynthetic processes. Expression of *Solyc08g043170.2.1* and *Solyc07g056570.1.1* encoding a Pyrroline-5-carboxylate synthetase (P5CS) and a 9-cis-epoxycarotenoid dioxygenase (NCED) respectively was evaluated by qPCR. In Dr1, P5CS was induced, while in RW and Dr2 no significant up-regulation was observed (Figure 5C). NCED was induced at comparable levels at Dr1 and Dr2, while at RW expression levels were similar to the controls (Figure 5D).

Transcriptomic Perturbations in Response to Drought Stress and Rehydration

To identify genes whose expression were altered by drought stress and rewatering in leaves, which could result in the observed physiological alterations, we carried out transcriptome sequencing. We used the Illumina platform on RNA samples extracted from leaves of M82 well-watered plants (WW) as well as in Dr1, RW, and Dr2 (Supplementary Table S2). RNA sequencing derived data were then subjected to gene expression

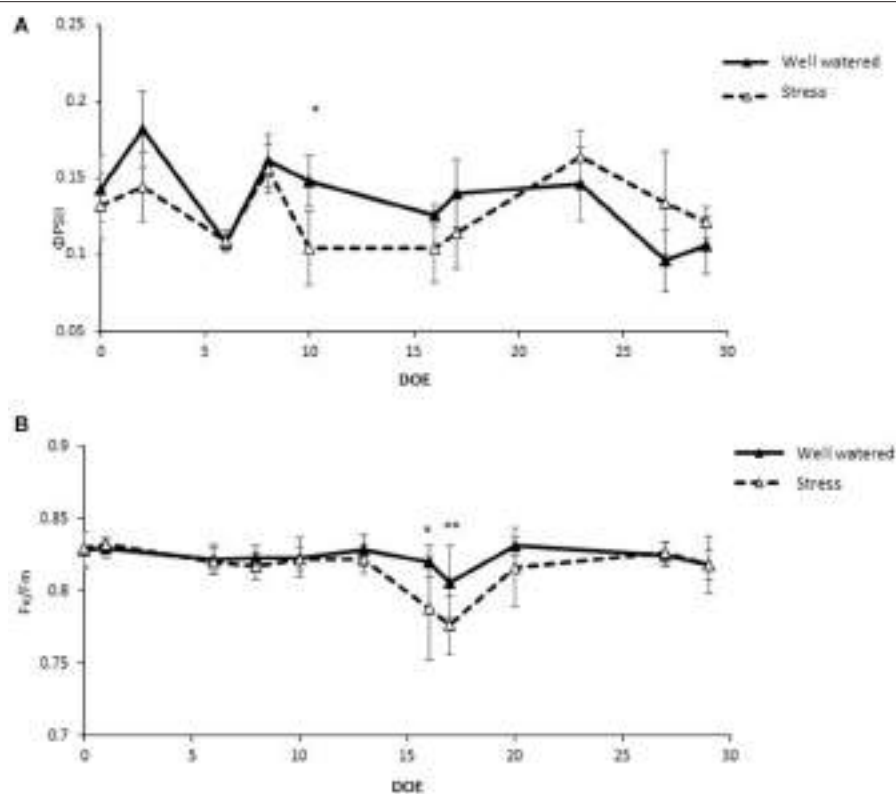


FIGURE 3 | Chlorophyll fluorescence parameters in well watered and drought stressed plants throughout the experiment. **(A)** Quantum yield of PSII (Φ_{PSII}); **(B)** Maximum quantum yield of PSII (Fv/Fm). Values represent average measurements \pm SD, $n \geq 5$. * and ** indicate significantly different values in drought stress compared to well-watered plants at $p \leq 0.05$ and $p \leq 0.01$, respectively. DOE, days of experiment.

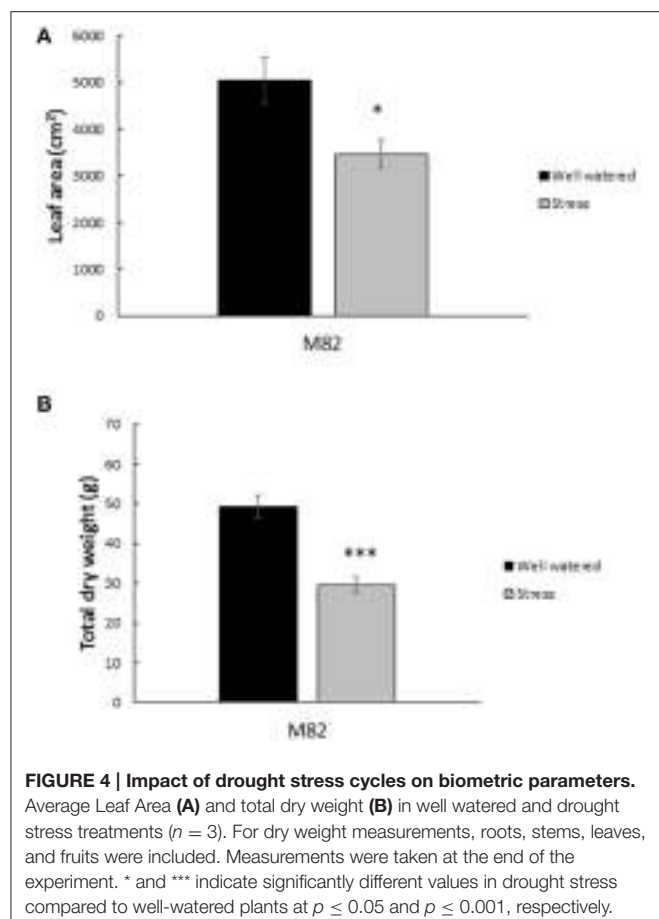
analyses followed by clustering of genes showing similar trends of expression by comparison of the four conditions, and by gene ontology (GO) enrichment analysis. By comparing the different treatments, we identified 966 genes that showed differential expression in at least one of the comparisons, which were therefore considered as Differentially Expressed Genes (DEGs) (Supplementary Table S3).

The analysis highlighted that a large number of DEGs were down-regulated during drought stress. Comparative analysis of drought stressed (Dr1 and Dr2) vs. watered plants (WW and RW) revealed 119 DEGs common to all 4 comparisons (Supplementary Table S4). These included several histone encoding genes (e.g., *Solyc10g008910*), cell wall modifying enzymes (e.g., *Solyc04g082140*) as well as heat shock proteins (e.g., *Solyc11g020330*) (Supplementary Table S4).

In order to classify transcripts based on their behavior in WW, Dr1, RW, and Dr2, a cluster analysis was performed on the DEGs using normalized expression values of the DEGs in each of the experimental conditions. Twenty clusters were identified which grouped transcripts with similar expression trends (Supplementary Table S5). RNA sequencing results and the cluster analysis were validated using qRT-PCR on genes selected from different clusters (Supplementary Table S6, Figure 6). Figures 6A,B show normalized expression values from RNA sequencing and qRT-PCR experiments, respectively. As

shown in Figure 6C, a good correlation was observed between the two sets of results. Seven clusters of DEGs were selected for further investigation based on their similar expression patterns (Supplementary Table S5, Figures 7A,B). Among them, clusters 1, 2, 14, 17, and 18 included genes with a higher expression level in WW and RW, while the remaining two clusters 7 and 20 were composed of transcripts with higher expression in Dr1 and Dr2 stressed plants (Figure 7A). Interestingly, clusters containing genes repressed during drought contained several histone variants and chlorophyll binding proteins. Several heat shock proteins and a heat shock factor also appeared to be induced by drought (Table 1). GO enrichment analyses were performed on clusters 1, 2, 14, 17, and 18 and clusters 7 and 20 independently (Figure 7B, Supplementary Tables S7, S8). These analyses showed that genes related to photosynthetic light harvesting (such as Chlorophyll a/b binding protein, *Solyc08g067320*) and to modification of cell wall (i.e., Pectinesterase, *Solyc09g075350*) were down-regulated in Dr1 and Dr2. Several genes encoding sucrose and starch metabolic processes were also down-regulated (Supplementary Table S6).

GO categories enriched in clusters 7 and 20, instead, were more specifically related to stress, including classes such as response to water stimulus (members included dehydrin, *Solyc01g109920.2*) and water deprivation (including genes such as 2 NAC domain encoding

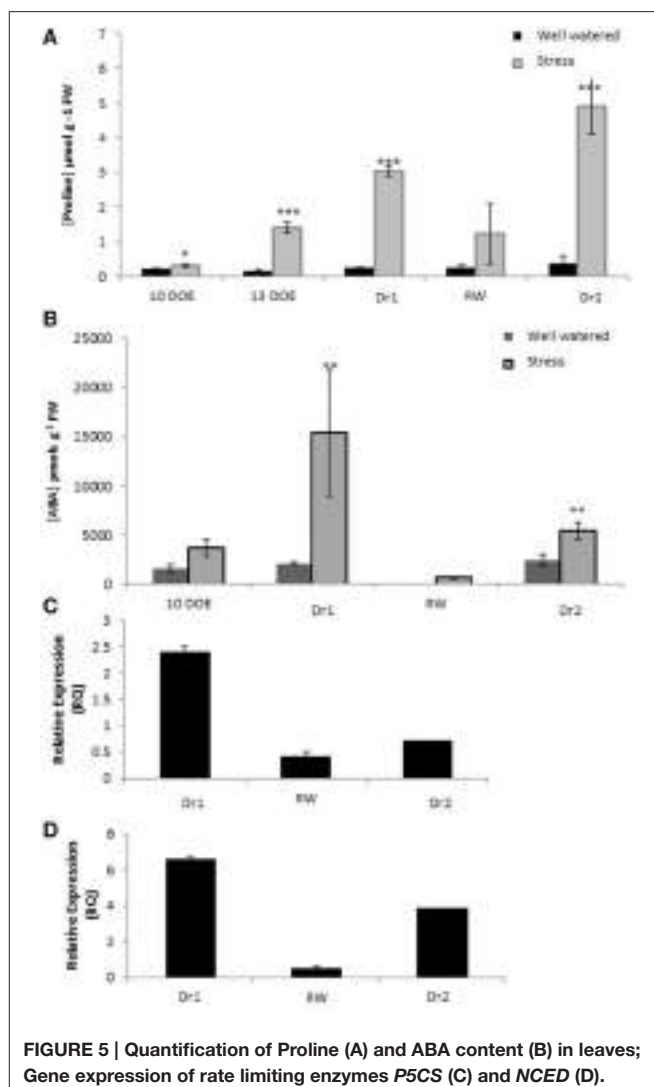
**FIGURE 4 | Impact of drought stress cycles on biometric parameters.**

Average Leaf Area (A) and total dry weight (B) in well watered and drought stress treatments ($n = 3$). For dry weight measurements, roots, stems, leaves, and fruits were included. Measurements were taken at the end of the experiment. * and *** indicate significantly different values in drought stress compared to well-watered plants at $p \leq 0.05$ and $p \leq 0.001$, respectively.

IPR003441- *Solyc12g013620.1/Solyc07g063410.2* (Figure 7, Supplementary Table S8). Transcripts coding for proteins involved in protein folding (Peptidyl-prolyl cis-trans isomerase *Solyc09g092690.2* and heat shock protein *Solyc03g117630.1*) were also induced by water stress.

DISCUSSION

In the present study, we have provided a detailed picture of physiological, metabolic and molecular adjustments employed by adult plants of tomato when exposed to events of prolonged water stress. The progression of stress was assessed by detailed monitoring of soil water content and stomatal conductance (g_s). Leaf water status was strongly impaired by drought stress, as indicated by the very low values of g_s observed at Dr1 and Dr2 (Figure 2B). Lutfor Rahman et al. (1999) found in four tomato genotypes that after ca. Ten days of interrupted irrigation, soil water content and g_s decreased to values quite similar to our data, and a leaf water potential ranging from -10 to -14 MPa, indicating severe water stress. On this basis, a condition of severe stress can be hypothesized when plants approached Dr1 or Dr2. As expected (Hsiao et al., 1976), both leaf area and dry weight of the entire plant were significantly reduced in response to water deficit (Figure 4). The reduction in photosynthetic rate also likely contributed to plant growth

**FIGURE 5 | Quantification of Proline (A) and ABA content (B) in leaves; Gene expression of rate limiting enzymes P5CS (C) and NCED (D).**

DOE, days of experiment. *, ** and *** indicate significantly different values in drought stressed compared to well-watered plants at $p \leq 0.05$, $p \leq 0.01$, and $p \leq 0.001$, respectively.

reduction (Figure 2; Chaves et al., 2002). We found that the CO_2 concentration inside the leaf (data not shown) was not affected during the first week of drought treatment, when soil water deficit (Figure 1) had no clear effect on both A and g_s (Figure 2). During subsequent days of stress, both stomatal conductance (Figure 2B) and intercellular $[\text{CO}_2]$ (data not shown) showed a decrease. This indicates the action of stomatal limitation to A, while concomitant non-stomatal limitations, especially during progression to Dr1 should not be ruled out (Tezara et al., 1999; Cifre et al., 2005). The efficiency of the electron transport in the photosystems also decreased as stress progressed (Figure 3). The low F_v/F_m ratio at Dr1 likely indicates that photoinactivation of PSII may have occurred (Baker, 2008). Therefore, we conclude that photochemical limitations contributed to the decline in CO_2 assimilation along with the altered metabolic content under severe drought (Cifre et al., 2005; Chaves et al., 2009).

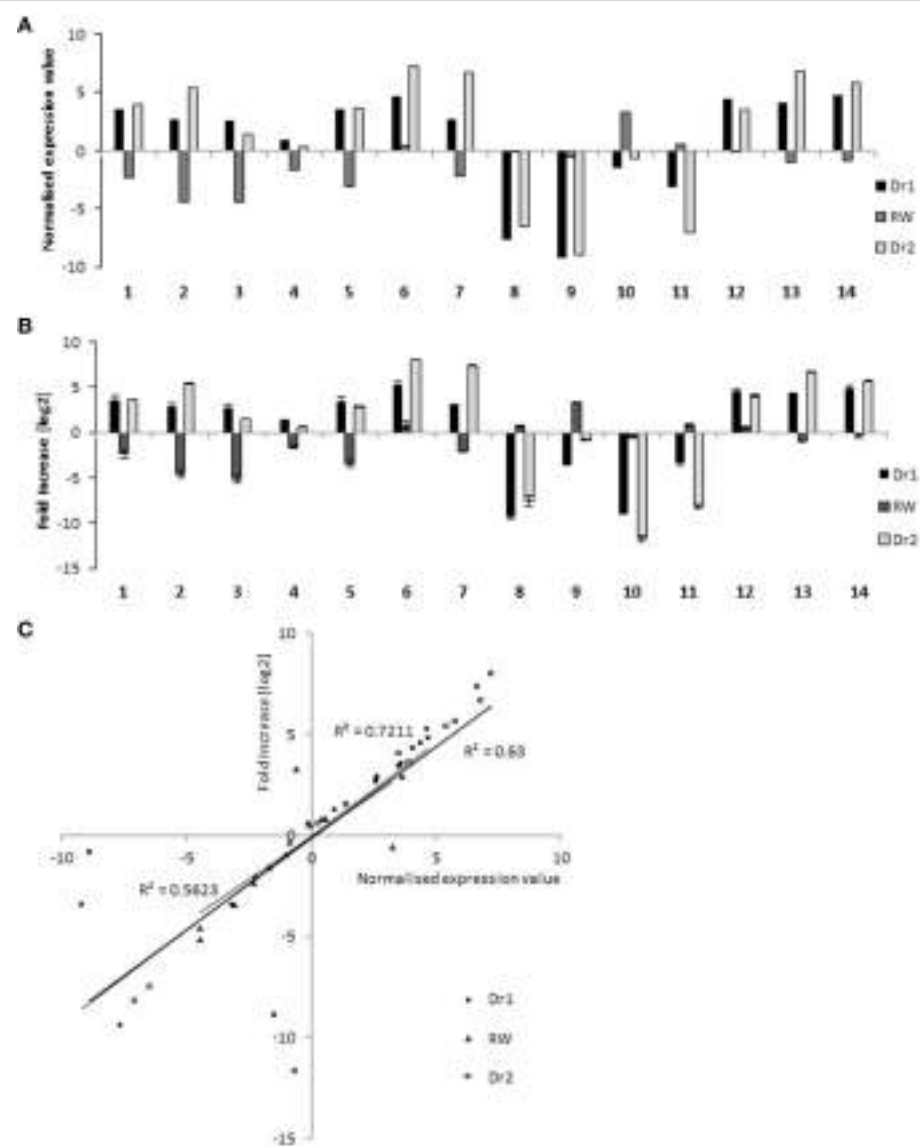


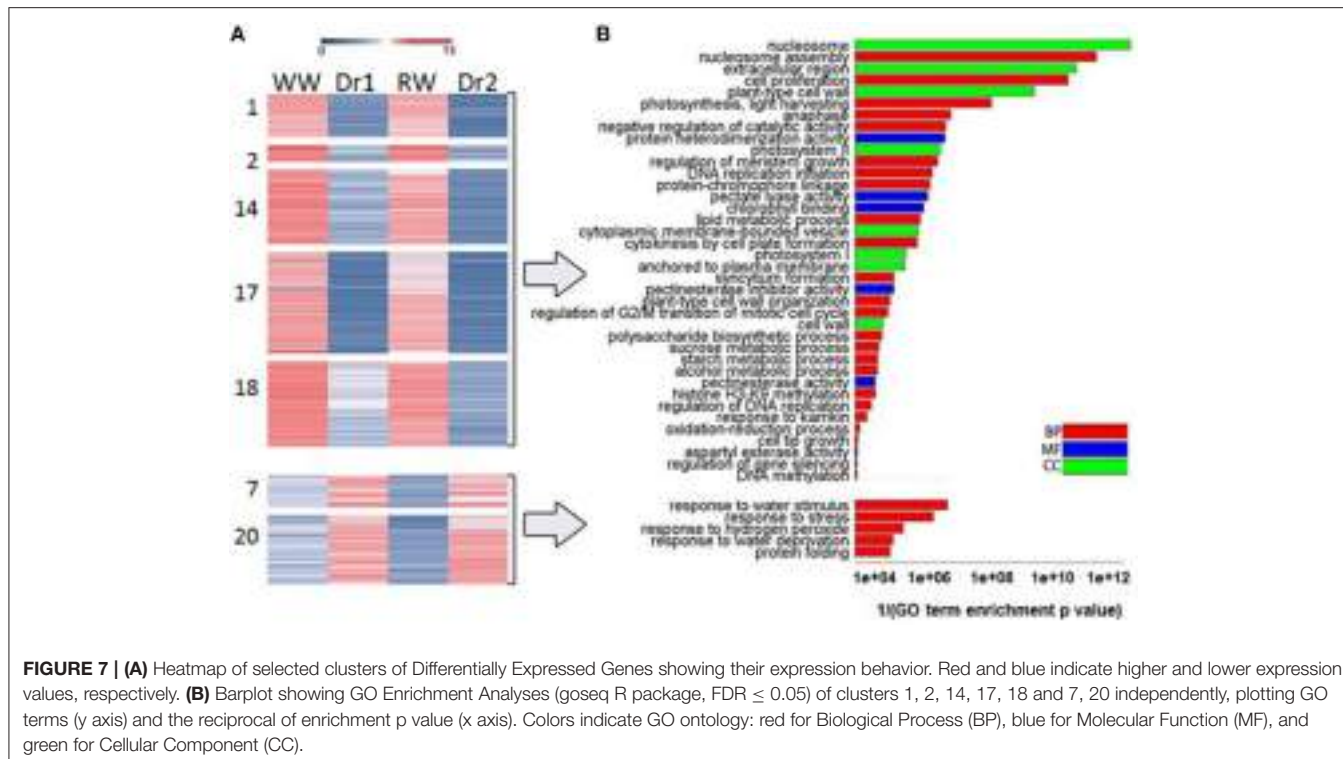
FIGURE 6 | qRT-PCR validation of RNA sequencing data on 14 selected genes (Supplementary Table S6). **(A)** Expression value detected by RNA-seq method. **(B)** Expression analysis conducted by qRT-PCR. Data have been plotted on a \log_2 scale. **(C)** Correlation between RNA-Sequencing and qRT-PCR data. The normalized expression value obtained with RNA sequencing (x axis) were compared to the \log_2 of fold increase by qRT-PCR (y axis). RNA from well-watered control plants was used as calibrator sample.

These inferences are consistent with the effects observed in response to rewatering. Upon rehydration, a prompt recovery of CO₂ assimilation in response to stomata reopening would indicate no significant impairment of the photosynthetic machinery (Cornic, 2000).

Chaves et al. (2009) reviewed that a recovery in CO₂ assimilation of about 50% within a day from rewatering indicates severe water stress and that a few more days are required to reestablish the photosynthetic machinery. Recently, a complete recovery of the photosynthetic rate 24 h after rewatering was observed when mild drought conditions were applied (Nilsen et al., 2014). The moderate recovery observed here in both A

and g_s after 1 day of soil rewatering is therefore an additional indication of severe drought stress conditions.

One of the goals of this study was to identify potential factors controlling growth under drought stress conditions. At the molecular level, several transcription factors were up-regulated during drought stress, which could also help to explain the observed drought-induced growth reduction, in addition to the induction of stress responses (Supplementary Table S5). We found that two isoforms of subunit A of Nuclear factor Y (NF-Y), encoding orthologs of Arabidopsis *NF-YA7* and *NF-YA10* were also induced by drought stress. NF-Y is a heterotrimetric transcription factor whose subunit A is



responsible for binding to DNA promoter sequences containing the CCAAT-box. Over-expression of NF-YAs, including NF-YA7 and NF-YA10, causes a dwarf phenotype and an increase in stress tolerance. Expression of NF-YA transcripts is stress-inducible and is inhibited in *Arabidopsis* in control conditions by miR169, a microRNA present in several isoforms (Li et al., 2008; Leyva-González et al., 2012). The changes in gene expression we observed in NF-Y isoforms likely play a role in growth retardation under the imposed drought conditions.

Our results also yielded other GO categories that contribute to growth and development. GO categories enriched in gene clusters down-regulated by drought stress included the cellular compartment “plant-type cell wall,” “cell wall” and the molecular function “pectate lyase activity” and “pectinesterase activity,” suggesting that cell wall modifying activities are repressed after prolonged drought stress. These categories included genes encoding cell wall modifying enzymes such as two laccase-22 (*Solyc02g065170.2*; *Solyc07g052240.2*), several pectinesterases and four expansins (*Solyc05g007830.2*, *Solyc06g005560.2*, *Solyc06g076220.2*, *Solyc07g054170.2*).

We observed that the tomato heat stress transcription factor *HsfA3* was also up-regulated in drought stress conditions. In *Arabidopsis* *HsfA3* is regulated by the dehydration-responsive element binding protein 2A (DREB2A). Plants overexpressing DREB2A are drought and heat tolerant and show increased levels of *HsfA3* (Yoshida et al., 2008). *HsfA3* is a powerful driver of heat shock protein expression and probably accounts for the observed up-regulation of several members of the Heat shock protein family, in several species including tomato (Table 1; Supplementary Table S5; Schramm et al., 2008; Li et al., 2013).

Over expression of *HSFA4a* and *HSFA9*, two targets of *HsfA3*, has been reported to increase desiccation tolerance in *Helianthus* (Personat et al., 2014). *HsfA3* may play a role in stress tolerance beyond heat tolerance and merits further study based on our results.

We found the presence of high levels of ABA (Figure 5) and of several targets of the ABA signal transduction pathway among the drought up-regulated genes. Included in these were *RD29B* (*Solyc03g025810.2*) and several LEA proteins indicating that the pathway is active in tomato after prolonged drought stress. The concomitant up-regulation of inhibitors of the ABA signaling cascade such as putative orthologs of *Arabidopsis PP2CA* (*Solyc03g096670.2*), *MFT* (*SELFPRUINING* 2G, *Solyc02g079290.2*), and *AFP3* (*Solyc05g012210.2*; Garcia et al., 2008) was also observed. The increased expression of these genes indicates that a negative feedback loop is also in place. This is analogous to reports in *Arabidopsis* plants exposed to moderate drought stress, where the up-regulation of effectors of the ABA response also led to expression of negative regulatory components (Clauw et al., 2015).

Drought stress caused induction of three NAC domain-containing transcription factors (Supplementary Table S5), two of which encode *JA2* (*Solyc12g013620*) and *JA2like* (*JA2L*, *Solyc07g063140*). These have been recently shown to have antagonistic roles in stomatal movements in tomato during pathogen attack (Du et al., 2014). *JA2* is induced by ABA and promotes stomatal closure through induction of expression of the ABA biosynthetic gene *NCED1*. In contrast, *JA2L* is induced by the bacterial virulence factor coronatine and is proposed to have a role in stomatal reopening by

TABLE 1 | Expression values (Log₂ RPKM) in WW, Dr1, RW, Dr2 of DEGs belonging to selected functional categories (down, histones, and chlorophyll binding proteins; up, heat shock proteins).

Gene ID	Cluster ID	Log ₂ RPKM				Function
		WW	Dr1	RW	Dr2	
HISTONES						
Solyc01g074000.2	14	7.478648295	1.438292852	6.699745948	0.941106311	Histone H3
Solyc01g079110.2	14	7.717402251	1.427606173	6.763411574	0.378511623	Histone H3
Solyc01g080600.2	17	5.459103696	0	4.09592442	0	Histone H3
Solyc01g086820.2	14	7.564835417	1.580145484	6.261530815	0.695993813	Histone H3
Solyc05g054610.1	17	6.787902559	0	5.704318678	0	Histone H4
Solyc06g074790.1	18	8.206526016	3.867896464	7.335211682	2.150559677	Histone H2B
Solyc06g084090.2	17	6.445428759	0.887525271	5.12763328	1.350497247	Histone H2A
Solyc09g074300.1	17	6.513332824	0.650764559	5.369466484	0.704871964	Histone H2A
Solyc10g008910.1	1	8.601436535	2.049630768	7.722807531	1.344828497	Histone H3
Solyc11g072840.1	17	6.533096079	0.35614381	5.329841177	0.687060688	Histone H4
Solyc11g072860.1	1	8.5389261	1.944858446	7.555969495	0.389566812	Histone H4
Solyc11g073260.1	14	6.958378712	3.207892852	5.529508641	1.339137385	Histone H2A
PHOTOSYSTEM COMPONENTS						
Solyc08g067330.1	1	9.419538892	2.316145742	9.05058332	0	Chlorophyll a-b binding protein 3C-like
Solyc08g067320.1	1	8.889716892	2.046141782	8.634847344	0	Chlorophyll a/b binding protein
Solyc03g005790.2	1	8.373561216	0.887525271	7.935695463	0.389566812	Chlorophyll a/b-binding protein
Solyc02g070990.1	2	14.18934198	5.337354298	12.9016928	3.370164281	Chlorophyll a/b binding protein
Solyc02g070950.1	2	14.38162474	4.700994494	13.43618319	4.017031081	Chlorophyll a/b binding protein
Solyc03g005780.1	2	14.70360028	3.926948248	14.60010223	3.491853096	Chlorophyll a-b binding protein 3C-like
HEAT SHOCK-RELATED PROTEINS						
Solyc12g042830.1	20	2.313245852	6.575766127	1.855989697	6.841218374	Class I heat shock protein
Solyc02g093600.2	20	3.097610797	7.172727518	1.859969548	7.400879436	Class I heat shock protein
Solyc03g113930.1	20	2.313245852	6.969127461	2.720278465	9.552822772	Class IV heat shock protein
Solyc06g053960.2	20	4.286881148	6.571373436	3.261530815	8.040289721	Heat stress transcription factor A3
Solyc09g015000.2	7	9.743252396	12.91458695	7.968263589	13.21605617	Class I heat shock protein
Solyc03g117630.1	7	6.822475232	10.43675318	5.586464526	12.58523251	Heat shock protein
Solyc03g123540.2	7	6.808256325	9.913577595	5.879950768	10.38608881	Class II heat shock protein

A full list of DEGs along with their expression in the four conditions is available in Supplementary Table S5.

regulating the expression of genes involved in Salicylic acid metabolism (Du et al., 2014). The presence of both JA2 and JA2L in our list of drought-induced genes indicates that these two TFs might also be involved in abiotic stress-triggered stomatal movements and represents a further indication that antagonistic pathways concur to the final balance of physiological adjustments.

The GO Enrichment analysis of the categories overrepresented in clusters showing interesting patterns allowed for the identification of specific functions regulated by drought stress (Figure 7, Supplementary Tables S7, S8). Several GO categories related to photosynthesis, such as “photosystem I,” “photosystem II,” “chlorophyll binding,” and “photosynthesis, light harvesting” were enriched in clusters containing genes with higher expression in well-watered rather than drought stressed samples. This possibly indicates a reduced synthesis of components of the photosynthetic machinery under stress conditions (Clusters 1, 2, 14, 17, 18; Table 1). These differences in expression correlated with the low photosynthetic assimilation rate observed in drought stressed plants (Figure 2). A similar down-regulation of photosynthetic genes was observed in a progressive drought stress treatment on *Arabidopsis* plants.

Moderate drought stress reduced the photosynthesis rate while expression of photosynthetic genes was not affected (Harb et al., 2010). This suggests that the mode of drought stress application and the severity of the stress influence the impact on the photosynthetic machinery. Concomitant with the downregulation of components of the photosystem under drought, we observed an upregulation of a FtsH homolog (*Solyc03g112590.2*) with a predicted chloroplast target peptide. FtsHs are ATP-dependent zinc metalloproteases, which, in chloroplasts, have been suggested to be involved in the turnover of the oxidized D1 protein of the PSII reaction center during recovery from photoinhibition (Lindahl et al., 2000; Bailey et al., 2002). Recently, Zhang et al. (2014) observed a progressive and constant upregulation of FtsH in *Medicago truncatula* subjected to drought stress and suggested a role in the repair of PSII damages resulting from drought-induced oxidative stress (Zhang et al., 2014).

Reduction of leaf growth occurs as a result of reduced cell division and/or cell expansion. Analysis of the GO enrichment categories suggests that both cell division and expansion are affected in tomato during drought stress. Categories such as “Cell Proliferation,” “Anaphase,” “Regulation of DNA replication” were

enriched in well-watered rather than drought stressed samples, indicating that cell division is very likely repressed during drought.

We also observed that histone s gene families were the most down-regulated group of functional categories (**Table 1**). Histone expression is regulated during the progression of the cell cycle and tightly connected to DNA replication (Meshi et al., 2000; Rattray and Müller, 2012). The repression of the expression of several H3 and H4 isoforms (**Table 1**, Supplementary Tables S5, S6), concomitant with repression of genes such as a DNA topoisomerase, two DNA polymerase, single-stranded DNA-binding replication protein A large subunit, single-stranded DNA binding protein p30 could be an indication of a reduction in cell division. This is in all probability one of the factors leading to growth reduction in stress conditions. The observed repression of histone expression under drought is consistent with a recent report in rice showing that expression of several histone isoforms was reduced upon salt and drought treatment (Hu and Lai, 2015).

This study has sought to establish the transcriptomic profile of severe drought treatment in tomato and subsequent recovery with physiological and metabolic measurements. This combined data provides a comprehensive picture of the plant's status under stress and opens avenues to better understand the mechanisms involved in drought tolerance.

Overall, the results presented in this work indicate that drought stress causes the repression of several genes implicated in photosynthesis/light harvesting and plant growth, which was concomitant with a reduction of CO₂ assimilation, electron transport efficiency through the photosystems and a growth reduction. In addition, we found several genes up-regulated by drought stress that encoded late effectors and early regulators

of ABA signaling. The expression of these genes was in parallel with an increase of ABA and osmolyte concentration as well as closure of stomata. Therefore, gene expression and physiological responses are intimately interconnected. Analysis of these results has yielded interesting candidate genes that could play novel roles in drought tolerance and adaptation.

AUTHOR CONTRIBUTIONS

MV, AC, MC, RA, PG, GB, and SG conceived the work and designed experiments. PI, PP, GG, CM, RN, HB, CC, PB, GB performed experiments, analyzed the results, contributed figures. PI, MV, RA, PG, GB, SG wrote the paper. All authors reviewed the manuscript.

ACKNOWLEDGMENTS

The authors thank all lab members for helpful discussions and Gaetano Guarino for technical assistance. This work was supported by the Italian Ministry of University and Research, projects GenoPOM (DM17732) and GenoPOM-PRO (PON02_00395_3082360), and by the Italian Ministry of Economy and Finance (Legge n.191/2009), to the National Research Council, project "Innovazione e Sviluppo del Mezzogiorno - Conoscenze Integrate per Sostenibilità ed Innovazione del Made in Italy Agroalimentare" (CISIA).

SUPPLEMENTARY MATERIAL

The Supplementary Material for this article can be found online at: <http://journal.frontiersin.org/article/10.3389/fpls.2016.00371>

REFERENCES

- Anders, S., and Huber, W. (2010). Differential expression analysis for sequence count data. *Genome Biol.* 11:R106. doi: 10.1186/gb-2010-11-10-r106
- Andolfo, G., and Ercolano, M. R. (2015). Plant innate immunity multicomponent model. *Front. Plant Sci.* 6:987. doi: 10.3389/fpls.2015.00987
- Bailey, S., Thompson, E., Nixon, P. J., Horton, P., Mullineaux, C. W., Robinson, C., et al. (2002). A critical role for the Var2 FtsH homologue of *Arabidopsis thaliana* in the photosystem II repair cycle *in vivo*. *J. Biol. Chem.* 277, 2006–2011. doi: 10.1074/jbc.M105878200
- Baker, N. R. (2008). Chlorophyll fluorescence: a probe of photosynthesis *in vivo*. *Ann. Rev. Plant Biol.* 59, 89–113. doi: 10.1146/annurev.arplant.59.032607.092759
- Barghini, E., Cossu, R. M., Cavallini, A., and Giordani, T. (2015). Transcriptome analysis of response to drought in poplar interspecific hybrids. *Genom. Data* 3, 143–145. doi: 10.1016/j.gdata.2015.01.004
- Bartels, D., and Sunkar, R. (2005). Drought and salt tolerance in plants. *CRC Crit. Rev. Plant Sci.* 24, 23–58. doi: 10.1080/07352680590910410
- Bosco De Oliveira, A., Mendes Alencar, N. L., and Gomes-Filho, E. (2012). "Physiological and biochemical responses of semiarid plants subjected to water stress" in *Water Stress*, ed M. R. Rahman (Rijeka: InTech), 43–58.
- Boyer, J. S. (1982). Plant productivity and environment. *Science* 218, 443–448. doi: 10.1126/science.218.4571.443
- Boyer, J. S., Byrne, P., Cassman, K. G., Cooper, M., Delmer, D., Grene, T., et al. (2013). The U.S. drought of 2012 in perspective: A call to action. *Global Food Security* 2, 139–143. doi: 10.1016/j.gfs.2013.08.002
- Canene-Adams, K., Campbell, J. K., Zaripheh, S., Jeffery, E. H., and Erdman, J. W. (2005). The tomato as a functional food. *J. Nutr.* 135, 1226–1230.
- Chaves, M. M., Flexas, J., and Pinheiro, C. (2009). Photosynthesis under drought and salt stress: regulation mechanisms from whole plant to cell. *Ann. Bot.* 103, 551–560. doi: 10.1093/aob/mcn125
- Chaves, M. M., Pereira, J. S., Maroco, J., Rodrigues, M. L., Ricardo, C. P. P., Osório, M. L., et al. (2002). How plants cope with water stress in the field? Photosynthesis and growth. *Ann. Bot.* 89, 907–916. doi: 10.1093/aob/mcf105
- Cifre, J., Bota, J. M., Escalona, J. M., Medrano, H., and Flexas, J. (2005). Physiological tools for irrigation scheduling in grapevine (*Vitis vinifera* L.): an open gate to improve water-use efficiency? *Agric. Ecosyst. Environ.* 106, 159–170. doi: 10.1016/j.agee.2004.10.005
- Claussen, W. (2005). Proline as a measure of stress in tomato plants. *Plant Sci.* 168, 241–248. doi: 10.1016/j.plantsci.2004.07.039
- Clauw, P., Coppens, F., De Beuf, K., Dhondt, S., Van Daele, T., Maleux, K., et al. (2015). Leaf responses to mild drought stress in natural variants of *Arabidopsis thaliana*. *Plant Physiol.* 167, 800–816. doi: 10.1104/pp.114.254284
- Conesa, A., and Götz, S. (2008). Blast2GO: a comprehensive suite for functional analysis in plant genomics. *Int. J. Plant Genomics* 2008:619832. doi: 10.1155/2008/619832
- Cornic, G. (2000). Drought stress inhibits photosynthesis by decreasing stomatal aperture—not by affecting ATP synthesis. *Trends Plant Sci.* 5, 187–188. doi: 10.1016/S1360-1385(00)01625-3
- Corrado, G., Sasso, R., Pasquariello, M., Iodice, L., Carretta, A., Cascone, P., et al. (2007). Systemin regulates both systemic and volatile signaling in tomato plants. *J. Chem. Ecol.* 33, 669–681. doi: 10.1007/s10886-007-9254-9

- Du, M., Zhai, Q., Deng, L., Li, S., Li, H., Yan, L., et al. (2014). Closely related NAC transcription factors of tomato differentially regulate stomatal closure and reopening during pathogen attack. *Plant Cell* 26, 3167–3184. doi: 10.1101/tpc.114.128272
- Dugas, D. V., Monaco, M. K., Olsen, A., Klein, R. R., Kumari, S., Ware, D., et al. (2011). Functional annotation of the transcriptome of *Sorghum bicolor* in response to osmotic stress and abscisic acid. *BMC Genomics* 12:514. doi: 10.1186/1471-2164-12-514
- Elliott, J., Deryng, D., Müller, C., Frieler, K., Konzmann, M., Gerten, D., et al. (2014). Constraints and potentials of future irrigation water availability on agricultural production under climate change. *Proc. Natl. Acad. Sci. U.S.A.* 111, 3239–3244. doi: 10.1073/pnas.1222474110
- Flexas, J., Bota, J., Cifre, J., Escalona, M. J., Galmés, J., Gulás, J., et al. (2004). Understanding down-regulation of photosynthesis under water stress: future prospects and searching for physiological tools for irrigation management. *Ann. Appl. Biol.* 144, 273–283. doi: 10.1111/j.1744-7348.2004.tb00343.x
- Foolad, M. R. (2007). Genome mapping and molecular breeding of tomato. *Int. J. Plant Genom.* 52:64358. doi: 10.1155/2007/64358
- Galmés, J., Conesa, M. Á., Ochogavia, J., Perdomo, J. A., Francis, D. M., Ribas-Carbó, M., et al. (2011). Physiological and morphological adaptations in relation to water use efficiency in mediterranean accessions of *Solanum lycopersicum*. *Plant Cell Environ.* 34, 245–260. doi: 10.1111/j.1365-3040.2010.02239.x
- Galmés, J., Ochogavia, J., Gago, J., Roldán, E. J., Cifre, J., and Conesa, M. Á. (2013). Leaf responses to drought stress in mediterranean accessions of *Solanum lycopersicum*: anatomical adaptations in relation to gas exchange parameters. *Plant Cell Environ.* 36, 920–935. doi: 10.1111/pce.12022
- Garcia, M. E., Lynch, T., Peeters, J., Snowden, C., and Finkelstein, R. (2008). A small plant-specific protein family of ABI five binding proteins (AFPs) regulates stress response in germinating *Arabidopsis* seeds and seedlings. *Plant Mol. Biol.* 67, 643–658. doi: 10.1007/s11103-008-9344-2
- Genty, B., Briantais, J. M., and Baker, N. R. (1989). The relationship between the quantum yield of photosynthetic electron transport and quenching of chlorophyll fluorescence. *Biochim. Biophys. Acta* 990, 87–92. doi: 10.1016/S0304-4165(89)80016-9
- Giorio, P., Nuzzo, V., Guida, G., and Albrizio, R. (2011). Black leaf-clips increased minimum fluorescence emission in clipped leaves exposed to high solar radiation during dark adaptation. *Photosynthetica* 50, 467–471. doi: 10.1007/s11099-012-0042-6
- Gong, P., Zhang, J., Li, H., Yang, C., Zhang, C., Zhang, X., et al. (2010). Transcriptional profiles of drought-responsive genes in modulating transcription signal transduction, and biochemical pathways in tomato. *J. Exp. Bot.* 61, 3563–3575. doi: 10.1093/jxb/erq167
- Harb, A., Krishnan, A., Ambavaram, M. M. R., and Pereira, A. (2010). Molecular and physiological analysis of drought stress in *Arabidopsis* reveals early responses leading to acclimation in plant growth. *Plant Physiol.* 154, 1254–1271. doi: 10.1104/pp.110.161752
- Hsiao, T. C., Acevedo, E., Fereres, E., and Henderson, D. W. (1976). Water stress, growth, and osmotic adjustment. *Philos. Trans. R. Soc. Lond. B Biol. Sci.* 273, 479–500. doi: 10.1098/rstb.1976.0026
- Hu, Y., and Lai, Y. (2015). Identification and expression analysis of rice histone genes. *Plant Physiol. Biochem.* 86, 55–65. doi: 10.1016/j.plaphy.2014.11.012
- Kakumanu, A., Ambavaram, M. M. R., Klumas, C., Krishnan, A., Batlang, U., Myers, E., et al. (2012). Effects of drought on gene expression in maize reproductive and leaf meristem tissue revealed by RNA-seq. *Plant Physiol.* 160, 846–867. doi: 10.1104/pp.112.200444
- Kaldenhoff, R. (2012). Mechanisms underlying CO₂ diffusion in leaves. *Curr. Opin. Plant Biol.* 15, 276–281. doi: 10.1016/j.pbi.2012.01.011
- Kim, D., Pertea, G., Trapnell, C., Pimentel, H., Kelley, R., and Salzberg, S. L. (2013). TopHat2: accurate alignment of transcriptomes in the presence of insertions, deletions and gene fusions. *Genome Biol.* 14:R36. doi: 10.1186/gb-2013-14-4-r36
- Kissoudis, C., Chowdhury, R., van Heusden, S., van de Wiel, C., Finkers, R., Visser, R. G. F., et al. (2015). Combined biotic and abiotic stress resistance in tomato. *Euphytica* 202, 317–332. doi: 10.1007/s10681-015-1363-x
- Kitajima, M., and Butler, W. L. (1975). Quenching of chlorophyll fluorescence and primary photochemistry in chloroplasts by dibromothymoquinone. *Biochim. Biophys. Acta* 376, 105–115. doi: 10.1016/0005-2728(75)90209-1
- Langmead, B., and Salzberg, S. L. (2012). Fast gapped-read alignment with Bowtie 2. *Nat. Methods* 9, 357–359. doi: 10.1038/nmeth.1923
- Langridge, P., and Reynolds, M. P. (2015). Genomic tools to assist breeding for drought tolerance. *Curr. Opin. Biotechnol.* 32, 130–135. doi: 10.1016/j.copbio.2014.11.027
- Leyva-González, M. A., Ibarra-Laclette, E., Cruz-Ramírez, A., and Herrera-Estrella, L. (2012). Functional and transcriptome analysis reveals an acclimatization strategy for abiotic stress tolerance mediated by *Arabidopsis* NF-YA family members. *PLoS ONE* 7:e48138. doi: 10.1371/journal.pone.0048138
- Li-Cor. (2011). *Using the Li-6400/Li-6400XT Portable Photosynthesis System*. Lincoln, NE.
- Li, W. X., Oono, Y., Zhu, J., He, X. J., Wu, J. M., Iida, K., et al. (2008). The *Arabidopsis* NYFA5 transcription factor is regulated transcriptionally and posttranscriptionally to promote drought resistance. *Plant Cell* 20, 2238–2251. doi: 10.1101/tpc.108.059444
- Li, Z., Zhang, L., Wang, A., Xu, X., and Li, J. (2013). Ectopic overexpression of SIHsfA3, a heat stress transcription factor from tomato, confers increased thermotolerance and salt hypersensitivity in germination in transgenic *Arabidopsis*. *PLoS ONE* 8:e54880. doi: 10.1371/journal.pone.0054880
- Lindahl, M., Spetea, C., Hundal, T., Oppenheim, A. B., Adam, Z., and Andersson, B. (2000). The thylakoid FtsH protease plays a role in the light-induced turnover of the photosystem II D1 protein. *Plant Cell* 12, 419–431. doi: 10.1101/tpc.12.3.419
- Livak, K. J., and Schmittgen, T. D. (2001). Analysis of relative gene expression data using real-time quantitative PCR and the 2^{-ΔΔCT} method. *Methods* 25, 402–408. doi: 10.1006/meth.2001.1262
- Lutfor Rahman, S. M., Nawata, E., and Sakurata, T. (1999). Effect of water stress on growth, yield and eco-physiological responses of four tomato (*Lycopersicon esculentum* Mill.) cultivars. *J. Jpn. Soc. Hortic. Sci.* 68, 499–504. doi: 10.2503/jjshs.68.499
- Ma, Y., Szostkiewicz, I., Korte, A., Moes, D., Yang, Y., Christmann, A., et al. (2009). Regulators of PP2C phosphatase activity function as abscisic acid sensors. *Science* 324, 1064–1068. doi: 10.1126/science.1172408
- MacQueen, J. B. (1967). "Some methods for classification and analysis of multivariate observations," in *Proceedings of 5th Berkeley Symposium on Mathematical Statistics and Probability*, Vol. 1 (Berkeley, CA), 281–297.
- Martin, M. (2011). Cutadapt removes adapter sequences from high-throughput sequencing reads. *EMBnet J.* 17, 10–12. doi: 10.14806/ej.17.1.200
- Mekonnen, M. M., and Hoekstra, A. Y. (2011). The green, blue and grey water footprint of crops and derived crop products. *Hydrol. Earth Syst. Sci.* 15, 1577–1600. doi: 10.5194/hess-15-1577-2011
- Meshi, T., Taoka, K. I., and Iwabuchi, M. (2000). Regulation of histone gene expression during the cell cycle. *Plant Mol. Biol.* 43, 643–657. doi: 10.1023/A:1006421821964
- Mickelbart, M. V., Hasegawa, P. M., and Bailey-Serres, J. (2015). Genetic mechanisms of abiotic stress tolerance that translate to crop yield stability. *Nat. Rev. Genet.* 16, 237–251. doi: 10.1038/nrg3901
- Nicot, N., Hausman, J.-F., Hoffmann, L., and Evers, D. (2005). Housekeeping gene selection for real-time RT-PCR normalization in potato during biotic and abiotic stress. *J. Exp. Bot.* 56, 2907–2914. doi: 10.1093/jxb/eri285
- Nilsen, E. T., Freeman, J., Greene, R., and Tokunaga, J. (2014). A rootstock provides water conservation for a grafted commercial tomato (*Solanum lycopersicum* L.) line in response to mild-drought conditions: a focus on vegetative growth and photosynthetic parameters. *PLoS ONE* 9:e115380. doi: 10.1371/journal.pone.0115380
- Nuruddin, M., Madramootoo, C. A., and Dodds, G. T. (2003). Effects of water stress at different growth stages on greenhouse tomato yield and quality. *Hortic. Sci.* 38, 1389–1393.
- Oono, Y., Yazawa, T., Kawahara, Y., Kanamori, H., Kobayashi, F., Sasaki, H., et al. (2014). Genome-wide transcriptome analysis reveals that cadmium stress signaling controls the expression of genes in drought stress signal pathways in rice. *PLoS ONE* 9:e96946. doi: 10.1371/journal.pone.0096946
- Osorio, S., Alba, R., Damasceno, C. M. B., Lopez-Casado, G., Lohse, M., Zanor, M. I., et al. (2011). Systems biology of tomato fruit development: combined transcript, protein, and metabolite analysis of tomato transcription factor (*nor*, *rin*) and ethylene receptor (*Nr*) mutants reveals novel regulatory interactions. *Plant Physiol.* 157, 405–425. doi: 10.1104/pp.111.175463

- Pantin, F., Monnet, F., Jannaud, D., Costa, J. M., Renaud, J., Muller, B., et al. (2013). The dual effect of abscisic acid on stomata *New Phytol.* 197, 65–72. doi: 10.1111/nph.12013
- Park, S. Y., Fung, P., Nishimura, N., Jensen, D. R., Fujii, H., Lumba, S., et al. (2009). Abscisic acid inhibits type 2C protein phosphatases via the PYR/PYL family of START proteins. *Science* 324, 1068–1071. doi: 10.1126/science.1173041
- Personat, J.-M., Tejedor-Cano, J., Prieto-Dapena, P., Almoguera, C., and Jordano, J. (2014). Co-overexpression of two Heat Shock Factors results in enhanced seed longevity and in synergistic effects on seedling tolerance to severe dehydration and oxidative stress. *BMC Plant Biol.* 14:56. doi: 10.1186/1471-2229-14-56
- Rai, G. K., Rai, N. P., Rathaur, S., Kumar, S., and Singh, M. (2013). Expression of rd29A::AtDREB1A/CBF3 in tomato alleviates drought-induced oxidative stress by regulating key enzymatic and non-enzymatic antioxidants. *Plant Physiol. Biochem.* 69, 90–100. doi: 10.1016/j.plaphy.2013.05.002
- Rattray, A. M. J., and Müller, B. (2012). The control of histone gene expression. *Biochem. Soc. Trans.* 40, 880–885. doi: 10.1042/BST20120065
- Saadi, S., Todorovic, M., Tanasijevic, L., Pereira, L. S., Pizzigalli, C., and Lionello, P. (2015). Climate change and mediterranean agriculture: impacts on winter wheat and tomato crop evapotranspiration, irrigation requirements and yield. *Agric. Water Manag.* 147, 103–115. doi: 10.1016/j.agwat.2014.05.008
- Sadder, M., Alsadon, A., and Wahb-Allah, M. (2014). Transcriptomic analysis of tomato lines reveals putative stress-specific biomarkers. *Turk. J. Agric. For.* 38, 700–715. doi: 10.3906/tar-1312-17
- Sakuraba, Y., Kim, Y. S., Han, S. H., Lee, B. D., and Paek, N. C. (2015). The Arabidopsis transcription factor NAC016 promotes drought stress responses by repressing AREB1 transcription through a trifurcate feed-forward regulatory loop involving NAP. *Plant Cell* 27, 1771–1787. doi: 10.1105/tpc.15.00222
- Sato, S., Tabata, S., Hirakawa, H., Asamizu, E., Shirasawa, K., Isobe, S., et al. (2012). The tomato genome sequence provides insights into fleshy fruit evolution. *Nature* 485, 635–641. doi: 10.1038/nature11119
- Schramm, F., Larkindale, J., Kiehlmann, E., Ganguli, A., Englich, G., Vierling, E., et al. (2008). A cascade of transcription factor DREB2A and heat stress transcription factor HsfA3 regulates the heat stress response of Arabidopsis. *Plant J.* 53, 264–274. doi: 10.1111/j.1365-313X.2007.03334.x
- Sharp, R. E., and LeNoble, M. E. (2002). ABA, ethylene and the control of shoot and root growth under water stress. *J. Exp. Bot.* 53, 33–37. doi: 10.1093/jexbot/53.366.33
- Solankey, S. S., Singh, R. K., Baranwal, D. K., and Singh, D. K. (2014). Integrated genomics, physio-chemical and breeding approaches for improving heat and drought tolerance in tomato. *Int. J. Veget. Sci.* 125, 625–645. doi: 10.1080/19315260.2014.902414
- Strasser, R., Srivastava, A., and Tsimilli-Michael, M. (2000). “The fluorescence transient as a tool to characterize and screen photosynthetic samples” in *Probing Photosynthesis: Mechanism, Regulation and Adaptation*, ed M. Yunus (London: CRC Press), 445–483.
- Suresh, B. V., Roy, R., Sahu, K., Misra, G., and Chattopadhyay, D. (2014). Tomato genomic resources database: an integrated repository of useful tomato genomic information for basic and applied research. *PLoS ONE* 9:e86387. doi: 10.1371/journal.pone.0086387
- Tezara, W., Mitchell, V. J., Driscoll, S. D., and Lawlor, D. W. (1999). Water stress inhibits plant photosynthesis by decreasing coupling factor and ATP. *Nature* 401, 914–917. doi: 10.1038/44842
- Thorndike, R. L. (1953). Who belongs in the family? *Psychometrika* 18, 267–276. doi: 10.1007/BF02289263
- von Caemmerer, S., and Farquhar, G. D. (1981). Some relationships between the biochemistry of photosynthesis and the gas exchange of leaves. *Planta* 153, 376–387. doi: 10.1007/BF00384257
- Yoshida, T., Sakuma, Y., Todaka, D., Maruyama, K., Qin, F., Mizoi, J., et al. (2008). Functional analysis of an Arabidopsis heat-shock transcription factor HsfA3 in the transcriptional cascade downstream of the DREB2A stress-regulatory system. *Biochem. Biophys. Res. Commun.* 368, 515–521. doi: 10.1016/j.bbrc.2008.01.134
- Young, M. D., Wakefield, M. J., Smyth, G. K., and Oshlack, A. (2010). Gene ontology analysis for RNA-seq: accounting for selection bias. *Genome Biol.* 11:R14. doi: 10.1186/gb-2010-11-2-r14
- Zhang, J.-Y., Cruz De Carvalho, M. H., Torres-Jerez, I., Kang, Y., Allen, S. N., Huhman, D. V., et al. (2014). Global reprogramming of transcription and metabolism in *Medicago truncatula* during progressive drought and after rewetting. *Plant Cell Environ.* 37, 2553–2576. doi: 10.1111/pce.12328

Conflict of Interest Statement: The authors declare that the research was conducted in the absence of any commercial or financial relationships that could be construed as a potential conflict of interest.

Copyright © 2016 Iovieno, Punzo, Guida, Mistretta, Van Oosten, Nurcato, Bostan, Colantuono, Costa, Bagnaresi, Chiusano, Albrizio, Giorio, Batelli and Grillo. This is an open-access article distributed under the terms of the Creative Commons Attribution License (CC BY). The use, distribution or reproduction in other forums is permitted, provided the original author(s) or licensor are credited and that the original publication in this journal is cited, in accordance with accepted academic practice. No use, distribution or reproduction is permitted which does not comply with these terms.



Heterologous Expression of AtWRKY57 Confers Drought Tolerance in *Oryza sativa*

Yanjuan Jiang¹, Yuping Qiu², Yanru Hu¹ and Diqu Yu^{1*}

¹ Key Laboratory of Tropical Plant Resources and Sustainable Use, Xishuangbanna Tropical Botanical Garden, Chinese Academy of Sciences, Kunming, China, ² National Plateau Wetlands Research Center, Southwest Forestry University, Kunming, China

OPEN ACCESS

Edited by:

Olivier Lamotte,
CNRS, UMR Agroécologie, Dijon,
France

Reviewed by:

Tong Zhu,
Syngenta Crop Protection, LLC., USA
Zhao Su,
Pennsylvania State University, USA

*Correspondence:

Diqu Yu
ydq@xtbg.ac.cn

Specialty section:

This article was submitted to
Plant Physiology,
a section of the journal
Frontiers in Plant Science

Received: 19 November 2015

Accepted: 28 January 2016

Published: 11 February 2016

Citation:

Jiang Y, Qiu Y, Hu Y and Yu D (2016)
Heterologous Expression
of AtWRKY57 Confers Drought
Tolerance in *Oryza sativa*.
Front. Plant Sci. 7:145.
doi: 10.3389/fpls.2016.00145

Drought stress is a severe environmental factor that greatly restricts plant distribution and crop production. Recently, we have found that overexpressing AtWRKY57 enhanced drought tolerance in *Arabidopsis thaliana*. In this study, we further reported that the *Arabidopsis* WRKY57 transcription factor was able to confer drought tolerance to transgenic rice (*Oryza sativa*) plants. The enhanced drought tolerance of transgenic rice was resulted from the lower water loss rates, cell death, malondialdehyde contents and relative electrolyte leakage while a higher proline content and reactive oxygen species-scavenging enzyme activities was observed during stress conditions. Moreover, further investigation revealed that the expression levels of several stress-responsive genes were up-regulated in drought-tolerant transgenic rice plants, compared with those in wild-type plants. In addition to the drought tolerance, the AtWRKY57 over-expressing plants also had enhanced salt and PEG stress tolerances. Taken together, our study indicates that over-expressing AtWRKY57 in rice improved not only drought tolerance but also salt and PEG tolerance, demonstrating its potential role in crop improvement.

Keywords: AtWRKY57, drought tolerance, *Oryza sativa*, Stress, ROS

INTRODUCTION

Drought is a critical abiotic stress that severely restricts crop production (Zhu, 2002). With the process of evolution, plants have gained a variety of strategies with the purpose of avoiding drought stress by reducing water loss or increasing water uptake. Nevertheless, other strategies need to protect plant cells from damage when water is exhausted and tissue dehydration unavoidable (Verslues et al., 2006). Additionally, the molecular, cellular, and whole-plant levels strategies should be coordinated to adapt to drought stress (Yu et al., 2008).

Under drought- or salt-stress conditions, plants accumulate reactive oxygen species (ROS) (Verslues et al., 2006). In living cells, ROS such as superoxide, hydrogen peroxide (H_2O_2), and hydroxyl radicals are generated as harmful substances via aerobic metabolism. Through partially reduced or activated derivatives of oxygen, ROS can destroy DNA, proteins and carbohydrates, resulting in cell death (Mittler et al., 2004). A master level of ROS gives rise to the oxidation of biomolecules, such as lipids, nucleic acids and proteins, which caused cellular damage. When CO_2 fixation is restricted under environmental stress conditions, the photosynthetic electron transport system generates ROS (Asada, 1999). To defend oxidative stress, organisms have

evolved an effective system to protect themselves. For example, numerous stress-related genes were induced by ROS in response to oxidative stress in these defensive systems (Demple and Amabile-Cuevas, 1991; Gasch et al., 2000; Desikan et al., 2002). As higher plants have the ability to coordinately regulate multiple antioxidant genes, they are much tolerant to oxidative stresses.

Normally, the maintenance of routine homeostasis is achieved through the ROS-scavenging system in plant cells, which is mainly mediated by enzymatic defenses, including superoxide dismutase (SOD), catalase (CAT), and peroxidases (POX) (Mittler et al., 2004). Generally, SODs, which catalyze the dismutation of superoxide into oxygen and H₂O₂, provide the first line of defense against ROS in various subcellular compartments, such as chloroplast, mitochondria and cytosol (Raychaudhuri and Deng, 2000). The physiological role of CAT is to break down H₂O₂ in the cell (Scandalios, 2002). Therefore, increased CAT activity would result in H₂O₂ degradation. PODs are a group of enzymes that catalyze the oxidation of many substrates (e.g., phenolic compounds) at the expense of H₂O₂ (Asada, 1987). The increased activity of these enzymes would decrease ROS levels. Recent reports have demonstrated that transgenic rice plants with enhanced ROS-scavenging abilities had improved drought tolerance (Ouyang et al., 2010; Zhang et al., 2011). For example, OsSIK1 functions in stress signaling through scavenging and detoxification of ROS. In OsSIK1-overexpressing plants, the high levels of POD and CAT enzymes resulted to low levels of H₂O₂ (Ouyang et al., 2010). Similarly, the improved drought tolerance of HRF1-overexpressing transgenic rice plants was partially resulted from the increased ROS-scavenging activities (Zhang et al., 2011).

Under environment stress conditions, the stress-related proteins not only function in protecting cells from damage but also regulate the expression of downstream genes for signal sensing, perception and transduction (Kreps et al., 2002; Seki et al., 2002). These proteins can be classified into two groups. The first group protein plays a crucial role to avoid cellular injury, such as detoxification enzymes, Late Embryogenesis Abundant (LEA) proteins, and the key enzymes for osmolyte biosynthesis (Kreps et al., 2002; Seki et al., 2002). The second group includes numerous transcription factors involved in further regulation of transcriptional control and signal transduction. The CBF/DREB factor, Basic Leucine Zipper families, CUC transcription factor, NAM, plant nuclear factor Y (NF-Y) B subunits, zinc finger and ATAF, belong to this group (Umezawa et al., 2006; Nelson et al., 2007; Takasaki et al., 2010). Studies on these transcription factors will contribute to uncover the respect for commercially improving drought tolerance in crops through genetic engineering.

The WRKY family consists of 74 and 102 members in *Arabidopsis thaliana* and *Oryza sativa*, respectively (Eulgem et al., 2000; Wu et al., 2005); and majority of them play critical roles in biotic and abiotic stress responses (Eulgem and Somssich, 2007; Miller et al., 2008). Recently, increasing evidences confirmed that numerous of WRKY genes are

involved in drought stress. For example, ABO3/WRKY63 plays a key role in plant responses to ABA and drought stress (Ren et al., 2010). Overexpression of a stress-induced OsWRKY45 significantly confer drought tolerance in *Arabidopsis* and rice (Qiu and Yu, 2008; Tao et al., 2011). Especially, our previous study demonstrated that overexpression of AtWRKY57 improved drought tolerance by directly targeting the promoter sequences of NCED3 to increase the content of ABA in *Arabidopsis* (Jiang et al., 2012). These evidences give us a hypothesis that the improvement of plant drought tolerance might be realized through gene manipulation approaches. To test this hypothesis, we further over-expressed AtWRKY57 in rice and demonstrated that the stress tolerance of the transgenic rice under drought conditions was significantly improved. 3,3'-Diaminobenzidine (DAB) and nitro blue tetrazolium (NBT) staining analyses showed that the ROS levels in transgenic lines were lower than in control plants after drought-stress treatment. Consistent with the low ROS levels, the antioxidative enzyme activities were also enhanced in the transgenic lines. Moreover, high expression levels of stress-responsive genes also supported the drought tolerance in transgenic lines. Overall, our results indicated that the over-expression of AtWRKY57 in rice conferred the adaptation of rice to drought tolerance by reducing ROS damage and up-regulating the expression of stress-responsive genes.

MATERIALS AND METHODS

Construction and Transformation of AtWRKY57 in Rice

The full-length cDNA sequence of AtWRKY57 was obtained from *Arabidopsis* using the same method as described in our previous study (Jiang et al., 2012). The full coding sequence of AtWRKY57 was cloned into pUN1301 in the sense orientation behind the Ubiquitin promoter. Then the T-DNA was transformed into ZH11 (*Oryza sativa* L. ssp. *japonica* cv. Zhonghua11) via the *Agrobacterium tumefaciens*-mediated method (Hiei et al., 1994). After transformation, the calli were selected from half-strength (MS) medium containing 100 µg/ml hygromycin. Seedlings with hygromycin-resistant were transplanted to soil in a growth chamber.

Plant Growth Conditions

The sterilized *Oryza* seeds sowed on medium and kept in a growth chamber at 22°C under long-day conditions [16 h light/8 h dark cycles]. One week generation, seedlings were then transplanted in soil and half-strength MS medium supplemented with 1.5% (W/V) sucrose for drought stress, NaCl and PEG treatments. The soils are commonly used loam, mixed 50% humus soil, 30% coconut tree branny, 20% red clay.

Drought-Tolerance Assays

Drought-tolerance assays were performed using 4-week-old plants. The transgenic rice and control seedlings were

transplanted in the same pot and treated with drought stress by withholding water for 20 days. Three independent pots repeated at the same time and a representative result displayed. Three independent experimental replications were conducted.

To evaluate the water loss rates, flag leaves were detached from the plants and weighed at designated time intervals at room temperature. The proportion of fresh weight lost was calculated based on the initial plant weight. At least three biological replicates for each sample were used for the calculation.

Trypan Blue, DAB and NBT Staining

For DAB staining, leaf sections of approximately 5 cm in length were cut and soaked in a 1% solution of DAB in 50 mM Tris-HCl buffer (pH 6.5). After 30 min vacuum infiltrating, the immersed leaves were incubated in the dark for 20 h at room temperature. And then the leaves were bleached by bath in boiling ethanol until the brown spots appeared clearly. The area of brown spots are represented the DAB reaction degree to H_2O_2 .

Leaf sections of approximately 5 cm in length were excised to detect superoxide accumulation by a 0.1% solution of NBT in 10 mM potassium phosphate buffer (pH 7.8) as described previously (Fitzgerald et al., 2004). After 15 min vacuum infiltrating, the immersed leaves were incubated overnight at room temperature. After incubation, the leaves were fixed and cleared in alcoholic lacto-phenol (2:1:1, 95% ethanol:lactic acid:phenol) at 65°C for 30 min, rinsed with 50% ethanol, and then rinsed with water. When NBT interacts with superoxide, a blue precipitate forms is visible in leaves.

Proline (Pro) Content, Malondialdehyde (MDA) Content, and Electrolyte Leakage Measurements

The proline concentration was determined as described (Bates, 1973). Approximately 0.5 g of transgenic and control leaf segments were homogenized in 10 ml 3% aqueous sulfosalicylic acid and centrifuged at 3,000 × g for 20 min. 2 ml of supernatant was reacted with 2 ml acid ninhydrin and 2 ml glacial acetic acid in a test tube at 100°C for 1 h, cooled on ice, and the absorbance at 520 was measured. L-Pro was used as a standard to calculate the proline concentration.

The MDA content was determined as described (Heath and Packer, 1968) with slight modifications. Approximately 1 g of transgenic and control leaf segments were homogenized in 10 ml of 10% trichloroacetic (v/v) and centrifuged at 5,000 × g for 10 min. 2 ml of supernatant was reacted with 2 ml thiobarbituric acid in a test tube at 100°C for 15 min, quickly cooled on ice, and the absorbance at 532 was measured. The MDA content was confirmed using the extinction coefficient of 155 $\text{nM}^{-1} \text{cm}^{-1}$, and expressed as nmol g^{-1} FW.

The relative ion leakage was checked following the method of Clarke et al. (2004). For the above assays, each data point is the average of three replicates. At least three experiments were performed, and the results are consistent. The result from one set of experiments is presented here.

Oxidative Enzyme Activity Measurements

The leaves of 4-week-old rice seedlings were dehydrated for 2 h, and then homogenized in a solution of 50 mM sodium phosphate buffer (pH 7.8) containing 1% polyvinylpyrrolidone and 10 mM β -mercaptoethanol in an ice-cold mortar. After centrifugation (13,000 × g, 15 min) at 4°C, the supernatant was used to identify SOD, POD and CAT activity levels. U $\text{min}^{-1} \text{mg}^{-1}$ protein was represented the enzyme activity of SOD, POD, and CAT.

The ability to inhibit the photochemical reduction of NBT chloride was used for the determination of the total SOD activity as described by Beauchamp and Fridovich (1971). The reduction of NBT by 50% of the quantity of enzyme required was defined as one unit of SOD activity.

The activity of POD was determined as described by Maehly and Chance (1954). Three milliliter of reaction mixture contained 30 μl enzyme extract, 5.4 mM guaiacol, 50 mM sodium acetate buffer (pH 5.6), and 15 mM H_2O_2 . The oxidation of guaiacol to tetraguaiacol was contributed to the increase in absorbance monitored at 470 nm. A 0.01 absorbance increase per min at 470 nm was defined as one unit of POD activity.

The activity of CAT was measured following the method of Cakmak and Marschner (1992) by determining the rate of H_2O_2 disappearance at 240 nm. Three milliliter of reaction mixture contained 30 μl enzyme extract, 10 mM H_2O_2 and 50 mM phosphate buffer (pH 7.0). A 0.01 absorbance decrease per min at 240 nm was defined as one unit of CAT activity.

For each enzyme's activity, the data points are the average of three replicates. Three experiments were performed, and the results are consistent. The result from one set of experiments is presented here.

Salt and Osmotic Tolerance Assays

For salt tolerance assays, 2-week-old seedlings grown on half-strength MS agar medium were transferred into half-strength MS liquid medium for 2 weeks growth and then transferred into half-strength MS liquid medium supplemented with 175 mM NaCl and incubated at 22°C under long-day conditions for 2 days. After 2 days of NaCl treatment, the seedlings were transferred into half-strength MS liquid medium for 7 days recovery.

For PEG tolerance assays, 2-week-old seedlings grown on half-strength MS agar medium were transferred into half-strength MS liquid medium for 2 weeks of growth and then transferred into half-strength MS liquid medium supplemented with 25% PEG6000 (m/v) and incubated at 22°C under long-day conditions for 4 days. After 4 days of PEG treatment, the seedlings were transferred into half-strength MS liquid medium for 7 days recovery.

The transgenic rice and control seedlings were transplanted in the same pot for NaCl and PEG treatments. Three independent pots repeated at the same time and a representative result displayed in the manuscript. Three independent experimental replications were conducted.

Real-Time RT-PCR Analysis

For the real-time RT-PCR analysis, the same method was used as described in our previous studies (Jiang et al., 2012, 2014). We conducted three independent experiments (three biological replications and three technological replications in every independent experiment) and one representative result was displayed. All of the primer sequences used in real-time RT-PCR analysis were listed in Supplementary Table 1.

Statistical Analysis

Statistically significant differences ($*P < 0.05$) based on the Student's test computed by the SigmaPlot10.0. Data are the means \pm SE of three independent experiments (3 biological replications and three technological replications in every independent experiment).

RESULTS

Constitutive Expression of AtWRKY57 in Transgenic Rice Lines

In our previous study, we confirmed that overexpression of *AtWRKY57* significantly enhanced drought tolerance in *Arabidopsis* (Jiang et al., 2012). To explore whether *AtWRKY57* plays an important role in improving the agronomic traits through gene manipulation approaches, we introduced this gene to rice. More than 20 transgenic lines were generated and five lines were randomly selected to check *AtWRKY57* expression by northern blotting (Supplementary Figure 1). And then two lines, Line 3 and Line 5, were chosen for further analysis (Supplementary Figure 1). There were no significant differences in morphology between the control and transgenic plants (Figure 1A).

Improved Drought Tolerance in AtWRKY57 Transgenic Plants

The transgenic lines and control seeds were germinated simultaneously on half-strength MS agar medium containing 2% sucrose with or without hygromycin at 100 μ g/ml and then planted in soil after 1 week. Four-week-old plants were treated with natural drought stress (not supplied with water). The control plants showed wilting symptoms 6 days before the transgenic lines. After 14 days treatment, the transgenic plants did not display any drought-stress symptoms, while the wild-type plants exhibited severe drought symptoms (Figure 1B). Up to 20 days of treatment, the control showed obvious drought-stress symptoms (Figure 1C). When plants were re-watered, only 12.3% of control plants were survived and most of them never recovered; however, all of the transgenic rice plants survived (Figures 1D,E). These results suggested that these transgenic rice plants acquired significantly improved drought tolerance. Soil moisture contents and their dynamics showed in Supplementary Figure 2.

Transpiration water loss is an important factor related to drought tolerance. Flag leaves were detached and the changes

of fresh weight were determined over a 200-min period to assess the water loss rate of transgenic and control plants. A slower water loss rate was displayed in the transgenic lines' leaves than the control' (Figure 1F). The reduced water loss rate is favorable for an increased drought tolerance in the transgenic lines. In response to drought stress, stomata often close to limit water loss by transpiration. Given that water loss rate were lower in two transgenic lines than in control plants, we further investigated whether stomata density and/or stomata aperture affects this progress. White nail polish blotting was used to count the stomata density and measure stomata aperture. The ratio of stomatal width to length indicated the degree of stomatal closure. The results showed that the stomata density didn't displayed significant difference between control and two transgenic plants leaf adaxial surface (Supplementary Figures 3A,B). However, two transgenic lines' stomata showed more quick closure than control' under dehydration treatments (Supplementary Figure 3C). These results suggest that more quick closure of stomata in two transgenic lines result in the lower water loss rate, which may be critical for transgenic plants to adapt to drought stress.

The accumulation of proline in plant is associated with adaptation to environmental stress through metabolic adjustments (Ábrahám et al., 2003). We also checked the proline contents of transgenic and control plants under normal growth and drought-stress conditions to characterize the physiological basis for the improved stress tolerance. No differences in the proline contents were observed in the leaves of transgenic and control plants under normal conditions (Figure 1G). However, under drought conditions, transgenic plants began to accumulate proline after 14 days and further accumulated an up to fourfold higher proline content compared with the levels prior to drought stress, whereas control plants showed a low increase in proline. This result demonstrates that the proline accumulation corresponded to the increased drought tolerance of transgenic plants.

Decreasing the ROS Damage in AtWRKY57 Transgenic Plants

Leaves of control plants began to produce brownish lesions after 14 days of drought stress (Figure 2A). In contrast, none of the transgenic plants exhibited lesion formation grown under the same conditions. Lesion formation was accompanied by significant trypan blue staining that indicates cell death in the control leaves (Figure 2B).

Stress usually causes damage via oxidative damage in plants including the generation of ROS, represented as H_2O_2 and superoxide (Zhu, 2001; Mittler, 2002; Xiong and Zhu, 2002). As activation of *AtWRKY57* enhanced the drought tolerance of transgenic rice plants, we further determined whether *AtWRKY57* is involved in drought tolerance via ROS detoxification. Transgenic rice and control seedlings were subjected to DAB staining and NBT staining to detect H_2O_2 and superoxides in their leaves. After 14 days of drought stress, the transgenic plants had very few brown H_2O_2 and superoxide

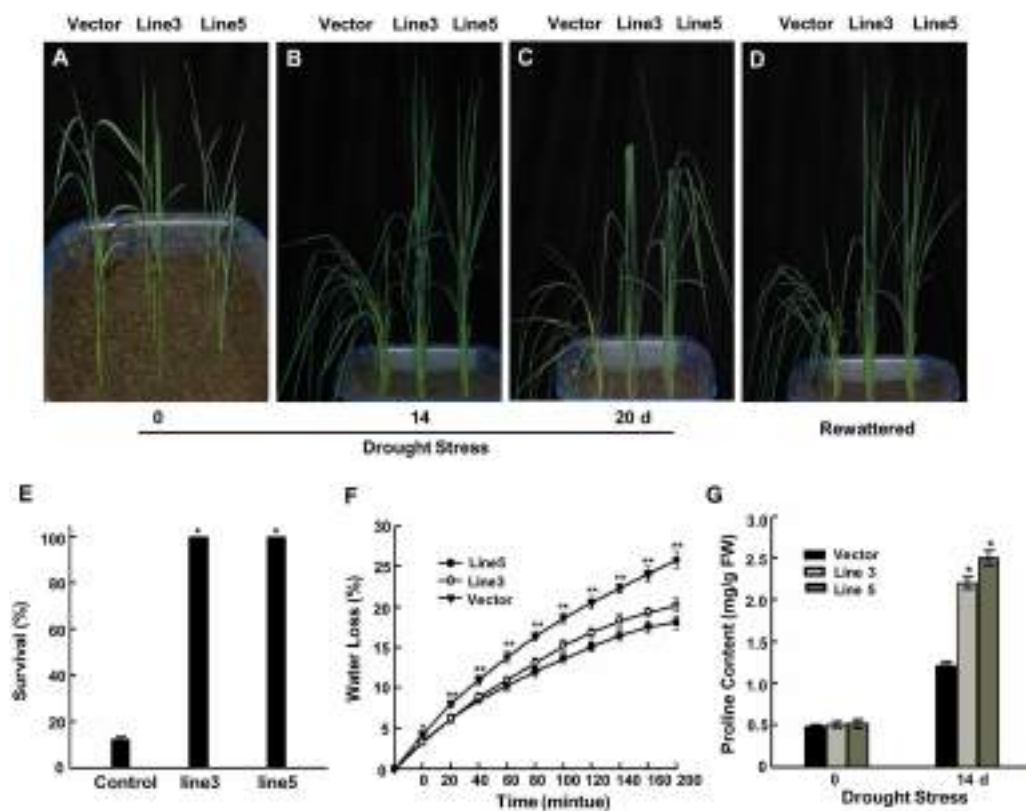


FIGURE 1 | Improved drought tolerance in AtWRKY57 transgenic rice. (A) Before drought treatment. **(B)** Drought for 14 days. **(C)** Drought for 20 days. **(D)** Recovery for 7 days after 20 days drought treatment. Drought stress was imposed on 4-week-old T3 transgenic seedlings in greenhouse. Drought experiments were repeated three times and at least 40 plants for each individual lines were used in each repeated experiment and one representative picture was shown. **(E)** Survival rate after 20 days drought stress. Values are mean \pm SE ($n = 40$ plants, $^*P < 0.05$). **(F)** Rate of water loss by detached leaves from control and transgenic plants. Values are the mean \pm SE ($n = 6$ plants, $^{**}P < 0.01$). **(G)** Proline content in the leaves of 4-week-old transgenic and control plants with or without drought treatments. Values are the mean \pm SE of three independent experiments ($^*P < 0.05$). FW, Fresh weight.

spots within the leaf segments, whereas more than half of the leaf area of the control plants became brown (Figures 2C,D). The leave segments of control plants displayed more brown areas than compared transgenic plants. These results confirmed that over-expressing *AtWRKY57* in rice could efficiently remove the H_2O_2 and superoxide produced during drought stress.

Malondialdehyde, acting as a biomarker for lipid peroxidation, is an effect of oxidative damage deriving from decomposition product of polyunsaturated fatty acid hydroperoxides. The MDA contents in transgenic lines and controls were similar under normal growth conditions, but there was a significant difference after drought stress. Then, the MDA contents of two *AtWRKY57* over-expressing lines were significantly lower than those of control plants (Figure 2E).

Electrolyte leakage, an indicator of membrane damage, was also measured following drought stress. The results showed that the leaves of two *AtWRKY57* over-expressing lines exhibited significantly lower electrolyte leakage levels, compared to those of control leaves (Figure 2F). After 14 days of drought stress, more than 60% of the ions leaked from cells in control plants, whereas the ion leakage of *AtWRKY57* over-expressing lines was less than 50%.

Overall, these results indicated that the over-expressing *AtWRKY57* gene in rice increased the tolerance to drought stress by decreasing ROS damage.

The Enhanced ROS-Scavenging Ability and High-Level Expression of Oxidative Enzyme Genes in *AtWRKY57* Transgenic Plants

A decreased cell viability and even cell death was resulted from the over-accumulation of ROS; therefore, scavenging ROS avoids or alleviates the harmful effects on plant under stress conditions. In the ROS-scavenging mechanisms of plants, POD, SOD, and CAT are key enzymes (Mittler, 2002; Xiong and Zhu, 2002; Apel and Hirt, 2004), and are involved in the H_2O_2 elimination. Following drought stress, the enzyme activities of seedlings were subjected to measurement. Under normal growth conditions, POD, SOD, and CAT activity levels were not different; however, after 14 days of drought stress, the activities of the antioxidative enzymes were all significantly enhanced in the *AtWRKY57*-overexpressing plants compared with those in the control plants (Figures 3A–C). These results suggested that over-expression of

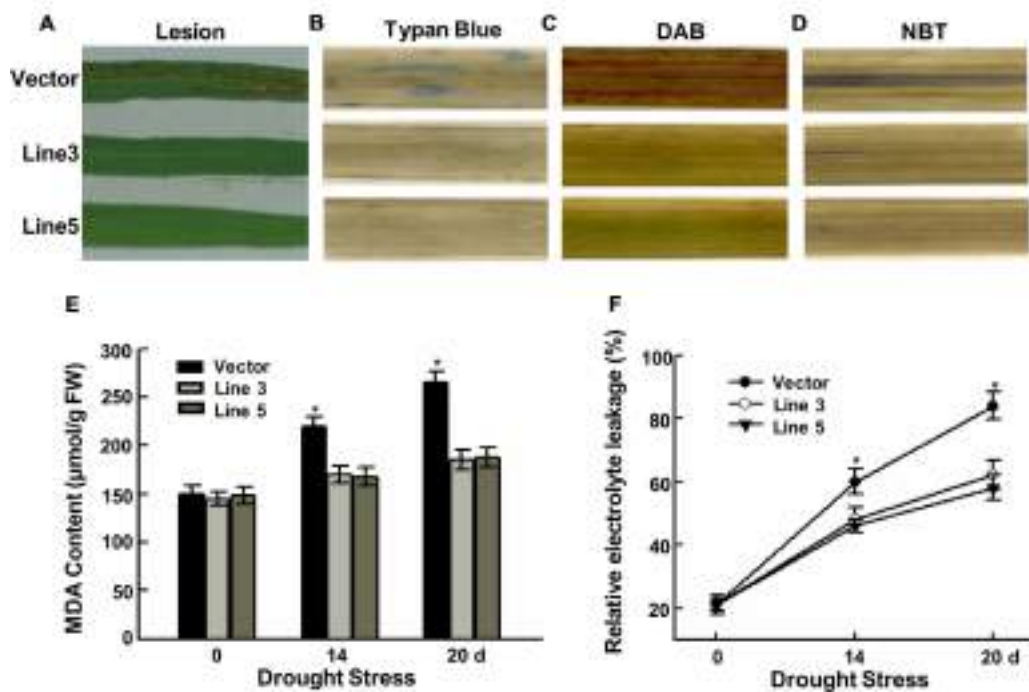


FIGURE 2 | Decreased the ROS damage in transgenic rice. Phenotype of brownish lesions (**A**), Typan blue staining (**B**), DAB staining (**C**) and NBT staining (**D**) after 14 days drought stress. (**E**) MDA content in the leaves of control and transgenic plants after 0, 14, and 20 days drought stress. Values are the mean \pm SE of three independent experiments (* $P < 0.05$). FW, Fresh weight. (**F**) Relative electrolyte leakage in the leaves of control and transgenic plants after 0, 14, and 20 days drought stress. Values are the mean \pm SE of three independent experiments (* $P < 0.05$).

AtWRKY57 gene may enhance the ROS-scavenging ability, which decreases ROS damage.

To test whether drought stress modifies transcript levels, the expression levels of several antioxidant genes were measured. Consistent with the increase of antioxidative enzymes activities, control and two transgenic plants up-regulated the transcript levels of *OsCAT B*, *OsCu/Zn-SOD1*, *OsCu/Zn-SOD2* and *OsPOD* in response to drought stress, with a greater increase in the transgenic plants (Figures 3D–G). This was enhancing the capacity to decompose H₂O₂ and superoxide in the leaves.

High-Level Expression of Stress-Response Genes in AtWRKY57 Transgenic Plants

To better understand the mechanisms of drought tolerance conferred by over-expressing *AtWRKY57*, the expressions of several stress-related genes were investigated. As shown in Figure 4A, the expression levels of a pyrroline-5-carboxylate synthesis gene (*OsP5CS*; Igarashi et al., 1997) were strongly induced in transgenic lines under drought stress compared with those in control plants. This higher expression level of *OsP5CS* was consistent with the higher proline content in two *AtWRKY57* overexpressing lines (Figure 1G). However, the expression level of an ABA synthesis gene (*OsNCED5*) was not significantly different in transgenic lines and control plants after drought stress (Figure 4B). Dehydration-responsive element-binding

(DREB) transcription factors play key important roles in plant-stress responses. DREB proteins encoding by *OsDREB1A* and *OsDREB2A* were strongly up-regulated in drought stress, with a greater increase in the transgenic plants compared to the control plants (Figures 4C,D). We also checked another two well-characterized drought resistance-related genes (*OsRab21* and *OsRab16D*), and found that they were significantly affected by water stress. Their expression levels were obviously higher in transgenic plants than in control after drought treatment (Figures 4E,F).

These results indicated that over-expressing *AtWRKY57* gene in rice may enhance the expression of some stress-response genes and finally increase the tolerance to drought stress.

Improved NaCl and PEG Tolerance in AtWRKY57 Transgenic Plants

Our results revealed that the constitutive expression of *AtWRKY57* enhanced the drought tolerance in rice (Figure 1). Given the function of WRKY-type regulators in abiotic stress, we further explored the functions of *AtWRKY57* in NaCl and PEG stress conditions. We tested the survival rates of transgenic and control plants on MS medium additionally added with 175 mM NaCl. The control plants displayed more severe phenotype, including leaf curves and dehydration, than the transgenic lines after 2 days of NaCl treatment (Figures 5A,B). When plants were recovered in fresh MS medium, none of the control plants survived but most of the transgenic lines reversed (Figure 5C;

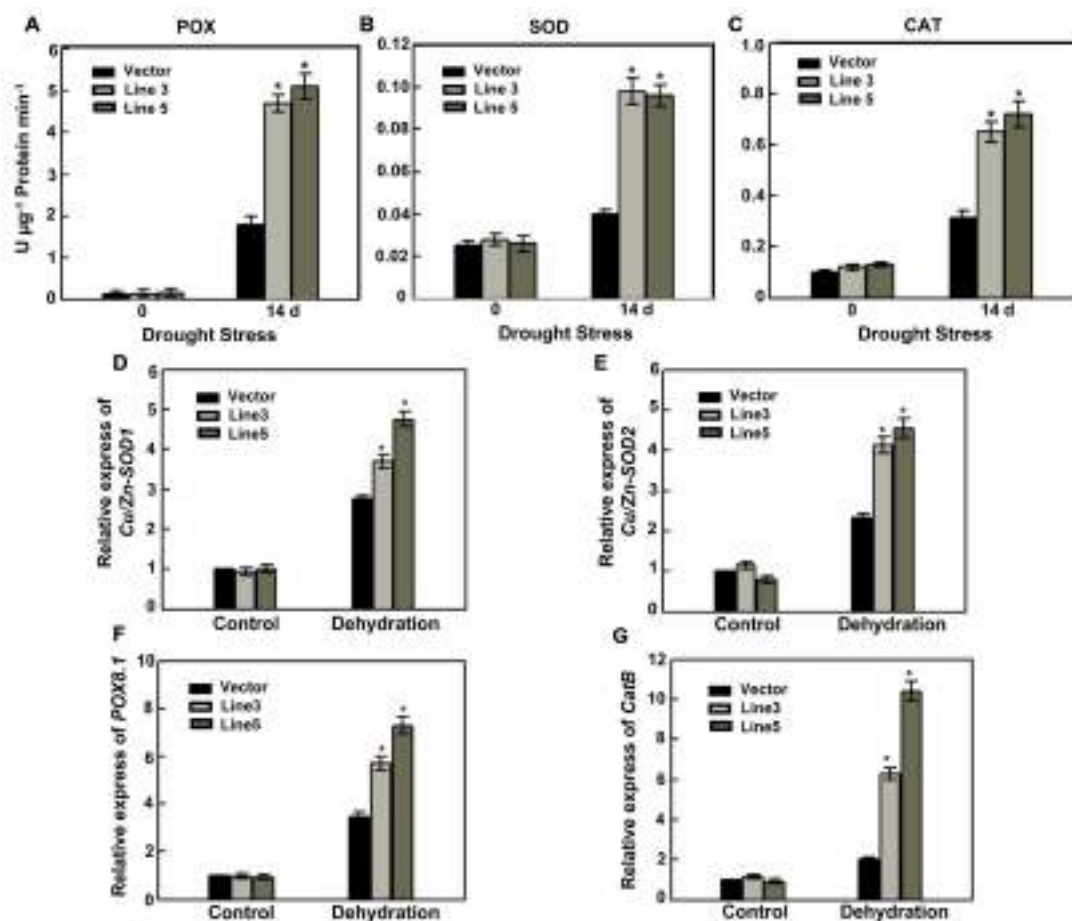


FIGURE 3 | Enhanced the ROS-scavenging ability and the expression of oxidative enzymes genes in transgenic rice. (A–C) POX, SOD, and CAT activities in the leaves of 4-week-old transgenic and control plants before and after drought stress. Values are the mean \pm SE of three independent experiments (* $P < 0.05$). FW, Fresh weight. Relative expression of oxidative enzymes genes *Cu/Zn-SOD1* (D), *Cu/Zn-SOD2* (E), *POX8.1* (F), and *CatB* (G) in the leaves of 4-week-old transgenic and control plants before and after drought stress. Values are the mean \pm SE of three independent experiments (* $P < 0.05$).

Supplementary Figure 4). We also tested the survival rate of transgenic lines and control plants on MS medium supplemented with 25% PEG6000. The control plants showed more severe phenotype than transgenic lines after 4 days PEG treatments (Figures 5D,E). When plants were recovered in fresh MS medium, none of the control plants survived, but all of the transgenic lines lived (Figures 5F,G; Supplementary Figure 5).

These results showed that consecutively expressing *AtWRKY57* enhanced not only drought tolerance but also the NaCl and PEG stress tolerance in rice.

DISCUSSION

Combination of abiotic and biotic stresses used to limit the production of crop. Drought severely restricts crop production as the most important abiotic stress (Boyer, 1982; Rockstrom and Falkenmark, 2000). In a previous study, we confirmed that over-expressing *AtWRKY57* significantly conferred drought tolerance in *Arabidopsis* (Jiang et al., 2012). These results suggested that

AtWRKY57 may improve crops' drought adaptability using gene manipulation. In this study, we evaluated the role of *AtWRKY57* in transgenic rice after drought stress.

The drought-tolerance phenotype of *AtWRKY57* transgenic rice plants were the result of a collection of physiological indexes observed in the over-expressing plants. *AtWRKY57* overexpressing plants displayed higher survival rates most likely because the water loss was reduced in these plants compared to control plants under drought conditions (Figure 1F). *P5CS*, catalyzing proline biosynthesis, is critical for the increasing of osmotolerance. Drought, salt, and abscisic acid induce the expression of *OsP5CS* and the conferred osmotolerance is resulting from an up-regulated expression of *OsP5CS* which increases proline content in transgenic plants (Xiang et al., 2007). The significantly higher transcript levels of *OsP5CS* were consistent with the high proline content in transgenic plants after drought stress (Figures 1G and 4A). These results confirmed that the transgenic plants' adaptation to drought stress was associated with mechanisms of dehydration avoidance through proline metabolic adjustments. Programmed

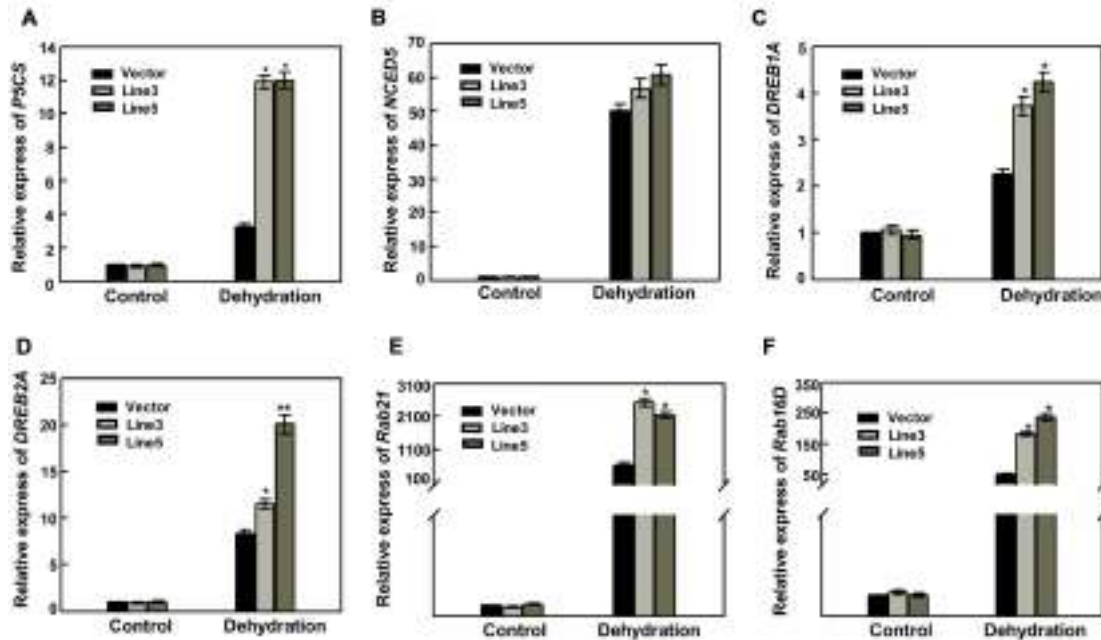


FIGURE 4 | High level expression of stress-responsive genes in transgenic rice. **(A–F)** Relative expression levels of *P5CS*, *NCED5*, *DREB1A*, *DREB2A*, *Rab21* and *Rab16D* in the leaves of 4-week-old transgenic and control plants before and after drought stress. Values are the mean \pm SE (* $P < 0.05$) of three independent experiments.

cell death (PCD) and lesion formation in some lesion mimic mutants, such as *lsl1*, was mainly caused from the elevated levels of extracellular superoxide (Jabs et al., 1996). We observed high levels of superoxide, H_2O_2 and cell death in control plants than in transgenic lines. We believe that the lesion formation in control plants results from their reduced capability to detoxify ROS compared with transgenic plants (Figure 2A). These results are similar to those of Yang et al. (2004), who reported that salicylic acid-deficient transgenic rice contains elevated levels of superoxide and H_2O_2 and exhibits spontaneous lesion formation in an age- and light-dependent manner.

Drought or salt-stress conditions promoted the accumulation of ROS in plants. MDA is often considered as a reflection of cellular membrane degradation or dysfunction and is also an important intermediary agent in ROS scavenging. Thus, high level of MDA causes PCD and induces toxicity to plant cells (Apel and Hirt, 2004; Hou et al., 2009). High ability of ROS-scavenging enzymes decreased over-accumulated ROS levels which induces PCD in plants (Mittler, 2002; Apel and Hirt, 2004; Chaves and Oliveira, 2004; Farooq et al., 2009; Hou et al., 2009). In *AtWRKY57* transgenic plants, lower levels of PCD, DAB and NBT staining, MDA content and relative electrolyte leakage were detected (Figures 2B–F), but increased SOD, POD, and CAT activity levels (Figures 3A–C) and elevated oxidative enzyme genes' transcript levels (Figures 3D–G) were detected after drought stress, demonstrating that they were better protected from oxidative damages through the enhanced capability to scavenge ROS.

The transcript levels for several stress-tolerant genes were more elevated in *AtWRKY57* transgenic rice than in control plants under drought-stress conditions (Figure 4). It is interesting that the relative transcript levels of *OsNCED5* and the ABA content were not significantly changed (Figure 4B; Supplementary Figure 6) in *AtWRKY57* transgenic plants under drought-stress conditions, which may demonstrate that there were different regulatory mechanisms in transgenic *Arabidopsis* and transgenic rice. Our previous study revealed that the activated expression of *AtWRKY57* conferred *Arabidopsis* transgenic plants drought tolerant by elevating the ABA contents through directly binding the promoter sequence of *AtNCED3* (Jiang et al., 2012). In this study, we found that the enhanced capability to scavenge ROS was important for *AtWRKY57* overexpressing transgenic rice plants to tolerate drought stress (Figures 2 and 3). Interestingly, there are increasing studies demonstrated that the same gene may have different regulatory functions and/or mechanisms when overexpressed in different plants species, such as in rice, cotton and *Arabidopsis*. For example, *OsWRKY45* overexpressing transgenic rice showed sensitivity to drought stress (Tao et al., 2011); however, heterologous overexpression of *OsWRKY45* in *Arabidopsis* conferred plants drought tolerant mainly resulting from the reduction of transpiration rate (Qiu and Yu, 2008). Overexpression of *OsSNAC1* enhanced drought tolerance of transgenic rice plants by targeting genes that control ROS homeostasis and stomatal closure (Yu et al., 2013), whereas overexpressing *OsSNAC1* rendered

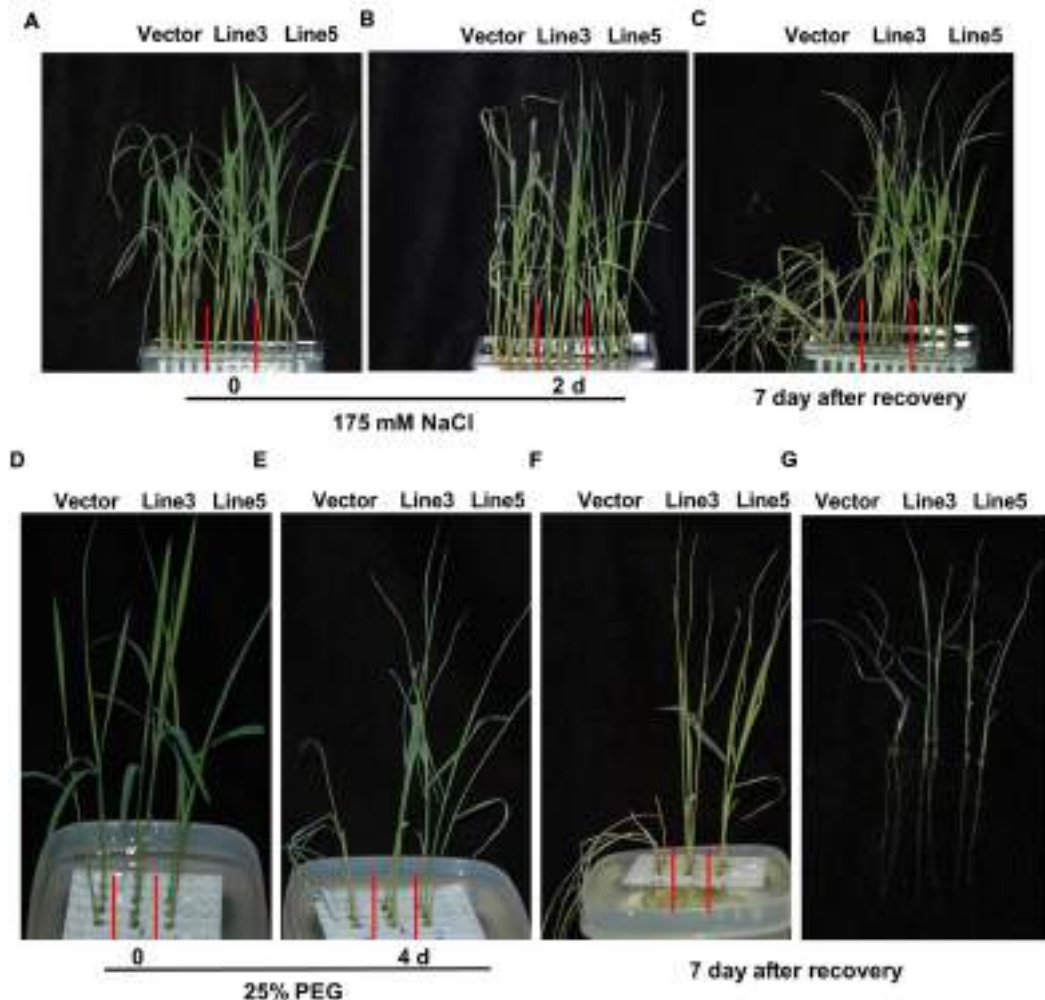


FIGURE 5 | Improved NaCl and PEG tolerance in transgenic rice. (A) Before NaCl treatment. **(B)** NaCl treatment for 2 days. **(C)** Recovery for 7 days after 2 days NaCl treatment. **(D)** Before PEG treatment. **(E)** PEG treatment for 4 days. **(F,G)** Recovery for 7 days after 4 days PEG treatment. NaCl and PEG stress was imposed on 4-week-old T3 transgenic seedlings under water culture conditions in greenhouse. Experiments were repeated three times and at least 30 plants for each individual lines were used in each repeated experiment and one representative picture was shown.

transgenic cotton plants more drought tolerance by reducing transpiration rate and enhancing root development (Liu et al., 2014). Heterologous expression of the *AtDREB1A* gene in peanut conferred transgenic plants drought and NaCl tolerance by upregulating proline synthesis to better osmotic adjustments (Sarkar et al., 2014), while the *AtDREB1A* transgenic *Arabidopsis* enhanced drought by activating some stress-related genes expression (Liu et al., 1998). Thus, it's possible that there may be diversified regulatory functions and/or mechanisms for one protein to regulate different physiological processes in different species under stress conditions.

WRKY transcription factors belong to a large family that functions under a variety of abiotic stresses. Our results provided evidences that overexpressing *AtWRKY57* also increased the tolerance to salt and PEG stresses (Figures 1 and 5), demonstrating that this is a potential candidate gene for

crop improvement. Recently, several studies confirmed that overexpression of some stress-related genes may enhance drought tolerance in rice (Dubouzet et al., 2003; Park et al., 2005; Chen et al., 2008; Hou et al., 2009; Huang et al., 2009; Cui et al., 2011; Gao et al., 2011; Yang et al., 2012; Zou et al., 2012). However, a persistent problem is that the constitutive over-expression of stress-related genes often result in abnormal development and thus reduces crop productivity (Kasuga et al., 1999; Hsieh et al., 2002; Dubouzet et al., 2003; Nakashima et al., 2007; Priyanka et al., 2010). The improvement in drought tolerance should be perfectible without limitation in plant growth and production (Cattivelli et al., 2008). Yu's study confirmed that the heterologous expression of *AtEDT1/HDG11* in rice significantly improved its drought tolerance and also simultaneously increased the grain yield under both normal and drought-stress conditions (Yu et al., 2013). In our study, *AtWRKY57* transgenic plants underwent normal development compared with controls

(Figure 1A), but we have not statistically analyzed the effects on productivity. Further studies should focus on the grain yield of transgenic plants under drought-stress conditions.

AUTHOR CONTRIBUTIONS

YJ designed and performed experiments, interpreted data, and wrote the article. DY designed experiments, and edited the article. YQ and YH interpreted data and edited the article. Both authors read and approved the final article.

REFERENCES

- Ábrahám, E., Rigó, G., Székely, G., Nagy, R., Koncz, C., and Szabados, L. (2003). Light dependent induction of proline biosynthesis by abscisic acid and salt stress is inhibited by brassinosteroid in *Arabidopsis*. *Plant Mol. Biol.* 51, 363–372. doi: 10.1023/A:1022043000516
- Apel, K., and Hirt, H. (2004). Reactive oxygen species: metabolism, oxidative stress, and signal transduction. *Annu. Rev. Plant Biol.* 55, 373–399. doi: 10.1146/annurev.arplant.55.031903.141701
- Asada, K. (1987). The water-water cycle in chloroplasts: scavenging of active oxygens and dissipation of excess photons. *Annu. Rev. Plant Physiol. Plant Mol. Biol.* 50, 601–639. doi: 10.1146/annurev.arplant.50.1.601
- Asada, K. (1999). The water-water cycle in chloroplasts: scavenging of active oxygen and dissipation of excess photons. *Annu. Rev. Plant Physiol. Plant Mol. Biol.* 50, 601–639. doi: 10.1146/annurev.arplant.50.1.601
- Bates, L. S. (1973). Rapid determination of free proline for water-stress studies. *Plant Soil* 39, 205–207. doi: 10.1016/j.dental.2010.07.006
- Beauchamp, C., and Fridovich, I. (1971). Superoxide dismutase: improved assays and an assay applicable to acrylamide gels. *Anal. Biochem.* 44, 276–287. doi: 10.1016/0003-2697(71)90370-8
- Boyer, J. S. (1982). Plant productivity and environment. *Science* 218, 443–448. doi: 10.1126/science.218.4571.443
- Cakmak, I., and Marschner, H. (1992). Magnesium deficiency and high light intensity enhance activities of superoxide dismutase, ascorbate peroxidase, and glutathione reductase in bean leaves. *Plant Physiol.* 98, 1222–1227. doi: 10.1104/pp.98.4.1222
- Cattivelli, L., Rizza, F., Badeck, F. W., Mazzucotelli, E., Mastrangelo, A. M., Francia, E., et al. (2008). Drought tolerance improvement in crop plants: an integrated view from breeding to genomics. *Field Crops Res.* 105, 1–14. doi: 10.3389/fpls.2015.00563
- Chaves, M. M., and Oliveira, M. M. (2004). Mechanisms underlying plant resilience to water deficits: prospects for water-saving agriculture. *J. Exp. Bot.* 55, 2365–2384. doi: 10.1093/jxb/erh269
- Chen, J. Q., Meng, X. P., Zhang, Y., Xia, M., and Wang, X. P. (2008). Over-expression of OsDREB genes lead to enhanced drought tolerance in Rice. *Biotechnol. Lett.* 30, 2191–2198. doi: 10.1007/s10529-008-9811-5
- Clarke, S. M., Mur, L. A. J., Wood, J. E., and Scott, I. M. (2004). Salicylic acid dependent signaling promotes basal thermotolerance but is not essential for acquired thermotolerance in *Arabidopsis thaliana*. *Plant J.* 33, 432–447. doi: 10.1111/j.1365-313X.2004.02054.x
- Cui, M., Zhang, W., Zhang, Q., Xu, Z., Zhu, Z., Duan, F., et al. (2011). Induced over-expression of the transcription factor OsDREB2A improves drought tolerance in rice. *Plant Physiol. Biochem.* 49, 1384–1391. doi: 10.1016/j.plaphy.2011.09.012
- Dempke, B., and Amabile-Cuevas, C. F. (1991). Redox redux: the control of oxidative stress responses. *Cell* 67, 837–839. doi: 10.1016/0092-8674(91)90355-3
- Desikan, R., Griffiths, R., Hancock, J. T., and Neill, S. (2002). A new role for an old enzyme: nitrate reductase-mediated nitric oxide generation is required for abscisic acid-induced stomatal closure in *Arabidopsis thaliana*. *Proc. Natl. Acad. Sci. U.S.A.* 99, 16314–16318. doi: 10.1073/pnas.252461999
- Dubouzet, J. G., Sakuma, Y., Ito, Y., Kasuga, M., Dubouzet, E. G., Miura, S., et al. (2003). OsDREB genes in rice, *Oryza sativa* L., encode transcription activators that function in drought-, high-salt- and cold-responsive gene expression. *Plant J.* 33, 751–763. doi: 10.1046/j.1365-313X.2003.01661.x
- Eulgem, T., Rushton, P. J., Robatzek, S., and Somssich, I. E. (2000). The WRKY superfamily of plant transcription factors. *Trends Plant Sci.* 5, 199–206. doi: 10.1016/S1360-1385(00)01600-9
- Eulgem, T., and Somssich, I. E. (2007). Networks of WRKY transcription factors in defense signaling. *Curr. Opin. Plant Biol.* 10, 366–371. doi: 10.1016/j.pbi.2007.04.020
- Farooq, M., Wahid, A., Lee, D. J., Ito, O., and Siddique, K. H. M. (2009). Advances in drought resistance of rice. *Crit. Rev. Plant Sci.* 28, 199–217. doi: 10.1080/07352680902952173
- Fitzgerald, H. A., Chern, M.-S., Navarre, R., and Ronald, P. C. (2004). Overexpression of (At)NPR1 in rice leads to a BTH- and environment-induced lesion-mimic/cell death phenotype. *Mol. Plant Microbe Interact.* 17, 140–151. doi: 10.1094/MPMI.2004.17.2.140
- Gao, T., Wu, Y., Zhang, Y., Liu, L., Ning, Y., Wang, D., et al. (2011). OsSDIR1 overexpression greatly improves drought tolerance in transgenic rice. *Plant Mol. Biol.* 76, 145–156. doi: 10.1007/s11103-011-9775-z
- Gasch, A. P., Spellman, P. T., Kao, C. M., Carmel-Harel, O., Eisen, M. B., Storz, G., et al. (2000). Genomic expression programs in the response of yeast cells to environmental changes. *Mol. Biol. Cell* 11, 4241–4257. doi: 10.1091/mbc.11.12.4241
- Heath, R. L., and Packer, L. (1968). Photoperoxidation in isolated chloroplasts. I. Kinetics and stoichiometry of fatty acid peroxidation. *Arch. Biochem. Biophys.* 125, 189–198. doi: 10.1016/0003-9861(68)90654-1
- Hiei, Y., Ohta, S., Komari, T., and Kumashiro, T. (1994). Efficient transformation of rice (*Oryza sativa* L.) mediated by Agrobacterium and sequence analysis of boundaries of the T-DNA. *Plant J.* 6, 271–282. doi: 10.1046/j.1365-313X.1994.6020271.x
- Hou, X., Xie, K., Yao, J., Qi, Z., and Xiong, L. (2009). A homolog of human skiing interacting protein in rice positively regulates cell viability and stress tolerance. *Proc. Natl. Acad. Sci. U.S.A.* 106, 6410–6415. doi: 10.1073/pnas.0901940106
- Hsieh, T. H., Lee, J. T., Charng, Y. Y., and Chan, M. T. (2002). Tomato plants ectopically expressing *Arabidopsis* CBF1 show enhanced resistance to water deficit stress. *Plant Physiol.* 130, 618–626. doi: 10.1104/pp.006783
- Huang, X. Y., Chao, D. Y., Gao, J. P., Zhu, M. Z., Shi, M., and Lin, H. X. (2009). A previously unknown zinc finger protein, DST, regulates drought and salt tolerance in rice via stomatal aperture control. *Genes Dev.* 23, 1805–1817. doi: 10.1101/gad.1812409
- Igarashi, Y., Yoshida, Y., Sanada, Y., Yamaguchi-Shinozaki, K., Wada, K., and Shinozaki, K. (1997). Characterization of the gene for D1-pyrrole-5-carboxylate synthetase and correlation between the expression of the gene and salt tolerance in *Oryza sativa* L. *Plant Mol. Biol.* 33, 857–865. doi: 10.1023/A:1005702408601
- Jabs, T., Dietrich, R. A., and Dangl, J. L. (1996). Initiation of runaway cell death in an *Arabidopsis* mutant by extracellular superoxide. *Science* 273, 1853–1856. doi: 10.1126/science.273.5283.1853

ACKNOWLEDGMENT

This work was supported by the Natural Science Foundation of China (31300252), the program for Innovative Research Team of Yunnan Province (2014HC017) and the West Light Foundation of Chinese Academy of Sciences.

SUPPLEMENTARY MATERIAL

The Supplementary Material for this article can be found online at: <http://journal.frontiersin.org/article/10.3389/fpls.2016.00145>

- Jiang, Y., Liang, G., Yang, S., and Yu, D. (2014). *Arabidopsis* WRKY57 functions as a node of convergence for jasmonic acid- and auxin-mediated signals in jasmonic acid-induced leaf senescence. *Plant Cell* 26, 230–245. doi: 10.1101/tpc.113.117838
- Jiang, Y. J., Liang, G., and Yu, D. Q. (2012). Activated expression of WRKY57 confers drought tolerance in *Arabidopsis*. *Mol. Plant* 5, 1375–1388. doi: 10.1093/mp/sss080
- Kasuga, M., Liu, Q., Miura, S., Yamaguchi-Shinozaki, K., and Shinozaki, K. (1999). Improving plant drought, salt, and freezing tolerance by gene transfer of a single stress-inducible transcription factor. *Nat. Biotechnol.* 17, 287–291. doi: 10.1038/7036
- Kreps, J. A., Wu, Y., Chang, H. S., Zhu, T., Wang, X., and Harper, J. F. (2002). Transcriptome changes for *Arabidopsis* in response to salt, osmotic, and cold stress. *Plant Physiol.* 130, 2129–2141. doi: 10.1104/pp.008532
- Liu, G., Jin, S., Liu, X., Zhu, L., Nie, Y., and Zhang, X. (2014). Overexpression of rice NAC gene SNAC1 improves drought and salt tolerance by enhancing root development and reducing transpiration rate in transgenic cotton. *PLoS ONE* 28:e86895. doi: 10.1371/journal.pone.0086895
- Liu, Q., Kasuga, M., Sakuma, Y., Abe, H., Miura, S., Yamaguchi-Shinozaki, K., et al. (1998). Two transcription factors, DREB1 and DREB2, with an EREBP/AP2 DNA binding domain separate two cellular signal transduction pathways in drought- and low-temperature-responsive gene expression, respectively, in *Arabidopsis*. *Plant Cell* 10, 1391–1406. doi: 10.2307/3870648
- Maehly, A., and Chance, B. (1954). The assay of catalases and peroxidases. *Methods Biochem. Anal.* 1, 357–424. doi: 10.1002/9780470110171.ch14
- Miller, G., Shulaev, V., and Mittler, R. (2008). Reactive oxygen signaling and abiotic stress. *Physiol. Plant.* 133, 481–489. doi: 10.1111/j.1399-3054.2008.01090.x
- Mittler, R. (2002). Oxidative stress, antioxidants and stress tolerance. *Trends Plant Sci.* 7, 405–410. doi: 10.1016/S1360-1385(02)02312-9
- Mittler, R., Vanderauwera, S., Gollery, M., and Breusegem, F. (2004). Reactive oxygen gene network of plants. *Trends Plant Sci.* 9, 490–498. doi: 10.1016/j.tplants.2004.08.009
- Nakashima, K., Tran, L. S., Nguyen, D., Fujita, M., Maruyama, K., Todaka, D., et al. (2007). Functional analysis of a NAC-type transcription factor OsNAC6 involved in abiotic and biotic stress responsive gene expression in rice. *Plant J.* 51, 617–630. doi: 10.1111/j.1365-313X.2007.03168.x
- Nelson, D. E., Repetti, P. P., Adams, T. R., Creelman, R. A., Wu, J., Warner, D. C., et al. (2007). Plant nuclear factor Y(NF-Y) B subunits confer drought tolerance and lead to improved corn yields on water-limited acres. *Proc. Natl. Acad. Sci. U.S.A.* 104, 16450–16455. doi: 10.1073/pnas.0707193104
- Ouyang, S. Q., Liu, Y. F., Liu, P., Lei, G., He, S. J., Ma, B., et al. (2010). Receptor-like kinase OsSIK1 improves drought and salt stress tolerance in rice (*Oryza sativa*) plants. *Plant J.* 62, 316–329. doi: 10.1111/j.1365-313X.2010.04146.x
- Park, S., Li, J. S., Pittman, J. K., Berkowitz, G. A., Yang, H. B., Undurraga, S., et al. (2005). Up-regulation of a H+-pyrophosphatase (H+-PPase) as a strategy to engineer drought-resistant crop plants. *Proc. Natl. Acad. Sci. U.S.A.* 102, 18830–18835. doi: 10.1073/pnas.0509512102
- Priyanka, B., Sekhar, K., Reddy, V. D., and Rao, K. V. (2010). Expression of pigeonpea hybrid-proline-rich protein encoding gene (CcHyPRP) in yeast and *Arabidopsis* affords multiple abiotic stress tolerance. *Plant Biotechnol. J.* 8, 76–87. doi: 10.1111/j.1467-7652.2009.00467.x
- Qiu, Y. P., and Yu, D. Q. (2008). Over-expression of the stress-induced OsWRKY45 enhances disease resistance and drought tolerance in *Arabidopsis*. *Environ. Exp. Bot.* 65, 35–47. doi: 10.1016/j.envexpbot.2008.07.002
- Raychaudhuri, S. S., and Deng, X. W. (2000). The role of superoxide dismutase in combating oxidative stress in higher plants. *Bot. Rev.* 66, 89–98. doi: 10.1007/BF02857783
- Ren, X. Z., Chen, Z. Z., Liu, Y., Zhang, H. R., Zhang, M., Liu, Q., et al. (2010). ABO3, a WRKY transcription factor, mediates plant responses to abscisic acid and drought tolerance in *Arabidopsis*. *Plant J.* 63, 417–429. doi: 10.1111/j.1365-313X.2010.04248.x
- Rockstrom, J., and Falkenmark, M. (2000). Semiarid crop production from a hydrological perspective: gap between potential and actual yields. *Crit. Rev. Plant Sci.* 19, 319–346. doi: 10.1080/07352680091139259
- Sarkar, T., Thankappan, R., Kumar, A., Mishra, G., and Dobarla, J. R. (2014). Heterologous expression of the atdreb1a gene in transgenic peanut-conferred tolerance to drought and salinity stresses. *PLoS ONE* 9:e110507. doi: 10.1371/journal.pone.0110507
- Scandalios, J. G. (2002). The rise of ROS. *Trends Biochem. Sci.* 27, 483–486. doi: 10.1016/S0968-0004(02)02170-9
- Seki, M., Narusaka, M., Ishida, J., Nanjo, T., Oono, Y., Kamiya, A., et al. (2002). Monitoring the expression profiles of 7000 *Arabidopsis* genes under drought, cold and high-salinity stresses using a full-length cDNA microarray. *Plant J.* 31, 279–292. doi: 10.1046/j.1365-313X.2002.01359.x
- Takasaki, H., Maruyama, K., Kidokoro, S., Ito, Y., Fujita, Y., Shinozaki, K., et al. (2010). The abiotic stress-responsive NAC-type transcription factor OsNAC5 regulates stress-inducible genes and stress tolerance in rice. *Mol. Genet. Genomics* 284, 173–183. doi: 10.1007/s00438-010-0557-0
- Tao, Z., Kou, Y. J., Liu, H. B., Li, X. H., Xiao, J. H., and Wang, S. P. (2011). OsWRKY45 alleles play different roles in abscisic acid signalling and salt stress tolerance but similar roles in drought and cold tolerance in rice. *J. Exp. Bot.* 62, 4863–4874. doi: 10.1093/jxb/err144
- Umezawa, T., Fujita, M., Fujita, Y., Yamaguchi-Shinozaki, K., and Shinozaki, K. (2006). Engineering drought tolerance in plants: discovering and tailoring genes to unlock the future. *Curr. Opin. Biotechnol.* 17, 113–122. doi: 10.1016/j.copbio.2006.02.002
- Verslues, P. E., Agarwal, M., Katiyar-Agarwal, S., Zhu, J. H., and Zhu, J. K. (2006). Methods and concepts in quantifying resistance to drought, salt and freezing, abiotic stresses that affect plant water status. *Plant J.* 45, 523–539. doi: 10.1111/j.1365-313X.2005.02593.x
- Wu, K. L., Guo, Z. J., Wang, H. H., and Li, J. (2005). The WRKY family of transcription factors in rice and *Arabidopsis* and their origins. *DNA Res.* 12, 9–26. doi: 10.1093/dnarese/12.1.9
- Xiang, Y., Huang, Y., and Xiong, L. (2007). Characterization of stress-responsive CIPK genes in rice for stress tolerance improvement. *Plant Physiol.* 144, 1416–1428. doi: 10.1104/pp.107.101295
- Xiong, L., and Zhu, J. K. (2002). Molecular and genetic aspects of plant responses to osmotic stress. *Plant Cell Environ.* 25, 131–139. doi: 10.1046/j.1365-3040.2002.00782.x
- Yang, A., Dai, X. Y., and Zhang, W. H. (2012). A R2R3-type MYB gene, OsMYB2, is involved in salt, cold, and dehydration tolerance in rice. *J. Exp. Bot.* 63, 2541–2556. doi: 10.1093/jxb/err431
- Yang, Y. N., Qi, M., and Mei, C. S. (2004). Endogenous salicylic acid protects rice plants from oxidative damage caused by aging as well as biotic and abiotic stress. *Plant J.* 40, 909–919. doi: 10.1111/j.1365-313X.2004.02267.x
- Yu, H., Chen, X., Hong, Y. Y., Wang, Y., Xu, P., Ke, S. D., et al. (2008). Activated expression of an *Arabidopsis* HD-START protein confers drought tolerance with improved root system and reduced stomatal density. *Plant Cell* 20, 1134–1151. doi: 10.1105/tpc.108.058263
- Yu, L. H., Chen, X., Wang, Z., Wang, S. M., Wang, Y. P., Zhu, Q. S., et al. (2013). *Arabidopsis* enhanced drought tolerance1/HOMEODOMAIN GLABROUS11 confers drought tolerance in transgenic rice without yield penalty. *Plant Physiol.* 162, 1378–1391. doi: 10.1104/pp.113.217596
- Zhang, L., Xiao, S. S., Li, W., Feng, W., Li, J., Wu, Z. D., et al. (2011). Overexpression of a Harpin-encoding gene hrfl in rice enhances drought tolerance. *J. Exp. Bot.* 62, 4229–4238. doi: 10.1093/jxb/err131
- Zhu, J. K. (2001). Plant salt tolerance. *Trends Plant Sci.* 6, 66–72. doi: 10.1016/S1360-1385(00)01838-0
- Zhu, J. K. (2002). Salt and drought stress signal transduction in plants. *Annu. Rev. Plant Biol.* 53, 247–273. doi: 10.1146/annurev.arplant.53.091401.143329
- Zou, J., Liu, C. F., Liu, A. L., Zou, D., and Chen, X. B. (2012). Overexpression of OsHsp17.0 and OsHsp23.7 enhances drought and salt tolerance in rice. *J. Plant Physiol.* 169, 628–635. doi: 10.1016/j.jplph.2011.12.014

Conflict of Interest Statement: The authors declare that the research was conducted in the absence of any commercial or financial relationships that could be construed as a potential conflict of interest.

Copyright © 2016 Jiang, Qiu, Hu and Yu. This is an open-access article distributed under the terms of the Creative Commons Attribution License (CC BY). The use, distribution or reproduction in other forums is permitted, provided the original author(s) or licensor are credited and that the original publication in this journal is cited, in accordance with accepted academic practice. No use, distribution or reproduction is permitted which does not comply with these terms.



Soybean C2H2-Type Zinc Finger Protein GmZFP3 with Conserved QALGGH Motif Negatively Regulates Drought Responses in Transgenic *Arabidopsis*

OPEN ACCESS

Edited by:

Olivier Lamotte,
Centre National de la Recherche
Scientifique, France

Reviewed by:

Lionel Verdoucq,
Centre National de la Recherche
Scientifique, France
Cheng Xianguo,
Chinese Academy of Agricultural
Sciences, China

*Correspondence:

Dayong Zhang
cotton.z@126.com;
Hongbo Shao
shaohongbuchu@126.com;
Hongxiang Ma
mahx@jaas.ac.cn

[†]These authors have contributed
equally to this work.

Specialty section:

This article was submitted to
Plant Physiology,
a section of the journal
Frontiers in Plant Science

Received: 16 September 2015

Accepted: 03 March 2016

Published: 18 March 2016

Citation:

Zhang D, Tong J, Xu Z, Wei P, Xu L,
Wan Q, Huang Y, He X, Yang J,
Shao H and Ma H (2016) Soybean
C2H2-Type Zinc Finger Protein
GmZFP3 with Conserved QALGGH
Motif Negatively Regulates Drought
Responses in Transgenic *Arabidopsis*.
Front. Plant Sci. 7:325.
doi: 10.3389/fpls.2016.00325

Dayong Zhang^{1*†}, Jinfeng Tong^{2†}, Zhaolong Xu¹, Peipei Wei¹, Ling Xu¹, Qun Wan¹,
Yihong Huang¹, Xiaolan He¹, Jiayin Yang³, Hongbo Shao^{1,4*} and Hongxiang Ma^{1*}

¹ Jiangsu Key Laboratory for Bioresources of Saline Soils, Provincial Key Laboratory of Agrobiology, Institute of Biotechnology, Jiangsu Academy of Agricultural Sciences, Nanjing, China, ² Institute of Botany, Chinese Academy of Sciences, Nanjing, China, ³ Huaiyin Institute of Agricultural Sciences of Xuhuai Region in Jiangsu, Huai'an, China, ⁴ Key Laboratory of Coastal Biology and Bioresources Utilization, Yantai Institute of Coastal Zone Research, Chinese Academy of Sciences, Yantai, China

Plant response to environmental stresses is regulated by a complicated network of regulatory and functional genes. In this study, we isolated the putative stress-associated gene *GmZFP3* (a C2H2-type Zinc finger protein gene) based on the previous finding that it was one of two genes located in the QTL region between the Satt590 and Satt567 markers related to soybean tolerance to drought. Temporal and spatial expression analysis using quantitative real-time PCR indicated that *GmZFP3* was primarily expressed in roots, stems and leaf organs and was expressed at low levels in flowers and soybean pods. Moreover, *GmZFP3* expression increased in response to polyethylene glycol (PEG) and Abscisic acid (ABA) treatments. In addition, subcellular localization analysis indicated that *GmZFP3* was ubiquitously distributed in plant cells. Transgenic experiments indicated that *GmZFP3* played a negative role in plant tolerance to drought. Analysis of ABA-related marker gene expression in *Arabidopsis* suggested that *GmZFP3* might be involved in the ABA-dependent pathway during the drought stress response. Taken together, these results suggest that soybean *GmZFP3* negatively regulates the drought response.

Keywords: Soybean, *GmZFP3*, transgenic *Arabidopsis*, drought response, negatively

INTRODUCTION

Plants are frequently exposed to a variety of stresses due to environmental changes, and they have evolved efficient mechanisms to adapt to these conditions. Drought is a serious environmental stress factor worldwide (Shao et al., 2009; Harrison et al., 2014). Consequently, it is important to maximize crop yield potential and maintain yield stability under drought conditions to guarantee a food supply for the increasing global population.

The zinc-finger protein (ZFP) family is one of the largest family of transcription factors in plants (Takatsuji, 1999; Iuchi et al., 2001). Among them, the Cys2/His2 (C2H2) zinc finger protein, which typically contains one to four conserved QALGGH motifs in the zinc-finger helices,

is a well-characterized eukaryotic transcription factor (Laity et al., 2001) that play various roles in the plant stress response (Kim et al., 2001; Sakamoto et al., 2004; de Lorenzo et al., 2007; Xu et al., 2007; Ciftci-Yilmaz and Mittler, 2008). In *Arabidopsis*, several C2H2-type ZFPs, such as AZF1, AZF2, AZF3, ZAT6, ZAT7, and ZAT10, have been reported to function in the drought and salt stress response (Sakamoto et al., 2000; Ciftci-Yilmaz et al., 2007). Expression of AZFs (AZF1-3) and STZ are strongly induced by dehydration, high-salt, cold stresses, and abscisic acid (ABA) treatment, and they function as transcriptional repressors to increase stress tolerance following growth retardation (Sakamoto et al., 2004). ZAT12 plays a role in ROS and abiotic stress signaling transduction (Davletova et al., 2005). ZAT10 has dual roles, as both overexpression and RNAi largely increased plant tolerance to environmental stresses (Mittler et al., 2006). AZF2 has been identified as an ABA-induced transcriptional repressor during seed germination (Kodaira et al., 2011). However, MPK6 phosphorylation regulates ZAT6 during seed germination under salt and osmotic stress (Liu et al., 2013).

Huang et al. (2009) cloned and characterized rice *DST* (Drought and salt tolerance) and found that it negatively regulated stomatal closure by binding to the TGCTANNATTG element and directly modulated H₂O₂ homeostasis-related gene. However, Jan et al. (2013) found that rice CCCH-Type OsTZF1 bound to the RNA poly(u) rich region in an *in vitro* RNA gel electrophoresis assay. Several recent reports used transgenic approaches to show that rice ZFP proteins, such as ZFP179 (Sun et al., 2010), ZFP182 (Zhang et al., 2012), and ZFP36 (Zhang et al., 2014), are involved in the ABA-dependent pathway to regulate the response to drought and salt and oxidative stresses. These reports revealed that zinc finger proteins play an important role in withstanding many stresses and plant growth and development.

Luo et al. (2012) cloned soybean *GsZFP1* from *Glycine soja* and found that it played a crucial role in the plant response to cold and drought stress. They further found that *GsZFP1* over-expression in *Arabidopsis* reduced ABA sensitivity and decreased stomata size under ABA treatment. Kim et al. (2001) found that the C2H2-type protein SCOF-1 was specifically induced by low temperature and ABA, but not by dehydration or salinity. Furthermore, SCOF-1 interacted with SGBF-1 in a yeast two-hybrid system, suggesting that SCOF-1 functions as a positive regulator of ABRE-mediated COR gene expression through protein-protein interactions, which in turn, enhances plant cold tolerance. Yu et al. (2014) reported that soybean GmZF1 enhanced *Arabidopsis* tolerance to cold stress by regulating cold-regulation gene expression.

Specht et al. (2001) identified a WUE (Water Use Efficiency)-related QTL region between the Satt590 and Satt567 markers on chromosome 7 in soybean, and the Glyma07g01900 and Glyma07g05820 gene loci were borders of this QTL region.

Abbreviations: PEG, Polyethylene glycol; GFP, Green Fluorescent Protein; ZFP, Zinc-finger protein; CTAB, hexadecyltrimethylammonium bromide; QTL, quantitative trait locus; RT-PCR, Reverse Transcription-Polymerase Chain Reaction; QRT-PCR, Quantitative reverse transcriptase Chain Reaction; ABA, Abscisic acid; SEM, Scanning electron microscope.

All 393 genes between these two loci were downloaded using the Perl program and isolated. One such gene was *GmZFP3*, a putative stress-associated gene, was selected for further study. *GmZFP3* was primarily expressed in the root and stem, while *GmZFP3* protein was ubiquitously distributed among plant cells. Transgenic experiments indicated that *GmZFP3* played a negative role in plant tolerance to drought and that it might be involved in the ABA-dependent pathway during response to drought stress.

MATERIALS AND METHODS

Plant Materials

The *Glycine max* var. Willimas 82 variety was used to grow seedlings and extract total RNA for *GmZFP3* gene cloning, tissue expression and induced expression analysis experiments. *Arabidopsis* ecotype Col-0 was used for transformation and protoplast preparation and grown in a 7:2:1(v/v/v) mixture of vermiculite: soilrite: perlite under a 16 h light/ 8 h dark regime. The day/light temperature was 23/20°C. Plants were watered every week.

DNA and RNA Isolation

Genomic DNA was extracted from fresh leaves using the cetyltrimethylammonium bromide (CTAB) method. Total RNA was extracted from soybean and *Arabidopsis* samples according to the TRIZOL Kit (Invitrogen, China) manual.

Gene Cloning and Sequence Analysis

The QTL region sequences between markers Satt590 and Satt567 related to soybean drought tolerance were downloaded from <http://www.phytozome.net/cgi-bin/gbrowse/soybean/> using the perl program. The functional annotation of genes was confirmed with BLAST2GO software. The *GmZFP3* gene primers (see Table 1) were designed according to the full-length coding sequence and used to clone the genes from soybean root tissue cDNA using RT-PCR (Reverse transcriptase-polymerase chain reaction).

The Neighbor Joining (NJ) tree of ZFPs from soybean and other plants was performed using MEGA4 software (Tamura et al., 2007).

RT-PCR and qPCR Analysis

The soybean root, stem, and leaf from three different stages, including young seedling stage, flowering stage, and podding stage, were harvested and frozen in liquid nitrogen for RNA extraction. The soybean roots were collected from plants treated with PEG6000 for 0, 2, 4, and 12 h or with 100 μM ABA for 10, 20, 30, 45, 60, 90, and 120 min. The method was the same for all samples, including *Arabidopsis*. Total RNA from all samples was isolated using TRIzol® reagent (Invitrogen) following the manufacturer's instructions. Single-stranded cDNA was synthesized using 2 μg total RNA and Oligo(dT)18 primer with the Takara RT-PCR system in a total volume of 25 μl according to the manufacturer's protocol (TaKaRa Bio Inc.) and used for RT-PCR and qRT-PCR analysis. RT-PCR and qPCR analysis was performed as described previously (Zhang et al., 2013).

TABLE 1 | Primer sequences used in this study.

Gene	Forward primer 5'-3'	Reverse primer 5'-3'	Purpose
GmZFP3	ATCAACACTCAAACAAAGACGAA	GAGTATGTGTGCCAAAATCTGC	Semi-RT-PCR and QRT-PCR
GmZFP3	CGCGTCGACATGCCCTCTGAAAATT	CGCCCATGGGAGCTTAAGGGACAAG	Subcellular localization in Arabidopsis protoplast
GmZFP3	CACCATGCCCTCTGAAAATTGAA	AGCTTAAGGGACAAGTCAAGCTT	Subcellular localization in tobacco leaf
GmZFP3	GGGGACAAGTTGTC AAAAAGCAGGCTTC ACCATGCCCTCTGAAAATTGAA	GGGGACCACCTTGACAA GAAAGCTGGGTT GAGCTTAAGGGACAAGTCAAG	Overexpression (OE)
GmActin	CGGTGGTCTATCTGGCATC	GTCTTCGCTCAATAACCCTA	qRT-PCR (internal control)

TABLE 2 | List of primers for stress-related genes and internal control in *Arabidopsis*.

Gene	Locus	Forward primer (5'-3')	Reverse primer (5'-3')
CCA1	AT2G46830	TGTGGCTCAAACACTCCG	GCAATTGACCCCTCGTCA
LHY	AT1G01060	AAGTCTCCGAAGAGGGTC	CATGTTCCAACACCGATC
UGT71B6	AT3G21780	TTTGATGGAGCAAGACAG	GTTTCCGACCAAGCAATA
DREB2A	AT5G05410	AACAGAAGGAGCAAGGGAT	ACATCGTCGCCATTAGG
MYB2	AT2G47190	ACGCCCAATCATTACCCA	AACCTGACCCGTTACCA
PAD3	AT3G26830	TATGCGATGGGTCGTGAT	TTGGCTTCCTCTGCTT
RCI3	AT1G05260	AGCCTCAACGATAACAAG	TGAAACAGACCTCTACGC
LTP3	AT5G59320	ATGTGGCACAGTGGCAGGTA	CTTGTGGCGGTCTGGTG
At5g02840	NM_120362	TATTCACCAGAACAGTGA	CACTCCCAATGAAGTTAT
AtActin2	NM_112764.3	CCTCCGTCTGACCTTGC	AGCGATACTGAGAACATAGTG

One microliter of the cDNA mix was used as a template in a 25 μ L PCR reaction volume. The RT-PCR condition was 94°C, 3 min, and 27 cycles of 94°C, 30 s; 55°C, 30 s; 72°C, 0.5 min, with a final extension of 10 min at 72°C. PCR products were separated on 1% agarose gel containing ethidium bromide and were photographed. For qPCR analysis, equal amount of cDNA prepared was analyzed by quantitative Real-Time PCR using a Roche 2.0 Real-Time PCR Detection System with the SYBR Green Supermix (Takara).

The assays were repeated three times. *Arabidopsis* primers are listed in **Table 2**.

Subcellular Localization

PCR-generated *Sal1-Nco1* and *Hind III-BamH1* fragments containing the open reading frame of *GmZFP3*, respectively, were subcloned in-frame upstream of the GFP gene in the pJIT166GFP plasmid. All constructs were validated by sequencing. The primer sequences are listed in **Table 1**.

Arabidopsis leaf protoplasts were isolated according to Yoo et al. (2007). The two resulting fusion constructs or empty control vector (p35S::GFP) were introduced into *Arabidopsis* protoplasts by the PEG4000-mediated method (Abel and Theologis, 1994). After incubation of transformed *Arabidopsis* protoplasts for 18–24 h at room temperature, GFP signal was detected by confocal fluorescence microscopy (Zeiss, LSM510 Meta, Carl Zeiss AG).

To further validate *GmZFP3* localization, full-length *GmZFP3* CDS lacking a stop codon (primers used are listed in **Table 1**) were amplified and cloned into the pMDC83 destination vector using the Gateway™ method. The in-frame GFP fusion

constructs were transformed into the *Agrobacterium tumefaciens* GV3101 strain by electroporation and injected into the tobacco leaf. GFP signal was examined by confocal fluorescence microscopy (Zeiss, LSM510 Meta, Carl Zeiss AG). Nuclei were stained with DAPI (4',6-diamidino-2-phenylindole).

Transformation of *Arabidopsis*

The *Agrobacterium* strain containing the pearlygate103-*GmZFP3* construct was grown on Luria-Bertani plates containing 50 mg/L kanamycin and 100 mg/L rifampicin at 28°C for 48 h. A single colony was transferred to 5 mL DYT medium containing the same antibiotics and was cultured overnight at 28°C with vigorous shaking (180 rpm). The overnight culture was added to 500 mL of the same medium and cultured overnight to an OD₆₀₀ of 0.5 to 1. *Agrobacterium* cells were harvested by centrifugation for 15 min (4000 rpm, 4°C) and re-suspended in infiltration medium (5.0% Suc and 0.05% Silwet L-77). *Arabidopsis* plants were transformed by the floral dip method (Clough and Bent, 1998). Transgenic plants were selected on selective medium containing kanamycin. Transgenic plants were transferred to soil and grown until seed harvest.

Architecture Parameter Measurements

Before treatment, the total root length, water loss rate from 0 to 24 h, stomatal width/length and density were measured in *GmZFP3*-overexpressing transgenic *Arabidopsis* plants and WT control plants. After air drought treatment application, including no watering and rewatering, the phenotype change of transgenic, and wild type were recorded using camera (Canon, Japan). The experiments were repeated independently at least three times.

SEM Observation and Statistical Analysis

Leaves from ~3-week-old non-transgenic and transgenic GmZFP3 *Arabidopsis* plants were stripped and serially dehydrated for 30 min each in 30, 50, 70, 80, 90, and 100% ethanol solutions. They were then placed in isoamyl acetate three times for 30 min each. Thereafter, samples were freeze-dried (Hitachi ES-2030, Tokyo, Japan) and sputter-coated with silver using an ion sputter (Hitachi E-1010/E-1020), then the specimens were observed by SEM (Hitachi S-3000N). Each specimen was observed at an accelerating voltage of 15 KV, and images were stored as TIF files. The width/length, density, and open/close status of stoma were measured using WinRhizo software (Regent Instruments, Montreal, QC, Canada).

Statistical Analysis

Data were analyzed using an one-way ANOVA test in Microsoft Excel. Significant differences among means were determined by the LSD (Least Significant Difference),* at $P < 0.05$ and ** at $P < 0.01$.

RESULTS

Isolation and Characterization of GmZFP3

We cloned and sequenced the putative drought-associated gene *GmZFP3* from soybean. Sequence analysis indicated that the GmZFP3 protein contains one zinc finger motif and one conserved QALGGH motif. Phylogenetic tree analysis of GmZFP3 and other ZFP proteins from other plants, including *Triticum aestivum*, *G. soja*, *Ricinus communis*, *Medicago truncatula*, and *Cicer arietinum*, showed that GmZFP3 was most similar to ZFP3 proteins from *M. truncatula* and *C. arietinum* (Figure 1). Thus, we designated GmZFP as GmZFP3. We then analyzed *GmZFP3* expression in various tissues/organs at different developmental stages of soybean cv. Willimas 82 by qRT-PCR. *GmZFP3* transcript was expressed in the root, stem, and leaf of young seedlings. Its expression increased in the stem and leaf but was weak in the flower at the blooming stage. Finally,

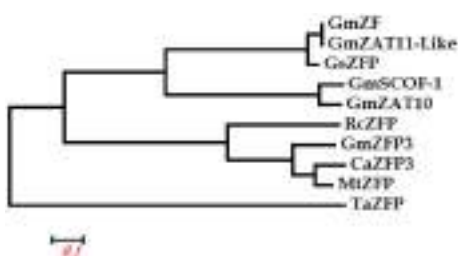


FIGURE 1 | Phylogenetic tree of GmZFP3 and other ZFP proteins from *Triticum aestivum* (TaZFP accession number: AEE81066), *Glycine max* (GmZF: DQ055134; GmSCOF-1: U68763; GmZAT11-Like: XM_003547379; GmZAT10: NM_001267693), *Glycine soja* (GsZFP:FJ417330), *Ricinus communis* (RcZFP:XM_002515403), *Medicago truncatula* (MtZFP:XM_003604157), and *Cicer arietinum* (CaZFP3:XM_004515472). The GmZFP3 cloned in this paper had the highest similarity with ZFP3 proteins from other plants. Thus, ZFP was designated GmZFP3.

it was primarily expressed in the root and stem at the podding stage (Figure 2).

To test whether drought stress induced *GmZFP3* expression, we treated the roots of soybean seedlings with PEG and ABA, then analyzed *GmZFP3* expression by quantitative real-time RT-PCR. ABA treatment (100 μ M) initially significantly suppressed *GmZFP3* expression after 30 min treatment ($p < 0.05$), but then it increased back to its initial expression level from 45 to 60 min, then continuously decreased from 90 to 120 min (Figure 3A). However, *GmZFP3* expression

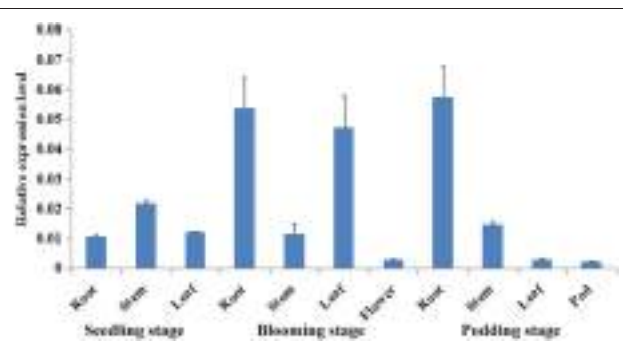


FIGURE 2 | The temporal and spatial expression pattern of *GmZFP3* in different organs and stages. The expression pattern of *GmZFP3* in root, stem, leaf, flower and pod at seedling, flowering, and podding stages, respectively using quantitative RT-PCR. The picture showed that *GmZFP3* expressed all the tested tissues including, root, stem, and leaf at young seedlings, and increased abundance in stem and leaf at blooming stage, but weak in flower, and kept the similar expression level in root and stem, but decreased in leaf and weak in pod at podding stage. The relative expression level at Y axis indicates the expression of *GmZFP3/GmActin*.

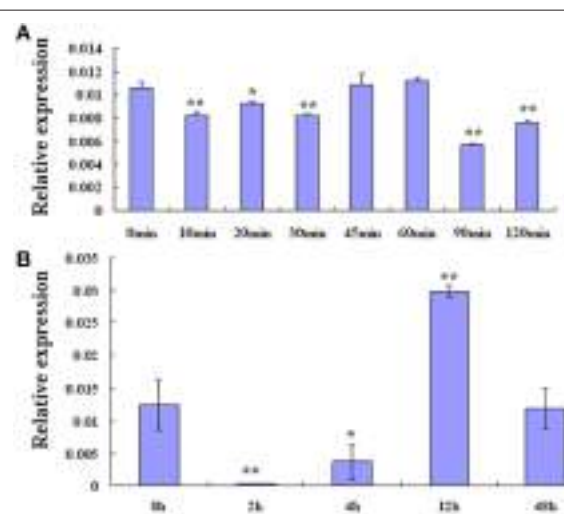


FIGURE 3 | The expression pattern of *GmZFP3* in soybean roots under PEG6000 (20%) and 100 μ M ABA treatments. **(A)** The expression pattern of *GmZFP3* in soybean roots under 100 μ M ABA for 10, 20, 30, 45, 60, 90, or 120 min. **(B)** The expression pattern of *GmZFP3* in soybean roots under PEG6000 (20%) for 2, 4, 12, or 48 h. * $p < 0.05$ level; ** $p < 0.01$. The relative expression level at Y axis indicates the expression of *GmZFP3/GmActin*.

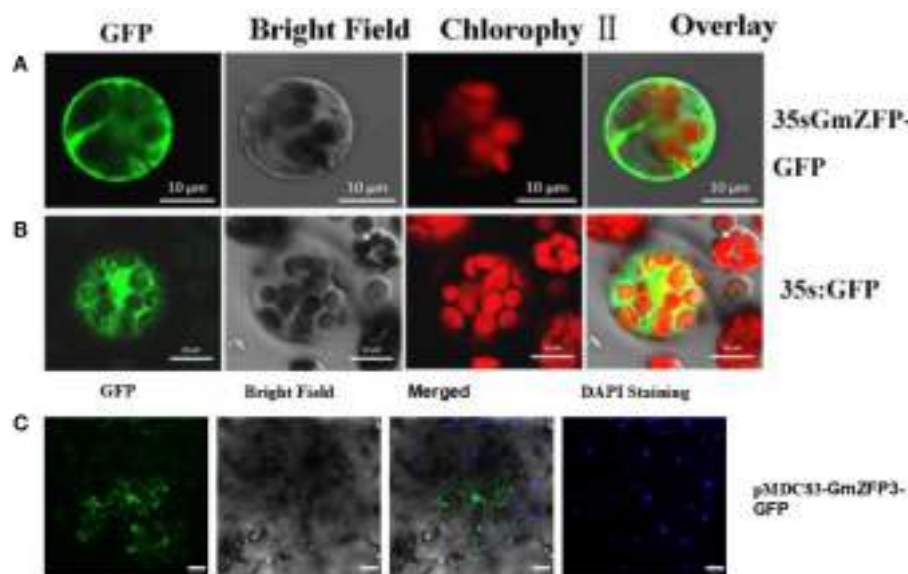


FIGURE 4 | Subcellular localization of GmZFP3 protein in *Arabidopsis* protoplasts and in tobacco leaf epidermal cells. The GmZFP3-green fluorescent protein (p35S::GmZFP3-GFP) fusion construct was generated by inserting GmZFP3 into pJIT166-GFP and pMDC83 vector without a termination codon to create an in-frame fusion between the CDS and GFP. p35S::GmZFP3-GFP and the GFP control plasmid (p35S::GFP) were transformed into *Arabidopsis* protoplasts by the PEG4000-mediated method respectively. In addition, the pMDC83-GmZFP3 construct was injected into the tobacco leaf epidermal cell respectively. **(A)** GmZFP3 distributed throughout the cell, especially nucleus **(B)**. The GFP control distributed throughout the whole cell (Con). Scale bars = 10 μ m. **(C)** Subcellular localization of GmZFP3 in tobacco leaf epidermal cells. GmZFP3 distributed throughout the cell, especially the plasma membrane and nucleus. Nuclei were stained with DAPI. Scale bars = 40 μ m.

decreased within 2 h of PEG-6000 (20%) treatment, then its mRNA expression continuously increased from 4 to 12 h and reached a maximum at 12 h. Finally, its expression decreased from 12 to 48 h (Figure 3B). Taken together, these data suggest that *GmZFP3* expression changed in response to PEG and ABA.

GmZFP3 Subcellular Localization

To examine GmZFP3 protein localization, we fused its coding sequences N-terminal to green fluorescent protein (GFP). We then transformed the fused proteins into *Arabidopsis* leaf protoplasts. The GmZFP3::GFP fluorescence signal was distributed throughout the cell, including the nucleus (Figure 4A), similar to the ubiquitous distribution of free GFP (Figure 4B). When we used the injected tobacco leaf method, GmZFP3 also distributed throughout the cell, especially the plasma membrane and nucleus (Figure 4C).

GmZFP3 Drought Response

To further validate GmZFP3 function in drought stress, we did not water 4-week-old transgenic *Arabidopsis* seedlings for 3 weeks and used wild type (WT) *Arabidopsis* plants as controls. Seedlings from transgenic *GmZFP3* *Arabidopsis* lines #5 and #6 grew worse compared to controls (Figure 5A). The survival rate of transgenic lines was significantly lower than that of

wild type(WT), suggesting that *GmZFP3* overexpression did not improve drought tolerance, likely due to the decreased root length and increased water loss rate in transgenic plants (Figures 5B,C).

To determine the function of GmZFP3 in drought response, we performed RT-PCR and qRT-PCR for nine genes related to stress/or ABA signaling pathway in transgenic lines #5 and #6, including *DREB2A*, *LHY1*, *AT5G02840*, *MYB2*, *RCI3*, *PAD3*, *CCA1*, and *UGT71B6*. Among the nine genes tested, six genes related to the ABA-dependent signaling pathway were up-regulated, with the exception of *DREB2A* related to the ABA-independent pathway and *AT5G02840* compared to wild-type (Figure 6). Because of the higher expression in transgenic line #5, we measured the relative germination rate, stoma width/length, and density for line #5 under different ABA concentrations. We found that leaf stoma in transgenic plants were primarily completely open (CO), while stoma in wild-type plants were primarily completely closed (CC) (Figures 7A–C). The relative germination rate was significantly lower in GmZFP3-overexpressing plants compared to wild-type after ABA treatment (Figure 7D), suggesting that GmZFP3-overexpressing plants were sensitive to ABA. Moreover, the width/length was significantly higher compared to wild-type, but the stoma density was significantly decreased under the same conditions (Figures 7E,F). Taken together, these data suggest that GmZFP3 functioned in the ABA-dependent pathway during the drought response.

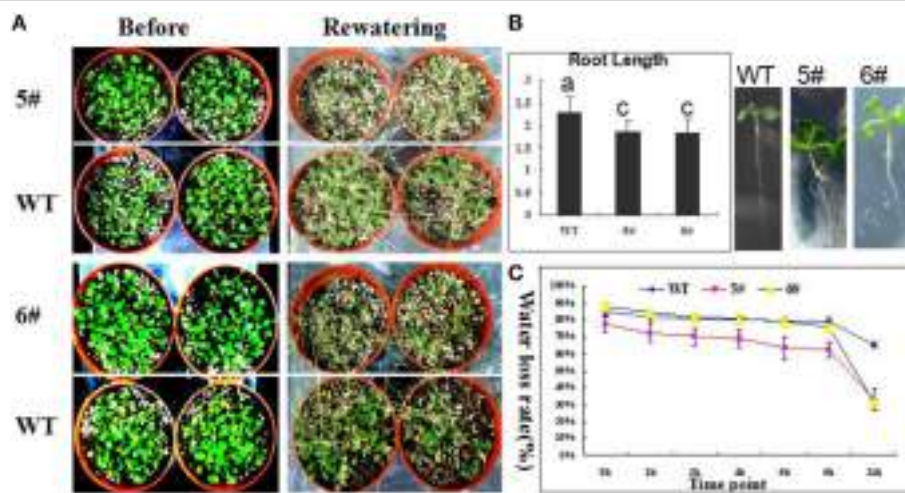


FIGURE 5 | Performance of transgenic *GmZFP3*- overexpressing *Arabidopsis* plants under drought stress. (A) The response of transgenic plants and wild type (WT) to drought stress. The transgenic plants (#5 and #6) showed the more sensitive to drought treatment compared with the WT plants. **(B)** The root length of transgenic was significantly shorter than that of WT. The roots of transgenic plants (#5 and #6) had the shorter primary root compared with the WT plants. **(C)** The water loss rate under air condition in transgenic and WT. When detached leaves from transgenic and WT plant were placed the air condition, the transgenic plants (#5 and #6) showed a faster water loss compared with the WT plants.

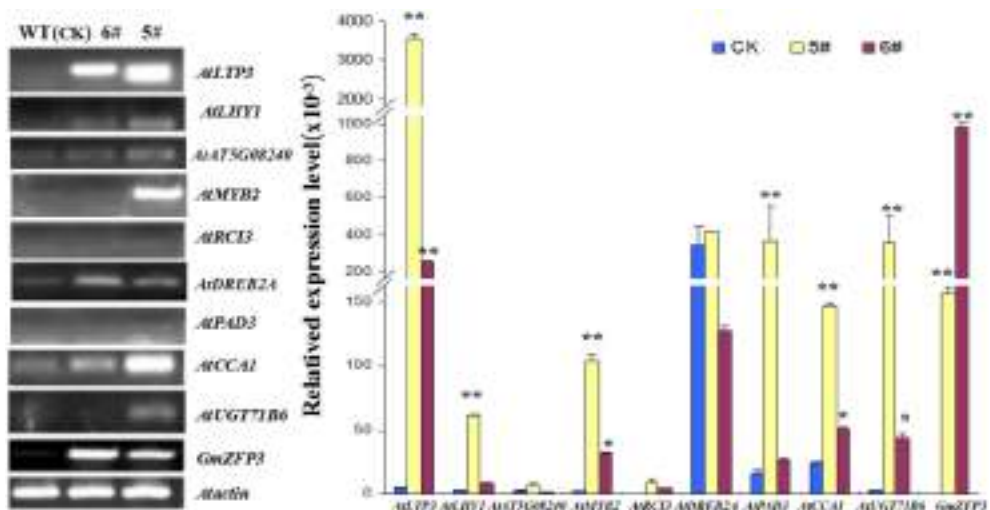


FIGURE 6 | RT-PCR and qRT-PCR results for the relative transcript abundance of nine stress-related genes in transgenic *GmZFP3*-overexpressing plants. Leaves of 2-week-old transgenic *GmZFP3*-overexpressing *Arabidopsis* seedlings. The *Actin* (NM_112764.3) gene was used as an internal control. The nine genes, including *AtLTP3*, *AtHY1*, *AtAT5G08240*, *AtMYB2*, *AtRCI3*, *AtDREB2A*, *AtPAD3*, *AtCCA1*, and *AtUGT71B6* related to abiotic stress or ABA signaling pathway were selected for comparative analysis of differential expression between transgenic plants(#5 and #6) and WT, among of which six genes showed the significant different expression except for *AtDREB2A*, *AtRCI3*, and *AtAT5G08240*. The relative expression level at Y axis indicates the genes expression above mentioned from *Arabidopsis/GmActin* respectively. *indicated significantly < 0.05 level, ** indicated significantly < 0.01 level.

DISCUSSION

Specht et al. (2001) identified a WUE (Water Use Efficiency)-related QTL region between the Satt590 and Satt567 markers on chromosome 7 in soybean. We searched the <http://www.phytozome.net/cgi-bin/gbrowse/soybean/> website using these two markers as probes and identified the Glyma07g01900 and Glyma07g05820 gene loci between these two markers.

We downloaded and isolated all 393 genes within these two loci using the Perl program. Function categorization analysis showed that the number of other function was 146(37%), enzyme was 95(24%), unknown function was 90(23%), transcription factor was 37(9%), and zinc finger was 13(3%). GO classification, including biological process, cellular component, and molecular function, indicated that oxidation reduction and regulation of transcription, mitochondrial, and

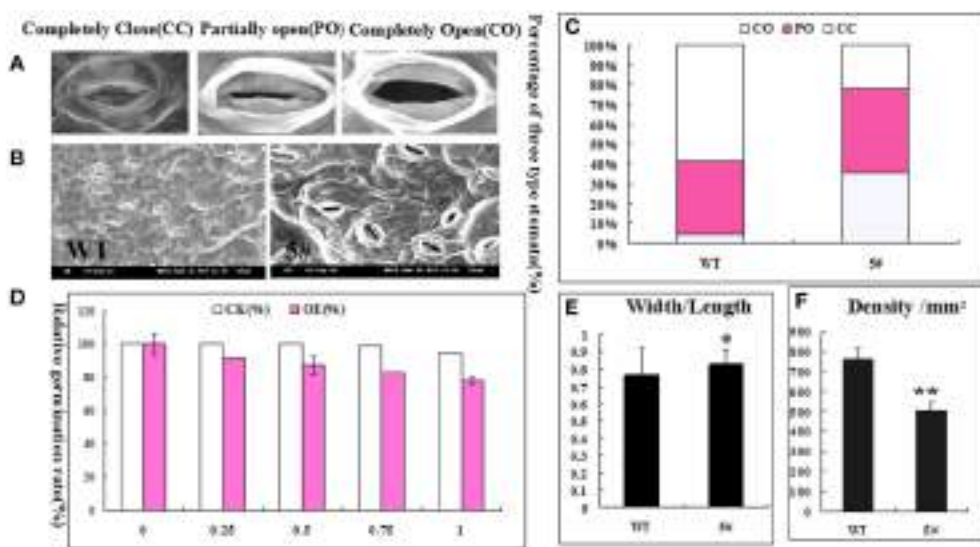


FIGURE 7 | The relationship between transgenic plant ABA-induced drought sensitivity and stomata. **(A)** Environmental scanning electron microscopy images of three stomatal levels. **(B)** Scanning electron microscopy images of transgenic line #5 and wild-type. **(C)** The percentage of the three types of stomatal opening in transgenic line #5 and wild-type. **(D)** The germination rate of transgenic line #5 and wild-type (WT) under different ABA concentrations. **(E)** The stomatal width/length in transgenic line #5 and wild-type. **(F)** The stomatal density in transgenic line #5 and wild-type. Significant difference at $*P < 0.05$ and $**P < 0.01$ level.

ATP binding were primarily related to this QTL (Figures S1, S2A–C).

Based on the many reports about plant drought tolerance, we selected two aquaporin gene TIP (TIP2;3, Glyma07g02060) and NIP (Glyma07g02800), six transcription factors HD (Homeodomain)-zip (Glyma07g01940), ERF (Glyma07g02380), bZIP38 (Glyma07g02050), Zinc Finger Protein (ZFP3, Glyma07g02880), bHLH (Glyma07g02120), and WRKY27 (Glyma07g02630) as candidate genes for soybean drought tolerance. Among them, the *GmTIP2;3* and *GmZFP3* genes showed similar spatial and temporal expression patterns after 10%PEG6000 or 100 μM ABA treatments for different time periods. More importantly, when we co-transformed pEarlygate103-HD-zip(OE), GmERF(OE), GmbZIP38(OE), GmZFP3(OE), bHLH(OE), and pGUS-GmTIP2;3-promoter(Zhang et al., 2016), only GmZFP3 could alter and inhibited GUS expression, leading to the lack of blue color(Data not shown), indicating that GmZFP3 inhibited the expression of *GmTIP2;3*.

In addition, GmZF1 contained a conserved QALGGH motif, which has been previously been shown to enhance *Arabidopsis* tolerance to cold stress (Yu et al., 2014). However, studies on *Arabidopsis* transformed with GsZFP1 lacking the typical QALGGH motif revealed that it played an important role in withstanding cold and drought stresses (Luo et al., 2012), suggesting that the QALGGH motif in the GsZFP1 protein was not necessary for adaptation to abiotic stress in wild soybean. In our study, GmZFP3 also had a plant-specific typical QALGGH motif, suggesting that this motif was crucial for plant response to abiotic stresses in cultivated soybean.

Xie et al. (2009) found that soybean trihelix transcription factors GmGT-2A and GmGT-2B improved plant tolerance to

abiotic stresses in transgenic *Arabidopsis*, as the expression of *CCA1*, *LHY1*, *MYB2*, and *AT5G02840* was down-regulated in transgenic plants compared to WT, while the expression of *PAD3*, *LTP3*, *RCI3*, *UGT71B6*, and *DREB2A* was up-regulated. In this study, we selected these nine stress-responsive genes for further quantitative real-time PCR analysis in transgenic and WT plants. Six genes, including *LHY1*, *MYB2*, *CCA1*, *PAD3*, *LTP3*, and *UGT71B6*, were up-regulated in transgenic lines expressing *GmZFP3.RCI3*, while *AT5G02840* expression did not significantly change between transgenic and WT plants, in contrast to the report by Xie et al, especially for *LHY1*, *MYB2*, and *CCA1*, implying a difference in gene function. *LTP3*, *PAD3*, and *UGT71B6* are involved in ABA responses (Arondel et al., 2000; Priest et al., 2006; Kaliff et al., 2007). *RCI3* encodes a peroxidase, and its overexpression conferred dehydration and salt tolerance (Llorente et al., 2002). *DREB2A* acts as a trans-acting factor in the signal transduction pathway under dehydration conditions, and dehydration induced its expression (Liu et al., 1998). *DREB2A* expression does not activate downstream genes under normal growth conditions. However, overexpression of its constitutively active form leads to drought stress tolerance and slight freezing tolerance (Sakuma et al., 2006). *LHY1*, *CCA1*, *At5g02840*, and *MYB2* have been found to be responsive to stress and/or ABA (Boxall et al., 2005). In our study, *GmZFP3*-overexpressing *Arabidopsis* plants were more sensitive to drought stress than wild-type plants, consistent with *AtMYB2* function, whose expression was induced by dehydration, high salt stress or exogenous ABA (Urao et al., 1993). However, transgenic plants overexpressing *MYB2* were more sensitive to ABA and showed stress tolerance, while co-expression of *AtMYB2* and *AtMYC2* conferred moderate stress tolerance (Abe et al., 2003). The seed germination rate of transgenic *GmZFP3* plants was influenced

by ABA and decreased as ABA concentrations increased. In addition, we observed the stomata by SEM to gain further insight into the mechanism of GmZFP3 during stress. Stomatal aperture (width/length) of transgenic plant leaves under drought conditions was significantly larger than wild-type, and the percentage of completely open (CO) stoma in transgenic plants was higher than wild-type. However, the stomatal density was lower in transgenic plants compared to wild-type. Huang et al. (2009) examined the percentage of three types of stomata, stomatal density, and stomatal conduction between ZH11 and *dst* mutants and found that the completely open level, stomatal density, and aperture in mutants was lower than in wild-type, which was consistent with the positive role under drought stress in *dst* mutants. Therefore, the *GmZFP*-overexpressing plants might lose large volumes of water by increasing the width/length and number of completely open stoma, but not the density, leading to drought stress sensitivity. Moreover, stomatal development and change are closely related to ABA (Trejo et al., 1993). By examining the expression pattern of marker genes related to stress or ABA and the effect of ABA on germination rate, we conclude that the function of GmZFP3 under drought stress involves the ABA pathway but not the ROS pathway.

AUTHOR CONTRIBUTIONS

DZ, PW, and LX conceived, designed and conducted the experiments. ZX, XH, QW, JY, and YH analyzed the data and results. DZ, HS, and JT wrote the manuscript. HS and HM

monitored the experiments and critically commented on the manuscript. All authors read and approved the final manuscript.

ACKNOWLEDGMENTS

This study was sponsored by the National Science Foundation of China (31101166, 31571695); Jiangsu Key Laboratory for Bioresources of Saline Soils (JKLBS2014002; JKLBS2014006), Shuangchuang Talent Plan of Jiangsu Province, the Jiangsu Natural Science Foundation, China (BK20151364) and Jiangsu Agriculture Science, and Technology Innovation Fund (JASTIE, CX(15)1005).

SUPPLEMENTARY MATERIAL

The Supplementary Material for this article can be found online at: <http://journal.frontiersin.org/article/10.3389/fpls.2016.00325>

Figure S1 | The results of function categorization of 393 genes between the Glyma07g01900 and Glyma07g05820 loci on soybean chromosome 7. (A) Most of them belong to other (146), the enzyme is 95, unknown function is 90 and 37 transcription factors respectively.

Figure S2 | The results of BLAST2GO analysis of 393 genes between the Glyma07g01900 and Glyma07g05820 loci on soybean chromosome 7. (A) Concerning the biological process, the top categories with the highest number were regulation of transcription (23), oxidation reduction (13), and amino acid phosphoglution (9), respectively. **(B)** Concerning the molecular function, the top categories with the highest number were ATP binding (15), transcription factor activity (13), iron binding (11), and binding (10), respectively. **(C)** Concerning cell component, the top categories with the highest number were mitochondrion (28), plastid(19), membrance (18), and nucleus(18), respectively.

REFERENCES

- Abe, H., Urao, T., Ito, T., Seki, M., Shinozaki, K., and Yamaguchi-Shinozaki, K. (2003). Arabidopsis AtMYC2 (bHLH) and AtMYB2 (MYB) function as transcriptional activators in abscisic acid signaling. *Plant Cell* 15, 63–78. doi: 10.1105/tpc.006130
- Abel, S., and Theologis, A. (1994). Transient transformation of Arabidopsis leaf protoplasts: a versatile experimental system to study gene expression. *Plant J.* 5, 421–427. doi: 10.1111/j.1365-313X.1994.00421.x
- Arondel, V. V., Vergnolle, C., Cantrel, C., and Kader, J. (2000). Lipid transfer proteins are encoded by a small multigene family in Arabidopsis thaliana. *Plant Sci.* 157, 1–12. doi: 10.1016/S0168-9452(00)00232-6
- Boxall, S. F., Foster, J. M., Bohnert, H. J., Cushman, J. C., Nimmo, H. G., and Hartwell, J. (2005). Conservation and divergence of circadian clock operation in a stress-inducible Crassulacean acid metabolism species reveals clock compensation against stress. *Plant Physiol.* 137, 969–982. doi: 10.1104/pp.104.054577
- Ciftci-Yilmaz, S., and Mittler, R. (2008). The zinc finger network of plants. *Cell Mol. Life Sci.* 65, 1150–1160. doi: 10.1007/s00018-007-7473-4
- Ciftci-Yilmaz, S., Morsy, M. R., Song, L., Coutu, A., Krizek, B. A., Lewis, M. W., et al. (2007). The EAR-motif of the Cys2/His2-type zinc finger protein Zat7 plays a key role in the defense response of Arabidopsis to salinity stress. *J. Biol. Chem.* 282, 9260–9268. doi: 10.1074/jbc.M611093200
- Clough, S. J., and Bent, A. F. (1998). Floral dip: a simplified method for Agrobacterium-mediated transformation of Arabidopsis thaliana. *Plant J.* 16, 735–743. doi: 10.1046/j.1365-313X.1998.00343.x
- Davletova, S., Schlauch, K., Coutu, J., and Mittler, R. (2005). The zinc-finger protein Zat12 plays a central role in reactive oxygen and abiotic stress signaling in Arabidopsis. *Plant Physiol.* 139, 847–856. doi: 10.1104/pp.105.068254
- de Lorenzo, L., Merchan, F., Blanchet, S., Megias, M., Frugier, F., Crespi, M., et al. (2007). Differential expression of the TFIIIA regulatory pathway in response to salt stress between *Medicago truncatula* genotypes. *Plant Physiol.* 145, 1521–1532. doi: 10.1104/pp.107.106146
- Harrison, M. T., Tardieu, F., Dong, Z., Messina, C. D., and Hammer, G. L. (2014). Characterizing drought stress and trait influence on maize yield under current and future conditions. *Glob. Change Biol.* 20, 867–878. doi: 10.1111/gcb.12381
- Huang, X. Y., Chao, D. Y., Gao, J. P., Zhu, M. Z., Shi, M., and Lin, H. X. (2009). A previously unknown zinc finger protein, DST, regulates drought and salt tolerance in rice via stomatal aperture control. *Genes Dev.* 23, 1805–1817. doi: 10.1101/gad.1812409
- Iuchi, S., Kobayashi, M., Taji, T., Naramoto, M., Seki, M., Kato, T., et al. (2001). Regulation of drought tolerance by gene manipulation of 9-cis-epoxycarotenoid dioxygenase, a key enzyme in abscisic acid biosynthesis in Arabidopsis. *Plant J.* 27, 325–333. doi: 10.1046/j.1365-313X.2001.01096.x
- Jan, A., Maruyama, K., Todaka, D., Kidokoro, S., Abo, M., Yoshimura, E., et al. (2013). OsTZF1, a CCCH-tandem zinc finger protein, confers delayed senescence and stress tolerance in rice by regulating stress-related genes. *Plant Physiol.* 161, 1202–1216. doi: 10.1104/pp.112.205385
- Kaliff, M., Staal, J., Myrenas, M., and Dixelius, C. (2007). ABA is required for *Leptosphaeria maculans* resistance via ABI1- and ABI4-dependent signaling. *Mol. Plant Microbe Interact.* 20, 335–345. doi: 10.1094/MPMI-20-4-0335
- Kim, J. C., Lee, S. H., Cheong, Y. H., Yoo, C. M., Lee, S. I., Chun, H. J., et al. (2001). A novel cold-inducible zinc finger protein from soybean, SCOF-1, enhances cold tolerance in transgenic plants. *Plant J.* 25, 247–259. doi: 10.1046/j.1365-313X.2001.00947.x
- Kodaira, K. S., Qin, F., Tran, L. S., Maruyama, K., Kidokoro, S., Fujita, Y., et al. (2011). Arabidopsis Cys2/His2 zinc-finger proteins AZF1 and AZF2 negatively regulate abscisic acid-repressive and auxin-inducible genes under abiotic stress conditions. *Plant Physiol.* 157, 742–756. doi: 10.1104/pp.111.182683

- Laity, J. H., Lee, B. M., and Wright, P. E. (2001). Zinc finger proteins: new insights into structural and functional diversity. *Curr. Opin. Struct. Biol.* 11, 39–46. doi: 10.1016/S0959-440X(00)00167-6
- Liu, Q., Kasuga, M., Sakuma, Y., Abe, H., Miura, S., Yamaguchi-Shinozaki, K., et al. (1998). Two transcription factors, DREB1 and DREB2, with an EREBP/AP2 DNA binding domain separate two cellular signal transduction pathways in drought- and low-temperature-responsive gene expression, respectively, in Arabidopsis. *Plant Cell* 10, 1391–1406. doi: 10.1105/tpc.10.8.1391
- Liu, X. M., Nguyen, X. C., Kim, K. E., Han, H. J., Yoo, J., Lee, K., et al. (2013). Phosphorylation of the zinc finger transcriptional regulator ZAT6 by MPK6 regulates Arabidopsis seed germination under salt and osmotic stress. *Biochem. Biophys. Res. Commun.* 430, 1054–1059. doi: 10.1016/j.bbrc.2012.12.039
- Llorente, F., Lopez-Cobollo, R. M., Catala, R., Martinez-Zapater, J. M., and Salinas, J. (2002). A novel cold-inducible gene from Arabidopsis, RCI3, encodes a peroxidase that constitutes a component for stress tolerance. *Plant J.* 32, 13–24. doi: 10.1046/j.1365-313X.2002.01398.x
- Luo, X., Cui, N., Zhu, Y., Cao, L., Zhai, H., Cai, H., et al. (2012). Over-expression of GsZFP1, an ABA-responsive C2H2-type zinc finger protein lacking a QALGGH motif, reduces ABA sensitivity and decreases stomata size. *J. Plant Physiol.* 169, 1192–1202. doi: 10.1016/j.jplph.2012.03.019
- Mittler, R., Kim, Y., Song, L., Coutu, J., Coutu, A., Ciftci-Yilmaz, S., et al. (2006). Gain- and loss-of-function mutations in Zat10 enhance the tolerance of plants to abiotic stress. *FEBS Lett.* 580, 6537–6542. doi: 10.1016/j.febslet.2006.11.002
- Priest, D. M., Ambrose, S. J., Vaistij, F. E., Elias, L., Higgins, G. S., Ross, A. R., et al. (2006). Use of the glucosyltransferase UGT71B6 to disturb abscisic acid homeostasis in Arabidopsis thaliana. *Plant J.* 46, 492–502. doi: 10.1111/j.1365-313X.2006.02701.x
- Sakamoto, H., Araki, T., Meshi, T., and Iwabuchi, M. (2000). Expression of a subset of the Arabidopsis Cys(2)/His(2)-type zinc-finger protein gene family under water stress. *Gene* 248, 23–32. doi: 10.1016/S0378-1119(00)00133-5
- Sakamoto, H., Maruyama, K., Sakuma, Y., Meshi, T., Iwabuchi, M., Shinozaki, K., et al. (2004). Arabidopsis Cys2/His2-type zinc-finger proteins function as transcription repressors under drought, cold, and high-salinity stress conditions. *Plant Physiol.* 136, 2734–2746. doi: 10.1104/pp.104.046599
- Sakuma, Y., Maruyama, K., Osakabe, Y., Qin, F., Seki, M., Shinozaki, K., et al. (2006). Functional analysis of an Arabidopsis transcription factor, DREB2A, involved in drought-responsive gene expression. *Plant Cell* 18, 1292–1309. doi: 10.1105/tpc.105.035881
- Shao, H. B., Chu, L. Y., Jaleel, C. A., Manivannan, P., Panneerselvam, R., and Shao, M. A. (2009). Understanding water deficit stress-induced changes in the basic metabolism of higher plants - biotechnologically and sustainably improving agriculture and the ecoenvironment in arid regions of the globe. *Crit. Rev. Biotechnol.* 29, 131–151. doi: 10.1080/07388550902869792
- Specht, J. E., Chase, K., Macrander, M., Graef, G. L., and Chung, J., Markwell, J. (2001). Soybean response to water: a QTL analysis of drought tolerance. *Crop Sci.* 41, 493–509.
- Sun, S. J., Guo, S. Q., Yang, X., Bao, Y. M., Tang, H. J., Sun, H., et al. (2010). Functional analysis of a novel Cys2/His2-type zinc finger protein involved in salt tolerance in rice. *J. Exp. Bot.* 61, 2807–2818. doi: 10.1093/jxb/erq120
- Takatsuji, H. (1999). Zinc-finger proteins: the classical zinc finger emerges in contemporary plant science. *Plant Mol. Biol.* 39, 1073–1078. doi: 10.1023/A:1006184519697
- Tamura, K., Dudley, J., Nei, M., and Kumar, S. (2007). MEGA4: Molecular Evolutionary Genetics Analysis (MEGA) software version 4.0. *Mol. Biol. Evol.* 24, 1596–1599. doi: 10.1093/molbev/msm092
- Trejo, C. L., Davies, W. J., and Ruiz, L. (1993). Sensitivity of Stomata to Abscisic Acid (An Effect of the Mesophyll). *Plant Physiol.* 102, 497–502.
- Urao, T., Yamaguchi-Shinozaki, K., Urao, S., and Shinozaki, K. (1993). An Arabidopsis myb homolog is induced by dehydration stress and its gene product binds to the conserved MYB recognition sequence. *Plant Cell* 5, 1529–1539. doi: 10.1105/tpc.5.11.1529
- Xie, Z. M., Zou, H. F., Lei, G., Wei, W., Zhou, Q. Y., Niu, C. F., et al. (2009). Soybean Trihelix transcription factors GmGT-2A and GmGT-2B improve plant tolerance to abiotic stresses in transgenic Arabidopsis. *PLoS ONE* 4:e6898. doi: 10.1371/journal.pone.0006898
- Xu, S., Wang, X., and Chen, J. (2007). Zinc finger protein 1 (ThZF1) from salt cress (*Thellungiella halophila*) is a Cys-2/His-2-type transcription factor involved in drought and salt stress. *Plant Cell Rep.* 26, 497–506. doi: 10.1007/s00299-006-0248-9
- Yoo, S. D., Cho, Y. H., and Sheen, J. (2007). Arabidopsis mesophyll protoplasts: a versatile cell system for transient gene expression analysis. *Nat. Protoc.* 2, 1565–1572. doi: 10.1038/nprot.2007.199
- Yu, G. H., Jiang, L. L., Ma, X. F., Xu, Z. S., Liu, M. M., Shan, S. G., et al. (2014). A soybean C2H2-type zinc finger gene GmZF1 enhanced cold tolerance in transgenic Arabidopsis. *PLoS ONE* 9:e109399. doi: 10.1371/journal.pone.0109399
- Zhang, D. Y., Ali, Z., Wang, C. B., Xu, L., Yi, J. X., Xu, Z. L., et al. (2013). Genome-wide sequence characterization and expression analysis of major intrinsic proteins in soybean (*Glycine max* L.). *PLoS ONE* 8:e56312. doi: 10.1371/journal.pone.0056312
- Zhang, D. Y., Tong, J. F., He, X. L., Xu, Z. L., Xu, L., Wei, P. P., et al. (2016). A novel soybean intrinsic protein gene, GmTIP2;3, involved in responding to osmotic stress. *Front. Plant Sci.* 6:1237. doi: 10.3389/fpls.2015.01237
- Zhang, H., Liu, Y., Wen, F., Yao, D., Wang, L., Guo, J., et al. (2014). A novel rice C2H2-type zinc finger protein, ZFP36, is a key player involved in abscisic acid-induced antioxidant defence and oxidative stress tolerance in rice. *J. Exp. Bot.* 65, 5795–5809. doi: 10.1093/jxb/eru313
- Zhang, H., Ni, L., Liu, Y., Wang, Y., Zhang, A., Tan, M., et al. (2012). The C2H2-type zinc finger protein ZFP182 is involved in abscisic acid-induced antioxidant defense in rice. *J. Integr. Plant Biol.* 54, 500–510. doi: 10.1111/j.1744-7909.2012.01135.x

Conflict of Interest Statement: The authors declare that the research was conducted in the absence of any commercial or financial relationships that could be construed as a potential conflict of interest.

Copyright © 2016 Zhang, Tong, Xu, Wei, Xu, Wan, Huang, He, Yang, Shao and Ma. This is an open-access article distributed under the terms of the Creative Commons Attribution License (CC BY). The use, distribution or reproduction in other forums is permitted, provided the original author(s) or licensor are credited and that the original publication in this journal is cited, in accordance with accepted academic practice. No use, distribution or reproduction is permitted which does not comply with these terms.



Mutation of OsGIGANTEA Leads to Enhanced Tolerance to Polyethylene Glycol-Generated Osmotic Stress in Rice

Shuai Li^{1,2}, Wenhao Yue¹, Min Wang¹, Wenmin Qiu¹, Lian Zhou¹ and Huixia Shou^{1*}

¹ State Key Laboratory of Plant Physiology and Biochemistry, College of Life Sciences, Zhejiang University, Hangzhou, China,

² College of Life Sciences, Qingdao Agricultural University, Qingdao, China

OPEN ACCESS

Edited by:

Olivier Lamotte,
Centre National de la Recherche
Scientifique, UMR Agroécologie,
France

Reviewed by:

Monica Höfte,
Ghent University, Belgium
Walter Alberto Vargas,
Consejo Nacional de Investigaciones
Científicas y Técnicas, Argentina

*Correspondence:

Huixia Shou
huixia@zju.edu.cn

Specialty section:

This article was submitted to
Plant Physiology,
a section of the journal
Frontiers in Plant Science

Received: 16 December 2015

Accepted: 24 March 2016

Published: 18 April 2016

Citation:

Li S, Yue W, Wang M, Qiu W, Zhou L
and Shou H (2016) Mutation of
OsGIGANTEA Leads to Enhanced
Tolerance to Polyethylene
Glycol-Generated Osmotic Stress in
Rice. *Front. Plant Sci.* 7:465.
doi: 10.3389/fpls.2016.00465

Water deficit is one of the most important environmental stresses limiting plant growth and crop yield. While the identification of many key factors involved in the plant water deficit response has greatly increased our knowledge about the regulation system, the mechanisms underlying dehydration tolerance in plants are still not well understood. In our current study, we investigated the roles of the key flowering time regulator, OsGIGANTEA (OsGI), in the osmotic stress tolerance in rice. Results showed that mutation of OsGI conferred tolerance to osmotic stress generated by polyethylene glycol (PEG), increased proline and sucrose contents, and accelerated stomata movement. In addition, qRT-PCR and microarray analysis revealed that the transcript abundance of some osmotic stress response genes, such as *OsDREB1E*, *OsAP37*, *OsAP59*, *OsLIP9*, *OsLEA3*, *OsRAB16A*, and *OsSalT*, was significantly higher in *osgi* than in WT plants, suggesting that OsGI might be a negative regulator in the osmotic stress response in rice.

Keywords: GIGANTEA, osmotic stress, water deficiency, stomata, rice

INTRODUCTION

Water availability is a critical environmental factor for plant growth and development. To cope with water shortages, plants have developed multiple mechanisms to preserve cellular water homeostasis, including morphological, physiological and biochemical modulations that enhance water uptake and reduce water loss (Hincha et al., 2002; Chaves et al., 2003; Villadsen et al., 2005; Valliyodan and Nguyen, 2006; Hadiarto and Tran, 2011). A promising approach to enhance plant tolerance to dehydration stresses is the modulation of genes responsive to water deficiency (Yamaguchi-Shinozaki et al., 1995; Shinozaki et al., 1998). In recent years, several instances of crosstalk between the osmotic stress response and other signaling pathways, such as abscisic acid (ABA) signaling and flowering time regulation, have been identified (Ikegami et al., 2009; Fujita et al., 2011). For example, genes involved in flowering time regulation, such as *phytochrome B* (*phyB*) and *timing of CAB expression 1* (*toc1*), have been shown to be negative regulators in the response to dehydration conditions (Legnaioli et al., 2009; Liu et al., 2012).

GIGANTEA (GI) is regarded as a key component of flowering time regulation in many plant species (Fowler et al., 1999; Hayama et al., 2003; Hecht et al., 2007; Higuchi et al., 2011). In *Arabidopsis*, GI, CONSTANS (CO), and FLOWERING LOCUS T (FT) control photoperiodic

flowering responses (Fowler et al., 1999; Mouradov et al., 2002; Srikanth and Schmid, 2011). Overexpression of *GI* promotes early flowering while *GI* mutants develop a large rosette of leaves and “gigantic” size under long day conditions due to a prolonged vegetative growth phase (Koornneef et al., 1991; Fowler et al., 1999; Park et al., 1999). The rice homolog of *GI*, *OsGI*, is also a circadian gene controlling diurnal rhythms of the global transcriptome and carbohydrate metabolism (Izawa et al., 2011), and mutation of *OsGI* causes late flowering under short day condition (Hayama et al., 2003; Izawa et al., 2011).

Besides its role in the regulation of flowering time and circadian rhythms, *GI* is also involved in processes such as sucrose signaling, starch accumulation and stress tolerance (Kurepa et al., 1998; Fowler and Thomashow, 2002; Dalchau et al., 2011; Kim et al., 2013; Riboni et al., 2013; Mishra and Panigrahi, 2015). In the past decade, *GI* has been shown to function in the response to several abiotic stressors including cold, salt, drought and oxidative stresses (Kurepa et al., 1998; Cao et al., 2005; Kim et al., 2013; Riboni et al., 2013). Expression of Arabidopsis *GI* was induced 5–8 fold by cold stress (Fowler and Thomashow, 2002). *GI* was proposed to regulate cold acclimation through a C-repeat Binding proteins (CBFs) independent pathway (Cao et al., 2005). *GI* mutants displayed increased cold sensitivity because the protective role of *GI* in cold tolerance was reduced (Cao et al., 2005). Recent evidence suggests that *GI* is a negative regulator for the tolerance to salt stress (Kim et al., 2013). Under normal conditions, Arabidopsis *GI* interacts with salt overly sensitive 2 (SOS2) to prevent SOS2-mediated SOS1 phosphorylation and activation (Kim et al., 2013). Under salt stress condition, *GI* is degraded and the freed SOS2 can interact with the Ca²⁺-activated sensor of sodium ions, SOS3, to activate and stabilize SOS1 (Kim et al., 2013; Park et al., 2013). Therefore, the *gi* mutant confers enhanced salt tolerance due to the constitutive activation of SOS1 (Shi et al., 2000; Kim et al., 2013; Park et al., 2013).

In addition, *GI* has been shown to regulate the response to oxidative stress which increases *GI* abundance and promotes flowering (Qian et al., 2014). *GI* mutants exhibit increased activation of superoxide dismutase (SOD) and ascorbate peroxidase (APX) and tolerance to a redox cycling agent, parquat, and H₂O₂ (Kurepa et al., 1998; Cao et al., 2006). Furthermore, it was recently discovered that *GI* can lead to early flowering and drought tolerance via the abscisic acid (ABA)-dependent activation of florigens under long day condition (Riboni et al., 2013).

Despite the increasing knowledge of *GI*'s role in Arabidopsis, little is known about the biochemical and molecular functions of its rice homolog, *OsGI*, in response to water deficits. In this study, we investigated the role of *OsGI* in osmotic stress in rice. We determined that mutation of *OsGI* confers tolerance to osmotic stress generated by polyethylene glycol (PEG). Mutation of *OsGI* results in increased proline and sucrose contents and more rapid stomata movement. In addition, transcription analysis revealed that the expression of many genes involved in drought response is altered in *osgi* plants.

MATERIALS AND METHODS

Plant Materials, Growth Conditions, and Stress Treatments

The rice (*Oryza sativa*) *osgi* mutant, *osgi*, was obtained from the Rice *Tos17* insertion mutant database at the Rice Genome Resource Center, Japan. *Osg*i and its wild type control, cv. *Nipponbare*, were used for all physiological experiments. For complementation of the *osgi* mutant, the *OsGI* coding sequence was expressed in a modified pCAMBIA1300 vector under control of the Cauliflower Mosaic virus 35S promoter (Wang et al., 2009). The construct was introduced into *osgi* mutants using a *Agrobacterium tumefaciens*-mediated transformation method (Wang et al., 2009). A modified culture medium containing 1.425 mM NH₄NO₃, 0.323 mM NaH₂PO₄, 0.513 mM K₂SO₄, 1.643 mM MgSO₄, 0.998 mM CaCl₂, 0.125 mM EDTA-Fe(II), 0.075 μM (NH₄)₆Mo₇O₂₄, 0.25 mM NaSiO₃, 0.009 mM MnCl₂, 0.019 μM H₃BO₃, 0.155 μM CuSO₄, and 0.152 μM ZnSO₄ was used at pH 5.5 for hydroponic experiments (Yoshida et al., 1976; Li et al., 2014). Rice plants were grown in a growth room with a 12 h light/12 h dark cycle, a daytime temperature of 30°C and nighttime temperature of 22°C.

Rice seeds were first germinated in tap water for 2 days before being transferred into the culture media. For osmotic stress tolerance experiments, seedlings were transferred to culture media containing 21% polyethylene glycol (PEG) 8000. For gene expression analysis, plants were transferred to culture media containing 18% PEG 8000. For microarrays, leaves from 14-day-old *osgi* and WT seedlings grown under normal growth condition were used.

Measurement of Proline and Sucrose Contents

Proline content was measured as previously described (Bates et al., 1973). Briefly, approximately 50 mg fresh leaves from 15-day-old rice plants grown in hydroponics were harvested for analysis. Samples were homogenized in 5 ml 3% sulfosalicylic acid, incubated at 100°C for 10 min and pelleted by centrifugation. The resulting supernatant was collected, mixed 1:1:1 (2 mL each) with glacial acetic acid and acidic ninhydrin, and incubated at 100°C for 30 min. The chromophore was toluene extracted, and absorption values for the solution were detected at 520 nm wavelength. Proline concentration was determined using a standard concentration curve and adjusted to the fresh weight of leaves.

For sucrose analysis, approximately 200 mg fresh leaves were homogenized in 2 ml deionized water and centrifuged at 4°C for 10 min. The resulting supernatant was incubated at 100°C for 3 min, and sucrose content was determined using ion chromatography (ICS-3000, DIONEX).

RNA Preparation, Quantitative Real-Time PCR

For microarray, total RNA was extracted from plant samples using RNeasy mini kits (Qiagen, USA, <http://www.qiagen.com>) according to the manufacturer's instructions. For quantitative reverse transcription PCR (qRT-PCR), total RNA was extracted

from leaf samples using TRIzol Reagent (Invitrogen, CA, USA) according to the manufacturer's instructions.

First-strand cDNAs were synthesized from 4 μ g total RNA using SuperScript II reverse transcriptase (Invitrogen), and qRT-PCR was performed using LightCycler 480 SYBR Green I Master Kit (Roche Diagnostics, USA) on a LightCycler480 thermocycler. The amplification steps and quantitative analysis of relative expression levels was performed as previously described (Li et al., 2014). RNA samples were collected from three biological replicates. Each sample was analyzed using three biological replicates and normalized to the housekeeping gene *OsACTIN*. All primers used for qRT-PCR analyses are listed in Supplementary Table 1.

Microarray Analyses

For the microarray analysis, leaves were sampled from plants grown for 14 days after germination (DAG) under normal condition. Genes were considered significantly differentially expressed when $p < 0.05$ and Posterior Probability of Differential Expression (PPDE) >0.95 with a 2 fold cut-off to correct for false discovery rates (Dalchau et al., 2011). Differentially expressed genes (up- or down-regulated) between *osgi* and WT were compared to a previously published microarray (Jain et al., 2007). The raw microarray data files have been supplied as Supplementary File 2.

Stomata Conductance (g_s) and Transpiration Rate (T_r) Measurements

Stomata conductance (g_s) and transpiration rate (T_r) were recorded in *osgi* and WT plants inside a growth chamber on fully expanded leaves using an Li-6400 portable gas-exchange system (LI-COR) according to the manufacturer's instructions. All measurements were conducted 9 h after lights-on in saturating light (1500 $\mu\text{mol m}^{-2} \text{s}^{-1}$) with 400 $\mu\text{mol mol}^{-1}$ CO₂ surrounding the leaf. Leaf temperature for all measurements was approximately 30°C (ambient temperature), and the leaf-to-air vapor pressure deficit (VPD) was kept abetween 1.5–2.5 kPa. To measure stomata movement in response to PEG treatment, *osgi* and WT plants were grown in hydroponics under normal condition for 5 weeks and then treated with 18% PEG 8000 at 4, 6, and 8 h after lights-on.

Statistical Analysis

Statistical significance was determined using the SAS program with *t*-test (SAS Institute Inc., <http://www.sas.com>).

RESULTS

Morphological Analysis of *osgi* Mutant Rice Plants

The *TOS17* insertion mutant of *osgi* was obtained and characterized. As shown in Figure 1, the cyclic expression pattern of *OsGI*, which peaks at dusk in wild type (WT) plants, was completely abolished in *osgi* mutant plants (Figure 1A). Circadian rhythm genes, such as *OsRFT1* and *OsHd3a*, were also suppressed in *osgi* plants (Supplementary Figure 1). *Osg* mutants displayed a growth inhibited phenotype (Figure 1B;

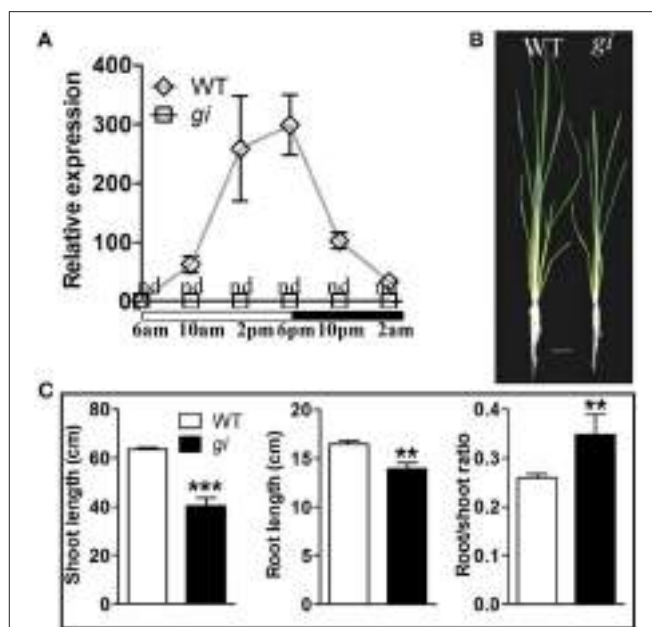


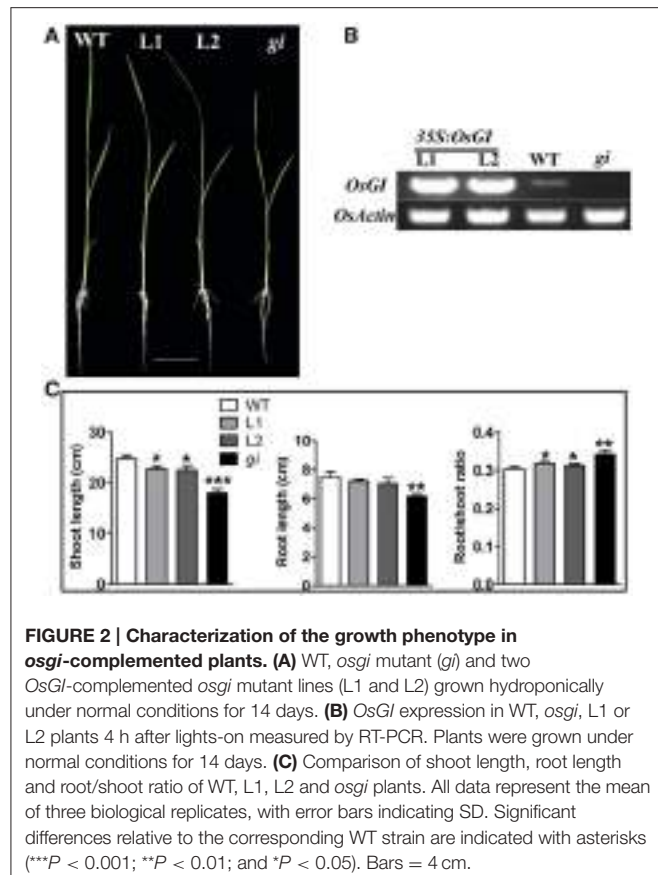
FIGURE 1 | Characterization of the growth phenotype of WT and *osgi* plants. (A) Expression of *OsGI* in WT and *osgi* (*gi*) plants throughout the day. Unfilled and filled bars below the x-axis indicate times of lights-on and lights-off, respectively. Gene expression was normalized to the expression level of *OsACTIN*. **(B)** WT and *osgi* plants were grown hydroponically under normal growth conditions for 30 days. **(C)** Shoot length, root length and root/shoot ratio of WT and *osgi* plants. All data represent the mean of three biological replicates, with error bars indicating SD. Significant differences relative to the corresponding WT strain are indicated with asterisks (** $P < 0.001$; and ** $P < 0.01$). Bars = 4 cm. nd, not detectable.

Itoh and Izawa, 2011). Shoot and root lengths of 30-day-old *osgi* plants were reduced by 35 and 15% compared to WT plants, respectively, resulting in an increased root-to-shoot ratio (Figure 1C).

To confirm that the growth defects were caused by the mutation in *OsGI*, genetic complementation was carried out by introducing the *OsGI* coding sequence under control of the CaMV35S promoter into *osgi* mutants in two transgenic events, L1 and L2. As shown in Figure 2A, the overexpression of *OsGI* in the *osgi* background rescued the growth defect observed in the mutant. The relative transcript abundance of *OsGI*, measured by reverse-transcription PCR (RT-PCR), was significantly higher in L1 and L2 than in either WT or *osgi* plants (Figure 2B, Supplementary Figure 2). Compared to *osgi* plants, the root and shoot lengths were increased in L1 and L2 while the root-to-shoot ratio decreased (Figure 2C). Based on these results, the L1 and L2 plants were used as overexpression lines in later experiments.

Mutation of *OsGI* Improved Plant Osmotic Stress Tolerance

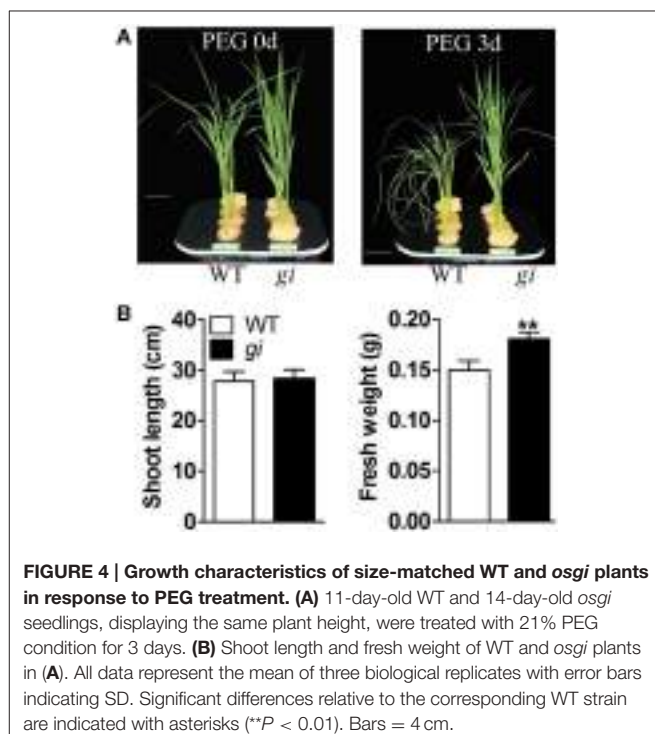
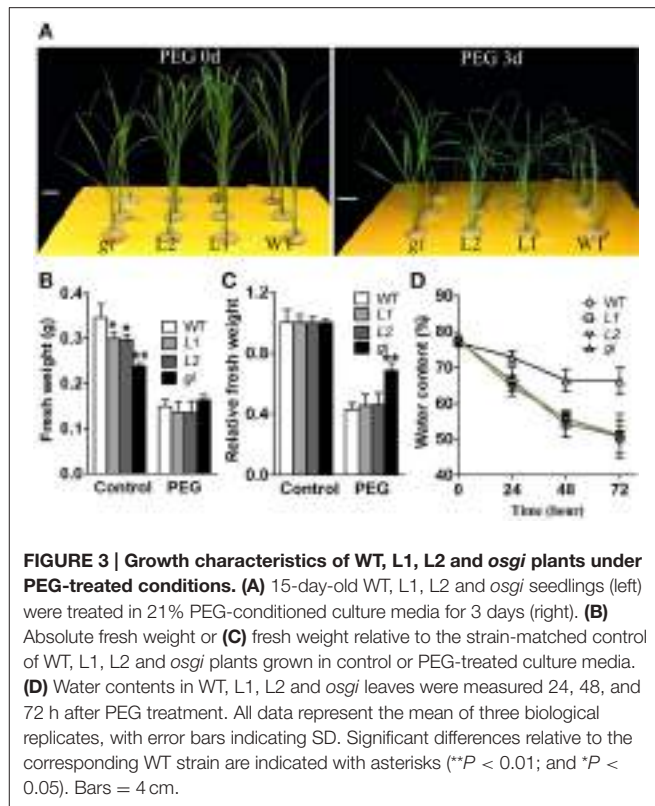
OsGI has been reported to be a molecular switch connecting flowering time regulation with multiple stress-response pathways, such as oxidative and salinity stresses (Kurepa et al., 1998; Kim et al., 2013). To investigate whether GI influences the



tolerance to osmotic stress, WT and *osgi* plants were grown for 15 days under normal growth condition and then treated with 21% PEG 8000 for 3 days. As shown in **Figure 3A**, *osgi* mutants displayed improved osmotic stress tolerance compared to WT. After 3 days of exposure to high concentrations of PEG, WT plants were completely wilted while *osgi* plants remained healthy. PEG treatment decreased the fresh weight of WT and *osgi* plants by 55 and 30%, respectively, compared to the corresponding plants grown under normal condition (**Figures 3B,C**). While the water content in both WT and *osgi* leaves decreased during PEG treatment, *osgi* plants maintained a significantly higher water content than WT (**Figure 3D**). However, *osgi* plants used for the analysis of resistance to drought in soil showed the same phenotype as WT (data not shown).

To exclude the possibility that the improved osmotic stress tolerance in *osgi* plants was due to its relatively smaller size (**Figures 1B, 3A**), additional osmotic stress tests were performed using size-matched WT plants and *osgi* seedlings at 11 DAG (WT) and 14 DAG (*osgi*), respectively (**Figures 4A,B**). Results showed that *osgi* plants still exhibited much higher tolerance to PEG treatment than WT plants (**Figure 4A**).

To confirm these results, the *OsGI* overexpression lines L1 and L2 were analyzed for their tolerance to osmotic stress. Results showed that L1 and L2 lines displayed increased sensitivity to osmotic stress under PEG exposure (**Figure 3**) compared to *osgi* mutants. However, we did not detect any differences between WT



and *OsGI* overexpressing plants in response to PEG treatment (**Figure 3**). These results confirmed that *OsGI* functions as a negative factor in the osmotic tolerance of rice.

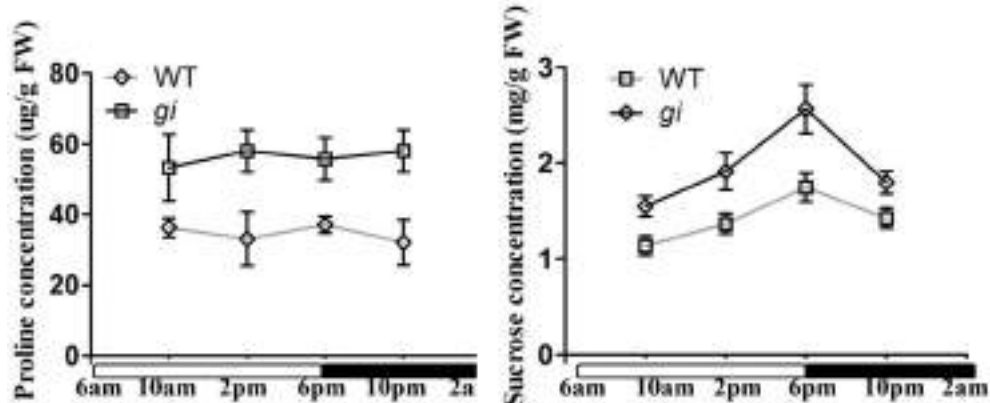


FIGURE 5 | Analysis of proline and sucrose contents in WT and *osgi* plants. Proline and sucrose contents in leaves of 15-day-old WT and *osgi* plants grown under normal conditions. All data represent the mean of three biological replicates, with error bars indicating SD. The unfilled and filled bars below the x-axis indicate times of lights-on and lights-off, respectively.

Mutation of OsGI Increases Proline and Sucrose Contents in Rice

It is generally accepted that under abiotic stress conditions, plants often accumulate compatible osmolytes to maintain osmotic balance and protect their subcellular structures from damage. Several studies have shown that the accumulation of free proline is positively correlated to plant tolerance to dehydration stress (Shinozaki and Yamaguchi-Shinozaki, 2007; Xiong et al., 2012). In order to assess whether mutation of *OsGI* can enhance the accumulation of osmotic protectants, the free proline content in WT and *osgi* plants was analyzed (Figure 5). Leaves from plants grown under normal conditions were collected at four different time points at 15 DAG and the proline content measured. At all times, the proline content was higher in *osgi* than in WT plants. For example, 8 h after lights-on, the proline levels in *osgi* plants were approximately 1.7 times higher than in WT plants (Figure 5). Moreover, while sucrose levels increased throughout the day and decreased at night in both WT and *osgi* plants, *osgi* plants had higher sucrose levels than WT plants at all times (Figure 5). The sucrose content in L1 and L2 plants was not altered compared to WT plants (Supplementary Figure 3). These results suggest that *osgi* plants possess a much higher osmotic potential, which could be beneficial in protecting plants against osmotic stress.

Stomata Movement in WT and *osgi* Plants

In *Arabidopsis*, *GI* has been shown to be involved in the regulation of stomata opening (Ando et al., 2013). To investigate whether *OsGI* participates in the regulation of stomata movement under dehydration stress conditions, the stomata conductance (g_s) and transpiration rate (T_r) in WT and *osgi* plants were measured using LI-6400. 35-day-old WT and *osgi* seedlings, grown under normal conditions or treated with 18% PEG 8000 at 4, 6, and 8 h after lights-on, were used for the experiment. The g_s and T_r were recorded 9 h after lights-on (1, 3, and 5 h after PEG treatment, respectively) using an LI-6400.

Under normal growth conditions, there was no difference in the g_s and T_r between WT and *osgi* plants (Figure 6). PEG treatment reduced the g_s and T_r in both WT and *osgi* plants. The g_s decreased by 70, 75, and 90% in WT plants after PEG treatment for 1, 3, and 5 h, respectively. In contrast, the g_s in *osgi* seedlings decreased rapidly by about 90% after only 1 h of PEG treatment and stayed at a similarly low level after 3 and 5 h of PEG exposure. The change in T_r in response to PEG treatment followed a similar pattern as g_s (Figure 6). These results indicate that under osmotic stress conditions, stomata movement changes faster in *osgi* mutant plants than in WT plants.

Mutation of OsGI Alters the Expression Pattern of Dehydration-Related Genes

To investigate the impact of *OsGI* mutation on the expression of genes involved in the response to dehydration stress, qRT-PCR was carried out on leaf samples of WT and *osgi* plants grown under normal or PEG treatment conditions. The expression of *OsGI* was not affected by osmotic stress (Figure 7, Supplementary Figure 4). *OsDREB1E*, *OsAP37*, *OsAP59*, *OsLEA3*, *OsRAB16A*, *OsLIP9*, and *OsSalT*, which have been shown to be positively associated with osmotic stress tolerance, were selected for analysis (Chaves et al., 2003; Umezawa et al., 2006; Valliyodan and Nguyen, 2006; Shinozaki and Yamaguchi-Shinozaki, 2007; Xiao et al., 2007; Fukao et al., 2011). As expected, the expression of *OsAP37*, *OsAP59*, *OsLEA3*, *OsRAB16A*, *OsLIP9*, and *OsSalT* were induced by osmotic stress (Figure 7). Under normal conditions, the transcript abundance of all tested genes was significantly higher in *osgi* mutants than in the WT. Osmotic stress conditions further increased the expression of *OsAP37*, *OsAP59*, and *OsSalT* in *osgi* mutants (Figure 7). These results suggest that dehydration-responsive genes are constitutively active in *osgi* mutant plants.

To elucidate the molecular function of *OsGI*, the expression profiles in *osgi* mutant and WT leaves were analyzed using Affymetrix GeneChip. Microarray analysis revealed that mutation of *osgi* results in substantial transcriptomic

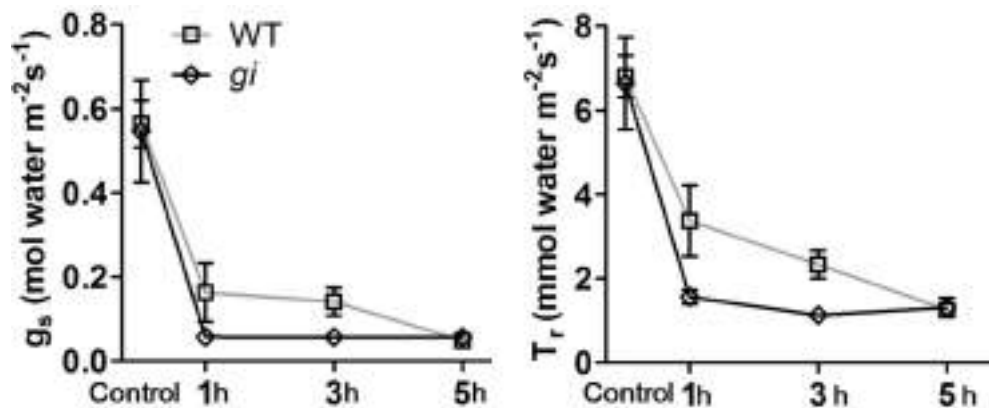


FIGURE 6 | Analysis of stomata conductance (gs) and transpiration rate (Tr) in WT and *osgi* plants. Stomata conductance (gs) and transpiration rate (Tr) in WT and *osgi* plants after PEG treatment for 1, 3, and 5 h. 35-day-old WT and *osgi* plants grown under normal conditions or treated with 18% PEG 8000 at 4, 6, and 8 h after lights-on, respectively, were used for the experiment. The gs and Tr were recorded in *osgi* and WT plants using an Li-6400 at 9 h after lights-on. All data represent the mean of three biological replicates, with error bars indicating SD.

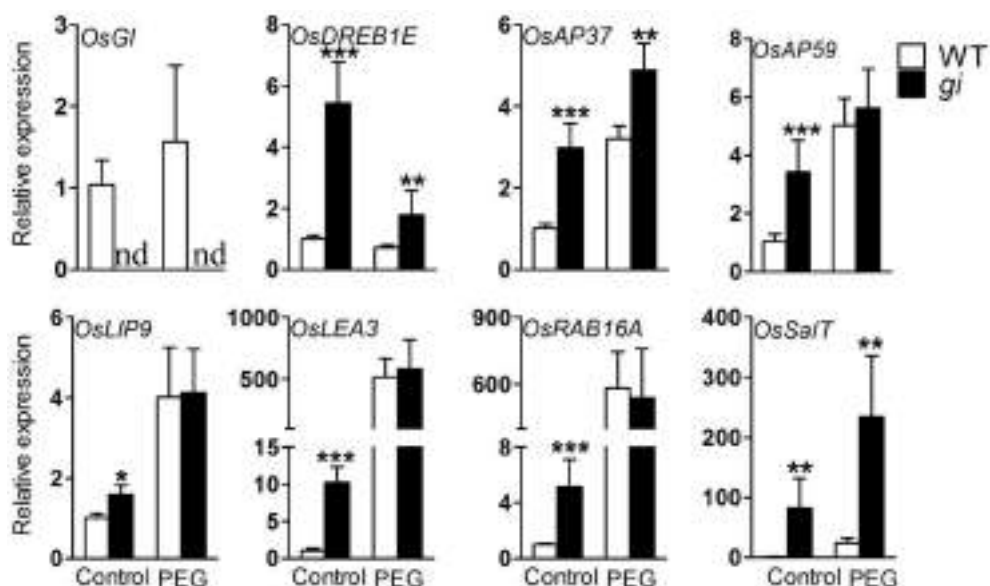


FIGURE 7 | Expression of water deficiency-related genes in WT and *osgi* leaves. WT and *osgi* plants were grown under normal conditions for 15 days and then cultured in 18% PEG 8000 or normal culture media for 2 days. Leaves were sampled 8 h after lights-on. Total RNA was extracted from the leaves and used for qRT-PCR. All data represent the mean of three biological replicates, with error bars indicating SD. Expression of OsACTIN was used as the internal control. Significant differences relative to the corresponding WT strain are indicated with asterisks (**P < 0.001; **P < 0.01; and *P < 0.05).

reprogramming. Indeed, 1870 genes were differentially expressed in the *osgi* mutant background compared to WT plants ($p < 0.05$, PPDE > 0.95 , 2-fold cut-off), of which 594 and 1267 genes were down- or up-regulated, respectively (Figure 8). Given the increased osmotic stress tolerance in *osgi* plants, we compared the mutant transcriptome to a dehydration-altered transcriptome of WT rice (Qian et al., 2014). In summary, 151 down-regulated and 257 up-regulated genes in *osgi* overlapped with the reported dehydration stress responses (Figure 8; Jain et al., 2007).

In order to further assess how *OsGI* mutation alters dehydration stress-related genes, we analyzed the expression pattern of water deficiency-related genes in leaves in our microarray. Abscisic acid (ABA) is thought to be involved in the regulation of stomata movement and plays a critical role in the response to drought (Chaves et al., 2003). Given the regulation of *OsGI* in stomata opening, the expression of ABA-related genes was examined in *osgi* plants (Table 1). A number of genes involved in ABA signaling displayed altered expression in *osgi* leaves, including several ABA-induced proteins and

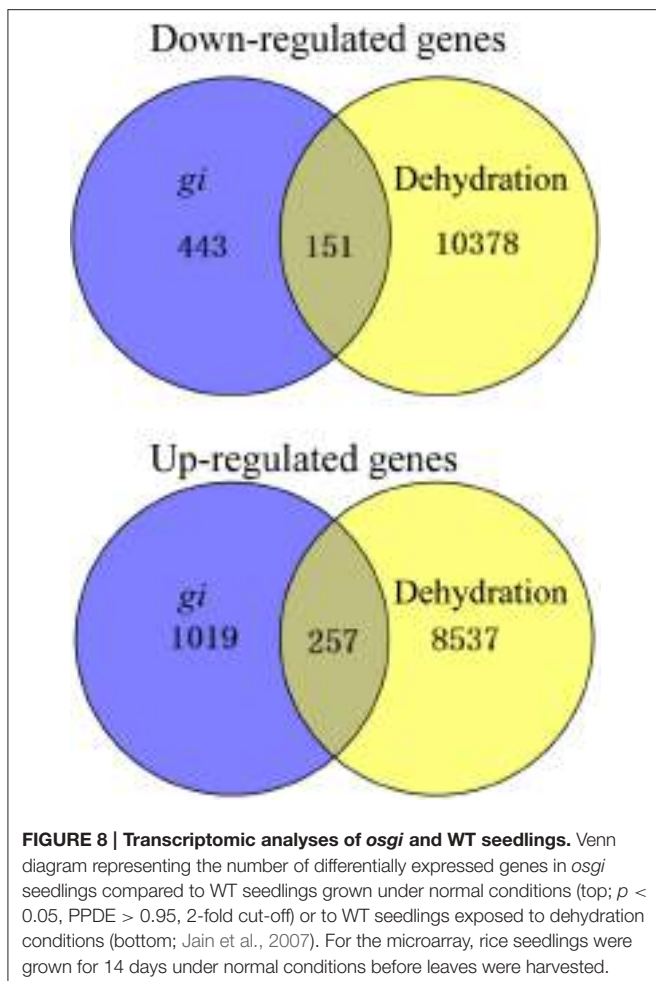


FIGURE 8 | Transcriptomic analyses of *osgi* and WT seedlings. Venn diagram representing the number of differentially expressed genes in *osgi* seedlings compared to WT seedlings grown under normal conditions (top; $p < 0.05$, PPDE > 0.95 , 2-fold cut-off) or to WT seedlings exposed to dehydration conditions (bottom; Jain et al., 2007). For the microarray, rice seedlings were grown for 14 days under normal conditions before leaves were harvested.

protein phosphatase 2C (PP2C) genes in subfamily A (Table 1; Schweighofer et al., 2004). Since improved antioxidant capacity is critical in order for plants to survive in water-limited conditions, the expression levels of antioxidant genes were investigated in the microarray (Mittler et al., 2004; Hu et al., 2008). Surprisingly, mutation of OsGI activated antioxidant genes including superoxide dismutase, peroxidase and thioredoxin (Table 2), indicating that *osgi* plants are strong Reactive Oxygen Species (ROS) scavengers. Furthermore, increased expression of chaperones which protect proteins from stress damage has been shown to improve plant tolerance to water deficits (Wang et al., 2004). Accordingly, the expression of various chaperone genes such as heat shock proteins increased in *osgi* plants (Table 3).

DISCUSSION

In the past decade, the identification of many key factors involved in the response to water deficits has greatly increased our understanding of molecular mechanisms participating in the osmotic response in plants. In our current study, we investigated the role of a key flowering time regulator, OsGI, in osmotic stress tolerance in rice. Our data revealed that OsGI plays a negative role in the rice response to water deficiency by regulating at both

TABLE 1 | ABA signaling-related genes with significantly altered transcript abundance in *osgi* compared to WT leaves ($p < 0.05$).

TIGR locus identifier	Fold change	Description
	<i>osgi</i> vs. WT	
ABA		
Os04g52090	2.54	OsAP2-39
Os03g09170	2.63	DRE binding factor
Os09g35010	2.11	HvCBF4
Os04g46440	3.23	DREB1C
Os11g30500	3.73	ABA induced protein
Os04g34600	1.58	ABA induced protein
Os06g14370	4.91	ABA induced protein
Os11g06720	1.63	Abscisic stress ripening protein (OsASR5)
Os07g07050	3.26	Abscisic-aldehyde oxidase
Os07g18120	1.75	Abscisic-aldehyde oxidase
Os02g52780	1.53	bZIP transcription factor AB15
Os05g50800	4.22	ABIL1 protein
Os02g03960	-2.52	Transcription factor, OsbZIP14
Os02g49860	-11.10	ABA induced plasma membrane protein PM 19
Os02g50140	-2.95	ABA-induced protein
Os09g07380	-1.35	ABI3-interacting protein 2
Os01g73250	-3.29	Abscisic stress-ripening (OsASR6)
PP2C		
Os01g40094	3.98	Protein phosphatase 2C
Os05g46040	1.47	Protein phosphatase 2C
Os03g16170	4.06	Protein phosphatase 2C
Os09g15670	7.29	Protein phosphatase 2C
Os01g62760	1.55	Protein phosphatase 2C
Os01g46760	1.52	Protein phosphatase 2C

TIGR locus identifiers are given for each transcript at the left. Expression ratio in *osgi* vs. WT leaves is shown. The annotation description of each gene is according to the TIGR and RAP general description. Positive numbers indicate increased gene expression whereas negative numbers indicate decreased gene expression.

physiological and transcriptional levels. Results from our analysis suggest that in *osgi* mutant plants, several components of the osmotic stress response are constitutively activated.

Alteration of OsGI could have improved the plant osmotic stress response in two ways. One, the osmotic potential in the *osgi* mutant could have increased due to the constitutively altered morphology, metabolism and gene expression which led to the accumulation of osmoprotectants such as sucrose and proline. It has been shown that increased sucrose and proline contents improve plant tolerance to osmotic stress (Hadiarto and Tran, 2011). In *osgi* seedlings, concentrations of sucrose and proline increased in the leaves (Figure 5), which could have increased the plants' osmotic potential to defend against dehydration. Alteration of OsGI could also play a role in the osmotic stress response because rapid physiological adjustment has been shown to decrease water loss and improve water utilization (Hirayama and Shinozaki, 2010; Hadiarto and Tran, 2011; Xiong et al., 2012). In plants, water loss mainly occurs in transpiration via stomata

TABLE 2 | Genes involved in antioxidant synthesis with significantly altered transcript abundance in *osgi* compared to WT leaves ($p < 0.05$).

TIGR locus identifier	Fold change	Description
	<i>osgi</i> vs. WT	
Os07g46990	1.59	Superoxide dismutase
Os08g44770	1.92	Superoxide dismutase
Os06g02500	2.21	Superoxide dismutase
Os05g25850	1.29	Superoxide dismutase
Os01g61320	2.19	Thioredoxin family protein
Os03g58630	1.24	Thioredoxin H-type 5 (OsTrx10)
Os01g07376	1.65	Thioredoxin H-type (OsTrx1)
Os02g56900	2.31	Thioredoxin family protein
Os08g29110	1.44	Thioredoxin family protein
Os02g53400	1.30	Thioredoxin-like 5, chloroplast precursor
Os05g11090	1.45	Thioredoxin-like 6, chloroplast precursor
Os04g15690	5.24	DSBA-like thioredoxin domain containing protein
Os06g37080	1.55	L-ascorbate oxidase precursor
Os11g42220	4.06	L-ascorbate oxidase precursor
Os08g44340	2.50	monodehydroascorbate reductase
Os07g49400	1.19	OsAPx2—Cytosolic Ascorbate Peroxidase gene
Os01g19020	15.16	Peroxidase 1 precursor
Os05g04380	18.38	Peroxidase 1 precursor
Os01g22370	1.62	Peroxidase 1 precursor
Os01g22230	2.37	Peroxidase 1 precursor
Os10g39170	1.33	Peroxidase 1 precursor
Os01g07770	2.62	Peroxidase 25 precursor
Os06g46799	2.18	Peroxidase 39 precursor
Os05g04500	9.58	Peroxidase 63 precursor
Os06g13050	1.50	Peroxidase family protein
Os06g09610	2.64	Peroxiredoxin bcp
Os02g09940	5.88	Peroxiredoxin-5, mitochondrial precursor
Os01g16152	1.77	Peroxiredoxin-5, mitochondrial precursor
Os02g33450	1.67	2-cys peroxiredoxin BAS1, chloroplast precursor

opening. Stomata movement is critical for plants to reduce transpiration and to rapidly respond to osmotic stress conditions (Chaves et al., 2003; Valliyodan and Nguyen, 2006). In *osgi* plants, the accelerated stomata closure could have greatly improved water utilization by rapidly decreasing the transpiration rate in leaves, resulting in decreased water loss (Figures 3D, 6).

Although GI shares no known functional domains with other proteins, it has been shown to function in many pathways at the protein level (Shi et al., 2000; Kim et al., 2013; Park et al., 2013). In our study, expression of OsGI is not affected by osmotic stress at the transcriptional level (Figure 7, Supplementary Figure 4), indicating that OsGI might function purely on a protein level in the response to dehydration stress. Further study to determine

TABLE 3 | Genes involved in chaperone synthesis with significantly different transcript abundance in *osgi* vs. WT leaves ($p < 0.05$).

TIGR locus identifier	Fold change	Description
	<i>osgi</i> vs. WT	
Os02g52150	2.93	Heat shock protein (OsHSP20)
Os06g11610	3.57	Heat shock protein
Os09g31486	2.20	Heat shock 70 kDa protein, mitochondrial precursor
Os02g53420	1.31	Heat shock 70 kDa protein, mitochondrial precursor
Os03g60620	1.25	Heat shock cognate 70 kDa protein 2
Os01g62290	2.36	Heat shock cognate 70 kDa protein
Os05g38530	2.25	Heat shock cognate 70 kDa protein
Os06g35960	3.03	Heat shock factor protein
Os04g48030	2.05	Heat shock factor protein
Os09g28354	4.39	Heat shock factor protein
Os01g43590	2.04	Heat shock factor protein HSF8
Os08g39140	1.30	Heat shock protein 81-1
Os03g18200	1.30	Heat shock protein DnaJ
Os12g31460	1.50	Heat shock protein DnaJ
Os01g53220	2.13	Heat shock factor protein (OshsfC1b)
Os03g16040	1.84	Heat shock protein (OsHsp17.7)
Os02g54140	2.82	Heat shock protein
Os10g32550	1.99	Chaperonin CPN60-1, mitochondrial precursor
Os03g04970	1.85	Chaperonin CPN60-1, mitochondrial precursor
Os05g46290	1.69	Chaperonin CPN60-2, mitochondrial precursor
Os06g09679	1.29	Chaperonin, chloroplast precursor
Os09g26730	1.54	Chaperonin, chloroplast precursor
Os03g25050	2.18	Chaperonin
Os07g44740	1.78	Chaperonin
Os03g25050	1.79	Chaperonin

the OsGI protein abundance under osmotic stress conditions will provide more insight into the molecular mechanisms by which OsGI responds to dehydration stress. Interestingly, mutation of OsGI resulted in substantial transcriptomic reprogramming, and 151 of the down- and 257 of the up-regulated genes in *osgi* leaves showed the same (down/up-regulated) response in WT leaves exposed to dehydration conditions (Figure 8). However, further studies are required to determine the mechanisms by which OsGI regulates the transcriptional response to osmotic pressure.

ABA is required for plants to adapt stomata movement to water-deficient conditions (Fujita et al., 2011). Because OsGI is involved in regulating stomata opening (Figure 6), ABA-related genes were examined in *osgi* plants. Results showed that a number of genes involved in ABA signaling were altered in *osgi* leaves (Table 1). Although the growth phenotype of rice *osgi* plants under ABA treatment was comparable to that of WT plants (data not shown), GI has been shown to function in ABA metabolism

(Penfield and Hall, 2009; Riboni et al., 2013). Indeed, *GI* has been suggested to play a role in drought response and seed dormancy in an ABA-dependent pathway (Penfield and Hall, 2009; Riboni et al., 2013). *GI* serves as a core gene in the circadian rhythm of plants, and recent research revealed that around 40% of ABA-related genes are controlled by the circadian clock (Covington et al., 2008; Legnaioli et al., 2009). The circadian gene TOC1 participates in ABA signaling by regulating ABA-Related gene (ABAR) and by interacting with Abscisic Acid Insensitive 3 (ABI3) and is degraded by ZEITLUPE (ZTL) (Kurup et al., 2000; Kim et al., 2007). It is possible that *GI* functions in ABA signaling via TOC1 regulation by directly interacting with ZTL (Kim et al., 2007). In addition, the *GI*-CO-FT flowering time regulatory system is also conserved in stomata regulation (Ando et al., 2013). FT is required for maintaining H⁺-ATPase activation to regulate stomata opening (Kinoshita et al., 2011). *GI* might therefore be involved in the H⁺-ATPase-dependent regulation of stomata movement. Our results suggest that *GI* could regulate stomata movement via multiple pathways but how *GI* regulates stomata movement in response to osmotic stress still needs further investigation.

ROS can quickly accumulate in plants under osmotic stress and cause oxidative damage to proteins. As a result, ROS scavenging is critical for plants in order to survive under water deficient condition (Umezawa et al., 2006). In Arabidopsis, increased levels of superoxide dismutase and ascorbate peroxidase confer oxidative stress tolerance in *Atgi* plants (Kurepa et al., 1998; Cao et al., 2006). In rice, superoxide dismutase, peroxidase and thioredoxin are constitutively active in *osgi* plants to defend against oxidative damage (Table 2). Moreover, molecular chaperones are key factors in protein stabilization, and the increased expression of chaperone genes in *osgi* leaves is speculated to protect proteins from dehydration damage (Table 3; Wang et al., 2004).

Compared to WT, a majority of the alterations in *osgi* plants, such as sucrose, were observed both in the field and greenhouse (Figure 5; Izawa et al., 2011). However, transcriptome and metabolome analysis revealed that *osgi* plants exhibited different responses in the field and greenhouse in some pathways. While stomata conductance was higher in field-grown *osgi* than WT plants, there was no difference between *osgi* and WT plants grown under normal conditions in the greenhouse (Figure 6; Izawa et al., 2011). Conversely, *osgi* plants grown in the greenhouse had higher proline contents than WT plants (Figure 5) while there was no difference in the proline contents of field-grown *osgi* and WT plants (Izawa et al., 2011). The TCA cycle intermediate malate was decreased in field-grown but increased in greenhouse-grown *osgi* plants (Izawa et al., 2011). In addition, Expressions of some key genes in the phenylpropanoid

pathway, a secondary metabolite pathway controlled by circadian clocks, was significantly upregulated in *osgi* plants in the field, but none of these genes were altered in our microarray, indicating that OsGI function is affected by the environment (Izawa et al., 2011).

The tolerance to osmotic stress prompted us to check whether *osgi* plants exhibit drought resistance but we did not detect any differences between WT and *osgi* plants grown in soil under drought condition (data not shown), nor did we find any differences between WT and *osgi* plants in response to salt stress. In Arabidopsis, *GI*-deficient plants exhibit increased sensitivity to drought but improved tolerance to salt stress (Han et al., 2013; Kim et al., 2013), suggesting divergent functions of *GI* in drought and salt resistance in rice and Arabidopsis. Seedlings encounter sudden dehydration stress when transferred from normal culture media to PEG-treated media, as opposed to soil-grown plants where water depletion and thus drought formation is much more gradual, commonly occurring over hours or even days. In conclusion, while *osgi* plants are capable of tolerating sudden osmotic stress to some degree, further study is needed to better understand the mechanisms by which OsGI is involved in drought response.

In summary, we have shown that OsGI is an essential regulator of the plant response to dehydration stress, and modification of OsGI expression might improve the osmotic tolerance of crop cultures. However, more work remains to be done to fully understand the mechanisms of action by which OsGI functions in the regulation of the plant stress response.

AUTHOR CONTRIBUTIONS

HS conceived and designed the research. SL, WY, MW, WQ, and LZ conducted the experiments and analyzed the data. SL and HS wrote the manuscript. All authors read and approved the manuscript.

ACKNOWLEDGMENTS

This work was supported by the National Natural Science Foundation (31172024, 31401934, 31572189). The authors thank the RGRC (Rice Genome Resource Center, Japan) for the *Tos17* insertion mutant NF8540.

SUPPLEMENTARY MATERIAL

The Supplementary Material for this article can be found online at: <http://journal.frontiersin.org/article/10.3389/fpls.2016.00465>

REFERENCES

- Ando, E., Ohnishi, M., Wang, Y., Matsushita, T., Watanabe, A., Hayashi, Y., et al. (2013). TWIN SISTER OF FT, GIGANTEA, and CONSTANS have a positive but indirect effect on blue light-induced stomatal opening in Arabidopsis. *Plant Physiol.* 162, 1529–1538. doi: 10.1104/pp.113.217984

- Bates, L. S., Waldren, R. P., and Teare, I. D. (1973). Rapid determination of free proline for water-stress studies. *Plant Soil* 39, 205–207. doi: 10.1007/BF00018060
 Cao, S., Jiang, S., and Zhang, R. (2006). The role of GIGANTEA gene in mediating the oxidative stress response and in Arabidopsis. *Plant Growth Regul.* 48, 261–270. doi: 10.1007/s10725-006-0012-8

- Cao, S., Ye, M., and Jiang, S. (2005). Involvement of GIGANTEA gene in the regulation of the cold stress response in Arabidopsis. *Plant Cell Rep.* 24, 683–690. doi: 10.1007/s00299-005-0061-x
- Chaves, M. M., Maroco, J. O. P., and Pereira, J. O. S. (2003). Understanding plant responses to drought—from genes to the whole plant. *Funct. Plant Biol.* 30, 239–264. doi: 10.1071/fp02076
- Covington, M. F., Maloof, J. N., Straume, M., Kay, S. A., and Harmer, S. L. (2008). Global transcriptome analysis reveals circadian regulation of key pathways in plant growth and development. *Genome Biol.* 9:R130. doi: 10.1186/gb-2008-9-8-r130
- Dalchow, N., Baek, S. J., Briggs, H. M., Robertson, F. C., Dodd, A. N., Gardner, M. J., et al. (2011). The circadian oscillator gene GIGANTEA mediates a long-term response of the Arabidopsis thaliana circadian clock to sucrose. *Proc. Natl. Acad. Sci. U.S.A.* 108, 5104–5109. doi: 10.1073/pnas.1015452108
- Fowler, S., Lee, K., Onouchi, H., Samach, A., Richardson, K., Morris, B., et al. (1999). GIGANTEA: a circadian clock-controlled gene that regulates photoperiodic flowering in Arabidopsis and encodes a protein with several possible membrane-spanning domains. *EMBO J.* 18, 4679–4688. doi: 10.1093/emboj/18.17.4679
- Fowler, S., and Thomashow, M. F. (2002). Arabidopsis transcriptome profiling indicates that multiple regulatory pathways are activated during cold acclimation in addition to the CBF cold response pathway. *Plant Cell* 14, 1675–1690. doi: 10.1105/tpc.003483
- Fujita, Y., Fujita, M., Shinozaki, K., and Yamaguchi-Shinozaki, K. (2011). ABA-mediated transcriptional regulation in response to osmotic stress in plants. *J. Plant Res.* 124, 509–525. doi: 10.1007/s10265-011-0412-3
- Fukao, T., Yeung, E., and Bailey-Serres, J. (2011). The submergence tolerance regulator SUB1A mediates crosstalk between submergence and drought tolerance in rice. *Plant Cell* 23, 412–427. doi: 10.1105/tpc.110.080325
- Hadiarto, T., and Tran, L.-S. (2011). Progress studies of drought-responsive genes in rice. *Plant Cell Rep.* 30, 297–310. doi: 10.1007/s00299-010-0956-z
- Han, Y., Zhang, X., Wang, Y., and Ming, F. (2013). The suppression of WRKY44 by GIGANTEA-miR172 pathway is involved in drought response of Arabidopsis thaliana. *PLoS ONE* 8:e73541. doi: 10.1371/journal.pone.0073541
- Hayama, R., Yokoi, S., Tamaki, S., Yano, M., and Shimamoto, K. (2003). Adaptation of photoperiodic control pathways produces short-day flowering in rice. *Nature* 422, 719–722. doi: 10.1038/nature01549
- Hecht, V., Knowles, C. L., Vander Schoor, J. K., Liew, L. C., Jones, S. E., Lambert, M. J., et al. (2007). Pea LATE BLOOMER1 is a GIGANTEA ortholog with roles in photoperiodic flowering, deetiolation, and transcriptional regulation of circadian clock gene homologs. *Plant Physiol.* 144, 648–661. doi: 10.1104/pp.107.096818
- Higuchi, Y., Sage-Ono, K., Sasaki, R., Ohtsuki, N., Hoshino, A., Iida, S., et al. (2011). Constitutive expression of the GIGANTEA ortholog affects circadian rhythms and suppresses one-shot induction of flowering in Pharbitis nil, a typical short-day plant. *Plant Cell Physiol.* 52, 638–650. doi: 10.1093/pcp/pcr023
- Hinch, D. K., Zuther, E., Hellwege, E. M., and Heyer, A. G. (2002). Specific effects of fructo- and gluco-oligosaccharides in the preservation of liposomes during drying. *Glycobiology* 12, 103–110. doi: 10.1093/glycob/12.2.103
- Hirayama, T., and Shinozaki, K. (2010). Research on plant abiotic stress responses in the post-genome era: past, present and future. *Plant J.* 61, 1041–1052. doi: 10.1111/j.1365-313X.2010.04124.x
- Hu, X., Wang, W., Li, C., Zhang, J., Lin, F., Zhang, A., et al. (2008). Cross-talks between Ca²⁺/CaM and H₂O₂ in abscisic acid-induced antioxidant defense in leaves of maize plants exposed to water stress. *Plant Growth Regul.* 55, 183–198. doi: 10.1007/s10725-008-9272-9
- Ikegami, K., Okamoto, M., Seo, M., and Koshiba, T. (2009). Activation of abscisic acid biosynthesis in the leaves of Arabidopsis thaliana in response to water deficit. *J. Plant Res.* 122, 235–243. doi: 10.1007/s10265-008-0201-9
- Itoh, H., and Izawa, T. (2011). A study of phytohormone biosynthetic gene expression using a circadian clock-related mutant in rice. *Plant Signal. Behav.* 6, 1932–1936. doi: 10.4161/psb.6.12.18207
- Izawa, T., Mihara, M., Suzuki, Y., Gupta, M., Itoh, H., Nagano, A. J., et al. (2011). Os-GIGANTEA confers robust diurnal rhythms on the global transcriptome of rice in the field. *Plant Cell* 23, 1741–1755. doi: 10.1105/tpc.111.083238
- Jain, M., Nijhawan, A., Arora, R., Agarwal, P., Ray, S., Sharma, P., et al. (2007). F-box proteins in rice. Genome-wide analysis, classification, temporal and spatial gene expression during panicle and seed development, and regulation by light and abiotic stress. *Plant Physiol.* 143, 1467–1483. doi: 10.1104/pp.106.091900
- Kim, W. Y., Ali, Z., Park, H. J., Park, S. J., Cha, J. Y., Perez-Hormaeche, J., et al. (2013). Release of SOS2 kinase from sequestration with GIGANTEA determines salt tolerance in Arabidopsis. *Nat. Commun.* 4:1352. doi: 10.1038/ncomms2357
- Kim, W. Y., Fujiwara, S., Suh, S. S., Kim, J., Kim, Y., Han, L., et al. (2007). ZEITLUPE is a circadian photoreceptor stabilized by GIGANTEA in blue light. *Nature* 449, 356–360. doi: 10.1038/nature06132
- Kinoshita, T., Ono, N., Hayashi, Y., Morimoto, S., Nakamura, S., Soda, M., et al. (2011). FLOWERING LOCUS T regulates stomatal opening. *Curr. Biol.* 21, 1232–1238. doi: 10.1016/j.cub.2011.06.025
- Koornneef, M., Hanhart, C. J., and van der Veen, J. H. (1991). A genetic and physiological analysis of late flowering mutants in Arabidopsis thaliana. *Mol. Gen. Genet.* 229, 57–66. doi: 10.1007/BF00264213
- Kurepa, J., Smalle, J., Van Montagu, M., and Inze, D. (1998). Oxidative stress tolerance and longevity in Arabidopsis: the late-flowering mutant gigantea is tolerant to paraquat. *Plant J.* 14, 759–764. doi: 10.1046/j.1365-313x.1998.00168.x
- Kurup, S., Jones, H. D., and Holdsworth, M. J. (2000). Interactions of the developmental regulator ABI3 with proteins identified from developing Arabidopsis seeds. *Plant J.* 21, 143–155. doi: 10.1046/j.1365-313x.2000.00663.x
- Legnaioli, T., Cuevas, J., and Mas, P. (2009). TOC1 functions as a molecular switch connecting the circadian clock with plant responses to drought. *EMBO J.* 28, 3745–3757. doi: 10.1038/emboj.2009.297
- Li, S., Wang, C., Zhou, L., and Shou, H. (2014). Oxygen deficit alleviates phosphate overaccumulation toxicity in OsPHR2 overexpression plants. *J. Plant Res.* 127, 433–440. doi: 10.1007/s10265-014-0628-0
- Liu, J., Zhang, F., Zhou, J., Chen, F., Wang, B., and Xie, X. (2012). Phytochrome B control of total leaf area and stomatal density affects drought tolerance in rice. *Plant Mol. Biol.* 78, 289–300. doi: 10.1007/s11103-011-9860-3
- Mishra, P., and Panigrahi, K. C. (2015). GIGANTEA - an emerging story. *Front. Plant Sci.* 6:8. doi: 10.3389/fpls.2015.00008
- Mittler, R., Vanderauwera, S., Gollery, M., and Van Breusegem, F. (2004). Reactive oxygen gene network of plants. *Trends Plant Sci.* 9, 490–498. doi: 10.1016/j.tplants.2004.08.009
- Mouradov, A., Cremer, F., and Coupland, G. (2002). Control of flowering time: interacting pathways as a basis for diversity. *Plant Cell* 14 (Suppl.), S111–S130. doi: 10.1105/tpc.001362
- Park, D. H., Somers, D. E., Kim, Y. S., Choy, Y. H., Lim, H. K., Soh, M. S., et al. (1999). Control of circadian rhythms and photoperiodic flowering by the Arabidopsis GIGANTEA gene. *Science* 285, 1579–1582. doi: 10.1126/science.285.5433.1579
- Park, H. J., Kim, W. Y., and Yun, D. J. (2013). A role for GIGANTEA: Keeping the balance between flowering and salinity stress tolerance. *Plant Signal. Behav.* 8:e24820. doi: 10.4161/psb.24820
- Penfield, S., and Hall, A. (2009). A role for multiple circadian clock genes in the response to signals that break seed dormancy in Arabidopsis. *Plant Cell* 21, 1722–1732. doi: 10.1105/tpc.108.064022
- Qian, H., Han, X., Peng, X., Lu, T., Liu, W., and Fu, Z. (2014). The circadian clock gene regulatory module enantioselectively mediates imazethapyr-induced early flowering in Arabidopsis thaliana. *J. Plant Physiol.* 171, 92–98. doi: 10.1016/j.jplph.2013.11.011
- Riboni, M., Galbiati, M., Tonelli, C., and Conti, L. (2013). GIGANTEA enables drought escape response via abscisic acid-dependent activation of the florigens and SUPPRESSOR OF OVEREXPRESSION OF CONSTANS. *Plant Physiol.* 162, 1706–1719. doi: 10.1104/pp.113.217729
- Schweighofer, A., Hirt, H., and Meskiene, I. (2004). Plant PP2C phosphatases: emerging functions in stress signaling. *Trends Plant Sci.* 9, 236–243. doi: 10.1016/j.tplants.2004.03.007
- Shi, H., Ishitani, M., Kim, C., and Zhu, J. K. (2000). The Arabidopsis thaliana salt tolerance gene SOS1 encodes a putative Na⁺/H⁺ antiporter. *Proc. Natl. Acad. Sci. U.S.A.* 97, 6896–6901. doi: 10.1073/pnas.120170197
- Shinozaki, K., and Yamaguchi-Shinozaki, K. (2007). Gene networks involved in drought stress response and tolerance. *J. Exp. Bot.* 58, 221–227. doi: 10.1093/jxb/erl164

- Shinozaki, K., Yamaguchi-Shinozaki, K., Mizoguchi, T., Urao, T., Katagiri, T., Nakashima, K., et al. (1998). Molecular responses to water stress in *Arabidopsis thaliana*. *J. Plant Res.* 111, 345–351. doi: 10.1007/BF02512195
- Srikanth, A., and Schmid, M. (2011). Regulation of flowering time: all roads lead to Rome. *Cell. Mol. Life Sci.* 68, 2013–2037. doi: 10.1007/s00018-011-0673-y
- Umezawa, T., Fujita, M., Fujita, Y., Yamaguchi-Shinozaki, K., and Shinozaki, K. (2006). Engineering drought tolerance in plants: discovering and tailoring genes to unlock the future. *Curr. Opin. Biotech.* 17, 113–122. doi: 10.1016/j.copbio.2006.02.002
- Valliyodan, B., and Nguyen, H. T. (2006). Understanding regulatory networks and engineering for enhanced drought tolerance in plants. *Curr. Opin. Biotech.* 9, 189–195. doi: 10.1016/j.pbi.2006.01.019
- Villadsen, D., Rung, J. H., and Nielsen, T. H. (2005). Osmotic stress changes carbohydrate partitioning and fructose-2,6-bisphosphate metabolism in barley leaves. *Funct. Plant Biol.* 32, 1033–1043. doi: 10.1071/FP05102
- Wang, C., Ying, S., Huang, H., Li, K., Wu, P., and Shou, H. (2009). Involvement of OsSPX1 in phosphate homeostasis in rice. *Plant J.* 57, 895–904. doi: 10.1111/j.1365-313X.2008.03734.x
- Wang, W., Vinocur, B., Shoseyov, O., and Altman, A. (2004). Role of plant heat-shock proteins and molecular chaperones in the abiotic stress response. *Trends Plant Sci.* 9, 244–252. doi: 10.1016/j.tplants.2004.03.006
- Xiao, B., Huang, Y., Tang, N., and Xiong, L. (2007). Over-expression of a LEA gene in rice improves drought resistance under the field conditions. *Theor. Appl. Genet.* 115, 35–46. doi: 10.1007/s00122-007-0538-9
- Xiong, J., Zhang, L., Fu, G., Yang, Y., Zhu, C., and Tao, L. (2012). Drought-induced proline accumulation is uninvolved with increased nitric oxide, which alleviates drought stress by decreasing transpiration in rice. *J. Plant Res.* 125, 155–164. doi: 10.1007/s10265-011-0417-y
- Yamaguchi-Shinozaki, K., Urao, T., and Shinozaki, K. (1995). Regulation of genes that are induced by drought stress in *Arabidopsis thaliana*. *J. Plant Res.* 108, 127–136. doi: 10.1007/BF02344316
- Yoshida, S., Forno, D. A., and Cock, J. H. K. G. (1976). *Laboratory Manual for Physiological Studies of Rice*, 3rd Edn. Manila: The International Rice Research Institute.

Conflict of Interest Statement: The authors declare that the research was conducted in the absence of any commercial or financial relationships that could be construed as a potential conflict of interest.

Copyright © 2016 Li, Yue, Wang, Qiu, Zhou and Shou. This is an open-access article distributed under the terms of the Creative Commons Attribution License (CC BY). The use, distribution or reproduction in other forums is permitted, provided the original author(s) or licensor are credited and that the original publication in this journal is cited, in accordance with accepted academic practice. No use, distribution or reproduction is permitted which does not comply with these terms.



Salinity and High Temperature Tolerance in Mungbean [*Vigna radiata* (L.) Wilczek] from a Physiological Perspective

Bindumadhava HanumanthaRao^{1*}, Ramakrishnan M. Nair² and Harsh Nayyar³

¹ Plant Physiology, World Vegetable Center, South Asia, Hyderabad, India, ² Vegetable Breeding – Legumes, World Vegetable Center, South Asia, Hyderabad, India, ³ Department of Botany, Panjab University, Chandigarh, India

OPEN ACCESS

Edited by:

Sylvain Jeandroz,
Agrosup Dijon, France

Reviewed by:

Michael Vincent Mickelbart,
Purdue University, USA
Anil Kumar Singh,
ICAR-Indian Institute of Agricultural
Biotechnology, India

*Correspondence:

Bindumadhava HanumanthaRao
bindu.madhava@worldveg.org

Specialty section:

This article was submitted to
Plant Physiology,
a section of the journal
Frontiers in Plant Science

Received: 18 January 2016

Accepted: 15 June 2016

Published: 29 June 2016

Citation:

HanumanthaRao B, Nair RM and
Nayyar H (2016) Salinity and High
Temperature Tolerance in Mungbean
[*Vigna radiata* (L.) Wilczek] from a
Physiological Perspective.

Front. Plant Sci. 7:957.

doi: 10.3389/fpls.2016.00957

Biotic and abiotic constraints seriously affect the productivity of agriculture worldwide. The broadly recognized benefits of legumes in cropping systems—biological nitrogen fixation, improving soil fertility and broadening cereal-based agro-ecologies, are desirable now more than ever. Legume production is affected by hostile environments, especially soil salinity and high temperatures (HTs). Among legumes, mungbean has acceptable intrinsic tolerance mechanisms, but many agro-physiological characteristics of the *Vigna* species remain to be explored. Mungbean has a distinct advantage of being short-duration and can grow in wide range of soils and environments (as mono or relay legume). This review focuses on salinity and HT stresses on mungbean grown as a fallow crop (mungbean-rice-wheat to replace fallow-rice-wheat) and/or a relay crop in cereal cropping systems. Salinity tolerance comprises multifaceted responses at the molecular, physiological and plant canopy levels. In HTs, adaptation of physiological and biochemical processes gradually may lead to improvement of heat tolerance in plants. At the field level, managing or manipulating cultural practices can mitigate adverse effects of salinity and HT. Greater understanding of physiological and biochemical mechanisms regulating these two stresses will contribute to an evolving profile of the genes, proteins, and metabolites responsible for mungbean survival. We focus on abiotic stresses in legumes in general and mungbean in particular, and highlight gaps that need to be bridged through future mungbean research. Recent findings largely from physiological and biochemical fronts are examined, along with a few agronomic and farm-based management strategies to mitigate stress under field conditions.

Keywords: salinity, high temperature, physiological mechanisms, Na and K uptake, cropping systems, mungbean

INTRODUCTION

Globally, agriculture productivity is inhibited by abiotic and biotic stresses, but abiotic stresses in particular (Gong et al., 2013) affect spreading of plant species across different environmental zones (Chaves et al., 2003). Under this situation, the widely accepted benefits of legumes in cropping systems are needed now more than ever (Arnoldi et al., 2014; Araujo et al., 2015). Legumes/pulses

Abbreviations: ABA, abscisic acid; ASC, ascorbic acid; HT, high temperature; MDA, melondealdehyde; NaCl, sodium chloride; ROS, reactive oxygen species; RuBisCO, Rubilose 1,5 Bisphosphate Carboxylase/Oxygenase.

are very important food and feed crops, known for their health benefits (Arnoldi et al., 2014) vital ingredient of Indian and Mediterranean diets and considered staple in other regions (Vaz Patto et al., 2014), have high demand as forage for producing high-quality meat and milk (Boelt et al., 2014).

The changing climate is expected to worsen abiotic factors globally and adaptation strategies need to be established for target crops to specific environments (Beebe et al., 2011). Connect between different stress factors will likely surge harm to crop yields (Beebe, 2012). As observed, the average yield of temperate legumes has moderately improved in past half a century, with about a 45–50% increase for most legumes (Araujo et al., 2015). The highest yield increase (~100%) was realized in groundnut etc, which is still lower than the jump achieved by major cereals (~140%) (FAOSTAT, 2013). The emphasis in last decade was on exploring ‘cause-effect’ (bio-physiological and molecular, etc.) relationships of abiotic stress responses of a broad range of crop species (Araujo et al., 2015). Although physiology given insights on plant responses referring stress tolerance, further dissection on the genetic basis of tolerance traits through integration of system biology approaches is needed to dissect the traits and ultimately obtain larger benefits (Mir et al., 2012; Araujo et al., 2015).

A recent review (Araujo et al., 2015) highlights the latest research accomplishments in understanding abiotic stress responses in model food and forage legumes, and supports the development of legumes that are better adapted to environmental constraints. The review emphasizes the need to address current demands on modern agriculture and food production activities impaired by global climate change. It mostly focused on mainstream crops such as soybean, common bean, chickpea, pea, cowpea and forage legumes such as alfalfa, but apparently less on abiotic stresses tolerance of other grain legumes like mungbean and black gram, probably largely due to the sparse availability of information on the diverse stress responses and the mechanisms of tolerance in these legume species.

Mungbean [*Vigna radiata* (L.) R. Wilczek] is cultivated on >6 million ha in the warmer regions of the world and is one of the most important pulse crops. It is a short duration (65–90 days) grain legume having wide adaptability and low input requirements (Nair et al., 2012). Cultivation of the crop extends across wide range of latitudes (40° N or S) in regions with diurnal temperatures of growing season are > 20°C (Lawn and Ahn, 1985). India is the largest producer and consumer, and accounts for about 65 and 54% of the world acreage and production respectively. Like other legumes, mungbean fixes atmospheric nitrogen (58–109 kg/ha) in symbiosis with *Rhizobium*, which not only meet its own nitrogen need, but also benefits following crops (Ali and Gupta, 2012). It requires relatively less water than other legumes for good growth and is important for its high nutritional value and for improving soil fertility (Parida and Das, 2005). Mungbean contains very low levels of oligosaccharides (sugars influence flatulence), is a good protein source (~23%) with high digestibility and suitable as baby food (Ihsan et al., 2013).

Mungbean is one of the common legume in most tropical and subtropical regions and grown after harvesting wheat and before ensuing autumn crops, and has a major role in ensuring the

nutrition security of developing countries such as India (Dhingra et al., 1991). Being rich in proteins, minerals and vitamins, it is an indispensable ingredient in majority of Indian diets. Regardless of such merits, mungbean often is cultivated on marginal soils with low inputs, that prone to numerous abiotic stresses that greatly hampers seed yield (Singh and Singh, 2011). Due to its short duration, in the Indo-Gangetic plains it easily fits into established cropping rotations of rice in *kharif* (monsoon) and wheat in *rabi* (winter), the major crops in the northern Indian states of Punjab, Haryana, and Uttar Pradesh.

Static mungbean yield in last decades is largely accounts for crop susceptibility to various biotic and abiotic stresses at different growth stages of the crop (Sehrawat et al., 2013a). Among them, salinity severely limits growth and yield worldwide; ~50 mM NaCl can cause >60% yield losses (Abd-Alla et al., 1998). It is expected that increased salinity will have an irresistible global effects, resulting ~50% loss of arable land by mid of the 21st century (Hasanuzzaman et al., 2012).

Thus there is a compulsion to continuously improve agricultural productivity of staple crops, legumes and specifically mungbean to ensure nutritional requirements for burgeoning human population, especially in developing countries. Mungbean often is grown on irrigated soils (as relay crop in cereal cropping systems) with salt deposits in upper layer due soil evaporation of water during dry season or from varying amounts of salinity in irrigation water. This accumulated salt decreases osmotic potential of soil, create water stress and imparts nutrient imbalances that trigger metabolic damage and cell death (Hasanuzzaman et al., 2013b).

In this paper, we focus on abiotic stress tolerance in legumes, particularly mungbean, and highlight any gaps that should be addressed in future mungbean research. We explore influence of salinity and HT on mungbean grown as a fallow crop (mungbean-rice-wheat) and/or as a relay crop in cereal cropping systems. Recent findings in physiology, biochemistry and molecular aspects of mungbean are presented along with several agronomic and farm-based mitigation strategies. We also briefly emphasize the role of exogenous protectants and growth-promoting microbes and the underlying physiological mechanisms for transduction of stress signals for salinity and HT stress tolerance.

Apart from salinity and heat stress, water deficit and waterlogging are also the key abiotic stresses that restrict growth, development and yield traits in mungbean, but they are outside the scope of this review. Consulting recent reviews/reports (Mirzaei et al., 2014; Araujo et al., 2015) for legumes and (Singh and Singh, 2011; Kumar et al., 2013; Naresh et al., 2013) for mungbean would provide necessary details.

SALINITY

Legumes are economically important crops and serve as sources of nutritious food, feed and raw-materials for humans, animals and industries respectively. Additionally, legumes have a symbiotic association with nitrogen-fixing rhizobia present in the root nodules, thus plants do not require external nitrogen

sources. However, legumes are highly salt-sensitive crops, and a high concentration of Na^+ and Cl^- ions around the root zone in water-scarce areas limits geographical range of legumes in arid and semiarid climates where evapotranspiration exceeds precipitation. Usually, salinity affects plants in two modes: osmotic stress and ion toxicity. However, for legume species particularly, there is a third mode: reduced nodulation by rhizobia, as salinity affects them either directly or indirectly. However, response of legumes/other plant species differ liable to prevailing conditions and extent of stress intensity. Therefore, it is necessary to enhance productivity of food grain legumes and to exploit valuable natural resources more efficiently to meet the demand for nutritious food from a growing population.

Salinity and its Effect on Crop Plants

Salinity limits the output of food crops and growth reduction is the main morphological effect on many biochemical mechanisms of the plant. Plants under high saline unable take up adequate water for metabolic processes or maintain turgidity due to low osmotic potential. Naturally, salt-alkalinized soils are complex that include various ions creating soil-salt-alkalization complex (Läuchli and Lüttge, 2002). Alkaline salts (NaHCO_3 and Na_2CO_3) were shown more damaging to plants than neutral salts (NaCl and Na_2SO_4) (Yang et al., 2007). Salt stress generally involves osmotic stress and ion injury (Ge and Li, 1990). Differential response of plants to salt and alkali stresses are largely due to high-pH associated stress (Munns, 2002; Li et al., 2012). Increased uptake of cations, such as Na, Mg, Ca, cause different kinds of nutritional imbalances leads to different ranges of toxicity. Under general NaCl toxic conditions, plants absorb a higher amount of Na, which thus decreases the K/Na^{-1} ratio (Ahmad and Umar, 2011; Ahmad and Prasad, 2012). In this review we focus and discuss only NaCl -induced salinity effects on general plant response.

Salinity Effect: Physiological and Biochemical Mechanisms

Salinity stress involves changes in various physiological and metabolic processes, varies with stress severity and its duration and ultimately inhibits crop production (Munns, 2005; Rozema and Flowers, 2008). Initially, soil salinity represses plant growth through osmotic stress, which is then followed by ion toxicity (Rahnama et al., 2010; James et al., 2011). During initial phases, the water absorption capacity of the root system decreases and water loss from leaves is accelerated due to osmotic stress, and therefore salinity stress is also considered hyperosmotic stress (Munns, 2005). Osmotic stress at the initial stage causes various physiological changes, such as interruption of membranes, nutrient imbalance, impaired ability to detoxify reactive oxygen species (ROS), differences in antioxidant enzymes, and decreased photosynthetic activity (Munns and Tester, 2008; Pang et al., 2010). One of the most damaging effects is accumulation of Na^+ and Cl^- ions in tissues of plants exposed to soils with high NaCl concentrations. Higher Na^+ blocks K^+ uptake, results in lower productivity and may even lead to cell death (Ahmad and Umar, 2011; James et al., 2011).

Plant adaptation or tolerance to salinity stress involves complex physiological traits, metabolic pathways and molecular or gene networks. Comprehensive knowledge of how plants respond to salinity stress at different levels and an integrated approach combining molecular, physiological, and biochemical techniques (Palao et al., 2014) are imperative for developing salt-tolerant varieties in salt-affected areas (Ashraf, 2014). Recent research revealed various adaptive responses to salinity stress at cellular, metabolic and physiological levels, although mechanisms underlying salinity tolerance are yet to be clearly understood (Gupta and Huang, 2014). Plants develop various physiological and biochemical mechanisms to survive in soils with high salt concentration. Principal mechanisms include, but are not limited to, ion transport, uptake and compartmentalization biosynthesis of osmoprotectants and compatible solutes, activation and synthesis of antioxidant enzymes/compounds, polyamines and hormonal modulation (Reddy et al., 1992; Roy et al., 2014) (Figure 1).

Salinity and Hormonal Regulation

Among the plant hormones, ABA plays a key role with ameliorating stress effects. As a first line of defense, ABA has long been recognized to synthesize in roots during soil water deficit (Popova et al., 1995; He and Cramer, 1996). ABA can mitigate inhibitory effects of salinity on photosynthesis (Yong et al., 2014), growth, and translocation of assimilates (Cabot et al., 2009). The positive link of ABA with salinity tolerance partially credited to K^+ , Ca^{2+} levels (Hussain et al., 2016) and compatible solutes in cytosol, which offset Na^+ and Cl^- uptake (Chen et al., 2001; Gurmani et al., 2011). Other compounds such as, salicylic acid (SA) and brassinosteroids (BR) also share abiotic stress responses (Fragnire et al., 2011; Khan et al., 2015). Ashraf et al. (2010) reviewed a possible role of BRs and SA in mitigating harmful effects of salt stress and discussed their exogenous applications in regulating various biochemical and physiological processes. Reddy et al. (2015) suggest over-production of proline eases salt stress and protects photosynthetic and antioxidant enzyme activities in transgenic sorghum [*Sorghum bicolor* (L.)]. The effect of salt stress on intrinsic physiological traits, malondialdehyde (MDA) levels and antioxidant enzyme activities were evaluated in 40-day-old transgenic lines and compared with wild type plants. The photosynthetic rate was reduced in wild type plants almost completely. Salinity induced cent percent stomatal closure in wild type, while it did only 64–81% in transgenic plants (after 4 days), indicating transgenic lines were better in coping up with salt stress than wild type.

Salinity: Effect on Physiological Traits

Largely in response to salt stress, crop varieties/genotypes vary in their inherent ability to adjust several physiological and biochemical processes (Grewal, 2010; Singh et al., 2014). Most observed both physiological (high Na^+ transport to shoot, favored storage of Na in older leaves, high Cl^- uptake, lower K^+ uptake, low P and Zn uptake, etc.) and biochemical (alteration in scavenging enzymes synthesis and their expression, rise in non-toxic compatible solutes, etc.) and their modifications. Ashraf (2014) described agronomic characters that represent,

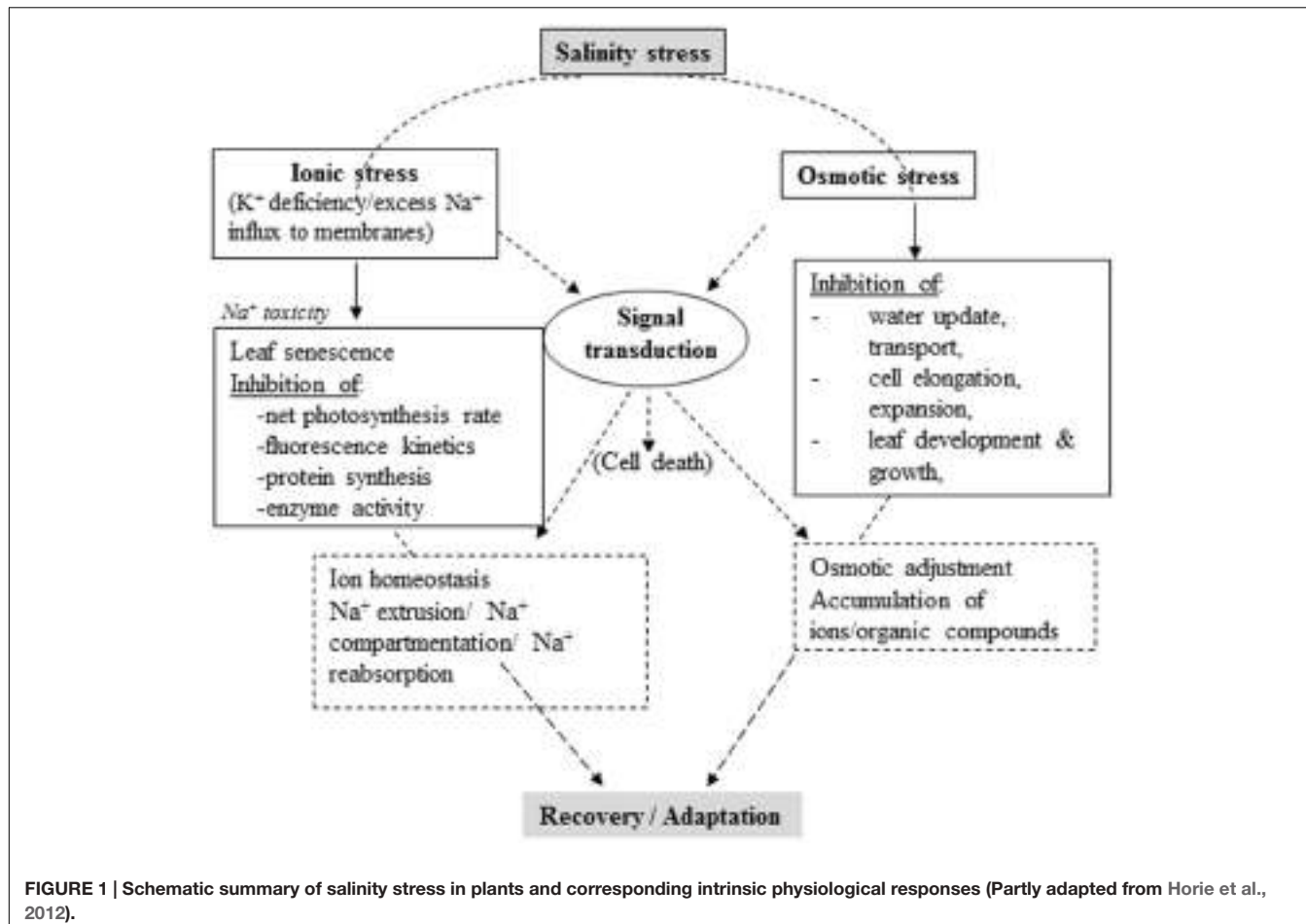


FIGURE 1 | Schematic summary of salinity stress in plants and corresponding intrinsic physiological responses (Partly adapted from Horie et al., 2012).

combined effects ($G \times E$) on plant growth, includes growth rates and physiological efficiencies related to salinity tolerance. Physiological traits lead to more reliable evidence than agronomic traits; thus, several reports mainly focused on water relations, carbon assimilatory functions and synthesis of various inorganic compounds and organic solutes in discrete crop species.

For assessing response to various abiotic stresses, effective indicator is yield; however, it may not capture underlying genetic mechanisms linked to strong environmental interaction. Intricate inheritance pattern and low heritability limit selection efficacy for yield or biomass under abiotic stresses (Ashraf, 1994; Noreen et al., 2010). Furthermore, dearth of a dependable trait for screening hinders developing salt tolerance in target crops (Palao et al., 2014) which is also true in mungbean (Mahdavi and Sanavy, 2007). Instead, it would be more sensible, if one can focus of using simply inherited morpho-physiological traits inked to yield. However, using physiological traits as selective markers to achieve success rest on strength of the relationship of such markers with salinity response of target plants (Roy et al., 2014). Yet, selection from pool of markers would be more effective than rely on a single marker. Tolerance of a genotype was found linked to its ability to confine assimilation potential toxic ions (such as Na⁺) and better balancing of ions (such as K⁺). Adding K⁺ to nutrient solution reduced negative effect of NaCl on

growth in barley (Roy et al., 2014). Although uptake of both Na and K are distinct, lower Na/K ratio is treated desirable. Na⁺ is transported to shoots from roots typically through passive uptake, while K⁺ through the active uptake (Hasegawa et al., 2000).

At entry level, plant roots experience salt stress when Na⁺ and Cl⁻ along with other cations are present in the soil in varying levels. Ion uptake depends upon the plant growth stage, genotype, temperature, RH and light intensity (Singh et al., 2002). Salt in excessive amount retards plant growth, decrease yield and may cause plant death (Garcia de Blas et al., 2003). It also induces production of ROS/intermediate viz., superoxide, H₂O₂ and OH⁻-radicals in chloroplasts and mitochondria. Plants have devised different systems for scavenging ROS by using enzymes such as SOD peroxidases and catalases. Under normal growth condition, ROS in cells is as low as 240 μMs^{-1} , however, under salinity, ROS production reaches to 720 μMs^{-1} (threefold) (Mittler, 2002; Mudgal et al., 2010). H₂O₂ concentration of 10 μM reduced net photosynthesis rate by 50%. Identifying a single criterion as an effective selection target is difficult, given the complexity of salt tolerance. However, some information is available on the use of these attributes as selection criteria for improving salt tolerance through breeding.

Salinity and Mungbean

Salinity stress causes a significant reduction in mungbean yield (Abd-Alla et al., 1998; Saha et al., 2010) through decline in seed germination, root and shoot lengths, fresh mass and seedling vigor and varies with different genotypes (Promila and Kumar, 2000; Misra and Dwivedi, 2004). Salt injury also leads to pronounced symptoms like enhanced chlorosis, necrosis and decreased content of chlorophyll and carotenoids in mungbean (Gulati and Jaiwal, 1993; Wahid and Ejaz, 2004). NaCl stress had more deleterious effect on roots than shoots, with a sudden dip in root growth associated traits (Friedman et al., 2006; Saha et al., 2010).

Most of the mungbean cultivars tolerate salt to an extent of 9–18 m mhos/cm than usual salt concentration of 5–6 m mhos/cm (at germination stage). Paliwal and Maliwal (1980) reported that mungbean seeds could tolerate 6 m mhos/cm salinity, compared to 3 m mhos/cm for black gram. In another study, 42 cultivars of mungbean and black gram were tested at five levels of salinity (3–18 mmhos/cm) in 1/5 Hoagland nutrient solution in plastic containers (Maliwal and Paliwal, 1982). Germination/seedling length of all the cultivars was delayed/decreased; salinity and its tolerance limit varied with the cultivar. Some varieties (S 72, H 45, No. 525, Madira and RS-4) were found to be more salt-tolerant. Mungbean accumulates compatible solutes like proline and betaine to mitigate damaging effects (Hoque et al., 2008), however, not at a high level to regulate osmotic potential in plants (Hamilton and Heckathorn, 2001; Hossain and Fujita, 2010). In one of the study (Phillips and Collins, 1979), callus from mungbean grown in sand culture with Hoagland's nutrient solution supplemented with 0–350 mol/m³ NaCl, showed tolerance to salt as that of whole plant, suggesting mungbean appears to have salt tolerance at cellular level.

In a field experiment, Reddy (1982) observed injury to mungbean cultivars with irrigation water containing EC of 4 m mhos/cm. More and Ghonikar (1984) determined that the critical level of salinity in irrigation water to cause injury to seed germination in mungbean was 3.5 m mhos/cm. We also observed similar results while field screening 45 elite mungbean accessions with different sources of irrigation water under field conditions in Punjab, India. The irrigation water (tube well water with 2200 μ mhos EC and residual sodium carbonate – RSC of 6.4 meqL⁻¹) resulted in growth retardation at the vegetative stage compared to irrigation (canal) water with EC of 290 μ mhos and RSC of 0.7 meqL⁻¹ (Bindumadhava et al., 2015). Lawn et al. (1988) reported from a pot study that some of the accessions of *V. radiata* var. *sublobata* showed no symptoms of chlorosis when grown on extremely alkaline (pH > 8.5) calcareous soils. Roychoudhury and Ghosh (2013) studied the physiological and biochemical responses of *V. radiata* seedlings to varying concentrations of cadmium chloride ($CdCl_2$) and NaCl. Both chemicals enhanced seedling mortality, notably at higher concentrations. A decline in normal growth, germination %, inhibition in root and shoot length and decreased fresh and dry weights of seedlings was observed. The activities of antioxidant enzymes, catechol-peroxidase and catalase increased progressively with an increase in $CdCl_2$ and NaCl concentrations.

Altering the level of biomolecules and modulating physiological and biochemical functions, *V. radiata* seedlings could overcome the cellular toxicity of $CdCl_2$ and NaCl (Roychoudhury and Ghosh, 2013). Degree of salt stress affects different crops differently. For mungbean, RSC beyond ~ 4 meq/L is considered moderate salinity while more than 7 meq/L is very high. Similarly, a pH of 8.5 – 9.1 is considered as non-stress, 9.2 – 9.8 as moderate stress, and ≥9.8 as high stress. Extremely high salt stress conditions damage the plant, but moderate to low salt stress affects plant growth rate and thereby manifests symptoms that could be associated with morphological, physiological, or biochemical change (Hasegawa, 2013). Singh et al. (1989) reported that four mungbean cultivars in plots salinized with 2,4, and 6 dS m⁻¹ gave average seed yield of 906, 504, and 370 kg/ha, respectively. Salinity occupies a prominent place among the soil problems that threaten the sustainability of agriculture in Pakistan. Out of 16.2 m ha of land under irrigation, more than 40,000 ha of land are lost each year (Yasin et al., 1998). Mungbean is planted in annual crop rotations on an increasingly large area of heavy clay soils in many regions of Pakistan frequently exposed to moderate to high levels of salts. Mungbean production (455 kg/ha) in Pakistan is very low compared to other countries (Agricultural Statistics of Pakistan, 2001). The major mungbean-growing areas in the country are affected by salt and to make effective use of salt-affected soils, it is important to select mungbean genotypes that can tolerate salt stress and produce substantial yields under saline environments.

Salinity Effect at Different Growth Stages of Mungbean

Germination and seedling growth

During germination under saline conditions, high osmotic pressure of saline water is created due to capillary rise leading to more salts density at seed depth than at lower soil profile, which reduces time and rate of germination (Mudgal et al., 2010). In mungbean seedlings, high salt concentration causes increased H_2O_2 content in both roots and leaves, hence salts should be removed to ensure proper growth and development (Saha et al., 2010). Both root and shoot lengths were reduced with increased NaCl concentration, but roots were more damaged, with an increase in number of lateral roots and increase in its thickness, compared to shoots (Misra et al., 1996). Photosynthetic activity of mungbean is reduced due to reduced function of electron transport and instability of pigment protein complex (Promila and Kumar, 2000). High salinity results in a decrease in total leaf area and stomatal opening (Nandini and Subhendu, 2002). Proline and glycinebetaine levels in roots and shoots increased in mungbean (tolerant) cultivar 'T 44' subjected to NaCl stress at seedling stage (Misra and Gupta, 2006). Increase was seen with a supply of 5 mM $CaCl_2$ to 200 mM NaCl. Calcium ions play a key role in osmoprotection and effects of Na^+ and Ca^{2+} are thus harmonizing the accretion of osmolytes (Hu and Schmidhalter, 2005). Increased proline levels occurred when proline oxidase activity was low and high production of P-5-CR and γ -glutamyl kinase in both roots and shoots. Thus, calcium facilitated osmolytes synthesis in NaCl-stressed mungbean seedlings (Misra and Gupta, 2006). When three

species of *Vigna* (*V. radiata*, *V. mungo*, and *V. unguiculata*) subjected to varied doses of NaCl (50, 75, 100, 125, and 150 mM), reduction in chlorophyll content, sugar, starch and peroxidase enzyme activity were observed in shoots and roots (Arulbalachandran et al., 2009). Germination %, seedling growth rate, RWC and photosynthesis decreased with increasing NaCl levels in all species. The growth decrease was higher in mungbean than in black gram and cowpea. However, increase of compatible solutes was higher in cowpea than in black gram and mungbean, suggesting cowpea is more salt-tolerant than other two. The effect of pre-soaking seed in 50, 100, and 1000 μM SA on growth parameters of two mungbean genotypes (NM 19-19 and NM 20-21) under salinity stress (50 and 100 mM NaCl) was studied (Shakeel and Mansoor, 2012) and found a reduced seedling length and fresh/dry weight of both genotypes. Pre-soaking treatments (100 μM) with SA reduced salinity-induced decline. However, pre-treatment with a high concentration (1000 μM) prior to salt treatment caused a significant reduction in mean seedling length. NM 19-19 respond better under salt stress than NM 20-21. In a pot experiment (from Bangladesh), effect of salinity levels (e.g., 0, 0.1, 0.2, 0.3, and 0.4% of NaCl) on germination, growth and nodulation of mungbean varieties (BARI Mung 4, BARI Mung 5 and BARI Mung 6) was observed. Salinity affected germination and root elongation. Root growth was significantly reduced with higher salt and BARI Mung 4 showed better performance than other varieties. All showed similar performance in yield traits at higher NaCl levels. No effect on nodulation at a higher (0.4% NaCl) dose was seen in BARI Mung 5. However (Naher and Alam, 2010), reported nodules per plant decreased but not nodule size with increase in salinity.

Nodulation and nitrogen metabolism

Salinity interfered with initiation, reduced number, weight and nitrogen-fixing efficiency of nodules in chickpea, cowpea and mungbean, (Balasubramanian and Sinha, 1976), causing significant reduction in leghaemoglobin content, which decreased with aging of nodules by irreversible oxidation. Inhibition of root colonization by *Rhizobium* was the main reason for poor nodulation (Mudgal et al., 2010). Although nodules were present, nitrogen fixation was inhibited completely in inoculated plants grown at 6 dS m⁻¹. These findings largely indicate process of symbiosis is salt-sensitive than both *Rhizobium* and the host plant (Zurayk, 1998). Plants in saline habitat accumulate proline and glutamine and increase concentration of amino di-carboxylic acid (Soussi et al., 1998; Munns et al., 2002). The ill effect on nitrogen metabolism is mainly observed in above ground plant parts (Munns et al., 2006; Munns and Tester, 2008). Symbiotic association of rhizobia with legume roots has specific advantages during different abiotic stresses; rhizobia aid N₂ fixation and facilitate water uptake, thereby helping withstand heat stress. Some strains of rhizobia which are resistant to salts, helped in solubilizing osmolytes/ions in the rhizosphere and thus improves salt tolerance. *Rhizobium* and *Bradyrhizobium* spp. vary in their tolerance to salinity, though they nodulate the same plant differ in salinity tolerance (Elsheikh and Wood, 1995; Elsheikh, 1998) The effect of salinity

on growth and survival of *Rhizobium* spp. suggests growth of these tested strains and species decreased when EC was raised from 1.2 to 6.7 mS cm⁻¹ or to 13.1 mS cm⁻¹ (Kaur D. et al., 2015), indicating that many strains of *rhizobia* can grow and survive at salt concentrations that inhibitory to most agricultural legumes. Hence focus should be more on exploiting salinity effect on symbiosis rather than survival of *Rhizobium* spp.

Growth, flowering yield pattern

Soil salinity delays and also reduces flowering and yield of crop plants (Maas, 1986). Salinity-induced reduction in yield was reported in many crops viz., wheat, barley, mungbean and cotton (Keating and Fisher, 1985). Mungbean showed decreased growth, photosynthesis and yield at a high salinity, but postponed pod ripening during the spring resulted in reduced pod shattering (Sehrawat et al., 2013a,d). A study by Hasanuzzaman et al. (2012) on screening mungbean germplasm for salt tolerance in the spring season identified a few resistant genotypes for saline areas. NaCl stress, combined with other types of stress, resulted in organ-specific changes in polyamine content in mungbean plants and affected enzyme activity. An excessive amount of salt can enter transpiring stream and cause injury to leaves, resulting in reduced photosynthesis of growing leaves (Mittler, 2002; Okuma et al., 2002; Tilman et al., 2002; Neelam and Dwivedi, 2004; Hossain and Fujita, 2010). Misra and Dwivedi (1995) reported a salt-tolerant cultivar was characterized by higher levels of total soluble carbohydrates than a salt-sensitive cultivar irrespective of salinity level. The physiological processes were compared in salt-tolerant ('Pusa Vishal') and sensitive ('T 44') mungbean cultivars and how SA effective in alleviate reduction in photosynthesis under salt stress (Nazar et al., 2011) was also explored. SA (0.5 mM) found effective as osmoprotectant as it increased nitrogen and sulfur assimilation and restricted Na⁺ and Cl⁻ content in leaves, maintained higher photosynthetic efficiency in 'Pusa Vishal.' However, diverse accessions resistant to salt stress within *Vigna* species could be useful source for exploring mechanism of salt tolerance was proposed (Zahir et al., 2010; Win et al., 2011). Saha et al. (2010) reported that pre-treatment with a sub-lethal dose of NaCl was able to overcome adverse effects of stress imposed by NaCl. Mungbean plants could acclimatize to lethal levels of salinity through pre-treatment with sub-lethal doses, which resulted in increased growth and photosynthesis in seedlings and modified the activities of antioxidant enzymes. Bourgault et al. (2010) demonstrated mungbean as a better adapted species to semi-arid and arid climates and able to maintain its photosynthetic rates, harvest index under water deficit and NaCl stress, than common bean. Further, addition of K⁺ was also examined to alleviate the stress effect and found higher levels of K⁺ improves water retention, growth and yield of mungbean (Wahid and Ejaz, 2004). In a separate study, Sehrawat et al. (2015) reported the effect of salt stress (two levels: 50 and 75 mM NaCl) on two mungbean varieties, 'Pusa Vishal' and 'Pusa Ratna' during summer season and found significant variations and adaptability in both varieties. The plants in early growth stages were more resistant compared at reproductive stages (Sehrawat et al., 2013b,c). Salinity and associated osmotic stress severely constrained plant growth,

physiology and yield traits. In general, the tolerant cultivar 'Pusa Vishal' exhibited less reduction in growth and yield traits than 'Pusa Ratna.'

Globally, ongoing research to address salt-related problems are based on: (a) changing the growing environment suitable for normal growth of plants, or (b) selecting crop and/or altering genetic makeup, so that it can be grown in such saline areas. The first method involves major tweaking in systems biology and soil amelioration, which demand considerable resources and are often out of reach. The second approach (biological; developing crop varieties tolerance to salts) is more promising, economical, and socially acceptable¹. Plants with high salt tolerance allow farmers to optimally manage their available resources. The latter approach is being attempted in mungbean by identifying intrinsic salt-associated traits and putative salt-tolerant lines from among world vegetable center's core and mini-core mungbean collections (Schafleitner et al., 2015) and further, developing salt-tolerant accessions to use as donor sources in future breeding programs (Bindumadhava et al., 2015). Once developed, such selections can be validated in saline soils in the field for survival, growth and yield performance. A third "fusion" approach combines modified environmental and biological methods, which is highly prolific, less resource intense and frugally viable. Current global soil reclamation programs involve both biology and fusion approaches to contest salinity-associated problems.

Salt-tolerant wild mungbean (*Vigna marina*, beach cowpea) is found on tropical and subtropical beaches around the world (Hawaii and islands in the Pacific Ocean, the Caribbean, along the Atlantic and Indian Ocean coasts of Africa, India and Sri Lanka, Australian coasts², United States Department of Agriculture [USDA] (2011). It has been domesticated, adapted and released as a dual-purpose legume in Bangladesh. *V. marina* is considered a light-sensitive type with profused vegetative growth habit showing tolerance to saline conditions (Hamid and Haque, 2007). Chankaew et al. (2014) reported quantitative trait loci (QTLs) for mapping salt tolerance in *V. marina*. QTL mapping in the F₂ population (*V. luteola* × *V. marina* subsp. *oblonga*) revealed that salt tolerance in *V. marina* subsp. *oblonga* is controlled by a single major QTL, however, segregation analysis indicated it is controlled by a few genes. *Vigna marina* would be a potential salt-tolerant donor for future *V. radiata* breeding programs (inter-species hybridization can be attempted) for its natural growing habitat and intrinsic salt resistance mechanisms.

Salinity Tolerance in Legumes from Molecular Perspective

In a review on salt tolerance in Asiatic *Vigna* species, Mishra et al. (2014) opined transgenic approach had made limited progress due to severe recalcitrance of these plants to genetic transformation and *in vitro* regeneration. Strategies discussed were overexpression of genes involved in (a) exclusion of toxic

sodium ions by plasma membrane Na⁺/H⁺ antiporter; SOS1 in legumes (Kido et al., 2013), (b) sequestration of sodium ions in vacuoles to reduce ionic toxicity by isolation and characterization of vacuolar Na⁺/H⁺ antiporters of legumes (Li et al., 2006), (c) encoding for compatible osmolytes by raising osmotic potential of cells (Porcel et al., 2004), (d) encoding for antioxidant enzymes to oxidative stress (Jiang et al., 2013). Role of regulatory genes include (a) upregulation of calcium in response to stress; isolation and characterization of novel calcineurin B-like proteins interacting with protein kinases (CIPKs) (Imamura et al., 2008) and (b) manipulation of transcription factors including AP2/ERF, bZIP, NAC, MYB, MYC, Cys₂His₂ zinc-finger and WRKY (Bhatnagar-Mathur et al., 2008). Use of activation tagging in model legume, *Medicago truncatula* for gene discovery, could extend to identify novel genes in Asiatic grain legumes (Scholte et al., 2002). RNAi mediated inactivation of a transcription factor of *M. truncatula*, MtNAC969, known to be associated with salt stress (de Zelicourt et al., 2012) is another strategy. However, gene-expression with constitutive promoters provide partial biological information than inducible or cell type-specific promoters. Choice of promoters can significantly affect the output from transgenic manipulation. Further, several findings on transformation for improving salinity tolerance focus toward genes controlling ion transport, as regulation of Na⁺ uptake and compartmentalization is critically important for plant survival and many candidate genes controlling this mechanism have been identified (Gupta and Huang, 2014).

Genetic variability and differential responses to stress enable to identify physiological mechanisms, sets of gene/s products that would impart stress tolerance and facilitate in incorporating under suitable background species to develop salt tolerant types.

Management Practices for Alleviating Salinity under Field Conditions

In the field, if the salinity level is less intense, the crop show lopsided in plant vigor. Moderate salinity, if uniform, display the restricted vegetative and reproductive growth without apparent injury *per se*. Leaves in salt-infested areas may appear smaller and darker blue-green in color (Richards, 1954).

Through avoiding leaching of salts from root zones, systematic monitoring farm management activities, and planting saline tolerant crop species, salinization can be controlled. Irrigation in agriculture can be sustained by efficient water management techniques (partial root zone drying methods, and by drip irrigation, etc.). Dry land salinity can be mitigated by reducing water infiltration beyond the root zones, which may restore the balance between water fall and water use, thus averting rising water tables and movement of salt to soil surface (Manchanda and Garg, 2008). Farming systems can alter in incorporating perennials in rotation with annual crops (phase-wise and rotation farming), in mixed plantings (inter-cropping), or in site-specific planting (precision farming) (Munns et al., 2002). Evolving efficient, low cost, easily adaptable methods for abiotic stress management is a major challenge. Worldwide, extensive studies

¹www.knowledgebank.irri.org

²<http://plants.usda.gov>

are being conducted to develop strategies to cope with abiotic stresses through the development of salt- and drought-tolerant varieties, by shifting crop calendars, and by improving resource management practices (Venkateswarlu and Shanker, 2009)³. The following approaches would aid in removing/reducing salts:

Soil Reclamation

Salt removal from root zone is perhaps most effective and long-lasting way to ameliorate or even eliminate detrimental effects of salinity. It involves substituting sodium in the soil with calcium ions (through applying large quantities of gypsum). The released sodium ions are then leached deep beyond the root zone using excess water and finally moved out of the field through drainage. Gypsum slowly mix with water releasing calcium ions, which replace sodium ions from the soil into the downward moving water (Ramajulu and Sudhakar, 2001)⁴.

Suitable Use of Ridges or Beds for Planting

Impact of salinity may be minimized by sowing seed or planting seedlings on ridges effectively. Planting plants on ridge shoulder than ridge top is effective in escaping from salt episodes as during water evaporation, salts concentrate only at top rather on shoulders thereby minimizing salt ill effects. However, for alternate furrow planting, ideal would be planting on one shoulder of the ridge closer to water source. (Goyal et al., 1999a,b)⁴.

In a recent review, Srivastava and Kumar (2015) explained how a range of adaptations and mitigation strategies help to cope with global salinity impacts³. These plans assume cost- and time-intensive but assures strength in developing simple, low-cost natural means for handling salinity episodes better in future soil management strategies.

Broad Management Practices to Reduce Salinity Impact

Additionally, following approaches may help in reducing negative effects of salinity (Qureshi et al., 2003).

(a) Adding crop residues/green manure as organic mulch improves soil health, structure, and water penetration, thus protects from adverse salinity effects. Steady mixing of organic matter to soil (crop residue, sludge and compost etc.) would reduce soil evaporation which lessens upward salt movement. Low evaporation demands less water which helps in lower accumulation of salts.

(b) Salt accumulation closer to the surface is a typical feature of saline soils. Deep tillage would mix salts present in surface zone into a much larger soil volume and reduce salt content and impact. Many soils have an impermeable hard pan, which hinders salt-leaching process. Under such circumstances, “chiseling” would improve water infiltration and the downward movement of salts⁴.

³www.ncbi.nlm.nih.gov

⁴www.plantstress.com

HIGH TEMPERATURE

High Temperature and its Effect in Crop Plants

The global air temperature is predicted to rise by 0.2°C per decade, which will lead to temperatures 1.8–4.0°C higher than the current level by 2100 (Intergovernmental Panel on Climate Change [IPCC], 2007)⁵. HTs are injurious to plants at all stages of development, resulting in severe loss of productivity (Lobell and Asner, 2003; Lobell and Field, 2007; Hasanuzzaman et al., 2010). In response to unfavorable temperatures, plant biomolecules (stress proteins, enzymatic and non-enzymatic antioxidants, osmolytes and phytohormones) come into rescue (Kaur R. et al., 2015). Typically, their endogenous levels shoot up as plant defense and expression depends on type of plant species exposed, and intensity/duration of the stress. Legumes show varying degrees of sensitivity, which reduces their potential performance at different developmental stages such as germination, seedling emergence, vegetative phase, flowering and pod/seed filling phase (Bhandari et al., 2016). To address ever-fluctuating temperature extremes, efforts are being made in developing tolerant genotypes in legume either by conventional breeding strategies and/or more newly, by molecular breeding methods.

High Temperature Effect on Photosynthesis and Growth

High temperatures can constrain growth, lower yield and truncate crop cycles (McKenzie et al., 1988; Araujo et al., 2015). Temperature range which is not sufficiently high to damage cells, may inhibit growth associated tissue water functions and carbon assimilation associated chloroplast functions coupled with impaired vigor, cellular respiration, N fixation and metabolism (Buxton, 1996).

Among several processes, photosynthesis (Ps) is one such important physiological process impaired by heat stress (Crafts-Brandner and Salvucci, 2002). HT impacted more on photosynthetic capacity of C₃ plants than C₄ (Yang et al., 2006). In chloroplasts, carbon metabolism and photochemical reactions are considered primary sites of injury (Wang et al., 2009). Major effect such as altered structural organization of leaf stromal and thylakoids assembly and functions under heat stress (Rodriguez et al., 2005).

The maintenance of leaf gas exchange (transpiration and CO₂ assimilation rates) under heat stress has a direct relationship with heat tolerance mechanisms of active leaves (Kumar et al., 2005). Heat markedly affects the leaf stomatal and CO₂ assimilatory functions driven by photosystem II-photochemistry (Greer and Weedon, 2012). The mean change in photosynthesis capacity of *Vitis vinifera* leaves was declined by 60% with growing temperature from 25 to 45°C. Heat imposes negative impacts on leaves, such as reduced water potential, leaf area and pre-mature senescence and drop in photosynthesis (Greer and Weedon, 2012). Other likely reasons believed to hamper photosynthesis under heat stress are reduction in soluble proteins, RuBisCO binding proteins, large-subunits (LS), and small-subunits (SS) of

⁵www.mdpi.com

RuBisCO in darkness, and increases of those in light (Sumesh et al., 2008)³. HT also affects starch and sucrose synthesis through reduced activity of sucrose phosphate synthase and ADP-glucose pyrophosphorylase (Rodriguez et al., 2005). Loss of productivity in heat stress is chiefly related to decreased assimilatory capacity by altered membrane stability (Zhang et al., 2006), enhanced maintenance respiration (Reynolds et al., 2007), and reduction in radiation use efficiency.

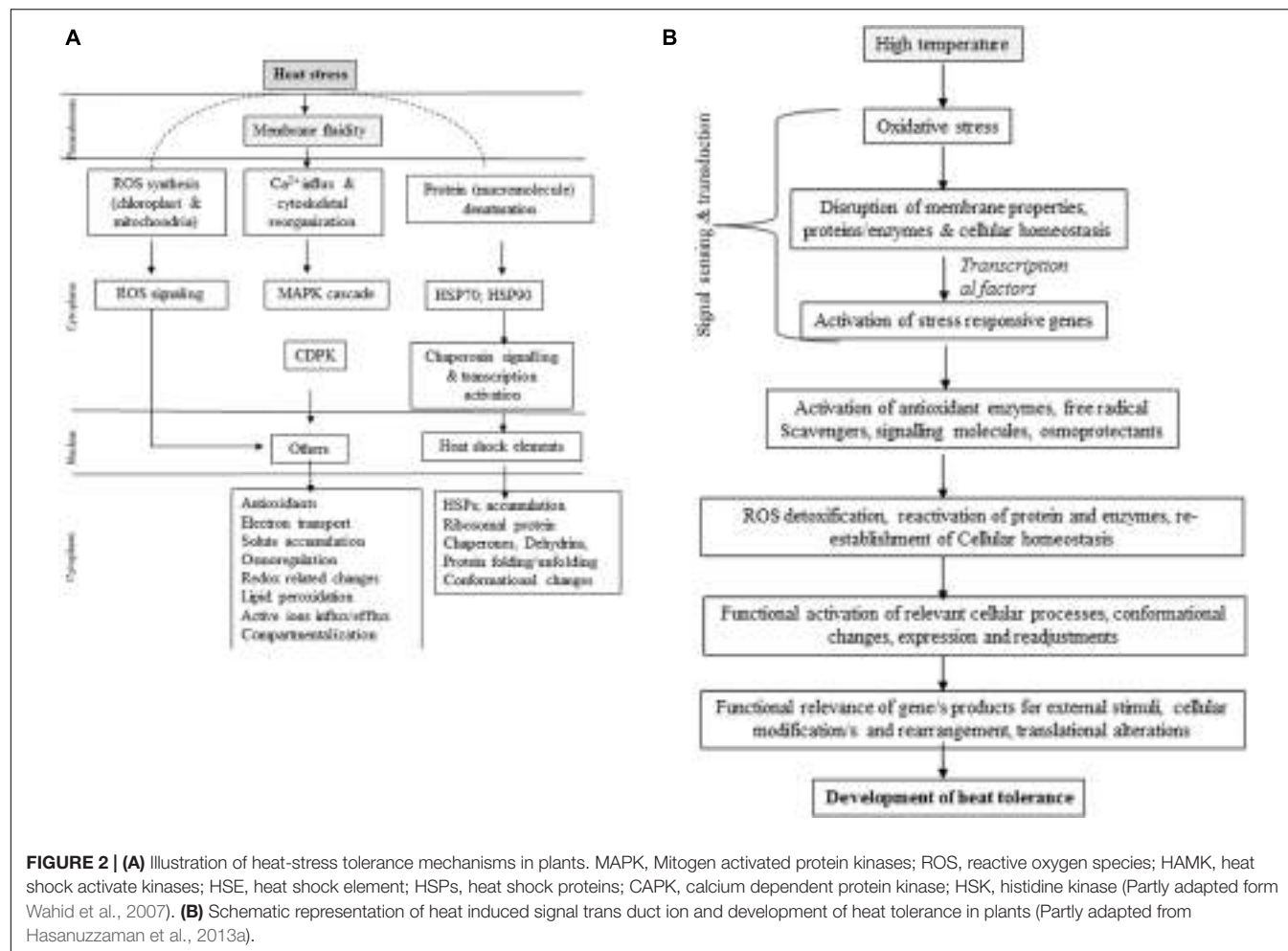
Among different growth stages, firstly germination is affected followed by other associated process related to seed hormones, though it is species specific and temperature range dependent (Johkan et al., 2011). Reduced germination percent, seedling emergence, cell size, poor vigor, reduced radicle and plumule growth were major impacts of heat stress reported in various plant species (Rodriguez et al., 2005; Piramila et al., 2012). Since there is a commonality in stress response at the cellular level, it is likely that thermo-tolerant lines might show tolerance to other stresses such as desiccation and salinity (Kumar et al., 1999). In common bean morphology (plant growth habit and height, leaf shape, – and physiological traits (phenology, water relations and shoot growth) were hampered by heat stress (Koini et al., 2009). Under excess heat stress, plants exhibit programmed death of specific cell and tissue types. Conversely, moderate HTs for extended duration leads to gradual death. Both types of injuries can lead to leaf shedding, flower/pod drop, abortion of reproductive organs and premature maturity or (Hasanuzzaman et al., 2010). HT also results in low yield, plant quality and seed viability (Anderson and Sonali, 2004; Khalil et al., 2009). In chickpea, it was shown that heat stress induced reproductive failure that would possibly impair sucrose metabolism in leaves, anthers and inhibit sucrose transporters; consequently, availability of trios phosphates (reducing and non-reducing sugars) to developing pollen would be upset, impairing its functions and causing reproductive failure (Kaushal et al., 2013). In model crops, such as *Arabidopsis* and tomato, tangible heat sensitive growth stage in crop cycle was elucidated and relevant proteins involved and their functions were described (Scharf et al., 2012). However, its implication for other legumes needs to be revealed to exploit trait-linked functionality. More recently, Gaur et al. (2015) highlighted that heat stress during reproductive stages is becoming a serious constraint to grain legumes productivity as their cultivation is expanding to warmer environments and temperatures are increasing due to climate change.

Plants characteristically have number of adaptive, avoidance or acclimation mechanisms to face HT. However, their survival depends on ability to perceive HT stimulus, generate and transmit the signal and initiate appropriate cellular, physiological and biochemical changes. Interestingly, breeding strategies aimed at enhancing drought tolerance will often capture plant responses to heat stress; hence heat tolerance may not be a specific target for improvement by most plant breeders (Hasanuzzaman et al., 2013a). Plants continuously tussle for survival under HT and alter their metabolism in various ways, particularly through compatible solutes and modify antioxidant systems (Munns and Tester, 2008).

Heat Stress Tolerance from Cell Signaling and Molecular Perspectives

As a multi-genic trait, several mechanisms are involved in heat tolerance, includes antioxidant activity, membrane lipid unsaturation, gene expression and translation, protein stability and accrual of compatible solutes (Kaya et al., 2001). In a review on heat stress, Bita and Gerats (2013), discussed activation of lipid based signaling cascades, increased Ca^{2+} influx (Saidi et al., 2011), heat shock proteins (HSPs) acting as molecular chaperones to prevent denaturation/aggregation of target proteins and facilitating protein refolding (Lohar and Peat, 1998) and transcriptional repression by repetitive DNA regions (Khraiwesh et al., 2012). Heat shock factors (HSFs) are transcriptional activators of HSPs (Banti et al., 2010). For e.g., in *Arabidopsis*, expression of APX gene family is heat stress dependent and regulated by HSF that links heat stress response with oxidative stress (Panchuk et al., 2002).

Molecular approaches are being adopted for developing HT tolerance. At a cell level, heat stress causes changes in expression of genes involved in direct plant defense (Chinnusamy et al., 2007; Shinozaki and Yamaguchi-Shinozaki, 2007; Hasanuzzaman et al., 2012; Mathur et al., 2014) thereby regulating expression of osmoprotectants, detoxifying enzymes and regulatory proteins (Semenov and Halford, 2009). Heat stress is sensed by plants through increase in membrane fluidity, and the sensors located in membranes detect this phase transition resulting in conformational changes and phosphorylation/dephosphorylation events (Plieth et al., 1999). Membranes perceive heat stress activates calcium channels to release Ca^{2+} into the cytosol, combined with calmodulin activates calcium dependent kinases and various transcription factors (von Koskull-Doring et al., 2007; Zhang et al., 2009) (**Figure 2A**). Heat stress causes activation of unfolded proteins (UPR) of endoplasmic reticulum (ER-UPR) and cytosol (Cyt-UPR) (Mittler et al., 2012). Activated ER-UPR joins bZIP transcription factor that enters into nucleus and leads to expression of genes related to brassinosteroid signaling (Deng et al., 2013). Conversely, Cyt-UPR becomes activated by HSF capable of binding HSF-binding element at the promoter region of heat shock responsive genes (Sugio et al., 2009). HTs influence histone occupancy by changing H_2A with $\text{H}_2\text{A.Z}$ in the nucleosome in *Arabidopsis* (Kumar and Wigge, 2010), where actin-related protein-6 (ARP6) is engaged in replacing histone (Erkina et al., 2010). Heat stress increases membrane fluidity to induce lipid signaling to activate two molecules, phosphatidic acid (PA) and D-myo-inositol-1,4,5-triphosphate (IP₃) (Mishkind et al., 2009). IP₃ and PA activate calcium channels located on ER to further release Ca^{2+} ions (Saidi et al., 2011). Based on duration and intensity of heat stress, release of Ca^{2+} ions and its expression pattern varies (calcium signatures). Calcium availability in cytosol during early hours of heat stress significantly reduced activation level of small HSP promoter and negatively influenced acquired thermo-tolerance. Heat stress does not trigger osmotic-responsive promoters, thus indicating heat- and osmo-sensors are specific, though they both require an influx of extracellular calcium. Such high specificity to heat and



osmotic stresses possibly relies on specific effectors of calcium like calmodulin. Since heat stress is often associated with osmotic stress, high possibility of cross-talk between various secondary messengers of two stresses is expected while retaining their specificity (Saidi et al., 2009). Heat sensing and signaling need to be explored to test specific receptors in cell membrane, activation of HSFs, CaM kinases and occupancy of nucleosome. Knowing how phytohormones, especially having thermo-protective roles mediate and/or regulated through heat sensing would be useful in addressing heat tolerance from a practical view point (Figure 2B).

Transgenics for Heat Tolerance

Heat stress leads to production of special group of proteins termed as HSP's, which on their molecular masses are further grouped into five classes; Hsp100, Hsp90, Hsp70, Hsp60 and small heat-shock proteins (sHsps). HSPs act as chaperones and prevent mis-folding and aggregation of native proteins. E.g., HSP101 from *Arabidopsis*, if over-expressed in rice plants, growth performance of rice was significantly enhanced during recovery from heat stress (Liu et al., 2011). The transcription of HSPs genes depends upon heat shock transcription factors, HSFs, which are located in the cytoplasm in inactive state and exist in three forms, HsfA1, HsfA2, HsfA3 (Tripp et al., 2009), which are vital to

acquire thermo-tolerance as evident in *Arabidopsis* (Charng et al., 2007).

Quantitative trait loci mapping has established a genetic relationship with tolerance of various types of abiotic stresses and molecular markers helped in exploring QTLs linked to stress protection (Foolad, 2005). In *Arabidopsis*, four genomic loci associated with thermo-tolerance were reported while in maize, 11 QTLs related to pollen tube and germination under heat stress were mapped. A protein synthesis elongation factor Tu (EF-Tu) has been implicated in thermo-tolerance (Fu et al., 2012). A single plastid EF-Tu gene (*tufA*) is identified (Fu et al., 2012) in *Arabidopsis* and *Oryza sativa*, whereas multiple copies in nuclear genome of other plants, ranging from two genes (*tufA* and *tufB*) in *Nicotiana sylvestris* to four (*tufA1*, *tufA2*, *tufB1*, and *tufB2*) in *Glycine max* (Fu et al., 2012), indicating EF-Tu acts as chaperone and protects chloroplast stromal proteins from heat stress (Momcilovic and Ristic, 2004). Largely, over-expression of stress proteins resulted in enhanced thermo-tolerance in *Arabidopsis* (Alia et al., 1998), tobacco (Yang et al., 2005) and alfalfa (Saurez et al., 2008). Introduction of the *APX1* (ascorbate peroxidase) gene from pea and the *HvAPX1* gene from barley (Shi et al., 2001) in *Arabidopsis* led to improved thermo-tolerance.

High Temperature Stress and Mungbean

From observations of the International Mungbean Nurseries, Poehlman (1978) suggested that a mean temperature of 28–30°C is optimum for this crop. Mungbean develops through nine distinct phenological phases as suggested by Carberry (2007) and Chauhan et al. (2010). The development of mungbean plants during stages 1–9 is mainly related to growing temperatures. The temperature requirement for different development stages is known as “thermal time” or day-degrees (unit °Cd) (Chauhan et al., 2010). The APSIM (Agricultural Production Systems sIMulator) mungbean model uses thermal time to drive phenological development and canopy expansion. The key temperatures used in thermal time calculations in the APSIM model were 7.5°C base, 30°C optimum and 40°C maximum (Carberry, 2007; Chauhan et al., 2010).

Under heat stress, activity of native housekeeping proteins in mungbean is suppressed while some specific proteins, known as heat shock proteins (Hsp70), are synthesized in leaves and in growing flower primordia (Schlesinger et al., 1982). HT (>40°C) has a direct effect on flower maintenance and pod formation (Kumari and Varma, 1983). Being a short-duration crop, possibly can be cultivated over a range of environments. Sensitivity of mungbean to varying photoperiod and temperature regimes necessitates developing thermo-photoperiod-insensitive varieties suit for both dry and wet seasons (Tickoo et al., 1996).

Among different stages, reproductive stage is most sensitive to HTs, resulting in loss of flower buds, pods and seed yield. The reproductive stage includes functioning of flowers to achieve pod set (viz., loss of pollen viability, germination, poor anther dehiscence, less pollen load on stigma and its sterility). The stigmatic surface also loses receptivity coupled with poor ovule viability (Kaushal et al., 2013). Therefore, pollen heat stress appears to be a crucial target for developing heat-tolerant mungbean (Rainey and Griffiths, 2005). Flower shedding is very common and the extent of flower shedding has been reported up to 79% (Kumari and Varma, 1983). However, little is known about HT driven floral and pod development mechanisms in mungbean (Tickoo et al., 1996). Khattak et al. (2009) reported no or less resistance to flower shedding under HTs. However, this relationship may not hold true for all genotypes (Aggarwal and Poehlman, 1977). Rawson and Craven (1979) reported temperature-flowering interactions in particular groups of genotypes with high mean temperatures (24–28°C) and long photoperiods (15–16 h). Similarly, 77 mutants derived from NM 92 and 51 recombinants selected from three crosses viz., VC1560D × NM92, VC1482C × NM92, and NM98 × VC3902A were also evaluated for this trait under HTs. No genotype showed absolute tolerance to flower shedding, while NM 92 showed susceptibility to the same trait under HTs (>40°C). Only the opened flowers shed under HTs and pods at any stage didn't and humidity fluctuations had no effect on flower shedding⁶.

Several reasons for failure in reproductive growth and seed yield are attributed to heat stress. HT results in leaf scorching, leading to marginal (mild) to complete (severe) browning of leaves. The plant loses leaf pigments and photosynthetic function

declines considerably (Kaushal et al., 2013; Awasthi et al., 2014). Leaf damage intensifies due to oxidative damage and reduction in antioxidative defense (Kumar et al., 2013). Truncated growth appears to be due to poor leaf expansion and growth. As reproductive parts (flowers, pods and seeds) rely on the leaves for sucrose and other macromolecules for nodulation and organelle function, maintenance of photosynthetic machinery of the leaves become vital under heat stress to sustain synthesis and transport of sucrose to these organs (Awasthi et al., 2014). Sucrose decreases in leaves and seeds owing to heat stress, which may link to reduced RuBisCO activity (or increased photorespiration) and sucrose synthesizing enzymes. Although useful information on the effect of heat stress on photosynthesis and photosynthesis exists for other crop plants, sparse in mungbean (Bindumadhava et al., 2015). Under HTs, RuBisCO though enzymatically active, RuBisCO activase (RA) suffers catalytic deactivation, which might trigger disruption of total turnover rates of the enzyme (Ray et al., 2003). Oxidative damage to leaves increases, impairing photosynthetic efficiency, which also affects nitrogen-fixing ability of mungbean rhizobia by restricting formation and spread of root hair (Bansal et al., 2014).

Terminal heat stress is a severe problem of mungbean in India, particularly in spring/summer. However, in the *kharif* crop, temperatures >40°C occur during early growth stage, causing a drastic reduction in seed yield due to pollen sterility, lack of fertilization and high or otherwise, complete flower shedding. Rainey and Griffiths (2005) reported abscission of reproductive organs as the primary determinant of yield under heat stress in many annual grain legumes. In subtropics or at higher altitudes, mungbean is sometime planted when mean night temperatures are <20°C – for instance, the spring/summer crop of northern India. In such environments, germination is delayed and reduced, plant growth becomes very slow. Hence, selection for rapid germination and growth would improve plant stand, promote early maturity and yield. Kumar et al. (2011) grew mungbean hydroponically at varying temperatures of 30/20°C (control), 35/25, 40/30, and 45/35°C (day/night; 12 h/12 h) with (50 µM) or without exogenous ASC to investigate effects on growth, membrane damage, leaf water status, components of oxidative stress and antioxidants. Among all the antioxidants, endogenous ASC content decreased maximum in 45/35°C grown plants, indicating its vital role in affecting the response of mungbean to heat stress. Exogenously applied ASC improves its endogenous levels along with glutathione and proline at 45/35°C. Thus indicating application of ASC overcomes heat stress-induced inhibition in growth and chlorosis triggered by oxidative stress.

To improve productivity of mungbean in warmer climates, it is crucial to decipher genetic variation for heat tolerance in the core germplasm and probe mechanisms governing therein. Recently, Kaur R. et al. (2015) elucidated the response of mungbean genotypes to heat stress on reproductive biology, leaf function and yield traits. Two genotypes (SML 832 and 668) were subjected to HTs (>40/25°C; day/night) during reproductive stage. A drastic reduction in pod set, number of filled pods (32–38%), seed number (43–47%) and seed yield (35–47%) was observed with no or less effect on phenology, flowering duration and podding. SML 668 was found to be more sensitive to heat

⁶www.pakbs.org

stress than SML 832. This is perhaps the first preliminary report on the mechanisms affecting reproductive failures as a result of heat stress attributed to impaired sucrose metabolism in leaves and anthers. Malaviarachchi et al. (2016) assessed sensitivity of mungbean yield to increasing temperatures across different growing locations representing natural temperature gradient over two varied cropping seasons. In second season, crop experienced a broader temperature range, led to significantly reduced seed yield. However, insight on whether HT triggers failure in pollination, flower shedding, are they related to pollen infertility?, are responses linked to pollen viability and germination?, whether the ovule or the pollen more sensitive to heat?, if so to what extent, etc., are to be answered to know more on effects of heat stress on reproductive functions, pod maturity and final yield traits. Efforts must be made toward examining functional viability of pollen developed under heat stress for crossing ability with female parents grown under normal temperatures for both normal and heat stress conditions. We consider this is perhaps a current research gap and our own research is underway to address them in different growing environments.

Evidently, no studies on molecular mechanisms related to heat tolerance have been indicated, hence appropriate depiction of gene/s function and action against heat stress is still illusive. Apparently, apart from exploiting genetic variation for heat stress in various legumes, functional relevance of genes/gene product imparting tolerance are to be elucidated at molecular level. The existing high yielding genotypes of various legumes can be screened for heat tolerance either by planting them at hot spots or under late-sown conditions and selecting progenies on the bases of growth and yield traits. Diverse source viz., wild relatives might provide vital clues on target gene/s for heat tolerance which may have competitive advantage in breeding. Conclusively, integrated approaches involving marker-assisted selection, high throughput phenotyping and genotyping would form crucial links to unravel mechanisms of heat tolerance, which may subsequently pave the way for developing heat tolerant types in legumes through novel breeding approaches.

Management Practices for Alleviating Heat Stress under Field Conditions

Although it is difficult to mitigate crop growth temperatures in open field, a few options can be applied with some success. There is a general crop management practice to adjust the method and date of sowing to ensure crops don't face adverse heat effects during critical growth periods. However, in the literature, management practices for alleviating drought and heat stress are always presented together. We have attempted to de-link this association. The following soil management and irrigation practices, methods of handling crop residues and mulching, and choice of crops/varieties can alleviate negative effects of drought and heat stresses.

Soil Management and Irrigation

Changes in the soil surface affect soil water and heat balance in terms of soil water evaporation, infiltration and heat exchange between soil and atmosphere (Ferrero et al., 2005; Sekhon et al., 2010). These changes can be induced by tillage, surface residue

management/mulching. The soil surface roughness, gradients in temperature and water vapor, and infiltration affect amount of water stored in soil and water uptake by plants (Lipiec et al., 2006, 2012). An increase in rooting depth in soils with definite hard subsoils can be attained by deep tillage. However, due to its high cost, practiced only in most dense soil paddocks (Siczek and Lipiec, 2011; Martinez et al., 2012). Use of surface organic mulch diminishes soil temperature for its low thermal conductivity (Khan et al., 2000) and favorably influence water content by controlling surface evaporation (Mulumba and Lal, 2008).

Modern irrigation techniques including sprinkling, drip and film hole irrigation save water (up to >50%) and improve grain yield and WUE compared to surface irrigation, but are less effective in terms of cost and energy requirements (Jensen, 2013).

Crop Management: Choice of Crops/Varieties and Sowing Date

Crops vary in their ability to tolerate drought and heat stress under water limited and HT conditions. Intrinsic genetic factors help plant to control these two stresses (Blum, 2005; Singh et al., 2010). Some crops/genotypes tolerate stress better than others do. In general, plant types and varieties that mature earlier perform better in drought-prone areas by escaping terminal drought (Singh et al., 2010). Moreover, crops and varieties with an ability to develop early crop stand and canopy structures perform better in drought- and heat-prone areas through reduction in soil evaporation and heating (Sekhon et al., 2010).

Waraich et al. (2012) highlighted that better plant nutrition can effectively alleviate adverse effects of temperature stress through a number of mechanisms. The management and regulated use of plant nutrients is very helpful to develop plant tolerance to temperature stress. HT stress results in increased generation of the ROS due to energy accumulation in stressed plants, which increases photo-oxidative effect and damage to chloroplast membranes. Addition of plant nutrients reduce toxicity of ROS by increasing concentration of antioxidants in plant cells. These antioxidants scavenge the ROS, maintain integrity of chloroplast membranes, and increase photosynthesis. These nutrients help to maintain high tissue water potential under temperature stress conditions⁷.

In temperate or subtropical zones, alteration in sowing date would help in increasing the probability that annual crop species will escape stressful HTs during sensitive stages of development. In some subtropical zones, the weather can be chilling in early spring and become progressively warmer, reaching very hot conditions in the middle of the summer (Ismail et al., 1997, 1999)⁴. Agroforestry, including concurrent production of trees and agricultural crops on the same piece of land, can be useful for sustaining stresses in the cropping zone (Khan et al., 2000). Change in temperatures and water limitations expected under climate change may have a significant effect on geographical distribution and occurrence of pests and diseases, as well as expansion of new pathogens limiting crop production (Vadez et al., 2011; Sharma, 2014), which implies a need for developing new control measures.

⁷www.scielo.cl

Exogenous Application of Thermo-Protectants

Recently, exogenous applications of protectants in the form of osmoprotectants (proline, glycine betaine, brassosteroids, SA, phytohormones (ABA), signaling molecules, trace elements (selenium, etc.) and nutrients (phosphorus, potassium etc.) have been projected and found effective (Akhtar et al., 2015) in mitigating HT stress-induced damage in plants (Hasanuzzaman et al., 2010; Waraich et al., 2012)³. These molecules show promise in protecting plants from adverse effects of temperature stresses (Awasthi et al., 2015) and impart defense by managing the ROS through upregulation of antioxidant capacity.

In a few controlled experiments, application of proline and ASC conferred protection to heat-stressed plants of chickpea (Kaushal et al., 2011) and mungbean (Kumar et al., 2011), respectively. The positive effects of these molecules may be associated with reduction in damage to leaf and root tissues due to oxidative stress and activation of various antioxidants. Proline and ASC improved the growth of heat-stressed plants significantly, thus indicating the potential of these thermo-protectants. Wahid and Shabbir (2005) reported that, bean seeds pre-treated with glycine-betaine led to plants with lower membrane damage, better photosynthetic rate, improved leaf water potential and greater shoot dry mass compared to untreated seeds. In tomato, exogenous application of 4 mM spermidine improved heat resistance through better chlorophyll fluorescence properties, under heat stress⁷ and higher level of Ca^{2+} is required to mitigate adverse effects of the stress (Kleinhenz and Palta, 2002).

COLLABORATIVE RESEARCH OF WORLD VEGETABLE CENTER AND PARTNERS ON ABIOTIC STRESS IN INDIA

Development of mungbean genotypes tolerant to salinity and HT has been a long-standing goal of most institutes focusing on legume research. The World Vegetable Center's mandate for mungbean research emphasizes establishing growth and yield records for elite accessions against salinity and HTs.

In Punjab regions of India and Pakistan, mungbean is grown during summer and *kharif* seasons. With introduction of short-duration varieties, production potential expanded to > 2 m ha. During spring, mungbean grown on about 60-80,000 hectares of area after potato, wheat, etc., is exposed to HTs, especially during reproductive stage. HT is detrimental to both vegetative and reproductive growth. Early maturing and short duration genotypes grown between rice-wheat cycles may experience temperatures >40°C, causing serious damage to intrinsic growth and yield performances.

To address them, we initiated a program for screening elite (45) lines [mungbean yellow mosaic disease (MYMD)-resistant for salinity and HT under field and controlled conditions at ICRISAT Hyderabad, Panjab University (PU), Chandigarh, and Punjab Agricultural University (PAU), Ludhiana, India. The lines were from AVRDC's own collection and from several

Indian agricultural research institutes. Initial efforts yielded in identifying a few putative salinity (11 lines) and HT tolerant accessions (10 lines). The study continues to evaluate and validate these accessions under field conditions in different Indian states. These accessions will serve as donor parents in future mungbean breeding programs. Improving salinity along with heat tolerance would increase yield stability against harsh environments and possibly helps in expanding the geographical cultivable area.

INFERENCES AND FUTURE PROJECTIONS

Tolerance to salinity in legumes involves a multifaceted responses at cellular, molecular, physiological and whole-plant levels. Its adverse effects include osmotic stress, ion toxicity and nutrient imbalances. Although mungbean has intrinsic tolerance through physiological mechanisms, much needs to be explored in this species. Mungbean has distinct advantage of being a short-duration crop; it can grow in a range of soils and environments as a solo or as a relay crop. However, because it is sensitive to thermo-photoperiods and salinity, it has not been widely adopted by farmers. It is hoped that increasing osmotic stress tolerance would provide impetus for mungbean production under saline conditions.

Under HTs, modification of physiological and biochemical processes would gradually lead to heat tolerance through acclimation or adaptation. Depending on extremity and duration of intrinsic variations in plant types and allied environmental factors, mungbean would expect to show dynamic responses to stresses. However, most current experiments are laboratory and short duration investigations. Field experiments that explore different biochemical and molecular approaches as well as agronomic interventions are very much needed to gain tangibly HT responses on maturity and final yield patterns. At the field level, manipulating cultural practices can mitigate adverse effects of HT stress. In recent decades, exogenous applications of protectants and growth-promoting microorganisms have proven to be beneficial under HTs for their growth-promoting and antioxidant actions. Molecular approaches that reveal response/tolerance mechanisms will facilitate modifying plants that are able to withstand HTs without compromising yield. Integration of genes from closely related species for resistance to temperature and soil-related stresses should be the top priority for mungbean breeders to identify donor sources. Invariably, these qualities will substantiate the scope for horizontal expansion of mungbean and be a bonus in agricultural lands that remain fallow for 2–3 months after the harvest of the main (wheat/rice) crop.

Apart from exploring physiological and biochemical regulations of salinity and HT stress, there must be a continuous effort to compile a whole profile of genes, proteins, and metabolites responsible for different mechanisms of salinity and HT tolerance. Marker-linked genes for MYMD, powdery mildew, bruchid resistance, and some important yield traits already have been identified. However, potential sources of resistance to

adverse climatic and soil conditions from wild relatives can also be integrated for crop improvement. With the availability of draft mungbean genome plus transcriptomic and metabolomics approaches, researchers are now well equipped to explore and exploit underlying molecular processes, which may pave the way to develop multi-stress tolerant mungbeans best suited to adverse growing environments.

AUTHOR CONTRIBUTIONS

BH made initial review framework and gather all information connected to abiotic stresses and implications. Refocused on effect of salinity and heat stress in legumes in general and mungbean in particular. Has made full efforts in writing, editing and revising the review. RN conceptualized the idea and supported in providing scientific literature linked to salinity and high temperatures from plant breeding point of view. He reviewed and revised the manuscript and helped to improve

the reading and final editing. HN supported to gather recent research advancement in heat temperature tolerance in legumes, specially in mungbean as his team has been involved in this area from the last decade. He reviewed the manuscript and added valuable comments to improve it that helped in final editing.

ACKNOWLEDGMENTS

The authors acknowledge Dr. Warwick Easdown, Regional Director, World Vegetable Center, South Asia, Hyderabad, for suggestions and support, and thank Maureen Mecozzi and Dr. Roland Schafleitner for editing the manuscript. Core funding to support World Vegetable Center activities worldwide is provided by the Republic of China (ROC), UK Department for International Development (UK/DFID), United States Agency for International Development (USAID), Germany, Thailand, Philippines, Korea, and Japan.

REFERENCES

- Abd-Alla, M. H., Vuong, T. D., and Harper, J. E. (1998). Genotypic differences in nitrogen fixation response to NaCl stress in intact and grafted soybean. *Crop Sci.* 38:72. doi: 10.2135/cropscl1998.0011183X003800010013x
- Aggarwal, V. D., and Poehlman, J. M. (1977). Effects of photoperiod and temperature on flowering in mungbean (*Vigna radiata* (L.) Wilczek). *Euphytica* 26, 207–219. doi: 10.1007/BF00032086
- Agricultural Statistics of Pakistan (2001). *Ministry of Food Agriculture and Livestock*. Islamabad: Government of Pakistan.
- Ahmad, P., and Prasad, M. N. V. (2012). *Abiotic Stress Responses in Plants: Metabolism, Productivity and Sustainability*. New York, NY: Springer.
- Ahmad, P., and Umar, S. (2011). *Oxidative Stress: Role of Antioxidants in Plants*. New Delhi: Stadium Press.
- Akhtar, S., Hazra, P., and Naik, A. (2015). Harnessing heat stress in vegetable crops towards mitigating impacts of climate change. *Clim. Dyn. Hortic Sci.* 1:419.
- Ali, M., and Gupta, S. (2012). Carrying capacity of Indian agriculture: pulse crops. *Curr. Sci.* 102, 874–881.
- Alia, H. H., Sakamoto, A., and Murata, N. (1998). Enhancement of the tolerance of *Arabidopsis* to high temperatures by genetic engineering of the synthesis of glycine-betaine. *Plant J.* 16, 155–161. doi: 10.1046/j.1365-313x.1998.00284.x
- Anderson, A. J., and Sonali, P. R. (2004). Protein aggregation, radical scavenging capacity, and stability of hydrogen peroxide defense system in heat stressed *Vinca* and sweet pea leaves. *J. Am. Soc. Hortic. Sci.* 129, 54–59.
- Araujo, S. S., Beebe, S., Crespi, M., Delbreli, B., Gonzaliz, E. M., Gruber, V., et al. (2015). Abiotic stress responses in legumes: strategies used to cope with environmental challenges. *Crit. Rev. Plant Sci.* 34, 237–280. doi: 10.1080/07352689.2014.898450
- Arnoldi, A., Zanoni, C., Lammi, C., and Boschin, G. (2014). The role of grain legumes in the prevention of hypercholesterolemia and hypertension. *Crit. Rev. Plant Sci.* 33, 1–3.
- Arulbalachandran, D., Sankar, G. K., and Subramani, A. (2009). Changes in metabolites and antioxidant enzyme activity of three *Vigna* species induced by NaCl stress. *Am. Eur. J. Agron.* 2, 109–116.
- Ashraf, M. (1994). Organic substances responsible for salt tolerance in *Eruca sativa*. *Biol. Plant* 36, 255–259. doi: 10.1007/BF02921095
- Ashraf, M. (2014). Some important physiological selection criteria for salt tolerance in plants. *Flora* 199, 361–376. doi: 10.1078/0367-2530-00165
- Ashraf, M., Akram, N. A., Arteca, R. N., and Foolad, M. R. (2010). The physiological, biochemical and molecular roles of brassinosteroids and salicylic acid in plant processes and salt tolerance. *Crit. Rev. Plant Sci.* 29, 162–190. doi: 10.1080/07352689.2010.483580
- Awasthi, R., Bhandari, K., and Nayyar, H. (2015). Temperature stress and redox homeostasis in agricultural crops. *Front. Environ. Sci.* 3:11. doi: 10.3389/fenvs.2015.00011
- Awasthi, R., Kaushal, N., Vadez, V., Turner, N. C., Berger, J., Siddique, K. H. M., et al. (2014). Individual and combined effects of transient drought and heat stress on carbon assimilation and seed filling in chickpea. *Funct. Plant Biol.* 41, 1148–1167. doi: 10.1071/FP13340
- Balasubramanian, V., and Sinha, S. K. (1976). Effects of salt stress on growth, nodulation and nitrogen fixation in cowpea and mungbean. *Physiol. Plant.* 36, 197–200. doi: 10.1111/j.1399-3054.1976.tb03935.x
- Bansal, M., Kukreja, K., Sunita, S., and Dudeja, S. S. (2014). Symbiotic effectiveness of high temperature tolerant mungbean (*Vigna radiata*) rhizobia under different temperature conditions. *Int. J. Curr. Microbiol. Appl. Sci.* 3, 807–821.
- Banti, V., Mafessoni, F., Loret, E., Alpi, A., and Perata, P. (2010). The heat inducible transcriptionfactorHsfA2 enhances anoxia tolerance in *Arabidopsis*. *Plant Physiol.* 152, 1471–1483. doi: 10.1104/pp.109.149815
- Beebe, S. (2012). “Common bean breeding in the tropics,” in *Plant Breeding Reviews* Vol. 36, Chap. 5, ed. J. Janick (Hoboken, NJ: John Wiley & Sons, Inc.), 357–426. doi: 10.1002/978111358566.ch5
- Beebe, S., Ramirez, J., Jarvis, A., Rao, I., Mosquera, G., Bueno, G., et al. (2011). “Genetic improvement of common beans and the challenges of climate change,” in *Crop Adaptation of Climate Change* 1st Edn, eds S. S. Yadav, R. J. Redden, J. L. Hatfield, H. Lotze-Campen, and A. E. Hall (New York, NY: Wiley), 356–369.
- Bhandari, K., Sharma, K., Bindumadhava, H., Siddique, K. H. M., Gaur, P., Kumar, S., et al. (2016). Temperature sensitivity of food legumes: a physiological insight. *Acta Physiol. Plant.* (in press).
- Bhatnagar-Mathur, P., Vadez, V., and Sharma, K. K. (2008). Transgenic approaches for abiotic stress tolerance in plants: retrospect and prospects. *Plant Cell Rep.* 27, 411–424. doi: 10.1007/s00299-007-0474-9
- Bindumadhava, H., Nair, R. M., and Easdown, W. (2015). *Physiology of Mungbean Accessions Grown under Saline and High Temperature Conditions*. AVRDC-Annual report, No. 74199. Tainan: Weihai Shanhua Carpet Group Co., Ltd., 1–46.
- Bitar, C. E., and Gerats, T. (2013). Plant tolerance to high temperature in a changing environment: scientific fundamentals and production of heat stress tolerant crops. *Front. Plant Sci.* 4:273. doi: 10.3389/fpls.2013.00273
- Blum, A. (2005). Drought resistance, water-use efficiency, and yield potential— are they compatible, dissonant, or mutually exclusive? *Aust. J. Agric. Res.* 56, 1159–1168. doi: 10.1071/AR05069
- Boelt, B., Julier, B., Karagic, D., and Hampton, J. (2014). Legume seed production meeting market requirements and economic impacts. *Crit. Rev. Plant Sci.* 33, 116–122.

- Bourgault, M., Madramootoo, C. A., Webber, H. A., Stulina, G., Horst, M. G., and Smith, D. L. (2010). Effects of deficit irrigation and salinity stress on common bean (*Phaseolus Vulgaris* L.) and Mungbean (*Vigna Radiata* (L.) Wilczek) Grown in a Controlled Environment. *J. Agron. Crop Sci.* 196, 262–272.
- Buxton, D. R. (1996). Quality related characteristics of forages as influenced by plant environment and agronomic factors. *Anim. Feed Sci. Technol.* 59, 37–49. doi: 10.1016/0377-8401(95)00885-3
- Cabot, C., Sibole, J. V., Barceló, J., and Poschenrieder, C. (2009). Abscisic acid decreases leaf Na⁺ exclusion in salt-treated *Phaseolus vulgaris* L. *J. Plant Growth Regul.* 28, 187–192. doi: 10.1007/s00344-009-9088-5
- Carberry, P. (2007). “Crop development models,” in *Encyclopedia of Water Science*, 2nd Edn, ed. Encyclopedia of Science (Boca Raton, FL: CRC Press), 121–124.
- Chankaew, S., Isemura, T., Naito, K., Ogiso-Tanaka, E., Tomooka, N., Somta, P., et al. (2014). QTL mapping for salt tolerance and domestication-related traits in *Vigna marina* subsp. *oblonga*, a halophytic species. *Theor. Appl. Genet.* 127, 691–702. doi: 10.1007/s00122-013-2251-1
- Charng, Y. Y., Liu, H. C., Liu, N. Y., Chi, W. T., Wang, C. N., Chang, S. H., et al. (2007). A heat-inducible transcription factor, HsfA2, is required for extension of acquired thermotolerance in *Arabidopsis*. *Plant Physiol.* 143, 251–262. doi: 10.1104/pp.106.091322
- Chauhan, Y. S., Douglas, C., Rachaputti, R. C. N., Agius, P., Martin, W., King, K., et al. (2010). “Physiology of mungbean and development of the mungbean crop model,” in *Proceedings of the 1st Australian Summer Grains Conference*, Australia, Gold Coast, QL.
- Chaves, M. M., Maroco, J. P., and Pereira, J. S. (2003). Understanding plant responses to drought – from genes to the whole plant. *Funct. Plant Biol.* 30, 239–264. doi: 10.1071/FP02076
- Chen, S., Li, J., Wang, S., Hüttermann, A., and Altman, A. (2001). Salt, nutrient uptake and transport, and ABA of *Populus euphratica*; a hybrid in response to increasing soil NaCl. *Trees Struct. Funct.* 15, 186–194. doi: 10.1007/s004680100091
- Chinnusamy, V., Zhu, J., Zhou, T., and Zhu, J. K. (2007). “Small RNAs: big role in abiotic stress tolerance of plants,” in *Advances in Molecular Breeding toward Drought and Salt Tolerant Crops*, eds M. A. Jenks, P. M. Hasegawa, and S. M. Jain (Dordrecht: Springer), 223–260.
- Crafts-Brandner, S. J., and Salvucci, M. E. (2002). Sensitivity of photosynthesis in a C4 plant, maize, to heat stress. *Plant Physiol.* 129, 1773–1780. doi: 10.1104/pp.002170
- de Zélicourt, A., Diet, A., Marion, J., Laffont, C., Ariel, F., Moison, M., et al. (2012). Dual involvement of a *Medicago truncatula* NAC transcription factor in root abiotic stress response and symbiotic nodule senescence. *Plant J.* 70, 220–230. doi: 10.1111/j.1365-313X.2011.04859.x
- Deng, Y., Srivastava, R., and Howell, S. H. (2013). Endoplasmic reticulum (ER) stress response and its physiological roles in plants. *Int. J. Mol. Sci.* 14, 8188–8212. doi: 10.3390/ijms14048188
- Dhingra, K. K., Dhillon, M. S., Grewal, K., and Shorma, K. (1991). Performance of maize and mungbean intercropping different planting patterns and row orientation. *Indian J. Agron.* 36, 207–212.
- Elsheikh, E. A. E. (1998). Effects of salt on rhizobia and bradyrhizobia: a review. *Annu. Appl. Biol.* 132, 507–524. doi: 10.1111/j.1744-7348.1998.tb05226.x
- Elsheikh, E. A. E., and Wood, M. (1995). Nodulation and nitrogen fixation by soybean inoculated with salt-tolerant rhizobia or salt-sensitive bradyrhizobia in saline soil. *Soil Biol. Biochem.* 27, 657–661. doi: 10.1016/0038-0717(95)98645-5
- Erkina, T. Y., Zou, Y., Freeling, S., Vorobyev, V. I., and Erkine, A. M. (2010). Functional interplay between chromatin remodeling complexes RSC, SWI/SNF and ISWI in regulation of yeast heat shock genes. *Nucleic Acids Res.* 38, 1441–1449. doi: 10.1093/nar/gkp1130
- FAOSTAT (2013). FAOSTAT. Available at: <http://faostat.fao.org>
- Ferrero, A., Usowicz, B., and Lipiec, J. (2005). Effects of tractor traffic on spatial variability of soil strength and water content in grass covered and cultivated sloping vineyard. *Soil Tillage Res.* 84, 127–138. doi: 10.1016/j.still.2004.10.003
- Foolad, M. R. (2005). “Breeding for abiotic stress tolerances in tomato,” in *Abiotic Stresses: Plant Resistance Through Breeding and Molecular Approaches*, eds M. Ashraf and P. J. C. Harris (New York, NY: The Haworth Press Inc), 613–684.
- Fragnire, C., Serrano, M., Abou-Mansour, E., Métraux, J.-P., and L'Haridon, F. (2011). Salicylic acid and its location in response to biotic and abiotic stress. *FEBS Lett.* 585, 1847–1852. doi: 10.1016/j.febslet.2011.04.039
- Friedman, R., Altman, A., and Nitsa, L. (2006). The effect of salt stress on polyamine biosynthesis and content in mung bean plants and in halophytes. *Physiol. Plant.* 76, 295–302. doi: 10.1111/j.1399-3054.1989.tb06194.x
- Fu, J., Momčilović, I., and Vara Prasad, P. V. (2012). Roles of protein synthesis elongation factor EF-Tu in heat tolerance in plants. *J. Bot.* 20, 1–8. doi: 10.1155/2012/835836
- Garciadebllás, B., Senn, M. E., Bañuelos, M. A., and Rodríguez-Navarro, A. (2003). Sodium transport and HKT transporters: the rice model. *Plant J.* 34, 788–801. doi: 10.1046/j.1365-313X.2003.01764.x
- Gaur, P. M., Samineni, S., Krishnamurthy, L., Kumar, S., Ghanem, M. E., Bebb, S., et al. (2015). High temperature tolerance in grain legumes. *Legume Perspect.* 7, 23–24. doi: 10.3389/fphys.2012.00179
- Ge, Y., and Li, J. D. (1990). A preliminary study on the effects of halophytes on salt accumulation and desalination in the soil of Songnen Plain, northeast China. *Acta Prat. Sin.* 1, 70–76.
- Gong, Y., Rao, L., and Yu, D. (2013). “Abiotic stress in plants,” in *Agricultural Chemistry*, ed. M. Stoytcheva (Rijeka: InTech).
- Goyal, S. S., Sharma, S. K., Rains, D. W., and Lauchli, A. (1999a). Long term reuse of drainage waters of varying salinities for crop irrigation in a cotton-safflower rotation system in the San Joaquin Valley of California - A nine year study: I. Cotton (*Gossypium hirsutum* L.). *J. Crop Prod.* 2, 181–213. doi: 10.1300/J144v02n02_07
- Goyal, S. S., Sharma, S. K., Rains, D. W., and Lauchli, A. (1999b). Long term reuse of drainage waters of varying salinities for crop irrigation in a cotton-safflower rotation system in the San Joaquin Valley of California - A nine year study: II. Safflower (*Carthamus tinctorius* L.). *J. Crop Prod.* 2, 215–227. doi: 10.1300/J144v02n02_08
- Greer, D. H., and Weedon, M. M. (2012). Modelling photosynthetic responses to temperature of grapevine (*Vitis vinifera* cv. Semillon) leaves on vines grown in a hot climate. *Plant Cell Environ.* 35, 1050–1064. doi: 10.1111/j.1365-3040.2011.02471.x
- Grewal, H. S. (2010). Water uptake, water use efficiency, plant growth and ionic balance of wheat, barley, canola and chickpea plants on a sodic vertisol with variable subsoil NaCl salinity. *Agric. Water Manag.* 97, 148–156. doi: 10.1016/j.agwat.2009.09.002
- Gulati, A., and Jaiwal, P. K. (1993). In vitro selection of salt resistant *Vigna radiata* (L.) Wilczek plants by adventitious shoot formation from cultured cotyledon explants. *J. Plant Physiol.* 142, 99–102. doi: 10.1016/S0176-1617(11)80114-8
- Gupta, B., and Huang, B. (2014). Mechanism of salinity tolerance in plants: physiological, biochemical, and molecular characterization. *Int. J. Genomics* 2014:701596. doi: 10.1155/2014/701596
- Gurmani, A. R., Bano, A., Khan, S. U., Din, J., and Zhang, J. L. (2011). Alleviation of salt stress by seed treatment with abscisic acid (ABA), 6-benzylaminopurine (BA) and chlormequat chloride (CCC) optimizes ion and organic matter accumulation and increases yield of rice (*Oryza sativa* L.). *Aust. J. Crop Sci.* 5, 1278–1285.
- Hamid, A., and Haque, M. M. (2007). “Adaptation and yield potential of dual purpose wild mungbean (*Vigna marina*)” in *Proceedings of the Acta Horticulturae 752: I International Conference on Indigenous Vegetables and Legumes. Prospectus for Fighting Poverty, Hunger and Malnutrition*. Belgium: International Society for Horticultural Science.
- Hamilton, L. I. I. E. W., and Heckathorn, S. A. (2001). Mitochondrial adaptations to NaCl stress: complex I is protected by anti-oxidants and small heat shock proteins, whereas Complex II is protected by proline and betaine. *Plant Physiol.* 126, 1266–1274. doi: 10.1104/pp.126.3.1266
- Hasanuzzaman, M., Hossain, M. A., da Silva, J. A. T., and Fujita, M. (2012). “Plant responses and tolerance to abiotic oxidative stress: antioxidant defenses is a key factor,” in *Crop Stress and Its Management: Perspectives and Strategies*, eds V. Bandi, A. K. Shanker, C. Shanker, and M. Mandapaka (Berlin: Springer), 261–316.
- Hasanuzzaman, M., Hossain, M. A., and Fujita, M. (2010). Physiological and biochemical mechanisms of nitric oxide induced abiotic stress tolerance in plants. *Am. J. Plant Physiol.* 5, 295–324. doi: 10.1016/j.niox.2013.03.004

- Hasanuzzaman, M., Nahar, K., and Fujita, M. (2013a). "Extreme temperatures, oxidative stress and antioxidant defense in plants," in *Abiotic Stress—Plant Responses and Applications in Agriculture*, eds K. Vahdati and C. Leslie (Rijeka: InTech), 169–205.
- Hasanuzzaman, M., Nahar, K., and Fujita, M. (2013b). "Plant response to salt stress and role of exogenous protectants to mitigate salt-induced damages," in *Ecophysiology and Responses of Plants under Salt Stress*, eds P. Ahmad, M. M. Azooz, and M. N. V. Prasad (New York, NY: Springer), 25–87.
- Hasegawa, P. M. (2013). Sodium (Na^+) homeostasis and salt tolerance of plants. *Environ. Exp. Bot.* 92, 19–31. doi: 10.1016/j.envexpbot.2013.03.001
- Hasegawa, P. M., Bressan, R. A., Zhu, J. K., and Bohnert, H. J. (2000). Plant cellular and molecular responses to high salinity. *Ann. Rev. Plant Biol.* 51, 463–499. doi: 10.1146/annurev.arplant.51.1.463
- He, T., and Cramer, G. R. (1996). Abscisic acid concentrations are correlated with leaf area reductions in two salt-stressed rapid cycling *Brassica* species. *Plant Soil* 179, 25–33. doi: 10.1007/BF00011639
- Hoque, M. A., Banu, M. N., Nakamura, Y., Shimoishi, Y., and Murata, Y. (2008). Proline and glycinebetaine enhance antioxidant defense and methylglyoxal detoxification systems and reduce NaCl-induced damage in cultured tobacco cells. *J. Plant Physiol.* 165, 813–824. doi: 10.1016/j.jplph.2007.07.013
- Horie, T., Karahara, I., and Katsuhara, M. (2012). Salinity tolerance mechanisms in glycophytes: an overview with the central focus on rice plants. *Rice J.* 5, 1–18. doi: 10.1186/1939-8433-5-11
- Hossain, M. A., and Fujita, M. (2010). Evidence for a role of exogenous glycinebetaine and proline in antioxidant defense and methylglyoxal detoxification systems in mung bean seedlings under salt stress. *Physiol. Mol. Biol. Plants* 16, 19–29. doi: 10.1007/s12298-010-0003-0
- Hu, Y., and Schmidhalter, U. (2005). Drought and salinity: a comparison of their effects on mineral nutrition of plants. *J. Plant Nutr. Soil Sci.* 168, 541–549. doi: 10.1002/jpln.200420516
- Hussain, M. I., Lyra, A. A., Farooq, M., Nikolaos, N., and Khalid, N. (2016). Salt and drought stresses in safflower; a review. *Agron. Sustain. Dev.* 36:4. doi: 10.1007/s13593-015-0344-8
- Ihsan, M. Z., Shahzad, N., Kanwal, S., Naeem, M., Khaliq, A., El-Nakhlawy, F. S., et al. (2013). Potassium as foliar supplementation mitigates moisture induced stresses in mung bean (*Vigna radiata* L.) as Revealed by Growth, Photosynthesis, Gas Exchange Capacity and Zn Analysis of Shoot. *Int. J. Agron. Plant Prod.* 4, 3828–3835.
- Imamura, M., Yuasa, T., Takahashi, T., Nakamura, N., Htwe, N. M. P. S., Zheng, S. H., et al. (2008). Isolation and characterization of a cDNA coding cowpea (*Vigna unguiculata* (L.) Walp.) calcineurin B-like protein-interacting protein kinase, VuCIPK1. *Plant Biotechnol.* 25, 437–445. doi: 10.5511/plantbiotechnology.25.437
- Intergovernmental Panel on Climate Change [IPCC] (2007). "The physical science basis," in *Contribution of Working Group-I to the Fourth Assessment Report of the Intergovernmental Panel on Climate Change*, eds S. Solomon, D. Qin, M. Manning, Z. Chen, M. Marquis, K. B. Averyt, et al. (Cambridge: Cambridge University Press).
- Ismail, A. M., Hall, A. E., and Close, T. J. (1997). Chilling tolerance during emergence of cowpea associated with a dehydrin and slow electrolyte leakage. *Crop Sci.* 37, 1270–1277. doi: 10.2135/cropsci1997.0011183X003700040041x
- Ismail, A. M., Hall, A. E., and Close, T. J. (1999). Purification and partial characterization of a dehydrin involved in chilling tolerance during seedling emergence of cowpea. *Plant Physiol.* 96, 13566–13570.
- James, R. A., Blake, C., Byrt, C. S., and Munns, R. (2011). Major genes for Na^+ exclusion, Nax1 and Nax2 wheatHKT1;4 and HKT1;5, decrease Na^+ accumulation in bread wheat leaves under saline and waterlogged conditions. *J. Exp. Bot.* 62, 2939–2947. doi: 10.1093/jxb/err003
- Jensen, R. (2013). "Some options for securing water resources for agricultural production," in *Plant Functioning under Environmental Stress*, eds M. Grzesiak, A. Rzepka, T. Hura, and S. Grzesiak (Cracow: Institute of Plant Physiology, PAS), 9–25.
- Jiang, J., Su, M., Chen, Y., Gao, N., Jiao, C., Sun, Z., et al. (2013). Correlation of drought resistance in grass pea (*Lathyrus sativus*) with reactive oxygen species scavenging and osmotic adjustment. *Biologia* 68, 231–240. doi: 10.2478/s11756-013-0003-y
- Johkan, M., Oda, M., Maruo, T., and Shinohara, Y. (2011). "Crop production and global warming," in *Global Warming Impacts - Case Studies on the Economy, Human Health, and on Urban and Natural Environments*, ed. S. Casalegno (Rijeka: InTech), 139–152.
- Kaur, D., Pallavi, M., Sharma, P., and Sharma, S. (2015). Symbiotic effectiveness of *Bradyrhizobium* ensifer strains on growth, symbiotic nitrogen fixation and yield in soybean. *Adv. Appl. Sci. Res.* 6, 122–129.
- Kaur, R., Bains, T. S., Bindumadhava, H., and Nayyar, H. (2015). Responses of mungbean (*Vigna radiata* L.) genotypes to heat stress: effects on reproductive biology, leaf function and yield traits. *Sci. Hortic.* 197, 527–541. doi: 10.1016/j.scientia.2015.10.015
- Kaushal, N., Awasthi, R., Gupta, K., Gaur, P., Siddique, K. H. M., and Nayyar, H. (2013). Heat-stress-induced reproductive failures in chickpea (*Cicer arietinum*) are associated with impaired sucrose metabolism in leaves and anthers. *Funct. Plant Biol.* 40, 1334–1349. doi: 10.1071/FP13082
- Kaushal, N., Gupta, K., Bhandhari, K., Kumar, S., Thakur, P., and Nayyar, H. (2011). Proline induces heat tolerance in chickpea (*Cicer arietinum* L.) plants by protecting vital enzymes of carbon and antioxidative metabolism. *Physiol. Mol. Biol. Plants* 17, 203–213. doi: 10.1007/s12298-011-0078-2
- Kaya, H., Shibahara, K., Taoka, K., Iwabuchi, M., Stillman, B., and Araki, T. (2001). FASCIATA genes for chromatin assembly factor-1 in *Arabidopsis* maintain the cellular organization of apical meristems. *Cell* 104, 131–142. doi: 10.1016/S0092-8674(01)00197-0
- Keating, B. A., and Fisher, M. J. (1985). Comparative tolerance of tropical grain legumes to salinity. *Aust. J. Agric. Res.* 36, 373–383. doi: 10.1071/AR9850373
- Khalil, S. I., El-Bassiouny, H. M. S., Hassanein, R. A., Mostafa, H. A., El-Khawas, S. A., and Abd El-Monem, A. A. (2009). Antioxidant defence system in heat shocked wheat plants previously treated with arginine or putrescine. *Aust. J. Basic Appl. Sci.* 3, 1517–1526.
- Khan, A. R., Chandra, D., Quraishiand, S., and Sinha, R. K. (2000). Soil aeration under different soil surface conditions. *J. Agron. Crop Sci.* 185, 105–112. doi: 10.1046/j.1439-037X.2000.00417.x
- Khan, M., Izbal, R., Mehar, F., Tasir, S. P., Naser, A. A., and Nafees, A. K. (2015). Salicilic acid induced abiotic stress tolerance and underlying mechanisms in plants. *Front. Plant Sci.* 6:462. doi: 10.3389/fpls.2015.00462
- Khattak, G. S. S., Saeed, I., and Muhammad, T. (2009). Flowers' shedding under high temperature in mungbean (*Vigna radiata* (L.) Wilczek). *Pak. J. Bot.* 41, 35–39.
- Khraiwesh, B., Zhu, J. K., and Zhu, J. (2012). Role of miRNAs and siRNAs in biotic and abiotic stress responses of plants. *Biochim. Biophys. Acta* 1819, 137–148. doi: 10.1016/j.bbagen.2011.05.001
- Kido, E. A., Neto, J. R. F., Silva, R. L., Belarmino, L. C., Neto, J. P. B., Soares-Cavalcanti, N. M., et al. (2013). Expression dynamics and genome distribution of osmoprotectants in soybean: identifying important components to face abiotic stress. *BMC Bioinformatics* 14:S7. doi: 10.1186/1471-2105-14-S1-S7
- Kleinhenz, M. D., and Palta, J. P. (2002). Root zone calcium modulates the response of potato plants to heat stress. *Physiol. Plant.* 115, 111–118. doi: 10.1034/j.1399-3054.2002.1150113.x
- Koini, M. A., Alvey, L., Allen, T., Tilley, C. A., Harberd, N. P., Whitelam, G. C., et al. (2009). High temperature-mediated adaptations in plant architecture require the bHLH transcription factor PIF4. *Curr. Biol.* 19, 408–413. doi: 10.1016/j.cub.2009.01.046
- Kumar, A., Omae, H., Egawa, Y., Kashiwaba, K., and Shono, M. (2005). "Some physiological responses of snap bean (*Phaseolus vulgaris* L.) to water stress during reproductive period," in *Proceedings of the International Conference on Sustainable Crop Production in Stress Environment: Management and Genetic Option*. (Jabarpur: JNKVV), 226–227.
- Kumar, G., Krishnaprasad, B. T., Savitha, M., Gopalakrishna, R., Mukhopadhyay, K., Ramamohan, G., et al. (1999). Enhanced expression of heat shock proteins in thermotolerant lines of sunflower and their progenies selected on the basis of temperature induction response (TIR). *Theor. App. Gen.* 99, 359–367. doi: 10.1007/s001220051245
- Kumar, S., Kaur, R., Kaur, N., Bhandhari, K., Kaushal, N., Gupta, K., et al. (2011). Heat-stress induced inhibition in growth and chlorosis in mungbean (*Phaseolus aureus* Roxb.) is partly mitigated by ascorbic acid application and is

- related to reduction in oxidative stress. *Acta Physiol. Plant.* 33, 2091–2101. doi: 10.1007/s11738-011-0748-2
- Kumar, S., Thakur, P., Kaushal, N., Malik, J. A., Gaur, P., and Nayyar, H. (2013). Effect of varying high temperatures during reproductive growth on reproductive function, oxidative stress and seed yield in chickpea genotypes differing in heat sensitivity. *Arch. Agron. Soil Sci.* 59, 823–843. doi: 10.1080/03650340.2012.683424
- Kumar, S. V., and Wigge, P. A. (2010). H2A.Z-containing nucleosomes mediate the thermosensory response in *Arabidopsis*. *Cell* 140, 136–147. doi: 10.1016/j.cell.2009.11.006
- Kumari, P., and Varma, S. K. (1983). Genotypic differences in flower production/shedding and yield in mungbean (*Vigna radiata*). *Indian J. Plant Physiol.* 26, 402–405.
- Läuchli, A., and Lüttge, U. (2002). “Salinity in the soil environment,” in *Salinity: Environment-Plants-Molecules*, ed. K. K. Tanji (Boston, MA: Boston Kluwer Academic Publishers), 21–23.
- Lawn, R. J., and Ahn, C. S. (1985). “Mungbean (*Vigna radiata* L. Wilczek/ *Vigna mungo* L. Hepper),” in *Grain Legume Crops*, eds R. Summerfield and E. H. Roberts (London: Collins), 584–623.
- Lawn, R. J., Williams, R. W., and Imrie, B. C. (1988). “Potential of wild germplasm as a source of tolerance to environmental stresses in mungbean,” in *Proceedings of the 2nd International Symposium on Mungbean*, eds J. Fernandez and S. Shanmugam (Tainan: Asian Vegetable Research and Development Centre), 136–145.
- Li, C., Wang, X., Wang, H., Ni, F., and Shi, D. (2012). Comparative investigation of single salts stresses and their mixtures on Eragrostoid (*Chloris virgata*) to demonstrate the relaxation effect of mixed anions. *Aust. J. Crop Sci.* 6, 839–845.
- Li, W. Y. F., Wong, F. L., Tsai, S. N., Phang, T. H., Shao, G., and Lam, H. M. (2006). Tonoplast located *GmCLC1* and *GmNHX1* from soybean enhance NaCl tolerance in transgenic bright yellow (BY) - 2 cells. *Plant Cell Environ.* 29, 1122–1137. doi: 10.1111/j.1365-3040.2005.01487.x
- Lipiec, J., Horn, R., Pietrusiewicz, J., and Siczek, A. (2012). Effects of soil compaction on root elongation and anatomy of different cereal plant species. *Soil Tillage Res.* 121, 74–81. doi: 10.1016/j.still.2012.01.013
- Lipiec, J., Kuoe, J., Słowińska-Jurkiewicz, A., and Nosalewicz, A. (2006). Soil porosity and water infiltration as influenced by tillage methods. *Soil Tillage Res.* 89, 210–220. doi: 10.1016/j.still.2005.07.012
- Liu, H. C., Liao, H. Y., and Charng, Y. Y. (2011). The role of class A1 heat shock factors (HSFA1s) in response to heat and other stresses in *Arabidopsis*. *Plant Cell Environ.* 34, 738–751. doi: 10.1111/j.1365-3040.2011.02278.x
- Lobell, D. B., and Asner, G. P. (2003). Climate and management contributions to recent trends in U.S. agricultural yields. *Science* 299:1032. doi: 10.1126/science.1077838
- Lobell, D. B., and Field, C. B. (2007). Global scale climate–Crop yield relationships and the impacts of recent warming. *Environ. Res. Lett.* 2:014002. doi: 10.1088/1748-9326/2/1/014002
- Lohar, D., and Peat, W. (1998). Floral characteristics of heat tolerant and heat sensitive tomato (*Lycopersicon esculentum* Mill.) cultivars at high temperature. *Sci. Hortic.* 73, 53–60. doi: 10.1016/S0304-4238(97)00056-3
- Maas, E. V. (1986). Salt tolerance of plants. *Appl. Agric. Res.* 1, 12–26.
- Mahdavi, B., and Sanavy, S. A. (2007). Developing salt tolerant mungbean varieties. *Pak. J. Biol. Sci.* 10, 273–279.
- Malaviarachchi, M. A. P. W. K., Costa, W. A. J. M., Kumara, J. B. D. A. P., Suriyagoda, D. B., and Fonseka, R. M. (2016). Response of Mung bean (*Vigna radiata* (L.) R. Wilczek) to an increasing natural temperature gradient under different crop management systems. *J. Agron. Crop Sci.* 202, 51–68. doi: 10.1111/jac.12131
- Maliwal, G. L., and Paliwal, K. V. (1982). Effect of different levels of bicarbonates alone and combination with carbonates in irrigation waters on the growth, mineral nutrition and quality of barley grown in sand culture. *Indian J. Agric. Sci.* 52, 593–597.
- Manchanda, G., and Garg, N. (2008). Salinity and its effects on the functional biology of legumes. *Acta Physiol. Plant.* 30, 595–618. doi: 10.1007/s11738-008-0173-3
- Martínez, I. G., Prat, C., Ovalle, C., del Pozo, A., Stolpe, N., and Zagal, E. (2012). Subsoiling improves conservation tillage in cereal production of severely degraded Alfisols under Mediterranean climate. *Geoderma* 18, 10–17. doi: 10.1016/j.geoderma.2012.03.025
- Mathur, S., Divya, A., and Anjana, J. (2014). Photosynthesis: response to high temperature stress. *J. Photochem. Photobiol.* 137, 116–126. doi: 10.1016/j.jphotobiol.2014.01.010
- McKenzie, J. S., Paquin, R., and Duke, S. K. (1988). “Cold and heat tolerance,” in *Alfalfa and Alfalfa Improvement, Agronomy Monograph*, eds A. A. Hanson, D. K. Barnes, and R. R. Hill (Madison, WI: ASA, CSSA, and SSSA), 259–302.
- Mir, R. R., Zaman-Alah, M., Sreenivasulu, N., Trethowan, R., and Varshney, R. K. (2012). Integrated genomics, physiology and breeding approaches for improving drought tolerance in crops. *Theor. Appl. Genet.* 125, 625–645. doi: 10.1007/s00122-012-1904-9
- Mirzaei, S., Farshadfar, E., and Mirzaei, Z. (2014). Evaluation of physiologic and metabolic indicators of drought resistance in chickpea. *Int. J. Biosci.* 5, 106–113. doi: 10.12692/ijb/5.2.106-113
- Mishkind, M., Vermeer, J. E., Darwish, E., and Munnik, T. (2009). Heat stress activates phospholipase D and triggers PIP2 accumulation at the plasma membrane and nucleus. *Plant J.* 60, 10–21. doi: 10.1111/j.1365-313X.2009.03933.x
- Mishra, S., Panda, S. K., and Sahoo, L. (2014). Transgenic Asiatic grain legumes for salt tolerance and functional genomics. *Rev. Agric. Sci.* 2, 21–36.
- Misra, N., and Dwivedi, U. N. (1995). Carbohydrate metabolism during seed germination and seedling growth in green gram under saline stress. *Plant Physiol. Biochem.* 33, 33–38.
- Misra, N., and Dwivedi, U. N. (2004). Genotypic difference in salinity tolerance of green gram cultivars. *Plant Sci.* 166, 1135–1142. doi: 10.1016/j.plantsci.2003.11.028
- Misra, N., and Gupta, A. K. (2006). Interactive effects of sodium and calcium on proline metabolism in salt tolerant green gram cultivar. *Am. J. Plant Physiol.* 1, 1–12. doi: 10.3923/ajpp.2006.1.12
- Misra, N., Murmu, B., Singh, P., and Misra, M. (1996). Growth and Proline accumulation in mungbean seedlings as affected by sodium chloride. *Biol. Plant.* 38, 531–536. doi: 10.1007/BF02890603
- Mittler, R. (2002). Oxidative stress, antioxidants and stress tolerance. *Trends Plant Sci.* 7, 405–410. doi: 10.1016/S1360-1385(02)02312-9
- Mittler, R., Finka, A., and Goloubinoff, P. (2012). How do plants feel the heat? *Trends Biochem. Sci.* 37, 118–125. doi: 10.1016/j.tibs.2011.11.007
- Momcilošević, I., and Ristić, Z. (2004). Localization and abundance of chloroplast protein synthesis elongation factor (EF-Tu) and heat stability of chloroplast stromal proteins in maize. *Plant Sci.* 166, 81–88. doi: 10.1016/j.plantsci.2003.08.009
- More, S. D., and Ghonikar, C. P. (1984). “Nitrogen use efficiency and its soil balance an influenced by sorghum-wheat and greengram-wheat cropping sequences,” in *Nitrogen in Soils, Crops and Fertilizers: Bulletin No. 13* (New Delhi: IOS Press), 346–350.
- Mudgal, V., Madaan, N., and Mudgal, A. (2010). Biochemical mechanisms of salt tolerance in plants: a review. *Int. J. Bot.* 6, 136–143. doi: 10.3923/ijb.2010.136.143
- Mulumba, L. N., and Lal, R. (2008). Mulching effects on selected soil physical properties. *Soil Tillage Res.* 98, 106–111. doi: 10.1016/j.still.2007.10.011
- Munns, R. (2002). Comparative physiology of salt and water stress. *Plant Cell Environ.* 25, 239–250. doi: 10.1046/j.0016-8025.2001.00808.x
- Munns, R. (2005). Genes and salt tolerance: bringing them together. *New Phytol.* 167, 645–663. doi: 10.1111/j.1469-8137.2005.01487.x
- Munns, R., Husain, S., Rivelli, A. R., James, R. A., Condon, A. G., Lindsay, M. P., et al. (2002). Avenues for increasing salt tolerance of crops, and the role of physiologically based selection traits. *Plant Soil* 247, 93–105. doi: 10.1023/A:1021119414799
- Munns, R., James, R. A., and Lauchli, A. (2006). Approaches to increasing salt tolerance of wheat and other cereals. *J. Exp. Bot.* 57, 1025–1043. doi: 10.1093/jxb/erj100
- Munns, R., and Tester, M. (2008). Mechanisms of salinity tolerance. *Annu. Rev. Plant Biol.* 59, 651–681. doi: 10.1146/annurev.arplant.59.032607.092911

- Naher, N., and Alam, A. K. (2010). Germination, growth and nodulation of mungbean (*Vigna radiata* L.) as affected by sodium chloride. *Int. J. Sustain. Crop Prod.* 5, 8–11.
- Nair, R. M., Schafleitner, R., Kenyon, L., Srinivasan, R., Easdown, W., Ebert, R. W., et al. (2012). Genetic improvement of mungbean. *SABRAO J. Breed. Genet.* 44, 177–190.
- Nandini, C., and Subhendu, M. (2002). Growth regulator mediated changes in leaf area and metabolic activity in mungbean under salt stress condition. *Indian J. Plant Physiol.* 7, 256–263.
- Naresh, R. K., Purushottam, Singh, S. P., Ashish Dwivedi, and Vineet Kumar. (2013). Effects of water stress on physiological processes and yield attributes of different mungbean (L.) varieties. *Afr. J. Biochem. Res.* 7, 55–62.
- Nazar, R., Iqbal, N., Syeed, S., and Khan, N. A. (2011). Salicylic acid alleviates decreases in photosynthesis under salt stress by enhancing nitrogen and sulfur assimilation and antioxidant metabolism differentially in two mungbean cultivars. *J. Plant Physiol.* 168, 807–815. doi: 10.1016/j.jplph.2010.11.001
- Neelam, M., and Dwivedi, U. N. (2004). Genotypic difference in salinity tolerance of green gram cultivars. *Plant Sci.* 166, 1135–1142. doi: 10.1016/j.plantsci.2003.11.028
- Noreen, Z., Ashraf, M., and Akram, N. A. (2010). Salt-induced modulation in some key physio-biochemical processes and their use as selection criteria in potential vegetable crop pea (*Pisum sativum* L.). *Crop Pasture Sci.* 61, 369–378. doi: 10.1071/CP09255
- Okuma, E., Soeda, K., Fukuda, M., Tada, M., and Murata, Y. (2002). Negative correlation between the ratio of K^+ to Na^+ and proline accumulation in tobacco suspension cells. *Soil Sci. Plant Nutr.* 48, 753–757. doi: 10.1080/00380768.2002.10409266
- Palao, D. C., De La Viña, C. B., Aiza Vispo, N., and Singh, R. K. (2014). “New phenotyping technique for salinity tolerance at reproductive stage in rice,” in *Proceedings of the 3rd International Plant Phenotyping Symposium*, Chennai.
- Paliwal, K. V., and Maliwal, G. L. (1980). Growth and nutrient uptake relationship of some crops in saline substrate. *Ann. Arid Zone* 19, 251–253.
- Panchuk, I. I., Volkov, R. A., and Schoffl, F. (2002). Heat stress and heat shock transcription factor dependent expression and activity of ascorbate peroxidase in *Arabidopsis*. *Plant Physiol.* 129, 838–885. doi: 10.1104/pp.001362
- Pang, Q., Chen, S., Dai, S., Chen, Y., Wang, Y., and Yan, X. (2010). Comparative proteomics of salt tolerance in *Arabidopsis thaliana* and *Thellungiella halophila*. *J. Proteome Res.* 9, 2584–2599. doi: 10.1021/pr100034f
- Parida, A. K., and Das, A. B. (2005). Salt tolerance and salinity effects on plants: a review. *Ecotoxicol. Environ. Saf.* 60, 324–349.
- Phillips, G. C., and Collins, G. B. (1979). In-vitro tissue culture of selected legumes and plant regeneration from callus cultures of red clover. *Crop Sci.* 19, 59–64. doi: 10.2135/cropscli1979.0011183X001900010014x
- Piramila, B. H. M., Prabha, A. L., Nandagopalan, V., and Stanley, A. L. (2012). Effect of heat treatment on germination, seedling growth and some biochemical parameters of dry seeds of black gram. *Int. J. Pharm. Phytopharacol. Res.* 1, 194–202.
- Plieth, C., Hansen, U. P., Knight, H., and Knight, M. R. (1999). Temperature sensing by plants: the primary characteristics of signal perception and calcium response. *Plant J.* 18, 491–497. doi: 10.1046/j.1365-313X.1999.00471.x
- Poehlman, J. M. (1978). “What we have learnt from the International Mungbean Nurseries?,” in *Proceedings of the 1st International Mungbean Symposium*, (Tainan: Asian Vegetable Research and Development Centre), 97–100.
- Popova, L. P., Stoinova, Z. G., and Maslenkova, L. T. (1995). Involvement of abscisic acid in photosynthetic process in *Hordeum vulgare* L. during salinity stress. *J. Plant Growth Regul.* 14, 211–218. doi: 10.1007/BF00204914
- Porcel, R., Azcón, R., and Ruiz-Lozano, J. M. (2004). Evaluation of the role of genes encoding for Δ^1 -pyrroline-5-carboxylate synthetase (P5CS) during drought stress in arbuscular mycorrhizal *Glycine max* and *Lactuca sativa* plants. *Physiol. Mol. Plant Pathol.* 65, 211–221. doi: 10.1016/j.pmp.2005.02.003
- Promila, K., and Kumar, S. (2000). *Vigna radiata* seed germination under salinity. *Biol. Plant.* 43, 423–426. doi: 10.1093/pcp/pcs040
- Qureshi, R. H., Aslam, M., and Akhtar, J. (2003). “Productivity enhancement in the salt-affected lands of Joint Satiana Pilot Project area of Pakistan,” in *Crop Production in Saline Environments: Global and Integrative perspectives*, eds S. S. Goyal, S. K. Sharma, and D. W. Rains (Binghamton, NY: The Food Products Press).
- Rahnama, A., James, R. A., Poustini, K., and Munns, R. (2010). Stomatal conductance as a screen for osmotic stress tolerance in durum wheat growing in saline soil. *Funct. Plant Biol.* 37, 255–263. doi: 10.1071/FP09148
- Rainey, K. M., and Griffiths, P. D. (2005). Differential responses of common bean genotypes to high temperatures. *J. Am. Soc. Hortic. Sci.* 130, 18–23.
- Ramajulu, S., and Sudhakar, C. (2001). Alleviation of NaCl salinity stress by calcium is partly related to the increased proline accumulation in Mulberry callus. *J. Plant Biol.* 28, 203–206.
- Rawson, H. M., and Craven, C. L. (1979). Variation between short duration mungbean cultivars (*Vigna radiata* (L.) Wilczek) in response to temperature and photoperiod. *Indian J. Plant Physiol.* 22, 127–136.
- Ray, D., Sheshshayee, M. S., Mukhopadhyay, K., Bindumadhava, H., Prasad, T. G., and Udayakumar, M. (2003). High Nitrogen use efficiency in rice genotypes is associated with higher net photosynthetic rate at lower RuBisCO content. *Biol. Plant.* 46, 251–256. doi: 10.1023/A:1022858828972
- Reddy, C. V. (1982). Note on the effect of saline water irrigation on green gram. *Curr. Agric.* 6, 183–185.
- Reddy, M. P., Sanish, S., and Iyengar, E. R. R. (1992). Photosynthetic studies and compartmentation of ions in different tissues of *Salicornia brachiata* Roxb under saline conditions. *Photosynthetica* 26, 173–179.
- Reddy, P. S., Jogeswar, G., Rasineni, G. K., Maheswari, M., Reddy, A. R., and Varshney, R. K. (2015). Proline over-accumulation alleviates salt stress and protects photosynthetic and antioxidant enzyme activities in transgenic sorghum [*Sorghum bicolor* (L.) Moench]. *Plant Physiol. Biochem.* 94, 104–113. doi: 10.1016/j.plaphy.2015.05.014
- Reynolds, M. P., Pierre, C. S., Saad, A. S. I., Vargas, M., and Condon, A. G. (2007). Evaluating potential genetic gains in wheat associated with stress-adaptive trait expression in elite genetic resources under drought and heat stress. *Crop Sci.* 47, 172–189. doi: 10.2135/cropscli2007.10.0022IPBS
- Richards, L. A. (ed.) (1954). *Diagnosis and Improvements of Saline and Alkali Soils, Agriculture Handbook* 60, Washington, DC: USDA, 160.
- Rodriguez, M., Canales, E., and Borrás-Hidalgo, O. (2005). Molecular aspects of abiotic stress in plants. *Biotechnol. Appl.* 22, 1–10.
- Roy, S. J., Negrão, S., and Tester, M. (2014). Salt resistant crop plants. *Curr. Opin. Biotechnol.* 26, 115–124. doi: 10.1016/j.copbio.2013.12.004
- Roychoudhury, A., and Ghosh, S. (2013). Physiological and biochemical responses of mungbean to varying concentrations of Cadmium Chloride or Sodium Chloride. *Unique J. Pharm. Biol. Sci.* 1, 11–21.
- Rozema, J., and Flowers, T. (2008). Ecology: crops for a salinized world. *Science* 322, 1478–1480. doi: 10.1126/science.1168572
- Saha, P., Chatterjee, P., and Biswas, A. K. (2010). NaCl pretreatment alleviates salt stress by enhancement of antioxidant defense and osmolyte accumulation in mungbean (*Vigna radiata* L. Wilczek). *Indian J. Exp. Biol.* 48, 593–600.
- Saidi, Y., Finka, A., and Goloubinoff, P. (2011). Heat perception and signaling in plants: a tortuous path to thermotolerance. *New Phytol.* 190, 556–565. doi: 10.1111/j.1469-8137.2010.03571.x
- Saidi, Y., Finka, A., Muriset, M., Bromberg, Z., Weiss, Y. G., Maathuis, F. J., et al. (2009). The heat shock response in moss plants is regulated by specific calcium-permeable channels in the plasma membrane. *Plant Cell* 21, 2829–2843. doi: 10.1105/tpc.108.065318
- Saurez, R., Calderon, C., and Iturriaga, G. (2008). Enhanced tolerance to multiple abiotic stresses in transgenic alfalfa accumulating trehalose. *Crop Sci.* 49, 1791–1799. doi: 10.2135/cropscli2008.09.0573
- Schafleitner, R., Nair, R. M., Rathore, A., Wang, Y.-W., Lin, C.-Y., Chu, S.-H., et al. (2015). The AVRDC – The World Vegetable Center mungbean (*Vigna radiata*) core and mini core collections. *BMC Genomics* 16:344. doi: 10.1186/s12864-015-1556-7
- Scharf, K. D., Berberich, T., Ebersberger, I., and Nover, L. (2012). The plant heat stress transcription factor (Hsf) family: structure, function and evolution. *Biochim. Biophys. Acta* 1819, 104–119. doi: 10.1016/j.bbagr.2011.10.002
- Schlesinger, M. J., Ashburner, M., and Tissieres, A. (eds). (1982). *Heat Shock: From Bacteria to Man*. Cold Spring Harbor, NY: Cold Spring Harbor Laboratory, 440.

- Scholte, M., d'Erfurth, I., Rippa, S., Mondy, S., Cosson, V., Durand, P., et al. (2002). T-DNA tagging in the model legume *Medicago truncatula* allows efficient gene discovery. *Mol. Breed.* 10, 203–215. doi: 10.1023/A:1020564612093
- Sehrawat, N., Bhat, K. V., Sairam, R. K., and Jaiwal, P. K. (2013b). Screening of mungbean (*Vigna radiata* L. Wilczek) genotypes for salt tolerance. *Int. J. Plant Anim. Environ. Sci.* 4, 36–43.
- Sehrawat, N., Bhat, K. V., Sairam, R. K., and Jaiwal, P. K. (2013d). Identification of salt resistant wild relatives of mungbean (*Vigna radiata* L. Wilczek). *Asian J. Plant Sci. Res.* 3, 41–49.
- Sehrawat, N., Bhat, K. V., Sairam, R. K., Tomooka, N., Kaga, A., Shu, Y., et al. (2013c). Diversity analysis and confirmation of intra-specific hybrids for salt tolerance in mungbean (*Vigna radiata* L. Wilczek). *Int. J. Integr. Biol.* 14, 65–73.
- Sehrawat, N., Jaiwal, P. K., Yadav, M., Bhat, K. V., and Sairam, R. K. (2013a). Salinity stress restraining mungbean (*Vigna radiata* L. Wilczek) production: gateway for genetic improvement. *Int. J. Agric. Crop Sci.* 6, 505–509.
- Sehrawat, N., Yadav, M., Bhat, K. V., Sairam, R. K., and Jaiwal, P. K. (2015). Effect of salinity stress on Mungbean [*Vigna radiata* (L.)] during consecutive summer and spring seasons. *J. Agric. Sci.* 60, 23–32. doi: 10.2298/JAS1501023S
- Sekhon, H. S., Singh, G., Sharma, P., and Bains, T. S. (2010). “Water use efficiency under stress environments,” in *Climate Change and Management of Cool Season Grain Legume Crops*, eds S. S. Yadav, D. L. Mc Neil, R. Redden, and S. A. Patil (New York, NY: Springer Press).
- Semenov, M. A., and Halford, N. G. (2009). Identifying target traits and molecular mechanisms for wheat breeding under a changing climate. *J. Exp. Bot.* 60, 2791–2804. doi: 10.1093/jxb/erp164
- Shakeel, S., and Mansoor, S. (2012). Salicylic acid prevents the damaging action of salt in mungbean seedlings. *Pak. J. Bot.* 44, 559–562.
- Sharma, H. C. (2014). Climate change effects on insects: implications for crop protection and food security. *J. Crop Improv.* 28, 229–259.
- Shi, W. M., Muramoto, Y., Ueda, A., and Takabe, T. (2001). Cloning of peroxisomal ascorbate peroxidase gene from barley and enhanced thermotolerance by overexpressing in *Arabidopsis thaliana*. *Gene* 273, 23–27. doi: 10.1016/S0378-1119(01)00566-2
- Shinozaki, K., and Yamaguchi-Shinozaki, K. (2007). Gene networks involved in drought stress response and tolerance. *J. Exp. Bot.* 58, 221–227. doi: 10.1093/jxb/erl164
- Shrivastava, P., and Kumar, R. (2015). Soil Salinity: a serious environmental issue and plant promoting bacteria as one of the tools for its alleviation. *Saudi J. Biol. Sci.* 22, 123–131. doi: 10.1016/j.sjbs.2014.12.001
- Siczek, A., and Lipiec, J. (2011). Soybean nodulation and nitrogen fixation in response to soil compaction and surface straw mulching. *Soil Tillage Res.* 114, 50–56. doi: 10.1016/j.still.2011.04.001
- Singh, A. K., Sopory, S. K., Wu, K., and Singla-Pareek, S. K. (2010). “Transgenic Approaches,” in *Abiotic Stress Adaptation in Plants: Physiological, Molecular and Genomic Foundation*, eds A. Pareek, S. K. Sopory, H. J. Bohnert, and Govindjee (New York, NY: Springer), 417–450.
- Singh, D. P., and Singh, B. B. (2011). Breeding for tolerance to abiotic stresses in mungbean. *J. Food Legumes* 24, 83–90.
- Singh, H. B., Mali, P. S., Sharma, H. C., and Singh, H. (1989). Relative performance of mungbean (*Vigna radiata* L. Wilczek) cultivars under varying levels of soil salinity. *Haryana J. Agron.* 5, 171–173.
- Singh, M., Kumar, J., Singh, V. P., and Prasad, S. M. (2014). Plant tolerance mechanism against salt stress: the nutrient management approach. *Biochem. Pharmacol.* 3:e165. doi: 10.4172/2167-0501.1000e165
- Singh, R. K., Mishra, B., Chauhan, M. S., Yeo, A. R., Flowers, S. A., Flowers, T. J., et al. (2002). Solution culture for screening rice varieties for sodicity tolerance. *J. Agric. Sci.* 139, 327–333. doi: 10.1017/S0021859602002447
- Soussi, M., Ocana, A., and Lluch, C. (1998). Effect of salt stress on growth, photosynthesis and nitrogen fixation in Chickpea. *J. Exp. Bot.* 49, 1329–1337. doi: 10.1093/jxb/49.325.1329
- Sugio, A., Dreos, R., Aparicio, F., and Maule, A. J. (2009). The cytosolic protein response as a subcomponent of the wider heat shock response in *Arabidopsis*. *Plant Cell* 21, 642–654. doi: 10.1105/tpc.108.062596
- Sumesh, K. V., Sharma-Natu, P., and Ghildiyal, M. C. (2008). Starch synthase activity and heat shock protein in relation to thermal tolerance of developing wheat grains. *Biol. Plant.* 52, 749–753. doi: 10.1007/s10535-008-0145-x
- Tickoo, J. L., Grajraj, R., Matho, M., and Manji, C. (1996). “Plant type in mungbean,” in *Proceedings of Recent Advances in Mungbean*, eds A. N. Asthana and D. H. Kum (Kanpur: Indian Society of Pulses Research), 197–213.
- Tilman, D., Cassman, K. G., Matson, P. A., Naylor, R., and Polasky, S. (2002). Agricultural sustainability and intensive production practices. *Nature* 418, 671–677. doi: 10.1038/nature01014
- Tripp, J., Mishra, S. K., and Scharf, K.-D. (2009). Functional dissection of the cytosolic chaperone network in tomato mesophyll protoplasts. *Plant Cell Environ.* 32, 123–133. doi: 10.1111/j.1365-3040.2008.01902.x
- United States Department of Agriculture [USDA] (2011). “Plants Profile for *Vigna marina* (Notched Cowpea)-USDA PLANTS,” Retrieved December 19, 2011 and “GRIN Taxonomy for Plants: *Vigna marina* (Burm.) Merr.” Germplasm Resources Information Network, USDA, Retrieved December 29, 2011. Available at: <http://plants.usda.gov>
- Vadez, V., Kholova, J., Choudhary, S., Zindy, P., Terrier, M., Krishnamurthy, L., et al. (2011). “Whole plant response to drought under climate change,” in *Crop Adaptation to Climate Change*, eds S. S. Yadav, R. Redden, J. L. Hatfield, H. Lotze-Campen, and A. E. Hall (Chichester: Wiley-Blackwell).
- Vaz Patto, M. C., Amarowicz, R., Aryee, A. N. A., Boye, J. I., Chung, H. J., Martín-Cabrejas, M. A., et al. (2014). Achievements and challenges in improving the nutritional quality of food legumes. *Crit. Rev. Plant Sci.* 33, 188–193.
- Venkateswarlu, B., and Shanker, A. K. (2009). Climate change and agriculture: adaptation and mitigation strategies. *Indian J. Agron.* 54, 226–230.
- von Koskull-Doring, P., Scharf, K. D., and Nover, L. (2007). The diversity of plant heat stress transcription factors. *Trends Plant Sci.* 12, 452–457. doi: 10.1016/j.tplants.2007.08.014
- Wahid, A., and Ejaz, M. H. R. (2004). Salt injury symptom, changes in nutrient and pigment composition and yield characteristics of mungbean. *Int. J. Agric. Biol.* 6, 1143–1152.
- Wahid, A., Gelani, S., Ashraf, M. R., and Foolad, M. R. (2007). Heat tolerance in plants: an overview. *Environ. Exp. Bot.* 61, 199–223. doi: 10.1016/j.envexpbot.2007.05.011
- Wahid, A., and Shabbir, A. (2005). Induction of heat stress tolerance in barley seedlings by pre-sowing seed treatment with glycinebetaine. *Plant Growth Regul.* 46, 133–141. doi: 10.1007/s10725-005-8379-5
- Wang, J. Z., Cui, L. J., Wang, Y., and Li, J. L. (2009). Growth, lipid peroxidation and photosynthesis in two tall fescue cultivars differing in heat tolerance. *Biol. Plant.* 53, 237–242. doi: 10.1007/s10535-009-0045-8
- Waraich, E. A., Ahmad, R., Halim, A., and Aziz, T. (2012). Alleviation of temperature stress by nutrient management in crop plants: a review. *J. Soil Sci. Plant Nutr.* 12, 221–244. doi: 10.4067/S0718-95162012000200003
- Win, T., Oo, A. Z., Hirasawa, T., Okawa, T., and Yutaka, H. (2011). Genetic analysis of Myanmar *Vigna* species in responses to salt stress at the seedling stage. *Afr. J. Biotechnol.* 10, 1615–1624.
- Yang, C., Chong, J., Kim, C., Li, C., Shi, D., and Wang, D. (2007). Osmotic adjustment and ion balance traits of an alkali resistant halophyte *Kochia sieversiana* during adaptation to salt and alkali conditions. *Plant Soil* 294, 263–276. doi: 10.1007/s11104-007-9251-3
- Yang, X., Chen, X., Ge, Q., Li, B., Tong, Y., Zhang, A., et al. (2006). Tolerance of photosynthesis to photoinhibition, high temperature and drought stress in flag leaves of wheat: a comparison between a hybridization line and its parents grown under field conditions. *Plant Sci.* 171, 389–397. doi: 10.1016/j.plantsci.2006.04.010
- Yang, X., Liang, Z., and Lu, C. (2005). Genetic engineering of the biosynthesis of glycine betaine enhances photosynthesis against high temperature stress in transgenic tobacco plants. *Plant Physiol.* 138, 2299–2309. doi: 10.1104/pp.105.063164
- Yasin, M., Zada, R., and Niazi, B. H. (1998). Effectiveness of chemical and biotic methods for reclamation of saline-sodic soil. *Pak. J. Soil Sci.* 15, 179–182.
- Yong, H., Shuya, Y., and Hyang, L. (2014). Towards plant salinity tolerance implications from ion transporters and biochemical regulation. *Plant Growth Regul.* 35, 133–143.
- Zahir, Z. A., Kashif Shah, M., Naveed, M., and Javed Akhter, M. (2010). Substrate-dependent auxin production by *Rhizobium phaseoli* improves the growth and yield of *Vigna radiata* L. Under Salt Stress Conditions. *J. Microbiol. Biotechnol.* 20, 1288–1294. doi: 10.4014/jmb.1002.02010

- Zhang, G. L., Chen, L. Y., Zhang, S. T., Zheng, H., and Liu, G. H. (2009). Effects of high temperature stress on microscopic and ultrastructural characteristics of mesophyll cells in flag leaves of rice. *Rice Sci.* 16, 65–71. doi: 10.1016/S1672-6308(08)60058-X
- Zhang, Y., Mian, M. A. R., and Bouton, J. H. (2006). Recent molecular and genomic studies on stress tolerance of forage and turf grasses. *Crop Sci.* 46, 497–511. doi: 10.2135/cropsci2004.0572
- Zurayk, R. (1998). Interactive effects of salinity and biological nitrogen fixation on chickpea (*Cicer arietinum* L.) growth. *J. Agron. Crop Sci.* 180, 249–258. doi: 10.1111/j.1439-037X.1998.tb00531.x

Conflict of Interest Statement: The authors declare that the research was conducted in the absence of any commercial or financial relationships that could be construed as a potential conflict of interest.

Copyright © 2016 HanumanthaRao, Nair and Nayyar. This is an open-access article distributed under the terms of the Creative Commons Attribution License (CC BY). The use, distribution or reproduction in other forums is permitted, provided the original author(s) or licensor are credited and that the original publication in this journal is cited, in accordance with accepted academic practice. No use, distribution or reproduction is permitted which does not comply with these terms.



Boron Toxicity Causes Multiple Effects on *Malus domestica* Pollen Tube Growth

Kefeng Fang[†], Weiwei Zhang[†], Yu Xing, Qing Zhang, Liu Yang, Qingqin Cao and Ling Qin*

Beijing Key Laboratory for Agricultural Application and New Technique, College of Plant Science and Technology, Beijing University of Agriculture, Beijing, China

OPEN ACCESS

Edited by:

Sylvain Jeandroz,
AgroSup Dijon, France

Reviewed by:

Frantisek Baluska,
University of Bonn, Germany
Jorge Muschietti,
Institute for Research
in Genetic Engineering and Molecular
Biology (INGEBI), Argentina

***Correspondence:**

Ling Qin
qinlingbac@126.com

[†]These authors have contributed
equally to this work.

Specialty section:

This article was submitted to
Plant Physiology,
a section of the journal
Frontiers in Plant Science

Received: 17 December 2015

Accepted: 06 February 2016

Published: 26 February 2016

Citation:

Fang K, Zhang W, Xing Y, Zhang Q,
Yang L, Cao Q and Qin L (2016)
Boron Toxicity Causes Multiple Effects
on *Malus domestica* Pollen Tube
Growth. *Front. Plant Sci.* 7:208.
doi: 10.3389/fpls.2016.00208

Boron is an important micronutrient for plants. However, boron is also toxic to cells at high concentrations, although the mechanism of this toxicity is not known. This study aimed to evaluate the effect of boron toxicity on *Malus domestica* pollen tube growth and its possible regulatory pathway. Our results showed that a high concentration of boron inhibited pollen germination and tube growth and led to the morphological abnormality of pollen tubes. Fluorescent labeling coupled with a scanning ion-selective electrode technique detected that boron toxicity could decrease $[Ca^{2+}]_c$ and induce the disappearance of the $[Ca^{2+}]_c$ gradient, which are critical for pollen tube polar growth. Actin filaments were therefore altered by boron toxicity. Immuno-localization and fluorescence labeling, together with fourier-transform infrared analysis, suggested that boron toxicity influenced the accumulation and distribution of callose, de-esterified pectins, esterified pectins, and arabinogalactan proteins in pollen tubes. All of the above results provide new insights into the regulatory role of boron in pollen tube development. In summary, boron likely plays a structural and regulatory role in relation to $[Ca^{2+}]_c$, actin cytoskeleton and cell wall components and thus regulates *Malus domestica* pollen germination and tube polar growth.

Keywords: *Malus domestica*, boron toxicity, calcium, actin, callose, pectin, arabinogalactan proteins

INTRODUCTION

Boron is an essential micronutrient for the normal development of higher plants (Blevins and Lukaszewski, 1998). Its main role is to form borate-diol ester bonds to link two rhamnogalacturonan II (RGII) chains of pectic polysaccharide (Pérez-Castro et al., 2012; Funakawa and Miwa, 2015). Recent research illustrated that boron also cross-link glycosylinositol phosphorylcer amides of the plasma membrane with arabinogalactan proteins (AGPs) of the cell wall, thereby attaching the membrane to the cell wall (Tenhaken, 2014; Vioxeur and Fry, 2014). Thus, boron is known to affect the mechanical properties of the cell wall (Dumont et al., 2014). There is a narrow range of favorable boron concentrations for plant development. Abnormal levels of boron can be toxic or can trigger deficiency symptoms (Pérez-Castro et al., 2012). The optimum boron level for one species can be either toxic or insufficient for other species (Blevins and Lukaszewski, 1998). Boron toxicity is an important agricultural problem that limits crop productivity (Nable et al., 1997) and attracts increase interest. Boron toxicity has been shown to affect several developmental or biochemical processes in plants (Sakamoto et al., 2011), including

inhibiting the formation of glutathione (Ruiz et al., 2003) and tocopherol (Keles et al., 2004), reducing root cell division (Aquea et al., 2012), and shoot cell wall expansion (Loomis and Durst, 1992), decreasing fruit number, size and weight, formatting reactive oxygen species(ROSSs) (Paull et al., 1992; Nable et al., 1997; Karabal et al., 2003; Cervilla et al., 2007), increasing oxidative damage (Gunes et al., 2006; Molassiotis et al., 2006; Sotiropoulos et al., 2006), affecting the photosynthesis and antioxidant apparatus (Landi et al., 2013), and leading to DNA damage (Sakamoto et al., 2011). A cDNA-AFLP analysis revealed that long-term boron stress induced changes related to signal transduction, metabolism of carbohydrate, energy, nucleic acid, protein, amino acid and lipid, cell wall and cytoskeleton modification, stress responses, and cell transport in *Citrus grandis* and *Citrus sinensis* (Guo et al., 2014). Furthermore, several genes involved in plant tolerance to boron stress have been identified, including *Arabidopsis thaliana* *BOR4* and *TIP5;1* (Miwa et al., 2007; Pang et al., 2010), barley (*Hordeum vulgare*) *Bot1* (Sutton et al., 2007), wheat and barley *HvBOR2* (Reid, 2007), and citrus (*Citrus macrophylla*) *CmBOR1* (Cañon et al., 2013). These genes encode transport molecules that exclude excess boron or regulate intracellular boron homeostasis to prevent boron stress (Sakamoto et al., 2011). Although a number of studies have been performed in this field, as described above, the effects of boron toxicity on sexual plant reproduction remain largely unknown.

Pollen tubes represent a fast growing system that requires boron to germinate and maintain tube elongation (Taylor and Hepler, 1997), making it a good system with which to investigate the influence of boron toxicity. Pollen tubes are cells that grow from their tips, whose elongation exhibits a polarized pattern (Hao et al., 2013). During the process of pollen tube growth, large amounts of membrane, and cell wall precursors are transported by the secretory vesicles derived from the Golgi apparatus to the tip to form the new cell wall and thus lead to pollen tube elongation (Taylor and Hepler, 1997; Ketelaar et al., 2008; Moscatelli and Idilli, 2009; Zhang et al., 2010; Bou and Geitmann, 2011). The pollen tube wall is mainly composed by cellulose, callose, and pectins, among which the pectins seem to be the major component of the cell wall (Li et al., 1996, 2002; Ferguson et al., 1998). The Golgi apparatus produced esterified pectin residues and the latter is secreted at the extreme apex of the pollen tube (Hasegawa et al., 1998). The esterified pectins are de-esterified by the enzyme pectin methyl-esterase (PME) when arrival at the cell wall (Geitmann, 1999; Li et al., 2002). De-esterification of pectin produces acidic residue which cross-links Ca^{2+} ions to form a semi rigid pectate gel (Braccini and Perez, 2001), thus providing mechanical support for the elongating tube. Esterified pectins are mainly present at the apex and speculated to allow tube expansion (Franklin-Tong, 1999). Therefore, de-esterified and esterified pectins control jointly the growth of plant cell (Wolf and Greiner, 2012).

Boron is necessary for pollen tubes (Obermeyer et al., 1996), and affects pollen tube morphology and tube growth (Dickinson, 1978; Holdaway-Clarke and Hepler, 2003). However, few data are available on the effects of boron toxicity on pollen germination

and tube growth. The detailed regulatory effects of boron toxicity on pollen tube development remain to be elucidated.

In the present study, *Malus domestica* pollen was chosen as the material with which to study the influence of boron toxicity on germination and pollen tube growth, focusing on the dynamics of calcium, actin, and cell wall components. Our results revealed that boron toxicity could interrupt the calcium gradient at the tip of a pollen tube and block its polar growth, likely via disturbing the actin organization and thus disturbing the cell wall material directional transportation and cell wall construction.

MATERIALS AND METHODS

Plant Materials and Pollen Culture

Mature pollen grains were collected from *Malus domestica* trees grown in Henan Province on April 10, 2014. The collected pollen grains were dried on paper towels and then stored in vials at -20°C until use.

The basal medium for pollen tube growth was composed by 20% (w/v) sucrose and 0.01% CaCl_2 , pH 6.8. Pollen grains was placed into culture medium in concentration of 1.0 mg mL^{-1} . Different concentrations of boric acid (Sigma, St. Louis, MO, USA) was added to the medium at the beginning of incubation. The culture with shake for 100 rpm at 30°C in the darkness.

Method of Dafni (2000) was used to determine the pollen germination rates under BX51 microscope which is equipped with a CoolSNAP HQ CCD camera (Photometrics) after 2 h of incubation. The lengths of pollen tubes were measured using MetaMorph (Universal Imaging) after 2 h of incubation. All experiments were performed in triplicate and at least 150 pollen tubes were measured in each experiment. Viability of the pollen tube was detect with fluorescein diacetate (FDA) according to Chebli et al. (2013).

Measurement of Extracellular Ca^{2+} Influx

Net Ca^{2+} fluxes of pollen tubes were measured in the Younger USANMT Service Center (Xuyue Beijing) using a Non-invasive Micro-test Technique (NMT-YG-100, Younger USALLC, Amherst, MA 01002, USA) with the ASET 2.0 (Sciencewares, Falmouth, MA 02540, USA) and the iFluxes 1.0 (Younger USA, LLC, Amherst, MA 01002, USA) software packages (Wang et al., 2013). Excel sheet (Microsoft) was employed to analyze the obtained data and convert data into ion influx ($\text{pmol cm}^{-2} \text{ sec}^{-1}$) accordingly.

Labeling of Cytoplasmic $[\text{Ca}^{2+}]_c$

Fluo-3/AM ester was loaded into pollen tubes to label cytoplasmic $[\text{Ca}^{2+}]_c$ at low temperature in the dark at a final concentration of $10 \mu\text{M}$, as described previously (Zhang and Renzel, 1998). After 1 h of incubation, the pollen tubes were washed with standard medium several times and placed under room temperature for 1 h. After that the pollen tubes photographed using a Leica TCS SP5 laser-scanning confocal microscope (LSCM) (Leica Co., Germany) with excitation at 488 nm and emission at 515 nm.

Fluorescent Labeling of Actin Filament

Fluorescent labeling of actin filament was according to Hao et al. (2013). Control and boron toxicity treated pollen tubes were fixed in a freshly prepared solution of 4% paraformaldehyde in PBS (pH 6.9) for 1.5 h at room temperature, followed by three washes with PBS, and treated with enzyme solution containing 1% cellulase R-10 and 1% pectinase at 37°C for 15 min. Then the pollen tubes were washed in PBS, and incubated in 1% Triton X-100 at room temperature for 1 h. After three times with PBS, the pollen tubes were incubated in 0.2 μM phalloidin-FITC (Sigma, USA) in PBS (pH 6.9) buffer for 2 h in darkness (Hao et al., 2013). Then, the pollen tubes were washed with PBS and observed under the LSCM with Excitation at 488 nm and emission at 515 nm.

Localization and Analysis of Cell Wall Components

Calcofluor was employed to stain cellulose as described by Lazzaro et al. (2003), callose was stained with 0.05% aniline blue according to Chen et al. (2007). The stained pollen tubes were observed and photographed under a FSX100 microscope (Olympus, Japan). Method described by Chen et al. (2007) was used to label pectins and AGPs of pollen tubes. The labeled pollen tubes were observed under the LSCM with excitation at 488 nm and emission at 515 nm. Values for fluorescence intensity was analyzed according to Chebli et al. (2013). At least 10 tubes were analyzed for each treatment, which was repeated three times. Fourier Transform Infrared (FTIR) spectroscopy analysis of wall components was performed according to Hao et al. (2013). At least 10 tubes were analyzed for each treatment, which was repeated three times.

RESULTS

Boron Toxicity Affected Pollen Germination and Tube Growth

Boron affected pollen tube morphology (Figure 1). In germination medium including 20% sucrose, 0.015% CaCl₂ and 0.01% H₃BO₃, pollen tubes appeared healthy with a regular shape. The constant diameter is illustrated in Figure 1A. The morphology of pollen tubes treated with high concentrations of boron was abnormal: the pollen tube was short, the tip of the tube swelled, and the diameter of the tube increased (Figures 1B,C). Strong FDA fluorescence indicated the viability of the swollen tube (Figure 1D).

Boron affects pollen germination and tube growth in a dose-dependent manner. Apple pollen grain has been reported to contain 55.45 μg/g boron (Gao et al., 2014), and our results showed that the endogenous levels were able to support pollen germination. At low concentrations, boron stimulated pollen germination and tube growth. Above 0.02%, boron inhibited pollen germination and tube growth. In the presence of 0.2% boric acid, the germination percentage was 12.87%, much lower than the 60.25% germination of the control pollen grains (Figure 2A). The average growth rate of pollen tubes treated with 0.2% boric acid was distinctly slower than for the control:

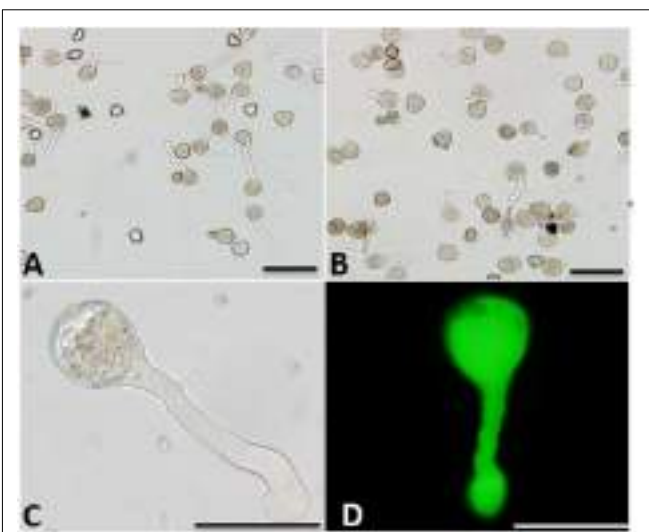


FIGURE 1 | Morphology of *Malus domestica* pollen tube under boron toxicity. (A) Morphology of a control pollen tube with slender diameter and straight shape. **(B)** Morphology of a pollen tube treated with 0.2% boric acid, showing an abnormal tube. **(C)** Abnormal pollen tubes showing the twisted morphology and swollen tip, respectively. **(D)** Fluorescein diacetate (FDA) fluorescence indicated viability of the swollen pollen tube. Scale bar: 50 μm.

the average growth rate of control pollen tubes was 163.7 μm/h, whereas the growth rate was only 30.65 μm/h in the presence of 0.2% boric acid (Figure 2B).

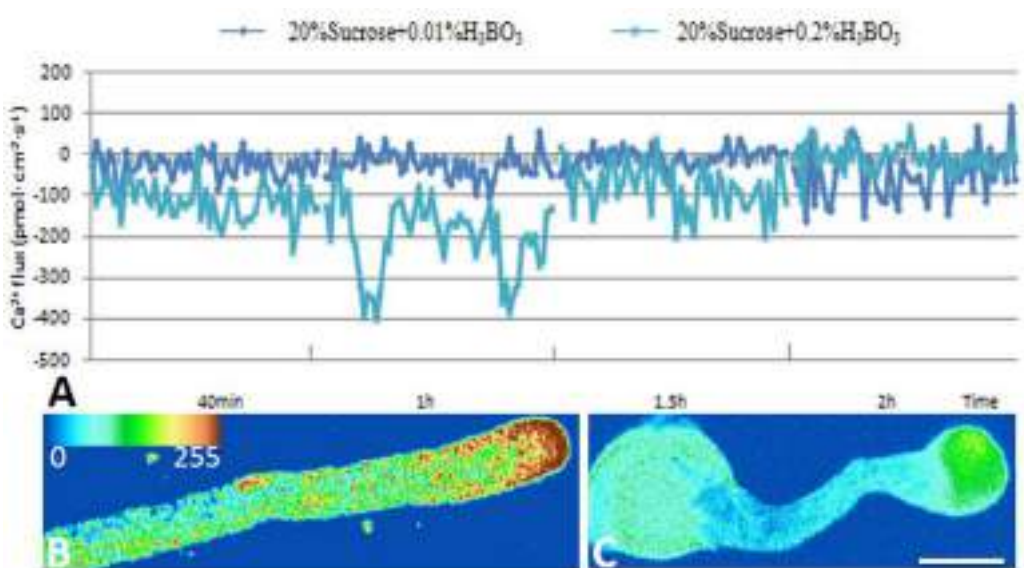
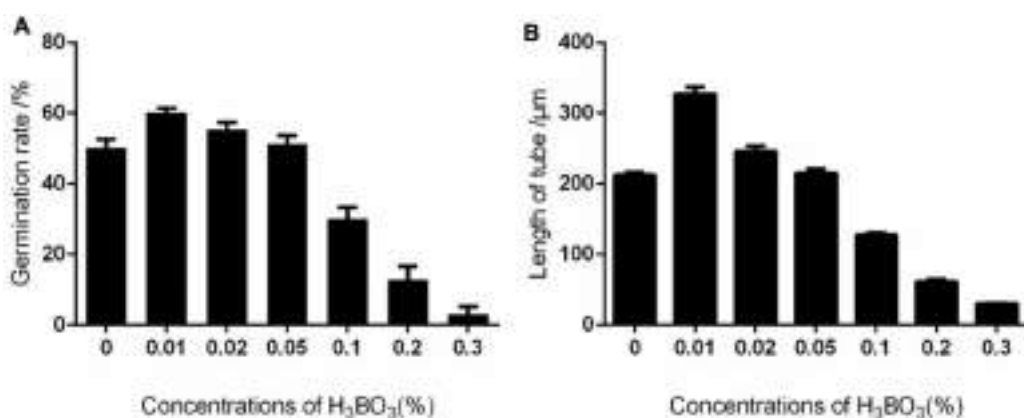
Boron Toxicity Induced a Decrease in [Ca²⁺]c Concentration and Disappearance of the [Ca²⁺]c Gradient

Ca²⁺ influx was measured at the extreme apex of the growing pollen tubes using a vibrating electrode technique (non-invasive micro-test technique). The results showed that Ca²⁺ influx was equal to efflux in the control tube apex at 2 h after culture. The magnitude of Ca²⁺ influx at the extreme apex was increased upon 0.2% boric acid treatment (Figures 3A,B).

Furthermore, [Ca²⁺]c was detected using Fluo-3/AM in pollen tubes. The control pollen tube tips showed a representative [Ca²⁺]c gradient within 20–30 μm (Figure 3B), while the pollen tubes treated with 0.2% boric acid showed very weak [Ca²⁺]c fluorescence in their swollen tips compared to the control, and the [Ca²⁺]c distribution was totally altered, (Figure 3C, Supplementary Figure S1a) indicating that boron toxicity led to the disappearance of the [Ca²⁺]c gradient.

Boron Toxicity Varied the Actin Filaments

Actin filaments take an active part in vesicle trafficking, cell wall construction, and tip growth of pollen tubes (Hao et al., 2013). Thus, the actin cytoskeleton in control and boron toxicity-treated pollen tubes was compared. As observed by LSCM, the actin filaments showed a contiguous bundle through the tube, which was parallel to the growth axis in the control pollen tubes (Figures 4A,A1). However, under boron toxicity, the actin filaments were clearly twisted and condensed. The disrupted



actin filament fragments accumulated into clusters with a very strong signal in the apical region (**Figures 4B,B1, Supplementary Figure S1b**).

Effect of Boron Toxicity on Cellulose and Callose Deposition on the Pollen Tube Wall

As shown in **Figure 5**, boron toxicity did not alter the distributive pattern and deposition of the cellulose in pollen tube wall (**Figures 5A,B,E**). Aniline blue staining showed that callose was present evenly along the tube except for the tip in control pollen tubes (**Figures 5C,C1**). On the contrary, strong fluorescence

was observed in the pollen tube tip treated by boron toxicity, suggesting enhanced callose deposition at the tip in response to boron toxicity (**Figures 5D,D1,F**).

Impact of Boron Toxicity on Pectin and AGP Deposition on Pollen Tube Wall

In the control pollen tubes, the distribution of JIM5-labeled (de-esterified or acid) pectin was relatively uniform, with much at the basal part near the grain and less at the tip (**Figures 6A,A1**), whereas the localization of JIM7-binding (esterified) pectin was relatively uniform, with stronger fluorescence at the apex of the growing tubes (**Figures 6C,C1,E**). Both types of pectin

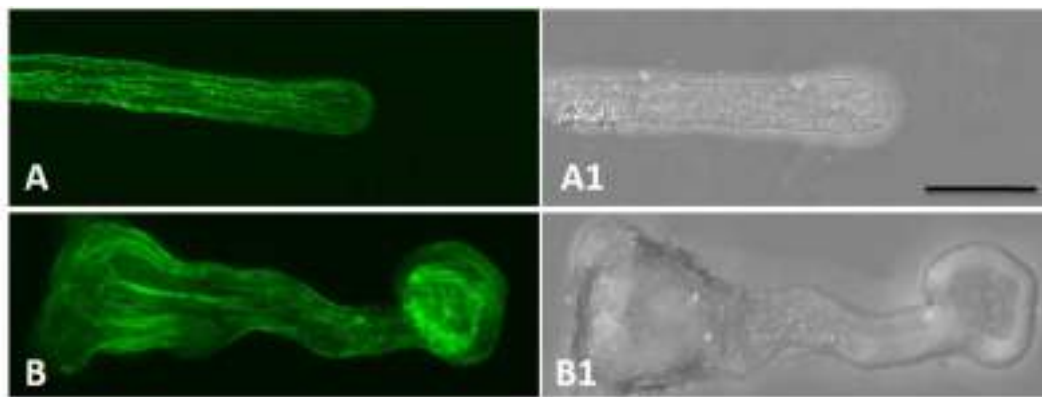


FIGURE 4 | Actin filaments of *Malus domestica* pollen tube in normal and boron toxicity media. **(A)** Actin filament paralleled with the pollen tube in the normal culture medium. **(A1)** Corresponding bright field image of **(A)**. **(B)** Actin filaments showed serious fracture at the apical part of the pollen tube treated with 0.2% boric acid. **(B1)** Corresponding bright field image of **B**. Scale bar: 25 μ m.

showed a polar distribution. By contrast, more de-esterified pectin was detected along the entire tube (**Figures 6B,B1**) and more esterified pectin was detected on the entire pollen tube under boron toxicity (**Figures 6D,D1,F**). That is, no obvious polar distribution of pectin was observed in these pollen tubes.

Boron toxicity clearly disrupted the distribution pattern of AGPs. The typical characteristic AGP distribution on the pollen tube wall is a periodic ring-like pattern with a stronger signal in the basal part and weaker signals at the apex (**Figures 7A,A1**). However, under boron toxicity, the typical pattern disappeared. Instead, continued but irregular deposition was observed (**Figures 7B,B1**). Quantitative analysis of the fluorescence signal of AGPs in the wall indicated that boron toxicity induced more AGP accumulation in the pole of the tube (**Figure 7C**).

FTIR Spectroscopy Analysis of Pollen Tube Wall Components

Representative FTIR spectra gained from the tip domain of control and 0.2% boric acid-treated pollen tubes are shown in **Figure 8**. For the control pollen, saturated esters absorbed at 1740 cm^{-1} , amide stretching bands of proteins absorbed at 1638 and 1529 cm^{-1} , carboxylic acid groups absorbed at 1457 cm^{-1} , and carbohydrates absorbed between 1200 and 900 cm^{-1} . In the presence of 0.2% boric acid, the ester peak at 1738 cm^{-1} was increased, free acid stretched at 1455 cm^{-1} , and the amide stretching bands of proteins absorbing at 1628 and 1515 cm^{-1} were increased, indicating that pollen tubes under boron toxicity showed increased esterified pectins, acid pectins and AGPs compared with the values in normal pollen tubes.

DISCUSSION

Boron toxicity has been reported to affect various developmental processes in plants (Nable et al., 1990, 1997; Reid, 2007; Guo et al., 2014). Baluška et al. (2003) reported that interactions

between pectins, boron, and the cytoskeleton were important for the assembly of the cell wall-cytoskeleton continuum as well as for its maintenance via signal-mediated processes. So the changes in boron concentrations may cause a mechanical cascade of signals extending into the cytoplasm via the cell wall-plasma membrane-cytoskeleton continuum, with the possible involvement of AGPs (Camacho-Cristóbal et al., 2008). The hypothesis is sustained by the researches that boron deficiency resulted in a varied polymerization pattern of cytoskeletal proteins (Yu et al., 2001, 2003) and in inhibition of the endocytic pathway for the internalization of B-cross-linked RG-II pectins (Yu et al., 2002). Our present work provides novel evidence for this proposal.

Boron Toxicity Induced a Decrease of $[\text{Ca}^{2+}]_c$ and Disappearance of the $[\text{Ca}^{2+}]_c$ Gradient

It has been appreciated that Ca^{2+} plays a key role in determining the structure and function of the cell wall (Hepler, 2005). The apical wall of normal pollen tube consists almost entirely of pectin, with cellulose and callose being located behind the apex (Ferguson et al., 1998). Ca^{2+} affected the mechanical properties of the cell wall through cross-linking de-esterified HG of pectin (Peaucelle et al., 2012). As a consequence, when the $[\text{Ca}^{2+}]$ is lowered sufficiently the pollen tube wall loses its structural integrity and therefore bursts, whereas when $[\text{Ca}^{2+}]$ is high, the pectin chains will be cross-linked and aggregated, and the wall maximally rigidified (Hepler and Winship, 2010). Picton and Steer (1983) stated that the permissive $[\text{Ca}^{2+}]$ for pollen tubes extends between 10 μM to 10 mM. Because 20–30% of the newly deposited pectin will be de-esterified, there will be always an immediate need for Ca^{2+} by the growing pollen tube (Hepler and Winship, 2010). Ca^{2+} has been reported to be involved in the signal transduction pathway of boron deficiency (González-Fontes et al., 2014), which was supported by the reports that boron deficiency increased the

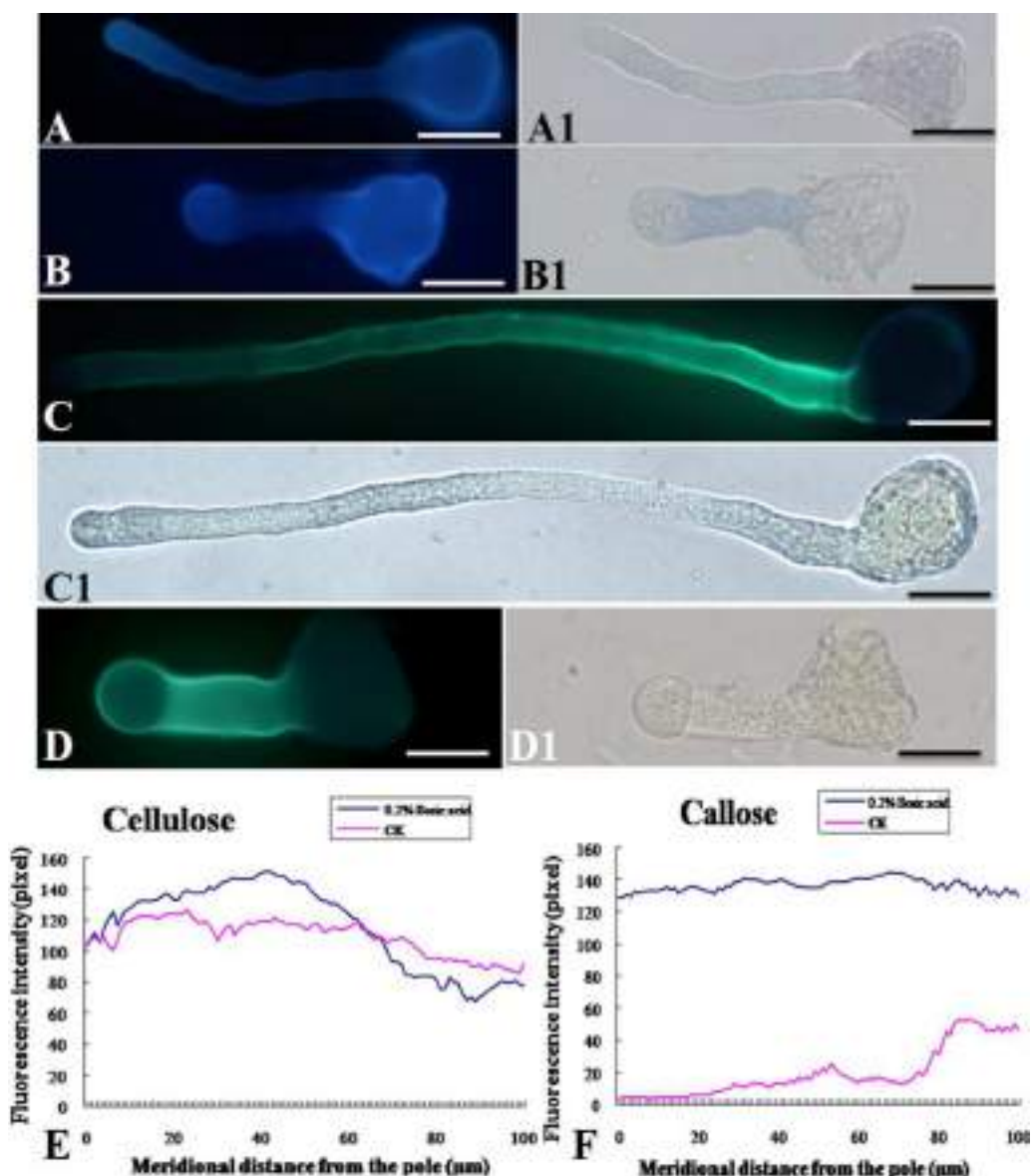


FIGURE 5 | Effect of boron toxicity on the distribution of cellulose and callose in the *Malus domestica* pollen tube. **(A)** Cellulose distributed on the whole control pollen tube indicated by fluorescence of calcofluor. **(A1)** Corresponding bright field image of A. **(B)** Boron toxicity treated pollen tube showed more cellulose at the pollen tube tip indicated by fluorescence of calcofluor. **(B1)** Corresponding bright field image of B. **(C)** Callose was distributed along the entire length of the control pollen tube except the apex. **(C1)** Corresponding bright field image of C. **(D)** Strong fluorescence was detected along the entire pollen tube treated by boron toxicity, including the apex, indicating more callose accumulation at the apex under boron toxicity. **(D1)** Corresponding bright field image of D. **(E)** Quantitative analysis of the fluorescent signal of cellulose in the wall of control pollen tubes (CK, pink line) and tubes under boron toxicity (0.2% boric acid, blue line). **(F)** Quantitative analysis of the fluorescent signal of callose in the wall of control pollen tubes (CK, pink line) and tubes under boron toxicity (0.2% boric acid, blue line). Scale bar: 25 μ m.

levels of cytosolic Ca^{2+} in tobacco BY-2 cells (Koshiba et al., 2010) and *Arabidopsis thaliana* roots (Quiles-Pando et al., 2013).

In the present study, we revealed that boron toxicity induced a decrease in $[\text{Ca}^{2+}]_c$ concentration and a disappearance of the $[\text{Ca}^{2+}]_c$ gradient, suggesting the sensitive and critical role of Ca^{2+} in boron signaling in the proposed mechanical cascade of signals which extended from cell wall to the cytoplasm via the

cell wall-plasma membrane-cytoskeleton continuum (Camacho-Cristóbal et al., 2008). Calcium is likely a major element in transmitting boron signals and modulating cytoplasmic activities. We speculate that excessive boron first binds to pectin in the wall of the pollen tube and provides many more binding sites for calcium, which results in a $[\text{Ca}^{2+}]_c$ decrease and the disappearance of the calcium gradient in the tip of the pollen tube, resulting in irregular pollen tube growth. Although

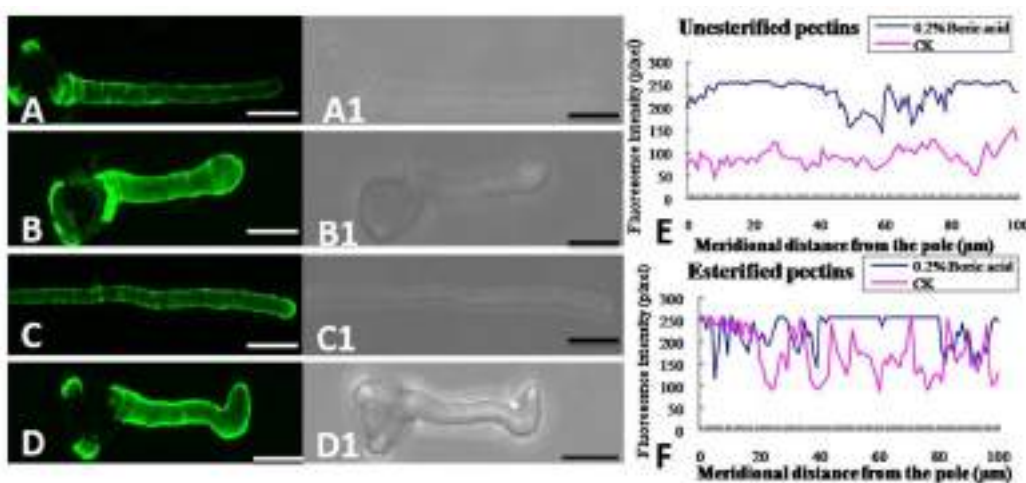


FIGURE 6 | Effect of boron toxicity on the distribution of acid and esterified pectins, respectively. **(A)** Fluorescence by JIM5 labeling of control pollen tubes with much acid pectin at the basal part and less in the apex. **(A1)** Corresponding bright field image of a. **(B)** Fluorescence indicated more acid pectins in the apex of the boron toxicity-treated pollen tube. **(B1)** Corresponding bright field image of b. **(C)** Fluorescence from JIM7 labeling of control pollen tube with much esterified pectin in the apex. **(C1)** Corresponding bright field image of c. **(D)** Fluorescence was observed evenly along the tube after antibody JIM7 labeling of pollen tubes in the presence of boron toxicity. **(D1)** Corresponding bright field image of d. **(E)** Quantitative analysis of the fluorescence signal of acid pectins in the wall of control pollen tubes (CK, pink line) and tubes under boron toxicity (0.2% boric acid, blue line). **(F)** Quantitative analysis of the fluorescence signal of esterified pectins in the wall of the control pollen tubes (CK, pink line) and tubes under boron toxicity (0.2% boric acid, blue line). Scale bar: 25 μm .

more evidence is needed to support this proposal, our results indicated that calcium might be involved in the responses to boron toxicity.

Boron Toxicity Disturbed the Actin Filaments

Boron deficiency induced alteration of cytoskeleton biosynthesis (Yu et al., 2001, 2002), suggesting that a linkage between boron and cytoskeleton may exist. Previous evidence indicates that actin filaments play an essential role in the transport of secretory vesicles and pollen tube growth (Cárdenas et al., 2008; Fu, 2015; Qu et al., 2015). In normal pollen tubes, actin filaments are reported to be arrayed in bundles and extend the subapical region (Shi and Yang, 2010). It was reported that there exists crosstalk between calcium signaling and cytoskeleton in the pollen tube, while Ca^{2+} is a central factor controlling the transition from G-actin in the tube apex to the F-actin cables in the shank (Shi and Yang, 2010). These results suggest that Ca^{2+} is critical for the actin organization in pollen tubes.

In the present research, we have revealed that actin organization is sensitive to boron toxicity. Both the specialized structure and distribution were clearly disturbed in pollen tubes under boron toxicity. This abnormal appearance of actin organization was coupled with decreased $[\text{Ca}^{2+}]_c$ and the disappearance of the $[\text{Ca}^{2+}]_c$ gradient in pollen tubes under boron toxicity. Based on the previous findings noted above, it is reasonable to speculate that actin organization abnormality might result from boron toxicity-induced low $[\text{Ca}^{2+}]_c$. It is likely that boron toxicity signaling is mediated by calcium dynamics to achieve the cytoplasmic response.

Boron Toxicity Altered the Deposition of Pollen Tube Wall Components

Boron toxicity affects the morphology of pollen tube, thus we want to know whether the tube wall composition was affected by boron toxicity. Results showed that cellulose was present throughout the pollen tube wall under normal conditions and under boron toxicity. Boron toxicity showed no obvious effect on the cellulose deposition of the pollen tube. Callose can be synthesized in the normal pollen tube walls (Qin et al., 2012). In addition, callose is distributed at the tips of abnormal pollen tubes (Hao et al., 2013). Our results showed that boron toxicity altered the deposition pattern of the callose in the pollen tube walls of *Malus domestica*. In the control pollen tube, callose was detected along the entire pollen tube except for the tip, but in the presence of boron toxicity, callose was distributed along the entire tube including the tip.

Beside cellulose and callose, pectin is an important composition of the pollen tube wall. Pectin is secreted mainly as methoxy-esters, and later de-esterified by the enzyme pectin methyl esterase (PME) (Bosch and Hepler, 2005; Peaucelle et al., 2012). Plant cell wall also contains essential minerals including calcium and boron, which are necessary for formation of networks of pectic polysaccharides in cell walls. The extent and strength of Ca^{2+} cross-linking depend on the acidic residue of the de-esterified pectins (Hepler and Winship, 2010). Research by Fang et al. (2008) illustrated that pectin associates with carboxyl moieties which participate in binding with free Ca^{2+} to form plastic gels. Ngouémazong et al. (2012) reported that at high $[\text{Ca}^{2+}]$, with a low degree of methoxylation, pectins reach maximum strength. According to the previous studies, pollen tube growth is speculated to depend on a balance between the

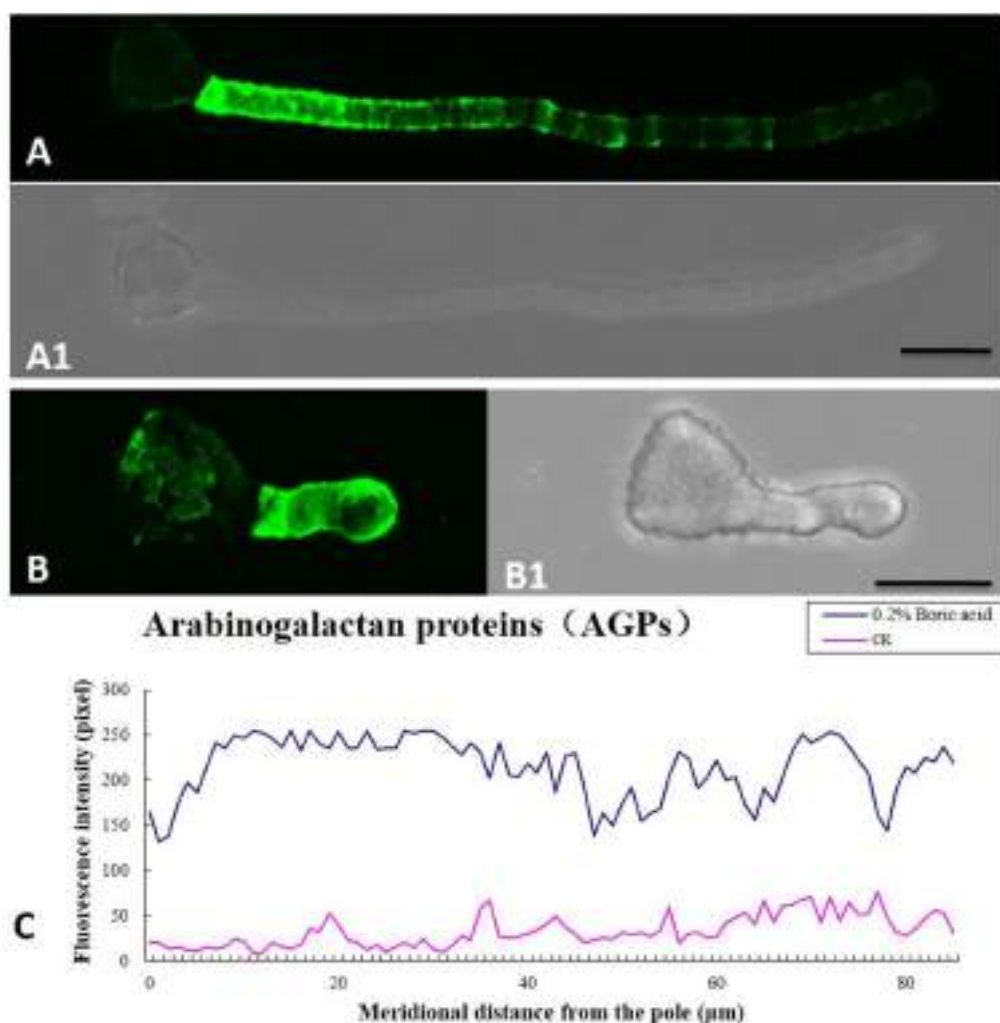


FIGURE 7 | Influence of boron toxicity on the distribution of arabinogalactan proteins (AGPs) in *Malus domestica* pollen tubes. (A) Fluorescence after antibody LM2 labeling of pollen tubes cultured in normal medium, indicating more AGPs in the basal part and decreasing levels from the base to the pollen tip. **(A1)** Corresponding bright field image of **(A)**. **(B)** Fluorescence was observed throughout the entire tube; note the irregular distribution. **(B1)** Corresponding bright field image of **(B)**. **(C)** Quantitative analysis of fluorescence signal of AGPs in the wall of control pollen tubes (CK, pink line) and boron toxicity-treated tubes (0.2% boric acid, blue line). Scale bar: 25 μ m.

number of available acidic residues and the $[Ca^{2+}]$. That is too few acidic groups or too little Ca^{2+} will lead to the pollen tube burst, but too many acidic groups and/or too much Ca^{2+} will result in overly cross-linked wall and therefore pollen tube can't extend (Hepler and Winship, 2010). Our immunolabeling results showed that in the boron toxicity-treated pollen tube, there was more acidic pectin, which could create more binding sites for calcium and thus result in less calcium ion in the cytoplasm. Therefore, the ratio of de-esterified pectin to esterified pectin plays a critical role in the adjustment of the cytoplasmic calcium level and in the transmission of boron toxicity-induced effects on pollen tube growth.

Arabinogalactan proteins are proteins which exist in plant and distribute through different developmental stages (Pereira et al., 2014). AGPs can interact with pectins or other

cell wall-localized proteins (Baldwin et al., 1993; Showalter, 2001). Recent researches have enhanced our understanding of AGPs' role in plant (Lampert and Várnai, 2013; Lampert et al., 2014). AGPs may play an essential role in the boron deficiency signal transduction by binding Ca^{2+} (González-Fontes et al., 2014). In the present study, AGPs were deposited by LM2, indicating that boron toxicity caused AGPs to accumulate throughout the pollen tube except the basal part near the grain, instead of the characteristic periodic ring-like deposits with less signal at the tip. Boron toxicity changed the distribution pattern and quantity of AGPs, which may interlink with calcium and actin alteration. More AGPs might bind to more calcium and result in low $[Ca^{2+}]_c$. These findings indicated that boron toxicity induced reconstruct of tip cell wall components, resulting in cell

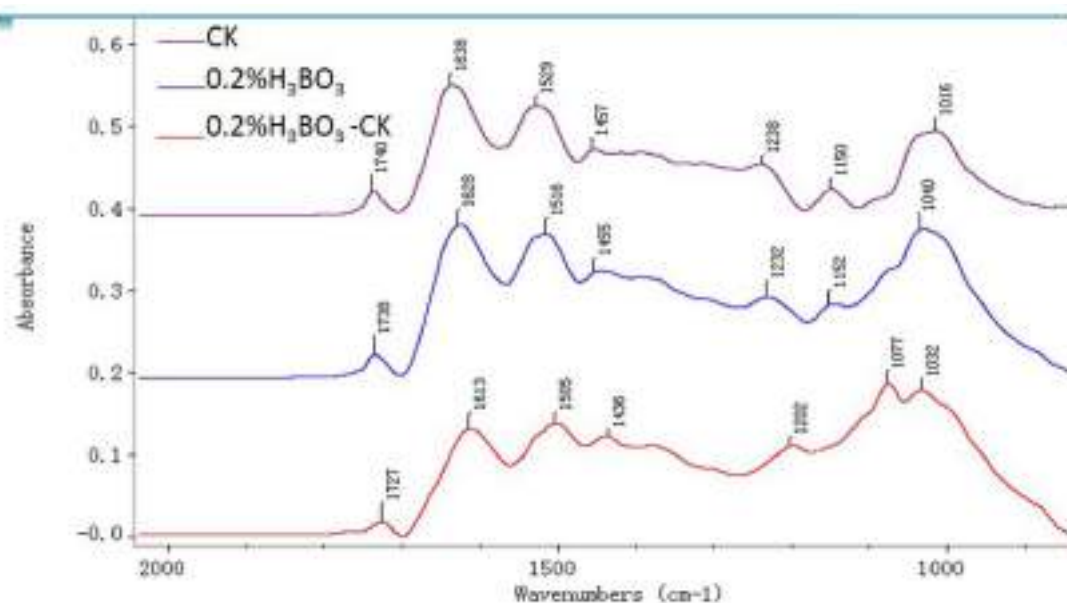


FIGURE 8 | Fourier-transform infrared analysis spectra from the tip regions of *Malus domestica* pollen tubes (control pollen tube: CK; pink), pollen tubes treated with 0.2% boric acid medium (blue, 0.2% H_3BO_3) and the FTIR differential spectrum (red) generated by digital subtraction of the pink spectra (CK) from the blue spectra (0.2% H_3BO_3).

wall rigidity/extensibility changes and subsequent slowing and cessation of growth.

It can be expected that boron toxicity alters the cell wall structure, and a rapid change in the mechanical strength of the cell wall occurs. This effect triggers a mechanical cascade of signals through the cell wall-plasma membrane-cytoskeleton continuum, in which AGPs most likely take an active part (Goldbach and Wimmer, 2007). This expectation agrees with the structural modification of the cell wall pectin and cytoskeleton under boron toxicity in this research.

Boron toxicity is an important agricultural problem that limits crop productivity, however, under boron stress condition, how much boron could accumulate in style and directly regulate pollen tube growth remains unknown. Therefore, *in vitro* test the influence of the high boron on pollen tube growth will provide useful clue to understand possible response of pollen tube to the stress.

In the low rainfall and on highly alkaline and saline soil where the rate of boron is over 2.0 mg/L, there is boron pollution and consequently decreases in production and defect in the products can be seen (Ozturk et al., 2010). When boron is present at high concentrations in the soil or ground water, plant growth, and reproduction can be affected by boron toxicity (Roessner et al., 2006). So boron toxicity has been recognized as an important problem limiting crop production. Following long-term exposure to high B concentrations, overall vegetative plant growth is retarded and this leads to either a reduction in or a complete lack of seed set (Roessner et al., 2006).

Application of boron fertilizer in soil and boron foliar application appear worthwhile in the field. Both of the methods increased the boron concentration in various parts of the plant

(Asad et al., 2003). There are no data on boron concentration in style and how much boron pollen tube could absorb from style so far. However, based on the previous study mentioned above, the concentration of boron in style increases if the plant grows under high boron. Whether the boron concentrations used in the present study is similar to the *in vivo* values need further research.

Our *in vitro* test illustrated that 0.2% boron inhibited *Malus domestica* pollen germination and arrested pollen tube growth. Based on this, if boron foliar application or boron in the soil at high concentrations leads to similar boron concentration in style, it will be harmful to pollen tube growth.

In brief, our investigation of the effects of boron toxicity on *Malus domestica* pollen tubes provides an extensive understanding of the role of boron in the polarized tip growth of pollen tubes. We found that boron toxicity decreases $[\text{Ca}^{2+}]_c$, inducing the disappearance of the $[\text{Ca}^{2+}]_c$ gradient and altering actin filament organization. The distorted actin filament may disturb transport of the wall precursor to the pollen tube wall, resulting in defects in cell wall construction and variations in pollen tube tip growth. This research provides new insights into the boron function in pollen tube growth and valuable evidence for the previous proposal that boron may lead to a mechanical cascade of signals from the wall to the cytoplasm through the cell wall-plasma membrane-cytoskeleton continuum.

AUTHOR CONTRIBUTIONS

The authors have made the following declarations regarding their contributions: Conceived and designed the experiments: KF. Performed the experiments: WZ, KF. Analyzed the data: KF,

WZ, YX, QZ, LY, and LQ. Contributed to the writing of the manuscript: KF, WZ, YX, QC, and LQ.

ACKNOWLEDGMENTS

This work was supported by the National Natural Science Foundation of China (31270719), the Importation and Development of High-Caliber Talents Project of Beijing Municipal Institutions (CIT&TCD201304095) and the Project of Construction of Innovative Teams and Teacher Career Development for Universities and Colleges under Beijing

Municipality (IDHT20140509). The authors thank AE for English editing.

SUPPLEMENTARY MATERIAL

The Supplementary Material for this article can be found online at: <http://journal.frontiersin.org/article/10.3389/fpls.2016.00208>

FIGURE S1 | (a) Weak fluorescence was detected at the apex of the pollen tube under boron toxicity for 1.5 h, no Ca^{2+} gradient was visible. **(b)** The actin deposition varied upon treatment with high boron for 1.5 h.

REFERENCES

- Aquea, F., Federici, F., Moscoso, C., Vega, A., Jullian, P., Haseloff, J., et al. (2012). A molecular framework for the inhibition of *Arabidopsis* root growth in response to boron stress. *Plant Cell Environ.* 35, 719–734. doi: 10.1111/j.1365-3040.2011.02446.x
- Asad, A., Blamey, F. P. C., and Edwards, D. G. (2003). Effect of Boron foliar applications on vegetative and reproductive growth of sunflower. *Ann. Bot.* 92, 565–570. doi: 10.1093/aob/mcg179
- Baldwin, T. C., McCann, M. C., and Roberts, K. (1993). A novel hydroxyproline deficient arabinogalactan protein secreted by suspension-cultured cells of *Daucus carota*. (purification and partial characterization). *Plant Physiol.* 103, 115–123. doi: 10.1104/pp.103.1.115
- Baluška, F., Šamaj, J., Wojtaszek, P., Volkmann, D., and Menzel, D. (2003). Cytoskeleton – plasma membrane – cell wall continuum in plants: emerging links revisited. *Plant Physiol.* 133, 482–491. doi: 10.1104/pp.103.027250
- Blevins, D. G., and Lukaszewski, K. (1998). Boron in plant structure and function. *Annu. Rev. Plant Physiol. Plant Mol. Biol.* 49, 481–500. doi: 10.1146/annurev.arplant.49.1.481
- Bosch, M., and Hepler, P. K. (2005). Pectin methylesterases and pectin dynamics in pollen tubes. *Plant Cell* 17, 3219–3226. doi: 10.1105/tpc.105.037473
- Bou, D. F., and Geitmann, A. (2011). Actin is involved in pollen tube tropism through redefining the spatial targeting of secretory vesicles. *Traffic* 12, 1537–1551. doi: 10.1111/j.1600-0854.2011.01256.x
- Braccini, I., and Perez, S. (2001). Molecular basis of Ca^{2+} induced gelation in alginates and pectins: the egg-box model revisited. *Biomacromolecules* 2, 1089–1096. doi: 10.1021/bm010008g
- Camacho-Cristóbal, J. J., Rexach, J., and González-Fontes, A. (2008). Boron in Plants: deficiency and toxicity. *J. Int. Plant Biol.* 50, 1247–1255. doi: 10.1111/j.1744-7909.2008.00742.x
- Cañón, P., Aquea, F., Rodríguez-Hoces de la Guardia, A., and Arce-Johnson, P. (2013). Functional characterization of *Citrus macrophylla* BOR1 as a boron transporter. *Physiol. Plant* 149, 329–339. doi: 10.1111/ppl.12037
- Cárdenas, L., Lovy-Wheeler, A., Kunkel, J. G., and Hepler, P. K. (2008). Pollen tube growth oscillations and intracellular calcium levels are reversibly modulated by actin polymerization. *Plant Physiol.* 146, 1611–1621. doi: 10.1104/pp.107.113035
- Cervilla, L. M., Blasco, B., Ríos, J. J., Romero, L., and Ruiz, J. M. (2007). Oxidative stress and antioxidants in tomato (*Solanum lycopersicum*) plants subjected to boron toxicity. *Ann. Bot.* 100, 747–756. doi: 10.1093/aob/mcm156
- Chebli, Y., Pujol, L., Shoaib, A., Brouwer, I., van Loon, J. J., and Geitmann, A. (2013). Cell wall assembly and intracellular trafficking in plant cells are directly affected by changes in the magnitude of gravitational acceleration. *PLoS ONE* 8:e58246. doi: 10.1371/journal.pone.0058246
- Chen, T., Teng, N. J., Wu, X. Q., Wang, Y. H., Tang, W., Šamaj, J., et al. (2007). Disruption of actin filaments by latrunculin B affects cell wall construction in *Picea meyeri* pollen tube by disturbing vesicle trafficking. *Plant Cell Physiol.* 48, 19–30. doi: 10.1093/pcp/pcl036
- Dafni, A. (2000). A new procedure to assess pollen viability. *Sex. Plant Reprod.* 12, 241–244. doi: 10.1007/s004970050008
- Dickinson, D. B. (1978). Influence of borate and pentaerythritol concentration on germination and tube growth of *Lilium longiflorum* pollen. *J. Am. Soc. Hortic. Sci.* 103, 263–269.
- Dumont, M., Lehner, A., Bouton, S., Kiefer-Meyer, M. C., Voyer, A., Pelloux, J., et al. (2014). The cell wall pectic polymer rhamnogalacturonan-II is required for proper pollen tube elongation: implications of a putative sialyltransferase-like protein. *Ann. Bot.* 114, 1177–1188. doi: 10.1093/aob/mcu093
- Fang, Y., Al-Assaf, S., Phillips, G. O., Nishinari, K., Funami, T., and Williams, P. A. (2008). Binding behavior of calcium to polyuronates: comparison of pectin with alginate. *Carbohydr. Polym.* 72, 334–341. doi: 10.1016/j.carbpol.2007.08.021
- Ferguson, C., Teeri, T. T., Siika-aho, M., Read, S. M., and Bacic, A. (1998). Location of cellulose and callose in pollen tubes and grains of *Nicotiana tabacum*. *Planta* 206, 452–460. doi: 10.1007/s004250050421
- Franklin-Tong, V. E. (1999). Signaling and the modulation of pollen tube growth. *Plant Cell* 11, 727–738. doi: 10.1105/tpc.11.4.727
- Fu, Y. (2015). The cytoskeleton in the pollen tube. *Curr. Opin. Plant Biol.* 6, 111–119. doi: 10.1016/j.pbi.2015.10.004
- Funakawa, H., and Miwa, K. (2015). Synthesis of borate cross-linked rhamnogalacturonan II. *Front. Plant Sci.* 6:223. doi: 10.3389/fpls.2015.00223
- Gao, S., Wang, J. L., Wang, J. J., Cao, Q. Q., Qin, L., and Fang, K. F. (2014). Comparison analysis of mineral elements composition on four pollens. *J. Agricul* 4, 77–80.
- Geitmann, A. (1999). “The rheological properties of the pollen tube cell wall,” in *Fertilization in Higher Plants*, eds M. Cresti, G. Cai, and A. Moscatelli (Berlin: Springer), 283–297.
- Goldbach, H. E., and Wimmer, M. A. (2007). Boron in plants and animals: is there a role beyond cell-wall structure? *J. Plant Nutr. Soil Sci.* 170, 39–48. doi: 10.1002/jpln.200625161
- González-Fontes, A., Navarro-Gochicoa, M. T., Camacho-Cristóbal, J. J., Herrera-Rodríguez, M. B., Quiles-Pando, C., and Rexach, J. (2014). Is Ca^{2+} involved in the signal transduction pathway of boron deficiency? New hypotheses for sensing boron deprivation. *Plant Sci.* 217–218, 135–139. doi: 10.1016/j.plantsci.2013.12.011
- Gunes, A., Soylemezoglu, G., Inal, A., Bagci, E. G., Coban, S., and Sahin, O. (2006). Antioxidant and stomatal responses of grapevine (*Vitis vinifera* L.) to boron toxicity. *Sci. Horticul.* 110, 279–284. doi: 10.1016/j.scienta.2006.07.014
- Guo, P., Qi, Y. P., Yang, L. T., Ye, X., Jiang, H. X., Huang, J. H., et al. (2014). cDNA-AFLP analysis reveals the adaptive responses of citrus to long-term boron-stress. *BMC Plant Biol.* 14:284. doi: 10.1186/s12870-014-0284-5
- Hao, H. Q., Chen, T., Fan, L., Li, R. L., and Wang, X. H. (2013). 2, 6-dichlorobenzonitrile causes multiple effects on pollen tube growth beyond altering cellulose synthesis in *Pinus bungeana* Zucc. *PLoS ONE* 8:e76660. doi: 10.1371/journal.pone.0076660
- Hasegawa, Y., Nakamura, S., Kakizoe, S., Sato, M., and Nakamura, N. (1998). Immunocytochemical and chemical analyses of Golgi vesicles isolated from the germinated pollen of *Camellia japonica*. *J. Plant Res.* 111, 421–429. doi: 10.1023/A:1010662911148
- Hepler, P. K. (2005). Calcium: a central regulator of plant growth and development. *Plant Cell* 17, 2142–2155. doi: 10.1105/tpc.105.032508

- Hepler, P. K., and Winship, L. J. (2010). Calcium at the cell wall-cytoplasm interface. *J. Int. Plant Biol.* 52, 147–160. doi: 10.1111/j.1744-7909.2010.00923.x
- Holdaway-Clarke, T. L., and Hepler, P. K. (2003). Control of pollen tube growth: role of ion gradients and fluxes. *New Phytol.* 159, 539–563. doi: 10.1016/j.bbamcr.2012.10.009
- Karabal, E., Yücel, M., and Ökçe, H. A. (2003). Antioxidants responses of tolerant and sensitive barley cultivars to boron toxicity. *Plant Sci.* 164, 925–933. doi: 10.1016/S0168-9452(03)00067-0
- Keles, Y., Öncel, I., and Yenice, N. (2004). Relationship between boron content and antioxidant compounds in Citrus leaves taken from fields with different water source. *Plant Soil* 265, 345–353. doi: 10.1007/s11104-005-0646-8
- Ketelaar, T., Galway, M. E., Mulder, B. M., and Emons, A. M. (2008). Rates of exocytosis and endocytosis in *Arabidopsis* root hairs and pollen tubes. *J. Microsci.* 231, 265–273. doi: 10.1111/j.1365-2818.2008.02031.x
- Koshiba, T., Kobayashi, M., Ishihara, A., and Matoh, T. (2010). Boron nutrition of cultured tobacco BY-2 cells. VI. Calcium is involved in early responses to boron deprivation. *Plant Cell Physiol.* 51, 323–327. doi: 10.1093/pcp/pcp179
- Lampert, D. T. A., and Várnai, P. (2013). Periplasmic arabinogalactan glycoproteins act as a calcium capacitor that regulates plant growth and development. *New Phytol.* 197, 58–64. doi: 10.1111/nph.12005
- Lampert, D. T. A., Várnai, P., and Seal, C. E. (2014). Back to the future with the AGP-Ca²⁺ flux capacitor. *Ann. Bot.* 114, 1069–1085. doi: 10.1093/aob/mcu161
- Landi, M., Remorini, D., Pardossi, A., and Guidi, L. (2013). Boron excess affects photosynthesis and antioxidant apparatus of greenhouse *Cucurbita pepo* and *Cucumis sativus*. *J. Plant Res.* 126, 775–786. doi: 10.1007/s10265-013-0575-1
- Lazzaro, M. D., Donohue, J. M., and Soodavar, F. M. (2003). Disruption of cellulose synthesis by isoxaben causes tip swelling and disorganizes cortical microtubules in elongating conifer pollen tubes. *Protoplasma* 220, 201–207. doi: 10.1007/s00709-002-0042-7
- Li, Y. Q., Mareck, A., Faleri, C., Moscatelli, A., Liu, Q., and Cresti, M. (2002). Detection and localization of pectin methylesterase isoforms in pollen tubes of *Nicotiana tabacum* L. *Planta* 214, 734–740. doi: 10.1007/s004250100664
- Li, Y. Q., Zhang, H. Q., Pierson, E. S., Huang, F. Y., Linskens, H. F., Hepler, P. K., et al. (1996). Enforced growth-rate fluctuation causes pectin ring formation in the cell wall of *Lilium longiflorum* pollen tubes. *Planta* 200, 41–49. doi: 10.1007/BF00196647
- Loomis, W. D., and Durst, R. W. (1992). Chemistry and biology of boron. *Biofactors* 3, 229–239.
- Miwa, K., Takano, J., Omori, H., Seki, M., Shinozaki, K., and Fujiwara, T. (2007). Plants tolerant of high boron levels. *Science* 318:1417. doi: 10.1126/science.1146634
- Molassiotis, A., Sotiropoulos, T. E., Tanou, G., Diamantidis, G., and Therios, I. (2006). Boron induced oxidative damage and antioxidant and nucleolytic responses in shoot tips culture of the apple rootstock EM9 (*Malus domestica* Borkh). *Environ. Exp. Bot.* 56, 54–62. doi: 10.1016/j.envexpbot.2005.01.002
- Moscatelli, A., and Idilli, A. I. (2009). Pollen tube growth: a delicate equilibrium between secretory and endocytic pathways. *J. Integr. Plant Biol.* 51, 727–739. doi: 10.1111/j.1744-7909.2009.00842.x
- Nable, O. R., Bañuelos, G. S., and Paull, J. G. (1997). Boron toxicity. *Plant Soil* 193, 181–198. doi: 10.1023/A:1004272227886
- Nable, O. R., Lance, R. C. M., and Cartwright, B. (1990). Uptake of boron and silicon by barley genotypes with differing susceptibilities to boron toxicity. *Ann. Bot. (Lond)* 66, 83–90.
- Ngouémazong, D. E., Jolie, R. P., Cardinaels, R., Fraeye, I., Van Loey, A., Moldenaers, P., et al. (2012). Stiffness of Ca²⁺-pectin gels: combined effects of degree and pattern of methylesterification for various Ca²⁺ concentrations. *Carbohydr. Res.* 348, 69–76. doi: 10.1016/j.carres.2011.11.011
- Obermeyer, G., Kriechbaumer, R., Strasser, D., Maschessning, A., and Bentrup, F. W. (1996). Boric acid stimulates the plasma membrane H⁺-ATPase of ungerminated lily pollen grains. *Physiol. Plant* 98, 281–290. doi: 10.1034/j.1399-3054.1996.980209.x
- Ozturk, M., Sakcali, S., Gucel, S., and Rombuloglu, H. (2010). “Boron and plants,” in *Plant Adaptation and Phytoremediation*, eds M. Ashrat, M. Ozturk, and M. S. A. Ahmad (Berlin: Springer), 275–311.
- Pang, Y., Li, L., Ren, F., Lu, P., Wei, P., Cai, J., et al. (2010). Overexpression of the tonoplast aquaporin AtTIP5;1 conferred tolerance to boron toxicity in *Arabidopsis*. *J. Genet. Genomics* 37, 389–397. doi: 10.1016/S1673-8527(09)60057-6
- Paull, J. G., Nable, R. O., and Rathjen, A. J. (1992). Physiological and genetic control of the tolerance of wheat to high concentrations of boron and implications for plant breeding. *Plant Soil* 146, 251–260. doi: 10.1007/BF00012019
- Peaucelle, A., Braybrook, S., and Höfte, H. (2012). Cell wall mechanics and growth control in plants: the role of pectins revisited. *Front. Plant Sci.* 3:121. doi: 10.3389/fpls.2012.00121
- Pereira, A. M., Masiero, S., Nobre, M. S., Costa, M. L., Solís, M. T., Testillano, P. S., et al. (2014). Differential expression patterns of arabinogalactan proteins in *Arabidopsis thaliana* reproductive tissues. *J. Exp. Bot.* 65, 5459–5471. doi: 10.1093/jxb/eru300
- Pérez-Castro, R., Kasai, K., Gainza-Cortés, F., Ruiz-Lara, S., Casaretto, J. A., Peña-Cortés, H., et al. (2012). VvBOR1, the grapevine ortholog of AtBOR1, encodes an efflux boron transporter that is differentially expressed throughout reproductive development of *Vitis vinifera* L. *Plant Cell Physiol.* 53, 485–494. doi: 10.1093/pcp/pcs001
- Picton, J. M., and Steer, M. W. (1983). Evidence for the role of Ca²⁺ ions in tip extension in pollen tubes. *Protoplasma* 115, 11–17. doi: 10.1007/BF01293575
- Qin, P., Ting, D., Shieh, A., and McCormick, S. (2012). Callose plug deposition patterns vary in pollen tubes of *Arabidopsis thaliana* ecotypes and tomato species. *BMC Plant Biol.* 12:178. doi: 10.1186/1471-2229-12-178
- Qu, X. L., Jiang, Y. X., Chang, M., Liu, X. N., Zhang, R. H., and Huang, S. J. (2015). Organization and regulation of the actin cytoskeleton in the pollen tube. *Front. Plant Sci.* 5:786. doi: 10.3389/fpls.2014.00786
- Quiles-Pando, C., Rexach, J., Navarro-Gochicoa, M. T., Camacho-Cristóbal, J. J., Herrera-Rodríguez, M. B., and González-Fontes, A. (2013). Boron deficiency increases the levels of cytosolic Ca²⁺ and expression of Ca²⁺-related genes in *Arabidopsis thaliana* roots. *Plant Physiol. Biochem.* 65, 55–60. doi: 10.1016/j.plaphy.2013.01.004
- Reid, R. (2007). Identification of boron transporter genes likely to be responsible for tolerance to boron toxicity in wheat and barley. *Plant Cell Physiol.* 48, 1673–1678. doi: 10.1093/pcp/pcm159
- Roessner, U., Patterson, J. H., Forbes, M. G., Fincher, G. B., Langridge, P., and Bacic, A. (2006). An investigation of boron toxicity in barley using metabolomics. *Plant Physiol.* 142, 1087–1101. doi: 10.1104/pp.106.04053
- Ruiz, J. M., Rivero, R. M., and Romero, L. (2003). Preliminary studies on the involvement of biosynthesis of cysteine and glutathione concentration in the resistance to B toxicity in sunflower plants. *Plant Sci.* 165, 811–817. doi: 10.1016/S0168-9452(03)00276-0
- Sakamoto, T., Inui, Y. T., Uraguchi, S., Yoshizumi, T., Matsumaga, S., Mastui, M., et al. (2011). Condensin II alleviates DNA damage and is essential for tolerance of boron overload stress in *Arabidopsis*. *Plant Cell* 23, 3533–3546. doi: 10.1105/tpc.111.086314
- Shi, D. Q., and Yang, W. C. (2010). “Pollen germination and tube growth,” in *Plant Developmental Biology – Biotechnological Perspectives*, eds E. C. Pua and M. R. Davey (Berlin: Springer), 245–282.
- Showalter, A. M. (2001). Arabinogalactan-proteins: structure, expression and function. *Cell. Mol. Life Sci.* 58, 1399–1417. doi: 10.1007/PL000000784
- Sotiropoulos, T. E., Molassiotis, A., Almaliotis, D., Mouhtaridou, G., Dimassi, K., Therios, I., et al. (2006). Growth, nutritional status, chlorophyll content, and antioxidant responses of the apple rootstock MM 111 shoots cultured under high boron concentrations in vitro. *J. Plant Nutr.* 29, 575–583. doi: 10.1080/01904160500526956
- Sutton, T., Baumann, U., Hayes, J., Collins, N. C., Shi, B. J., Schnurbusch, T., et al. (2007). Boron-toxicity tolerance in barley arising from efflux transporter amplification. *Science* 30, 1446–1449. doi: 10.1126/science.1146853
- Taylor, L. P., and Hepler, P. K. (1997). Pollen germination and tube growth. *Annu. Rev. Plant Physiol. Plant Mol. Biol.* 48, 461–491. doi: 10.1146/annurev.applant.48.1.461

- Tenhaken, R. (2014). Cell wall remodeling under abiotic stress. *Front. Plant Sci.* 5:771. doi: 10.3389/fpls.2014.00771
- Voxeur, A. A., and Fry, S. C. (2014). Glycosylinositol phosphorylceramides from Rosa cell cultures are boron-bridged in the plasma membrane and form complexes with rhamnogalacturonan II. *Plant J.* 79, 139–149. doi: 10.1111/tpj.12547
- Wang, M. J., Wang, Y., Sun, J., Ding, M. Q., Deng, S. R., Hou, P. C., et al. (2013). Overexpression of PeHA1 enhances hydrogen peroxide signaling in salt-stressed *Arabidopsis*. *Plant Physiol. Biochem.* 71, 37–48. doi: 10.1016/j.plaphy.2013.06.020
- Wolf, S., and Greiner, S. (2012). Growth control by cell wall pectins. *Protoplasma* 249, 169–175. doi: 10.1007/s00709-011-0371-5
- Yu, Q., Baluska, F., Jasper, F., Menzel, D., and Goldbach, H. E. (2003). Short term boron deprivation enhances levels of cytoskeletal proteins in maize, but not zucchini, root apices. *Physiol. Plant* 117, 270–278. doi: 10.1034/j.1399-3054.2003.00029.x
- Yu, Q., Hlavacka, A., Matoh, T., Volkmann, D., Menzel, D., Goldbach, H. E., et al. (2002). Short-term boron deprivation inhibits endocytosis of cell wall pectins in meristematic cells of maize and wheat root apices. *Plant Physiol.* 130, 415–421. doi: 10.1104/pp.006163
- Yu, Q., Wingender, R., Schulz, M., Baluska, F., and Goldbach, H. (2001). Short-term boron deprivation induces increased levels of cytoskeletal proteins in *Arabidopsis* roots. *Plant Biol.* 3, 335–340. doi: 10.1007/0-306-47624-X_77
- Zhang, W. H., and Renzel, Z. (1998). Determination of intracellular Ca²⁺ in cells of intact wheat root: loading of acetoxymethyl ester of Fluo-3 under low temperature. *Plant J.* 15, 147–151. doi: 10.1046/j.1365-313X.1998.0188.x
- Zhang, Y., He, J., Lee, D., and McCormick, S. (2010). Interdependence of endomembrane trafficking and actin dynamics during polarized growth of *Arabidopsis* pollen tubes. *Plant Physiol.* 152, 2200–2210. doi: 10.1104/pp.109.142349

Conflict of Interest Statement: The authors declare that the research was conducted in the absence of any commercial or financial relationships that could be construed as a potential conflict of interest.

Copyright © 2016 Fang, Zhang, Xing, Zhang, Yang, Cao and Qin. This is an open-access article distributed under the terms of the Creative Commons Attribution License (CC BY). The use, distribution or reproduction in other forums is permitted, provided the original author(s) or licensor are credited and that the original publication in this journal is cited, in accordance with accepted academic practice. No use, distribution or reproduction is permitted which does not comply with these terms.



Pronounced Phenotypic Changes in Transgenic Tobacco Plants Overexpressing Sucrose Synthase May Reveal a Novel Sugar Signaling Pathway

Quynh Anh Nguyen¹, Sheng Luan², Seung G. Wi³, Hanhong Bae⁴, Dae-Seok Lee³ and Hyeun-Jong Bae^{1,3*}

¹ Department of Bioenergy Science and Technology, Chonnam National University, Gwangju, South Korea, ² Department of Plant and Microbial Biology, University of California, Berkeley, Berkeley, CA, USA, ³ Bio-Energy Research Center, Chonnam National University, Gwangju, South Korea, ⁴ School of Biotechnology, Yeungnam University, Gyeongsan, South Korea

OPEN ACCESS

Edited by:

Sylvain Jeandroz,
Agrosup Dijon, France

Reviewed by:

Clay Carter,
University of Minnesota Twin Cities,
USA

Axel Tiessen,

Centro de Investigación y de Estudios
Avanzados del Instituto Politécnico
Nacional, Mexico

*Correspondence:

Hyeun-Jong Bae
baehj@chonnam.ac.kr

Specialty section:

This article was submitted to
Plant Physiology,
a section of the journal
Frontiers in Plant Science

Received: 18 September 2015

Accepted: 17 December 2015

Published: 11 January 2016

Citation:

Nguyen QA, Luan S, Wi SG, Bae H,
Lee D-S and Bae H-J (2016)
Pronounced Phenotypic Changes in
Transgenic Tobacco Plants
Overexpressing Sucrose Synthase
May Reveal a Novel Sugar Signaling
Pathway. *Front. Plant Sci.* 6:1216.
doi: 10.3389/fpls.2015.01216

Soluble sugars not only serve as nutrients, but also act as signals for plant growth and development, but how sugar signals are perceived and translated into physiological responses in plants remains unclear. We manipulated sugar levels in transgenic plants by overexpressing sucrose synthase (SuSy), which is a key enzyme believed to have reversible sucrose synthesis and sucrose degradation functions. The ectopically expressed SuSy protein exhibited sucrose-degrading activity, which may change the flux of sucrose demand from photosynthetic to non-photosynthetic cells, and trigger an unknown sucrose signaling pathway that lead to increased sucrose content in the transgenic plants. An experiment on the transition from heterotrophic to autotrophic growth demonstrated the existence of a novel sucrose signaling pathway, which stimulated photosynthesis, and enhanced photosynthetic synthesis of sucrose, which was the direct cause or the sucrose increase. In addition, a light/dark time treatment experiment, using different day length ranges for photosynthesis/respiration showed the carbohydrate pattern within a 24-h day and consolidated the role of sucrose signaling pathway as a way to maintain sucrose demand, and indicated the relationships between increased sucrose and upregulation of genes controlling development of the shoot apical meristem (SAM). As a result, transgenic plants featured a higher biomass and a shorter time required to switch to reproduction compared to those of control plants, indicating altered phyllotaxis and more rapid advancement of developmental stages in the transgenic plants.

Keywords: sucrose synthase, sucrose-degrading SuSy activity, endogenous sucrose, enhanced photosynthesis, shoot apical meristems, WUSCHEL, CycD cyclin, sucrose signaling pathway

INTRODUCTION

The transition from heterotrophic to autotrophic growth is one of the most important processes during the plant life cycle, as plants survive and develop independently from the quantities of carbohydrate and nutrients that accumulate in seeds (Koornneef et al., 2002; Finch-Savage and Leubner-Metzger, 2006). Light-induced biomass production during autotrophic

growth occurs through chlorophyll in chloroplasts to produce photosynthetically fixed carbon compounds (such as triose phosphates—TP), which are later released into the cytosol (Bédard and Jarvis, 2005; Philipp et al., 2007). Sucrose is a primary sugar synthesized mainly from TP through the catalytic action of sucrose-phosphate synthase (SPS) and sucrose-phosphatase (SPP) in the cytosol. As a disaccharide formed by the combination of a glucosyl and fructosyl moiety, sucrose is a major transport carbohydrate, transported from photosynthetic to non-photosynthetic cells (Geigenberger and Stitt, 2000; Salerno and Curatti, 2003; Rolland et al., 2006; Wind et al., 2010). Thus, sucrose acts as the primary energy source and as a plant growth and development signal (Eveland and Jackson, 2012; Lastdrager et al., 2014). However, only invertase (INV; IC 3.2.1.16) and sucrose synthase (SuSy; IC 2.4.1.13), have sucrose-catalyzing ability in plants. It is generally believed that INV hydrolyzes sucrose to glucose and fructose in the cell wall, vacuolar, and cytosolic fractions, whereas SuSy is localized in sink tissues and has reversible functions of both sucrose synthesis and degradation (Geigenberger and Stitt, 1991, 1993; Fernie et al., 2002; Koch, 2004; Rolland et al., 2006; Bieniawska et al., 2007; Angeles-Núñez and Tiessen, 2012; Eveland and Jackson, 2012). The structure of At.SuSy1 provides insight into its functions (Zheng et al., 2011), but it is unclear how SuSy actually affects sucrose metabolism.

Sucrose is a major photosynthetic product that is actively transported by the phloem and affects cell growth and division; thus, sucrose has a pivotal role in plant growth and development. Plant growth is a highly energy-demanding process that requires optimal sugar balance, particularly that of sucrose, between photosynthetic and non-photosynthetic cells. Numerous sugar signaling pathways have been identified which involve in the maintaining the balance between the sugar production and consumption, which helps avoid energy stress (Tiessen and Padilla-Chacon, 2013; Lastdrager et al., 2014). Starch regulates sugar status through biosynthesis and degradation during day and night, respectively (Chourey et al., 1998; Smith and Stitt, 2007; Angeles-Núñez and Tiessen, 2010; Graf and Smith, 2011; Farré and Weise, 2012). A relationship between sugar status and cell growth and development has been demonstrated in *Arabidopsis* via the SnRKs and TOR signaling pathways. SnRK1 is activated when plants have low sugar status (Chiou and Bush, 1998; Halford et al., 2003; Rolland et al., 2006; Coello et al., 2011), whereas TOR is activated in the presence of high levels of sucrose (Deprost et al., 2007; Robaglia et al., 2012; Lastdrager et al., 2014). Sucrose induces the expression of phytochrome-interacting factors (PIFs; Leivar and Quail, 2011), whereas degradation of PIFs is promoted by light-activated phytochromes (Castillon et al., 2007). This finding has helped bridge the gap to determine how plants alter growth through different day length (Nagel and Kay, 2012; Shin et al., 2013). Such sugar signaling pathways help to explain how plants sense and adapt to their energy source to regulate growth. However, there are still gaps in our understanding of how plants regulate and respond to sucrose

level and the demand of sucrose flux to maintain the sucrose balance between photosynthetic and non-photosynthetic cells. In addition, changes in the morphology and development of plants occur after directly adding exogenous sucrose to plant culture media (Rolland et al., 2006; Wind et al., 2010; Liu et al., 2011; Eveland and Jackson, 2012); however, how plants regulate sucrose production and consumption for responses and the effects of increased endogenous sucrose on plant metabolism are poorly understood.

Plants possess pluripotent stem cells located in specialized regions called meristems that are capable of producing new cells to drive organogenesis. Stem cells are located in the center zone (CZ) of shoot apical meristems (SAMs) and receive energy (i.e., sucrose from source cells) and signals (e.g., phytohormones) to stimulate the production of new cells, thus making important contributions to plant growth and organogenesis. The populations of stem cells and their progenitors are tightly controlled during proliferation by a negative feedback loop between the WUSCHELL (WUS) transcription factor and the CLAVATA (CLV) pathway (Schoof et al., 2000; Grandjean et al., 2004; Traas and Bohn-Courseau, 2005; Williams and Fletcher, 2005; Francis and Halford, 2006). WUS promotes an increase in the number of stem cells, whereas the CLV pathway limits the number of stem cells by inhibiting WUS. The exogenous sucrose supply promotes WUS expression by stimulating cell division (Wu et al., 2005) and *CycD* expression (Riou-Khamlichi et al., 2000), which can increase cell division and, consequently, increase the number of stem cells, and thus plant development.

Several studies have suggested that heterologous overexpression of the *SuSy* gene in plants promotes the production of biomass (Coleman et al., 2006, 2009; Barojas-Fernández et al., 2009; Jiang et al., 2012; Xu et al., 2012; Li et al., 2013). These studies focused on changes in soluble sugars and biomass in ectopically expressed SuSy transgenic plants; however, the mechanism of how the changes in soluble sugars affect plant growth and development is poorly understood. Herein, we present the following results after transforming six *SuSy* genes (S1–S6) into *Nicotiana tabacum*: (1) sucrose-degrading sucrose synthase (SuSy) activity increased significantly in transgenic plants compared to that in wild-type (WT) plants; (2) total soluble sugars (TSS), particularly sucrose and fructose, increased markedly in the transgenic plants; and (3) increased chlorophyll content, a higher rate of photosynthetic efficiency, and the upregulated expression levels of the genes involved in the photosynthetic sucrose synthesis were observed in the transgenic plants compared to those in WT plants. These results suggest the existence of a novel sucrose signaling pathway. This novel signaling pathway involves unknown factors that stimulate photosynthesis in the photosynthetic cells, thereby securing the sucrose flux demanded from photosynthetic to non-photosynthetic cells. Consequently, the increase in sucrose upregulated the transcription of genes controlling growth, division, and elongation of stem cells in the SAM, resulting in pronounced changes in the development and phenotype of the transgenic plants.

MATERIALS AND METHODS

Plant Materials and Growth Conditions for Transformation

We used WT *Arabidopsis thaliana* Columbia ecotype (Col-0) and tobacco (*Nicotiana tabacum* SR1). WT *Arabidopsis* plants and tobacco seedlings were grown on MS medium (Murashige and Skoog, 1962) in culture room at $25 \pm 3^\circ\text{C}$ under a 16 h/8 h light/dark photoperiod, and light intensity of $60 \text{ mmol m}^{-2} \text{ s}^{-1}$.

Gene Cloning, Plasmid Construction, Plant Transformation, and Molecular Analyses

We used the lithium chloride method and superscript reverse transcriptase (Invitrogen, Carlsbad, CA, USA) to obtain the mRNA and six full-length of *SuSy* genes from *A. thaliana* (Auffray and Rougeon, 1980) by using forward primer (FP) and reverse primer (RP; Supplementary Table S1). The cloned genes were inserted into pCambia 2300 with HA-NOS downstream, under regulation of the 35S promoter. *Agrobacterium tumefaciens* strain GV3013 was used for transformation of tobacco (*N. tabacum* cv. SR1) using the leaf disk method (Helmer et al., 1984).

Total genomic DNA was extracted from T₁ generation transgenic plant leaves to confirm the presence of the heterologous *SuSy* in the transgenic plants, and the heterologous *SuSy* proteins were examined by Western blotting with a mouse HA antibody (LF-MA0048, Ab frontiers) as the primary antibody, and goat anti-mouse IgG (HRP, LF-SA5001, Ab frontiers) as the secondary antibody.

Growth Conditions, Sampling, and Phenotypic Observations

At least 10 transgenic lines were confirmed in each *SuSy* transgenic plant (S1–S6). Three lines from each transgenic plant that had the highest sucrose-degrading *SuSy* activity were used for further analysis. Thirty individuals from each line were transferred to a greenhouse in 10-L pots in soil–perlite mixtures at $25 \pm 3^\circ\text{C}$ under a 16 h/8 h light/dark photoperiod and light intensity of $100 \text{ mmol m}^{-2} \text{ s}^{-1}$. The first-day germination of each plant was recorded.

The tenth leaf from the top of ten individual of each chosen transgenic lines and those from WT plants were harvested after each 10 days, from 30 to 120 DAG, stored at -70°C and ground in liquid N₂ to analyze *SuSy* enzymatic activities, soluble sugars, and chlorophyll contents.

The phenotypic characteristics of the transgenic and WT plants were also measured, and the carbohydrate content of each plant part was determined by gas chromatography (GC). A weight of 30 mg of each non- and popping-pretreated biomass samples were treated with 0.25 mL of 72% sulfuric acid (H₂SO₄) for 45 min at 30°C and diluted with 67.9 mL of distilled water to 4% H₂SO₄. Hydrolysis step was carried out at 121°C for 1 h in an autoclave machine. A solution containing a known amount of myo-inositol was used as an internal standard and was neutralized with ammonia solution by vortex mixing. Sodium borohydride solution (1 mL) and 0.1 mL of glacial acetic acid

(18 M) were added to degrade the sodium tetrahydroborate. Next, 0.2 mL of methyl immidazol and 2.0 mL of anhydrous acetic acid were sequentially added. Finally, 5.0 mL of deionized water were added and extracted with 2.0 mL of dichloromethane. The samples were analyzed using GC (GC-2010; Shimadzu, Otsu, Japan) with a DB-225 capillary column (30 m \times 0.25 mm i.d., 0.25 lm film thickness, J&W; Agilent, Folsom, CA, USA) operating with helium. The operating conditions were as follows: injector temperature of 220°C , flame ionization detector (FID) at 250°C , and an oven temperature of 100°C for 1.5 min with a constant increase of $5^\circ\text{C}/\text{min}$ to 220°C .

A 2-cm long segment from the top of the shoot tip was harvested from the transgenic and WT plants (three individuals from each transgenic line and WT plants) to measure soluble sugars in the shot tip, at 60 DAG. All leaves at the shoot tip were eliminated, and only the stem including SAM was ground in N₂ liquid. The powder was used to measure soluble sugars as mentioned below.

The experiment to demonstrate enhanced photosynthesis and photosynthetic sucrose synthesis was conducted as follow: Seeds from the three S1 transgenic lines which had the highest sucrose content and WT were sprayed in petri dishes with MS media without sucrose for seeding (kanamycin added for the transgenic). The dishes were placed in the dark (in a box) at $25 \pm 3^\circ\text{C}$ until germination, and the germinated seeds were transferred immediately to new MS media without sucrose. The dishes were placed in the dark for the next 7 days. The transgenic and WT plants were sampled before the light treatment at eight DAG. After the light treatment started, whole seedlings samples (at least 0.5 g) were obtained every 6 h for 48 h and analyzed for chlorophyll, starch, and soluble sugar contents. The transgenic and WT seedlings were harvested after 48 h to extract RNA, synthesize cDNA, and examine *CHLG*, *SPS* and *SPP* genes expression levels by RT-PCR.

Different light/dark time treatment experiment was set up as described above, except that the seedlings were transferred to new MS without sucrose media after germination and exposed to different light/dark periods. The light/dark treatments were: L.3/D.21 (3 h in light/21 h in dark); L.6/D.18; L.9/D.15; L.12/D.12; and L.24/D.0 (full-time light continuously). The dishes were placed in the dark for 14 days after finishing their respective time for light treatment, and then transferred to the light again the next day. Samplings were obtained at three time points beginning on day 15: start of the light treatment, after the light treatment, and after the dark treatment, according to the assigned times. Fresh seedlings were harvested, ground in liquid N₂, and the powder was used to analyze sucrose-degrading *SuSy* activity, starch and soluble sugar contents. Cross sections of stems and vertical sections of the shoot apical were prepared as described below for the light microscope analysis.

Enzyme Activity Assay

The tenth leaf from the tops of three individuals from each chosen transgenic line and wild-type (WT) plants was harvested at 7:00 a.m. at 10 day intervals from 30 to 120 DAG, stored at -70°C and ground in liquid N₂ to analyze *SuSy*, *SPS*, and *SPP* enzymatic activities, and soluble sugars.

SuSy enzymatic activity was determined through sucrose-degrading and sucrose-synthesizing SuSy activities, according to the previous methods (Geigenberger and Stitt, 1991, 1993; King et al., 1997; Hauch and Magel, 1998; Ruan, 2003; Koch, 2004; Bieniawska et al., 2007). Briefly, leaf powder was used to extract protein in a buffer containing of 50 mM Na₂HPO₄, pH 8.0, 1 mM EDTA, 5 mM DTT, 20 mM mercaptoethanol, and 10% glycerol. The triphenyltetrazolium chloride (TTC; ~95%; Cas. No. 298-96-4, Sigma Aldrich, USA) solution contained 0.25% (w/v) TTC, 1 M NaOH, and 0.08% Triton-X. The supernatant was collected and checked for total soluble protein by the Bradford method before measuring fructose produced in the reaction with TTC. Sucrose-degrading SuSy activity was determined by adding 10 µg protein from the supernatant to 200 µl of solution containing 10 mM sucrose and 10 mM UDP, pH 5.0, followed by a 1 h incubation at 37°C. Meanwhile, the same reaction without adding UDP was conducted to measure sucrose-degrading activity caused by other enzymes existing in the supernatant. Sucrose-synthesizing SuSy activity was determined by adding 10 µg proteins from the supernatant to 200 µl of solution containing 10 mM UDP-Glc and 10 mM fructose in the same condition. Control samples were conducted without adding the supernatant to detect fructose content. Fructose reacted with TTC and changes to a red color. Absorbance levels were obtained by measuring optical density (OD) at 495 nm by Multiskan EX spectrophotometer (ThermoScience, Rockford, IL, USA).

Sucrose phosphate synthase (SPS) enzymatic activity was measured by quantifying the sucrose fructosyl moiety using the anthrone test (Lunn and Furbank, 1997; Baxter et al., 2003), whereas sucrose phosphate phosphatase (SPP) was determined by following the release of orthophosphate from Suc6P (Ames, 1966; Lunn et al., 2000; Chen et al., 2005). SPS activity was determined by adding 10 µg protein of supernatant in a 200 µl buffer containing 50 mM HEPES-KOH pH 7.5, 20 mM KCl, and 4 mM MgCl₂, 10 mM UDP-Glc and 10 mM Fru6P, incubated at 37°C for 1 h. The mixtures then were boiled for 5 min to stop the reaction before added 100 µl of 0.14% (w/v) anthrone reagent (in 14.6 M H₂SO₄), and absorbance was measured at OD 620 nm. SPP activity was determined by adding 10 µg protein of supernatant in a 200 µl the same buffer plus 1.25 mM Suc6P ~98% (Cas. No. 36064-19-4, Sigma Aldrich, USA) and incubated at 30°C for 1 h, and stopped by adding 30 µl of 2 M trichloroacetic acid. A 100 µl of 0.42% ammonium molybdate in 1 M H₂SO₄ was added, incubated for 10 min, and the solution was read at OD 820 nm.

Soluble Sugars and Starch Analyses

The ground powder used to measure the enzymatic activities described above was used to analyze soluble sugar and starch contents. Sucrose, glucose and fructose were measured in 0.5 g of frozen powder that was re-suspended in 1 mL of ethanol 90%, left at 70°C for 90 min and centrifuged at 13,000 × g for 10 min. The supernatants were then filtered and subjected to high performance liquid chromatography with pulsed amperometric detection on a DX-500 Dionex system (Li et al., 2013). The pellet from the above sugar analysis was washed three times with ethanol 90% and then three times with distilled water before

being assayed using an amyloglucosidase-based test kit (Sigma Aldrich, St. Louis, MO, USA) to determine starch content.

Chlorophyll Fluorescence and Chlorophyll Content

All six transgenic plant lines (S1–S6) were used to determine which has the highest sucrose content based on photosynthesis capability and chlorophyll content. Photosynthetic activity was measured at early morning in the tenth leaf from the top of the transgenic and WT plant was measured using the OS1-FL (OPTI—Sciences Co. Ltd., Hudson, NH, USA) as described previously (Hajirezaei et al., 2002). Chlorophyll was extracted from the frozen leaf powder using ethanol 90%, boiled for 5 min and measured absorbance at OD 620 nm to calculate chlorophyll concentration (Lichtenthaler, 1987).

Light Microscopy

Transgenic and WT 15 DAG seedlings were fixed in a freshly prepared mixed of 2% (w/v) glutaraldehyde and 4% (w/v) paraformaldehyde in 50 mM sodium cacodylate buffer (pH 7.4) to compare cell morphology. The samples were de-gassed and fixed under a vacuum for 4 h at room temperature. After washing in the same buffer, dehydration was done through a graded ethanol series. The specimens were then infiltrated and embedded in a LR-White resin (Wi et al., 2006), semi-thin sections (1–2 µm) were stained 1% toluidine blue and examined under a Carl Zeiss microscope (Axilab; Carl Zeiss Inc., Jena, Germany).

Tobacco stems were fixed in FAA (formaldehyde, acetic acid, and ethanol) solution under vacuum to observe the general structure and starch distribution. After washing in distilled water, sections were cut on a rotary microtome using a disposable blade and stained with 1% toluidine blue and Lugol's solution (6 mM iodine, 42 mM KI, and 0.2 N HCl) to detect structure and starch granules, respectively (Hayashi et al., 2011).

RESULTS AND DISCUSSION

Soluble Sugars, Particularly Sucrose, and Sucrose-Degrading SuSy Activity Increase in Transgenic Plants, Probably Due to Enhanced Photosynthesis and Photosynthetic Sucrose Synthesis

Although it is generally accepted that SuSy possesses reversible functions, clarifying how this enzyme affects soluble sugars is complex. In particular, multi-gene families encoding SuSy isoforms exist in many plant species, but each of the six isoforms identified in *A. thaliana* has different expression patterns during development (Baud et al., 2004; Bieniawska et al., 2007). Six *At.SuSy* genes were heterologous overexpressed into *N. tabacum* to elucidate the function of SuSy isoforms in sucrose management and the mechanism by which soluble sugars, particularly sucrose, is affected. The six constructed vectors, each carrying one *SuSy* gene (S1–S6) driven by the 35S promoter, were introduced into tobacco plants by *Agrobacterium*-mediated

transformation. Each successful transgene produced more than ten transgenic lines, and three were chosen for analysis. The constructed vectors and transgene expression levels were determined and shown in Supplementary Figures S1A,B.

SuSy enzymatic activity was measured as sucrose-degrading and sucrose-synthesizing sucrose synthase (SuSy) activities. The sucrose-degrading and sucrose-synthesizing SuSy activity profiles revealed that successful heterologous overexpressed SuSy markedly upregulated sucrose-degrading SuSy activity in transgenic plants compared to in the WT plants (see Figure 1A for a comparison of S1 transgenic and WT plants

and Supplementary Figure S1C for S1–S6 transgenic and WT plants), whereas low sucrose-synthesizing SuSy activity was detected, with no difference in the activity between WT and the transgenic plants (Figure 1B and Supplementary Figure S1E). Sucrose-degrading activities caused by other enzymes existing in the supernatant, including INVs, were low, and particularly, no different results between WT and the transgenic plants (Supplementary Figure S1D), suggested that others sucrose-degrading enzymes, particularly INVs did not involve in the upgraded sucrose-degrading activity. Sucrose-degrading SuSy activity was higher in shoots, stems, and roots of the transgenic

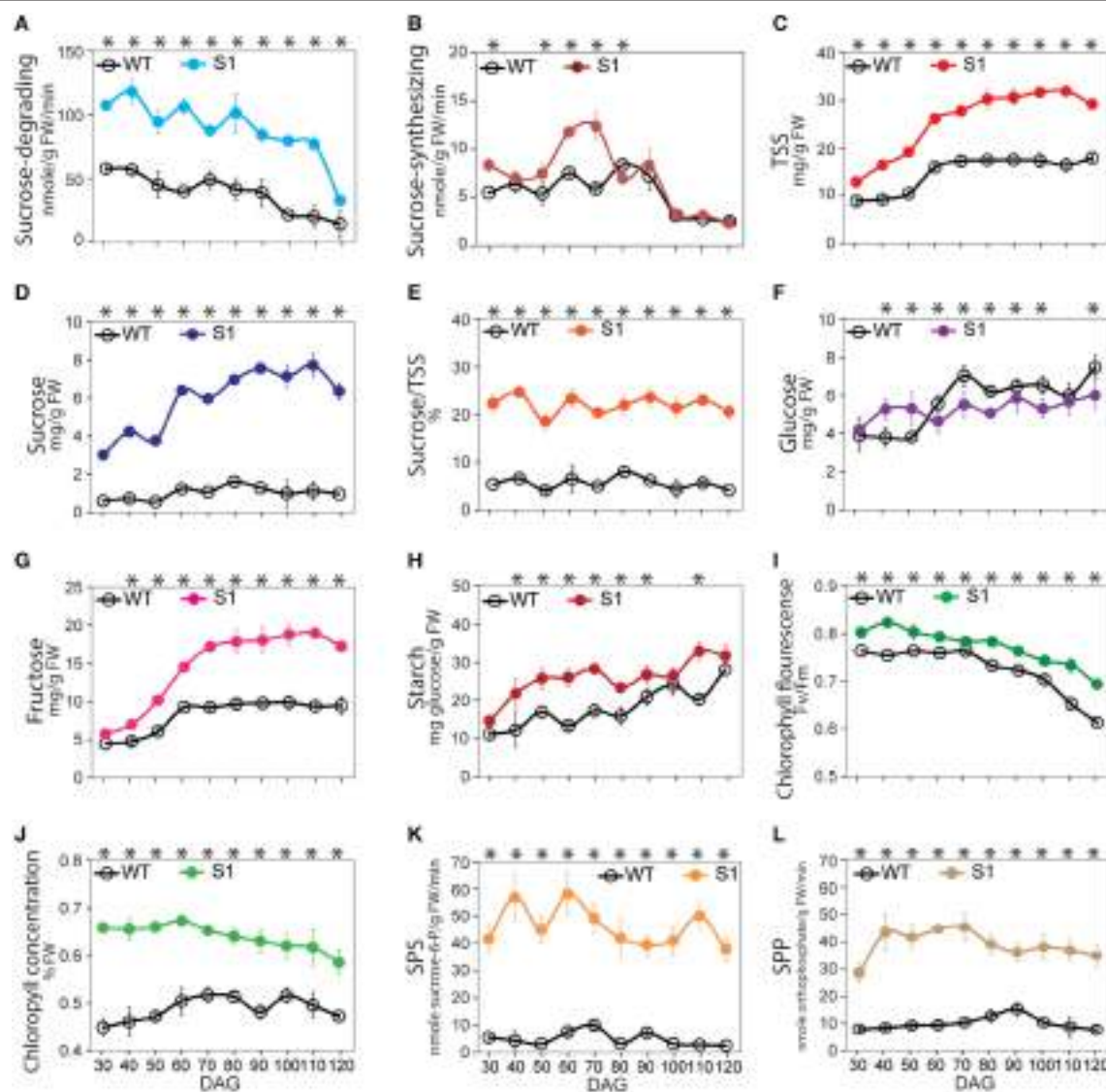


FIGURE 1 | Pattern of the sucrose synthase (SuSy) enzymatic activity, soluble sugar, starch, photosynthesis, chlorophyll concentration, sucrose-phosphate synthase (SPS) and sucrose-phosphatase synthase (SPP) activity profiles of S1 transgenic and wild-type (WT) plants from 30 to 120 days after germination (DAG). (A) Sucrose-degrading SuSy activity. **(B)** Sucrose-synthesizing SuSy activity. **(C)** Total soluble sugar content (TSS), determined as the sum of sucrose (**D**), glucose (**F**), and fructose (**G**) contents. **(E)** Percentage of sucrose in TSS (%). **(H)** Starch content. **(I)** Photosynthetic capability, represented by chlorophyll fluorescence (Fv/Fm). **(J)** Chlorophyll concentration (% FW). **(K)** SPS activity. **(L)** SPP activity. Average values were calculated from triplicate ($n = 3$) from transgenic line which had highest sucrose-degrading SuSy activity. Asterisks (*) indicate significant differences from the control (WT), determined by a Student's *t*-test ($*P < 0.05$).

plants than that in the WT (Supplementary Figure S1F), whereas no difference in sucrose-synthesizing SuSy activity was observed (Supplementary Figure S1G), indicating that the increase in sucrose-degrading SuSy activity occurred in all transgenic plants. Clearly sucrose-degrading SuSy activity, rather than sucrose-synthesizing SuSy activity, was exhibited in all heterologous overexpressed SuSy transgenic plants.

TSS, including soluble sucrose, glucose, and fructose, was distinctly elevated in the transgenic plants relative to that in the WT plants (**Figure 1C** and Supplementary Figure S1H), due to significant increase in sucrose and fructose (**Figures 1D,G**, respectively), whereas no difference in glucose was detected (**Figure 1F**). Consequently, sucrose made up the greatest proportion of TSS (**Figure 1E**), revealing that the TSS component has basically changed. The proportion of fructose was consistently higher in the transgenic than in the WT plants (**Figure 1G**), suggesting that increased sucrose in the transgenic plants may not be involved with sucrose-synthesizing SuSy activity. Sugar status can be influenced by starch biosynthesis and degradation (Smith and Stitt, 2007; Graf and Smith, 2011; Farré and Weise, 2012), but we found that starch increased significantly in the transgenic plants compared to the WT plants (**Figure 1H**), indicating that the increase in sucrose was not due to starch degradation. Notably, the same patterns were observed in sucrose and starch extracted from leaves, stems, and roots of the transgenic and WT plants (Supplementary Figures S1I,J, respectively), with higher sucrose-degrading SuSy activity occurring in these organs in the transgenic than in the WT plants. This demonstrates that the flux of sucrose delivery occurred at a higher rate in the transgenic than in the WT plants to distribute sucrose from photosynthetic to non-photosynthetic cells.

Autotroph means self-provided, thus, autotroph plants can synthesize almost all of their required carbohydrates from photosynthetically fixed carbon released from chloroplasts. The known sugar signaling pathways explain how plants control their growth to adapt to energy stress, but a mechanism must exist that allows plants to synthesize carbohydrates to compensate for any loss when they experience an unbalanced energy status. Analyses of the SuSy enzymatic activity, TSS, and starch patterns in the transgenic and WT plants at the same time after germination provided novel evidence that the increase in TSS, particularly sucrose, was not derived from either the sucrose-synthesizing SuSy activity or starch degradation, but was influenced by other factors that induced a series of reactions leading to the increase in sucrose. Before detecting the existence of the novel signaling pathway, we examined the directed responses that led to increased sucrose. We first proposed that the increased sucrose was driven by enhanced photosynthesis and photosynthetic sucrose synthesis. This enhancement of photosynthesis led to increased production of photosynthetically fixed carbon, such as TP in chloroplasts, which was delivered to the cytosol and utilized to synthesize sucrose, leading to overall enhancement of photosynthetic sucrose synthesis.

An abundance of chlorophyll in chloroplasts generally indicates proper photosynthesis (Beale, 1999; Bauer et al., 2001; Tanaka et al., 2001; Philipp et al., 2007; Moon et al., 2008; Shalygo et al., 2009; Berry et al., 2013). Of the six transgenic plants

tested (S1–S6), the transgenic lines with the highest sucrose content were used to measure photosynthetic capability and chlorophyll content (see Materials and Methods). Consistent with our prediction, higher chlorophyll fluorescence (Fv/Fm) and chlorophyll concentration values were recorded in the transgenic lines (**Figures 1I,J**, respectively), indicating enhanced photosynthetic capability in the transgenic plants as compared to WT.

Enhanced photosynthetic efficiency leads to increased production of TP precursors for sugar synthesis (Bauer et al., 2001; Salerno and Curatti, 2003; Rolland et al., 2006). However, photosynthetic sucrose synthesis requires the participation of two other enzymes, sucrose phosphate synthase (SPS; E.C. 2.4.1.14) and sucrose phosphate phosphatase (SPP; EC 3.1.3.24; Rolland et al., 2006). Reverse-genetic approaches have demonstrated that reduced expression of these enzymes inhibits photosynthesis, indicating that sugar metabolism can also regulate the photosynthesis through downstream signaling (Baxter et al., 2003; Prasad et al., 2004; Chen et al., 2005) because decreased expression of these genes leads to a surplus of TP, followed by inhibited chloroplast function to cope with the sugar demand. We hypothesized that the increase in TP driven by enhanced photosynthesis upregulates *SPS* and *SPP*. Some studies have demonstrated an association between increased CO₂ increased photosynthesis, and *SPS* expression (Farrar and Williams, 1991; Hussain et al., 1999; Vu et al., 2001; Prasad et al., 2004). Moreover, although *SPS* and *SPP* expression are regulated by day/night length (Huber and Huber, 1996; Chen et al., 2005; Sun et al., 2011), a clear correlation between enhanced photosynthesis and the expression levels of these genes is still missing. Herein, *SPS* and *SPP* activities were significantly higher in the transgenic than in the WT plants (**Figures 1K,L**, respectively, and Supplementary Figures S1K,L), in accordance with our hypothesis. These results indicate that *SPS* and *SPP* were upregulated in the transgenic plants.

To summarize, combined with the increased sucrose levels shown above (**Figures 1D,E**), our data suggest that enhanced photosynthesis and photosynthetic sucrose synthesis occur as a response in the condition of the increased sucrose-degrading SuSy activity in the transgenic plants.

Increased Endogenous Sucrose Content May Upregulate of *WUS* and *CycD3*, Which Induce the SAM and Trigger Pronounced Phenotypic and Morphological Changes in Transgenic Plants

All aboveground plant tissues and organs are derived from the SAM, which is located in the shoot tips and harbors sets of pluripotent stem cells embedded in the CZ. The number of stem cells and their progeny population, which is tightly regulated by energy signals, determine the size of the CZ (Bodson and Outlaw, 1985; Medford et al., 1991; Pien et al., 2001). Here, we wanted to link the increase in sucrose to the remarkable SAM development of transgenic plants than in the WT plants. Samples were harvested from the shoot tips of the transgenic and WT plants 60 days after germination (DAG) to measure soluble sugar.

Significant higher in sucrose-degrading SuSy activity, but low and no difference in sucrose-synthesizing SuSy activity were obtained in the shoot tips of the transgenic and WT plants (**Figure 2A**). The SuSy transgenic plants contained more TSS (35.5 mg/g FW in S1 compared to 19.0 mg/g FW in WT plants, **Figure 2B**), with significantly higher sucrose content (10.2 mg/g FW in S1 compared to 1.7 mg/g FW in WT plants), which led to a higher proportion of sucrose in the TSS in the transgenic plants than in the WT plants (about 28.9% in S1 compared to 9.4% in WT plants, **Figure 2C**). Sucrose and fructose contents were also higher in the transgenic than in the WT plants (Supplementary Figure S2A). These data are similar to the results above, and show basic changes in the TSS component in the SAM, with higher sucrose in the transgenic than WT plants, derived from photosynthetic cells via sucrose flux demanded.

Stem cells in the SAM are controlled by WUS and exogenous sucrose promotes WUS expression by stimulating cell division (Wu et al., 2005) and inducing the expression of *CycD* genes, leading to increased cell division (Gaudin et al., 2000; Riou-Khamlichi et al., 2000). Our results show an abundance of endogenous sucrose in the SAM of the transgenic plants, which may affect *WUS* and *CycD3.1* expression levels. Reverse transcription–polymerase chain reaction (RT-PCR) analysis revealed dramatic upregulation of relative *WUS* and *CycD3.1* expression in the S1 transgenic plants compared to that in the WT plants (**Figure 2D**).

Our data suggest that the abundance of endogenous sucrose driven by enhanced photosynthesis and photosynthetic sucrose synthesis was sufficient to induce the expression of genes controlling stem cell development, which lead to pronounced

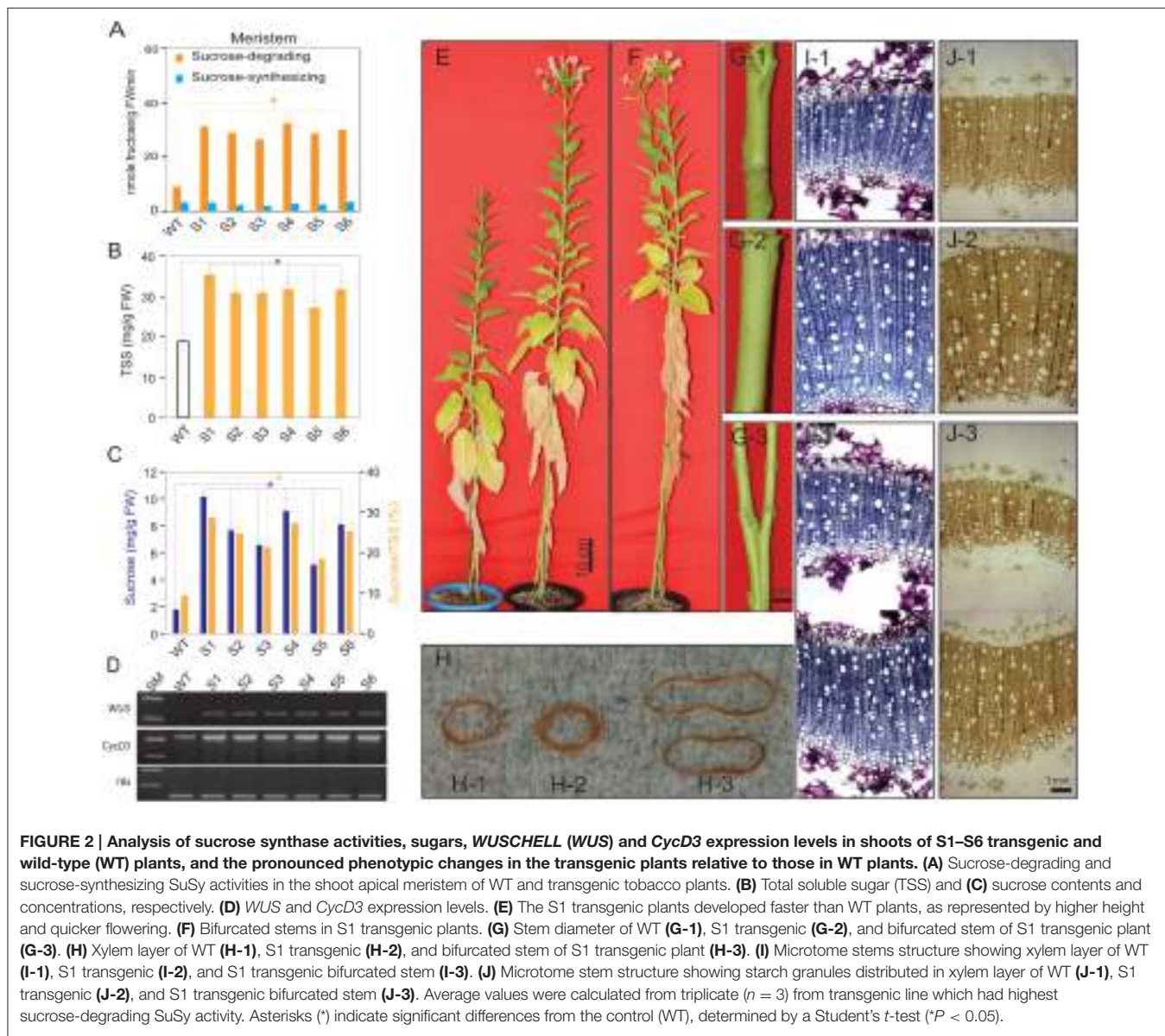


TABLE 1 | Time required for germination to initial bud generation (BG), initial flowering (F), and from BG to F in the wild-type (WT) and transgenic plants.

Line	Time required (DAG)		
	Initial buds generation (BG)	Initial flowering (F)	From BG to F
WT	124.1 ± 4.7	137.8 ± 3.9	13.7 ± 2.1
S1	97.5 ± 4.1*	108.6 ± 3.5*	11.1 ± 1.0*
S2	101.4 ± 3.4*	113.4 ± 3.1*	12.0 ± 2.0*
S3	102.1 ± 3.1*	114.6 ± 4.4*	12.3 ± 1.5*
S4	102.6 ± 3.7*	115.8 ± 4.6*	12.6 ± 1.2*
S5	99.6 ± 2.9*	112.4 ± 1.7*	12.9 ± 2.0*
S6	102.8 ± 3.1*	116.8 ± 3.1*	12.6 ± 1.3*

Mean values were calculated from data obtained from individuals ($n = 10$) in each chosen transgenic line and WT. Asterisks (*) indicate significant differences determined by a Student's t-test (* $P < 0.05$).

changes in the phenotypes of the transgenic plants; i.e., longer stem height (Figure 2E and Supplementary Figure S2B), thicker stem diameter (Figure 2G and Supplementary Figure S2C), shorter time to generate the initial bud and to flowering (Table 1), and enhanced reproduction and biomass production (Table 2). These results are similar to those of previous studies, which demonstrated the effects of exogenous sucrose supply on plant development and physiology. For example, a study (Bodson and Outlaw, 1985) reported that the accumulation of sucrose in the meristem is an early physiological event in floral transition, which was later reviewed (Bernier et al., 1993), who hypothesized a regulatory loop between sucrose and cytokinins to control the transition to flowering at the SAM. Later, a study stated that sugar signals may also regulate meristematic proliferation at the G2 to M transition (Skylar et al., 2011). In our study, the secondary xylem was thicker in the transgenic than in the WT plants (Figure 2G). Particularly, bifurcated stems (Figure 2F) formed in all transgenic lines (more than 30% of all six transgenic plants had bifurcated stems, Supplementary Figure S2D), and xylem morphology was also affected (Figures 2H,I). The first demonstration about the formation of bifurcated stems and the involvement of an oligosaccharide signal molecule to the formation was introduced without a clear mechanism (Schmidt et al., 1993). We observed these features in all six transgenic lines tested, suggesting that the stem cells and SAM structural development patterns were altered by the increased endogenous sucrose content. More predominant starch granules were observed in the stem section of transgenic plants, clearly indicating that starch content was also higher in the transgenic than in WT plants (Figure 2J).

Plant biomass was harvested and analyzed by gas chromatography (GC) to examine carbohydrates that accumulated in the plant cell walls after complete maturation (Coleman et al., 2009). The argument was that different SuSy isoforms can have different effects on carbohydrate accumulation in the cell wall. The results showed higher total carbohydrate contents in all parts of the plant (leaves, stems, and roots) in the transgenic than in WT plants (Table 3). The highest glucose content was observed in leaves, compared to that in stems and

roots. Glucose was significantly higher in the transgenic than in WT plants, whereas xylose was lower in leaves but higher in the stems and roots. These data confirm no differences in the effects of the SuSy isoforms on carbohydrate accumulation in plant cell walls, as all of the isoforms revealed altered carbohydrate content in the transgenic plants, consistent with previous studies (Coleman et al., 2009; Jiang et al., 2012; Xu et al., 2012; Li et al., 2013).

Evidence for a Novel Sucrose Signaling Pathway Leading to Enhanced Photosynthesis and Photosynthetic Sucrose Synthesis

Sucrose is a photosynthetic product, produced in photosynthetic cells and transported to non-photosynthetic cells, and the synthesis, transport from source to sink cells, and use of sucrose are tightly regulated (Koch, 2004; Rolland et al., 2006; Wind et al., 2010). A proper balance between hexose (glucose and fructose) and sucrose is required for normal plant development. As reported previously, expression of *SnRKs* genes is upregulated in culture media without sucrose, whereas *TOR* genes are upregulated in media with an abundance of sucrose (Chiou and Bush, 1998; Halford et al., 2003; Rolland et al., 2006; Coello et al., 2011; Robaglia et al., 2012; Lastdrager et al., 2014). In contrast, our hypothesis about the existence of an unknown sucrose signaling pathway is strongly supported by the higher levels of TSS and each of its sugars, as well as enhanced photosynthesis and photosynthetic sucrose synthesis leading to increased sucrose content. We conducted an experiment to detect the relationship between the transition from heterotrophic to autotrophic growth and the variations in chlorophyll content and soluble sugars to determine the existence of a sucrose signaling pathway. Accordingly, when the carbohydrate reserved in the seed is depleted, seedlings must synthesize their own carbohydrates (Baker et al., 2006; Rolland et al., 2006; Stitt and Zeeman, 2012). We also conducted an experiment to analyze the changes when plants are transferred from dark to light conditions. Harvested samples were analyzed for chlorophyll, starch, and soluble sugar contents, and *CHLG*, *SPS* and *SPP* gene expression levels were determined by RT-PCR after 48 h.

As shown in Figure 3A, the leaves of the S1 transgenic seedlings turned nearly green, whereas leaves of the WT plants remained yellowish after 48 h of light treatment. *CHLG*, *SPS*, and *SPP* expression levels were also higher in the S1 transgenic seedlings than in the WT plants (Figure 3B), reinforcing our hypothesis. Chlorophyll concentration (% FW) revealed that chlorophyll was synthesized faster after light treatment (Figure 3C), suggesting that the setup or recovery of photosynthetic capacity within 48 h was stronger in the S1 transgenic than in the WT seedlings. In addition, sucrose-degrading SuSy activity was also higher in the S1 transgenic than in the WT seedlings (Figure 3D). Almost no difference in TSS content were observed between transgenic and WT seedlings for light treatments of 0–6 h, whereas TSS in the S1 transgenic seedlings was clearly higher than that in the WT seedlings beginning at 12 h (Figure 3E). In more detailed,

TABLE 2 | Comparison of reproduction and biomass weight characteristics between the wild-type (WT) and transgenic plants.

Line	SuSy-degrading activity at flowering (nmol fructose/g FW/min)	Phenotype						
		Number of buds/flowers (unit)	Total harvested seed weight (g/plant)	100-seeds weight (mg/100 seeds)	After freeze drying—Weight (g/plant)			
					Leaves	Stem	Roots	Total dried biomass
T	23.2 ± 1.2	38.8 ± 4.3	1.1 ± 0.0	11.0 ± 0.1	7.2 ± 0.9	6.9 ± 1.1	2.5 ± 0.5	16.7 ± 1.5
S1	60.2 ± 4.6*	50.7 ± 6.1*	1.8 ± 0.1*	12.0 ± 0.1*	9.8 ± 0.0*	12.9 ± 0.1*	5.2 ± 0.3*	28.0 ± 0.2*
S2	54.5 ± 3.9*	47.1 ± 4.3*	1.3 ± 0.0*	11.8 ± 0.2*	9.6 ± 0.6*	11.3 ± 0.8*	3.9 ± 0.0*	24.8 ± 1.5*
S3	67.4 ± 2.4*	46.1 ± 2.9*	1.3 ± 0.1*	11.7 ± 0.4*	9.6 ± 0.4*	10.9 ± 0.6*	5.0 ± 0.2*	25.5 ± 0.0*
S4	53.8 ± 3.5*	49.3 ± 2.5*	1.6 ± 0.1*	12.0 ± 0.1*	9.9 ± 0.0*	11.5 ± 1.4*	6.1 ± 0.2*	27.7 ± 1.2*
S5	69.2 ± 1.0*	48.6 ± 4.0*	1.5 ± 0.2*	11.7 ± 0.3*	9.6 ± 0.3*	10.9 ± 0.3*	5.4 ± 0.0*	26.0 ± 0.6*
S6	50.2 ± 1.3*	48.8 ± 3.8*	1.5 ± 0.2*	11.8 ± 0.3*	9.7 ± 0.6*	11.3 ± 0.3*	4.2 ± 0.0*	25.3 ± 0.9*

Mean values were calculated from the data obtained from individuals ($n = 10$) of each chosen transgenic line and WT. Asterisks (*) indicate significant differences determined by a Student's *t*-test (* $P < 0.05$).

TABLE 3 | Comparison of carbohydrate content in leaves, stem, and roots between the wild-type (WT) and transgenic plants.

	(%)	WT	S1	S2	S3	S4	S5	S6
Leaves	Rhamnose	2.4 ± 0.6	2.7 ± 0.7*	2.7 ± 0.5*	2.6 ± 0.6*	2.3 ± 0.3	2.4 ± 0.4	2.5 ± 0.5
	Arabinose	1.2 ± 0.1	1.3 ± 0.4	1.4 ± 0.1	1.3 ± 0.0	1.1 ± 0.1	1.2 ± 0.1	1.0 ± 0.1
	Xylose	1.5 ± 0.3	1.7 ± 0.2*	1.6 ± 0.1	1.4 ± 0.0	1.2 ± 0.1*	1.3 ± 0.1*	1.1 ± 0.0*
	Mannose	0.9 ± 0.4	1.3 ± 0.7	0.9 ± 0.4	0.9 ± 0.1	0.8 ± 0.2	0.9 ± 0.2	0.8 ± 0.0
	Galactose	2.8 ± 0.2	2.8 ± 1.1	3.1 ± 0.5*	2.8 ± 0.4	2.6 ± 0.3*	2.7 ± 0.5	2.3 ± 0.1*
	Glucose	46.5 ± 1.2	62.6 ± 4.4*	55.5 ± 1.0*	50.5 ± 0.8*	49.8 ± 2.2	47.0 ± 1.1	45.5 ± 2.4
	Total	55.4 ± 5.6	72.5 ± 8.4*	65.3 ± 4.4*	59.4 ± 4.4*	57.8 ± 2.4	55.5 ± 6.1	53.3 ± 2.7
Stems	Rhamnose	1.8 ± 0.4	1.3 ± 0.1*	1.3 ± 0.4*	1.2 ± 0.2*	1.1 ± 0.2*	1.2 ± 0.1*	1.3 ± 0.2*
	Arabinose	0.7 ± 0.2	0.6 ± 0.0	0.7 ± 0.0	0.7 ± 0.0	0.6 ± 0.0	0.6 ± 0.1	0.5 ± 0.1
	Xylose	5.6 ± 0.9	8.2 ± 1.5*	8.4 ± 0.6*	9.7 ± 1.1*	9.8 ± 0.1*	9.0 ± 0.9*	8.8 ± 0.9*
	Mannose	1.0 ± 0.2	1.4 ± 0.3*	1.4 ± 0.3*	1.6 ± 0.0*	1.6 ± 0.1*	1.7 ± 0.1*	1.5 ± 0.1*
	Galactose	1.5 ± 0.1	1.3 ± 0.2	1.3 ± 0.2	1.3 ± 0.1	1.1 ± 0.1*	1.1 ± 0.1*	1.0 ± 0.2*
	Glucose	43.5 ± 1.2	50.9 ± 6.1*	49.7 ± 5.7*	52.8 ± 2.9*	52.7 ± 2.9*	46.9 ± 3.6*	46.2 ± 2.5
	Total	54.2 ± 3.4	63.6 ± 4.5*	62.7 ± 5.4*	67.3 ± 1.1*	67.0 ± 3.3*	60.4 ± 3.6*	59.4 ± 1.5*
Roots	Rhamnose	1.2 ± 0.6	1.2 ± 0.1	1.3 ± 0.3	1.4 ± 0.3*	1.3 ± 0.1	1.0 ± 0.2*	1.2 ± 0.5
	Arabinose	0.7 ± 0.2	0.9 ± 0.1*	0.9 ± 0.0*	1.0 ± 0.1*	0.9 ± 0.1*	0.9 ± 0.2*	1.0 ± 0.1*
	Xylose	6.4 ± 3.5	9.1 ± 1.1*	9.8 ± 1.1*	8.8 ± 0.3*	8.1 ± 0.7*	6.9 ± 0.4	8.9 ± 1.9*
	Mannose	1.1 ± 0.5	1.1 ± 0.1	0.9 ± 0.0	0.9 ± 0.0	0.8 ± 0.0	0.7 ± 0.0*	0.9 ± 0.2
	Galactose	1.3 ± 0.1	1.0 ± 0.3*	1.0 ± 0.1*	1.2 ± 0.0	1.0 ± 0.2*	1.1 ± 0.1*	1.3 ± 0.3
	Glucose	42.0 ± 3.8	47.7 ± 2.6*	46.1 ± 1.3*	50.0 ± 1.5*	48.9 ± 4.1*	45.1 ± 1.8*	51.4 ± 7.8*
	Total	52.7 ± 3.6	61.1 ± 6.4*	60.0 ± 3.4*	63.2 ± 2.4*	61.0 ± 4.5*	55.8 ± 3.5*	64.7 ± 4.6*

Mean values were calculated from the data obtained from individuals ($n = 3$) of each chosen transgenic line and WT. Asterisks (*) indicate significant differences determined by a Student's *t*-test (* $P < 0.05$).

sucrose increased slowly in the WT seedlings during the first 24 h of the light treatment, but we found almost no change (or slight reduction) in the transgenic seedlings, which can be explained by the sucrose-degrading function of heterologous S1; however, sucrose increased strongly beginning at 24 h of light treatment in the transgenic seedlings relative to in the WT seedlings (Figure 3F). It appears that glucose increased by 36 h of the light treatment (Figure 3G). Fructose and

starch also increased (Figures 3H,I, respectively), strengthen the argument that the increased sucrose was not derived from either degradation of starch or sucrose synthesis with fructose as precursor. These data suggest that the sucrose signaling pathway induces the prompt setup or recovery of photosynthesis and photosynthetic sucrose synthesis, leading to the impressive increase in TSS, particularly sucrose, observed in the transgenic plants. Moreover, the sucrose signaling pathway was activated

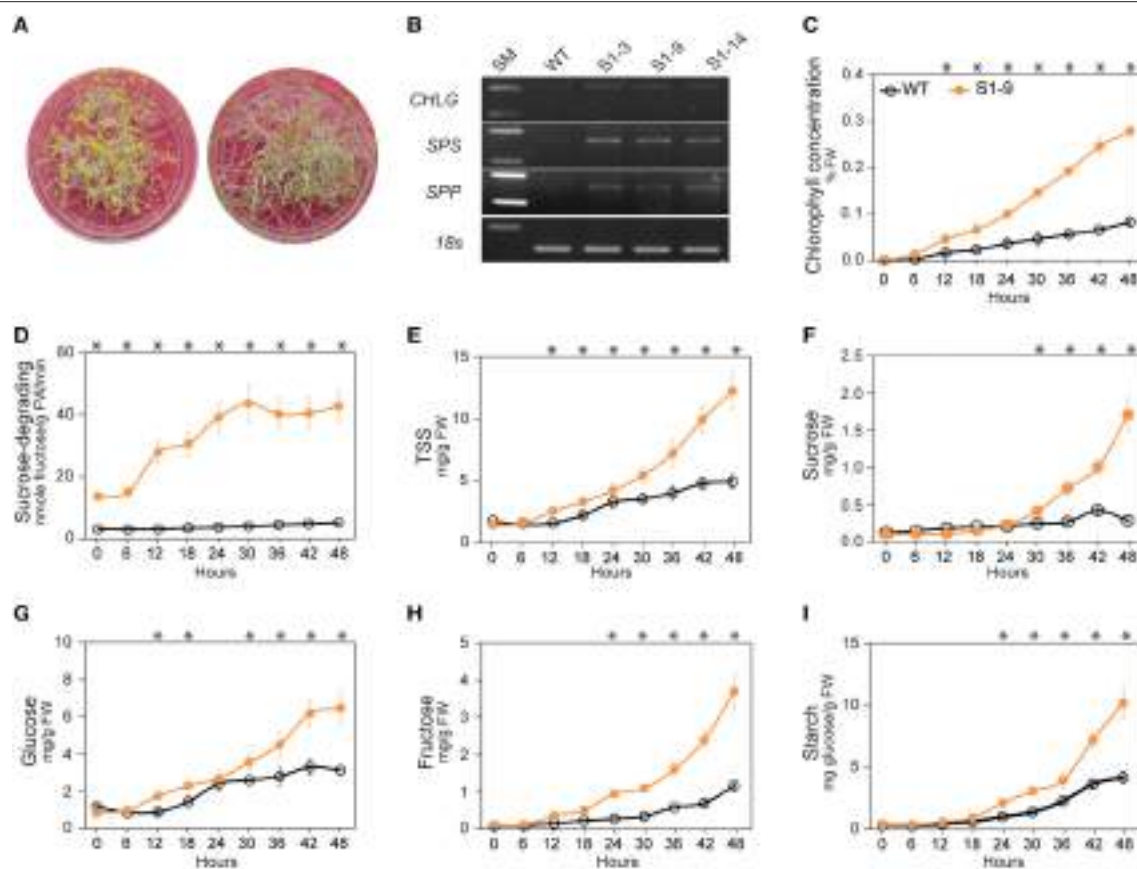


FIGURE 3 | Results of experiment demonstrating enhanced photosynthesis and photosynthetic sucrose synthesis in sucrose synthase (SuSy) transgenic plants. (A) Leaves of S1 transgenic seedlings turned nearly green color, whereas WT seedlings remained yellowish after the 48 h light treatment. **(B)** Chlorophyll synthase (CHLG), sucrose-phosphate synthase (SPS) and sucrose-phosphatase (SPP) expression levels after the 48 h light treatment. **(C)** Pattern of chlorophyll concentration (% FW), 6 h intervals from 0 to 48 h after starting the light treatment. **(D)** Sucrose-degrading SuSy activity. **(E)** Total soluble sugar (TSS) content, represented by the sum of content of sucrose (**F**), glucose (**G**), and fructose (**H**) contents. **(I)** Starch content. Average values were calculated from triplicate ($n = 3$). Asterisks (*) indicate significant differences from the control (WT), determined by a Student's *t*-test ($*P < 0.05$).

soon after transferring the seedlings from heterotrophic to autotrophic growth conditions (from dark to light treatment), which caused a dramatic shift in the photosynthetic setup. Once the setup was completed, chlorophyll was synthesized, and photosynthetic sucrose synthesis started in the photosynthetic cells.

Sugar metabolism in plants is regulated primarily by light/dark duration. Synthesis of soluble sugars, particularly sucrose, and starch occur by photosynthesis in the presence of light, and decomposition occurs during respiration in the dark. Starch synthesis and degradation are key mechanisms used to maintain the balance of sugars (Smith and Stitt, 2007; Kötting et al., 2010; Graf and Smith, 2011; Farré and Weise, 2012; Stitt and Zeeman, 2012). Thus, we conducted an experiment with variable light/dark time to determine the influence of different day lengths on sugar metabolism, how variations in sugars affects plant growth and development, and how increased sucrose under light conditions may not be driven by starch degradation in the SuSy transgenic plants. Seedlings were transferred to new MS without sucrose media and exposed to different light/dark

periods. The light (L)/dark (D) treatments were: L.3/D.21 (3 h light/21 h dark); L.6/D.18; L.9/D.15; and L.12/D.12. The dishes were put in the dark after completing the respective times under light treatment for 14 days and then transferred to light again the next day. Plants exposed to L.24/D.0 were given light all the time. Samples were collected at three time points starting day 15: start of the light treatment, after the light treatment, and after the dark treatment, according to the assigned times. The samples were analyzed for sucrose-degrading SuSy activity and starch and soluble sugar contents. The fresh samples were photographed to compare phenotypes and to analyze stem cross and SAM vertical sections. Evaluation of seedlings development revealed that the longer light treatment resulted in faster development and faster growth rates in the S1 transgenic plants compared to those in the WT seedlings (Figure 4A). The phenotypic characteristics were also higher in the S1 transgenic plants than those in the WT for the same setting (Table S2). Stem xylem layer morphology varied based on the cross-sections (Supplementary Figure S3A), indicating that a higher growth rate was achieved with longer photosynthesis times in the

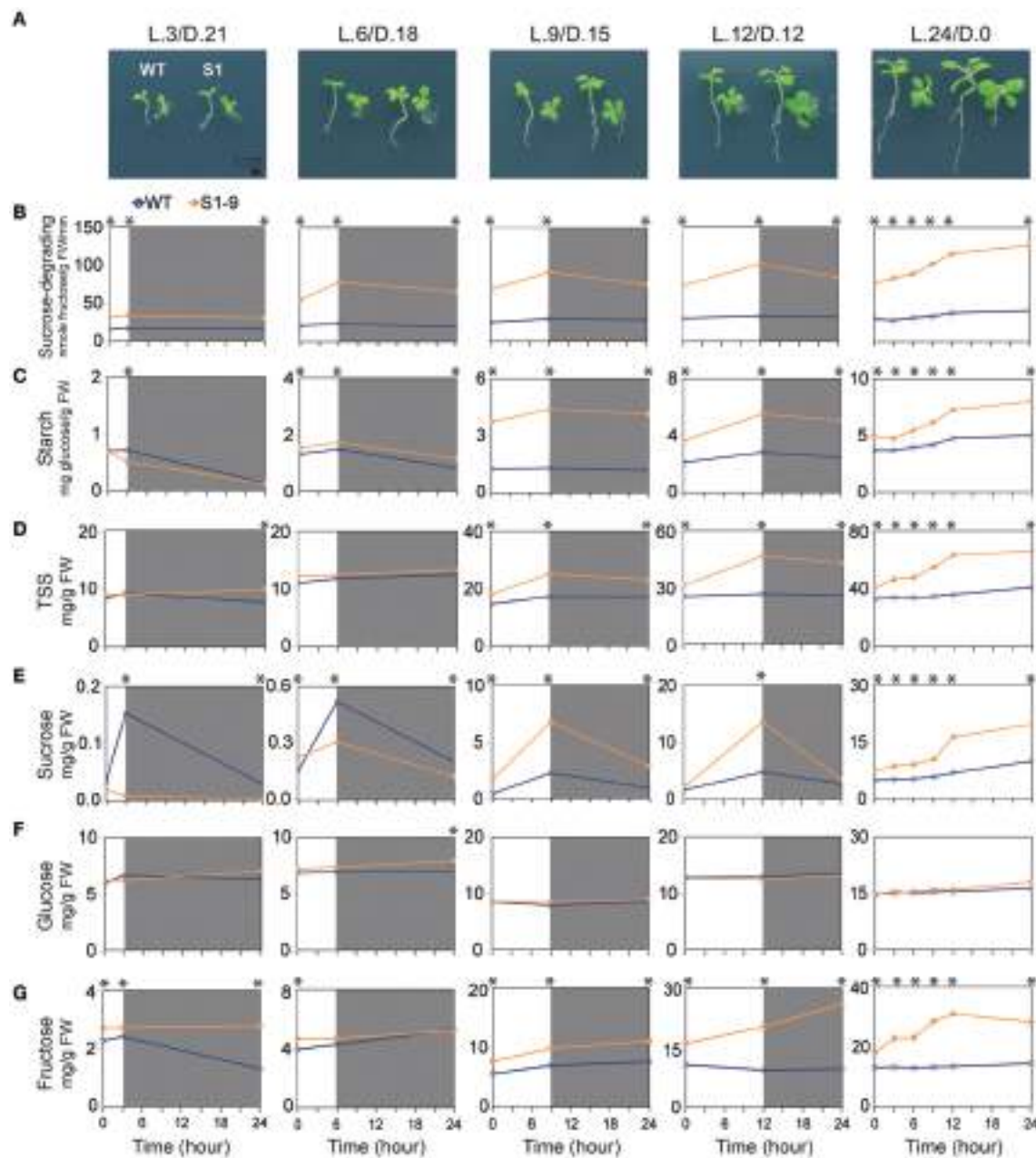
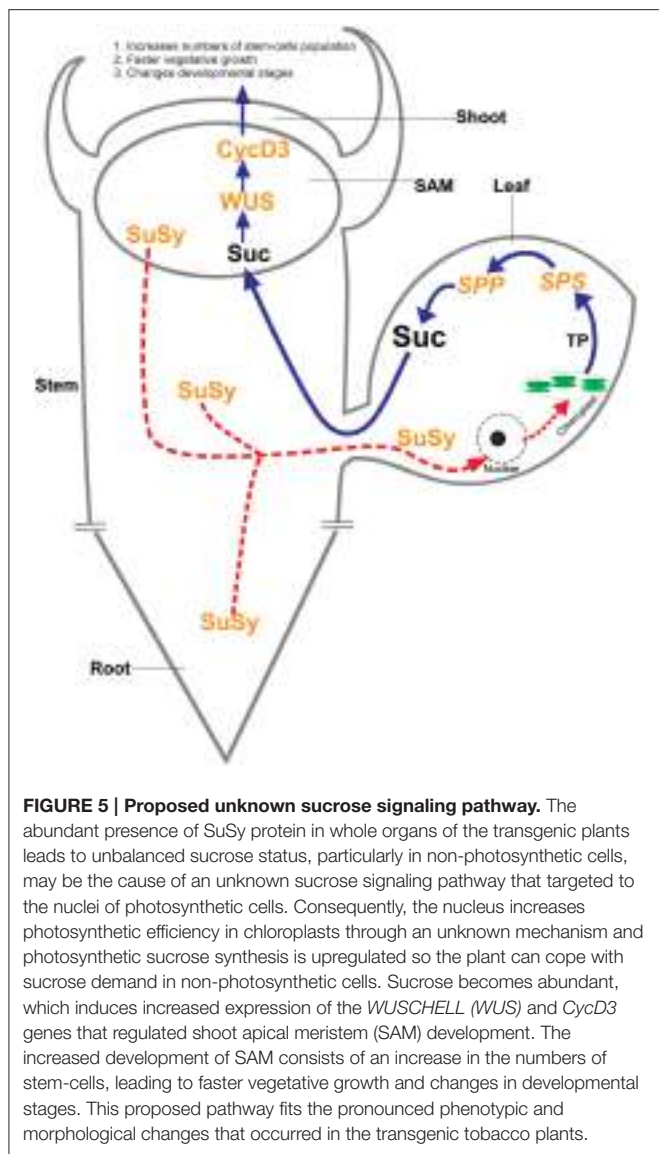


FIGURE 4 | Different phenotypes and sucrose-degrading sucrose synthase (SuSy) activity pattern, starch and sugar contents in the transgenic and wild-type (WT) seedlings exposed to different light/dark time treatment. **(A)** Transgenic seedlings developed faster than wild-type (WT) seedlings under all light/dark treatments, as represented by larger transgenic than WT seedling (bar = 1 cm). Detailed are shown detailed in Supplementary Table S2. **(B)** Sucrose-degrading SuSy activity. **(C)** Starch content. **(D)** Total soluble sugar (TSS) content, represented by the sum of sucrose (**E**), glucose (**F**), and fructose (**G**) contents. Average values were calculated from triplicate ($n = 3$). Asterisks (*) indicate significant differences from the control (WT), determined by a Student's *t*-test ($^*P < 0.05$).

transgenic than in the WT plants. Thicker xylem layers in the transgenic plants exposed to L.9/D.15, L.12/D.12, and L.24/D.0, suggested improved secondary xylem formation, derived from the primary xylem. Vertical sections revealed differences in the size of the shoot apical structure, as evidenced by longer vertical and horizontal lines. Calculations using Photoshop CS6 software showed that the shoot apical area was larger in the S1 transgenic

than in the WT plants (Supplementary Figures S3B,C), indicating enhanced development of the SAM in the transgenic plants, which helps explain the faster vegetative growth of the transgenic plants.

Sucrose-degrading SuSy activity showed an increasing trend during light treatment, but a decreasing trend during the dark treatment, with higher sucrose-degrading SuSy activity



achieved during the longer light treatment times. These features were clearly observed in the transgenic plants exposed to L.24/D.0, indicating that heterologous *SuSy* isoforms were induced during photosynthesis (Figure 4B). The same patterns were also observed for starch content (Figure 4C). Significantly higher rates of synthesized and total starch content (about 3.4 times higher; 4.4 mg glucose/g FW in S1 transgenic compared to 1.3 mg glucose/g FW in WT seedlings after 9 h, and about twice higher; 5.5 mg glucose/g FW in S1 transgenic compared to 2.8 mg glucose/g FW in WT seedlings after 12 h of light treatment, respectively) were detected after the light treatment in transgenic seedlings exposed to L.9/D.15 and L.12/D.12 than in the WT seedlings. Seedlings exposed to L.24/D.0 showed a 63% increase in starch (from 4.9 to 8.0 mg glucose/g FW) in the S1 transgenic, compared to 37% (from 3.7 to 5.0 mg glucose/g FW) in the WT seedlings after 24 h of light treatment. We found no difference in starch degradation rate after the dark treatment, but

starch content was higher in the transgenic than in WT seedlings. These data suggest that, degradation of starch is not involved in the increase of sucrose during the light treatment, as presented below.

The variations in soluble sugars are shown in Figures 4D–G, and sucrose revealed the most interesting results. Small quantities of sucrose were detected in the S1 transgenic and WT seedlings after 3 and 6 h of light during the day, but the respective trends were differed. The WT seedlings tended to increase sucrose, whereas the transgenic seedlings showed a decreasing trend, clearly indicating the function of upregulated sucrose-degrading SuSy activity in the transgenic seedlings. However, we found significantly more sucrose in transgenic than in the WT seedlings after 9 and 12 h of light during the day. About three times more (6.8 mg/g FW in S1 transgenic compared to 2.3 mg/g FW in WT seedlings) was detected after light treatment for 9 h, and 2.9 times more (13.5 mg/g FW in S1 transgenic compared to 4.7 mg/g FW in WT seedlings) were detected after 12 h of light (Figure 4E), which contributed to the dramatic increase in TSS in the transgenic relative to that in the WT seedlings (Figure 4D). As mentioned, starch was also significantly higher in the samples (Figure 4C), confirming that the increased sucrose was not the result of starch degradation. Sucrose tended to decrease after the dark treatment in both the transgenic and WT seedlings, but the rate of decrease was significantly higher in the transgenic than in WT seedlings, suggesting that the ectopically expressed SuSy properly displayed a sucrose-degrading SuSy function after photosynthetic sucrose synthesis was interrupted. The results also showed that, about two times more sucrose was produced in the exposed to L.24/D.0 transgenic than in the WT seedlings (19.7 mg/g FW in the S1 transgenic compared to 9.9 mg/g FW in the WT; Figure 4E). These data suggest that photosynthetic sucrose synthesis was strongly induced in the transgenic seedlings receiving light for 9 h/day, which was closely related to upregulated SPS and SPP activities in the source cells (Figures 1J,K). This resulted in the production of large amounts of sucrose. In addition, insufficient amounts of sucrose in the transgenic seedlings seemed to be due to the effects of ectopically expressed SuSy, shown by the reduced quantity of sucrose produced in a plants exposed to short day length. Similarly, a significantly higher quantity of fructose was detected in the transgenic than in WT seedlings: about 1.4 times higher (9.9 mg/g FW in S1 transgenic compared to 7.0 mg/g FW in WT seedlings), and about 2.2 times higher (20.4 mg/g FW in S1 transgenic compared to 9.4 mg/g FW in WT seedlings), after 9 and 12 h of light/day, respectively (Figure 4G), but no difference in glucose was observed (Figure 4F). The data from different light/dark treatment experiment show that variations in sucrose indicate the existence of a sucrose signaling pathway and show how seedlings are influenced by different durations of photosynthesis.

In summary, we first demonstrated that the increase in sucrose during upregulated sucrose-degrading SuSy activity was directly due to enhanced photosynthesis and photosynthetic sucrose synthesis. However, these improvements were triggered and driven by an unknown sucrose signaling pathway that exists in the condition of the more abundant of SuSy protein is presented in whole organs of the transgenic tobacco plants.

We propose that the sucrose signaling pathway triggers the following photosynthetic response cells in order: (1) acceleration of photosynthetic efficiency by increasing chlorophyll synthesis enhances the production and releases of TP from chloroplasts into the cytosol; and (2) the abundance of TP leads to upregulated photosynthetic sucrose synthesis by enhancing *SPS* and *SPP* transcriptional levels, leading to increased sucrose.

Photosynthetic and non-photosynthetic cells in plants communicate to convey nutrient status within the plant body; however, the nature of the nutrient signals and how such signals activate meristems to provide a sustained supply of new cells for plant growth is poorly understood. Our results strongly support the vital role of sucrose during plant growth and development. The more abundant presence of SuSy protein may be the cause of a novel sucrose signaling pathway, which, in turn, increases photosynthetic efficiency, and stimulates photosynthetic sucrose synthesis to allow the plants to cope with the sucrose demand. Our data help explain why heterologous SuSy activity leads to increased sucrose content and pronounced phenotypic and morphological changes in the transgenic tobacco plants (Figure 5).

CONCLUSION

Sucrose is synthesized in photosynthetic cells and transported to non-photosynthetic cells and other regions to cope with energy demands during plant growth and development. Sucrose also acts as a signal to regulate its status between photosynthetic

and non-photosynthetic cells. Besides the previously known sugar signaling mechanisms, which help plants change their development to adapt to energy conditions and the surrounding environment, we describe a novel sucrose signaling pathway that allows plants to respond to constant changes in sucrose status by regulating photosynthesis and photosynthetic sucrose synthesis. The existence of this signaling pathway is strengthened by the same phenomena during sugar metabolism, by chlorophyll, photosynthetic efficiency, and photosynthetic sucrose synthesis, and also by the pronounced phenotypic changes corresponding to increased sucrose in all six SuSy transgenic plants examined herein, which had a preference for sucrose-degrading SuSy activity. Future studies should focus on understanding the precise nature of the signaling and control mechanisms associated with increased plant sugar synthesis and biomass accumulation.

ACKNOWLEDGMENTS

This work was supported by Priority Centers Program (2010-0020141) through the National Research Foundation of Korea (NRF) funded by the Ministry of Education, Science and technology, Republic of Korea.

SUPPLEMENTARY MATERIAL

The Supplementary Material for this article can be found online at: <http://journal.frontiersin.org/article/10.3389/fpls.2015.01216>

REFERENCES

- Ames, B. N. (1966). “[10] Assay of inorganic phosphate, total phosphate and phosphatases,” in *Methods in Enzymology*, ed V. G. Elizabeth and F. Neufeld (Amsterdam: Academic Press), 115–118.
- Angeles-Núñez, J., and Tiessen, A. (2010). Arabidopsis sucrose synthase 2 and 3 modulate metabolic homeostasis and direct carbon towards starch synthesis in developing seeds. *Planta* 232, 701–718. doi: 10.1007/s00425-010-1207-9
- Angeles-Núñez, J., and Tiessen, A. (2012). Regulation of AtSUS2 and AtSUS3 by glucose and the transcription factor LEC2 in different tissues and at different stages of Arabidopsis seed development. *Plant Mol. Biol.* 78, 377–392. doi: 10.1007/s11103-011-9871-0
- Auffray, C., and Rougeon, F. (1980). Purification of mouse immunoglobulin heavy-chain messenger RNAs from total myeloma tumor RNA. *Eur. J. Biochem.* 107, 303–314. doi: 10.1111/j.1432-1033.1980.tb06030.x
- Baker, A., Graham, I. A., Holdsworth, M., Smith, S. M., and Theodoulou, F. L. (2006). Chewing the fat: β-oxidation in signalling and development. *Trends Plant Sci.* 11, 124–132. doi: 10.1016/j.tplants.2006.01.005
- Baroja-Fernández, E., Muñoz, F. J., Montero, M., Etxeberria, E., Sesma, M. T., Ovecka, M., et al. (2009). Enhancing sucrose synthase activity in transgenic potato (*Solanum tuberosum* L.) tubers results in increased levels of starch, ADPGlucose and UDPGlucose and total yield. *Plant Cell Physiol.* 50, 1651–1662. doi: 10.1093/pcp/pcp108
- Baud, S., Vaultier, M. N., and Rochat, C. (2004). Structure and expression profile of the sucrose synthase multigene family in *Arabidopsis*. *J. Exp. Bot.* 55, 397–409. doi: 10.1093/jxb/erh047
- Bauer, J., Hiltbrunner, A., and Kessler, F. (2001). Molecular biology of chloroplast biogenesis: gene expression, protein import and intraorganellar sorting. *Cell. Mol. Life Sci.* 58, 420–433. doi: 10.1007/PL00000867
- Baxter, C. J., Foyer, C. H., Turner, J., Rolfe, S. A., and Quick, W. P. (2003). Elevated sucrose-phosphate synthase activity in transgenic tobacco sustains photosynthesis in older leaves and alters development. *J. Exp. Bot.* 54, 1813–1820. doi: 10.1093/jxb/erg196
- Beale, S. (1999). Enzymes of chlorophyll biosynthesis. *Photosyn. Res.* 60, 43–73. doi: 10.1023/A:1006297731456
- Bédard, J., and Jarvis, P. (2005). Recognition and envelope translocation of chloroplast preproteins. *J. Exp. Bot.* 56, 2287–2320. doi: 10.1093/jxb/eri243
- Bernier, G., Havelange, A., Houssa, C., Petitjean, A., and Lejeune, P. (1993). Physiological signals that induce flowering. *Plant Cell* 5, 1147–1155. doi: 10.1105/tpc.5.10.1147
- Berry, J. O., Yerramsetty, P., Zielinski, A., and Mure, C. (2013). Photosynthetic gene expression in higher plants. *Photosyn. Res.* 117, 91–120. doi: 10.1007/s11120-013-9880-8
- Bieniawska, Z., Paul Barratt, D. H., Garlick, A. P., Thole, V., Kruger, N. J., Martin, C., et al. (2007). Analysis of the sucrose synthase gene family in *Arabidopsis*. *Plant J.* 49, 810–828. doi: 10.1111/j.1365-313X.2006.03011.x
- Bodson, M., and Outlaw, W. H. (1985). Elevation in the sucrose content of the shoot apical meristem of *Sinapis alba* at floral evocation. *Plant Physiol.* 79, 420–424. doi: 10.1104/pp.79.2.420
- Castillon, A., Shen, H., and Huq, E. (2007). Phytochrome interacting factors: central players in phytochrome-mediated light signaling networks. *Trends Plant Sci.* 12, 514–521. doi: 10.1016/j.tplants.2007.10.001
- Chen, S., Hajirezaei, M., Peisker, M., Tschiersch, H., Sonnewald, U., and Börnke, F. (2005). Decreased sucrose-6-phosphate phosphatase level in transgenic tobacco inhibits photosynthesis, alters carbohydrate partitioning, and reduces growth. *Planta* 221, 479–492. doi: 10.1007/s00425-004-1458-4
- Chiou, T.-J., and Bush, D. R. (1998). Sucrose is a signal molecule in assimilate partitioning. *Proc. Natl. Acad. Sci. U.S.A.* 95, 4784–4788. doi: 10.1073/pnas.95.8.4784
- Chourey, P. S., Taliercio, E. W., Carlson, S. J., and Ruan, Y. L. (1998). Genetic evidence that the two isozymes of sucrose synthase present in developing maize

- endosperm are critical, one for cell wall integrity and the other for starch biosynthesis. *Mol. Gen. Genet.* 259, 88–96. doi: 10.1007/s004380050792
- Coello, P., Hey, S. J., and Halford, N. G. (2011). The sucrose non-fermenting-1-related (SnRK) family of protein kinases: potential for manipulation to improve stress tolerance and increase yield. *J. Exp. Bot.* 62, 883–893. doi: 10.1093/jxb/erq331
- Coleman, H. D., Ellis, D. D., Gilbert, M., and Mansfield, S. D. (2006). Up-regulation of sucrose synthase and UDP-glucose pyrophosphorylase impacts plant growth and metabolism. *Plant Biotechnol. J.* 4, 87–101. doi: 10.1111/j.1467-7652.2005.00160.x
- Coleman, H. D., Yan, J., and Mansfield, S. D. (2009). Sucrose synthase affects carbon partitioning to increase cellulose production and altered cell wall ultrastructure. *Proc. Natl. Acad. Sci. U.S.A.* 106, 13118–13123. doi: 10.1073/pnas.0900188106
- Deprost, D., Yao, L., Sormani, R., Moreau, M., Leterreux, G., Nicolaï, M., et al. (2007). The *Arabidopsis* TOR kinase links plant growth, yield, stress resistance and mRNA translation. *EMBO Rep.* 8, 864–870. doi: 10.1038/sj.embo.7401043
- Eveland, A. L., and Jackson, D. P. (2012). Sugars, signalling, and plant development. *J. Exp. Bot.* 63, 3367–3377. doi: 10.1093/jxb/err379
- Farré, E. M., and Weise, S. E. (2012). The interactions between the circadian clock and primary metabolism. *Curr. Opin. Plant Biol.* 15, 293–300. doi: 10.1016/j.pbi.2012.01.013
- Farrar, J. F., and Williams, M. L. (1991). The effects of increased atmospheric carbon dioxide and temperature on carbon partitioning, source-sink relations and respiration. *Plant Cell Environ.* 14, 819–830. doi: 10.1111/j.1365-3040.1991.tb01445.x
- Fernie, A. R., Tiessen, A., Stitt, M., Willmitzer, L., and Geigenberger, P. (2002). Altered metabolic fluxes result from shifts in metabolite levels in sucrose phosphorylase-expressing potato tubers. *Plant Cell Environ.* 25, 1219–1232. doi: 10.1046/j.1365-3040.2002.00918.x
- Finch-Savage, W. E., and Leubner-Metzger, G. (2006). Seed dormancy and the control of germination. *New Phytol.* 171, 501–523. doi: 10.1111/j.1469-8137.2006.01787.x
- Francis, D., and Halford, N. (2006). Nutrient sensing in plant meristems. *Plant Mol. Biol.* 60, 981–993. doi: 10.1007/s11103-005-5749-3
- Gaudin, V., Lunness, P. A., Fobert, P. R., Towers, M., Riou-Khamlichi, C., Murray, J., et al. (2000). The expression of D-cyclin genes defines distinct developmental zones in snapdragon apical meristems and is locally regulated by the cycloidea gene. *Plant Physiol.* 122, 1137–1148. doi: 10.1104/pp.122.4.1137
- Geigenberger, P., and Stitt, M. (1991). A “futile” cycle of sucrose synthesis and degradation is involved in regulating partitioning between sucrose, starch and respiration in cotyledons of germinating *Ricinus communis* L. seedlings when phloem transport is inhibited. *Planta* 185, 81–90. doi: 10.1007/bf00194518
- Geigenberger, P., and Stitt, M. (1993). Sucrose synthase catalyses a readily reversible reaction *in vivo* in developing potato tubers and other plant tissues. *Planta* 189, 329–339. doi: 10.1007/BF00194429
- Geigenberger, P., and Stitt, M. (2000). Diurnal changes in sucrose, nucleotides, starch synthesis and AGPS transcript in growing potato tubers that are suppressed by decreased expression of sucrose phosphate synthase. *Plant J.* 23, 795–806. doi: 10.1046/j.1365-313x.2000.00848.x
- Graf, A., and Smith, A. M. (2011). Starch and the clock: the dark side of plant productivity. *Trends Plant Sci.* 16, 169–175. doi: 10.1016/j.tplants.2010.12.003
- Grandjean, O., Vernoux, T., Laufs, P., Belcram, K., Mizukami, Y., and Traas, J. (2004). *In vivo* analysis of cell division, cell growth, and differentiation at the shoot apical meristem in *Arabidopsis*. *Plant Cell* 16, 74–87. doi: 10.1105/tpc.017962
- Hajirezaei, M.-R., Peisker, M., Tschersch, H., Palatnik, J. F., Valle, E. M., Carrillo, N., et al. (2002). Small changes in the activity of chloroplastic NADP+-dependent ferredoxin oxidoreductase lead to impaired plant growth and restrict photosynthetic activity of transgenic tobacco plants. *Plant J.* 29, 281–293. doi: 10.1046/j.0960-7412.2001.01209.x
- Halford, N. G., Hey, S., Jhurreea, D., Laurie, S., McKibbin, R. S., Paul, M., et al. (2003). Metabolic signalling and carbon partitioning: role of Snf1-related (SnRK1) protein kinase. *J. Exp. Bot.* 54, 467–475. doi: 10.1093/jxb/erg038
- Hauch, S., and Magel, E. (1998). Extractable activities and protein content of sucrose-phosphate synthase, sucrose synthase and neutral invertase in trunk tissues of *Robinia pseudoacacia* L. are related to cambial wood production and heartwood formation. *Planta* 207, 266–274. doi: 10.1007/s004250050482
- Hayashi, L., Faria, G. M., Nunes, B., Zitta, C., Scariot, L., Rover, T., et al. (2011). Effects of salinity on the growth rate, carrageenan yield, and cellular structure of *Kappaphycus alvarezii* (Rhodophyta, Gigartinales) cultured *in vitro*. *J. Appl. Phycol.* 23, 439–447. doi: 10.1007/s10811-010-9595-6
- Helmer, G., Casadaban, M., Bevan, M., Kayes, L., and Chilton, M.-D. (1984). A new chimeric gene as a marker for plant transformation: the expression of *Escherichia coli* [beta]-galactosidase in sunflower and tobacco Cells. *Nat. Biotech.* 2, 520–527. doi: 10.1038/nbt0684-520
- Huber, S. C., and Huber, J. L. (1996). Role and regulation of sucrose-phosphate synthase in higher plants. *Annu. Rev. Plant Physiol. Plant Mol. Biol.* 47, 431–444. doi: 10.1146/annurev.applant.47.1.431
- Hussain, M., Hartwell Allen L. Jr., and Bowes, G. (1999). Up-regulation of sucrose phosphate synthase in rice grown under elevated CO₂ and temperature. *Photosyn. Res.* 60, 199–208. doi: 10.1023/A:1006242001390
- Jiang, Y., Guo, W., Zhu, H., Ruan, Y. L., and Zhang, T. (2012). Overexpression of GhSusA1 increases plant biomass and improves cotton fiber yield and quality. *Plant Biotechnol. J.* 10, 301–312. doi: 10.1111/j.1467-7652.2011.00662.x
- King, S. P., Lunn, J. E., and Furbank, R. T. (1997). Carbohydrate content and enzyme metabolism in developing canola siliques. *Plant Physiol.* 114, 153–160.
- Koch, K. (2004). Sucrose metabolism: regulatory mechanisms and pivotal roles in sugar sensing and plant development. *Curr. Opin. Plant Biol.* 7, 235–246. doi: 10.1016/j.pbi.2004.03.014
- Koornneef, M., Bentsink, L., and Hilhorst, H. (2002). Seed dormancy and germination. *Curr. Opin. Plant Biol.* 5, 33–36. doi: 10.1016/S1369-5266(01)00219-9
- Kötting, O., Kossmann, J., Zeeman, S. C., and Lloyd, J. R. (2010). Regulation of starch metabolism: the age of enlightenment? *Curr. Opin. Plant Biol.* 13, 320–328. doi: 10.1016/j.pbi.2010.01.003
- Lastdrager, J., Hanson, J., and Smeekens, S. (2014). Sugar signals and the control of plant growth and development. *J. Exp. Bot.* 65, 799–807. doi: 10.1093/jxb/ert474
- Leivar, P., and Quail, P. H. (2011). PIFs: pivotal components in a cellular signaling hub. *Trends Plant Sci.* 16, 19–28. doi: 10.1016/j.tplants.2010.08.003
- Li, J., Barroja-Fernández, E., Bahaji, A., Munoz, F. J., Ovecka, M., Montero, M., et al. (2013). Enhancing sucrose synthase activity results in increased levels of starch and ADP-glucose in maize (*Zea mays* L.) seed endosperms. *Plant Cell Physiol.* 54, 282–294. doi: 10.1093/pcp/pcs180
- Lichtenthaler, H. K. (1987). “[34] Chlorophylls and carotenoids: pigments of photosynthetic biomembranes,” in *Methods in Enzymology*, ed R. D. Lester (Packer: Academic Press), 350–382.
- Liu, Z., Zhang, Y., Liu, R., Hao, H., Wang, Z., and Bi, Y. (2011). Phytochrome interacting factors (PIFs) are essential regulators for sucrose-induced hypocotyl elongation in *Arabidopsis*. *J. Plant Physiol.* 168, 1771–1779. doi: 10.1016/j.jplph.2011.04.009
- Lunn, J. E., Ashton, A. R., Hatch, M. D., and Heldt, H. W. (2000). Purification, molecular cloning, and sequence analysis of sucrose-6F-phosphate phosphohydrolase from plants. *Proc. Natl. Acad. Sci. U.S.A.* 97, 12914–12919. doi: 10.1073/pnas.230430197
- Lunn, J. E., and Furbank, R. T. (1997). Localisation of sucrose-phosphate synthase and starch in leaves of C4 plants. *Planta* 202, 106–111. doi: 10.1007/s004250050108
- Medford, J. I., Elmer, J. S., and Klee, H. J. (1991). Molecular cloning and characterization of genes expressed in shoot apical meristems. *Plant Cell* 3, 359–370. doi: 10.1101/tpc.3.4.359
- Moon, J., Zhu, L., Shen, H., and Huq, E. (2008). PIF1 directly and indirectly regulates chlorophyll biosynthesis to optimize the greening process in *Arabidopsis*. *Proc. Natl. Acad. Sci. U.S.A.* 105, 9433–9438. doi: 10.1073/pnas.0803611105
- Murashige, T., and Skoog, F. (1962). A revised medium for rapid growth and bio assays with tobacco tissue cultures. *Physiol. Plant.* 15, 473–497. doi: 10.1111/j.1399-3054.1962.tb08052.x
- Nagel, D. H., and Kay, S. A. (2012). Complexity in the wiring and regulation of plant circadian networks. *Curr. Biol.* 22, R648–R657. doi: 10.1016/j.cub.2012.07.025
- Philipp, K., Geis, T., Ilkavets, I., Oster, U., Schwenkert, S., Meurer, J., et al. (2007). Chloroplast biogenesis: the use of mutants to study the etioplast-chloroplast transition. *Proc. Natl. Acad. Sci. U.S.A.* 104, 678–683. doi: 10.1073/pnas.0610062104

- Pien, S., Wyrzykowska, J., and Fleming, A. J. (2001). Novel marker genes for early leaf development indicate spatial regulation of carbohydrate metabolism within the apical meristem. *Plant J.* 25, 663–674. doi: 10.1046/j.1365-313x.2001.01002.x
- Prasad, P. V. V., Boote, K. J., Vu, J. C. V., and Allen, L. H. Jr. (2004). The carbohydrate metabolism enzymes sucrose-P synthase and ADG-pyrophosphorylase in phaseolus bean leaves are up-regulated at elevated growth carbon dioxide and temperature. *Plant Sci.* 166, 1565–1573. doi: 10.1016/j.plantsci.2004.02.009
- Riou-Khamlich, C., Menges, M., Healy, J. M., and Murray, J. A. (2000). Sugar control of the plant cell cycle: differential regulation of arabidopsis D-type cyclin gene expression. *Mol. Cell. Biol.* 20, 4513–4521. doi: 10.1128/MCB.20.13.4513-4521.2000
- Robaglia, C., Thomas, M., and Meyer, C. (2012). Sensing nutrient and energy status by SnRK1 and TOR kinases. *Curr. Opin. Plant Biol.* 15, 301–307. doi: 10.1016/j.pbi.2012.01.012
- Rolland, F., Baena-Gonzalez, E., and Sheen, J. (2006). Sugar sensing and signaling in plants: conserved and novel mechanisms. *Annu. Rev. Plant Biol.* 57, 675–709. doi: 10.1146/annurev.arplant.57.032905.105441
- Ruan, Y. L. (2003). Suppression of sucrose synthase gene expression represses cotton fiber cell initiation, elongation, and seed development. *Plant Cell* 15, 952–964. doi: 10.1105/tpc.010108
- Salerno, G. L., and Curatti, L. (2003). Origin of sucrose metabolism in higher plants: when, how and why? *Trends Plant Sci.* 8, 63–69. doi: 10.1016/S1360-1385(02)00029-8
- Schmidt, J., Röhrig, H., John, M., Wienke, U., Stacey, G., Koncz, C., et al. (1993). Alteration of plant growth and development by Rhizobium nodA and nodB genes involved in the synthesis of oligosaccharide signal molecules. *Plant J.* 4, 651–658. doi: 10.1046/j.1365-313X.1993.04040651.x
- Schoof, H., Lenhard, M., Haecker, A., Mayer, K. F. X., Jürgens, G., and Lax, T. (2000). The stem cell population of arabidopsis shoot meristems is maintained by a regulatory loop between the CLAVATA and WUSCHEL genes. *Cell* 100, 635–644. doi: 10.1016/S0092-8674(00)80700-X
- Shalysko, N., Czarnecki, O., Peter, E., and Grimm, B. (2009). Expression of chlorophyll synthase is also involved in feedback-control of chlorophyll biosynthesis. *Plant Mol. Biol.* 71, 425–436. doi: 10.1007/s11103-009-9532-8
- Shin, J., Anwer, M. U., and Davis, S. J. (2013). Phytochrome-Interacting Factors (PIFs) as bridges between environmental signals and the circadian clock: diurnal regulation of growth and development. *Mol. Plant* 6, 592–595. doi: 10.1093/mp/sst060
- Skylar, A., Sung, F., Hong, F., Chory, J., and Wu, X. (2011). Metabolic sugar signal promotes Arabidopsis meristematic proliferation via G2. *Dev. Biol.* 351, 82–89. doi: 10.1016/j.ydbio.2010.12.019
- Smith, A. M., and Stitt, M. (2007). Coordination of carbon supply and plant growth. *Plant Cell Environ.* 30, 1126–1149. doi: 10.1111/j.1365-3040.2007.01708.x
- Stitt, M., and Zeeman, S. C. (2012). Starch turnover: pathways, regulation and role in growth. *Curr. Opin. Plant Biol.* 15, 282–292. doi: 10.1016/j.pbi.2012.03.016
- Sun, J., Zhang, J., Larue, C. T., and Huber, S. C. (2011). Decrease in leaf sucrose synthesis leads to increased leaf starch turnover and decreased RuBP regeneration-limited photosynthesis but not Rubisco-limited photosynthesis in Arabidopsis null mutants of SPSA1. *Plant Cell Environ.* 34, 592–604. doi: 10.1111/j.1365-3040.2010.02265.x
- Tanaka, R., Koshino, Y., Sawa, S., Ishiguro, S., Okada, K., and Tanaka, A. (2001). Overexpression of chlorophyllide a oxygenase (CAO) enlarges the antenna size of photosystem II in *Arabidopsis thaliana*. *Plant J.* 26, 365–373. doi: 10.1046/j.1365-313X.2001.2641034.x
- Tiessen, A., and Padilla-Chacon, D. (2013). Subcellular compartmentation of sugar signalling: links among carbon cellular status, route of sucrolysis, sink-source allocation, and metabolic partitioning. *Front. Plant Sci.* 3:306. doi: 10.3389/fpls.2012.00306
- Traas, J., and Bohn-Courseau, I. (2005). Cell proliferation patterns at the shoot apical meristem. *Curr. Opin. Plant Biol.* 8, 587–592. doi: 10.1016/j.pbi.2005.09.004
- Vu, J. C. V., Gesch, R. W., Pennanen, A. H., Allen Hartwell, L. Jr., Boote, K. J., and Bowes, G. (2001). Soybean photosynthesis, Rubisco, and carbohydrate enzymes function at supraoptimal temperatures in elevated CO₂. *J. Plant Physiol.* 158, 295–307. doi: 10.1078/0176-1617-00290
- Wi, S., Chung, B., Kim, J.-S., Chae, H., Park, Y., An, B., et al. (2006). Immuno-localization of peroxidase in pumpkin (*Cucurbita ficifolia* Bouché) seedlings exposed to high-dose gamma ray. *J. Plant Biol.* 49, 180–185. doi: 10.1007/BF03031015
- Williams, L., and Fletcher, J. C. (2005). Stem cell regulation in the Arabidopsis shoot apical meristem. *Curr. Opin. Plant Biol.* 8, 582–586. doi: 10.1016/j.pbi.2005.09.010
- Wind, J., Smeeekens, S., and Hanson, J. (2010). Sucrose: metabolite and signaling molecule. *Phytochemistry* 71, 1610–1614. doi: 10.1016/j.phytochem.2010.07.007
- Wu, X., Dabi, T., and Weigel, D. (2005). Requirement of homeobox gene STIMPY/WOX9 for Arabidopsis meristem growth and maintenance. *Curr. Biol.* 15, 436–440. doi: 10.1016/j.cub.2004.12.079
- Xu, S. M., Brill, E., Llewellyn, D. J., Furbank, R. T., and Ruan, Y. L. (2012). Overexpression of a potato sucrose synthase gene in cotton accelerates leaf expansion, reduces seed abortion, and enhances fiber production. *Mol. Plant* 5, 430–441. doi: 10.1093/mp/ssr090
- Zheng, Y., Anderson, S., Zhang, Y., and Garavito, R. M. (2011). The structure of sucrose synthase-1 from *Arabidopsis thaliana* and its functional implications. *J. Biol. Chem.* 286, 36108–36118. doi: 10.1074/jbc.M111.275974

Conflict of Interest Statement: The authors declare that the research was conducted in the absence of any commercial or financial relationships that could be construed as a potential conflict of interest.

Copyright © 2016 Nguyen, Luan, Wi, Bae, Lee and Bae. This is an open-access article distributed under the terms of the Creative Commons Attribution License (CC BY). The use, distribution or reproduction in other forums is permitted, provided the original author(s) or licensor are credited and that the original publication in this journal is cited, in accordance with accepted academic practice. No use, distribution or reproduction is permitted which does not comply with these terms.



How Very-Long-Chain Fatty Acids Could Signal Stressful Conditions in Plants?

Antoine De Bigault Du Granrut¹ and Jean-Luc Cacas^{1,2*}

¹ UMR1318 Institut National de la Recherche Agronomique-AgroParisTech, Centre Institut National de la Recherche Agronomique de Versailles-Grignon, Institut Jean-Pierre Bourgin, Versailles, France, ² Département Sciences de la Vie et Santé, AgroParisTech, UFR de Physiologie Végétale, Paris, France

Although encountered in minor amounts in plant cells, very-long-chain fatty acids exert crucial functions in developmental processes. When their levels are perturbed by means of genetic approaches, marked phenotypic consequences that range from severe growth retardation to embryo lethality was indeed reported. More recently, a growing body of findings has also accumulated that points to a potential role for these lipids as signals in governing both biotic and abiotic stress outcomes. In the present work, we discuss the latter theory and explore the ins and outs of very-long-chain fatty acid-based signaling in response to stress, with an attempt to reconcile two supposedly antagonistic parameters: the insoluble nature of fatty acids and their signaling function. To explain this apparent dilemma, we provide new interpretations of pre-existing data based on the fact that sphingolipids are the main reservoir of very-long-chain fatty acids in leaves. Thus, three non-exclusive, molecular scenarii that involve these lipids as membrane-embedded and free entities are proposed.

Keywords: very-long-chain fatty acids, biotic and abiotic stress, signaling cascades, sphingolipids, membrane microdomains, plasma membrane, endoplasmic reticulum, secretory pathway

OPEN ACCESS

Edited by:

Sylvain Jeandroz,
Agrosup Dijon, France

Reviewed by:

Christina Kuehn,
Humboldt University of Berlin,
Germany

Susanne Hoffmann-Benning,
Michigan State University, USA

*Correspondence:

Jean-Luc Cacas
jean-luc.cacas@agroparistech.fr;
cacasjl@yahoo.fr

Specialty section:

This article was submitted to
Plant Physiology,
a section of the journal
Frontiers in Plant Science

Received: 02 July 2016

Accepted: 20 September 2016

Published: 18 October 2016

Citation:

De Bigault Du Granrut A and Cacas J-L (2016) How Very-Long-Chain Fatty Acids Could Signal Stressful Conditions in Plants? *Front. Plant Sci.* 7:1490.
doi: 10.3389/fpls.2016.01490

INTRODUCTION

Both abiotic and biotic stresses, as well as developmental cues, have long been known to drastically modify lipid composition—including fatty acid (FA) content—at the organ level. For instance, it is well-documented that phosphate starvation reorients lipid anabolism from phospholipid toward galactolipid synthesis (Kobayashi et al., 2006), likely for maintaining plant cell homeostasis until the constraint is relieved. Likewise, temperature-induced stress provokes changes in plasma membrane (PM) physico-chemical properties due to modification of sterol concentration and FA double bond index (Los and Murata, 2004). Progressive loss of chloroplast galactolipids is also a well-defined hallmark of foliar senescence processes (Jia and Li, 2015). Furthermore, plant resistance to pathogens can cause the consumption of chloroplast-originating polyunsaturated fatty acids for supplying an oxidative pathway that orchestrates host cell dismantling (Cacas et al., 2005). Obviously, all these events, whether or not associated with stress acclimation, are relevant to profound structural alterations and mobilize huge amounts of lipids that can be readily quantified by regular biochemical methods. By contrast, one can easily imagine that lipid-contingent signaling events relies on more subtle changes. This is perfectly illustrated by the case of phosphatidic acid, a conserved stress signaling molecule produced by either phospholipase D or the coordinated action of phospholipase C and diacylglycerol kinase (Guo et al., 2011). Because of its low abundance, phosphatidic acid is commonly evidenced by *in vivo* isotopic labeling experiments

(Arisz et al., 2009; Cacas et al., 2016a). Another example that could be cited is that of the FA-derived hormonal signal jasmonic acid that requires highly sensitive liquid chromatography-based methods for efficient quantification (Glauser and Wolfender, 2013; Cacas et al., 2016b). Additionally, to the best of our knowledge, marked degradation of the respective lipid substrates alimenting the two latter signaling cascades were rarely correlated with signal generation. Hence, this hints the importance of carefully considering, whenever possible, absolute concentrations of metabolites involved when discriminating among signaling events and structural changes. What about very-long-chain fatty acids (VLCFA)? How are they synthesized? And, how their levels are affected in response to stress?

BIOSYNTHESIS OF VERY-LONG-CHAIN FATTY ACIDS IN PLANT CELLS

In plants, lipid metabolism is highly compartmentalized and this intricate organellar networks allows fine-tuned regulation of the intracellular catabolic/anabolic balance for approximately several thousands of molecular lipid species. Biosynthesis of FA-containing lipids—mostly phospholipids, galactolipids, sphingolipids, triacylglycerides, and to a lesser extent, acylsteryl-glycosides—relies on two interacting metabolic routes: the “*prokaryotic pathway*” that resides in plastids and the “*eukaryotic pathway*” that is localized to endoplasmic reticulum (ER). Basically, production of FA-building units is initiated in plastids by the fatty acid synthase (FAS) complex II that uses malonyl-CoA and acetyl-CoA as co-substrates and NADPH as reductant. Each FAS-mediated cycle adds 2 carbons to acyl-CoA chains until molecules reaches a length of 16 or 18 carbons. Combined thioesterase and acyl-CoA synthetase activities are then invoked in active export of aliphatic chains from stroma to cytoplasm, where this pool of activated molecules is used by the ER for further chain length extension (Li-Beisson et al., 2010).

Very-long-chain fatty acids, formally defined as FA longer than 18 carbons, are extended by an ER membrane-embedded protein complex of 4 enzymes, acting presumably on the cytosolic side (see Haslam and Kunst, 2013 for an updated review). Fatty acid elongase activity results in successive action of β -ketoacyl-CoA synthase (KCS), β -ketoacyl-CoA reductase (KCR), β -hydroxyacyl-CoA dehydratase (HCD), and enoyl-CoA

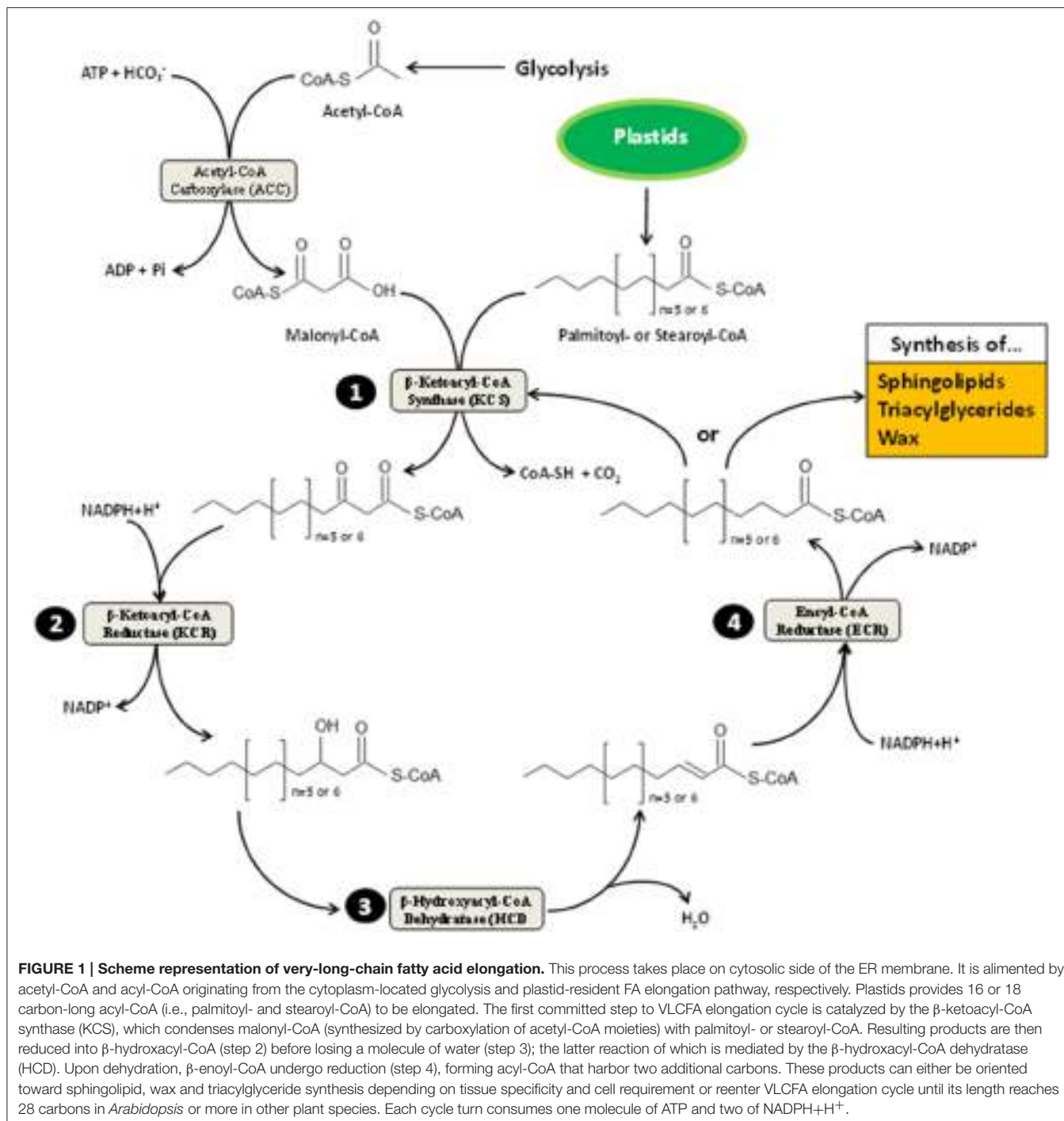
reductase (ECR). Each of these enzymes utilizes as substrate the product of the previous one in cycles beginning by malonyl-CoA condensation to long-chain acyl-CoA (Figure 1). Except for ECR, which is a single copy-encoded gene in *Arabidopsis thaliana*, a huge multigenic family composed of 21 members codes for tissue-specific KCS enzymes (Joubès et al., 2008) that are thought to dictate the length of acyl-CoA chains produced by the complex (Fehling and Mukherjee, 1991; Millar and Kunst, 1997). Both KCR and HCD are encoded by 2 independent genes, dubbed *KCS1/KCS2* and *PASTICCINO2/PTPLA*, respectively (Table 1). Such a complexity could suggest that multiple elongase complexes, which differ by their relative composition, coexist in ER membranes. In other words, functionally spatialized-domains with large metabolon units could orient the lipid class into which very-long-acyl chains are incorporated. But, only indirect evidence for this kind of ER sub-compartmentation were reported so far (Shockley et al., 2006). VLCFA are mainly present in the impermeable cuticular wax layer deposited at the plant aerial organ surface, in triacylglycerides found in seed oil and in sphingolipids, which act as structural elements in lipid bilayers forming endomembranes and PM (Bach and Faure, 2010).

CHANGES IN VERY-LONG-CHAIN FATTY ACID LEVELS IN PLANT CELLS UNDERGOING STRESS

With respect to modifications of VLCFA concentrations under stressful conditions, sparse data have been obtained but clear trends are currently emerging (Table 2). Overall, numerous abiotic constraints (salt, cold, hypoxia, heavy metal exposure...) were reported to increase VLCFA contents in distinct plant species. Induced *Arabidopsis* resistance to bacterial pathogens seems also associated with an augmentation of endogenous VLCFA levels (Raffaele et al., 2008). Not surprisingly, detailed lipid analysis revealed that VLCFA, which are both components and precursors of epicuticular wax, are affected by drought stress and bacterial infection in proportions which are clearly relevant to structural changes (Raffaele et al., 2008; Zhu and Xiong, 2013). This experimental fact makes full sense as cuticle is involved in limiting stomata-independent evaporation in shoots, suggesting a reinforcement of this hydrophobic layer under water stress. In the context of pathogen invasion, strengthening the apoplastic barrier is also a well-known defense phenomenon (Garcion et al., 2014), believed to prevent further micro-organism penetration and spreading.

Pioneering works pointed out the transcriptional activation of genes coding for members of the *Arabidopsis* ER-localized elongase complex in response to stress. It has been demonstrated that multiple KCS-encoding genes were responsive to light conditions, dehydration, salt, cold, and osmotic stresses (Joubès et al., 2008). Mutants deficient for the transcription factor MYB30 were proven to be unable to accumulate WT levels of VLCFA under hypoxia (Xie et al., 2015). In addition, microarray experiments showed that 3 out of the 21 KCS genes (*KCS1*, *KCS2*, and *KCS10*), one HCD gene (*PASTICCINO 2*)

Abbreviations: ACBP, Acyl-CoA Binding Protein; ACD5/11, ACCELERATED CELL DEATH 5/11; BII, BAX INHIBITOR 1; Cer, ceramide; Cer-P, ceramide phosphate; CerS, ceramide synthase; CoA, coenzyme A; DIM, detergent-insoluble membranes; ECR, enoyl-CoA reductase; EIX2, ETHYLENE-INDUCING XYLANASE 2; ER, endoplasmic reticulum; ES, endomembrane system; FAH1, fatty acid hydroxylase 1; FFAR/GPAR, FREE FATTY ACID RECEPTORS/G PROTEIN-COUPLED RECEPTORS; FA, fatty acid; FAH, fatty acid hydroxylase; FAS, fatty acid synthase; GA, Golgi apparatus; GFP, green fluorescent protein; GIPC, glycosyl-inositolphosphoryl-ceramide; GluCer, glucosylceramide; HCD, hydroxyacyl-CoA dehydratase; (h)VLCFA, (2-hydroxy-)very-long-chain fatty acid; IPCS, inositolphosphoryl-ceramide synthase; KCR, β -ketoacyl-CoA reductase; KCS, β -ketoacyl-CoA synthase; LCB, long-chain base; LCB-P, long-chain base phosphate; LOH, LAG ONE HOMOLOG; MPK6, MITOGEN-ACTIVATED PROTEIN KINASE 6; NADPH, Nicotinamide Adénine Dinucléotide Phosphate; PM, plasma membrane; PR1, PATHOGENESIS-RELATED 1; SPT, serine-palmitoyl-CoA transferase; TGN, trans-Golgi network.



and the only *ECR* gene (*CER10*) were transcriptionally up-regulated during incompatible interaction with bacteria, and the consecutive increase in VLCFA levels was confirmed by biochemical approach. This transcriptional reprogramming was further shown to be under the control of *MYB30* (Raffaele et al., 2008). Although elongase regulation could account for cuticle structure readjustment, one cannot rule out the possibility that it could reflect an unusual context where VLCFA-contingent changes hide signaling cascades. Arguing in favor of this idea

are several lines of evidence. Firstly, concentrations of VLCFA mobilized in many instances described in the literature are all the more sufficient for signaling purposes (Table 2). Secondly, except for drought stress (Zhu and Xiong, 2013), no data can currently explain clearly the role of VLCFA in certain specific abiotic contexts (like cold stress, mechanical injury and others) by the solely bias of cuticle. Thirdly, other lipids than wax components, such as complex sphingolipids that are potential reservoirs of signal molecules (Gronnier et al., 2016), exhibit

TABLE 1 | Nomenclature of the VLCFA elongase complex-encoding genes.

Gene names	Other gene names	Loci (AGI)	Protein activity	Protein length (aa)	M.W. (kDa)	pI
KCS1	-	At1g01120	β -ketoacyl-CoA synthase (catalyzes the first committed step to VLCFA synthesis)	528	59.28	8.9
KCS2	-	At1g04220		528	59.53	9.6
KCS3	-	At1g07720		478	54.33	9.5
KCS4	-	At1g19440		516	57.84	9.1
KCS5	CER60	At1g25450		492	55.65	8.9
KCS6	CER6, CUT1, POP1	At1g68530		497	56.40	9.1
KCS7	-	At1g71160		460	51.50	8.3
KCS8	-	At2g15090		481	54.19	9.4
KCS9	-	At2g16280		512	57.97	9.4
KCS10	FDH	At2g26250		550	61.96	9.3
KCS11	-	At2g26640		509	57.81	9.6
KCS12	-	At2g28630		476	53.97	9.0
KCS13	HIC	At2g46720		466	52.18	9.3
KCS14	-	At3g10280		459	51.63	9.4
KCS15	-	At3g52160		451	51.11	9.7
KCS16	-	At4g34250		493	55.78	9.1
KCS17	-	At4g34510		487	54.91	9.7
KCS18	FAE1	At4g34520		506	56.26	9.8
KCS19	-	At5g04530		464	52.61	8.6
KCS20	-	At5g43760		529	59.31	9.2
KCS21	-	At5g49070		464	52.56	9.3
KCR1	-	At1g67730	ketoacyl-CoA reductase	318	35.76	9.9
KCR2	-	At1g24470		312	35.00	9.8
HCD	PAS2	At5g10480	β -hydroxyacyl-CoA dehydratase	230	26.41	9.7
PTPLA	-	At5g59770		272	30.96	10
ECR	CER10, GLH6	At3g55360	enoyl-CoA reductase	310	35.72	9.7

This table provides information on regular gene names, additional designations found in the literature and referenced loci based on the *Arabidopsis* Genome Initiative (AGI). Demonstrated or potential enzymatic activities of the corresponding proteins are also indicated. Protein length is expressed as the number of amino acids (aa). M.W. and pI refers to molecular weight and isoelectric point, respectively. Most data were retrieved from The *Arabidopsis* Information Resource (TAIR) website (<https://www.arabidopsis.org/>) and crossed with the *Arabidopsis* book chapter dedicated to acyl-lipid metabolism (Li-Beisson et al., 2010). Abbreviations: CER6, 10 and 60, ECRIFERUM 6, 10 and 60; CUT1, CUTICULAR 1; FAE1, FATTY ACID ELONGATION 1; FDH, FIDDLEHEAD; GLH6, GLASSY HAIR 6; HIC, HIGH CARBON DIOXIDE; PAS2, PASTICCINO 2; POP1, POLLEN-PISTIL INCOMPATIBILITY 1; PTPLA, PROTEIN-TYROSINE PHOSPHATASE-LIKE.

significant changes in their VLCFA contents following stress (Table 2). Lastly, transgenic lines that displayed VLCFA over-accumulation correlated with enhanced pathogen-contingent cell death phenotype (Raffaele et al., 2008). Given that cuticle-related processes are unlikely to control programmed cell death, it must be envisaged that VLCFA exert their putative effects on cell fate in an alternative manner. Thus, it seems reasonable to investigate the concept that VLCFA could participate to stress signaling pathway.

ARE FREE VERY-LONG-CHAIN FATTY ACIDS GENUINE SIGNALING MOLECULES?

In humans, lipid homeostasis is tightly controlled, and its long-term perturbation can have severe deleterious effects on health. Free FA contribute to the regulation of organ

and tissue homeostasis by acting as signaling molecules through autocrine or paracrine cell non-autonomous modes. Extracellular free FA concentrations can be finely perceived by plasma membrane-localized protein receptors that discriminate among chain lengths. These are named FREE FATTY ACID RECEPTORS (FFAR)/G PROTEIN-COUPLED RECEPTORS (GPAR) (Ichimura et al., 2014). In plant genomes, no genes coding for such orthologous receptors could be retrieved by sequence comparison (unpublished data). Besides, even when a number of long-chain acyl-CoA binding proteins (ACBP) were reported to participate in plant stress tolerance (Xiao and Chye, 2011), it seems that they rather function as general regulators of lipid metabolism than as cognate signaling partners of acyl chains in challenged cells. For instance, AtACBP2 and AtACBP4 were found to physically interact with an ethylene-responsive transcription factor (Li and Chye, 2004; Li et al., 2008), possibly controlling by this means lipid-related gene expression. Another issue for VLCFA to be considered as genuine signals relies on

TABLE 2 | Changes in VLCFA levels under stressful conditions.

Plant models	Stresses	FA phenotypes	Affected lipid classes*	Analyzed organs	References
<i>Nigella sativa</i> L.	Mild Zn ²⁺ exposure	Increase in 20:0, 22:0 and 24:0	n.d.	Seeds	Marichali et al., 2016
		Increase in 20:0, 22:0 and 24:0 Decrease in 20:1	n.d.	Leaves	
		Increase in 20:1, 22:0 and 24:0 Decrease in 20:0	n.d.	Stems	
		Increase in 20:0, 22:0 and 24:0 Decrease in 20:1	n.d.	Roots	
<i>Noccaea caerulescens</i> , ecotype Mezica	Cd ²⁺ exposure	Decrease 26:0, 28:0 and 30:0	n.d.	-	Zemanová et al., 2015
		Increase in 20:2 and 20:3			
<i>Tetraselmis</i> sp. M8	Salt	Increase in 20:4 and 20:5	n.d.	-	Adarme-Vega et al., 2014
<i>Artemisia annua</i>	Long-term salinity	Decrease in 22:0 and 24:0 Increase in 22:1	n.d.	Leaves	Qureshi et al., 2013
<i>Taxus chinensis</i> cv. <i>mairei</i>	Shear stress	Increase in 20:0, 20:1, 22:0, 24:0 and 25:0	n.d.	Suspension cell culture from stem	Han et al., 2009
Rice (<i>Oriza sativa</i>)	Drought	Increase in 26:0 and 28:0	Cuticular wax	Leaves	Zhu and Xiong, 2013
<i>Arabidopsis thaliana</i>	Hypoxia	Increase in 22:0, 24:0 and 24:1	GIPC and GluCer	Leaves	Xie et al., 2015
<i>Arabidopsis thaliana</i>	Oxidative stress	Increase in total hVLCFA	n.d.	Leaves	Nagano et al., 2012
<i>Arabidopsis thaliana</i>	Cold	n.d.	Increase in GIPC	Shoots	Nagano et al., 2014
<i>Arabidopsis thaliana</i>	Pst DC3000::AvrRpm1	Total VLCFA	n.d.	Leaves	Raffaele et al., 2008

This table provides an overview of selected publications dealing with abiotic stress. Of note, to the best of our knowledge, the only published work reporting on biotic stress and VLCFA content is that of Raffaele et al. (2008). Nomenclature for fatty acids (FA) is as follows: the first number indicates the carbon chain length and the second the number of unsaturation (example: 24:1 is 24 carbon-long FA which possesses one double bond). n.d., not determined, * refers to the lipid classes whose VLCFA content is altered. Pst refers to *Pseudomonas syringae* pv. *tomato*.

their amphipathic nature that renders them strong membrane destabilizers and not prone to cross lipid bilayers. This certainly prevents unmodified VLCFA from functioning as soluble signals at both the intra—and extra-cellular levels. Therefore, alternative hypotheses must be imagined for explaining how these lipids could regulate plant stress responses. What could be the molecular mechanisms invoked? Based on the literature, three potentially interconnected scenarios taking into account the observed relatively high amounts of VLCFA mobilized during stress response are described hereafter.

“THE INDIRECT SPHINGOLIPID SIGNALING HYPOTHESES”–HOW TO RECONCILE VERY-LONG-CHAIN FATTY ACIDS WITH STRESS SIGNALING?

Plant sphingolipids encompass four major classes: long-chain bases (LCB), ceramides (Cer), glucosylceramides (GluCer), and

more complex glycosylated sphingolipids, known as glycosyl-inositolphosphoryl-ceramides (GIPC) (Figure 2A). Apart from GIPC, the synthesis of which is initiated in the ER and completed in the Golgi apparatus (GA), the three other classes are produced in the ER (Figure 2B). Neo-synthesis of LCB results from the condensation of serine and palmitoyl-CoA moieties catalyzed by a protein complex, so-called the serine-palmitoyl-CoA transferase (SPT). Subsequent reduction of the SPT product results in the synthesis of sphinganine, the precursor of the eight other LCB found in plants. Ceramide synthases (CerS), encoded by a multigenic family named after the yeast protein LAG ONE HOMOLOG (LOH), are responsible for the formation of the amide bond that links (V)LCA to LCB, leading to Cer formation. Ceramides can then be used as backbone for the production of GluCer and GIPC by addition of a glucose molecule or an inositolphosphoryl group followed by one or several glycosylation steps, respectively (Markham et al., 2013). Noteworthy, it can be inferred, on the basis of their biosynthetic pathway (Li-Beisson et al., 2010), and additional data (Pata

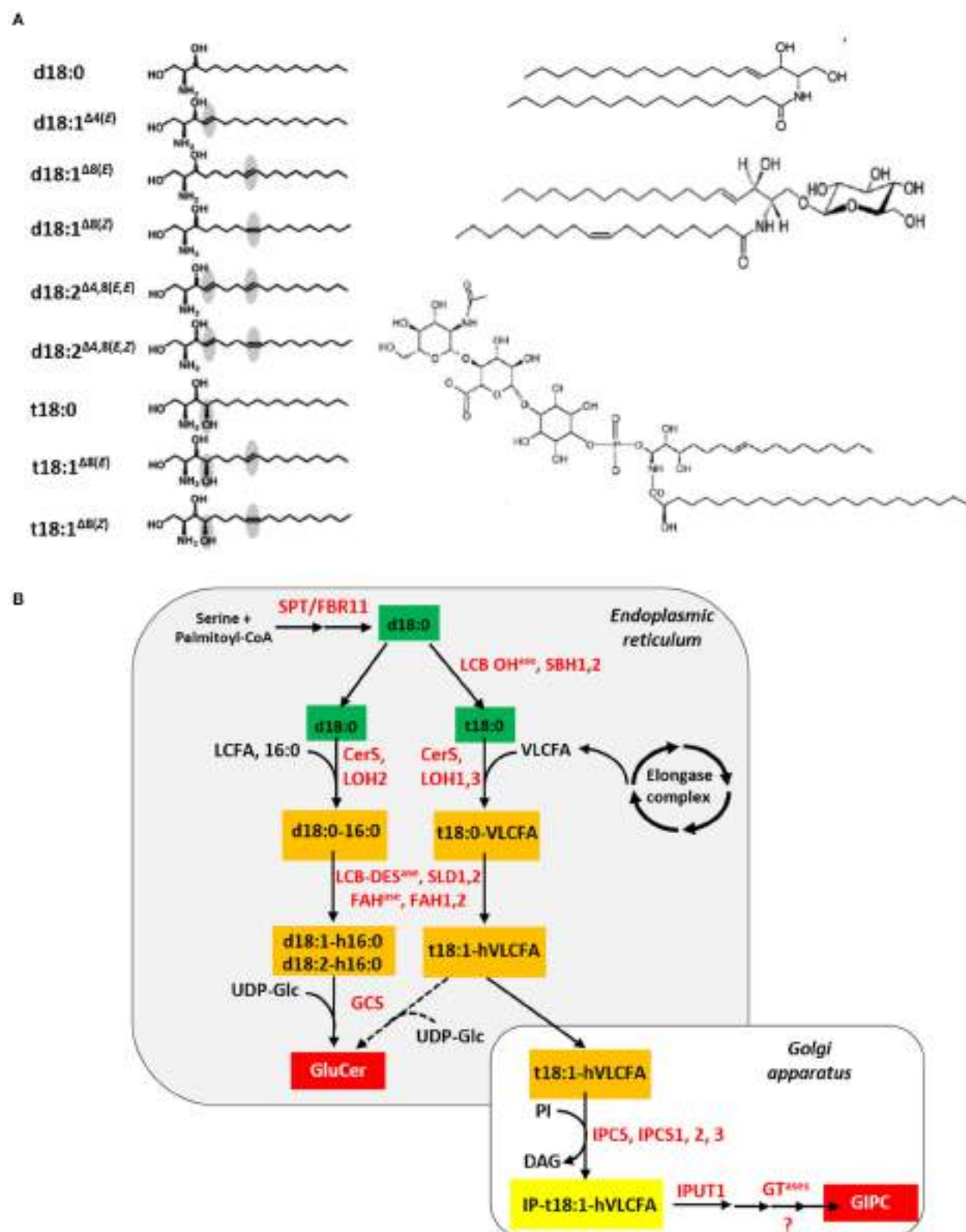


FIGURE 2 | Plant sphingolipid synthesis. (A) The four classes of plant sphingolipids (from Cacás et al., 2012a). The left panel displays the nine molecular species of long-chain bases found in plants, from top to bottom: sphinganine/dihydroosphingosine, d18:0; sphingosine/sphing-4(*trans*)-enine, d18:1 $\Delta^4(E)$; sphing-8(*trans*)-enine, d18:1 $\Delta^8(E)$; sphing-8(*cis*)-enine, d18:1 $\Delta^8(Z)$; sphinga-4,8(*trans, trans*)-dienine, d18:1 $\Delta^4,8(E,E)$; sphinga-4,8(*trans, cis*)-dienine, d18:1 $\Delta^4,8(E,Z)$; (Continued)

FIGURE 2 | Continued

phytosphingosine/4-hydroxy sphinganine, t18:0; 4-hydroxy sphing-8(*trans*)-enine, t18:1 Δ 8(*E*); 4-hydroxy sphing-8(*cis*)-enine, t18:1 Δ 8(*Z*). On the right panel (from top to bottom) are showed a ceramide (sphing-4(*trans*)-enine-*N*-octadecanoic acid), a glucosylceramide (Glucosyl-O- β -ceramide (sphing-4(*trans*)-enine-*N*-octadec-9(*cis*)-enoic acid)) and a glycosyl-inositolphosphoryl-ceramide (N-acetylglucosamine-glucuronic acid-inositolphosphoryl-ceramide (4-hydroxy sphing-8(*cis*)-enine-*N*-tetracosanoic acid)). **(B)** *In situ* simplified view of the plant sphingolipid biosynthesis pathway. Except for the serine and palmitoyl-CoA precursors, sphingolipid metabolites appear in colored rectangles: green for long-chain bases, orange for ceramides and red for final products like glucosylceramides (GluCer) and glycosyl-inositolphosphoryl-ceramides (GIPC). Nomenclature for ceramide is as follows: for instance, d18:0-16:0 indicates that the long-chain base corresponds to sphinganine and the fatty acid is a palmitoyl moiety, respectively. Enzymes are written in red. Abbreviations: CerS, ceramide synthase; DAG, diacylglycerol; FAH^{ase}, fatty acid hydroxylase; GCS, glucosylceramide synthase; GT^{ase}, glycosyl-transferase; IPCS, inositolphosphoryl-ceramide synthase; INPUT1, INOSITOLPHOSPHORYL-CERAMIDE GLUCURONOSYL-TRANSFERASE 1; LCB, long-chain base; LCB DES^{ase}, LCB desaturase; LCB OH^{ase}, LCB hydroxylase; LCFA, long-chain fatty acid; LOH, LAG ONE HOMOLOG; PI, phosphatidylinositol; SPT/FBR11, serine palmitoyl-CoA transferase/FUMONISIN-RESISTANT 11; SLD1,2, SPHINGOLIPID LCB Δ 8 DESAUTRASE 1,2; UDP-Glc, uridine diphosphate-glucose; VLCFA, very-long-chain fatty acid.

et al., 2010; Cacas et al., 2016c), that sphingolipids contain most VLCFA produced in leaves.

Scenario 1: Interplay between Very-Long-Chain Fatty Acids and the Ceramide and LCB Signals

Schematically, GIPC represent two third of total sphingolipids within photosynthetic plant cells whereas Glucer accounts for the other third (Markham et al., 2006). This is coherent with their role as structural membrane elements. By contrast, free Cer and LCB, as intermediate metabolites, are weakly present in leaf organs (Markham et al., 2006). Defining genuine molecular signals as locally- and timely-produced molecules that act at infinitesimal concentrations, it might not be surprising that the signaling function of both LCB and ceramides under stressful conditions could be conserved across kingdoms. Even though exact molecular substratum for sphingolipid control of cell fate is far from being deciphered, it is assumed that, in plants, like in animals, accumulation of free Cer or LCB would kill cells whereas that of their phosphorylated counterparts would have survival-promoting effects in response to stress. In plants, when chemically-perturbed or genetically-disrupted, most steps of the sphingolipid biosynthesis pathway can lead to conditional cell death phenotypes or spontaneous pathogen resistance-mimicking hypersensitive-like foliar lesions. These observations can be tentatively explained by a disequilibrium of the tightly-regulated intracellular balance between unfettered LCB and LCB-phosphate (LCB-P). Compelling evidence for this notion was provided by exogenous LCB application, the use of the mycotoxin fumonisin B1 that inhibits CerS and mutation (*fumonisin-resistant 11, fbr11*) in a subunit of the LCB-forming enzyme SPT (Alden et al., 2011; Berkey et al., 2012). Another crucial regulatory node may also rely on the Cer/Cer-phosphate (Cer-P) ratio, as substantiated by genetic data regarding the ceramide kinase ACCELERATED CELL DEATH 5 (Liang et al., 2003), the Cer-P transferase ACCELERATED CELL DEATH 11 (Simanshu et al., 2014) and inositolphosphoryl-ceramide synthase (IPCS) (Wang et al., 2008).

Recent work addressing *Arabidopsis* CerS specificity toward FA chain length *in vitro* established that LOH1/3 preferentially use VLCFA as substrates whereas LOH2 rather forms sixteen carbon-long fatty acid (16:0)-containing Cer (Luttgehrm et al., 2016). While LOH1/3 overexpressing lines showed only little changes in their sphingolipid profiles, a strong enrichment in Cer molecular species with 16:0 FA was recorded

for those that overexpressed LOH2. Additional phenotypical traits of the latter overexpressor plants were reminiscent of lesion-mimic mutants that exhibit enhanced disease resistance and develop hypersensitive cell death symptoms under restrictive environment, despite the absence of pathogens. These traits included increased salicylic acid concentrations and *PATHOGENESIS-RELATED 1* (PR1) gene expression, localized programmed cell death and severe dwarfism (Luttgehrm et al., 2015). Consistently, *loh1* null mutants displayed discrete spontaneous foliar lesions correlated with strong constitutive PR1 expression and significant elevation in 16:0-containing Cer and GluCer contents (Ternes et al., 2011). Although FA-mediated structural effects cannot totally be ruled out for explaining the aforementioned phenotypes (see below), these data may also pinpoint the importance of the aliphatic chain length present in Cer destined to signaling purposes, suggesting the occurrence of a supplementary regulatory level to that driven by the solely balance of phosphorylated/non-phosphorylated metabolites. In line with this postulate, it is thus tempting to speculate that stress-induced rise in VLCFA concentrations might alter intracellular Cer pool composition and, subsequently, impact related signaling routes. Moving further this way, it is also plausible that, following stress exposure, quantitative and/or qualitative modifications of VLCFA pool indirectly influence LCB synthesis due to metabolic reorientation, as suggested by the analysis of LCB hydroxylase mutants (Chen et al., 2008). The existence for two *Arabidopsis* sphingosine kinases with sharply different substrate specificity also reinforces the idea that both VLCFA and LCB chains could matter when it comes to signaling stress (Guo et al., 2011). Since the *Arabidopsis* MITOGEN-ACTIVATED PROTEIN KINASE 6 (MPK6) has been recently described as a downstream effector of sphingolipid-induced cell death (Saucedo-García et al., 2011), it could represent a privileged target for investigating the interplay between VLCFA and LCB/Cer-contingent signaling under stressful conditions.

Scenario 2: The Membrane Trafficking Link

The plant endomembrane system (ES) is a complex, dynamic and intricate membrane-composed web that encompasses the ER, Golgi apparatus (GA), trans-Golgi network (TGN), the endocytic, vacuolar, and autophagic compartments, the plasma membrane (PM) and all vesicles that shuttle in between these organelles. It provides infrastructure for the secretory pathway which is dedicated to both protein and lipid sorting (Cacas, 2010). Apart from its crucial role in maintaining cellular homeostasis,

the ES has also recently emerged as an essential component of plant tolerance to stress (for review, see Cacas, 2015) and, this may be linked to VLCFA-containing sphingolipids, like GluCer and GIPC.

Early indirect insights into a potential relationships between GluCer and protein trafficking came from clinical studies focused on molecular mechanisms underpinning Gaucher disease. A bench of mutations that totally or partially invalidate the two glucocerebrosidases-encoding genes—involved in lysosomal degradation of GluCer—was found to cause ER to dysfunction, leading to enzyme sorting impairment (Yu et al., 2007). In plants, regulation of GluCer homeostasis is as essential as in animal models. In *Arabidopsis*, only one gene codes for the ER-localized glucosylceramide synthase, or GCS. Null *gcs* mutants fail to develop beyond seedling stage and are defective for organogenesis. In addition, *gcs* ($-/-$) cells display altered GA morphology indicative of a probable perturbed cell secretion activity (Msanne et al., 2015). Accordingly, groundbreaking work carried out by the team of Dr. Moreau (CNRS, Bordeaux, France) pointed out that chemical blunting of GCS activity resulted in (i) GA disaggregation into vesicles, (ii) reduced externalization of an apoplastic fluorescent protein ectopically expressed (N-SecYFP), and (iii) both mislocalization and secretion diminishment of the PM-located H⁺-ATPase PMA4 (Melser et al., 2010). Transient overexpression of the two latter proteins (N-SecYFP and PMA4) in a WT genetic background was further reported to augment sterol and GluCer contents whereas that of soluble proteins and membrane proteins which do not traffic beyond GA was unable to do so (Melser et al., 2010). Combined, these findings put forward the case for GluCer, along with sterols, as potent protein sorting mediators in the late secretory pathway. Two main explanations can be envisaged in this context. On the one hand, one can assume that GluCer and sterols exerts their function through a chaperone-like activity, stabilizing native structure of specific integral membrane cargo proteins that they escort from GA to PM. On the other hand, it has been proposed that glycosphingolipids could impose positive curvature to membranes, thereby facilitating vesicle fusion (Barth et al., 2010; Molino et al., 2014). In this regard, the few data that are currently available in the literature do not allow discriminating among these two hypotheses yet.

Joined study between our team (Faure's lab, INRA, Versailles, France) and that of Markham (Danforth Plant Science Center, Saint Louis, Missouri, USA) documented the impact of *loh* mutations on *Arabidopsis* root architectural modifications in relation with sphingolipid profile and secretion of PM-resident proteins (Markham et al., 2011). As corroborated latter on by Luttgehrm et al. (2016), it was demonstrated that double *loh1/loh3* mutants overaccumulated 16:0-containing complex glycosphingolipids at the expense of VLCFA-containing ones, reflecting the substrate specificity of the remaining CerS activity borne by LOH2. Remarkably, this marked trend was correlated with PM-targeting default for two auxin carrier proteins; the latter of which being characterized by a loss of cell polarity, a strong inhibition of hormonal transport and the absence of lateral root initiation at macroscopic level. Again, experimental data argued in favor of a post-Golgi trafficking defect when

sphingolipid synthesis was manipulated (Markham et al., 2011). Together with those of Melser's work, our results provide unequivocal evidence for the requirement of VLCFA-containing sphingolipids for protein transport, even though the respective contribution of GluCer and GIPC in this process could not have been ascertained. Back to signaling topic, it is possible that VLCFA anabolism adjustment participate in accommodating cell secretory activity to challenging environmental conditions. In fact, several published examples already indicate that effective intracellular membrane trafficking is necessary for transducing specific protein-based signals during plant immunity (for reviews, see Berkey et al., 2012; Teh and Hofius, 2014). Among them can be cited the immune receptor EIX2 (ETHYLENE-INDUCING XYLANASE 2) from tomato plants, the endosomal internalization of which is necessary for mounting proper defense response (Sharfman et al., 2011). Another striking example is that of the relocalization of the RPW8 resistance protein to extrahaustorial membranes at the host-pathogen interface in response to specific fungi and oomycetes (Wang et al., 2009). Moreover, numerous protein regulators that control cell death outcome in response to abiotic and biotic stress are distributed along the ES (Cacas, 2015). This sustains the idea that VLCFA could define a late secretory pathway dedicated to some stress signaling components. One of the main challenges in next future will be to understand the role of one such path under abiotic constraints. Distinguishing how VLCFA could, respectively, influence antimicrobial protein burden to be excreted and transport of specific regulatory proteins following pathogen infection will probably represent a difficult task too.

Scenario 3: The Membrane Microdomain Hypothesis

Membrane microdomains can be defined as islands composed of lipids and proteins that laterally segregate from the rest of the PM. They are highly enriched in sterols, sphingolipids and signaling proteins (Boutté and Grebe, 2009). Their size was described to fit nanometer to micrometer scales. Originally named raft, microdomains were identified in mammalian systems where they notably act as platforms responsible for the launching of apoptotic and inflammation signaling cascades (Malorni et al., 2007; George and Wu, 2012). First experimental evidence for their occurrence in plants was provided by biochemical approaches based on the purification of detergent-insoluble membranes (DIM) through floatation on step sucrose gradient (Mongrand et al., 2004). Since then, accumulation of pharmacological, proteomic, microscopy, and genetic data ended the controversy on plant microdomain existence. Thus, it is now broadly accepted that DIM do not represent functional equivalents of microdomains, but rather constitutes one way of assessing their chemical composition (Cacas et al., 2012a).

Previously, a strong enrichment in tri-hydroxylated LCB in PM fractions purified from two plant species was reported (Borner et al., 2005; Lefebvre et al., 2007). Given that this class of LCB is mainly encountered in GIPC (for review, see Pata et al., 2010), this led the plant lipid community to the reasonable hypothesis that GIPC reside, for the most part,

in PM. Having established methods for purifying GIPC and characterizing their composition (Buré et al., 2011; Casas et al., 2012b), we tested for this assumption using tobacco plants and cell cultures. Not astonishingly, we found that (i) tobacco GIPC contain the large majority of the intracellular VLCFA

pool, and (ii) VLCFA moieties engaged in these lipids were predominantly hydroxylated on carbon position 2 (noted hVLCFA). Exploiting this unique opportunity for probing GIPC repartition within the ES uncovered a marked hVLCFA gradient along the secretory pathway that reaches an optimum in DIM

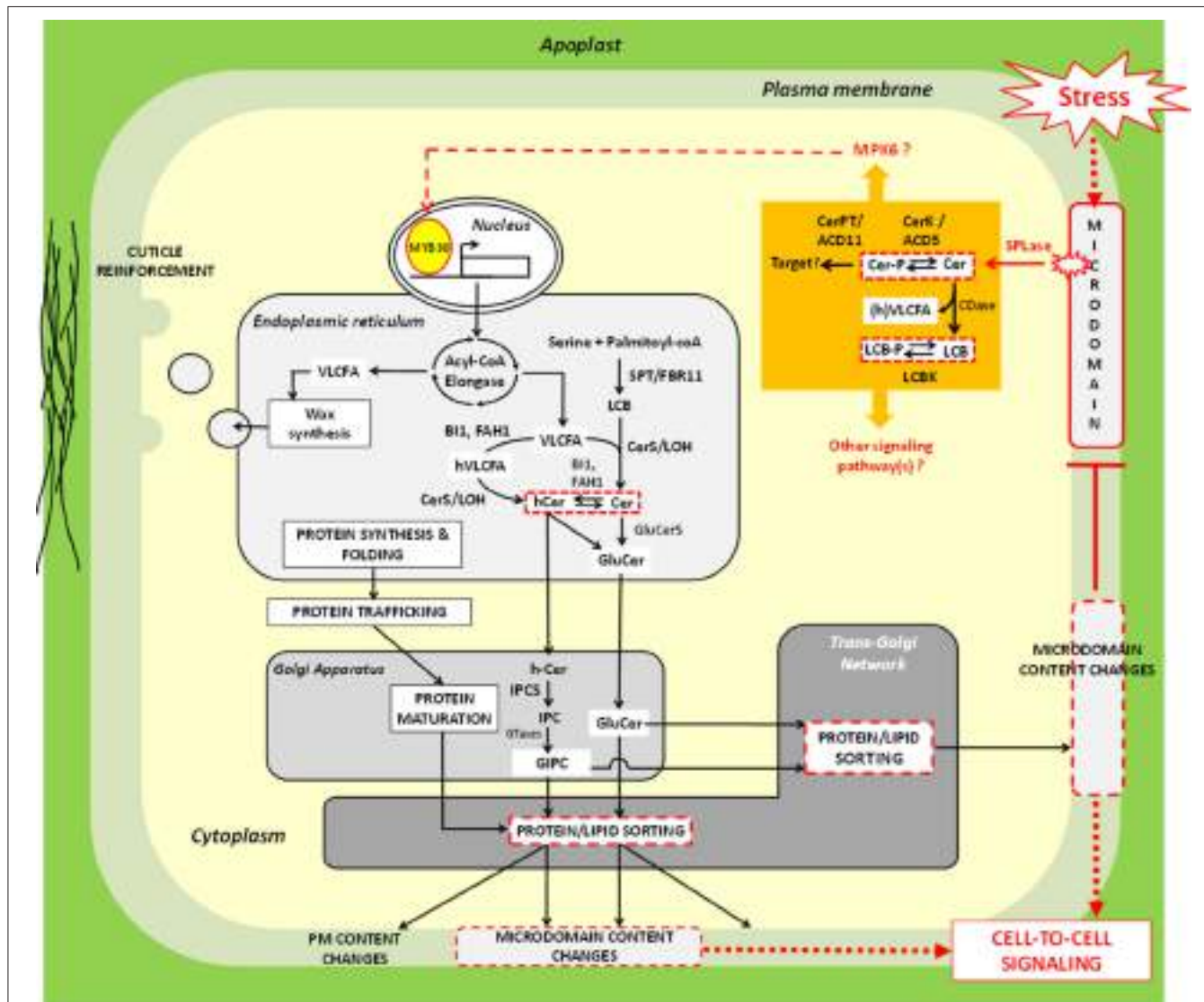


FIGURE 3 | Molecular model explaining how very-long-chain fatty acids could participate in stress signaling response in plant cells. In mammalian systems, extrinsic cues can be perceived at the plasma membrane by means of microdomains. A comparable hypothesis can be emitted for plant models. It is possible that “sphingolipase D” (SPLase) like the one identified by Tanaka et al. (2013) is recruited to microdomains following stress exposure, and releases ceramide (Cer) molecules from complex glycosphingolipids *in situ*. Free Cer could either directly act as signals or be processed into Cer-P by the kinase ACCELERATED CELL DEATH 5 (ACD5). The ceramide-1-phosphate transesterase ACCELERATED CELL DEATH 11 (ACD11) may participate to this signaling cascade as well, though its exact mode of action remains to be clarified. In addition, Cer could also be hydrolyzed by ceramidase (CDase) into LCB that can, in turn, be phosphorylated; one such activity have indeed been documented in plants (Pata et al., 2010). Although little is still known about molecular actors that relay LCB/Cer signals (orange part of the figure), the work of Saucedo-García et al. (2011) identified MITOGEN-ACTIVATED PROTEIN KINASE 6 (MPK6) as a good candidate for exerting this function. The transcription factor MYB30 represents a potential downstream target of sphingolipid-induced phosphorylation events, since it was found to up-regulate acyl-CoA elongase genes in response to environmental cues. Resulting very-long-chain fatty acid (VLCFA) production could then be utilized for strengthening cuticle, especially epicuticular wax. Alternatively, VLCFA could be incorporated into sphingolipids. Modifications of sphingolipid composition and/or level can impact protein sorting at the TGN and, therefore, probably modulate targeting of specific stress responsive signaling proteins to PM. From this postulate, it seems coherent to envisage that modifications of the secreted lipids and proteins influence PM lateral segregation. Expected consequences of this segregation phenomenon could be changes in microdomain content that could feature extracellular signaling process(es) and/or negative feedback regulation. Of note, elements in the picture that represent regulatory nodes involving VLCFA (Hypotheses 1–3) are delineated by red continue or discontinued lines. Red discontinued arrows indicate steps which has not been experimentally demonstrated. For additional abbreviations, refer to the legend of Figure 2.

fractions. Further investigations brought to light that GIPC amount to approximately 60 mole % of total DIM lipids; the polyglycosylated forms being only present in the external hemilayer and clustering in 35 nm-sized microdomains. Combined biophysical and modeling strategies also showed that hVLCFA could strongly interact with sterols and interdigitate between the two membrane leaflets, which likely explains the synergistic effect of GIPC and sterol in structuring membrane *in vitro* (Cacas et al., 2016c). Hence, in addition to their postulated role in protein sorting at the TGN, glycosphingolipids may also be involved in stress response with respect to their lateral segregation within PM.

Nagano et al. (2009, 2012) shed light on possible links between hVLCFA and stress acclimation. Working on the conserved family of ER-resident cell death regulators, known as BAX INHIBITORS (BI), the authors showed that At-BI1 interacts with the electron donor, cytochrome b5, the latter of which can in turn associate with FATTY ACID HYDROXYLASE1 (FAH1) catalyzing the hydroxylation of VLCFA. Overexpression of At-BI1 was also correlated with higher hVLCFA contents and decreased cell death under stressful conditions. Conversely, knock-down FAH1 plants displayed decreased hVLCFA amounts and enhanced sensitivity to hydrogen peroxide, suggesting that At-BI1 protects cells by activating FAH1. Now, given that hCer exhibit pro-survival properties in animal cells (Young et al., 2013), one can hypothesize that the hCer/Cer balance under the control of BI1/FAH1 dictates the progression rate of hypersensitive foliar lesions in response to pathogen attack. This attractive theory cannot, however, justify by itself MYB30-driven transcriptional induction of the elongase complex genes (Raffaele et al., 2008) and the resulting massive increase in VLCFA concentrations reported in this context. Alternatively, one can envisage that modulating hVLCFA synthesis could affect GIPC composition and/or concentration and, consequently, impact raft signaling events. *In vivo* and *in vitro* experiments have proven that lateral segregation of membrane proteins is dependent on that of lipids, and vice versa (for review, see Volmer and Ron, 2015). In animal systems, recruitment or disassembly of signaling actors can be achieved through respective coalescence or dissociation of microdomains, thereby provoking initiation or termination of signaling cascades at the PM (Malorni et al., 2007; George and Wu, 2012). A comparable situation has already been proposed to take place in BI1-overexpressing transgenics (Ishikawa et al., 2015) and during plant innate immunity (Keinath et al., 2010). In addition, both biotic and abiotic stresses are known to provoke changes in protein content of microdomains (Minami et al., 2009; Stanislas et al., 2009).

Findings that elongase complex-encoding genes are under transcriptional control upon environmental cues (Joubès et al., 2008; Raffaele et al., 2008; Xie et al., 2015) implies that modulation of hVLCFA steady-state levels is implicated in a secondary signaling wave, possibly regulating microdomain-coordinated events. Indeed, for transcriptional reprogramming to occur, stress perception must be completed and signal transduction engaged. This is quite distinct from, but not incompatible with the regular picture documented in the mammalian literature where external constraints are generally

described to promote rapid relocation of sphingolipid-modifying enzymes to microdomains, freeing Cer or LCB moieties and, *per se*, generating primary signals relayed by downstream effectors. Actually, one can expect that both situations could cohabit in the same challenged plant cell with different timing. In this case, raft sphingolipids could feature a reservoir of signals to be mobilized early following stress application, as sustained by the recent discovery of sphingolipase D activities in plants (Tanaka et al., 2013). Once initiated, such signaling cascades would contribute to activate hVLCFA neo-synthesis, ultimately fine-tuning microdomain composition. The latter phenomena could either benefit to intercellular communication or simply operate as a negative feedback that abrogate the production of signaling molecules by microdomains. Testing for this seductive concept will require a careful *in situ* dosage of hVLCFA-containing sphingolipids over time. With the recent advances in mass spectrometry-based chemical imaging, this deadlock should be broken in a close future.

TENTATIVE MODEL—PUZZLING OUT VERY-LONG-CHAIN FATTY ACID-CONTINGENT SIGNALING PATHWAYS

Although the involvement of VLCFA in stress response is not contestable, interpretation of this experimental fact may remain delicate in light of the currently available data. Pleiotropic consequences of VLCFA level alterations also render this task complicated. Based on the observation that VLCFA are highly enriched in sphingolipids, we have, however, suggested, and explored three non-exclusive, molecular scenarios to tentatively explain how insoluble molecules —like VLCFA—could participate in stress signaling response. These hypotheses, which are experimentally testable, are summarized in a model presented in the Figure 3. By analogy with animal systems, it is envisaged that stress perception could trigger recruitment of yet-to-be cloned “sphingolipases” to microdomains. Enzymatically-released Cer(-P) skeletons could then either directly serve as signals or be further processed, activating a potent downstream effector, the kinase MPK6. One possible target of this phosphorylation cascade could be the transcription factor MYB30, which is known to up-regulate expression of the elongase complex-encoded genes upon pathogen attack and hypoxia. As also supported by several studies, changes in the composition and/or level of VLCFA-containing lipids impact protein sorting at the TGN. This could represent a potential regulatory mechanism whereby targeting of specific signaling proteins to PM could be spatio-temporally modulated depending on stressed cell requirements. Adding a supplemental layer of regulation, these changes in sphingolipids certainly alter microdomain content, and consequently, should also influence PM-coordinated signaling events. Beyond the response plasticity conferred to plant cells by a dual lipid/protein-based rheostat, this model raises the interesting question as to how this molecular scheme

contributes to stress acclimation. Is this linked to intercellular communication, negative feedback control of microdomain-dependent signaling or both?

AUTHOR CONTRIBUTIONS

AD provided **Table 2**, JC defined hypotheses, wrote the manuscript, and drew figures.

REFERENCES

- Adarme-Vega, T. C., Thomas-Hall, S. R., Lim, D. K., and Schenk, P. M. (2014). Effects of long chain fatty acid synthesis and associated gene expression in microalga *Tetraselmis* sp. *Mar. Drugs.* 12, 3381–3398. doi: 10.3390/MD12063381
- Alden, K. P., Dhondt-Cordelier, S., McDonald, K. L., Reape, T. J., Ng, C. K., McCabe, P. F., et al. (2011). Sphingolipid long chain base phosphates can regulate apoptotic-like programmed cell death in plants. *Biochem. Biophys. Res. Commun.* 410, 574–580. doi: 10.1016/j.bbrc.2011.06.028
- Arisz, S. A., Testerink, C., and Munnik, T. (2009). Plant PA signaling via diacylglycerol kinase. *Biochim. Biophys. Acta.* 1791, 869–875. doi: 10.1016/j.bbalip.2009.04.006
- Bach, L., and Faure, J. D. (2010). Role of very-long-chain fatty acids in plant development, when chain length does matter. *C. R. Biol.* 333, 361–370. doi: 10.1016/j.crvi.2010.01.014
- Barth, B. M., Gustafson, S. J., Young, M. M., Fox, T. E., Shanmugavelandy, S. S., Kaiser, J. M., et al. (2010). Inhibition of NADPH oxidase by glucosylceramide confers chemoresistance. *Cancer Biol. Ther.* 10, 1126–1136. doi: 10.4161/cbt.10.11.13438
- Berkey, R., Bendigeri, D., and Xiao, S. (2012). Sphingolipids and plant defense/disease: the “death” connection and beyond. *Front. Plant Sci.* 3:68. doi: 10.3389/fpls.2012.00068
- Borner, G. H. H., Sherrier, J. D., Weimar, T., Michaelson, L. V., Hawkins, N. D., MacAskill, A., et al. (2005). Analysis of detergent-resistant membranes in *Arabidopsis*. Evidence for plasma membrane lipid rafts. *Plant Physiol.* 137, 104–116. doi: 10.1104/pp.104.053041
- Boutté, Y., and Grebe, M. (2009). Cellular processes relying on sterol function in plants. *Curr. Opin. Plant Biol.* 12, 705–713. doi: 10.1016/j.pbi.2009.09.013
- Buré, C., Casas, J. L., Wang, F., Domergue, F., Mongrand, S., and Schmitter, J. M. (2011). Fast screening of highly glycosylated plant sphingolipids by tandem mass spectrometry. *Rapid Commun. Mass Spectrom.* 25, 3131–3145. doi: 10.1002/rcm.5206
- Casas, J. L. (2010). Devil inside: does plant programmed cell death involve the endomembrane system? *Plant Cell Env.* 33, 1453–1473. doi: 10.1111/j.1365-3040.2010.02117.x
- Casas, J. L. (2015). “Out for a walk along the secretory pathway during programmed cell death,” in *Plant Programmed Cell Death*, eds A. H. Gunawardena and P. F. McCabe (Powell, WY: Springer), 123–161.
- Casas, J. L., Buré, C., Grosjean, K., Gerbeau-Pisot, P., Lherminier, J., Rombouts, Y., et al. (2016c). Revisiting plant plasma membrane lipids in tobacco: a focus on sphingolipids. *Plant Physiol.* 170, 367–384. doi: 10.1104/pp.15.00564
- Casas, J. L., Furt, F., Le Guédart, M., Bayer, E., Schmitter, J. M., Buré, C., et al. (2012a). Lipids of plant membrane rafts. *Prog. Lipid Res.* 51, 272–299. doi: 10.1016/j.plipres.2012.04.001
- Casas, J. L., Gerbeau-Pisot, P., Fromentin, J., Cantrel, C., Thomas, D., Jeannette, E., et al. (2016a). Diacylglycerol kinases activate tobacco NADPH oxidase-dependent oxidative burst in response to cryptogein. *Plant Cell Environ.* doi: 10.1111/pce.12771. [Epub ahead of print].
- Casas, J. L., Melser, S., Domergue, F., Joubès, J., Bourdenx, B., Schmitter, J. M., et al. (2012b). Rapid nanoscale quantitative analysis of plant sphingolipid long chain bases by GC-MS. *Anal. Bioanal. Chem.* 403, 2745–2755. doi: 10.1007/s00216-012-6060-1
- Casas, J. L., Pré, M., Pizot, M., Cissoko, M., Diedhiou, I., Jalloul, A., et al. (2016b). GhERF-IIb3 regulates accumulation of jasmonate and leads to enhanced cotton resistance to blight disease. *Mol. Plant Pathol.* doi: 10.1111/mpp.12445. [Epub ahead of print].
- Casas, J. L., Vailleau, F., Davoine, C., Ennar, N., Agnel, J. P., Tronchet, M., et al. (2005). The combined action of 9 lipoxygenase and galactolipase is sufficient to bring about programmed cell death during tobacco hypersensitive response. *Plant Cell Env.* 28, 1367–1378. doi: 10.1111/j.1365-3040.2005.01369.x
- Chen, M., Markham, J. E., Dietrich, C. R., Jaworski, J. G., and Cahoon, E. B. (2008). Sphingolipid long-chain base hydroxylation is important for growth and regulation of sphingolipid content and composition in *Arabidopsis*. *Plant Cell* 20, 1862–1878. doi: 10.1105/tpc.107.057851
- Fehling, E., and Mukherjee, K. D. (1991). Acyl-CoA elongase from a higher plant (*Lunaria annua*): metabolic intermediates of very-long chain acyl-CoA products and substrate specificity. *Biochim. Biophys. Acta* 1082, 239–246. doi: 10.1016/0005-2760(91)90198-q
- Garcion, C., Lamotte, O., Casas, J. L., and Métraux, J. P. (2014). “Mechanisms of defence to pathogens: biochemistry and physiology,” in *Induced Resistance For Plant Defence: A Sustainable Approach For Crop Protection*, eds D. Walters, A. Newton, and G. Lyon (West Sussex: Wiley-Blackwell), 106–136.
- George, K. S., and Wu, S. (2012). Lipid raft: a floating island of death or survival. *Toxicol. Appl. Pharmacol.* 259, 311–319. doi: 10.1016/j.taap.2012.01.007
- Glauser, G., and Wolfender, J. L. (2013). A non-targeted approach for extended liquid chromatography-mass spectrometry profiling of free and esterified jasmonates after wounding. *Methods Mol. Biol.* 1011, 123–134. doi: 10.1007/978-1-62703-414-2_10
- Gronnier, J., Germain, V., Gouguet, P., Casas, J. L., and Mongrand, S. (2016). GIPC: Glycosyl Inositol Phospho Ceramides, the major sphingolipids on earth. *Plant Signal. Behav.* 11:e1152438. doi: 10.1080/15592324.2016.1152438
- Guo, L., Mishra, G., Taylor, K., and Wang, X. (2011). Phosphatidic acid binds and stimulates *Arabidopsis* sphingosine kinases. *J. Biol. Chem.* 286, 13336–13345. doi: 10.1074/jbc.M110.190892
- Han, P. P., Zhou, J., and Yuan, Y. J. (2009). Analysis of phospholipids, sterols, and fatty acids in *Taxus chinensis* var. *mairei* cells in response to shear stress. *Biotechnol. Appl. Biochem.* 54, 105–112. doi: 10.1042/BAB20090102
- Haslam, T. M., and Kunst, L. (2013). Extending the story of very-long-chain fatty acid elongation. *Plant Sci.* 210, 93–107. doi: 10.1016/j.plantsci.2013.05.008
- Ichimura, A., Hasegawa, S., Kasubuchi, M., and Kimura, I. (2014). Free fatty acid receptors as therapeutic targets for the treatment of diabetes. *Front. Pharmacol.* 5:236. doi: 10.3389/fphar.2014.00236
- Ishikawa, T., Aki, T., Yanagisawa, S., Uchimiya, H., and Kawai-Yamada, M. (2015). Overexpression of BAX INHIBITOR-1 links plasma membrane microdomain proteins to stress. *Plant Physiol.* 169, 1333–1343. doi: 10.1104/pp.15.00445
- Jia, Y., and Li, W. (2015). Characterisation of lipid changes in ethylene-promoted senescence and its retardation by suppression of phospholipase D δ in *Arabidopsis* leaves. *Front. Plant Sci.* 6:1045. doi: 10.3389/fpls.2015.01045
- Joubès, J., Raffaele, S., Bourdenx, B., Garcia, C., Laroche-Traineau, J., Moreau, P., et al. (2008). The VLCFA elongase gene family in *Arabidopsis thaliana*: phylogenetic analysis, 3D modelling and expression profiling. *Plant Mol. Biol.* 67, 547–566. doi: 10.1007/s11103-008-9339-z
- Keinath, N. F., Kierszniewska, S., Lorek, J., Bourdais, G., Kessler, S. A., Shimosato-Asano, H., et al. (2010). PAMP (pathogen-associated molecular pattern)-induced changes in plasma membrane compartmentalization reveal novel components of plant immunity. *J. Biol. Chem.* 285, 39140–39149. doi: 10.1074/jbc.M110.160531

ACKNOWLEDGMENTS

We would like to warmly thank Dr. Palauqui JC (INRA, Versailles) for critical reading and enthusiastic discussions. We also would like to thank the editors for inviting us contributing to this special issue. We declare no conflict of interest with any works cited in this article. We apologize in advance for not citing colleagues’ research due to space limitation.

- Kobayashi, K., Masuda, T., Takamiya, K., and Ohta, H. (2006). lipid alteration during phosphate starvation is regulated by phosphate signaling and auxin/cytokinin cross-talk. *Plant J.* 47, 238–248. doi: 10.1111/j.1365-313X.2006.02778.x
- Lefebvre, B., Furt, F., Hartmann, M. A., Michaelson, L. V., Carde, J. P., Sargueil-Boiron, F., et al. (2007). Characterization of Lipid Rafts from *Medicago truncatula* root plasma membranes: a proteomic study reveals the presence of a raft-associated redox system. *Plant Physiol.* 144, 402–418. doi: 10.1104/pp.106.094102
- Li, H. Y., and Chye, M. L. (2004). *Arabidopsis* acyl-CoA-binding protein ACBP2 interacts with an ethylene-responsive element-binding protein, AtEBP, via its ankyrin repeats. *Plant Mol. Biol.* 54, 233–243. doi: 10.1023/B:PLAN.0000028790.75090.ab
- Li, H. Y., Xiao, S., and Chye, M. L. (2008). Ethylene- and pathogen-inducible *Arabidopsis* acyl-CoA-binding protein 4 interacts with an ethylene-responsive element binding protein. *J. Exp. Bot.* 59, 3997–4006. doi: 10.1093/jxb/ern241
- Liang, H., Yao, N., Song, J. T., Luo, S., Lu, H., and Greenberg, J. T. (2003). Ceramides modulate programmed cell death in plants. *Genes Dev.* 17, 2636–2641. doi: 10.1101/gad.1140503
- Li-Beisson, Y., Shorrosh, B., Beisson, F., Andersson, M. X., Arondel, V., Bates, P. D., et al. (2010). Acyl-Lipid Metabolism. *Arabidopsis Book* 8:e0133. doi: 10.1199/tab.0133
- Los, D. A., and Murata, N. (2004). Membrane fluidity and its roles in the perception of environmental signals. *Biochim. Biophys. Acta* 1666, 142–157. doi: 10.1016/j.bbamem.2004.08.002
- Luttgeharm, K. D., Cahoon, E. B., and Markham, J. E. (2016). Substrate specificity, kinetic properties and inhibition by fumonisin B1 of ceramide synthase isoforms from *Arabidopsis*. *Biochem. J.* 473, 593–603. doi: 10.1042/BJ20150824
- Luttgeharm, K. D., Chen, M., Mehra, A., Cahoon, R. E., Markham, J. E., and Cahoon, E. B. (2015). Overexpression of *Arabidopsis* ceramide synthases differentially affects growth, sphingolipid metabolism, programmed cell death, and mycotoxin resistance. *Plant Physiol.* 169, 1108–1117. doi: 10.1104/pp.15.00987
- Malorni, W., Giammarioli, A. M., Garofalo, T., and Sorice, M. (2007). Dynamics of lipid raft components during lymphocyte apoptosis: the paradigmatic role of GD3. *Apoptosis* 12, 941–949. doi: 10.1007/s10495-007-0757-1
- Marichali, A., Dallali, S., Ouerghemmi, S., Sebei, H., Casabianca, H., and Hosni, K. (2016). Responses of *Nigella sativa* L. to Zinc excess: focus on germination, growth, yield and yield components, lipid and terpene metabolism, and total phenolics and antioxidant activities. *J. Agric. Food Chem.* 64, 1664–1675. doi: 10.1021/acs.jafc.6b00274
- Markham, J. E., Li, J., Cahoon, E. B., and Jaworski, J. G. (2006). Separation and identification of major plant sphingolipid classes from leaves. *J. Biol. Chem.* 281, 22684–22694. doi: 10.1074/jbc.M604050200
- Markham, J. E., Lynch, D. V., Napier, J. A., Dunn, T. M., and Cahoon, E. B. (2013). Plant sphingolipids: function follows form. *Curr. Opin. Plant Biol.* 16, 350–357. doi: 10.1016/j.pbi.2013.02.009
- Markham, J. E., Molino, D., Gissot, L., Bellec, Y., Hématy, K., Marion, J., et al. (2011). Sphingolipids containing very-long-chain fatty acids define a secretory pathway for specific polar plasma membrane protein targeting in *Arabidopsis*. *Plant Cell* 23, 2362–2378. doi: 10.1105/tpc.110.080473
- Melser, S., Batailler, B., Peypelut, M., Poujol, C., Bellec, Y., Wattelet-Boyer, V., et al. (2010). Glucosylceramide biosynthesis is involved in Golgi morphology and protein secretion in plant cells. *Traffic* 11, 479–490. doi: 10.1111/j.1600-0854.2009.01030.x
- Millar, A. A., and Kunst, L. (1997). Very-long-chain fatty acid biosynthesis is controlled through the expression and specificity of the condensing enzyme. *Plant J.* 12, 121–131. doi: 10.1046/j.1365-313X.1997.12010121.x
- Minami, A., Fujiwara, M., Furuto, A., Fukao, Y., Yamashita, T., Kamo, M., et al. (2009). Alterations in detergent-resistant plasma membrane microdomains in *Arabidopsis thaliana* during cold acclimation. *Plant Cell Physiol.* 50, 341–359. doi: 10.1093/pcp/pcn202
- Molino, D., Van der Giessen, E., Gissot, L., Hématy, K., Marion, J., Barthelemy, J., et al. (2014). Inhibition of very long acyl chain sphingolipid synthesis modifies membrane dynamics during plant cytokinesis. *Biochim. Biophys. Acta* 1842, 1422–1130. doi: 10.1016/j.bbalip.2014.06.014
- Mongrand, S., Morel, J., Laroche, J., Claverol, S., Carde, J. P., Hartmann, M. A., et al. (2004). Lipid rafts in higher plant cells: purification and characterization of Triton X-100-insoluble microdomains from tobacco plasma membrane. *J. Biol. Chem.* 279, 36277–36286. doi: 10.1074/jbc.m403440200
- Msanne, J., Chen, M., Luttgeharm, K. D., Bradley, A. M., Mays, E. S., Paper, J. M., et al. (2015). Glucosylceramides are critical for cell-type differentiation and organogenesis, but not for cell viability in *Arabidopsis*. *Plant J.* 84, 188–201. doi: 10.1111/tpj.13000
- Nagano, M., Ihara-Ohori, Y., Imai, H., Inada, N., Fujimoto, M., Tsutsumi, N., et al. (2009). Functional association of cell death suppressor, *Arabidopsis* Bax inhibitor-1, with fatty acid 2-hydroxylation through cytochrome b₅. *Plant J.* 58, 122–134. doi: 10.1111/j.1365-313X.2008.03765.x
- Nagano, M., Ishikawa, T., Ogawa, Y., Iwabuchi, M., Nakasone, A., Shimamoto, K., et al. (2014). *Arabidopsis* Bax inhibitor-1 promotes sphingolipid synthesis during cold stress by interacting with ceramide-modifying enzymes. *Planta* 240, 77–89. doi: 10.1007/s00425-014-2065-7
- Nagano, M., Takahara, K., Fujimoto, M., Tsutsumi, N., Uchimiya, H., and Kawai-Yamada, M. (2012). *Arabidopsis* sphingolipid fatty acid 2-hydroxylases (AtFAH1 and AtFAH2) are functionally differentiated in fatty acid 2-hydroxylation and stress responses. *Plant Physiol.* 159, 1138–1148. doi: 10.1104/pp.112.199547
- Pata, M. O., Hannun, Y. A., and Ng, C. K. (2010). Plant sphingolipids: decoding the enigma of the Sphinx. *New Phytol.* 185, 611–630. doi: 10.1111/j.1469-8137.2009.03123.x
- Qureshi, M. I., Abdin, M. Z., Ahmad, J., and Iqbal, M. (2013). Effect of long-term salinity on cellular antioxidants, compatible solute and fatty acid profile of Sweet Annie (*Artemisia annua* L.). *Phytochemistry* 95, 215–223. doi: 10.1016/j.phytochem.2013.06.026
- Raffaele, S., Vailleau, F., Léger, A., Joubès, J., Miersch, O., Huard, C., et al. (2008). A MYB transcription factor regulates very-long chain fatty acid biosynthesis for activation of the hypersensitive cell death response in *Arabidopsis*. *Plant Cell* 20, 752–767. doi: 10.1105/tpc.107.054858
- Saucedo-García, M., Guevara-García, A., González-Solís, A., Cruz-García, F., Vázquez-Santana, S., Markham, J. E., et al. (2011). MPK6, sphinganine and the LCB2a gene from serine palmitoyltransferase are required in the signaling pathway that mediates cell death induced by long chain bases in *Arabidopsis*. *New Phytol.* 191, 943–957. doi: 10.1111/j.1469-8137.2011.03727.x
- Sharfman, M., Bar, M., Ehrlich, M., Schuster, S., Melech-Bonfil, S., Ezer, R., et al. (2011). Endosomal signaling of the tomato leucine-rich repeat receptor-like protein LeEix2. *Plant J.* 68, 413–423. doi: 10.1111/j.1365-313X.2011.04696.x
- Shockey, J. M., Gidda, S. K., Chapital, D. C., Kuan, J. C., Dhanoa, P. K., Bland, J. M., et al. (2006). Tung tree DGAT1 and DGAT2 have non redundant functions in triacylglycerol biosynthesis and are localized to different subdomains of the endoplasmic reticulum. *Plant Cell* 18, 2294–2313. doi: 10.1105/tpc.106.043695
- Simanshu, D. K., Zhai, X., Munch, D., Hofius, D., Markham, J. E., Bielawski, J., et al. (2014). *Arabidopsis* accelerated cell death 11, ACD11, is a ceramide-1-phosphate transfer protein and intermediary regulator of phytoceramide levels. *Cell Rep.* 6, 388–399. doi: 10.1016/j.celrep.2013.12.023
- Stanislas, T., Bouyssie, D., Rossignol, M., Vesa, S., Fromentin, J., Morel, J., et al. (2009). Quantitative proteomics reveals a dynamic association of proteins to detergent-resistant membranes upon elicitor signaling in tobacco. *Mol. Cell. Proteomics* 8, 2186–2198. doi: 10.1074/mcp.M900090-MCP200
- Tanaka, T., Kida, T., Imai, H., Morishige, J., Yamashita, R., Matsuoka, H., et al. (2013). Identification of a sphingolipid-specific phospholipase D activity associated with the generation of phytoceramide-1-phosphate in cabbage leaves. *FEBS J.* 280, 3797–3809. doi: 10.1111/febs.12374
- Teh, O. K., and Hofius, D. (2014). Membrane trafficking and autophagy in pathogen-triggered cell death and immunity. *J. Exp. Bot.* 65, 1297–1312. doi: 10.1093/jxb/ert441
- Ternes, P., Feussner, K., Werner, S., Lerche, J., Iven, T., Heilmann, I., et al. (2011). Disruption of the ceramide synthase LOH1 causes spontaneous cell death in *Arabidopsis thaliana*. *New Phytol.* 192, 841–854. doi: 10.1111/j.1469-8137.2011.03852.x
- Volmer, R., and Ron, D. (2015). Lipid-dependent regulation of unfolded protein response. *Curr. Opin. Cell Biol.* 33, 67–73. doi: 10.1016/j.ceb.2014.12.002
- Wang, W., Wen, Y., Berkey, R., and Xiao, S. (2009). Specific targeting of the *Arabidopsis* resistance protein RPW8.2 to the interfacial membrane encasing the fungal haustorium renders broad-spectrum resistance to powdery mildew. *Plant Cell* 21, 2898–2913. doi: 10.1105/tpc.109.067587

- Wang, W., Yang, X., Tangchaiburana, S., Ndeh, R., Markham, J. E., Tsegaye, Y., et al. (2008). An inositolphosphorylceramide synthase is involved in regulation of plant programmed cell death associated with defense in *Arabidopsis*. *Plant Cell* 20, 3163–3179. doi: 10.1105/tpc.108.060053
- Xiao, S., and Chye, M. L. (2011). New roles for acyl-CoA-binding proteins (ACBPs) in plant development, stress responses and lipid metabolism. *Prog. Lipid Res.* 50, 141–151. doi: 10.1016/j.plipres.2010.11.002
- Xie, L. J., Yu, L. J., Chen, Q. F., Wang, F. Z., Huang, L., Xia, F. N., et al. (2015). *Arabidopsis* acyl-CoA-binding protein ACBP3 participates in plant response to hypoxia by modulating very-long-chain fatty acid metabolism. *Plant J.* 81, 53–67. doi: 10.1111/tpj.12692
- Young, M. M., Kester, M., and Wang, H. G. (2013). Sphingolipids: regulators of crosstalk between apoptosis and autophagy. *J. Lipid Res.* 54, 5–19. doi: 10.1194/jlr.R031278
- Yu, Z., Sawkar, A. R., and Kelly, J. W. (2007). Pharmacologic chaperoning as a strategy to treat Gaucher disease. *FEBS J.* 274, 4944–4950. doi: 10.1111/j.1742-4658.2007.06042.x
- Zemanová, V., Pavlík, M., Kyjaková, P., and Pavlíková, D. (2015). Fatty acid profiles of ecotypes of hyperaccumulator *Noccaea caerulescens* growing under cadmium stress. *J. Plant Physiol.* 180, 27–34. doi: 10.1016/j.jplph.2015.02.012
- Zhu, X., and Xiong, L. (2013). Putative megaenzyme DWA1 plays essential roles in drought resistance by regulating stress-induced wax deposition in rice. *Proc. Natl. Acad. Sci. U.S.A.* 110, 17790–17795 doi: 10.1073/pnas.1316412110

Conflict of Interest Statement: The authors declare that the research was conducted in the absence of any commercial or financial relationships that could be construed as a potential conflict of interest.

Copyright © 2016 De Bigault Du Granrut and Cacas. This is an open-access article distributed under the terms of the Creative Commons Attribution License (CC BY). The use, distribution or reproduction in other forums is permitted, provided the original author(s) or licensor are credited and that the original publication in this journal is cited, in accordance with accepted academic practice. No use, distribution or reproduction is permitted which does not comply with these terms.



Carbon Monoxide as a Signaling Molecule in Plants

Meng Wang and Weibiao Liao*

College of Horticulture, Gansu Agricultural University, Lanzhou, China

Carbon monoxide (CO), a gaseous molecule, has emerged as a signaling molecule in plants, due to its ability to trigger a series of physiological reactions. This article provides a brief update on the synthesis of CO, its physiological functions in plant growth and development, as well as its roles in abiotic stress tolerance such as drought, salt, ultraviolet radiation, and heavy metal stress. CO has positive effects on seed germination, root development, and stomatal closure. Also, CO can enhance plant abiotic stress resistance commonly through the enhancement of antioxidant defense system. Moreover, CO shows cross talk with other signaling molecules including NO, phytohormones (IAA, ABA, and GA) and other gas signaling molecules (H_2S , H_2 , CH_4).

Keywords: abiotic stress, carbon monoxide (CO), growth and development, antioxidant defense, physiological role, signaling transduction

OPEN ACCESS

Edited by:

Sylvain Jeandroz,
AgroSup Dijon, France

Reviewed by:

John Hancock,
University of the West of England,
Bristol, UK
Gaurav Zinta,
Shanghai Center for Plant Stress
Biology, China

*Correspondence:

Weibiao Liao
liaowb@gsau.edu.cn

Specialty section:

This article was submitted to
Plant Physiology,
a section of the journal
Frontiers in Plant Science

Received: 23 February 2016

Accepted: 13 April 2016

Published: 29 April 2016

Citation:

Wang M and Liao W (2016) Carbon Monoxide as a Signaling Molecule in Plants. *Front. Plant Sci.* 7:572.
doi: 10.3389/fpls.2016.00572

INTRODUCTION

Carbon monoxide (CO), which has long been widely considered as a poisonous gas ("the silent killer") since 17th century, is a low molecular weight diatomic gas that occurs ubiquitously in nature. However, CO has been recently proven to be one of the most essential cellular components regulating a variety of biological processes both in animals and plants (Xie et al., 2008). Generally speaking, CO arises in biological systems principally during heme degradation as the oxidation product of the α -methylene bridge of heme, and this process is catalyzed by heme oxygenase enzymes (HOs, EC 1.14.14.18; Bilban et al., 2008). CO plays a critical role as neurotransmitter (Boehning et al., 2003), inhibitor of platelet aggregation (Brüne and Ullrich, 1987) and suppressor of acute hypertensive (Motterlini et al., 1998) in animals. Similarly, involvement of CO gas in different biological processes has also been found in plants. For instance, it acts as a compound with hormonal effects, affecting seed germination (Dekker and Hargrove, 2002), root development (Cui et al., 2015), and inducing stomatal closure (Cao et al., 2007a). In natural environments, plants develop inducible defence systems to survive biotic and abiotic threats, thus producing a wide variety of defense-related hormones to unlock the defense-related regulatory networks. CO is also generated against oxidant damage under abiotic stress, such as drought stress (Liu et al., 2010), salt stress (Ling et al., 2009), and heavy metal stress (Meng et al., 2011). In addition, CO not only acts as a signaling molecule during plant growth and development, but also interacts with other signaling molecules in plant stress response, growth and development (Santa-Cruz et al., 2010; Lin et al., 2014; Xie et al., 2014). In view of the evidence described above, we provide a brief update here on CO synthesis, physiological function in plant growth and development and its response to abiotic stresses. Furthermore, the cross-talk between CO and other signaling molecules including phytohormone, hydrogen peroxide (H_2O_2), and other small gas signaling molecules is also discussed.

SYNTHESIS OF CO IN PLANTS

Carbon monoxide is primarily generated by incomplete combustion of organic materials in atmosphere, and it is also a significant component of tobacco smoke and vehicle exhaust fumes (Figure 1). In animals and plants, the generation of intracellular CO and its actions are closely connected with HOs. As shown in Figure 1, HOs catalyze the oxidative conversion of heme to CO, free iron (Fe^{2+}), and biliverdin (BV) in presence of molecular oxygen and electrons supplied by NADPH (Bilban et al., 2008). BV is then converted to the potent antioxidant bilirubin (BR) by biliverdin reductase. To date, three isoforms of HO have been detected in animals, including HO1 (32 kDa), HO2 (36 kDa), and HO3 (33 kDa) (Maines, 1997). HO1 is the highly inducible isozyme which increases rapidly to diverse stimuli and protects tissues against a wide range of injuries (Ryter and Choi, 2015). HO2 and HO3 are constitutively expressed with very low activity. Although the most investigated mechanism for CO production in animals involves HOs, much smaller amounts of CO can derive from other sources, like lipid peroxidation (Vreman et al., 2001; Figure 1).

In plants, the presence of CO biosynthesis was first reported by Wilks (1959) and subsequently the photoproduction of CO in living plants was also identified (Schade et al., 1999; Figure 1). Furthermore, Muramoto et al. (2002) found a plastid heme oxygenase (AtHO1) recombinant protein which was able to catalyze the formation of CO from heme molecules *in vitro*. To date, HOs are still viewed as the main enzymatic source of CO in plants (Xuan et al., 2008; Figure 1). Recent researches provided exciting evidence that the genes for HOs have been identified in a variety of plant species (Erborg et al., 2006; Wang et al., 2014). It comprises a small family with four members in total, which

can be classified into two sub-families: HY1 (HO1), HO3 and HO4 all belong to the HO1 sub-family, while HO2 is the only member of the HO2 sub-family (Shekhawat and Verma, 2010). All members of the HO1 sub-family (HY1, HO3, and HO4) can convert heme to BV with a concomitant release of CO and Fe^{2+} , whereas HO2 sub-family does not exhibit HO activity (Figure 1). Despite the enzymatically catalyzed reaction by HOs has been considered as the main productive route of CO in plants, the opposite results have been proposed in soybean (Zilli et al., 2014). The authors suggested that HOs are not the main source of CO in soybean plants, and lipid peroxidation and ureide metabolism could also be considered as potential sources of CO (Figure 1). Additionally, heme methylene bridges could be broken and CO released when exogenous H_2O_2 or ascorbic acid was supplied (Dulak and Józkowicz, 2003; Figure 1). Collectively, CO synthetic is a complex physiological process and more non-enzymatic biosynthetic processes of CO need to be elucidated.

ROLE OF CO IN PLANT GROWTH AND DEVELOPMENT

A high level of exogenous CO is toxic in plants and animals, however, CO at a proper level involves in many important physiological processes as an active signaling mediator. In animals, the amazing progress in our understanding of the biology of CO has developed rapidly. It was convincingly reported that exogenous CO gas could exert the beneficial effects on modulating a number of physiological events including neurotransmission (Boehning et al., 2003), vasodilation (Motterlini, 2007), and platelet aggregation (Brüne and Ullrich, 1987). More importantly, application of exogenous CO is

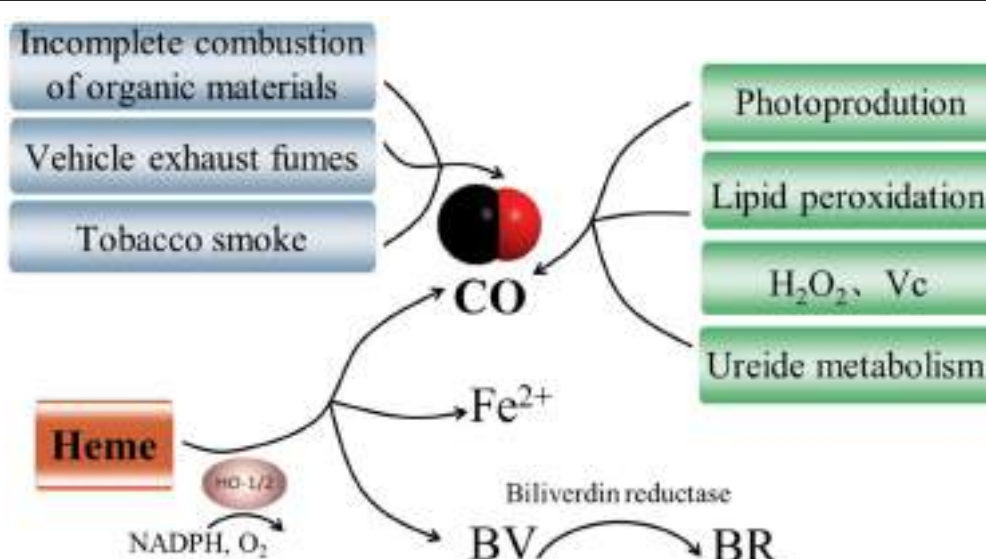


FIGURE 1 | Pathways of generation of carbon monoxide (CO). There are three synthetic routes for CO. Heme source is viewed as the main productive route of CO in animals and plants (Bilban et al., 2008). CO is also generated via incomplete combustion of organic materials, tobacco smoke and vehicle exhaust fumes in atmosphere. Additionally, non-heme sources including photoproduction (Schade et al., 1999), lipid peroxidation (Zilli et al., 2014), hydrogen peroxide (H_2O_2) and ascorbic acid (Vc; Dulak and Józkowicz, 2003), and ureide metabolism have been proposed in plants (Zilli et al., 2014).

developing a new therapeutic strategy for treatment of numerous clinical conditions (Fagone et al., 2015). Also in plants, CO has been studied to elucidate the roles of this enigmatic signaling molecule in plant growth and development. Accumulating evidence in plants has shown that CO is used for a number of intercellular and intracellular biological functions. For instance, CO was likely to delay gibberellins (GA)-triggered programmed cell death (PCD) in wheat aleurone cells by up-regulating of *ascorbate peroxidase (APX)* and *catalase (CAT)* expression, and decreasing H₂O₂ overproduction (Wu et al., 2010; **Table 1**). Until now, the studies of roles of CO in plants mostly focus on seed germination, root development, and stomatal closure.

Seed Germination

Seed germination, which is a highly specialized phase in plant life, is essential for seedling establishment. It is a critical step in a plant's life cycle and is regulated by a wide range of endogenous and environment factors (Kong et al., 2015). Several researches demonstrated that CO exerted an advantageous effect on promoting seed germination in a dose-dependent manner and in many plants. The application of low levels of exogenous CO (0.1 or 1%) stimulated seed germination of foxtail (*Setaria faberii*) under favorable temperature and moisture conditions, while germination decreased with the addition of 75% CO due to the inhibition of mitochondrial respiration (Dekker and Hargrove, 2002; **Table 1**). Both CO donor heme and CO aqueous dose-dependently accelerated the physiological process of seed germination in *Oryza sativa* via activating amylase activity and increasing the formation of energy resources (Liu et al., 2007; **Table 1**). Similarly, CO as a positive regulator was also involved in the process of seed germination in wheat (Liu et al., 2010) and *Brassica nigra* (Amooaghiae et al., 2015; **Table 1**).

Root Development

The root systems have been identified to play important roles in plant nutrient and water acquisition. CO has exhibited positive

effects on regulating plant root development. For example, the promoting effects of auxin (IAA) or nitric oxide (NO) on root elongation were mimicked by application of aqueous solution of CO with different saturations in wheat seedlings (Xuan et al., 2007; **Table 1**). In tomato, exogenous CO promoted root hair density and elongation, which increased 3.38- and 2.48-folds compared with the control. Genetic analyses have shown that CO was able to affect the root hair formation by up-regulating *LeExt1* gene expression (Guo et al., 2009; **Table 1**). Actually, previous studies of CO-induced root development mostly concentrated on lateral root (LR) and adventitious root (AR).

LR Development

Lateral root is derived from the pericycle of parent root, in which mature cells are stimulated to dedifferentiate and proliferate to form a LR primordium, finally leading to the emergence of LR. LR plays an indispensable role in the development of plant root system responsible for water-use efficiency and the extraction of nutrients from soils (Guo et al., 2008). CO has been shown to induce the formation of LR. In rapeseed seedlings, the total length and number of LR increased significantly in a dose-dependent manner with the CO donor hematin or CO aqueous, while the positive effects were fully reversed by the addition of the CO scavenger hemoglobin (Hb) or the CO-specific synthetic inhibitor zinc protoporphyrin-IX (ZnPPIX; Cao et al., 2007b; **Table 1**). Treatment with exogenous CO up-regulated heme oxygenase-1 (*LeHO-1*) expression and the amount of LeHO-1 proteins, then stimulated the formation of tomato LR (Guo et al., 2008; **Table 1**). Above results indicate that exogenous CO is, at least partially, correlated with the formation process of LR in plants.

AR Development

Adventitious root development is an essential step for vegetative propagation which involves the reestablishment of a meristematic tissue after removal of the primary root system (Liao et al., 2012). AR formation is affected by multiple endogenous and

TABLE 1 | Overview of CO-mediated physiological processes in plants.

Physiological process	Plant species	Tissue	CO-induced effect	Reference
Seed germination	<i>Setaria faberii</i>	Seed	+	Dekker and Hargrove, 2002
	<i>Oryza sativa</i>			Liu et al., 2007
	<i>Triticum aestivum</i>			Liu et al., 2010
	<i>Brassica nigra</i>			Amooaghiae et al., 2015
Lateral root formation	<i>Solanum lycopersicum</i>	LR	+	Guo et al., 2008
	<i>Brassica napus</i>			Cao et al., 2007b
Adventitious root development	<i>Cucumis sativus</i>	AR	+	Xuan et al., 2008
	<i>Phaseolus radiatus</i>			Xu J. et al., 2006
	<i>Cucumis sativus</i>			Cui et al., 2015
	<i>Cucumis sativus</i>			Lin et al., 2014
	<i>Cucumis sativus</i>			Xuan et al., 2012
Root hair development	<i>Solanum lycopersicum</i>	Root hair	+	Guo et al., 2009
Root elongation	<i>Triticum aestivum</i>	Root tip segments	+	Xuan et al., 2007
Programmed cell death	<i>Triticum aestivum</i>	Aleurone layers	-	Wu et al., 2010
Stomatal closure	<i>Vicia faba</i>	Leaf	+	Cao et al., 2007a; She and Song, 2008; Song et al., 2008

exogenous factors, wherein IAA is viewed as one of the most important phytohormones in mediating AR (Xuan et al., 2008). The investigation of CO-induced AR formation can be dated back to the year 2006 that CO exhibited positive effects on AR formation in mung bean seedling (Xu J. et al., 2006; **Table 1**). Then, more attention has been given to highlight AR formation induced by CO. Xuan et al. (2008) discovered that CO dose-dependently promoted AR number and length in IAA-depleted cucumber seedlings by up-regulating the expression of target genes (CSDNAJ-1 and CSCDPK1/5) during AR (**Table 1**). It has also been demonstrated that the induction of AR formation by methane-rich water (MRW) was blocked by ZnPPIX, and further reversed by CO aqueous (Cui et al., 2015; **Table 1**). In addition, CO could up-regulate NO production, and thereafter promoting AR formation in IAA-depleted seedlings (Xuan et al., 2012; **Table 1**). Previous results also exposed that endogenous HO-1 might be involved in hydrogen-rich water (HRW)-induced AR formation in cucumber explants (Lin et al., 2014; **Table 1**). Thus, HRW or NO-induced AR formation may require the involvement of CO (Xuan et al., 2012; Lin et al., 2014).

Stomatal Closure

Stomatal movement critically controls the plant water status, and it can be triggered by numerous environment or hormonal factors. Among these, the stress hormone abscisic acid (ABA) is a key player in regulating stomatal movement under drought and humidity stress (Grondin et al., 2015). ABA treatment was found to increase CO content and HO activity in *vicia faba* leaves, and then researchers began to investigate the relationship between CO and stomatal closure. Interestingly, further results

showed that exogenously applied hematin and CO aqueous not only resulted in the enhancement of CO release, but also induced stomatal closure in dose- and time-dependent manners (Cao et al., 2007a; **Table 1**). The CO effects in stomatal movement are similar to NO and H₂O₂ (She and Song, 2008; Song et al., 2008; **Table 1**).

RESPONSE OF CO IN ABIOTIC STRESS

Abiotic stresses are major constraint to plant growth, survival, yield, and distribution, which also result in the oxidative stress and reactive oxygen species (ROS) overproduction by disrupting cellular redox homeostasis. It has been known that ABA is a key regulator involved in plant developmental processes and responses to biotic and abiotic stresses (Raghavendra et al., 2010). Similar to ABA, CO is also required for the alleviation of abiotic stress-induced oxidative stress (Cao et al., 2007a).

Salt Stress

Salt stress has become an ever-present threat to crop yields often causing many unfortunate consequences in plants, such as growth inhibition, ionic phyto-toxicity and ROS overproduction. Low concentrations of CO alleviated the inhibition of seed germination and the damage of seedling leaves produced by salt stress through enhancing antioxidant enzyme activities including superoxide dismutase (SOD), CAT, APX, and guaiacol peroxidase (GPOX) in wheat (Huang et al., 2006; Xu S. et al., 2006; **Table 2**). Similar result was confirmed in rice. CO enhanced the activities of CAT and SOD and

TABLE 2 | Overview of the responses of CO in abiotic stress.

Plant species	Tissue	Abiotic stress	CO-mediated effect	CO-mediated antioxidant enzyme	CO-mediated gene	Reference
<i>Triticum aestivum</i>	Seed	Drought	Maintain antioxidative capability/ROS-scavenging activity	CAT, APX, SOD, DHAR	HO-1	Liu et al., 2010
<i>Triticum aestivum</i>	Seed	Salt	Counteract lipid peroxidation	CAT, APX, SOD, GPOX	–	Xu S. et al., 2006
<i>Triticum aestivum</i>	Leaf	Salt	Alleviate oxidative damage	CAT, APX, SOD, GPOX	–	Huang et al., 2006
<i>Oryza sativa</i>	Seed	Salt	Alleviate oxidative damage	CAT, SOD	HO-1, CAT, SOD, APX	Liu et al., 2007
<i>Triticum aestivum</i>	Root	Salt	Maintain ion homeostasis/up-regulate antioxidant defense	APX, GR, SOD, MDHAR, DHAR	SOD, GR, DHAR	Xie et al., 2008
<i>Triticum aestivum</i>	Root	Salt	Inhibition superoxide anion overproduction	SOD	SOD	Ling et al., 2009
<i>Cassia obtusifolia</i>	Seeds/seedlings	Salt	Increase osmotic substances/antioxidant enzyme activities	SOD, POD, CAT, APX	–	Zhang et al., 2012
<i>Glycine max</i>	Leaf	UVB	Prevent oxidative stress	CAT, APX	HO-1	Yannarelli et al., 2006
<i>Medicago sativa</i>	Root	Hg	Alleviate oxidative damage	GR, MDHAR, SOD	HO-1/2	Han et al., 2007
<i>Chlamydomonas reinhardtii</i>	–	Hg	Suppress reactive oxygen species	SOD, CAT, APX	HO-1	Wei et al., 2011
<i>Brassica juncea</i>	Root	Hg	Alleviate oxidative stress	SOD, POD, CAT, APX	SOD, POD, CAT, APX	Meng et al., 2011
<i>Medicago sativa</i>	Root	Cd	Alleviate oxidative damage	SOD, POD, APX, GR	HO-1, APX, GR	Han et al., 2008
<i>Chlamydomonas reinhardtii</i>	–	Cu	Alleviate oxidative damage	SOD, CAT, APX	SOD, CAT, APX	Zheng et al., 2011
<i>Arabidopsis</i>	–	Fe	Maintain iron-homeostasis	–	HO-1	Kong et al., 2010

up-regulated the expression of *CAT* and *Cu/Zn-SOD* genes, thus resulting in alleviating salt-induced oxidative damage and finally decreasing the inhibition of seed germination (Liu et al., 2007; **Table 2**). CO might increase the tolerance of wheat seedling to salt stress, and its alleviation of PCD and root growth inhibition was linked to the maintenance of ion homeostasis and the decrease of superoxide anion (O_2^-) overproduction (Xie et al., 2008; Ling et al., 2009; **Table 2**). In *Cassia obtusifolia*, hematin or CO-saturated aqueous solution increased the level of cytosolic osmotic substances (total soluble sugars, free proline, and soluble protein) and antioxidant enzyme activities (SOD, POD, CAT, and APX), and lightened the damage of photosynthetic system under salt stress, consequently alleviating the inhibition of seed germination and seedling growth deriving from salinity stress (Zhang et al., 2012; **Table 2**).

Drought Stress

Drought stress is a widely present environmental factor which affects negatively on seed germination, seedling growth and even plant productivity. Application of exogenous hematin brought about marked increase in the activities of amylase and antioxidant enzyme such as CAT, APX, SOD, and dehydroascorbate reductase (DHAR), which were responsible for the mitigation of drought stress-induced wheat seed germination inhibition and lipid peroxidation (Liu et al., 2010; **Table 2**). To date, the investigations of CO in plant tolerance to drought stress are scarce.

Ultraviolet Radiation Stress

The stratospheric ozone layer is thinning resulting in more ultraviolet-B (UV-B) radiation reaching the surface of the earth. UV-B exposure increases the amount of ROS and oxygen-derived free radicals, thus leading to cellular damage and apoptosis. UV-B radiation provoked an increase of the expression of HO-1 and its transcript levels in a dose-dependent manner, which was regarded as a cell protection mechanism against UV-B radiation-induced oxidative damage (Yannarelli et al., 2006). Moreover, CO production was closely related with HO-mediated heme catabolism, implying that CO probably exerted potential functions in modulating the defense response of plants to UV-B stress (Yannarelli et al., 2006; **Table 2**).

Heavy Metals Stress

Heavy metals such as mercury (Hg), cadmium (Cd), iron (Fe), and copper (Cu) result in serious environmental pollution in many places worldwide and lead to a threat to human health and plant development. Heavy metal-induced oxidative stress in plants could be attenuated in the presence of small reactive gaseous molecules such as NO. Like NO, the vital role of CO in relieving heavy metals stress in plants has been verified (Han et al., 2007; Zheng et al., 2011). Hematin and CO supplementation to HgCl₂-treated alfalfa root reduced lipid peroxidation and increased root elongation via activating antioxidant enzymes including glutathione reductase (GR), monodehydroascorbate reductase (MDHRR) and SOD activities, as well as decreasing lipoxygenase activity (LOX;

Han et al., 2007; **Table 2**). CO also enhanced the tolerance of algae to Hg exposure which was closely related to the lower accumulation of Hg and free radical species (Wei et al., 2011; **Table 2**). The detrimental effect by Hg stress could be partially reversed by administration of CO in Indian mustard through suppressing the production of O_2^- and H₂O₂ and increasing the accumulation of proline (Meng et al., 2011; **Table 2**). Also, Cd-induced oxidative damage was alleviated by CO pretreatment via modulating glutathione metabolism in alfalfa, which accelerated the exchange of oxidized glutathione (GSSG) to glutathione (GSH) to restore GSH: GSSG ratio and further decreased the oxidative damage (Han et al., 2008; **Table 2**). In addition, Cu-induced oxidative damage in algae was alleviated by CO mainly via the improvement of CAT activity (Zheng et al., 2011; **Table 2**). Moreover, the up-regulating expression of genes related to Fe acquisition such as *AtLRT1*, *AtFRO2*, *AtF1T1*, and *AtFER1* by CO were responsible for preventing the Fe deficient-induced chlorosis and improving chlorophyll accumulation (Kong et al., 2010; **Table 2**).

CROSS-TALK BETWEEN CO AND OTHER SIGNALING MOLECULES

Carbon monoxide has been highly appreciated for its versatile properties as a signaling molecule regulating diverse physiological processes in animals and plants. A number of studies have shown that CO signal transduction is extremely complex which usually doesn't operate as the linear pathways but that extensive cross-talk occurs between various signal transduction. Thus, we provide here a brief overview of the interaction between CO signaling molecule and other signaling molecules.

Cross-talk between CO and NO

Carbon monoxide signal transduction pathways don't always work independently, but it is rather closely linked to NO. The two endogenously produced gasses share many common downstream signaling pathways and have some similar properties. For example, CO in animals, like NO, binded to the iron atom of heme proteins of soluble guanylate cyclase (sGC) to activate the enzyme and increase intracellular second messenger cyclic guanosine monophosphate (cGMP) production, thus exerting many of their biological functions including regulating vascular tone, inhibiting platelet aggregation, and decreasing blood pressure (Snyder et al., 1998). However, whether the phenomenon exists in plants still has no sufficient evidence to confirm. CO was also able to mimic to some extent the effect of NO in dose-dependently inducing stomatal closure (Song et al., 2008) and K-to-Na ration (Xie et al., 2008). Increasing evidence in animals supports that there exist an intimate connection in the expression of HO and NOS responsible for generating CO and NO, indicating possible interaction between the CO- and NO-generating systems. Also, it is becoming increasingly clear that CO can potentiate the activity of NO synthase (NOS) in plants. Song et al. (2008) implied that there might be existing

HO-1 enzyme and NOS-like enzyme activity in *V. faba* guard cells. CO was involved in darkness-induced NO synthesis via the NOS-like enzyme (Song et al., 2008; **Figure 2**). NaCl-treated wheat seedling roots resulted in a moderate enhancement of endogenous NO level, whereas a very strong increase of NO appeared when adding 50% CO-saturated aqueous solution (Xie et al., 2008; **Figure 2**). Conversely, CO could directly bind to and inactivate NOS, decreasing the enzyme activity probably due to the competition of CO with NO for binding to its targets such as sCG (Ding et al., 1999). Interestingly, recent research showed that NOS enzymes only exist in a few algal species but appear to not be conserved in land plants, suggesting the production of NO may rely mainly on nitrate assimilation in land plants (Jeandroz et al., 2016). Thus, NO synthesis is a complex process in plants and the interaction between the CO- and NO-generating systems via NOS enzymes also needs further validation. Furthermore, a functional interaction of NO and CO has been demonstrated in regulating plant growth and development. For example, CO alleviated osmotic-induced wheat seed germination inhibition and lipid peroxidation which required participation of NO (Liu et al., 2010; **Figure 2**). Santa-Cruz et al. (2010) proposed that NO was implicated in the HO signaling pathway which might directly potentiate UV-B-induced HO-1 transcription in soybean plants. Meanwhile, NO might act as a downstream signal molecule in hemin-induced cucumber AR process (Xuan et al., 2012; **Figure 2**).

Cross-talk between CO and Phytohormone

It has been demonstrated that CO may partially involve in IAA-induced tomato LR development via altering biosynthesis/perception in some way (Guo et al., 2008; **Figure 2**). Meanwhile, Xuan et al. (2008) strongly confirmed that there exists a serial linkage IAA → HO/CO → AR. IAA could activate HO/CO signaling system, and then triggered the signal transduction events, thus leading to AR formation in cucumber (**Figure 2**). Also, CO might be involved in ABA-induced stomatal closure which NO and cGMP may function as downstream intermediates in CO signal transduction network (Cao et al., 2007a; **Figure 2**). In addition, HO/CO might be a component or signaling system of hydrogen sulfide (H₂S)-induced cytoprotective role against GA-induced PCD (Xie et al., 2014; **Figure 2**). Thus, phytohormone could induce various distinct developmental responses in plants, which are dependent on CO.

Cross-talk between CO and Other Small Signaling Molecules

Similar to NO, H₂O₂, and other small signaling molecules also play an indispensable role in CO-mediated physiological responses. She and Song (2008) directly illustrated for the first time that CO-induced stomatal closure probably was mediated by H₂O₂ signaling pathways in *V. faba* (**Figure 2**). Up-regulation of HO expression protected aleurone layers against GA-induced PCD in wheat implicating an alteration of H₂O₂ metabolism (Wu et al., 2010; **Figure 2**). There is adequate evidence to support

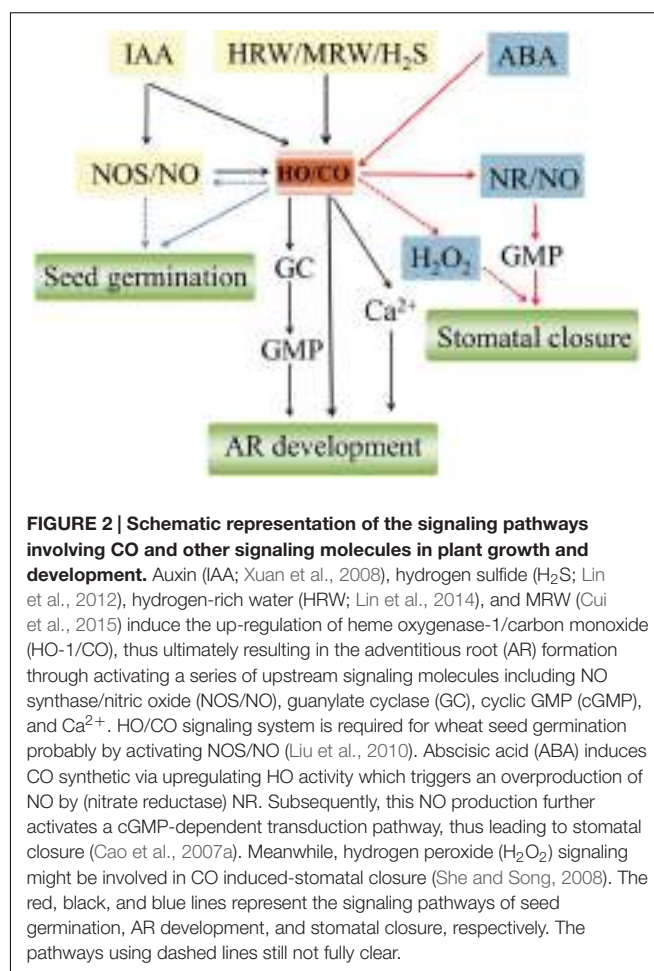


FIGURE 2 | Schematic representation of the signaling pathways involving CO and other signaling molecules in plant growth and development. Auxin (IAA; Xuan et al., 2008), hydrogen sulfide (H₂S; Lin et al., 2012), hydrogen-rich water (HRW; Lin et al., 2014), and MRW (Cui et al., 2015) induce the up-regulation of heme oxygenase-1/carbon monoxide (HO-1/CO), thus ultimately resulting in the adventitious root (AR) formation through activating a series of upstream signaling molecules including NO synthase/nitric oxide (NOS/NO), guanylate cyclase (GC), cyclic GMP (cGMP), and Ca²⁺. HO/CO signaling system is required for wheat seed germination probably by activating NOS/NO (Liu et al., 2010). Abscisic acid (ABA) induces CO synthetic via upregulating HO activity which triggers an overproduction of NO by (nitrate reductase) NR. Subsequently, this NO production further activates a cGMP-dependent transduction pathway, thus leading to stomatal closure (Cao et al., 2007a). Meanwhile, hydrogen peroxide (H₂O₂) signaling might be involved in CO induced-stomatal closure (She and Song, 2008). The red, black, and blue lines represent the signaling pathways of seed germination, AR development, and stomatal closure, respectively. The pathways using dashed lines still not fully clear.

that HO/CO signaling system mediating cucumber AR formation interacts closely with H₂S, H₂, and CH₄. For example, HO-1 as a downstream component was involved in H₂S-induced AR cucumber formation through the modulation of expression of *DNAJ-1* and *CDPK1/5* genes (Lin et al., 2012; **Figure 2**). Likewise, HRW-induced AR formation was heme oxygenase-1/ CO (HO-1/CO)-dependent by up-regulating target genes related to auxin signaling and AR formation including *CsDNAJ-1*, *CsCDPK1/5*, *CsCDC6*, and *CsAUX22B/D* (Lin et al., 2014; **Figure 2**). More recently, it was suggested that MRW might serve as a stimulator of AR, which was partially mediated by HO-1/CO and Ca²⁺ pathways (Cui et al., 2015; **Figure 2**).

CONCLUSION

Carbon monoxide as a gaseous signaling molecule is well studied in animals, but the current situation of CO research in plants is at an early stage. Despite the presence of CO biosynthesis in plants was first reported by Wilks (1959) and HO was claimed as its main productive route, the experimental evidence of non-enzymatic biosynthetic processes of CO is still quite limited. CO has been recognized as a signal or bio-effector involved in plant

growth and development under normal and stress conditions. CO can enhance plant abiotic stress resistance in relation to the cross-talk with other signaling molecules, but the exact biological roles of CO in plants and its detail signal transduction pathway are largely unknown. Thus, more work need to be done to further elucidate the above questions by using pharmacological, physiological, and molecular approaches in the future.

AUTHOR CONTRIBUTIONS

All authors listed, have made substantial, direct and intellectual contribution to the work, and approved it for publication.

REFERENCES

- Amooaghaie, R., Tabatabaei, F., and Ahadi, A. M. (2015). Role of hematin and sodium nitroprusside in regulating *Brassica nigra* seed germination under nanosilver and silver nitrate stresses. *Ecotox. Environ. Safe.* 113, 259–270. doi: 10.1016/j.ecoenv.2014.12.017
- Bilban, M., Haschemi, A., Wegiel, B., Chin, B.Y., Wagner, O., and Otterbein, L.E. (2008). Heme oxygenase and carbon monoxide initiate homeostatic signaling. *J. Mol. Med.* 86, 267–279. doi: 10.1007/s00109-007-0276-0
- Boehning, D., Moon, C., Sharma, S., Hurt, K. J., Hester, L. D., Ronnett, G. V., et al. (2003). Carbon monoxide neurotransmission activated by CK2 phosphorylation of heme oxygenase-2. *Neuron* 40, 129–137. doi: 10.1016/S0896-6273(03)00596-8
- Brüne, B., and Ullrich, V. (1987). Inhibition of platelet aggregation by carbon monoxide is mediated by activation of guanylate cyclase. *Mol. Pharmacol.* 32, 497–504
- Cao, Z. Y., Huang, B. K., Wang, Q. Y., Xuan, W., Ling, T. F., Zhang, B., et al. (2007a). Involvement of carbon monoxide produced by heme oxygenase in ABA-induced stomatal closure in *Vicia faba* and its proposed signal transduction pathway. *Chinese Sci. Bull.* 52, 2365–2373. doi: 10.1007/s11434-007-0358-y
- Cao, Z.Y., Xuan, W., Liu, Z.Y., Li, X.N., Zhao, N., Xu, P., et al. (2007b). Carbon monoxide promotes lateral root formation in rapeseed. *J. Integr. Plant Biol.* 49, 1070–1079. doi: 10.1111/j.1672-9072.2007.00482.x
- Cui, W. T., Qi, F., Zhang, Y. H., Cao, H., Zhang, J., Wang, R., et al. (2015). Methane-rich water induces cucumber adventitious rooting through heme oxygenase1/carbon monoxide and Ca²⁺ pathways. *Plant Cell Rep.* 34, 435–445. doi: 10.1007/s00299-014-1723-3
- Dekker, J., and Hargrove, M. (2002). Weedy adaptation in *Setaria* spp.V. Effects of gaseous environment on giant foxtail (*Setaria faberii*) (Poaceae) seed germination. *Am. J. Bot.* 89, 410–416. doi: 10.3732/ajb.89.3.410
- Ding, Y., McCoubrey, W. K. Jr., and Maines, M. D. (1999). Interaction of heme oxygenase-2 with nitric oxide donors. Is the oxygenase an intracellular ‘sink’ for NO? *Eur. J. Biochem.* 264, 854–861. doi: 10.1046/j.1432-1327.1999.00677.x
- Dulak, J., and Józkowicz, A. (2003). Carbon monoxide: a “new” gaseous modulator of gene expression. *Acta Biochim. Pol.* 50, 31–48.
- Emborg, T. J., Walker, J. M., Noh, B., and Vierstra, R. D. (2006). Multiple heme oxygenase family members contribute to the biosynthesis of the phytochrome chromophore in *Arabidopsis*. *Plant Physiol.* 140, 856–868. doi: 10.1104/pp.105.074211
- Fagone, P., Mangano, K., Mammana, S., Cavalli, E., Marco, R. D., and Barcellona, M. L., et al. (2015). Carbon monoxide-releasing molecule-A1 (CORM-A1) improves clinical signs of experimental autoimmune uveoretinitis (EAU) in rats. *Clin. Immunol.* 157, 198–204. doi: 10.1016/j.clim.2015.02.002
- Grondin, A., Rodrigues, O., Verdoucq, L., Merlot, S., Leonhardt, N., and Maurel, C. (2015). Aquaporins contribute to ABA-triggered stomatal closure through OST1-mediated phosphorylation. *Plant Cell* 27, 1945–1954. doi: 10.1105/tpc.15.00421
- Guo, K., Kong, W. W., and Yang, Z. M. (2009). Carbon monoxide promotes root hair development in tomato. *Plant Cell Environ.* 32, 1033–1045. doi: 10.1111/j.1365-3040.2009.01986.x
- Guo, K., Xia, K., and Yang, Z. M. (2008). Regulation of tomato lateral root development by carbon monoxide and involvement in auxin and nitric oxide. *J. Exp. Bot.* 59, 3443–3452. doi: 10.1093/jxb/ern194
- Han, Y., Xuan, W., Yu, T., Fang, W. B., Lou, T. L., Gao, Y., et al. (2007). Exogenous hematin alleviates mercury-induced oxidative damage in the roots of *Medicago sativa*. *J. Integr. Plant Bio.* 49, 1703–1713. doi: 10.1111/j.1744-7909.2007.00592.x
- Han, Y., Zhang, J., Chen, X. Y., Gao, Z. Z., Xuan, W., Xu, S., et al. (2008). Carbon monoxide alleviates cadmium-induced oxidative damage by modulating glutathione metabolism in the roots of *medicago sativa*. *New Phytol.* 177, 155–166. doi: 10.1111/j.1469-8137.2007.02251.x
- Huang, B. K., Xu, S., Xuan, W., Li, M., Cao, Z. Y., Liu, K. L., et al. (2006). Carbon monoxide alleviates salt-induced oxidative damage in wheat seedling leaves. *J. Integr. Plant Biol.* 48, 249–254. doi: 10.1111/j.1744-7909.2006.00220.x
- Jeandroz, S., Wipf, D., Stuehr, D. J., Lamattina, L., Melkonian, M., Tian, Z., et al. (2016). Occurrence, structure, and evolution of nitric oxide synthase-like proteins in the plant kingdom. *Sci. Signal.* 417, re2. doi: 10.1126/scisignal.aad4403
- Kong, D. D., Ju, C. L., Parihar, A., Kim, S., Cho, D., and Kwak, J. M. (2015). Arabidopsis glutamate receptor homolog3.5 modulates cytosolic Ca²⁺ level to counteract effect of abscisic acid in seed germination. *Plant Physiol.* 167, 1630–1642. doi: 10.1104/pp.114.251298
- Kong, W. W., Zhang, L. P., Guo, K., Liu, Z. P., and Yang, Z. M. (2010). Carbon monoxide improves adaptation of arabidopsis to iron deficiency. *Plant Biotechnol. J.* 8, 88–99. doi: 10.1111/j.1467-7652.2009.00469.x
- Liao, W. B., Zhang, M. L., Huang, G. B., and Yu, J. H. (2012). Ca²⁺ and CaM are involved in NO- and H₂O₂-induced adventitious root development in marigold. *J. Plant Growth Regul.* 31, 253–264. doi: 10.1007/s00344-011-9235-7
- Lin, Y. T., Li, M. Y., Cui, W. T., Lu, W., and Shen, W. B. (2012). Haem oxygenase-1 is involved in hydrogen sulfide-induced cucumber adventitious root formation. *J. Plant Growth Regul.* 31, 519–528. doi: 10.1007/s00344-012-9262-z
- Lin, Y. T., Zhang, W., Qi, F., Cui, W. T., Xie, Y. J., and Shen, W. B. (2014). Hydrogen-rich water regulates cucumber adventitious root development in a heme oxygenase-1/carbon monoxide-dependent manner. *J. Plant Physiol.* 171, 1–8. doi: 10.1016/j.jplph.2013.08.009
- Ling, T. F., Zhang, B., Cui, W. T., Wu, M. Z., Lin, J. S., and Zhou, W. T. (2009). Carbon monoxide mitigates salt-induced inhibition of root growth and suppresses programmed cell death in wheat primary roots by inhibiting superoxide anion overproduction. *Plant Sci.* 177, 331–340. doi: 10.1016/j.plantsci.2009.06.004
- Liu, K. L., Xu, S., Xuan, W., Ling, T. F., Cao, Z. Y., Huang, B. K., et al. (2007). Carbon monoxide counteracts the inhibition of seed germination and alleviates oxidative damage caused by salt stress in *Oryza sativa*. *Plant Sci.* 172, 544–555. doi: 10.1016/j.plantsci.2006.11.007
- Liu, Y. H., Xu, S., Ling, T. F., Xu, L. L., and Shen, W. B. (2010). Heme oxygenase/carbon monoxide system participates in regulating wheat seed

ACKNOWLEDGMENTS

We thank Dr. Claudio Pasian (The Ohio State University, Columbus, OH, USA) for critical reading of the manuscript. This research was supported by the National Natural Science Foundation of China (Nos. 31160398 and 31560563), the Post Doctoral Foundation of China (Nos. 20100470887 and 2012T50828), the Key Project of Chinese Ministry of Education (No. 211182), the Research Fund for the Doctoral Program of Higher Education (No. 20116202120005), the Natural Science Foundation of Gansu Province, China (Nos. 1308RJZA179 and 1308RJZA262), the Fundamental Research Funds for Universities in Gansu, P. R. China.

- germination under osmotic stress involving the nitric oxide pathway. *J. Plant Physiol.* 167, 1371–1379. doi: 10.1016/j.jplph.2010.05.021
- Maines, M. D. (1997). The heme oxygenase system: a regulator of second messenger gases. *Annu. Rev. Pharmacol.* 37, 517–554. doi: 10.1146/annurev.pharmtox.37.1.517
- Meng, D. K., Chen, J., and Yang, Z. M. (2011). Enhancement of tolerance of Indian mustard (*Brassica juncea*) to mercury by carbon monoxide. *J. Hazard. Mater.* 186, 1823–1829. doi: 10.1016/j.jhazmat.2010.12.062
- Motterlini, R. (2007). Carbon monoxide-releasing molecules (CO-RMs): vasodilatory, anti-ischaemic and anti-inflammatory activities. *Biochem. Soc. T.* 35, 1142–1146. doi: 10.1042/BST0351142
- Motterlini, R., Gonzales, A., Foresti, R., Clark, J. E., Green, C. J., and Winslow, R. M. (1998). Heme oxygenase-1 derived carbon monoxide contributes to the suppression of acute hypertensive responses in vivo. *Circ. Res.* 83, 568–577. doi: 10.1161/01.RES.83.5.568
- Muramoto, T., Tsurui, N., Terry, M. J., Yokota, A., and Kohchi, T. (2002). Expression and biochemical properties of a ferredoxin-dependent heme oxygenase required for phytochrome chromophore synthesis. *Plant Physiol.* 130, 1958–1966. doi: 10.1104/pp.008128
- Raghavendra, A. S., Gonugunta, V. K., Christmann, A., and Grill, E. (2010). ABA perception and signaling. *Trends Plant Sci.* 15, 395–401. doi: 10.1016/j.tplants.2010.04.006
- Ryter, S. W., and Choi, A. M. K. (2015). Targeting heme oxygenase-1/carbon monoxide for therapeutic modulation of inflammation. *Transl. Res.* 167, 7–34. doi: 10.1016/j.trsl.2015.06.011
- Santa-Cruz, D. M., Pacienza, N. A., Polizzi, A. H., Balestrasse, K. B., Tomaro, M. L., and Yannarelli, G. G. (2010). Nitric oxide synthase-like dependent no production enhances heme oxygenase up-regulation in ultraviolet-B-irradiated soybean plants. *Phytochemistry* 71, 1700–1707. doi: 10.1016/j.phytochem.2010.07.009
- Schade, G. W., Hofmann, R. W., and Crutzen, P. J. (1999). CO emissions from degrading plant matter. *Tellus. B.* 51, 889–908. doi: 10.1034/j.1600-0889.1999.t01-4-00003.x
- She, X. P., and Song, X. G. (2008). Carbon monoxide-induced stomatal closure involves generation of hydrogen peroxide in *Vicia faba* guard cells. *J. Integr. Plant Biol.* 50, 1539–1548. doi: 10.1111/j.1744-7909.2008.00716.x
- Shekhawat, G. S., and Verma, K. (2010). Haem oxygenase (HO): an overlooked enzyme of plant metabolism and defence. *J. Exp. Bot.* 61, 2255–2270. doi: 10.1093/jxb/erq074
- Snyder, S. H., Jaffrey, S. R., and Zakhary, R. (1998). Nitric oxide and carbon monoxide: parallel roles as neural messengers. *Brain Res. Rev.* 26, 167–175. doi: 10.1016/S0165-0173(97)00032-5
- Song, X. G., She, X. P., and Zhang, B. (2008). Carbon monoxide-induced stomatal closure in *vicia faba* is dependent on nitric oxide synthesis. *Physiol. Plant.* 132, 514–525. doi: 10.1111/j.1399-3054.2007.01026.x
- Vreman, H. J., Wong, R. J., and Stevenson, D. K. (2001). “Sources, sinks and measurement of carbon monoxide,” in *Carbon Monoxide and Cardiovascular Functions*, ed. R. Wang (Boca Raton, FL: CRC Press LLC), 273–307.
- Wang, L. J., Ma, F., Xu, S., Zheng, T. Q., Wang, R., Chen, H. P., et al. (2014). Cloning and characterization of a heme oxygenase-2 gene from rice (*Oryza sativa* L.), and its expression analysis in response to some abiotic stresses. *Acta Physiol. Plant.* 36, 893–902. doi: 10.1007/s11738-013-1468-6
- Wei, Y. Y., Zheng, Q., Liu, Z. P., and Yang, Z. M. (2011). Regulation of tolerance of *Chlamydomonas reinhardtii* to heavy metal toxicity by heme oxygenase-1 and carbon monoxide. *Plant Cell Physiol.* 52, 1665–1675. doi: 10.1093/pcp/pcr102
- Wilks, S. S. (1959). Carbon monoxide in green plants. *Science* 129, 964–966. doi: 10.1126/science.129.3354.964
- Wu, M. Z., Huang, J. J., Xu, S., Ling, T. F., Xie, Y. J., and Shen, W. B. (2010). Haem oxygenase delays programmed cell death in wheat aleurone layers by modulation of hydrogen peroxide metabolism. *J. Exp. Bot.* 62, 235–248. doi: 10.1093/jxb/erq261
- Xie, Y. J., Ling, T. F., Han, Y., Liu, K. L., Zheng, Q. S., Huang, L. Q., et al. (2008). Carbon monoxide enhances salt tolerance by nitric oxide-mediated maintenance of ion homeostasis and up-regulation of antioxidant defence in wheat seedling roots. *Plant Cell Environ.* 31, 1864–1881. doi: 10.1111/j.1365-3040.2008.01888.x
- Xie, Y. J., Zhang, C., Lai, D. W., Sun, Y., Samma, M. K., Zhang, J., et al. (2014). Hydrogen sulfide delays GA-triggered programmed cell death in wheat aleurone layers by the modulation of glutathione homeostasis and heme oxygenase-1 expression. *J. Plant Physiol.* 171, 53–62. doi: 10.1016/j.jplph.2013.09.018
- Xu, J., Xuan, W., Huang, B. K., Zhou, Y. H., Ling, T. F., Xu, S., et al. (2006). Carbon monoxide-induced adventitious rooting of hypocotyl cuttings from mung bean seedling. *Chinese Sci. Bull.* 51, 668–674. doi: 10.1007/s11434-006-0668-5
- Xu, S., Sa, Z., Cao, Z. S., Xuan, W., Huang, B. K., Ling, T. F., et al. (2006). Carbon monoxide alleviates wheat seed germination inhibition and counteracts lipid peroxidation mediated by salinity. *J. Integr. Plant Biol.* 48, 1168–1176. doi: 10.1111/j.1744-7909.2006.00337.x
- Xuan, W., Huang, L. Q., Li, M., Huang, B. K., Xu, S., Liu, H., et al. (2007). Induction of growth elongation in wheat root segments by heme molecules: a regulatory role of carbon monoxide: a regulatory role of carbon monoxide in plants? *Plant Growth Regul.* 52, 41–51. doi: 10.1007/s10725-007-9175-1
- Xuan, W., Xu, S., Li, M. Y., Han, B., Zhang, B., Zhang, J., et al. (2012). Nitric oxide is involved in hemin-induced cucumber adventitious rooting process. *J. Plant Physiol.* 169, 1032–1039. doi: 10.1016/j.jplph.2012.02.021
- Xuan, W., Zhu, F. Y., Xu, S., Huang, B. K., Ling, T. F., Qi, J. Y., et al. (2008). The heme oxygenase/carbon monoxide system is involved in the auxin-induced cucumber adventition rooting process. *Plant Physiol.* 148, 881–893. doi: 10.1104/pp.108.125567
- Yannarelli, G. G., Noriega, G. O., Batlle, A., and Tomaro, M. L. (2006). Heme oxygenase up-regulation in ultraviolet-B irradiated soybean plants involves reactive oxygen species. *Planta* 224, 1154–1162. doi: 10.1007/s00425-006-0297-x
- Zhang, C. P., Li, Y. C., Yuan, F. G., Hu, S. J., and He, P. (2012). Effects of hematin and carbon monoxide on the salinity stress responses of cassia obtusifolia L. seeds and seedlings. *Plant Soil.* 359, 85–105. doi: 10.1007/s11104-012-1194-7
- Zheng, Q., Meng, Q., Wei, Y. Y., and Yang, Z. M. (2011). Alleviation of copper-induced oxidative damage in *chlamydomonas reinhardtii* by carbon monoxide. *Arch. Environ. Con. Tox.* 61, 220–227. doi: 10.1007/s00244-010-9602-6
- Zilli, C. G., Santa-Cruz, D. M., and Balestrasse, K. B. (2014). Heme oxygenase-independent endogenous production of carbon monoxide by soybean plants subjected to salt stress. *Environ. Exp. Bot.* 102, 11–16. doi: 10.1016/j.envexpbot.2014.01.012

Conflict of Interest Statement: The authors declare that the research was conducted in the absence of any commercial or financial relationships that could be construed as a potential conflict of interest.

Copyright © 2016 Wang and Liao. This is an open-access article distributed under the terms of the Creative Commons Attribution License (CC BY). The use, distribution or reproduction in other forums is permitted, provided the original author(s) or licensor are credited and that the original publication in this journal is cited, in accordance with accepted academic practice. No use, distribution or reproduction is permitted which does not comply with these terms.



Ammonium Inhibits Chromomethylase 3-Mediated Methylation of the *Arabidopsis* Nitrate Reductase Gene *NIA2*

Joo Yong Kim¹, Ye Jin Kwon¹, Sung-II Kim¹, Do Youn Kim¹, Jong Tae Song² and Hak Soo Seo^{1,3,4*}

¹ Department of Plant Science and Research Institute for Agriculture and Life Sciences, Seoul National University, Seoul, South Korea, ² School of Applied Biosciences, Kyungpook National University, Daegu, South Korea, ³ Plant Genomics and Breeding Institute, Seoul National University, Seoul, South Korea, ⁴ Bio-MAX Institute, Seoul National University, Seoul, South Korea

OPEN ACCESS

Edited by:

Sylvain Jeandroz,
Agrosup Dijon, France

Reviewed by:

Serena Varotto,
University of Padova, Italy
Hong-Gu Kang,
Texas State University, USA

*Correspondence:

Hak Soo Seo
seohs@snu.ac.kr

Specialty section:

This article was submitted to
Plant Physiology,
a section of the journal
Frontiers in Plant Science

Received: 10 September 2015

Accepted: 07 December 2015

Published: 21 January 2016

Citation:

Kim JY, Kwon YJ, Kim S-I, Kim DY,
Song JT and Seo HS (2016)
Ammonium Inhibits Chromomethylase
3-Mediated Methylation of the
Arabidopsis Nitrate Reductase Gene
NIA2. *Front. Plant Sci.* 6:1161.
doi: 10.3389/fpls.2015.01161

Gene methylation is an important mechanism regulating gene expression and genome stability. Our previous work showed that methylation of the nitrate reductase (NR) gene *NIA2* was dependent on chromomethylase 3 (CMT3). Here, we show that CMT3-mediated *NIA2* methylation is regulated by ammonium in *Arabidopsis thaliana*. CHG sequences (where H can be A, T, or C) were methylated in *NIA2* but not in *NIA1*, and ammonium $[(\text{NH}_4)_2\text{SO}_4]$ treatment completely blocked CHG methylation in *NIA2*. By contrast, ammonium had no effect on *CMT3* methylation, indicating that ammonium negatively regulates CMT3-mediated *NIA2* methylation without affecting *CMT3* methylation. Ammonium upregulated *NIA2* mRNA expression, which was consistent with the repression of *NIA2* methylation by ammonium. Ammonium treatment also reduced the overall genome methylation level of wild-type *Arabidopsis*. Moreover, CMT3 bound to specific promoter and intragenic regions of *NIA2*. These combined results indicate that ammonium inhibits CMT3-mediated methylation of *NIA2* and that of other target genes, and CMT3 selectively binds to target DNA sequences for methylation.

Keywords: ammonium, CMT3, DNA methylation, gene expression, *NIA2*, nitrogen assimilation, plant growth

INTRODUCTION

DNA methylation is an important epigenetic mechanism that regulates gene expression and genome stability in plants and animals (Herman and Baylin, 2003). DNA methylation in plants occurs at symmetric CG and CHG sequences and non-symmetric CHH sequences (where H can be A, C, or T). Three types of DNA methyltransferases (DNMTs) have been identified in plants, namely chromomethylase (CMT), methyltransferase (MET), and domain-rearranged methyltransferase (DRM) (Cao and Jacobsen, 2002b; Ronemus et al., 1996; Lindroth et al., 2001).

Chromomethylases contain six conserved motifs (I, IV, VI, VIII, IX, and X), a bromo adjacent homology (BAH) domain, and a chromodomain. The BAH domain is located at the N-terminal region, and the chromodomain is embedded between catalytic motifs I and IV. All DNMT1/MET1 proteins contain two BAH domains, whereas CMTs contain only one BAH domain. BAH domains are involved in protein–protein interactions, recognition of methylated histones, and

nucleosome binding in animal systems (Armache et al., 2011; Kuo et al., 2012; Yang and Xu, 2013). Chromodomains function as methylated histone lysine-binding domains, facilitating recruitment to chromatin in animals (Sanchez and Zhou, 2009; Yap and Zhou, 2012). In plants, the BAH domain and chromodomain of CMT3 mediate its specific binding to histone H3 lysine 9 dimethylation (H3K9me2) (Du et al., 2012). Mutations in the BAH domain or chromodomain caused a failure of CMT3 binding to nucleosomes and a complete loss of CMT3 activity *in vivo*, suggesting that CMT3 associates with H3K9me2-containing nucleosomes through dual binding of its BAH and chromo domains to H3K9me2 to target DNA methylation.

Arabidopsis has three *CMT* genes, namely, *CMT1*, *CMT2*, and *CMT3* (Henikoff and Comai, 1998; Finnegan and Kovac, 2000; McCallum et al., 2000). In the ecotype Wassilewskija (WS), *CMT2* and *CMT3* are predicted to encode functional proteins (Henikoff and Comai, 1998), whereas *CMT1* encodes a non-functional protein (Jones et al., 2001). *CMT* genes have been identified in several plant species, including tobacco and maize, but they have not been identified in fungal or animal systems (Rose et al., 1998; Finnegan and Kovac, 2000). This indicates that *CMT* is a plant-specific DNMT. *CMT2* and *CMT3* have DNA methylation activity at CHG sites (Jones et al., 2001; Lindroth et al., 2001), and maintain CHH methylation at certain genomic loci (Cao and Jacobsen, 2002a; Cokus et al., 2008; Stroud et al., 2013). *Zea mays* methyltransferase 2 (ZMET2) and the *Nicotiana benthamiana* CMT3 homolog NbCMT3 were identified as CHG-specific DNMTs (Papa et al., 2001; Hou et al., 2013). MET1 is a homolog of mammalian DNMT1 that catalyzes symmetric CG methylation (Jones et al., 2001). MET1 has little effect on CHG methylation levels and it cannot substitute for CMT3 (Cokus et al., 2008; Stroud et al., 2013). The DRM DNMTs, which include DRM1, DRM2, and DRM3, have *de novo* DNA methylation activity at CG, CHG, and CHH sites through RNA-directed methylation pathways (Cao et al., 2003; Cokus et al., 2008; Henderson et al., 2010; Greenberg et al., 2011; Stroud et al., 2013). DRMs also maintain CHG and CHH methylation at specific genomic loci (Cao et al., 2003; Cokus et al., 2008; Henderson et al., 2010; Stroud et al., 2013). These combined results indicate that plant CHG and CHH methylation is controlled by CMT and DRM DNMTs (Chan et al., 2005; Stroud et al., 2013; Zemach et al., 2013).

The roles of plant MET1, DRM2, and CMT3 are well characterized. The expression patterns and levels of these DNMTs differ in different tissues and during different developmental stages. Mutation of these DNMTs causes severe loss of DNA methylation, which leads to abnormal development. For example, plants defective in CMT3 activity display abnormal embryo development (Pillot et al., 2010). Loss of MET1 activity delays flowering and reduces fertility, and these effects become more severe in the presence of CMT3 or DRM2 mutations (Xiao et al., 2006; Zhang and Jacobsen, 2006). A recent GUS study reported that these DNMTs are expressed in specific tissues or ubiquitously expressed at specific developmental stages (Huang et al., 2014). CMT3 is expressed only in specific organ regions that co-express DRM2 and MET1.

Nitrogen assimilation is a fundamental biological process that is essential for plant growth and development. Plants utilize nitrate as a source of environmental nitrogen, and nitrate is a potent signal that regulates nitrogen and carbon metabolism, plant growth, and development (Crawford and Forde, 2002; Forde, 2002; Stitt et al., 2002; Foyer et al., 2003). Nitrate is actively transported into cells from the soil by a nitrate transporter and then sequentially reduced to ammonia, which enters amino acid metabolic pathways primarily via the action of glutamine synthetase. NR, a key enzyme of the plant nitrogen assimilation pathway, forms homodimers that catalyze the NAD(P)H-dependent reduction of nitrate to nitrite (Campbell and Kinghorn, 1990; Solomonson and Barber, 1990). Therefore, the regulation of NR expression and NR activity is important for nitrate assimilation. A recent study reported that the *Arabidopsis* NRs NIA1 and NIA2 are positively regulated by sumoylation through the activity of the E3 SUMO ligase AtSIZ1 (Park et al., 2011). CMT3 sumoylation by AtSIZ1 is suggested to control NR gene expression (Kim et al., 2015a).

In the present study, we investigated the effect of ammonium on CMT3-mediated methylation of NR genes. We report that ammonium inhibits CMT3-mediated *NIA2* methylation without affecting on *CMT3* methylation. In addition, CMT3 binds to specific regions of *NIA2*. Our results provide evidence that CMT3-mediated *NIA2* methylation is negatively modulated by ammonium.

MATERIALS AND METHODS

Plant Materials, Growth Conditions, and Ammonium Treatment

Arabidopsis thaliana Columbia-0 ecotype (wild-type, Col-0) was used in this study. For *in vitro* culture in artificial media, seeds were surface-sterilized for 10 min using commercial bleach containing 5% sodium hypochlorite and 0.1% Triton X-100, rinsed five times in sterilized distilled water, and then stratified for 3 days at 4°C in the dark. Seeds were then sown on agar plates containing Murashige and Skoog medium (pH 5.7), 2% sucrose, and 0.8% agar. For plants grown in a non-agar substrate, seeds were sown and grown on sterile vermiculite. All plants were grown in a growth chamber at 22°C under a 16 h light/8 h dark cycle. To examine the effect of ammonium, three different ammonium sources $[(\text{NH}_4)_2\text{SO}_4$, NH_4Cl , and NH_4NO_3] were used with similar results. Thus, $(\text{NH}_4)_2\text{SO}_4$ was used for all experiments.

Immunoprecipitation of Methylated DNA

Wild-type plants were grown in vermiculite for 3 weeks, treated with 5 mM $(\text{NH}_4)_2\text{SO}_4$, and grown for an additional 12 h at 22°C. Then, genomic DNA was isolated from individual plants and sonicated to produce random fragments of 200–600 bp. The fragmented DNA (4 mg) was used in a standard methylated DNA immunoprecipitation (IP) (MeDIP) assay as described previously (Pomraning et al., 2009). Methylated DNA was recovered as described previously (Kim et al., 2015a).

Illumina Genome Analyzer Sequencing

To perform second-strand synthesis of MeDIP-enriched ssDNA fragments, approximately 200 ng of MeDIP-enriched ssDNA fragments and 500 ng of random primers were mixed in a final volume of 57.9 μ L, incubated at 70°C for 10 min, and then cooled gradually for 40 min. Subsequent experiments were performed as described previously (Kim et al., 2015a). End-repair of DNA fragments, addition of an adenine residue to the 3' fragment ends, adaptor ligation, and PCR amplification using Illumina paired-end primers were performed as described previously (Pomraning et al., 2009). The products were analyzed by agarose gel electrophoresis, and bands were excised to produce libraries with 250–350 bp insert sizes, which were quantified using Quant-iT PicoGreen dsDNA Reagent and Kit (Invitrogen). Flow cells were prepared with 8 pM DNA according to the manufacturer's recommended protocol and sequenced for 36 cycles on an Illumina Genome Analyzer II (Illumina). The obtained images were analyzed and base-called using GA pipeline software (version 1.3) with default settings (Illumina).

Mapping Reads

The reads obtained from Illumina sequencing were mapped onto the *Arabidopsis* genome reference sequence (Bioconductor¹) using Bowtie2 as described previously (Kim et al., 2015a). The sequence reads of untreated Col-0 wild-type plants were used as controls and to categorize the methylation sequences of $(\text{NH}_4)_2\text{SO}_4$ -treated wild-type plants.

Bisulfite Sequencing

Genomic DNA was isolated from rosette leaves of 3-week-old wild-type plants treated with 5 mM $(\text{NH}_4)_2\text{SO}_4$ or untreated plants (control). Bisulfite treatment and sample recovery were performed using the EpiTect Bisulfite Kit (QIAGEN) according to the manufacturer's instructions. The primers were designed using MethPrimer software². The percentage methylation (% C) was calculated as $100 \times C/(C + T)$. Cytosine methylation in CG, CHG, and CHH contexts was analyzed and displayed using CyMATE (Hetzl et al., 2007).

Analysis of CMT3 Pull-Down of *NIA2*

CMT3 binding to *NIA2* was examined by *in vivo* pull-down using a plant expression vector construct. The full-length CMT3 cDNA was amplified by PCR using FLAG₄-tagged forward and reverse primers, and inserted into the plant expression vector pBA002. This generated the construct 35S-CMT3-FLAG₄. Then, 3-week-old wild-type plants were infiltrated with transformed agrobacteria carrying 35S-CMT3-FLAG₄ and sequentially treated with 5 mM $(\text{NH}_4)_2\text{SO}_4$. Plants were incubated for 12 h at 22°C, and genomic DNA and total protein were extracted

from rosette leaves of the transformed plants. CMT3-FLAG₄ expression was examined by western blotting using an anti-FLAG antibody.

For the binding assay, genomic DNA was sonicated to produce random fragments of 200 – 600 bp. The fragmented DNA (4 mg) was used in the IP assay. Anti-FLAG antibody (20 μ g) was added to each sample of fragmented DNA, reactions were brought to a final volume of 1 ml in IP buffer [10 mM sodium phosphate (pH 7.0), 140 mM NaCl, and 0.05% Triton X-100], and the mixture was incubated for 2 h at 4°C. Then, samples were incubated with 40 μ l of protein A agarose beads for 12 h at 4°C and then washed seven times with 1 ml of IP buffer. DNA was recovered from the beads by phenol-chloroform extraction and ethanol precipitation. Purified DNA was amplified with specific primers for *NIA1* and *NIA2*, and then the DNA levels were examined by 1.2% agarose gel electrophoresis. The primers used for quantitative PCR were as follows: *NIA1*, 5'-GCTAGTAAGCATAGGAGAG-3' (forward) and 5'-CCTTCACGTTGTAACCCATCTTCT-3' (reverse); *NIA2*, 5'-TGTCTCAGTACCTAGACTCTTGC-3' (forward) and 5'-TGTCTCAGTACCTAGACTCTT-3' (reverse).

The site of CMT3 binding to *NIA2* was determined using genomic DNA isolated from 3-week-old wild-type plants, which was sonicated to produce 200 – 600 bp fragments. The fragmented DNA (4 mg) was immunoprecipitated and analyzed as described above. Purified DNA was amplified with gene-specific primers, and the DNA levels were examined by 1.2% agarose gel electrophoresis. The following forward and reverse primers (21 oligonucleotides) were designed for PCR amplification of different regions (fragments) of *NIA2*: fragment – 3,000 to – 2,500 bp, 5'-TCAATAAGAGGAGGCCA CAAA-3' (forward) and 5'-ATTGTATTATATATCAAAG-3' (reverse); fragment – 2,499 to – 2,000 bp, 5'-CTGGCCAACATC TATTCACTTA-3' (forward) and 5'-ATATATATGATTTTATA TAC-3' (reverse); fragment – 1,999 to – 1,500 bp, 5'-TGAAACT GCTATATGCAAGTA-3' (forward) and 5'-CTAATTTGGGT AACCAATAT-3' (reverse); fragment – 1,499 to – 1,000 bp, 5'-A AGTTACAAGAAAATCAATA-3' (forward) and 5'-TTTCTT ATTAAACGTTATTTT-3' (reverse); fragment – 999 to – 500 bp, 5'-ATAAAATATTGTATGATTATTA-3' (forward) and 5'-TTTCCTTTTATTTAGTCG-3' (reverse); fragment – 499 to – 1 bp, 5'-TGTGTTGATCACATTTTATA-3' (forward) and 5'-TTGGAAAGTGTATAATCGTAA-3' (reverse); fragment 1 to 500 bp, 5'-CATGGCGGCCTGTAGATAA-3' (forward) and 5'-GTTGACGAATCCGGTCACCT-3' (reverse); fragment 501–1,000 bp, 5'-GGCCCATGAAATTCAACCATGG-3' (forward) and 5'-GTTGTCCTGAAATGGTAGAA-3' (reverse); fragment 1,001–1,500 bp, 5'-AGAGTTTACCTCTTTGGTA-3' (forward) and 5'-ACCTCCACACGGGTACTTT-3' (reverse); fragment 1,501–2,000 bp, 5'-CACGGTAGATGGTGG AGAGAC-3' (forward) and 5'-ATCGTGTACAATCATAGATAT-3' (reverse); fragment 2,001–2,500 bp, 5'-TCCTTATGGATC ACCCGGGTG-3' (forward) and 5'-TGGGTGGACACCGCCA AAGTA-3' (reverse); fragment 2,501–3,412 bp, 5'-AGATTCCCTAACGGCGGGCTC-3' (forward) and 5'-ATGA AAAATGAACATATTCA-3' (reverse).

¹<https://bioconductor.org/packages/release/data/annotation/html/BSgenome.Athaliana.TAIR.TAIR9.html>

²<http://www.urogene.org/methprimer/>

Examination of DNA Methylation by McrBC-PCR

The methylation analysis procedure involved 5-methylcytosine-specific restriction enzyme (McrBC)-based PCR using a previously published protocol (Lippman et al., 2003). Genomic DNA (500 ng) was isolated from wild-type plants treated with 5 mM $(\text{NH}_4)_2\text{SO}_4$ or untreated plants (control) and digested with 30 units of McrBC endonuclease (New England Biolabs) for 3 h at 37°C. Then, quantitative PCR analyses were performed as described previously (Kim et al., 2015a). The primers used for quantitative PCR were as follows: *NIA1*, 5'-GCTAGTAAGCATAAGGAGAG-3' (forward) and 5'-CCTTCA CGTTGTAACCCATCTTCT-3' (reverse); *NIA2*, 5'-TGTCTC AGTACCTAGACTCTTGC-3' (forward) and 5'-TGTCTCA GTACCTAGACTCTT-3' (reverse); *CMT3*, 5'-GCTAGTAAGC ATAAGGAGAG-3' (forward) and 5'-CCTTCACGTTGTAAC CCATCTTCT-3' (reverse); tubulin, 5'-GTGAGCGAACAGITTC ACAGC-3' (forward) and 5'-TTATTGCTCCTCCTGCACTT-3' (reverse).

Transcript Level Analysis for Genes Involved in NR Pathways and *CMT3*

Wild-type plants were grown for 3 weeks in vermiculite and treated with or without 5 mM $(\text{NH}_4)_2\text{SO}_4$ for 12 h. Total RNA was extracted from rosette leaves, quantified, and divided into equal amounts. First-strand cDNA was synthesized from 5 µg of total RNA using an iScript cDNA Synthesis Kit (Bio-Rad), and cDNA was amplified by real-time qRT-PCR (MyIQ, Bio-Rad) according to the manufacturer's instructions. PCR analysis and sequencing were performed as described previously (Kim et al., 2015b). The primers used for quantitative PCR were the same as those described in the previous section.

RESULTS

Ammonium Reduces Genome Methylation Levels

Nitrogen is an essential element for plant growth, and plants take up nitrogen as nitrate or ammonium through roots or leaves to support biosynthetic production. Nitrate, the uptake of which is mediated by nitrate transporters, is converted to ammonia by NR and nitrite reductase, indicating that ammonia affects plant development as an end product before its incorporation into glutamine by glutamine synthase. Therefore, we first examined the effect of ammonium on genome methylation. For this experiment, wild-type plants were grown for 3 weeks in vermiculite and treated with or without 5 mM $(\text{NH}_4)_2\text{SO}_4$ before being subjected to MeDIP sequencing analysis to determine the methylation level of the whole genome. The results showed that CpG and C methylation were lower in $(\text{NH}_4)_2\text{SO}_4$ -treated plants than in control plants (Table 1).

The number of reads that overlapped with CpG islands was determined to quantify the genomic coverage, which showed that the CpG coverage and sequence pattern coverage were lower in $(\text{NH}_4)_2\text{SO}_4$ -treated plants than in control plants (Figure 1).

TABLE 1 | CpG and C enrichment analysis of ammonium-treated plants by MeDIP sequencing.

	No treatment	$(\text{NH}_4)_2\text{SO}_4$
CG regions	15,407,837	13,311,909
C regions	105,277,236	98,704,801
Total base(bp)	3,101,970,144	3,938,852,604
Alignment rate(%)	79.67	91.72

Therefore, the chromosomal distribution of methylated DNA was analyzed in wild-type plants treated with and without 5 mM $(\text{NH}_4)_2\text{SO}_4$. Extensive DNA methylation was detected in the heterochromatic regions of each of the five chromosomes of control plants, although some noisy peaks were detected in other regions (Figure 2, left panel). This methylation pattern was similar to that reported previously (Zhang et al., 2006). In $(\text{NH}_4)_2\text{SO}_4$ -treated plants, methylation levels in the heterochromatic regions were lower than those in control plants (Figure 2, right panel). A comparison of whole genome methylation indicated that the methylation levels of 6,070 gene loci were downregulated in $(\text{NH}_4)_2\text{SO}_4$ -treated plants compared with those in control plants (Supplementary Table S1). This suggests that gene methylation status can be regulated by ammonium and lead to the upregulation of gene expression.

Similar results were obtained by performing replicate experiments using other ammonium sources including NH_4Cl , indicating that changes in DNA methylation levels in response to treatment with 5 mM $(\text{NH}_4)_2\text{SO}_4$ are caused by ammonium and not by sulfate.

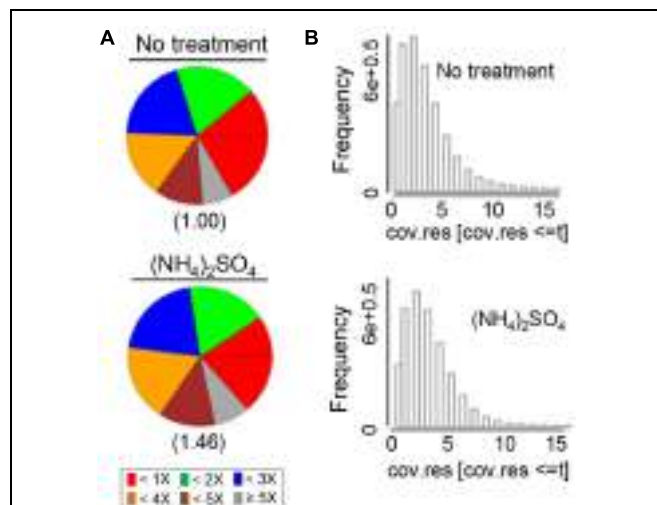


FIGURE 1 | MeDIP sequencing was used to detect whole genome methylation in ammonium-treated and untreated control *Arabidopsis* plants. Genomic coverage was quantified by the number of DNA methylation measurements that overlapped with CpG islands. (A) CpG coverage was determined by counting the number of reads. CpG islands were identified using the program MEDIPS. The numbers below the diagrams indicate “pattern not covered.” (B) The methylation pattern is presented as sequence pattern coverage. The parameter t indicates the maximal coverage depth to be plotted (15 reads per sequence pattern).

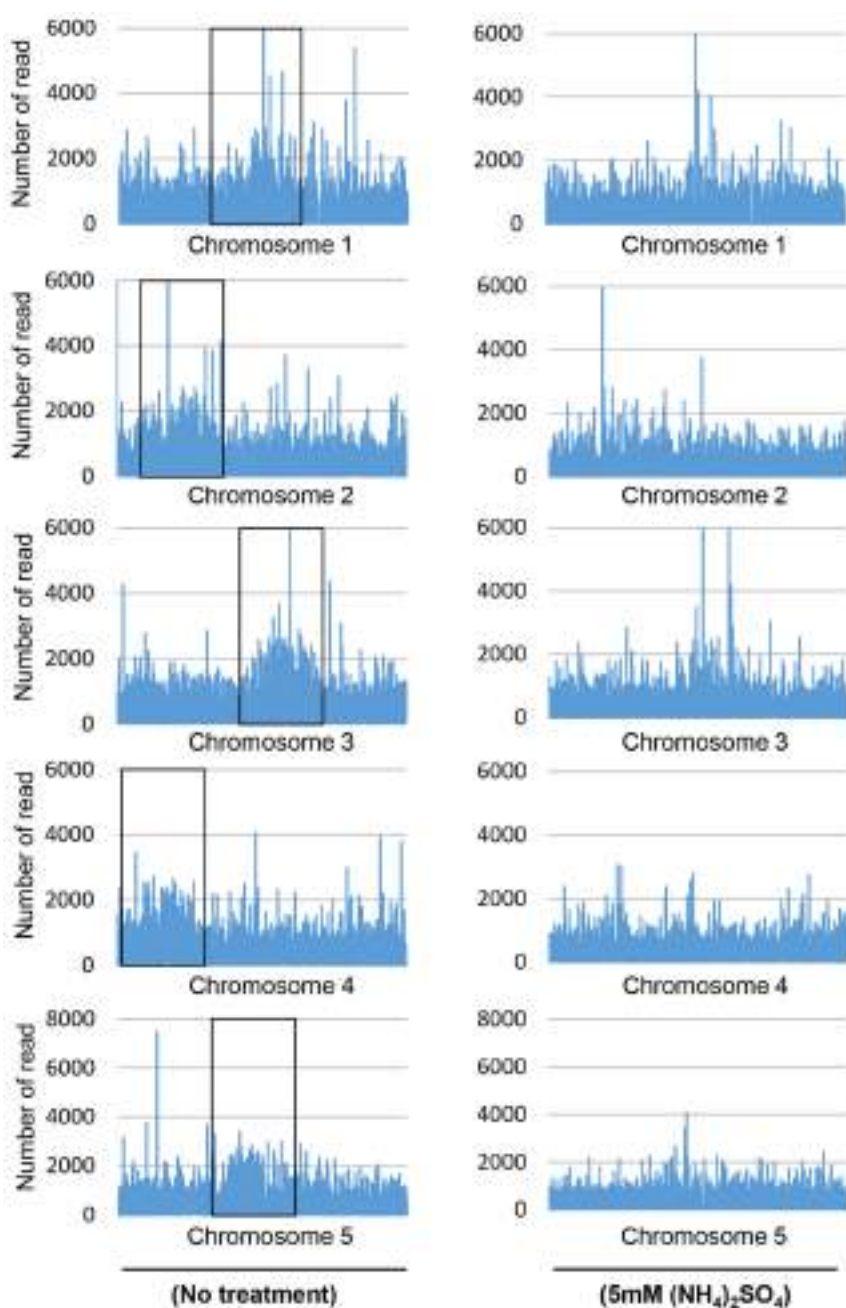


FIGURE 2 | DNA methylation landscape in the genome of ammonium-treated plants. MeDIP sequencing was performed using whole genomic DNA isolated from wild-type and 5 mM $(\text{NH}_4)_2\text{SO}_4$ -treated plants. Each peak shows the distribution of sequenced read count in chromosome. Boxes indicate heterochromatic regions in each of the five chromosomes.

Ammonium Treatment Reduces *NIA2* Methylation Levels

MeDIP sequencing analyses indicated that the whole genome methylation level was lower in $(\text{NH}_4)_2\text{SO}_4$ -treated plants than in control plants. Therefore, we examined the methylation level of *NR* genes, which encode the first enzyme in the nitrate reduction pathway. The *Arabidopsis* genome database contains

two *NR* genes, *NIA1* and *NIA2*, and their methylation levels were analyzed by bisulfite sequencing of genomic DNA isolated from control and $(\text{NH}_4)_2\text{SO}_4$ -treated plants. The results showed that *NIA1* and *NIA2* CG methylation levels were lower in $(\text{NH}_4)_2\text{SO}_4$ -treated plants than in control plants (Table 2; Supplementary Table S2). CHG methylation of *NIA1* was not detected in control and $(\text{NH}_4)_2\text{SO}_4$ -treated plants, whereas CHG methylation of *NIA2* was significantly reduced from 11.11 to 0% in response

TABLE 2 | Methylation analysis of *NIA1* and *NIA2* genes by bisulfite sequencing after ammonium treatment.

(A) <i>NIA1</i>		(B) <i>NIA2</i>			
No treatment		No treatment			
Methylated (%)	Non-methylated (%)	Methylated (%)	Non-methylated (%)		
CG	10.00	90.00	CG	11.11	88.88
CHG	0.00	100.00	CHG	11.11	88.88
CHH	0.00	100.00	CHH	16.66	83.33
All	1.89	98.11	All	14.81	85.19
$(\text{NH}_4)_2\text{SO}_4$		$(\text{NH}_4)_2\text{SO}_4$			
Methylated (%)	Non-methylated (%)	Methylated (%)	Non-methylated (%)		
CG	5.55	94.44	CG	5.88	94.11
CHG	0.00	100.00	CHG	0.00	100.00
CHH	1.28	98.71	CHH	0.00	100.00
All	1.90	98.10	All	1.01	98.99

The region of *NIA1* corresponds to positions from 1751st to 2128th (from transcription start site), and the region of *NIA2* corresponds to positions from 1552nd to 1898th (from transcription start site).

to $(\text{NH}_4)_2\text{SO}_4$ treatment (Table 2; Supplementary Table S2). CHH methylation was slightly increased from 0 to 1.28% in *NIA1* in response to $(\text{NH}_4)_2\text{SO}_4$, whereas CHH methylation was not detected in *NIA2* even after $(\text{NH}_4)_2\text{SO}_4$ treatment (Table 2; Supplementary Table S2). The overall *NIA2* methylation level was reduced by $(\text{NH}_4)_2\text{SO}_4$ treatment, but this had no effect on *NIA1* methylation (Table 2; Supplementary Table S2). The same results were obtained in replicate experiments with other ammonium sources.

Ammonium Inhibits CMT3 Binding to *NIA2*

The complete loss of CHG methylation in *NIA2* in response to $(\text{NH}_4)_2\text{SO}_4$ led us to investigate the effect of $(\text{NH}_4)_2\text{SO}_4$ on CMT3 binding to *NIA2*. The plant expression vector 35S-CMT3-FLAG4 was constructed and introduced into *Agrobacterium*, which was used to transform 3-week-old wild-type plants by infiltration. Then, CMT3-FLAG4 expression was analyzed in transformed plants after sequential treatment with 5 mM $(\text{NH}_4)_2\text{SO}_4$ for 12 h and isolation of genomic DNA and total proteins. Western blot analysis showed that CMT3-FLAG4 was expressed in both untreated control and $(\text{NH}_4)_2\text{SO}_4$ -treated plants (Figure 3A). On the basis of this result, a DNA/protein-binding assay was performed using sonicated genomic DNA and an anti-FLAG antibody, and the pull-down DNA amount was estimated by PCR analysis with gene-specific primers for *NIA1* and *NIA2*. The results showed that complex formation between CMT3 and *NIA2* was inhibited in $(\text{NH}_4)_2\text{SO}_4$ -treated plants, whereas complex formation between CMT3 and *NIA1* was not affected by $(\text{NH}_4)_2\text{SO}_4$ treatment (Figure 3B).

The methylation levels of *NIA1*, *NIA2*, and *CMT3* in $(\text{NH}_4)_2\text{SO}_4$ -treated plants were examined by McrBC digestion and PCR analysis with gene-specific primers. The gels showed similar band intensities for *NIA1* and *CMT3* in untreated control

and $(\text{NH}_4)_2\text{SO}_4$ -treated plants, indicating that *NIA1* and *CMT3* methylation levels did not change in response to $(\text{NH}_4)_2\text{SO}_4$ treatment (Figure 3C). However, the *NIA2* band intensity increased in $(\text{NH}_4)_2\text{SO}_4$ -treated plants, indicating that *NIA2* methylation was reduced in response to $(\text{NH}_4)_2\text{SO}_4$ treatment (Figure 3C). Similar binding patterns and methylation levels were observed in response to treatment with other ammonium sources.

Ammonium Upregulates *NIA2* Gene Expression

Our results showed that *NIA2* methylation was inhibited by ammonium treatment, which suggests that ammonium induces *NIA2* expression. *NIA2* transcription was examined by qRT-PCR, which showed approximately 2-fold higher *NIA2* transcript levels in $(\text{NH}_4)_2\text{SO}_4$ -treated plants than in control plants (Figure 4A). This indicates that *NIA2* upregulation in $(\text{NH}_4)_2\text{SO}_4$ -treated plants resulted from low methylation levels caused by the lack of CHG methylation of *NIA2*. However, because low *NIA2* methylation levels could also be caused by low *CMT3* expression, we evaluated *CMT3* expression levels and detected no differences in *CMT3* transcript levels between $(\text{NH}_4)_2\text{SO}_4$ -treated and control plants (Figure 4B). These data indicate that low methylation levels and high transcription levels of *NIA2* in response to $(\text{NH}_4)_2\text{SO}_4$ were caused by impaired CHG methylation of *NIA2*. Similar gene expression patterns were detected with other ammonium sources.

CMT3 Binds to Specific Regions of *NIA2*

CMT3 catalyzed the CHG methylation of *NIA2* but not that of *NIA1*. Therefore, the CMT3-binding region in *NIA2* was detected using IP and PCR analysis. Wild-type *Arabidopsis* plants were transformed by infiltration with *Agrobacterium* carrying 35S-CMT3-FLAG4, and the DNA/CMT3-FLAG4 complex was pulled down with an anti-FLAG antibody. DNA

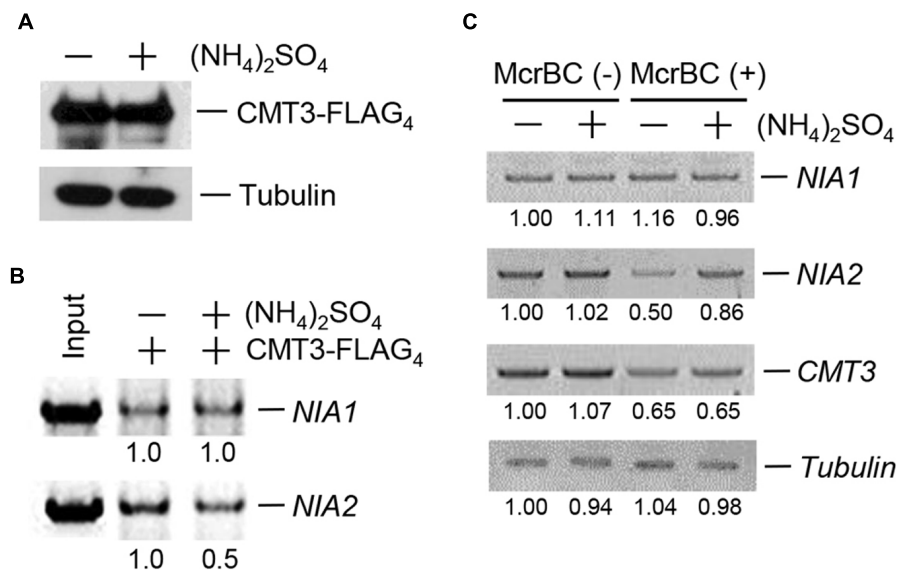


FIGURE 3 | CMT3 binding to NIA2 decreased in response to ammonium. **(A)** Wild-type *Arabidopsis* was infiltrated by Agrobacteria transformed with 35S-CMT3-FLAG₄, and then treated with or without 5 mM (NH₄)₂SO₄. CMT3-FLAG₄ expression was examined by western blotting with anti-FLAG antibody. Tubulin was used as the loading control. **(B)** CMT3-FLAG₄ was pulled down with an anti-FLAG antibody, and DNA was extracted. The purified DNA was analyzed by PCR using gene-specific primers, and *NIA1* and *NIA2* levels were examined by agarose gel electrophoresis. Numbers under lanes indicate relative intensities. DNA levels were normalized to a value of 1.00 for DNA level in the “—” (NH₄)₂SO₄ lane in each panel. **(C)** Genomic DNA was isolated from wild-type *Arabidopsis* treated with or without 5 mM (NH₄)₂SO₄ and then digested with McrBC. The remaining DNA was used for PCR amplification with specific primers for *NIA1*, *NIA2*, and *CMT3*. Numbers under lanes indicate relative intensities. DNA levels were normalized to a value of 1.00 for DNA level in the “—” McrBC and “—” (NH₄)₂SO₄ lane in each panel. Tubulin was used as the loading control.

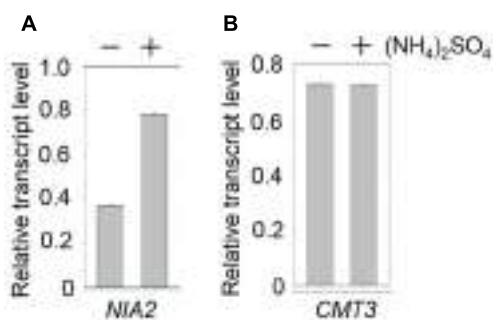


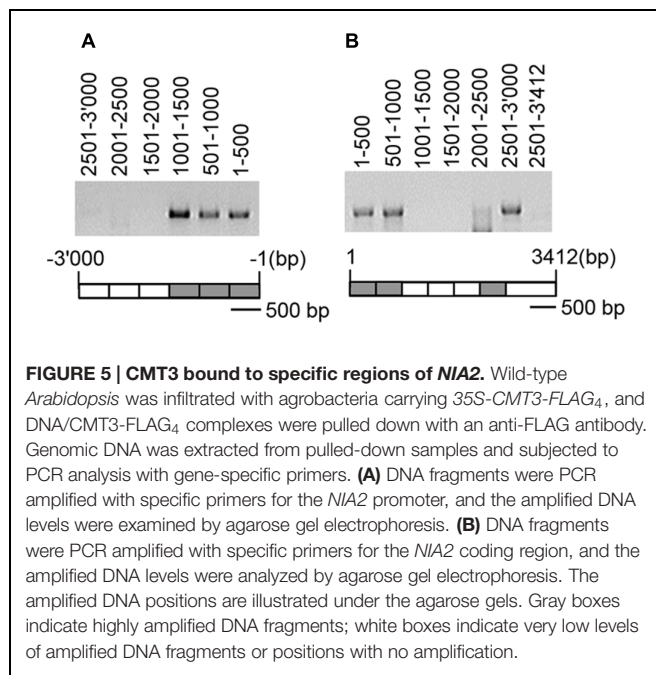
FIGURE 4 | NIA2 expression was upregulated by ammonium. Total RNA was isolated from wild-type *Arabidopsis* plants treated with and without 5 mM (NH₄)₂SO₄, and then subjected to real-time qRT-PCR analysis with specific primers for *NIA2* **(A)** and *CMT3* **(B)**.

was then amplified by PCR using specific primers for the promoter and coding regions of *NIA2*. The following three regions formed complexes with CMT3-FLAG₄: the 1.5 kb promoter region from -1,500 to -1 bp (**Figure 5A**), the 1.0 kb coding region from 1 to 1,000 bp, and the 0.5 kb coding region from 2,501 to 3,000 bp (**Figure 5B**). These results indicate that CMT3 binds to specific regions in the *NIA2* promoter and coding sequence, suggesting that CMT3 catalyzes *NIA2* methylation at specific sequences or structures.

DISCUSSION

The current study aimed to define the role of CMT3 in nitrogen assimilation. We examined the effect of ammonium on whole genome methylation and observed that ammonium reduced the levels of whole genome methylation (**Table 1** and Supplementary Table S1). Plants utilize ammonium for carbon metabolism, nitrogen fixation, and biosynthesis of metabolic building blocks. Therefore, the effect of ammonium on reducing genome methylation suggests that high intracellular nitrogen concentration induces gene demethylation or represses gene methylation, thereby upregulating the expression of numerous genes involved in nitrogen metabolism. The carbohydrate-to-nitrogen (CN) ratio has a central and interactive role in regulating post-germination growth because the level of nitrogen is regulated with respect to that of carbohydrate during development (Huppe and Turpin, 1994). This suggests that ammonium treatment increases the intracellular nitrogen concentration, which affects nitrogen-sensitive metabolic networks. These combined data indicate that ammonium treatment induces the expression of genes involved in nitrogen assimilation by activating DNA demethylases or inactivating DNMTs.

CMT3-mediated genome methylation is a critical epigenetic modification that regulates plant growth and development. CMT3 functions in flower and reproductive organ development, embryogenesis, seed viability (Xiao et al., 2006; Pillot et al., 2010), organogenesis, and shoot regeneration from root explants



(Shemer et al., 2015). CMT3 is involved in shoot growth regulation in *Arabidopsis* (Lin et al., 2015) and plays a role in tobacco leaf development by modulating the jasmonate pathway (Coustham et al., 2014). In addition, CMT3 acts as a functional regulator of oxidative stress to prevent genome instability and the accumulation of mutations caused by ionizing irradiation (Sidler et al., 2015). These data indicate that CMT3 catalyzes the methylation of numerous genes and may methylate and silence transposable elements (Kato et al., 2003). Therefore, CMT3 functions as a plant-specific DNMT that modulates growth, development, and differentiation throughout the plant life cycle from germination to seed maturation.

Our previous study showed that CHG methylation occurs on *NIA2* but not on *NIA1* and that CMT3 catalyzes CHG methylation of *NIA2* (Kim et al., 2015a). In the present study, CHG methylation of *NIA2* was not detected in ammonium-treated plants (Table 2), suggesting that ammonium treatment inactivates CMT3 activity or represses CMT3 expression. The mechanism of CMT3 methylation of target genes has not been completely elucidated. Three possible mechanisms are proposed to explain how CMT3 distinguishes target DNA sequences. First, CMT3 may distinguish target genes through specific siRNAs in a siRNA/CMT3 complex, leading to CHG methylation of the specific target genes. This is similar to the recently reported DRM2 methylation of genes with target sequence homology to specific siRNAs as an AGO4/siRNA/DRM2 complex (Matzke and Mosher, 2014; Zhong et al., 2014). Since AGO4/siRNA complex formation is a prerequisite for the interaction of siRNAs with other components including methylases, identification of AGO4/siRNA complex interacting with CMT3 may provide the mechanism that CMT3 distinguishes target DNA sequences.

Second, the BAH domain and chromodomain of CMT3 recognize H3K9me2, leading to CMT3 binding to nucleosomes

to methylate target DNA sequences (Du et al., 2012). This indicates that the BAH domain and chromodomain guide CMT3 to specific genomic regions by interacting with specific chromatin modifications. Therefore, examination of H3K9me2 of *NIA1* and *NIA2* genes *in vivo* may also provide clues as to why CMT3 selectively methylates the *NIA2* gene.

Third, the citrullination of DNMT3A by peptidylarginine deiminase (PADI4) stimulates its DNMT activity (Deplus et al., 2014). Citrullination affects protein structure and function (Lee et al., 2005; Gyorgy et al., 2006; Guo and Fast, 2011). CMT3 can be citrullinated by a plant PADI4 homolog. Therefore, CMT3 citrullination can modulate its ability to interact with partners involved in CMT3 targeting to specific genes and DNA methylation, suggesting that citrullination can help CMT3 discriminate among potential target sequences.

CHG methylation of *NIA2* in control wild-type plants but not in ammonium-treated plants (Table 2) indicated that CMT3-mediated CHG methylation of *NIA2* was blocked by ammonium treatment, suggesting that ammonium treatment represses CMT3 expression. However, CMT3 transcript levels and methylation levels were not affected by ammonium treatment (Figure 4B). This indicates that repression of CMT3-mediated CHG methylation of *NIA2* in response to ammonium treatment may not result from changes in CMT3 levels, but may be caused by changes in CMT3 activity due to post-translational modification. Our previous study showed that the DNMT activity of CMT3 was increased by sumoylation by the E3 SUMO ligase of AtSIZ1 (Kim et al., 2015a). This suggests that ammonium treatment may block AtSIZ1-mediated CMT3 sumoylation or other CMT3 modifications that are required for CMT3 activation.

CHG methylation correlates with H3K9m2 (Bernatavichute et al., 2008; Deleris et al., 2012), and the H3K9m2 histone MET triple mutant *kyp/suvh5/suvh6* shows a reduction in CHG methylation similar to that found in the *cmt3* mutant (Edds and Bender, 2006; Stroud et al., 2013). Some CHG sites also lost methylation in the *met1* mutant, indicating that CHG methylation partly depends on CG methylation (Stroud et al., 2013). A lack of CHG methylation correlates with a lack of the H3K9m2 marker, which is maintained by the histone methylase INCREASE IN BONSAI METHYLATION1 (IBM1) (Saze and Kakutani, 2011). These results suggest that the reduction in genome methylation levels in response to ammonium treatment can be affected by other DNA and histone METs. Therefore, further investigation of these mutants is needed to discover how ammonium regulates gene methylation or demethylation, including that of *NIA2*.

CONCLUSION

The present study showed that ammonium has no effect on CMT3 methylation and expression, whereas it blocks CMT3-mediated CHG methylation of *NIA2*, which induces *NIA2* expression. Future studies should be aimed at identifying CMT3-interacting factors, including siRNAs and proteins, and at examining the modulation of CMT3 DNMT activity by

phytohormones or chemicals including ammonium. This may help elucidate specific mechanisms regulating CMT3-mediated genome methylation during specific growth and developmental stages, as well as during nitrogen assimilation.

AUTHOR CONTRIBUTIONS

HSS designed the studies. JYK, and DYK performed experiments. JYK, SIK, YJK, JTS, and HSS interpreted data. JYK and HSS wrote the manuscript. All authors commented on the results and the manuscript.

REFERENCES

- Armache, K. J., Garlick, J. D., Canzio, D., Narlikar, G. J., and Kingston, R. E. (2011). Structural basis of silencing: Sir3 BAH domain in complex with a nucleosome at 3.0 Å resolution. *Science* 334, 977–982. doi: 10.1126/science.1210915
- Bernatavichute, Y. V., Zhang, X., Cokus, S., Pellegrini, M., and Jacobsen, S. E. (2008). Genome-wide association of histone H3 lysine nine methylation with CHG DNA methylation in *Arabidopsis thaliana*. *PLoS ONE* 3:e3156. doi: 10.1371/journal.pone.0003156
- Campbell, W. H., and Kinghorn, K. R. (1990). Functional domains of assimilatory nitrate reductases and nitrite reductases. *Trends Biochem. Sci.* 15, 315–319. doi: 10.1016/0968-0004(90)90021-3
- Cao, X., Aufsatz, W., Zilberman, D., Mette, M. F., Huang, M. S., Matzke, M., et al. (2003). Role of the DRM and CMT3 methyltransferases in RNA-directed DNA methylation. *Curr. Biol.* 13, 2212–2217. doi: 10.1016/j.cub.2003.11.052
- Cao, X., and Jacobsen, S. E. (2002a). Locus-specific control of asymmetric and CpNpG methylation by the DRM and CMT3 methyltransferase genes. *Proc. Natl. Acad. Sci. U.S.A.* 99, 16491–16498. doi: 10.1073/pnas.1623199
- Cao, X., and Jacobsen, S. E. (2002b). Role of the *Arabidopsis* DRM methyltransferases in de novo DNA methylation and gene silencing. *Curr. Biol.* 9, 1138–1144. doi: 10.1016/S0960-9822(02)00925-9
- Chan, S. W., Henderson, I. R., and Jacobsen, S. E. (2005). Gardening the genome: DNA methylation in *Arabidopsis thaliana*. *Genetics* 6, 351–360.
- Cokus, S. J., Feng, S., Zhang, X., Chen, Z., Merriman, B., Haudenschild, C. D., et al. (2008). Shotgun bisulphite sequencing of the *Arabidopsis* genome reveals DNA methylation patterning. *Nature* 452, 215–219. doi: 10.1038/nature06745
- Coustham, V., Vlad, D., Deremetz, A., Gy, I., Cubillos, F. A., Kerdaffrec, E., et al. (2014). SHOOT GROWTH1 maintains *Arabidopsis* epigenomes by regulating IBM1. *PLoS ONE* 9:e84687. doi: 10.1371/journal.pone.0084687
- Crawford, N. M., and Forde, B. G. (2002). “Molecular and developmental biology of inorganic nitrogen nutrition,” in *The Arabidopsis Book*, Vol. 1, eds E. Meyerowitz and C. Somerville (Rockville, MD: American Society of Plant Biologists Press), e0011. doi: 10.1199/tab.0011
- Deleris, A., Stroud, H., Bernatavichute, Y., Johnson, E., Klein, G., Schubert, D., et al. (2012). Loss of the DNA methyltransferase MET1 Induces H3K9 hypermethylation at Pcg target genes and redistribution of H3K27 trimethylation to transposons in *Arabidopsis thaliana*. *PLoS Genet.* 8:e1003062. doi: 10.1371/journal.pgen.1003062
- Deplus, R., Denis, H., Putmans, P., Calonne, E., Fourrez, M., Yamamoto, K., et al. (2014). Citrullination of DNMT3A by PADI4 regulates its stability and controls DNA methylation. *Nucleic Acids Res.* 42, 8285–8296. doi: 10.1093/nar/gku522
- Du, J., Zhong, X., Bernatavichute, Y. V., Stroud, H., Feng, S., Caro, E., et al. (2012). Dual binding of chromomethylase domains to H3K9me2-containing nucleosomes directs DNA methylation in plants. *Cell* 151, 167–180. doi: 10.1016/j.cell.2012.07.034
- Ebbs, M. L., and Bender, J. (2006). Locus-specific control of DNA methylation by the *Arabidopsis* SUVH5 histone methyltransferase. *Plant Cell* 18, 1166–1176. doi: 10.1105/tpc.106.041400
- Finnegan, E. J., and Kovac, K. A. (2000). Plant DNA methyltransferases. *Plant Mol. Biol.* 43, 189–201. doi: 10.1023/A:1006427226972
- Forde, B. G. (2002). Local and long-range signaling pathways regulating plant responses to nitrate. *Annu. Rev. Plant Biol.* 53, 203–224. doi: 10.1146/annurev.arplant.53.100301.135256
- Foyer, C. H., Parry, M., and Noctor, G. (2003). Markers and signals associated with nitrogen assimilation in higher plants. *J. Exp. Bot.* 54, 585–593. doi: 10.1093/jxb/erg053
- Greenberg, M. V., Ausin, I., Chan, S. W., Cokus, S. J., Cuperus, J. T., Feng, S., et al. (2011). Identification of genes required for de novo DNA methylation in *Arabidopsis*. *Epigenetics* 6, 344–354. doi: 10.4161/epi.6.3.14242
- Guo, Q., and Fast, W. (2011). Citrullination of inhibitor of growth 4 (ING4) by peptidylarginine deminase 4 (PAD4) disrupts the interaction between ING4 and p53. *J. Biol. Chem.* 286, 17069–17078. doi: 10.1074/jbc.M111.230961
- Gyorgy, B., Toth, E., Tarcsa, E., Falus, A., and Buzas, E. I. (2006). Citrullination: a posttranslational modification in health and disease. *Int. J. Biochem. Cell Biol.* 38, 1662–1677. doi: 10.1016/j.biocel.2006.03.008
- Henderson, I. R., Deleris, A., Wong, W., Zhong, X., Chin, H. G., Horwitz, G. A., et al. (2010). The de novo cytosine methyltransferase DRM2 requires intact UBA domains and a catalytically mutated paralog DRM3 during RNA-directed DNA methylation in *Arabidopsis thaliana*. *PLoS Genet.* 6:e1001182. doi: 10.1371/journal.pgen.1001182
- Henikoff, S., and Comai, L. (1998). A DNA methyltransferase homolog with a chromodomain exists in multiple polymorphic forms in *Arabidopsis*. *Genetics* 149, 307–318.
- Herman, J. G., and Baylin, S. B. (2003). Gene silencing in cancer in association with promoter hypermethylation. *N. Engl. J. Med.* 349, 2042–2054. doi: 10.1056/NEJMra023075
- Hetzl, J., Foerster, A. M., Raidl, G., and Mittelsten Scheid, O. (2007). CyMATE : a new tool for methylation analysis of plant genomic DNA after bisulphite sequencing. *Plant J.* 51, 526–536. doi: 10.1111/j.1365-313X.2007.03152.x
- Hou, P. Q., Lee, Y. I., Hsu, K. T., Lin, Y. T., Wu, W. Z., Lin, J. Y., et al. (2013). Functional characterization of *Nicotiana benthamiana* chromomethylase 3 in developmental programs by virus-induced gene silencing. *Physiol. Plant.* 150, 119–132. doi: 10.1111/ppl.12071
- Huang, J. J., Wang, H. H., Liang, W. H., Xie, X. J., and Guo, G. Q. (2014). Developmental expression of *Arabidopsis* methyltransferase genes MET1, DRM2 and CMT3. *Mol. Biol.* 48, 782–789. doi: 10.1134/S0026893314050057
- Huppe, H. C., and Turpin, D. H. (1994). Integration of carbon and nitrogen metabolism in plant and algal cells. *Annu. Rev. Plant Physiol. Plant Mol. Biol.* 45, 577–607. doi: 10.1146/annurev.pp.45.060194.003045
- Jones, L., Ratcliff, F., and Baulcombe, D. C. (2001). RNA-directed transcriptional gene silencing in plants can be inherited independently of the RNA trigger and requires Met1 for maintenance. *Curr. Biol.* 11, 747–757. doi: 10.1016/S0960-9822(01)00226-3
- Kato, M., Miura, A., Bender, J., Jacobsen, S. E., and Kakutani, T. (2003). Role of CG and non-CG methylation in immobilization of transposons in *Arabidopsis*. *Curr. Biol.* 13, 421–426. doi: 10.1016/S0960-9822(03)00106-4
- Kim, D. Y., Han, Y. J., Kim, S., Song, J. T., and Seo, H. S. (2015a). *Arabidopsis* CMT3 activity is positively regulated by AtSIZ1-mediated sumoylation. *Plant Sci.* 239, 209–215. doi: 10.1016/j.plantsci.2015.08.003
- Kim, S. I., Park, B. S., Kim, D. Y., Yeo, S. Y., Ong, S. I., Song, J. T., et al. (2015b). E3 SUMO ligase AtSIZ1 positively regulates SLY1-mediated GA signaling and plant development. *Biochem. J.* 469, 299–314. doi: 10.1042/BJ20141302

ACKNOWLEDGMENTS

This work was supported by a grant from the Next-Generation BioGreen 21 Program (Plant Molecular Breeding Center no. PJ01108701), Rural Development Administration, Republic of Korea.

SUPPLEMENTARY MATERIAL

The Supplementary Material for this article can be found online at: <http://journal.frontiersin.org/article/10.3389/fpls.2015.01161>

- Kuo, A. J., Song, J., Cheung, P., Ishibe-Murakami, S., Yamazoe, S., Chen, J. K., et al. (2012). The BAH domain of ORC1 links H4K20me2 to DNA replication licensing and Meier-Gorlin syndrome. *Nature* 484, 115–119. doi: 10.1038/nature10956
- Lee, Y. H., Coonrod, S. A., Kraus, W. L., Jelinek, M. A., and Stallcup, M. R. (2005). Regulation of coactivator complex assembly and function by protein arginine methylation and demethylation. *Proc. Natl. Acad. Sci. U.S.A.* 102, 3611–3616. doi: 10.1073/pnas.0407159102
- Lin, Y. T., Wei, H. M., Lu, H. Y., Lee, Y. I., and Fu, S. F. (2015). Developmental- and tissue-specific expression of NbCMT3-2 encoding a chromomethylase in *Nicotiana benthamiana*. *Plant Cell Physiol.* 56, 1124–1143. doi: 10.1093/pcp/pcv036
- Lindroth, A. M., Cao, X., Jackson, J. P., Zilberman, D., McCallum, C. M., Henikoff, S., et al. (2001). Requirement of CHROMOMETHYLASE3 for maintenance of CpXpG methylation. *Science* 292, 2077–2080. doi: 10.1126/science.1059745
- Lippman, Z., May, B., Yordan, C., Singer, T., and Martienssen, R. (2003). Distinct mechanisms determine transposon inheritance and methylation via small interfering RNA and histone modification. *PLoS Biol.* 1:e67. doi: 10.1371/journal.pbio.0000067
- Matzke, M. A., and Mosher, R. A. (2014). RNA-directed DNA methylation: an epigenetic pathway of increasing complexity. *Nat. Rev. Genet.* 15, 394–408. doi: 10.1038/nrg3683
- McCallum, C. M., Comai, L., Greene, E. A., and Henikoff, S. (2000). Targeted screening for induced mutations. *Nat. Biotechnol.* 18, 455–457. doi: 10.1038/74542
- Papa, C. M., Springer, N. M., Muszynski, M. G., Meeley, R., and Kaepller, S. M. (2001). Maize chromomethylase Zea Methyltransferase2 is required for CpNpG methylation. *Plant Cell* 13, 1919–1928. doi: 10.2307/3871328
- Park, B. S., Song, J. T., and Seo, H. S. (2011). *Arabidopsis* nitrate reductase activity is stimulated by the E3 SUMO ligase AtSIZ1. *Nat. Commun.* 2, 400. doi: 10.1038/ncomms1408
- Pillot, M., Baroux, C., Vazquez, M. A., Autran, D., Leblanc, O., Vielle-Calzada, J. P., et al. (2010). Embryo and endosperm inherit distinct chromatin and transcriptional states from the female gametes in *Arabidopsis*. *Plant Cell* 22, 307–320. doi: 10.1105/tpc.109.071647
- Pomraning, K. R., Smith, K. M., and Freitag, M. (2009). Genome-wide high throughput analysis of DNA methylation in eukaryotes. *Methods* 47, 142–150. doi: 10.1016/j.ymeth.2008.09.022
- Ronemus, M. J., Galbiati, M., Ticknor, C., Chen, J., and Dellaporta, S. L. (1996). Demethylation-induced developmental pleiotropy in *Arabidopsis*. *Science* 273, 654–657. doi: 10.1126/science.273.5275.654
- Rose, T. M., Schultz, E. R., Henikoff, J. G., Pietrovski, S., McCallum, C. M., and Henikoff, S. (1998). Consensus-degenerate hybrid oligonucleotide primers for amplification of distantly related sequences. *Nucleic Acids Res.* 26, 1628–1635. doi: 10.1093/nar/26.7.1628
- Sanchez, R., and Zhou, M. M. (2009). The role of human bromodomains in chromatin biology and gene transcription. *Curr. Opin. Drug Discov. Devel.* 12, 659–665.
- Saze, H., and Kakutani, T. (2011). Differentiation of epigenetic modifications between transposons and genes. *Curr. Opin. Plant Biol.* 14, 81–87. doi: 10.1016/j.pbi.2010.08.017
- Shemer, O., Landau, U., Candela, H., Zemach, A., and Eshed Williams, L. (2015). Competency for shoot regeneration from *Arabidopsis* root explants is regulated by DNA methylation. *Plant Sci.* 238, 251–261. doi: 10.1016/j.plantsci.2015.06.015
- Sidler, C., Li, D., Kovalchuk, O., and Kovalchuk, I. (2015). Development-dependent expression of DNA repair genes and epigenetic regulators in *Arabidopsis* plants exposed to ionizing radiation. *Radiat. Res.* 183, 219–232. doi: 10.1667/RR13840.1
- Solomonson, L. P., and Barber, M. J. (1990). Assimilatory nitrate reductase-functional properties and regulation. *Annu. Rev. Plant Physiol. Plant Mol. Biol.* 41, 225–253. doi: 10.1146/annurev.pp.41.060190.001301
- Stitt, M., Müller, C., Matt, P., Gibon, Y., Carillo, P., Morcuende, R., et al. (2002). Steps towards an integrated view of nitrogen metabolism. *J. Exp. Bot.* 53, 959–970. doi: 10.1093/jexbot/53.370.959
- Stroud, H., Greenberg, M. V., Feng, S., Bernatavichute, Y. V., and Jacobsen, S. E. (2013). Comprehensive analysis of silencing mutants reveals complex regulation of the *Arabidopsis* methylome. *Cell* 152, 352–364. doi: 10.1016/j.cell.2012.10.054
- Xiao, W., Custard, K. D., Brown, R. C., Lemmon, B. E., Harada, J. J., Goldberg, R. B., et al. (2006). DNA methylation is critical for *Arabidopsis* embryogenesis and seed viability. *Plant Cell* 18, 805–814. doi: 10.1105/tpc.105.08836
- Yang, N., and Xu, R. M. (2013). Structure and mechanisms of lysine methylation recognition by the chromodomain in gene transcription. *Crit. Rev. Biochem. Mol. Biol.* 48, 211–221. doi: 10.1021/bi101885m
- Yap, K. L., and Zhou, M. M. (2012). Structure and mechanisms of lysine methylation recognition by the chromodomain in gene transcription. *Biochemistry* 50, 1966–1980. doi: 10.1021/bi101885m
- Zemach, A., Kim, M. Y., Hsieh, P. H., Coleman-Derr, D., Eshed-Williams, L., Thao, K., et al. (2013). The *Arabidopsis* nucleosome remodeler DDM1 allows DNA methyltransferases to access H1-containing heterochromatin. *Cell* 153, 193–205. doi: 10.1016/j.cell.2013.02.033
- Zhang, X., and Jacobsen, S. E. (2006). Genetic analyses of DNA methyltransferase in *Arabidopsis thaliana*. *Cold Spring Harb. Symp. Quant. Biol.* 71, 439–447. doi: 10.1101/sqb.2006.71.047
- Zhang, X., Yazaki, J., Sundaresan, A., Cokus, S., Chan, S. W.-L., Chen, H., et al. (2006). Genome-wide high-resolution mapping and functional analysis of DNA methylation in *Arabidopsis*. *Cell* 126, 1189–1201. doi: 10.1016/j.cell.2006.08.003
- Zhong, X., Du, J., Hale, C. J., Gallego-Bartolome, J., Feng, S., Vashisht, A. A., et al. (2014). Molecular mechanism of action of plant DRM de novo DNA methyltransferases. *Cell* 157, 1050–1060. doi: 10.1016/j.cell.2014.03.056

Conflict of Interest Statement: The authors declare that the research was conducted in the absence of any commercial or financial relationships that could be construed as a potential conflict of interest.

Copyright © 2016 Kim, Kwon, Kim, Kim, Song and Seo. This is an open-access article distributed under the terms of the Creative Commons Attribution License (CC BY). The use, distribution or reproduction in other forums is permitted, provided the original author(s) or licensor are credited and that the original publication in this journal is cited, in accordance with accepted academic practice. No use, distribution or reproduction is permitted which does not comply with these terms.



Protein Phosphatase 2A in the Regulatory Network Underlying Biotic Stress Resistance in Plants

Guido Durian¹, Moona Rahikainen¹, Sara Alegre¹, Mikael Brosché² and Sajaliisa Kangasjärvi^{1*}

¹ Department of Biochemistry, Molecular Plant Biology, University of Turku, Turku, Finland, ² Division of Plant Biology, Department of Biosciences, Viikki Plant Science Centre, University of Helsinki, Helsinki, Finland

OPEN ACCESS

Edited by:

Olivier Lamotte,
UMR Agroécologie, France

Reviewed by:

Alison DeLong,
Brown University, USA
Ben M. Long,
Australian National University,
Australia
Girdhar Kumar Pandey,
University of Delhi, India

*Correspondence:

Sajaliisa Kangasjärvi
sajaliisa.kangasjarvi@utu.fi

Specialty section:

This article was submitted to
Plant Physiology,
a section of the journal
Frontiers in Plant Science

Received: 25 February 2016

Accepted: 25 May 2016

Published: 10 June 2016

Citation:

Durian G, Rahikainen M, Alegre S, Brosché M and Kangasjärvi S (2016)
Protein Phosphatase
2A in the Regulatory Network
Underlying Biotic Stress Resistance
in Plants. *Front. Plant Sci.* 7:812.
doi: 10.3389/fpls.2016.00812

Biotic stress factors pose a major threat to plant health and can significantly deteriorate plant productivity by impairing the physiological functions of the plant. To combat the wide range of pathogens and insect herbivores, plants deploy converging signaling pathways, where counteracting activities of protein kinases and phosphatases form a basic mechanism for determining appropriate defensive measures. Recent studies have identified Protein Phosphatase 2A (PP2A) as a crucial component that controls pathogenesis responses in various plant species. Genetic, proteomic and metabolomic approaches have underscored the versatile nature of PP2A, which contributes to the regulation of receptor signaling, organellar signaling, gene expression, metabolic pathways, and cell death, all of which essentially impact plant immunity. Associated with this, various PP2A subunits mediate post-translational regulation of metabolic enzymes and signaling components. Here we provide an overview of protein kinase/phosphatase functions in plant immunity signaling, and position the multifaceted functions of PP2A in the tightly inter-connected regulatory network that controls the perception, signaling and responding to biotic stress agents in plants.

Keywords: protein phosphatase 2a, plant immunity, signaling, metabolism, protein phosphorylation

INTRODUCTION

Modern agricultural practices and breeding programs have significantly increased crop yields over the past century. Compared to their wild ancestors, however, modern crops suffer from reduced stress resistance, since plant breeding has largely focused on increasing yield in monocultural farming. A combination of environmental challenges, such as light stress, drought or plant disease pose major threats for plant health, and the urgent need to control plant disease has recently been exemplified by headlines reporting yield losses caused by the Panama disease of banana or head blight of cereals, caused by the detrimental fungal pathogens *Fusarium oxysporum* and *F. graminearum*, respectively. Besides causing severe symptoms or even death of the plant, biotic and abiotic stresses may deteriorate plant productivity by limiting plant growth and development through impaired physiological functions (Krasensky and Jonak, 2012).

To survive in sub-optimal conditions, plants have evolved a repertoire of mechanisms to combat harmful external cues (Boller and Felix, 2009; Yamazaki and Hayashi, 2015). Recognition of attempted infection or insect infestation leads to reprogramming of basic metabolism and production of deterring chemical compounds to prevent pathogens and pests from colonizing the host plant tissue. Organellar metabolism and signaling are vital in reinforcing these protective reactions, but the exact mechanisms remain poorly understood (Trotta et al., 2014). It is well-known, however, that exposure of plants to excess

light promotes formation of protective pigments, such as anthocyanins and other phenolic compounds with distinct antioxidant activities. Such stress-induced plant-derived protective compounds can have both deleterious and beneficial effects in human nutrition, and provide a vast repertoire of molecular structures for discovery of novel bioactive compounds from the plant kingdom. Understanding how the signals arising from recognition of pathogen infection cross-communicate with organelle signaling and become translated into appropriate metabolic adjustments, and how this supports the physiology of the whole cell and disease resistance in the entire plant still requires future research efforts.

Identification of stress-inducible biosynthetic pathways and modeling their integration with the metabolic and regulatory networks governing basic production, stress resistance and growth are increasing trends in modern plant biology (Allahverdiyeva et al., 2015). In these interactions, reversible protein phosphorylation, catalyzed by counteracting activities of protein kinases and protein phosphatases, connects stress perception and the immediate down-stream cascades with the signaling networks that ultimately regulate gene expression profiles and metabolic activities in the cell (Uhrig et al., 2013; van Wijk et al., 2014).

Protein dephosphorylation is emerging as a key regulatory mechanism in plant immunity. In plants, as in other eukaryotic organisms, protein phosphatases can be grouped into four families: PPP (phosphoprotein phosphatase), PPM/PP2C (Mg^{2+} - or Mn^{2+} -dependent protein phosphatase/protein phosphatase 2C), PTP (phosphotyrosine phosphatase), and aspartate-dependent phosphatase families (reviewed by Uhrig et al., 2013). PPPs and PPM/PP2Cs dephosphorylate serine and threonine residues, and it is believed that the evolutionarily highly conserved PPPs are responsible for catalyzing about 80% of eukaryotic protein dephosphorylation (Moorhead et al., 2009; Lillo et al., 2014). In plants, the PPP family of serine-/threonine phosphatases can be further divided into nine subfamilies: PP1 (protein phosphatase type one), PP2A (protein phosphatase 2A), PP4, PP5, PP6, PP7, SLP (*Shewanella*-like protein) phosphatase, and PPKL (protein phosphatase with Kelch-like repeat domains) (Uhrig et al., 2013). This review highlights the multifaceted function of PP2A in controlling the sensing, signaling and responding to biotic stress agents in plants.

SENSING AND SIGNALING OF PATHOGEN INFECTION: JOINT ACTION AMONG DIFFERENT CELLULAR COMPARTMENTS

Phosphorelay Signaling from the Plasma Membrane to the Nucleus

Plants monitor their biotic environment through plasma membrane pattern recognition receptors, which act as receptor-like kinases (RLKs) or receptor-like proteins (RLPs) (Jones and Dangl, 2006; Gust and Felix, 2014) that can sense the

presence of conserved pathogen-associated molecular patterns (PAMPs), such as bacterial flagella and peptidoglycans, the fungal cell wall constituent chitin or the saliva of aphids (Gómez-Gómez and Boller, 2000; Liu et al., 2012; Prince et al., 2014; Zipfel, 2014; **Figure 1**). After binding their specific PAMPs, RLKs undergo homo-dimerization or hetero-dimerize with plasma-membrane bound coreceptors, allowing signal initiation by the activated receptor complex. RLPs in turn associate with their corresponding cytoplasmic adaptor kinases either before or after binding their individual pathogen derived ligands to form an active signaling component when the ligand is perceived (Gust and Felix, 2014; Macho and Zipfel, 2014).

Through the cytoplasmic kinase function of RLKs, the recognition rapidly elicits downstream signaling effects that manifest themselves as transient increases in cytosolic calcium concentration, activation of the plasma membrane NADPH oxidases, a consequent burst of reactive oxygen species (ROS) in the apoplast, and concomitant activation of phosphorelay cascades employing mitogen-activated protein kinases (MAPKs) or calcium-dependent protein kinases (CDPKs, or in *Arabidopsis thaliana* CPKs) (Asai et al., 2002; Zhang et al., 2007; Boudsocq et al., 2010; Ranf et al., 2011; Schulz et al., 2013; Savatin et al., 2014). Even though the sequence of events is not yet fully established, these regulatory actions trigger the first line of transcriptional reprogramming in the nucleus. The initial and transient onset of defense gene expression is followed by more persisting changes in hormonal signaling notably through salicylic acid (SA), jasmonic acid (JA), and ethylene (ET), sealing of inter-cellular connections at plasmodesmata, and reprogramming of primary and secondary metabolism (Boller and Felix, 2009; Lee et al., 2011; Chaouch et al., 2012; Wang et al., 2013). To evade PAMP-triggered immunity (PTI), pathogens deliver effector proteins into plant cells to facilitate pathogenesis. As a counter measure, plants have evolved RESISTANCE (R) proteins, which recognize the presence of pathogen effectors and mount a second, stronger response termed effector-triggered immunity (ETI), that is commonly associated with programmed cell death called hypersensitive response (HR) (Jones and Dangl, 2006; Boller and Felix, 2009).

In the context of innate immunity, the MAPKs, which include both positive and negative regulators of PAMP-triggered immunity (PTI), have been well studied (Li et al., 2015). As an example of a defense-executing MPK-phosphorelay cascade, upstream MAPKK-Kinases (MAPKKKs) phosphorylate the MAPK-Kinases (MAPKKs) MKK4 and MKK5, which in turn phosphorylate two closely related MPKs, MPK3 and MPK6 that directly phosphorylate the stress-inducible transcription factor WRKY33. The phosphorylated WRKY33 drives the expression of its immunity-related target genes, such as 1-AMINOCYCLOPROPANE-1-CARBOXYLIC ACID SYNTHASE (ACS) to activate the committing step in ethylene biosynthesis, and PHYTOALEXIN DEFICIENT 3 (PAD3), required to trigger the production of the antimicrobial phytoalexin camalexin (Ishihama and Yoshioka, 2012; Guan et al., 2015). In a recent study, Kang et al. (2015)

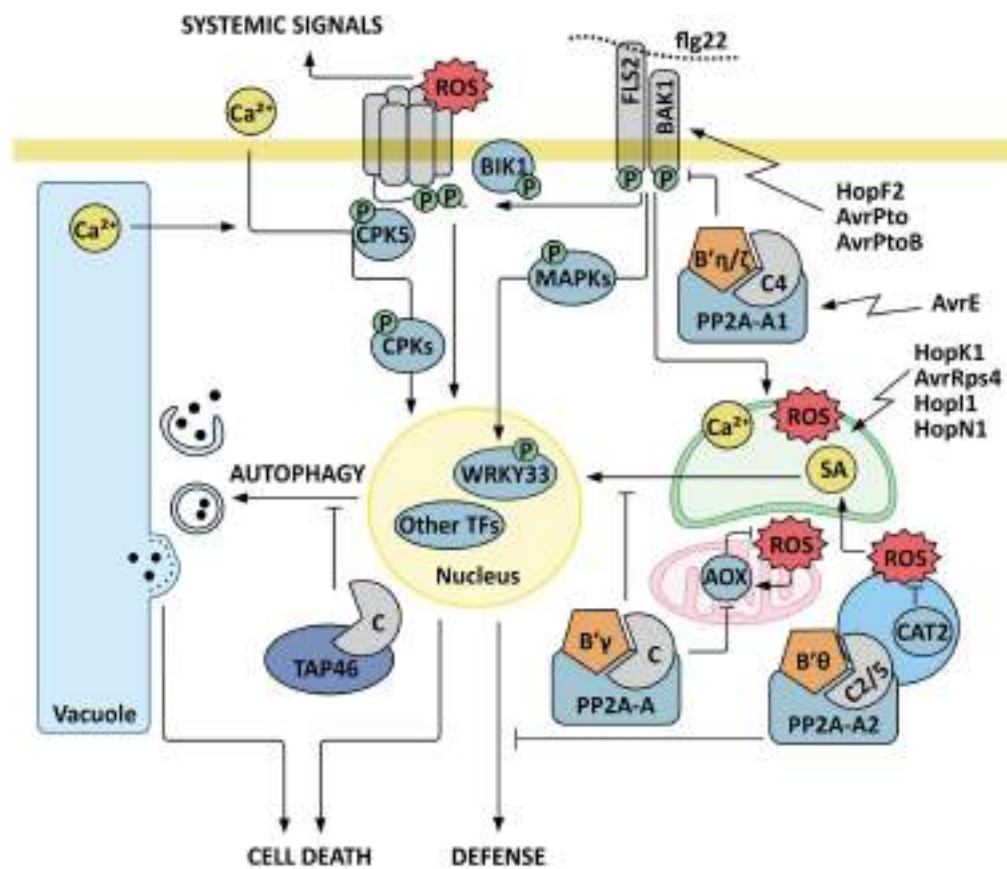


FIGURE 1 | Model for PP2A as a regulatory component in plant immunity signaling. Trimeric PP2A protein phosphatase composed of catalytic subunit C4, scaffold subunit A1 and regulatory B subunit B'η or B'γ negatively regulates the receptor-like kinase BRI1-ASSOCIATED KINASE 1 (BAK1), which is an essential coreceptor of the FLAGELLIN SENSING RECEPTOR 2 (FLS2), and targeted by bacterial effectors HopF2, AvrPto, and AvrPtoB. Activation of FLS2 signaling upon recognition of flagellin (flg22) rapidly elicits transient increases in cytosolic calcium concentration, activation of plasma membrane NADPH oxidases, a consequent burst of reactive oxygen species (ROS) in the apoplast, and activation of MAPKs and calcium-dependent protein kinases (CPKs), which trigger defense gene expression in the nucleus. As an example of a defense-executing phosphorelay cascade, phosphorylation of the transcription factor (TF) WRKY33 by MPKs is depicted. CPK5 additionally mediates systemic ROS signals to distal tissues by activating the NADPH-oxidase RBOHD. Flagellin-induced signals are also rapidly relayed into the chloroplasts, where calcium-dependent signaling interactions trigger chloroplast retrograde signals that further modulate plant immunity. The *P. syringae* effectors HopK1, AvrRps4 Hopl1 and HopN1 are indicated as examples that target chloroplastic functions. The PP2A-B'-subfamily members B'θ and B'γ function as negative regulators of plant immunity. PP2A-B'-B'γ controls a feed-back loop where increased abundance of alternative oxidases AOX1A and AOX1D result in reduced ROS production. PP2A-B'γ is also required to control salicylic acid (SA)-dependent pathogenesis responses and cell death triggered by intracellular ROS signals. Another important layer of regulation is provided by the PP2A regulatory protein TAP46, which interacts with PP2A catalytic subunits and negatively regulates autophagy and the associated programmed cell death.

showed that activated MPK6 additionally phosphorylates the transcription factor BRASSINOSTEROID INSENSITIVE1-ETHYL METHANESULFONATE-SUPPRESSOR1 (BES1) and that this phosphorylation is needed for full resistance against the hemibiotrophic bacterial pathogen *Pseudomonas syringae* pv. *tomato* DC3000 (*Pst*) in *A. thaliana*. Intriguingly, BES1 is a core component of the brassinosteroid signaling pathway, where its brassinosteroid-induced dephosphorylation promotes plant growth through activation of the major gibberellic acid biosynthesis genes (Unterholzner et al., 2015). Together, these signaling interactions illustrate examples of intricate branching among mechanisms that modulate plant growth and defense via key transcriptional regulators.

Parallel to the MPK-mediated signaling mechanisms, transient and presumably highly localized oscillations in cytosolic Ca²⁺ concentration activate a second branch of signal transduction, which is mediated by CDPKs. In *A. thaliana*, concerted action of CPK4, CPK5, CPK6, and CPK11 activates transcription of the immunity-marker genes *NHL10* and *PHI-1* (Boudsocq et al., 2010). CPK5 also initiates systemic signals to distal tissues by mediating Ca²⁺-dependent activation of the NADPH-oxidase RBOHD and a ROS-wave that proceeds in the apoplastic space, leading to the activation of defense responses in non-infected tissues (Dubiella et al., 2013; Figure 1). Analysis of calcium signaling interactions in rice, in turn, revealed an intriguing kinase–kinase interaction, where Ca²⁺-activated CPK18 phosphorylates rice MPK5 on threonine 14 and threonine

32, residues that are not part of the general TXY-motif that provides the well-known phosphorylation side for the activation of MAPKs by MAPKKs, and this multi-phosphorylated MPK mediates both activating and repressing effects on its downstream target genes (Xie et al., 2014). Collectively, the delicate regulatory interactions among different types of protein kinases allow subtle changes in gene expression profiles and metabolic pathways, and may therefore specifically adjust the plants' defense programs against the variety of biotic stress agents.

While protein kinases and their regulation mechanisms have long been intensively studied, the importance of protein phosphatases in plant immunity has been established more recently. The general involvement of protein dephosphorylation in early PTI responses was underscored by quantitative phosphoproteomic analysis of flagellin-treated *A. thaliana* plants, which showed reduced phosphorylation of a number of metabolic enzymes already 15 min after the application of the commonly utilized model for bacterial PAMP, the flagellin epitope flg22 (Rayapuram et al., 2014). In addition to metabolic adjustments, protein phosphatases are evidently also required to limit the activation state of PAMP-triggered phosphorelay cascades. However, even though the transient nature of early defense gene activation (Lewis et al., 2015) speaks for the importance of protein dephosphorylation in limiting the extent of defensive measures, only a few protein kinase–phosphatase pairs with counteracting effects on stress responses in plants have been identified (Schweighofer et al., 2007; Qiu et al., 2008; Geiger et al., 2009; Lee et al., 2009).

An example of a regulatory kinase–phosphatase interaction was provided by Bartels et al. (2009), who showed that the dual-specificity phosphatase MAP KINASE PHOSPHATASE1 (MKP1), together with the PROTEIN TYROSINE PHOSPHATASE1 (PTP1) regulate the phosphorylation status and hence the activity of MPK6. In line with this finding, null mutation of MKP1 resulted in constitutive defense responses and resistance to *P. syringae* (Bartels et al., 2009). Subsequently, Lumbrreras et al. (2010) identified MAP KINASE PHOSPHATASE2 (MKP2) as a negative regulator of a programmed cell death, elicited by ectopic overexpression of the *A. thaliana* MPK6 in *Nicotiana tabacum* (Lumbrreras et al., 2010). In effector triggered immunity, a MAPK-phosphatase INDOLE-3-BUTYRIC ACID RESPONSE 5 (IBR5) modulates the plant defense response and associated gene expression profiles in response to the bacterial effectors AvrRps4 and AvrRpm1 (Liu et al., 2015). PAMP-induced regulation of gene expression is also controlled through MAPKs that activate cyclin-dependent kinases (CDKCs), which in turn phosphorylate the C-terminal domain of RNA polymerase II, with a consequent activation of defense gene expression Li et al. (2014a). The phosphorylation of these residues is counteracted by dephosphorylation by the protein phosphatase C-terminal domain (CTD) phosphatase-like 3 (CPL3), which functions as a negative regulator of PAMP-induced immune responses (Li et al., 2014a).

Taken together, plant immunity is governed by converging signaling pathways where protein kinases and phosphatases collectively determine the extent of defense reactions. Tight

control of immune responses is also critical in preventing unnecessary investment of resources to energy-consuming metabolic changes, such as biosynthesis of secondary metabolites. Connecting the variety of protein kinases to their counteracting protein phosphatases, revealing their target proteins and understanding the physiological significance of the interactions therefore represent outstanding future research questions in plant biology.

The Centrality of Organelle Biology in Plant Immunity

A few recent studies have provided compelling evidence indicating that chloroplasts, peroxisomes, and mitochondria, with their cross-communicating enzymatic machineries, form active metabolic and regulatory hubs in plant immunity. PAMP-triggered signals are rapidly relayed into the chloroplasts, where calcium-dependent signaling interactions are needed to trigger additional signaling events, which further modulate immunity related gene expression in the nucleus (Nomura et al., 2012; Caplan et al., 2015). It was also recently discovered that stromules, which extend from the chloroplasts to the nucleus during innate immunity, form an important route for defense-associated chloroplast retrograde signaling (Caplan et al., 2015). de Torres Zabala et al. (2015) proposed a scenario where PAMP-triggered signals maintain Photosystem II activity in chloroplasts in order to facilitate a chloroplastic ROS burst and the consequent activation of PTI. On the other hand, suppression of chloroplast-associated genes within the nuclear genome displays another fast defense response in the framework of PTI (Lewis et al., 2015). Since chloroplasts form an essential signaling compartment in plant immunity, pathogens have evolved secreted chloroplast-targeted effector molecules to manipulate the chloroplastic defense mechanisms (Kangasjärvi et al., 2014; Li et al., 2014b; Trotta et al., 2014; de Torres Zabala et al., 2015). For example, the *P. syringae* effectors HopK1 and AvrRps4 localize to chloroplasts in their processed forms and require chloroplast transit peptides to suppress plant immunity, inferring that their target proteins are present in the chloroplast (Li et al., 2014b). The chloroplast-targeted effectors Hop11 and HopN1 in turn exert their actions by suppressing chloroplastic ROS burst and SA-mediated defenses (Jones et al., 2006; Rodríguez-Hervá et al., 2012).

Given that photosynthetic redox signals and oxidative signaling have long been recognized central in triggering abiotic stress responses, notably during light stress (Pogson et al., 2008), it is not surprising that biotic and abiotic stress responses may have partially overlapping outcomes. Besides the initiating signals arising from the photosynthetic electron transfer chain, a level of cross-talk occurs also within cytosolic stress signaling networks, where light acclimation and biotic stress signaling also appear to share common components. Vogel et al. (2014) reported that MPK6, together with APETALA2/ETHYLENE RESPONSIVE FACTOR- (AP2/ERF-) transcription factors, both of which are commonly associated with plant defense signaling, also mediate light-stress-induced signals that promote rapid and transient light acclimation responses in *A. thaliana*.

Pre-exposure to high light stress has also been shown to enhance plant resistance to subsequent infection by virulent strains of *P. syringae* (Mühlenbock et al., 2008), or infestation by green peach aphid (*Myzus persicae*, Rasool et al., 2014). Even though the concept of such cross-tolerance has become commonly accepted, the developmental and metabolic readjustments that ultimately promote broad-range stress resistance in plants remain to be elaborated (Bowler and Fluhr, 2000; Bostock, 2005). By contrast, the establishment of long term systemic acquired resistance (SAR), which renders uninfected tissue of an infected plant resistant to future infections, is known to involve hydrogen peroxide (H_2O_2) and nitric oxide (NO) as well as mono- and digalactosyldiacylglycerol lipids (Gao et al., 2014; Wang et al., 2014). Moreover, the three main regulators of SAR comprise azealic acid, SA, and pipecolic acid (Jung et al., 2009; Bernsdorff et al., 2016), the latter two of which rely on metabolic intermediates derived from the chloroplast.

Besides the generally accepted roles of chloroplasts, peroxisomes and mitochondria in reinforcing plant defenses (Chaouch et al., 2010; Trotta et al., 2014), a signaling role has been realized for foliar lipid bodies, which are small organelles surrounded by a monolayer membrane and which have earlier been regarded as a compartment for lipid storage in seeds. The surface of lipid bodies can accommodate signaling components, such as the pathogen-responsive calcium-dependent protein kinase CPK1 (Coca and San Segundo, 2010). Lipid bodies also store phytosterol esters, which promote plant immunity by modulating the permeability of the plasma membrane, and perform the biosynthesis of the anti-fungal phytoalexin 2-hydroxyoctadecatrienoic acid (2-HOT). Being highly mobile organelles, lipid bodies may also shuttle metabolites and proteins to specific cellular sites of action, hence providing an important addition to the plant's defense strategies (van der Schoot et al., 2011; Kopischke et al., 2013; Shimada et al., 2014).

Plant immunity is a multilevel process executed through tight communication and metabolic interaction between different cellular compartments, and is highly dependent on the physiological status of the plant. Here we focus on the emerging functions of PP2A in controlling the initiation and transduction of stress signals as well as in modulating organellar signaling and metabolic responses. These actions are vital in ensuring appropriate activation of the plasma membrane sensory systems, downstream signaling cascades and defense gene expression, as well as in the execution of defensive measures through biosynthesis of antimicrobial and insecticidal compounds according to the prevailing environmental cues.

PROTEIN PHOSPHATASE 2A AS A REGULATORY ENZYME

Trimeric type 2A protein phosphatases, composed of a catalytic subunit C, scaffold subunit A and regulatory subunit B, are evolutionarily conserved signaling components that essentially regulate stress signaling in animals and plants. The high level

of conservation can be exemplified by the *Homo sapiens* PP2A catalytic subunit termed 3FGA_C, which displays approximately 80% amino acid identity with its *A. thaliana* counterparts (Rasool et al., 2014).

Structural analysis of the *H. sapiens* PP2A holoenzyme has shown that the scaffold subunit A forms a horseshoe-shaped fold with its 15 tandem internal repeats of the HEAT (huntingtin-elongation-A subunit-TOR) motif binding the catalytic C subunit (Cho and Xu, 2007). The PP2A-C subunit attains an active conformation upon dimerization with the A subunit, and forms a platform for interaction with the regulatory B subunit. The consensus on PP2A function is that the regulatory B subunit plays the key role in determining specificity of the phosphatase holoenzyme for a substrate (reviewed by Sents et al., 2013). Hence, the regulatory B subunit is commonly referred to as the "specificity unit" that determines the target specificity of the trimeric PP2A holoenzyme (for a review, see Farkas et al., 2007). For a more detailed discussion and comparison of PP2A and its homologs in mammalian and yeast cells we refer the reader to excellent recent reviews by Uhrig et al. (2013) and Lillo et al. (2014).

In plants, each PP2A subunit is encoded by multiple genes (Kerk et al., 2002). The *A. thaliana* genome contains five different genes encoding C subunits, three genes for the A subunits and 17 genes encoding the variable regulatory B subunits, which are further classified as B, B', and B'' based on their structural characteristics (Farkas et al., 2007; **Table 1**). It is worth noting, however, that the nomenclature for B''-subunits in Farkas et al., (2007) differs from that indicated in the GenBank database¹ and followed, e.g., by Leivar et al. (2011; **Table 1**). Phylogenetic analysis of plant PP2A catalytic subunits from diverse plant species in turn clustered the C-subunits into two subfamilies designated I and II (He et al., 2004). Within these clusters, the *Arabidopsis* PP2A catalytic subunits C1, C2, and C5 belong to subfamily I while C3 and C4 belong to subfamily II (He et al., 2004). The trimeric holoenzyme compositions provide extensive variability and versatility for PP2A in regulatory networks. What determines the trimeric PP2A subunit composition of a specific holoenzyme is currently not well understood.

Computational analysis indicated that the amino acids located on PP2A-C/A/B interfaces are highly conserved, and hence unlikely to determine the different trimeric compositions of *A. thaliana* PP2A (Rasool et al., 2014). This conclusion is also supported by BiFC experiments in *Nicotiana benthamiana* cells where all three *A. thaliana* scaffold PP2A-A-subunits interacted with all five catalytic PP2A-C-subunits *in vivo* (Waadt et al., 2015). Spatiotemporal gene expression patterns and subcellular localization may instead provide important regulatory levels that determine the availability of the different PP2A subunits for holoenzyme formation (Pernas et al., 2007; Konert et al., 2015a). Indeed, the regulatory PP2A-B subunits have been detected in distinct subcellular localizations, albeit most of them seem to reside in

¹<http://www.ncbi.nlm.nih.gov/genbank>

TABLE 1 | Subcellular localisations of *Arabidopsis thaliana* PP2A regulatory B subunits.

<i>A. thaliana</i> PP2A B-subunit	AGI code	Localization	Promoter	Fusion protein	Expression system	Reference
B- subfamily						
B alpha (B α)	AT1G51690	-Cytoplasm -Nucleus -Punctate structures	<i>UBQ10</i> AT4G05310	mTurquoise and mVenus	<i>Nicotiana benthamiana</i> leaf epidermis	Waadt et al., 2015
B beta (B β)	AT1G17720	-Cytoplasm -Nucleus -Punctate structures	<i>UBQ10</i>	mTurquoise and mVenus	<i>N. benthamiana</i> leaf epidermis	Waadt et al., 2015
B'-subfamily						
B' alpha (B' α)	AT5G03470	-Cytoplasm	<i>pPP2AB'</i> α	YFP	<i>A. thaliana</i> (stably transformed)	Tang et al., 2011
		-Cytoplasm -Nucleus	<i>UBQ10</i>	mTurquoise and mVenus	<i>N. benthamiana</i> leaf epidermis	Waadt et al., 2015
B' beta (B' β)	AT3G09880	-Cytoplasm	<i>pPP2AB'</i> β	YFP	<i>A. thaliana</i> (stably transformed)	Tang et al., 2011
		-Cytoplasm -Nucleus	<i>UBQ10</i>	mTurquoise and mVenus	<i>N. benthamiana</i> leaf epidermis	Waadt et al., 2015
B' gamma (B' γ)	AT4G15415	-Cytoplasm	CaMV 35S	YFP	<i>A. thaliana</i> protoplasts (made from leaves)	Trotta et al., 2011
		-Cytoplasm -Nucleus	CaMV 35S	YFP	<i>A. thaliana</i> protoplasts (made from suspension culture cells)	Matre et al., 2009
B' delta (B' δ)	AT3G26030	-Cytoplasm -Punctate structures	<i>UBQ10</i>	mTurquoise and mVenus	<i>N. benthamiana</i> leaf epidermis	Waadt et al., 2015
		-Cytoplasm -Nucleus	<i>UBQ10</i>	mTurquoise and mVenus	<i>N. benthamiana</i> leaf epidermis	Waadt et al., 2015
B' epsilon (B' ϵ)	AT3G54930	-Cytoplasm -Nucleus -PM	<i>UBQ10</i>	mTurquoise and mVenus	<i>N. benthamiana</i> leaf epidermis	Waadt et al., 2015
B' zeta (B' ζ)	AT3G21650	-Cytoplasm -Mitochondria	CaMV 35S	YFP (YFP at C-terminus)	<i>A. thaliana</i> leaf epidermis (particle bombardment)	Matre et al., 2009
		-Cytoplasm -Nucleus	CaMV 35S	YFP (YFP at N-terminus)	<i>N. tabacum</i> leaf epidermis (particle bombardment)	Matre et al., 2009
		-Cytoplasm -Nucleus -Nucleolus	<i>UBQ10</i>	mTurquoise and mVenus	<i>N. benthamiana</i> leaf epidermis	Waadt et al., 2015
B' eta (B' η)	AT3G26020	-Cytoplasm	<i>pPP2AB'</i> η	YFP	<i>A. thaliana</i> (stably transformed)	Tang et al., 2011
		-Cytoplasm -Nucleolus	CaMV 35S	YFP	<i>A. thaliana</i> protoplasts (made from suspension culture cells)	Matre et al., 2009
		-Cytoplasm -Nucleus -Nucleolus -PM -Punctate structures	<i>UBQ10</i>	mTurquoise and mVenus	<i>N. benthamiana</i> leaf epidermis	Waadt et al., 2015
B' theta (B' θ)	AT1G13460	-Peroxisomes	CaMV 35S	YFP (YFP at N-terminus)	<i>A. thaliana</i> protoplasts (made from suspension culture cells)	Matre et al., 2009
		-Cytoplasm -Nucleus	CaMV 35S	YFP (YFP at C-terminus)	<i>A. thaliana</i> protoplasts (made from suspension culture cells)	Matre et al., 2009

(Continued)

TABLE 1 | Continued

<i>A. thaliana</i> PP2A B-subunit	AGI code	Localization	Promoter	Fusion protein	Expression system	Reference
		-Peroxisome-like structures (in leaves and roots)	CaMV 35S	eYFP	<i>A. thaliana</i> (stably transformed)	Kataya et al., 2015b
		-Cytoplasm -Nucleus -Nucleolus -PM	<i>UBQ10</i>	mTurquoise and mVenus	<i>N. benthamiana</i> leaf epidermis	Waadt et al., 2015
B' kappa (B' κ) *B' iota (B' ι) in GenBank	AT5G25510	-Cytoplasm -Nucleus -Nucleolus -PM -Punctate structures	<i>UBQ10</i>	mTurquoise and mVenus	<i>N. benthamiana</i> leaf epidermis	Waadt et al., 2015
B''-subfamily						
B'' alpha (B'' α)	AT5G44090	-Cytoplasm -Nucleus	<i>UBQ10</i>	mTurquoise and mVenus	<i>N. benthamiana</i> leaf epidermis	Waadt et al., 2015
B'' epsilon (B'' ϵ) *B'' beta in GenBank and Leivar et al. (2011)	AT5G28850	-Cytoplasm -Nucleus	<i>UBQ10</i>	mTurquoise and mVenus	<i>N. benthamiana</i> leaf epidermis	Waadt et al., 2015
B'' delta (B'' δ) *B'' gamma in GenBank and Leivar et al. (2011)	AT5G28900	-Cytoplasm -Nucleus	<i>UBQ10</i>	mTurquoise and mVenus	<i>N. benthamiana</i> leaf epidermis	Waadt et al., 2015
B'' gamma (B'' γ) *B'' delta in GenBank and Leivar et al. (2011)	AT1G54450	-Nucleus -Punctate structures	<i>UBQ10</i>	mTurquoise and mVenus	<i>N. benthamiana</i> leaf epidermis	Waadt et al., 2015
B'' beta (B'' β) *B'' epsilon in GenBank and Leivar et al. (2011)	AT1G03960	-Cytoplasm -Nucleus	<i>UBQ10</i>	mTurquoise and mVenus	<i>N. benthamiana</i> leaf epidermis	Waadt et al., 2015
TON 2 (FASS)	AT5G18580	-Cytoplasm - Mitotic preprophase (root tip cells) -Cytoplasm -Cytoplasm -Nucleus	CaMV 35S <i>UBQ10</i>	GFP mTurquoise and mVenus	<i>A. thaliana</i> (stably transformed) <i>N. benthamiana</i> leaf epidermis <i>N. benthamiana</i> leaf epidermis	Spinner et al., 2013 Spinner et al., 2013 Waadt et al., 2015

The fusion proteins were examined in transient expression systems unless "stably transformed" is stated. The nomenclature is based on Farkas et al. (2007). For PP2A-B' subunits and AT5G25510, alternative nomenclature according to either GenBank (<http://www.ncbi.nlm.nih.gov/genbank>) or GenBank and Leivar et al. (2011) is indicated by asterisks (*).

more than one compartment, at least in the over-expression systems currently available for studies on protein localization (**Table 1**).

Clues to transcriptional regulation of genes encoding PP2A subunits can be obtained by querying publicly available microarray datasets of mRNA abundance available in Genevestigator² (Hruz et al., 2008) for various experimental conditions (**Figure 2**). Of the catalytic PP2A subunits, *PP2A-C5*, and to some extent also *PP2A-C2* transcript abundance increases in response to various plant pathogens, ozone fumigation that mimics pathogen infection by promoting

extracellular ROS burst (Vainonen and Kangasjärvi, 2015) and various pathogenic elicitors, whereas abiotic stresses appear to decrease the expression of the catalytic PP2A subunits. The genes encoding the scaffold A subunits in turn do not seem to be transcriptionally highly responsive. Of the regulatory PP2A-B subunits, the transcript abundance for *B' ζ* , *B' η* , *B' θ* , and to some extent also *B'' α* , follows that of *PP2A-C5*, being increased by biotic cues and reduced by abiotic stress conditions. The transcript abundance for *B' α* , *B' β* , *B' γ* , and *B' δ* in contrast decreases in response to both biotic factors and abiotic stress agents. Hence, transcriptional regulation may provide an important level of regulation of PP2A function.

²www.genevestigator.com

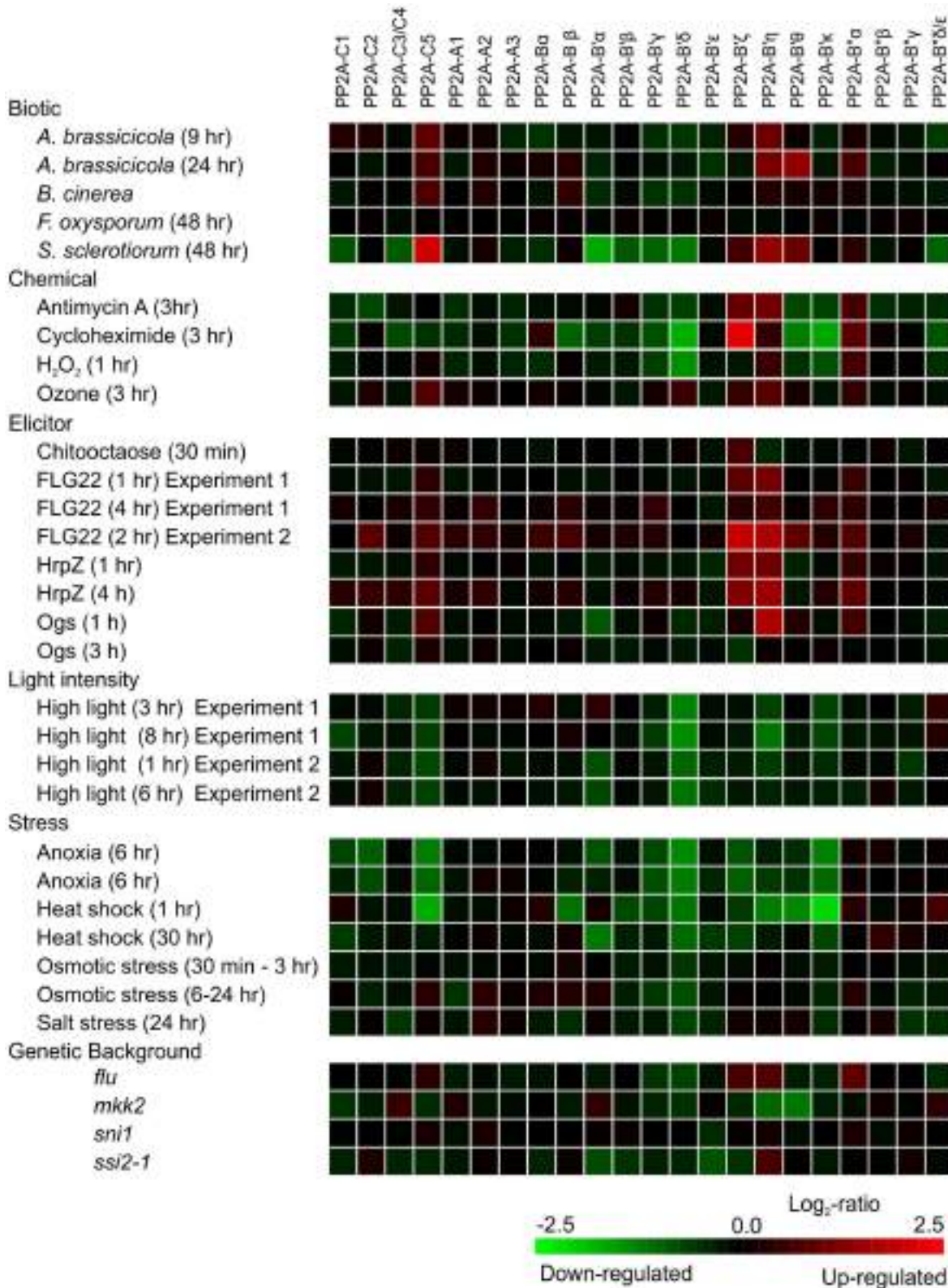


FIGURE 2 | Expression of PP2A subunits as visualized by investigating selected treatments in Genevestigator using the Perturbations tool. Green indicates decreased expression and red increased expression. The probes on the Affymetrix ATH1 chip cannot distinguish between PP2A-C3 and C4, PP2A-B'δ, and ε subunits (as named according to Farkas et al., 2007); hence for these genes the indicated expression is the sum of the corresponding genes.

On the protein level, PP2A activity is modulated through interactions with regulatory proteins, which may be mutually exclusive with PP2A regulatory subunits (Yang et al., 2007; Xing et al., 2008; Wu et al., 2011; Sents et al., 2013). PP2A becomes activated through reversible methylation of a conserved C-terminal leucine residue by the leucine carboxylmethyltransferase (De Baere et al., 1999), which in *A. thaliana* was identified as SUPPRESSOR OF BRI1 (SBI1) in a screen for brassinosteroid signaling components (Wu et al., 2011). This methylation event relies on yet another regulator, the *Arabidopsis* PHOSPHOTYROSYL PHOSPHATASE ACTIVATOR (AtPTPA) (Chen et al., 2014). The elucidation of the *in vivo* function of the PP2A regulator PTPA began originally in yeast and PTPA was shown to be conserved also in mammals (reviewed in Sents et al., 2013). Moreover, both animals and plants also possess other regulatory components, such as the mammalian $\alpha 4$ /yeast tap42 (type 2A-phosphatase-associated protein 42 kD) and their homolog TAP46 of *A. thaliana*, which may further modulate the phosphatase activity of PP2A (Harris et al., 1999; Ahn et al., 2011; Sents et al., 2013; Hu et al., 2014). In plants, TAP46 was first described as an interactor of PP2A and PP2A-like phosphatases by Harris et al. (1999). More recent studies have demonstrated key roles for TAP46 in developmental programs and stress responses, but whether and how the TAP46 interaction impacts the catalytic phosphatase activity and/or the target specificity of the protein phosphatase has not yet been indisputably demonstrated (Ahn et al., 2011; Hu et al., 2014; Rexin et al., 2015). Altogether, PP2A is a versatile protein phosphatase that is functionally controlled at multiple levels to ensure specificity in cellular signaling. Furthermore, it is plausible that different nodes of signaling cascades and regulatory networks are controlled by PP2A phosphatases with different heterotrimeric compositions.

PP2A AS A REGULATOR OF PLASMA MEMBRANE SENSORY SYSTEMS

Several recent studies have assigned functions for PP2A in plant immunity. Segonzac et al. (2014) revealed a mechanistic connection between a trimeric PP2A, composed of the catalytic subunit C4, the scaffold subunit A1 and the regulatory B subunits B' η or B' ζ , and the receptor-like kinase BRI1-ASSOCIATED KINASE 1 (BAK1), which is an essential coreceptor of the two extensively studied RLKs FLAGELLIN SENSING RECEPTOR 2 (FLS2) and EF-TU RECEPTOR (EFR) (Segonzac et al., 2014; Figure 1). FLS2 and EFR perceive flagellin and the elongation factor (EF-) Tu, respectively, both PAMPs of bacterial pathogens. The PP2A-holoenzyme limits the autophosphorylation and hence the activity of BAK1 (Segonzac et al., 2014). Accordingly, knock-out mutants deficient in the catalytic C4 subunit or the scaffold A1 subunit are hypersensitive to bacterial PAMPs, as demonstrated by increased apoplastic ROS burst upon exposure of leaves to elf18 or flg22, elicitor-active peptides derived from EF-Tu and flagellin, respectively. Associated with this, *pp2a-c4* and *pp2a-a1* show increased resistance to virulent *P. syringae* pv.

tomato DC3000 (Segonzac et al., 2014). These findings are highly significant, given that BAK1 is a key component in various plant-biotic interactions, including the recently discovered resistance to aphids (Prince et al., 2014). The importance of BAK1 as a coreceptor for the key RLKs FLS2 and EFR in the ongoing evolutionary arms-race between plants and their pathogens is also highlighted by the immunity-suppressing effects of the bacterial effectors HopF2, AvrPto and AvrPtoB on BAK1 function (Zhou et al., 2014).

The PAMP-triggered ROS-burst is brought about by the NADPH-oxidase RBOHD, which is activated by the kinases BOTRYTIS-INDUCED KINASE1 (BIK1) and CPK5 (Dubiella et al., 2013; Kadota et al., 2014; Li et al., 2014c), but the protein phosphatases counteracting these phosphorylations for deactivation of RBOHD are yet to be identified. Intriguingly, application of the PP2A-inhibitor cantharidin leads to a ROS-burst with an intensity comparable to that induced by flg22 in *A. thaliana* wild type plants (Segonzac et al., 2014), suggesting that PP2A activity is required to control the NADPH oxidase driven ROS burst. Taken together, PP2A is a key regulatory component that controls PAMP-triggered immunity at receptor level. It is therefore noteworthy that, based on yeast two-hybrid data, Degrave et al. (2015) postulated that a special class of bacterial effectors (AvrEs) may bind to PP2A to promote its function as a negative regulator of plant immunity.

One of the unresolved outstanding questions is how PP2A, which in many cases appears to function as a negative regulator, becomes transiently inactivated upon infection in order to allow elicitation of appropriate defensive or adaptive measures. One possibility is that PP2A becomes a target for a plasma membrane receptor-like kinase, which phosphorylates the attached PP2A phosphatase with a consequent inactivation of the PP2A holoenzyme. Alternatively, pathogen induced ROS signaling could lead to inactivation of PP2A phosphatase activity through oxidative modifications and further nitration or nitrosylation of cysteines of the PP2A proteins. This scenario is supported by a recent report by Van Breusegem et al. (2008), who identified the PP2A regulatory subunit B- α as a target for H₂O₂-mediated cysteine oxidation (Waszcak et al., 2014). Such hypothetical regulatory mechanisms, however, call for experimental verification.

PP2A AS A REGULATOR OF INTRACELLULAR SIGNALING NETWORKS AND CELL DEATH

Protein Phosphatase 2A has also been associated with intracellular signaling interactions (Figure 1). Apart from the involvement of B' η and B' ζ in containing BAK1-triggered receptor signaling (Segonzac et al., 2014), two other members of the PP2A-B'-subfamily function as negative regulators in plant defense pathways. A mutant deficient in B' θ displays increased resistance toward *P. syringae* pv. *tomato* (Kataya et al., 2015a). B' θ co-localizes with PP2A-C2, PP2A-C5, and PP2A-A2 in peroxisomes, where its positive impact maintains

β -oxidation of fatty acids and protoauxins (Kataya et al., 2015b). Whether B'θ-dependent regulation of β -oxidation has an impact on plant immunity, however, remains to be established. The subunit B'γ in turn mainly localizes to the cytoplasm where it is required for transcriptional and post-translational control of immune processes, and hence negatively regulates defenses against green peach aphid (*M. persicae*) and the necrotrophic fungus *Botrytis cinerea* (Trotta et al., 2011; Rasool et al., 2014).

Since in *A. thaliana* each regulatory B subunit may theoretically bind 15 different compositions of PP2A, trimeric holoenzymes with different B subunits may regulate cellular functions in both redundant and opposing ways. For example, the regulatory PP2A subunit B'ζ exerts counteracting effects on B'γ-mediated regulation of aphid resistance and cell death in *A. thaliana* (Rasool et al., 2014; Konert et al., 2015a). When compared to wild type, aphid fecundity was decreased in the *pp2a-b'γ* single mutant but not in the *pp2a-b'γζ* double mutants (Rasool et al., 2014). Acclimation to high light, on the other hand, led to a similar decrease in aphid fecundity in all genotypes (Rasool et al., 2014). These phenotypes are peculiar, given that the B'γ and B'ζ subunits are closely related with 80% amino acid sequence identity (Rasool et al., 2014), albeit their different gene expression profiles speak for differential regulatory roles under biotic stresses (Figure 2). Moreover, the saliva-triggered induced resistance against green peach aphid deploys BAK1, which is negatively regulated by B'ζ (Prince et al., 2014; Segonzac et al., 2014). Based on this, B'ζ should rather negatively regulate plant resistance to aphids. Such contradictory phenotypic outcomes presumably reflect the fact that each regulatory PP2A-B subunit is likely to interact with a multitude of target phosphoproteins.

Analysis of plant immunity by using the *pp2a-b'γ* single mutant as a tool is further complicated by its highly conditional phenotype, which depends on light intensity and relative humidity (Trotta et al., 2011; Li et al., 2014d; Rasool et al., 2014; Konert et al., 2015a). When grown under 50% humidity and 130 μ mol of photons $m^{-2}s^{-1}$ light intensity, *pp2a-b'γ* displays premature yellowing, constitutive accumulation of ROS, SA- and JA-related defense responses, and increased abundance and phosphorylation of pathogenesis related (PR) proteins (Trotta et al., 2011). These phenotypic properties suggest that PP2A-B'γ is required to control both transcriptional and post-translational responses. Growth under 800 μ mol of photons $m^{-2}s^{-1}$ and elevated temperature, however, partially abolishes the constitutive defense phenotypes and rather promotes enhanced abiotic stress responses and acclimation to high light (Trotta et al., 2011; Konert et al., 2015a; reviewed by Rahikainen et al., 2016). Later studies showed that increasing the growth light from 130 to 200 μ mol of photons $m^{-2}s^{-1}$ at 65% relative humidity is sufficient to annul the yellowing *pp2a-b'γ* mutant phenotype (Li et al., 2014d). Even though it is evident that PP2A-B'γ is required to control the extent of light acclimation and biotic stress responses in *A. thaliana* leaves (Trotta et al., 2011), these characteristics complicate the interpretation of *pp2a-b'γ* single mutant phenotypes and

the understanding of PP2A-regulated processes by mutant approaches.

By taking advantage of pharmacological approaches and selected reaction monitoring (SRM) mass spectrometry, Konert et al. (2015b) showed that *pp2a-b'γ* may partially circumvent oxidative stress through a feed-back loop, where the mitochondrial alternative oxidases AOX1A and AOX1D channel electrons to a bypass pathway with a consequent reduction in ROS production. AOX1A and AOX1D are well known to be transcriptionally responsive to organellar ROS and SA signaling (De Clercq et al., 2013; Sewelam et al., 2014; Figure 1). PP2AB'γ, however, exerts its effects on the abundance of AOX1A and AOX1D and mediates post-translational control of the bypass pathway, albeit the molecular mechanism remains unresolved (Konert et al., 2015b). Even so, it is clear that PP2A-B'γ forms a key component within the regulatory network that controls intracellular ROS homeostasis and the involved hormonal signaling responses in *A. thaliana*.

Li et al. (2014d) generated a *catalase 2* (*cat2*) *pp2a-b'γ* double mutant to study the impact of oxidative signaling in the *pp2a-b'γ* mutant background. CATALASE 2 is a major scavenging enzyme that quenches photorespiratory H₂O₂ in peroxisomes, and hence provides a highly informative system to study factors involved in intracellular ROS signaling in C3 plants (Mhamdi et al., 2010; Kaurilind et al., 2015). In *cat2*, the oxidative stress induced pathogenesis responses, such as accumulation of SA and phytoalexins, expression of PR genes, lesion formation, and cell death, are conditioned by day length and are more pronounced under long day conditions (Queval et al., 2007, 2012; Chaouch et al., 2010; Li et al., 2014d). Li et al. (2014d) showed that under short photoperiod these ROS-induced pathogenesis responses become suppressed through pathways that require the activity of PP2AB'γ. Physiological and biochemical characterization of *cat2 pp2a-b'γ* double mutants revealed enhanced cell death and reprogramming of primary metabolism, and these adjustments associated with elevated levels of SA and camalexin in short day photoperiods (Li et al., 2014d). Introduction of *sid2* (a mutation in ISOCHORISMATE SYNTHASE1, the major SA biosynthesis enzyme in *A. thaliana*) into the *cat2 pp2a-b'γ* background, however, suppressed the cell death phenotype, demonstrating that the observed pathogenesis responses in *cat2 pp2a-b'γ* were driven by SA signaling (Li et al., 2014d). Hence, PP2A-B'γ is required to control SA-dependent pathogenesis responses triggered by intracellular ROS signals (Figure 1).

Besides the regulatory PP2A-B subunits, another important layer of cell death regulation is provided by the PP2A regulatory protein TAP46, which negatively regulates autophagy and the associated programmed cell death, but this pathway appears to be at least partially SA independent (Ahn et al., 2011). In yeast and mammalian cells, Tap42/α4 acts as a downstream component in the target of rapamycin (TOR) protein kinase dependent pathway, which promotes basic cellular functions, such as protein synthesis, transcription and ribosome biogenesis under favorable nutritional conditions. Starvation-induced inactivation of TOR in turn leads to repression of translational activity and recycling

of nutrients through the process of autophagy (for a review on TOR signaling, see Jacinto and Hall, 2003; Rexin et al., 2015).

TAP46 was shown to interact with the *A. thaliana* PP2A catalytic subunits, and depletion of TAP46 by virus-induced gene silencing (VIGS) in *N. benthamiana* or RNA interference (RNAi) in *A. thaliana* resulted in global modulations in PP2A activities, albeit the regulatory mode of interaction remains unclear (Ahn et al., 2011). The induced silencing of TAP46 promoted a transient increase in total PP2A activity, which, however, declined in the course of the experiment, leading the authors to conclude that TAP46 may have a more prominent role as an activator of PP2A activity in this experimental system (Ahn et al., 2011). At 7 days of induced silencing, strong depletion of TAP46 mRNA coincided with reduced PP2A activity and appearance of visually observable cell death on transgenic *A. thaliana* leaves (Ahn et al., 2011). Hence, TAP46 is required to maintain PP2A activity, which in turn prevents unnecessary mounting of the cell death response (**Figure 1**). In the *N. benthamiana* system, depletion of TAP46 mRNA likewise resulted in growth arrest, activation of autophagy, and programmed cell death, with hallmark features including DNA fragmentation, reduced mitochondrial membrane potential, and decline in chlorophyll fluorescence (Ahn et al., 2011). Hence, depletion of TAP46 phenocopies the physiological effects attributable to inactivation of TOR. Co-expression of the SA-catabolising enzyme NahG delayed the onset of cell death by 4 days, demonstrating that the TAP46-regulated cell death was only partially attributable to SA signaling (Ahn et al., 2011). Rather, the time-dependent modulation of PP2A activity in TAP46-silenced plants coincided with that observed in TOR-deficient plants, and phosphorylation of TAP46 by TOR *in vitro* further inferred that TAP46 may be functionally connected with TOR signaling (Ahn et al., 2011). Even though the exact mechanisms of TAP46/TOR/PP2A interaction remain to be defined, this study highlighted the relevance of PP2A catalytic activity in determining cell death responses in plants.

Catalytic PP2A subunits have also been related to ETI (He et al., 2004), a defense response which commonly includes the HR, a particular type of programmed cell death in plants. By taking advantage of VIGS of subfamily I PP2A catalytic subunits in *N. benthamiana*, He et al. (2004) demonstrated that reduced PP2A activity correlated with increased expression of the pathogens-related genes PR1a, PR1b and PR5 and with localized cell death, which became visually observable in the stems and leaves of the PP2A-silenced plants. Accordingly, the PP2A-silenced *N. benthamiana* plants displayed a 20-fold reduced growth of virulent *P. syringae* pv. *tabaci* as compared to vector-infected control plants, suggesting that the decline in PP2A activity enhances a complex array of mechanisms essential in the impediment of *P. syringae* growth (He et al., 2004).

By taking advantage of *N. benthamiana* transiently expressing the Resistance (R) gene/effector pairs tomato Pto/*P. syringae* pv. *tomato* AvrPto or tomato Cf9/*Cladosporium fulvum* Avr9 in PP2A silenced plants, He et al. (2004)

could demonstrate that PP2A also negatively controls HR signaling downstream of different R-genes. Furthermore, in response to infection by *P. syringae* pv. *tomato* expressing AvrPto, transcript abundance for the catalytic PP2A subunit *LePP2Ac1* increased in tomato lines capable of recognizing this bacterial effector (Mysore et al., 2002). He et al. (2004) suggested that such transcriptional activation of a negative immune regulator may allow precise regulation of defense pathways to prevent uncontrolled damage to the host tissue. Altogether, PP2A activity is an important contributor to negative regulation of a variety of plant defense responses, notably cell death.

EXECUTING PLANT IMMUNITY: PP2A IN THE CONTROL OF METABOLIC RESPONSES

Since biotrophic and hemibiotrophic plant pathogens rely on a supply of metabolites by living plant cells, basic defense mechanisms of the plant employ reprogramming of primary and secondary metabolism as a key mechanism of defense. Such metabolomic restructuring is not only essential in channeling metabolic intermediates for production of deterring secondary compounds, but also in ensuring the supply of energy for the energy-consuming biosynthetic pathways and the withdrawal of nutritional nitrogen-rich compounds from the infection zone. Chaouch et al. (2012) showed that the most highly induced metabolites detected in *A. thaliana* upon infection by virulent or avirulent (i.e., successfully parried by the plant after recognition of a specific pathogen effector) strains of *P. syringae* include the stress hormone SA as well as the monosaccharides ribose and fructose, the amino acids threonine, O-acetylserine, tyrosine, leucine, isoleucine and phenylalanine, and nicotinic acid. These findings reflect the centrality of primary metabolism in plant immunity. In basal defense, metabolic rearrangements are at least partially mediated by PAMP-induced transcriptional activation of genes related to biosynthesis of aromatic amino acids and the down-stream steps for the biosynthesis of secondary metabolites, including anthocyanins, lignins, flavonols, and the phytoalexin camalexin (Truman et al., 2007).

Reprogramming of the plant secondary metabolome with increased amounts of camalexin, agmantine derivatives, and glucosinolates can be triggered by induced expression of constitutively active forms of MPK3 and MPK6 and the ensuing changes in the phosphoproteome, even in the absence of pathogen infection (Lassowskat et al., 2014). This finding highlights protein phosphorylation as the key mechanism in triggering inducible chemical defenses in plants. Cruciferous plants harbor a particularly complex set of secondary compounds, of which camalexin and indole glucosinolates have well-documented antimicrobial effects in different *Arabidopsis* accessions, which have been instrumental in the identification of the underlying biosynthetic pathways (Sønderby et al., 2010). Post-translational regulation and its

impact on defense-associated metabolism in contrast remains less well understood.

PP2A in the Regulation of Primary Metabolism

Proteomic and metabolomic analysis of *pp2a-b'γ* and *cat2 pp2a-b'γ* mutants provided insights into potential PP2A targets in post-translational regulation of immune reactions (Trotta et al., 2011; Li et al., 2014d). Besides the recognized key players in pathogenesis responses, such as the pathogenesis-related proteins PR2 and PR5, these studies revealed enzymes of primary metabolism as potential PP2A targets, and suggested that PP2A-B'γ influences the post-translational regulation of oxidative-stress-triggered modulations in primary and secondary metabolism.

Attempts to identify the molecular mechanisms underlying PP2A dependent metabolic adjustments revealed that PP2A-B'γ interacts with and regulates the phosphorylation level of the cytosolic form of ACONITASE 3 (Konert et al., 2015b; Figure 3). The *A. thaliana* genome encodes three aconitase isoforms that are all dually localized to mitochondria and cytosol. Like ACONITASE 1 and ACONITASE 2, ACONITASE 3 also operates in the mitochondrial citric acid cycle, but it is additionally the key isoform that executes cytoplasmic functions and essentially contributes to energy metabolism at least in young *A. thaliana* seedlings (Hooks et al., 2014). Cytosolic aconitases act in a metabolic cascade where the aconitase-driven reaction is followed by successive activities of

isocitrate dehydrogenase (ICDH) and glutamine synthase, both of which have been functionally connected with plant immunity (Mhamdi et al., 2010; Seifi et al., 2013). Intriguingly, PP2A-B'γ exerts a control over transcript and protein abundance of cytosolic glutamine synthase 1;1 (GLN1;1), which functions in remobilization of nitrogen-rich amino acids and may have a key role in maintaining chloroplast redox balance in infected leaves (Liu et al., 2010; Trotta et al., 2011; Figure 3). Even though the exact mechanisms remain to be reported, PP2A and primary carbon metabolism appear to be tightly intertwined in triggering defensive measures in plants.

Besides the role in primary carbon metabolism, aconitases also contribute to the regulation of cellular redox balance and cell death in plants (Moeder et al., 2007). *A. thaliana* *aconitase 3* mutants and *N. benthamiana* plants with reduced aconitase levels displayed increased resistance against methyl viologen induced oxidative stress (Moeder et al., 2007). This effect may be at least partially connected to the fact that aconitases possess iron in their active center, and this iron may be readily released upon attack of the iron-sulfur cluster by ROS. Such ROS-induced release of iron forms a potential for an even more drastic ROS burst through formation of hydroxyl radicals in the Fenton reaction (Navarre et al., 2000). This provides a plausible explanation for the observed oxidative stress tolerance of the aconitase-deficient plants, and raises a question whether PP2A-mediated dephosphorylation of ACONITASE 3 contributes to cellular ROS homeostasis by modulating the stability of the iron-sulfur cluster.

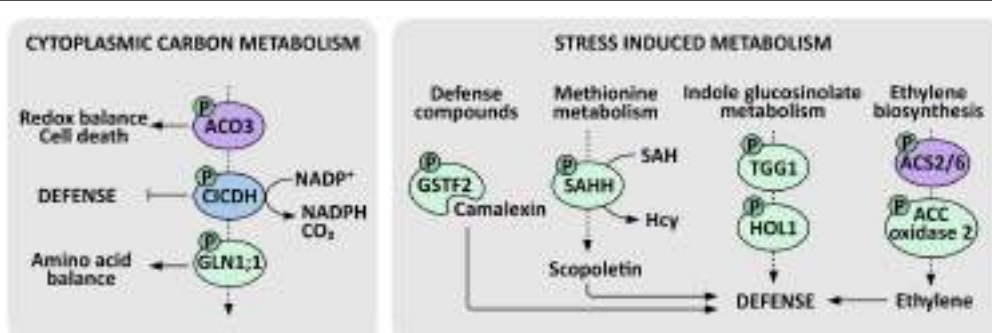


FIGURE 3 | PP2A-regulated enzymes in defense metabolism. Cytosolic aconitase (ACO), isocitrate dehydrogenase (ICDH) and glutamine synthase form a metabolic cascade that is tightly connected with defensive responses in plants. PP2A-B'γ regulates the phosphorylation of cytosolic ACONITASE 3, which contributes to redox balance and cell death regulation. ICDH prevents over-amplification of defense responses and its activity yields α -ketoglutarate, CO_2 , and NADPH. Further down-stream, PP2A-B'γ exerts a control over mRNA and protein abundance of a defense-associated GLUTAMINE SYNTHASE 1;1 (GLN1;1), which contributes to remobilization of amino acids by assimilating α -ketoglutarate and ammonia, and may have a key role in the maintenance of redox balance in chloroplasts. Primary metabolism is also tightly connected with stress-induced metabolism. PP2A-B'γ controls the mRNA and protein abundance of the camalexin binding protein GSTF2, which is a phosphoprotein possibly involved in the transport of this deterring defense compound. PP2A-B'γ also controls the key activated methyl cycle enzyme S-adenosyl-homocysteine hydrolase (SAHH), which contributes to the recycling of S-adenosylmethionine (SAM), hence maintaining transmethylation reactions essential in the biosynthesis of a vast range of protective compounds, such as scopoletin and methylated indole glucosinolates. PP2A-B'γ is also required to control the accumulation and phosphorylation of the myrosinase TGG1 and the thiocyanate methyltransferase 1 (HOL1), which methylates the thiocyanate arising from the degradation of indole glucosinolates. SAM also serves as a precursor for the biosynthesis of the stress hormone ethylene, where the ACC synthases ACS2 and ACS6 and possibly also ACC oxidase 2 are controlled by PP2A. Demonstrated PP2A targets are indicated by violet, and enzymes with increased protein amount and/or phosphorylation in a *pp2a-b'γ* mutant background are indicated by green. ICDH has been identified as a phosphoprotein in the *Arabidopsis* Protein Phosphorylation Site Database (<http://phosphat.uni-hohenheim.de/>) but its regulation has not been connected with PP2A and is hence indicated in blue. P denotes phosphoprotein.

The Impact of PP2A on Stress-induced Secondary Metabolism and Hormonal Signaling

The *cat2 pp2a-b'γ* double mutant proved instrumental in the analysis of PP2A-dependent regulation of secondary metabolism (Li et al., 2014d). Metabolite profiling and subsequent hierarchical clustering of the quantified metabolites revealed only minor impacts caused by the *pp2a-b'γ* and *cat2* single mutations on the global metabolite contents when examined in short-day conditions, which are non-permissive for induction of pathogenesis responses in *cat2* (Li et al., 2014d). The *cat2 pp2a-b'γ* double mutant in contrast showed a striking metabolic signature, which significantly over-lapped with those obtained in long day grown *cat2* or the *P. syringae* challenged wild type leaves (Chaouch et al., 2010, 2012). This signature included marked changes in the contents of amino acids and their derivatives, exemplified by tryptophan, SA and camalexin (Li et al., 2014d). As discussed above, camalexin biosynthesis becomes transcriptionally activated in PTI upon infection of *A. thaliana* plants by a large variety of microorganisms, including bacteria, fungi, and oomycetes, and is commonly recognized as an outcome of SA and ROS signaling (Glawischnig, 2007; Van Breusegem et al., 2008). However, perturbations in the function of PP2A-B'γ did not significantly alter the expression of camalexin-related genes, with the exception of the gene encoding the camalexin binding protein GSTF2 (Trotta et al., 2011; Li et al., 2014d), which also displayed increased abundance and phosphorylation in *pp2a-b'γ* (Li et al., 2014d). This further associated with a slight increase in camalexin content in the constitutively defense-active *pp2a-b'γ* single mutant and a significant accumulation in *cat2 pp2a-b'γ* (Li et al., 2014d; Figure 3). Thus, PP2A-B'γ appears to be required for post-translational control of oxidative-signal-induced metabolic alterations in *A. thaliana* leaves.

2D-gel electrophoresis and subsequent mass spectrometry analysis identified a number of proteins the abundance and/or phosphorylation of which was altered in *cat2 pp2a-b'γ* (Li et al., 2014d; Figure 3). These proteins included the central activated methyl cycle enzyme S-adenosyl-homocysteine hydrolase (SAHH), which contributes to the recycling of methionine, a metabolic function essential in plant resistance to pathogens. Stress-induced biosynthetic processes involve a vast range of transmethylation reactions, which form a significant sink for the methyl donor S-adenosylmethionine (SAM). The reaction product S-adenosyl-homocysteine (SAH) is toxic and must be continuously hydrolyzed by SAHH, making this an essential step in the recycling of methionine and SAM and the associated production of a wide range of defense-related secondary metabolites (Moffatt and Weretilnyk, 2001). In *cat2 pp2a-b'γ*, SAM is consumed in the biosynthesis of scopoletin, a coumarin that accumulates in response to biotic stress

agents (Chong et al., 2002; Li et al., 2014d). On protein level, *cat2 pp2a-b'γ* mutants exhibit increased accumulation and phosphorylation of the myrosinase TGG1 involved in the catabolism of indole glucosinolates, and the thiocyanate methyltransferase 1 (HOL1), which in turn methylates the thiocyanate arising from the *in vivo* degradation of indole glucosinolates (Nagatoshi and Nakamura, 2009), suggesting that indole glucosinolate metabolism is under the control of PP2A-B'γ (Li et al., 2014d; Figure 3).

Yet another sink for SAM is the biosynthesis of ethylene, which plays a role in plant resistance against bacterial and fungal pathogens (Guan et al., 2015). Ethylene biosynthesis is highly induced in both PTI and ETI, and a recent report by Guan et al. (2015) showed that this induction is potentiated by SA signaling through a pathway that largely depends on MPK3 and MPK6 and their downstream targets, the ACC synthases ACS2 and ACS6. Using the *roots curl in naphthalphthalamic acid 1 (rcn1)* mutant as a tool, Alison DeLong and co-workers showed that the same ACS2 and ACS6 isoforms are negatively controlled by PP2A-dependent dephosphorylation (Skottke et al., 2011). As a consequence, *rcn1* mutants display constitutive ethylene production, which was, however, not further enhanced in response to flagellin-induced signals (Skottke et al., 2011). Li et al. (2014d) found that also ACC oxidase 2, which mediates the next enzymatic step in the biosynthesis of ethylene, is a phosphoprotein with significantly elevated protein level in *cat2 pp2a-b'γ* double mutants. Hence, PP2A may, directly or indirectly, negatively regulate multiple enzymatic steps in stress-induced ethylene biosynthesis.

In conclusion, the multitude of PP2A-dependent metabolic adjustments reflect the intimate connections between primary and secondary metabolism and cellular signaling. These interactions can be readily adjusted by protein kinases and protein phosphatases that delicately fine-tune different levels of plant immunity.

AUTHOR CONTRIBUTIONS

All authors listed, have made substantial, direct and intellectual contribution to the work, and approved it for publication.

FUNDING

The work was funded by Academy of Finland Centre of Excellence (CoE) in the Molecular Biology of Primary Producers (2014–2019) (decision #271832), the research funds (#135751, #140981, and #273132) to MB and the post-doctoral fund (#289687) to GD. MR and SA were supported University of Turku Doctoral Programme in Molecular Life Sciences.

REFERENCES

- Ahn, C. S., Han, J.-A., Lee, H.-S., Lee, S., and Pai, H.-S. (2011). The PP2A regulatory subunit Tap46, a component of the TOR signaling pathway, modulates growth and metabolism in plants. *Plant Cell* 23, 185–209. doi: 10.1105/tpc.110.074005
- Allahverdiyeva, Y., Battchikova, N., Brosché, M., Fujii, H., Kangasjärvi, S., Mulo, P., et al. (2015). Integration of photosynthesis, development and stress as an opportunity for plant biology. *New Phytol.* 208, 647–655. doi: 10.1111/nph.13549
- Asai, T., Tena, G., Plotnikova, J., Willmann, M. R., Chiu, W.-L., Gomez-Gomez, L., et al. (2002). MAP kinase signalling cascade in *Arabidopsis* innate immunity. *Nature* 415, 977–983. doi: 10.1038/415977a
- Bartels, S., Anderson, J. C., Gonzalez Besteiro, M. A., Carreri, A., Hirt, H., Buchala, A., et al. (2009). MAP KINASE PHOSPHATASE1 and PROTEIN TYROSINE PHOSPHATASE1 are repressors of salicylic acid synthesis and SNC1-mediated responses in *Arabidopsis*. *Plant Cell* 21, 2884–2897. doi: 10.1105/tpc.109.067678
- Bernsdorff, F., Doering, A.-C., Gruner, K., Schuck, S., Bräutigam, A., and Zeier, J. (2016). Pipecolic acid orchestrates plant systemic acquired resistance and defense priming via salicylic acid-dependent and independent pathways. *Plant Cell* 28:tc.15.00496. doi: 10.1105/tpc.15.00496
- Boller, T., and Felix, G. (2009). A renaissance of elicitors: perception of microbe-associated molecular patterns and danger signals by pattern-recognition receptors. *Annu. Rev. Plant Biol.* 60, 379–406. doi: 10.1146/annurev.arplant.57.032905.105346
- Bostock, R. M. (2005). Signal crosstalk and induced resistance: straddling the line between cost and benefit. *Annu. Rev. Phytopathol.* 43, 545–580. doi: 10.1146/annurev.phyto.41.052002.095505
- Boudsocq, M., Willmann, M. R., McCormack, M., Lee, H., Shan, L., He, P., et al. (2010). Differential innate immune signalling via Ca^{2+} sensor protein kinases. *Nature* 464, 418–422. doi: 10.1038/nature08794
- Bowler, C., and Fluhr, R. (2000). The role of calcium and activated oxygens as signals for controlling cross-tolerance. *Trends Plant Sci.* 5, 241–246. doi: 10.1016/S1360-1385(00)01628-9
- Caplan, J. L., Kumar, A. S., Park, E., Padmanabhan, M. S., Hoban, K., Modla, S., et al. (2015). Chloroplast stromes function during innate immunity. *Dev. Cell* 34, 45–57. doi: 10.1016/j.devcel.2015.05.011
- Chaouch, S., Queval, G., and Noctor, G. (2012). AtRbohF is a crucial modulator of defence-associated metabolism and a key actor in the interplay between intracellular oxidative stress and pathogenesis responses in *Arabidopsis*. *Plant J.* 69, 613–627. doi: 10.1111/j.1365-313X.2011.04816.x
- Chaouch, S., Queval, G., Vanderauwera, S., Mhamdi, A., Vandorpé, M., Langlois-Meurinne, M., et al. (2010). Peroxisomal hydrogen peroxide is coupled to biotic defense responses by ISOCHORISMATE SYNTHASE1 in a daylength-related manner. *Plant Physiol.* 153, 1692–1705. doi: 10.1104/pp.110.153957
- Chen, J., Hu, R., Zhu, Y., Shen, G., and Zhang, H. (2014). *Arabidopsis* PHOSPHOTYROSYL PHOSPHATASE ACTIVATOR is essential for protein phosphatase 2A holoenzyme assembly and plays important roles in hormone signaling, salt stress response, and plant development. *Plant Physiol.* 166, 1519–1534. doi: 10.1104/pp.114.250563
- Cho, U. S., and Xu, W. (2007). Crystal structure of a protein phosphatase 2A heterotrimeric holoenzyme. *Nature* 445, 53–57. doi: 10.1038/nature05351
- Chong, J., Baltz, R., Schmitt, C., Beffa, R., Fritig, B., Saindrenan, P., et al. (2002). Downregulation of a pathogen-responsive tobacco UDP-Glc?: phenylpropanoid glucosyltransferase reduces scopoletin glucoside accumulation, enhances oxidative stress, and weakens virus resistance. *Plant Cell* 14, 1093–1107. doi: 10.1105/tpc.010436.2
- Coca, M., and San Segundo, B. (2010). AtCPK1 calcium-dependent protein kinase mediates pathogen resistance in *Arabidopsis*. *Plant J.* 63, 526–540. doi: 10.1111/j.1365-313X.2010.04255.x
- De Baere, I., Derua, R., Janssens, V., Van Hoof, C., Waelkens, E., Merlevede, W., et al. (1999). Purification of porcine brain protein phosphatase 2A leucine carboxyl methyltransferase and cloning of the human homologue. *Biochemistry* 38, 16539–16547. doi: 10.1021/bi991646a
- De Clercq, I., Vermeirissen, V., Van Aken, O., Vandepoele, K., Murcha, M. W., Law, S. R., et al. (2013). The membrane-bound NAC transcription factor ANAC013 functions in mitochondrial retrograde regulation of the oxidative stress response in *Arabidopsis*. *Plant Cell* 25, 3472–3490. doi: 10.1105/tpc.113.117168
- de Torres Zabala, M., Littlejohn, G., Jayaraman, S., Studholme, D., Bailey, T., Lawson, T., et al. (2015). Chloroplasts play a central role in plant defence and are targeted by pathogen effectors. *Nat. Plants* 1:15074. doi: 10.1038/nplants.2015.74
- Degrave, A., Siamer, S., Boureau, T., and Barny, M. A. (2015). The AvrE superfamily: ancestral type III effectors involved in suppression of pathogen-associated molecular pattern-triggered immunity. *Mol. Plant Pathol.* 16, 899–905. doi: 10.1111/mpp.12237
- Dubiella, U., Seybold, H., Durian, G., Komander, E., Lassig, R., Witte, C.-P., et al. (2013). Calcium-dependent protein kinase/NADPH oxidase activation circuit is required for rapid defense signal propagation. *Proc. Natl. Acad. Sci. U.S.A.* 110, 8744–8749. doi: 10.1073/pnas.1221294110
- Farkas, I., Dombrádi, V., Miskei, M., Szabados, L., and Koncz, C. (2007). *Arabidopsis* PPP family of serine/threonine phosphatases. *Trends Plant Sci.* 12, 169–176. doi: 10.1016/j.tplants.2007.03.003
- Gao, Q. M., Yu, K., Xia, Y., Shine, M. B., Wang, C., Navarre, D., et al. (2014). Mono- and digalactosyldiacylglycerol lipids function nonredundantly to regulate systemic acquired resistance in plants. *Cell Rep.* 9, 1681–1692. doi: 10.1016/j.celrep.2014.10.069
- Geiger, D., Scherzer, S., Mumm, P., Stange, A., Marten, I., Bauer, H., et al. (2009). Activity of guard cell anion channel SLAC1 is controlled by drought-stress signaling kinase-phosphatase pair. *Proc. Natl. Acad. Sci. U.S.A.* 106, 21425–21430. doi: 10.1073/pnas.0912021106
- Glawischning, E. (2007). Camalexin. *Phytochemistry* 68, 401–406. doi: 10.1016/j.phytochem.2006.12.005
- Gómez-Gómez, L., and Boller, T. (2000). FLS2: an LRR receptor-like kinase involved in the perception of the bacterial elicitor flagellin in *Arabidopsis*. *Mol. Cell* 5, 1003–1011. doi: 10.1016/S1097-2765(00)80265-8
- Guan, R., Su, J., Meng, X., Li, S., Li, Y., Xu, J., et al. (2015). Multi-layered regulation of ethylene induction plays a positive role in *Arabidopsis* resistance against *Pseudomonas syringae*. *Plant Physiol.* 169, 299–312. doi: 10.1104/pp.115.00659
- Gust, A. A., and Felix, G. (2014). Receptor like proteins associate with SOBIR1-type of adaptors to form bimolecular receptor kinases. *Curr. Opin. Plant Biol.* 21, 104–111. doi: 10.1016/j.pbi.2014.07.007
- Harris, D. M., Myrick, T. L., and Rundle, S. J. (1999). The *Arabidopsis* homolog of yeast TAP42 and mammalian alpha4 binds to the catalytic subunit of protein phosphatase 2A and is induced by chilling. *Plant Physiol.* 121, 609–617. doi: 10.1104/pp.121.2.609
- He, X., Anderson, J. C., Del Pozo, O., Gu, Y. Q., Tang, X., and Martin, G. B. (2004). Silencing of subfamily I of protein phosphatase 2A catalytic subunits results in activation of plant defense responses and localized cell death. *Plant J.* 38, 563–577. doi: 10.1111/j.1365-313X.2004.02073.x
- Hooks, M. A., Allwood, J. W., Harrison, J. K., Kopka, J., Erban, A., Goodacre, R., et al. (2014). Selective induction and subcellular distribution of ACONITASE 3 reveal the importance of cytosolic citrate metabolism during lipid mobilization in *Arabidopsis*. *Biochem. J.* 317, 309–317. doi: 10.1042/BJ20140430
- Hruz, T., Laule, O., Szabo, G., Wessendorp, F., Bleuler, S., Oertle, L., et al. (2008). Genevestigator V3: a reference expression database for the meta-analysis of transcriptomes. *Adv. Bioinformatics* 2008, 1–5. doi: 10.1155/2008/420747
- Hu, R., Zhu, Y., Shen, G., and Zhang, H. (2014). TAP46 plays a positive role in the ABSCISIC ACID INSENSITIVE5-regulated gene expression in *Arabidopsis*. *Plant Physiol.* 164, 721–734. doi: 10.1104/pp.113.233684
- Ishihama, N., and Yoshioka, H. (2012). Post-translational regulation of WRKY transcription factors in plant immunity. *Curr. Opin. Plant Biol.* 15, 431–437. doi: 10.1016/j.pbi.2012.02.003
- Jacinto, E., and Hall, M. N. (2003). Tor signalling in bugs, brain and brawn. *Nat. Rev. Mol. Cell Biol.* 4, 117–126. doi: 10.1038/nrm1018
- Jones, A. M. E., Thomas, V., Bennett, M. H., Mansfield, J., and Grant, M. (2006). Modifications to the *Arabidopsis* defense proteome occur prior to significant transcriptional change in response to inoculation with *Pseudomonas syringae*. *Plant Physiol.* 142, 1603–1620. doi: 10.1104/pp.106.086231
- Jones, J. D. G., and Dangl, J. L. (2006). The plant immune system. *Nat. Rev.* 444, 323–329. doi: 10.1038/nature05286
- Jung, H. W., Tschaplinski, T. J., Wang, L., Glazebrook, J., and Greenberg, J. T. (2009). Priming in systemic plant immunity. *Science* 324, 89–91. doi: 10.1126/science

- Kadota, Y., Sklenar, J., Derbyshire, P., Stransfeld, L., Asai, S., Ntoukakis, V., et al. (2014). Direct regulation of the NADPH Oxidase RBOHD by the PRR-associated kinase BIK1 during plant immunity. *Mol. Cell* 54, 43–55. doi: 10.1016/j.molcel.2014.02.021
- Kang, S., Yang, F., Li, L., Chen, H., Chen, S., and Zhang, J. (2015). The *Arabidopsis* transcription factor BRASSINOSTEROID INSENSITIVE1-ETHYL METHANESULFONATE-SUPPRESSOR1 is a direct substrate of MITOGEN-ACTIVATED PROTEIN KINASE6 and regulates immunity. *Plant Physiol.* 167, 1076–1086. doi: 10.1104/pp.114.250985
- Kangasjärvi, S., Tikkkanen, M., Durian, G., and Aro, E. M. (2014). Photosynthetic light reactions – an adjustable hub in basic production and plant immunity signaling. *Plant Physiol. Biochem.* 81, 128–134. doi: 10.1016/j.plaphy.2013.12.004
- Kataya, A. R., Behzad, H., and Cathrine, L. (2015a). Protein phosphatase 2A regulatory subunits affecting plant innate immunity, energy metabolism, and flowering time – joint functions among B'γ subfamily members. *Plant Signal. Behav.* 10, 37–41. doi: 10.1080/15592324.2015.1026024
- Kataya, A. R., Heidari, B., Hagen, L., Kommedal, R., Slupphaug, G., and Lillo, C. (2015b). Protein phosphatase 2A holoenzyme is targeted to peroxisomes by piggybacking and positively affects peroxisomal β-oxidation. *Plant Physiol.* 167, 493–506. doi: 10.1104/pp.114.254409
- Kaurilind, E., Xu, E., and Brosché, M. (2015). A genetic framework for H₂O₂ induced cell death in *Arabidopsis thaliana*. *BMC Genomics* 16:837. doi: 10.1186/s12864-015-1964-8
- Kerk, D., Bulgrien, J., Smith, D. W., Barsam, B., Veretnik, S., and Grabskov, M. (2002). The complement of protein phosphatase catalytic subunits encoded in the genome of *Arabidopsis*. *Plant Physiol.* 129, 908–925. doi: 10.1104/pp.004002
- Konert, G., Rahikainen, M., Trotta, A., Durian, G., Salojärvi, J., Khorobrykh, S., et al. (2015a). Subunits B'γ and B'ζ of protein phosphatase 2A regulate photo-oxidative stress responses and growth in *A. thaliana*. *Plant. Cell Environ.* 38, 2641–2651. doi: 10.1111/pce.12575
- Konert, G., Trotta, A., Kouvonnen, P., Rahikainen, M., Durian, G., Blokhina, O., et al. (2015b). Protein phosphatase 2A (PP2A) regulatory subunit B'γ interacts with cytoplasmic ACONITASE 3 and modulates the abundance of AOX1A and AOX1D in *Arabidopsis thaliana*. *New Phytol.* 205, 1250–1263. doi: 10.1111/nph.13097
- Kopischke, M., Westphal, L., Schneeberger, K., Clark, R., Ossowski, S., Wewer, V., et al. (2013). Impaired sterol ester synthesis alters the response of *Arabidopsis thaliana* to *Phytophthora infestans*. *Plant J.* 73, 456–468. doi: 10.1111/tpj.12046
- Krasensky, J., and Jonak, C. (2012). Drought, salt, and temperature stress-induced metabolic rearrangements and regulatory networks. *J. Exp. Bot.* 63, 1593–1608. doi: 10.1093/jxb/err460
- Lassowska, I., Böttcher, C., Eschen-Lippold, L., Scheel, D., and Lee, J. (2014). Sustained mitogen-activated protein kinase activation reprograms defense metabolism and phosphoprotein profile in *Arabidopsis thaliana*. *Front. Plant Sci.* 5:554. doi: 10.3389/fpls.2014.00554
- Lee, J.-Y., Wang, X., Cui, W., Sager, R., Modla, S., Czymmek, K., et al. (2011). A plasmodesmata-localized protein mediates crosstalk between cell-to-cell communication and innate immunity in *Arabidopsis*. *Plant Cell* 23, 3353–3373. doi: 10.1105/tpc.111.087742
- Lee, S. C., Lan, W., Buchanan, B. B., and Luan, S. (2009). A protein kinase-phosphatase pair interacts with an ion channel to regulate ABA signaling in plant guard cells. *Proc. Natl. Acad. Sci. U.S.A.* 106, 21419–21424. doi: 10.1073/pnas.0910601106
- Leivar, P., Antolín-Llovera, M., Ferrero, S., Closa, M., Arró, M., Ferrer, A., et al. (2011). Multilevel control of *Arabidopsis* 3-hydroxy-3-methylglutaryl coenzyme A reductase by protein phosphatase 2A. *Plant Cell* 23, 1494–1511. doi: 10.1105/tpc.110.074278
- Lewis, L. A., Polanski, K., de Torres-Zabala, M., Jayaraman, S., Bowden, L., Moore, J., et al. (2015). Transcriptional dynamics driving MAMP-triggered immunity and pathogen effector-mediated immunosuppression in *Arabidopsis* leaves following infection with *Pseudomonas syringae* pv tomato DC3000. *Plant Cell* 27:tc.15.00471. doi: 10.1105/tpc.15.00471
- Li, B., Jiang, S., Yu, X., Cheng, C., Chen, S., Cheng, Y., et al. (2015). Phosphorylation of trihelix transcriptional repressor ASR3 by MAP kinase4 negatively regulates *Arabidopsis* immunity. *Plant Cell* 27, 839–856. doi: 10.1105/tpc.114.134809
- Li, F., Cheng, C., Cui, F., De Oliveira, M. V. V., Yu, X., Meng, X., et al. (2014a). Modulation of RNA polymerase II phosphorylation downstream of pathogen perception orchestrates plant immunity. *Cell Host Microbe* 16, 748–758. doi: 10.1016/j.chom.2014.10.018
- Li, G., Froehlich, J. E., Elowsky, C., Msanne, J., Ostosh, A. C., Zhang, C., et al. (2014b). Distinct *Pseudomonas* type-III effectors use a cleavable transit peptide to target chloroplasts. *Plant J.* 77, 310–321. doi: 10.1111/tpj.12396
- Li, L., Li, M., Yu, L., Zhou, Z., Liang, X., Liu, Z., et al. (2014c). The FLS2-Associated Kinase BIK1 Directly Phosphorylates the NADPH Oxidase RbohD to Control Plant Immunity. *Cell Host Microbe* 15, 329–338. doi: 10.1016/j.chom.2014.02.009
- Li, S., Mhamdi, A., Trotta, A., Kangasjärvi, S., and Noctor, G. (2014d). The protein phosphatase subunit PP2A-B'γ is required to suppress day length-dependent pathogenesis responses triggered by intracellular oxidative stress. *New Phytol.* 202, 145–160. doi: 10.1111/nph.12622
- Lillo, C., Kataya, A. R. A., Heidari, B., Creighton, M. T., Nemie-Feyissa, D., Ginbot, Z., et al. (2014). Protein phosphatases PP2A, PP4 and PP6: mediators and regulators in development and responses to environmental cues. *Plant Cell Environ.* 37, 2631–2648. doi: 10.1111/pce.12364
- Liu, G., Ji, Y., Bhuiyan, N. H., Pilot, G., Selvaraj, G., Zou, J., et al. (2010). Amino Acid Homeostasis modulates salicylic acid – associated redox status and defense responses in *Arabidopsis*. *Plant Cell* 22, 3845–3863. doi: 10.1105/tpc.110.079392
- Liu, J., Yang, H., Bao, F., Ao, K., Zhang, X., Zhang, Y., et al. (2015). IBR5 modulates temperature-dependent r protein CHS3-mediated defense responses in *Arabidopsis*. *PLoS Genet.* 11:e1005584. doi: 10.1371/journal.pgen.1005584
- Liu, T., Liu, Z., Song, C., Hu, Y., Han, Z., She, J., et al. (2012). Chitin-induced dimerization activates a plant immune receptor. *Science* 336, 1160–1164. doi: 10.1126/science.1218867
- Lumbrales, V., Vilela, B., Irar, S., Solé, M., Capellades, M., Valls, M., et al. (2010). MAPK phosphatase MKP2 mediates disease responses in *Arabidopsis* and functionally interacts with MPK3 and MPK6. *Plant J.* 63, 1017–1030. doi: 10.1111/j.1365-313X.2010.04297.x
- Macho, A. P., and Zipfel, C. (2014). Plant PRRs and the activation of innate immune signaling. *Mol. Cell* 54, 263–272. doi: 10.1016/j.molcel.2014.03.028
- Matre, P., Meyer, C., and Lillo, C. (2009). Diversity in subcellular targeting of the PP2A B'η subfamily members. *Planta* 230, 935–945. doi: 10.1007/s00425-009-0998-z
- Mhamdi, A., Mauve, C., Gouia, H., Saindrenan, P., Hodges, M., and Noctor, G. (2010). Cytosolic NADP-dependent isocitrate dehydrogenase contributes to redox homeostasis and the regulation of pathogen responses in *Arabidopsis* leaves. *Plant Cell Environ.* 33, 1112–1123. doi: 10.1111/j.1365-3040.2010.02133.x
- Moeder, W., del Pozo, O., Navarre, D. A., Martin, G. B., and Klessig, D. F. (2007). Aconitase plays a role in regulating resistance to oxidative stress and cell death in *Arabidopsis* and *Nicotiana benthamiana*. *Plant Mol. Biol.* 63, 273–287. doi: 10.1007/s11103-006-9087-x
- Moffatt, B. A., and Weretilnyk, E. A. (2001). Sustaining S-adenosyl-l-methionine-dependent methyltransferase activity in plant cells. *Physiol. Plant* 113, 435–442. doi: 10.1034/j.1399-3054.2001.1130401.x
- Moorhead, G. B., De Wever, V., Templeton, G., and Kerk, D. (2009). Evolution of protein phosphatases in plants and animals. *Biochem. J.* 417, 401–409. doi: 10.1042/BJ20081986
- Mühlenbock, P., Szechynska-Hebda, M., Plaszczyc, M., Baudo, M., Mateo, A., Mullineaux, P. M., et al. (2008). Chloroplast signaling and LESION SIMULATING DISEASE1 regulate crosstalk between light acclimation and immunity in *Arabidopsis*. *Plant Cell* 20, 2339–2356. doi: 10.1105/tpc.108.059618
- Mysore, K. S., Crasta, O. R., Tuori, R. P., Folkerts, O., Swirsky, P. B., and Martin, G. B. (2002). Comprehensive transcript profiling of Pto- and Prf-mediated host defense responses to infection by *Pseudomonas syringae* pv. tomato. *Plant J.* 32, 299–315. doi: 10.1046/j.1365-313X.2002.01424.x
- Nagatoshi, Y., and Nakamura, T. (2009). *Arabidopsis* HARMLESS to OZONE LAYER protein methylates a glucosinolate breakdown product and functions in resistance to *Pseudomonas syringae* pv. maculicola. *J. Biol. Chem.* 284, 19301–19309. doi: 10.1074/jbc.M109.001032
- Navarre, D. A., Wendehenne, D., Durner, J., Noad, R., and Klessig, D. F. (2000). Nitric Oxide modulates the activity of tobacco aconitase. *Plant Physiol.* 122, 573–582. doi: 10.1104/pp.122.2.573
- Nomura, H., Komori, T., Uemura, S., Kanda, Y., Shimotani, K., Nakai, K., et al. (2012). Chloroplast-mediated activation of plant immune signalling in *Arabidopsis*. *Nat. Commun.* 3:926. doi: 10.1038/ncomms1926

- Pernas, M., García-Casado, G., Rojo, E., Solano, R., and Sánchez-Serrano, J. J. (2007). A protein phosphatase 2A catalytic subunit is a negative regulator of abscisic acid signalling. *Plant J.* 51, 763–778. doi: 10.1111/j.1365-313X.2007.03179.x
- Pogson, B. J., Woo, N. S., Förster, B., and Small, I. D. (2008). Plastid signalling to the nucleus and beyond. *Trends Plant Sci.* 13, 602–609. doi: 10.1016/j.tplants.2008.08.008
- Prince, D. C., Drurey, C., Zipfel, C., and Hogenhout, S. A. (2014). The leucine-rich repeat receptor-like kinase brassinosteroid insensitive1-associated kinase1 and the cytochrome p450 phytoalexin deficient3 contribute to innate immunity to aphids in *Arabidopsis*. *Plant Physiol.* 164, 2207–2219. doi: 10.1104/pp.114.235598
- Qiu, J.-L., Zhou, L., Yun, B.-W., Nielsen, H. B., Fiil, B. K., Petersen, K., et al. (2008). *Arabidopsis* mitogen-activated protein kinase kinases MKK1 and MKK2 have overlapping functions in defense signaling mediated by MEKK1, MPK4, and MKS1. *Plant Physiol.* 148, 212–222. doi: 10.1104/pp.108.120006
- Queval, G., Issakidis-Bourguet, E., Hoeberichts, F. A., Vandorpe, M., Gakière, B., Vanacker, H., et al. (2007). Conditional oxidative stress responses in the *Arabidopsis* photorespiratory mutant cat2 demonstrate that redox state is a key modulator of daylength-dependent gene expression, and define photoperiod as a crucial factor in the regulation of H₂O₂-induced cel. *Plant J.* 52, 640–657. doi: 10.1111/j.1365-313X.2007.03263.x
- Queval, G., Neukermans, J., Vanderauwera, S., van Breusegem, F., and Noctor, G. (2012). Day length is a key regulator of transcriptomic responses to both CO₂ and H₂O₂ in *Arabidopsis*. *Plant Cell Environ.* 35, 374–387. doi: 10.1111/j.1365-3040.2011.02368.x
- Rahikainen, M., Pascual, J., Alegre, S., Durian, G., and Kangasjärvi, S. (2016). PP2A Phosphatase as a regulator of ROS signaling in plants. *Antioxidants* 5:8. doi: 10.3390/antiox5010008
- Ranf, S., Eschen-Lippold, L., Pecher, P., Lee, J., and Scheel, D. (2011). Interplay between calcium signalling and early signalling elements during defence responses to microbe- or damage-associated molecular patterns. *Plant J.* 68, 100–113. doi: 10.1111/j.1365-313X.2011.04671.x
- Rasool, B., Karpinska, B., Konert, G., Durian, G., Denessiouk, K., Kangasjärvi, S., et al. (2014). Effects of light and the regulatory B-subunit composition of protein phosphatase 2A on the susceptibility of *Arabidopsis thaliana* to aphid (*Myzus persicae*) infestation. *Front. Plant Sci.* 5:405. doi: 10.3389/fpls.2014.00405
- Rayapuram, N., Bonhomme, L., Bigeard, J., Haddadou, K., Przybylski, C., Hirt, H., et al. (2014). Identification of novel PAMP-triggered phosphorylation and dephosphorylation events in *Arabidopsis thaliana* by quantitative phosphoproteomic analysis. *J. Proteome Res.* 13, 2137–2151. doi: 10.1021/pr040268v
- Rexin, D., Meyer, C., Robaglia, C., and Veit, B. (2015). TOR signalling in plants. *Biochem. J.* 470, 1–14. doi: 10.1042/BJ20150505
- Rodríguez-Hervá, J. J., González-Melendi, P., Cuartas-Lanza, R., Antúnez-Lamas, M., Río-Alvarez, I., Li, Z., et al. (2012). A bacterial cysteine protease effector protein interferes with photosynthesis to suppress plant innate immune responses. *Cell. Microbiol.* 14, 669–681. doi: 10.1111/j.1462-5822.2012.01749.x
- Savatin, D. V., Bisceglia, N. G., Martí, L., Fabbri, C., Cervone, F., and De Lorenzo, G. (2014). The *Arabidopsis* NUCLEUS- AND PHRAGMOPLAST-LOCALIZED KINASE1-related protein kinases are required for elicitor-induced oxidative burst and immunity. *Plant Physiol.* 165, 1188–1202. doi: 10.1104/pp.114.236901
- Schulz, P., Herde, M., and Romeis, T. (2013). Calcium-dependent protein kinases: hubs in plant stress signaling and development. *Plant Physiol.* 163, 523–530. doi: 10.1104/pp.113.222539
- Schweighofer, A., Kazanaviciute, V., Scheikl, E., Teige, M., Doczi, R., Hirt, H., et al. (2007). The PP2C-type phosphatase AP2C1, which negatively regulates MPK4 and MPK6, modulates innate immunity, jasmonic acid, and ethylene levels in *Arabidopsis*. *Plant Cell* 19, 2213–2224. doi: 10.1105/tpc.106.049585
- Segonzac, C., Macho, A. P., Sanmartín, M., Ntoukakis, V., Sánchez-Serrano, J. J., and Zipfel, C. (2014). Negative control of BAK1 by protein phosphatase 2A during plant innate immunity. *EMBO J.* 33, 1–11. doi: 10.15252/embj.201488698
- Seifi, H. S., Van Bockhaven, J., Angenon, G., and Höfte, M. (2013). Glutamate metabolism in plant disease and defense: friend or foe? *Mol. Plant. Microbe Interact.* 26, 475–485. doi: 10.1094/MPMI-07-12-0176-CR
- Sents, W., Ivanova, E., Lambrecht, C., Haesen, D., and Janssens, V. (2013). The biogenesis of active protein phosphatase 2A holoenzymes: a tightly regulated process creating phosphatase specificity. *FEBS J.* 280, 644–661. doi: 10.1111/j.1742-4658.2012.08579.x
- Sewelam, N., Jaspert, N., Van Der Kelen, K., Tognetti, V. B., Schmitz, J., Frerigmann, H., et al. (2014). Spatial H₂O₂ signaling specificity: H₂O₂ from chloroplasts and peroxisomes modulates the plant transcriptome differentially. *Mol. Plant* 7, 1191–1210. doi: 10.1093/mp/suu070
- Shimada, T. L., Takano, Y., Shimada, T., Fujiwara, M., Fukao, Y., Mori, M., et al. (2014). Leaf oil body functions as a subcellular factory for the production of a phytoalexin in *Arabidopsis*. *Plant Physiol.* 164, 105–118. doi: 10.1104/pp.113.230185
- Skottke, K. R., Yoon, G. M., Kieber, J. J., and DeLong, A. (2011). Protein phosphatase 2A controls ethylene biosynthesis by differentially regulating the turnover of ACC synthase isoforms. *PLoS Genet.* 7:e1001370. doi: 10.1371/journal.pgen.1001370
- Sønderby, I. E., Geu-Flores, F., and Halkier, B. A. (2010). Biosynthesis of glucosinolates - gene discovery and beyond. *Trends Plant Sci.* 15, 283–290. doi: 10.1016/j.tplants.2010.02.005
- Spinner, L., Gadeyne, A., Belcram, K., Goussot, M., Moison, M., Duroc, Y., et al. (2013). A protein phosphatase 2A complex spatially controls plant cell division. *Nat. Commun.* 4:1863. doi: 10.1038/ncomms2831
- Tang, W., Yuan, M., Wang, R., Yang, Y., Wang, C., Oses-Prieto, J. A., et al. (2011). PP2A activates brassinosteroid-responsive gene expression and plant growth by dephosphorylating BZR1. *Nat. Cell Biol.* 13, 124–131. doi: 10.1038/ncb2151
- Trotta, A., Rahikainen, M., Konert, G., Finazzi, G., and Kangasjärvi, S. (2014). Signalling crosstalk in light stress and immune reactions in plants. *Philos. Trans. R. Soc. Lond. B. Biol. Sci.* 369:20130235. doi: 10.1098/rstb.2013.0235
- Trotta, A., Wrzaczek, M., Scharte, J., Tikkkanen, M., Konert, G., Rahikainen, M., et al. (2011). Regulatory subunit B'gamma of protein phosphatase 2A prevents unnecessary defense reactions under low light in *Arabidopsis*. *Plant Physiol.* 156, 1464–1480. doi: 10.1104/pp.111.178442
- Truman, W., Bennett, M. H., Kubigsteltig, I., Turnbull, C., and Grant, M. (2007). *Arabidopsis* systemic immunity uses conserved defense signaling pathways and is mediated by jasmonates. *Proc. Natl. Acad. Sci. U.S.A.* 104, 1075–1080. doi: 10.1073/pnas.0605423104
- Uhrig, R. G., Labandera, A. M., and Moorhead, G. B. (2013). *Arabidopsis* PPP family of serine/threonine protein phosphatases: many targets but few engines. *Trends Plant Sci.* 18, 505–513. doi: 10.1016/j.tplants.2013.05.004
- Unterholzner, S. J., Rozhon, W., Papacek, M., Ciomas, J., Lange, T., Kugler, K. G., et al. (2015). Brassinosteroids are master regulators of gibberellin biosynthesis in *Arabidopsis*. *Plant Cell* 27, 1–13. doi: 10.1105/tpc.15.00433
- Vainonen, J. P., and Kangasjärvi, J. (2015). Plant signalling in acute ozone exposure. *Plant Cell Environ.* 38, 240–252. doi: 10.1111/pce.12273
- Van Breusegem, F., Bailey-Serres, J., and Mittler, R. (2008). Unraveling the tapestry of networks involving reactive oxygen species in plants. *Plant Physiol.* 147, 978–984. doi: 10.1104/pp.108.122325
- van der Schoot, C., Paul, L. K., Paul, S. B., and Rinne, P. L. H. (2011). Plant lipid bodies and cell-cell signaling: a new role for an old organelle? *Plant Signal. Behav.* 6, 1732–1738. doi: 10.4161/psb.6.11.17639
- van Wijk, K. J., Friso, G., Walther, D., and Schulze, W. X. (2014). Meta-Analysis of *Arabidopsis thaliana* phospho-proteomics data reveals compartmentalization of phosphorylation motifs. *Plant Cell* 26, 2367–2389. doi: 10.1105/tpc.114.125815
- Vogel, M. O., Moore, M., König, K., Pecher, P., Alsharafa, K., Lee, J., et al. (2014). Fast retrograde signaling in response to high light involves metabolite export, MITOGEN-ACTIVATED PROTEIN KINASE6, and AP2/ERF transcription factors in *Arabidopsis*. *Plant Cell* 26, 1151–1165. doi: 10.1105/tpc.113.121061
- Waadt, R., Manalansan, B., Rauniyar, N., Munemasa, S., Booker, M. A., Brandt, B., et al. (2015). Identification of open stomatal-interacting proteins reveals interactions with sucrose non-fermenting1-related protein kinases2 and with type 2a protein phosphatases that function in abscisic acid responses. *Plant Physiol.* 169, 760–779. doi: 10.1104/pp.15.00575
- Wang, C., El-Shetehy, M., Shine, M. B., Yu, K., Navarre, D., Wendehenne, D., et al. (2014). Free radicals mediate systemic acquired resistance. *Cell Rep.* 7, 348–355. doi: 10.1016/j.celrep.2014.03.032
- Wang, X., Sager, R., Cui, W., Zhang, C., Lu, H., and Lee, J. (2013). Salicylic acid regulates Plasmodesmata closure during innate immune responses in *Arabidopsis*. *Plant Cell* 25, 2315–2329. doi: 10.1105/tpc.113.110676

- Waszczak, C., Akter, S., Eeckhout, D., Persiau, G., Wahni, K., Bodra, N., et al. (2014). Sulfenome mining in *Arabidopsis thaliana*. *Proc. Natl. Acad. Sci. U.S.A.* 111, 11545–11550. doi: 10.1073/pnas.1411607111
- Wu, G., Wang, X., Li, X., Kamiya, Y., Otegui, M. S., and Chory, J. (2011). Methylation of a phosphatase specifies dephosphorylation and degradation of activated brassinosteroid receptors. *Sci. Signal.* 4:ra29. doi: 10.1126/scisignal.2001258
- Xie, K., Chen, J., Wang, Q., and Yang, Y. (2014). Direct phosphorylation and activation of a mitogen-activated protein kinase by a calcium-dependent protein kinase in rice. *Plant Cell* 26, 1–14. doi: 10.1105/tpc.114.126441
- Xing, Y., Li, Z., Chen, Y., Stock, J. B., Jeffrey, P. D., and Shi, Y. (2008). Structural mechanism of demethylation and inactivation of protein phosphatase 2A. *Cell* 133, 154–163. doi: 10.1016/j.cell.2008.02.041
- Yamazaki, A., and Hayashi, M. (2015). Building the interaction interfaces: host responses upon infection with microorganisms. *Curr. Opin. Plant Biol.* 23, 132–139. doi: 10.1016/j.pbi.2014.12.003
- Yang, J., Roe, S. M., Prickett, T. D., Brautigan, D. L., and Barford, D. (2007). The structure of Tap42/α4 reveals a tetratricopeptide repeat-like fold and provides insights into PP2A regulation. *Biochemistry* 46, 8807–8815. doi: 10.1021/bi7007118
- Zhang, J., Shao, F., Li, Y., Cui, H., Chen, L., Li, H., et al. (2007). A *Pseudomonas syringae* effector inactivates MAPKs to suppress PAMP-induced immunity in plants. *Cell Host Microbe* 1, 175–185. doi: 10.1016/j.chom.2007.03.006
- Zhou, J., Wu, S., Chen, X., Liu, C., Sheen, J., Shan, L., et al. (2014). The *Pseudomonas syringae* effector HopF2 suppresses *Arabidopsis* immunity by targeting BAK1. *Plant J.* 77, 235–245. doi: 10.1111/tpj.12381
- Zipfel, C. (2014). Plant pattern-recognition receptors. *Trends Immunol.* 35, 345–351. doi: 10.1016/j.it.2014.05.004

Conflict of Interest Statement: The authors declare that the research was conducted in the absence of any commercial or financial relationships that could be construed as a potential conflict of interest.

Copyright © 2016 Durian, Rahikainen, Alegre, Brosché and Kangasjärvi. This is an open-access article distributed under the terms of the Creative Commons Attribution License (CC BY). The use, distribution or reproduction in other forums is permitted, provided the original author(s) or licensor are credited and that the original publication in this journal is cited, in accordance with accepted academic practice. No use, distribution or reproduction is permitted which does not comply with these terms.



Regulation of WRKY46 Transcription Factor Function by Mitogen-Activated Protein Kinases in *Arabidopsis thaliana*

OPEN ACCESS

Edited by:

Olivier Lamotte,
Centre National de la Recherche
Scientifique, France

Reviewed by:

Hirofumi Yoshioka,
Nagoya University, Japan
Andrea Pitzschke,
University of Salzburg, Austria

*Correspondence:

Justin Lee
jlee@ipb-halle.de

†Present address:

Arsheed H. Sheikh,
School of Life Sciences, Gibbet Hill
Campus, The University of Warwick,
Coventry, CV4 7AL, UK;
Pascal Pecher,
Department of Cell and
Developmental Biology, John Innes
Centre, Norwich Research Park,
Norwich NR4 7UH, UK

[‡]These authors have contributed
equally to this work.

Specialty section:

This article was submitted to
Plant Physiology,
a section of the journal
Frontiers in Plant Science

Received: 07 October 2015

Accepted: 14 January 2016

Published: 04 February 2016

Citation:

Sheikh AH, Eschen-Lippold L,
Pecher P, Hoehenwarter W, Sinha AK,
Scheel D and Lee J (2016) Regulation
of WRKY46 Transcription Factor
Function by Mitogen-Activated
Protein Kinases in *Arabidopsis*
thaliana. *Front. Plant Sci.* 7:61.
doi: 10.3389/fpls.2016.00061

Arsheed H. Sheikh^{1†‡}, Lennart Eschen-Lippold^{1†‡}, Pascal Pecher^{1†},
Wolfgang Hoehenwarter¹, Alok K. Sinha², Dierk Scheel¹ and Justin Lee^{1*}

¹ Department of Stress and Developmental Biology, Leibniz Institute of Plant Biochemistry, Halle/Saale, Germany, ² National Institute of Plant Genome Research, New Delhi, India

Mitogen-activated protein kinase (MAPK) cascades are central signaling pathways activated in plants after sensing internal developmental and external stress cues. Knowledge about the downstream substrate proteins of MAPKs is still limited in plants. We screened *Arabidopsis* WRKY transcription factors as potential targets downstream of MAPKs, and concentrated on characterizing WRKY46 as a substrate of the MAPK, MPK3. Mass spectrometry revealed *in vitro* phosphorylation of WRKY46 at amino acid position S168 by MPK3. However, mutagenesis studies showed that a second phosphosite, S250, can also be phosphorylated. Elicitation with pathogen-associated molecular patterns (PAMPs), such as the bacterial flagellin-derived flg22 peptide led to *in vivo* destabilization of WRKY46 in *Arabidopsis* protoplasts. Mutation of either phosphorylation site reduced the PAMP-induced degradation of WRKY46. Furthermore, the protein for the double phosphosite mutant is expressed at higher levels compared to wild-type proteins or single phosphosite mutants. In line with its nuclear localization and predicted function as a transcriptional activator, overexpression of WRKY46 in protoplasts raised basal plant defense as reflected by the increase in promoter activity of the PAMP-responsive gene, *NHL10*, in a MAPK-dependent manner. Thus, MAPK-mediated regulation of WRKY46 is a mechanism to control plant defense.

Keywords: mitogen-activated protein kinase, WRKY transcription factors, phosphorylation, protein stability, defense, pathogen-associated molecular patterns (PAMPs)

INTRODUCTION

Upon pathogen encounter, plants respond through two layers of immunity: PTI (pattern-triggered immunity) and ETI (effector-triggered immunity; Jones and Dangl, 2006). PTI is the generalized defense mechanism in which conserved pathogen-associated molecular patterns (PAMPs) like bacterial flagellin, elongation factor Tu (EF-Tu) and fungal chitin are recognized at the cell surface by specialized pattern-recognition receptors (PRRs; Boller and Felix, 2009). One of the best studied plant PAMP-PRR interactions is that of the elicitor-active 22-amino acid peptide derived from bacterial flagellin (flg22) and the flg22 receptor, FLAGELLIN-SENSING 2 (FLS2), in *Arabidopsis thaliana*. FLS2 contains an extracellular leucine-rich repeat (LRR) domain for ligand binding, a transmembrane domain and a cytoplasmic serine/threonine kinase domain

(Gómez-Gómez and Boller, 2002). After activation by flg22, FLS2 interacts with BRI1-ASSOCIATED RECEPTOR KINASE 1 (BAK1) to initiate PTI (Chinchilla et al., 2007). The general cellular responses in PTI include Ca^{2+} fluxes, reactive oxygen species (ROS) production, activation of mitogen-activated protein kinases (MAPKs), transcriptional reprogramming like *PR-1* and *WRKY* gene expression and production of antimicrobial compounds like phytoalexins (Dodds and Rathjen, 2010). However, adapted pathogens are able to suppress PTI through effector molecules, which are mostly delivered into the plant cell. During plant-pathogen co-evolution, some plants have developed intracellular LRR-receptors to recognize, such effectors or the modifications they cause, and subsequently initiate the typically stronger ETI defense response (Chisholm et al., 2006). ETI usually results in localized cell death (hypersensitive response, HR) to restrict the growth of biotrophic pathogens.

Activation of MAPK signaling is vital for mounting an appropriate PTI response. A typical MAPK cascade consists of a modular complex comprising a MAPK kinase kinase (MAPKKK), phosphorylating a MAPK kinase (MAPKK), which phosphorylates a MAPK (Sinha et al., 2011; Meng and Zhang, 2013). Then, the activated MAPK specifically phosphorylates various substrate proteins, such as transcription factors, at conserved amino acid residues (S/T-P motif). After flg22 perception, two *Arabidopsis* MAPK pathways are activated. One pathway involves the MAPKKs, MKK4, and MKK5, which act upstream of the MAPKs, MPK3 and MPK6, leading to the activation of WRKY transcription factors that positively regulate defense gene expression (Asai et al., 2002). The second flg22-activated MAPK cascade is composed of MEKK1, MKK1/MKK2 (two redundant MAPKKs), and MPK4. Based on both genetic and biochemical studies, MPK4 exhibits negative control of salicylic acid (SA)-regulated plant defense (Petersen et al., 2000). A recent study identified a more complex scheme of MAPK-dependent defense gene expression. Here, MPK3 and MPK4 influenced subsets of defense-related genes both negatively and positively in their expression (Frei dit Frey et al., 2014). A fourth MAPK, MPK11, is also activated by flg22 treatment (Bethke et al., 2012) or other PAMPs (Eschen-Lippold et al., 2012).

Knowledge regarding the downstream targets of MAPKs is still fragmentary and high-throughput methods have been employed to identify the potential MAPK substrates. The various strategies used include yeast-two hybrid screens, protein microarrays and *in vitro* kinase assays. Microarray-based testing of 1690 *Arabidopsis* proteins identified 48 *in vitro* substrates for MPK3 and 39 for MPK6, with an overlapping set of 26 candidates (Feilner et al., 2005). High-density protein microarrays used to determine the phosphorylation targets of 10 different MAPKs identified 570 potential MAPK targets out of 2158 candidates (Popescu et al., 2009). Some of the well characterized MAPK targets relevant to pathogen response include the 1-aminocyclopropane-1-carboxylic acid synthase (ACS), ethylene response factor 104 (ERF104), tandem zinc finger 9 (TZF9), VirE1-interacting protein 1 (VIP1), WRKY33 transcription factor, MPK4 substrate 1 (MKS1), and

several related proteins with so-called “VQ-motifs” (Meng and Zhang, 2013; Maldonado-Bonilla et al., 2014; Pecher et al., 2014).

WRKY transcription factors control transcriptional reprogramming to mediate cellular responses to diverse environmental cues (Eulgem and Somssich, 2007) and many WRKYS are targets of *Arabidopsis* MAPKs (Popescu et al., 2009). Besides regulating plant development, WRKYS are important positive and negative regulators of both PTI and ETI (van Verk et al., 2011). The defining feature of WRKYS is their DNA binding WRKY domain. The WRKY domain comprises the highly conserved WRKYGQK peptide sequence and a zinc finger motif (CX_{4–7}-CX_{22–23}-HXH/C, where X represents any amino acid and C/H are the conserved zinc-coordinating cysteine or histidine residues). This domain is responsible for binding to the W-box element with the consensus “(C/T)TGAC(T/C)” nucleotide sequence, although flanking DNA sequences appear to contribute to binding specificities (Ciolkowski et al., 2008). The 74 members of *Arabidopsis* WRKYS are divided into three groups based on the number of WRKY domains (two domains in group I, and one in groups II and III) and the arrangement of conserved cysteine/histidine residues of their zinc fingers (C-C-H-H in group I/II but C-C-H-C in group III; Rushton et al., 2010). In *Arabidopsis*, it has been shown that WRKY33 exists in nuclear complexes with MPK4 and MKS1. PAMP perception activates MPK4, leading to the nuclear dissociation of the MPK4-MKS1-WRKY33 complex and thereby releasing WRKY33 and MKS1. WRKY33 then activates expression of *PAD3* (*Phytoalexin Deficient 3*), a key enzyme for the synthesis of antimicrobial camalexin (Qiu et al., 2008). Additionally, MPK3 and MPK6 are major contributors to fungus-induced camalexin accumulation by phosphorylating WRKY33 (Mao et al., 2011). Taken together, these two studies suggest transcriptional regulation of camalexin biosynthesis gene expression through a release of WRKY33 from an inhibitory MPK4-containing protein complex and a positive effect on WRKY33 function through MPK3/6-mediated WRKY33 phosphorylation.

In the current study, 48 *Arabidopsis* WRKY proteins were investigated as *in vitro* MPK3 and MPK6 phosphorylation targets; and one member, WRKY46 was selected for further characterisation since its importance in plant pathogen response and abiotic stresses is indicated in numerous studies (van Verk et al., 2011; Moreau et al., 2012; Ding et al., 2013, 2014; Gao et al., 2013). Our findings establish WRKY46 as an MAPK phospho-target mediating plant defense responses.

MATERIALS AND METHODS

Plant Growth Conditions and Genotypes

All plants were grown in growth chambers with a photoperiod of 8 h light ($120 \mu\text{mol m}^{-2} \text{s}^{-1}$; 22°C) and 16 h dark (20°C). *Arabidopsis thaliana* ecotype Col-0 was used as wild type. The *mpk3* and *mpk6* mutants (in Col-0 background) were described previously (Wang et al., 2008; Bethke et al., 2009). *Nicotiana benthamiana* was used for *Agrobacterium tumefaciens*-mediated transient expression experiments.

Site-Directed Mutagenesis

The *WRKY46*^{S168A}, *WRKY46*^{S250A}, and *WRKY46*^{S168A,S250A} phosphorylation site variants were generated as described (Palm-Forster et al., 2012; Eschen-Lippold et al., 2014). Briefly, mutagenesis primers (as listed in **Table 1**) with a flanking *Bsa*I site were used to amplify the entire pDONR220 vector harboring *WRKY46*. After *Dpn*I digestion of the template plasmid, the amplified vector was gel-purified, digested with *Bsa*I and ligated. The mutated *WRKY46* variants were then transferred to destination vectors by standard GatewayTM LR-recombination-based cloning (Invitrogen). For the phosphomimetic *WRKY46*^{S168D,S250D} variant, two fragments were amplified by PCR using the primer pairs, W46-S168D_3/W46-S250D_5 and W46-S168D_5/W46-S250D_3, and *pUGW15-WRKY46* as a template. Both fragments were gel-purified and mixed and incubated in the presence of *Lgu*I and T4-DNA ligase in a PCR cycler machine (10 cycles of 10 min 37°C and 10 min 22°C).

Preparation of Recombinant Proteins and *In Vitro* Phosphorylation Assay

The 48 WRKY coding sequences were cloned in-frame into expression vector pDEST-N110 (Dyson et al., 2004) to generate N-terminally His₁₀-tagged recombinant proteins. The vectors were transformed into *KRX* competent cells (Promega). Cells were grown in 2xYT media (16 g L⁻¹ Bacto tryptone, 10 g L⁻¹ Bacto yeast extract, 5 g L⁻¹ NaCl, pH 7.2) to OD₆₀₀ of 0.5–0.6 and protein expression was induced at 24°C overnight by adding 1 mM rhamnose. Denaturing purification was performed by resuspending the pellet from 100 mL culture in 20 mL of lysis buffer (100 mM sodium phosphate, 10 mM Tris, 6 M GuHCl, pH 8) and incubated at room temperature for 30 min. After centrifugation the supernatant was incubated for 1 h with 100 μL of equilibrated Ni-NTA-Agarose beads (Thermo Scientific). The beads were washed thrice with wash buffer (100 mM sodium

phosphate, 10 mM Tris, 8 M Urea, pH 6.3). The proteins were refolded on the beads as previously described (Feilner et al., 2005). Briefly, 130 μL, 260 μL and 1 mL of native buffer (10 mM Tris pH 7.5, 1 mM PMSF) was consecutively added within a period of 30 min (on ice) to reduce urea concentration to <0.5 M. The supernatant after a brief centrifugation pulse was removed and 1 mL of native buffer added and refolding of the proteins allowed to proceed for another 2 h on ice.

In vitro kinase assay was performed as described (Feilner et al., 2005; Pecher et al., 2014) with slight modifications. Briefly, after visual estimation (by coomassie staining) of the amount of proteins purified, 5–10 μL of the Ni-NTA resin containing the bound protein was mixed with reaction buffer to give a final volume of 15 μL containing 25 mM Tris-Cl (pH 7.5), 10 mM MgCl₂, 1 mM DTT, 1 mM PMSF, 25 μM ATP, 1 μCi [γ-³²P]ATP and ~100 ng of active MAPKs. After 30 min incubation at 30°C, the reaction was stopped by addition of one volume of 2x SDS sample buffer. Samples were boiled at 95°C for 5 min and then separated on 10% SDS-PAGE gel and phosphorylation of the protein substrates visualized by phosphor-imaging (Typhoon Phosphorimaging System, GE Healthcare) after drying the gel.

ProQ Diamond Staining of Phosphoproteins

The MPK:WRKY proteins were incubated at approximately 1:10 (w/w) ratio for 30 min as described above (except for the lack of radioactive ATP). After separation by SDS-PAGE, the gel was fixed with 50% methanol and 10% acetic acid overnight. The gel was washed with water for 30 min and stained with 3x diluted Pro-Q diamond stain (Invitrogen) in the dark for 2 h. The gel was destained four times for 30 min each with 20% acetonitrile, 50 mM sodium-acetate (pH 4.2). The gel was washed again with water for 10 min and was scanned at 400 V using a Typhoon Scanner (GE Healthcare).

Mass Spectrometric Analysis

Phosphorylated proteins were separated by 10% SDS-PAGE. The gel was stained with Colloidal Coomassie Blue Stain (Life Technologies) and washed with water. The corresponding gel bands were excised, destained by multiple washes with 30% acetonitrile, 100 mM NH₄HCO₃ and finally rinsed twice with water. After standard reduction and alkylation (Pecher et al., 2014), the proteins in the gel pieces were digested overnight at 37°C by incubation in 5% acetonitrile, 10 mM NH₄HCO₃ with 3 ng μL⁻¹ modified trypsin (Promega). Peptides were extracted into 35% acetonitrile with 0.4% TFA, dried down in a Speed-vac and finally resuspended in 20 μL of 0.1% TFA. After 5 min of sonication in a sonifier water bath, the peptides were either frozen for storage or immediately analyzed on an LC-MS system consisting of a split-free nano-LC (Easy-nLC II, Proxeon, Thermo Scientific) coupled to a hybrid-FT-mass spectrometer (Orbitrap Velos Pro, Thermo Scientific). Additional targeted LC-MS measurements of selected phosphopeptides were performed using an inclusion list in a data dependent acquisition (DDA) scan method. Peptide fragmentation was achieved using CID with MSA (multi-stage

TABLE 1 | Primers used for site-directed mutagenesis.

Name	Primer*	Purpose
WRKY46PSM1 F	TT <u>GGTCTC</u> A AGATCTTGCTCCTG CAACATCA	S250A mutation
WRKY46PSM1 R	TT <u>GGTCTC</u> A ATCTTCCACGAAATT CCCCAGA	S250A mutation
WRKY46PSM2 F	TT <u>GGTCTC</u> A TCACAGCCCCGAAGA CGACGAC	S168A mutation
WRKY46PSM2 R	TT <u>GGTCTC</u> A GTGATGTTACAAG TGTGGTTCC	S168A mutation
W46-S168D_5	AAAAAA <u>GCTCTTC</u> C ACAGATCCGAA GACGACGACG	S168D mutation
W46-S168D_3	AAAAAA <u>GCTCTTC</u> A TGTGATGTTGT TACAAGTGTG	S168D mutation
W46-S250D_5	AAAAAA <u>GCTCTTC</u> T GATCCTGCAAC ATCAGGGTCT	S250D mutation
W46-S250D_3	AAAAAA <u>GCTCTTC</u> G ATCAAGATCTT CCACGAAATT	S250D mutation

*Note that the Type IIs restriction sites (*Bsa*I or *Lgu*I) are underlined.

activation). Proteins were identified and phosphorylation sites were identified using Mascot V.2.3.02 and the Phospho RS module in Proteome Discoverer v1.3.

In Silico Prediction of MAPK Targets

In silico functional prediction was performed with WRKY-family proteins. First, they were classified according to functional annotation clustering using DAVID 6.7 software¹ (Huang et al., 2009). All known and predicted WRKY protein-protein interactions were retrieved from STRING 9.1 software² (Franceschini et al., 2013). The data from both STRING 9.1 and DAVID 6.7 were integrated, analysed and visualized using CYTOSCAPE 3.0.2 software³ (Shannon et al., 2003). The WRKYS were broadly categorized into the functional groups of “general transcription” and “defense-regulated transcription factors.”

In Vivo Phosphorylation of WRKY46

For examining phosphorylation of WRKY46 *in vivo*, the WRKY46 coding sequence was cloned into *pUGW15* (Nakagawa et al., 2007) to generate *p35S-WRKY46* (which expresses an N-terminal HA-tagged WRKY46 under the control of the Cauliflower Mosaic Virus 35S promoter). Transformation of *Arabidopsis* mesophyll protoplasts was performed as described (Yoo et al., 2007; Ranf et al., 2011). After overnight incubation in the dark at 22°C, protoplasts were treated with either water or 100 nM flg22 for 15 min. Protoplasts were harvested by centrifugation and immediately frozen in liquid nitrogen. Dephosphorylation assays were performed as described (Maldonado-Bonilla et al., 2014). Briefly, lambda phosphatase (400 units; Upstate-Millipore) was added to the protoplast extracts for 1 h to dephosphorylate the proteins. After SDS-PAGE, the proteins were transferred to a nitrocellulose membrane (Macherey and Nagel) and immunoblotted against anti-HA.11 antibody (Eurogentec).

In Vivo Stability of WRKY46

To check the stability of WRKY46 after PAMP elicitation, protoplasts were transfected with *p35S-WRKY46* constructs as described above. Protoplasts were treated with 2.5 μM cycloheximide to stop the translation and immediately elicited with 100 nM flg22. Samples were harvested by centrifugation at the indicated time points and were subjected to immunoblotting with anti-HA11 antibody to check the levels of WRKY46 proteins.

Promoter-Luciferase (LUC) Assay

The promoter-LUC assay was performed as described earlier (Ranf et al., 2011). Briefly, protoplasts were isolated and co-transformed with three vectors: an effector construct for WRKY46 overexpression, *pNHL10-LUC* (reporter construct)

and *pUBQ10-GUS* (normalization construct). After overnight incubation in the dark at 22°C, 200 μM luciferin were added and mixed gently by inverting the tubes. Then, 100 μL of protoplasts were transferred into 96-well microtiter plates suitable for luminescence measurements (Greiner) and were elicited with 100 nM flg22/elf18, 200 μg/mL chitin or water as control. The luciferase activity kinetics were measured for 3 h with a 96-well plate luminescence reader (Luminoscan, Thermo Scientific). After the measurement, protoplast samples were directly lysed by adding 10 μL of 10-fold concentrated GUS extraction buffer (final concentration: 50 mM NaPO₄ pH 7.0, 1 mM EDTA, 0.1% Triton X-100, 10 mM beta-mercaptoethanol) and vortexing. GUS-activity was measured upon incubation with 4-methylumbelliferyl glucuronide (4-MUG; 15 min at 37°C), based on the fluorometric detection of the reaction product 4-methyl umbelliferone (4-MU). Values are expressed as LUC/GUS ratios relative to the CFP-transfected controls (at timepoint 0 min).

Localization of WRKY46

WRKY46 was cloned into *pEXSG-YFP* vector (Feys et al., 2005) to express WRKY46 with a C-terminal YFP-tag. ERF104-CFP (Bethke et al., 2009) was used as a nuclear marker. Protoplasts were isolated, transfected with *WRKY46-YFP* with or without *ERF104-CFP* constructs, incubated overnight and observed under a laser scanning confocal microscope (LSM 710 Laser Scanning System; Carl Zeiss) as described Reddy et al. (2014). For YFP detection, excitation wavelength, and emission filters were 514 nm/band-pass 520–540 nm. For CFP detection, excitation wavelength and emission filters were 458 nm/band-pass 465–500 nm. Chloroplast auto-fluorescence was recorded using band-pass 650–710 nm settings.

Statistical Analyses

All statistical analyses were performed using GraphPad Prism 5⁴.

RESULTS

Arabidopsis MPK3 Phosphorylates WRKY46 In Vitro

We expressed 48 members out of the 74 WRKYS, covering all three WRKY groups, as recombinant proteins. MPK3 and MPK6 were also prepared and activated by incubating with a constitutively active MAPKK (abbreviated as MKK5^{DD}; Lee et al., 2004). *In vitro* kinase assays were performed using the 48 purified WRKY proteins as substrates for MPK3 or MPK6 (Figure 1). Most of the WRKYS (or their truncated products) were phosphorylated by both kinases. The WRKYS showed differential phosphorylation intensities, possibly reflecting either the strength of their interaction with MPK3/MPK6 or the number of putative MAPK-targeted (SP/TP) sites present in them.

¹<http://david.abcc.ncifcrf.gov/>

²<http://string-db.org/>

³<http://www.cytoscape.org/>

⁴www.graphpad.com

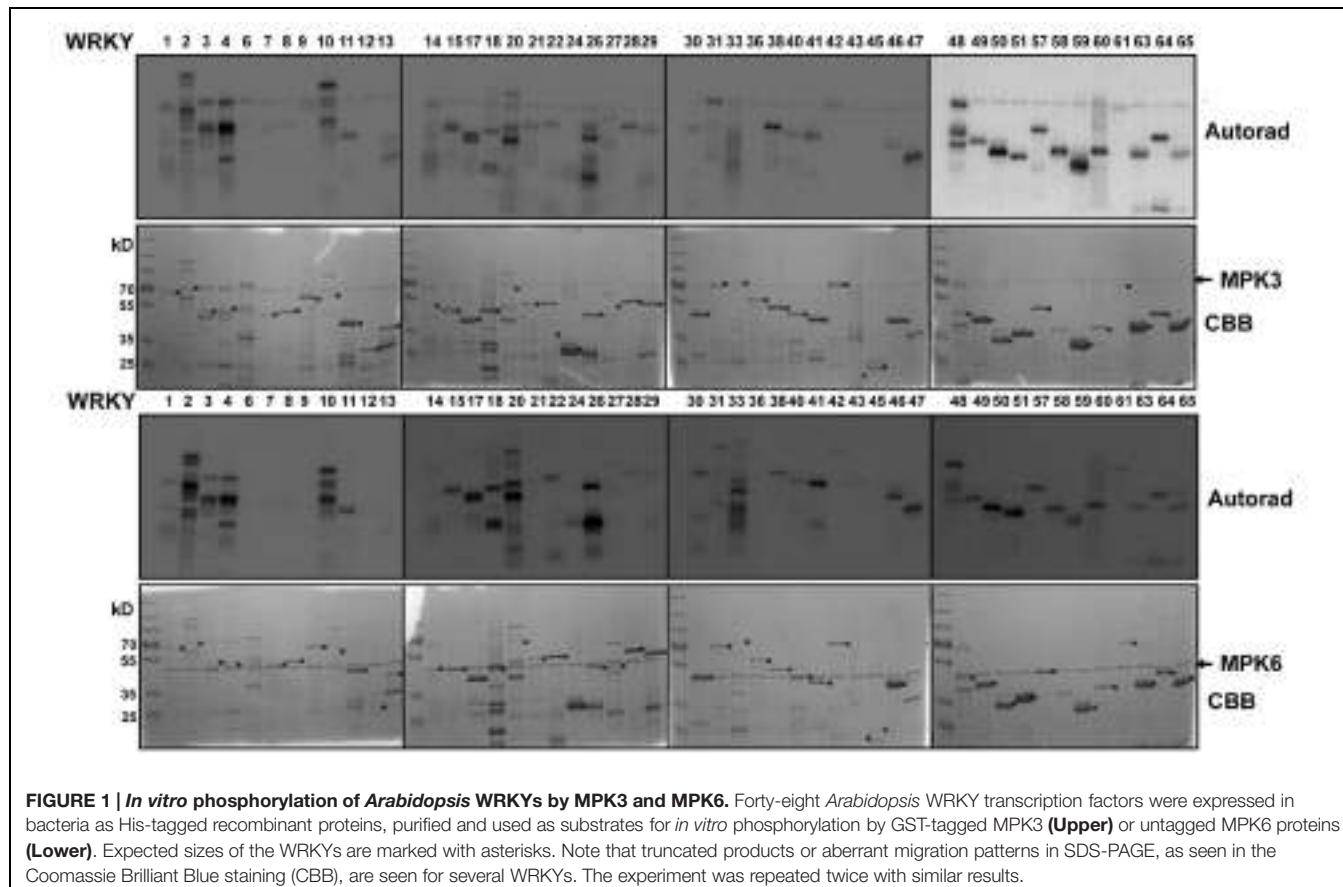


FIGURE 1 | *In vitro* phosphorylation of *Arabidopsis* WRKYs by MPK3 and MPK6. Forty-eight *Arabidopsis* WRKY transcription factors were expressed in bacteria as His-tagged recombinant proteins, purified and used as substrates for *in vitro* phosphorylation by GST-tagged MPK3 (**Upper**) or untagged MPK6 proteins (**Lower**). Expected sizes of the WRKYs are marked with asterisks. Note that truncated products or aberrant migration patterns in SDS-PAGE, as seen in the Coomassie Brilliant Blue staining (CBB), are seen for several WRKYs. The experiment was repeated twice with similar results.

To narrow down the candidate WRKYs possibly involved in plant defense responses, *in silico* data-mining for protein-protein interaction (STRING 9.1, Franceschini et al., 2013) and functional annotation of roles in defense or transcriptional regulation (DAVID 6.7, Huang et al., 2009) was carried out with the WRKYs and MAPKs used in this study. A network of at least eight WRKYs, including WRKY46, was linked to MPK3 and may be involved in plant defense responses (Figure 2A).

Arabidopsis WRKY46 is a group III WRKY of 295 amino acids (molecular weight of 33.6 kDa) and contains two consensus MAPK phosphorylation sites at positions S168 and S250. We performed site-directed mutagenesis to change these two sites from Ser to Ala. To determine which phosphorylation site of WRKY46 can be phosphorylated by MAPKs *in vitro*, His-tagged recombinant WRKY46 protein variants were purified and used for MAPK phosphorylation assays. Using MPK3, MPK4 and MPK6 with comparable kinase activities (estimated by kinase assays with artificial myelin-basic protein as substrate), MPK3 showed the strongest phosphorylation of WRKY46 (Figure 2B). The observation was also confirmed by using a non-radioactive kinase assay with MPK3 and subsequent Pro-Q diamond phosphoprotein staining (Figure 2C). The MPK3-phosphorylated WRKY46 bands were excised from the non-radioactive gel, trypsin-digested and subjected to mass spectrometry (MS) analysis. A phospho-peptide

containing phosphorylated S168 was detected (Figure 2D). Phosphorylation at S250, however, cannot be excluded since the peptide coverage of the MS analysis did not include this region of the protein. Nevertheless, MPK3-mediated phosphorylation of the WRKY46^{S168A} variant was strongly reduced compared to WRKY46^{S250A} (Figures 2B,C), so that S168 may be the preferred *in vitro* phospho-site. The recombinant WRKY46^{S168A,S250A} double mutant was, unfortunately, poorly expressed in bacteria and it was difficult to purify sufficient amounts for comparison in the *in vitro* kinase assay. Curiously, the phosphorylated WRKY46 band(s) often show a double band, except for the WRKY46^{S250A} variant; this may mean that phosphorylation at S250 results in a mobility shift in SDS-PAGE (Figures 2B,C).

In Vivo Phosphorylation of WRKY46

To determine whether WRKY46 is phosphorylated *in vivo*, WRKY46 was cloned into a vector expressing HA-tagged proteins under control of the Cauliflower Mosaic Virus 35S promoter and transfected into *Arabidopsis* protoplasts. After an overnight incubation (~15 h) to enable protein expression, protoplasts were treated with flg22 (100 nM) or an equivalent volume of water (as control) for 15 min. Protoplasts were harvested, proteins extracted, and immunoblotted against an anti-HA antibody. An aliquot of proteins from the flg22-treated sample was incubated with lambda phosphatase to

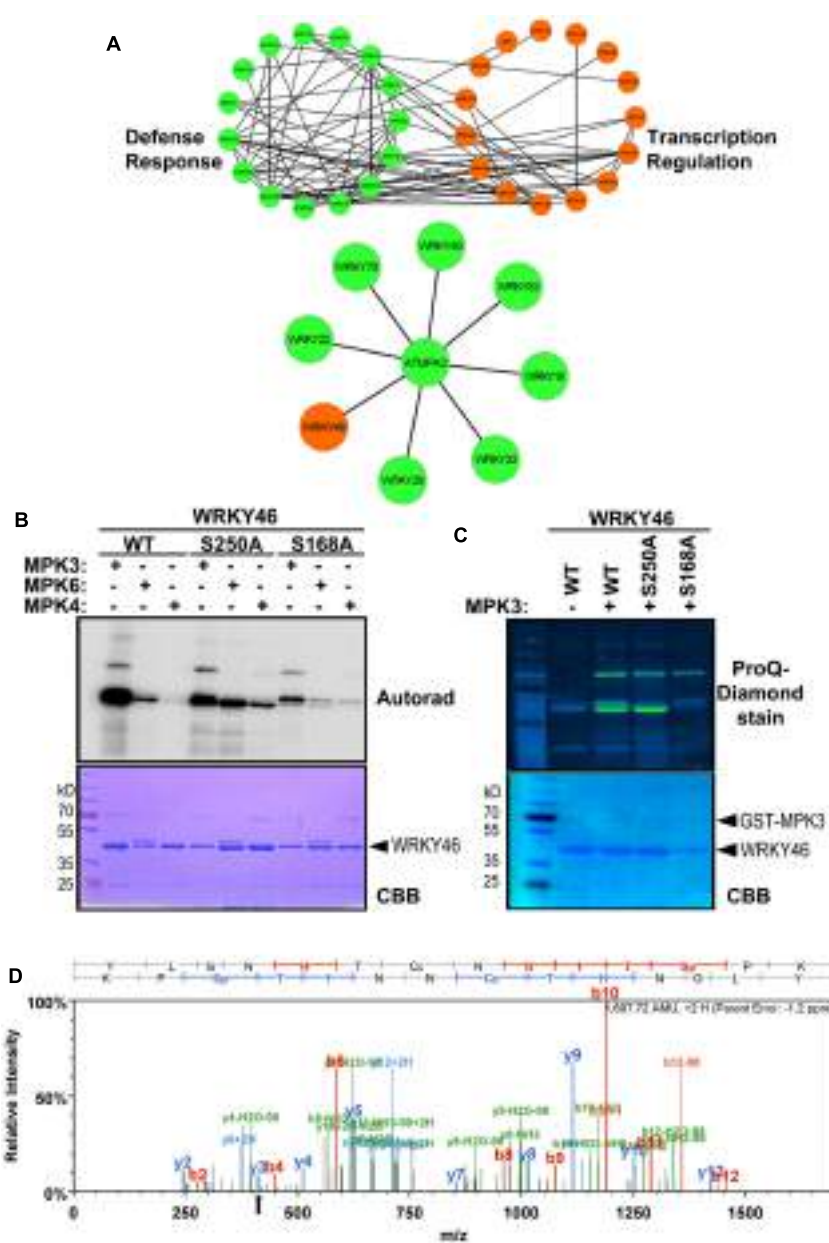


FIGURE 2 | WRKY46 is a potential defense-related phosphorylation target of MPK3. **(A)** The functional annotation of all WRKYs was performed using DAVID 6.7 tool dividing all WRKYs into two groups (defense response, DR, or transcriptional regulation, TR; top network). The known and the predicted protein-protein interactions were analyzed by STRING 9.1 tool. Finally, all the information was integrated, analyzed and visualized using CYTOSCAPE 3.0.2 program. The (bottom) network shows WRKY46 as a potential defense-related MPK3 target along with many known MPK3 interaction partners. **(B)** *In vitro* phosphorylation of WRKY46 by MAPKs and phospho-site mapping. His-tagged WRKY46 and its phospho-site variants (S168A and S250A) were expressed using bacterial expression systems and used as substrates for phosphorylation by GST-MPK3, GST-MPK4, and tag-free MPK6 proteins, which were pre-activated with constitutively active MKK5^{DD}. The proteins from the *in vitro* kinase assays were separated by SDS-PAGE and phosphorylation visualized by autoradiography (Autorad). Note that the MAPK bands can be seen above the WRKY46 proteins (GST-MPK3 or -MPK4 = ~70 kD; MPK6 = ~48 kD) The experiment was repeated twice with similar results. **(C)** Phosphorylation of WRKY46 and its variants by MPK3 was performed as described in **(B)**; but using non-radioactive ATP. ProQ diamond® staining was used to visualize phosphorylated proteins. CBB of the gels was performed as loading control. **(D)** Mass spectrometry (MS) analysis of WRKY46. The phosphorylated WRKY46 bands (from **C**) were excised from the gels, trypsin digested and analyzed by LC-MS/MS. A phosphopeptide demonstrating phosphorylation of WRKY46 at position S168 (as reflected by y3 peak at 411 m/z) is shown.

dephosphorylate the proteins. As reflected by a mobility shift in SDS-PAGE, which is abolished by the phosphatase treatment, WRKY46 is already phosphorylated before any PAMP elicitation

(Figure 3A). Since the MAPKs are typically not activated prior to PAMP treatment, it appears that there are other kinase(s) that target WRKY46. As there is no additional

phospho-shift after PAMP treatment, it is also not possible to use this assay as an indicator for *in vivo* phosphorylation by PAMP-activated MAPKs, such as MPK3 or MPK6 (see below).

Phosphorylation of WRKY46 Alters Its *In Vivo* Stability

The half-life of proteins is critical for the regulation of various signaling pathways and stability of several MAPK substrates has been shown to be regulated through phosphorylation after PAMP treatment (Liu and Zhang, 2004; Maldonado-Bonilla et al., 2014; Pecher et al., 2014). Therefore, as an alternative to using phospho-shift in gels, we investigated WRKY46 stability after elicitation of transiently transformed protoplasts with flg22. To facilitate visualization of the reduced protein levels after PAMP addition, cycloheximide was also added to block protein translation. Protoplasts were harvested at different time points after elicitation and subjected to immunoblotting. Reduction in wild type WRKY46 levels was seen 1 h after flg22 treatment, with little-to-no WRKY46 detectable after 2 h (Figure 3B). By contrast, flg22-induced reduction in protein levels was less pronounced for the WRKY46^{S168A}, WRKY46^{S250A} and WRKY46^{S168A,S250A} mutant variants over the tested period of 3 h. In general, the highest level of protein expression was observed for the WRKY46^{S168A,S250A} double phosphorylation site mutant (Figure 3B). Taken together, phosphorylation of WRKY46 (at S168 and/or S250) is required for the flg22-induced degradation *in vivo* and the non-phosphorylatable WRKY46 is more stable.

To directly link this destabilization effect to MAPK activities, we co-expressed MKK5-DD, a constitutively active MAPK kinase that activates MPK3 and MPK6 (Lee et al., 2004, 2015; Lassowska et al., 2014) together with WRKY46. We also performed these experiments in the *mpk3* or *mpk6* mutant backgrounds to specifically activate only MPK6 or MPK3, respectively. As seen in Figure 3C, specific activation of MPK3 and/or MPK6 led to reduced WRKY46 protein levels – thus pointing to a direct effect of MPK3/MPK6-mediated phosphorylation on WRKY46 stability. As *mpk3mpk6* double mutants are embryo-lethal and even the so-called “rescued” mutants have severe growth defects (Wang et al., 2007, 2008), it is difficult to test the effect of knocking-out both MAPKs on WRKY46 stability. The data therefore also suggests functional redundancy between MPK3 and MPK6 in regulating WRKY46 destabilization.

WRKY46 is a Nuclear Protein and Elevates the Basal Plant Defense Status

To examine WRKY46 subcellular localization, we transiently expressed WRKY46-YFP in *Arabidopsis* protoplasts. To visualize the nucleus, protoplasts were co-transfected with a CFP-tagged ERF104 that was previously shown to be nuclear-localized (Bethke et al., 2009). The resulting CFP and YFP

fluorescence signals were both in the nuclei (Figure 4A). To exclude that WRKY46 might have been tethered to the ERF104 nuclear protein, WRKY46 was expressed alone where the WRKY46-YFP signals were also in the nucleus (Supplementary Figure S1). Western blotting using an anti-GFP monoclonal antibody revealed predominantly protein bands with the expected molecular weights for intact WRKY46-YFP and ERF104-CFP fusion proteins (Figure 4A), so that the nuclear fluorescence signals detected is not due to free CFP/YFP cleavage products. In addition, we also tested the non-phosphorylatable WRKY46^{S168A,S250A} variant, which is also localized in the nucleus (Supplementary Figure S1). These findings are in agreement with WRKY46 functioning as a putative transcription factor in the nucleus (Ding et al., 2014, 2015) and also the increased protein stability of WRKY46^{S168A,S250A} (Figure 3A) is not due to its mislocalization.

To investigate the role of WRKY46 in plant defense, we analyzed expression of a luciferase (LUC) reporter driven by a routinely used W-box-containing defense-related promoter, *NDR1/HIN1-like 10* (*NHL10*), in *Arabidopsis* protoplasts co-expressing either different variants of WRKY46 or CFP (as a control for expression of a defense-unrelated protein). Protoplasts were treated with either water, bacterial (flg22/elf18) or fungal (chitin) elicitors and luciferase activity was measured. In protoplasts expressing any WRKY46 variant, an elevated basal promoter activity (time point 0 min) was observed for the water and also the PAMP-treated samples (Figure 4B). Also at later time points, all treatments showed an overall elevation of *NHL10* promoter activity in the WRKY46-expressing protoplasts. This suggests that WRKY46 is a positive regulator of the defense-related *NHL10* gene. Interestingly, the S168A variant consistently showed a higher boost on the *NHL10* promoter activity. Since western blotting showed comparable expression of the respective WRKY46 variants (Figure 4B, right), the enhanced activity of WRKY46^{S168A} is not simply due to enhanced protein stability/expression (see Figure 3B). To further test if phosphorylation of WRKY46 influences its effect on transcription controlled by the *NHL10* promoter, we created a WRKY46^{S168D,S250D} phospho-mimic. For simplicity, we tested only flg22 and concentrated only on the peak *NHL10* promoter activity. As seen in Figure 4C, there was no difference in activities of the phospho-mimic (WRKY46^{S168D,S250D}) or the non-phosphorylatable (WRKY46^{S168A,S250A}) variants compared to wild type WRKY46. However, in line with the role of phosphorylation in regulating WRKY46 stability (compare Figure 3B), the phospho-mimic variant is expressed at lower levels (Figure 4C). We therefore compared the stability of WRKY46 phosphosite-mutated variants. While trace levels of wild type WRKY46 are expressed 2 h post flg22 treatment, the phospho-mimetic WRKY46 is hardly detectable (Figure 4D). Thus, this serves as indirect evidence that mutated residues are functionally mimicking the phosphorylated serines. Taken together, transcriptional activity of WRKY46 does not seem to be directly controlled by its phosphorylation status.

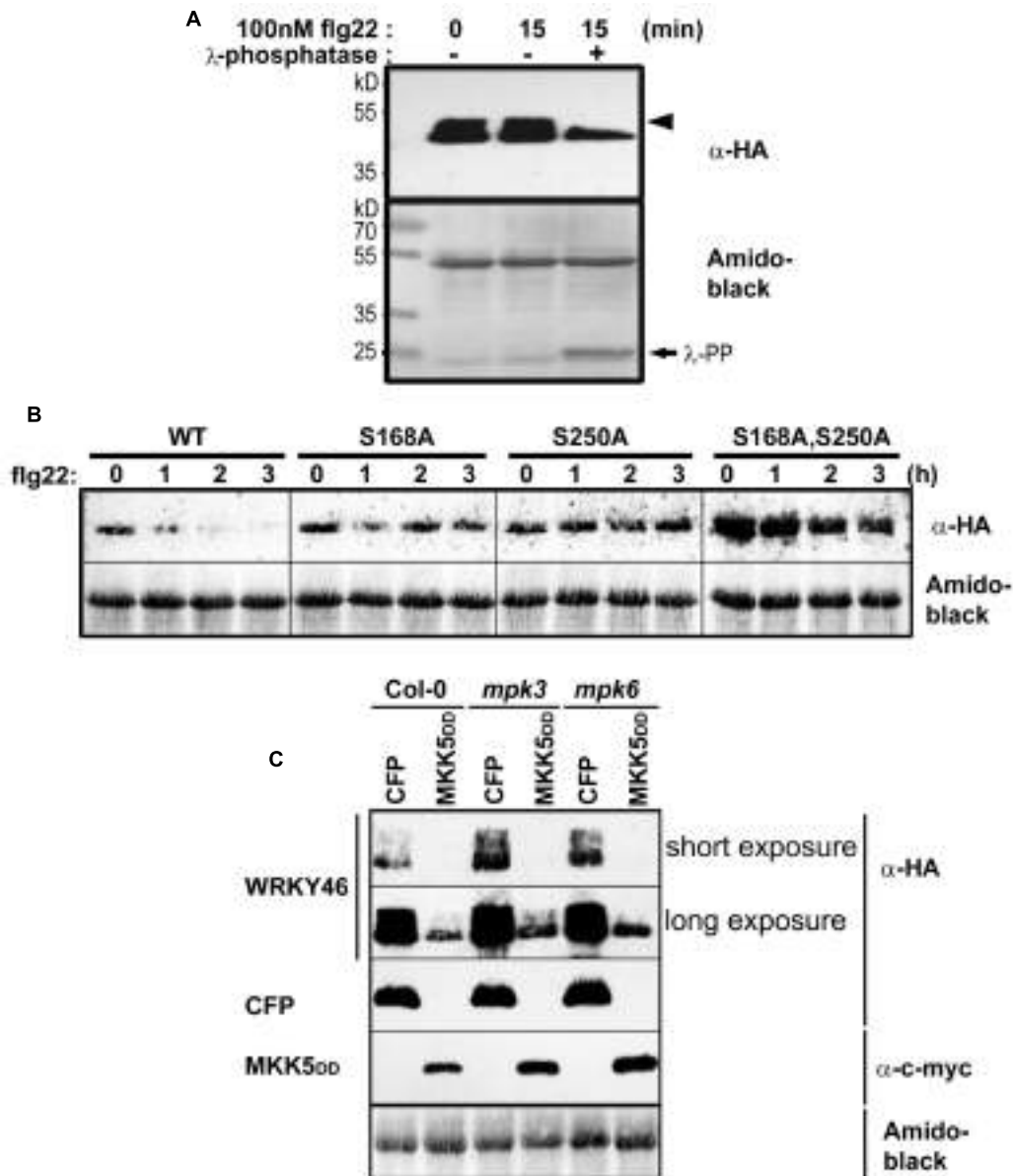


FIGURE 3 | *In vivo* phosphorylation and alteration in WRKY46 stability. **(A)** *Arabidopsis* mesophyll protoplasts were transfected with p35S-WRKY46 (expressing an HA-tagged protein). After overnight incubation, protoplasts were elicited with 100 nM flg22 for 15 min. Total protein extracts were incubated with or without lambda phosphatase (λ -PP) for 1 h (37°C), separated by SDS-PAGE and western blot analysis was performed using anti-HA antibodies. Amido black staining was used to monitor equal loading of the proteins. The experiment was performed twice. Note a mobility shift of WRKY46 (indicative of phosphorylation) is marked by an arrowhead. **(B)** *Arabidopsis* mesophyll protoplasts expressing different WRKY46 variants were simultaneously treated with 100 nM flg22 and 2.5 μ M cycloheximide (to block translation) and harvested at the time points indicated. The protein levels of WRKY46 variants were estimated by immunoblotting using anti-HA antibody. Amido black staining (showing the Rubisco large subunit band) was performed to monitor equal loading of proteins. The experiment was repeated at least five times. Note that the gels were blotted on the same membrane to allow direct comparison of band intensities. **(C)** *Arabidopsis* mesophyll protoplasts derived from the indicated genotype were co-transfected with p35S-WRKY46 and either p35S-mycMKK5^{DD} (expressing a constitutively active MAPK kinase that activates MPK3 and MPK6) or a as control, a CFP-expressing plasmid. Immunoblot with the indicated antibodies and loading control monitoring by amido black staining were performed as described above.

Since the *NHL10* reporter is often used as a reporter for MAPK impact on defense gene expression (Boudsocq et al., 2010), it is possible that there is a feedback regulation on MAPK activities after WRKY46 overexpression. This has been shown for the MAPK substrate, MYC2, which

exerts feedback regulation on its phosphorylating MAPK, MPK6, during blue light-induced signaling (Sethi et al., 2014). To investigate whether also WRKY46 affects MAPK activities *in planta*, protoplasts expressing either WRKY46 (or CFP as a control) were treated with water or flg22

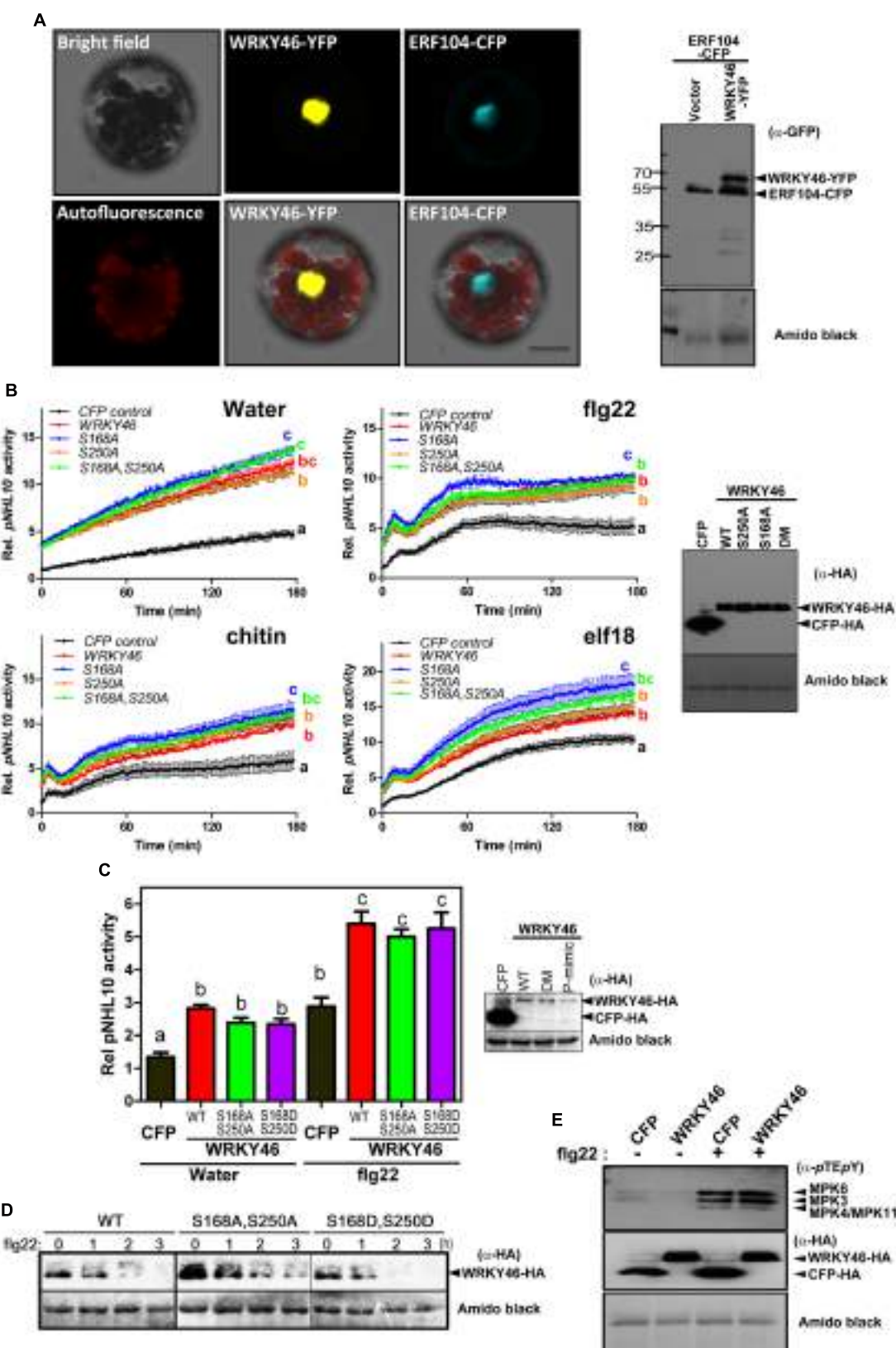


FIGURE 4 | Continued

FIGURE 4 | Continued

WRKY46 is nuclear localized and boosts defense-related promoter activity. (A) *Arabidopsis* Col-0 mesophyll protoplasts were co-transfected with WRKY46-YFP and ERF104-CFP constructs, with ERF104 serving as a nuclear marker. Confocal laser scanning micrographs of the protoplasts show the nuclear localization of WRKY46. Chlorophyll autofluorescence is also included to visualize chloroplasts. Scale Bar = 20 μm . (B) p35S-WRKY46 wild type and mutant variants were transfected into *Arabidopsis* mesophyll protoplasts along with pNHL10-LUC and pUBQ10-GUS reporter constructs. After overnight incubation, protoplasts were elicited with water, 100 nM flg22/elf18 or 200 $\mu\text{g mL}^{-1}$ crab shell chitin. Luciferase activity was measured for 3 h. After the measurements, GUS-assays were performed with total protein extracts. The data are presented as LUC/GUS ratios relative to the untreated CFP-expressing control (at timepoint 0 min) with error bars indicating standard deviation (SD) of the mean. Different letters indicate statistically significant differences at time point 60 min [two-way repeated measures (RM) ANOVA with Bonferroni post tests, $p < 0.01$]. The experiment was performed three times with similar results (DM = S168A, S250A double phospho-site mutant). (C) Experiments after transfection with the indicated WRKY46 variants or CFP as a control were conducted as described in (B) above and the peak pNHL10 activities (typically at ~40 min post elicitation with flg22) plotted. The different alphabets mark statistically distinct groups after one-way ANOVA analysis with Bonferroni's multiple comparison test. Right panel is the immunoblot analysis of HA-tagged proteins. (P-mimic = S168D, S250D double phospho-mimic mutant). (D) WRKY46 protein stability after flg22 treatment was analyzed as described in Figure 3B. (E) Overexpression of WRKY46 does not alter MAPK activation. *Arabidopsis* mesophyll protoplasts were either transfected with constructs for expressing CFP (as a control) or WRKY46. After overnight incubation, protoplasts were treated with either water or 100 nM flg22 for 10 min. The SDS-PAGE-separated proteins were immunoblotted with anti-pTEpY antibody to check for MAPK activation. The experiment was performed twice with similar results. In all cases, equivalent expression of (intact) proteins in the protoplasts was tested by immunoblotting with the indicated antibodies. Amido black staining of the nitrocellulose membranes was used to estimate equal loading (The staining of the Rubisco large subunit is shown).

for 10 min and MAPK activation was analyzed. Treatment with flg22 leads to strong activation of MPK6, MPK3, and MPK4/11 in both WRKY46 and CFP expressing samples without obvious differences (Figure 4E). Thus, WRKY46 does not seem to have feedback regulatory activity on the MAPK pathway; and the enhanced *NHL10* promoter activity is likely due to direct action of the overexpressed WRKY46.

Transgenic WRKY46-overexpressing *Arabidopsis* plants have been shown to be more resistant to bacterial pathogens (Hu et al., 2012). To validate this, we transiently overexpressed *Arabidopsis* WRKY46 in *Nicotiana benthamiana* leaves by agro-infiltration. After 24 h, the leaves were challenged with *Pseudomonas syringae* pv. *tabaci* and harvested 2 days later. Significantly less bacteria were counted in the leaves overexpressing WRKY46 compared to leaves expressing CFP as a control (Figure 5A). Taken together, these observations suggest that WRKY46 is a positive regulator of plant defense.

MAPKs, and Particularly MPK3, are Required for the Transcriptional Activity of WRKY46

As mentioned above, we could not use the protein mobility phospho-shift in SDS-PAGE to demonstrate an *in vivo* PAMP-activated MAPK phosphorylation of WRKY46, which we routinely use for several other MAPK substrates (Bethke et al., 2009; Maldonado-Bonilla et al., 2014; Pecher et al., 2014). To alternatively address the role of MPK3 and MPK6 in the function of WRKY46, we investigated *NHL10* promoter activities in the respective *mpk* mutants. In protoplasts derived from *mpk3* or *mpk6* plants, a statistically significant reduction of the WRKY46-mediated boost of the *NHL10* promoter activity was observed in comparison to the wild type for both the water (control) or flg22 treatments (Figure 5B), indicating that both kinases are important for full WRKY46 activity. Notably, *mpk3* showed a more dramatic effect than the *mpk6* mutant, where the WRKY46-mediated boost on the basal *NHL10* promoter activity was completely abolished (See

Figure 5B left, compare the green trace to the blue trace). Furthermore, the flg22-activation of *NHL10* promoter was also compromised compared to the CFP control (Figure 5B, right, blue and black traces, respectively) in the *mpk3* background. Thus, despite functional redundancy between MPK3 and MPK6 (Figure 3C), MPK3 may play a stronger *in vivo* role in regulating the transcriptional activity of WRKY46 (on the *NHL10* promoter). This observation is in agreement to a preferential *in vitro* phosphorylation of WRKY46 by MPK3 than MPK6 (Figure 2B).

DISCUSSION

In order to adapt to new environmental conditions, plants have to reprogram transcription of the appropriate genes. Transcription factors play major roles in the control of gene expression. The WRKY family is among the ten largest families of transcription factors in higher plants and is found throughout the green lineage (green algae and land plants; Rushton et al., 2010). WRKY proteins are involved in growth development, such as embryogenesis (Lagace and Matton, 2004), trichome development (Johnson et al., 2002), senescence (Robatzek and Somssich, 2001), and plant responses to various biotic and abiotic stresses (Cai et al., 2008; Wu et al., 2009). Only a few components of signaling pathways interacting with WRKY transcription factors have been identified. In addition to histone deacetylases and calmodulin (CaM)-binding domain proteins, MAP kinases are one of the major protein classes interacting with WRKY transcription factors (Kim and Zhang, 2004). The ability of WRKY proteins to interact with many other proteins makes it challenging to decipher the entire pathways regulated by them. WRKY proteins can interact among themselves, with VQ-domain proteins, calmodulin-like proteins, chromatin remodeling proteins and most importantly with MAP kinases (Chi et al., 2013). MAP kinase pathways are involved in regulating the activity of WRKY33 and WRKY34 to control the plant defense response and pollen development, respectively (Mao et al., 2011; Guan et al., 2014). It is plausible that the MPK3/6

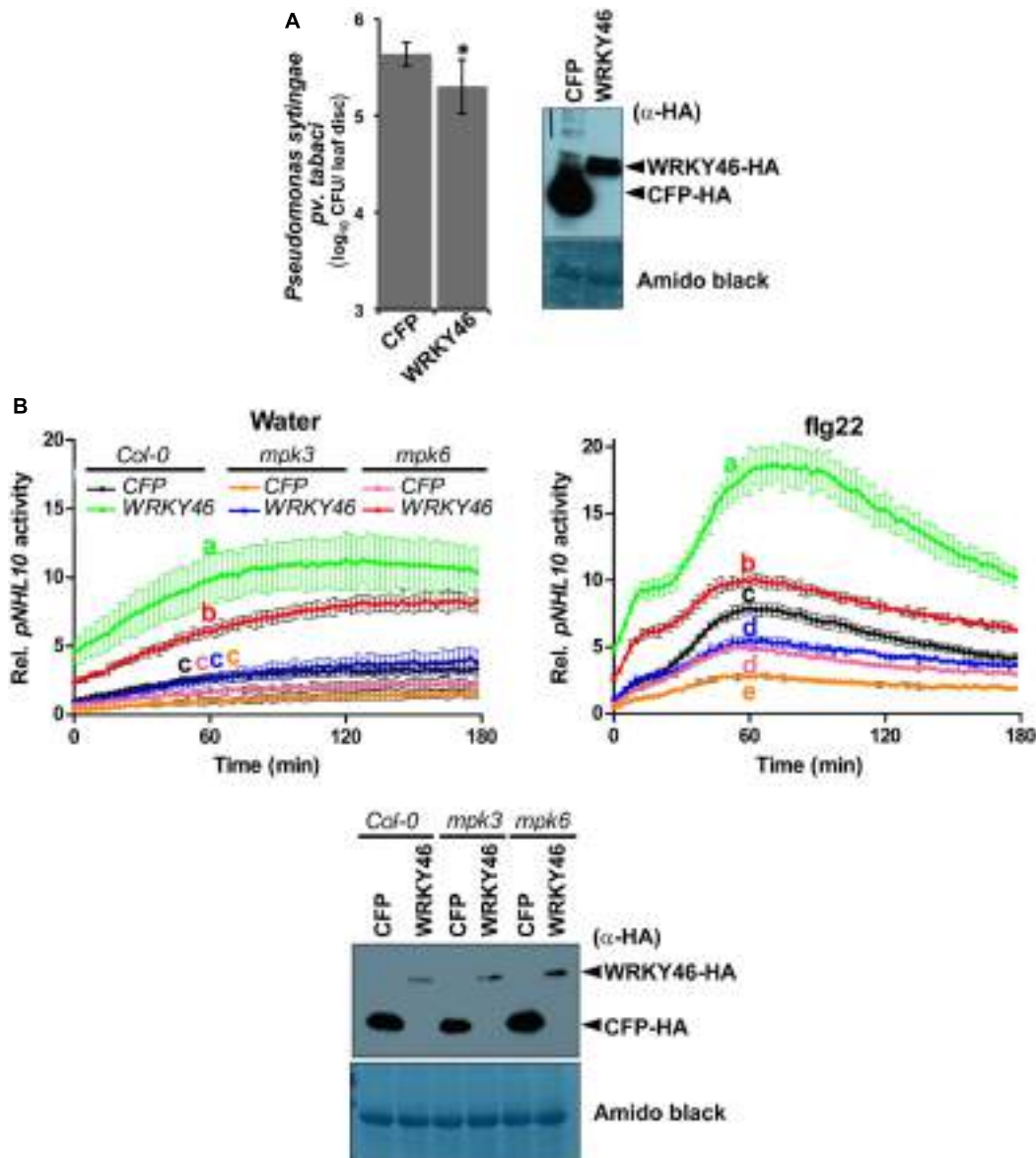


FIGURE 5 | WRKY46 enhances bacterial resistance and MPK3/6 are required for the WRKY46-mediated boost of *NHL10*-promoter activity.

(A) WRKY46 overexpression slightly enhances resistance against *P. syringae* in tobacco. WRKY46 was transiently expressed in *N. benthamiana* leaves by Agrobacterium-mediated delivery. After 48 h, leaves were challenged with *P. syringae* pv. *tabaci*. Colony forming units (CFU) were calculated for samples harvested 2 days post infection. Data shown is the average of three triplicates with error bars indicating standard deviation (* $p < 0.05$; Student's *t*-test). **(B)** *p35S-WRKY46* was transfected together with *pNHL10-LUC* and *pUBQ10-GUS* constructs into protoplasts derived from *Arabidopsis* Col-0, *mpk3* and *mpk6*, and analyzed as described above **(B)**. Error bars indicate standard deviation. Different letters indicate statistically significant differences at time point 60 min (two-way RM ANOVA with Bonferroni post tests, $p < 0.01$). The experiment was performed three times with similar results. In all cases, protein expression is validated by western blotting as described above.

cascade acts as a molecular hub to integrate different signaling networks of WRKY transcription factors with different upstream cues. This is further substantiated by the fact that almost 70% of the WRKYs are differentially regulated by bacterial pathogens or SA treatment, which also activates the MPK3/6 pathway (Dong et al., 2003).

In the current study, 48 out of 74 WRKY members were identified as *in vitro* phosphorylation substrates of

MPK3 and MPK6. *In silico* analysis revealed that WRKY46 may be a putative target of MPK3, which is supported by *in vitro* kinase assays showing a stronger phosphorylation by MPK3 compared to MPK6. MS analysis identified S168 of WRKY46 as a phosphorylation site targeted by MPK3. However, subsequent experiments suggest that S250, the other putative phosphorylation site, is also phosphorylated. Direct *in vivo* MPK3 or MPK6 activation by expressing a constitutively

active MKK5 led to destabilization of WRKY46 protein. Thus, MPK3 and/or MPK6 (or perhaps also other unknown kinases activated by these MAPKs) phosphorylate S168, S250 and other positions to regulate its stability. In this respect, a *WRKY46* promoter-based reporter assay revealed transcription activation of *WRKY46* by the calcium-dependent protein kinases, CPK-3, -4, -5, -6, -10, -11, and -30 and several WRKYS were directly phosphorylated by CPKs (Gao et al., 2013).

WRKY46 regulates responses to several abiotic stresses in *Arabidopsis*. For instance, it controls the expression of several genes involved in osmoprotection and redox homeostasis under dehydration stress (Ding et al., 2015). It is also involved in controlling the light-dependent stomatal opening in guard cells (Ding et al., 2014), which may serve as potential entry points for pathogens and therefore contribute to responses to pathogens. Indeed, *WRKY46* is also involved in biotic stresses. Similar to the *NHL10* gene shown in this work, over-expression of *WRKY46* in protoplasts was found to increase the expression of endogenous *AVRPPHB SUSCEPTIBLE 3 (PBS3)* gene, which plays an important role in SA metabolism (van Verk et al., 2011). *WRKY46* acts in concert with other WRKYS, including *WRKY54* as a positive regulator and *WRKY70* as a negative defense regulator, to resist infection by the necrotrophic *Erwinia amylovora* (Moreau et al., 2012). It also coordinates with *WRKY53* and *WRKY70* to control defense response against the hemi-biotrophic pathogen, *Pseudomonas syringae* (Hu et al., 2012). In general, expression of many WRKY genes is induced by pathogen-related stimuli, possibly in a feedback amplification loop. For instance, the expression of *WRKY46* was highly induced within hours after *P. syringae* and SA treatments (Dong et al., 2003). *WRKY46* transcripts accumulated in protoplasts expressing *avrRpm1*, *avrB*, or *avrRpt2* in an RPM1- or RPS2- dependent manner, thereby making it an early marker gene in ETI signaling and candidate ETI regulator (Gao et al., 2013). The induction of its expression by PAMPs (Figure 4B) also makes it a PTI marker gene. Since *WRKY46* can contribute to both PTI and ETI signaling, it is plausible that it mediates interplay between PTI and ETI and this will be an interesting question to address in the future.

The MAPK phosphorylation could control the function of transcription factors or their associated proteins by regulating their *in planta* stability (Pecher et al., 2014; Weyhe et al., 2014). Recently, phosphorylation of LIP5 (LYST-INTERACTING PROTEIN5), a positive regulator of multivesicular body (MVB) biogenesis by MPK6 was found to increase its stability (Wang et al., 2015). Similarly, phosphorylation of *Arabidopsis* ERF6, ACS2, and ACS6 by MPK3/MPK6 increase the stability of these substrates (Li et al., 2012). In case of *WRKY46*, our data provides evidence that MAPK-mediated phosphorylation upon flg22-treatment controls its stability *in vivo*. The phosphorylation at both S168 and S250 positions seems to be very important for the half-life of the protein, since ablation of phosphorylation at either position leads to increased stability upon elicitation. Hence, the phosphorylation-dependent

regulation of protein substrate stability appears to be a common mechanism through which MAPKs regulate plant defense responses.

Localization studies revealed that *WRKY46* is localized in the nucleus. This result is consistent with the fact that it acts as a transcription factor, possibly regulating the transcription of defense-related genes. Accordingly, *WRKY46* overexpression boosts the defense responsive *NHL10* promoter activity (in the absence of pathogens or PAMPs). Since there are WRKY DNA-binding elements in the *NHL10* promoter (Zheng et al., 2004), which have been shown to be important for regulation of PAMP-induced expression (Pecher et al., 2014), it is likely that *WRKY46* acts directly as a positive transcriptional activator *via* such *cis*-elements. The compromised activation of the *NHL10* promoter by *WRKY46* overexpression in the *mpk3* or *mpk6* mutants suggests the importance of these two MAPKs, particularly MPK3, in controlling *WRKY46* activity. This may seem puzzling for the water-treated samples since no enhanced MAPKs activities are usually detected prior to PAMP elicitation. However, we cannot exclude that some handling stress did, in fact, initiate a transient MAPK activation in the protoplast system and this may trigger a long-lasting effect on the subsequently expressed *WRKY46* proteins. This would mean that effect of *WRKY46* on the *NHL10* promoter is indirect or at least acts only in synergy with the general stress-induced MAPK activities. In support of the latter, the *WRKY46*-induction of the *NHL10* promoter in the flg22-treated protoplasts (Figure 5B, right) – where MAPKs as well as other signaling pathways are activated – is also compromised by *mpk3* or *mpk6* mutations. In summary, the mode of the *WRKY46*-MAPKs regulation of *NHL10* promoter is currently unknown but it appears to be unrelated to *WRKY46* protein stability or its phospho-status (Note: the phospho-mimic *WRKY46* did not show enhanced transcriptional activity). Future experiments could reveal if the MPK3/MPK6 effect may be due to altered affinity of *WRKY46* to the promoter or direct impact on its transcriptional activity. Alternatively, a more likely scenario would be that there may be other MPK3/MPK6 targets that influence *WRKY46* activity. Furthermore, as already discussed, there may be additional kinase(s) that phosphorylate *WRKY46*. Likely candidates include members of the calcium-dependent protein kinase family – especially those that have been shown to regulate *WRKY46* expression (Gao et al., 2013). It will be crucial to identify these kinase(s) and understand how they, in concert with MAPKs, control the multiple functions of *WRKY46* in developmental processes, abiotic and biotic stress responses.

AUTHOR CONTRIBUTIONS

AS and LE designed and performed the experiments shown. PP cloned the WRKYS into the bacterial expression system and screened them for recombinant protein expression. WH performed the LC-MS/MS determination of the phosphorylation sites. DS, AS, and JL supervised the project and all authors contributed to writing the manuscript.

FUNDING

AS is supported by a German Academic Exchange (DAAD) fellowship (A/11/75070). Research in our laboratory is financed by the German Research Foundation through the Collaborative Research Centre SFB648/TP-B1 “Molecular mechanisms of information processing in plants.” The BMBF project ProNET-T3 (03ISO2211B) supported LE.

ACKNOWLEDGMENTS

We thank Imre Somssich for providing the Gateway-compatible *pENTR* clones of the WRKY transcription factors, Mubashir Ahmad (University of Ulm) for helping with in-silico studies,

Nicole Bauer for excellent technical assistance and all members from our laboratory for constructive discussions.

SUPPLEMENTARY MATERIAL

The Supplementary Material for this article can be found online at: <http://journal.frontiersin.org/article/10.3389/fpls.2016.00061>

FIGURE S1 | Nuclear localization of WRKY46: (A) Confocal laser scanning micrographs of *Arabidopsis* Col-0 mesophyll protoplasts transfected with the indicated WRKY46-YFP constructs. To visualize the nucleus, nuclear DNA was stained with $1 \mu\text{g mL}^{-1}$ of 4',6-Diamidino-2-Phenylindole (DAPI) in the presence of 0.05 % Triton-X100 (to permeabilize the membranes). Scale Bar = 10 μm . **(B)** Western blot analysis with α -GFP to show intactness of WRKY46-GFP fusion proteins.

REFERENCES

- Asai, T., Tena, G., Plotnikova, J., Willmann, M. R., Chiu, W. L., Gómez-Gómez, L., et al. (2002). MAP kinase signalling cascade in *Arabidopsis* innate immunity. *Nature* 415, 977–983. doi: 10.1038/415977a
- Bethke, G., Pecher, P., Eschen-Lippold, L., Tsuda, K., Katagiri, F., Glazebrook, J., et al. (2012). Activation of the *Arabidopsis thaliana* mitogen-activated protein kinase MPK11 by the flagellin-derived elicitor peptide, flg22. *Mol. Plant Microbe Interact.* 25, 471–480. doi: 10.1094/MPMI-11-11-0281
- Bethke, G., Unthan, T., Uhrig, J. F., Pöschl, Y., Gust, A. A., Scheel, D., et al. (2009). Flg22 regulates the release of an ethylene response factor substrate from MAP kinase 6 in *Arabidopsis thaliana* via ethylene signaling. *Proc. Natl. Acad. Sci. U.S.A.* 106, 8067–8072. doi: 10.1073/pnas.0810206106
- Boller, T., and Felix, G. (2009). A renaissance of elicitors: perception of microbe-associated molecular patterns and danger signals by pattern-recognition receptors. *Annu. Rev. Plant Biol.* 60, 379–406. doi: 10.1146/annurev.arplant.57.032905.105346
- Boudsocq, M., Willmann, M. R., McCormack, M., Lee, H., Shan, L., He, P., et al. (2010). Differential innate immune signalling via Ca^{2+} sensor protein kinases. *Nature* 464, 418–422. doi: 10.1038/nature08794
- Cai, M., Qiu, D., Yuan, T., Ding, X., Li, H., Duan, L., et al. (2008). Identification of novel pathogen-responsive cis-elements and their binding proteins in the promoter of OsWRKY13, a gene regulating rice disease resistance. *Plant Cell Environ.* 31, 86–96. doi: 10.1111/j.1365-3040.2007.01739.x
- Chi, Y., Yang, Y., Zhou, Y., Zhou, J., Fan, B., Yu, J. Q., et al. (2013). Protein-protein interactions in the regulation of WRKY transcription factors. *Mol. Plant* 6, 287–300. doi: 10.1093/mp/sst026
- Chinchilla, D., Zipfel, C., Robatzek, S., Kemmerling, B., Nürnberger, T., Jones, J. D., et al. (2007). A flagellin-induced complex of the receptor FLS2 and BAK1 initiates plant defence. *Nature* 448, 497–500. doi: 10.1038/nature05999
- Chisholm, S. T., Coaker, G., Day, B., and Staskawicz, B. J. (2006). Host-microbe interactions: shaping the evolution of the plant immune response. *Cell* 124, 803–814. doi: 10.1016/j.cell.2006.02.008
- Ciolkowski, I., Wanke, D., Birkenbihl, R. P., and Somssich, I. E. (2008). Studies on DNA-binding selectivity of WRKY transcription factors lend structural clues into WRKY-domain function. *Plant Mol. Biol.* 68, 81–92. doi: 10.1007/s11103-008-9353-1
- Ding, Z. J., Yan, J. Y., Li, C. X., Li, G. X., Wu, Y. R., and Zheng, S. J. (2015). Transcription factor WRKY46 modulates the development of *Arabidopsis* lateral roots in osmotic/salt stress conditions via regulation of ABA signaling and auxin homeostasis. *Plant J.* 84, 56–69. doi: 10.1111/tpj.12958
- Ding, Z. J., Yan, J. Y., Xu, X. Y., Li, G. X., and Zheng, S. J. (2013). WRKY46 functions as a transcriptional repressor of ALMT1, regulating aluminum-induced malate secretion in *Arabidopsis*. *Plant J.* 76, 825–835. doi: 10.1111/tpj.12337
- Ding, Z. J., Yan, J. Y., Xu, X. Y., Yu, D. Q., Li, G. X., Zhang, S. Q., et al. (2014). Transcription factor WRKY46 regulates osmotic stress responses and stomatal movement independently in *Arabidopsis*. *Plant J.* 79, 13–27. doi: 10.1111/tpj.12538
- dit Frey, N., Garcia, A. V., Bigeard, J., Zaag, R., Bueso, E., Garmier, M., et al. (2014). Functional analysis of *Arabidopsis* immune-related MAPKs uncovers a role for MPK3 as negative regulator of inducible defences. *Genome Biol.* 15:R87. doi: 10.1186/gb-2014-15-6-r87
- Dodds, P. N., and Rathjen, J. P. (2010). Plant immunity: towards an integrated view of plant-pathogen interactions. *Nat. Rev. Genet.* 11, 539–548. doi: 10.1038/nrg2812
- Dong, J., Chen, C., and Chen, Z. (2003). Expression profiles of the *Arabidopsis* WRKY gene superfamily during plant defense response. *Plant Mol. Biol.* 51, 21–37. doi: 10.1023/A:1020780022549
- Dyson, M. R., Shadbolt, S. P., Vincent, K. J., Perera, R. L., and McCafferty, J. (2004). Production of soluble mammalian proteins in *Escherichia coli*: identification of protein features that correlate with successful expression. *BMC Biotechnol.* 4:32. doi: 10.1186/1472-6750-4-32
- Eschen-Lippold, L., Bauer, N., Lohr, J., Palm-Forster, M. A., and Lee, J. (2014). Rapid mutagenesis-based analysis of phosphorylation sites in mitogen-activated protein kinase substrates. *Methods Mol. Biol.* 1171, 183–192. doi: 10.1007/978-1-4939-0922-3_15
- Eschen-Lippold, L., Bethke, G., Palm-Forster, M. A., Pecher, P., Bauer, N., Glazebrook, J., et al. (2012). MPK11-a fourth elicitor-responsive mitogen-activated protein kinase in *Arabidopsis thaliana*. *Plant Signal. Behav.* 7, 1203–1205. doi: 10.4161/psb.21323
- Eulgem, T., and Somssich, I. E. (2007). Networks of WRKY transcription factors in defense signaling. *Curr. Opin. Plant Biol.* 10, 366–371. doi: 10.1016/j.pbi.2007.04.020
- Feilner, T., Hultschig, C., Lee, J., Meyer, S., Immink, R. G. H., Koenig, A., et al. (2005). High throughput identification of potential *Arabidopsis* mitogen-activated protein kinases substrates. *Mol. Cell. Proteomics* 4, 1558–1568. doi: 10.1074/mcp.M500007-MCP200
- Feys, B. J., Wiermer, M., Bhat, R. A., Moisan, L. J., Medina-Escobar, N., Neu, C., et al. (2005). Arabidopsis SENESCENCE-ASSOCIATED GENE101 stabilizes and signals within an ENHANCED DISEASE SUSCEPTIBILITY1 complex in plant innate immunity. *Plant Cell* 17, 2601–2613. doi: 10.1105/tpc.105.033910
- Franceschini, A., Szklarczyk, D., Frankild, S., Kuhn, M., Simonovic, M., Roth, A., et al. (2013). STRING v9.1: protein-protein interaction networks, with increased coverage and integration. *Nucleic Acids Res.* 41, D808–D815. doi: 10.1093/nar/gks1094
- Gao, X., Chen, X., Lin, W., Chen, S., Lu, D., Niu, Y., et al. (2013). Bifurcation of *Arabidopsis* NLR immune signaling via Ca^{2+} -dependent protein kinases. *PLoS Pathog.* 9:e1003127. doi: 10.1371/journal.ppat.1003127
- Gómez-Gómez, L., and Boller, T. (2002). Flagellin perception: a paradigm for innate immunity. *Trends Plant Sci.* 7, 251–256. doi: 10.1016/S1360-1385(02)02261-6
- Guan, Y., Lu, J., Xu, J., McClure, B., and Zhang, S. (2014). Two mitogen-activated protein kinases, MPK3 and MPK6, are required for funicular guidance of pollen

- tubes in *Arabidopsis*. *Plant Physiol.* doi: 10.1104/pp.113.231274 [Epub ahead of print].
- Hu, Y., Dong, Q., and Yu, D. (2012). *Arabidopsis* WRKY46 coordinates with WRKY70 and WRKY53 in basal resistance against pathogen *Pseudomonas syringae*. *Plant Sci.* 185–186, 288–297. doi: 10.1016/j.plantsci.2011.12.003
- Huang, D. W., Sherman, B. T., and Lempicki, R. A. (2009). Systematic and integrative analysis of large gene lists using DAVID bioinformatics resources. *Nat. Protoc.* 4, 44–57. doi: 10.1038/nprot.2008.211
- Johnson, C. S., Kolevski, B., and Smyth, D. R. (2002). TRANSPARENT TESTA GLABRA2, a trichome and seed coat development gene of *Arabidopsis*, encodes a WRKY transcription factor. *Plant Cell* 14, 1359–1375. doi: 10.1105/tpc.001404
- Jones, J. D., and Dangl, J. L. (2006). The plant immune system. *Nature* 444, 323–329. doi: 10.1038/nature05286
- Kim, C. Y., and Zhang, S. (2004). Activation of a mitogen-activated protein kinase cascade induces WRKY family of transcription factors and defense genes in tobacco. *Plant J.* 38, 142–151. doi: 10.1111/j.1365-313X.2004.02033.x
- Lagace, M., and Matton, D. P. (2004). Characterization of a WRKY transcription factor expressed in late torpedo-stage embryos of *Solanum chacoense*. *Planta* 219, 185–189. doi: 10.1007/s00425-004-1253-2
- Lassowska, I., Böttcher, C., Eschen-Lippold, L., Scheel, D., and Lee, J. (2014). Sustained mitogen-activated protein kinase activation reprograms defense metabolism and phosphoprotein profile in *Arabidopsis thaliana*. *Front. Plant Sci.* 5:554. doi: 10.3389/fpls.2014.00554
- Lee, J., Eschen-Lippold, L., Lassowska, I., Boettcher, C., and Scheel, D. (2015). Cellular reprogramming through mitogen-activated protein kinases. *Front. Plant Sci.* 6:940. doi: 10.3389/fpls.2015.00940
- Lee, J., Rudd, J. J., Macioszek, V. K., and Scheel, D. (2004). Dynamic changes in the localization of MAPK cascade components controlling pathogenesis-related (PR) gene expression during innate immunity in parsley. *J. Biol. Chem.* 279, 22440–22448. doi: 10.1074/jbc.M401099200
- Li, G., Meng, X., Wang, R., Mao, G., Han, L., Liu, Y., et al. (2012). Dual-level regulation of ACC synthase activity by MPK3/MPK6 cascade and its downstream WRKY transcription factor during ethylene induction in *Arabidopsis*. *PLoS Genet.* 8:e1002767. doi: 10.1371/journal.pgen.1002767
- Liu, Y. D., and Zhang, S. Q. (2004). Phosphorylation of 1-aminocyclopropane-1-carboxylic acid synthase by MPK6, a stress-responsive mitogen-activated protein kinase, induces ethylene biosynthesis in *Arabidopsis*. *Plant Cell* 16, 3386–3399. doi: 10.1105/tpc.104.026609
- Maldonado-Bonilla, L. D., Eschen-Lippold, L., Gago-Zachert, S., Tabassum, N., Bauer, N., Scheel, D., et al. (2014). The *Arabidopsis* tandem zinc finger 9 protein binds RNA and mediates pathogen-associated molecular pattern-triggered immune responses. *Plant Cell Physiol.* 55, 412–425. doi: 10.1093/pcp/pct175
- Mao, G., Meng, X., Liu, Y., Zheng, Z., Chen, Z., and Zhang, S. (2011). Phosphorylation of a WRKY transcription factor by two pathogen-responsive MAPKs drives phytoalexin biosynthesis in *Arabidopsis*. *Plant Cell* 23, 1639–1653. doi: 10.1105/tpc.111.084996
- Meng, X., and Zhang, S. (2013). MAPK cascades in plant disease resistance signaling. *Annu. Rev. Phytopathol.* 51, 245–266. doi: 10.1146/annurev-phyto-082712-102314
- Moreau, M., Degrave, A., Vedel, R., Bitton, F., Patriot, O., Renou, J. P., et al. (2012). EDS1 contributes to nonhost resistance of *Arabidopsis thaliana* against *Erwinia amylovora*. *Mol. Plant Microbe Interact.* 25, 421–430. doi: 10.1094/MPMI-05-11-0111
- Nakagawa, T., Kurose, T., Hino, T., Tanaka, K., Kawamukai, M., Niwa, Y., et al. (2007). Development of series of gateway binary vectors, pGWBs, for realizing efficient construction of fusion genes for plant transformation. *J. Biosci. Bioeng.* 104, 34–41. doi: 10.1263/jbb.104.34
- Palm-Forster, M. A., Eschen-Lippold, L., and Lee, J. (2012). A mutagenesis-based screen to rapidly identify phosphorylation sites in mitogen-activated protein kinase substrates. *Anal. Biochem.* 427, 127–129. doi: 10.1016/j.ab.2012.05.015
- Pecher, P., Eschen-Lippold, L., Herklotz, S., Kuhle, K., Naumann, K., Bethke, G., et al. (2014). The *Arabidopsis thaliana* mitogen-activated protein kinases MPK3 and MPK6 target a subclass of 'VQ-motif'-containing proteins to regulate immune responses. *New Phytol.* 203, 592–606. doi: 10.1111/nph.12817
- Petersen, M., Brodersen, P., Naested, H., Andreasson, E., Lindhart, U., Johansen, B., et al. (2000). *Arabidopsis* map kinase 4 negatively regulates systemic acquired resistance. *Cell* 103, 1111–1120. doi: 10.1016/S0092-8674(00)00213-0
- Popescu, S. C., Popescu, G. V., Bachan, S., Zhang, Z., Gerstein, M., Snyder, M., et al. (2009). MAPK target networks in *Arabidopsis thaliana* revealed using functional protein microarrays. *Genes Dev.* 23, 80–92. doi: 10.1101/gad.174009
- Qiu, J. L., Fiil, B. K., Petersen, K., Nielsen, H. B., Botanga, C. J., Thorgrimsen, S., et al. (2008). *Arabidopsis* MAP kinase 4 regulates gene expression through transcription factor release in the nucleus. *EMBO J.* 27, 2214–2221. doi: 10.1038/emboj.2008.147
- Ranf, S., Eschen-Lippold, L., Pecher, P., Lee, J., and Scheel, D. (2011). Interplay between calcium signalling and early signalling elements during defence responses to microbe- or damage-associated molecular patterns. *Plant J.* 68, 100–113. doi: 10.1111/j.1365-313X.2011.04671.x
- Reddy, P. S., Kavi Kishor, P. B., Seiler, C., Kuhlmann, M., Eschen-Lippold, L., Lee, J., et al. (2014). Unraveling regulation of the small heat shock proteins by the heat shock factor HvHsfB2c in barley: its implications in drought stress response and seed development. *PLoS ONE* 9:e89125. doi: 10.1371/journal.pone.089125
- Robatzek, S., and Somssich, I. E. (2001). A new member of the *Arabidopsis* WRKY transcription factor family, AtWRKY6, is associated with both senescence- and defence-related processes. *Plant J.* 28, 123–133. doi: 10.1046/j.1365-313X.2001.01131.x
- Rushton, P. J., Somssich, I. E., Ringler, P., and Shen, Q. J. (2010). WRKY transcription factors. *Trends Plant Sci.* 15, 247–258. doi: 10.1016/j.tplants.2010.02.006
- Sethi, V., Raghuram, B., Sinha, A. K., and Chattopadhyay, S. (2014). A mitogen-activated protein kinase cascade module, MKK3-MPK6 and MYC2, is involved in blue light-mediated seedling development in *Arabidopsis*. *Plant Cell* 26, 3343–3357. doi: 10.1105/tpc.114.128702
- Shannon, P., Markiel, A., Ozier, O., Baliga, N. S., Wang, J. T., Ramage, D., et al. (2003). Cytoscape: a software environment for integrated models of biomolecular interaction networks. *Genome Res.* 13, 2498–2504. doi: 10.1101/gr.123930
- Sinha, A. K., Jaggi, M., Raghuram, B., and Tuteja, N. (2011). Mitogen-activated protein kinase signalling in plants under abiotic stress. *Plant Signal. Behav.* 6, 196–203. doi: 10.4161/psb.6.2.14701
- van Verk, M. C., Bol, J. F., and Linthorst, H. J. (2011). WRKY transcription factors involved in activation of SA biosynthesis genes. *BMC Plant Biol.* 11:89. doi: 10.1186/1471-2229-11-89
- Wang, F., Yang, Y., Wang, Z., Zhou, J., Fan, B., and Chen, Z. (2015). A critical role of lyst-interacting protein5, a positive regulator of multivesicular body biogenesis, in plant responses to heat and salt stresses. *Plant Physiol.* 169, 497–511. doi: 10.1104/pp.15.00518
- Wang, H., Liu, Y., Bruffett, K., Lee, J., Hause, G., Walker, J. C., et al. (2008). Haplotype insufficiency of MPK3 in MPK6 mutant background uncovers a novel function of these two MAPKs in *Arabidopsis* ovule development. *Plant Cell* 20, 602–613. doi: 10.1105/tpc.108.058032
- Wang, H., Ngwenyama, N., Liu, Y., Walker, J. C., and Zhang, S. (2007). Stomatal development and patterning are regulated by environmentally responsive mitogen-activated protein kinases in *Arabidopsis*. *Plant Cell* 19, 63–73. doi: 10.1105/tpc.106.048298
- Weyhe, M., Eschen-Lippold, L., Pecher, P., Scheel, D., and Lee, J. (2014). Ménage à trois: the complex relationships between mitogen-activated protein kinases, WRKY transcription factors and VQ-motif-containing proteins. *Plant Signal. Behav.* 9:e29519. doi: 10.4161/psb.29519
- Wu, X., Shiroto, Y., Kishitani, S., Ito, Y., and Toriyama, K. (2009). Enhanced heat and drought tolerance in transgenic rice seedlings overexpressing OsWRKY11 under the control of HSP101 promoter. *Plant Cell Rep.* 28, 21–30. doi: 10.1007/s00299-008-0614-x
- Yoo, S. D., Cho, Y. H., and Sheen, J. (2007). Arabidopsis mesophyll protoplasts: a versatile cell system for transient gene expression analysis. *Nat. Protoc.* 2, 1565–1572. doi: 10.1038/nprot.2007.199
- Zheng, M. S., Takahashi, H., Miyazaki, A., Hamamoto, H., Shah, J., Yamaguchi, I., et al. (2004). Up-regulation of *Arabidopsis thaliana* NHL10 in the hypersensitive response to Cucumber mosaic virus infection and

in senescing leaves is controlled by signalling pathways that differ in salicylate involvement. *Planta* 218, 740–750. doi: 10.1007/s00425-003-1169-2

Conflict of Interest Statement: The authors declare that the research was conducted in the absence of any commercial or financial relationships that could be construed as a potential conflict of interest.

Copyright © 2016 Sheikh, Eschen-Lippold, Pecher, Hoehenwarter, Sinha, Scheel and Lee. This is an open-access article distributed under the terms of the Creative Commons Attribution License (CC BY). The use, distribution or reproduction in other forums is permitted, provided the original author(s) or licensor are credited and that the original publication in this journal is cited, in accordance with accepted academic practice. No use, distribution or reproduction is permitted which does not comply with these terms.



Overexpression of Soybean Isoflavone Reductase (*GmIFR*) Enhances Resistance to *Phytophthora sojae* in Soybean

Qun Cheng^{1†}, Ninghui Li^{1,2†}, Lidong Dong^{1†}, Dayong Zhang¹, Sujie Fan¹, Liangyu Jiang¹, Xin Wang^{1,3}, Pengfei Xu^{1*} and Shuzhen Zhang^{1*}

¹ Key Laboratory of Soybean Biology of Chinese Education Ministry, Soybean Research Institute, Northeast Agricultural University, Harbin, China; ² Jiamusi Branch Academy of Heilongjiang Academy of Agricultural Sciences, Jiamusi, China,

³ Heilongjiang Academy of Land Reclamation Sciences, Harbin, China

OPEN ACCESS

Edited by:

Sylvain Jeandroz,
Agrosup Dijon, France

Reviewed by:

Raimund Tenhaken,
University of Salzburg, Austria
Haitao Shi,
Hainan University, China

*Correspondence:

Pengfei Xu
xupengfei@neau.edu.cn;
Shuzhen Zhang
zhangshuzhen@neau.edu.cn

[†]These authors have contributed
equally to this work.

Specialty section:

This article was submitted to
Plant Physiology,
a section of the journal
Frontiers in Plant Science

Received: 30 July 2015

Accepted: 05 November 2015

Published: 23 November 2015

Citation:

Cheng Q, Li N, Dong L, Zhang D, Fan S, Jiang L, Wang X, Xu P and Zhang S (2015) Overexpression of Soybean Isoflavone Reductase (*GmIFR*) Enhances Resistance to *Phytophthora sojae* in Soybean. *Front. Plant Sci.* 6:1024.
doi: 10.3389/fpls.2015.01024

Isoflavone reductase (IFR) is an enzyme involved in the biosynthetic pathway of isoflavonoid phytoalexin in plants. IFRs are unique to the plant kingdom and are considered to have crucial roles in plant response to various biotic and abiotic environmental stresses. Here, we report the characterization of a novel member of the soybean isoflavone reductase gene family *GmIFR*. Overexpression of *GmIFR* transgenic soybean exhibited enhanced resistance to *Phytophthora sojae*. Following stress treatments, *GmIFR* was significantly induced by *P. sojae*, ethephon (ET), abscisic acid (placeCityABA), salicylic acid (SA). It is located in the cytoplasm when transiently expressed in soybean protoplasts. The daidzein levels reduced greatly for the seeds of transgenic plants, while the relative content of glyceollins in transgenic plants was significantly higher than that of non-transgenic plants. Furthermore, we found that the relative expression levels of reactive oxygen species (ROS) of transgenic soybean plants were significantly lower than those of non-transgenic plants after incubation with *P. sojae*, suggesting an important role of *GmIFR* might function as an antioxidant to reduce ROS in soybean. The enzyme activity assay suggested that *GmIFR* has isoflavone reductase activity.

Keywords: *Glycine max*, isoflavone reductase, *Phytophthora sojae*, isoflavonoid, gene expression, antioxidant properties

INTRODUCTION

A major response of soybean to attack by fungal pathogens and oomycetes is production of isoflavonoid phytoalexin glyceollins (Partridge and Keen, 1977; Yoshikawa et al., 1978; Banks and Dewick, 1983; Ng et al., 2011; Kim et al., 2012). They are valuable secondary metabolites produced primarily in leguminous plants and are rarely found in other plant families (Wang et al., 2006; Kim et al., 2010b), and are synthesized by the isoflavonoid branch of the central phenylpropanoid pathway (Ng et al., 2011). Moreover, glyceollins in general protect plant tissues from environmental challenge possibly by reducing the oxidative damage induced by stress factors; therefore, the compounds can possess considerable cellular antioxidant properties (Nwachukwu et al., 2013). A huge variety of enzymes are thought to be involved in their biosynthetic pathways (Somerville and Somerville, 1999). Isoflavone reductase (IFR) is identified as a crucial enzyme

involved in the synthesis of the glyceollins from daidzein (Graham et al., 1990; Oliver et al., 2003), and catalyzes a stereospecific NADPH-dependent reduction to (3R)-isoflavanone (Guo et al., 1994; Cooper et al., 2002). In addition, IFR is a monomeric, cytosolic reductase, and the enzyme can use 2'-hydroxydaidzein, 2'-hydroxyformononetin, and 2'-hydroxygenistein as substrates in soybean (Wang et al., 2006).

IFRs are members of a large protein family, and their cDNAs cloned from leguminous plants such as alfalfa (*Medicago sativa*; Paiva et al., 1991), pea (*Pisum sativum*; Sun et al., 1991), kidney bean (*Phaseolus vulgaris*; Rípodas et al., 2013) share high levels of sequence identity, and they participate specifically in isoflavonoid phytoalexin biosynthesis. IFR was first identified as a key enzyme involved in the latter part of the isoflavanoid phytoalexins pathway in alfalfa (Paiva et al., 1991). In pea, the enzyme has been purified and used to raise polyclonal antibodies (Sun et al., 1991). The levels of IFR in response to *Ascochyta rabiei* in chickpea were higher than those of control, suggesting that IFR may play a role in determining resistance to fungal (Daniel et al., 1990). In kidney bean, the reduction of IFR levels affected the growth, lateral root elongation and the number of nodules developed (Rípodas et al., 2013). However, beyond the purification to apparent homogeneity of IFR from elicitor-challenged soybean cell cultures and some physical and kinetic properties of this enzyme (Fischer et al., 1990; Wang et al., 2006), the gene function is still unclear in soybean.

In addition, IFR-like (IRL) proteins from non-leguminous plants, which are also part of the IFR family (Kim et al., 2010b), have also been cloned from tobacco (*Nicotiana tabacum*; Shoji et al., 2002), rice (*Oryza sativa*; Kim et al., 2003), Arabidopsis (Babiychuk et al., 1995), Ginkgo (*Ginkgo biloba*; Cheng et al., 2013), etc. They show amino acid sequence homology with those of legumes IFRs. Moreover, several IRL proteins have been implicated in response to biotic or abiotic stresses (Babiychuk et al., 1995; Lers et al., 1998; Shoji et al., 2002; Kim et al., 2003, 2010b). For instance, *OsIRL* gene was induced with an expression pattern similar to methyl jasmonic acid (MeJA) induction after *Pyricularia grisea* inoculation of rice (Kim et al., 2003). It has been proposed that AtIRL might have an important role as an antioxidant in yeast (Babiychuk et al., 1995). A recent study showed that OsIRL may behave as an antioxidant in response to reactive oxygen species (ROS) in suspension-cultured cells as well as during root development in rice (Kim et al., 2010b).

In a previous study, a cDNA library enriched for mRNAs encoding ESTs that increased in abundance during infection with *Phytophthora sojae* was constructed by suppression subtractive hybridization from leaf tissues of a high resistant soybean cultivar “Suinong 10,” and an EST homologous to an isoflavanone reductase from white lupin (*Lupinus albus*) was identified to be up-regulated by microarray and real-time PCR (Xu et al., 2012). In this study, the full-length EST, designated *GmIFR* (GenBank accession no. NM_001254100, NCBI protein no. NP_001241029), was isolated through RT-PCR from “Suinong 10” soybean, and the transgenic soybean plants over-expressing *GmIFR* gene under the control of 35S promoter were produced. The expression patterns of *GmIFR* induced under biotic stresses

were also examined. Moreover, the function of *GmIFR* and the content of daidzein, genistein, glycine, the relative content of glyceollins and the ROS in transgenic plants were investigated. *GmIFR* protein could catalyze a distinct NADPH-dependent oxidoreductase reaction by enzyme activity assay, suggesting that *GmIFR* has isoflavanone reductase activity. Together, we report insights into the function of an isoflavanone reductase (IFR) in soybean, namely *GmIFR*, in host responses to *P. sojae*.

MATERIALS AND METHODS

Plant Materials and Stress Treatments

The soybean cultivar “Suinong10,” resistant to the predominant race 1 of *P. sojae* in Heilongjiang, China (Zhang et al., 2010), was used in this study. The seeds of “Suinong10” were grown with a photoperiod of 16/8 h light/dark and maintained at 22°C with 70% relative humidity in the greenhouse. Fourteen days after planting, seedlings at the first-node stage (V1; Fehr et al., 1971) were used for various treatments.

For abiotic treatments, the seedlings were exposed to one of the five different stresses, namely wounding, ET, ABA, SA, or MeJA. For wounding treatment, the edges of leaves were cut by about 0.2 cm with scissors and incubated at room temperature for 0, 1, 3, 6, 9, 12 or 24 h; the intact leaves of soybean were used as controls. The ABA (200 μM), SA (2 mM), and MeJA (100 μM) were dissolved in 0.01% Tween 20 and sprayed onto young leaves for 0, 1, 3, 6, 9, 12 or 24 h. Ethylene treatment was performed with a concentration of 200 μL L⁻¹ by injection of gaseous ethylene in a sealed plexiglass chamber for 0, 1, 3, 6, 9, 12, or 24 h. The control leaves were sprayed with an equivalent volume of 0.01% (v/v) Tween 20.

For *P. sojae* treatment, the soybean plants were inoculated with *P. sojae* zoospores following the method described by Ward et al. (1979) and Morris et al. (1991) with minor modifications. Mock inoculations were carried out with equivalent amounts of sterile water. Zoospores were developed with the procedure of Ward et al. (1979), and the concentration was estimated using hemacytometer to approximately 1 × 10⁵ spores mL⁻¹. The unifoliolate leaves were also treated for 0, 3, 6, 9, 12, 24, 36, 48, 64, 72 h. “Dongnong50” soybean, which was susceptible to *P. sojae* race 1, obtained from the Key Laboratory of Soybean Biology in Chinese Ministry of Education, Harbin, was used for gene transformation experiments.

Isolation of the *GmIFR* Gene

A suppression subtractive hybridization library coupled with cDNA microarrays was queried using a soybean EST encoding an EST homologous to an isoflavanone reductase from white lupin (*L. albus*), previously shown to be up-regulated in “Suinong 10” soybean inoculated with *P. sojae* (Xu et al., 2012). Here, the full-length cDNA (named *GmIFR*, GenBank accession no. NM_001254100, NCBI protein no. NP_001241029) of the EST was amplified by RT-PCR from cDNA of “Suinong 10” using the primer pairs *GmIFRF* and *GmIFRR* (Supplementary Table S1). PCR was performed as follows: 94°C for 5 min, followed 30 cycles of 94°C for 30 s, 60°C

for 30 s, and 72°C for 90 s, with a final extension at 72°C for 10 min. The amplification product was gel purified and cloned into the pMD18-T vector (TaKaRa, Dalian, China). An analysis of protein structure was performed using Smart (<http://smart.embl-heidelberg.de/>). Sequence alignments were performed using DNAMAN software (<http://www.lynnon.com/>). A phylogenetic analysis of *GmIFR* and various heterologous IFR proteins was performed using MEGA4 software (Tamura et al., 2007).

Quantitative RT-PCR Analysis

Quantitative real-time PCR analysis was performed to determine the transcript abundance of *GmIFR*. Total RNA was isolated from “Suinong 10” soybean leaves using Trizol reagent (Invitrogen, Shanghai, China). The synthesis of cDNA was conducted using an oligo(dT) primer and a M-MLV reverse transcriptase kit (Takara, Dalian, China) according to the manufacturer’s instructions. qRT-PCR was performed on a CFX96 Touch™ Real-Time PCR machine (Biobad, USA) using the real-time PCR kit (ToYoBo, Japan). DNA accumulation was measured using SYBR Green as the reference dye. The soybean housekeeping gene *Gmactin4* (GenBank accession no. AF049106) was used as the internal control (see **Supplementary Table S1** for primer sequences). For tissue distribution analysis, the transcript level of *GmEF1* gene (GenBank accession no. NM_001248778) was used as quantitative control (see **Supplementary Table S1** for primer sequence). The relative expression of target gene in different tissues of soybean was calculated using the $2^{-\Delta\Delta CT}$ method. For each sample, three biological replicates were analyzed with their respective technical replicates.

Subcellular Localization of GmIFR Protein

To determine the subcellular localization of GmIFR, the coding region of GmIFR was fused to the N-terminus of GFP under the control of the CaMV 35S promoter in the PCAMBIA1302 vector. Soybean protoplasts were obtained according to the method described by Lin (1983). Soybean protoplast transformation described by Yoo et al. (2007) was performed with minor modifications.

Expression and Purification of Fusion Protein

The full-length cDNA of *GmIFR* was fused to the N-terminus of the 6 × His-tag, at the *Nco*I and *Xho*I restriction sites of the vector pET28a (+) (Novagen, Germany). The recombinant fusion plasmid was expressed into *Tranetta* (DE3) cells (TransGen Biotech, China). His-tagged proteins were induced with 0.5 mM isopropyl-β-D-thiogalactoside (IPTG) at 37°C for 4 h. The fusion protein was purified at room temperature and quantified according to the pET System Manual (Novagen). The fusion GmIFR protein was subsequently analyzed by sodium dodecyl sulfate polyacrylamide gel electrophoresis (SDS-PAGE) and western blotting using anti-His antibody.

Enzyme Assays

In order to determine whether GmIFR has isoflavone reductase activity, the enzyme assays of GmIFR was analyzed. The fusion

protein was used in the enzyme assays. GmIFR activity was analyzed according to the method described by Paiva et al. (1991) with minor modifications. High Performance Liquid Chromatography (HPLC) was used to separate the substrate and product.

Plasmid Construction and Transformation of Soybean

For gene overexpression analysis, the full length *GmIFR* coding region was amplified with gene specific primers *GmIFRTF* and *GmIFRTR* (**Supplementary Table S1**). The PCR conditions were as follows: 94°C for 2 min followed by 30 cycles at 94°C for 30 s, 55°C for 30 s, and 72°C for 1 min and a final extension at 72°C for 10 min. Then the *GmIFR* open reading frame was cloned into the vector pCAMBIA3301 under the control of a CaMV35S promoter. The constructs were transferred into the *Agrobacterium tumefaciens* strain LBA4404 via tri-parental mating. For “Dongnong 50” soybean transformation, the cotyledonary nodes were used as explants for the transformation using the *Agrobacterium*-mediated transformation method described by Paz et al. (2004). Transgenic soybean plants (T7) were identified by PCR amplification and southern hybridization using the DIG High Prime DNA Labeling and Detection Starter Kit II (Roche Cat., Germany), and they were developed to T8 transgenic soybean plants for further analysis.

Pathogen Response Assays of Transgenic Soybean Plants

To investigate whether the *GmIFR*-transformed plants resist pathogen infection, artificial inoculation procedures were performed according to the methods described by Dou et al. (2003) and Morrison and Thorne (1978) with some modifications. The living cotyledons of three T8 transgenic soybean plants (numbered T8-80, T8-88, and T8-96) were treated with a *P. sojae* inoculum. For infection assays, three biological replicates were analyzed with their respective technical replicates. The living cotyledons were incubated in a mist chamber at 25°C with 90% relative humidity under a 14 h photoperiod at a light intensity of 350 μmol photons m⁻² s⁻¹ for investigation. The cotyledons of non-transformed plants were used as controls. Disease symptoms on each cotyledon were observed and photographed after inoculation using a Nikon D7000 camera.

Measurement of Reactive Oxygen Species (ROS) Generation

To investigate whether the *GmIFR*-transformed plants respond to oxidative stresses, the hypocotyls of three T8 transgenic soybean plants (numbered T8-31, T8-39, and T8-47) and non-transgenic soybean plants were treated with *P. sojae* zoospores of approximately 1×10^5 spores mL⁻¹ for 0, 3, 6, 12, 24, 48 h following the method described by Ward et al. (1979) and Morris et al. (1991) with minor modifications. The ROS were measured according to the instructions supplied with the Reactive Oxygen Species Assay Kit (Beyotime Institute

of Biotechnology, Haimen, China). In this kit, the non-fluorescent probe 2',7'-dichlorofluorescein diacetate (H2DCF-DA) passively diffuses into cells and is deacetylated to form nonfluorescent 2',7'-dichlorofluorescein (DCFH). DCFH reacts with ROS to form the fluorescent product DCF, which is trapped inside the cells. Fluorescence was detected at 485 nm for excitation and 530 nm for emission with a fluorescence microplate reader (Bio-TEK, USA; Qian et al., 2009).

Isoflavone and Glyceollins Analysis

Approximately 0.1 g sample of seeds (numbered S-T8-80, S-T8-88, S-T8-96) developed from T8-80, T8-88 and T8-96 transgenic soybean plants, and that of non-transgenic soybean plants were ground to a fine power using a commercial coffee grinder. Daidzein, genistein, and glycitein were extracted from flour and separated using HPLC as described previously (Zeng et al., 2009). Measurements were done as micrograms of isoflavone per gram of seeds plus and minus the standard deviations.

Glyceollins were extracted from the seeds (namely S-T8-80, S-T8-88, S-T8-96) developed from T8-80, T8-88, and T8-96 transgenic soybean plants and non-transgenic soybean with 80% ethanol following the method described by Boue et al. (2000) and isolated using HPLC as described previously (Zeng et al., 2009).

RESULTS

Isolation and Bioinformatic Analysis of GmIFR

The full-length cDNA sequence of *GmIFR* (GenBank Accession No. NM_001254100) was isolated from total RNA of “Suinong10” soybean by RT-PCR and cloned into pMD-18T vector. Sequence analysis showed that *GmIFR* has an open reading frame (ORF) of 939 bp and encodes a polypeptide of 312 amino acids (**Supplementary Figure S1**) with a predicted molecular mass of 34.92 kDa and a isoelectric point (pI) of 6.33. The deduced protein has a central 107 amino acid NAD (P) domain (**Supplementary Figure S1**). The predicted three-dimensional model of the *GmIFR* consists of 13 α -helices and 10 β -strands (**Supplementary Figure S2A**). To further explore the evolutionary relationship among plant NAD (P) proteins, a phylogenetic tree was constructed using MEGA 4.0 (Tamura et al., 2007) based on the amino acid sequences. Alignment and phylogenetic tree analysis of leguminous plants sequences revealed that *GmIFR* has 44–94% identity for overall amino acid sequence to *Phaseolus vulgaris* PvIFR, *Cicer arietinum* CaIFR, *Medicago truncatula* MtIFR, *Lotus japonicus* LjIFR, *Glycine soja* GsIFR, *Medicago sativa* MsIFR, *Pisum sativum* PsIFR (**Supplementary Figure S2B**). Analysis of the conserved NAD (P) domain of 107 aa showed that *GmIFR* shared 86–90% amino acid identity with others (**Supplementary Figure S2C**). The analysis of homologs of *GmIFR* in the soybean genome, based on data obtained from the Phytozome database (<http://www.phytozome.net/> soybean), indicated that the two genes

were clustered on two linkage groups, namely one each on Gm 01 and Gm 09 and had three introns.

Accumulation of the GmIFR Transcript under Different Stress Treatments

To determine the expression pattern of *GmIFR*, quantitative real-time reverse transcription-PCR (qRT-PCR) was performed to examine the transcript levels of *GmIFR* in “Suinong 10” soybean plant. The examination of tissue-specific transcript abundance in “Suinong 10” soybean showed that *GmIFR* was constitutively and highly expressed in the cotyledons, followed by roots, stems, and leaves (**Figure 1**). Quantitative real-time PCR showed that *GmIFR* was responsive to ET, SA, MeJA, ABA, wounding and *P. sojae* treatments (**Figure 2**). *GmIFR* mRNA rapidly increased under ET and SA treatments, reaching a maximum level at 12 h after the treatment followed by a rapid decline (**Figure 2**). Under wounding, ABA, MeJA, and *P. sojae* treatments, *GmIFR* mRNA accumulated and reached a maximum level at 1, 3, 9 and 48 h, respectively (**Figure 2**).

Subcellular Localization of the GmIFR Protein

The Psort program predicted a cytoplasmic localization of *GmIFR* with 45% certainty (<http://psort.hgc.jp/form.html>). To determine the subcellular localization of *GmIFR* protein, *GmIFR*-GFP (for green fluorescent protein) fusion protein driven by the cauliflower mosaic virus 35S promoter was introduced into soybean protoplast by transient transformation. Analysis of the subcellular localization of the *GmIFR*-GFP fusion proteins by confocal laser scanning microscopy revealed that a strong fluorescent signal derived from GFP alone was observed in the cytoplasm, nuclei and cell membrane, whereas transformed cells carrying *GmIFR*-GFP showed a strong green fluorescence signal in the cytoplasm (**Figure 3**), demonstrating the cytoplasm localization of *GmIFR*.

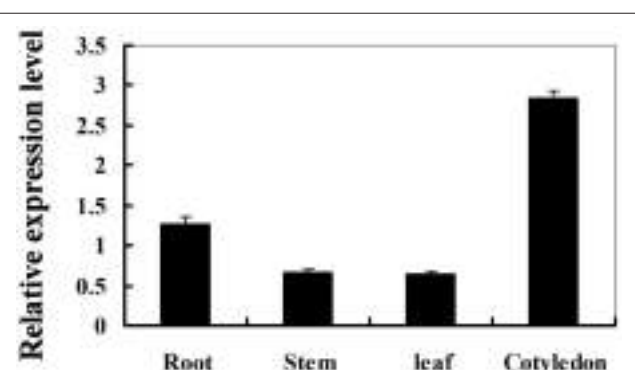


FIGURE 1 | Expression patterns of the *GmIFR* genes in various tissues of “Suinong” 10 soybean under normal condition. The roots, stems or leaves were prepared from 14-day-old seedlings, and the cotyledons from 7-day-old seedlings. The amplification of the soybean *EF1* (*GmEF1*) gene was used as an internal control to normalize all the data. For each sample, three biological replicates were analyzed with their respective three technical replicates, bars indicate standard error of the mean.

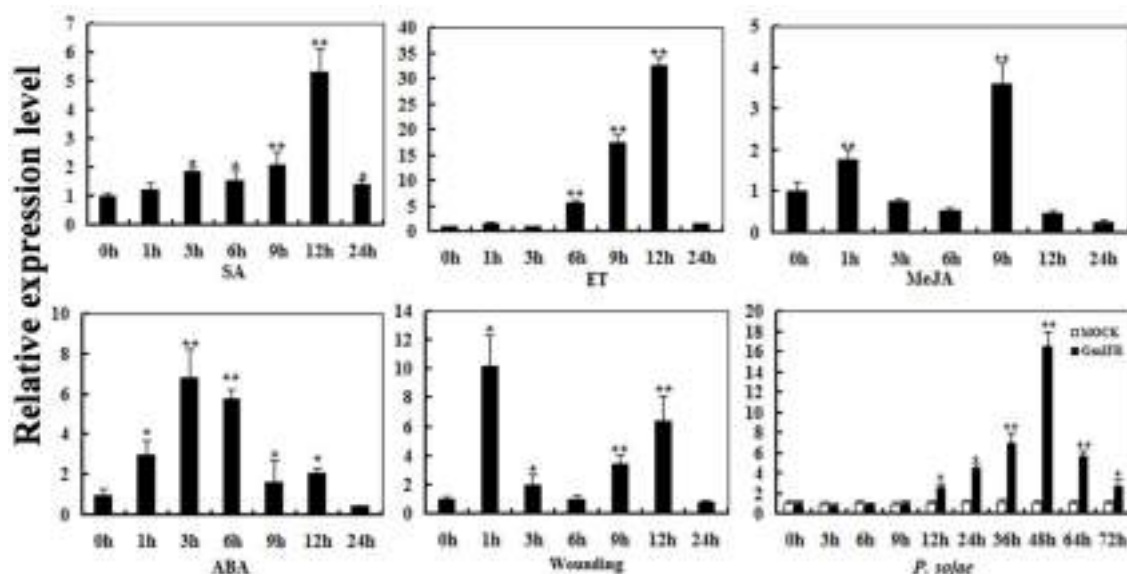


FIGURE 2 | Relative quantities of *GmIFR* mRNA at various time points post-treatment with ET, SA, MeJA, ABA, wounding, and *P. sojae*.

Fourteen-day-old plants were used for treatments and analyses. Water treatment were used as control for *P. sojae* treatments. The amplification of the soybean *Actin* (*GmActin4*) gene was used as an internal control to normalize all the data. Relative transcript levels of *GmIFR* were quantified compared with mock plants at the same time point. The experiment was performed on three biological replicates with their respective three technical replicates and statistically analyzed using Student's *t*-test (**P* < 0.05; ***P* < 0.01). Bars indicate standard error of the mean.

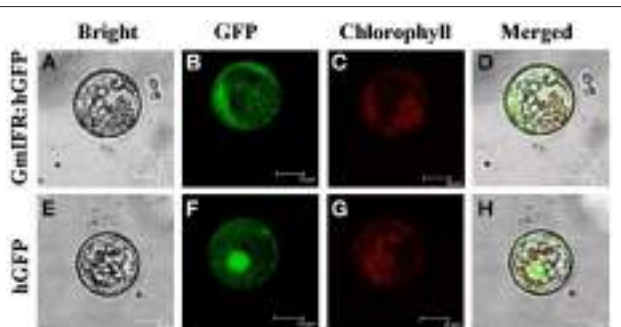


FIGURE 3 | Subcellular localization of the IFR-GFP fusion protein in Soybean protoplasts. *GmIFR*-GFP expression was driven by the cauliflower mosaic virus 35S promoter and transiently expressed in Soybean protoplasts. The images of bright-field (A,E), the GFP fluorescence (green) only (B,F), the chlorophyll autofluorescence (red) only (C,G), cytoplasmic marker fluorescence localization, and combined ones (D,H) are shown. Bars = 10 mm.

The Activity of *GmIFR* In vitro

To express *GmIFR* in *Transetta* (DE3) cells, the coding sequence of *GmIFR* was cloned into pET-28a that was an expression vector with a His-tag. Upon induction by IPTG, *GmIFR* was expressed as a major soluble protein product at 1, 2, 4, 6 h (Figure 4A, Lane 2, 3, 4, 5). The molecular weight of the purified protein was about 34 kDa in SDS-PAGE, consistent with the calculated molecular mass (34 kDa) (Figure 4A, lane 6). Western blotting of the purified recombinant *GmIFR* protein confirmed its specific immune reactivity to anti-His antibodies (Figure 4A, lane Western blot).

In order to determine whether *GmIFR* has isoflavone reductase activity, the enzyme assays of *GmIFR* was analyzed. The reductase reactions in the presence of NADPH were measured by reversed-phase HPLC: the formation of the product from the substrate. As shown in Figures 4B,C, the protein purified from *Transetta* (DE3) expressing the fusion protein showed clear isoflavone reductase activity, with 2'-hydroxyformononetin as the substrate. These results proved that *GmIFR* is an isoflavone reductase.

Overexpression of *GmIFR* Enhanced Resistance to *P. sojae* in Soybean

To investigate whether overexpression of *GmIFR* in soybean has an effect on Phytophthora root rot resistance, the living cotyledons of three T8 transgenic soybean plants (T8-80, T8-88, T8-96) were selected by Real-time PCR (Figure 5A).

As shown in Figure 5B, the cotyledons of the non-transgenic soybean plants detached and exhibited clear and large water-soaked lesions compared with those of the transgenic plants after 72 h of incubation with *P. sojae* (Figure 5B). The lesion area of the three transgenic lines was significantly (*P* < 0.01) smaller than that of non-transgenic soybean plants at 72 h after inoculation (Figure 5C). These results indicated that constitutive expression of the *GmIFR* enhances resistance toward *P. sojae*.

Expression of *GmIFR* in Soybean Seed Affects ROS Levels

It is known that pathogen infection is associated with the production of ROS (Hückelhoven and Kogel, 2003; Soosaar et al.,

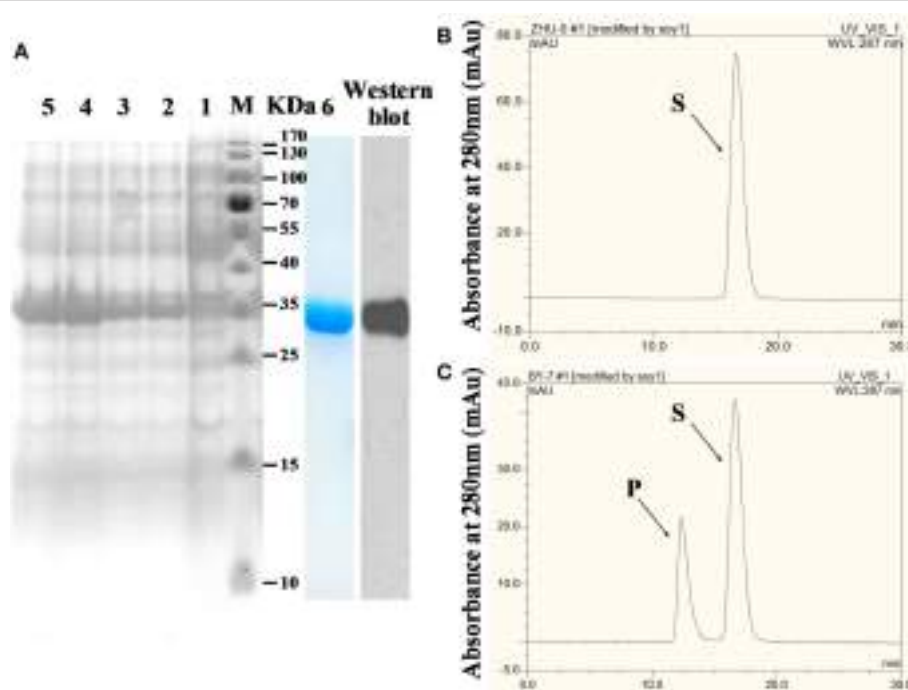


FIGURE 4 | Analysis of GmIFR activity by HPLC. (A) After IPTG induction, *Tranetta* cells containing pET28a-IFR were grown at 37°C for 1, 2, 4, 6 h. Lane 1 protein of total cells without IPTG induction, lane 2 protein of total cells with IPTG induction for 1 h, lane 3 protein of total cells with IPTG induction for 2 h, lane 4 induction for 4 h, lane 5 induction for 6 h, lane 6 purified recombinant GmIFR protein with Nickel-CL agarose affinity chromatography and used for enzyme activity assay; *M*, molecular marker; *Lane Western blot* western blotting of the purified recombinant GmIFR protein with an anti-His tag primary antibody probe. **(B)** The reaction with 2'-hydroxyformononetin. **(C)** The reaction harboring the GmIFR protein and with 2'-hydroxyformononetin as the substrate. S, substrate; P, product.

2005; Takabatake et al., 2007; Shetty et al., 2008). Therefore, the ROS relative expression levels was detected in three T8 transgenic soybean plants (T8-31, T8-39, and T8-47) and non-transgenic plants at 0, 3, 6, 12, 24, 48 h after incubation with *P. sojae*. The results showed that the relative expression levels of ROS gradually increased in transgenic plants and non-transgenic plants with the incubation period (Figure 6). The relative expression levels of ROS in the transgenic plants were significantly lower than those of non-transgenic plants at the same time point (Figure 6), suggesting that an important role of *GmIFR* might function as an antioxidant to reduce ROS in soybean.

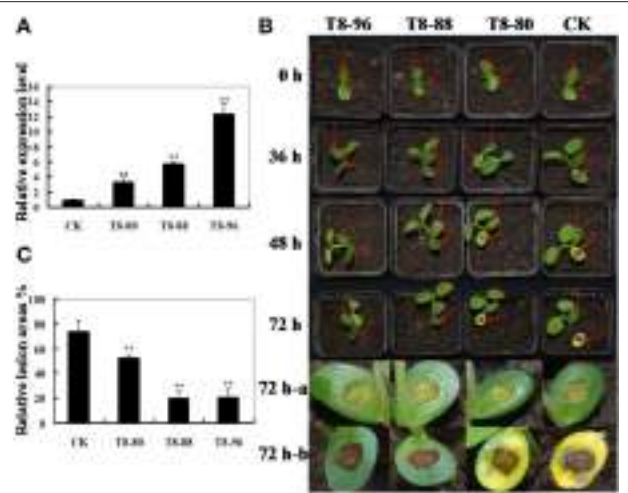
Overexpression of GmIFR in Soybean Seed Affects Isoflavone and Glyceollins Expression Levels

It is well known that daidzein, genistein, and glycinein were the essential components of isoflavones (Wang et al., 2014) and IFR was a crucial enzyme involved in the synthesis of the glyceollins from daidzein (Graham et al., 1990; Oliver et al., 2003). Thus, changes in the IFR expression level may cause change of isoflavanoid and glyceollins content in soybean. To study the relationship between isoflavanoid and glyceollins content in soybean seeds and the *GmIFR* gene expression level, the isoflavanoid content and the relative content of the glyceollins were measured in the seeds of transgenic soybean plants and

non-transgenic soybean plants. As shown in Figure 7A, the daidzein levels in the seeds (numbered S-T8-80, S-T8-88, and S-T8-96) developed from the three independent transformed lines T8-80, T8-88, and T8-96 reduced greatly, while levels of genistein and glycinein had little change compared to those of control (Figures 7B,C). The relative content of glyceollins in the transgenic plants was significantly higher than that of non-transgenic plants (Figure 7D), suggesting that an important role of *GmIFR* involved in the synthesis of the glyceollins from daidzein in soybean.

Over-expressing of GmIFR Affected the Transcriptional Level of Multiple Genes Involved in Phenylpropanal Pathway

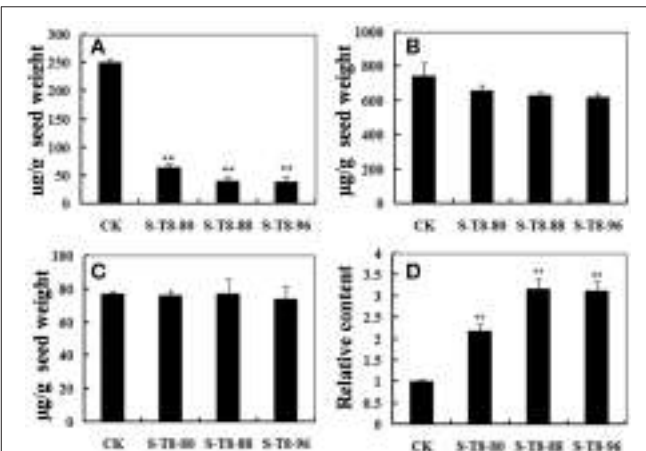
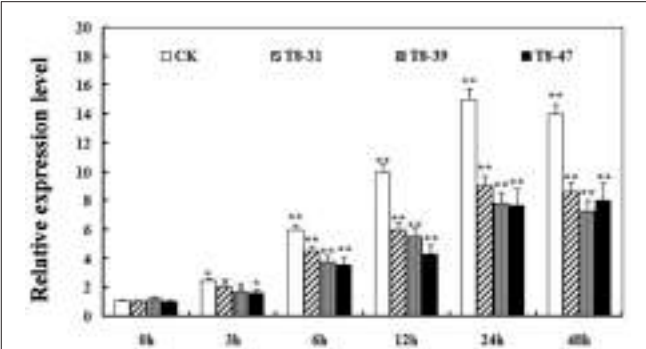
To test whether GmIFR protein could regulate stress-related genes expression in the isoflavonoids synthesis pathway, the expression of *GmIFR* and three stress-related genes (*GmPAL*, *Gm4CL*, *GmCHS*) was analyzed in transgenic soybean plants and non-transgenic plants using qRT-PCR at 0, 6, 12, 24, 48, 64 h after incubation with *P. sojae*. As shown in Figure 8, the transcript levels of *GmPAL*, *Gm4CL*, *GmCHS* were induced after incubation with *P. sojae* in transgenic soybean plants and non-transgenic soybean, and the transcript levels of the three genes were significantly higher than those of non-transgenic soybean plants at the same time point.



DISCUSSION

In this study, we identified a novel *GmIFR* gene that encodes for a NAD(P)H -dependant oxidoreductase, enhances resistance to *P. sojae* when over-expressed in soybean. The gene encoding isoflavanoid reductase (IFR), one of the key enzymes in isoflavanoid phytoalexin biosynthesis, was first cloned from alfalfa (*Medicago sativa* L.; Paiva et al., 1991). However, there is little knowledge about the biological function of IFR in soybean. Here, we report for the first time that *GmIFR* transgenic soybean plants inoculated with *P. sojae* display significantly altered responses to pathogen infection.

Plants encounter a range of environmental stresses in their natural environments and have evolved a wide range of mechanisms to cope with them (Dixon and Paiva, 1995; Zhang et al., 2008). There are multiple stress perception and signaling pathways, some of which are specific, whereas others cross-talk at various steps (Kunkel and Brooks, 2002; Chinnusamy et al., 2004; Fujita et al., 2006; Rípodas et al., 2013). It has been reported that higher levels of IFR determining fungal resistance in response to *A. rabiei* in chickpea (Daniel et al., 1990). In the present study, we demonstrated that overexpression of the *GmIFR* gene improved resistance to *P. sojae* in soybean.



Moreover, the genes with high sequence similarity to IFRs have been identified in non-leguminous plants and are called isoflavanone reductases like (IRL; Shoji et al., 2002). In most cases, IRLs might involve in responses to biotic or abiotic stresses (Shoji et al., 2002; Zhu et al., 2009; Cheng et al., 2013). A recent study suggested that GbIRL is involved in regulating ABA, JA, and ET stress responses in Ginkgo (Cheng et al., 2013). In this study, the expression of *GmIFR* following various stress treatments was analyzed. The results showed that inoculation with *P. sojae* as biotic stress and woundings as abiotic stress

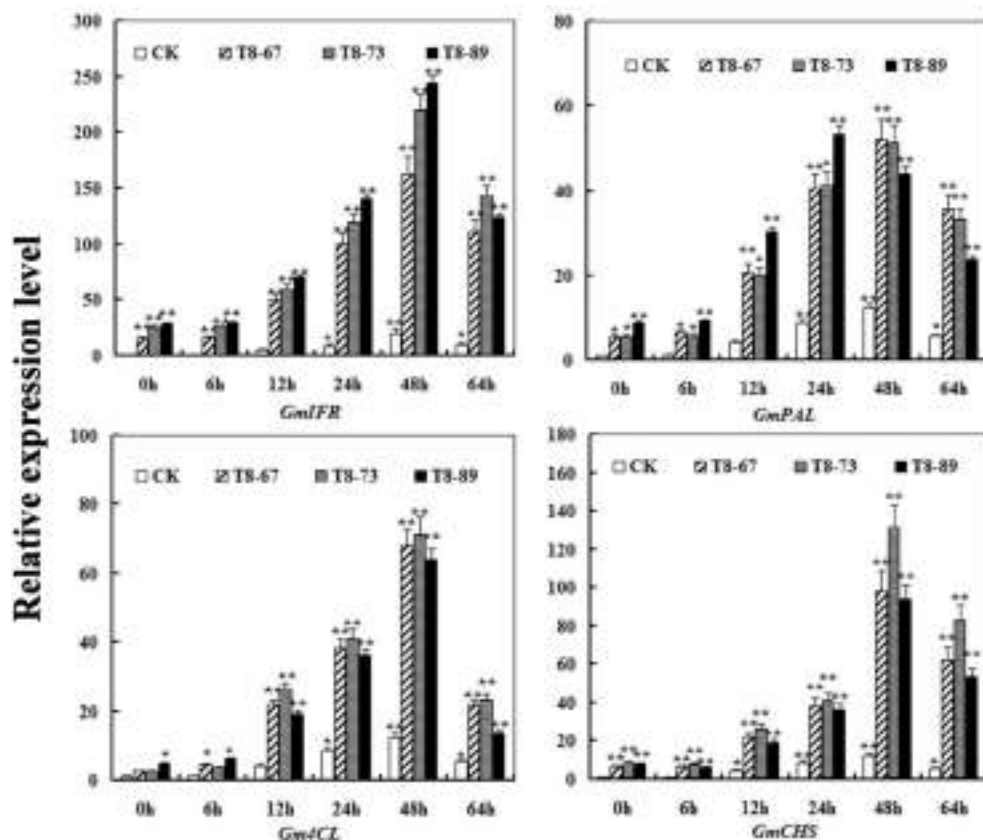


FIGURE 8 | The transcript levels of the three genes (*GmPAL*, *Gm4CL*, *GmCHS*) in *GmIFR* transgenic and non-transgenic soybean plants after *P. sojae* infection using quantitative RT-PCR analysis. The amplification of the soybean *Actin* (*GmActin4*) gene was used as an internal control to normalize all the data. The relative transcript levels of the genes were quantified compared with mock plants at the same time point. The experiment was performed on three biological replicates with their respective three technical replicates and statistically analyzed using Student's *t*-test (**P* < 0.05; ***P* < 0.01). Bars indicate standard error of the mean.

significantly increased the transcript levels of *GmIFR* in soybean plants. The expression of *GmIFR* was also induced by treatments with SA, ET, JA, and ABA. ABA is a phytohormone that is extensively involved in responses to abiotic stresses such as drought and low temperature, as well as osmotic stress (Skriver and Mundy, 1990). In contrast, the phytohormones SA, JA, and ET play central roles in biotic stress signaling following pathogen infection (Pieterse et al., 2009; Robert-Seilaniantz et al., 2011; Sugano et al., 2013). Therefore, it is possible to speculate that *GmIFR* likely plays an important role in responsive to biotic stresses in soybean. Moreover, it has been reported that IFR proteins as the key enzymes can catalyze reductase reactions (Paiva et al., 1991; Gang et al., 1999). For instance, IFR can convert 2'-hydroxyformononetin of the isoflavanoid substrates to (3R)-vestitone in alfalfa (Paiva et al., 1991). In Ginkgo, the recombinant GbIRL1 protein could catalyze the formation of the TDDC, IDDDC from DDDC, DDC (Cheng et al., 2013). In this work, we determined the recombinant *GmIFR* protein could catalyze oxidoreductase reaction using enzyme assays. Therefore, it is proven that *GmIFR* has isoflavone reductase activity.

There have been some reports about the inhibition of glyceollin on several lines of pathogen species (Lyne et al.,

1976; Kim et al., 2010a, 2012; Nwachukwu et al., 2013). More specifically, the glyceollin can resist to *Phytophthora megasperma* var. *sojae* in soybean (Lyne et al., 1976; Hahn et al., 1985; Lygin et al., 2010, 2013). In addition, Boue and Raina (2003) noted that the fungi *Aspergillus flavus*, *Aspergillus niger*, *Aspergillus oryzae*, and *Aspergillus flavus* were all able to induce glyceollin in soybean. Glyceollin revealed a remarkable antimicrobial effect against *Phytophthora capsici* and *Sclerotinia scotiorum* by Kim et al. (2010a). Moreover, It has been reported that IFR was a key enzyme involved in the synthesis of the glyceollins from daidzein which was the essential component of the isoflavones (Graham et al., 1990; Oliver et al., 2003). In this work, we detected the content of daidzein, genistein, glycinein and the relative content of glyceollins in transgenic soybean seeds and non-transgenic soybean seeds. The results showed that the daidzein content greatly reduced in transgenic soybean seeds, while levels of genistein and glycinein had little change compared to those of the non-transgenic soybean seeds. The relative content of glyceollins in the transgenic plants was significantly higher than that of non-transgenic plants. Therefore, we suggested that *GmIFR* might improve the resistance to *P. sojae* in soybean when overexpression likely by increasing the accumulation of

glyceollins. It has been reported that the biosynthesis of glyceollin via the isoflavanoid branch of the phenylpropanoid pathway (Ng et al., 2011) and glyceollin as a phytoalexin could response to pathogen invasion (Hahn et al., 1985; Lygin et al., 2010; Kim et al., 2012). PAL, 4CL, and CHS play an important role in the isoflavanoid branch of the phenylpropanoid pathway (Vogt, 2010; Yi et al., 2010). Here, we studied the transcript levels change of the three genes (*GmPAL*, *GmCHS*, *Gm4CL*) after incubation with *P. sojae* in transgenic and non-transgenic soybean plants. We found that these genes were induced after incubation with *P. sojae* and there was up-regulation of the transcript in transgenic soybean plants. We speculated that the three genes (*GmPAL*, *GmCHS*, *Gm4CL*) might play a cooperation role on the biosynthesis of glyceollin which might improve resistance to *P. sojae* in soybean.

Plants experience a variety of environmental stresses likely leading to the generation of ROS (Sies, 1991). Although ROS may be essential to maintain homoeostasis, the generation of ROS, within certain boundaries, is harmful at the high concentration (Kim et al., 2012). However, glyceollins as major isoflavanoid phytoalexin in leguminous plants, showed strong antioxidant activity and ROS scavenging potential when assessed by an *in vitro* model (Kim et al., 2010a, 2012). Moreover, Kim et al. (2010b) reported that overexpression of *OsIRL* in transgenic rice plants promotes resistance to ROS. A possible interpretation is that the IRLs contain a putative NAD (P) domain related to oxidation/reduction properties (Babiychuk et al., 1995; Petrucco et al., 1996). The different roles of ROS in plants interactions with special emphasis on fungal and oomycete pathogens have also been reported (Shetty et al., 2008). For example, *Blumeria graminis* f. sp. *hordei* can induce ROS accumulation in barley (Hückelhoven and Kogel, 2003) and *Septoria tritici* can induce ROS accumulation in wheat (Shetty et al., 2003). Thus, it can be deduced that the plants can improve resistance to pathogen by scavenge excess ROS. Consistent with these, we detected the relative expression levels of ROS in transgenic soybean plants and non-transgenic plants after incubation with *P. sojae*, and found that the

relative expression levels of ROS in transgenic plants were significantly lower than those of control plants. Overexpression of *GmIFR* in transgenic soybean plants can increase the content of glyceollins or *GmIFR* itself behave as an antioxidant to scavenge ROS, which might improve resistance to *P. sojae* in soybean.

ACKNOWLEDGMENTS

The research was supported through funding from the Heilongjiang Province outstanding youth fund (JC201308), NSFC Projects (30971811, 31071439, 31171577, 31101167), Natural Science Foundation of Heilongjiang Province (C2015010), the Specialized Research Fund for the Doctoral Program of Higher Education (20112325120005), the Science and Technology Innovation Project in Harbin (2012RFQXN011, 2012RFXXN019), and the Research Fund for Young Teachers through NEAU (2012 RCB 08).

SUPPLEMENTARY MATERIAL

The Supplementary Material for this article can be found online at: <http://journal.frontiersin.org/article/10.3389/fpls.2015.01024>

Supplementary Table S1 | Oligonucleotide primers used in this study.

Supplementary Figure S1 | The nucleotide sequence of GmIFR cDNA together with its predicted amino acid sequence. The NAD (P) domain is underlined.

Supplementary Figure S2 | Phylogenetic analysis and sequence alignment of GmIFR in the leguminous plants genome. **(A)** The predicted three-dimensional model of the IFR. **(B)** Phylogenetic relationships of GmIFR with IFRs proteins; the phylogenetic tree was constructed using amino acid sequences of the IFRs protein from other species. The plant species and GenBank accession numbers were as follows: *Glycine max* GmIFR (NM_001254100); *Phaseolus vulgaris* PvIFR (XP_007156276.1), *Cicer arietinum* CaIFR (XP_004509553.1), *Medicago truncatula* MtIFR (AFK37791.1), *Lotus japonicus* LjIFR (BAF34845.1), *Glycine soja* GsIFR (KHN36092.1), *Medicago sativa* MsIFR (CAA41106), *Pisum sativum* PsIFR (P52576.1). **(C)** The conserved NAD (P) domain of the IFR group proteins.

REFERENCES

- Babiychuk, E., Kushnir, S., Belles-Boix, E., Van Montagu, M., and Inz'e, D. (1995). *Arabidopsis thaliana* NADPH oxidoreductase homologs confer tolerance of yeast toward the thiol-oxidizing drug diamide. *J. Biol. Chem.* 270, 26224–26231. doi: 10.1074/jbc.270.44.26224
- Banks, S. W., and Dewick, P. M. (1983). Biosynthesis of glyceollins I, II and III in soybean. *Phytochemistry* 22, 2729–2733. doi: 10.1016/S0031-9422(00)97682-9
- Boue, S. M., Carter, C. H., Ehrlich, K. C., and Clevell, T. E. (2000). Induction of the soybean phytoalexins coumestrol and glyceollin by *Aspergillus*. *J. Agric. Food Chem.* 48, 2167–2172. doi: 10.1021/jf9912809
- Boue, S. M., and Raina, A. K. (2003). Effects of plant flavonoids on fecundity, survival, and feeding of the Formosan subterranean termite. *J. Chem. Ecol.* 29, 2575–2584. doi: 10.1023/A:1026318203775
- Cheng, H., Li, L. L., Xu, F., Wang, Y., Yuan, H. H., Wu, C. H., et al. (2013). Expression patterns of an isoflavone reductase-like gene and its possible roles in secondary metabolism in *Ginkgo biloba*. *Plant Cell Rep.* 32, 637–650. doi: 10.1007/s00299-013-1397-2
- Chinnusamy, V., Schumaker, K., and Zhu, J. K. (2004). Molecular genetic perspectives on cross-talk and specificity in abiotic stress signalling in plants. *J. Exp. Bot.* 55, 225–236. doi: 10.1093/jxb/erh005
- Cooper, J. D., Qiu, F., and Paiva, N. L. (2002). Biotransformation of an exogenously supplied isoflavanoid by transgenic tobacco cells expressing alfalfa isoflavone reductase. *Plant Cell Rep.* 20, 876–884. doi: 10.1007/s00299-001-0404-1
- Daniel, S., Tiemann, K., Wittkampf, U., Bless, W., Hinderer, W., and Barz, W. (1990). Elicitor-induced metabolic changes in cell cultures of chickpea (*Cicer arietinum* L.) cultivars resistant and susceptible to *Ascochyta rabiei*. *Planta* 182, 270–278.
- Dixon, R. A., and Paiva, N. L. (1995). Stress-induced phenylpropanoid metabolism. *Plant Cell* 7, 1085–1097. doi: 10.1105/tpc.7.7.1085
- Dou, D. L., Wang, B. S., Zhu, S. W., Tang, Y. X., Wang, Z. X., Sun, J. S., et al. (2003). Transgenic tobacco with NDR1 gene improved its resistance to two fungal disease. *Sci. Agric. Sin.* 36, 1120–1124.
- Fehr, W. R., Caviness, C. E., Burmood, D. T., and Pennington, J. (1971). Stage of development descriptions for soybeans, *Glycine max* (L.) Merrill. *Crop Sci.* 11, 929–931. doi: 10.2135/cropsci1971.0011183X001100060051x

- Fischer, D., Ebeanau-Jehle, C., and Grisebach, H. (1990). Phytoalexin synthesis in soybean: purification and characterization of NADPH: 20-hydroxydaidzein oxidoreductase from elicitor-challenged soybean cellcultures. *Arch. Biochem. Biophys.* 276, 390–395. doi: 10.1016/0003-9861(90)90737-J
- Fujita, M., Fujita, Y., Noutoshi, Y., Takahashi, F., Narusaka, Y., Yamaguchi-Shinozaki, K., et al. (2006). Crosstalk between abiotic and biotic stress responses: a current view from the points of convergence in the stress signaling networks. *Curr. Opin. Plant Biol.* 9, 436–442. doi: 10.1016/j.pbi.2006.05.014
- Gang, D. R., Kasahara, H., Xia, Z. Q., Vander Mijnsbrugge, K., Bauw, G., Boerjan, W., et al. (1999). Evolution of plant defense mechanisms: relationships of phenylcoumaran benzylic ether reductases to pinoresinol lariciresinol and isoflavone reductases. *J. Biol. Chem.* 274, 7516–7527. doi: 10.1074/jbc.274.11.7516
- Graham, T. L., Kim, J. E., and Graham, M. Y. (1990). Role of constitutive isoflavone conjugates in the accumulation of glyceollin in soybean infected with *Phytophthora megasperma*. *Mol. Plant Microbe* 3, 157–166. doi: 10.1094/MPMI-3-157
- Guo, L., Dixon, R. A., and Paiva, N. L. (1994). Conversion of vestitone to medicarpin in alfalfa (*Medicago sativa* L.) is catalyzed by two independent enzymes. *J. Biol. Chem.* 269, 22372–22378.
- Hahn, M. G., Bonhoff, A., and Grisebach, H. (1985). Quantitative localization of the phytoalexin glyceollinI in relation to fungal hyphae in soybean roots infected with *Phytophthora megasperma* f. sp. *glycinea*. *Plant Physiol.* 77, 591–601. doi: 10.1104/pp.77.3.591
- Hückelhoven, R., and Kogel, K. H. (2003). Reactive oxygen intermediates in plant-microbe interactions: who is who in powdery mildew resistance? *Planta* 216, 891–902. doi: 10.1007/s00425-003-0973-z
- Kim, H. J., Lim, J. S., Kim, W. K., and Kim, J. S. (2012). Soybean glyceollins: biological effects and relevance to human health. *Proc. Nutr. Soc.* 71, 166–174. doi: 10.1017/S0029665111003272
- Kim, H. J., Suh, H. J., Kim, J. H., Park, S., Joo, Y. C., and Kim, J. S. (2010a). Antioxidant activity of glyceollins derived from soybean elicited with *Aspergillus sojae*. *Agric. Food Chem.* 58, 11633–11638. doi: 10.1021/jf102829z
- Kim, S. G., Kim, S. T., Wang, Y. M., Kim, S. K., Lee, C. H., Kim, K. K., et al. (2010b). Overexpression of rice isoflavone reductase-like gene (*OsIRL*) confers tolerance to reactive oxygen species. *Physiol. Plant* 138, 1–9. doi: 10.1111/j.1399-3054.2009.01290.x
- Kim, S. T., Cho, K. S., Kim, S. G., Kang, S. Y., and Kang, K. Y. (2003). A rice isoflavone reductase-like gene, *OsIRL*, is induced by rice blast fungal elicitor. *Mol. Cells* 16, 224–231.
- Kunkel, B. N., and Brooks, D. M. (2002). Cross talk between signaling pathways in pathogen defense. *Curr. Opin. Plant Biol.* 5, 325–331. doi: 10.1016/S1369-5266(02)00275-3
- Lers, A., Bud, S., Lomanic, E., Droby, S., and Chalutz, E. (1998). The expression of a grapefruit gene encoding an isoflavone reductase-like protein is induced in response to UV-irradiation. *Plant Mol. Biol.* 36, 847–856. doi: 10.1023/A:1005996515602
- Lin, W. (1983). Isolation of mesophyll protoplasts from mature leaves of soybeans. *Plant Physiol.* 73, 1067–1069. doi: 10.1104/pp.73.4.1067
- Lygin, A. V., Hill, C. B., Zernova, O. V., Crull, L., Widholm, J. M., Hartman, G. L., et al. (2010). Response of soybean pathogens to glyceollin. *Phytopathology* 100, 897–903. doi: 10.1094/PHYTO-100-9-0897
- Lygin, A. V., Zernova, O. V., Hill, C. B., Kholina, N. A., Widholm, J. M., Hartman, G. L., et al. (2013). Glyceollin is an important component of soybean plant defense against *Phytophthora sojae* and *Macromomina phaseolina*. *Phytopathology* 103, 984–994. doi: 10.1094/PHYTO-12-12-0328-R
- Lyne, R. L., Mulheirn, L. J., and Leworthy, D. P. (1976). New pterocarpinoid phytoalexins of soybean. *J. Chem. Soc. Chem. Commun.* 13, 497–498. doi: 10.1039/c39760000497
- Morris, P. F., Savard, M. E., and Ward, E. W. B. (1991). Identification and accumulation of isoflavonoids and isoflavone glucosides in soybean leaves and hypocotyls in resistance responses to *Phytophthora megasperma* f. sp. *glycinea*. *Physiol. Mol. Plant* 39, 229–224. doi: 10.1016/0885-5765(91)9006-4
- Morrison, R. H., and Thorne, J. C. (1978). Inoculation of detached cotyledons for screening soybeans against two races of *Phytophthora megasperma* var. *sojae*. *Crop Sci.* 18, 1089–1091. doi: 10.2135/cropsci1978.0011183X001800060049x
- Ng, T. B., Ye, X. J., Wong, J. H., Fang, E. F., Chan, Y. S., Pan, W. L., et al. (2011). Glyceollin, a soybean phytoalexin with medicinal properties. *Appl. Microbiol. Biotechnol.* 90, 59–68. doi: 10.1007/s00253-011-3169-7
- Nwachukwu, I. D., Luciano, F. B., and Udenigwe, C. C. (2013). The inducible soybean glyceollin phytoalexins with multifunctional health-promoting properties. *Food Res. Int.* 54, 1208–1216. doi: 10.1016/j.foodres.2013.01.024
- Oliver, Y., Shi, J., Hession, A. O., Maxwell, C. A., McGongigle, B., and Odell, J. T. (2003). Metabolic engineering to increase isoflavone biosynthesis in soybean seed. *Phytochemistry* 63, 753–763. doi: 10.1016/S0031-9422(03)00345-5
- Paiva, N. L., Edwards, R., Sun, Y. J., Hrazdina, G., and Dixon, R. A. (1991). Stress responses in alfalfa (*Medicago sativa* L.) 11. Molecular cloning and expression of alfalfa isoflavone reductase, a key enzyme of isoflavonoid phytoalexin biosynthesis. *Plant Mol. Biol.* 17, 653–667. doi: 10.1007/BF00037051
- Partridge, J. E., and Keen, N. T. (1977). Soybean phytoalexins: rates of synthesis are not regulated by activation of initial enzymes in flavonoid biosynthesis. *J. Physiol. Biochem.* 67, 50–55. doi: 10.1094/phyto-67-50
- Paz, M. M., Shou, H. X., Guo, Z. B., Zhang, Z. Y., Banerjee, A. K., and Wang, K. (2004). Assessment of conditions affecting *Agrobacterium*-mediated soybean transformation using the cotyledonary node explant. *Euphytica* 136, 167–179. doi: 10.1023/B:EUPH.0000030669.75809.dc
- Petrucco, S., Bolchi, A., Foroni, C., Percudani, R., Rossi, G. L., and Ottonello, S. (1996). A maize gene encoding an NADPH binding enzyme highly homologous to isoflavone reductases is activated in response to sulfur starvation. *Plant Cell* 8, 69–80. doi: 10.1105/tpc.8.1.69
- Pieterse, C. M. J., Leon-Reye, A., Van der Ent, S., and Van Wees S. C. (2009). Networking by smallmolecule hormones in plant immunity. *Nat. Chem. Biol.* 5, 308–316. doi: 10.1038/nchembio.164
- Qian, H. F., Chen, W., Sun, L. W., Jin, Y. X., Liu, W. P., and Fu, Z. W. (2009). Inhibitory effects of paraquat on photosynthesis and the response to oxidative stress in *Chlorella vulgaris*. *Ecotoxicology* 18, 537–543. doi: 10.1007/s10646-009-0311-8
- Ripodas, C., Via, V. D., Aguilar, O. D., Zanetti, M. E., and Blanco, F. A. (2013). Knock-down of a member of the isoflavone reductase gene family impairs plant growth and nodulation in *Phaseolus vulgaris*. *Plant Physiol. Bioch.* 68, 81–89. doi: 10.1016/j.jplphys.2013.04.003
- Robert-Seilaniantz, A., Grant, M., and Jones, J. D. G. (2011). Hormone crosstalk in plant disease and defense: more than just jasmonate-salicylate antagonism. *Annu. Rev. Phytopathol.* 49, 317–343. doi: 10.1146/annurev-phyto-073009-114447
- Shetty, N. P., Kristensen, B. K., Newman, M. A., Møller, K., Gregersen, P. L., and Jørgensen, H. J. L. (2003). Association of hydrogen peroxide with restriction of *Septoria tritici* in resistant wheat. *Physiol. Mol. Plant* 62, 333–346. doi: 10.1016/S0885-5765(03)00079-1
- Shetty, N. P., Lyngs Jørgensen, H. J., Jensen, J. D., Collinge, D. B., and Shetty, H. S. (2008). Roles of reactive oxygen species in interactions between plants and pathogens. *Eur. J. Plant Pathol.* 121, 267–280. doi: 10.1007/s10658-008-9302-5
- Shoji, T., Winz, R., Iwase, T., Nakajima, K., Yamada, Y., and Hashimoto, T. (2002). Expression patterns of two tobacco isoflavone reductase-like genes and their possible roles in secondary metabolism in tobacco. *Plant Mol. Biol.* 50, 427–440. doi: 10.1023/A:1019867732278
- Sies, H. (1991). Oxidative stress: from basic research to clinical application. *Am. J. Med.* 91, 31–38. doi: 10.1016/0002-9343(91)90281-2
- Skriver, K., and Mundy, J. (1990). Gene expression in response to abscisic acid and osmotic stress. *Plant Cell* 2:503. doi: 10.1105/tpc.2.6.503
- Somerville, C., and Somerville, S. (1999). Plant functional genomics. *Science* 285, 380–383. doi: 10.1126/science.285.5426.380
- Soosaar, J. L. M., Burch-Smith, T. M., and Dinesh-Kumar, S. P. (2005). Mechanisms of plant resistance to viruses. *Nat. Rev. Microbiol.* 3, 789–798. doi: 10.1038/nrmicro1239
- Sugano, S., Sugimoto, T., Takatsujii, H., and Jiang, J. (2013). Induction of resistance to *Phytophthora sojae* in soybean (*Glycine max*) by salicylic acid and ethylene. *Plant Pathol.* 62, 1048–1056. doi: 10.1111/ppa.12011
- Sun, Y. J., Wu, Q. D., VanEtten, H. D., and Hrazdina, G. (1991). Stereoisomerism in plant disease resistance: induction and isolation of the 7, 20-dihydroxy-40, 50-methylenedioxyisoflavone reductase, an enzyme introducing chirality during synthesis of isoflavanoid phytoalexins in pea (*Pisum sativum* L.). *Arch. Biochem. Biophys.* 284, 167–173. doi: 10.1016/0003-9861(91)90279-R

- Takabatake, R., Ando, Y., Seo, S., Katou, S., Tsuda, S., Ohashi, Y., et al. (2007). MAP kinases function downstream of HSP90 and upstream of mitochondria in TMV resistance gene *N*-mediated hypersensitive cell death. *Plant Cell Physiol.* 48, 498–510. doi: 10.1093/pcp/pcm021
- Tamura, K., Dudley, J., Nei, M., and Kumar, S. (2007). MEGA4: molecular evolutionary genetics analysis (MEGA) software version 4.0. *Mol. Biol. Evol.* 24, 1596–1599. doi: 10.1093/molbev/msm092
- Vogt, T. (2010). Phenylpropanoid biosynthesis. *Mol. Plant* 3, 2–20. doi: 10.1093/mp/ssp106
- Wang, X. Q., He, X. Z., Lin, J. Q., Shao, H., Chang, Z. Z., and Dixon, R. A. (2006). Crystal structure of isoflavone reductase from alfalfa (*Medicago sativa* L.). *J. Mol. Biol.* 358, 1341–1352. doi: 10.1016/j.jmb.2006.03.022
- Wang, Y., Han, Y. P., Teng, W. L., Zhao, X., Li, Y. G., Wu, L., et al. (2014). Expression quantitative trait loci infer the regulation of isoflavone accumulation in soybean (*Glycine max* L. Merr.) seed. *BMC Genomics* 15:680. doi: 10.1186/1471-2164-15-680
- Ward, E. W. B., Lazarovits, G., Unwin, C. H., and Buzzell, R. I. (1979). Hypocotyl reactions and glyceollin in soybeans inoculated with zoospores of *Phytophthora megaspuma* var. *sojae*. *Phytopathology* 69, 951–955. doi: 10.1094/Phyto-69-951
- Xu, P. F., Chen, W. Y., Lv, H. Y., Fan, S. J., Wang, X., Jiang, L. Y., et al. (2012). Differentially expressed genes of soybean during infection by *Phytophthora sojae*. *J. Integr. Agric.* 11, 368–377. doi: 10.1016/S2095-3119(12)60021-5
- Yi, J. X., Derynck, M. R., Li, X. Y., Telmer, P., Marsolais, F., and Dhaubhadel, S. (2010). A single-repeat MYB transcription factor, GmMYB176, regulates CHS8 gene expression and affects isoflavanoid biosynthesis in soybean. *Plant J.* 62, 1019–1034. doi: 10.1111/j.1365-313x.2010.04214.x
- Yoo, S. D., Cho, Y. H., and Sheen, J. (2007). Arabidopsis mesophyll protoplasts: a versatile cell system for transient gene expression analysis. *Nat. Protoc.* 2, 1565–1572. doi: 10.1038/nprot.2007.199
- Yoshikawa, M., Yamauchi, K., and Masago, H. (1978). Glyceollin: its role in restricting fungal growth in resistant soybean hypocotyls infected with *Phytophthora megasperma* var. *sojae*. *Physiol. Mol. Plant* 12, 73–82. doi: 10.1016/0048-4059(78)90020-6
- Zeng, G. L., Li, D. M., Han, Y. P., Teng, W. L., Wang, J., Qiu, L. Q., et al. (2009). Identification of QTL underlying isoflavone contents in soybean seeds among multiple environments. *Theor. Appl. Genet.* 118, 1455–1463. doi: 10.1007/s00122-009-0994-5
- Zhang, G. Y., Chen, M., Chen, X. P., Xu, Z. S., Guan, S., Li, L. C., et al. (2008). Phylogeny, gene structures, and expression patterns of the ERF gene family in soybean (*Glycine max* L.). *J. Exp. Bot.* 59, 4095–4107. doi: 10.1093/jxb/ern248
- Zhang, S. Z., Xu, P. F., Wu, J. J., Allen, X., Zhang, J. X., Li, W. B., et al. (2010). Races of *Phytophthora sojae* and their virulences on commonly grown soybean varieties in Heilongjiang, China. *Plant Dis.* 94, 87–91. doi: 10.1094/PDIS-94-1-0087
- Zhu, Q., Guo, T., Sui, S., Liu, G., Lei, X., Luo, L., et al. (2009). Molecular cloning and characterization of a novel isoflavone reductase-like gene (*FcIRL*) from high flavonoids-producing callus of *Fagopyrum cymosum*. *Acta Pharmacol. Sin.* 44, 809–819.

Conflict of Interest Statement: The authors declare that the research was conducted in the absence of any commercial or financial relationships that could be construed as a potential conflict of interest.

Copyright © 2015 Cheng, Li, Dong, Zhang, Fan, Jiang, Wang, Xu and Zhang. This is an open-access article distributed under the terms of the Creative Commons Attribution License (CC BY). The use, distribution or reproduction in other forums is permitted, provided the original author(s) or licensor are credited and that the original publication in this journal is cited, in accordance with accepted academic practice. No use, distribution or reproduction is permitted which does not comply with these terms.



The Novel Gene *VpPR4-1* from *Vitis pseudoreticulata* Increases Powdery Mildew Resistance in Transgenic *Vitis vinifera* L.

Lingmin Dai^{1,2,3}, Dan Wang^{1,2,3}, Xiaoqing Xie^{1,2,3}, Chaohong Zhang^{1,2,3}, Xiping Wang^{1,2,3}, Yan Xu^{1,2,3}, Yuejin Wang^{1,2,3*} and Jianxia Zhang^{1,2,3*}

¹ College of Horticulture, Northwest A&F University, Yangling, China, ² Key Laboratory of Horticultural Plant Biology and Germplasm Innovation in Northwest China, Ministry of Agriculture, Yangling, China, ³ State Key Laboratory of Crop Stress Biology in Arid Areas, Northwest A&F University, Yangling, China

OPEN ACCESS

Edited by:

Sylvain Jeandroz,
Agrosup Dijon, France

Reviewed by:

Anil Kumar Singh,
ICAR-Indian Institute of Agricultural
Biotechnology, India
Sophie Trouvelot,
University of Burgundy, France

*Correspondence:

Yuejin Wang
wangyj@nwsuaf.edu.cn;
Jianxia Zhang
zhangjx666@126.com

Specialty section:

This article was submitted to
Plant Physiology,
a section of the journal
Frontiers in Plant Science

Received: 24 December 2015

Accepted: 06 May 2016

Published: 27 May 2016

Citation:

Dai L, Wang D, Xie X, Zhang C, Wang X, Xu Y, Wang Y and Zhang J (2016) The Novel Gene *VpPR4-1* from *Vitis pseudoreticulata* Increases Powdery Mildew Resistance in Transgenic *Vitis vinifera* L. Front. Plant Sci. 7:695. doi: 10.3389/fpls.2016.00695

Pathogenesis-related proteins (PRs) can lead to increased resistance of the whole plant to pathogen attack. Here, we isolate and characterize a PR-4 protein (*VpPR4-1*) from a wild Chinese grape *Vitis pseudoreticulata* which shows greatly elevated transcription following powdery mildew infection. Its expression profiles under a number of abiotic stresses were also investigated. Powdery mildew, salicylic acid, and jasmonic acid methyl ester significantly increased the *VpPR4-1* induction while NaCl and heat treatments just slightly induced *VpPR4-1* expression. Abscisic acid and cold treatment slightly affected the expression level of *VpPR4-1*. The *VpPR4-1* gene was overexpressed in 30 regenerated *V. vinifera* cv. Red Globe via *Agrobacterium tumefaciens*-mediated transformation and verified by the Western blot. The 26 transgenic grapevines exhibited higher expression levels of PR-4 protein content than wild-type vines and six of them were inoculated with powdery mildew which showed that the growth of powdery mildew was repressed. The powdery mildew-resistance of Red Globe transformed with *VpPR4-1* was enhanced inoculated with powdery mildew. Moreover, other powdery mildew resistant genes were associated with feedback regulation since *VpPR4-1* is in abundance. This study demonstrates that PR-4 protein in grapes plays a vital role in defense against powdery mildew invasion.

Keywords: grapevine, pathogenesis-related protein-4 (PR-4), transformation, powdery mildew, qRT-PCR

INTRODUCTION

Pathogenesis-related proteins (PRs) are involved in higher-plant responses to environment stress. They can be triggered by a large amount of pathogens including fungi, bacteria, and viruses (Van Loon, 1985; Lamb et al., 1989; Linthorst and Van Loon, 1991). Pathogenesis-related proteins were first detected in tobacco leaves under tobacco mosaic virus attack (Van Loon and Van Kammen, 1970). A large number of PRs have since been isolated from a range of other plant species (Sels et al., 2008). Currently, 17 families of PRs have been classified, based on their amino acid sequence similarities, enzymatic activities and other biological properties. These families have been numbered in sequence of discovery (Sels et al., 2008; Sinha et al., 2014). Usually, PRs possess enzymatic functions – so, for example, PR-2 is a 1,3-β-glucanase (Kauffmann et al., 1987),

PR-7 has endoprotease activity, PR-9 is a peroxidase, and PR-10 is a ribonuclease (Lagrimini et al., 1987; Vera and Conejero, 1988; Park et al., 2004; Xu et al., 2010). Moreover, a number of them, e.g., PR-1 and PR-6, have been identified as having antifungal and proteinase inhibitory properties (Green and Ryan, 1972; Niderman et al., 1995). In addition, chitinase activity has been detected in PR-3, PR-4, PR-8, and PR-11 (Van Loon, 1982; Métraux et al., 1988; Melchers et al., 1994), with PR-4 being referred to as chitin-binding proteins.

The PR-4 proteins were first described as wound-inducible proteins and were termed win-1 and win-2 in potato (Stanford et al., 1989; Friedrich et al., 1991). Since then, several PR-4 proteins have been isolated and characterized. PR-4 is not only induced by wounding but also by ethanol, abscisic acid (ABA), salicylic acid (SA), 2,6-dichloroisonicotinic acid, methyl jasmonate (MeJA), sugar starvation, viruses, and fungi (Broekaert et al., 1990; Boll, 1991; Friedrich et al., 1991; Linthorst and Van Loon, 1991; Potter et al., 1993; Melchers et al., 1994; Chevalier et al., 1995; Gregersen et al., 1997; Lee et al., 2001; Bravo et al., 2003; Hamada et al., 2005; Park et al., 2005; Guevara-Morato et al., 2010). The PR-4 proteins possess a Barwin domain in the C-terminal which comes from a barley seed protein related to the wound-induced proteins (Svensson et al., 1992). The secondary structure analysis of the barley seed protein shows the protein contains a large four-stranded antiparallel β -sheet and a small parallel β -sheet (Ludvigsen and Poulsen, 1992a). The binding site of the Barwin domain to the tetramer N-acetyl glucosamine was investigated by three-dimensional structural analysis (Ludvigsen and Poulsen, 1992b). The PR-4 proteins are classified into classes I and II based on whether they have an N-terminal Hevein domain or not (Neuhaus et al., 1996). Wheatwin1 and wheatwin2 belong to class II of the PR-4 proteins and show antifungal activity by inhibiting fungal hyphal growth (Caruso et al., 1996, 2001; Huet et al., 2013). Furthermore, wheatwin1 is able to digest RNA from wheat and *Fusarium culmorum* (Caporale et al., 2004). The ribonuclease activity of wheat PR-4 proteins contributes to their antifungal activity (Bertini et al., 2009). In addition, a PR-4 in *Capsicum chinense* has been shown to exhibit deoxyribonuclease and ribonuclease in *in vitro* assays (Guevara-Morato et al., 2010). AtHEL, a class I PR-4 protein of *Arabidopsis*, was found to interact with a fungal lectin having deoxyribonuclease and ribonuclease activities (Bertini et al., 2012; Huet et al., 2013).

Grape production is principally of *Vitis vinifera* cultivars and is also principally geared toward winemaking. Fungal disease is a critical factor in this major international industry, leading to heavy financial penalties due to reductions in both fruit yield and in fruit quality. When infected by fungi, a number of grape PRs are induced, including PR-4 (Kortekamp, 2006). *V. pseudoreticulata* accession Baihe 35-1 is a distinct accession of Chinese wild grape, which possesses high resistance to Erysiphe necator and powdery mildew-induced genes had been isolated from the cDNA library of the high powdery mildew resistant Baihe-35-1 inoculated by Erysiphe necator (Yu et al., 2013). Moreover, *VpPR4* is different from the powdery

mildew resistance gene of *V. pseudoreticulata* that we have already studied before (Yu et al., 2013; Dai et al., 2015) or other PR4 gene from similar species in sequence. Powdery mildew can induce abundant expression of PR-4 in *V. vinifera* (Fung et al., 2008). However, the expression of *VpPR4* gene was significant higher than the *PR4* detected in the European grapevine control by cDNA library analyzing in our previous study (Zhu et al., 2012) which suggested that the characterization and expression of *VpPR4* is different compared with *VvPR4*. Moreover, the detailed function of PR-4 proteins in grape is unclear.

This study describes the detection and characterization of a PR-4 protein induced by powdery mildew (*Erysiphe necator* [Schw.] Burr) in the leaves of *V. pseudoreticulata* Baihe-35-1, and this gene expression profile following exposure to a range of plant hormones and abiotic stresses. The *PR-4* gene was overexpressed in the powdery mildew susceptible variety Red Globe which shows enhanced resistance to powdery mildew and disarranged expression patterns of related defense genes.

MATERIALS AND METHODS

Plant Materials and Stress Treatments

Grapevines (wild Chinese *V. pseudoreticulata* accession Baihe 35-1) were propagated by tissue culture and plantlets were transplanted to pots grown in a culture room (Yu et al., 2013). The inoculation of vine leaves with powdery mildew was carried out as previously described (Guan et al., 2011). The young leaves were inoculated by touching the adaxial surface of the leaves with PM cv. NAFU1 (KJ539202) colonies maintained on the greenhouse-grown grapes. Young grapevine plantlets (*V. pseudoreticulata* Baihe 35-1) 20–25 cm in height were selected for hormone treatments and the leaves were allowed to expand in a greenhouse. Treatments with 100 μ M SA, 50 μ M MeJA, or 100 μ M ABA were imposed by spraying these onto the fully expanded leaves. The solution of SA was 100 μ M in distilled water (Wang and Li, 2006), solution of MeJA was 50 μ M in 0.1% ethanol (Repka et al., 2004), and the solution of ABA was 100 μ M in distilled water (Seong et al., 2007). For the environmental treatments, grapevine plantlets (*V. pseudoreticulata* Baihe 35-1) were incubated in 4°C (cold) or 40°C (hot). For NaCl treatment, the grapevines in pots were watered with 500 mM NaCl (Yang et al., 2012).

Isolation of Full-length Coding Sequences of *VpPR4-1*

The well-known PR-4s were used to blast search the grape genome on <http://www.genoscope.cns.fr/externe/GenomeBrowser/Vitis/>. Three homologous sequences were isolated from the grape genome. One was a pseudogene and the other two were used as templates for homology-based cloning of *PR-4s* from *V. pseudoreticulata*. The amplified primers are listed in **Table 1**.

TABLE 1 | Primers used for RT-PCR or PCR reactions.

Gene	Primer sequence	Tm (°C)	Amplicon length (bp)
VpPR4-1 (JN977472) (Construct overexpression plasmid)	Forward: CCCTCGAGATGGAGAGGAGAGGCA Reverse: GCTCTAGATTAGTCACCACAGTTC	62.5 55.7	450
NPTII (AF485783) (Detect transgenic lines)	Forward: CCCTGAATGAACTGCAGGACG Reverse: CAATATCACGGGTAGCCAACG	56.3 54.4	520
VpPR4-1 (RT-PCR)	Forward: TCAGGCAACAGTGAGAATAGTG Reverse: TTAAGATGACCTGGCATAGC	53 53	114
NPR1 (XM_002281439) (RT-PCR)	Forward: GCGGAAGAGGCCAACGATTA Reverse: CTGGTGAGCCTTTGCTATT	51.8 52.4	107
PR1 (XM_002274239) (RT-PCR)	Forward: GGTTGTGTAGGAGTCCATTAG Reverse: TGTGAGCATTGAGGTAGTCTTG	54.8 53	103
PAL (JN858957) (RT-PCR)	Forward: CTGCGAGAAGGACTTGCTAAA Reverse: ACCTTCTGCATCAGTGGATATG	52.4 53	95
GAPDH (EF192466) (RT-PCR)	Forward: TCAAGGTCAAGGACTCTAACACC Reverse: CCAACAACGAAACATAGGAGCA	55.3 52.4	225

Alignment and Phylogenetic Analysis of PR-4 Proteins

Protein sequences of VpPR4-1 and other well-known PR-4s were aligned by DNAMAN using default parameters. The phylogenetic tree was constructed by Neighbor-joining method using Mega 5.0 software (Tamura et al., 2011). Bootstrap analysis was carried out using 1000 replicates.

Quantification of Gene Expression by Real-time PCR (qRT-PCR)

A modified SDS/phenol method was used to extract total RNA (Reid et al., 2006). First-strand cDNA synthesis and quantitative RT-PCR were carried out as Hou et al. (2013). The grape GAPDH gene (GenBank accession No. EF192466) was amplified as a normalized control. According to Dai et al. (2015), gene expression analysis was carried out by qRT-PCR with a Bio-Rad IQ5 Real-Time PCR Detection System (Hercules, CA, USA) using TaKaRa SYBR Premix Ex TaqTM II (Perfect Real Time). The qRT-PCR reaction was conducted in triplicate following parameters: 95°C for 10 s; 40 cycles of 94°C for 5 s and 60°C for 30 s. The normalized fold expression of RNA was calculated by comparison with the normalized control.

Binary Vector Construction and Genetic Transformation of Grape

Binary vector construction was carried out as Yu et al. (2013). The VpPR4-1 gene was PCR cloned in-frame into plasmid pART-CAM-S (Xu et al., 2014) using *Xba* I and *Xba* I restriction enzymes to generate 35S::VpPR4-1, which contained a kanamycin resistance selective marker. The binary construct was introduced into *Agrobacterium* strain GV3101 using electroporation.

Proembryonic masses of *V. vinifera* L. Red Globe, initiated from immature stamens and maintained from a previous study, were used for genetic transformation with VpPR4-1. Transformation was carried out via the *Agrobacterium*-mediated transformation system as described previously (Zhou et al., 2014; Dai et al., 2015).

Western Blotting

Total protein was extracted using phenol-based protocols as described previously (Vincent et al., 2006). The protein was fractionated by 5–10% SDS-PAGE and blotted to polyvinyl difluoride membranes (Roche) using a semi-dry blot apparatus as described by the manufacturer (Bio-Rad). The purified polyclonal antisera antibody of VpPR4-1 protein obtained from New Zealand rabbits immunized by purification of the prokaryotic expressed VpPR4-1 protein in our previously study (data not shown), and the polyclonal antisera was used at 1:2,000 dilution and secondary goat anti-rabbit IgG (TransGen Biotech) conjugated with alkaline phosphatase at 1:5,000 dilution. Detection was carried out using Pierce ECL Western Blotting Substrate (Thermo scientific) and imaged with Image Lab Software (Bio-Rad).

Trypan Blue Staining

The trypan blue staining is used for observing powdery mildew hyphal development and carried out according to Xiao et al. (2003) with minor modification. Briefly, grape leaves were picked and stained with the Trypan blue staining solution in a boiling water bath for 15 min and then allowed to rest at room temperature for 24 h. The samples were then incubated in chloral hydrate solution for 2–6 h at room temperature with the chloral hydrate saturated solution changed once and then incubated for a further 8 h at room temperature. The chloral hydrate solution was then removed and the tissue immersed in 70% glycerol and examined using a compound light microscope.

Statistical Analysis

Experimental results in Figures 2, 5, and 7 are mean values of triplicate experiments; error bars in Figures 2 and 5 indicate standard deviations (SD). Mean values and SD were calculated using SPSS 18.0 software (SPSS Inc, Chicago, IL, USA).

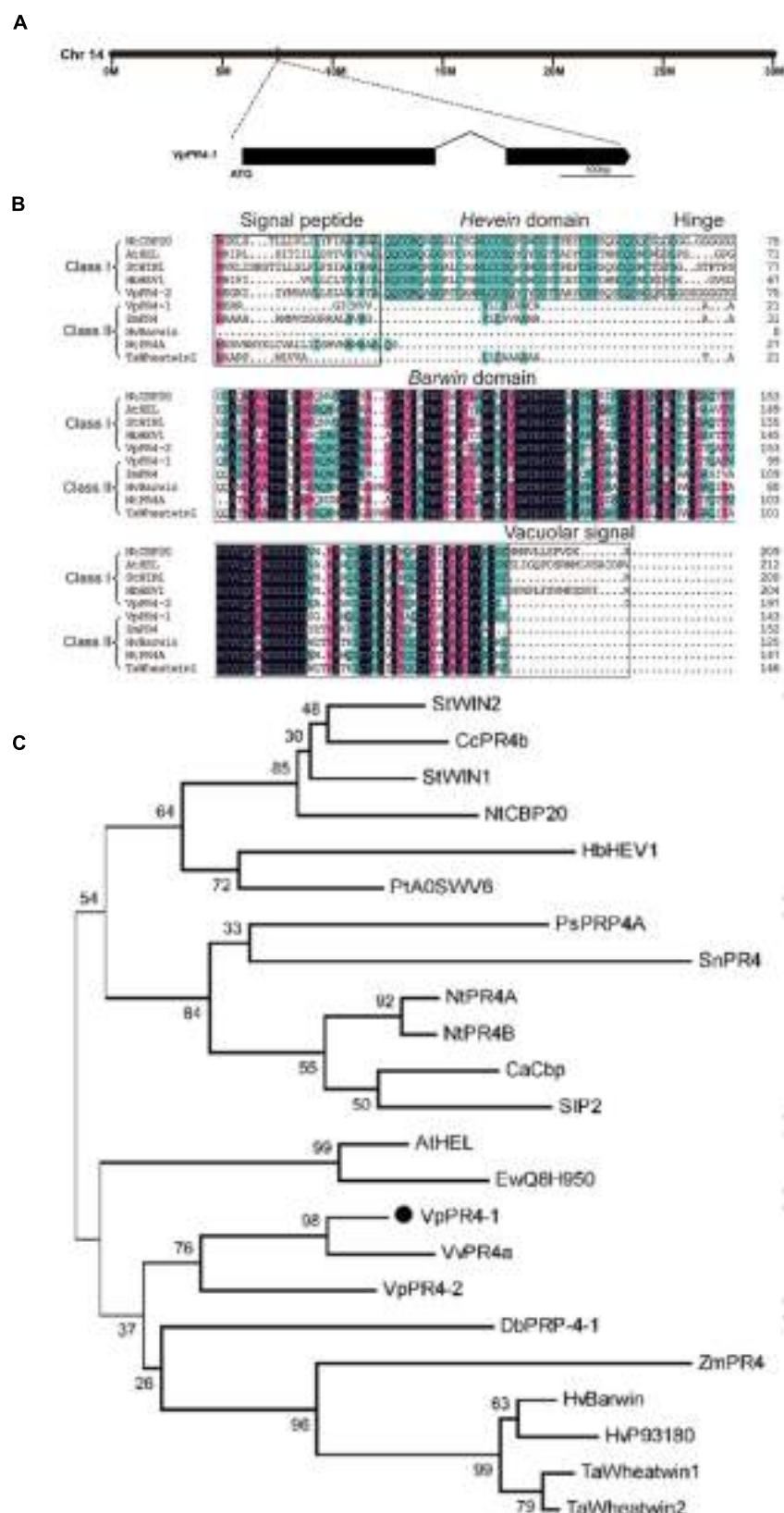


FIGURE 1 | Continued

FIGURE 1 | Continued

Phylogenetic analysis and alignment of PR-4 proteins. **(A)** Location on the chromosome and schematic representation of the *VpPR4-1* gene. **(B)** Sequence alignment of *VpPR4-1*. The conserved domains are shown above the sequences. Identical amino acids are shaded with black, and similar amino acids are shaded with pink (<100 and ≥75%) or blue (<75 and ≥50%). **(C)** Phylogenetic analysis of various PR-4-1 proteins. Class I, subgroup of PR-4 proteins which contain a *Hevein* domain. Class II, subgroup of PR-4s which do not have a *Hevein* domain. Accession numbers are: *VpPR4-1* (AEW12795; *Vp*, *Vitis pseudoreticulata*), *VpPR4-2* (KP274873), *StWIN2* (NP_001275628; *St*, *Solanum tuberosum*), *CcPR4b* (BAD11073; *Cc*, *Capsicum chinense*), *StWIN1* (XP_006347743), *NtCBP20* (AAB29960; *Nt*, *Nicotiana tabacum*), *HbHEV1* (P02877; *Hb*, *Hevea brasiliensis*), *PtA0SW6* (ABK63195; *Pt*, *Populus tremula* × *Populus alba*), *PsPRP4A* (AAF61434; *Ps*, *Pisum sativum*), *SnPR4* (CAA87070; *Sn*, *Sambucus nigra*), *NtPR4A* (XP_009763689), *NtPR4B* (XP_009614804), *CaCbp* (AFN21550; *Capsicum annuum*), *SIP2* (NP_001234083; *Sl*, *Solanum lycopersicum*), *AtHEL* (NP_187123; *At*, *Arabidopsis thaliana*), *EwQ8H950* (BAC16357; *Ew*, *Eutrema wasabi*), *VvPR4* (AAC33732; *Vv*, *Vitis vinifera*), *DbPRP-4-1* (AAB94514; *Db*, *Dioscorea bulbifera*), *ZmPR4* (AFW60484; *Zm*, *Zea mays*), *HvBarwin* (BAK04328; *Hv*, *Hordeum vulgare*), *HvP93180* (CAA71774), *TaWheatwin1* (O64392; *Ta*, *Triticum aestivum*), and *TaWheatwin2* (O64393).

RESULTS

Sequence Analysis of *VpPR4-1* from Wild Chinese *V. pseudoreticulata*

The full-length cDNA of *VpPR4-1* was homologous cloned from the cDNA library of high powdery mildew resistant *V. pseudoreticulata* Baihe 35-1 inoculated by powdery mildew (Zhu et al., 2012). The *VpPR4-1* gene is on the chromosome 14 of the whole genome of PN40024 (Jaillon et al., 2007), it is 432 base pairs (bp) long and codes for a unique polypeptide of 143 amino acids with two exons (Figure 1A) and possesses a Barwin domain (Figure 1B).

Numerous PR-4 proteins have been detected from a variety of different species. To understand the evolutionary relationships between these PR-4 proteins, alignment and phylogenetic analyses were carried out. Alignment analysis of PR-4s showed that all contained a Barwin domain. However, PR-4s can be divided into two classes on the basis of whether they have a Hevein domain. *VpPR4-1* fell into class II according to this classification scheme (Figure 1B). Phylogenetic analysis indicated that the PR-4s fell into two subgroups. The *VpPR4-1* is closely referred to the PR-4 protein (BAK04328) from *Hordeum vulgare* subsp. at the amino acid level (Figure 1C). *Vulgare* sharing 79.3% of sequence identity (Matsumoto et al., 2011). For other PR-4 proteins used for alignment and phylogenetic analyses, the sequence identities ranged from 61.7 to 76.7%.

Induction of *VpPR4-1* by Powdery Mildew, Exogenous Hormones, and Abiotic Stresses

PRs are usually induced by pathogen attack. Expression of the *VpPR4-1* induced by powdery mildew was demonstrated in the powdery mildew resistant genotype *V. pseudoreticulata* Baihe 35-1 (Figure 2A). Under normal conditions, the transcript level of *VpPR4-1* was very low. Upon infection with powdery mildew *VpPR4-1* transcript levels increased significantly, reaching a maximum 24 h post inoculation (hpi) and then declined. The induction increase of *VpPR4-1* transcript level was very high, showing a nearly 800-fold increase compared with the normal level.

To determine the upstream pathway of *VpPR4-1*, exogenous hormones and abiotic stresses were imposed for RT-PCR. The *VpPR4-1* responded differently to the applications of three

exogenous hormones and three abiotic stresses (Figures 2B–G). The PR gene responds differently to different stresses in *V. pseudoreticulata* Baihe 35-1. ABA and cold treatment slightly affected the expression level of *VpPR4-1*. SA increased the level *VpPR4-1* induction, which peaked at 24 hpi. MeJA increased *VpPR4-1* induction strongly, with a peak at 12 hpi. This was about a 33-fold increase above normal. However, following NaCl and heat treatments, *VpPR4-1* expression increased only about 3-fold.

Molecular Analysis of Overexpression

To further understand the functional response of *VpPR4-1* in grapevine, in relation to powdery mildew attack, functional analyses of *VpPR4-1* in transgenic *V. vinifera* L. Red Globe were carried out with the overexpression construct *VpPR4-1* (Figure 3) via *Agrobacterium*-media transformation (Supplementary Figure 1). A total of 30 independent transgenic Red Globe plantlets were obtained. Genomic DNA was extracted from the transgenic grapevines of *VpPR4-1* and used to amplify the 520 bp fragment of *NPTII*. *NPTII* was detected in all transgenic lines and positive plasmid control, whereas no amplification was detected in the wild-type (WT) plant line (Figure 4A). The expression profiles of *VpPR4-1* in transgenic plant lines were studied using the Western-blot method. Total proteins were extracted from the WT plant line and transgenic plant lines of *VpPR4-1* under the same growth condition and blotting using polyclonal antibody. Twenty-six of *VpPR4-1* transgenic lines showed higher expression levels of *VpPR4-1* than the WT plant line (Figures 4B,C). However, expression levels of *VpPR4-1* of transgenic lines 13, 14, 15, and 21 were lower than the WT grape. Transgenic lines *VpPR4-1-4* and *VpPR4-1-5* showed relatively higher levels of PR4 protein and were selected for further experiments.

Enhanced Tolerance to Powdery Mildew of Transgenic Plants

To confirm that *VpPR4-1* actually participates in antifungal activity, we compared the growth rates of powdery mildew hyphae between the six overexpression lines of the higher PR4 protein level and WT plants after powdery mildew infection. Hyphal growth during a 12-day period infection with powdery mildew revealed enhanced tolerance of transgenic plants to the fungus than of none transgenic plants. The *VpPR4-1-2*, *VpPR4-1-3* showed better resistance than other transgenic lines (Figure 5). To investigate the growth of powdery mildew, light microscopy with trypan blue staining was used as previously

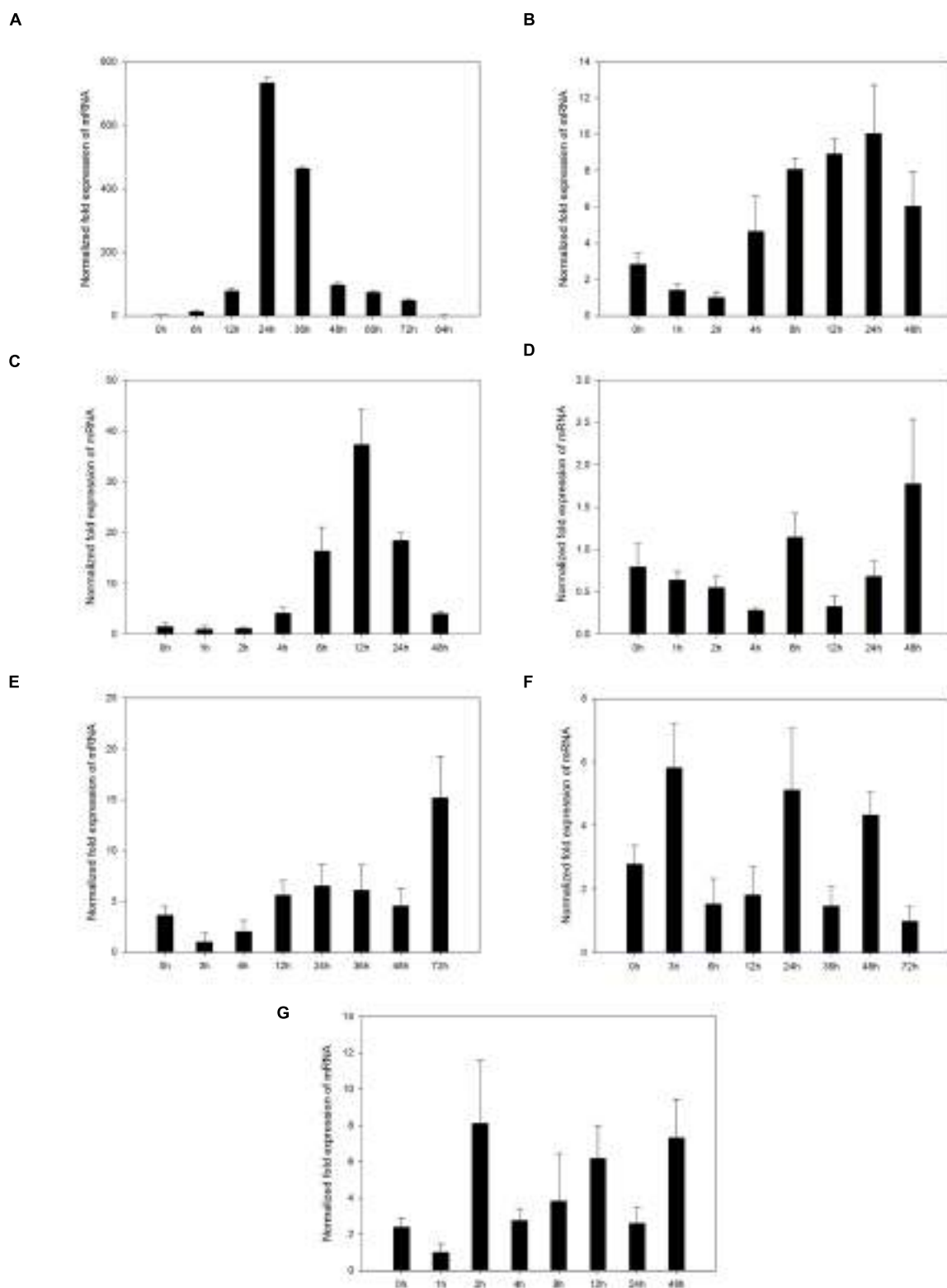


FIGURE 2 | Accumulation of mRNA of *VpPR4-1* was assessed by quantitative RT-PCR in leaves under a number of stresses. (A) Expression profiles of *VpPR4-1* infection with powdery mildew. **(B)** Expression profiles of *VpPR4-1* under SA treatment. **(C)** Expression profiles of *VpPR4-1* under MeJA treatment. **(D)** Expression profiles of *VpPR4-1* under ABA treatment. **(E)** Expression profiles of *VpPR4-1* under NaCl treatment. **(F)** Expression profiles of *VpPR4-1* under 4°C treatment. **(G)** Expression profiles of *VpPR4-1* under 42°C treatment. Error bars indicate SD, from three independent experiments.

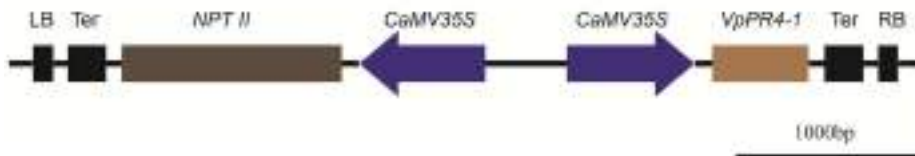


FIGURE 3 | Physical maps of plant transformation vector *VpPR4-1*. LB, Left border of T-DNA; Ter, terminator; *NPTII*, neomycin phosphotransferase gene; CaMV35S, Cauliflower mosaic virus 35S promoter; *VpPR4-1*, pathogen-related protein gene from *Vitis pseudoreticulata* Baihe 35-1; RB, Right border of T-DNA.

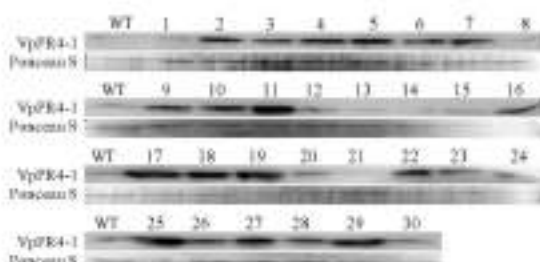
A**B****C**

FIGURE 4 | Molecular analysis of transgenic *Vitis vinifera* L. Red Globe by overexpression *VpPR4-1* from *V. pseudoreticulata*. **(A)** PCR analysis of *NPTII* from transgenic *V. vinifera* L. Red Globe of *VpPR4-1*. **(B)** Western blotting analysis of transgenic *V. vinifera* L. Red Globe by overexpression *VpPR4-1*, showing the Western blotting of VpPR4-1 in transgenic lines; Ponceau S, showing the protein stained by Ponceau S. **(C)** Quantitative analysis for VpPR4-1 protein expression of Western blotting analysis of transgenic *V. vinifera* L. Red Globe by overexpression *VpPR4-1* **(B)** were performed by Image lab 4.1 software. WT, wild-type line; 1–30, 30 transgenic lines of *VpPR4-1*.

described (Xiao et al., 2003). Images at 24, 72, 120, and 168 hpi are shown in **Figure 6**. In the WT lines, more hyphal growth was observed than in the transgenic plants, and the overexpression lines significantly reduced powdery mildew hyphal growth but did not inhibit the fungal completely (**Figure 6**).

To investigate expression changes of disease-resistance associated genes in the transgenic lines, *NPR1*, *PR1*, *PR10*, and *PAL* genes transcript levels were measured in the *VpPR4-1-4*, *VpPR4-1-5*, and WT lines inoculated with powdery mildew. These showed that the expression of disease-resistance associated genes was induced by powdery mildew and peaked between 12 and 48 hpi, before returning to the low baseline level in

the WT line by 72 hpi. However, compared with WT grapes, the defense related genes were disturbed to different degrees by the *VpPR4-1* overexpression when inoculated with powdery mildew. In transgenic lines, the expression of the *NPR1*, *PR1*, and *PAL* genes displayed a lower transcription level, and the peak of the *PR10* gene transcript was delayed when inoculated with powdery mildew (**Figure 7**). Specifically, in the WT plants, *NPR1* was induced and reached a 30-fold peak at 12 hpi but there was no significant change in the overexpression lines. Correspondingly, in WT, *PR1* showed a double peak expression pattern while in the *VpPR4-1* transgenic lines this was suppressed and showed a delayed response. However, *PAL* was not materially affected since both the WT and overexpression

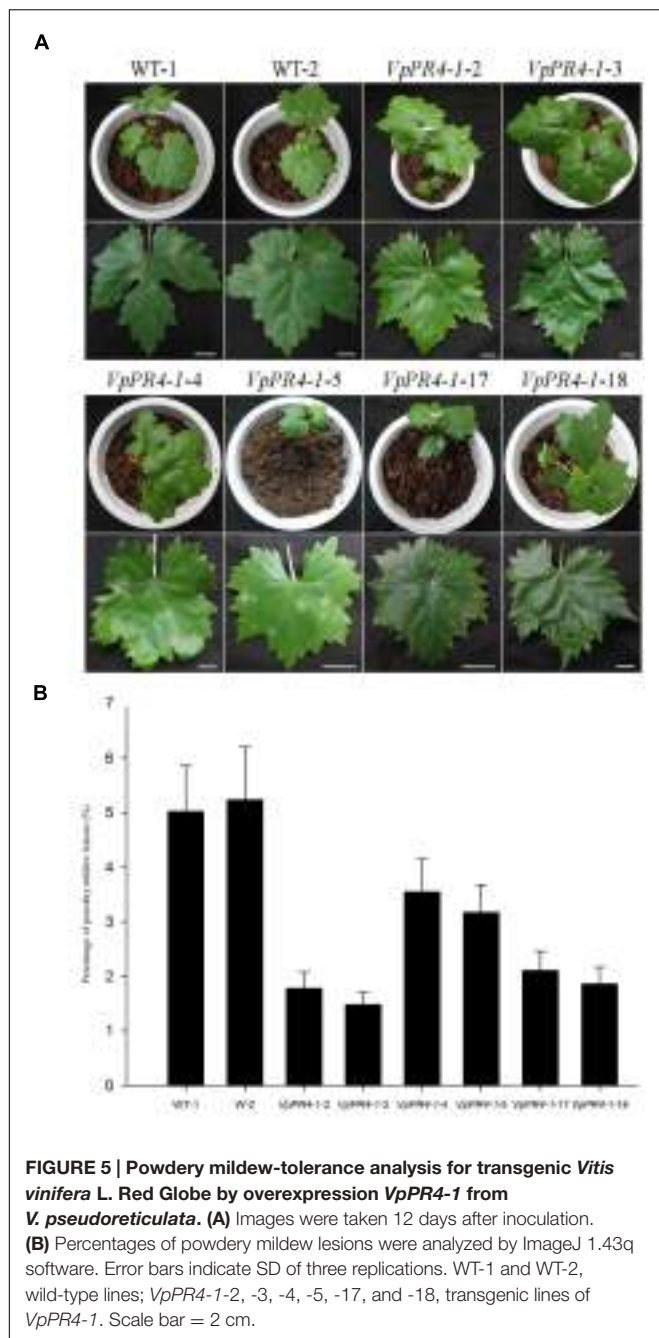


FIGURE 5 | Powdery mildew-tolerance analysis for transgenic *Vitis vinifera* L. Red Globe by overexpression *VpPR4-1* from *V. pseudoreticulata*. (A) Images were taken 12 days after inoculation. (B) Percentages of powdery mildew lesions were analyzed by ImageJ 1.43q software. Error bars indicate SD of three replications. WT-1 and WT-2, wild-type lines; *VpPR4-1*-2, -3, -4, -5, -17, and -18, transgenic lines of *VpPR4-1*. Scale bar = 2 cm.

lines showed a tendency to rise at first but then decline later.

Further gene function and the role of powdery mildew resistance of *VpPR4-1* including the disease resistance tests in the vineyard will be studied in our future study based on the current work and the transgenic lines of *VpPR4-1* obtained.

DISCUSSION

Powdery mildew is one of the most damaging fungal diseases of the European grapevines. Since powdery mildew resistance is

regulated by multi-gene, grapevine is still recalcitrant to powdery mildew resistance and the genes from the cDNA library of the high powdery mildew resistant Baihe 35-1 is worth researching. In our study, detection and characterization of a PR-4 protein induced by powdery mildew in the leaves of *V. pseudoreticulata* Baihe 35-1 were detected, sequence analyses and expression patterns of *VpPR4-1* were carried out. Finally, *VpPR4-1* was overexpressed in the powdery mildew susceptible variety Red Globe to exhibit its resistance to powdery mildew.

VpPR4-1 Belongs to the Class II PR-4 Proteins

Vitis pseudoreticulata shows high resistance to powdery mildew. The PR-4 proteins, *VpPR4-1*, were isolated from *V. pseudoreticulata* and characterized. *VpPR4-1* has previously been cloned from expressed sequence tags (Shi et al., 2010). The PR-4 protein precursor has a short signal peptide and the mature protein format undergoes a strict cutoff. Based on the lack of a *Hevein* domain near the N terminal, *VpPR4-1* belongs to class II. The class II PR-4 proteins are proposed to have evolved from the class I PR-4 proteins because of the highly conserved sequences in the C terminal and the deletion of the only *Hevein* domain (Friedrich et al., 1991; Ponstein et al., 1994). And sequence alignment and phylogenetic analysis indicate that *VpPR4-1* belongs to class II and shows a high level of sequence conservation with these well characterized class II PR-4 proteins.

VpPR4-1 Was More Strongly Induced by Powdery Mildew than by the Other Stresses

PR-4 mRNA expression level in grape increased during powdery mildew incubation. However, the induction patterns in susceptible and non-susceptible cultivars are quite different (Fung et al., 2008). Wild Chinese grape *V. pseudoreticulata* is an accession having high resistance to powdery mildew. The PR-4 gene expression levels are significantly higher in leaves of *V. pseudoreticulata* following inoculation with powdery mildew than that under normal conditions. Nevertheless, SA, MeJA, ABA, cold, heat, or NaCl stresses do not stimulate *VpPR4-1* to a similar extent to powdery mildew attack although they do lead to PR-4 up-regulation. A possible explanation for the expression profile is that powdery mildew regulates *VpPR4-1* in an independent or crossover pathway to these six abiotic stresses. It is well known that SA and JA have positive roles in disease resistance, while ABA has a negative role (Kunkel and Brooks, 2002; Mauch-Mani and Mauch, 2005). In this study, *VpPR4-1* was induced by SA and MeJA (by 3- to 30-fold) but was insensitive to ABA. A different result was observed with ABA treatment in rice which shows threefold to ninefold change in the expression levels of the PR-4 genes. The expression profiles of *VpPR4-1* were also induced by a number of environment stresses (including by salt, cold and heat shock) but the responses were slow. Together, these results suggest that *VpPR4-1* has a positive role in stress responses in *V. pseudoreticulata*, which may be regulated by SA- and JA

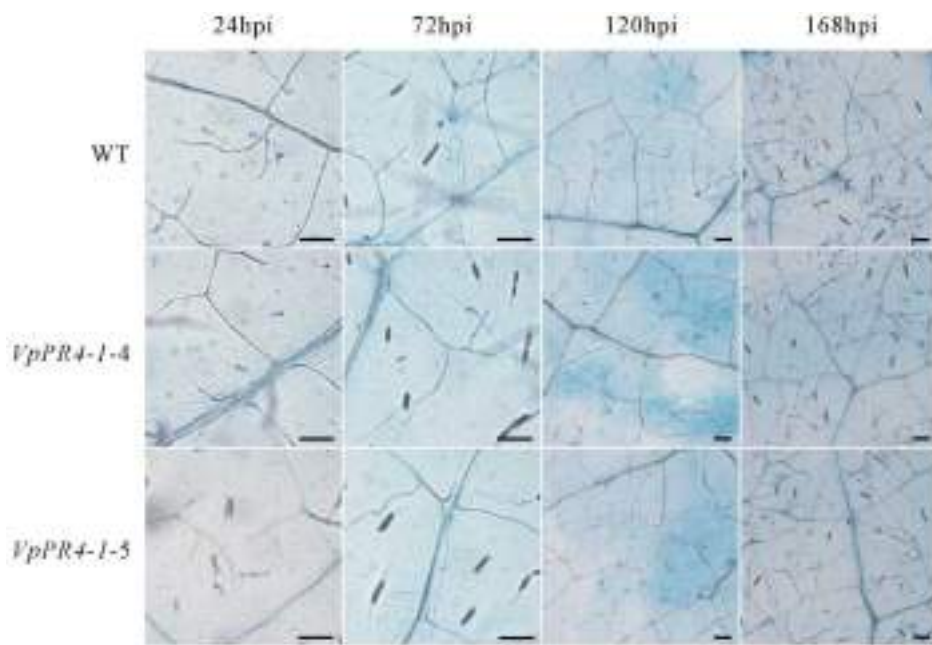


FIGURE 6 | Powdery mildew invaded the leaves of transgenic *Vitis vinifera* L. Red Globe by overexpression *VpPR4-1* from *V. pseudoreticulata*. WT, wild-type line; *VpPR4-1-4* and *VpPR4-1-5*, transgenic line 4 and 5 of *VpPR4-1*, respectively. Scale bar = 100 μ m.

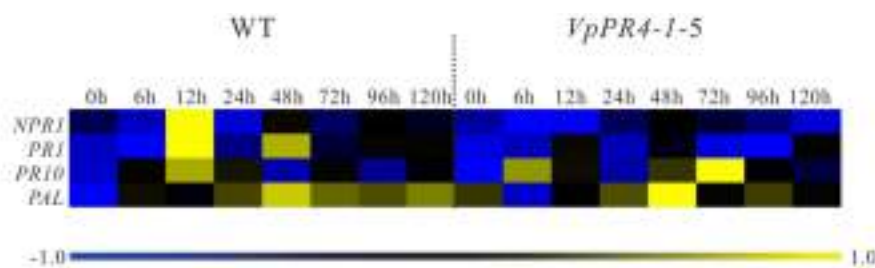


FIGURE 7 | qPCR expression analysis for disease-resistance associated genes in leaves of transgenic *Vitis vinifera* L. Red Globe by overexpression *VpPR4-1* from *V. pseudoreticulata* under powdery mildew treatment. WT, wild-type grapevines; *VpPR4-1-5*, transgenic line 5 containing *VpPR4-1*. The color heat map was created according to the standardized RT-PCR expression data by median normalization method using MeV 4.9.0 software, and the color coded showed the differences in gene expression (see key, bottom). The color scale represents relative expression levels: blue represents decreased transcript abundance and yellow represents increased transcript abundance.

networks. Moreover, our results are consistent with Wang et al. (2011).

Overexpression of *VpPR4-1* Increases Powdery Mildew Resistance of *V. vinifera*

The Ribonuclease activity of PR-4 proteins has been reported a number of times and many experiments have confirmed that they can repress fungal growth *in vitro* (Bai et al., 2013; Vaghefi et al., 2013; Menezes et al., 2014). To expand our knowledge about PR-4 proteins and create resistant table-grape germplasm, we overexpressed the *VpPR4-1* gene in *V. vinifera* cv. Red Globe. In spite of PR-4 proteins having been implicated in stress responses (Wang et al., 2011), no direct evidence has been reported previously showing that the PR-4 proteins participate in powdery mildew resistance in an important food

crop such as grapevines. The *VpPR4-1* gene was overexpressed in 30 regenerated *V. vinifera* cv. Red Globe via *Agrobacterium tumefaciens*-mediated transformation and confirmed by PCR of *NPTII*. The 26 transgenic grapevines exhibited higher expression levels of PR-4 protein content than WT vines verified by the Western blot. It is probably that the target gene between the right and left border of T-DNA in *Agrobacterium* was randomly transformed into the chromosome of host cell via *Agrobacterium tumefaciens*-mediated transformation and even multicopy of target genes transformation which could make gene expression different from each other or even gene silencing in transgenic lines (Bouquet et al., 2007), the expression of PR4 protein were not the same in all transgenic lines and the transgenic lines *VpPR4-1-13*, 14, 15, and 21 were lower than the WT grape, that is consistent with other gene transformation of grapevine

(Zhou et al., 2014; Dai et al., 2015; Cheng et al., 2016). To confirm that VpPR4-1 actually participates in antifungal activity, we compared the growth rates of powdery mildew hyphae between the six overexpression lines of the higher PR4 protein level and WT plants after powdery mildew infection. The overexpression lines showed relatively high gene expression levels (**Figures 4B,C**) and significant reduced powdery mildew hyphal growth but not inhibited the fungal completely (**Figure 6**) which is probably due to powdery mildew resistance is regulated by multi-gene complex network and not by a dominant gene (Fung et al., 2008), and the result is similar with Bertini et al. (2012). Various related genes exhibit different expressions under normal or stress conditions when genes are overexpressed *in vivo* (Tillett et al., 2012; Xu et al., 2014). The PR-4 proteins are pathogenesis-related proteins involved in pathogen defense response. Since powdery mildew resistance is regulated by multi-gene of SA and/or MeJA pathways and other network (Fung et al., 2008), it is supposed that the significantly higher expression of PR4 protein may lead to affect the expression of other pathogen relative genes which also play important role in powdery mildew resistance network. Therefore, we detected the influences of overexpression of VpPR4-1 on related genes transcripts, including: *NPR1*, *PR1*, and *PAL*. In the overexpression lines, the expression level of *NPR1* which plays a positive role in inducible plant disease resistance, was obviously down-regulated. The results may be associated with feedback regulation since *PR-4* is in abundance. Accordingly, *PR1* was also suppressed to some extent. It was different for *PAL*, this key enzyme catalyzes the rate-limiting step of phenylpropanoid biosynthesis in plants, that occurred negligibly during the long incubation period. And it is supposed that the higher expression of PR4 protein leading to the suppression expression of other disease resistant genes which resulted in that VpPR4-1-4 and VpPR4-1-5 with higher PR4 levels were not so resistant for powdery mildew as VpPR4-1-2 (**Figure 5**). Though numerous details for the regulation mechanism of VpPR4-1

in bestowing resistance to abiotic and biotic stress remains unclear (Wang et al., 2011), the twin facts that VpPR4-1 is responsive to powdery mildew inoculation and that the VpPR4-1 overexpression lines showed enhanced powdery mildew resistance in *V. vinifera* cv. Red Globe indicate that they do nevertheless play an important role in increasing fungal resistance.

AUTHOR CONTRIBUTIONS

LD had made the substantial contributions to the conception, design of the work, and the acquisition, analysis. DW had done interpretation of data for the work. XX did the revising manuscript critically for important intellectual content. JZ did drafting the work of the manuscript. YW gave final approval of the version to be published; XW, YX, and CZ made the agreement to be accountable for all aspects of the work in ensuring that questions related to the accuracy or integrity of any part of the work are appropriately investigated and resolved.

ACKNOWLEDGMENTS

This work was supported by the National Natural Science Foundation of China (grant no. 31171924) and the Program for Innovative Research Team of Grape Germplasm Resource and Breeding (2013KCT-25). The authors thank Dr. Alexander (Sandy) Lang from RESCRIPT Co. New Zealand for useful comments and language editing which have greatly improved the manuscript.

SUPPLEMENTARY MATERIAL

The Supplementary Material for this article can be found online at: <http://journal.frontiersin.org/article/10.3389/fpls.2016.00695>

REFERENCES

- Bai, S., Dong, C., Li, B., and Dai, H. (2013). A PR-4 gene identified from *Malus domestica* is involved in the defense responses against *Botryosphaeria dothidea*. *Plant Physiol. Biochem.* 62, 23–32. doi: 10.1016/j.plaphy.2012.10.016
- Bertini, L., Caporale, C., Testa, M., Proietti, S., and Caruso, C. (2009). Structural basis of the antifungal activity of wheat PR4 proteins. *FEBS Lett.* 583, 2865–2871. doi: 10.1016/j.febslet.2009.07.045
- Bertini, L., Proietti, S., Aleandri, M. P., Mondello, F., Sandini, S., Caporale, C., et al. (2012). Modular structure of HEL protein from *Arabidopsis* reveals new potential functions for PR-4 proteins. *Biol. Chem.* 393, 1533–1546. doi: 10.1515/hzs-2012-0225
- Boll, J. F. (1991). Tobacco and tomato PR proteins homologous to win and Prohevein lack the “Hevein”. *Domain. Mol. Plant Microbe Interact.* 4, 586–592. doi: 10.1094/MPMI-4-586
- Bouquet, A., Torregrosa, L., Iocco, P., and Thomas, M. R. (2007). *Grapevine (Vitis vinifera L.) Agrobacterium Protocols*, Vol. 2. (Berlin: Springer), 273–285.
- Bravo, J., Campo, S., Murillo, I., Coca, M., and San Segundo, B. (2003). Fungus- and wound-induced accumulation of mRNA containing a class II chitinase of the pathogenesis-related protein 4 (PR-4) family of maize. *Plant Mol. Biol.* 52, 745–759. doi: 10.1023/A:1025016416951
- Broekaert, I., Lee, H. I., Kush, A., Chua, N. H., and Raikhel, N. (1990). Wound-induced accumulation of mRNA containing a hevein sequence in laticifers of rubber tree (*Hevea brasiliensis*). *Proc. Natl. Acad. Sci. U.S.A.* 87, 7633–7637. doi: 10.1073/pnas.87.19.7633
- Caporale, C., Di Berardino, I., Leonardi, L., Bertini, L., Cascone, A., Buonocore, V., et al. (2004). Wheat pathogenesis-related proteins of class 4 have ribonuclease activity. *FEBS Lett.* 575, 71–76. doi: 10.1016/j.febslet.2004.07.091
- Caruso, C., Bertini, L., Tucci, M., Caporale, C., Nobile, M., Leonardi, L., et al. (2001). Recombinant wheat antifungal PR4 proteins expressed in *Escherichia coli*. *Protein Exp. Purif.* 23, 380–388. doi: 10.1006/prep.2001.1512
- Caruso, C., Caporale, C., Chilosì, G., Vacca, F., Bertini, L., Magro, P., et al. (1996). Structural and antifungal properties of a pathogenesis-related protein from wheat kernel. *J. Protein Chem.* 15, 35–44. doi: 10.1007/BF01886809
- Cheng, S., Xie, X., Xu, Y., Zhang, C., Wang, X., Zhang, J., et al. (2016). Genetic transformation of a fruit-specific, highly expressed stilbene synthase gene from Chinese wild *Vitis quinquangularis*. *Planta* 243, 1041–1053. doi: 10.1007/s00425-015-2459-1

- Chevalier, C., Bourgeois, E., Pradet, A., and Raymond, P. (1995). Molecular cloning and characterization of six cDNAs expressed during glucose starvation in excised maize (*Zea mays* L.) root tips. *Plant Mol. Biol.* 28, 473–485. doi: 10.1007/BF00020395
- Dai, L., Zhou, Q., Li, R., Du, Y., He, J., Wang, D., et al. (2015). Establishment of a picloram-induced somatic embryogenesis system in *Vitis vinifera* cv. chardonnay and genetic transformation of a stilbene synthase gene from wild-growing *Vitis* species. *Plant Cell Tissue Organ Cult.* 121, 397–412. doi: 10.1007/s11240-015-0711-9
- Friedrich, L., Moyer, M., Ward, E., and Ryals, J. (1991). Pathogenesis-related protein 4 is structurally homologous to the carboxy-terminal domains of hevein, Win-1 and Win-2. *Mol. Gen. Genet.* 230, 113–119. doi: 10.1007/BF00290658
- Fung, R. W., Gonzalo, M., Fekete, C., Kovacs, L. G., He, Y., Marsh, E., et al. (2008). Powdery mildew induces defense-oriented reprogramming of the transcriptome in a susceptible but not in a resistant grapevine. *Plant Physiol.* 146, 236–249. doi: 10.1104/pp.107.108712
- Green, T. R., and Ryan, C. A. (1972). Wound-induced proteinase inhibitor in plant leaves: a possible defense mechanism against insects. *Science* 175, 776–777. doi: 10.1126/science.175.4023.776
- Gregersen, P. L., Thordal-Christensen, H., Förster, H., and Collinge, D. B. (1997). Differential gene transcript accumulation in barley leaf epidermis and mesophyll in response to attack by *Blumeria graminis* sp. Hordei (syn. *Erysiphe graminis* sp. hordei). *Physiol. Mol. Plant Pathol.* 51, 85–97. doi: 10.1006/pmpp.1997.0108
- Guan, X., Zhao, H., Xu, Y., and Wang, Y. (2011). Transient expression of glyoxal oxidase from the Chinese wild grape *Vitis pseudoreticulata* can suppress powdery mildew in a susceptible genotype. *Protoplasma* 248, 415–423. doi: 10.1007/s00709-010-0162-4
- Guevara-Morato, M. Á., De Lacoba, M. G., García-Luque, I., and Serra, M. T. (2010). Characterization of a pathogenesis-related protein 4 (PR-4) induced in Capsicum chinensis L3 plants with dual RNase and DNase activities. *J. Exp. Bot.* 61, 3259–3271. doi: 10.1093/jxb/erq148
- Hamada, H., Takeuchi, S., Kiba, A., Tsuda, S., Suzuki, K., Hikichi, Y., et al. (2005). Timing and extent of hypersensitive response are critical to restrict local and systemic spread of Pepper mild mottle virus in pepper containing the L3 gene. *J. Gen. Plant Pathol.* 71, 90–94. doi: 10.1007/s10327-004-0164-1
- Hou, H., Li, J., Gao, M., Singer, S. D., Wang, H., Mao, L., et al. (2013). Genomic organization, phylogenetic comparison and differential expression of the SBP-box family genes in grape. *PLoS ONE* 8:e59358. doi: 10.1371/journal.pone.0059358
- Huet, J., Teinkela Mbosso, E., Soror, S., Meyer, F., Looze, Y., Wintjens, R., et al. (2013). High-resolution structure of a papaya plant-defence barwin-like protein solved by in-house sulfur-SAD phasing. *Acta Crystallogr. D Biol. Crystallogr.* 69, 2017–2026. doi: 10.1107/S0907444913018015
- Jaillon, O., Aury, J.-M., Noel, B., Pollicetti, A., Clepet, C., Casagrande, A., et al. (2007). The grapevine genome sequence suggests ancestral hexaploidization in major angiosperm phyla. *Nature* 449, 463–467. doi: 10.1038/nature06148
- Kauffmann, S., Legrand, M., Geoffroy, P., and Fritig, B. (1987). Biological function of ‘pathogenesis-related’ proteins: four PR proteins of tobacco have 1,3-β-glucanase activity. *EMBO J.* 6, 3209–3212.
- Kortekamp, A. (2006). Expression analysis of defence-related genes in grapevine leaves after inoculation with a host and a non-host pathogen. *Plant Physiol. Biochem.* 44, 58–67. doi: 10.1016/j.plaphy.2006.01.008
- Kunkel, B. N., and Brooks, D. M. (2002). Cross talk between signaling pathways in pathogen defense. *Curr. Opin. Plant Biol.* 5, 325–331. doi: 10.1016/S1369-5266(02)00275-3
- Lagrimini, L. M., Burkhart, W., Moyer, M., and Rothstein, S. (1987). Molecular cloning of complementary DNA encoding the lignin-forming peroxidase from tobacco: molecular analysis and tissue-specific expression. *Proc. Natl. Acad. Sci. U.S.A.* 84, 7542–7546. doi: 10.1073/pnas.84.21.7542
- Lamb, C. J., Lawton, M. A., Dron, M., and Dixon, R. A. (1989). Signals and transduction mechanisms for activation of plant defenses against microbial attack. *Cell* 56, 215–224. doi: 10.1016/0092-8674(89)90894-5
- Lee, S. C., Kim, Y. J., and Hwang, B. K. (2001). A pathogen-induced chitin-binding protein gene from pepper: its isolation and differential expression in pepper tissues treated with pathogens, ethephon, methyl jasmonate or wounding. *Plant Cell Physiol.* 42, 1321–1330. doi: 10.1093/pcp/pcf168
- Linthorst, H. J. M., and Van Loon, L. C. (1991). Pathogenesis-related proteins of plants. *Crit. Rev. Plant Sci.* 10, 123–150. doi: 10.1080/07352689109382309
- Ludvigsen, S., and Poulsen, F. M. (1992a). Secondary structure in solution of barwin from barley seed using proton nuclear magnetic resonance spectroscopy. *Biochemistry* 31, 8771–8782. doi: 10.1021/bi0152a013
- Ludvigsen, S., and Poulsen, F. M. (1992b). Three-dimensional structure in solution of barwin, a protein from barley seed. *Biochemistry* 31, 8783–8789. doi: 10.1021/bi0152a013
- Matsumoto, T., Tanaka, T., Sakai, H., Amano, N., Kanamori, H., Kurita, K., et al. (2011). Comprehensive sequence analysis of 24,783 barley full-length cDNAs derived from 12 clone libraries. *Plant Physiol.* 156, 20–28. doi: 10.1104/pp.110.171579
- Mauch-Mani, B., and Mauch, F. (2005). The role of abscisic acid in plant-pathogen interactions. *Curr. Opin. Plant Biol.* 8, 409–414. doi: 10.1016/j.pbi.2005.05.015
- Melchers, L. S., Groot, M. A.-D., Van Der Knaap, J. A., Ponstein, A. S., Sela-Buurlage, M. B., Bol, J. F., et al. (1994). A new class of tobacco chitinases homologous to bacterial exo-chitinases displays antifungal activity. *Plant J.* 5, 469–480. doi: 10.1046/j.1365-313X.1994.05040469.x
- Menezes, S. P., de Andrade Silva, E. M., Lima, E. M., de Sousa, A. O., Andrade, B. S., Lemos, L. S. L., et al. (2014). The pathogenesis-related protein PR-4b from Theobroma cacao presents RNase activity, Ca²⁺ and Mg²⁺ dependent-DNase activity and antifungal action on *Moniliophthora perniciosa*. *BMC Plant Biol.* 14:161. doi: 10.1186/1471-2229-14-161
- Métraux, J. P., Streit, L., and Staub, T. (1988). A pathogenesis-related protein in cucumber is a chitinase. *Physiol. Mol. Plant Pathol.* 33, 1–9. doi: 10.1016/0885-5765(88)90038-0
- Neuhaus, J. M., Fritig, B., Linthorst, H. J. M., Meins, F., Mikkelsen, J. D., and Ryals, J. (1996). A revised nomenclature for chitinase genes. *Plant Mol. Biol. Rep.* 14, 102–104. doi: 10.1007/BF02684897
- Niderman, T., Genetet, I., Bruyere, T., Gees, R., Stintzi, A., Legrand, M., et al. (1995). Pathogenesis-related PR-1 proteins are antifungal (Isolation and Characterization of Three 14-Kilodalton Proteins of Tomato and of a Basic PR-1 of Tobacco with Inhibitory Activity against *Phytophthora infestans*). *Plant Physiol.* 108, 17–27. doi: 10.1104/pp.108.1.17
- Park, C.-J., Kim, K.-J., Shin, R., Park, J. M., Shin, Y.-C., and Paek, K.-H. (2004). Pathogenesis-related protein 10 isolated from hot pepper functions as a ribonuclease in an antiviral pathway. *Plant J.* 37, 186–198. doi: 10.1046/j.1365-313X.2003.01951.x
- Park, Y., Jeon, M. H., Lee, S., Moon, J. S., Cha, J., Kim, H. Y., et al. (2005). Activation of defense responses in Chinese cabbage by a nonhost pathogen, *Pseudomonas syringae* pv. tomato. *J. Biochem. Mol. Biol.* 38:748. doi: 10.5483/BMBRep.2005.38.6.748
- Ponstein, A. S., Bres-Vloemans, S. A., Sela-Buurlage, M. B., van den Elzen, P. J., Melchers, L. S., and Cornelissen, B. J. (1994). A novel pathogen-and wound-inducible tobacco (*Nicotiana tabacum*) protein with antifungal activity. *Plant Physiol.* 104, 109–118. doi: 10.1104/pp.104.1.109
- Potter, S., Uknas, S., Lawton, K., Winter, A. M., Chandler, D., DiMaio, J., et al. (1993). Regulation of a hevein-like gene in *Arabidopsis*. *Mol. Plant Microbe Interact.* 6, 680–685. doi: 10.1094/MPMI-6-680
- Reid, K. E., Olsson, N., Schlosser, J., Peng, F., and Lund, S. T. (2006). An optimized grapevine RNA isolation procedure and statistical determination of reference genes for real-time RT-PCR during berry development. *BMC Plant Biol.* 6:27. doi: 10.1186/1471-2229-6-27
- Repka, V., Ficherova, I., and Siharova, K. (2004). Methyl jasmonate is a potent elicitor of multiple defense responses in grapevine leaves and cell-suspension cultures. *Biol. Plant.* 48, 273–283. doi: 10.1023/B:BIOP.0000033456.27521.e5
- Sels, J., Mathys, J., De Coninck, B. M. A., Cammue, B. P. A., and De Bolle, M. F. C. (2008). Plant pathogenesis-related (PR) proteins: a focus on PR peptides. *Plant Physiol. Biochem.* 46, 941–950. doi: 10.1016/j.plaphy.2008.06.011
- Seong, E., Choi, D., Cho, H., Lim, C., Cho, H., and Wang, M. (2007). Characterization of a stress-responsive ankyrin repeat-containing zinc finger protein of *Capsicum annuum* (CaKR1). *J. Biochem. Mol. Biol.* 40, 952–958. doi: 10.5483/BMBRep.2007.40.6.952
- Shi, J.-L., Wang, Y.-J., Zhu, Z.-G., and Zhang, C.-H. (2010). The EST analysis of a suppressive subtraction cDNA Library of Chinese Wild *Vitis pseudoreticulata*

- Inoculated with *Uncinula necator*. *Agric. Sci. China* 9, 233–241. doi: 10.1016/S1671-2927(09)60088-2
- Sinha, M., Singh, R. P., Kushwaha, G. S., Iqbal, N., Singh, A., Kaushik, S., et al. (2014). Current overview of allergens of plant pathogenesis related protein families. *Sci. World J.* 2014:19. doi: 10.1155/2014/543195
- Stanford, A., Bevan, M., and Northcote, D. (1989). Differential expression within a family of novel wound-induced genes in potato. *Mol. Gen. Genet.* 215, 200–208. doi: 10.1007/BF00339718
- Svensson, B., Svendsen, I., Hoejrup, P., Roepstorff, P., Ludvigsen, S., and Poulsen, F. M. (1992). Primary structure of barwin: a barley seed protein closely related to the C-terminal domain of proteins encoded by wound-induced plant genes. *Biochemistry* 31, 8767–8770. doi: 10.1021/bi00152a012
- Tamura, K., Peterson, D., Peterson, N., Stecher, G., Nei, M., and Kumar, S. (2011). MEGA5: molecular evolutionary genetics analysis using maximum likelihood, evolutionary distance, and maximum parsimony methods. *Mol. Biol. Evol.* 28, 2731–2739. doi: 10.1093/molbev/msr121
- Tillett, R. L., Wheatley, M. D., Tattersall, E. A., Schlauch, K. A., Cramer, G. R., and Cushman, J. C. (2012). The *Vitis vinifera* C-repeat binding protein 4 (VvCBF4) transcriptional factor enhances freezing tolerance in wine grape. *Plant Biotechnol. J.* 10, 105–124. doi: 10.1111/j.1467-7652.2011.00648.x
- Vaghefi, N., Mustafa, B. M., Dulal, N., Selby-Pham, J., Taylor, P. W. J., and Ford, R. (2013). A novel pathogenesis-related protein (LcPR4a) from lentil, and its involvement in defence against *Ascochyta lenti*s. *Phytopathol. Mediter.* 52, 192–201.
- Van Loon, L. C. (1982). “Regulation of changes in proteins and enzymes associated with active defence against virus infection,” in *Active Defense Mechanisms in Plants*, ed. R. K. S. Wood (Berlin: Springer), 247–273.
- Van Loon, L. C. (1985). Pathogenesis-related proteins. *Plant Mol. Biol.* 4, 111–116. doi: 10.1007/BF02418757
- Van Loon, L. C., and Van Kammen, A. (1970). Polyacrylamide disc electrophoresis of the soluble leaf proteins from *Nicotiana tabacum* var. ‘Samsun’ and ‘Samsun NN’: II. Changes in protein constitution after infection with tobacco mosaic virus. *Virology* 40, 199–211. doi: 10.1016/0042-6822(70)90395-8
- Vera, P., and Conejero, V. (1988). Pathogenesis-related proteins of tomato: P-69 as an alkaline endoprotease. *Plant Physiol.* 87, 58–63. doi: 10.1104/pp.87.1.58
- Vincent, D., Wheatley, M. D., and Cramer, G. R. (2006). Optimization of protein extraction and solubilization for mature grape berry clusters. *Electrophoresis* 27, 1853–1865. doi: 10.1002/elps.200500698
- Wang, L., and Li, S. (2006). Thermotolerance and related antioxidant enzyme activities induced by heat acclimation and salicylic acid in grape (*Vitis vinifera* L.) leaves. *Plant Growth Regul.* 48, 137–144. doi: 10.1007/s10725-005-6146-2
- Wang, N., Xiao, B., and Xiong, L. (2011). Identification of a cluster of PR4-like genes involved in stress responses in rice. *J. Plant Physiol.* 168, 2212–2224. doi: 10.1016/j.jplph.2011.07.013
- Xiao, S., Brown, S., Patrick, E., Brearley, C., and Turner, J. G. (2003). Enhanced transcription of the *Arabidopsis* disease resistance genes *rpw8.1* and *rpw8.2* via a salicylic acid-dependent amplification circuit is required for hypersensitive cell death. *Plant Cell* 15, 33–45. doi: 10.1105/tpc.006940
- Xu, W., Zhang, N., Jiao, Y., Li, R., Xiao, D., and Wang, Z. (2014). The grapevine basic helix-loop-helix (bHLH) transcription factor positively modulates CBF-pathway and confers tolerance to cold-stress in *Arabidopsis*. *Mol. Biol. Rep.* 41, 1–14. doi: 10.1007/s11033-014-3404-2
- Xu, Y., Yu, H., He, M., Yang, Y., and Wang, Y. (2010). Isolation and expression analysis of novel pathogenesis-related protein 10 gene from Chinese wild *Vitis pseudoreticulata* induced by *Uncinula necator*. *Biologia* 65, 653–659. doi: 10.2478/s11756-010-0056-0
- Yang, Y., He, M., Zhou, Z., Li, S., Zhang, C., Singer, S., et al. (2012). Identification of the dehydrin gene family from grapevine species and analysis of their responsiveness to various forms of abiotic and biotic stress. *BMC Plant Biol.* 12:140. doi: 10.1186/1471-2229-12-140
- Yu, Y., Xu, W., Wang, J., Wang, L., Yao, W., Yang, Y., et al. (2013). The Chinese wild grapevine (*Vitis pseudoreticulata*) E3 ubiquitin ligase Erysiphe necator-induced RING finger protein 1 (EIRP1) activates plant defense responses by inducing proteolysis of the VpWRKY11 transcription factor. *New Phytol.* 200, 834–846. doi: 10.1111/nph.12418
- Zhou, Q., Dai, L., Cheng, S., He, J., Wang, D., Zhang, J., et al. (2014). A circulatory system useful both for long-term somatic embryogenesis and genetic transformation in *Vitis vinifera* L. cv. Thompson Seedless. *Plant Cell Tissue Organ Cult.* 118, 157–168. doi: 10.1007/s11240-014-0471-y
- Zhu, Z., Shi, J., He, M., Cao, J., and Wang, Y. (2012). Isolation and functional characterization of a transcription factor VpNAC1 from Chinese wild *Vitis pseudoreticulata*. *Biotechnol. Lett.* 34, 1335–1342. doi: 10.1007/s10529-012-0890-y

Conflict of Interest Statement: The authors declare that the research was conducted in the absence of any commercial or financial relationships that could be construed as a potential conflict of interest.

Copyright © 2016 Dai, Wang, Xie, Zhang, Wang, Xu, Wang and Zhang. This is an open-access article distributed under the terms of the Creative Commons Attribution License (CC BY). The use, distribution or reproduction in other forums is permitted, provided the original author(s) or licensor are credited and that the original publication in this journal is cited, in accordance with accepted academic practice. No use, distribution or reproduction is permitted which does not comply with these terms.



Gene Expression Changes during the Gummosis Development of Peach Shoots in Response to *Lasiodiplodia theobromae* Infection Using RNA-Seq

Lei Gao¹, Yuting Wang¹, Zhi Li², He Zhang¹, Junli Ye¹ and Guohuai Li^{1*}

¹ Key Laboratory of Horticultural Plant Biology, Ministry of Education, Huazhong Agricultural University, Wuhan, China, ² State Key Laboratory of Crop Stress Biology in Arid Areas, College of Horticulture, Northwest Agriculture and Forestry University, Yangling, China

OPEN ACCESS

Edited by:

Olivier Lamotte,
UMR Agroécologie, Dijon, France

Reviewed by:

Guus Bakkeren,
Agriculture and Agri-Food Canada,
Canada

Manuel Acosta,
Universidad de Murcia, Spain

*Correspondence:

Guohuai Li
liuohuai@mail.hzau.edu.cn

Specialty section:

This article was submitted to
Plant Physiology,
a section of the journal
Frontiers in Physiology

Received: 01 February 2016

Accepted: 25 April 2016

Published: 09 May 2016

Citation:

Gao L, Wang Y, Li Z, Zhang H, Ye J and Li G (2016) Gene Expression Changes during the Gummosis Development of Peach Shoots in Response to *Lasiodiplodia theobromae* Infection Using RNA-Seq. *Front. Physiol.* 7:170.
doi: 10.3389/fphys.2016.00170

Lasiodiplodia theobromae is a causal agent of peach (*Prunus persica* L.) tree gummosis, a serious disease affecting peach cultivation and production. However, the molecular mechanism underlying the pathogenesis remains unclear. RNA-Seq was performed to investigate gene expression in peach shoots inoculated or mock-inoculated with *L. theobromae*. A total of 20772 genes were detected in eight samples; 4231, 3750, 3453, and 3612 differentially expressed genes were identified at 12, 24, 48, and 60 h after inoculation, respectively. Furthermore, 920 differentially co-expressed genes (515 upregulated and 405 downregulated) were found, respectively. Gene ontology annotation revealed that phenylpropanoid biosynthesis and metabolism, uridine diphosphate-glucosyltransferase activity, and photosynthesis were the most differentially regulated processes during gummosis development. Significant differences were also found in the expression of genes involved in glycometabolism and in ethylene and jasmonic acid biosynthesis and signaling. These data illustrate the dynamic changes in gene expression in the inoculated peach shoots at the transcriptome level. Overall, gene expression in defense response and glycometabolism might result in the gummosis of peach trees induced by *L. theobromae*.

Keywords: gummosis, *Prunus*, *L. theobromae*, RNA-Seq, defense response, glycometabolism

INTRODUCTION

Fungal gummosis of peach (*Prunus persica* L.) trees was first reported in 1974 in Central Georgia (Weaver, 1974). Three species of *Botryosphaeria* fungus cause this disease, namely, *Lasiodiplodia theobromae*, *Diplodia seriata*, and *Fusicoccum aesculi* were identified and reported in follow-up studies (Britton and Hendrix, 1982; Wang et al., 2011). Previous studies suggested that the pathogenicity of *L. theobromae* JMB-122 was stronger than other species (Wang et al., 2011). The hyphae of *L. theobromae* were observed on the phloem of peach shoots at 2 days post-inoculation (Li et al., 2014b). In cashew gummosis caused by *L. theobromae*, hyphae were often colonized in the rays, vessels and parenchyma cells (Muniz et al., 2011). *Botryosphaeria* spp. are capable of degrading lignin and pectin (Alves da Cunha et al., 2003). Degradation of cell walls was observed in peach

shoots and cashew branches infected by *L. theobromae* (Muniz et al., 2011; Li et al., 2014b). In addition, *L. theobromae* induced the expression of cell wall degrading-related genes and triggered cell death of the inoculated peach shoots (Li et al., 2014b). A serious case of peach gummosis can cause tree death, which significantly affects agronomy and economics (Beckman et al., 2003; Wang et al., 2011). The main symptom of peach gummosis is gum exudation from tree trunks, branches, and fruits. The main components of gum are polysaccharides (Simas et al., 2008; Simas-Tosin et al., 2010). A recent study has observed polysaccharide accumulation and investigated carbohydrate metabolism changes in peach shoots infected with *L. theobromae* (Li et al., 2014a). These results suggest that glycometabolism directly relates to peach gum formation.

Pathogen attack in plants alters the levels of various secondary metabolites, among which, phenylpropanoid compounds contribute to pathogen resistance (Dixon et al., 2002). Plant hormones such as ethylene (ET) and jasmonates [mainly jasmonic acid (JA) and methyl jasmonate (JA-ME)] are essential factors in gum formation. Ethephon (ETH, 2-chloroethylphosphonic acid, ET-releasing compound) can induce sour cherry gummosis (Olien and Bukovac, 1982), and ET can initiate gum duct formation in almond fruits (Morrison et al., 1987). The application of ET in tulip bulbs leads to gum formation, and the effect can be prevented through pretreatment with the ET receptor inhibitor 1-methylcyclopropane (1-MCP) (de Wild et al., 2002). JA can induce gummosis in tulip (Skrzypek et al., 2005a,b) and grape hyacinth (Miyamoto et al., 2010), as well as in various species of stone-fruit trees such as plum shoots and fruits (Saniewski et al., 2002), apricot (Saniewski et al., 2001), and peach shoots (Saniewski et al., 1998; Li et al., 2015).

High-throughput sequencing technologies have been recently developed for transcriptome profiling, referred to as RNA-Seq (Wang et al., 2009; Marguerat and Bähler, 2010). RNA-Seq has been widely applied to study plant diseases caused by bacteria (Kim et al., 2011; Socquet-Juglard et al., 2013), fungi (Xu et al., 2011; de Jonge et al., 2012; Kunjeti et al., 2012; Windram et al., 2012; Czermel et al., 2015), and viruses (Zhang et al., 2012; Rubio et al., 2015) because of its capacity to elucidate the molecular mechanism underlying plant-pathogen interactions.

The molecular mechanism underlying peach fungal gummosis remains unclear to date. Thus, we used high-throughput Illumina sequencing in the present study to analyze the transcriptome of peach shoots at 12, 24, 48, and 60 h after inoculation (HAI) with *L. theobromae*. We analyzed differentially expressed genes (DEGs) and their significantly enriched pathways after pathogen infection, and discussed possible factors influencing gummosis development. The global view of the host transcriptional changes could contribute to our understanding of gum symptom development in peach shoots infected with *L. theobromae*.

MATERIALS AND METHODS

Plant Material and Pathogen Material

Peach plants (*P. persica* L. "Spring Snow") was grafted onto wild peach rootstocks and cultivated in the experiment field

of Huazhong Agricultural University (Wuhan, Hubei Province, China). Current-year shoots approximately 6 mm in diameter were collected from 4-year-old peach plants in 2012. *L. theobromae* strain JMB-122 was isolated from Hubei Province, China (Wang et al., 2011). Before inoculation, *L. theobromae* JMB-122 was cultured on potato dextrose agar (PDA) medium at 28°C for 3 days.

Inoculation of Peach Shoots with *L. theobromae*

The inoculation method was based on a previous study (Li et al., 2014b). In brief, after surface-sterilized peach shoots were cut into 15 cm-long segments and then wounded with a sterilized needle. A single mycelial plug (4 mm in diameter) of *L. theobromae* was placed onto the wound point. Shoot segments inoculated with sterile PDA medium without *L. theobromae* were treated as controls. The inoculated and control shoots were placed in glass bottles containing 100 mL of sterilized water. The shoots and glass bottles were covered with clear plastic wrap and then placed in a light incubator at 28°C, 90% relative humidity with a photoperiod of 12/12 h light (20,000 lux)/dark.

Measurement of ET Production

The inoculated and mock-inoculated shoots were used to measure the ET production rate. The mycelial plug or the PDA medium was removed before the shoots were placed in a 500 mL Erlenmeyer flask. Each Erlenmeyer flask containing about 15 shoots was sealed airtight by a rubber stopper. The shoots were sealed for up to 6 h at 28°C at 0, 1, 2, 3, and 4 days after inoculation. Then, 1 mL gas was extracted from the airtight Erlenmeyer flask by using gas-tight syringes. ET was detected using a gas chromatograph (Agilent, 7890A, USA) equipped with a DB-624 column and a flame ionization detector (FID). The injection, FID, and column temperature was 250°C, 250 and 40°C, respectively. The pressure in the column was 2.8109 Pa. The carrier gas was pure nitrogen (N₂) with a rate of 16 mL·min⁻¹. The external standard method was used in this study; the retention time of the standard sample (from Newradar special GAS Co., Ltd., China) and the peak area were used as qualitative and quantitative data, respectively. The rate of ET production was expressed as $\mu\text{L}\cdot\text{kg}^{-1}\cdot\text{h}^{-1}$. The results of ET production rate are shown as the means \pm SD of three independent biological replicates.

Plant Sample Preparation and RNA Preparation

Peach shoot tissues were collected within a 0.5–1.0 cm range from the wound point of the inoculated shoots (J) and the mock-inoculated shoots (C) at 12, 24, 48, and 60 HAI. The samples were immediately frozen in liquid nitrogen and stored at -80°C. Both infected and control samples were collected from eight peach shoots in a randomized manner. The J and C samples at 12, 24, 48, and 60 HAI were used to extract RNA. The total RNA was extracted using the EASYspin Plus RNA kit (Aidlab, Beijing, China). Any genomic DNA was removed by DNase (TaKaRa, Dalian, China). The RNA yield and purity were checked

through NANODROP 2000 (Thermo, USA), and RNA integrity was verified through electrophoresis on 1.5% agarose gel.

cDNA Library Construction and RNA-Seq

The eight RNA samples were sent for RNA-Seq using the Illumina Genome Analyzer at ABLife (Wuhan, China) in 2012. For each sample, 10 µg of total RNA was used for RNA-Seq library preparation. Polyadenylated mRNAs were purified and concentrated with dT-conjugated magnetic beads (Invitrogen) before used for directional RNA-Seq library preparation. The purified mRNAs were iron-fragmented at 95°C followed by end repair and 5' adaptor ligation. Then, reverse transcription was performed with RT primer harboring 3' adaptor sequence and randomized hexamer. The cDNAs were purified and amplified, and PCR products corresponding to 200–500 bp were purified, quantified, and stored at –80°C until used for sequencing. The libraries for high-throughput sequencing were prepared following the manufacturer's protocol and then applied to the Illumina GAIx system for 80-nucleotide single-end sequencing. Raw data were collected by the sequencer. Reads containing two N were removed, the adaptor was trimmed on the basis of adapter information, and low-quality reads were trimmed. After these steps, reads with lengths ≥20 nt were considered clean.

Mapping Reads to the Genome and Identification of Differentially Expressed Genes (DEGs)

The *P. persica* v1.0 genome dataset was used as a reference. The abundance of each gene was normalized to reads per kilo bases per million reads (RPKM) for between-sample comparison purposes. The edgeR software was applied to identify DEGs. Fold change ($|log_2FC| \geq 1$) and *p*-value ($p \leq 0.01$) were used as statistical significance indexes.

Validation of RNA-Seq Analysis by Quantitative Real-Time Polymerase Chain Reaction (qRT-PCR)

First-strand cDNA was synthesized from 1.0 µg of RNA using oligo (dT) primers by using a PrimeScript® RT Reagent Kit with gDNA Eraser (TaKaRa, Dalian, China) in accordance with the manufacturer's protocol. The cDNA was diluted to a final concentration of 300 ng·µL^{−1} and used as the template for qRT-PCR. qRT-PCR was performed on the LightCycler® 480 real-time detection system (Roche Diagnostics, Switzerland). The intercalation dye SYBR Green (TransStart®) was used as a fluorescent reporter. Translation elongation factor 2 was used as a reference gene to normalize gene expression in according with a previously published report (Sherif et al., 2012). In brief, 15 µL of the PCR system contained 300 ng of cDNA, 10 mmol of each primer, and 7.5 µL of 2 × TransStart® Top Green qPCR SuperMix (TransGen, Beijing, China). The reaction was performed at 95°C for 30 s, followed by 45 cycles of 95°C for 5 s, 60°C for 30 s, 72°C for 30 s. Relative gene expression was calculated using the comparative $2^{-\Delta\Delta CT}$ method (Livak and Schmittgen, 2001). The qRT-PCR results are shown as the means ± SD of three independent biological replicates.

RESULTS

Symptom Changes in Peach Shoots Infected with *L. theobromae*

A typical symptom observed in the inoculated peach shoots was the increased lesions compared with the mock-inoculated peach shoots. At 12 HAI, the lesion diameter was about 5 mm. From 24 HAI to 48 HAI, lesions developed at a comparatively rapid speed. The lesions were 17.3 ± 1.0 mm at 60 HAI (Figure 1B). Another typical symptom was the distinct red color surrounding the lesions at the beginning of 24 h. Importantly, the gum exudation was visible on the inoculated point at 60 h (Figure 1A), with a 29.3 ± 4.7 mg gum weight (Figure 1B) per inoculated shoot in average. When peach shoots were inoculated with *L. theobromae*, the maximum production rate of ET was reached at 1 day, but this rate declined during 2–4 days. ET production in the control plants on days 1–4 fell lower than the minimum detectable concentration. Thus, gas chromatography failed to generate any efficient data.

Analyses of RNA-Seq Data

In total, eight cDNA preparations were sequenced. The number of raw reads produced for each library exceeded 10 million (Table 1). After filtering, most of the clean reads were still more than 80% of the raw data, except C12 (66.15%) and C24 (79.24%). The useful length of the vast majority of the sequence was 66–67 bp, indicating few number of low-quality bases. The trimmed RNA-Seq reads were mapped on the v1.0 *P. persica* reference genome. Approximately 72–81% of the clean reads were mapped to the genome, except C12 (59.20%). The unique mapped reads accounted for more than 94% of the total mapped reads, indicating the low proportion of rRNA contamination. The clean reads were distributed mainly (an average of 75.1%) in the coding sequence of the genomic regions (Supplementary Table 1). A total of 20771 genes were detected as being expressed using the eight samples, or 74.58% of the total 27852 predicted genes of the v1.0 peach genome (Verde et al., 2013). In general, the RPKM value of the 60–70% reads of each sample was below 20, indicating a greater proportion of lowly expressed genes than highly expressed genes.

DEGs in J and C

The selection standards for DEGs are the fold change ≥ 2 or ≤ -2 and $p \leq 0.01$ (Supplementary Figure 1). Of the 20771 genes detected in this transcriptome, 4231, 3750, 3453, and 3612 were differentially expressed at $p \leq 0.01$ and $|log_2FC| \geq 1$ between J12 and C12, J24 and C24, J48 and C48, and J60 and C60, respectively. Then, 515 and 405 DEGs were co-upregulated and co-downregulated among the four comparisons, respectively (Table 2; Supplementary Table 2). The number of upregulated genes was less than that of downregulated genes between J24 and C24, and J60 and C60. The top 10 upregulated and top 10 downregulated genes in each of the four post-inoculated stages are listed in the Supplementary Table 3. A total of 1662, 645, 527, and 964 DEGs were specific for J12 vs. C12, J24 vs. C24, J48 vs. C48, and J60 vs. C60, respectively (Figure 2; Supplementary Table 4). In addition, the number of upregulated genes was

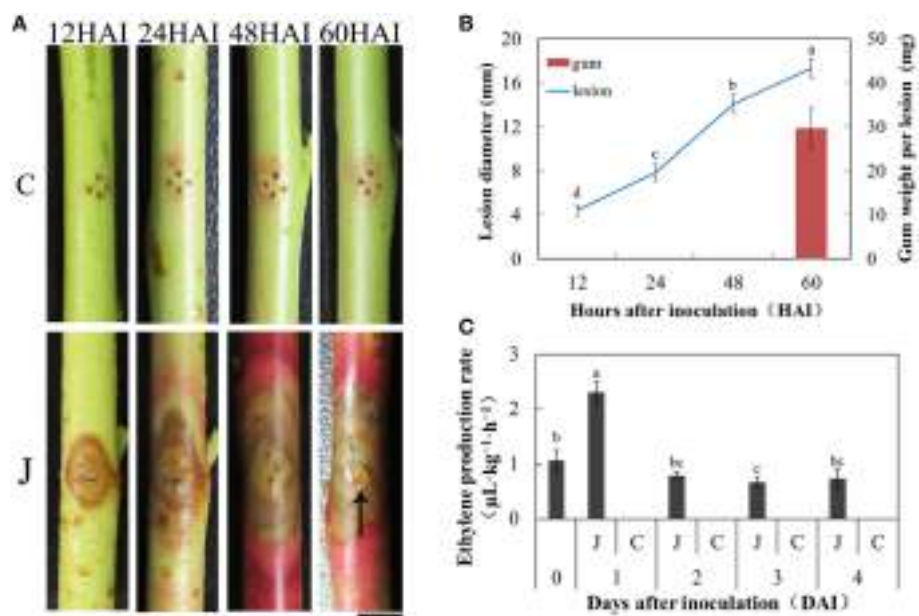


FIGURE 1 | Peach gummosis development and ethylene production rate. **(A)** Development of symptoms of peach current-year detached shoots inoculated with *L. theobromae*. C, mock-inoculated peach shoots; J, inoculated peach shoots; HAI, hours after inoculation; The black arrow indicates gum exudation; Bar is 5 mm. **(B)** Dynamic changes in lesion diameter at different hours and gum weight per lesion at 60 HAI. The values presented are the means \pm SD of six independent determinations. **(C)** ET production rate of the inoculated and mock-inoculated current-year peach shoots. At 0 days, the shoots were only wounded. In the days following, no ET was detectable in control shoots. Data were analyzed by ANOVA using SAS program package (version 8.1; SAS Institute, Cary, NC) to determine differences in lesion diameter **(B)** and ET production rate **(C)**. Means with the same letters are not significantly different at the 5% level by Duncan's multiple range test.

TABLE 1 | Summary of RNA-Seq data collected from the inoculated (J) and the mock-inoculated (C) peach shoots at the four selected hours after inoculation (HAI) and assemblies.

Sample		Raw reads	Clean reads	Reads mapped <i>P. persica</i> v 1.0	Unique mapped
12 HAI	J	10620646	8763947 (82.52%)	6320708 (72.12%)	6012821 (95.13%)
	C	14403060	9527620 (66.15%)	5640474 (59.20%)	5360326 (95.03%)
24 HAI	J	12457518	10567109 (84.83%)	7859332 (74.38%)	7501716 (95.45%)
	C	10672969	8456836 (79.24%)	6083248 (71.93%)	5774232 (94.92%)
48 HAI	J	13085397	11608410 (88.71%)	9428886 (81.22%)	8998979 (95.44%)
	C	12063922	9 888030 (81.96%)	7513771 (75.99%)	7140544 (95.03%)
60 HAI	J	12290504	10417691 (84.76%)	8248739 (79.18%)	7869553 (95.40%)
	C	10015740	8434545 (84.21%)	6604147 (78.30%)	6306888 (95.50%)

almost the same as that of the downregulated genes for J12 vs. C12, J24 vs. C24, and J48 vs. C48, respectively. However, in the comparison of J60 vs. C60, 288 (30%), and 676 (70%) of the 964 specific DEGs were up- and downregulated, respectively (Table 2).

Functional Analysis of DEGs in J and C

The Database for Annotation, Visualization and Integrated Discovery (DAVID) online platform (<https://david.ncifcrf.gov/>) was used to analyze the function of the DEGs. The up- and down-regulated cluster groups of the DEGs were subjected to gene ontology (GO) term analysis. Among the upregulated clusters, the DEGs were significantly enriched in “phenylpropanoid biosynthetic and metabolic

process.” Glycosyltransferase, especially the relevant uridine diphosphate (UDP)-glucosyltransferase genes were highly enriched from 24 h in the inoculated shoots. At 12 HAI, the genes involved in JA biosynthesis were highly enriched. Among the downregulated clusters of the GO term analysis, chloroplast, plastid, and photosynthesis were significantly enriched (Supplementary Table 5). In the comparison of “J12 vs. C12,” the metabolic process of starch, glucan, and polysaccharides was downregulated. Furthermore, the expression levels of relevant DEGs controlling the catabolic process of starch, glucan, and polysaccharide were downregulated in the inoculated shoots (detailed data in Supplementary Table 6). The same tendency was also observed on three other comparisons.

TABLE 2 | Distribution of differentially expressed genes (DEGs) between the inoculated (J) and control (C) peach shoots at each of the four selected hours after inoculation (HAI).

	J12 vs. C12	J24 vs. C24	J48 vs. C48	J60 vs. C60	J vs. C
Total DEGs	4231	3750	3453	3612	920
Upregulated	2257	1860	1768	1437	515
Downregulated	1974	1980	1685	2175	405
Shared DEGs	2569	3105	2926	2648	
Specific DEGs	1662	645	527	964	
Upregulated	880	360	248	288	
Downregulated	782	285	279	676	

J12 vs. C12 indicates a comparison between J and C at 12 HAI; J vs. C represents the co-DEGs (co-upregulated and co-downregulated) among the four comparisons performed.

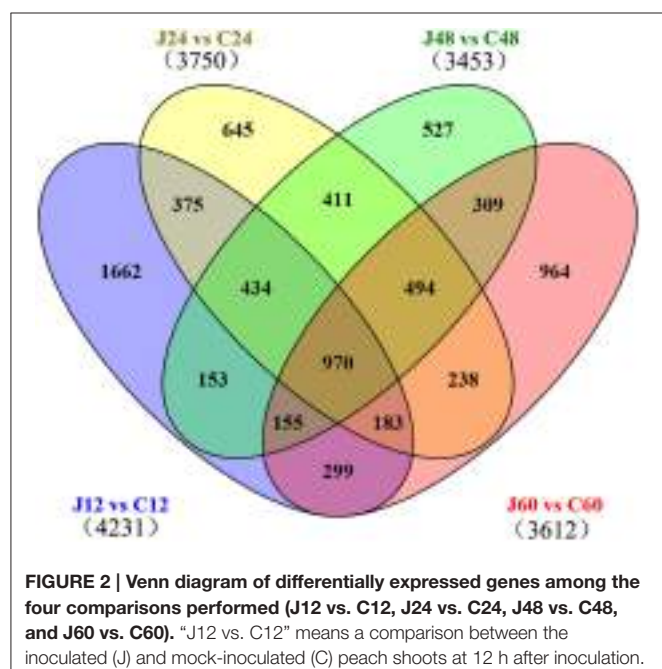


FIGURE 2 | Venn diagram of differentially expressed genes among the four comparisons performed (J12 vs. C12, J24 vs. C24, J48 vs. C48, and J60 vs. C60). “J12 vs. C12” means a comparison between the inoculated (J) and mock-inoculated (C) peach shoots at 12 h after inoculation.

GO terms were assigned to gain an overall understanding of the 920 DEGs identified in the J vs. C analysis. The broad categories for the three major GO functional domains (biological process, cellular component, and molecular function) are shown in **Figure 3**. The categories “metabolic process,” “cellular process,” “response to stimulus,” “biological regulation,” and “pigmentation” were the five representative categories based on the biological process (406 DEGs). The categories “cell,” “cell part,” “organelle,” “organelle part,” and “extracellular region,” captured most of these genes based on cellular component (416 DEGs), and the categories “catalytic activity,” “binding,” “transcription regulator activity,” and “transporter activity” captured most of these genes based on molecular function (442 DEGs) (**Figure 3**). Detailed information was obtained through the DAVID online platform (Supplementary Table 5). The terms “phenylpropanoid biosynthetic and metabolic process,” “oxidation reduction,” “UDP-glucosyltransferase activity,” and

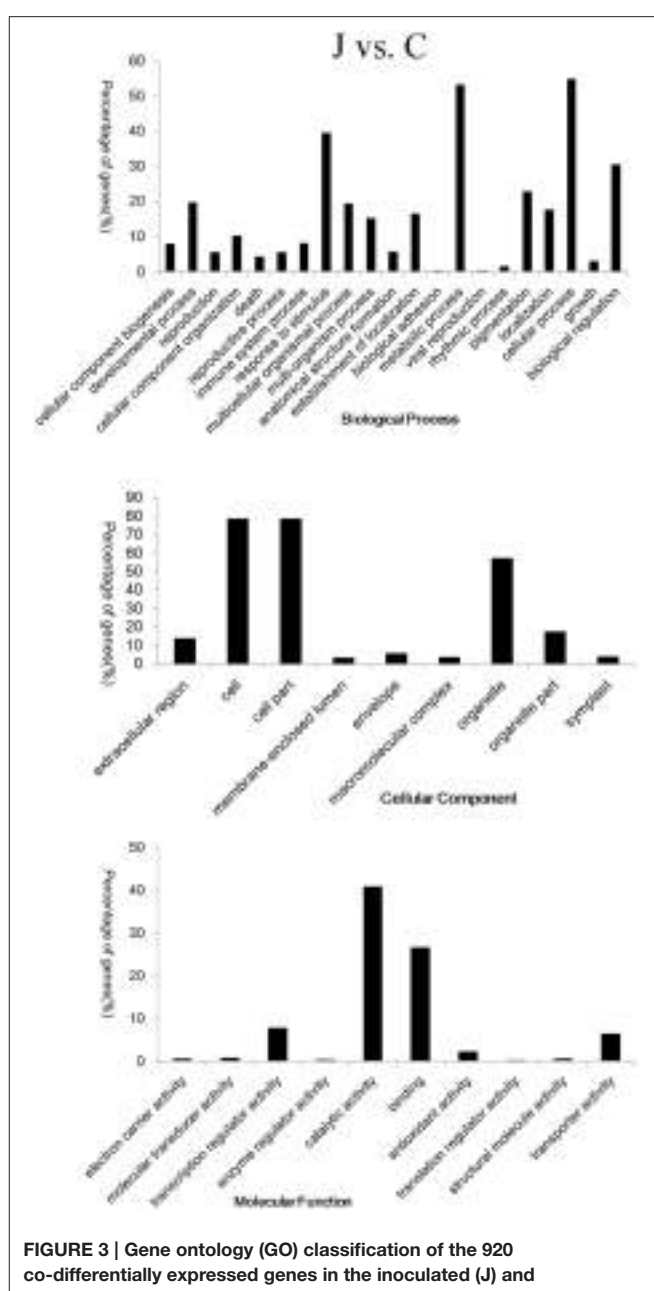


FIGURE 3 | Gene ontology (GO) classification of the 920 co-differentially expressed genes in the inoculated (J) and mock-inoculated (C) peach shoots. Annotations are grouped by biological process, cellular component, and molecular function. The percentage of genes (%) is listed for each category.

“carbohydrate transport and metabolism or signal transduction mechanisms” were significantly enriched in the upregulated clusters. Photosynthesis was obviously inhibited in the inoculated peach shoots.

L. *Theobromae* Infection Significantly Increased the Expression of Genes Involved in Biosynthesis and Metabolism of Phenylpropanoid and the Activity of UDP-Glucosyltransferase

The qRT-PCR analysis of several genes (**Figure 4C**) and the heat map diagram of DEGs involved in phenylpropanoid biosynthesis

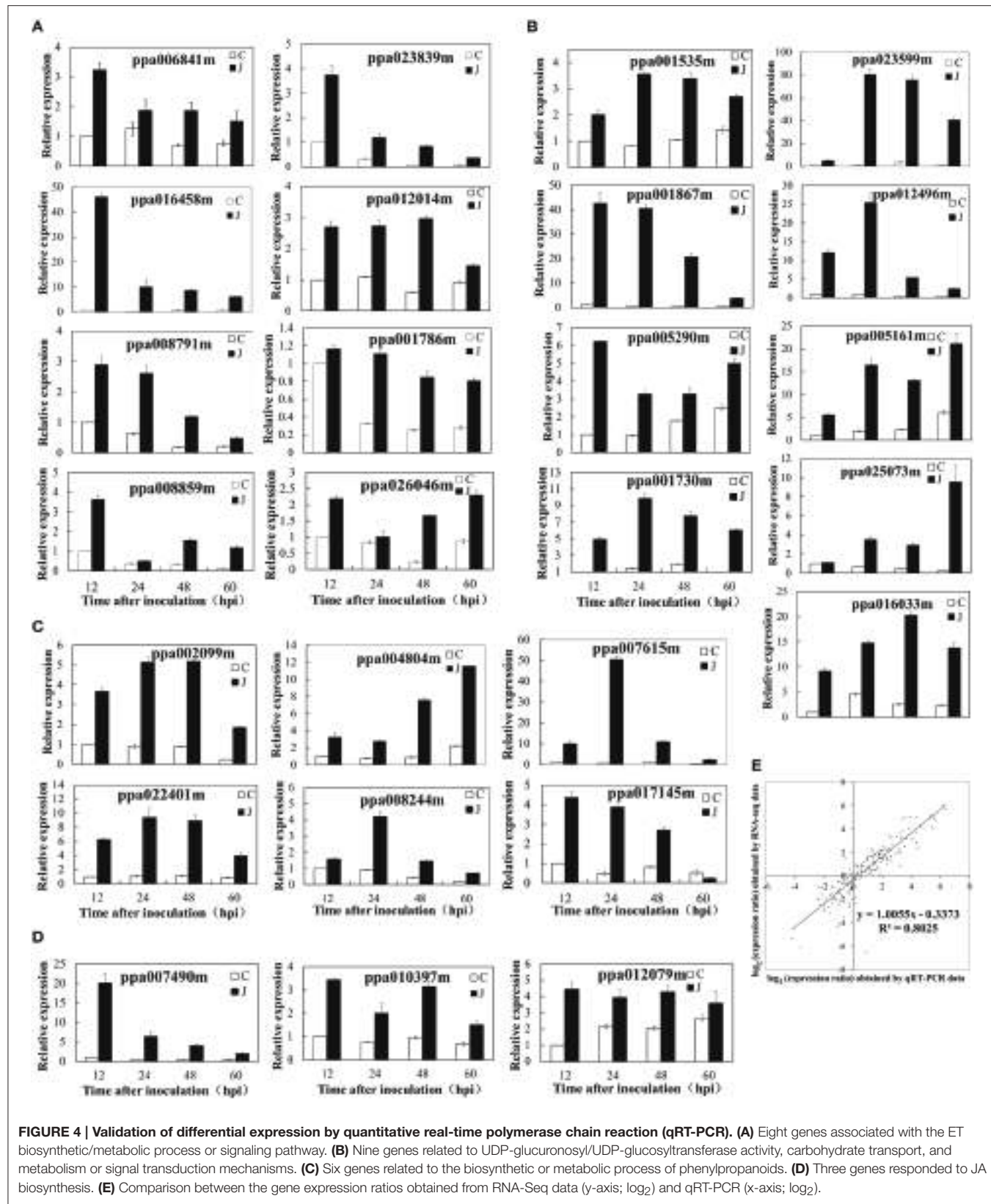


FIGURE 4 | Validation of differential expression by quantitative real-time polymerase chain reaction (qRT-PCR). (A) Eight genes associated with the ET biosynthetic/metabolic process or signaling pathway. (B) Nine genes related to UDP-glucuronosyl/UDP-glucosyltransferase activity, carbohydrate transport, and metabolism or signal transduction mechanisms. (C) Six genes related to the biosynthetic or metabolic process of phenylpropanoids. (D) Three genes responded to JA biosynthesis. (E) Comparison between the gene expression ratios obtained from RNA-Seq data (y-axis; \log_2) and qRT-PCR (x-axis; \log_2).

and metabolism (Supplementary Figure 2) also revealed the same result. Higher patterns of expression were exhibited by genes involved in the anthocyanin biosynthetic pathway. These genes include phenylalanine ammonia lyase (ppa002099m), cinnamate-4-hydroxylase (ppa018282m and ppa004544m), 4-coumarate: CoA ligase (ppa003854m and ppa022401m), chalcone synthase (ppa006888m, ppa006899m, ppa008402m, and ppa023080m), chalcone-flavanone isomerase (ppa011276m), flavanone 3-hydroxylase (ppa007636m), dihydroflavonol 4-reductase (ppa008069m), and leucoanthocyanidin dioxygenase (ppa007738m) (**Figure 4C**; Supplementary Table 8). An overview of genes involved in anthocyanin biosynthetic pathway was presented in Supplementary Figure 3. Genes encoding galactosyltransferase (ppa006755m, ppa022137m, and ppa015950m), UDP-glycosyltransferase and UDP-glucosyltransferase were upregulated several to hundreds-fold in the inoculated peach shoots compared with the control shoots (Supplementary Table 9).

Genes Related to Carbohydrate Metabolism are Differentially Expressed during *L. theobromae* Infection

Cellulose and pectin are the main components of plant cell walls. The expression levels of ppa004653 and ppa004719m (*cellulase* genes) increased in the inoculated peach shoots compared with those in the control shoots at 24 HAI (2- and 4.6-fold, respectively) and 48 HAI (7.5- and 2.8-fold, respectively). Ppa000557m (*cellulose synthase* 6) was downregulated at 12 HAI. However, several cellulose synthase-like genes were upregulated simultaneously (Supplementary Table 10). The expression of most of the pectin lyase-related genes was promoted within 12–48 HAI in the inoculated peach shoots. Interestingly, pectin methylesterase inhibitor-related genes were almost upregulated as well. At 60 HAI, the number of downregulated genes increased. Meanwhile, ppa007271m (gene encoding pectin lyase-like superfamily protein) was significantly upregulated at all HAI periods (Supplementary Table 10).

A comprehensive illustration of carbohydrate metabolism based on the transcriptomic changes during *L. theobromae* infection is presented in Supplementary Figure 4. The expression levels of Sucrose synthase (SS) genes (ppa001535m, ppa017606m, and ppa001135m) were higher in the inoculated peach shoots than in the control shoots. At 60 HAI, ppa001535m, and ppa017606m were downregulated in the inoculated peach shoots. Sucrose phosphate synthase (SPS) genes were also upregulated (ppa000622m) or showed this tendency (ppa000636m and ppa000639m) at 60 HAI. The expression levels of *glucose 6-phosphate translocator* genes (ppa006608m and ppa006795m) increased in the inoculated peach shoots (Supplementary Figure 5). Ppa007136m (*alpha-galactosidase* 2) was downregulated in the inoculated peach shoots, indicating that galactose hydrolysis was inhibited. Meanwhile, the expression of ppa008032 (*UDP-D-glucose 4-epimerase* 5) was promoted. UDP-D-glucose 4-epimerase (UGE) is the key enzyme in UDP-D-galactose biosynthesis (Seifert et al., 2002; Rösti et al., 2007). The expression levels of ppa008317m (*UDP-xylose synthase* 4) and ppa001692m (*beta-D-xylosidase* 4) were also enhanced,

especially at 48 HAI. Higher patterns of expression were observed in genes involved in the catabolism of fructose in the inoculated peach shoots relative to the control shoots. These genes include *hexokinase* (ppa004471m), *phosphofructokinase* (ppa003994m and ppa004086m), and *mannose-6-phosphate isomerase* (ppa005846m). However, ppa007744m, ppa025195m, and ppa006746m (encoding aldolase) were downregulated. This result indicates that the further decomposition of fructose-1,6-bisphosphate was inhibited in the inoculated peach shoots. Fructose-6-bisphosphate can participate in the biosynthesis of D-mannose-6-phosphate (Supplementary Figure 6). In addition, genes related to the degradation of glycosaminoglycan and other glycans were downregulated in the inoculated peach shoots.

Genes Involved in ET and JA Biosynthesis and Signaling were Mainly Upregulated in the Inoculated Peach Shoots

An overview of genes involved in ET and JA biosynthetic pathway was presented in Supplementary Figure 7. The *SAM synthetase* (ppa006841m) was overexpressed in the inoculated peach shoots. Higher patterns of expression were also observed (RPKM values) or obtained (qRT-PCR values) in pivotal genes related to the ET biosynthesis. These genes include *1-aminocyclopropane-1-carboxylate (ACC) synthase* 6 (ppa016458) and ET-forming enzyme (ppa008791m) (Supplementary Figure 8A; **Figure 4A**). The expression pattern of ppa016458 and ppa008791m was consistent with the variation trend of ET production. Several DEGs encoding ET signaling components have also been identified. The expression levels of ppa023839m and ppa012014m (genes encoding ET response factor) and ppa001786m (ET sensor) determined by qRT-PCR were increased several times to 10 times after *L. theobromae* infection, this result is consistent with the RNA-Seq data (**Figure 4A**). Other DEGs involved in the ethylene signaling pathway were listed in Supplementary Figure 8A. The protein involved in JA biosynthesis (12-oxophytodienoate reductase 2, ppa007490m) was overexpressed in the inoculated peach shoots. The expression levels (RPKM values) of other genes, such as *allene oxide synthase* (ppa025045m), *allene oxide cyclase* 3 (ppa010397m), and *allene oxide cyclase* 4 (ppa012079m) were higher (two to five-fold) in the inoculated peach shoots than in the control shoots at 12, 24, and 48 HAI, although no difference (ppa010397m and ppa012079m) or lower expression (ppa025045m) was observed at 60 HAI. JA-ME is catalyzed by JA carboxyl methyltransferase, this gene (ppa017829m) was upregulated at 12 and 24 HAI and downregulated at 48 and 60 HAI in the inoculated peach shoots (Supplementary Figure 8B). The qRT-PCR results were similar to the RPKM values (**Figure 4D**).

Verification of Gene Expression Profiles Using qRT-PCR

At 12, 24, 48, and 60 HAI, we collected samples from eight shoots and pooled them for RNA extraction and subsequent RNA-Seq analysis. A one-to-one correspondence exists between J and C in this experiment. To confirm the accuracy and reproducibility of the transcriptome analysis

results, 26 representative genes were selected for real-time qRT-PCR validation in a separate experiment. The primers of these genes are shown in Supplementary Table 7, and the qRT-PCR results are shown in **Figure 4**. The fold change of the gene expression ratios between RNA-Seq and qRT-PCR was analyzed by linear regression. The overall correlation coefficient was 0.8025, indicating the reliability of the RNA-Seq data (**Figure 4E**).

DISCUSSION

Phenylpropanoid Metabolism and Glycosyltransferase Activity of the Inoculated Peach Shoots

In general, a marked induction of genes is involved in the biosynthesis of phenylpropanoids in plants as a response to pathogens (Shetty et al., 2011; Xu et al., 2011; Kostyn et al., 2012; Muñoz-Bodnar et al., 2014). Phenylpropanoids play important roles in plant resistance to pathogen attacks (Dixon et al., 2002; Korkina, 2007; Naoumkina et al., 2010; Boubakri et al., 2013). In addition, the protective action of phenylpropanoids in plants is assumed to be based on their antioxidant and free radical scavenging properties. Flavonoids are representative substances of phenylpropanoid derivatives in plants (Tahara, 2007). Flavonoids are natural defense compounds in plants against pathogens. Anthocyanins represent one class of flavonoids that are significantly accumulated around the lesions of the inoculated peach shoots, resulting in a red coloration on infected peach shoots (**Figure 1A**; Li et al., 2014b). As important secondary metabolites, anthocyanins contribute to protect plants against pathogenic attack (Winkel-Shirley, 2001). As a type of abiotic stress, wounds can also induce the flavonoids accumulation. Therefore, a slight red coloration appeared around the wound site of the control shoots (**Figure 1A**). However, the effect was much less than the stress response induced by *L. theobromae*. Plant UDP-glycosyltransferases and UDP-glucosyltransferases can be involved in the modification of phenylpropanoids (Vogt and Jones, 2000). The glycosylated form of these compounds exhibits enhanced solubility, stability, and transport properties (Li et al., 2001), and can be stored as preformed defense compounds. The glycosylated defense compounds (e.g., flavonoids) involved during pathogen attacks are activated by deglycosylation (Jasiński et al., 2009). Several genes encoding UGTs play important roles in plant defense against pathogens (Chong et al., 2002; Poppenberger et al., 2003; von Saint Paul et al., 2011). For example, UGT73B3 and UGT73B5 supposedly participate in the regulation of redox status and general detoxification of reactive oxygen species and contribute to the resistance of *Arabidopsis* to *Pseudomonas syringae* pv. *tomato* (Simon et al., 2014).

Carbohydrate Metabolism and Gum Formation of the Inoculated Peach Shoots

Some pathogens can secrete polygalacturonases and endopolygalacturonases which enable them to penetrate the host plant by degrading the plant cell wall pectin. *Botryosphaeria* spp. belonging to ascomycetous fungi can degrade lignin and

pectin (Alves da Cunha et al., 2003). The pectinase produced by these fungi could degrade the cell wall structures (Srivastava et al., 2013). PMEIs (pectin methylesterase inhibitors) can inhibit pectin methylesterases. Lionetti et al. (2007) reported that PMEIs contributed to the defense of *Arabidopsis* to *B. cinerea*. In the present study, the transcript levels of genes encoding PMEIs increased, especially during the early and middle infection periods. The defense response of the peach shoot tissues was stimulated by *L. theobromae* infection. However, some genes encoding pectin lyase-like superfamily protein were also upregulated (Supplementary Table 10). Hence, PMEIs could not completely prevent the breakdown of pectin. Overall, the new biosynthesis of cellulose can be assumed to be accompanied by degradation. The monosaccharide components of peach gum polysaccharides are galactose, arabinose, xylose, mannose, and glucuronic acid (Simas et al., 2008; Simas-Tosin et al., 2009). β -1,4-linked glucose, xyloglucan, rhamnogalacturonan I, homogalacturonan, rhamnogalacturonan II, and arabinan are representative components of plant cell wall polysaccharides (Vorwerk et al., 2004). A previous study speculated that peach gum arises from the degradation of parenchyma cells around the periderm and vascular cambium (Biggs and Britton, 1988). Recent research has shown that the cell walls were severely degraded in the lesion of inoculated peach shoots (Li et al., 2014b). A follow-up study indicated that not only the infection site but also the glycometabolism of tissues around the lesion of the inoculated peach shoots greatly contributes to peach gum formation (Li et al., 2014a). Therefore, the degradation of plant cell walls after inoculation with *L. theobromae* is just one reason for gum formation.

The expression changes of starch metabolism-related genes indicate that amylose decomposition was promoted in the inoculated peach shoots while starch synthesis was inhibited. A previous report indicated that the amyloplast was disappeared during later infection (Li et al., 2014b). SS and SPS are key enzymes in sucrose metabolism (Winter and Huber, 2000; Ruan, 2014). SS has a dual function although it was previously believed to play a major role in sucrose cleavage (Chourey and Nelson, 1979; Geigenberger and Stitt, 1993; Heim et al., 1993). The measurement results of sucrose content (Li et al., 2014a) indicated that sucrose decomposition was promoted before 60 HAI and then biosynthesis reaction was increased. At 60 HAI, the peach gum spilled out, and then the increased biosynthesis of sucrose may compensate for the consumed sucrose. Glucose 6-phosphate, provided by the catabolism of sucrose and starch, was an important precursor in the biosynthesis of monosaccharide components of peach gum. The upregulated expression of glucose 6-phosphate translocator will contribute to the biosynthesis of monosaccharide components of peach gum. Our RNA-Seq results revealed that the biosynthesis of UDP-D-galactose, UDP-D-xylose, and D-mannose-6-phosphate was increased in the inoculated peach shoots. Previous study showed that the biosynthesis of UDP-D-arabinose and L-arabinose was also enhanced (Li et al., 2014a).

Glycosyltransferases can catalyze the transfer of sugar residue from an activated nucleotide sugar donor to specific acceptor molecules. This process leads to the formation of

glycosidic bonds that play important roles in the biosyntheses of disaccharides, oligosaccharides, polysaccharides, and glycoconjugates (Campbell et al., 1997; Breton et al., 2006). Common glycosyl donors in plants are UDP-glucose (Jones and Vogt, 2001; Jones et al., 2003), UDP-galactose (Ishikura and Mato, 1993; Miller et al., 1999), UDP-rhamnose (Bar-Peled et al., 1991; Jones et al., 2003), UDP-xylose (Martin et al., 1999), and UDP-glucuronate (Sawada et al., 2005). Interestingly, galactose, arabinose, xylose, mannose, and glucuronic acid are the main monosaccharide components of peach gum polysaccharides (Simas et al., 2008; Simas-Tosin et al., 2009). In the present study, the amount of these glycosyl donors (UDP-glucose, UDP-galactose, UDP-xylose, and UDP-arabinose) was increased. The high expression of genes encoding relevant galactosyltransferases in the inoculated peach shoots may promote the biosynthesis of peach gum polysaccharides.

Involvement of ET and JA in Peach Gummosis Development

ET is an important plant hormone signal in plant-pathogen interactions (Bleecker and Kende, 2000). ET production of plant tissues can be enhanced by pathogen invasion (Penninckx et al., 1998; Cohn and Martin, 2005). Consistent results were also determined in our study (Figure 1C). That is, ET biosynthesis was promoted, especially at 24 HAI. S-adenosylmethionine (SAM) is a general donor of methyl groups in the transmethylation reactions and is also an important precursor substance of ET synthesis. Tsuchisaka and Theologis (2004) reported that wounding the hypocotyl tissue of Arabidopsis induces the expression of *AtACS2*, 4, 6, 7, 8, and 11. In the present study, in addition to wound-treatments, the pathogen challenge aside from wound treatments promoted the expression of *ppa016458*, as proven in the endogenous production of ET (Figure 1C). Li et al. (2014c) reported that ETH application on peach shoots pre-inoculated with *L. theobromae* promotes gum formation. ETH treatments accelerated the senescence of peach shoots and rapidly increased the contents of sucrose, glucose, and fructose (Li et al., 2014c), which may promote disease development and facilitate gum formation.

In general, the expression data showed that the genes involved in JA biosynthesis were rapidly induced. A similar result has been observed in Arabidopsis defense against *B. cinerea* (Birkenbihl et al., 2012; Windram et al., 2012). In *Plum pox virus* inoculated peach leaves without visible symptoms, JA biosynthesis and signaling genes were upregulated, indicating that JA stimulate plant defense response (Rubio et al., 2015). Interestingly, JA was first isolated from cultures of the fungus *L. theobromae* (Aldridge et al., 1971). JA biosynthesis in *L. theobromae* is similar to that in plants (Tsukada et al., 2010). Thus, JA might play a role in the interaction between peach shoots and *L. theobromae*. Skrzypek et al. (2005b) pointed out that JA-ME substantially reduces the amount of sucrose and reducing sugars in tulips, contributing to gum formation. Li et al. (2015) also speculated that JA-ME treatments cause new synthesis of polysaccharides.

In conclusion, inoculation with *L. theobromae* can induce typical gummosis on current-year peach shoots *in vitro*. We

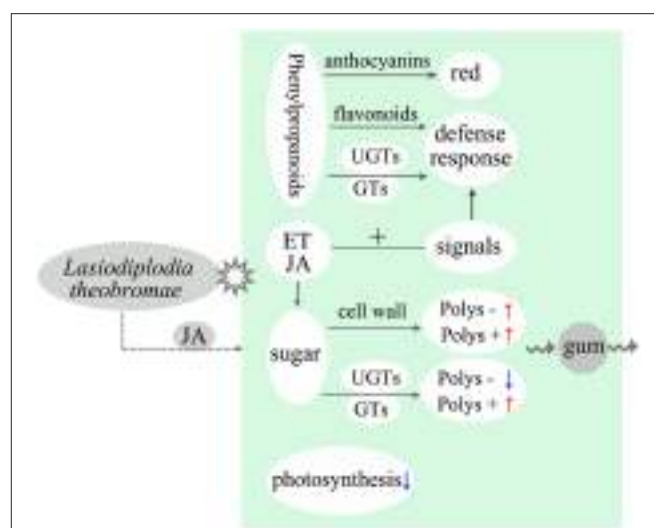


FIGURE 5 | Model illustrating the main molecular response and gum polysaccharide formation of peach shoots infected with *L. theobromae*.

theobromae. “Polys –” means polysaccharide degradation. “Polys +” indicates polysaccharide biosynthesis. Red and blue arrows represent upregulation and downregulation, respectively. Dotted arrow shows a supposed interaction.

analyzed gene expression changes of the peach shoots at different phases after inoculation through RNA-Seq. The main results of this study are summarized in Figure 5. Plant tissues usually exhibit strong defense responses during *L. theobromae* infection. Genes related to the glycometabolism of the inoculated peach shoots were activated, indicating that polysaccharide biosynthesis was increased. In addition, the expression of genes involved in the degradation of cell walls was promoted, but the degradation of glycosaminoglycan and glycan was inhibited. The above factors might be the main cause of the formation of gum polysaccharides induced by *L. theobromae*. Our study provided insights into the mechanisms of peach gummosis caused by *L. theobromae*. However, the role of gum in peach tree response to pathogen attacks requires further investigation.

AUTHOR CONTRIBUTIONS

LG and YW were responsible for generating the RNA-seq data and for the interpretation of the data. LG carried out qRT-PCR experiments and measured ethylene content, and drafted the manuscript. GL conceived the study and supervised the research. ZL and JY participated in its design and helped to draft the manuscript. HZ participated in the statistical analyses. All authors approved the final manuscript and approved it for publication.

FUNDING

This study was supported by the National Natural Science Foundation of China (Grant No. 31471840) and China Agriculture Research System (Grant No. CARS-31-2-4).

ACKNOWLEDGMENTS

Thanks the members of my group and ZL for helpful discussions. The raw data of the RNA-Seq has been uploaded to the Sequence Read Archive (SRA). The accession number is SRR3112581.

REFERENCES

- Aldridge, D. C., Galt, S., Giles, D., and Turner, W. B. (1971). Metabolites of *Lasioidiploida theobromae*. *J. Chem. Soc. C* 1623–1627. doi: 10.1039/j39710001623
- Alves da Cunha, M. A., Barbosa, A. M., Giese, E. C., and Dekker, R. F. (2003). The effect of carbohydrate carbon sources on the production of constitutive and inducible laccases by *Botryosphaeria* sp. *J. Basic Microbiol.* 43, 385–392. doi: 10.1002/jobm.200310250
- Bar-Peled, M., Lewinsohn, E., Fluhr, R., and Gressel, J. (1991). UDP-rhamnose: flavanone-7-O-glucoside-2'-O-rhamnosyltransferase. Purification and characterization of an enzyme catalyzing the production of bitter compounds in citrus. *J. Biol. Chem.* 266, 20953–20959.
- Beckman, T. G., Pusey, P. L., and Bertrand, P. F. (2003). Impact of fungal gummosis on peach trees. *HortScience* 38, 1141–1143.
- Biggs, A. R., and Britton, K. O. (1988). Presymptom histopathology of peach trees inoculated with *Botryosphaeria obtusa* and *B. dothidea*. *Phytopathology* 78, 1109–1118. doi: 10.1094/Phyto-78-1109
- Birkenbihl, R. P., Diezel, C., and Somssich, I. E. (2012). Arabidopsis WRKY33 is a key transcriptional regulator of hormonal and metabolic responses toward *Botrytis cinerea* infection. *Plant Physiol.* 159, 266–285. doi: 10.1104/pp.111.192641
- Bleecker, A. B., and Kende, H. (2000). Ethylene: a gaseous signal molecule in plants. *Annu. Rev. Cell Dev. Biol.* 16, 1–18. doi: 10.1146/annurev.cellbio.16.1.1
- Boubakri, H., Poutaraud, A., Wahab, M. A., Claveux, C., Baltenweck-Guyot, R., Steyer, D., et al. (2013). Thiamine modulates metabolism of the phenylpropanoid pathway leading to enhanced resistance to *Plasmopara viticola* in grapevine. *BMC Plant Biol.* 13:31. doi: 10.1186/1471-2229-13-31
- Breton, C., Šnajdrová, L., Jeanneau, C., Koča, J., and Imbert, A. (2006). Structures and mechanisms of glycosyltransferases. *Glycobiology* 16, 29R–37R. doi: 10.1093/glycob/cwj016
- Britton, K. O., and Hendrix, F. F. (1982). Three species of *Botryosphaeria* cause peach tree gummosis in Georgia. *Plant Dis.* 66, 1120–1121. doi: 10.1094/PD-66-1120
- Campbell, J. A., Davies, G. J., Bulone, V., and Henrissat, B. (1997). A classification of nucleotide-diphospho-sugar glycosyltransferases based on amino acid sequence similarities. *Biochem. J.* 326, 929–939. doi: 10.1042/bj3260929u
- Chong, J., Baltz, R., Schmitt, C., Beffa, R., Fritig, B., and Saindrenan, P. (2002). Downregulation of a pathogen-responsive tobacco UDP-Glc: phenylpropanoid glycosyltransferase reduces scopoletin glucoside accumulation, enhances oxidative stress, and weakens virus resistance. *Plant Cell* 14, 1093–1107. doi: 10.1105/tpc.010436
- Chourey, P. S., and Nelson, O. E. (1979). Interallelic complementation at the sh locus in maize at the enzyme level. *Genetics* 91, 317–325.
- Cohn, J. R., and Martin, G. B. (2005). *Pseudomonas syringae* pv. *tomato* type III effectors *AvrPto* and *AvrPtoB* promote ethylene-dependent cell death in tomato. *Plant J.* 44, 139–154. doi: 10.1111/j.1365-313X.2005.02516.x
- Czemmel, S., Galarneau, E. R., Travadon, R., McElrone, A. J., Cramer, G. R., and Baumgartner, K. (2015). Genes expressed in grapevine leaves reveal latent wood infection by the fungal pathogen *Neofusicoccum parvum*. *PLoS ONE* 10:e0121828. doi: 10.1371/journal.pone.0121828
- de Jonge, R., van Esse, H. P., Maruthachalam, K., Bolton, M. D., Santhanam, P., Saber, M. K., et al. (2012). Tomato immune receptor Ve1 recognizes effector of multiple fungal pathogens uncovered by genome and RNA sequencing. *Proc. Natl. Acad. Sci. U.S.A.* 109, 5110–5115. doi: 10.1073/pnas.1119623109
- de Wild, H. P., Gude, H., and Peppelenbos, H. W. (2002). Carbon dioxide and ethylene interactions in tulip bulbs. *Physiol. Plant.* 114, 320–326. doi: 10.1034/j.1399-3054.2002.1140219.x
- Dixon, R. A., Achtnine, L., Kota, P., Liu, C. J., Reddy, M. S., and Wang, L. (2002). The phenylpropanoid pathway and plant defence—a genomics perspective. *Mol. Plant Pathol.* 5, 371–390. doi: 10.1046/j.1364-3703.2002.00131.x
- Geigenberger, P., and Stitt, M. (1993). Sucrose synthase catalyses a readily reversible reaction *in vivo* in developing potato tubers and other plant tissues. *Planta* 189, 329–339. doi: 10.1007/BF00194429
- Heim, U., Weber, H., Bäumlein, H., and Wobus, U. (1993). A sucrose-synthase gene of *Vicia faba* L.: expression pattern in developing seeds in relation to starch synthesis and metabolic regulation. *Planta* 191, 394–401. doi: 10.1007/BF00195698
- Ishikura, N., and Mato, M. (1993). Partial purification and some properties of flavonol 3-O-glycosyltransferases from seedlings of *Vigna mungo*, with special reference to the formation of kaempferol 3-O-galactoside and 3-O-glucoside. *Plant Cell Physiol.* 34, 329–335.
- Jasiński, M., Kachlicki, P., Rodzikiewicz, P., Figlerowicz, M., and Stobiecki, M. (2009). Changes in the profile of flavonoid accumulation in *Medicago truncatula* leaves during infection with fungal pathogen *Phoma medicaginis*. *Plant Physiol. Biochem.* 47, 847–853. doi: 10.1016/j.plaphy.2009.05.004
- Jones, P., Messner, B., Nakajima, J. I., Schäffner, A. R., and Saito, K. (2003). UGT73C6 and UGT78D1, glycosyltransferases involved in flavonol glycoside biosynthesis in *Arabidopsis thaliana*. *J. Biol. Chem.* 278, 43910–43918. doi: 10.1074/jbc.M303523200
- Jones, P., and Vogt, T. (2001). Glycosyltransferases in secondary plant metabolism: tranquilizers and stimulant controllers. *Planta* 213, 164–174. doi: 10.1007/s004250000492
- Kim, K. H., Kang, Y. J., Kim, D. H., Yoon, M. Y., Moon, J. K., Kim, M. Y., et al. (2011). RNA-Seq analysis of a soybean near-isogenic line carrying bacterial leaf pustule-resistant and-susceptible alleles. *DNA Res.* 18, 483–497. doi: 10.1093/dnares/dsr033
- Korkina, L. G. (2007). Phenylpropanoids as naturally occurring antioxidants: from plant defense to human health. *Cell Mol. Biol.* 53, 15–25. doi: 10.1170/T772
- Kostyn, K., Czemplik, M., Kulma, A., Bortniczuk, M., Skala, J., and Szopa, J. (2012). Genes of phenylpropanoid pathway are activated in early response to *Fusarium* attack in flax plants. *Plant Sci.* 190, 103–115. doi: 10.1016/j.plantsci.2012.03.011
- Kunjetti, S. H., Evans, T. A., Marsh, A. G., Gregory, N. F., Kunjetti, S., Meyers, B. C., et al. (2012). RNA-Seq reveals infection-related global gene changes in *Phytophthora phaseoli*, the causal agent of lima bean downy mildew. *Mol. Plant Pathol.* 13, 454–466. doi: 10.1111/j.1364-3703.2011.00761.x
- Li, M., Liu, M., Peng, F., and Fang, L. (2015). Influence factors and gene expression patterns during MeJa-induced gummosis in peach. *J. Plant Physiol.* 182, 49–61. doi: 10.1016/j.jplph.2015.03.019
- Li, Y., Baldau, S., Lim, E. K., and Bowles, D. J. (2001). Phylogenetic analysis of the UDP-glycosyltransferase multigene family of *Arabidopsis thaliana*. *J. Biol. Chem.* 276, 4338–4343. doi: 10.1074/jbc.M007447200
- Li, Z., Gao, L., Wang, Y. T., Zhu, W., Ye, J. L., and Li, G. H. (2014a). Carbohydrate metabolism changes in *Prunus persica* gummosis infected with *Lasioidiploida theobromae*. *Phytopathology* 104, 445–452. doi: 10.1094/PHYTO-01-13-0025-R
- Li, Z., Wang, Y. T., Gao, L., Wang, F., Ye, J. L., and Li, G. H. (2014b). Biochemical changes and defence responses during the development of peach gummosis caused by *Lasioidiploida theobromae*. *Eur. J. Plant Pathol.* 138, 195–207. doi: 10.1007/s10658-013-0322-4
- Li, Z., Zhu, W., Fan, Y. C., Ye, J. L., and Li, G. H. (2014c). Effects of pre- and post-treatment with ethephon on gum formation of peach gummosis caused by *Lasioidiploida theobromae*. *Plant Pathol.* 63, 1306–1315. doi: 10.1111/ppa.12214
- Lionetti, V., Raiola, A., Camardella, L., Giovane, A., Obel, N., and Pauly, M., et al. (2007). Overexpression of pectin methylesterase inhibitors in *Arabidopsis* restricts fungal infection by *Botrytis cinerea*. *Plant Physiol.* 143, 1871–1880. doi: 10.1104/pp.106.090803

SUPPLEMENTARY MATERIAL

The Supplementary Material for this article can be found online at: <http://journal.frontiersin.org/article/10.3389/fphys.2016.00170>

- Livak, K. J., and Schmittgen, T. D. (2001). Analysis of relative gene expression data using real-time quantitative PCR and the $2^{-\Delta\Delta CT}$ method. *Methods* 25, 402–408. doi: 10.1006/meth.2001.1262
- Marguerat, S., and Bähler, J. (2010). RNA-seq: from technology to biology. *Cell Mol. Life Sci.* 67, 569–579. doi: 10.1007/s00018-009-0180-6
- Martin, R. C., Mok, M. C., and Mok, D. W. (1999). A gene encoding the cytokinin enzyme zeatinO-xylosyltransferase of *Phaseolus vulgaris*. *Plant Physiol.* 120, 553–558. doi: 10.1104/pp.120.2.553
- Miller, K. D., Guyon, V., Evans, J. N., Shuttleworth, W. A., and Taylor, L. P. (1999). Purification, cloning, and heterologous expression of a catalytically efficient flavonol 3-O-galactosyltransferase expressed in the male gametophyte of *Petunia hybrida*. *J. Biol. Chem.* 274, 34011–34019. doi: 10.1074/jbc.274.48.34011
- Miyamoto, K., Kotake, T., Sasamoto, M., Saniewski, M., and Ueda, J. (2010). Gummosis in grape hyacinth (*Muscari armeniacum*) bulbs: hormonal regulation and chemical composition of gums. *J. Plant Res.* 123, 363–370. doi: 10.1007/s10265-009-0273-1
- Morrison, J. C., Labavitch, J. M., and Greve, L. C. (1987). The role of ethylene in initiating gum duct formation in almond fruit. *J. Am. Soc. Hort. Sci.* 112, 364–367.
- Muniz, C. R., Freire, F. C. O., Viana, F. M. P., Cardoso, J. E., Cooke, P., and Wood, D., et al. (2011). Colonization of cashew plants by *Lasiodiplodia theobromae*: microscopical features. *Micron* 42, 419–428. doi: 10.1016/j.micron.2010.12.003
- Muñoz-Bodnar, A., Perez-Quintero, A. L., Gomez-Cano, F., Gil, J., Michelmore, R., Bernal, A., et al. (2014). RNAseq analysis of cassava reveals similar plant responses upon infection with pathogenic and non-pathogenic strains of *Xanthomonas axonopodis* pv. *manihotis*. *Plant Cell Rep.* 33, 1901–1912. doi: 10.1007/s00299-014-1667-7
- Naoumkina, M. A., Zhao, Q., Gallego-Giraldo, L., Dai, X., Zhao, P. X., and Dixon, R. A. (2010). Genome-wide analysis of phenylpropanoid defence pathways. *Mol. Plant Pathol.* 11, 829–846. doi: 10.1111/j.1364-3703.2010.00648.x
- Olien, W. C., and Bulkovac, M. J. (1982). Ethephon-induced gummosis in sour cherry (*Prunus cerasus* L.) I. Effect on xylem function and shoot water status. *Plant Physiol.* 70, 547–555. doi: 10.1104/pp.70.2.547
- Penningckx, I. A., Thomma, B. P., Buchala, A., Métraux, J. P., and Broekaert, W. F. (1998). Concomitant activation of jasmonate and ethylene response pathways is required for induction of a plant defensin gene in *Arabidopsis*. *Plant Cell* 10, 2103–2113. doi: 10.1105/tpc.10.12.2103
- Poppenberger, B., Berthiller, F., Lucyshyn, D., Sieberer, T., Schuhmacher, R., Krská, R., et al. (2003). Detoxification of the *Fusarium mycotoxin* deoxynivalenol by a UDP-glucosyltransferase from *Arabidopsis thaliana*. *J. Biol. Chem.* 278, 47905–47914. doi: 10.1074/jbc.M30755220
- Rösti, J., Barton, C. J., Albrecht, S., Dupree, P., Pauly, M., and Findlay, K., et al. (2007). UDP-glucose 4-epimerase isoforms UGE2 and UGE4 cooperate in providing UDP-galactose for cell wall biosynthesis and growth of *Arabidopsis thaliana*. *Plant Cell* 19, 1565–1579. doi: 10.1105/tpc.106.049619
- Ruan, Y. L. (2014). Sucrose metabolism: gateway to diverse carbon use and sugar signaling. *Annu. Rev. Plant Biol.* 65, 33–67. doi: 10.1146/annurev-arplant-050213-040251
- Rubio, M., Rodriguez-Moreno, L., Ballester, A. R., Moura, M. C., Bonghi, C., and Candresse, T., et al. (2015). Analysis of gene expression changes in peach leaves in response to *Plum pox virus* infection using RNA-Seq. *Mol. Plant Pathol.* 16, 164–176. doi: 10.1111/mpp.12169
- Saniewski, M., Miyamoto, K., and Ueda, J. (1998). Methyl jasmonate induces gums and stimulates anthocyanin accumulation in peach shoots. *J. Plant Growth Regul.* 17, 121–124. doi: 10.1007/PL00007024
- Saniewski, M., Miyamoto, K., and Ueda, J. (2002). “Gum induction by methyl jasmonate in fruits, stems and petioles of *Prunus domestica* L.” in XXVI International Horticultural Congress: Key Processes in the Growth and Cropping of Deciduous Fruit and Nut Trees, Vol. 636 (Toronto, ON), 151–158.
- Saniewski, M., Ueda, J., Horbowicz, M., Miyamoto, K., and Puchalski, J. (2001). Gum in apricot (*Prunus armeniaca* L.) shoots induced by methyl jasmonate. *Acta Agrobot.* 54, 27–34. doi: 10.5586/aa.2001.020
- Sawada, S. Y., Suzuki, H., Ichimaida, F., Yamaguchi, M. A., Iwashita, T., and Fukui, Y., et al. (2005). UDP-glucuronic acid: anthocyanin glucuronosyltransferase from red daisy (*Bellis perennis*) flowers enzymology and phylogenetics of a novel glucuronosyltransferase involved in flower pigment biosynthesis. *J. Biol. Chem.* 280, 899–906. doi: 10.1074/jbc.M410537200
- Seifert, G. J., Barber, C., Wells, B., Dolan, L., and Roberts, K. (2002). Galactose biosynthesis in *Arabidopsis*: genetic evidence for substrate channeling from UDP-D-galactose into cell wall polymers. *Curr. Biol.* 12, 1840–1845. doi: 10.1016/S0960-9822(02)01260-5
- Sherif, S., Palijath, G., and Jayasankar, S. (2012). Molecular characterization of peach PR genes and their induction kinetics in response to bacterial infection and signaling molecules. *Plant Cell Rep.* 31, 697–711. doi: 10.1007/s00299-011-1188-6
- Shetty, R., Fretté, X., Jensen, B., Shetty, N. P., Jensen, J. D., and Jørgensen, H. J. L., et al. (2011). Silicon-induced changes in antifungal phenolic acids, flavonoids, and key phenylpropanoid pathway genes during the interaction between miniature roses and the biotrophic pathogen *Podosphaera pannosa*. *Plant Physiol.* 157, 2194–2205. doi: 10.1104/pp.111.185215
- Simas, F. F., Gorin, P. A., Wagner, R., Sasaki, G. L., Bonkerner, A., and Iacomini, M. (2008). Comparison of structure of gum exudate polysaccharides from the trunk and fruit of the peach tree (*Prunus persica*). *Carbohydr. Polym.* 71, 218–228. doi: 10.1016/j.carbpol.2007.05.032
- Simas-Tosin, F. F., Barraza, R. R., Petkowicz, C. L. O., Silveira, J. L. M., Sasaki, G. L., and Santos, E. M. R., et al. (2010). Rheological and structural characteristics of peach tree gum exudate. *Food Hydrocolloid.* 24, 486–493. doi: 10.1016/j.foodhyd.2009.12.010
- Simas-Tosin, F. F., Wagner, R., Santos, E. M. R., Sasaki, G. L., Gorin, P. A. J., and Iacomini, M. (2009). Polysaccharide of nectarine gum exudate: comparison with that of peach gum. *Carbohydr. Polym.* 76, 485–487. doi: 10.1016/j.carbpol.2008.11.013
- Simon, C., Langlois-Meurinne, M., Didierlaurent, L., Chaouch, S., Bellvert, F., and Massoud, K., et al. (2014). The secondary metabolism glycosyltransferases UGT73B3 and UGT73B5 are components of redox status in resistance of *Arabidopsis* to *Pseudomonas syringae* pv. *tomato*. *Plant Cell Environ.* 37, 1114–1129. doi: 10.1111/pce.12221
- Skrzypek, E., Miyamoto, K., Saniewski, M., and Ueda, J. (2005a). Identification of jasmonic acid and its methyl ester as gum-inducing factors in tulips. *J. Plant Res.* 118, 27–30. doi: 10.1007/s10265-004-0190-2
- Skrzypek, E., Miyamoto, K., Saniewski, M., and Ueda, J. (2005b). Jasmonates are essential factors inducing gummosis in tulips: mode of action of jasmonates focusing on sugar metabolism. *J. Plant Physiol.* 162, 495–505. doi: 10.1016/j.jplph.2004.09.007
- Socquet-Juglard, D., Kamber, T., Pothier, J. F., Christen, D., Gessler, C., and Duffy, B., et al. (2013). Comparative RNA-seq analysis of early-infected peach leaves by the invasive phytopathogen *Xanthomonas arboricola* pv. *pruni*. *PLoS ONE* 8:e54196. doi: 10.1371/journal.pone.0054196
- Srivastava, P., Andersen, P. C., Marois, J. J., Wright, D. L., Srivastava, M., and Harmon, P. F. (2013). Effect of phenolic compounds on growth and ligninolytic enzyme production in *Botryosphaeria* isolates. *Crop Prot.* 43, 146–156. doi: 10.1016/j.cropro.2012.09.015
- Tahara, S. (2007). A journey of twenty-five years through the ecological biochemistry of flavonoids. *Biosci. Biotechnol. Biochem.* 71, 1387–1404. doi: 10.1271/bbb.70028
- Tsuchisaka, A., and Theologis, A. (2004). Unique and overlapping expression patterns among the *Arabidopsis* 1-amino-cyclopropane-1-carboxylate synthase gene family members. *Plant Physiol.* 136, 2982–3000. doi: 10.1104/pp.104.049999
- Tsukada, K., Takahashi, K., and Nabeta, K. (2010). Biosynthesis of jasmonic acid in a plant pathogenic fungus, *Lasiodiplodia theobromae*. *Phytochemistry* 71, 2019–2023. doi: 10.1016/j.phytochem.2010.09.013
- Verde, I., Abbott, A. G., Scalabrin, S., Jung, S., Shu, S., and Marroni, F. (2013). The high-quality draft genome of peach (*Prunus persica*) identifies unique patterns of genetic diversity, domestication and genome evolution. *Nat. Genet.* 45, 487–494. doi: 10.1038/ng.2586
- Vogt, T., and Jones, P. (2000). Glycosyltransferases in plant natural product synthesis: characterization of a supergene family. *Trends Plant Sci.* 5, 380–386. doi: 10.1016/S1360-1385(00)01720-9
- von Saint Paul, V., Zhang, W., Kanawati, B., Geist, B., Faus-Kefler, T., and Schmitt-Kopplin, P., et al. (2011). The *Arabidopsis* glucosyltransferase UGT76B1

- conjugates isoleucic acid and modulates plant defense and senescence. *Plant Cell* 23, 4124–4145. doi: 10.1105/tpc.111.088443
- Vorwerk, S., Somerville, S., and Somerville, C. (2004). The role of plant cell wall polysaccharide composition in disease resistance. *Trends Plant Sci.* 9, 203–209. doi: 10.1016/j.tplants.2004.02.005
- Wang, F., Zhao, L. N., Li, G. H., Huang, J. B., and Hsiang, T. (2011). Identification and Characterization of *Botryosphaeria* spp. Causing Gummosis of Peach Trees in Hubei Province, Central China. *Plant Dis.* 95, 1378–1384. doi: 10.1094/PDIS-12-10-0893
- Wang, Z., Gerstein, M., and Snyder, M. (2009). RNA-Seq: a revolutionary tool for transcriptomics. *Nat. Rev. Genet.* 10, 57–63. doi: 10.1038/nrg2484
- Weaver, D. J. (1974). A gummosis disease of peach trees caused by *Botryosphaeria dothidea*. *Phytopathology* 64, 1429–1432. doi: 10.1094/Phyto-6-1429
- Windram, O., Madhou, P., McHattie, S., Hill, C., Hickman, R., and Cooke, E., et al. (2012). Arabidopsis defense against *Botrytis cinerea*: chronology and regulation deciphered by high-resolution temporal transcriptomic analysis. *Plant Cell* 24, 3530–3557. doi: 10.1105/tpc.112.102046
- Winkel-Shirley, B. (2001). Flavonoid biosynthesis. A colorful model for genetics, biochemistry, cell biology, and biotechnology. *Plant Physiol.* 126, 485–493. doi: 10.1104/pp.126.2.485
- Winter, H., and Huber, S. C. (2000). Regulation of sucrose metabolism in higher plants: localization and regulation of activity of key enzymes. *Crit. Rev. Plant Sci.* 19, 31–67. doi: 10.1016/S0735-2689(01)80002-2
- Xu, L., Zhu, L. F., Tu, L. L., Liu, L. L., Yuan, D. J., and Jin, L., et al. (2011). Lignin metabolism has a central role in the resistance of cotton to the wilt fungus *Verticillium dahliae* as revealed by RNA-Seq-dependent transcriptional analysis and histochemistry. *J. Exp. Bot.* 62, 5607–5621. doi: 10.1093/jxb/err245
- Zhang, Y. Q., Pei, X. W., Zhang, C., Lu, Z. F., Wang, Z. X., and Jia, S. R., et al. (2012). *De novo* foliar transcriptome of *Chenopodium amaranticolor* and analysis of its gene expression during virus-induced hypersensitive response. *PLoS ONE* 7:e45953. doi: 10.1371/journal.pone.0045953

Conflict of Interest Statement: The authors declare that the research was conducted in the absence of any commercial or financial relationships that could be construed as a potential conflict of interest.

Copyright © 2016 Gao, Wang, Li, Zhang, Ye and Li. This is an open-access article distributed under the terms of the Creative Commons Attribution License (CC BY). The use, distribution or reproduction in other forums is permitted, provided the original author(s) or licensor are credited and that the original publication in this journal is cited, in accordance with accepted academic practice. No use, distribution or reproduction is permitted which does not comply with these terms.



RNA-Seq Analysis of Differential Gene Expression Responding to Different Rhizobium Strains in Soybean (*Glycine max*) Roots

Songli Yuan^{1,2}, Rong Li^{1,2}, Shuilian Chen^{1,2}, Haifeng Chen^{1,2}, Chanjuan Zhang^{1,2}, Limiao Chen^{1,2}, Qingnan Hao^{1,2}, Zhihui Shan^{1,2}, Zhonglu Yang^{1,2}, Dezhen Qiu^{1,2}, Xiaojuan Zhang^{1,2} and Xinan Zhou^{1,2*}

¹ Key Laboratory of Oil Crop Biology, Ministry of Agriculture, Wuhan, China, ² Oil Crops Research Institute of Chinese Academy of Agriculture Sciences, Wuhan, China

OPEN ACCESS

Edited by:

Olivier Lamotte,
UMR Agroécologie, France

Reviewed by:

Uener Kolukisaoglu,
University of Tübingen, Germany
Alexandre Boscarini,
Institut National de la Recherche
Agronomique, France

*Correspondence:

Xinan Zhou
zhouocri@sina.com

Specialty section:

This article was submitted to
Plant Physiology,
a section of the journal
Frontiers in Plant Science

Received: 14 January 2016

Accepted: 10 May 2016

Published: 30 May 2016

Citation:

Yuan S, Li R, Chen S, Chen H, Zhang C, Chen L, Hao Q, Shan Z, Yang Z, Qiu D, Zhang X and Zhou X (2016) RNA-Seq Analysis of Differential Gene Expression Responding to Different Rhizobium Strains in Soybean (*Glycine max*) Roots. *Front. Plant Sci.* 7:721.
doi: 10.3389/fpls.2016.00721

The root nodule symbiosis (RNS) between legume plants and rhizobia is the most efficient and productive source of nitrogen fixation, and has critical importance in agriculture and mesology. Soybean (*Glycine max*), one of the most important legume crops in the world, establishes a nitrogen-fixing symbiosis with different types of rhizobia, and the efficiency of symbiotic nitrogen fixation in soybean greatly depends on the symbiotic host-specificity. Although, it has been reported that rhizobia use surface polysaccharides, secretion proteins of the type-three secretion systems and nod factors to modulate host range, the host control of nodulation specificity remains poorly understood. In this report, the soybean roots of two symbiotic systems (*Bradyrhizobium japonicum* strain 113-2-soybean and *Sinorhizobium fredii* USDA205-soybean) with notable different nodulation phenotypes and the control were studied at five different post-inoculation time points (0.5, 7–24 h, 5, 16, and 21 day) by RNA-seq (Quantification). The results of qPCR analysis of 11 randomly-selected genes agreed with transcriptional profile data for 136 out of 165 (82.42%) data points and quality assessment showed that the sequencing library is of quality and reliable. Three comparisons (control vs. 113-2, control vs. USDA205 and USDA205 vs. 113-2) were made and the differentially expressed genes (DEGs) between them were analyzed. The number of DEGs at 16 days post-inoculation (dpi) was the highest in the three comparisons, and most of the DEGs in USDA205 vs. 113-2 were found at 16 dpi and 21 dpi. 44 go function terms in USDA205 vs. 113-2 were analyzed to evaluate the potential functions of the DEGs, and 10 important KEGG pathway enrichment terms were analyzed in the three comparisons. Some important genes induced in response to different strains (113-2 and USDA205) were identified and analyzed, and these genes primarily encoded soybean resistance proteins, NF-related proteins, nodulins and immunity defense proteins, as well as proteins involving flavonoids/flavone/flavonol biosynthesis and plant-pathogen interaction. Besides, 189 candidate genes are largely expressed in roots and/or nodules. The DEGs uncovered in this study provides molecular candidates for better understanding the mechanisms of

symbiotic host-specificity and explaining the different symbiotic effects between soybean roots inoculated with different strains (113-2 and USDA205).

Keywords: Soybean, symbiotic specificity, different nodulation phenotypes, RNA-seq, differential gene expression responding

INTRODUCTION

The root nodule symbiosis (RNS) between legume plants and rhizobia is the most efficient and productive source of nitrogen fixation, and has critical importance in agriculture and mesology (Biswas and Gresshoff, 2014). Rhizobium-legume symbiosis is established under tight regulation to coordinate bacterial infection steps with re-activation of root cortical cells. The process is triggered by rhizobia-secreted specific lipo-chitin-oligosaccharide signal molecules to host secreted flavonoids, and accompanied by a series of signal transduction inside the root cells (Oldroyd and Downie, 2004, 2008; Libault et al., 2010; Hayashi et al., 2012b). Rhizobium-legume symbiosis is highly host-specific, meaning that one rhizobium strain could only establish a symbiotic system with a limited set of host plants and vice versa (Hayashi et al., 2012a). Such a symbiotic characteristic is very pronounced and has led to the definition of different legume–rhizobia associations, which always associated with distinct nodulation phenotype and/or symbiotic effects (Jones et al., 2008; Hayashi et al., 2012a).

The symbiotic specificity is determined by exchanging species-specific signals between a host plant and its symbiotic rhizobium (Perret et al., 2000). It is well known that rhizobia utilizes surface polysaccharides, secreted proteins/type III secretion system (T3SS) and nod factor to modulate host range (Lerouge et al., 1990; Schultze et al., 1992; Stacey, 1995; Bec-Ferte et al., 1996; Deakin and Broughton, 2009; Yang et al., 2010; Okazaki et al., 2013), while the mechanisms underlying the corresponding recognition of these rhizobial signals and compatibility control of the legume–rhizobia interaction in the host legume are not well understood. To unravel such mechanisms, it is critical to investigate the differences of nod factor signaling reception and transduction in the host legume inoculated with different rhizobia strains.

Soybean (*Glycine max*), one of the most important legume crops in the world, normally establishes a nitrogen-fixing symbiosis with different types of rhizobia, such as *Bradyrhizobium japonicum*, *Bradyrhizobium elkanii*, *Bradyrhizobium liaoningense*, *Bradyrhizobium yuanmingense*, *E. fredii/Sinorhizobium fredii*, *Rhizobium tropici*, *R. oryzae* and *Mesorhizobium tianshanense*, and the efficiency of symbiotic nitrogen fixation in soybean by application of inoculates greatly depends on the symbiotic host-specificity (Yang et al., 2010; Hayashi et al., 2012a). The various species of *Rhizobium* make up two broad groups of fast- and slow-growing strains based

on their growth rate and other characteristics (Sadowsky and Bohlool, 1986). The best studied rhizobium-soybean symbiotic models are *B. japonicum*-soybean (Hennecke, 1990; Meakin et al., 2006; Wei et al., 2008; Mesa et al., 2009; Quelas et al., 2010; Tang et al., 2016) and *S. fredii*-soybean (Annapurna and Krishnan, 2003; Krishnan et al., 2011; Margaret et al., 2011; Jiao et al., 2016), while the differences of the molecular events of nodulation in soybean inoculated with these two rhizobia strains remain unclear.

In most cases, soybean genotypes restrict nodulation with their specific strains (or sero-groups; Keyser and Cregan, 1987; Cregan et al., 1989) and several dominant genes (Rj2, Rj3, Rj4, and Rfg1) have been designated to control the host specificity in the soybean–rhizobia symbiosis (Kanazin et al., 1996; Yang et al., 2010). Besides, comparative analysis of genome sequences of six legumes revealed a large number of symbiotic genes in soybean (Zhu et al., 2013) and RNA-Seq transcription data predicted several nodulation-related gene regulatory networks (Zhu et al., 2013). However, these results cannot explain why different symbiotic effects existed among different soybean–rhizobia associations. To improve our understanding of the host legume control of nodulation specificity, we (1) investigated the molecular events of nodulation in soybean roots inoculated with *B. japonicum* strain 113-2 or *S. fredii* strain USDA205, (2) identified a large number of differentially expressed genes (DEGs), and (3) analyzed the DEGs that are associated with the flavonoids biosynthesis pathway and the plant-pathogen interaction pathway. Our results provide fundamental clues to the mechanisms underlying the host-specific manners of rhizobial signals reception and transduction and shed new light on the host legume control of nodulation specificity.

MATERIALS AND METHODS

Plant Materials and Growth Conditions

Seeds of Soybean Tian long No.1 (stored in our lab) were surface-sterilized and germinated on moistened filter paper for 2–3 d at 28°C in an incubator with 70% relative humidity (RH) and a 16-h light/8-h dark photoperiod. They were then grown in pots filled with sterilized vermiculite and perlite (1:1) supplemented with half-strength B&D medium in a chamber with a 16/8 h day/night cycle at 28°C for 1–2 day before inoculation with rhizobium strain 113-2 (stored in our lab) and USDA205 (provided by Huazhong Agricultural University in China). After inoculation, plants were kept under the same growth conditions. Their growth situations at 12, 30, and 42 days of post-inoculation (dpi) and roots at 12 and 42 dpi were photographed. Chlorophyll contents in the first trifoliolate leaf were measured by SPAD-502 Plus Chlorophyll Meter. The mean values of nodule number and

Abbreviations: RNS, (The root nodule symbiosis); T3SS, (the type III secretion system); qPCR, (Quantitative real-time PCR); DEGs, (Differentially Expressed Genes); FDR, (False Discovery Rate); HR, (Hypersensitive response); WEGO, (Gene Ontology functional classification); RH, (relative humidity); CT, (cycle threshold).

nodule dry weight were calculated using software SPSS Statistics 17.0.

Samples for RNA isolation were collected from soybean roots (1) at 0.5 h; (2) 7 h/24 h; (3) 5 day; (4) 16 day and (5) 21 day of post inoculation. The former three time points represent the period that soybean root hairs recognize the rhizobium signals, the period that soybean root hairs are infected by Rhizobium (root hairs curling at 7 h of post inoculation (hpi) and cortical cells dividing at 24 hpi) and the nodule primordia formation period, respectively, and the latter two time points represent two early nodule development periods. Samples collected at 7 and 24 hpi were mixed as one sample. Each collection was performed with three biological replicates. RNAs isolated from the three replicates were mixed at 1:1:1 ratio for subsequent library construction and sequencing.

RNA Extraction and cDNA Library Preparation

Total RNA was isolated using TRIzol reagent (Invitrogen, USA) and stored in a -80°C for downstream gene-expression analysis. Potential genomic DNA were removed using RNeasy plant mini kit (QIAGEN, Germany) and RNA quantity and quality were measured using an Epoch Multi-Volume Spectrophotometer system, NanoDrop and Agilent 2100 Bioanalyzer (Agilent Technologies, Palo Alto, CA, USA). All samples had A₂₆₀/A₂₈₀ and A₂₆₀/A₂₃₀ ratios of 2.13~2.23, RIN value above 8.5 and 28S/18S above 1.6 except one.

To obtain a comprehensive range of transcripts, an equal amount of total RNA from each sample was pooled for RNA-Seq. mRNAs were enriched using oligo (dT) magnetic beads, fragmented in fragmentation buffer to about 200 bp and reverse-transcribed into single strand cDNA using random hexamer primers. After RNaseH digestion, the cDNA were converted into double strand cDNAs with DNA polymerase I and purified using magnetic beads. After end repair and addition of single nucleotide A (adenine) at 3'-end, cDNA were ligated to adaptors and prepared as libraries. After qualification and quantification using an Agilent 2100 Bioanaylzer and ABI Step One Plus Real-Time PCR System, the libraries were subjected to sequencing on Illumina HiSeq™ 2000.

Clean Reads Library Formation

Raw reads which include partial adaptor sequences and/or low quality reads were generated from the original image data from Illumina Hi Seq™ 2000 and filtered into high quality (clean) reads after (1) trimming off the adaptor sequences; (2) eliminating the reads with higher than 10% unknown bases and reads with higher than 50% low quality bases (base with quality value ≤ 5). The clean reads were then mapped to reference genes and genome (ftp://ftp.jgi-psf.org/pub/compgen/phytozome/v9.0/Gmax/annotation/Gmax_189_transcript.fa.gz and ftp://ftp.jgi-psf.org/pub/compgen/phytozome/v9.0/Gmax/assembly/Gmax_189.fa.gz) using SOAP aligner/SOAP2 (Li et al., 2009) with threshold that no more than two mismatches were permitted in the alignment. The mapping results are shown in Supplemental Table S2.

Function Annotation and Pathway Analysis

To understand function distribution of genes at macro-level, gene ontology (GO) annotation of DEGs was performed using software Blast2GO and used for GO functional classification of DEGs using software WEGO.

Kyoto Encyclopedia of Genes and Genomes (KEGG) is the major public pathway-related database, the significant differences between different groups were calculated using the formula

$$P = 1 - \sum_{i=0}^{m-1} \frac{\binom{M}{i} \binom{N-M}{n-i}}{\binom{N}{n}}$$

Where N is the number of all genes with KEGG annotation, n is the number of DEGs in N, M is the number of all genes annotated to specific pathways, and m is the number of DEGs in M. Besides the list of the most meaningful pathways, the detailed pathway information in KEGG database can be obtained by clicking the hyperlinks on KEGG pathways. The gene identifiers mapped to the pathway were used as the gene sets, and the lists of DEGs in each of the comparisons were used as the test sets.

Quantitative Real-Time PCR (qPCR)

DEGs were further evaluated using qPCR. In brief, RNA samples were treated with DNase I (Takara) and reverse-transcribed using a Prime Script RT reagent Kit (Perfect Real Time) with gDNA Eraser (Takara Bio, Inc) and oligo (dT) as the primer. cDNA from the reverse transcription of approximately 1 μg of RNA was used as the template for qPCR using primer sets listed in Supplemental Table S5 and cycling conditions of 30 s at 95°C followed by 40 cycles of 5 s at 95°C, 15 s at 60°C and 12 s at 72°C and final 5 s at 72°C. The polyubiquitin transcript was used as the internal control. Sample cycle threshold (CT) values were standardized for each template using the reference gene as control, and the 2^{-ΔΔCT} method was used to analyze the relative changes in gene expression from the qPCR experiments. Three replicate reactions per sample were used to ensure statistical credibility.

RESULTS

Symbiotic Phenotypic Characterization of Soybean Inoculated with Rhizobium Strains 113-2 or USDA205 at Roots

Soybean can establish nitrogen-fixing symbiosis with different species of rhizobium strains (Hayashi et al., 2012a). The best studied rhizobium-soybean symbiotic models are *B. japonicum*—soybean and *S. fredii*—soybean (Israel et al., 1986; Annapurna and Krishnan, 2003; Sanz-Saez et al., 2015). The symbiotic phenotype was different between soybean Tian long No.1 inoculated with slow-growing rhizobium strains *B. japonicum* 113-2 and fast-growing rhizobium strains *S. fredii* USDA205 (Figure 1, Supplemental Table S1). At 12 dpi, the control (CK, inoculated with media only) had slightly better growth and higher chlorophyll content than the two symbionts (Figures 1A,B, Supplemental Table S1), mainly because the symbiotic process needed more energy from the host plant and

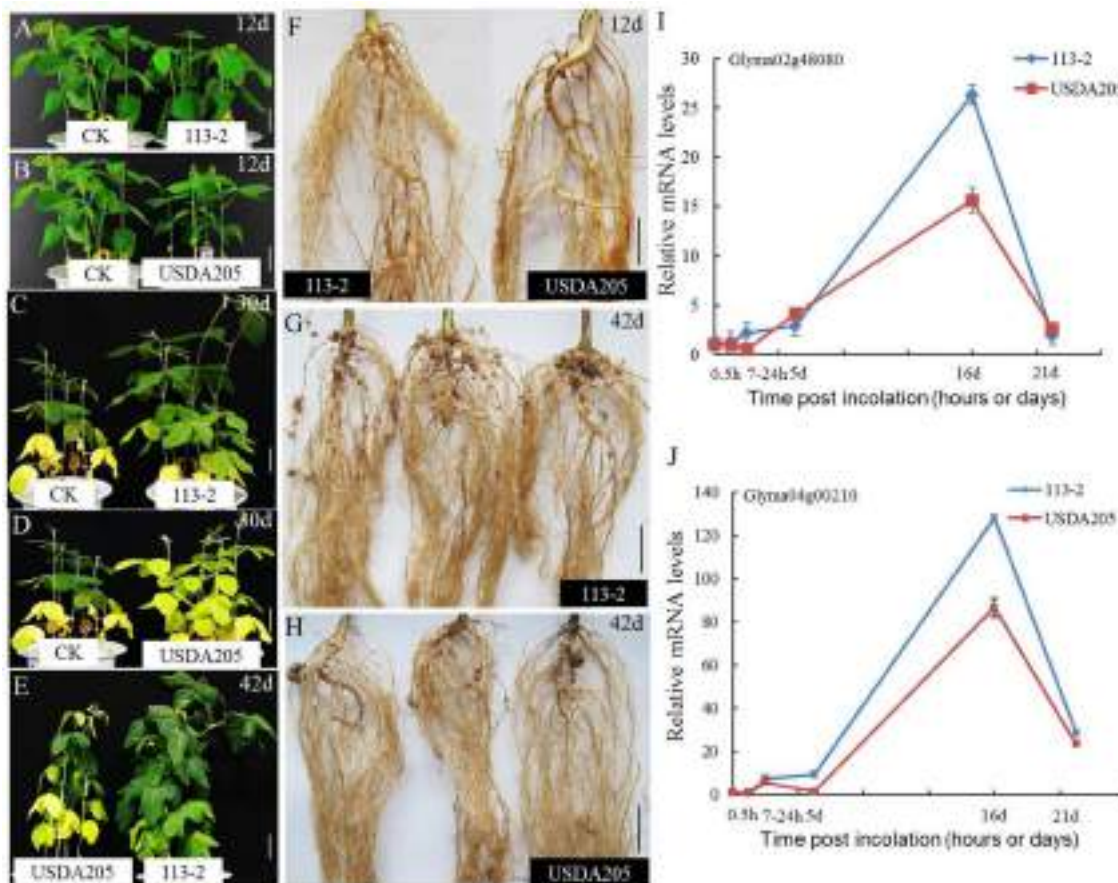


FIGURE 1 | Symbiotic phenotypic features of *B. japonicum* 113-2-soybean and *S. fredii* USDA205-soybean symbionts. Slow-growing rhizobium strains *B. japonicum* 113-2 was originated from southern China and fast-growing rhizobium strains *S. fredii* USDA205 was from USA. The soybean cultivar is Tian long No.1 (China). **(A–E)** The growth of plants without inoculation (12 and 30 day) and the two symbiosis (12, 30, and 42 day). **(F–H)** Nodulation phenotypes were examined at 12 and 42 day after inoculation with 113-2 or USDA205. **(I,J)** The expression levels of *GmNIN*-like genes (*Glyma02g48080* and *Glyma04g00210*) in soybean roots at five time points (0.5 h, 7–24 h, 5 day, 16 day, and 21 day) after inoculation with rhizobium strains 113-2 or USDA205. Bars, 4 cm **(A,B,D)**; 4.5 cm **(C)**; 5.0 cm **(E,F,G,H)**; d, days; h, hours.

the nitrogen fixation function was weak during this period. At 30 and 42 dpi (Figures 1C,D, Supplemental Table S1), the control had no additional nitrogen supply, thus its growth and chlorophyll synthesis was limited by insufficient nitrogen in cotyledon. Comparison of the two symbionts showed that *S. fredii* USDA205-soybean symbiont had much less nodule numbers per root system (0 vs. 13) at 12 dpi (Figure 1F, Supplemental Table S1), although they had similar growth and chlorophyll content (Figures 1A,B, Supplemental Table S1). In addition, compared with *B. japonicum* 113-2-soybean symbiont, *S. fredii* USDA205-soybean symbiont had (1) obviously more yellow leaves and less chlorophyll content at 30 dpi (Figures 1C,D, Supplemental Table S1); (2) worse growth (Figure 1E), less chlorophyll content (Supplemental Table S1), fewer nodule per root system (16.64 vs. 51.52, Figure 1G) and larger nodules (3-fold) (Figure 1H, Supplemental Table S1) at 42 dpi, and (3) lower expression of *GmNIN*-like genes (*Glyma02g48080* and *Glyma04g00210*), which are required for nodulation (Borisov et al., 2003), in soybean roots at almost all the tested time points (Figures 1I,J). These results

suggest that the soybean roots of these two symbiotic systems have differential cellular responses.

RNA-Seq Quality Assessment and Identification of DEGs

The above-mentioned different symbiotic phenotypes are related to the symbiotic host-specificity and maybe mainly due to the molecular events of nodulation (Marioni et al., 2008). To investigate the causes of these different symbiotic phenotypes, RNA-Seq was performed for soybean root samples at five important time points: 0.5, 7–24 hpi, 5, 16, and 21 dpi. The statistic results of alignment (Supplemental Table S2), randomness assessment (Supplemental Figure S1), the proportion of clean reads among the total acquired reads was more than 99.6%, and sequencing saturation analysis (Supplemental Figure S2) indicated that the sequencing was of good quality and contained sufficient information for gene expression analysis.

To judge the significance of differences of DEGs in soybean roots inoculated with different rhizobium strains, the false discovery rate (FDR) ≤ 0.001 and $|\log_2 \text{ratio}| \leq 1$ were used as criteria for the following three comparisons: (1) comparison between soybean roots uninoculated vs. inoculated with rhizobium strains 113-2 at 0.5, 7–24 hpi, 5, 16, and 21 dpi (Group 1); (2) comparison between soybean roots uninoculated vs. inoculated with rhizobium strain USDA205 at 0.5, 7–24 h, 5, 16, and 21 day post inoculation (Group 2); and (3) comparison between soybean roots inoculated with rhizobium strain USDA205 vs. inoculated with rhizobium strain 113-2 at 0.5, 7–24 h, 5, 16, and 21 day post inoculation (Group 3). DEGs in these comparisons are shown in Supplemental Table S3.

The numbers of up-regulated and down-regulated DEGs in the three comparisons are shown in **Figure 2A**. The number of DEG at 16 dpi was the highest in Group 1 (that was 3346) and Group 2 (that was 1161), indicating the beginning of a series of new processes. Most of the DEGs in Group 3 were found at 16 dpi and 21 dpi, indicating that most of the differential gene expression responses in soybean roots to rhizobia strains 113-2 and USDA205 happened at 16 and 21 dpi. The numbers of DEGs found at two or more time points in the three comparisons were showed in **Figure 2B**. Twenty two gene sets were analyzed and DEGs in $16\text{dR} \cap 21\text{dR}$ gene set was proportional to the highest number, besides, there were no DEGs consistently found at five time points ($0.5\text{hR} \cap 7\text{-24hR} \cap 5\text{dR} \cap 16\text{dR} \cap 21\text{dR}$) in the three comparisons.

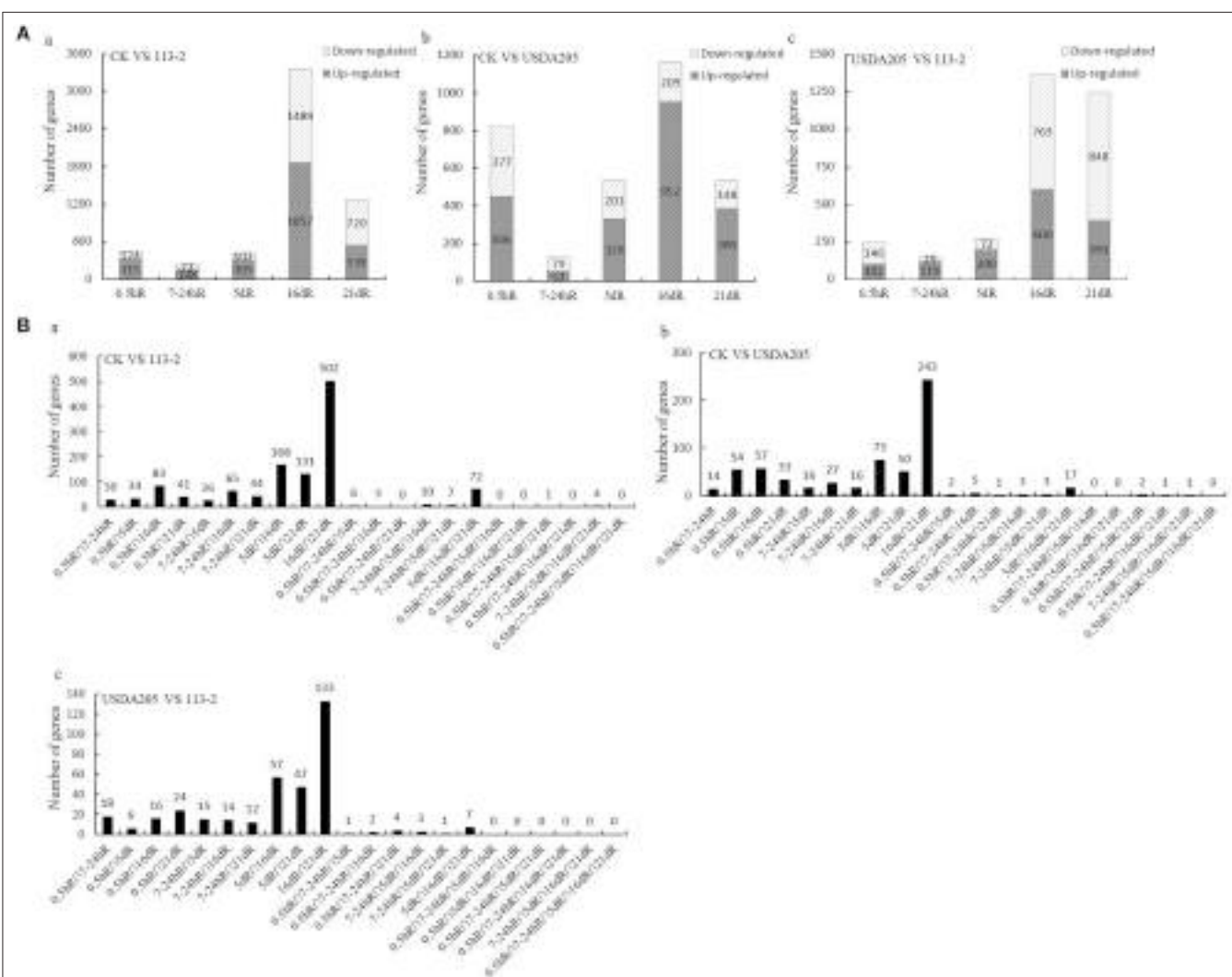


FIGURE 2 | Genes differentially expressed in soybean roots at five time points in the three Groups (CK vs. 113-2, CK vs. USDA205, and USDA205 vs. 113-2). (A) Genes differentially expressed in soybean roots at different time points were separated into two groups according to whether they were significantly up-regulated or down-regulated. a, CK vs. 113-2 (Group 1); b, CK vs. USDA205 (Group 2); c, USDA205 vs. 113-2 (Group 3). (B) The numbers of differentially expressed genes in 22 gene sets in the three groups. Five different post-inoculation time points (0.5 h, 7–24 h, 5 d, 16 d, and 21 d) are included and the division of DEGs into different gene sets depends on which time points (two or more) the DEGs were identified. a, CK vs. 113-2 (Group 1); b, CK vs. USDA205 (Group 2); c, USDA205 vs. 113-2 (Group 3).

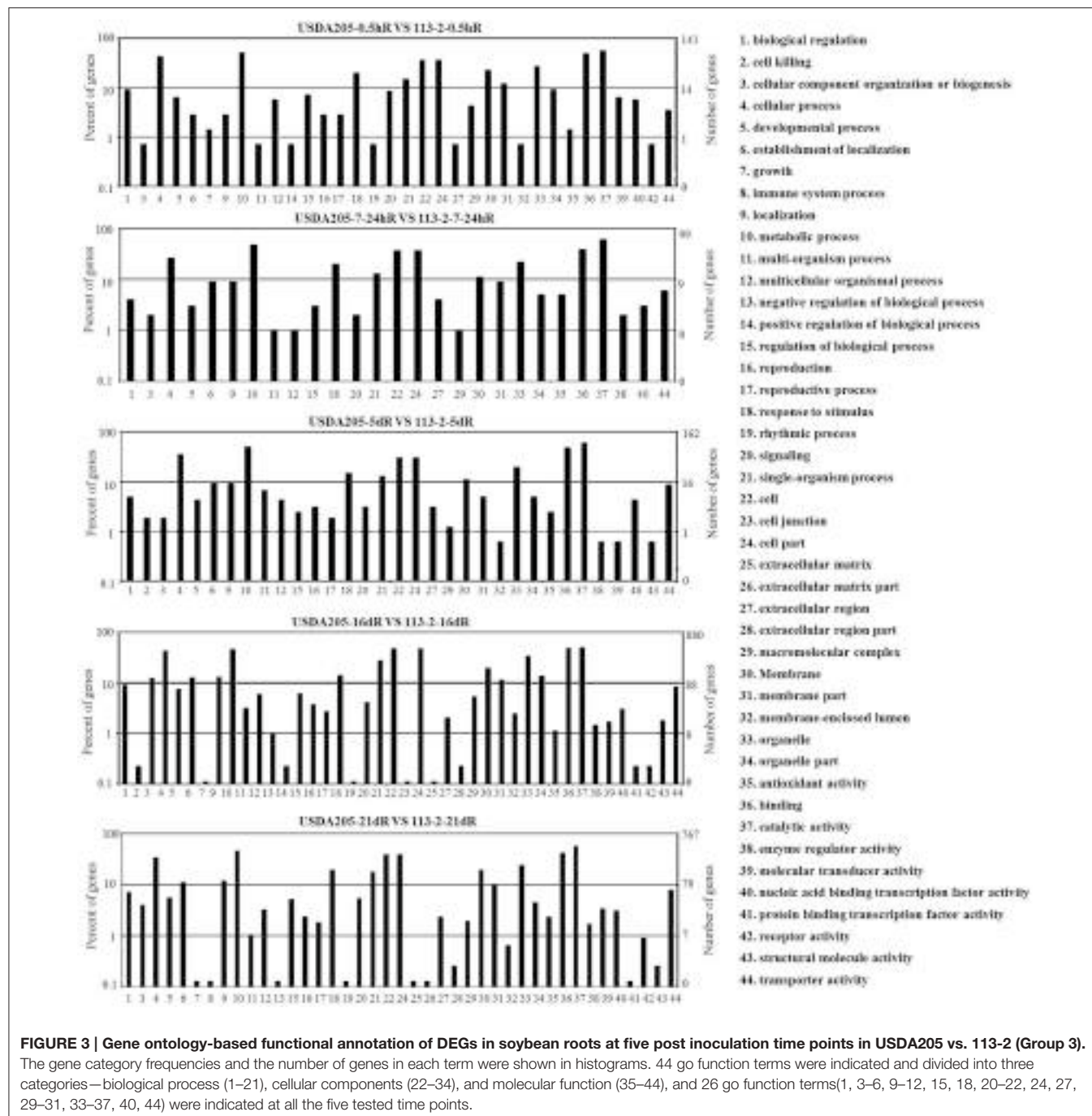


FIGURE 3 | Gene ontology-based functional annotation of DEGs in soybean roots at five post inoculation time points in USDA205 vs. 113-2 (Group 3).

The gene category frequencies and the number of genes in each term were shown in histograms. 44 go function terms were indicated and divided into three categories—biological process (1–21), cellular components (22–34), and molecular function (35–44), and 26 go function terms(1, 3–6, 9–12, 15, 18, 20–22, 24, 27, 29–31, 33–37, 40, 44) were indicated at all the five tested time points.

Function Ontology and KEGG Pathway Enrichment Analysis of DEGs

To evaluate the potential functions of the DEGs between the two symbiotic systems, DEGs with > 2-fold expression change in Group 3 were assigned to different GO categories such as biological process, molecular function, and cellular location, and 44 functional GO terms were analyzed (Figure 3). For all the five tested time points, the biological processes associated with the DEGs mainly focused on metabolic process, cellular process,

response to stimulus and single-organism process. The cellular components mainly included cell, cell part and organelle. The main molecular functions of the DEGs were binding and catalytic activity. Most of the DEGs involved in these 44 functional GO terms were identified in USDA205-16dR vs. 113-2-16dR and USDA205-21dR vs. 113-2-21dR, moreover, only two GO terms (immune system process and extracellular matrix part) were not found in USDA205-16dR vs. 113-2-16dR and three (cell killing, positive regulation of biological process and cell junction) were

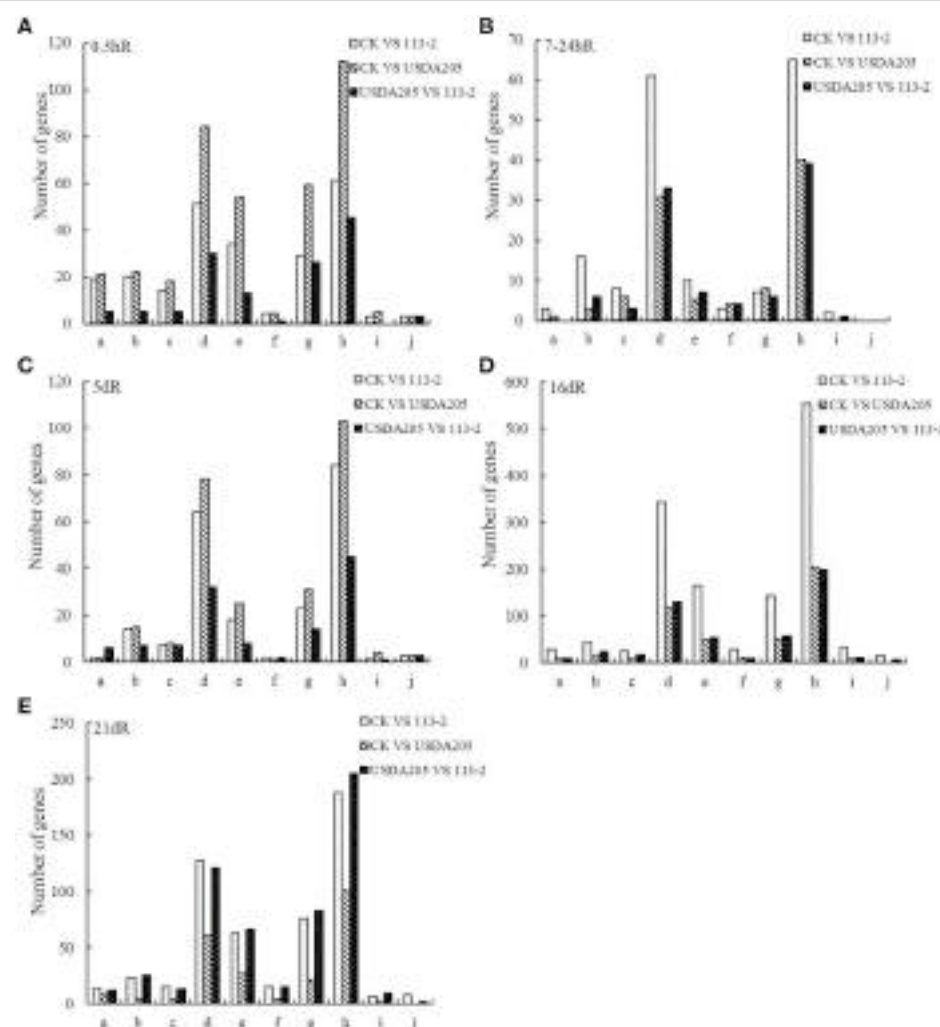


FIGURE 4 | KEGG pathway enrichment analyses of DEGs for 10 KEGG pathways in the three groups. The x- and y-axes represent pathway categories and the number of genes in each pathway, respectively. a, ABC transporters; b, Flavonoid biosynthesis; c, Flavone and flavonol biosynthesis; d, Biosynthesis of secondary metabolites; e, Plant hormone signal transduction; f, Nitrogen metabolism; g, Plant-pathogen interaction; h, Metabolic pathways; i, Ubiquitin mediated proteolysis; j, RNA transport.

not in USDA205-21dR vs. 113-2-21dR. Besides, 26 go function terms were indicated at all the five tested time points and revealed no high shift in the distribution (Figure 3).

KEGG is the major public pathway-related database. Therefore, we analyzed 10 KEGG pathways (Figure 4). In these pathways, the metabolic pathways were most prominent, followed by biosynthesis of secondary metabolites. Other two pathways: plant hormone signal transduction and plant-pathogen interaction, were also main enrichment pathways in the three groups. More DEGs at 7–24 hpi, 16 and 21 dpi in Group 1 were involved in these 10 KEGG pathways than those in Group 2 (Figures 4B,D,E). By contrast, more DEGs at 0.5 and 5 dpi in Group 2 were involved in these 10 KEGG pathways than those in Group 1 (Figures 4A,C). Moreover, most of DEGs in Group 3 involved in these 10 KEGG pathways were identified at 16 and 21 dpi (Figures 4D,E).

DEGs Associated with the Flavonoids/Flavone/Flavonol Biosynthesis Pathway and the Plant-Pathogen Interaction Pathway

In order to evaluate whether the recognition of different rhizobia to host legume is related to the secreted flavonoids, we analyzed the DEGs associated with the flavonoids biosynthesis pathway and flavone and flavonol biosynthesis pathway in Group 1 and Group 2 at 0.5 hpi in more detail (Table 1). The results showed that changes in expression levels of 28 DEGs were significantly different between the two groups (Table 1), more DEGs and higher change folds were found in Group 2 than Group 1, indicating that the flavonoids/flavone/flavonol biosynthesis pathways are more sensitive to the surface substance produced by USDA205.

TABLE 1 | The DEGs associated with flavonoids biosynthesis pathway in soybean at 0.5 h of post inoculation based on log2 ratio.

Gene code	Group 1	Group 2
Glyma01g29930		2.58
Glyma01g42350	1.6	
Glyma02g05470		-3.48
Glyma02g42180	1.8	
Glyma02g42470		1.8
Glyma03g07680	2.6	3.4
Glyma04g04270	1	
Glyma05g36210		1.48
Glyma06g43970		2
Glyma07g18280		4
Glyma08g19290		-1.2
Glyma08g42440	-2.2	-3.4
Glyma08g42450		-1.9
Glyma10g16790		-1.2
Glyma11g05680		-1.5
Glyma13g37810		-1.4
Glyma14g04800		-1.1
Glyma14g06710	1.2	
Glyma15g38670		-1.4
Glyma16g03760		-1.4
Glyma18g12180		-1.4
Glyma18g12210		-1.1
Glyma18g12280		-2.2
Glyma18g40186	-2.2	
Glyma18g49240	-1.3	-2.1
Glyma19g03760	-2.5	-4.3
Glyma19g03770	-2.3	-3.5
Glyma19g37116		-1

In the absence of Nod factor signal, legume plants terminate the infection process perhaps via a defense response (Jones et al., 2008). To explore the differential cell defense responses between soybean roots inoculated with rhizobium strains 113-2 and USDA205, the plant-pathogen interaction KEGG pathway was analyzed in more detail in Group 3 (Figure 5, Table 2). Among the DEGs annotated to this pathway, 7 were identified at 0.5 hpi, of which 4 were down-regulated; 6 were identified at 7–24 hpi, all of which were up-regulated; 10 were identified at 5 dpi, of which only 1 was down-regulated; 8 were identified at 16 dpi, of which 4 were down-regulated, and 10 were identified at 21 dpi, of which 6 were down-regulated (Figure 5), and the detailed expression information of 55 important DEGs associated with this pathway in Group 3 was shown in Table 2. These results indicated differential defense responses in soybean roots is related to the process of soybean responding to rhizobium strains 113-2 and USDA205.

Analysis of DEGs Encoding Resistance Proteins in Soybean Roots Inoculated with Rhizobium Strains 113-2 or USDA205

The genetic loci of soybean, namely Rj (s) or rj (s), have been identified responsive to the nodule formation (Hayashi et al.,

2012a), and several of these genes (e.g., Rj2, Rj4, and Rfg1) are found involving in restrict nodulation with specific rhizobial strains (Yang et al., 2010). To investigate whether resistance (R) proteins are involved in control of the nodulation phenotypes in soybean inoculated with rhizobium strains 113-2 or USDA205, DEGs encoding R proteins in soybean roots were analyzed in more detail (Figure 6). Figure 6A shows the numbers of DEGs encoding R proteins in each set. A total of 24 such genes were only found in one group (7, 7, and 10 in Groups 1–3, respectively), 22 genes were found in two groups (5 in Group 1 and 2; 4 in Group 2 and 3; 13 in Group 1 and 3) and 3 genes (Glyma05g17470, Glyma12g01420, and Glyma19g35270) were found in all three groups. Figure 6B shows the number of R genes differentially expressed at the five different time points in soybean roots in the three groups. It can be seen that more R genes were found in Group 1 than in Group 2 at each time point, especially at 16 dpi and not all differentially expressed R genes in Group 1 and/or Group 2 are also found in Group 3 (Figures 6A,B), indicating that they participate in nodulation but not in restriction of specific rhizobial strains. Besides, some differentially expressed R genes in Group 3 were not found in Group 1 and Group 2, indicating that these R genes may be associated with T3SS of rhizobium and/or defense responses in soybean roots.

Analysis of Selected Nodulation Factor (NF)-Related Genes and Nodulin Genes in Soybean Roots Inoculated with Different Rhizobium Strains 113-2 and/or USDA205

Twenty-five DEGs responsible for broad NF signal pathway and nodulation were identified in three groups by searching for homologs of *M. truncatula* and *L. japonicus* NF-related genes in soybean genome sequence database (Table 3; Kevei et al., 2007; Mbengue et al., 2010; Schmutz et al., 2010; Kim et al., 2013). Because same proteins may be encoded by one or more DEGs, only 14 NF-related genes are listed (Table 3), and the identified orthologs in these three legumes were named according to the given nomenclature in cloning studies in *M. truncatula*, *L. japonicus* and soybean.

Nodulins are legume genes whose expression is induced by rhizobium bacteria upon nodulation (Denance et al., 2014). Twenty-nine nodulin genes have been analyzed in *M. truncatula* and most of them play key roles in nodulation (Gamas et al., 1996; Denance et al., 2014). In this study, 25 soybean nodulin genes were identified as DEGs in soybean roots (Table 4). Among them, only three were not differentially expressed in soybean roots inoculated with rhizobia strains 113-2 and USDA205 (Table 4), and the detailed expression information of these nodulin genes at all the tested time points in the three groups was shown in Supplemental Table S4. However, their functions have not been well understood.

Verification of RNA-Seq Results by qPCR and Expression Analysis of 189 Candidate Genes in Roots and/or Nodules

To verify the RNA-Seq results, the expression stability of five reference genes (ELF1b, Qact, G6PD, Fbox and Ubiquitin) was evaluated (Supplemental Figure S3), of which, Ubiquitin, ELF1b

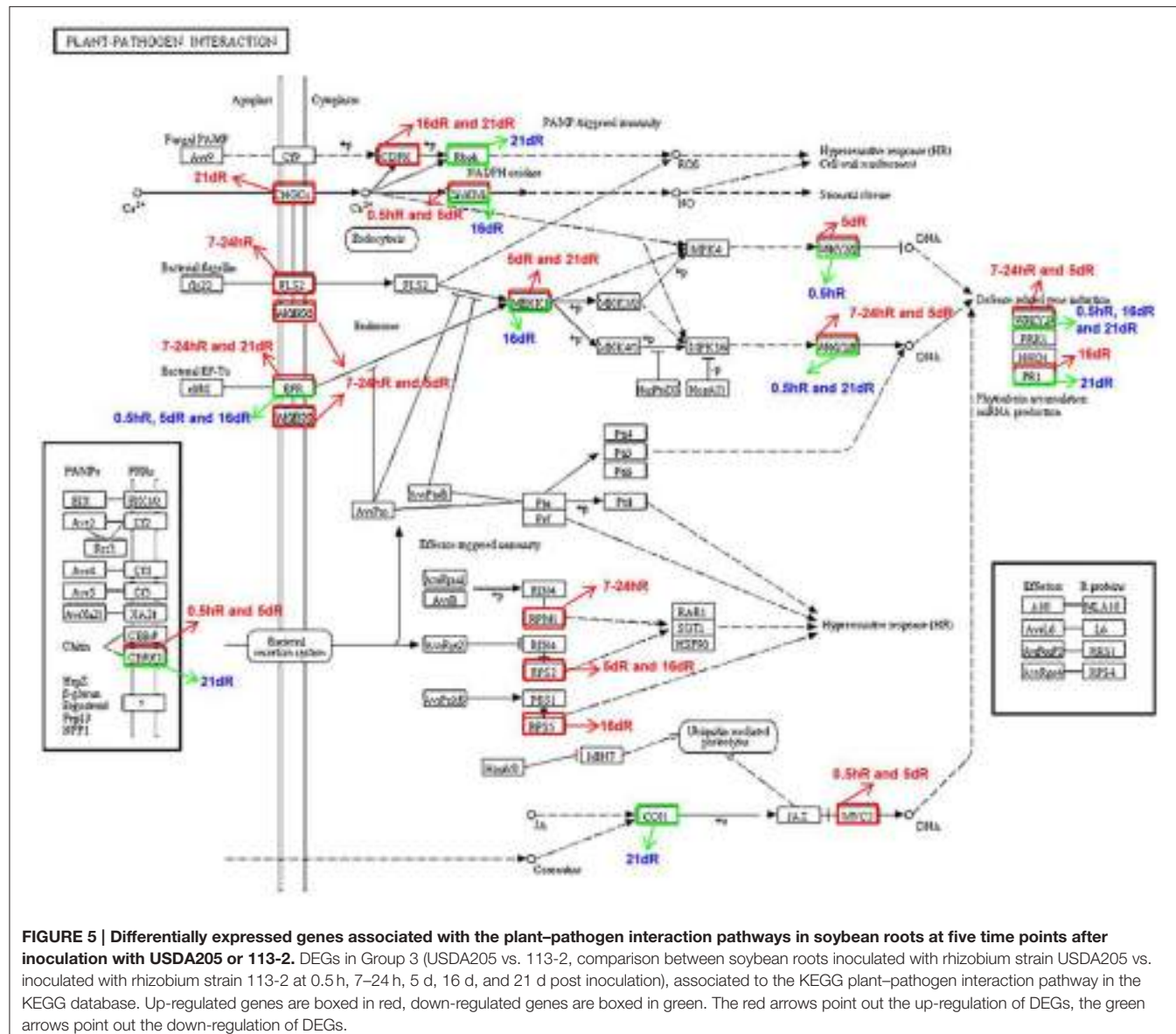


FIGURE 5 | Differentially expressed genes associated with the plant-pathogen interaction pathways in soybean roots at five time points after inoculation with USDA205 or 113-2. DEGs in Group 3 (USDA205 vs. 113-2, comparison between soybean roots inoculated with rhizobium strain USDA205 vs. inoculated with rhizobium strain 113-2 at 0.5 h, 7–24 h, 5 d, 16 d, and 21 d post inoculation), associated to the KEGG plant-pathogen interaction pathway in the KEGG database. Up-regulated genes are boxed in red, down-regulated genes are boxed in green. The red arrows point out the up-regulation of DEGs, the green arrows point out the down-regulation of DEGs.

and Qact were most stable in all samples, while GmG6PD and Fbox were consistently unstable (Supplemental Figure S3). Thus, Ubiquitin was selected as reference gene for quantitative real-time PCR (qPCR) experiment. A total of 11 DEGs were randomly selected based on the transcriptional profile analysis and measured by qPCR. The results were in agreement with the transcriptional profile data for 136 out of 165 (82.42%) data points (Figure 7). Although, the fold-changes were not exactly identical, both methods yielded identical expression trends for most data points. The sequences of the specific primers used for qPCR are given in Supplemental Table S5.

To confirm the candidate genes whether or not play roles in nodulation, the expressions of 189 candidate genes (78 from Tables 1–3, others are protein kinases and/or transcription factors) in roots and/or nodules were analyzed according to two databases (Phytozome v10.3 and Soybase) (Supplemental Table

S6). The results showed that only two genes (Glyma04g06470 and Glyma18g42610) nearly have no expression in roots and\ or nodules, indicating that most of these candidate genes might be indeed regulated or have a role in nodulation.

DISCUSSIONS

In this study, RNA-Seq was utilized to investigate the causes of different symbiotic phenotypes in soybean roots inoculated with different rhizobium strains *B. japonicum* 113-2 and *S. fredii* USDA205. RNA-Seq is an effective method that produces quantitative data related to transcripts with greater sensitivity, higher repeatability, and wider dynamic range (Jiang et al., 2014) than conventional methods. This method has also been shown to have relatively little variation between technical replicates to identify DEGs (Marioni et al., 2008). Consistent with the

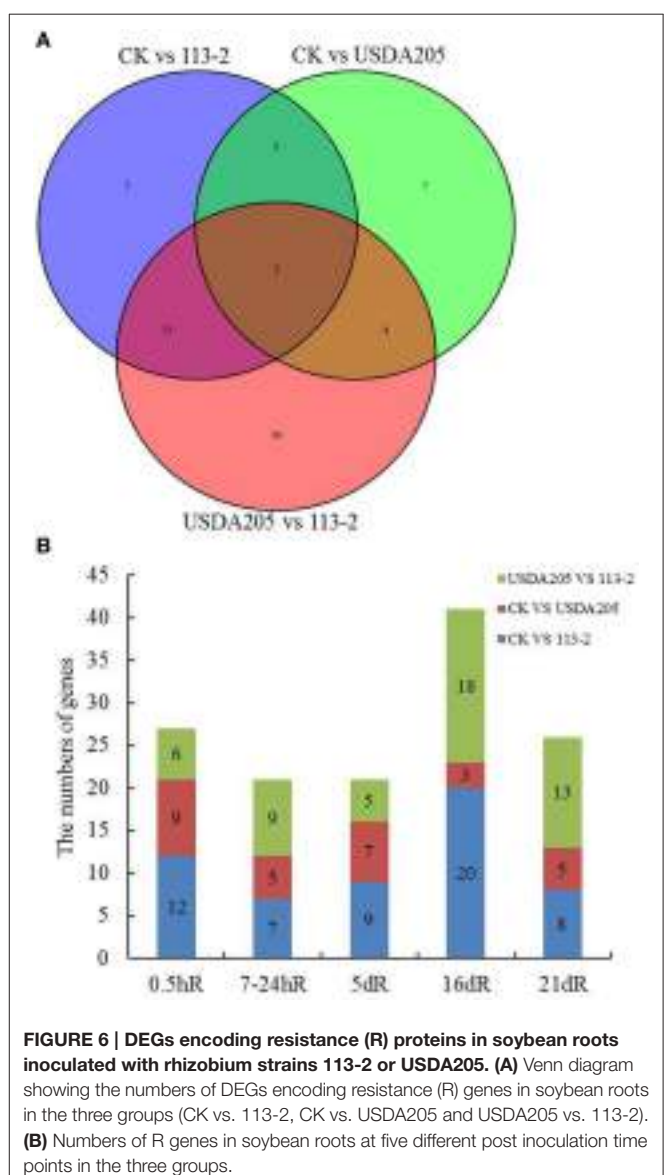
TABLE 2 | The DEGs associated with the plant-pathogen interaction pathway in group3 (USDA205 vs. 113-2) based on the log2 ratio.

Gene	Gene code in soybean	0.5hR	7-24hR	5dR	16dR	21dR
<i>CERK1</i>	Glyma11g06740	1.1				
	Glyma13g39880			1.3		
	Glyma17g36630					-1.6
<i>MYC2</i>	Glyma06g09670	2				
	Glyma08g21130	1				
	Glyma12g33751			1.4		
<i>CALM</i>	Glyma19g41730	1.4				
	Glyma05g07720			1.7	-1.4	
<i>EFR</i>	Glyma09g35011	-6.2				
	Glyma05g25360	-1.1				
	Glyma08g08360		1.5	-1.5		
	Glyma04g40080				-1	
	Glyma09g35090					1.2
	Glyma06g25110					1.2
<i>WRKY25</i>	Glyma05g25770	-1.7				
	Glyma03g05220	-1.6				
	Glyma01g31921	-1				
	Glyma15g00570	-1				
	Glyma18g16170			3.3		
<i>WRKY29/22</i>	Glyma05g37390	-1.4				
	Glyma05g36970	-1.3				
	Glyma09g06980	-1.3				
	Glyma08g02580	-1.3				
	Glyma13g00380	-1.2				
	Glyma17g06450	-1.2				
	Glyma04g41701	-1				
	Glyma19g44380		1.4			-1.3
	Glyma16g02960		1.1			
	Glyma09g24080				-1.4	
	Glyma03g00460			1.9	-1.3	
	Glyma03g41750					-1.6
<i>FLS2</i>	Glyma16g27260	1.8				
<i>BAK1</i>	Glyma17g07440	3.7				
	Glyma16g32600			4.2		
	Glyma09g27600			4		
<i>RPM1</i>	Glyma09g34381	1				
<i>MEKK1P</i>	Glyma14g08801		1		1	
	Glyma19g42340			-1.1		
	Glyma01g39380				2.1	
<i>CDPK</i>	Glyma10g30940			1.2		
	Glyma11g34000				1.1	
<i>PR1</i>	Glyma15g06830			3.2		
	Glyma13g32510			2.9		
	Glyma15g06780			1.1	-1.9	
	Glyma13g32560				-3.4	
	Glyma15g06770				-2.9	
	Glyma13g01250				-2.8	
	Glyma15g06790				-2.3	
<i>RPS2</i>	Glyma01g31550			1.2		
	Glyma05g17470			1.2	1.2	

(Continued)

TABLE 2 | Continued

Gene	Gene code in soybean	0.5hR	7-24hR	5dR	16dR	21dR
<i>RPS5</i>	Glyma01g05710					5.9
<i>CNGF</i>	Glyma17g12740					1.1
	Glyma08g24960					1.1
<i>RBOH</i>	Glyma05g00420					-1.2
<i>COI-1</i>	Glyma18g03420					-1



previous reports, our qPCR results agree with the transcriptional profile data for 136 out of 165(82.42%) data points (**Figure 7**), and 189 candidate genes are largely expressed in roots and/or nodules (Supplemental Table S6), suggesting our RNA-Seq data are reliable.

TABLE 3 | List of 14 NF-related genes in soybean roots inoculated with rhizobium strains 113-2 or USDA205.

Gene name	<i>M. truncatula</i>	<i>L. japonicus</i>	<i>Glycine max</i>	Group 3	Group 2	Group 1
<i>MtERN1</i>	Medtr7g102550	Lj1.CM0104.2670.r2.m	Glyma16g04410	Glyma16g04410	Glyma19g29000	Glyma06g06930
	Medtr6g031080		Glyma19g29000		Glyma06g06930	Glyma06g06930
<i>MtFLOT2</i>	Medtr3g137870		Glyma06g06930	Glyma06g06930	Glyma06g06930	Glyma06g06930
	Medtr1g099720					
<i>MtIPD3</i>	Medtr5g027010	Lj2.CM0803.150.r2.m	Glyma01g35255		Glyma02g06700	Glyma01g35255
			Glyma09g34695		Glyma11g06740	Glyma09g34695
<i>MtLIN</i>	Medtr1g112060	Lj5.CM0909.400.r2.m	Glyma10g33851			Glyma10g33851
<i>MtLYR3</i>	Medtr5g019000	Lj2.CM0323.420.r2.d	Glyma02g06700		Glyma02g06700	
<i>MtNFP</i>	Medtr5g018990	Lj2.CM0323.400.r2.d	Glyma11g06740	Glyma11g06740	Glyma11g06740	
	Medtr8g093910					
<i>MtNIN</i>	Medtr5g106690	Lj2.CM0102.250.r2.m	Glyma06g00240	Glyma04g00210	Glyma04g00210	Glyma06g00240
			Glyma04g00210		Glyma02g48080	Glyma04g00210
<i>MtNSP1</i>	Medtr8g025000	Lj3.CM0416.1260.r2.d	Glyma16g01020	Glyma02g48080	Glyma02g48080	Glyma02g48080
	Medtr5g015580		Glyma05g22460		Glyma05g22460	Glyma05g22460
<i>MtNSP2</i>	Medtr3g097800	Lj1.CM1976.90.r2.m	Glyma04g43090	Glyma13g02840	Glyma04g43090	
	Medtr5g065380		Glyma13g02840		Glyma13g02840	Glyma13g02840
<i>MtNup133</i>	Medtr5g097260	Lj2.CM0191.150.nc	Glyma14g01130	Glyma02g47560	Glyma02g47560	
			Glyma02g47560		Glyma02g47560	Glyma02g47560
<i>MtPUB1</i>	Medtr5g083030		Glyma02g43190	Glyma02g43190	Glyma11g09330	Glyma11g09330
<i>MtHMGR1</i>	Medtr5g026500		Glyma11g09330		Glyma11g09330	Glyma11g09330
<i>GmN56</i>	Medtr1g146810	Lj5.CM0492.390.r2.m Lj1.CM0001.650.r2.m Lj1.CM0001.690.r2.m Lj1.CM0001.710.r2.m	Glyma19g29880	Glyma05g29880 Glyma20g38950 Glyma13g12484	Glyma19g29880	Glyma19g29880
			Glyma20g38950		Glyma13g12484	Glyma20g38950
			Glyma13g12484			Glyma13g12484
<i>GmENOD93</i>	Medtr8g119590		Glyma05g08400	Glyma05g08400 Glyma17g12610	Glyma05g08400	Glyma05g08400
			Glyma06g24760		Glyma17g12610	Glyma17g12610
			Glyma17g12610		Glyma06g24760	Glyma06g24760

The efficiency of symbiotic nitrogen fixation in soybean by application of inoculants greatly depends on the symbiotic host-specificity. To identify the genes that can control the host specificity and elucidate the molecular mechanisms for the host-restriction of nodulation, we focused on DEGs in response to different rhizobium strains (*B. japonicum* strain 113-2 and *S. fredii* strain USDA205) in soybean roots, and identified a large number of DEGs from RNA-Seq data. Our results for the first time identified DEGs that could be involved in the molecular events of nodulation in soybean roots inoculated with different strains. Among these DEGs, many are associated with the flavonoids biosynthesis pathway and the plant-pathogen interaction pathway.

DEGs Involved in Nod Factor and EPS Signals Transduction in Soybean Root Cells

In the legume-rhizobium symbiosis, rhizobium exo-poly-saccharides (EPS), which act as nod factors, are also essential for bacterial infection (Jones et al., 2008). An EPS receptor (EPR3) identified in *L. japonicus* could selectively bind to compatible

EPS to control rhizobium infection in bacterial competition studies (Kawaharada et al., 2015). The symbiotic specificity is thus regulated by a two-stage mechanism involving sequential receptor-mediated recognition and transduction of nod factors and EPS signals.

In connection with the soybean genome-based information and the information obtained from the model legumes, the nodulation signaling transduction pathway of soybean is clear and the NF-related genes are shown in Supplemental Table S7. In this report, the NF-related genes were not differentially expressed after 113-2 and/or USDA205 inoculation, except six in Group 1 and five in Group 2 (Table 3), suggesting that these genes were not changed at the five time points. Interestingly, *GmNIN-Like* genes were differentially expressed in the three groups. The results indicate that this gene was induced by nod factors and responded differently to different nod factors, which partly explains the differences in nodulation and/or nitrogen-fixation time and nodule numbers per root system between soybean roots inoculated with 113-2 and with USDA205 (Figure 1, Supplemental Table S1).

EPS signals are shared by pathogenic and symbiotic bacteria and play important roles in the legume-rhizobium symbiosis.

TABLE 4 | Twenty-five differentially expressed nodulin genes identified in soybean roots by RNA-Seq.

Gene name	Gene ID in soybean	Group 1	Group 2	Group 3
Early nodulin-like protein 1	Glyma06g42110	+		
	Glyma12g32270	+	+	
	Glyma12g34100	+		
Early nodulin-like protein 2	Glyma13g38150	+		
	Glyma12g13130	+		+
Nodulin-16	Glyma02g43320	+	+	+
	Glyma02g43330		+	+
Nodulin-20	Glyma13g40400	+	+	+
Nodulin-21	Glyma05g25010	+	+	+
	Glyma08g08120	+	+	
Nodulin-22	Glyma15g05010	+	+	+
Nodulin-24	Glyma02g43341	+	+	+
Nodulin-26	Glyma08g12650	+	+	+
	Glyma13g40820	+	+	+
Nodulin-36	Glyma01g03470	+	+	+
Nodulin-44	Glyma15g41445	+	+	
Nodulin-50	Glyma10g34280	+	+	+
Nodulin-51	Glyma20g02921	+	+	+
Nodulin-61	Glyma10g06810	+	+	+
Early nodulin-70	Glyma18g02230	+	+	+
Early nodulin-93	Glyma05g08400	+	+	+
	Glyma06g24760	+	+	
Other nodulins	Glyma02g04180	+	+	+
	Glyma06g06930	+	+	+
	Glyma17g08110	+	+	+

"+" Indicates that the gene were different expressed in the group.

However, their signal recognition and transduction mechanisms in soybean are not well explored (D'haeze and Holsters, 2004; Staehelin et al., 2006; Jones et al., 2008). In this report, we analyzed DEGs associated with flavonoids/flavone/flavonol biosynthesis pathway (**Table 1**) and plant-pathogen interaction pathway (**Figure 5**), with the hope that these DEGs might provide fundamental clues to the mechanisms underlying EPS signal recognition and transduction. The physiological activities of rhizobia are usually related to their EPS components, which change among different *E. fredii/S. fredii* and *B. japonicum* strains (Hotter and Scott, 1991). Thus, different EPS receptors may exist in legume for responses to different rhizobium strains.

DEGs Involved in the Flavonoids/Flavone/Flavonol Biosynthesis and Plant Immunity Defense

Isoflavonoids, a subclass of much more common flavonoids, are the signals released by the soybean to attract rhizobium (Rolle,

1988). They are secreted in host-specific manner, but formed by the same flavonoids biosynthetic pathway (Deavours and Dixon, 2005; Barnes, 2010), which is associated with flavone and flavonol biosynthesis pathway. The analyses of DEGs associated with the flavonoids/flavone/flavonol biosynthesis pathway indicated that the biosynthesis and secretion of isoflavonoids may be related to the recognition of different Rhizobia to host legume.

Rhizobia can adopt pathogenic systems to modulate the host range in a genotype-specific manner (Okazaki et al., 2013). For example, T3SS, which is known as an introducer of virulence factors from plant pathogens (Hueck, 1998), can be induced by legume-derived flavonoids, affecting symbiosis with host legumes (Okazaki et al., 2013). In this report, we analyzed the DEGs involved in the plant-pathogen interaction KEGG pathway in Group 3 (**Figure 5, Table 2**) and found that Ca²⁺ signal, MAPK cascade, hypersensitive response (HR) and defense related gene induction are associated with the molecular events of nodulation in soybean roots. These data uncovered some important genes in the tightly regulated soybean nodulation process that coordinates nod factors signal transduction with the host soybean immunity defense. However, the mechanism of this co-regulation remains to be determined.

R Genes Differential Expression in Soybean Roots Inoculated with 113-2 or USDA205

Rhizobia can act as plant pathogens to infect legumes and cause a series of host immune responses (Okazaki et al., 2013), along with changes in expression of resistance (R) proteins inside soybean roots. Plant resistance (R) genes can specifically recognize the corresponding pathogen effectors or their associated protein(s) to activate plant immune responses at the site of infection (Liu et al., 2007), including a series of defense signaling cascades and pathogenesis-related (PR) gene expression (Durrant and Dong, 2004). In this report, 49 DEGs encoding broad resistance (R) proteins and six R-response genes were identified in soybean roots (**Figure 6**, Supplemental Table S3). The relationships among these six R-response genes and 49 R genes will help us to understand the immunity defenses mechanism in soybean roots. Their interactions will be determined by *in vitro* and *in vivo* assays.

In summary, to explain the different nodulation phenotypes, we analyzed the differential gene expression responses in uninoculated soybean roots and in soybean roots inoculated with 113-2 or USDA205 using RNA-seq, and found that DEGs associated with the flavonoids biosynthesis pathway and plant-pathogen interaction pathway could be used to understand the receptor-mediated recognition and transduction of nod factor and EPS signals. The DEGs uncovered in this study and their analyses shed new light on the host legume control of nodulation specificity, and provided a molecular basis for further investigations of the mechanisms underlying the host-specific manners of nod factor and EPS signals reception and transduction.

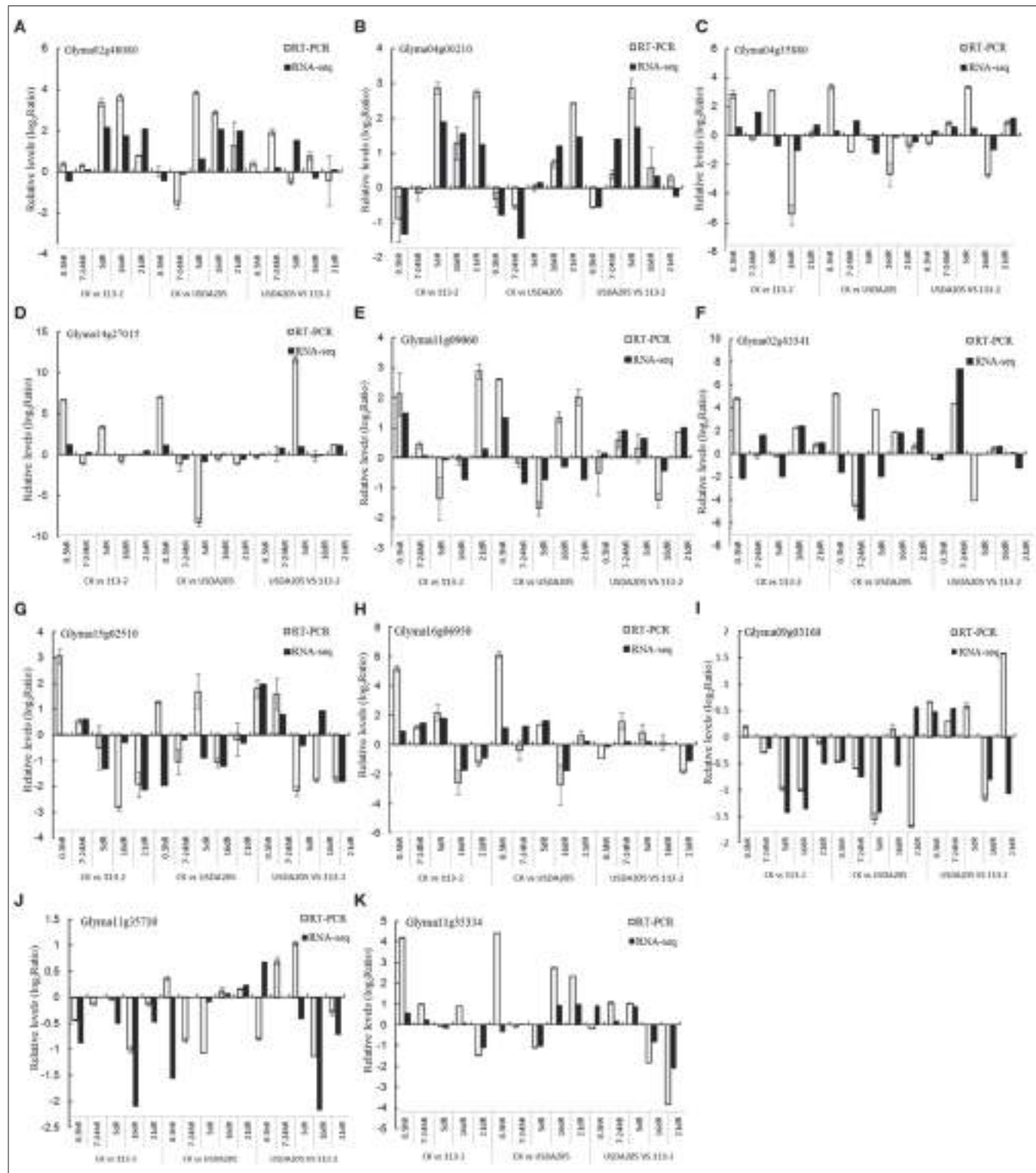


FIGURE 7 | Comparison of expression rates determined by RNA-Seq and qPCR on 11 genes in soybean roots. All qPCR reactions were repeated three times and the data are presented as the mean \pm SD. **(A)**, Glyma02g48080; **(B)**, Glyma04g00210; **(C)**, Glyma04g35880; **(D)**, Glyma14g27015; **(E)**, Glyma11g09060; **(F)**, Glyma02g43341; **(G)**, Glyma15g02510; **(H)**, Glyma16g06950; **(I)**, Glyma09g03160; **(J)**, Glyma11g35710; **(K)**, Glyma11g35334.

AUTHOR CONTRIBUTIONS

SY, XZ designed this work, SY wrote the manuscript, SY, RL performed most of the experiments, SC, HC, CZ, LC, ZS, XZ, ZY, and DQ contributed substantially to the completion of this work. All the authors read and approved the final Manuscript.

ACKNOWLEDGMENTS

We thank Prof. Zhongming Zhang (Huazhong Agricultural University in China) for USDA205 strain, and this work was supported by funds from the China Agriculture Research

System (CAAS-04-PS08), the National Transgenic Project of China (2014ZX08004-005), the Agricultural Science and Technology Innovation Program of CAAS, and the Scientific and Technological Support Project of Soybean Breeding and Propagation (2011BAD35B06). The National Natural Science Foundation of China (grant no. 31400213).

SUPPLEMENTARY MATERIAL

The Supplementary Material for this article can be found online at: <http://journal.frontiersin.org/article/10.3389/fpls.2016.00721>

REFERENCES

- Annapurna, K., and Krishnan, H. B. (2003). Molecular aspects of soybean cultivar-specific nodulation by *Sinorhizobium fredii* USDA257. *Indian J. Exp. Biol.* 41, 1114–1123.
- Barnes, S. (2010). The biochemistry, chemistry and physiology of the isoflavones in soybeans and their food products. *Lymphat. Res. Biol.* 8, 89–98. doi: 10.1089/lrb.2009.0030
- Bec-Ferte, M. P., Krishnan, H. B., Savagnac, A., Pueppke, S. G., and Prome, J. C. (1996). *Rhizobium fredii* synthesizes an array of lipooligosaccharides, including a novel compound with glucose inserted into the backbone of the molecule. *FEBS Lett.* 393, 273–279. doi: 10.1016/0014-5793(96)00903-9
- Biswas, B., and Gresshoff, P. M. (2014). The role of symbiotic nitrogen fixation in sustainable production of biofuels. *Int. J. Mol. Sci.* 15, 7380–7397. doi: 10.3390/ijms15057380
- Borisov, A. Y., Madsen, L. H., Tsyganov, V. E., Umehara, Y., Voroshilova, V. A., Batagov, A. O., et al. (2003). The Sym35 gene required for root nodule development in pea is an ortholog of Nin from *Lotus japonicus*. *Plant Physiol.* 131, 1009–1017. doi: 10.1104/pp.102.016071
- Cregan, P. B., Keyser, H. H., and Sadowsky, M. J. (1989). Host plant effects on nodulation and competitiveness of the *Bradyrhizobium japonicum* serotype strains constituting serocluster 123. *Appl. Environ. Microbiol.* 55, 2532–2536.
- Deakin, W. J., and Broughton, W. J. (2009). Symbiotic use of pathogenic strategies: rhizobial protein secretion systems. *Nat. Rev. Microbiol.* 7, 312–320. doi: 10.1038/nrmicro2091
- Deavours, B. E., and Dixon, R. A. (2005). Metabolic engineering of isoflavanoid biosynthesis in alfalfa. *Plant Physiol.* 138, 2245–2259. doi: 10.1104/pp.105.062539
- Denance, N., Szurek, B., and Noel, L. D. (2014). Emerging functions of nodulin-like proteins in non-nodulating plant species. *Plant Cell Physiol.* 55, 469–474. doi: 10.1093/pcp/pct198
- D'haeze, W., and Holsters, M. (2004). Surface polysaccharides enable bacteria to evade plant immunity. *Trends Microbiol.* 12, 555–561. doi: 10.1016/j.tim.2004.10.009
- Durrant, W. E., and Dong, X. (2004). Systemic acquired resistance. *Annu. Rev. Phytopathol.* 42, 185–209. doi: 10.1146/annurev.phyto.42.040803.140421
- Gamas, P., Niebel Fde, C., Lescure, N., and Cullimore, J. (1996). Use of a subtractive hybridization approach to identify new *Medicago truncatula* genes induced during root nodule development. *Mol. Plant Microbe Interact.* 9, 233–242. doi: 10.1094/MPMI-9-0233
- Hayashi, M., Saeki, Y., Haga, M., Harada, K., Kouchi, H., and Umehara, Y. (2012a). Rj (rj) genes involved in nitrogen-fixing root nodule formation in soybean. *Breed. Sci.* 61, 544–553. doi: 10.1270/jbsbs.61.544
- Hayashi, S., Reid, D. E., Lorenc, M. T., Stiller, J., Edwards, D., Gresshoff, P. M., et al. (2012b). Transient Nod factor-dependent gene expression in the nodulation-competent zone of soybean (*Glycine max* [L.] Merr.) roots. *Plant Biotechnol. J.* 10, 995–1010. doi: 10.1111/j.1467-7652.2012.00729.x
- Hennecke, H. (1990). Nitrogen fixation genes involved in the *Bradyrhizobium japonicum*-soybean symbiosis. *FEBS Lett.* 268, 422–426. doi: 10.1016/0014-5793(90)81297-2
- Hotter, G. S., and Scott, D. B. (1991). Exopolysaccharide mutants of *Rhizobium loti* are fully effective on a determinate nodulating host but are ineffective on an indeterminate nodulating host. *J. Bacteriol.* 173, 851–859.
- Hueck, C. J. (1998). Type III protein secretion systems in bacterial pathogens of animals and plants. *Microbiol. Mol. Biol. Rev.* 62, 379–433.
- Israel, D. W., Mathis, J. N., Barbour, W. M., and Elkan, G. H. (1986). Symbiotic Effectiveness and Host-Strain Interactions of *Rhizobium fredii* USDA 191 on Different Soybean Cultivars. *Appl. Environ. Microbiol.* 51, 898–903.
- Jiang, L., Romero-Carvajal, A., Haug, J. S., Seidel, C. W., and Piotrowski, T. (2014). Gene-expression analysis of hair cell regeneration in the zebrafish lateral line. *Proc. Natl. Acad. Sci. U.S.A.* 111, E1383–E1392. doi: 10.1073/pnas.1402898111
- Jiao, J., Wu, L. J., Zhang, B., Hu, Y., Li, Y., Zhang, X. X., et al. (2016). MucR is required for transcriptional activation of conserved ion transporters to support nitrogen fixation of *Sinorhizobium fredii* in soybean nodules. *Mol. Plant Microbe Interact.* 29, 352–361. doi: 10.1094/MPMI-01-16-0019-R
- Jones, K. M., Sharopova, N., Lohar, D. P., Zhang, J. Q., Vandembosch, K. A., and Walker, G. C. (2008). Differential response of the plant *Medicago truncatula* to its symbiont *Sinorhizobium meliloti* or an exopolysaccharide-deficient mutant. *Proc. Natl. Acad. Sci. U.S.A.* 105, 704–709. doi: 10.1073/pnas.0709338105
- Kanazin, V., Marek, L. F., and Shoemaker, R. C. (1996). Resistance gene analogs are conserved and clustered in soybean. *Proc. Natl. Acad. Sci. U.S.A.* 93, 11746–11750. doi: 10.1073/pnas.93.21.11746
- Kawahara, Y., Kelly, S., Nielsen, M. W., Hjuler, C. T., Gysel, K., Muszynski, A., et al. (2015). Receptor-mediated exopolysaccharide perception controls bacterial infection. *Nature* 523, 308–312. doi: 10.1038/nature14611
- Kevei, Z., Lougnon, G., Mergaert, P., Horvath, G. V., Kereszt, A., Jayaraman, D., et al. (2007). 3-hydroxy-3-methylglutaryl coenzyme a reductase 1 interacts with NORK and is crucial for nodulation in *Medicago truncatula*. *Plant Cell* 19, 3974–3989. doi: 10.1105/tpc.107.053975
- Keyser, H. H., and Cregan, P. B. (1987). Nodulation and Competition for Nodulation of Selected Soybean Genotypes among *Bradyrhizobium japonicum* Serogroup 123 Isolates. *Appl. Environ. Microbiol.* 53, 2631–2635.
- Kim, D. H., Parupalli, S., Azam, S., Lee, S. H., and Varshney, R. K. (2013). Comparative sequence analysis of nitrogen fixation-related genes in six legumes. *Front. Plant Sci.* 4:300. doi: 10.3389/fpls.2013.00300
- Krishnan, H. B., Natarajan, S. S., and Kim, W. S. (2011). Distinct cell surface appendages produced by *Sinorhizobium fredii* USDA257 and *S. fredii* USDA191, cultivar-specific and nonspecific symbionts of soybean. *Appl. Environ. Microbiol.* 77, 6240–6248. doi: 10.1128/AEM.05366-11
- Lerouge, P., Roche, P., Faucher, C., Maillet, F., Truchet, G., Prome, J. C., et al. (1990). Symbiotic host-specificity of *Rhizobium meliloti* is determined by a sulphated and acylated glucosamine oligosaccharide signal. *Nature* 344, 781–784. doi: 10.1038/344781a0
- Li, R., Yu, C., Li, Y., Lam, T. W., Yiu, S. M., Kristiansen, K., et al. (2009). SOAP2: an improved ultrafast tool for short read alignment. *Bioinformatics* 25, 1966–1967. doi: 10.1093/bioinformatics/btp336
- Libault, M., Farmer, A., Joshi, T., Takahashi, K., Langley, R. J., Franklin, L. D., et al. (2010). An integrated transcriptome atlas of the crop model *Glycine max*, and its use in comparative analyses in plants. *Plant J.* 63, 86–99. doi: 10.1111/j.1365-313x.2010.04222.x

- Liu, J., Liu, X., Dai, L., and Wang, G. (2007). Recent progress in elucidating the structure, function and evolution of disease resistance genes in plants. *J. Genet. Genomics* 34, 765–776. doi: 10.1016/S1673-8527(07)60087-3
- Margaret, I., Becker, A., Blom, J., Bonilla, I., Goesmann, A., Gottfert, M., et al. (2011). Symbiotic properties and first analyses of the genomic sequence of the fast growing model strain *Sinorhizobium fredii* HH103 nodulating soybean. *J. Biotechnol.* 155, 11–19. doi: 10.1016/j.jbiotec.2011.03.016
- Marioni, J. C., Mason, C. E., Mane, S. M., Stephens, M., and Gilad, Y. (2008). RNA-seq: an assessment of technical reproducibility and comparison with gene expression arrays. *Genome Res.* 18, 1509–1517. doi: 10.1101/gr.079558.108
- Mbengue, M., Camut, S., De Carvalho-Niebel, F., Deslandes, L., Froidure, S., Klaus-Heisen, D., et al. (2010). The *Medicago truncatula* E3 ubiquitin ligase PUB1 interacts with the LYK3 symbiotic receptor and negatively regulates infection and nodulation. *Plant Cell* 22, 3474–3488. doi: 10.1105/tpc.110.075861
- Meakin, G. E., Jepson, B. J., Richardson, D. J., Bedmar, E. J., and Delgado, M. J. (2006). The role of *Bradyrhizobium japonicum* nitric oxide reductase in nitric oxide detoxification in soya bean root nodules. *Biochem. Soc. Trans.* 34, 195–196. doi: 10.1042/BST0340195
- Mesa, S., Reutimann, L., Fischer, H. M., and Hennecke, H. (2009). Posttranslational control of transcription factor FixK2, a key regulator for the *Bradyrhizobium japonicum*-soybean symbiosis. *Proc. Natl. Acad. Sci. U.S.A.* 106, 21860–21865. doi: 10.1073/pnas.0908097106
- Okazaki, S., Kaneko, T., Sato, S., and Saeki, K. (2013). Hijacking of leguminous nodulation signaling by the rhizobial type III secretion system. *Proc. Natl. Acad. Sci. U.S.A.* 110, 17131–17136. doi: 10.1073/pnas.1302360110
- Oldroyd, G. E., and Downie, J. A. (2004). Calcium, kinases and nodulation signalling in legumes. *Nat. Rev. Mol. Cell Biol.* 5, 566–576. doi: 10.1038/nrm1424
- Oldroyd, G. E., and Downie, J. A. (2008). Coordinating nodule morphogenesis with rhizobial infection in legumes. *Annu. Rev. Plant Biol.* 59, 519–546. doi: 10.1146/annurev.arplant.59.032607.092839
- Perret, X., Staehelin, C., and Broughton, W. J. (2000). Molecular basis of symbiotic promiscuity. *Microbiol. Mol. Biol. Rev.* 64, 180–201. doi: 10.1128/MMBR.64.1.180-201.2000
- Quelas, J. I., Mongiardini, E. J., Casabuono, A., Lopez-Garcia, S. L., Althabeoiti, M. J., Covelli, J. M., et al. (2010). Lack of galactose or galacturonic acid in *Bradyrhizobium japonicum* USDA 110 exopolysaccharide leads to different symbiotic responses in soybean. *Mol. Plant Microbe Interact.* 23, 1592–1604. doi: 10.1094/MPMI-05-10-0122
- Rolfe, B. G. (1988). Flavones and isoflavones as inducing substances of legume nodulation. *Biofactors* 1, 3–10.
- Sadowsky, M. J., and Bohlool, B. B. (1986). Growth of fast- and slow-growing rhizobia on ethanol. *Appl. Environ. Microbiol.* 52, 951–953.
- Sanz-Saez, A., Heath, K. D., Burke, P. V., and Ainsworth, E. A. (2015). Inoculation with an enhanced N₂-fixing *Bradyrhizobium japonicum* strain (USDA110) does not alter soybean (*Glycine max* Merr.) response to elevated [CO₂]. *Plant Cell Environ.* 38, 2589–2602. doi: 10.1111/pce.12577
- Schmutz, J., Cannon, S. B., Schlueter, J., Ma, J., Mitros, T., Nelson, W., et al. (2010). Genome sequence of the palaeopolyploid soybean. *Nature* 463, 178–183. doi: 10.1038/nature08670
- Schultze, M., Quiclet-Sire, B., Kondorosi, E., Virelizer, H., Glushka, J. N., Endre, G., et al. (1992). Rhizobium meliloti produces a family of sulfated lipooligosaccharides exhibiting different degrees of plant host specificity. *Proc. Natl. Acad. Sci. U.S.A.* 89, 192–196. doi: 10.1073/pnas.89.1.192
- Stacey, G. (1995). *Bradyrhizobium japonicum* nodulation genetics. *FEMS Microbiol. Lett.* 127, 1–9. doi: 10.1111/j.1574-6968.1995.tb07441.x
- Staelelin, C., Forsberg, L. S., D'haeze, W., Gao, M. Y., Carlson, R. W., Xie, Z. P., et al. (2006). Exo-oligosaccharides of *Rhizobium* sp. strain NGR234 are required for symbiosis with various legumes. *J. Bacteriol.* 188, 6168–6178. doi: 10.1128/JB.00365-06
- Tang, F., Yang, S., and Zhu, H. (2016). Functional analysis of alternative transcripts of the soybean Rj2 gene that restricts nodulation with specific rhizobial strains. *Plant Biol. (Stuttg.)* 18, 537–541. doi: 10.1111/plb.12442
- Wei, M., Yokoyama, T., Minamisawa, K., Mitsui, H., Itakura, M., Kaneko, T., et al. (2008). Soybean seed extracts preferentially express genomic loci of *Bradyrhizobium japonicum* in the initial interaction with soybean, *Glycine max* (L.) Merr. *DNA Res.* 15, 201–214. doi: 10.1093/dnare/dsn012
- Yang, S., Tang, F., Gao, M., Krishnan, H. B., and Zhu, H. (2010). R gene-controlled host specificity in the legume-rhizobia symbiosis. *Proc. Natl. Acad. Sci. U.S.A.* 107, 18735–18740. doi: 10.1073/pnas.1011957107
- Zhu, M., Dahmen, J. L., Stacey, G., and Cheng, J. (2013). Predicting gene regulatory networks of soybean nodulation from RNA-Seq transcriptome data. *BMC Bioinformatics* 14:278. doi: 10.1186/1471-2105-14-278

Conflict of Interest Statement: The authors declare that the research was conducted in the absence of any commercial or financial relationships that could be construed as a potential conflict of interest.

Copyright © 2016 Yuan, Li, Chen, Chen, Zhang, Chen, Hao, Shan, Yang, Qiu, Zhang and Zhou. This is an open-access article distributed under the terms of the Creative Commons Attribution License (CC BY). The use, distribution or reproduction in other forums is permitted, provided the original author(s) or licensor are credited and that the original publication in this journal is cited, in accordance with accepted academic practice. No use, distribution or reproduction is permitted which does not comply with these terms.



Calcium Sensors as Key Hubs in Plant Responses to Biotic and Abiotic Stresses

Benoît Ranty, Didier Aldon, Valérie Cotelle, Jean-Philippe Galaud, Patrice Thuleau and Christian Mazars*^{*}

Laboratoire de Recherche en Sciences Végétales, Université de Toulouse, CNRS, UPS, Auzeville, Castanet-Tolosan, France

The Ca^{2+} ion is recognized as a crucial second messenger in signaling pathways coupling the perception of environmental stimuli to plant adaptive responses. Indeed, one of the earliest events following the perception of environmental changes (temperature, salt stress, drought, pathogen, or herbivore attack) is intracellular variation of free calcium concentrations. These calcium variations differ in their spatio-temporal characteristics (subcellular location, amplitude, kinetics) with the nature and strength of the stimulus and, for this reason, they are considered as signatures encrypting information from the initial stimulus. This information is believed to drive a specific response by decoding via calcium-binding proteins. Based on recent examples, we illustrate how individual calcium sensors from the calcium-dependent protein kinase and calmodulin-like protein families can integrate inputs from various environmental changes. Focusing on members of these two families, shown to be involved in plant responses to both abiotic and biotic stimuli, we discuss their role as key hubs and we put forward hypotheses explaining how they can drive the signaling pathways toward the appropriate plant responses.

OPEN ACCESS

Edited by:

Olivier Lamotte,
Centre National de la Recherche
Scientifique – Unité Mixte
de Recherche Agroécologie, France

Reviewed by:

Gerald Alan Berkowitz,
University of Connecticut, USA
Lorella Navazio,
University of Padova, Italy

***Correspondence:**

Christian Mazars
mazars@lrsv.ups-tlse.fr

Specialty section:

This article was submitted to
Plant Physiology,
a section of the journal
Frontiers in Plant Science

Received: 22 January 2016

Accepted: 03 March 2016

Published: 16 March 2016

Citation:

Ranty B, Aldon D, Cotelle V, Galaud J-P, Thuleau P and Mazars C (2016) Calcium Sensors as Key Hubs in Plant Responses to Biotic and Abiotic Stresses. *Front. Plant Sci.* 7:327.
doi: 10.3389/fpls.2016.00327

INTRODUCTION

Plants as sessile organisms have to continuously face environmental cues coming from abiotic and biotic challenges. Their survival depends on their ability to discriminate each stimulus among the diverse challenging environmental changes in order to prepare a specific response. Plants have evolved sophisticated signaling strategies allowing them, in most cases, to withstand these stresses and survive deleterious conditions. Among the strategies employed, plants use an intricate signaling network involving calcium as a second messenger. It is now well acknowledged that the Ca^{2+} ion plays a crucial role, as a mediator, in regulating and specifying the cellular responses to environmental stresses (Sanders et al., 2002; White and Broadley, 2003; Dodd et al., 2010). Each stimulus perceived by the plant is generally followed by an immediate increase in intracellular Ca^{2+} concentration occurring either simultaneously or after a lag time in a single or several intracellular compartments of the cell (cytosol, nucleus, mitochondria, etc.). Such Ca^{2+} transients, each linked to a particular stimulus, differ in their spatio-temporal patterns, being therefore considered as signatures (McAinsh and Hetherington, 1998). Each Ca^{2+} signature contributes to a first layer of specificity through its tissue and sub-cellular location, amplitude and frequency and the calcium

pool involved in producing it (Allen et al., 2001; Miwa et al., 2006). However, to be fully significant in terms of signaling, decoding Ca^{2+} signals by Ca^{2+} -modulated proteins (usually termed calcium sensors) is mandatory. Calcium sensor proteins estimated to number over 250 in *Arabidopsis* (Day et al., 2002) are represented by three main families, i.e., the calcineurin-B-like proteins (CBLs) (Luan, 2009), the calmodulin (CaM), and calmodulin-like proteins (CMLs) (Yang and Poovaiah, 2003; Bender and Snedden, 2013), the calcium-dependent protein kinases (CPKs) and the calcium and calmodulin-dependent protein kinase (CCaMK) (Cheng et al., 2002; Wang et al., 2015).

These proteins display various affinities for calcium ions and this property, combined with their sub-cellular location within the cell, will control their behavior. Calcium binding to Ca^{2+} sensors will induce a conformational change that triggers either their association to downstream target proteins or a direct stimulation of the kinase activity when CPKs are considered (Harmon et al., 2000). The diversity of Ca^{2+} sensors and their downstream targets contributes to a second layer of specificity, allowing the transduction of various primary stimuli into distinct biological responses (Hashimoto and Kudla, 2011). In addition, the hypothesis of signaling microdomains gathering calcium signaling components as described in animal cells (Good et al., 2011; Gueguinou et al., 2015) can also be proposed to contribute to response specificity in plants.

In this mini-review, we focus on calcium sensors lying at the crossroads of signaling pathways initiated by either abiotic or biotic stimuli. Due to the paucity of reported data concerning the role of the CBL/CIPK family in biotic stress responses, we will only consider CPK and CML protein families as common components of both biotic and abiotic stress signaling. We will discuss how a single Ca^{2+} sensor may direct the flow of signaling information toward distinct adaptive responses.

CMLS AT THE CROSSROADS OF BIOTIC AND ABIOTIC SIGNALING PATHWAYS

In addition to CaM, which has been well conserved through evolution, plant genomes are predicted to encode a broad range of CML proteins (McCormack et al., 2005; Boonburapong and Buaboocha, 2007; Zhu et al., 2015). Like CaM, most CMLs contain 4 EF-hand calcium-binding motifs and no other functional domains; they share at least 16% overall amino acid identity with CaM in *Arabidopsis* (McCormack and Braam, 2003). Several CMLs were shown to display biochemical properties typical of proteins that function as Ca^{2+} sensors, including, upon calcium binding, a shift in their electrophoretic mobility, and changes in secondary structure and in exposed surface hydrophobicity (Kohler and Neuhaus, 2000; Chiasson et al., 2005; Bender et al., 2014; Scholz et al., 2015). Thus, CMLs are believed to act as calcium sensors, and the Ca^{2+} -induced conformational changes likely increase their interaction affinity to downstream effectors, as described for CaM. Search for CML targets has allowed the identification of diverse CML-binding proteins including protein kinases, transcription factors, metabolic enzymes, and transporters (Yamaguchi et al., 2005;

Popescu et al., 2007; Perochon et al., 2010). Although regulation of these targets by CMLs is most often presumptive, CMLs likely function as calcium sensors/relays by tuning the activity of downstream effectors. Diverse roles for CMLs in plant development and stress responses have been reported, (Perochon et al., 2011; Bender and Snedden, 2013; Cheval et al., 2013; Zeng et al., 2015).

Our work on Ca^{2+} -mediated stress signaling in the model plant *Arabidopsis*, has identified AtCML9 as both a positive and negative regulator of plant immune response and drought stress tolerance, respectively (Magnan et al., 2008; Leba et al., 2012). AtCML9 was found to be induced early in plants exposed to salt, cold, or dehydration treatment, to a bacterial pathogen and to application of stress-associated phytohormones including abscisic acid (ABA) and salicylic acid (SA). Salt-responsive expression of AtCML9 is dependent on ABA production, while its expression in response to a virulent strain of *Pseudomonas syringae* is dependent on SA synthesis, suggesting that this CML is involved in stress hormone-mediated responses. In this respect, Atcml9 null mutants exhibit a hypersensitive response to ABA during early growth stages that could be correlated with the enhanced tolerance to drought and salt stress in adult plants. Atcml9 mutants also show alterations in the expression of several stress and ABA-responsive genes as well as defense-related genes. These data indicate that AtCML9 contributes to both abiotic and biotic stress responses in conjunction with hormone signaling, and suggest a role for AtCML9 in the regulation of stress/defense-related genes. AtCML9 was reported to interact with diverse transcription factors including WRKY53 and TGA3 two factors that participate in plant defense responses (Popescu et al., 2007). However, the biological relevance of these physical interactions requires further analysis.

Among other CMLs shown to be linked to stress signaling, AtCML37 and 42, appear to play dual roles in abiotic stress responses and defense against herbivorous insects. Loss of function of AtCML42 in *Arabidopsis* mutants results in enhanced resistance to *Spodoptera littoralis*, up-regulation of jasmonic acid (JA)-responsive genes and an increased accumulation of aliphatic glucosinolates (Vadassery et al., 2012). Thus, AtCML42 acts negatively on herbivore resistance by decreasing the expression of JA-responsive genes and the accumulation of defense secondary metabolites. Atcml42 null mutants also show a reduced content in flavonol glucosides that play a role in UV-B protection. As a consequence, Atcml42 mutant seedlings are less resistant to UV-B exposure. In contrast to AtCML42, AtCML37 acts positively on defense against *S. littoralis* (Scholz et al., 2014). AtCML37 loss-of-function mutants exhibit an enhanced susceptibility to herbivory correlated with a lower level of the bioactive form of jasmonate (JA-Ile), an important hormone in plant defense against herbivores, and lower expression of JA-responsive genes encoding proteins involved in the synthesis of molecules toxic for insects. In addition, Atcml37 null mutants show a decrease in drought stress tolerance correlated with a low content in ABA, whereas Atcml42 null mutants are not impaired in drought stress response (Scholz et al., 2015). Collectively, these data reveal opposite roles for AtCML37 and 42 in insect herbivory resistance and distinct functions of these two CMLs in abiotic

stress responses. It can also be noted that these particular CMLs, at the crossroads of biotic and abiotic signaling pathways, play antagonistic roles for the plant, being generally protective in one pathway and deleterious in the second. Due to their dual role in distinct signaling pathways, these Ca^{2+} sensors are interesting tools that can help in understanding how specificity is achieved in plant responses to environmental cues. Identification of their interacting partners will be helpful to clarify how these CMLs exert their action at a molecular level and will shed light on the mechanisms controlling their antagonistic effects in defense against herbivores.

CPKs AS SIGNALING NODES MEDIATING PLANT RESPONSES TO BIOTIC AND ABIOTIC STRESSES

Calcium-dependent protein kinase and CMLs share a similar broad distribution in the plant kingdom (Valmonte et al., 2014; Zhu et al., 2015). They possess a CaM-like and a kinase domain that make them direct effectors upon activation by Ca^{2+} binding. Their conserved molecular structure consists of a variable N-terminal domain joined to a Ser/Thr kinase domain associated to a CPK activation domain (CAD). CAD comprises an inhibitory junction domain (also termed pseudosubstrate region) fused to a CaM-like domain (Harper et al., 2004). The current *in vivo* activation model of CPKs states that, upon Ca^{2+} binding, the conformational change induced will release the pseudosubstrate region from the active site of the kinase domain (Liese and Romeis, 2013). Like CMLs, and according to their tissue and sub-cellular location or Ca^{2+} affinity, CPKs participate as Ca^{2+} sensors in the regulation of various plant functions ranging from plant growth and development to plant defense and adaptation against pathogens, pests, and environmental cues (Asano et al., 2012a; Boudsocq and Sheen, 2013; Schulz et al., 2013; Romeis and Herde, 2014). A number of studies have been performed to find substrates of CPKs (Rodriguez Milla et al., 2006; Uno et al., 2009; Mehlmer et al., 2010; Berendzen et al., 2012), but only a few have led to “*in vivo*” confirmation. Among them, the NADPH oxidase RBOHD, shown to be activated by AtCPK5 in *Arabidopsis* (Dubiella et al., 2013) is involved in ROS-mediated long distance signaling in response to several stimuli (Miller et al., 2009; Gilroy et al., 2014; Romeis and Herde, 2014). Other targets are located in guard cells where they display ion transport activity (Schroeder and Hagiwara, 1990; Pei et al., 1996; Brandt et al., 2012; Scherzer et al., 2012; Zhang et al., 2014). Interestingly, as for CMLs, some members of the CPK family appear to play a dual role in both biotic and abiotic stress responses.

In a recent study, aiming at understanding how calcium can regulate sphingolipid-induced programmed cell death (PCD), we identified AtCPK3 as a crucial effector in this process (Lachaud et al., 2013). Long chain bases (LCBs) which are precursors of more complex sphingolipids, have been proposed to mediate immune responses in plants (Peer et al., 2010). Some natural analogs mimicking LCBs, such as mycotoxins produced by necrotrophic *Fusarium* fungi, likely interfere

with the sphingolipid signaling pathway and plant immunity processes. Indeed, fumonisin B1 (FB1) produced by *Fusarium moniliforme*, is able to quickly increase the level of free LCBs in the cell thus mimicking a LCB treatment (Saucedo-Garcia et al., 2011). In addition FB1 induces a Ca^{2+} burst that activates AtCPK3 which forms a complex with dimeric 14-3-3 proteins in resting conditions. Upon activation, AtCPK3 phosphorylates a conserved serine residue located at the N-terminal part of each 14-3-3 monomer. Phosphorylation of 14-3-3 proteins at the dimer interface results in disruption of their dimeric structure, promoting AtCPK3 release and cell death induction. Using *Atcpk3* null lines, we demonstrate that AtCPK3 is required for full development of PCD symptoms in leaves infiltrated with this mycotoxin (Lachaud et al., 2013). In parallel studies, using co-expression assays in *Nicotiana benthamiana*, AtCPK3 was also shown to be involved in biotic stress responses during plant-insect interactions. In wild-type plants exposed to *Spodoptera littoralis*, AtCPK3 is able to phosphorylate the heat-shock transcription factor B2a (HsfB2a) that likely activates the transcription of the defensin gene *PDF1.2*, known to be induced as a resistance mechanism (Kanchiswamy et al., 2010). Besides participation of AtCPK3 in signaling processes associated with biotic stresses, various studies also describe its involvement in the transduction of abiotic signals. Indeed, genetic approaches have shown that this kinase, together with AtCPK6, mediates ABA responses in guard cells. They participate in Ca^{2+} activation of plasma membrane slow-type anion channels (Mori et al., 2006). In the *Atcpk3/Atcpk6* double mutant, ABA-induced stomatal closure is impaired while long-term Ca^{2+} -programmed stomatal closure is not. In addition, AtCPK3 binds and can phosphorylate the *Arabidopsis* vacuolar two-pore K⁺ channel TPK1, thereby contributing to its regulation during salt stress response (Latz et al., 2013) whereas during the same stress, AtCPK3 was shown to modulate the membrane phosphoproteome likely in a MAPK-independent pathway (Mehlmer et al., 2010).

Another example illustrating the dual role of CPKs in plant responses to biotic and abiotic stimuli concerns AtCPK1, which when over-expressed confers a SA-mediated resistance phenotype in *Arabidopsis* toward both necrotrophic fungi (*Botrytis cinerea*, *Fusarium oxysporum*) and biotrophic bacteria (*Pseudomonas syringae*), while its suppression (null mutants) results in an enhanced susceptibility to these pathogens (Coca and San Segundo, 2010). Like AtCPK3, AtCPK1 is thought to mediate responses to other environmental physical cues such as light. Using *Vicia faba* vacuoles and a patch-clamp approach, Schroeder's group showed that recombinant AtCPK1 was able to activate a vacuolar chloride channel that could be, according to the authors, an important player in light-mediated stomatal opening (Pei et al., 1996).

Finally, in an elegant and exhaustive work, Boudsocq et al. (2010) identified several CPKs activated by flg22, a 22-amino acid peptide derived from flagellin known to induce plant immune responses (Boudsocq et al., 2010). By transiently expressing constitutively active *Arabidopsis* CPKs, five AtCPKs (AtCPK4,5,6,11,26) were found able to activate the expression of the Ca^{2+} -dependent flg22-responsive reporter gene NHL10-LUC (NDR1/Hin1-Like10-LUCiferase), in the same manner as flg22

(Boudsocq et al., 2010). In the light of the presumed functions of AtCPKs (Boudsocq and Sheen, 2013), it is interesting to note that the AtCPKs mentioned above play a dual role being also involved in abiotic signaling pathways. AtCPK4 and AtCPK11 were shown to promote the expression of the reporter luciferase (LUC) under the control of an ABA-responsive promoter (*RD29A*). The activity of LUC was synergistically increased upon co-expression of AtCPK4 with the ABA-responsive bZIP transcription factor ABF2, whereas AtCPK11 which shares more than 95% identity with AtCPK4 was unable to enhance the LUC response through ABF2 (Lu et al., 2013).

HOW CAN A SINGLE CALCIUM SENSOR CONTRIBUTE SPECIFIC RESPONSES TO BOTH BIOTIC AND ABIOTIC STRESSES

From the different examples described above, it appears that CPKs as CMLs, share the property of being hubs, able to integrate signals triggered by both biotic and abiotic stimuli and to drive the signaling pathway toward the appropriate response. This property that seems common to related Ca^{2+} sensors in other plant species, including monocots (Asano et al., 2012b), raises the question of the mechanisms involved in the

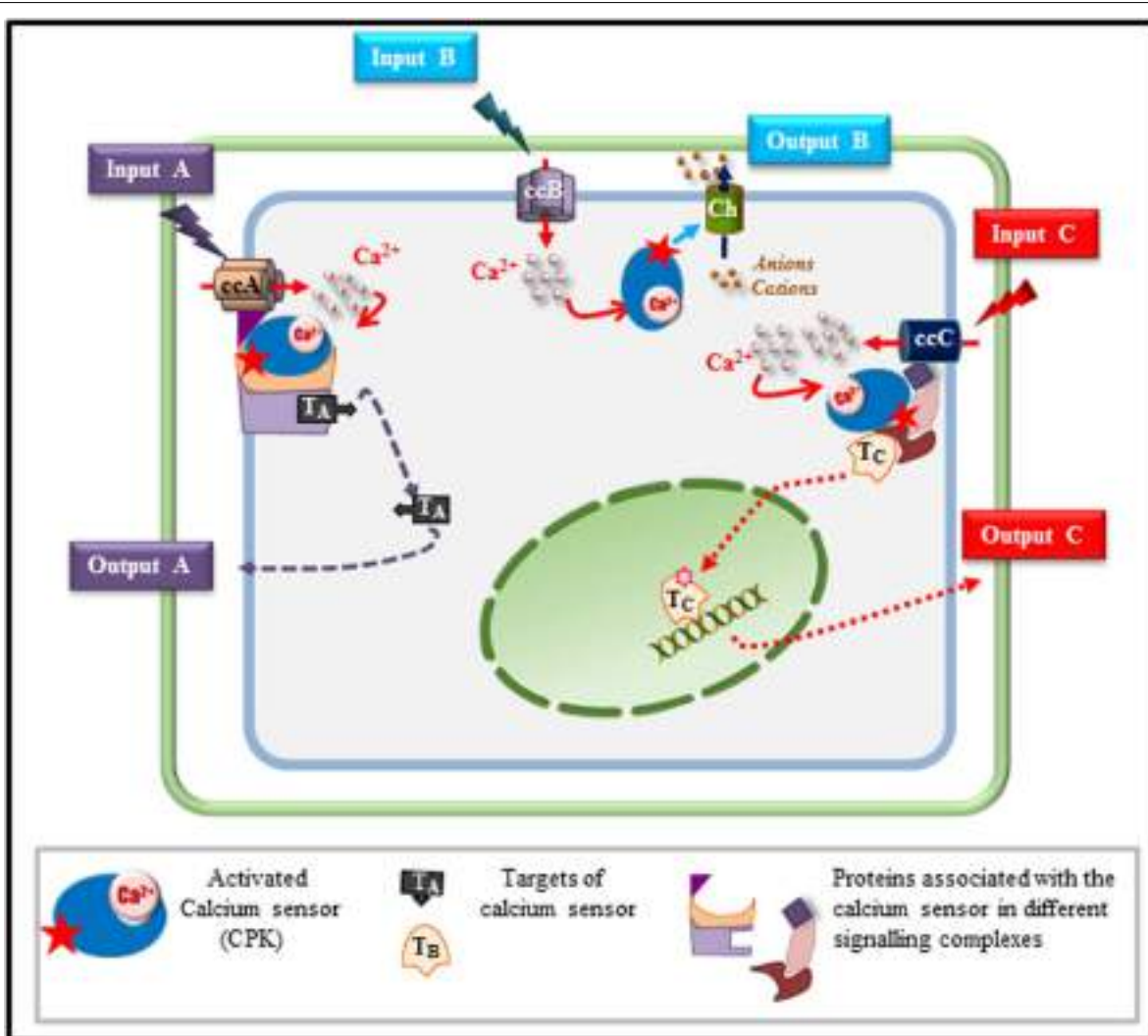


FIGURE 1 | Model depicting how a single calcium sensor can handle various cell signaling inputs and outputs. Based on the results described in this mini-review, we depict various possible scenarios explaining how a single calcium sensor such as a calcium-dependent protein kinase (CPK), can drive signaling pathways toward specific responses in a single cell exposed to different stimuli. In response to a stimulus A (input A), a specific calcium channel (ccA) is activated and generates a calcium flux that will activate the CPK that will phosphorylate target A (TA) involved in output A. In response to a second stimulus (input B), a specific calcium channel is activated (ccB) and calcium released into the cytosol will activate the CPK that can directly regulate an effector (Ch) such as an ion transporter (channel, pump, exchanger) leading, according to the charge of the transported ions, to membrane depolarisation or hyperpolarisation contributing to the final response (output B). The same calcium sensor can be associated, in the same cell, with a different scaffold tethered to a different calcium channel (ccC) that is activated only by stimulus C (input C). Upon ccC activation, the calcium sensor is activated and can lead, through this specific signaling module, to the activation of a different target (T_c) migrating to the nucleus in order to control the adaptive response C through gene reprogramming for instance (output C).

switching functions that these CPKs or CMLs are expected to play. While it is quite difficult to answer this question from studies performed on CMLs, mainly due to our lack of knowledge concerning their downstream targets, different hypotheses can be drawn from existing knowledge on CPKs (**Figure 1**). Taking AtCPK3, as a model, we can speculate on the way in which a single Ca^{2+} sensor can wire the flow of signaling information toward the right adaptive response upon challenging the plant with different stimuli. Beyond the importance of the specific Ca^{2+} signature generated in response to a given stimulus, it is clear that specificity of the routing will be achieved only if the calcium sensor, its downstream targets and putative partner proteins are co-localized and expressed at the same time. In guard cells, AtCPK3 can be activated by calcium ions flowing through non-selective calcium channels in response to environmental cues (e.g., drought) (Schroeder and Hagiwara, 1990) and can phosphorylate S-type anion channels resulting in stomatal closure. When located in mesophyll cells, the situation is more complex if we consider that these cells can be challenged by different stimuli (e.g., herbivores and mycotoxins) leading to different outputs (e.g., defense and cell death). Exposure of these cells to the chewing action of *S. littoralis* is reported to stimulate glutamate receptors (Mousavi et al., 2013) that have been shown to mediate Ca^{2+} influx (Kwaaitaal et al., 2011; Manzoor et al., 2013). These Ca^{2+} fluxes in mesophyll cells will probably account for AtCPK3 activation which in turn will phosphorylate HsfB2a, a transcription factor up-regulating the defensin gene involved in responses against herbivores (Kanchiswamy et al., 2010). However, if glutamate channels can be suspected in the case of *S. littoralis* attack, they are most probably not involved in the cytosolic Ca^{2+} transients observed in response to FB1/LCBs. Indeed, ionotropic glutamate channel inhibitors did not inhibit the cytosolic Ca^{2+} responses when cells were challenged with LCBs (Lachaud et al., 2010). A different type of Ca^{2+} channel could be involved in FB1-induced calcium increase leading to PCD. Therefore, in this particular case, the switching mode of AtCPK3, leading either to PCD or basal defense mechanisms, can rather be related to the origin of Ca^{2+} and/or the nature of the channels involved in shaping the Ca^{2+} signatures triggered by each stimulus (insect or sphingolipid). It can then be hypothesized that these different classes of activated channels can engage AtCPK3 in different signaling modules that are specifically associated to each type of channel. Such an association will favor the interaction of

AtCPK3 with its downstream substrates specifically dedicated to one output (defense or cell death). Similar assemblies of signaling proteins defined as signaling complexes or scaffolds have been shown for a few signaling proteins in plants. Indeed AtCPK21 was shown to interact in an ABA-dependent manner with the slow anion channel 1 (SLAC1) homolog 3 (SLAH3) in microdomains of the guard cell plasma membrane. The activity of AtCPK21, which is crucial for SLAH3 activation, seems to be regulated by a protein scaffold involving protein phosphatase 2C (PP2C) ABI1 and an ABA receptor of the RCAR1/PYR/PYL family (Demir et al., 2013). This scaffold hypothesis has got a much larger scientific audience in animals (Good et al., 2011) where clustering of Ca^{2+} channels in membrane microdomains and association with their downstream signaling complexes have been reported (Dart, 2010; Gueguinou et al., 2015).

CONCLUDING REMARKS

The operating mode of these signaling hubs remains a challenging question that needs further investigation. Emerging imaging techniques at nanoscale resolution (Curthoys et al., 2015; Komis et al., 2015) and new proteomics approaches dedicated to deciphering protein complexes (Boeri Erba, 2014; Liu and Heck, 2015; Politis and Borysik, 2015) are very promising and should lead to a better understanding of the mechanisms underlying how a single Ca^{2+} sensor acts at the crossroads of various signaling pathways to help plants to cope with various environmental challenges.

AUTHOR CONTRIBUTIONS

CM and BR contributed to the writing of the manuscript. DA and CM participated in drawing **Figure 1** and in critically revising the manuscript with PT, J-PG, and VC.

FUNDING

This work was supported by the Université Paul Sabatier (Toulouse, France), the CNRS (France) and by the French Laboratory of Excellence project “TULIP” (ANR-10-LABX-41; ANR-11-IDEX-0002-02).

REFERENCES

- Allen, G. J., Chu, S. P., Harrington, C. L., Schumacher, K., Hoffmann, T., Tang, Y. Y., et al. (2001). A defined range of guard cell calcium oscillation parameters encodes stomatal movements. *Nature* 411, 1053–1057. doi: 10.1038/35082575
- Asano, T., Hayashi, N., Kikuchi, S., and Ohsugi, R. (2012a). CDPK-mediated abiotic stress signalling. *Plant Signal. Behav.* 7, 817–821. doi: 10.4161/psb.20351
- Asano, T., Hayashi, N., Kobayashi, M., Aoki, N., Miyao, A., Mitsuhashi, I., et al. (2012b). A rice calcium-dependent protein kinase OsCPK12 oppositely modulates salt-stress tolerance and blast disease resistance. *Plant J.* 69, 26–36. doi: 10.1111/j.1365-313X.2011.04766.x
- Bender, K. W., Dobney, S., Ogunrinde, A., Chiasson, D., Mullen, R. T., Teresinski, H. J., et al. (2014). The calmodulin-like protein CML43 functions as a salicylic-acid-inducible root-specific $\text{Ca}(2+)$ sensor in *Arabidopsis*. *Biochem. J.* 457, 127–136. doi: 10.1042/bj20131080
- Bender, K. W., and Snedden, W. A. (2013). Calmodulin-related proteins step out from the shadow of their namesake. *Plant Physiol.* 163, 486–495. doi: 10.1104/pp.113.221069
- Berendzen, K. W., Bohmer, M., Wallmeroth, N., Peter, S., Vesic, M., Zhou, Y., et al. (2012). Screening for in planta protein-protein interactions combining bimolecular fluorescence complementation with flow cytometry. *Plant Methods* 8, 25. doi: 10.1186/1746-4811-8-25
- Boeri Erba, E. (2014). Investigating macromolecular complexes using top-down mass spectrometry. *Proteomics* 14, 1259–1270. doi: 10.1002/pmic.201300333

- Boonburapong, B., and Buaboocha, T. (2007). Genome-wide identification and analyses of the rice calmodulin and related potential calcium sensor proteins. *BMC Plant Biol.* 7:4. doi: 10.1186/1471-2229-7-4
- Boudsocq, M., and Sheen, J. (2013). CDPKs in immune and stress signaling. *Trends Plant Sci.* 18, 30–40. doi: 10.1016/j.tplants.2012.08.008
- Boudsocq, M., Willmann, M. R., McCormack, M., Lee, H., Shan, L., He, P., et al. (2010). Differential innate immune signalling via Ca^{2+} sensor protein kinases. *Nature* 464, 418–422. doi: 10.1038/nature08794
- Brandt, B., Brodsky, D. E., Xue, S., Negi, J., Iba, K., Kangasjarvi, J., et al. (2012). Reconstitution of abscisic acid activation of SLAC1 anion channel by CPK6 and OST1 kinases and branched ABI1 PP2C phosphatase action. *Proc. Natl. Acad. Sci. U.S.A.* 109, 10593–10598. doi: 10.1073/pnas.1116590109
- Cheng, S. H., Willmann, M. R., Chen, H. C., and Sheen, J. (2002). Calcium signaling through protein kinases. The *Arabidopsis* calcium-dependent protein kinase gene family. *Plant Physiol.* 129, 469–485. doi: 10.1104/pp.005645
- Cheval, C., Aldon, D., Galaud, J. P., and Ranty, B. (2013). Calcium/calmodulin-mediated regulation of plant immunity. *Biochim. Biophys. Acta* 1833, 1766–1771. doi: 10.1016/j.bbamcr.2013.01.031
- Chiasson, D., Ekengren, S. K., Martin, G. B., Dobney, S. L., and Snedden, W. A. (2005). Calmodulin-like proteins from *Arabidopsis* and tomato are involved in host defense against *Pseudomonas syringae* pv. tomato. *Plant Mol. Biol.* 58, 887–897. doi: 10.1007/s11103-005-8395-x
- Coca, M., and San Segundo, B. (2010). AtCPK1 calcium-dependent protein kinase mediates pathogen resistance in *Arabidopsis*. *Plant J.* 63, 526–540. doi: 10.1111/j.1365-313X.2010.04255.x
- Curthoys, N. M., Parent, M., Mlodzianoski, M., Nelson, A. J., Lilieholm, J., Butler, M. B., et al. (2015). Dances with membranes: breakthroughs from super-resolution imaging. *Curr. Top. Membr.* 75, 59–123. doi: 10.1016/bs.ctm.2015.03.008
- Dart, C. (2010). Lipid microdomains and the regulation of ion channel function. *J. Physiol.* 588, 3169–3178. doi: 10.1111/jphysiol.2010.191585
- Day, I. S., Reddy, V. S., Shad Ali, G., and Reddy, A. S. (2002). Analysis of EF-hand-containing proteins in *Arabidopsis*. *Genome Biol.* 3, RESEARCH0056. doi: 10.1186/gb-2002-3-10-research0056
- Demir, F., Horrnrich, C., Blachutzik, J. O., Scherzer, S., Reinders, Y., Kierszniewska, S., et al. (2013). *Arabidopsis* nanodomain-delimited ABA signaling pathway regulates the anion channel SLAH3. *Proc. Natl. Acad. Sci. U.S.A.* 110, 8296–8301. doi: 10.1073/pnas.1211667110
- Dodd, A. N., Kudla, J., and Sanders, D. (2010). The language of calcium signaling. *Annu. Rev. Plant Biol.* 61, 593–620. doi: 10.1146/annurev-arplant-070109-104628
- Dubiella, U., Seybold, H., Durian, G., Komander, E., Lassig, R., Witte, C. P., et al. (2013). Calcium-dependent protein kinase/NADPH oxidase activation circuit is required for rapid defense signal propagation. *Proc. Natl. Acad. Sci. U.S.A.* 110, 8744–8749. doi: 10.1073/pnas.1221294110
- Gilroy, S., Suzuki, N., Miller, G., Choi, W. G., Toyota, M., Devireddy, A. R., et al. (2014). A tidal wave of signals: calcium and ROS at the forefront of rapid systemic signaling. *Trends Plant Sci.* 19, 623–630. doi: 10.1016/j.tplants.2014.06.013
- Good, M. C., Zalatan, J. G., and Lim, W. A. (2011). Scaffold proteins: hubs for controlling the flow of cellular information. *Science* 332, 680–686. doi: 10.1126/science.1198701
- Gueguinou, M., Gambade, A., Felix, R., Chantome, A., Fourbon, Y., Bougnoux, P., et al. (2015). Lipid rafts, KCa/ClCa/ Ca^{2+} channel complexes and EGFR signaling: novel targets to reduce tumor development by lipids? *Biochim. Biophys. Acta* 1848, 2603–2620. doi: 10.1016/j.bbapm.2014.10.036
- Harmon, A. C., Gribskov, M., and Harper, J. F. (2000). CDPKs – a kinase for every Ca^{2+} signal? *Trends Plant Sci.* 5, 154–159. doi: 10.1016/S1360-1385(00)01577-6
- Harper, J. F., Breton, G., and Harmon, A. (2004). Decoding Ca^{2+} signals through plant protein kinases. *Annu. Rev. Plant Biol.* 55, 263–288. doi: 10.1146/annurev.arplant.55.031903.141627
- Hashimoto, K., and Kudla, J. (2011). Calcium decoding mechanisms in plants. *Biochimie* 93, 2054–2059. doi: 10.1016/j.biochi.2011.05.019
- Kanchiswamy, C. N., Takahashi, H., Quadro, S., Maffei, M. E., Bossi, S., Berteau, C., et al. (2010). Regulation of *Arabidopsis* defense responses against *Spodoptera littoralis* by CPK-mediated calcium signaling. *BMC Plant Biol.* 10:97. doi: 10.1186/1471-2229-10-97
- Kohler, C., and Neuhaus, G. (2000). Characterisation of calmodulin binding to cyclic nucleotide-gated ion channels from *Arabidopsis thaliana*. *FEBS Lett.* 471, 133–136. doi: 10.1016/S0014-5793(00)01383-1
- Komis, G., Samajova, O., Ovecka, M., and Samaj, J. (2015). Super-resolution microscopy in plant cell imaging. *Trends Plant Sci.* 20, 834–843. doi: 10.1016/j.tplants.2015.08.013
- Kwaaitaal, M., Huisman, R., Maintz, J., Reinstadler, A., and Panstruga, R. (2011). Ionotropic glutamate receptor (iGluR)-like channels mediate MAMP-induced calcium influx in *Arabidopsis thaliana*. *Biochem. J.* 440, 355–365. doi: 10.1042/BJ20111112
- Lachaud, C., Da Silva, D., Cotelle, V., Thuleau, P., Xiong, T. C., Jauneau, A., et al. (2010). Nuclear calcium controls the apoptotic-like cell death induced by d-erythro-sphinganine in tobacco cells. *Cell Calcium* 47, 92–100. doi: 10.1016/j.ceca.2009.11.011
- Lachaud, C., Prigent, E., Thuleau, P., Grat, S., Da Silva, D., Briere, C., et al. (2013). 14-3-3-regulated Ca^{2+} -dependent protein kinase CPK3 is required for sphingolipid-induced cell death in *Arabidopsis*. *Cell Death Differ.* 20, 209–217. doi: 10.1038/cdd.2012.114
- Latz, A., Mehlmer, N., Zapf, S., Mueller, T. D., Wurzinger, B., Pfister, B., et al. (2013). Salt stress triggers phosphorylation of the *Arabidopsis* vacuolar K⁺ channel TPK1 by calcium-dependent protein kinases (CDPKs). *Mol. Plant* 6, 1274–1289. doi: 10.1093/mp/sss158
- Leba, L. J., Cheval, C., Ortiz-Martin, I., Ranty, B., Beuzon, C. R., Galaud, J. P., et al. (2012). CML9, an *Arabidopsis* calmodulin-like protein, contributes to plant innate immunity through a flagellin-dependent signalling pathway. *Plant J.* 71, 976–989. doi: 10.1111/j.1365-313X.2012.05045.x
- Liese, A., and Romeis, T. (2013). Biochemical regulation of in vivo function of plant calcium-dependent protein kinases (CDPK). *Biochim. Biophys. Acta* 1833, 1582–1589. doi: 10.1016/j.bbamcr.2012.10.024
- Liu, F., and Heck, A. J. (2015). Interrogating the architecture of protein assemblies and protein interaction networks by cross-linking mass spectrometry. *Curr. Opin. Struct. Biol.* 35, 100–108. doi: 10.1016/j.sbi.2015.10.006
- Lu, Y., Chen, X., Wu, Y., Wang, Y., He, Y., and Wu, Y. (2013). Directly transforming PCR-amplified DNA fragments into plant cells is a versatile system that facilitates the transient expression assay. *PLoS ONE* 8:e57171. doi: 10.1371/journal.pone.0057171
- Luan, S. (2009). The CBL-CIPK network in plant calcium signaling. *Trends Plant Sci.* 14, 37–42. doi: 10.1016/j.tplants.2008.10.005
- Magnan, F., Ranty, B., Charpentier, M., Sotta, B., Galaud, J. P., and Aldon, D. (2008). Mutations in AtCML9, a calmodulin-like protein from *Arabidopsis thaliana*, alter plant responses to abiotic stress and abscisic acid. *Plant J.* 56, 575–589. doi: 10.1111/j.1365-313X.2008.03622.x
- Manzoor, H., Kelloniemi, J., Chiltz, A., Wendehenne, D., Pugin, A., Poinsot, B., et al. (2013). Involvement of the glutamate receptor AtGLR3.3 in plant defense signaling and resistance to *Hyaloperonospora arabidopsis*. *Plant J.* 76, 466–480. doi: 10.1111/tpj.12311
- McAinsh, M. R., and Hetherington, A. M. (1998). Encoding specificity in Ca^{2+} signalling systems. *Trends Plant Sci.* 3, 32–36. doi: 10.1016/S1360-1385(97)01150-3
- McCormack, E., and Braam, J. (2003). Calmodulins and related potential calcium sensors of *Arabidopsis*. *New Phytol.* 159, 585–598. doi: 10.1046/j.1469-8137.2003.00845.x
- McCormack, E., Tsai, Y. C., and Braam, J. (2005). Handling calcium signaling: *Arabidopsis* CaMs and CMLs. *Trends Plant Sci.* 10, 383–389. doi: 10.1016/j.tplants.2005.07.001
- Mehlmer, N., Wurzinger, B., Stael, S., Hofmann-Rodrigues, D., Csaszar, E., Pfister, B., et al. (2010). The Ca^{2+} -dependent protein kinase CPK3 is required for MAPK-independent salt-stress acclimation in *Arabidopsis*. *Plant J.* 63, 484–498. doi: 10.1111/j.1365-313X.2010.04257.x
- Miller, G., Schlauch, K., Tam, R., Cortes, D., Torres, M. A., Shulaev, V., et al. (2009). The plant NADPH oxidase RBOHD mediates rapid systemic signaling in response to diverse stimuli. *Sci. Signal.* 2, ra45. doi: 10.1126/scisignal.2000448
- Miwa, H., Sun, J., Oldroyd, G. E., and Downie, J. A. (2006). Analysis of calcium spiking using a cameleon calcium sensor reveals that nodulation gene expression is regulated by calcium spike number and the developmental status of the cell. *Plant J.* 48, 883–894. doi: 10.1111/j.1365-313X.2006.02926.x
- Mori, I. C., Murata, Y., Yang, Y., Munemasa, S., Wang, Y. F., Andreoli, S., et al. (2006). CDPKs CPK6 and CPK3 function in ABA regulation of guard cell S-type

- anion- and Ca(2+)-permeable channels and stomatal closure. *PLoS Biol.* 4:e327. doi: 10.1371/journal.pbio.0040327
- Mousavi, S. A., Chauvin, A., Pascaud, F., Kellenberger, S., and Farmer, E. E. (2013). GLUTAMATE RECEPTOR-LIKE genes mediate leaf-to-leaf wound signalling. *Nature* 500, 422–426. doi: 10.1038/nature12478
- Peer, M., Stegmann, M., Mueller, M. J., and Waller, F. (2010). *Pseudomonas syringae* infection triggers de novo synthesis of phytosphingosine from sphinganine in *Arabidopsis thaliana*. *FEBS Lett.* 584, 4053–4056. doi: 10.1016/j.febslet.2010.08.027
- Pei, Z. M., Ward, J. M., Harper, J. F., and Schroeder, J. I. (1996). A novel chloride channel in Vicia faba guard cell vacuoles activated by the serine/threonine kinase, CDPK. *EMBO J.* 15, 6564–6574.
- Perchon, A., Aldon, D., Galaud, J. P., and Ranty, B. (2011). Calmodulin and calmodulin-like proteins in plant calcium signaling. *Biochimie* 93, 2048–2053. doi: 10.1016/j.biochi.2011.07.012
- Perchon, A., Dieterle, S., Pouzet, C., Aldon, D., Galaud, J. P., and Ranty, B. (2010). Interaction of a plant pseudo-response regulator with a calmodulin-like protein. *Biochem. Biophys. Res. Commun.* 398, 747–751. doi: 10.1016/j.bbrc.2010.07.016
- Politis, A., and Borysik, A. J. (2015). Assembling the pieces of macromolecular complexes: hybrid structural biology approaches. *Proteomics* 15, 2792–2803. doi: 10.1002/pmic.201400507
- Popescu, S. C., Popescu, G. V., Bachan, S., Zhang, Z., Seay, M., Gerstein, M., et al. (2007). Differential binding of calmodulin-related proteins to their targets revealed through high-density *Arabidopsis* protein microarrays. *Proc. Natl. Acad. Sci. U.S.A.* 104, 4730–4735. doi: 10.1073/pnas.0611615104
- Rodriguez Milla, M. A., Uno, Y., Chang, I. F., Townsend, J., Maher, E. A., Quilici, D., et al. (2006). A novel yeast two-hybrid approach to identify CDPK substrates: characterization of the interaction between AtCPK11 and AtDi19, a nuclear zinc finger protein. *FEBS Lett.* 580, 904–911. doi: 10.1016/j.febslet.2006.01.013
- Romeis, T., and Herde, M. (2014). From local to global: CDPKs in systemic defense signaling upon microbial and herbivore attack. *Curr. Opin. Plant Biol.* 20, 1–10. doi: 10.1016/j.pbi.2014.03.002
- Sanders, D., Pelloux, J., Brownlee, C., and Harper, J. F. (2002). Calcium at the crossroads of signaling. *Plant Cell* 14, S401–S417. doi: 10.1105/tpc.002899
- Saucedo-Garcia, M., Guevara-Garcia, A., Gonzalez-Solis, A., Cruz-Garcia, F., Vazquez-Santana, S., Markham, J. E., et al. (2011). MPK6, sphinganine and the LCB2a gene from serine palmitoyltransferase are required in the signaling pathway that mediates cell death induced by long chain bases in *Arabidopsis*. *New Phytol.* 191, 943–957. doi: 10.1111/j.1469-8137.2011.03727.x
- Scherzer, S., Maierhofer, T., Al-Rasheid, K. A., Geiger, D., and Hedrich, R. (2012). Multiple calcium-dependent kinases modulate ABA-activated guard cell anion channels. *Mol. Plant* 5, 1409–1412. doi: 10.1093/mp/ssr084
- Scholz, S. S., Reichelt, M., Vadassery, J., and Mithofer, A. (2015). Calmodulin-like protein CML37 is a positive regulator of ABA during drought stress in *Arabidopsis*. *Plant Signal. Behav.* 10, e1011951. doi: 10.1080/15592324.2015.1011951
- Scholz, S. S., Vadassery, J., Heyer, M., Reichelt, M., Bender, K. W., Snedden, W. A., et al. (2014). Mutation of the *Arabidopsis* calmodulin-like protein CML37 deregulates the jasmonate pathway and enhances susceptibility to herbivory. *Mol. Plant* 7, 1712–1726. doi: 10.1093/mp/ssr102
- Schroeder, J. I., and Hagiwara, S. (1990). Repetitive increases in cytosolic Ca²⁺ of guard cells by abscisic acid activation of nonselective Ca²⁺ permeable channels. *Proc. Natl. Acad. Sci. U.S.A.* 87, 9305–9309. doi: 10.1073/pnas.87.23.9305
- Schulz, P., Herde, M., and Romeis, T. (2013). Calcium-dependent protein kinases: hubs in plant stress signaling and development. *Plant Physiol.* 163, 523–530. doi: 10.1104/pp.113.222539
- Uno, Y., Rodriguez Milla, M. A., Maher, E., and Cushman, J. C. (2009). Identification of proteins that interact with catalytically active calcium-dependent protein kinases from *Arabidopsis*. *Mol. Genet. Genomics* 281, 375–390. doi: 10.1007/s00438-008-0419-1
- Vadassery, J., Reichelt, M., Hause, B., Gershenson, J., Boland, W., and Mithofer, A. (2012). CML42-mediated calcium signaling coordinates responses to *Spodoptera* herbivory and abiotic stresses in *Arabidopsis*. *Plant Physiol.* 159, 1159–1175. doi: 10.1104/pp.112.198150
- Valmonte, G. R., Arthur, K., Higgins, C. M., and Macdiarmid, R. M. (2014). Calcium-dependent protein kinases in plants: evolution, expression and function. *Plant Cell Physiol.* 55, 551–569. doi: 10.1093/pcp/pct200
- Wang, J. P., Munyampundu, J. P., Xu, Y. P., and Cai, X. Z. (2015). Phylogeny of plant calcium and calmodulin-dependent protein kinases (CCaMKs) and functional analyses of tomato CCaMK in disease resistance. *Front. Plant Sci.* 6:1075. doi: 10.3389/fpls.2015.01075
- White, P. J., and Broadley, M. R. (2003). Calcium in plants. *Ann. Bot.* 92, 487–511. doi: 10.1093/aob/mcg164
- Yamaguchi, T., Aharon, G. S., Sottosanto, J. B., and Blumwald, E. (2005). Vacuolar Na⁺/H⁺ antiporter cation selectivity is regulated by calmodulin from within the vacuole in a Ca²⁺- and pH-dependent manner. *Proc. Natl. Acad. Sci. U.S.A.* 102, 16107–16112. doi: 10.1073/pnas.0504437102
- Yang, T., and Poovaiah, B. W. (2003). Calcium/calmodulin-mediated signal network in plants. *Trends Plant Sci.* 8, 505–512. doi: 10.1016/j.tplants.2003.09.004
- Zeng, H., Xu, L., Singh, A., Wang, H., Du, L., and Poovaiah, B. W. (2015). Involvement of calmodulin and calmodulin-like proteins in plant responses to abiotic stresses. *Front. Plant Sci.* 6:600. doi: 10.3389/fpls.2015.00600
- Zhang, T., Chen, S., and Harmon, A. C. (2014). Protein phosphorylation in stomatal movement. *Plant Signal. Behav.* 9, e972845. doi: 10.4161/15592316.2014.972845
- Zhu, X., Dunand, C., Snedden, W., and Galaud, J. P. (2015). CaM and CML emergence in the green lineage. *Trends Plant Sci.* 20, 483–489. doi: 10.1016/j.tplants.2015.05.010

Conflict of Interest Statement: The authors declare that the research was conducted in the absence of any commercial or financial relationships that could be construed as a potential conflict of interest.

Copyright © 2016 Ranty, Aldon, Cotelle, Galaud, Thuleau and Mazars. This is an open-access article distributed under the terms of the Creative Commons Attribution License (CC BY). The use, distribution or reproduction in other forums is permitted, provided the original author(s) or licensor are credited and that the original publication in this journal is cited, in accordance with accepted academic practice. No use, distribution or reproduction is permitted which does not comply with these terms.



Concurrent Drought Stress and Vascular Pathogen Infection Induce Common and Distinct Transcriptomic Responses in Chickpea

Ranjita Sinha, Aarti Gupta and Muthappa Senthil-Kumar*

National Institute of Plant Genome Research, New Delhi, India

OPEN ACCESS

Edited by:

Olivier Lamotte,
CNRS, UMR Agroécologie, France

Reviewed by:

Serge Delrot,
University of Bordeaux, France
Biswapiya Biswas Misra,
Texas Biomedical Research Institute,
USA

*Correspondence:

Muthappa Senthil-Kumar
skmuthappa@nipgr.ac.in

Specialty section:

This article was submitted to
Plant Physiology,
a section of the journal
Frontiers in Plant Science

Received: 21 November 2016

Accepted: 27 February 2017

Published: 14 March 2017

Citation:

Sinha R, Gupta A and Senthil-Kumar M (2017) Concurrent Drought Stress and Vascular Pathogen Infection Induce Common and Distinct Transcriptomic Responses in Chickpea. *Front. Plant Sci.* 8:333.
doi: 10.3389/fpls.2017.00333

Chickpea (*Cicer arietinum*); the second largest legume grown worldwide is prone to drought and various pathogen infections. These drought and pathogen stresses often occur concurrently in the field conditions. However, the molecular events in response to that are largely unknown. The present study examines the transcriptome dynamics in chickpea plants exposed to a combination of water-deficit stress and *Ralstonia solanacearum* infection. *R. solanacearum* is a potential wilt disease causing pathogen in chickpea. Drought stressed chickpea plants were infected with this pathogen and the plants were allowed to experience progressive drought with 2 and 4 days of *R. solanacearum* infection called short duration stress (SD stresses) and long duration stress (LD stresses), respectively. Our study showed that *R. solanacearum* multiplication decreased under SD-combined stress compared to SD-pathogen but there was no significant change in LD-combined stress compared to LD-pathogen. The microarray analysis during these conditions showed that 821 and 1039 differentially expressed genes (DEGs) were unique to SD- and LD-combined stresses, respectively, when compared with individual stress conditions. Three and fifteen genes were common among all the SD-stress treatments and LD-stress treatments, respectively. Genes involved in secondary cell wall biosynthesis, alkaloid biosynthesis, defense related proteins, and osmo-protectants were up-regulated during combined stress. The expression of genes involved in lignin and cellulose biosynthesis were specifically up-regulated in SD-combined, LD-combined, and LD-pathogen stress. A close transcriptomic association of LD-pathogen stress with SD-combined stress was observed in this study which indicates that *R. solanacearum* infection also exerts drought stress along with pathogen stress thus mimics combined stress effect. Furthermore the expression profiling of candidate genes using real-time quantitative PCR validated the microarray data. The study showed that down-regulation of defense-related genes during LD-combined stress resulted in an increased bacterial multiplication as compared to SD-combined stress. Overall, our study highlights a sub-set of DEGs uniquely expressed in response to combined stress, which serve as potential candidates for further functional characterization to delineate the molecular response of the plant to concurrent drought-pathogen stress.

Keywords: *Ralstonia solanacearum*, microarray, unique response, cellulose and lignin biosynthesis, combined stress, drought-pathogen stress, molecular response

INTRODUCTION

Chickpea (*Cicer arietinum*) is second largest cultivated legume crop in world. The crop is vulnerable to drought stress (Gaur et al., 2012) as well as to wilt diseases like Fusarium wilt caused by *Fusarium oxysporum* f. sp. *ciceris* (Nene et al., 2012). Under field conditions drought and pathogen stress often occurs simultaneously. Moreover, the combination of drought and pathogen stress has been noted to be devastating for growth and yield of crop plants (Olson et al., 1990; McElrone et al., 2001). These two stressors are noted for their influence on each other's interaction with plant, which might result in either negative or positive impact on the plants. Several studies in Arabidopsis, bean, grapevine have shown that drought stress makes the plant vulnerable to pathogen infection (McElrone et al., 2001; Mayek-Pérez et al., 2002; Mohr and Cahill, 2003; Prasch and Sonnewald, 2013). Conversely, reports also indicate that drought stress enhances the defense response of plants against pathogen (Achuo et al., 2006; Ramegowda et al., 2013; Hatmi et al., 2015). Pathogen infection has also been shown to alter the response of plants to water-deficit conditions. For example, wilt causing pathogens inhabit the xylem tissues, resulting in vascular dysfunction, and consequently causes a drought-like effect in plants (Douglas and MacHardy, 1981; Genin, 2010).

Overall, it is observed that the water deprivation induced during combined occurrence of drought and vascular pathogen infection increases the susceptibility of plants against pathogen as well as drought stress (McElrone et al., 2001; Kavak and Boydak, 2011; Choi et al., 2013; Ochola et al., 2015). Therefore it is important to understand the impact of combined stress and the cognate defense strategies adopted by plants to circumvent the concurrent onslaught of drought and vascular pathogen. However, the studies to understand the underlying molecular responses to combined drought and vascular pathogen are limited (Choi et al., 2013). At this juncture, in our present study we tried to dissect the molecular response of chickpea under combined drought and *Ralstonia solanacearum* infection. *R. solanacearum* is one of the most devastating wilt causing vascular pathogen having a broad host range and known to invade more than 200 different plants species (Genin, 2010). *R. solanacearum* colonizes xylem tissue and secretes massive amount of exopolysaccharides, which subsequently interrupts xylem function and leads to the wilting of the plant (Genin, 2010). *R. solanacearum* infection in chickpea was observed to result in a mild to severe disease symptoms which include yellowing, wilting and cell death; however, it was also observed that *R. solanacearum* does not provoke sudden plant death in leaf-inoculated plants (Sinha et al., 2016). The molecular responses of plants against *R. solanacearum* infection has been extensively studied (Hwang et al., 2011; Ishihara et al., 2012; Chen et al., 2014; Prasath et al., 2014; Zuluaga et al., 2015); however, so far no attempt has been made to understand the transcriptomic responses of plant to combined drought and *R. solanacearum* infection.

Recently, Sinha et al. (2016) showed that drought restricts the multiplication of *R. solanacearum* in chickpea which suggests that combined stress can induce robust defense responses in chickpea,

thus proposes the need to explore transcriptomic responses of chickpea under combined drought and *R. solanacearum* infection. Since *R. solanacearum* infection in chickpea causes disease symptoms after 6 days post infection (dpi) (Sinha et al., 2016), it has been hypothesized that *R. solanacearum* probably induces early and late defense responses at 2 and 4 dpi, respectively.

In the present study, transcriptomic responses of chickpea toward combined and individual *R. solanacearum* infection and drought stress was investigated using microarray at two time points namely short duration (SD) and long duration (LD). The transcriptomic changes induced during LD and SD combined stresses were categorized as unique (responses observed only during combined stress) and common (responses overlapping between individual and combined stresses) responses.

MATERIALS AND METHODS

Plant Material and Growth Conditions

Chickpea plants (variety ICC 4958) were grown in pots (5 inches diameter and 5 inches height) containing 500 gm of 3:1 mixture (vol/vol) of air dried peat (Prakruthi Agri Coco peat Industries, Karnataka, India) and vermiculite (Keltch Energies Pvt Ltd., Maharashtra, India) in an environmentally controlled growth chamber (PGR15, Conviron, Winnipeg, MB, Canada) with diurnal cycle of 12-h-light/12-h-dark, $200 \mu\text{Em}^{-2}\text{s}^{-1}$ photon flux intensity, 22°C temperature and 75% relative humidity. Pots were bottom irrigated every 2 days with half strength Hoagland's medium (TS1094, Hi-media Laboratories, Mumbai, India).

Inoculum Preparation for Pathogen Infection

Ralstonia solanacearum procured from Indian Type Culture Collection (ITCC# BI0001), IARI, New Delhi, India was grown in LB medium (without antibiotic) at 28°C to $\text{OD}_{600} = 0.6$ with a continuous shaking of 200 rpm for 2.5 h. Culture was pellet down by centrifuging at $3500 \times g$ for 10 min, washed thrice with sterile distilled water, and re-suspended in sterile distilled water to $\text{OD}_{600} = 0.005$ corresponding to 7×10^5 colony forming units (cfu)/ml.

Stress Treatments

Pathogen stresses namely SD-pathogen (2 days post *R. solanacearum* infection) and LD-pathogen (4 days post *R. solanacearum* infection) and drought stress namely SD-drought, SD or fast drought imposition and LD-drought, LD or slow drought imposition were used for this study. The two drought methods were included with incite that duration of drought imposition determines the plant's biochemical and molecular responses and therefore may affect the combined stress outcome. With SD- and LD-drought and SD- and LD-pathogen stresses, two combinations of combined stress treatments namely SD-combined (fast drought with 2 days of *R. solanacearum* infection) and LD-combined stress (slow drought with 4 days of *R. solanacearum* infection) were considered. Altogether, six

stress treatments were SD-combined (SD drought stress with 2 days of *R. solanacearum* infection), SD-pathogen (2 days of *R. solanacearum* infection), SD-drought [SD drought stress, 35% field capacity (FC)], LD-combined (LD drought with 4 days of *R. solanacearum* infection), LD-pathogen (4 days of *R. solanacearum* infection) and LD-drought (30% FC). Four plants were maintained for each stress treatment, along with absolute control and mock control and were placed in growth chamber using completely randomized design (CRD).

Drought stress was imposed by withholding the water, and stress level was assessed by measuring pot mix using gravimetric method following Sinha et al. (2016). For SD- and LD-drought stress treatments, water was withheld for 10 and 15 days for 29- and 24-day-old plants to attain 35% (SD-drought) and 30% FC (LD-drought), respectively, on 39th day of plant growth. *R. solanacearum* inoculation was done by vacuum infiltration, in which the plants were upturned in a beaker placed in vacuum chamber containing *R. solanacearum* culture (7×10^5 cfu/ml) with 0.02% Silwet L77 (Lehle seeds, Fisher Scientific, Waltham, MA, USA) and vacuum of 8.7 psi was applied for 10 min. Plants were briefly rinsed instantly after infiltration. To avoid the entry of bacterial suspension into the pot mix, the pot surface was covered with polythene wrap prior to infiltration. *R. solanacearum* was infiltrated into 35- and 37-day-old plants and samples were collected after 4 and 2 days of infiltration for LD- and SD-pathogen stress treatments, respectively. In case of LD- and SD-combined stress treatments, water was withheld for 8 and 11 days for 29- and 24-day-old plants to attain 40 and 35% FC, respectively. Following this, plants were vacuum infiltrated with 7×10^5 cfu/ml of *R. solanacearum* culture and were allowed for 2 and 4 days of progressive drought stress post *R. solanacearum* infection. After 2 and 4 days of progressive drought stress, FC of SD- and LD-combined stressed plants were 35 and 30%, respectively. Since plants at 60% FC showed better growth than 100% FC because of the high water holding capacity of pot mix, absolute and mock controls were maintained at 60% FC. For mock control, plants were infiltrated with water containing 0.02% Silwet L77. Leaf samples for all the treatment were collected from 39 days old plant for microarray analysis. The methodology of stress imposition is diagrammatically illustrated in Supplementary Figure S2.

Assessment of *In planta* Bacterial Numbers

Total *in planta* colony forming units (cfu) of *R. solanacearum* were counted at 0 and 2 days post treatment (dpt) for SD-pathogen and SD-combined stress, and at 0, 2, and 4 dpt for LD-pathogen and LD-combined stress experiments. The leaflets harvested from infiltrated plants were weighed and surface sterilized with 0.01% H₂O₂ for 5 s and subsequently homogenized in 100 µl of sterile water. After serial dilution in sterile water, leaflet homogenate was plated on LB medium without antibiotics. Since there was no significant difference in

dry weight (DW) as well as fresh weight (FW) ratio for individual pathogen and combined stressed plants, FW was accounted in calculating bacterial numbers. Bacterial count was expressed as log transformed values of cfu/mg FW of leaflet.

Cfu/mg was calculated using the following formula:

$$\text{CFU/mg} = \frac{\frac{\text{Number of colonies} \times \text{volume of homogenate (ml)} \times \text{dilution factor}}{\text{volume plated (ml)}}}{\text{weight of the leaflet (mg)}}$$

Relative Water Content

For all the six stress treatments and controls, relative water content (RWC) was measured at the end of the experiment (39-day-old plant). Moreover, RWC was also measured for SD- and LD-drought at 8 and 11 days after start of drought imposition, respectively. To measure the RWC, FW of leaflet samples was measured immediately after sample collection and samples were hydrated by floating on de-ionized water. Turgid weight (TW) was noted once leaflets attained full turgidity after 6 h at 22°C temperature. Samples were then oven dried at 60°C until they reach constant weight after 3 days, and DW was measured. RWC was calculated using the formula:

$$\text{RWC(}\%) = \frac{\text{FW} - \text{DW}}{\text{TW} - \text{DW}} * 100$$

Microarray Analysis

Microarray analysis for all treatments was performed in two biological replicates after taking clue from previous studies with two biological replicates (Yang et al., 2012; Liu et al., 2014; Chan et al., 2016). Leaf samples from two plants were pooled to make one biological replicate following recommendation by Kendzierski et al. (2005). The pooled leaves were mixed properly and a part of it was used for RNA isolation. Customized chickpea microarray chip with 60 mer oligonucleotide probe (Agilent_AMADID – 037094, Agilent technologies, Palo Alto, CA, USA) was used for the study. Entire experiment was performed once. The sampling method is thoroughly described in Supplementary Figure S3 and a flow chart describing the steps in the microarray analysis is shown in Supplementary Figure S4.

RNA Isolation

Total RNA from leaf tissue for all the treatments and controls was isolated using TRIzol reagent (Cat# 15596026, Invitrogen, Carlsbad, CA, USA) following manufacturers' protocol. Further, RNA was purified using RNeasy minikit (Cat# 74104, Qiagen, Hilden, Germany) and quantified using NanoDrop ND-1000 spectrophotometer (Thermo Scientific, Waltham, MA, USA). Quality of RNA was assessed on a Bioanalyzer (Agilent technologies, Palo Alto, CA, USA).

Labeling

Samples for transcriptome analysis were labeled using Agilent Quick-Amp labeling Kit (Cat# 5190-0442, Agilent Technologies, Palo Alto, CA, USA). Total RNA (RIN numbers 6–8, 500 ng) was reverse transcribed at 40°C using oligo(dT) primer tagged to a T7 polymerase promoter and converted to double stranded cDNA to be used as template for cRNA generation. cRNA was

generated by *in vitro* transcription and the dye Cy3 CTP was incorporated during this step. The cDNA synthesis and *in vitro* transcription procedures were carried out at 40°C. Labeled cRNA was purified using Qiagen RNeasy columns (Cat# 74106, Qiagen, Hilden, Germany) and quality was assessed for yields and quality using the Nanodrop ND-1000.

Hybridization and Scanning

Labeled cRNA (600 ng) was fragmented at 60°C and hybridized on to a Chickpea GXP_8X60K (AMADID: 037094) microarray chip. Fragmentation of labeled cRNA and hybridization were done using Gene Expression Hybridization Kit (Cat# 5190-0404, Agilent Technologies, California, USA). Hybridization was carried out in SureHyb Microarray Hybridization Chamber (Cat# G2534A, Agilent Technologies, Palo Alto, CA, USA) at 65°C for 16 h. The hybridized slides were washed with Agilent Gene Expression Wash Buffers (Cat# 5188-5327, Agilent technologies, Palo Alto, CA, USA) and scanned using the Agilent microarray scanner (Model# G2600D, Agilent Technologies, Palo Alto, CA, USA).

Data Analysis

Scanned images were quantified using Feature Extraction Software (Version-11.5 Agilent technologies, Palo Alto, CA, USA). Feature extracted raw data was analyzed using GeneSpring GX software (Version 12.1, Agilent technologies, Palo Alto, CA, USA). Normalization of the data was done in GeneSpring GX using the 50th percentile shift (where n has a range from 0 to 100 and $n = 50$ is the median) and differential expression patterns were identified for each sample. Fold expression values for combined stresses and pathogen stresses were obtained with respect to mock control and for drought stresses were obtained with respect to absolute control samples. Statistical unpaired student's *t*-test was applied among the replicates and *p*-value was calculated based on volcano plot algorithm (GeneSpring GX, Agilent technologies, Palo Alto, CA, USA). Microarray dataset was submitted to Gene Expression Omnibus (GSE89228). Differentially expressed genes (DEGs) with *p*-value < 0.05 were selected. Different fold change cut off values ranging from 0.5 to 1.5 were tried with intention of including genes with high fold change expression. Also we looked for the fold change value which did not eliminate genes related to hormone, biotic stress, abiotic stress and xylem modification. Consequently, up-regulated genes with fold > 1 (log base2) and down-regulated genes with fold > -1 (log base2) were selected for further studies.

Annotation of Transcripts and *In silico* Expression Profiling

Gene annotation data was retrieved from chickpea transcriptome database¹ (Verma et al., 2015). Further, annotation of some of the genes was updated by performing BLASTN search against chickpea database (taxid: 3827) available in NCBI. Differentially regulated genes were clustered using hierarchical clustering based on Pearson coefficient correlation algorithm².

¹<http://www.nipgr.res.in/ctdb.html>

²<https://software.broadinstitute.org/morpheus/>

Venn diagrams were generated to view the common and unique genes in various conditions (Venny 2.0³). Orthologous genes of *Arabidopsis thaliana* were obtained from chickpea transcriptome database⁴ (Verma et al., 2015) and their GO enrichment was performed using AgriGO singular enrichment analysis⁵ with default setting of Arabidopsis gene model (TAIR10) background and other parameters (statistical test method: Fisher; multi-test adjustment method: Yekutieli FDR under dependency; significance level: 0.05⁵). Finally, heat maps were generated using GENE-E software⁶.

Real-Time PCR Analysis

RNA from leaf tissue (100 mg FW) was isolated by TRIzol reagent (Cat# 15596018, Thermo Fisher Scientific, Waltham, MA, USA) following manufacturer's guidelines. Quality, quantity and integrity of RNA were verified by agarose gel electrophoresis and NanoDrop (Thermo Scientific, Waltham, MA, USA). The RNA samples with O.D. ratios at 260/280 nm in the range of 1.9–2.1, and at 260/230 nm in the range of 2.0–2.3 were used for RT-qPCR. First strand cDNA was synthesized from 5 µg of DNase treated total RNA in a reaction volume of 50 µl using Verso cDNA synthesis kit (Cat# K1621, Thermo Fisher Scientific, Waltham, MA, USA). Primers were obtained from Sigma-Aldrich, St. Louis, MO, USA. Details of gene-specific primers used for the RT-qPCR are provided in Supplementary Table S1. Reaction mix was prepared by adding 1 µl of two fold-diluted cDNA and 1 µl of each of the specific primers (10 µM/µl) to 5 µl of SYBR Green PCR master mix (Cat# 4309155, Thermo Fisher Scientific, Waltham, MA, USA) and final volume was made to 10 µl. The reaction was run in ABI Prism 7000 sequence detection system (Applied Biosystems, Foster City, CA, USA). Relative fold change in gene expression was quantified using $2^{-\Delta\Delta Ct}$ method (Livak and Schmittgen, 2001) using *CaActin1* (EU529707.1) as endogenous control to normalize the data. For all the RT-qPCR experiments, three independent biological replicates and two technical replicates were included. For statistical analysis, the relative quantification value (RQ) was transformed to log₂ value and test of significance was performed by one sample *t*-test.

RESULTS

Differential Transcriptomic Response of Chickpea under Combined and Individual Drought and *Ralstonia solanacearum* Stresses

To understand the transcriptomic responses of chickpea to combined drought and vascular pathogen *Ralstonia solanacearum*, combined stress experiments were conducted by imposing two levels of drought and pathogen stress. The study was conducted with two types of drought stress namely

³<http://bioinfogp.cnb.csic.es/tools/venny/>

⁴<http://www.nipgr.res.in/ctdb.html>

⁵<http://bioinfo.cau.edu.cn/agriGO/analysis.php>

⁶<http://www.broadinstitute.org/cancer/software/GENE-E/>

SD drought or fast drought (SD-drought) and LD drought or slow drought (LD-drought) with the premise that duration and severity of drought stress determines the plants biochemical and molecular responses and therefore may differentially influence the combined stress response in chickpea. Two time points in *R. solanacearum* growth, i.e., 2 days post infiltration (dpi) (SD-pathogen stress) and 4 dpi (LD-pathogen stress) were selected for the evaluation of transcriptomic response of chickpea against *R. solanacearum*. With the two types of drought stress and two time points of *R. solanacearum* multiplication, we imposed two types of combined stress namely SD (SD-combined stress, fast drought with 2 days post combined stress treatment, dpt) and LD (LD-combined stress, slow drought with 4 dpt) (Supplementary Figure S2A). Before initiating the combined stress study, *R. solanacearum* was first assessed for its pathogenicity in chickpea. It was found that at an infiltrated concentration of 7×10^5 cfu/ml, *R. solanacearum* was multiplying *in planta* and caused disease symptoms varying from mild water soaked lesions and yellowing to severe cell death and wilting. Also, bacterial ooze was noticed from base of the leaflet (Supplementary Figure S1). In the present study, drought stress was observed to induce reduction in leaf RWC. LD-drought stress showed more reduction in leaf water, i.e., 64% RWC after 11 days of water-withholding compared to SD-drought stress after 8 days of water withholding, i.e., 75% RWC (Supplementary Figure S2D) indicating an increased severity of drought stress with increased drought duration. Plants exposed to SD drought (FC-35%) and LD drought (FC-30%) showed 73 and 52% RWC, respectively, compared to 86% RWC in control plants after 10 and 15 days of drought treatment, respectively. *R. solanacearum* infiltration resulted in water soaking leading to 86% RWC in SD-combined stressed and 87% RWC in LD-combined stressed plants which were close to those of SD-pathogen (86%) and LD-pathogen (83%) stressed plants after 2 and 4 days post combined stress treatment (Supplementary Figure S2E). Notable reduction *in planta* multiplication of *R. solanacearum* was observed under SD-combined stress compared to SD-pathogen stress (Supplementary Figure S2B). However, *in planta* bacterial count was unchanged under LD-combined stress compared to LD-pathogen stress treatments (Supplementary Figure S2C).

Transcriptomic alterations in chickpea plants challenged with combined drought and *R. solanacearum* stress (SD- and LD-combined) and individual drought (SD- and LD-drought) and *R. solanacearum* stress (SD- and LD-pathogen) were studied by microarray analysis. Microarray data was submitted to Gene Expression Omnibus (GEO# GSE89228). The DEGs ($\log_2 FC \geq \pm 1$) under drought stress compared to absolute control, and under combined and pathogen stresses compared to mock control were screened using unpaired *t*-test ($p \leq 0.05$). Putative annotation of DEGs were obtained from chickpea transcriptome database⁷ (Verma et al., 2015) and also by homolog search using nucleotide BLAST⁸ against chickpea (NCBI taxid: 3827) database. The DEGs for which putative annotation could not be obtained by BLASTN or BLASTX were termed as unannotated

DEGs (Supplementary Table S2). Under both SD-pathogen and LD-pathogen stress treatments, many genes involved in defense response (WRKY33, MAP KINASE 11, and DEFENSIN) were up-regulated. Similarly, under SD-drought and LD-drought stress treatments, genes involved in signaling, biosynthesis of abscisic acid (ABA) and osmo-protectants namely the genes encoding for LATE EMBRYOGENESIS ABUNDANT 5 (LEA5), LOW-TEMPERATURE-INDUCED 65 KDA PROTEIN were up-regulated. Concordant with these observations, genes involved in both defense responses and abiotic stress tolerance (genes encoding for LEA and RESPIRATORY BURST OXIDASE HOMOLOG B) were differentially expressed in SD-combined and LD-combined stresses, which conforms to the nature of the stressors (Supplementary Figure S5 and File S1). The majority of top most up-regulated genes were belonging to stress responsive and cell wall modification categories under combined stress (Supplementary Figure S5 and File S1).

The number of up- and down-regulated genes under each stress condition is shown in **Figure 1**. The maximum numbers of DEGs were found in LD drought stress (1426 genes). Comparison of DEGs among SD stress treatments showed 821 genes (31.8%) out of 1011 genes to be uniquely up-regulated in response to SD-combined stress whereas, SD-combined stress treatment had 129 and 58 DEGs in common with the SD-pathogen and SD-drought stress, respectively (**Figure 1B**). Similarly, 1039 genes (31.5%) out of 1287 total DEGs were uniquely expressed under LD combined stress (**Figure 1C**). LD-combined stress and LD-drought stress had 102 DEGs in common, and both LD-combined and LD-pathogen had 131 genes in common (**Figure 1C**). The overlapping (common) and unique genes were also examined between SD-combined and LD-combined; SD-drought and LD-drought; SD-combined and LD-combined stress transcripts (**Figures 1D–F**). As a result a substantial variation in stress responsive transcriptome under SD- and LD-stresses was observed. The number of DEGs was more in LD stresses over SD stresses. For instance, number of DEGs under LD-pathogen was 841 compared to 594 under SD-pathogen stress treatment. Similarly, LD-drought stress treatment exhibited 1333 DEGs against 1111 DEGs under SD-drought stress. The LD-combined stress resulted in differential expression of 1196 genes over 959 DEGs under SD-combined stress. Each stress transcriptome had more number of unique DEGs and less number of common DEGs. LD-pathogen, LD-drought and LD-combined stress had 707, 1000, and 946 unique DEGs, respectively, as compared to 460, 778, and 709 unique DEGs in response to SD-pathogen, SD-drought and SD-combined stress, respectively. Moreover, very small percentages (10–15%) of genes were common between the respective SD and LD treatments (**Figures 1D–F**).

The overlapping genes showed differential expression under different stresses. A few common genes between LD combined and LD drought stress (genes encoding for LEA5, E3 UBIQUI TIN-PROTEIN LIGASE, PP2C37, INOSITOL 3 PHOSPHATASE SYNTHASE LIKE, and MATE EFFULUX FAMILY PROTEIN 5) had higher expression in LD-combined stress as compared to LD-drought stress. On the other hand, genes encoding for PATHOGENESIS RELATED (PR), DEFENSIN, PROTEIN TRRXL LIKE, and UDP-GLYCOSYLTRANSFERASE 73C2

⁷<http://www.nipgr.res.in/ctdb.html>

⁸<https://blast.ncbi.nlm.nih.gov/Blast.cgi>

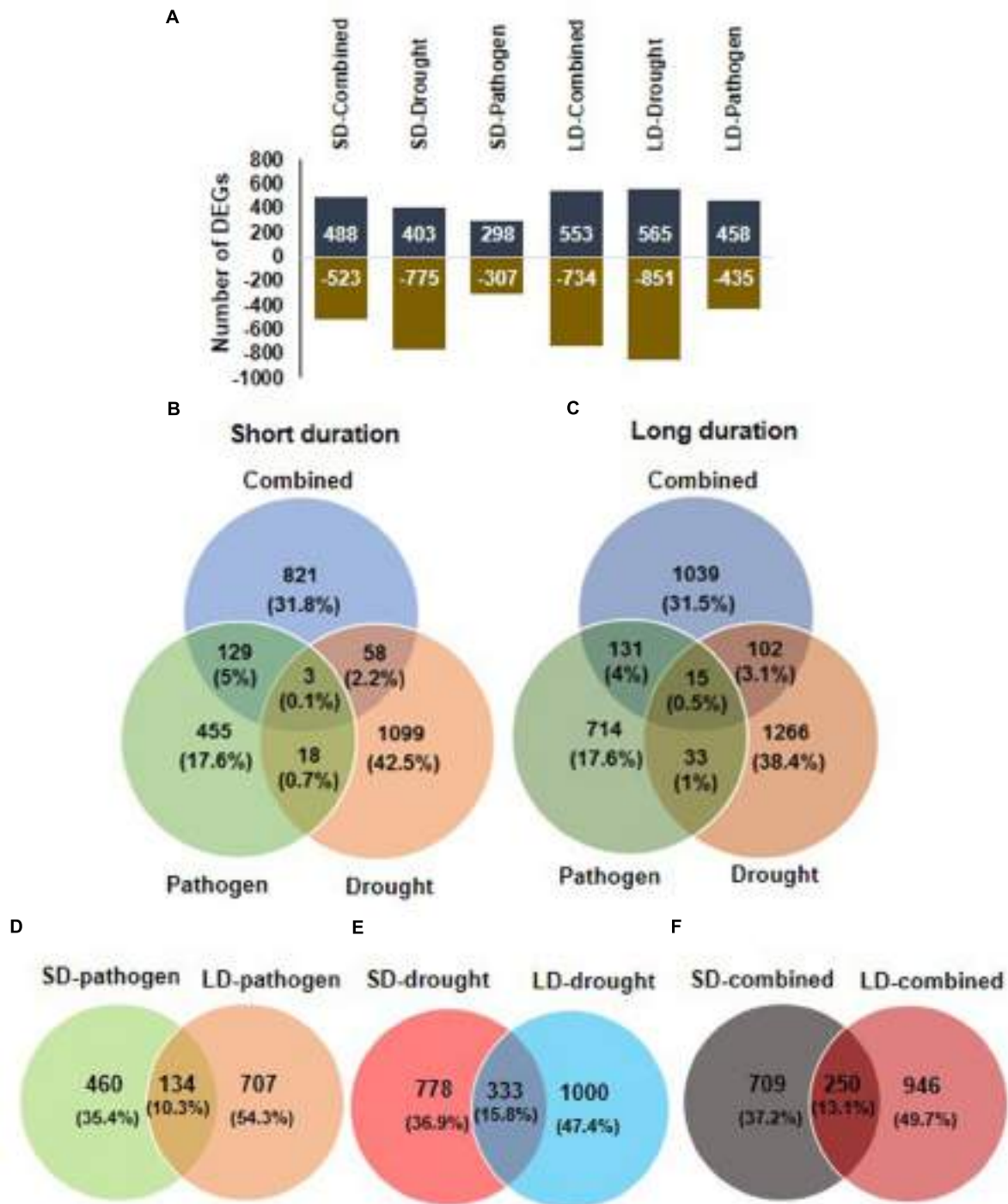


FIGURE 1 | Overview of differentially expressed genes (DEGs) in chickpea transcriptome in response to combined and individual stresses. To study the transcriptomic changes in chickpea ICC4958 in response to pathogen (*Ralstonia solanacearum*), drought and combination of *R. solanacearum* and drought stress, chickpea plants were imposed with drought alone, pathogen alone and combined stress for short duration (SD; 2 days) and long duration (LD; 4 days) and named as SD-stresses and LD-stresses, respectively. DEGs over control in drought only treated plant and over mock in pathogen treated and combined stresses plants were obtained by microarray analysis. Total number of DEGs having a minimum fold change of 1 (Log_2 transformed) and $p < 0.05$ under all six stress treatments, SD stresses (SD-pathogen, SD-drought, SD-combined) and LD stresses (LD-pathogen, LD-drought, LD-combined) are represented in graph (A). Positive values in chart shows number of up-regulated and negative values represents number of down-regulated DEGs. The number of common and unique genes among different SD stresses and LD stresses are shown in Venn diagram (B,C), respectively. Number of DEGs unique and common in SD- and LD-pathogen (D), SD- and LD-drought (E) and SD- and LD-combined stress (F) are shown.

(UGT73C2) proteins showed down-regulation in LD-combined stress as compared to their up-regulation in LD-pathogen stress. However, some of the down-regulated genes encoding for proteins in SD-pathogen stress like CYTOCHROME P450 73A1 (CYP73A1) and GTP BINDING PROTEIN 1 were induced in SD-combined stress (**Figure 2**). All the LD stress treatments (combined and individual) had 15 genes in common where four genes exhibited similar expression and 11 others exhibited tailored expression (**Figures 1B, 2** and Supplementary File S5).

The results obtained from microarray were verified by real time qPCR analysis of 14 genes, which were up-regulated in SD-combined stress. The differential expression of genes noted from qPCR and microarray are represented in **Figure 3** for the comparison. We also checked the expression of these 14 genes in other stress treatments to determine their relevance under other combined or individual stress treatments. We observed up-regulation of genes encoding CYTOCHROME C OXIDASE and RETICULIN OXIDASE LIKE under SD-combined, LD-combined and LD-pathogen stresses. Similarly, genes encoding CARVEOL DEHYDROGENASE and VICILLIN LIKE had a very high up-regulation under SD-combined, LD-combined and LD-pathogen stresses when compared to SD and LD drought treatments. BETA-GLUCOSIDASE 12 LIKE, ACETYLTRANSFERASE, PROLINE DEHYDROGENASE 2, and ASPARTYL PROTEASE 1 encoding genes exhibited high up-regulation in both SD and LD combined stresses. DIRIGENT PROTEIN 22 and LACCASE 7 LIKE encoding genes had high expression under SD-combined, SD-pathogen and LD-pathogen stresses. Gene for VEIN PATTERNING 1 (VEP1) was equally up-regulated in all treatments (Supplementary Figure S6). With the qPCR results we show that except VEP1, all other genes selected from SD-combined dataset were either specifically expressed or had higher expression under SD-combined stress, LD-combined stress and LD-pathogen stress treatments as compared to rest of the treatments.

We further categorized the DEGs under each stress treatments based on gene ontology (GO) using Arabidopsis orthologs of chickpea genes (Supplementary Table S3). Overall, we found enrichment of up-regulated DEGs (from all stress treatments) in GO biological processes like response to stimulus, biological regulation, metabolic process, developmental process, transport, signaling, reproduction, cell death, cell division, negative regulation of biological process. Up-regulated DEGs were enriched in GO molecular functions like catalytic activity, protein, ion and nucleic acid binding, and cellular components like membrane, cell wall and symplast (**Figure 4**). Furthermore, SD- and LD-pathogen stressed transcriptomes exhibited up-regulated DEGs belonging to specific categories like ‘response to wounding/chitin/salt stress’ and ‘response to jasmonic acid (JA) and ABA’, while up-regulated DEGs under LD-pathogen stress were also enriched under ‘respiratory burst during defense response’ and ‘response to water deprivation’ category (Supplementary Figure S7). These results indicate that *R. solanacearum* infected plants manifest pathogen mediated drought stress like symptoms and oxidative burst to combat the pathogen at high titer. The down-regulated DEGs under SD- and LD- pathogen stress showed enrichment in categories

like carbohydrate transmembrane transporter activity, fatty acid biosynthetic process, coumarin biosynthetic process, SA mediated signaling, negative regulation of defense response, systemic acquired resistance (SAR) and regulation of meristem growth (Supplementary Figure S7). Up-regulated DEGs under SD- and LD-drought stress were enriched in categories like response to water deprivation, ABA stimulus, negative regulation of biological process, cellular polysaccharide biosynthetic process whereas LD-drought treatment also showed enrichment in plasma membrane part, sugar and secondary active transporter activity and response to other organism categories. The down-regulated genes under SD- and LD-drought were enriched with GO processes: such as plant hypersensitive response, response to biotic stimulus, SA biosynthetic process, negative regulation of PCD, negative regulation of defense response, SAR, ligand gated ion channel activity and positive regulation of flavonoid biosynthetic process (Supplementary Figure S7).

The up-regulated DEGs under SD-combined stress genes were enriched under GO categories: mitochondrial membrane part, phosphorylation, response to temperature stimulus and oxidative stress, oxidation of organic compound and glutamine family amino acid metabolic process, while up-regulated DEGs under LD-combined stress, were enriched in secondary cell wall (SCW) biogenesis, response to water deprivation, ABA stimulus, lipid metabolic process regulation, hyperosmotic salinity response, hormone mediated signaling, glucosinolate biosynthesis and defense response GO categories. Down-regulated genes under SD- and LD-combined stress were majorly enriched in inorganic anion transmembrane transporter activity, protein serine/threonine kinase activity, negative regulation of cell death, MAPKK cascade, regulation of hypersensitive response, defense response to fungus, salicylic acid (SA) biosynthetic process, SAR and positive regulator of flavonoid biosynthetic process (Supplementary Figure S7).

Combined Stress and *R. solanacearum* Induces Transcriptome Changes Involved in Osmo-Protectant Accumulation

The genes involved in osmo-protectant biosynthesis, like those genes encoding for LEA, RAFFINOSE SYNTHASE, STACHYOSE SYNTHASE, VERBASCOSE SYNTHASE, DELTA 1-PYRROLINE-5-CARBOXYLATE SYNTHASE (P5CS), and PROLINE OXIDASE (involved in proline catabolism) were up-regulated in SD and LD-drought and SD and LD combined stress treatments. Moreover, the genes encoding RAFFINOSE BIOSYNTHESIS and LEA were also up-regulated in LD-pathogen stress indicating *R. solanacearum* mediated drought stress in the chickpea plants. Therefore, *R. solanacearum* infection itself mimics a dual abiotic and biotic stress in chickpea (Supplementary Figure S8). Results on hierachal clustering among different treatments (based on differential gene expression) revealed closeness of LD-pathogen with SD-combined stress (Supplementary Figure S9) substantiating that *R. solanacearum* infection exerts both drought and pathogen stress in chickpea.

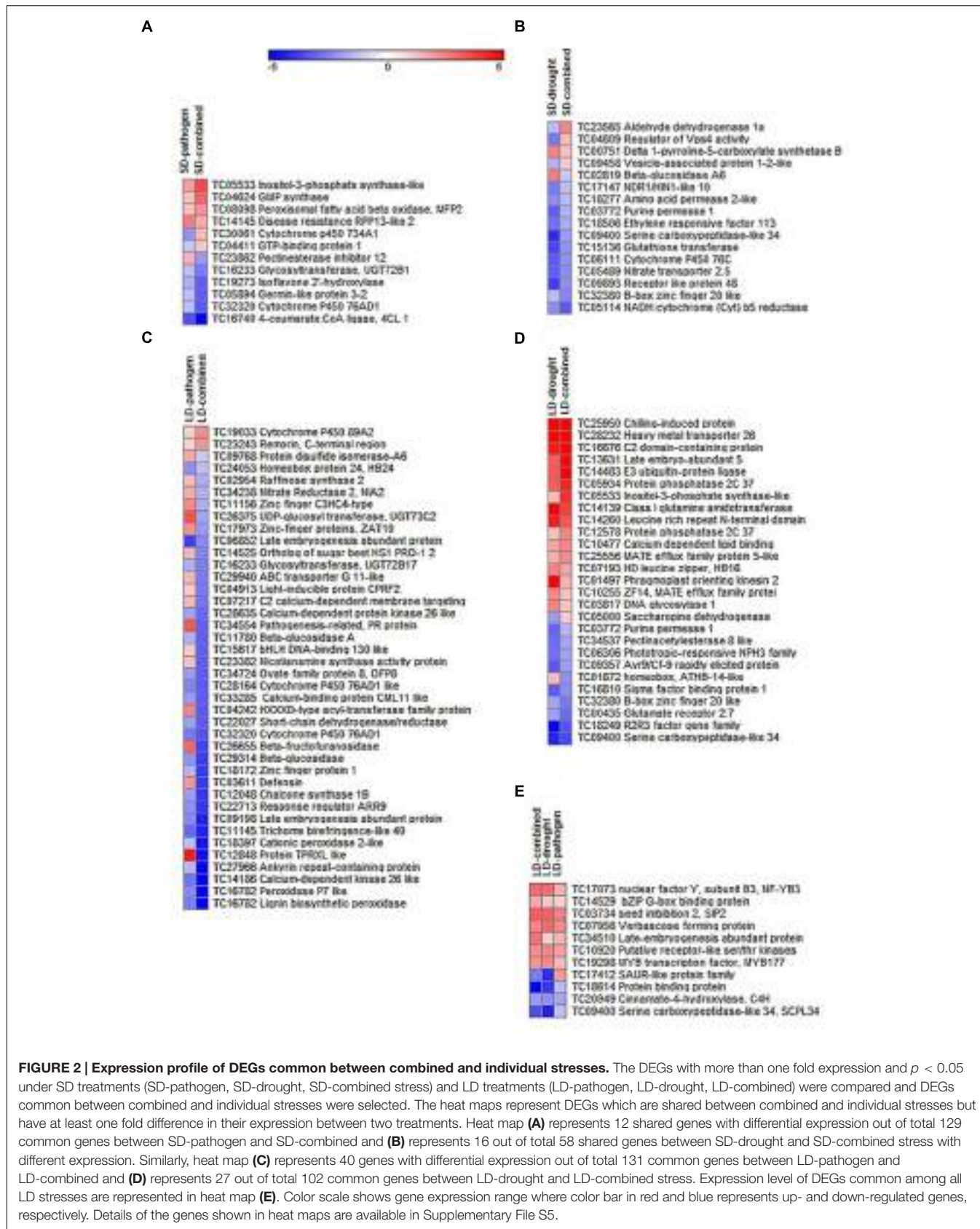


FIGURE 2 | Expression profile of DEGs common between combined and individual stresses. The DEGs with more than one fold expression and $p < 0.05$ under SD treatments (SD-pathogen, SD-drought, SD-combined stress) and LD treatments (LD-pathogen, LD-drought, LD-combined) were compared and DEGs common between combined and individual stresses were selected. The heat maps represent DEGs which are shared between combined and individual stresses but have at least one fold difference in their expression between two treatments. Heat map **(A)** represents 12 shared genes with differential expression out of total 129 common genes between SD-pathogen and SD-combined and **(B)** represents 16 out of total 58 shared genes between SD-drought and SD-combined stress with different expression. Similarly, heat map **(C)** represents 40 genes with differential expression out of total 131 common genes between LD-pathogen and LD-combined and **(D)** represents 27 out of total 102 common genes between LD-drought and LD-combined stress. Expression level of DEGs common among all LD stresses are represented in heat map **(E)**. Color scale shows gene expression range where color bar in red and blue represents up- and down-regulated genes, respectively. Details of the genes shown in heat maps are available in Supplementary File S5.

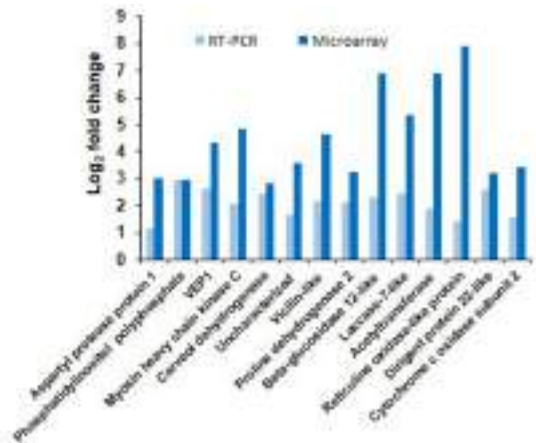


FIGURE 3 | Validation of microarray results by RT-qPCR. Transcript expression pattern of selected genes from microarray data was validated by RT-qPCR. Bar chart represents fold change expression (\log_2 FC) of the genes by RT-qPCR (light blue) and microarray (dark blue) under SD-combined stress. CaActin was used as reference gene for the qPCR normalization. Fold change was calculated over mock control. Each bar represents average of two biological and two technical replicates. Results presented are from one experiment.

Combined Stress Differentially Induces Genes Involved in Xylem Differentiation and Cellulose and Lignin Deposition

Differentially expressed genes in each stress category were mapped onto pathways involved in xylem differentiation based on available literature information (Růžička et al., 2015; Rybel et al., 2016). During SD-combined stress, we observed down-regulation of the gene *KANADI* (one clade of the GARP family of transcription factors) that act as negative regulator of procambium/cambium and vascular tissue formation (Růžička et al., 2015; Rybel et al., 2016). *KANADI* also indirectly suppresses expression of HD-ZIPIII transcription factor which promotes meristem function and xylem tissue formation (Růžička et al., 2015; Rybel et al., 2016). Down-regulation of *KANADI* thus enhances the possibility of either cambial proliferation or xylem trans-differentiation in SD-combined stressed plants. Another gene encoding PHLOEM INTERCALATED WITH XYLEM (PXY) receptor which is responsible for the BRASSINAZOLE-RESISTANT 1 (BES) mediated signaling (Růžička et al., 2015; Rybel et al., 2016) was up-regulated in SD-combined stressed plants (Figure 5, Supplementary Figure S10 and File S2). This may result either in increased cambial proliferation or xylem differentiation. Moreover, the mapping of DEGs onto pathway for SCW synthesis during xylem formation revealed high and unique up-regulation of gene encoding for SECONDARY WALL-ASSOCIATED NAC DOMAIN 2 (SND2), a tier 3 gene regulator in cellulose synthesis (Růžička et al., 2015; Taylor-Teeple et al., 2015) under SD-combined stress. However, genes encoding CELLULOSE SYNTHASE 8 (CESA 8), COBRA LIKE 2, and COBRA LIKE 4 which are directly involved in cellulose biosynthesis (McFarlane et al., 2014)

were not differentially expressed in SD-combined stress but were highly and uniquely up-regulated in LD-combined stress (Figure 5, Supplementary Figure S10). Among genes involved in lignin biosynthesis, the gene encoding for CINNAMYL-ALCOHOL DEHYDROGENASE 9 (CAD9) which catalyzes the terminal step of monolignol biosynthesis (Bonawitz and Chapple, 2010) showed high up-regulation under SD-combined and LD-pathogen stresses. Also, very high up-regulation of *LACCASE7* which is involved in polymerization of monolignol to lignin (Bonawitz and Chapple, 2010) was observed in SD-combined and LD-pathogen stress. Similarly, *LACCASE17* showed up-regulation in SD-combined, LD-combined and LD-pathogen stresses. However, the genes involved in earlier steps of phenylpropanoid pathway for monolignol biosynthesis were down-regulated in both SD-combined and LD-combined stress (Figure 5, Supplementary Figures S10, S11, and File S3). The genes acting at later stage or regulating lignin polymerization were up-regulated under SD-combined, LD-combined, and LD-pathogen stress. Therefore, we assume that genes involved in initial step of lignin synthesis (phenylpropanoid pathway) is up-regulated at early time point during combined stress for initiating lignin synthesis pathway and later may be down-regulated to maintain the metabolic load. This could possibly be because of feedback regulation mediated by high monolignol titer in the cell at 2 and 4 dpi. PAL which catalyzes first step in phenylpropanoid pathway for lignin biosynthesis has been reported to work under sophisticated regulatory control. Both PAL activity and *PAL* gene transcription are negatively regulated by *trans*-cinnamic acid (t-CA) (Zhang and Liu, 2015). A transient induction in *PAL* gene expression has been observed in many studies. In *A. thaliana*, the expression of *PAL1* and *CAD* genes upon *Pseudomonas syringae* pv. tomato DC3000 (Psd) infection had highest expression at 2 h post infection (hpi). However, *PAL* expression declined at 4 hpi and later time points, i.e., 8, 12, 24 hpi (Arabidopsis eFP Browser⁹). Schmelzer et al. (1989) reported a rapid and transient increase in *PAL* and *4CL* mRNA level from 4 to 8 hpi followed by rapid decline in Parsley leaves upon *Phytophthora megasperma* f. sp. *glycinnea* (Pmg) infection. The transient increase followed by decline in *PAL* activity at 12 h post *R. solanacearum* infection in resistant and 18–30 h post *R. solanacearum* infection in susceptible tomato variety was also reported by (Vanitha and Umesha, 2009). Kubasek et al. (1992) suggested that flavonoid genes are sequentially induced in the order of the biosynthetic steps in the flavonoid pathway and this level of regulation may be achieved by feed-forward or feedback mechanisms utilizing phenylpropanoid intermediates themselves. These evidences indirectly support our argument of sequential and transient expression of genes involved in lignin biosynthesis.

Hemi-cellulose deposition in cell wall is another important step in xylem biosynthesis. We observed up-regulation of gene *GLYCOGENIN-LIKE STARCH INITIATION 3* (*PGSIP3*) also called GUX2 regulating hemi-cellulose biosynthesis (Mortimer et al., 2010) in only LD-pathogen stress. Whereas, the hemi-cellulose biosynthesis gene; *IRREGULAR XYLEM 15*

⁹<http://bbc.botany.utoronto.ca/efp/cgi-bin/efpWeb.cgi>

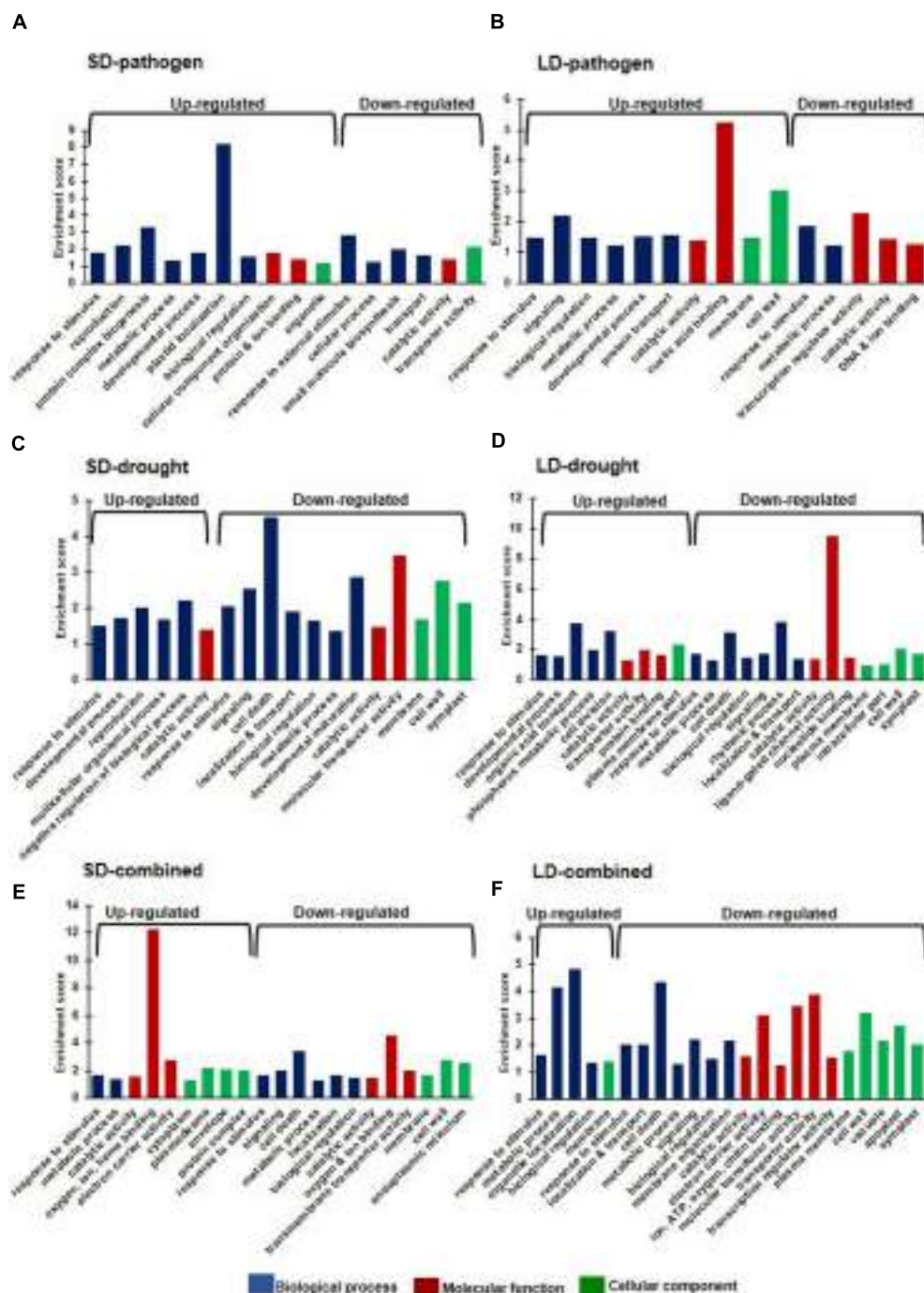


FIGURE 4 | Gene ontology (GO) enrichment analysis of individual and combined stress transcriptomes. The *Arabidopsis thaliana* orthologs of chickpea genes were used for GO enrichment. *A. thaliana* orthologs were obtained for chickpea DEGs with more than one fold (\log_2 converted) and $p < 0.05$ under six stress treatments (Supplementary Figure S2) from Chickpea Transcriptome Database (<http://www.nipgr.res.in/ctdb.html>). GO enrichment was done using AgriGO singular enrichment analysis with default settings (<http://bioinfo.cau.edu.cn/agriGO/analysis.php>). The enriched broad GO terms under each stress category are represented as bar diagram. Enrichment score of the GO terms are based on ratio of sample frequency and background frequency. Blue, red, and green color represents GO under biological process, molecular function and cellular component, respectively. Graphs show GO enrichment of DEGs under SD-pathogen (A), SD-drought (B) SD-combined stress (C), LD-pathogen (D), LD-drought (E), and LD-combined (F) stress categories. Number of *A. thaliana* orthologs obtained against total DEGs in each treatment is mentioned in Supplementary Table S2.

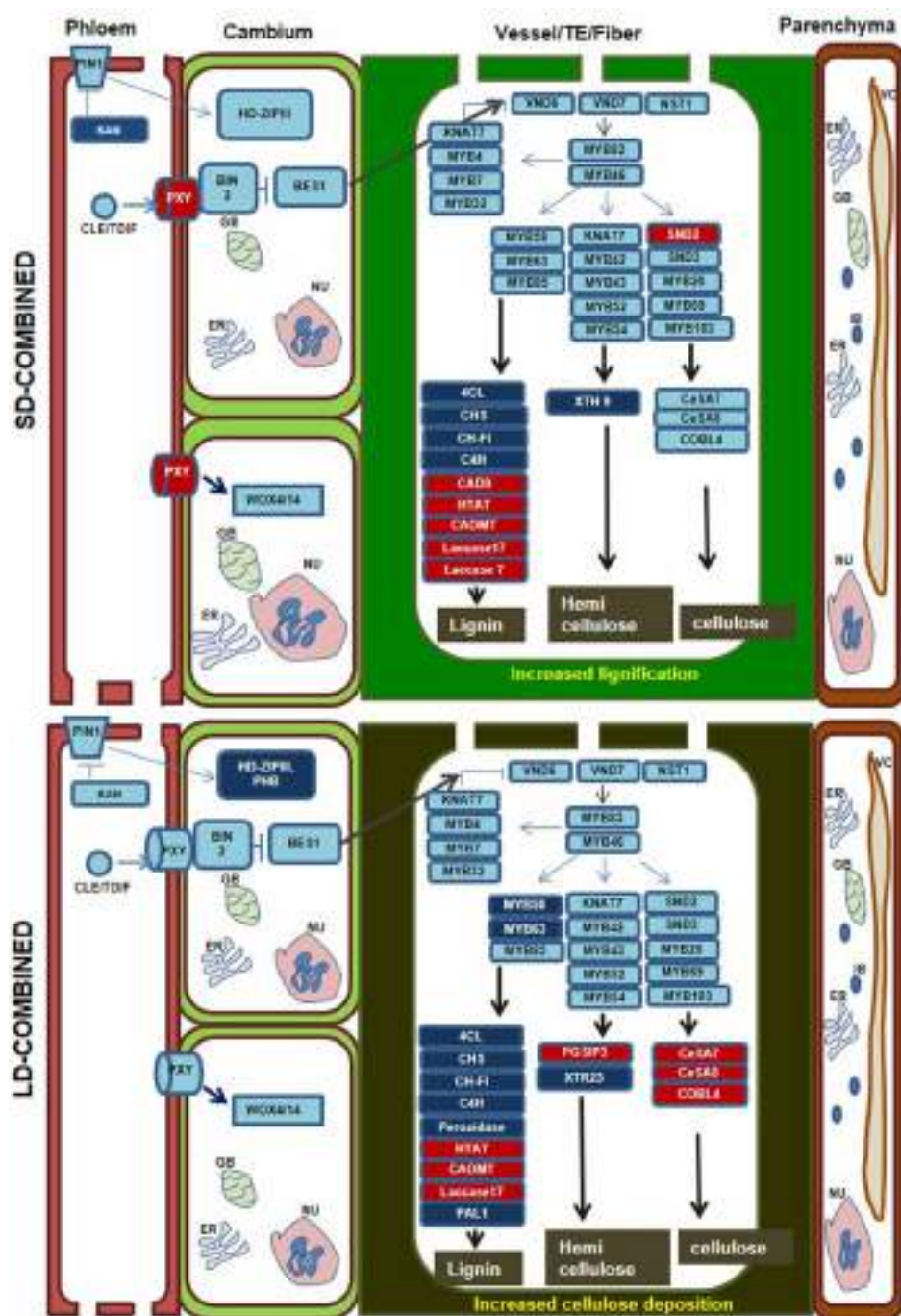


FIGURE 5 | Overview of differential expression of xylem differentiation and secondary cell wall (SCW) related genes in SD- and LD-combined stress treatments. Diagrams represent vascular bundle structure with phloem, cambium and xylem vessel/fiber and xylem parenchyma. The order of the cell in the diagram is likely following the order present in dicot leaf where phloem is placed on abaxial followed by cambium and xylem on adaxial surface. DEGs with minimum fold change 1 (Log_2 converted) were identified in each individual and combined stressed transcriptome over their respective controls. DEGs were mapped onto 'xylem development and SCW deposition' pathways based on literature information. Major molecular events related to xylem differentiation and SCW synthesis in xylem vessel, tracheary element and fiber are represented once in the same box. The SCW synthesis pathway is representing only those genes which are differentially expressed in the SD-combined and LD-combined stress transcriptome. Thickening of SCW in xylem vessel and TE are represented as thick green wall. Genes in red boxes represents up-regulated expression and in dark blue boxes represents down-regulated expression. Genes in the boxes with the light blue color has no differential expression. Details of the genes in the boxes are mentioned in the Supplementary File S2.

(*IRX15*-like) (Brown et al., 2011) showed unique and high up-regulation in SD-combined stress only. Two hemicellulose biosynthetic genes encoding for PURVUS/GLZ1 and PECTIN METHYLESTERASE (PME) (Scheller and Ulvskov, 2010) were up-regulated during SD- and LD-drought stress, respectively (**Figure 5**, Supplementary Figures S10, S11 and Files S2, S3). This strongly suggests that combined stress results in induction of lignin biosynthesis and modification in xylem SCW.

Furthermore, we wanted to explore if up-regulation of genes involved in SCW formation is a general consensus under combined stress. Therefore we looked for the expression of genes encoding for CAFFEIC ACID O-METHYLTRANSFERASE (COAMT), LACCASE 7 and 17 and CESA7 and 8 genes in combined drought and Psd transcriptomic data from Gupta et al. (2016). We found absence of those genes in differentially expressed transcriptome of both drought first Psd later (DP) and Psd first and drought later (PD) treatments (Gupta et al., 2016) (Supplementary Figure S12). This indicates that combined drought and foliar pathogen stress may not employ SCW modification for combined stress tolerance.

Combined Drought and *R. solanacearum* Stress Differentially Induces Phytohormone Biosynthesis and Signaling Genes

The combined stress mediated alteration in hormone biosynthesis, catabolism, transport, and signaling were studied by mapping the DEGs onto hormone pathways based on available literature information. We found up-regulation of ABA biosynthesis genes in all stress treatments. We observed the stress treatment specific differential expression of ABA biosynthetic genes. ABA biosynthesis gene encoding 9-CIS-EPOXYCAROTENOID DIOXYGENASE 3 (NCED3) was specifically induced during SD- and LD-pathogen stress whereas during SD- and LD-drought stress, ABA biosynthetic genes encoding ZEAXANTHIN EPOXIDASE (ZEP) and NCED1 were induced. During SD-combined stress, ALDEHYDE OXIDASE (AAO) was specifically up-regulated, similarly in LD-combined stress only ZEP is found to be up-regulated. Down-regulation of gene encoding for ABA transporter ATP-BINDING CASSETTE G40 (ABCG40) was observed only during SD- and LD-drought. ABA receptor encoding genes were up-regulated in SD- and LD-pathogen stress and signaling genes *PP2C6* and *PP2C37* were up-regulated in SD-pathogen, SD-drought, LD-drought, and LD-combined stressed plants (**Figure 6A** and Supplementary File S4). PP2C is negative regulator of ABA signaling, however, has been shown to confer abiotic stress tolerance in many plants in ABA insensitive manner (Bhaskara et al., 2012; Zhang et al., 2013; Singh et al., 2015). Another negative regulator of ABA signaling gene *ABI5*-interacting protein (*AFP3*) was also specifically up-regulated in LD-combined stress. The up-regulation of *PP2C* and *AFP3* under drought stress has been previously reported (Garcia et al., 2008) but its role under combined stress has not been seen yet. These results indicate that ABA signaling plays a major part in plant response under drought, *R. solanacearum* and combined stress.

Short duration- and long duration-pathogen stresses in chickpea induced up-regulation of SA and ethylene (ET) signaling genes encoding for TGACG (TGA) MOTIF-BINDING PROTEIN 10 (TGA10), PATHOGENESIS-RELATED GENE, WRKY54, ETHYLENE RESPONSE FACTOR104 LIKE (ERF104), and ERF1B (**Figures 6B,D** and Supplementary File S4). Contrastingly, we also encountered up-regulation of SA catabolism gene encoding for UDP-GLYCOSYLTRANSFERASE 74 F1 (UGT74F1) in LD-pathogen stress. SD- and LD-pathogen stress in chickpea also induced up-regulation of JA biosynthetic genes encoding ACYL-COA OXIDASE 1 and 2, respectively, but signaling genes were un-induced. SD-combined stress showed up-regulation of JA biosynthesis gene (*OPCL1*), down-regulation of SA repressor (*PROTEIN TYROSINE PHOSPHATASE1* (*PTP1*), Bartels et al., 2009) and up-regulation of SA and ET signaling genes *PR* and *MULTIPROTEIN BRIDGING FACTOR-1c* (*MBF1c*), respectively (**Figure 6C** and Supplementary File S4). LD-combined stress treatment exhibited up-regulation of both JA biosynthetic genes *OPCL1*, *AOS*, and catabolism gene *CYTOCHROM P450 94C1* (**Figure 6C**). While, LD-combined stress had up-regulation of SA biosynthetic gene *MES1* (METHYLESTERASE 1), which converts methyl salicylate (MeSA) to SA (Dempsey et al., 2011), it showed down-regulation of SA signaling genes WRKY53, PR like, *CBP60* and ET signaling genes *MYB22* and *ERF104* (**Figures 6B,D**). Altogether, they indicate toward suppression of immunity in LD combined stress (Supplementary Figure S13C). Collectively, our results on transcriptome analysis of phytohormone related genes suggest an involvement of ABA, SA, and ET mediated signaling in modulating combined stress response in these plants.

Both SD- and LD-combined stress showed up-regulation of brassinosteroid (BR) inactivator *CYP734A1* (Vriet et al., 2013). Genes encoding for BR receptors BRASSINOSTEROID INSENSITIVE 1 (BRI1) and BRASSINOSTEROID INSENSITIVE 1 LIKE 2 (BRI1like 2) were up-regulated under LD-combined and SD-pathogen stresses, respectively (Supplementary Figure S13B). LD-combined stress also showed up-regulation of gibberellin (GA) biosynthesis gene GIBBERELLIN 3-BETA-DIOXYGENASE 1 (*GA1*), catabolism gene CYTOCHROME P450 714ALIKE (*CYP714Alike*) and negative regulator of GA signaling gene; GIBBERELLIC ACID INSENSITIVE (*GAI*) indicating a loss of GA signaling in LD-combined stress (Supplementary Figure S13A). SD-combined stress resulted in up-regulation of genes encoding Auxin receptor; TOLL-INTERLEUKIN-RESISTANCE (TIR) and auxin transporter; ATP-BINDING CASSETTE B4 (ABCB4) (Supplementary Figures S13D and File S4).

Differential Expression of Defense Related Genes in SD- and LD-Combined Stress Influences *R. solanacearum* Multiplication

We looked for the differential expression of biotic stress responsive genes in the all the six treatments. We found up-regulated expression of genes encoding PLEIOTROPIC DRUG

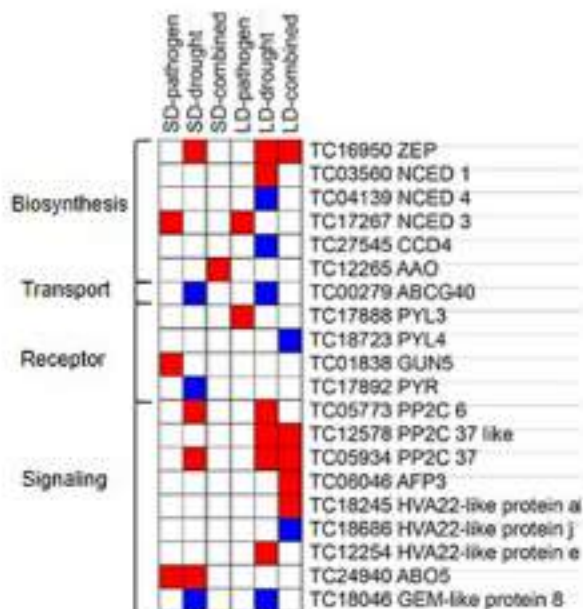
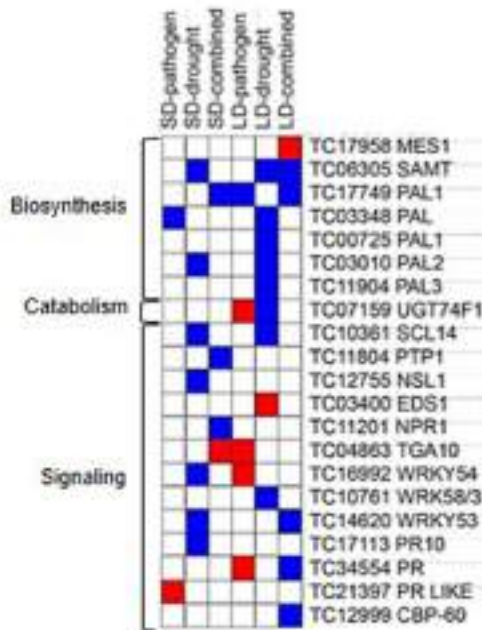
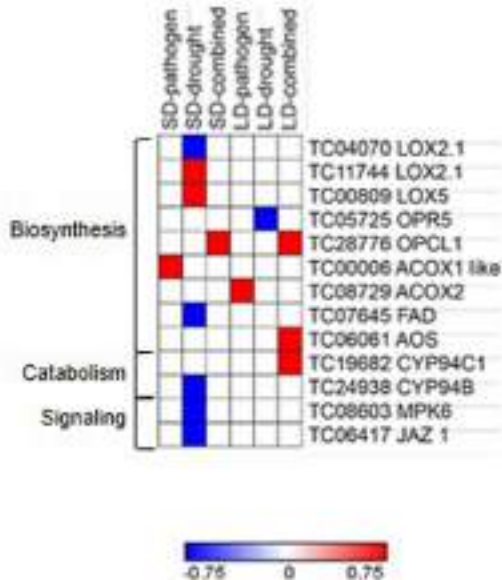
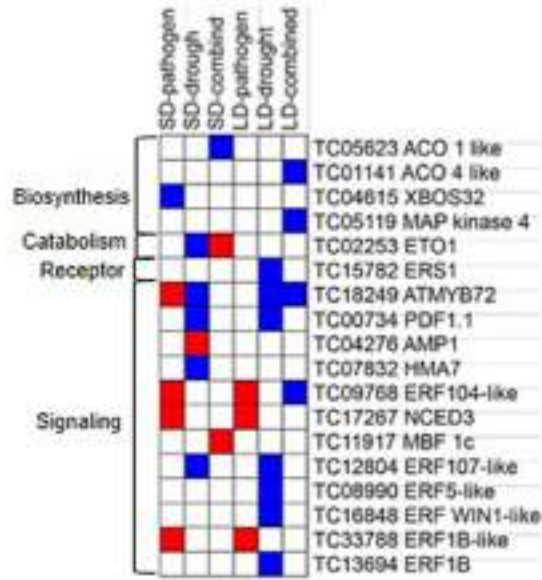
A**Abscisic Acid****B****Salicylic Acid****C****Jasmonic Acid****D****Ethylene**

FIGURE 6 | Expression profile of hormone related genes in individual and combined stressed chickpea leaves. DEGs with minimum fold change 1 (\log_2 converted) were identified in each individual and combined stressed plants over their respective controls. DEGs were mapped onto ‘hormone related’ pathways using MAPMAN and KEGG softwares, literature and Arabidopsis hormone database (<http://lifecenter.sgst.cn/orib/resourceDetail.do?resource.id=32682>). Heat maps represent expression profile of hormone biosynthesis, catabolism, receptor, transport and signaling genes related to abscisic acid (A), salicylic acid (B), jasmonic acid (C), and ethylene (D) under individual and combined stresses. Fold change values (over respective controls) were used to plot heat maps where color bar in red and blue represents up- and down-regulated genes, respectively, and white represents no differential expression. Details are mentioned in the Supplementary File S4.

RESISTANCE 3, ZINC FINGER PROTEIN, DOF ZINC FINGER PROTEIN DOF1.1, SER/THR-PROTEIN KINASE EDR1, (STPKEDR1) RESPIRATORY BURST OXIDASE HOMOLOG B (RBOHB), TIR CLASS DISEASE RESISTANCE, and NITRATE REDUCTASE under SD-pathogen stress. LD-pathogen stress showed up-regulation of defense related genes encoding RETICULIN OXIDASE LIKE PROTEIN, DISEASE RESISTANCE-RESPONSIVE (dirigent-like protein), GLUTAMINE AMIDO TRANSFERASE, PR, BOTRYTIS SUSCEPTIBLE 1, WRKY70, and RPP13. SD-combined stressed plants exhibited high up-regulation of genes encoding RETICULIN OXIDASE LIKE PROTEIN (also called BERBERINE BRIDGE ENZYME) involved in alkaloid biosynthesis, DISEASE RESISTANCE-RESPONSIVE (DIRIGENT-LIKE PROTEIN), LACCASE 7 involved in lignan and antioxidant synthesis to confer defense response in plant (**Figures 5, 7**) (Dittrich and Kutchan, 1991; Zhao et al., 2013). SD-combined stress also exhibited high up-regulation of defense related genes encoding GLUTAMINE AMIDO TRANSFERASE, RBOHE like, STPK25, WRKY4, DOF5.4, and MAJOR LATEX PROTEIN LIKE 28 (MLP28) (**Figure 7**). SD-combined stressed transcriptome exhibited more number of up-regulated genes involved in defense response with high amplitude of expression as compared to SD-pathogen stress. This justifies the activated defense leading to decreased bacterial growth in SD-combined stress as compared to SD-pathogen. In LD-combined stress, we observed up-regulation of genes encoding for RBOHE like, GLUTAMINE AMIDOTRANSFERASE C13C5.04, ZINC FINGER PROTEIN DOF5.4, CYS-RICH RECEPTOR KINASE 25, however, several defense related genes such as genes encoding DEFENSIN, MLO LIKE PROTEIN, BOTRYTIS-SUSCEPTIBLE1, PR5, CHITINASE, RETICULINE OXIDASE-LIKE, DIRIGENT-LIKE PROTEIN, WRKY12/47/33/31/35/75, RESISTANCE TO LEPTOSPHAERIA MACULANS 3 (RLM3), TIR-NBS-LRR FAMILY PROTEIN, SUPPRESSOR OF NPR1-1 (SNC4), and DISEASE RESISTANCE PROTEIN RPM1 were down-regulated which otherwise were up-regulated under either SD-pathogen, LD-pathogen or SD-combined stress (**Figure 7**). Therefore, we conclude that the imposition of slow drought has a different impact on defense related transcriptome and disease resistance capacity of plant when compared to fast drought.

DISCUSSION

Xylem invading pathogens induce physiological drought stress in plants by blocking xylem and resultantly induce wilt (Genin, 2010). When wilt disease co-occurs with drought, plants are either resistant (Pennypacker et al., 1991; Sinha et al., 2016) or susceptible to the wilt pathogen (Abd El-Rahim et al., 1998; Choi et al., 2013). The combined occurrence of drought and vascular pathogen is often reported to reduce the plant height, total leaf area and decrease the hydraulic conductance, RWC and transpiration (Pennypacker et al., 1991; Abd El-Rahim et al., 1998; Choi et al., 2013). In our previous study (Sinha et al., 2016), the vascular pathogen *Ralstonia solanacearum* multiplication was shown to be significantly decreased after 6 days of infection

under severe drought stress when compared to *R. solanacearum* infection alone in chickpea. In the present study, LD-combined stress did not change bacterial multiplication, however, SD-combined stress lead to decreased bacterial multiplication. The transcriptomic study under both SD- an LD-combined stresses unraveled responses unique to combined stress as well as responses common to both combined and individual stresses. Also SD- and LD-combined stress displayed very little overlap in transcriptomic responses between them which indicated that different durations of drought imposition in combined stress induces different transcriptomic changes in chickpea, consequently changing the overall effect on bacterial multiplication. Also, with increasing severity, the transcriptome complexity increased as reflected in more number of DEGs in LD-combined stress compared to SD-combined stress. Earlier, Gupta et al. (2016) reported increased resistance of *A. thaliana* to Psd under combined drought and Psd stress and they also reported that combined stress response differs with order of combined stress imposition (Gupta et al., 2016). However, Bidzinski et al. (2016) reported an increased susceptibility of rice plants toward *Magnaporthe oryzae* under intermittent drought and *M. oryzae* combined stress. Together these studies indicate that the plant's response toward combined stress varies with the severity and order of stresses and the plant's transcriptomic response also varies with continuous or intermittent drought stress. We also looked for the expression of certain unique genes from our study in transcriptomic data under combined drought and Psd (DPsd stress) stress in *A. thaliana* (Gupta et al., 2016) to compare if response to drought-foliar pathogen combination differs with drought-wilt pathogen combination. We could not find the differential expression of genes like LACCASE involved in lignin modification and flavonoid formation (Zhao et al., 2013) and CELLULOSE SYNTHASE involved in cellulose synthesis in DPsd transcriptome data. This suggests that unlike plant's response toward combined drought and wilt pathogen, combined stress with drought and foliar pathogen does not involve SCW modification. Gupta et al. (2016) suggested the priming of basal defenses due to interaction of drought and pathogen derived responses in combined stressed plants as a contributory factor for the resistance response observed under combined stress.

In the present study, we observed that *R. solanacearum* infection induces expression of genes involved in SA and ET signaling, biotic stress response and cell wall modification in chickpea. Earlier *R. solanacearum* infection to potato (*Solanum commersonii*) was also found to induce genes related to SA, ET, biotic stress and cell wall modification (Zuluaga et al., 2015). Narancio et al. (2013) also reported the *R. solanacearum* defense in potato (*S. commersonii* Dun) to be mediated by ET and SA mediated responses. They also reported up-regulation of *ERF*, *PR*, and *WRKY* genes. It was evident through transcriptome of LD-pathogen that *R. solanacearum* alone induces drought like symptoms. LD-pathogen stress showed highly up-regulated expression of genes encoding RAFFINOSE SYNTHASE, LEA14, MYOINOSITOL OXYGENASE, and CPRF2. The transcriptomic responses were close to SD-combined stress transcriptome indicating that chickpea upon *R. solanacearum* infection feels

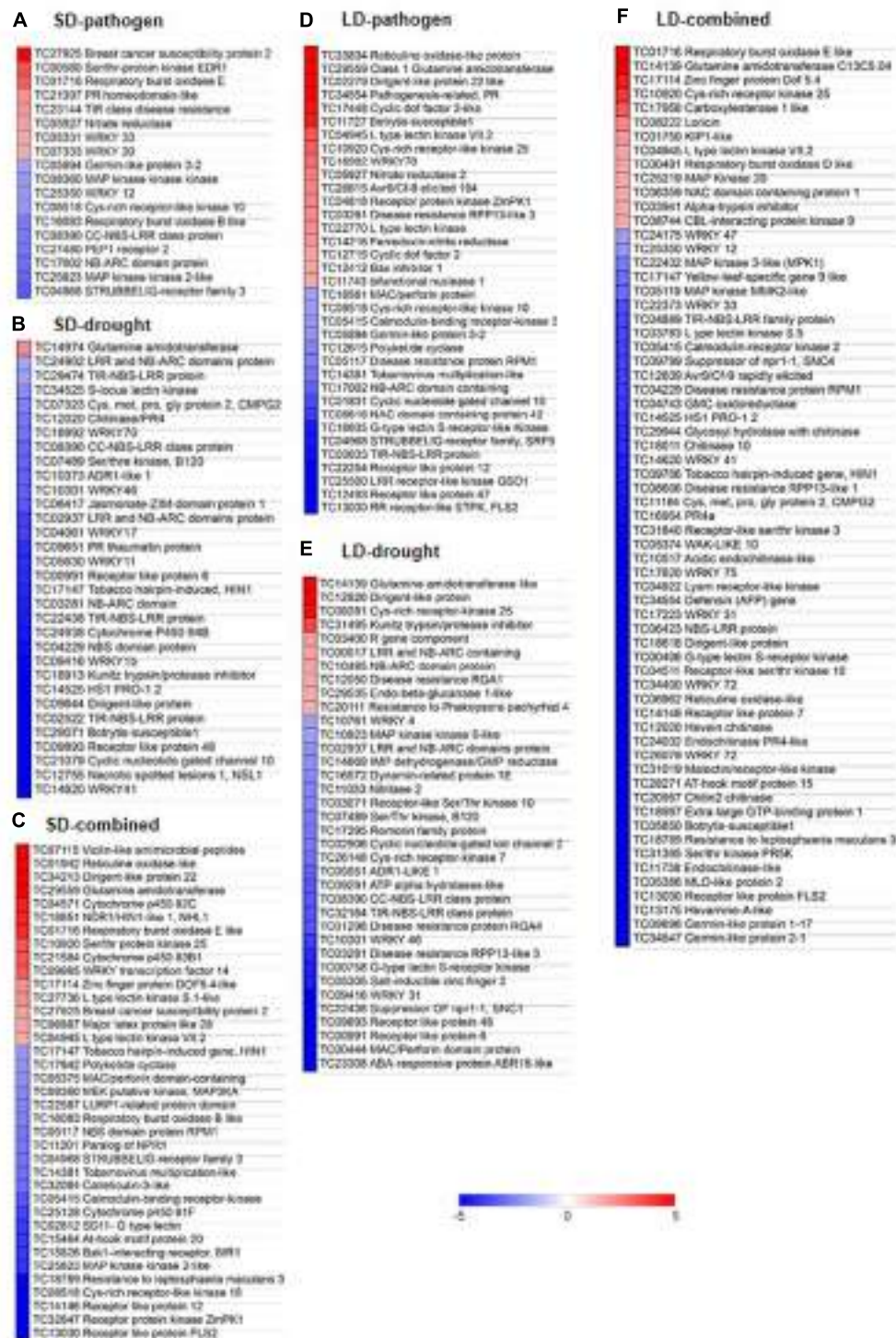


FIGURE 7 | Expression profile of genes involved in defense responses under individual and combined stress transcriptome. DEGs with minimum fold change 1 (Log₂ converted) were identified in each individual and combined stressed plants over their respective controls. DEGs involved in defense responses were identified using MAPMAN software and literature survey. Heat map represent expression profile of 'defense response related' genes under SD-pathogen (**A**), SD-drought (**B**), SD-combined (**C**), LD-pathogen (**D**), LD-drought (**E**), and LD-combined stresses (**F**). Fold change values (over respective controls) are represented in heat maps where color bar in red and blue represents up- and down-regulated genes, respectively.

drought stress like effect. Xylem invading *Xylella fastidiosa* was also found to invoke drought like response as it up-regulated expression ABA biosynthesis genes and two galactinol synthase genes involved in synthesis of galactinol and raffinose osmoprotectants (Choi et al., 2013).

The transcriptomic changes under SD-combined stress in this study directed toward defense response mediated SA and ET signaling and lignin and flavonoid accumulation. Contrastingly, LD-combined stress showed repressed expression of SA and ET signaling genes along with various defense related genes and thus induced the susceptibility of plant. We noted differential expression of various genes unique to SD- and LD-combined stresses. One of the unique responses under SD-combined stress was specific up-regulation of ET signaling gene Multiprotein Bridging Factor-1c (*MBF1c*). *MBF1* is a DNA-binding protein transcriptional coactivator which is involved in regulating metabolic and development pathways (Suzuki et al., 2011). Earlier, up-regulation of *MBF1c* was noticed in *A. thaliana* under pathogen infection, salinity, drought, heat, hydrogen peroxide, ABA, and SA application (Rizhsky et al., 2004; Tsuda and Yamazaki, 2004). Moreover, its constitutive expression was reported to increase the tolerance of transgenic plants to bacterial infection, salinity, heat, and osmotic stress and combined heat and osmotic stress (Suzuki et al., 2005). Similarly, genes encoding for auxin receptor TIR, transporters ABCB4, HP4, ARR17, PXY, and SND2 showed up-regulation only under SD-combined stress.

Xylem being conductor of water in plant is the most affected tissue under drought (De Souza et al., 2013) and wilt diseases (Yadeta and Thomma, 2013). While inhabiting the xylem, vascular pathogen exploits all inorganic and sugar resources present in the xylem (Yadeta and Thomma, 2013). Also, it enzymatically digests xylem cell wall to fulfill its nutritional needs (Yadeta and Thomma, 2013). The plant in turn, induces vascular coating as well as metabolic changes like secretion of PR proteins, peroxidases, proteases, xyloglucan-endotransglycosylase (XET), and xyloglucan-specific endoglucanase inhibitor protein (XEGIP), phenols, phytoalexins, and lignin-like compounds as a part of the plant defense toward the pathogen (Yadeta and Thomma, 2013). Primary and SCW also modulate ET, JA, SA, and ABA hormone signaling and thus have role in drought stress tolerance and regulation of defense response (Schulze-Lefert, 2004; Somerville et al., 2004; Hernández-Blanco et al., 2007; Denancé et al., 2013). In this regard, we looked for the expression of genes involved in xylem differentiation and SCW modification to understand if plant is utilizing xylem modification or re-differentiation as defense mechanism against combined stress. We observed that SD-combined stress had up-regulated expression of genes involved in xylem differentiation and SCW modification especially genes involved in lignin biosynthesis. During LD-combined stress the genes involved in cellulose biosynthesis were up-regulated. Increased lignin accumulation has been shown to increase the plants defense mechanism (Bhuiyan et al., 2009; Xu et al., 2011). However, on contrary increased cellulose synthesis is known to

increase the susceptibility of plants toward pathogen. Hernández-Blanco et al. (2007) showed that mutation in cellulose synthase encoding genes (*CeSA4*, *CeSA7*, and *CeSA8*) for cellulose deposition in SCW enhanced resistance of *A. thaliana* toward *R. solanacearum*. In our study, we could partly correlate increased lignification during SD-combined stress with the enhanced defense under this stress and up-regulation of *CeSA7* with the compromised disease resistance in LD-combined stressed plants.

CONCLUSION

The study highlights that combined drought and *R. solanacearum* stress invokes transcriptome changes unique to combined stress and also transcriptome common between combined and individual stresses in chickpea. SD-combined stress in chickpea causes up-regulation of genes involved in SA, ET signaling, and lignin biosynthesis. LD-combined stress down-regulates the expression of defense related genes and increases expression of genes involved in cellulose biosynthesis resulting in susceptibility of chickpea toward *R. solanacearum*. Transcriptome under *R. solanacearum* infection exhibit up-regulated expression of various abiotic stress related genes and displays closeness with the SD-combined stress transcriptome.

AUTHOR CONTRIBUTIONS

MS-K conceived the idea. MS-K and RS designed the study. RS and AG performed the experiments. RS analyzed the data with the input from MS-K. MS-K and RS wrote the manuscript.

FUNDING

We thank Science and Engineering Research Board (SERB), Department of Science and Technology (DST) for providing grant and fellowship for this study (SB/YS/LS-237/2013) to RS. Projects at MS-K lab are supported by National Institute of Plant Genome Research core funding and DBT-Ramalingaswami re-entry fellowship grant (BT/RLF/re-entry/23/2012).

ACKNOWLEDGMENTS

Authors thank Dr. Mehanathan Muthamilarasan and Mr. Joel L. Fernandes for critical reading of the manuscript. Microarray analysis was outsourced to Genotypic India Pvt. Ltd, Bangalore, India.

SUPPLEMENTARY MATERIAL

The Supplementary Material for this article can be found online at: <http://journal.frontiersin.org/article/10.3389/fpls.2017.00333/full#supplementary-material>

REFERENCES

- Abd El-Rahim, M. F., Fahmy, G. M., and Fahmy, Z. M. (1998). Alterations in transpiration and stem vascular tissues of two maize cultivars under conditions of water stress and late wilt disease. *Plant Pathol.* 47, 216–223. doi: 10.1046/j.1365-3059.1998.00211.x
- Achuo, E. A., Prinsen, E., and Hofte, M. (2006). Influence of drought, salt stress and abscisic acid on the resistance of tomato to *Botrytis cinerea* and *Oidium neolyopersici*. *Plant Pathol.* 55, 178–186. doi: 10.1111/j.1365-3059.2005.01340.x
- Bartels, S., Jeffrey, C. A., Marina, A. G., Scott, C. P., Alessandro, C., Heribert, H., et al. (2009). MAP KINASE PHOSPHATASE1 and PROTEIN TYROSINE PHOSPHATASE1 are repressors of salicylic acid synthesis and SNC1-mediated responses in *Arabidopsis*. *Plant Cell* 21, 2884–2897. doi: 10.1105/tpc.109.067678
- Bhaskara, G. B., Thao, T. N., and Paul, E. V. (2012). Unique drought resistance functions of the highly ABA-induced clade a protein phosphatase 2Cs. *Plant Physiol.* 160, 379–395. doi: 10.1104/pp.112.202408
- Bhuiyan, N. H., Selvaraj, G., Wei, Y., and King, J. (2009). Role of lignification in plant defense. *Plant Signal. Behav.* 4, 158–159. doi: 10.4161/psb.4.2.7688
- Bidzinski, P., Ballini, E., Ducasse, A., Michel, C., Zuluaga, P., Genga, A., et al. (2016). Transcriptional basis of drought-induced susceptibility to the rice blast fungus *Magnaporthe oryzae*. *Front. Plant Sci.* 7:1558. doi: 10.3389/fpls.2016.01558
- Bonawitz, N. D., and Chapple, C. (2010). The genetics of lignin biosynthesis?: connecting genotype to phenotype. *Annu. Rev. Genet.* 44, 337–363. doi: 10.1146/annurev-genet-102209-163508
- Brown, D., Wightman, R., Zhang, Z., Gomez, L. D., Atanassov, I., Bukowski, J.-P., et al. (2011). *Arabidopsis* genes *IRREGULAR XYLEM* (*IRX15*) and *IRX15L* encode DUF579-containing proteins that are essential for normal xylan deposition in the secondary cell wall. *Plant J.* 66, 401–413. doi: 10.1111/j.1365-313X.2011.04501.x
- Chan, Z., Wang, Y., Cao, M., Gong, Y., Mu, Z., Wang, H., et al. (2016). RDM4 modulates cold stress resistance in *Arabidopsis* partially through the *CBF*-mediated pathway. *New Phytol.* 209, 1527–1539. doi: 10.1111/nph.13727
- Chen, Y., Ren, X., Zhou, X., Huang, L., Yan, L., Lei, Y., et al. (2014). Dynamics in the resistant and susceptible peanut (*Arachis hypogaea* L.) root transcriptome on infection with the *Ralstonia solanacearum*. *BMC Genomics* 15:1078. doi: 10.1186/1471-2164-15-1078
- Choi, H. K., Alberto, I., Francisco, G. S., and Douglas, C. (2013). Water deficit modulates the response of *Vitis vinifera* to the Pierce's disease pathogen *Xylella fastidiosa*. *Mol. Plant Microbe Interact.* 26, 1–46. doi: 10.1094/MPMI-09-12-0217-R
- De Souza, T. C., de Castro, E. M., Magalhães, P. C., Lino, L. D. O., Alves, E. T., and Albuquerque, P. E. P. (2013). Morphophysiology, morphoanatomy, and grain yield under field conditions for two maize hybrids with contrasting response to drought stress. *Acta Physiol. Plant.* 35, 3201–3211. doi: 10.1007/s11738-013-1355-1
- Dempsey, D. A., Vlot, A. C., Wildermuth, M. C., and Klessig, D. F. (2011). Salicylic acid biosynthesis and metabolism. *Arabidopsis Book* 9:e0156. doi: 10.1199/tab.0156
- Denancé, N., Ranocha, P., Oria, N., Barlet, X., Rivière, M.-P., Yadeta, K. A., et al. (2013). *Arabidopsis wai1* (walls are thin1)-mediated resistance to the bacterial vascular pathogen, *Ralstonia solanacearum*, is accompanied by cross-regulation of salicylic acid and tryptophan metabolism. *Plant J.* 73, 225–239. doi: 10.1111/tpj.12027
- Dittrich, H., and Kutchan, T. M. (1991). Molecular cloning, expression, and induction of berberine bridge enzyme, an enzyme essential to the formation of benzophenanthridine alkaloids in the response of plants to pathogenic attack. *Proc. Natl. Acad. Sci. U.S.A.* 88, 9969–9973. doi: 10.1073/pnas.88.22.9969
- Douglas, S. M., and MacHardy, W. E. (1981). The relationship between vascular alterations and symptom development in *Verticillium* wilt of *Chrysanthemum*. *Physiol. Plant Pathol.* 19, 31–39. doi: 10.1016/S0048-4059(81)80005-7
- Garcia, M. E., Lynch, T., Peeters, J., Snowden, C., and Ruth, F. (2008). A small plant-specific protein family of ABI five binding proteins (AFPs) regulates stress response in germinating *Arabidopsis* seeds and seedlings. *Plant Mol. Biol.* 67, 643–658. doi: 10.1007/s11103-008-9344-2
- Gaur, P. M., Jukanti, A. K., and Varshney, R. K. (2012). Impact of genomic technologies on chickpea breeding strategies. *Agronomy* 2, 199–221. doi: 10.3390/agronomy2030199
- Genin, S. (2010). Molecular traits controlling host range and adaptation to plants in *Ralstonia solanacearum*. *New Phytol.* 187, 920–928. doi: 10.1111/j.1469-8137.2010.03397.x
- Gupta, A., Sarkar, A. K., and Senthil-Kumar, M. (2016). Global transcriptional analysis reveals unique and shared responses in *Arabidopsis thaliana* exposed to combined drought and pathogen stress. *Front. Plant Sci.* 7:686. doi: 10.3389/fpls.2016.00686
- Hatmi, S., Charlotte, G., Patricia, T. A., Sandra, V., Fanja, R., Fabienne, B., et al. (2015). Drought stress tolerance in grapevine involves activation of polyamine oxidation contributing to improved immune response and low susceptibility to *Botrytis cinerea*. *J. Exp. Bot.* 66, 775–787. doi: 10.1093/jxb/eru436
- Hernández-Blanco, C., Feng, D. X., Hu, J., Sánchez-Vallet, A., Deslandes, L., Llorente, F., et al. (2007). Impairment of cellulose synthases required for *Arabidopsis* secondary cell wall formation enhances disease resistance. *Plant Cell* 19, 890–903. doi: 10.1105/tpc.106.048058
- Hwang, J., Choi, Y., Kang, J., Kim, S., Cho, M., Mihalte, L., et al. (2011). Microarray analysis of the transcriptome for bacterial wilt resistance in pepper (*Capsicum annuum* L.). *Notulae Botanicae Horti Agrobotanici Cluj Napoca* 39, 49–57. doi: 10.15835/nbha3926820
- Ishihara, T., Mitsuhasha, I., Takahashi, H., and Nakaho, K. (2012). Transcriptome analysis of quantitative resistance-specific response upon *Ralstonia solanacearum* infection in tomato. *PLoS ONE* 7:e46763. doi: 10.1371/journal.pone.0046763
- Kavak, H., and Boydak, E. (2011). Trends of sudden wilt syndrome in sesame plots irrigated with delayed intervals. *Afr. J. Microbiol. Res.* 5, 1837–1841. doi: 10.5897/AJMR11.289
- Kendziorski, C., Irizarry, R. A., Chen, K. S., Haag, J. D., and Gould, M. N. (2005). On the utility of pooling biological samples in microarray experiments. *PNAS* 102, 4252–4257. doi: 10.1073/pnas.0500607102
- Kubasek, W., Shirley, B., McKillop, A., Goodman, H., Briggs, W., and Ausubel, F. (1992). Regulation of flavonoid biosynthetic genes in germinating *Arabidopsis* seedlings. *Plant Cell* 4, 1229–1236. doi: 10.1105/tpc.4.10.1229
- Liu, W., Tai, H., Li, S., Gao, W., Zhao, M., Xie, C., et al. (2014). *bHLH122* is important for drought and osmotic stress resistance in *Arabidopsis* and in the repression of ABA catabolism. *New Phytol.* 201, 1192–1204. doi: 10.1111/nph.12607
- Livak, K. J., and Schmittgen, T. D. (2001). Analysis of relative gene expression data using real-time quantitative PCR and the 2 (-Delta Delta C(T)) method. *Methods* 25, 402–408. doi: 10.1006/meth.2001.1262
- Mayek-Pérez, N., García-Espínosa, R., López-Castañeda, C., Acosta-Gallegos, J., and Simpson, J. (2002). Water relations, histopathology and growth of common bean (*Phaseolus vulgaris* L.) during pathogenesis of *Macrophomina phaseolina* under drought stress. *Physiol. Mol. Plant Pathol.* 60, 185–195. doi: 10.1006/pmp.2001.0388
- McElrone, A. J., Sherald, J. L., and Forseth, L. N. (2001). Effects of water stress on symptomatology and growth of *Parthenocissus quinquefolia* infected by *Xylella fastidiosa*. *Plant Dis.* 85, 1160–1164. doi: 10.1094/PDIS.2001.85.11.1160
- McFarlane, H. E., Doring, A., and Persson, S. (2014). The cell biology of cellulose synthesis. *Annu. Rev. Plant Biol.* 65, 69–94. doi: 10.1146/annurev-ap-050213040240
- Mohr, P. G., and Cahill, D. M. (2003). Abscisic acid influences the susceptibility of *Arabidopsis thaliana* to *Pseudomonas syringae* pv. *tomato* and *Peronospora parasitica*. *Funct. Plant Biol.* 30, 461–469. doi: 10.1071/FP02231
- Mortimer, J. C., Miles, G. P., Brown, D. M., Zhang, Z., Segura, M. P., Weimar, T., et al. (2010). Absence of branches from xylan in *Arabidopsis gux* mutants reveals potential for simplification of lignocellulosic biomass. *Proc. Natl. Acad. Sci. U.S.A.* 107, 17409–17414. doi: 10.1073/pnas.1005456107
- Narancio, R., Zorrilla, P., Robello, C., Gonzalez, M., Vilardo, F., Pritsch, C., et al. (2013). Insights on gene expression response of a characterized resistant genotype of *Solanum commersonii* Dun against *Ralstonia solanacearum*. *J. Plant Pathol.* 136, 823–835. doi: 10.1007/s10658-013-0210-y
- Nene, Y. L., Reddy, M. V., Haware, M. P., Ghanekar, A. M., Amin, K. S., Pande, S., et al. (2012). *Field Diagnosis of Chickpea Diseases and Their Control. Information Bulletin No. 28 (revised)*. Technical Report. Patancheru: International Crops Research Institute for the Semi-Arid Tropics.

- Ochola, D., Ocimati, W., Tinzaara, W., Blomme, G., and Karamura, E. B. (2015). Effects of water stress on the development of banana *Xanthomonas* wilt disease. *Plant Pathol.* 64, 552–558. doi: 10.1111/ppa.12281
- Olson, A. J., Pataky, J. K., D'Arcy, C. J., and Ford, R. E. (1990). Effects of drought stress and infection by maize dwarf mosaic virus on sweet corn. *Plant Dis.* 74, 147–151. doi: 10.1094/PD-74-0147
- Pennypacker, B. W., Leath, K. T., and Hill, R. R. Jr. (1991). Impact of drought stress on the expression of resistance to *Verticillium albo-atrum* in Alfalfa. *Phytopathology* 81, 1014–1024. doi: 10.1094/Phyto-81-1014
- Prasath, D., Karthika, R., Habeeba, N. T., Suraby, E. J., Rosana, O. B., Shaji, A., et al. (2014). Comparison of the transcriptomes of ginger (*Zingiber officinale* Rosc.) and mango ginger (*Curcuma amada* Roxb.) in response to the bacterial wilt infection. *PLoS ONE* 9:e99731. doi: 10.1371/journal.pone.0099731
- Prasch, C. M., and Sonnewald, U. (2013). Simultaneous application of heat, drought, and virus to Arabidopsis plants reveals significant shifts in signaling networks. *Plant Physiol.* 162, 1849–1866. doi: 10.1104/pp.113.221044
- Ramegowda, V., Senthil-Kumar, M., Ishiga, Y., Kaundal, A., Udayakumar, M., and Mysore, K. S. (2013). Drought stress acclimation imparts tolerance to *Sclerotinia sclerotiorum* and *Pseudomonas syringae* in *Nicotiana benthamiana*. *Int. J. Mol. Sci.* 14, 9497–9513. doi: 10.3390/ijms14059497
- Rizhsky, L., Liang, H., Shuman, J., Shulaev, V., Davletova, S., and Mittler, R. (2004). When defense pathways collide. The response of Arabidopsis to a combination of drought and heat stress. *Plant Physiol.* 134, 1683–1696. doi: 10.1104/pp.103.03431.1
- Růžička, K., Ursache, R., Hejátko, J., and Helariutta, Y. (2015). Xylem development – from the cradle to the grave. *New Phytol.* 207, 519–535. doi: 10.1111/nph.13383
- Rybél, B. D., Mähönen, A. P., Helariutta, Y., and Weijers, D. (2016). Plant vascular development?: from early specification to differentiation. *Nat. Rev. Mol. Cell Biol.* 17, 30–40. doi: 10.1038/nrm.2015.6
- Scheller, H. V., and Ulvskov, P. (2010). Hemicelluloses. *Annu. Rev. Plant Biol.* 61, 263–289. doi: 10.1146/annurev-arplant-042809-112315
- Schmelzer, E., Kruger-Lebus, S., and Hahlbrock, K. (1989). Temporal and spatial patterns of gene expression around sites of attempted fungal infection in parsley leaves. *Plant Cell* 1, 993–1001. doi: 10.1105/tpc.1.10.993
- Schulze-Lefert, P. (2004). Knocking on the heaven's wall: pathogenesis of and resistance to biotrophic fungi at the cell wall. *Curr. Opin. Plant Biol.* 7, 377–383. doi: 10.1016/j.pbi.2004.05.004
- Singh, A., Saroj, K. J., Jayram, B., and Pandey, G. K. (2015). ABA inducible rice protein phosphatase 2C confers ABA insensitivity and abiotic stress tolerance in *Arabidopsis*. *PLoS ONE* 10:e0125168. doi: 10.1371/journal.pone.0125168
- Sinha, R., Gupta, A., and Senthil-Kumar, M. (2016). Understanding the impact of drought on foliar and xylem invading bacterial pathogen stress in chickpea. *Front. Plant Sci.* 7:902. doi: 10.3389/fpls.2016.00902
- Somerville, C., Bauer, S., Brininstool, G., Facette, M., Hamann, T., Milne, J., et al. (2004). Toward a systems approach to understanding plant cell walls. *Curr. Opin. Plant Biol.* 7, 2206–2212. doi: 10.1016/j.pbi.2004.05.004
- Suzuki, N., Rizhsky, L., Liang, H., Shuman, J., Shulaev, V., and Mittler, R. (2005). Enhanced tolerance to environmental stress in transgenic plants expressing the transcriptional coactivator multiprotein bridging factor 1c. *Plant Physiol.* 139, 1313–1322. doi: 10.1104/pp.105.070110
- Suzuki, N., Sejima, H., Tam, R., Schlauch, K., and Mittler, R. (2011). Identification of the MBF1 heat-response regulon of *Arabidopsis thaliana*. *Plant J.* 66, 844–851. doi: 10.1111/j.1365-313X.2011.04550.x
- Taylor-Teeples, M., Lin, L., de Lucas, M., Turco, G., Toal, T. W., Gaudinier, A., et al. (2015). An *Arabidopsis* gene regulatory network for secondary cell wall synthesis. *Nature* 517, 571–575. doi: 10.1038/nature14099
- Tsuda, K., and Yamazaki, K. (2004). Structure and expression analysis of three subtypes of *Arabidopsis* MBF1 genes. *Biochim. Biophys. Acta* 1680, 1–10. doi: 10.1016/j.bbapex.2004.08.004
- Vanitha, S. C., and Umesh, S. (2009). Variations in defense related enzyme activities in tomato during the infection with bacterial wilt pathogen. *J. Plant Interact.* 3, 245–253. doi: 10.1080/17429140802032863
- Verma, M., Kumar, V., Patel, R. K., Garg, R., and Jain, M. (2015). CTDB: an integrated chickpea transcriptome database for functional and applied genomics. *PLoS ONE* 10:e0136880. doi: 10.1371/journal.pone.0136880
- Vriet, C., Russinova, E., and Reuzeau, C. (2013). From squalene to brassinolide: the steroid metabolic and signaling pathways across the plant kingdom. *Mol. Plant* 6, 1738–1757. doi: 10.1093/mp/sst096
- Xu, L., Zhu, L., Tu, L., Liu, L., Yuan, D., Jin, L., et al. (2011). Lignin metabolism has a central role in the resistance of cotton to the wilt fungus *Verticillium dahliae* as revealed by RNA-Seq-dependent transcriptional analysis and histochemistry. *J. Exp. Bot.* 62, 5607–5621. doi: 10.1093/jxb/err245
- Yadeta, K. A., and Thomma, B. P. H. J. (2013). The xylem as battleground for plant hosts and vascular wilt pathogens. *Front. Plant Sci.* 4:97. doi: 10.3389/fpls.2013.00097
- Yang, A., Dai, X., and Zhang, W. H. (2012). A R2R3-type MYB gene, OsMYB2, is involved in salt, cold, and dehydration tolerance in rice. *J. Exp. Bot.* 63, 2541–2556. doi: 10.1093/jxb/err431
- Zhang, X., and Liu, C. J. (2015). Multifaceted regulations of gateway enzyme phenylalanine ammonia-lyase in the biosynthesis of phenylpropanoids. *Mol. Plant* 8, 17–27. doi: 10.1016/j.molp.2014.11.001
- Zhang, Y., Wang, X., Li, Y., Wu, L., Zhou, H., Zhang, G., et al. (2013). Ectopic expression of a novel ser/thr protein kinase from cotton (*Gossypium barbadense*), enhances resistance to *Verticillium dahliae* infection and oxidative stress in *Arabidopsis*. *Plant Cell Rep.* 32, 1703–1713. doi: 10.1007/s00299-013-1481-7
- Zhao, Q., Nakashima, J., Chen, F., Yin, Y., Fu, C., Yun, J., et al. (2013). Laccase is necessary and nonredundant with peroxidase for lignin polymerization during vascular development in *Arabidopsis*. *Plant Cell* 25, 3976–3987. doi: 10.1105/tpc.113.117770
- Zuluaga, A. P., Solé, M., Lu, H., Góngora-Castillo, E., Vaillancourt, B., Coll, N., et al. (2015). Transcriptome responses to *Ralstonia solanacearum* infection in the roots of the wild potato *Solanum commersonii*. *BMC Genomics* 16:246. doi: 10.1186/s12864-015-1460-1

Conflict of Interest Statement: The authors declare that the research was conducted in the absence of any commercial or financial relationships that could be construed as a potential conflict of interest.

Copyright © 2017 Sinha, Gupta and Senthil-Kumar. This is an open-access article distributed under the terms of the Creative Commons Attribution License (CC BY). The use, distribution or reproduction in other forums is permitted, provided the original author(s) or licensor are credited and that the original publication in this journal is cited, in accordance with accepted academic practice. No use, distribution or reproduction is permitted which does not comply with these terms.



Responses of *In vitro*-Grown Plantlets (*Vitis vinifera*) to Grapevine leafroll-Associated Virus-3 and PEG-Induced Drought Stress

Zhen-Hua Cui^{1,2}, Wen-Lu Bi¹, Xin-Yi Hao¹, Yan Xu^{1*}, Peng-Min Li¹, M. Andrew Walker² and Qiao-Chun Wang^{1*}

¹ State Key Laboratory of Crop Stress Biology for Arid Areas, Key Laboratory of Genetic Improvement of Horticultural Crops of Northwest China, College of Horticulture, Northwest A&F University, Yangling, China, ² Department of Viticulture and Enology, University of California, Davis, Davis, CA, USA

OPEN ACCESS

Edited by:

Olivier Lamotte,
UMR Agroécologie, France

Reviewed by:

Walter Chittarra,
National Research Council, Italy
Giorgio Gambino,
National Research Council, Italy

*Correspondence:

Yan Xu
yan.xu@nwsuaf.edu.cn;
Qiao-Chun Wang
qiaochunwang@nwsuaf.edu.cn

Specialty section:

This article was submitted to
Plant Physiology,
a section of the journal
Frontiers in Physiology

Received: 20 December 2015

Accepted: 19 May 2016

Published: 02 June 2016

Citation:

Cui Z-H, Bi W-L, Hao X-Y, Xu Y, Li P-M, Walker MA and Wang Q-C (2016) Responses of *In vitro*-Grown Plantlets (*Vitis vinifera*) to Grapevine leafroll-Associated Virus-3 and PEG-Induced Drought Stress. *Front. Physiol.* 7:203.
doi: 10.3389/fphys.2016.00203

Stresses caused by viral diseases and drought have long threatened sustainable production of grapevine. These two stresses frequently occur simultaneously in many of grapevine growing regions of the world. We studied responses of *in vitro*-grown plantlets (*Vitis vinifera*) to *Grapevine leafroll associated virus-3* (GLRaV-3) and PEG-induced drought stress. Results showed that stress induced by either virus infection or drought had negative effects on vegetative growth, caused significant decreases and increases in total soluble protein and free proline, respectively, induced obvious cell membrane damage and cell death, and markedly increased accumulations of O_2^- and H_2O_2 . Co-stress by virus and drought had much severer effects than single stress on the said parameters. Virus infection alone did not cause significant alternations in activities of POD, ROS, and SOD, and contents of MDA, which, however, markedly increased in the plantlets when grown under single drought stress and co-stress by the virus and drought. Levels of ABA increased, while those of IAA decreased in the plantlets stressed by virus infection or drought. Simultaneous stresses by the virus and drought had co-effects on the levels of ABA and IAA. Up-regulation of expressions of ABA biosynthesis genes and down-regulation of expressions of IAA biosynthesis genes were responsible for the alternations of ABA and IAA levels induced by either the virus infection or drought stress and co-stress by them. Experimental strategies established in the present study using *in vitro* system facilitate investigations on ‘pure’ biotic and abiotic stress on plants. The results obtained here provide new insights into adverse effects of stress induced by virus and drought, in single and particularly their combination, on plants, and allow us to re-orientate agricultural managements toward sustainable development of the agriculture.

Keywords: cell damage, drought, grapevine leafroll virus, physiological metabolism, plant hormones, *Vitis vinifera*

INTRODUCTION

Stresses caused by abiotic and biotic factors have long threatened sustainable development of agricultural production. Drought, one of the greatest abiotic stresses, was reported to cause agricultural losses of 50 billion dollars between 1980 and 2012 in United States alone (Suzuki et al., 2014). It is estimated that more than 6% of the world’s land and 30% of the world’s irrigated

areas also face salinity problems (UNESCO Water Portal, 2007). Viral disease, a biotic stress, causes serious economic losses to agricultural crops (Hadidi and Barba, 2011).

The influence of stress by either virus infection (Sampol et al., 2003; Moutinho-Pereira et al., 2012; Li et al., 2013; Cui et al., 2015) or drought (Zhu, 2002; Suzuki et al., 2014) has been well-demonstrated on plant development, growth, photosynthetic capability and various physiological metabolisms, eventually resulting in reduction of crop yield and quality. However, studies on their combining effects have been quite limited (Atkinson and Urwin, 2012; Prasch, 2013; Suzuki et al., 2014). Plants grown in nature are exposed simultaneously to abiotic and biotic stresses. Abiotic stress was shown to alter the ability of plants resist/tolerate pathogens (Atkinson and Urwin, 2012; Prasch, 2013). Similarly, biotic stress was found to alter resistance/tolerance of hosts to abiotic stress (Xu et al., 2008; Atkinson and Urwin, 2012; Prasch, 2013). Therefore, responses of plants to single stress differ from those to multiple stresses (Atkinson and Urwin, 2012; Suzuki et al., 2014), and the simultaneous occurrence of multiple stresses can cause complex plant responses (Atkinson and Urwin, 2012; Prasch, 2013; Suzuki et al., 2014). Thus, better understanding of effects of combining abiotic with biotic stress is of great significance and would allow us to orientate agricultural management strategies to ensure sustainable development of agricultural production.

Grapevine (*Vitis vinifera*) is an economically important fruit crop worldwide. Virus disease and drought stress are the two key factors limiting high yield and quality production of grapevine (Martelli, 2012). Co-occurrence of drought and virus infection is common in many of grapevine-growing regions. However, most of the previous studies on the said issues addressed single stress, while the co-stress by virus and drought has been far less studied.

The objective of the present study was, therefore, to study responses of grapevines (*Vitis vinifera*) to *Grapevine leafroll-associated virus-3* (GLRaV-3) and PEG-induced drought stress using *in vitro* culture system. The overall goal was to better understand the effect of abiotic and biotic stress, in single and particularly in combination, on growth, physiological metabolic processes and cell damage, thus providing valuable data upon which agricultural management strategies could be adjusted to allow more sustainable viticultural production.

MATERIALS AND METHODS

Maintenance of *In vitro* Healthy and GLRaV-3 Infected Stock Plantlets and Establishment of PEG-Induced Drought Stress

Vitis vinifera L. ‘Cabernet Sauvignon’, a major red wine cultivar grown worldwide and susceptible to GLRaV-3, was used in this

Abbreviations: ABA, abscisic acid; BM, basal medium; CAT, catalase; DAB, 3, 3'-diaminobenzidine; DW, dry weight; EL, electrolytic leakage; FW, fresh weight; GLRaV-3, *Grapevine leafroll-associated virus-3*; IAA, indoleacetic acid; MDA, Methane Dicarboxylic Aldehyde; MS, Murashige and Skoog medium; NBT, nitroblue tetrazolium; PCD, Programmed cell death; PEG, polyethylene glycol; POD, peroxidase; ROS, Reactive oxygen species; SOD, superoxide dismutase.

study. *In vitro* shoots suspected of GLRaV-3 infection were established *in vitro*, according to Cui et al. (2015). After 6 months of *in vitro* establishment, the suspected shoots were screened again by RT-PCR for their virus status including GVA, GVB, GRSPaV, GFkV, GFLV, and ArMV, which are among the grapevine viruses reported in China (Ren et al., 2013). Samples showing a positive response only to GLRaV-3 were maintained and others discarded. The GLRaV-3 infected shoots (scions) were micrografted on to the healthy *in vitro* shoots (rootstocks). Micrografts developed into plantlets after 3 months of micrografting. GLRaV-3 was confirmed by RT-PCR in the micrografted rootstocks (Cui et al., 2015) and shoot segments were excised from the virus-infected rootstocks were proliferated to establish the diseased *in vitro* stock shoots. Thus, the healthy and diseased *in vitro* stock shoots were produced from the same mother plants. Both the healthy and virus-infected the cultures were maintained on a basal medium (BM) containing half-strength Murashige and Skoog (1962) medium (MS) with 30 g l⁻¹ sucrose and 7 g l⁻¹ agar. The pH of the medium was adjusted to 5.8 prior to autoclaving at 121°C for 20 min. The cultures were maintained at a constant temperature of 24 ± 2°C under a 16-h photoperiod with a light intensity of 50 μmol s⁻¹ m⁻² provided by cool-white fluorescent tubes. Subculture was done once every 6 weeks.

Shoot segments (1.5–2.0 cm in length) with 2 fully-opened leaves were excised from *in vitro* 6-week-old healthy and virus-infected stock plantlets, respectively, and cultured on BM containing 0, 2, or 4% (w/v) of polyethylene glycol (PEG) 8000, according to Cui et al. (2015), under the same cultural conditions as used for *in vitro* stock plantlets. Water potentials of medium containing 2 and 4% PEG were -2.4 MPa and -2.7 MPa, respectively, as calculated by Michel (1983). Unless stated otherwise, samples were taken after 4 weeks of culture and used for the following experiments.

Vegetative Growth of *In vitro* GLRaV-3 Infected Plantlets with and without Drought Stress

Vegetative growth including time required for axillary bud elongation, shoot length, number of roots, length of the longest root, and fresh weight (FW) and dry weight (DW) of shoots and roots were measured after 6 weeks of culture. Axillary bud elongation was defined when ≥50% of shoots showed bud elongation.

Analysis of Total Soluble Protein

Shoots with leaves of (0.5 g FW) were extracted with 3 ml of 50 mM phosphate buffer (pH 7.0), followed by centrifugation at 10,000 rpm for 10 min. The supernatant was collected and absorbance was recorded at 595 nm in a spectrophotometer (Thermo Multiskan MK3, USA) with bovine serum albumin (BSA) as a standard, according to Bradford (1976).

Analysis of Free Proline

Free proline content was determined according to the method of Bates et al. (1973). Shoots with leaves (0.5 g FW) were homogenized with 10 ml of 3% (w/v) sulfosalicylic acid. The

homogenate was centrifuged at 3000 rpm for 20 min. The supernatant was treated with acid ninhydrin in boiling water for 1 h. The reaction was terminated in a water bath at a room temperature for 10 min. The reaction mixture was extracted with 4 ml of toluene and vortexed for 15 s. The absorbance was determined at 520 nm in a spectrophotometer (Thermo Multiskan MK3, USA) using L-proline as a standard.

Analysis of Cell Membrane Damage (CMD) and Cell Death

Roots (0.5 g FW) were used for analysis of cell membrane damage (CMD) by measuring relative electrolytic leakage (EL), according to the method of Sullivan (1972). Cell death was detected by Evan's blue staining method (Gaff and Okong'O-Ogola, 1971). Samples were immersed in 0.1% Evan's blue solution for 30 min, and then washed with distilled water for 3 times to stop the color reaction. Staining reaction was photographed using a digital camera (PowerShot G9, Canon, Japan).

O_2^- and H_2O_2 Localization *In situ*

Fresh leaves were used for O_2^- and H_2O_2 localization *in situ*, according to the method of Romero-Puertas et al. (2004), with some modifications. For O_2^- localization, leaves were immersed in 0.1% solution of nitroblue tetrazolium (NBT) in 10 mM K-phosphate buffer (pH 7.6), vacuum-infiltrated for 30 min and illuminated for 2 h, followed by bleaching in 95% boiling ethanol for 5 min. For H_2O_2 localization, leaves were immersed in a 0.1% filtered solution of 3, 3'-diaminobenzidine (DAB) in 10 mM MES buffer (pH 5), vacuum-infiltrated for 30 min and then incubated at room temperature for 4 h in the dark, followed by bleached in 95% boiling ethanol for 5 min. Photographs were captured by a digital camera (PowerShot G9, Canon, Japan).

Analysis of Antioxidant Enzyme Activities

The activities of superoxide dismutase (SOD), peroxidase (POD), catalase (CAT) were measured, as described by Li et al. (2011). Fresh leaves (0.5 g FW) were harvested from 2-week-old plantlets grown at 0 and 4% PEG, ground in liquid nitrogen and extracted with following extraction media: 100 mM potassium phosphate buffer (pH 7.8) containing 0.1 mM EDTA, 1% (w/v) PVP and 0.1% (v/v) Triton x100. The extracts were centrifuged at 10,000 rpm for 15 min at 4°C. The supernatants were collected and used for the enzyme activity assays.

The SOD activity was determined by measuring its ability to inhibit photochemical reduction of nitrobluetetrazolium (NBT). The reaction mixture (3 ml) contained 0.3 ml each of 20 μ M riboflavin, 150 mM l-methionine, 600 μ M NBT and 0.1 ml extract, and performed under irradiance of 170 μ mol photons $m^{-2} s^{-1}$ provided by white fluorescent lamps. The absorbance was determined at 560 nm. The extract volume causing 50% inhibition of NBT reduction was taken as one unit of activity. The POD activity was measured in the reaction mixture (3 ml) containing 50 mM phosphate buffer (pH 7.0), 0.2 mM guaiacol, 10 mM H_2O_2 . The reaction was initiated by adding 200 μ l of enzyme extract to the reaction mixture. The oxidation of guaiacol was measured upon an increase in absorbance at 470 nm for 1 min. The CAT activity was determined by directly measuring

the decomposition of H_2O_2 at 240 nm in a spectrophotometer (Thermo Multiskan MK3, USA). The reaction mixture (3 ml) contained 0.05 M Na phosphate buffer (pH 7.0) supplemented with 1 mM EDTA, H_2O_2 (3%) and 100 μ l of enzyme extract.

Analysis of Methane Dicarboxylic Aldehyde (MDA)

The MDA content was determined according to Li et al. (2011). Briefly, leaves (1.0 g FW) taken from 2-week-old plantlets grown at 0 and 4% PEG were homogenized in 10 ml of 10% trichloroacetic acid, followed by centrifugation at 10000 rpm for 10 min. After then, 2 ml of 0.6% thiobarbituric acid in 10% trichloroacetic acid were added to 2 ml of the supernatant. The mixture was heated in boiling water for 15 min, and then quickly cooled in an ice bath. After centrifugation at 10,000 rpm for 10 min, the absorbance of the supernatant was recorded at 450 nm, 532 nm and 600 nm in a spectrophotometer (Thermo Multiskan MK3, USA). The MDA concentration was calculated using the following formula: $6.45(OD\ 532 - OD\ 600) - 0.56OD450$.

Analysis of Endogenous Hormones

Contents of endogenous ABA and IAA were analyzed in the *in vitro* plantlets grown at 0 and 4% PEG. Shoots with leaves were taken from 1-week-old plantlets and divided into two groups. One group was used for analysis of ABA and IAA, and the other for measurement of transcription level of ABA and IAA biosynthetic genes, as described below. Samples were frozen in liquid nitrogen and stored at -80°C until usage. Abscisic acid (ABA) and indoleactic acid (IAA) were provided by Sigma (St. Louis, MO, USA). At the beginning of extraction, 1000 Bq of each ABA and IAA, accordingly, were added to monitor the losses during purification. The extraction and purification of ABA and IAA were conducted, according to Dobrev et al. (2005). The purified extract solution was transferred into 2-ml centrifuge tubes containing 0.3 g polyvinylpolypyrrolidone (PVPP) and then kept at -20°C for the measurements of ABA and IAA in water breeze HPLC system (Waters 2489 UV/Visible Detector), using wavelength at 254 nm, velocity at 0.7 ml min^{-1} and sample quantity of 10 μm and column temperature at 30°C . The dried fraction containing ABA and IAA were, respectively, injected into the HPLC system for measurements, as described by Li et al. (2013).

Analysis of Transcription Level of ABA and IAA Biosynthetic Genes

The transcription levels of several major genes responsible for biosynthesis of ABA and IAA were analyzed in the *in vitro* plantlets grown at 0 and 4% PEG at different time durations. RNA was isolated from shoots with leaves (1 g FW), as described by Davies and Robinson (1996). RNA quality was evaluated by optical density (OD) value (1.9–2.1) at 260/280 nm. After removal of DNA using DNA Eraser (Takara, Japan), cDNA was synthesized using the reagent kits (RR047A, Takara, Japan) according to the manufacturer's instructions. All the candidate primers and reference genes of ABA and IAA biosynthesis pathway were selected according to the existing studies (**Table 1**). The reagent kits (RR047A, Takara) were used for qPCR reaction

TABLE 1 | Primers used for qRT-PCR analysis of ABA and IAA in *in vitro* plantlets of grape 'Cabernet Sauvignon'.

Primer names	References	Sequence 5'-3' (forward/reverse)	PN40024 12X V1 ID*	Coordinates*
VvNCED1	Wheeler et al., 2009	GAGACCCCAACTCTGGCAGG/ AAGGTGCCGTGGAATCCATAG	VIT_19s0093g00550	chr19:17645348..17647649
VvNCED2	Wheeler et al., 2009	AGTTCCATACTGGGTTCATGG/ CCATTTCCAATCCAGGGTGT	VIT_10s0003g03750	chr10:6374432..6376728
VvZEP	Wheeler et al., 2009	TACCGGGTATTTGGGACA/ CTTCTTCATCCGTGGCAAGT	VIT_07s0031g00620	chr7:16795707..16804559
VvTAR2	Böttcher et al., 2013	CAGCAATGAAGCATATTGAAGG/ GAGTGAGAGCACCAGGAAATG	VIT_17s0000g08990	chr17:10559797..10565113
VvTAR3	Böttcher et al., 2013	CCCAAGATGACT TTGATATGCTG/ TGATCAACTGATTGTTGATTCCACT	VIT_18s0157g00090	chr18:18858918..18864125
VvTAR4	Böttcher et al., 2013	CAGCCTCATCAAGACCCAAGAT/ TGACGGTTGATTCTTCTCG	VIT_18s0157g00170	chr18:18980507..18985732
VvYUC1	Böttcher et al., 2013	CAGGAAACTGTCGCAATAGTGG/ CAAGAACATGTTGGTATTGAGAGG	VIT_07s0104g01250	chr7:2276803..2279543
VvACTIN2	Böttcher et al., 2011	GCACCCTTCG CACGATATGA/ TGACGCAAGGCAAGGACTGA	VIT_04s0044g00580	chr4:21427077..21431176

*Means V1 annotations obtained from CRIBI (<http://genomes.cribi.unipd.it/grape/>) by a BLAST search of the gene sequence provided by NCBI (<http://www.ncbi.nlm.nih.gov>).

(IQ5, BIO-RAD, USA) in a 25 μ l reaction mixture containing 12.5 μ l of 2 \times SYBR Green I Master Mix, 1 μ l of each primer (0.4 μ M), 2 μ l of cDNA (100 ng) and 8.5 μ l of RNase-free water according to the kits instructions. The following program was used: an initial denaturation step at 94°C for 30 s, 45 cycles at 94°C for 10 s, 56°C for 10 s and 72°C for 30 s. A melting curve analysis was carried out over the range 65–97°C to verify the specificity of amplicons. Two controls (no-RT and no-template) were included in the designs. Transcript levels of each gene were normalized according to the reference gene, using the 2-(Δ -Delta C (T) method (Livak and Schmittgen, 2001).

Experimental Design and Data Analysis

Since some of the leaves at the basal part of the diseased shoots showed GLRaV-3 symptoms when grown under PEG-induced stress (Cui et al., 2015), symptomless leaves were used in all experiments. The experiments determining effects of virus and drought stress on vegetative growth of *in vitro* plantlets were designed as a completely randomized design. Ten samples were included in each of three replicates and the whole experiment was repeated at least twice. In all experiments measuring contents of total soluble protein, proline and MDA, activities of SOD, POD and CAT, endogenous hormones and transcript levels of ABA and IAA biosynthetic genes, each treatment contained five biological replicates and repeated three times in each experiment. Statistical analysis of the data was performed with the SPSS-19 for Windows statistics software package. Significant differences among means were calculated by the least significant difference (LSD) at $P \leq 0.05$. Two-way ANOVA, including GLRaV-3 infection and drought as factors, was performed to analyze the combined effects of these two factors on some selected parameters. Two-way MANOVA was performed for the vegetative growth. Significant differences were analyzed at $P \leq 0.05$ and $P \leq 0.01$, respectively.

RESULTS

Vegetative Growth and Root Formation

Without PEG stress, time duration required for axillary bud elongation was much shorter in the healthy shoots (4.5 days) than in GLRaV-3 infected ones (6.1 days; **Figure 1A**). No significant

differences were found in this parameter in the healthy shoots grown at 0% and 2% PEG, but PEG at 4% considerably delayed the time duration for axillary bud elongation (5.8 days). A similar pattern in axillary bud elongation was found in the diseased shoots grown at 2–4% PEG, but the negative effect was much stronger (**Figure 1A**). Shoot length was similar between the healthy and diseased shoots without PEG stress (**Figure 1B**). In the healthy shoots, shoot length markedly decreased as PEG concentrations increased from 0 to 4% (**Figure 1B**). This inhibitory effect exerted by PEG stress was much stronger on the infected shoots than on the healthy shoots (**Figure 1B**). When grown at 0% PEG, the healthy and virus infected shoots produced a similar number of roots (**Figure 1C**). Number of roots significantly decreased in the healthy shoots when grown at 2–4% PEG (**Figure 1C**). Negative effects of PEG concentrations on the number of roots were much pronounced in the infected shoots than in the healthy ones (**Figure 1C**). The healthy shoots without PEG stress produced greater length of the longest roots than the virus infected ones (**Figure 1D**). Length of the longest roots was similar in the healthy shoots grown at 0 and 2% PEG (**Figure 1D**), but 4% PEG resulted in much shorter length of the longest roots (**Figure 1D**). Co-stress by the virus and 4% PEG resulted in the shortest length of roots (**Figure 1D**). Without PEG stress, fresh weight (FW) of shoots was significantly greater in the healthy shoots than that of the virus infected ones (**Figure 1E**), and markedly reduced in the healthy shoots as PEG concentrations increased from 0 to 4%. Influences exerted by co-stress of the virus and drought on FW of roots were similar to those of FW of shoots (**Figure 1F**). Without PEG, the dry weight (DW) of the healthy shoots was greater than that of the virus infected shoots (**Figure 1G**), and it decreased when grown at 2–4% PEG. The DW of the infected shoots also decreased as PEG concentrations increased from 2 to 4%. There was no significant difference in DW of roots between the healthy and diseased shoots without PEG stress (**Figure 1H**). The DW of roots in both the healthy and infected shoots considerably reduced as PEG concentrations elevated from 0 to 2–4% (**Figure 1H**). Two-way MANOVA of all data on vegetative growth showed that single GLRaV-3 infection and PEG-induced drought, singly, and GLRaV-3 in combination with PEG all had significantly ($P \leq 0.01$) negative effects on vegetative growth (**Table 2**).

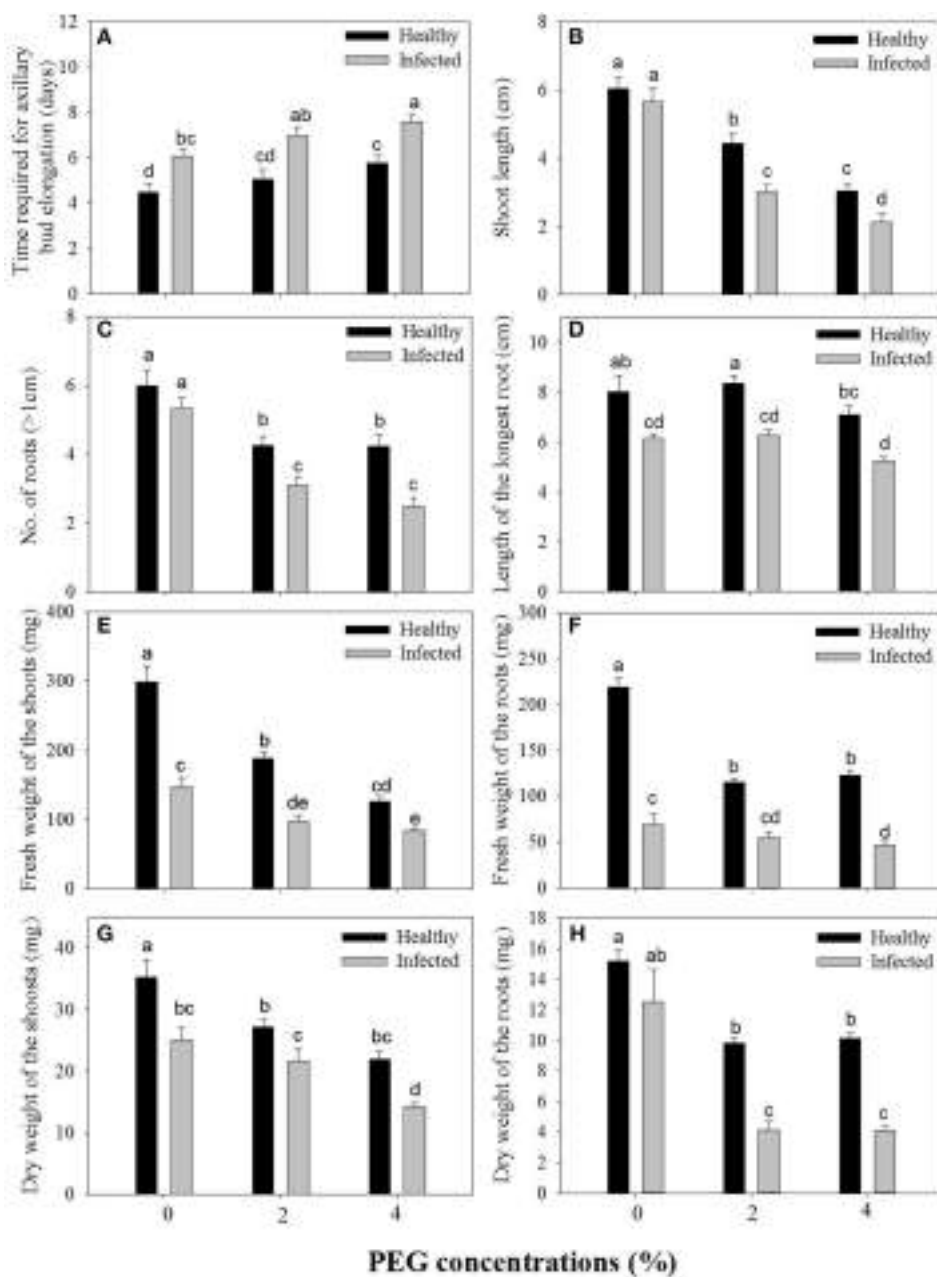


FIGURE 1 | Effects of GLRaV-3 infection and drought stress on shoot growth and root formation of *in vitro* plantlets of grape 'Cabernet Sauvignon'. (A) Time required for axillary bud elongation. (B) Shoot length. (C) Number of roots. (D) Length of the longest root. (E) Fresh weight of the shoots. (F) Fresh weight of the roots. (G) Dry weight of the shoots. (H) Dry weight of the roots. Data were presented as means \pm SE and with different letters within the same parameter are significantly different at $P \leq 0.05$.

Content of Total Soluble Protein and Free Proline

A significant difference was found in content of total soluble protein between the healthy and virus-infected shoots without PEG stress (Figure 2A). In the healthy shoots, marked reductions were found in content of total soluble protein only when grown at 4% PEG. In the infected shoots, PEG concentrations at 2–4% caused considerable decreases in contents of total soluble

protein (Figure 2A). Content of free proline was similar in the healthy and diseased shoots without PEG stress (Figure 2B). In the healthy shoots, PEG at 2–4% significantly increased accumulations of free proline (Figure 2B). Levels of free proline considerably increased in the virus-infected shoots as PEG concentrations increased from 0 to 4% (Figure 2B). Two-way ANOVA showed that virus infection and PEG stress, and virus infection in combination with PEG stress had significant negative

TABLE 2 | Two-way MANOVA of effects of GLRaV-3 and PEG-induced drought, and their combining effects on all variables of vegetative growth of *in vitro* plantlets of grape 'Cabernet Sauvignon'.

Parameters	Wilks' Lambda	F	p
Virus	0.031	66.690	**
Drought	0.008	22.241	**
Virus-drought	0.003	37.855	**

**Significant difference at $P \leq 0.01$.

effects on contents of both total soluble protein and free proline (Table 3).

Cell Membrane Damage and Cell Death

Relative electrolytic leakage (EL) was similar in the healthy and diseased shoots without any stress (Figure 2C). Stress by PEG concentrations at 2 and 4% produced increased EL comparing to 0% PEG in the healthy shoots. The similar pattern of EL was found in the diseased shoots grown under 2–4% PEG concentrations, but the negative effect was much more obvious.

Blue color forms when dead cells are stained by Evan's blue solution. Without PEG stress, almost no blue color was seen in the healthy roots (Figure 3A), but some light blue color was observed in GLRaV-3 infected roots (Figure 3B). Density and areas of blue color formation increased with increasing PEG concentrations from 2 to 4% in both the healthy (Figures 3C,E) and virus-infected roots (Figures 3D,F). The virus-infected roots had a much stronger blue color and larger areas than the healthy roots that were treated by the same concentrations of PEG. When grown at 4% PEG, almost the whole roots infected by GLRaV-3 became blue (Figure 3F).

O_2^- and H_2O_2 Localization *In situ*

Production of O_2^- in the leaves is visualized with NBT staining to give rise to dark blue spots. Without PEG stress, O_2^- accumulation was hardly detected in the healthy leaves (Figure 4A), but it was easily seen in the diseased leaves (Figure 4B). In the healthy leaves, O_2^- accumulation considerably increased with an increase in PEG concentrations from 2% (Figure 4C) to 4% (Figure 4E). A similar pattern was found in the diseased leaves, but staining density and stained areas were much stronger (Figure 4D) and larger (Figure 4F) than in the corresponding healthy samples. Production of H_2O_2 in the leaves is visualized with DAB staining to give rise to brown spots. Without PEG, H_2O_2 accumulation in the virus-infected leaves (Figure 5B) was stronger than that in the healthy leaves (Figure 5A). Although, PEG stress at 2–4% markedly increased H_2O_2 accumulation in both the healthy and infected leaves, staining density and strained areas were much stronger and larger in the virus-infected leaves than in the healthy leaves that were stressed by the corresponding PEG concentrations (Figures 5C–F).

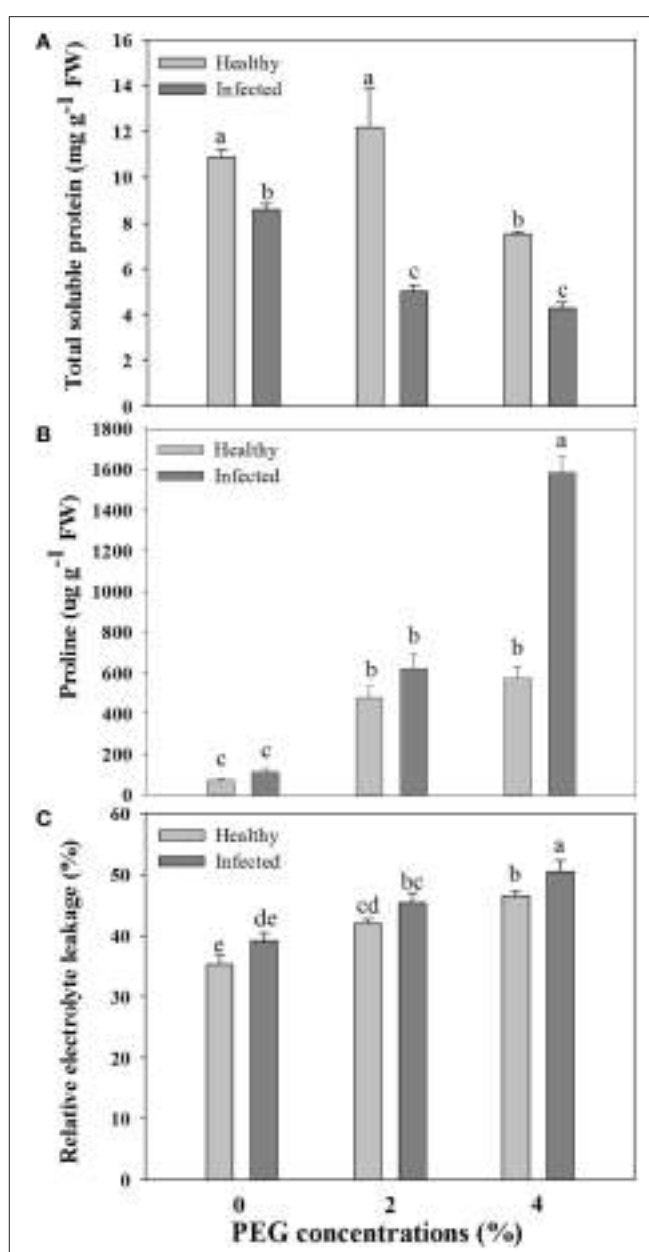


FIGURE 2 | Effects of GLRaV-3 infection and drought stress on contents of total soluble protein (A), proline (B), and relative electrolyte leakage (C) of *in vitro* plantlets of grape 'Cabernet Sauvignon'. Data are presented as means \pm SE and with different letters are significantly different at $P \leq 0.05$.

Activities of Antioxidant Enzymes and Content of MDA

Without PEG stress, no significant differences were found in the activities of SOD, POD, and CAT between the virus-infected and healthy plantlets (Figures 6A–C). For the healthy plantlets, 4% PEG resulted in significant increases in the activities of SOD and POD, although not in CAT (Figures 6A–C). For the diseased plantlets, the activities of SOD, POD, and CAT significantly increased when stressed by PEG 4%. No differences were found

TABLE 3 | Two-way ANOVA of effects of GLRaV-3 and drought, and their combining effects on indexes of in vitro plantlets shoots of grape ‘Cabernet Sauvignon’.

Contents of Influenced indexes	Virus	Drought	Virus-Drought
Total soluble protein	**	**	*
Proline	**	**	**
SOD	**	**	*
POD	**	**	**
CAT	**	**	**
MDA	**	**	**
ABA	**	**	**
IAA	**	**	ns

**Significant difference with levels of $P \leq 0.01$; *Significant difference with levels of $P \leq 0.05$; ns = no significant difference.

in MDA contents between the healthy and diseased plantlets without PEG stress (Figure 6D). MDA contents were found much higher both in the healthy and the diseased plantlets grown at 4% PEG, (Figure 6D). Two-way ANOVA showed that single stress by either the virus or PEG significantly ($P \leq 0.01$) changed the activities of SOD, POD, and CAT, and increased MDA content (Table 3). Co-stress by the virus and PEG had significantly ($P \leq 0.01$) negative effects on those of POD, CAT and MDA, as well as on SOD ($P \leq 0.05$) (Table 3).

Contents of ABA and IAA, and Expression Levels of ABA and IAA Biosynthetic Genes

Without PEG stress, virus infection caused significant ($P \leq 0.05$) increase and decrease in the content of ABA and IAA (Figures 7A,B), respectively. For the healthy plantlets, the content of ABA was significantly higher, while that of IAA was much lower, in the plantlets grown at 4% PEG than at 0% PEG (Figures 7A,B). Similar patterns of ABA and IAA levels were found in the virus-infected plantlets grown at 0 and 4% PEG (Figures 7A,B). Two-way ANOVA showed that PEG stress or the virus infection and their co-stress all significantly ($P \leq 0.01$) increased ABA content; the virus infection or drought stress significantly ($P \leq 0.01$) decreased IAA level, but there was no interaction between them on IAA level (Table 3).

For ABA biosynthesis genes, without PEG stress, expression levels of NCED1 were relatively stable in the healthy plantlets during 1 week of culture, and peaked at 96 h of culture and then reduced in the virus infected plantlets (Figure 8A). Patterns of expression levels of NCED2 and ZEP were similar to those of NCED1 in the healthy plantlets (Figures 8B,C). In the diseased plantlets, expression levels of NCED2 started to increase at 48 h of culture and the increased levels maintained up to 1 week of culture (Figure 8B). Expression levels of ZEP were hardly detected until 48 h of culture, and relatively increased during 96 h and 1 week of culture (Figure 8C). PEG stress markedly induced expression levels of NCED1, NCED2, and ZE in both the healthy and diseased plantlets (Figures 8A–C). The highest expression levels appeared for NCED1 between 48 to 96 h in both the healthy and diseased plantlets (Figure 8A), for NCED2 at 48 and 96 h in the infected and healthy plantlets, respectively

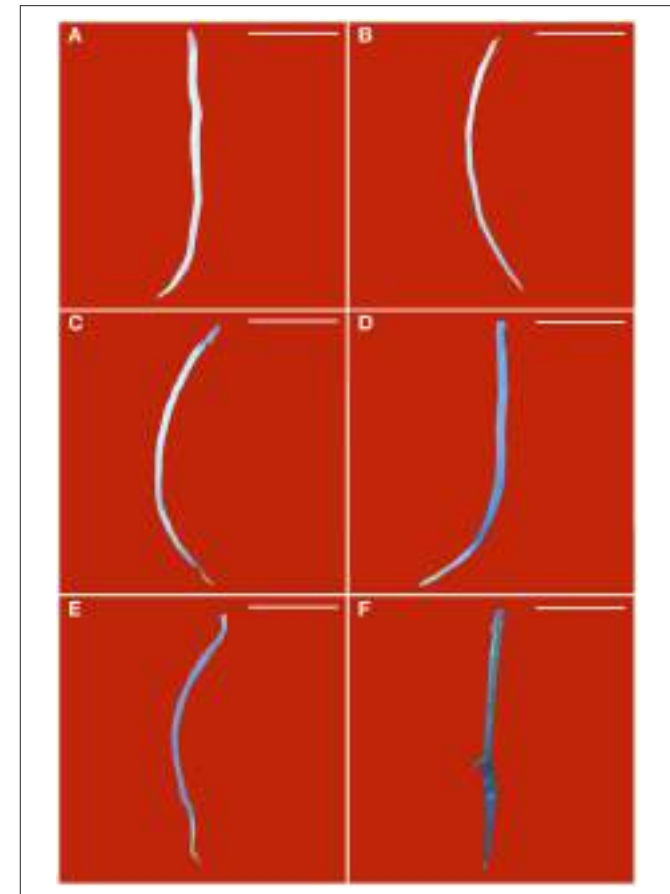


FIGURE 3 | Histochemical detection of cell death in roots of *in vitro* plantlets of grape ‘Cabernet Sauvignon’. Cell death in the roots was revealed by the blue precipitates produced by staining with Evan’s blue. Roots of the healthy shoots cultured at 0% (A), 2% (C), and 4% PEG (E). Roots of GLRaV-3-infected shoots cultured at 0% (B), 2% (D), and 4% PEG (F). Bar scale = 1 cm.

(Figure 8B), for ZEP at 96 h in the two types of plantlets (Figure 8C). For IAA biosynthesis genes, without PEG stress, higher expression levels of TAR2, TAR3, TAR4, and YUC1 were detected in the healthy than in the diseased plantlets during the whole culture time durations (Figures 9A–D). Expression levels of TAR2, TAR3, and TAR4 started to increase at 24 h, peaked at 96 h of culture and then decreased, while those of YUC1 peaked at 24 h and gradually decreased during 24 h to 1 weeks of culture (Figure 9D). PEG stress consistently reduced the expression levels of all the four genes in both the healthy and diseased plantlets during the whole culture durations, with more obviously reduced levels found in the diseased plantlets (Figures 9A–D).

DISCUSSION

Although, *in vitro* culture conditions largely differ from the field environments and responses of *in vitro* cultures to abiotic or biotic stress may differ from those of the field-grown plants in some cases (Suzuki et al., 2014), the former has been widely used

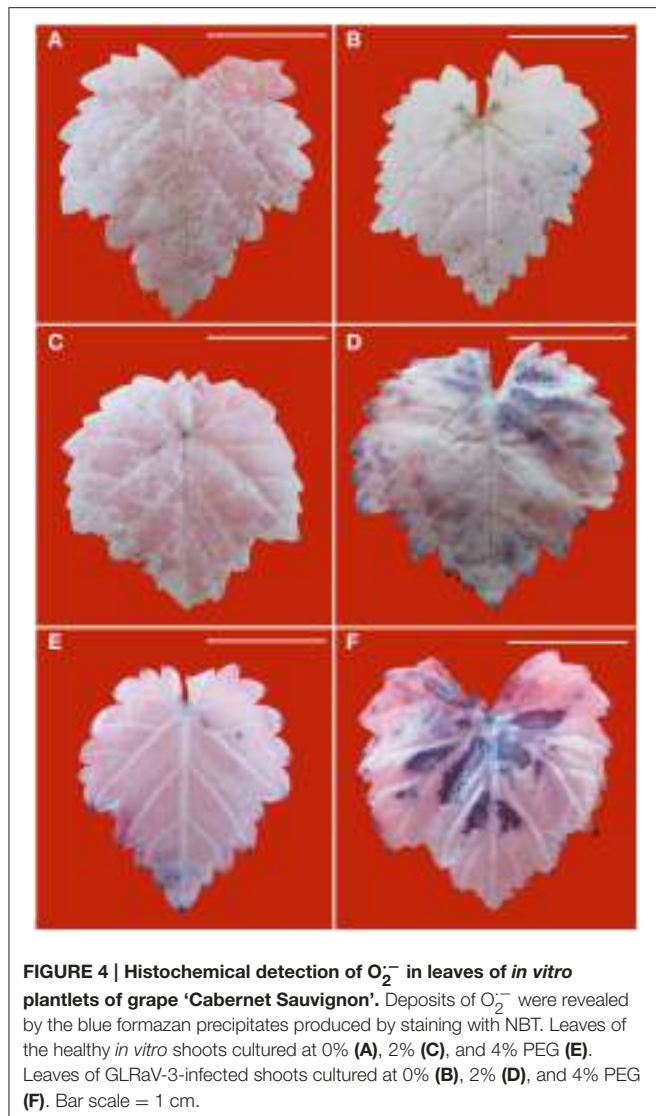


FIGURE 4 | Histochemical detection of O_2^- in leaves of *in vitro* plantlets of grape 'Cabernet Sauvignon'. Deposits of O_2^- were revealed by the blue formazan precipitates produced by staining with NBT. Leaves of the healthy *in vitro* shoots cultured at 0% (A), 2% (C), and 4% PEG (E). Leaves of GLRaV-3-infected shoots cultured at 0% (B), 2% (D), and 4% PEG (F). Bar scale = 1 cm.

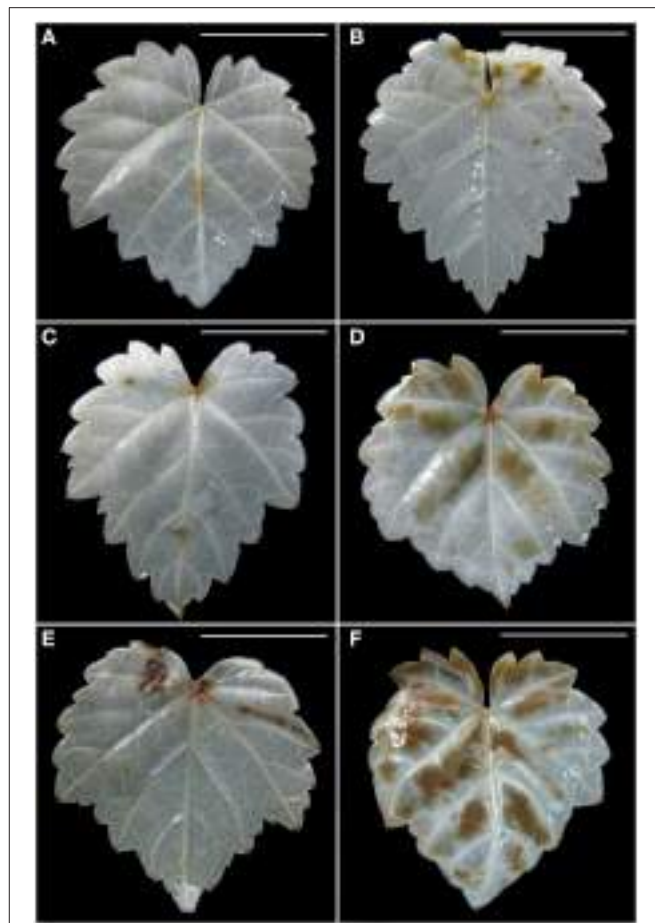


FIGURE 5 | Histochemical detection of H_2O_2 in leaves of *in vitro* plantlets of grape 'Cabernet Sauvignon'. H_2O_2 deposits were revealed by the brown precipitates produced by staining with DAB. Leaves of the healthy shoots cultured at 0% (A), 2% (C), and 4% PEG (E). Leaves of GLRaV-3-infected shoots cultured at 0% (B), 2% (D), and 4% PEG (F). Bar scale = 1 cm.

for studies on the said subjects (Watanabe et al., 2000; Khristov et al., 2001; Christov et al., 2007; Lu et al., 2007; Lokhande et al., 2010, 2011; Faraloni et al., 2011; Li et al., 2013; Marković et al., 2014; Cui et al., 2015), mainly due to its advantages that can avoid other variables such as light, temperature and nutrients, and by attacks of other pathogens facing in the field, in addition to its effects of efficient, rapid and low cost, thus facilitating studies of 'pure' biotic or abiotic stress (Watanabe et al., 2000; Khristov et al., 2001; Christov et al., 2007; Lokhande et al., 2010, 2011; Li et al., 2013; Cui et al., 2015). A recent study of Faraloni et al. (2011) found a high accordance between the *in vitro* and *in vivo* chlorophyll fluorescence measurements in monitoring changes in photosynthetic activity in response to drought stress.

Effects of single stress by either virus or drought on plant growth have been well-documented, but co-stress by pathogens like virus and drought to plants has been far less studied. Working on the several grapevine cultivars, Marković et al. (2014) found that the healthy *in vitro*-grown shoots had much better shoot growth than the GLRaV-3 or other virus infected

ones. Similar results have been reported in *in vitro* grapevine shoots infected by GLRaV-3 (Cui et al., 2015), *Grapevine leafroll* (Tanne et al., 1996), and *Grapevine fanleaf virus* (GFLV) (Abracheva et al., 1994). A number of examples of negative effects of virus infection on plant growth can be found in the publications of Watanabe et al. (2000), Li et al. (2013), and Cui et al. (2015). Reduced vegetative growth and slow rooting were observed in the *in vitro* grapevine shoots stressed by 2–6% PEG (Dami and Hughes, 1997) and by 4% sorbitol or 2–4% mannitol (Tanne et al., 1996). Inhibitory effects exerted by drought or osmotic stress on vegetative growth were much stronger in the grapevine leafroll infected shoots than in the healthy ones (Chaves et al., 2007; Cui et al., 2015). All of these results were consistent with ours.

Virus infection or drought stress has been found to influence levels of soluble protein. An increased level of soluble protein was noted in grapevine infected with GFLV and GLRaV-3 (Sampol et al., 2003) or GLRV (Bertamini et al., 2004; Moutinho-Pereira et al., 2012), in banana infected with BBTBV (Haq et al., 2012)

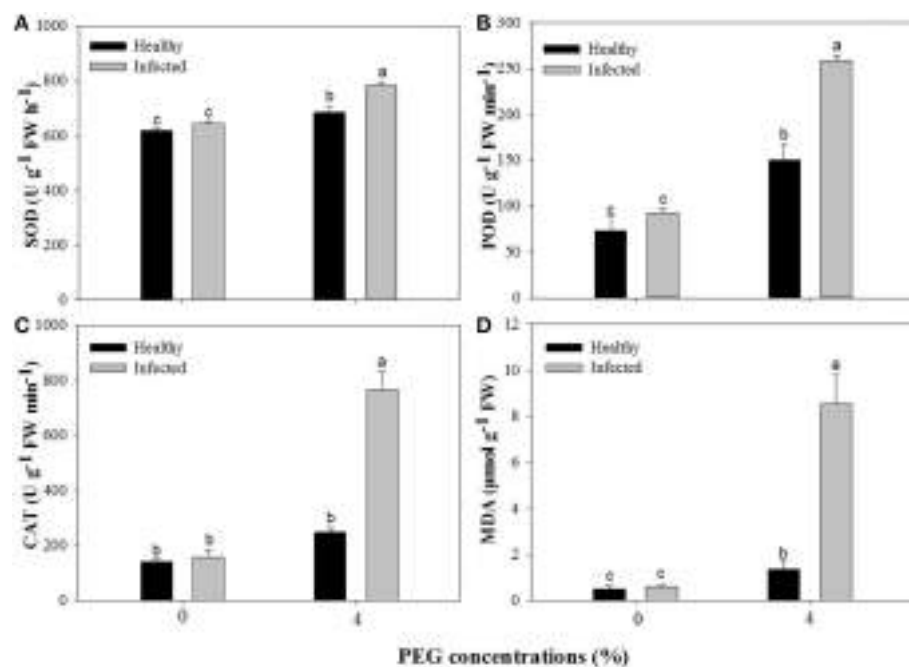


FIGURE 6 | Activities of superoxide dismutase (SOD, A), peroxidase (POD, B), catalase (CAT, C), and content of methane dicarboxylic aldehyde (MDA, D) of *in vitro* plantlets of grape 'Cabernet Sauvignon'. Data were presented as means \pm SE and with different letters within the same parameter are significantly different at $P \leq 0.05$.

and in potato infected with PLRV or PVY (Li et al., 2013). Similar results were also found in the present study. The decrease in synthesis of ribulose-1,5-bisphosphate (RuBP) carboxylase was found responsible for the marked reduction in the content of soluble proteins in the GLRV-infected samples (Bertamini et al., 2004). Decreased contents of total protein were observed in drought-stressed grapevine (Maroco et al., 2002) and other plants such as *Zea mays* (Hsiao, 1970), and *Gossypium hirsutum* (Parida et al., 2007). These data were again confirmed in our study. Drought stress caused marked changes in the protein synthesizing apparatus of plant tissue, thus reducing capacity for protein synthesis (Hsiao, 1970; Parida et al., 2007).

Our study found that drought stress and GLRaV-3 infection, singly or in combination, significantly increased proline contents. Increased proline contents by drought have been found in other plant species such as *Populus euphratica* (Watanabe et al., 2000), *Eucalyptus camaldulensis* (Woodward and Bennett, 2005) and *Capsicum annuum* (Fu et al., 2009), or by virus such as *Zucchini yellow mosaic virus* (ZYMV, Radwan et al., 2007). Proline accumulation generally is considered as a drought tolerance mechanism in plants (Chutia and Borah, 2012; Sun et al., 2013). Increased accumulation of proline was believed to be as an adaptive response to the stress, thus helping to maintain cell membrane integrity and protecting subcellular structures in drought-stressed plants (Chutia and Borah, 2012; Sun et al., 2013), and to activate a hypersensitive response (HR) to virus infection (Radwan et al., 2007).

Our results showed that GLRaV-3 infection did not significantly cause cell membrane damage and cell death,

but drought, singly or in combination with the virus, markedly increased cell membrane damage and induced cell death, particularly when GLRaV-3 infected shoots were stressed by 4% PEG. Programmed cell death (PCD) has been widely observed in response of the plants to pathogenic infection (Greenberg and Yao, 2004). The HR in response to virus infection is a typical example of PCD (Greenberg and Yao, 2004). Increased cell membrane damage and cell death have been well established in the plants infected with various viruses such as *Tobacco mosaic virus* (TMV)-infected *Nicotiana tabacum* (del Pozo and Lam, 2003), *Groundnut bud necrosis virus* (GBNV)-infected *Vigna unguiculata* (Permar et al., 2014) and *Soybean mosaic virus* (SMV)-infected *Glycine max* (Zhang et al., 2014). The HR is typically induced upon virus infection as in interaction between host encoded resistance (R) proteins and pathogen encoded avirulence proteins and functions to limit virus replication and thereby its eventual movement inside the host (Padder, 2014). Increased cell membrane damage and induced cell death by drought stress has also been found in other plants including *Saccharum officinarum* (Patade et al., 2008), *Arabidopsis* (Duan et al., 2010), and *Cucumis sativus* (Zhang et al., 2013). Drought stress-induced root cell death was suggested to be an adaptive response to the stress (Duan et al., 2010). Expression of *BAX inhibitor-1* (*AtB1I*) increased in response to water stress in roots of *Arabidopsis*, indicating that *AtB1I* and the endoplasmic reticulum (ER) response pathway reduced water stress-induced PCD (Duan et al., 2010).

MDA, a marker for lipid peroxidation, is frequently used as an indicator for measurement of cellular membrane damage (Masia,

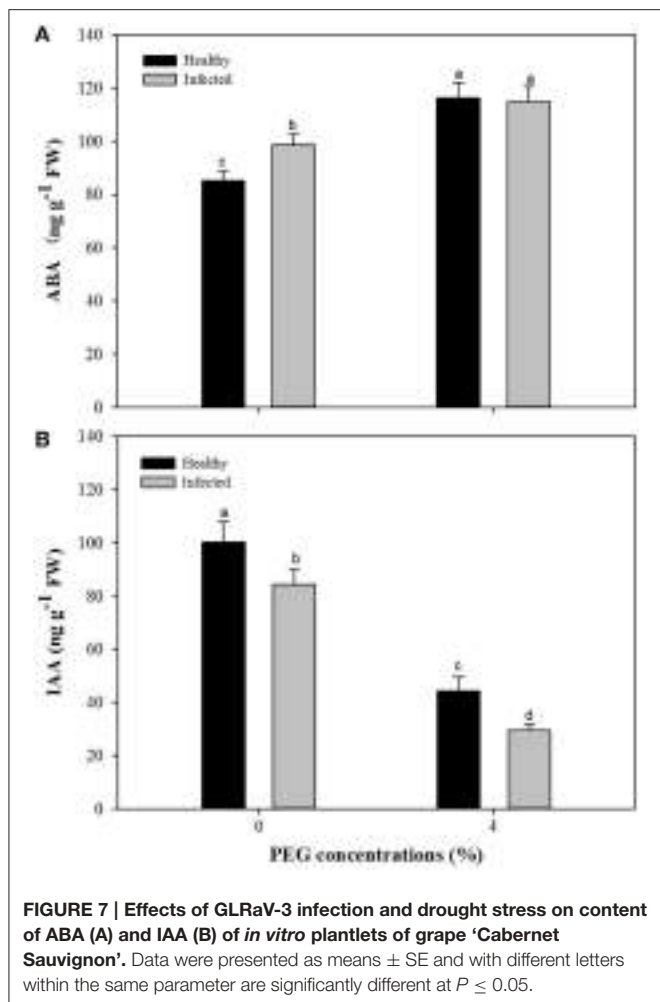


FIGURE 7 | Effects of GLRaV-3 infection and drought stress on content of ABA (A) and IAA (B) of *in vitro* plantlets of grape ‘Cabernet Sauvignon’. Data were presented as means \pm SE and with different letters within the same parameter are significantly different at $P \leq 0.05$.

2003). There have been many studies on drought-induced MDA, but data on virus-induced MDA have been quite limited. Huang et al. (2008) and Li et al. (2011) found the MDA level markedly increased in the plants under drought, indicating the occurrence of damage to cell membranes. These data were consistent with ours. In our study, virus infection did not cause significant accumulation of MDA, while 4% PEG resulted in significant increase in MAD and the increased MAD was much obvious in plantlets co-stressed by drought and the virus, indicating extra injury to cell membranes by the interaction of drought stress and virus-infection.

Reactive oxygen species (ROS), particularly O_2^- and H_2O_2 , are subproducts responding to abiotic and biotic stress (Bolwell et al., 1999). A number of studies have shown that accumulation of O_2^- and H_2O_2 considerably increased in plants infected by virus (Evans et al., 2006; Zhang et al., 2014) or stressed by drought (Duan et al., 2010; Gill and Tuteja, 2010; Sun et al., 2013; Noctor et al., 2014). In the present study, we found that stress by GLRaV-3 infection or drought increased the accumulation of O_2^- and H_2O_2 , and that accumulation was much greater when the *in vitro* shoots were stressed simultaneously by GLRaV-3 and PEG-induced drought. ROS has

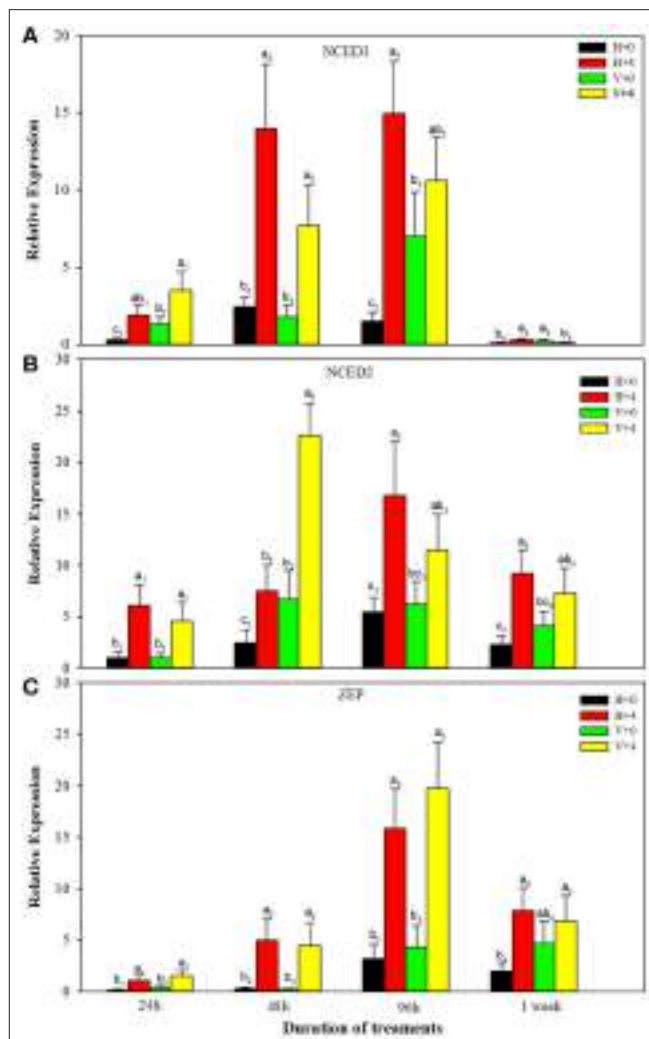
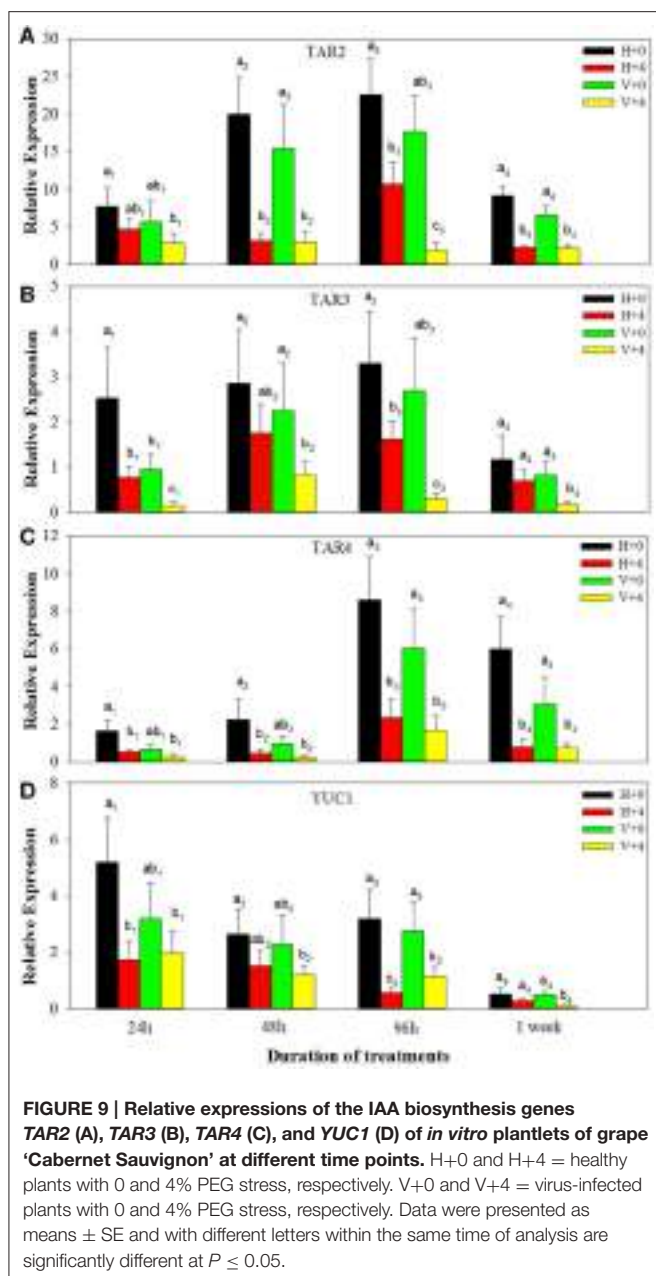


FIGURE 8 | Relative expressions of the ABA biosynthesis genes NCED1 (A), NCED2 (B), and ZEP (C) of *in vitro* plantlets of grape ‘Cabernet Sauvignon’ at different time points. H+0 and H+4 = healthy plantlets with 0 and 4% PEG stress, respectively. V+0 and V+4 = virus-infected plants with 0 and 4% PEG stress, respectively. Data were presented as means \pm SE and with different letters within the same time of analysis are significantly different at $P \leq 0.05$.

been shown to influence the expression of a number of genes and therefore manipulate various processes including growth, PCD, abiotic stress responses and pathogen defense (Gill and Tuteja, 2010). The production of ROS is the first response when plants are under biotic and abiotic stress (Gara et al., 2003; Evans et al., 2006), and as the stress continues, massive and prolonged ROS production, called an oxidative burst, occurs in the stressed cells (Gara et al., 2003). Accumulation of ROS in the virus-infected (Evans et al., 2006) or in abiotic-stressed plants may be associated with stress-induced oxidative bursts (Gara et al., 2003; Evans et al., 2006). Such oxidative bursts serve a number of protective functions activating defense responses of plants to biotic and abiotic stress (Gara et al., 2003).



Numerous studies have demonstrated that plants are able to protect against abiotic stress (Gill and Tuteja, 2010; Li et al., 2011) or biotic stress (Gonçalves et al., 2013; Kyseláková et al., 2013) by increasing the activities of antioxidant enzymes such as SOD, CAT, and POD. In the present study, we found that drought stress significantly increased the activities of SOD, POD, and CAT in both the healthy and diseased plantlets, but single virus infection increased slightly the activity of antioxidant enzymes. The increased activities of three antioxidant enzymes were much higher in the plantlets co-stressed by the drought and virus, indicating a strong need for ROS removal. Transgenic plants that showed increase in CAT or POD or SOD activity exhibited enhanced tolerance to drought or pathogen resistance

(Gill and Tuteja, 2010). SOD was believed to be the first line of defense against the toxic effects of elevated levels of ROS caused by abiotic or biotic stress (Gill and Tuteja, 2010).

ABA generally inhibits plant growth and is thought to act as a messenger when plants were stressed by either drought or virus (Jameson and Clarke, 2002; Zhu, 2002). Increased accumulation in ABA in plants under drought stress has been well-documented (Zhu, 2002), whereas there existed only a few studies on virus-induced ABA and no studies on changes of ABA levels in plants co-stressed by drought and virus (Jameson and Clarke, 2002). The present study confirmed again grapevine *in vitro* plantlets responded to drought stress by increasing ABA level, and found the level of ABA was higher in the GLRaV-3 infected plantlets than in the healthy ones. Similar results were also reported in plants infected with other viruses (Fraser and Whigham, 1989; Wang et al., 2011; Alazem et al., 2014). The increased levels of ABA were associated with up-regulation of ABA biosynthesis genes including NCED1, NCED2, and ZEP, which were the major genes for ABA biosynthesis in grapevine (Wheeler et al., 2009). These findings supported the speculation of Alazem et al. (2014) that the induction of ABA and up-regulation of the ABA biosynthesis genes may be common features of RNA virus infection. Increased levels of ABA in plants stressed by drought or infected with virus may eventually result in reduced growth, as found in the present study.

IAA can regulate diverse processes including growth, development and physiological metabolisms of plants (Kieffer et al., 2010; Swarup and Péret, 2012). Decreased IAA levels induced by drought stress have been reported in *Brassica napus* (Qaderi et al., 2006), *Phaseolus vulgaris* (Figueiredo et al., 2008), and *Cotinus coggygria* (Li et al., 2011). Reduced levels of IAA by virus infection were also found by Smith et al. (1968), Lockhart and Semancik (1970), Rao and Narasimham (1974), Rajagopal (1977), and Li et al. (2013). The results reported here were consistent with those mentioned above. The present study further found that co-stress by drought and virus resulted in much lower levels of IAA than single stress by either drought or virus, and down-regulation of expressions of IAA biosynthetic genes including TAR2, TAR3, TAR4, and YUC1 was associated with the decreased levels of IAA. Systemic virus infection was shown to influence the intercellular transport of the infected plants (Jameson and Clarke, 2002), which may prevent directional transport of auxin out of its source tissues, thus resulting in inhibition of shoot growth and root formation, as reported in the present study.

In conclusion, GLRaV-3 infection or drought stress reduced vegetative growth, affected physiological metabolisms, enhanced cell membrane damage and cell death, increased accumulation of H_2O_2 and O_2^- . Co-stresses by virus infection and drought cause much more deleterious effects, than either single stress, on the studied parameters. Analysis of total soluble protein, free proline, activities of antioxidant enzymes, MDA, levels of ABA and IAA and expressions of their biosynthetic genes provide insights into better understanding of the adverse effects of virus infection and drought, in single and in combination, on the grapevine *in vitro* plantlets. Results obtained in the present study address

use of virus-free plants and good irrigation toward achieving sustainable development of the grapevine.

AUTHOR CONTRIBUTIONS

ZC main work of all the experiments, data analysis and manuscript. WB phytohormone analysis and ROS gene expression analysis. XH the activity of the antioxidant enzymes YX design of the experiment and the financial support PL valuable discussion. AW the guide of the experiment and

manuscript revision. QW design of the experiment, revision of the manuscript and the financial support.

ACKNOWLEDGMENTS

The authors gratefully acknowledge financial supports through “948” program from State Forestry Administration of China (project No. 2013-4-41) and through from Department of Science & Technology of Shaanxi Province of China (Project No. 2013KTCL02-01).

REFERENCES

- Abracheva, P., Rozenova, L., and Todorova, M. (1994). The influence of grapevine fanleaf virus and stem pitting on *in vitro* grapevine cultures. *Vitis* 33, 181–182.
- Alazem, M., Lin, K.-Y., and Lin, N. S. (2014). The abscisic acid pathway has multifaceted effects on the accumulation of *Bamboo mosaic virus*. *Mol. Plant Microbe Interact.* 27, 177–189. doi: 10.1094/MPMI-08-13-0216-R
- Atkinson, N. J., and Urwin, P. E. (2012). The interaction of plant biotic and abiotic stresses: from genes to the field. *J. Exp Bot.* 63, 3523–3543. doi: 10.1093/jxb/ers100
- Bates, L. S., Waldren, R. P., and Teare, I. D. (1973). Rapid determination of free proline for water stress studies. *Plant Soil* 39, 205–208. doi: 10.1007/BF00018060
- Bertamini, M., Muthuchelian, K., and Nedunchezhian, N. (2004). Effect of grapevine leafroll on the photosynthesis of field grown grapevine plants (*Vitis vinifera* L. cv. Lagrein). *J. Phytopathol.* 152, 145–152. doi: 10.1111/j.1439-0434.2004.00815.x
- Bolwell, G. P., Blee, K. A., Butt, V. S., Davies, D. R., Gardner, S. L., Gerrish, C., et al. (1999). Recent advances in understanding the origin of the apoplastic oxidative burst in plant cells. *Free Radic. Res.* 31, S137–S145. doi: 10.1080/1071576990301431
- Böttcher, C., Boss, P. K., and Davies, C. (2011). Acyl substrate preferences of an IAA-amido synthetase account for variations in grape (*Vitis vinifera* L.) berry ripening caused by different auxinic compounds indicating the importance of auxin conjugation in plant development. *J. Exp. Bot.* 62, 4267–4280. doi: 10.1093/jxb/err134
- Böttcher, C., Burbidge, C. A., Boss, P. K., and Davies, C. (2013). Interactions between ethylene and auxin are crucial to the control of grape (*Vitis vinifera* L.) berry ripening. *BMC Plant Biol.* 13:222. doi: 10.1186/1471-2229-13-222
- Bradford, M. M. (1976). A rapid and sensitive method for the quantization of microgram quantities of protein utilizing the principle of protein-dye binding. *Anal. Biochem.* 72, 248–254. doi: 10.1016/0003-2697(76)90527-3
- Chaves, M. M., Santos, T., Souza, C. R., Ortúñoz, M. F., Rodrigues, M. L., Lopes, C., et al. (2007). Deficit irrigation in grapevine improves water-use efficiency while controlling vigour and production quality. *Ann. Appl. Biol.* 150, 237–252. doi: 10.1111/j.1744-7348.2006.00123.x
- Christov, I., Stefanov, D., Velinov, T., Goltsev, V., Georgieva, K., Abracheva, P., et al. (2007). The symptomless leaf infection with grapevine leafroll associated virus 3 in grown *in vitro* plants as a simple model system for investigation of viral effects on photosynthesis. *J. Plant Physiol.* 164, 1124–1133. doi: 10.1016/j.jplph.2005.11.016
- Chutia, J., and Borah, S. P. (2012). Water stress effects on leaf growth and chlorophyll content but not the grain yield in traditional rice (*Oryza sativa* Linn.) genotypes of Assam, India II. Protein and proline status in seedlings under PEG induced water stress. *Am. J. Plant Sci.* 3, 971–980. doi: 10.4236/ajps.2012.37115
- Cui, Z. H., Bi, W. L., Chen, P., Xu, Y., and Wang, Q. C. (2015). Abiotic stress improves *in vitro* biological indexing of Grapevine leafroll-associated virus-3 in red grapevine cultivars. *Aust. J. Grape Wine Res.* 21, 490–495. doi: 10.1111/ajgw.12146
- Dami, I., and Hughes, H. G. (1997). Effects of PEG-induced water stress on *in vitro* hardening of ‘Valiant’ grape. *Plant Cell Tiss. Org. Cult.* 47, 97–101. doi: 10.1007/BF02318944
- Davies, C., and Robinson, S. (1996). Sugar accumulation in grape berries: cloning of two putative vacuolar invertase cDNAs and their expression in grapevine tissues. *Plant Physiol.* 111, 275–283.
- del Pozo, O., and Lam, E. (2003). Expression of the baculovirus p35 protein in tobacco affects cell death progression and compromises N gene-mediated disease resistance response to Tobacco mosaic virus. *Mol. Plant Microbe Interact.* 16, 485–494. doi: 10.1094/MPMI.2003.16.6.485
- Dobrev, P. I., Havíček, L., Vágner, M., Malbeck, J., and Kaminek, M. (2005). Purification and determination of plant hormones auxin and abscisic acid using solid phase extraction and two-dimensional high performance liquid chromatography. *J. Chromat. A.* 1075, 159–166. doi: 10.1016/j.chroma.2005.02.091
- Duan, Y. F., Zhang, W. S., Li, B., Wang, Y. N., Li, K. X., Sodmergen, et al. (2010). An endoplasmic reticulum response pathway mediates programmed cell death of root tip induced by water stress in *Arabidopsis*. *New Phytol.* 186, 681–695. doi: 10.1111/j.1469-8137.2010.03207.x
- Evans, C., Malin, G., Graham, P., and Mills, G. P. (2006). Viral infection of *Emilia huxleyi* (Prymnesiophyceae) leads to elevated production of reactive oxygen species. *J. Phycol.* 42, 1040–1047. doi: 10.1111/j.1529-8817.2006.00256.x
- Faraloní, C., Cutino, I., Petruccelli, R., Leva, A. R., Lazzeri, S., and Torzillo, G. G. (2011). Chlorophyll fluorescence technique as a rapid tool for *in vitro* screening of olive cultivars (*Olea europaea* L.) tolerant to drought stress. *Environ. Experi. Bot.* 73, 49–56. doi: 10.1016/j.enexpbot.2010.10.011
- Figueiredo, M. V., Burity, H. A., Martínez, C. R., and Chanway, C. P. (2008). Alleviation of drought stress in the common bean (*Phaseolus vulgaris* L.) by co-inoculation with *Paenibacillus polymyxa* and *Rhizobium tropici*. *Appl. Soil Ecol.* 40, 182–188. doi: 10.1016/j.apsoil.2008.04.005
- Fraser, R. S. S., and Whennham, R. J. (1989). Abscisic-acid metabolism in tomato plants infected with tobacco mosaic virus: relationships with growth, symptoms and the *Tm-1* gene for TMV resistance. *Physiol. Mol. Plant Pathol.* 34, 215–226. doi: 10.1016/0885-5765(89)90045-3
- Fu, Q. S., Li, H. L., Cui, J., Zhao, B., and Guo, Y. D. (2009). Effects of water stress on photosynthesis and associated physiological characters of *Capsicum annuum* L. *Sci. Agric. Sin.* 42, 1859–1866. doi: 10.3864/j.issn.0578-1752.2009.05.046
- Gaff, D. F., and Okong’O-Ogola, O. (1971). The use of non-permeating pigments for testing the survival of cells. *J. Exp. Bot.* 22, 756–758.
- Gara, L. D., de Pinto, M. C., and Tommasi, F. (2003). The antioxidant systems vis-à-vis reactive oxygen species during plant-pathogen interaction. *Plant Physiol. Biochem.* 41, 863–870. doi: 10.1016/S0981-9428(03)00135-9
- Gill, S. S., and Tuteja, N. (2010). Reactive oxygen species and antioxidant machinery in abiotic stress tolerance in crop plants. *Plant Physiol. Biochem.* 48, 909–930. doi: 10.1016/j.plaphy.2010.08.016
- Gonçalves, L. S. A., Rodrigues, R., Diz, M. S. S., Robaina, R. R., do Amaral Júnior, A. T., Carvalho, A. O., et al. (2013). Peroxidase is involved in Pepper yellow mosaic virus resistance in *Capsicum baccatum* var. Pendulum. *Genet. Mol. Res.* 12, 1411–1420. doi: 10.4238/2013.April.26.3
- Greenberg, J. T., and Yao, N. (2004). The role and regulation of programmed cell death in plant-pathogen interactions. *Cell. Microbiol.* 6, 201–211. doi: 10.1111/j.1462-5822.2004.00361.x

- Hadidi, A., and Barba, M. (2011). "Economic impact of pome and stone fruit viruses and viroids," in *Virus and Virus-like Diseases of Pome and Stone Fruits*, eds A. Hadidi, M. Barba, T. Candresse, and W. Jelkman (St. Paul, MN: American Phyto pathological Society), 1–7.
- Haq, I. U., Nazia, P., Muhammad, T. R., and Muhammad, U. D. (2012). Comparative characteristics of micropropagated plantlets of banana from BBTV-infected explants to its normal and saline stressed cultures. *Pak. J. Bot.* 44, 1127–1130.
- Hsiao, T. C. (1970). Rapid changes in the levels of polyribosomes in *Zea mays* in response to water stress. *Plant Physiol.* 46, 281–285. doi: 10.1104/pp.46.2.281
- Huang, X., Yin, C., Duan, B., and Li, C. (2008). Interactions between drought and shade on growth and physiological traits in *Populus Cathayana* populations. *Can. J. Forest Res.* 38, 1877–1887. doi: 10.1139/X08-040
- Jameson, P. E., and Clarke, S. F. (2002). Hormone-virus interactions in plants. *Crit. Rev. Plant Sci.* 21, 205–228. doi: 10.1080/0735-260291044241
- Khrustov, I. K., Stefanov, D., Goltsev, V. N., and Abrasheva, P. (2001). Effects of grapevine fanleaf and stem pitting viruses on the photosynthetic activity of grapevine plants grown *in vitro*. *Russ. J. Plant Physiol.* 48, 473–477. doi: 10.1023/A:1016799329371
- Kieffer, M., Neve, J., and Kepinski, S. (2010). Defining auxin response contexts in plant development. *Curr. Opin. Plant Biol.* 13, 12–20. doi: 10.1016/j.pbi.2009.10.006
- Kyseláková, H., Sedlářová, M., Kubala, M., Nožková, V., Piterková, J., Luhová, L., et al. (2013). Reactive oxygen and nitrogen species and hormone signalling in systemic infection of pea by *Pea enation mosaic virus*. *Plant Protect. Sci.* 49, 105–119.
- Li, J. W., Wang, B., Song, X. M., Wang, R. R., Zhang, H., Zhang, Z. B., et al. (2013). Potato leafroll virus (PLRV) and Potato virus Y (PVY) influence vegetative, physiological metabolism of *in vitro*-cultured shoots of potato (*Solanum tuberosum* L.). *Plant Cell Tiss.* 114, 313–324. doi: 10.1007/s11240-013-0327-x
- Li, Y., Zhao, H., Duan, B., Korpelainen, H., and Li, C. (2011). Effect of drought and ABA on growth, photosynthesis and antioxidant system of *Cotinus coggygria* seedlings under two different light conditions. *Environ. Exp. Bot.* 71, 107–113. doi: 10.1016/j.enexpbot.2010.11.005
- Livak, K. J., and Schmittgen, T. D. (2001). Analysis of relative gene expression data using real-time quantitative PCR and the 2-(Delta Delta C (T)) method. *Methods* 25, 402–408. doi: 10.1006/meth.2001.1262
- Lockhart, B. E., and Semancik, J. S. (1970). Growth inhibition, peroxidase and 3-indoleacetic acid oxidase activity and ethylene production in cowpea mosaic virus infected cowpea seedlings. *Phytopathology* 60, 553–554. doi: 10.1094/Phyto-60-553
- Lokhande, V. H., Nikam, T. D., Patade, V. Y., Ahire, M. L., and Suprasanna, P. (2011). Effects of optimal and supra-optimal salinity stress on antioxidative defence, osmolytes and *in vitro* growth responses in *Sesuvium portulacastrum* L. *Plant Cell Tiss. Organ. Cult.* 104, 41–49. doi: 10.1007/s11240-010-9802-9
- Lokhande, V. H., Nikam, T. D., and Penna, S. (2010). Biochemical, physiological and growth changes in response to salinity in callus cultures of *Sesuvium portulacastrum* L. *Plant Cell Tiss. Organ. Cult.* 102, 17–25. doi: 10.1007/s11240-010-9699-3
- Lu, S., Peng, X., Guo, Z., Zhang, G., Wang, Z., Wang, C., et al. (2007). *In vitro* selection of salinity tolerant variants from triploid bermudagrass (*Cynodon transvaalensis* x *C. dactylon*) and their physiological responses to salt and drought stress. *Plant Cell Rep.* 26, 1413–1420. doi: 10.1007/s00299-007-0339-2
- Marković, Z., Preiner, D., Bošnjak, A. M., Safner, T., Stupić, D., Andabaka, Ž., et al. (2014). *In vitro* introduction of healthy and virus-infected genotypes of native Croatian grapevine cultivars. *Cent. Eur. J. Biol.* 9, 1087–1098. doi: 10.2478/s11535-014-0337-7
- Maroco, J. P., Rodrigues, M. L., Lopes, C., and Chaves, M. (2002). Limitations to leaf photosynthesis in field-grown grapevine under drought-metabolic and modeling approaches. *Funct. Plant Biol.* 29, 451–459. doi: 10.1071/PP01040
- Martelli, G. P. (2012). "Grapevine virology highlights: 2010–2012," in *Proceedings of the 17th Congress of ICSV* (Davis, CA), 13–31.
- Masia, A. (2003). "Physiological effects of oxidative stress in relation to ethylene in postharvest produce," in *Postharvest Oxidative Stress in Horticultural Crops*, ed D. M. Hodges (New York, NY: Food Products Press), 165–197.
- Michel, B. L. (1983). Evaluation of the water potentials of solutions of polyethylene glycol 8000 both in the absence and presence of other solutes. *Plant Physiol.* 72, 66–70. doi: 10.1104/pp.72.1.66
- Moutinho-Pereira, J., Correia, C. M., Gonçalves, B., Bacelar, E. A., Coutinho, J. F., Ferreira, H. F., et al. (2012). Impacts of leafroll-associated viruses (GLRaV-1 and -3) on the physiology of the Portuguese grapevine cultivar 'Touriga Nacional' growing under field conditions. *Annu. Appl. Biol.* 160, 237–249. doi: 10.1111/j.1744-7348.2012.00536.x
- Murashige, T., and Skoog, F. (1962). A revised medium for rapid growth and bioassays with tobacco cell cultures. *Physiol. Plant.* 15, 473–497. doi: 10.1111/j.1399-3054.1962.tb08052.x
- Noctor, G., Mhamdi, A., and Foyer, C. H. (2014). Roles of reactive oxygen metabolism in drought: not so cut and dried. *Plant Physiol.* 164, 1636–1648. doi: 10.1104/pp.113.233478
- Padder, B. A. (2014). Plant disease resistance genes: from perception to signal transduction. *Plant Signal.* 20, 345–354. doi: 10.1007/978-81-322-1542-4_20
- Parida, A. K., Dagaonkar, V. S., Phalak, M. S., Umalkar, G. V., and Aurangabadkar, L. P. (2007). Alterations in photosynthetic pigments, protein and osmotic components in cotton genotypes subjected to short-term drought stress followed by recovery. *Plant Biotech. Rep.* 1, 37–48. doi: 10.1007/s11816-006-0004-1
- Patade, V. Y., Suprasanna, P., and Bapat, V. A. (2008). Effects of salt stress in relation to osmotic adjustment on sugarcane (*Saccharum officinarum* L.) callus cultures. *Plant Growth Regul.* 55, 169–173. doi: 10.1007/s10725-008-9270-y
- Permar, V., Singh, A., Pandey, V., Alatar, A. A., Faisal, M., Jain, R. K., et al. (2014). Tospo viral infection instigates necrosis and premature senescence by micro RNA controlled programmed cell death in *Vigna unguiculata*. *Physiol. Mol. Plant Pathol.* 88, 77–84. doi: 10.1016/j.pmpp.2014.09.004
- Prasch, C. M. (2013). Simultaneous application of heat, drought, and virus to *Arabidopsis* plants reveals significant shifts in signaling networks. *Plant Physiol.* 162, 1849–1866. doi: 10.1104/pp.113.221044
- Qaderi, M. M., Kurepin, L. V., and Reid, D. M. (2006). Growth and physiological responses of canola (*Brassica napus*) to three components of global climate change: temperature, carbon dioxide and drought. *Physiol. Plant.* 128, 710–721. doi: 10.1111/j.1399-3054.2006.00804.x
- Radwan, D. E. M., Fayed, K. A., Mahmoud, S. Y., Hamad, A., and Lu, G. Q. (2007). Physiological and metabolic changes of *Cucurbita pepo* leaves in response to zucchini yellow mosaic virus (ZYMV) infection and salicylic acid treatments. *Plant Physiol. Biochem.* 45, 480–489. doi: 10.1016/j.plaphy.2007.03.002
- Rajagopal, R. (1977). Effect of tobacco mosaic virus infection on the endogenous levels of indoleacetic, phenylacetic and abscisic acids of tobacco leaves in various stages of development. *Z. Pflanzenphysiol.* 83, 403–409. doi: 10.1016/S0044-328X(77)80046-9
- Rao, M. R. K., and Narasimham, B. (1974). Endogenous auxin levels as influenced by infectious variegation in Lisbon lemon leaves. *South Ind. Hort.* 22, 138–139.
- Ren, F., Dong, Y.-F., Zhang, Z.-P., Fan, X.-D., Hu, G.-J., and Zhu, H.-J. (2013). Review of advances and perspectives in virus-resistant transgenic grapevine studies. *J. Hortic. Sci.* 40, 1633–1644.
- Romero-Puertas, M. C., Rodríguez-Serrano, M., Corpas, F. J., Gómezó, M., del Río, L. A., and Sandalio, L. M. (2004). Cadmium-induced subcellular accumulation of O²⁻ and H₂O₂ in pea leaves. *Plant Cell Environ.* 27, 1122–1134. doi: 10.1111/j.1365-3040.2004.01217.x
- Sampol, B., Bota, J., Riera, D., Medrano, H., and Flexas, J. (2003). Analysis of the virus-induced inhibition of photosynthesis in malmsey grapevines. *New Phytol.* 160, 403–412. doi: 10.1046/j.1469-8137.2003.00882.x
- Smith, S. H., McCall, S. R., and Harris, J. H. (1968). Auxin transport in curly top virus-infected tomato. *Phytopathology* 58, 1669–1670.
- Sullivan, C. Y. (1972). "Mechanism of heat and drought resistance in grain sorghum and methods of measurement," in *Sorghum in the seventies*, eds N. G. P. Rao and L. R. House (New Delhi: Oxford and IBH), 247–264.
- Sun, J., Guo, J., Zeng, J., Han, S., Song, A., Chen, F., et al. (2013). Changes in leaf morphology, antioxidant activity and photosynthesis capacity in two different drought-tolerant cultivars of chrysanthemum during and after water stress. *Sci. Hortic.* 161, 249–258. doi: 10.1016/j.scientia.2013.07.015
- Suzuki, N., Rivero, R. M., Shulaev, V., Blumwald, E., and Mittler, R. (2014). Abiotic and biotic stress combinations. *New Phytol.* 203, 32–43. doi: 10.1111/nph.12797
- Swarup, R., and Péret, B. (2012). AUX/LAX family of auxin influx carriers – an overview. *Front. Plant Sci.* 3:225. doi: 10.3389/fpls.2012.00225

- Tanne, E., Spiegel-Roy, P., and Shlamovitz, N. (1996). Rapid *in vitro* indexing of grapevine viral diseases: the effect of stress-inducing agents on the diagnosis of leafroll. *Plant Dis.* 80, 72–974. doi: 10.1094/P.D.-80-0972
- UNESCO Water Portal (2007). Available online at: <http://www.unesco.org/water> (Accessed 25 October 2007).
- Wang, S.-M., Hou, X.-L., Ying, L., Cao, X.-W., Zhang, S., and Wang, F. (2011). Effects of Turnip mosaic virus (TuMV) on endogenous hormones and transcriptional level of related genes in infected non-heading Chinese cabbage. *J. Nanjing Agric. Univ.* 5, 13–19. doi: 10.7685/j.issn.1000-2030.2011.05.003
- Watanabe, S., Kojima, K., Ide, Y., and Sasaki, S. (2000). Effects of saline and osmotic stress on proline and sugar accumulation in *Populus euphratica* *in vitro*. *Plant Cell Tiss.* 63, 199–206. doi: 10.1023/A:1010619503680
- Wheeler, S., Loveys, B., Ford, C., and Davies, C. (2009). The relationship between the expression of abscisic acid biosynthesis genes, accumulation of abscisic acid and the promotion of *Vitis vinifera* L. berry ripening by abscisic acid. *Aust. J. of Grape Wine Res.* 15, 195–204. doi: 10.1111/j.1755-0238.2008.00045.x
- Woodward, A. J., and Bennett, I. J. (2005). The effect of salt stress and abscisic acid on proline production, chlorophyll content and growth of *in vitro* propagated shoots of *Eucalyptus camaldulensis*. *Plant Cell Tiss.* 82, 189–200. doi: 10.1007/s11240-005-0515-4
- Xu, P., Chen, F., Mannas, J. P., Feldman, T., Sumner, L. W., and Roossinck, M. J. (2008). Virus infection improves drought tolerance. *New Phytol.* 180, 911–921. doi: 10.1111/j.1469-8137.2008.02627.x
- Zhang, K., Song, Y. P., Wang, Y., Li, K., Gao, L., Zhong, Y. K., et al. (2014). Differential necrotic lesion formation in soybean cultivars in response to Soybean mosaic virus. *Eur. J. Plant Pathol.* 139, 525–534. doi: 10.1007/s10658-014-0408-7
- Zhang, N., Zhao, B., Zhang, H. J., Weeda, S., Yang, C., Yang, Z. C., et al. (2013). Melatonin promotes water-stress tolerance, lateral root formation, and seed germination in cucumber (*Cucumis sativus* L.). *J. Pineal Res.* 54, 15–23. doi: 10.1111/j.1600-079X.2012.01015.x
- Zhu, J. K. (2002). Salt and drought stress signal transduction in plants. *Annu. Rev. Plant Biol.* 53, 247–273. doi: 10.1146/annurev.arplant.53.091401.143329

Conflict of Interest Statement: The authors declare that the research was conducted in the absence of any commercial or financial relationships that could be construed as a potential conflict of interest.

Copyright © 2016 Cui, Bi, Hao, Xu, Li, Walker and Wang. This is an open-access article distributed under the terms of the Creative Commons Attribution License (CC BY). The use, distribution or reproduction in other forums is permitted, provided the original author(s) or licensor are credited and that the original publication in this journal is cited, in accordance with accepted academic practice. No use, distribution or reproduction is permitted which does not comply with these terms.



A Halotolerant Bacterium *Bacillus licheniformis* HSW-16 Augments Induced Systemic Tolerance to Salt Stress in Wheat Plant (*Triticum aestivum*)

Rajnish P. Singh and Prabhat N. Jha*

Department of Biological Science, Birla Institute of Technology and Science, Pilani, India

OPEN ACCESS

Edited by:

Olivier Lamotte,
Centre Nationale de la Recherche
Scientifique – UMR Agroécologie,
France

Reviewed by:

Ashok Kumar,
Banaras Hindu University, India
Henk-jan Schoonbeek,
John Innes Centre (BBSRC), UK

***Correspondence:**

Prabhat N. Jha
prabhatn.jha@gmail.com;
prabhatjha@pilanibits-pilani.ac.in

Specialty section:

This article was submitted to
Plant Physiology,
a section of the journal
Frontiers in Plant Science

Received: 11 September 2016

Accepted: 30 November 2016

Published: 16 December 2016

Citation:

Singh RP and Jha PN (2016)
A Halotolerant Bacterium *Bacillus licheniformis* HSW-16 Augments
Induced Systemic Tolerance to Salt
Stress in Wheat Plant (*Triticum aestivum*). *Front. Plant Sci.* 7:1890.
doi: 10.3389/fpls.2016.01890

Certain plant growth promoting bacteria can protect associated plants from harmful effects of salinity. We report the isolation and characterization of 1-aminocyclopropane-1-carboxylic acid (ACC) deaminase bacterium *Bacillus licheniformis* HSW-16 capable of ameliorating salt (NaCl) stress in wheat plants. The bacterium was isolated from the water of Sambhar salt lake, Rajasthan, India. The presence of ACC deaminase activity was confirmed by enzyme assay and analysis of *AcdS* gene, a structural gene for ACC deaminase. Inoculation of *B. licheniformis* HSW-16 protected wheat plants from growth inhibition caused by NaCl and increased plant growth (6–38%) in terms of root length, shoot length, fresh weight, and dry weight. Ionic analysis of plant samples showed that the bacterial inoculation decreased the accumulation of Na⁺ content (51%), and increased K⁺ (68%), and Ca²⁺ content (32%) in plants at different concentration of NaCl. It suggested that bacterial inoculation protected plants from the effect of NaCl by decreasing the level of Na⁺ in plants. Production of exopolysaccharide by the *B. licheniformis* HSW-16 can also protect from Na⁺ by binding this ion. Moreover, application of test isolate resulted in an increase in certain osmolytes such as total soluble sugar, total protein content, and a decrease in malondialdehyde content, illustrating their role in the protection of plants. The ability of *B. licheniformis* HSW-16 to colonize plant root surface was examined by staining the bacterium with acridine orange followed by fluorescence microscopy and polymerase chain reaction-based DNA finger printing analysis. These results suggested that *B. licheniformis* HSW-16 could be used as a bioinoculant to improve the productivity of plants growing under salt stress.

Keywords: ACC deaminase, exopolysaccharide (EPS), *AcdS*, osmolytes, salt-stress, ERIC-PCR

INTRODUCTION

Soil salinity is one of the most important abiotic factors adversely affecting soil microbial activities and crop productivity. Reports suggest that >20% agricultural land worldwide is affected by salt (Pitman and Läuchli, 2002). It is estimated that the salinization will cause to the loss of 50% arability of agricultural land by middle of the 21st century (Wang et al., 2003). Saline soil adversely affects the plant growth and productivity by altering the normal metabolism of plants.

In plants, one of the effects of salt stress is an increase in the pool of 1-aminocyclopropane-1-carboxylic acid (ACC), a precursor of ethylene, which results in accumulation of ethylene. Increase in the level of ethylene beyond a threshold level is termed as 'stress ethylene', which inhibits growth of root and shoot (Penrose and Glick, 2003), suppresses leaf expansion (Peterson et al., 1991), alters photosynthesis and photosynthetic components (Koryo, 2006), and promotes epinasty (Abeles et al., 1992). In addition to salt stress, other stressors such as flood, drought, wounding, pathogen attack, temperature stress, and mechanical stress also lead to significant rise in the level of endogenous 'stress ethylene' (Morgan and Drew, 1997; Stearns and Glick, 2003).

Association of plant growth promoting bacteria (PGPB) equipped with ACC deaminase activity can have a tremendous effect on mitigating plant growth inhibition resulting from stress ethylene. Under salt stress condition, much of the ACC exudes out from plant roots where ACC deaminase (ACCD) bacteria can sequester and degrade ACC to α -ketobutyrate and ammonia, thus, decreasing the building up of stress ethylene in plants. Improvement in the growth of groundnut and red pepper plants by ACCD containing *Pseudomonas fluorescens* TDK1 and *Bacillus* sp. under salt stress have been reported in earlier studies (Saravanakumar and Samiyappan, 2007; Siddikee et al., 2011). Similarly, Nadeem et al. (2007) also reported a protective effect of ACC deaminase containing bacteria *Pseudomonas syringae*, *Enterobacter aerogenes* and *Pseudomonas fluorescens* on the growth of maize under salt stress conditions. Another experimental report of Gamalero et al. (2008) also suggested a plant growth stimulatory effect of *Pseudomonas putida* UW4 and *Gigaspora rosea* BEG9 on the growth of cucumber under salt stress condition. PGPB isolated from saline habitats can be adapted to tolerate the salt and hence increase plant resistance to salt stress. Mayak et al. (2004) reported that salt tolerant ACC deaminase bacteria help plants to overcome stress effects. Hence, higher ACC deaminase activity could be one of the primary mechanisms by which bacteria support plant growth under salt stress (Saleem et al., 2007).

High salinity induces both ionic and osmotic stresses on plants by stimulating the generation of reactive oxygen species (ROS), which finally cause the deleterious oxidative damage (Munns and Tester, 2008; Gill and Tuteja, 2010) in plants. It also alters gene expression in plants at both transcription and translation level (Fujita et al., 2006). A number of genes reported to be up-regulated by salt stress in plants have also been shown to be up-regulated by other types of abiotic stressors. However, many elements of gene regulation remain to be poorly understood (Huang et al., 2012). The plants have developed several physiological and biochemical mechanisms to combat salt and other stress conditions. These mechanisms include osmotic adjustment by secretion of osmolytes, selective ion uptake and compartmentalization of ions (Shabala et al., 2014). Plants accumulate low molecular weight compatible solutes termed as 'osmolytes' such as proline, sugars, polyols, trehalose, and quaternary ammonium compounds (QACs) such as glycine betaine, alanine betaine, proline betaine, hydroxyproline betaine, choline *o*-sulfate, and pipecolate betaine for osmotic adjustment to cope with salt stress (Wang et al., 2003; Parida and Das,

2005; Ashraf and Foolad, 2007). Certain PGPB can enable plants to cope with the salt stress by augmenting above mentioned strategies which protect plants from the damages caused by salt stress. Osmolytes mediated protective mechanism is still not fully understood, however, it generally favors the osmotic adjustment (Colmer et al., 1995). In addition, its role in stabilizing membrane lipids (Hincha et al., 2003), maintenance of redox potential (Yancey, 2005), free radicals scavenging (Smirnoff and Cumbes, 1989), binding toxic metals (Sharma and Dietz, 2006), and induction of transcription factors under stress responses (Gupta et al., 2012) have also been reported. To cope with salinity-induced oxidative damage, an increase in osmolytes is essential for mitigation of oxidative stress (Liu et al., 2011).

Other than the accumulation of stress ethylene, an increase in salinity also causes restriction of water uptake and toxicity of Na^+ (Mayak et al., 2004). Increased accumulation of Na^+ in salt-rich agricultural land promotes senescence of older leaves (Munns and Tester, 2008). PGPB can overcome the harmful effects of salinity by maintaining a favorable ratio of Na^+/K^+ ions amenable for plants growth and development under high salt levels (Mayak et al., 2004). Moreover, exopolysaccharides secreted by PGPB also reduce the amount of Na^+ available for plants uptake (Sutherland and Geddie, 1993; Lee and Han, 2005). It also acts as a protectant against ROS generated by stress conditions (Fujishige et al., 2006; Cooper, 2007) and is involved in other additional functions such as biofilm formation and colonization in plants (Cooper, 2007; Irie et al., 2012).

It is evident that PGPB can play an effective role in mitigating the unfavorable effect of stressors particularly salt stress through one or more mechanisms. Therefore, it requires the exploration of suitable bacterial strain(s) which can ameliorate salt stress in plants through one or more properties. The presence of plant growth promoting properties in PGPB includes nitrogen fixation, phosphate solubilization, phytohormone production, siderophore production, and biocontrol activities which help the plant grow in a sustainable manner. Therefore, the aim of the present work was to isolate and characterize salt tolerant bacterium with ACCD activity and other plant growth promoting properties, helpful in protecting plants from salt stress. In addition, evaluation of certain compatible solutes "osmolytes" responsible for the plant to tolerate salt stress in the presence of bacterial inoculation was also investigated.

MATERIALS AND METHODS

Isolation of Bacteria

The hypersaline water was collected from different sites of Sambhar lake, India ($26^\circ 58' \text{N}$, and $75^\circ 5' \text{E}$) using random sampling design. The sampling was done in the month of July (2013) and water samples were brought to the lab in ice packs. For the isolation of bacteria, water samples were serially diluted (decimally) up to 10^{-9} in sterile DF (Dworkin and Foster, 1958) minimal salt medium and plated on DF agar medium supplemented with 4% NaCl. Composition per liter of DF medium was as follows: KH_2PO_4 4.0 g, Na_2HPO_4 6.0 g, $\text{MgSO}_4 \cdot 7\text{H}_2\text{O}$ 0.2 g, glucose 2.0 g, gluconic acid 2.0 g, citric

acid 2.0 g, trace elements: $\text{FeSO}_4 \cdot 7\text{H}_2\text{O}$ 1 mg, H_3BO_3 10 μg , $\text{MnSO}_4 \cdot \text{H}_2\text{O}$ 11.19 μg , $\text{ZnSO}_4 \cdot 7\text{H}_2\text{O}$ 124.6 μg , $\text{CuSO}_4 \cdot 5\text{H}_2\text{O}$ 78.22 μg , MoO_3 10 μg , pH 7.2). Bacterial colonies with distinct morphology were selected and further cultured on solid DF salt minimal medium containing 3 mM ACC (Sigma—Aldrich, USA) and incubated for 48 to 72 h at 30°C. Based on rich growth on selective medium, isolate HSW-16 was selected and subcultured several times on DF-ACC agar plate to ensure its ability to use ACC as nitrogen source. The test isolate HSW-16 was assayed for ACC deaminase activity and other plant growth promoting properties. Glycerol stock (15% w/v) of the isolate was prepared and stored at -70°C until further use.

Biochemical Characterization

Biochemical tests such as Gram staining, starch agar test, IMViC (Indole, Methyl Red, Voges-Proskauer, Citrate Utilization test), and catalase were performed for the test organism following standard protocol (Prescott and Harley, 2002). Ability of the bacterium to utilize various carbon sources was tested using carbohydrate utilization test kit (KB 009, Himedia, India). The sensitivity to antibiotics gentamicin (30 μg), vancomycin (30 μg), kanamycin (5 μg), tetracycline (10 μg), and chloramphenicol (30 μg) was tested by placing antibiotic disks (HTM 002, Himedia, India) on bacterial culture spread on LB medium. Interpretation of result was done using zone inhibitive chart provided by the manufacturer.

Amplification and Sequencing of 16S rRNA

To identify the bacterium at the molecular level, 16S rRNA gene was amplified by PCR using standard method (Singh et al., 2015). Amplified product was then purified using Qiaquick PCR purification kit (Qiagen, Germany). Sequencing of the resulting amplicons was done by Xcelris Genomics Labs Ltd (Xcelris Ahmedabad, India). The nucleotide sequence was analyzed by comparing with 16S rRNA genes available at GenBank database of National Centre for Biological Information (NCBI) using BLAST algorithm¹ to find the closest match to type strain. The pairwise evolutionary distance between 16S rRNA gene sequence of the test isolate HSW-16 and related bacterial strains was calculated, and a phylogenetic tree was constructed by the Neighbor-Joining method using a software MEGA version 6.0 (Tamura et al., 2013). The bootstrap of 1000 replicates was used to cluster the associated taxa.

Screening for Salt Tolerance

The tolerance of bacterium HSW-16 against salt stress was tested by growing it in tryptic soy broth (Himedia Laboratories, India) amended with different concentrations of NaCl (2–11% w/v). After 24 h, absorbance of the culture was determined at 600 nm in a spectrophotometer (Jasco Corporation, Japan). Bacterial culture was inoculated in triplicate. The uninoculated medium was used as blank.

¹<http://www.ncbi.nlm.nih.gov/BLAST>

ACC Deaminase Assay

The test organism was grown in 15 ml of Tryptic soy broth (Himedia, India) to late log phase at 200 rpm for 24 h at 30°C. Then the cells were harvested by centrifugation, washed with 0.1 M Tris-HCl (pH 7.6) and incubated overnight in 7.5 ml DF-minimal medium containing 3 mM ACC as sole nitrogen source. The bacterial cells were returned to shaking water bath for induction of ACCD at 200 rpm for 24 h at 30°C. Then, cells were harvested by centrifugation, washed with 0.1 M Tris-HCl (pH 7.6), and resuspended in 600 μl of 0.1 M Tris-HCl (pH 8.5). Thirty microliter of toluene was added to the cell suspension and homogenized for 30 s. At this point, 100 μl of toluenized cells were set aside for protein assay and stored at 4°C. The remaining toluenized cell suspension was used immediately for ACC deaminase assay. ACC deaminase activity was assayed by measuring the amount of α -ketobutyric acid produced by the hydrolytic cleavage of ACC following the protocol of Penrose and Glick (2003). The quantity of α -ketobutyrate (KB) was determined at 540 nm by comparing an absorbance of the test sample with a standard curve of pure α -ketobutyrate (Sigma—Aldrich, USA).

Amplification and Sequencing of *AcdS* Gene

Total genomic DNA of HSW-16 was isolated by Qiagen genomic DNA isolation kit (Qiagen, USA). *AcdS*, the structural gene encoding ACCD was amplified by polymerase chain reaction (PCR) using universal primers (Duan et al., 2009). Sequences of primers were: (F) 5'-GGCAAGGTCGACATCTATC-3' and (R) 5'-GGCTTGCCATTCAAGCTATG-3'. Amplification was performed in a final volume of 50 μl containing genomic DNA (50 ng), 20 picomoles each of forward and reverse primers, 200 μM of each dNTP (Genei, India), 1X Taq polymerase buffer and 2.5 U of Taq DNA polymerase (Genei, India). The thermal profile of PCR was set with an initial denaturation at 94°C for 3 min, 35 cycles of denaturation at 94°C for 1 min, annealing at 58°C for 1 min and primer extension at 72°C for 3 min, followed by a final extension at 72°C for 5 min in a thermal cycler (T100, BioRad, USA). The *AcdS* gene sequence was determined by sequencing of PCR product at Xcelris Genomics Labs Ltd (Xcelris, India). The gene sequence was analyzed using BLASTn search program² for nucleotide sequence homology. The *AcdS* nucleotide sequence of *Bacillus* sp. and other bacterial strains was obtained from the NCBI database. The nucleotide sequences were aligned by ClustalW using MEGA 6.0 software and a Neighbor-Joining (NJ) tree with the bootstrap value 1000 was generated using the software.

Screening for Plant Growth Promoting Traits

Production of Phytohormones

The test isolate HSW-16 was tested for production of indole-3-acetic acid (IAA) following the method of Gordon and Weber (1951). Briefly, the culture was grown in Nutrient broth

²<http://www.ncbi.nlm.nih.gov>

containing 100 µg ml⁻¹ tryptophan at 30°C with shaking at 180 rpm in a bacteriological incubator. After growth for 72 h, the culture was harvested by centrifugation at 10,000 g for one min. One ml of resulting supernatant was mixed with 2 ml Salkowsky's reagent (35% HClO₄, 0.01 M FeCl₃) and kept at room temperature in the dark for 20 min. Optical density (OD) was measured spectrophotometrically in a UV-visible spectrophotometer at 530 nm (Jasco, Japan). The concentration of IAA was determined from the standard curve of pure IAA (Merck, Germany). It was also tested for another phytohormone gibberellic acid using the method of Holbrook et al. (1961). Briefly, HSW-16 was grown in nutrient medium, centrifuged, and pH of the culture supernatant was adjusted to 2.5 using 2 N HCl and extracted with equal volume of ethyl acetate for 2 to 3 times in a separating funnel. After mixing 1.5 ml extract with 0.2 ml of 5 mM potassium ferrocyanide and 9.8 M HCl, absorbance was measured at 254 nm in a UV-Visible spectrophotometer (Jasco, Japan) using gibberellic acid (10–100 µg ml⁻¹) as standard.

Mineral Phosphate Solubilizing Activity

Phosphate solubilizing activity was screened by growing the test isolate on National Botanical Research Institute's Phosphate Medium (NBRIP) containing insoluble tricalcium phosphate [composition per liter: glucose 10 g, Ca₃(PO₄)₂ 5 g, MgCl₂.6H₂O 5 g, MgSO₄.7H₂O 0.25 g, KCl 0.2 g, (NH₄)₂SO₄ 0.1 g, pH 7.0] (Mehta and Nautiyal, 2001). The culture was spot inoculated on NBRIP-agar plate containing bromophenol blue and incubated at 30°C for a week. Observation of halo zone around bacterial growth on the plate was considered as positive for phosphate solubilization activity (Frey-Klett et al., 2005). Solubilized phosphate was quantified according to the method of Ames (1964) keeping the various concentration of K₂HPO₄ as standard.

Siderophore Production

For the test of siderophore production, 2 µl overnight-grown culture of HSW-16 was spot inoculated on chrome azurole S (CAS) agar plates (Schwyn and Neilands, 1987) and incubated at 30°C for 4–5 days. After the experimental period, bacterial colony was observed for the appearance of orange color around its growth. The experiment was performed in triplicate.

Nitrogen fixation

In order to test the ability of HSW-16 to fix nitrogen, a preliminary test for nitrogen fixation was done by growing it in minimal medium devoid of fixed nitrogen sources. HSW-16 was grown in LB media overnight and harvested at 8,000 g for 5 min. Bacterial pellet was washed two times with phosphate buffer saline (PBS). The JNFb⁻ agar plates (Döbereiner, 1995) were streaked with above culture and incubated at 28°C for 4 days and appearance of bacterium growth was observed as qualitative evidence of atmospheric nitrogen fixation. Composition of JNFb⁻ per liter was: malic acid 5.0 g, K₂HPO₄ 0.6 g, KH₂PO₄ 1.8 g, MgSO₄.7H₂O 0.2 g, NaCl 0.1 g, CaCl₂ 0.02 g, 0.5% of bromothymol blue in 0.2 N KOH, vitamin solution 2 ml, micronutrient solution 1 ml, 1.64% Fe-EDTA (w/v) solution 2 ml, and KOH 4.5 g. One-hundred milliliters of vitamin

solution contained 10 mg of biotin and 20 mg of pyridoxal-HCl. The micronutrient solution contained (per liter) CuSO₄ 0.4 g, ZnSO₄.7H₂O 0.12 g, H₃BO₃ 1.4 g, Na₂MoO₄.2H₂O 1.0 g, and MnSO₄.H₂O 1.5 g, pH was adjusted to 5.8. Subculturing was repeated three times to ensure diazotrophy in given isolate. In addition, *nif H* gene was amplified using specific primers: Pol F (5'-TGCAGCCSARGCBGACTC-3') and Pol R (5'-ATSGCCATCATYTCRCCGGA-3') (Sigma-Aldrich), where Y = C/T, S = G/C, R = A/G, B = G/T/C (Poly et al., 2001). PCR reaction mix contained 1× Taq DNA polymerase buffer, 50 pmol of each primer, 125 µM each dNTP, 1 U Taq DNA polymerase and 50 ng of template DNA. Thermal cycling used were: 94°C for 5 min; 30 cycles of 94°C for 1 min, 55°C for 1 min, and 72°C for 30 s followed by extension at 72°C for 5 min. The amplified product was analyzed on 1.8% agarose gel (w/v).

Ammonia Production

The freshly grown culture of the test organism was inoculated into 10 ml peptone water and incubated for 48 h at 37°C. After the bacterial growth, Nessler's reagent (0.5 ml) was added to each tube. Development of brown to yellow color was observed as a positive for ammonia production (Cappuccino and Sherman, 1992). The uninoculated medium was used as blank for comparison.

Antagonism Test

Antagonistic activity of HSW-16 was evaluated by using agar well diffusion method against pathogenic fungal species namely *Aspergillus flavus*, *Candida albicans*, *Colletotrichum capsici*, *Fusarium oxysporum*, *Fusarium moniliforme*, *Fusarium graminearum*, and *Penicillium citrinum*. Antagonistic activity against certain bacterial pathogens such as *Bacillus cereus*, *Erwinia carotovora*, *Enterobacter* sp., *Escherichia coli*, *Klebsiella pneumoniae*, and *Staphylococcus aureus* was also determined. Standard bacterial/fungal strains were procured from Microbial type culture collection (MTCC), Chandigarh, India. Briefly, freshly grown cultures of fungal and bacterial species were spread on potato dextrose agar and tryptic soy agar plates, respectively. After adsorption, well size of 6 mm was made by metallic borer and filled with 100 µl (10⁸ CFU/ml) of the freshly grown culture of HSW-16 in tryptic soy broth medium. The plates were incubated for 7 days at 28°C for fungal species and 24 h at 37°C for bacteria. Antagonistic activity was determined by measuring zone of inhibition for which parameter used as: <10 mm = poor (+), between 10 to 20mm = good (++).

Exopolysaccharide (EPS) Production Assay

For EPS assay, HSW-16 was inoculated into an Erlenmeyer flask containing 200 ml broth supplemented with 4% NaCl and grown for 5 days at 25°C with shaking at 150 rpm. Growth medium consisted following constituents (per liter): yeast extract 10 g, casamino acids 7.5 g, trisodium citrate 3.0 g, KCl 2.0 g, MgSO₄.7H₂O 20 g, MnCl₂.4H₂O 0.36 mg, and FeSO₄.7H₂O 50 mg (Nicolaus et al., 1999). After incubation, the culture was heated at 100°C for 15 min to denature EPS-degrading enzyme and then centrifuged at 9,000g for 30 min at 4°C. Three volume

of chilled isopropanol was added to 1 vol of the supernatant and kept at 4°C for overnight precipitation. The precipitate was washed with 70% ethanol (v/v), and kept for drying in a desiccator. Residual protein was removed from the sample using 20% (v/v) trichloroacetic acid (TCA) and precipitate was redissolved in ultra-pure (Milli-q) water. The resultant sample was dialyzed to remove extra salts. Purified EPS was quantified using phenol-sulphuric acid test (Dubois et al., 1956). Detection of functional groups of purified EPS was done by FTIR (Fourier transform infrared spectroscopy) (Brucker Tensor -27) following micro-potassium bromide (KBr) pellet method. The pellet for infrared analysis was obtained by grinding a mixture of 2 mg exopolysaccharide with 200 mg dry KBr followed by pressing the mixture into a 16 mm diameter mold. The FTIR spectra were recorded in the region of 4000–400 cm⁻¹.

Motility Test

Motility of bacteria is involved in the colonization behavior. Therefore, test organism was tested for its motility following the standard protocol of Connelly et al. (2004).

(i) Swimming

Tryptone swim plates containing 1% tryptone (w/v), 0.5% NaCl (w/v), 0.3% agar (w/v) were spot inoculated with test organism using a sterile toothpick and incubated for 16 h at 25°C. Motility was then assessed qualitatively by examining the circular turbid zone formed by the bacterial cells migrating away from the point of inoculation.

(ii) Swarming

Cells were point inoculated with a sterile toothpick on swarm plates and incubated at 30 °C for 24 h. Medium used for the test of swarming consisted of 0.5% Bacto-agar (w/v) and 8 g l⁻¹ of nutrient broth (both from Difco, USA) supplemented with 5 g l⁻¹ of dextrose.

(iii) Twitching

Cells were stab inoculated with a toothpick through a thin (approximately 3 mm) LB agar layer containing 1% agar (w/v) to the bottom of the Petri dish. After incubation for 24 to 48 h at 30°C, a hazy zone of growth at the interface between the agar and the polystyrene surface was observed.

Effect of HSW-16 on Plant Growth Under NaCl Stress Condition

Physiochemical Characteristics of Soil

Soil sample used for plant growth studies was analyzed for its various physico-chemical properties. The pH and electrical conductivity of soil were analyzed by digital pH and EC meter on a 1:2.5 ratio of soil and water, respectively. Estimation of organic carbon was done by the method of Walkey and Black (1934) using 1N potassium dichromate for titration and 0.5 N ferrous ammonium sulfate for back titration. Available soil phosphorus (Olsen P) was determined by chlorostannus-reduced molybdophosphoric blue color method after extraction with 0.5 M sodium bicarbonate as described by Olsen et al. (1954). Available nitrogen, potassium, and other micronutrients

(Fe, Cu, Zn, and Mn) were estimated by the method of Jackson (1967).

Preparation of Bacterial Inoculum and Seed Treatment

The halotolerant bacterium HSW-16 was tested for its plant growth promoting effect on wheat (*Triticum aestivum* L., variety C-309) plants. Preparation of bacterial inoculum and seed bacterization was performed according to Penrose and Glick (2003) with slight modification. Briefly, HSW-16 was grown in 15 ml DF medium with 3 mM ACC as sole nitrogen source with 4% NaCl (w/v) for optimum growth of the isolate. The culture was incubated for 24 h at 30°C with shaking at 130 rpm in a bacteriological incubator (Labtech, India). After incubation, cells were harvested and re-suspended in 0.5 ml sterile 0.03 M MgSO₄ and diluted two to three times to obtain the bacterial population of 1×10^8 CFU/ml. Wheat seeds were surface sterilized by treating with 70% ethanol (v/v) for 2 min followed by three times washing with sterilized water. Then, the seeds were subjected to 1% (w/v) sodium hypochlorite (NaOCl) solution for 3 min followed by three consecutive washing with sterile water to remove all traces of sodium hypochlorite. Twenty seeds were treated with above-mentioned bacterial suspension for 1 h. Seeds treated with sterile 0.03 M MgSO₄ served as a control. Following treatment, twenty seeds were sown in plastic pots filled with soil in a plant growth chamber (Labtech, India) with 16:8 day/night photoperiod up to 15 days at 28 ± 2°C with a humidity of 65–70%. The soil used for the pot studies was sterilized by autoclaving at 121°C for 1 h for three consecutive days and 300 g sterilized soil was filled in each plastic pot. Hoagland medium supplemented with NaCl (150 mM, 175 mM, 200 mM) was used for providing nutrient as well as imposing the salt stressorss (Hoagland and Boyer, 1936). Pots were arranged in completely randomized block design with three replications in each treatment. The experiment was conducted for 15 days after the germination of seeds. The growth of plants was measured in terms of root length, shoot length, fresh weight, and dry weight. For measurement of Chlorophyll a/b, fresh leaf samples (1 g) were homogenized in 80% acetone (v/v), and pigments were extracted and quantified (Duxbury and Yentsch, 1956). The absorbance at 480, 510, and 663 nm was measured on a UV-Vis spectrophotometer (Jasco, Japan). Five randomly selected plants from each experimental set up were also used for tests namely ionic accumulation, analysis of osmolytes, and confirmation of colonization as described in following sections.

Ionic Accumulation Analysis

For analysis of ionic elements, 1 g of shoot tissue from each sample was ground in liquid N₂ and digested in 100 ml mixture of perchloric acid, sulphuric acid, and distilled water with the ratio of 10:1:2, respectively. Twenty milliliter of digested sample was used for analysis of Na⁺, K⁺, and Ca²⁺ by an Atomic Absorption Spectrophotometer (AAS 2380, Perkin Elmer, USA) at National Horticultural Research and Development Foundation (Nashik, India). For accuracy and precision, each sample was analyzed in triplicate sets.

Biochemical Analysis for Osmolytes in Plant After NaCl and Bacterial Inoculation

Proline content in the leaves was determined following the standard protocol (Bates et al., 1973) with minor modifications. A 0.5 g fresh leaves of experimental plant samples were homogenized in 3 ml of 5% (w/v) sulfosalicylic acid and centrifuged at 8,500g for 10 min. To 500 μ l of the resulting supernatant, 1 volume of water and 2 volumes 2% ninhydrin (w/v) were added. The mixture was incubated at 100°C for 30 min. After cooling, an equal volume (2 ml) of toluene was added to the mixture and upper aqueous phase was used for measuring absorbance at 520 nm in a spectrophotometer (Jasco, Japan). The proline content was calculated by comparing with a standard curve of pure L-proline (Sigma-Aldrich, USA).

Total soluble sugar (TSS) was estimated by anthrone reagent according to Irigoyen et al. (1992). 0.1 ml of alcoholic leaf extract prepared by homogenized 0.5 g leaf with 3 ml of 80% ethanol (v/v) was mixed with 3 ml of freshly prepared anthrone reagent and placed in a boiling water bath for 10 min. The absorbance of the resultant sample was measured at 620 nm. 20–400 μ g ml⁻¹ of glucose was used as a standard for making calibration curve for quantification of soluble sugar present in plants. Lipid peroxidation was determined by estimating the malondialdehyde (MDA) content produced by the thiobarbituric acid (TBA) reaction as per Hodges et al. (1999) with minor modification. Briefly, 1 ml of alcoholic extract (80%) prepared with 0.5 g of leaves was mixed with 1 ml of 0.5% (w/v) TBA containing 20% (w/v) TCA. The mixture was heated up to 90°C for 30 min in a water bath. After cooling at the room-temperature sample was centrifuged at 4,500 g for 5 min and absorbance was measured at 400, 532, and 600 nm. After subtracting the non-specific absorbance, the MDA concentration was determined by its molar extinction coefficient (155 nm⁻¹ cm⁻¹) and the results were expressed as mmol g⁻¹ FW.

Similarly, alcoholic extract of shoot tissue was used for measuring the auxin content as per Andreea and Ysselstein (1959). One ml of alcoholic extract of shoot tissue was mixed with 2 ml of Salkowsky reagent in the dark and incubated for 20 min. The absorbance was measured at 535 nm and compared with the standard curve of IAA. For the estimation of total protein content (TPC), protein was extracted by homogenizing 0.5 g plant tissue in extraction buffer containing Tris-HCl 50 mM (pH 8.3), EDTA 1 mM, DTT 3 mM, ascorbic acid 0.08% (w/v), and PMSF 1 mM and quantified by Bradford method (Bradford, 1976).

Test of Colonization

For monitoring the colonization of bacterium, soil particles adhering to the root surface were gently removed. The roots were cut into 1 cm long segments and 1 g of root segments were dipped into 5 ml of sterilized PBS buffer, and vortexed 5–6 times to release the bacteria into the buffer. Dilutions of bacterial suspensions were poured on Nutrient agar to evaluate the population of the indigenous bacterium. The colony forming units were counted after 24 to 48 h of incubation at 28 ± 1°C. For confirming identity of colonized bacterium, enterobacterial repetitive intergenic consensus- (ERIC) PCR was performed in a 50 μ l reaction volume containing 50 ng

bacterial DNA, 125 μ M each dNTP (Genei, India), 1 X Taq DNA polymerase buffer (Genei, India) with 1.5 mM MgCl₂, 20 pmol of each primers and 1.5 U of Taq DNA polymerase in a DNA thermal cycler (T 100, BIO-RAD, USA). Primers of ERIC 1R F' (ATGTAAGCTCCTGGGGATTAC) and ERIC 2R R' (AAGTAAGTGACTGGGTGAGCG) (Sigma-Aldrich, USA) were used for amplification. The thermal cycling condition was: initial denaturation for 3 min at 94°C, 35 cycles each consisting of denaturation for 1 min at 94°C, primer annealing for 1 min at 52°C and extension at 72°C for 5 min and a final extension of 7 min at 72°C. PCR product was analyzed on 2% agarose gel containing 0.5 μ g ml⁻¹ ethidium bromide using a gel documentation system (Bio-Rad, USA).

Statistical Analysis

Data on the growth parameters of wheat was analyzed by a DPS statistical software package (version 11.0) by one-way ANOVA followed by Student's *t*-test (*p* < 0.05). The statistical analysis was performed between 2 × 4 groups, by taking one groups of control and other with bacterial inoculated. Statistical difference between control and HSW-16 mean at each treatment were assessed by Student's *t*-test (*p* < 0.05).

RESULTS

Isolation, Biochemical Characterization, and Identification of HSW-16

Based on colony morphology, overall 13 different bacterial isolates were recovered from hypersaline Sambhar lake water. Out of these 13 isolates, one isolate namely HSW-16 showing consistent growth on minimal medium supplemented with ACC as the sole source of nitrogen was selected for detailed characterization. The ACC deaminase activity of HSW-16 was determined as 267.50 ± 19 nmol of α -KB mg⁻¹ protein h⁻¹. Basic microbiological and biochemical tests of the isolate HSW-16 indicated that it is a Gram-positive bacterium, which showed positive results for the test of Voges-Proskauer, lipase, nitrate reductase and negative for indole, methyl red, amylase, catalase, and urease. Moreover, antibiotic sensitivity profiling of HSW-16 showed its resistance to chloramphenicol, kanamycin, vancomycin and sensitivity to tetracycline and gentamicin (Table 1). The test organism HSW-16 was able to utilize various carbon sources such as xylose, maltose, fructose, dextrose, galactose, raffinose, trehalose, sucrose, L-arabinose, mannose, glycerol, salicin, inositol, sorbitol, mannitol, adonitol, α -Methyl-D-glucoside, rhamnose, cellobiose, ONPG, esculin hydrolysis, D-arabinose, sorbose, and inulin (Table 1). The carbohydrate utilization pattern of the test organism tallied with a standard strain of *B. licheniformis* reported by Salkinoja-Salonen et al. (1999). The tolerance of HSW-16 to NaCl was also assessed which showed NaCl tolerance in the range of 2–11% while optimal growth was observed at 8% of NaCl. To ascertain taxonomic affiliation of HSW-16 on a molecular level, it was subjected to 16S rRNA gene sequence analysis, which showed its closest match of 99% to the 16S rRNA gene sequence of *B. licheniformis* strain PF3-1.1 (Figure 1). It indicates that the test isolate

TABLE 1 | Biochemical and physiological characteristic feature of isolate HSW-16.

Characteristic (s)	Activity	Carbohydrate	Utilization
Gram test	+	Sucrose	+
Indole	-	L-arabinose	+
MR	-	Sodium gluconate	-
VP	+	Glycerol	+
Amylase	-	Salicin	+
Lipase	+	Dulcitol	-
Urease	-	Inositol	+
Catalase	-	Sorbitol	+
Nitrate reductase	+	Mannitol	+
+ positive, - negative		Adonitol	+
Antibiotic resistance		Arabitol	-
Chloramphenicol	+	Erythritol	-
Tetracyclin	-	a-methyl-D-glucoside	+
Kanamycin	+	Rhamnose	+
Gentamycin	-	Cellobiose	+
Vancomycin	+	Melezitose	-
- sensitive, + resistant		a-methyl-D-mannoside	-
Carbohydrate	Utilization	Xylitol	-
Lactose	-	ONPG	+
Xylose	+	Esculin hydrolysis	+
Maltose	+	D-Arabinose	+
Fructose	+	Citrate utilization	-
Dextrose	+	Malonate utilization	-
Galactose	+	Sorbose	+
Raffinose	+	Inulin	+
Trehalose	+	Mannose	+
Melibiose	-		

probably belongs to *B. licheniformis*. The obtained sequence was submitted to the NCBI Genbank under the accession number KJ950717.

Molecular Characterization of ACC Deaminase

An 800 bp amplicon was obtained by PCR from genomic DNA of the isolate HSW-16 using *AcdS* gene specific primers (Figure 2A). Sequence analysis of the amplicon confirmed its identity where it showed 98% similarity with *AcdS* sequence of *B. cereus* AcdSPB4. The obtained sequence was submitted under the accession number KM501059. Sequence analysis of *AcdS* gene obtained from HSW-16 and other bacterial species revealed that *AcdS* sequence of HSW-16 is closely related to *B. cereus* AcdSPB4, *B. subtilis*, and strains belonging to other genera including *Klebsiella*, *Pseudomonas*, *Burkholderia*, *Achromobacter*, and *Serratia*. It also showed 99% similarity with one of the most characterized ACCD bacteria *Pseudomonas putida* UW4 (Figure 2B). Nucleotide sequence analysis suggests that *AcdS* gene found in *B. licheniformis* HSW-16 encodes a true ACC deaminase. Phylogenetic analysis revealed that nucleotide sequence of *AcdS* of genus *Bacillus* clustered together along with other species belonging to genera *Serratia*, *Klebsiella*, and *Pseudomonas*. The accuracy

of placement in the tree of HSW-16 and MBPSP207 is possibly mitigated due to the use of partial sequences in the alignment.

Plant Growth Promoting Features

The test organism *B. licheniformis* HSW-16 formed a clear zone on solid agar medium supplemented with an insoluble form of phosphate (tricalcium phosphate) which indicated mineral phosphate solubilizing activity. Phosphate solubilization was quantified after 72 h of growth which showed solubilization of $11.04 \pm 2.44 \mu\text{g ml}^{-1}$ phosphate. For phytohormone production, it showed positive for the production of IAA while negative for gibberellic acid. It produced $2.89 \pm 0.03 \mu\text{g ml}^{-1}$ IAA after 72 h of bacterial growth. Ability to fix atmospheric nitrogen was tested by growing it on selective medium lacking any source of fixed nitrogen (Table 2). Continuous growth for several generations on N⁻ medium indicated its ability to fix atmospheric nitrogen fixation. Furthermore, the amplification of the *nifH* gene supports the nitrogen-fixing potential of HSW-16 at the molecular level. The desired band of 350 bp corresponding to the *nifH* gene was obtained by using universal primers for the *nifH* gene (Supplementary Figure S1). In addition, it was also positive for the test of ammonia production (Table 2). However, it gave a negative result for the test of siderophore production. Biocontrol potential of test organism was evaluated by testing antagonistic activity against various fungal and bacterial pathogens. The test organism HSW-16 inhibited the growth of *Aspergillus flavus*, *Fusarium oxysporum*, *Fusarium graminearum*, and *Penicillium citrinum*. Among the bacterial pathogens tested, it was found inhibitory against *Enterobacter* sp., *Klebsiella pneumoniae*, *Erwinia carotovora*, and *Escherichia coli* (Table 3). The test isolate showed the swimming, swarming and twitching motility (Figure 3)

Effect of HSW-16 on Plant Growth Under NaCl Stress

Physicochemical Characteristics of Soil and Plant Growth Studies

The soil was analyzed for its nutritional status for the plant growth study. The various parameters of soil were as follows: pH 7.20, EC 0.162ds m⁻¹, Olsen P 34.6 mg kg⁻¹, OC (organic C) 0.2%, total N 61 mg kg⁻¹, K 140.6 mg kg⁻¹, Zn 0.218 mg kg⁻¹, Cu 0.124 mg kg⁻¹, Fe 2.61 mg kg⁻¹, and Mn 0.948 mg kg⁻¹. To evaluate the effect of salt stress in control and HSW-16-treated plants, we carried out Student's *t*-test ($p < 0.05$), which demonstrated that the inoculation of HSW-16 resulted in significant increase in wheat plants growth under different concentration of NaCl. The growth was assessed by measuring shoot length, root length, fresh weight, and dry weight. In presence of bacterium, the shoot length increased significantly by 27.82% at 200 mM (1.17%) of NaCl as compared to uninoculated plants, whereas, it increased 13.26 and 13.35% at 150 and 175 mM of NaCl, respectively (Figure 4A). Similarly, a significant increase in root length (22.55%) was recorded at 200 mM of NaCl in response to bacterium inoculation.

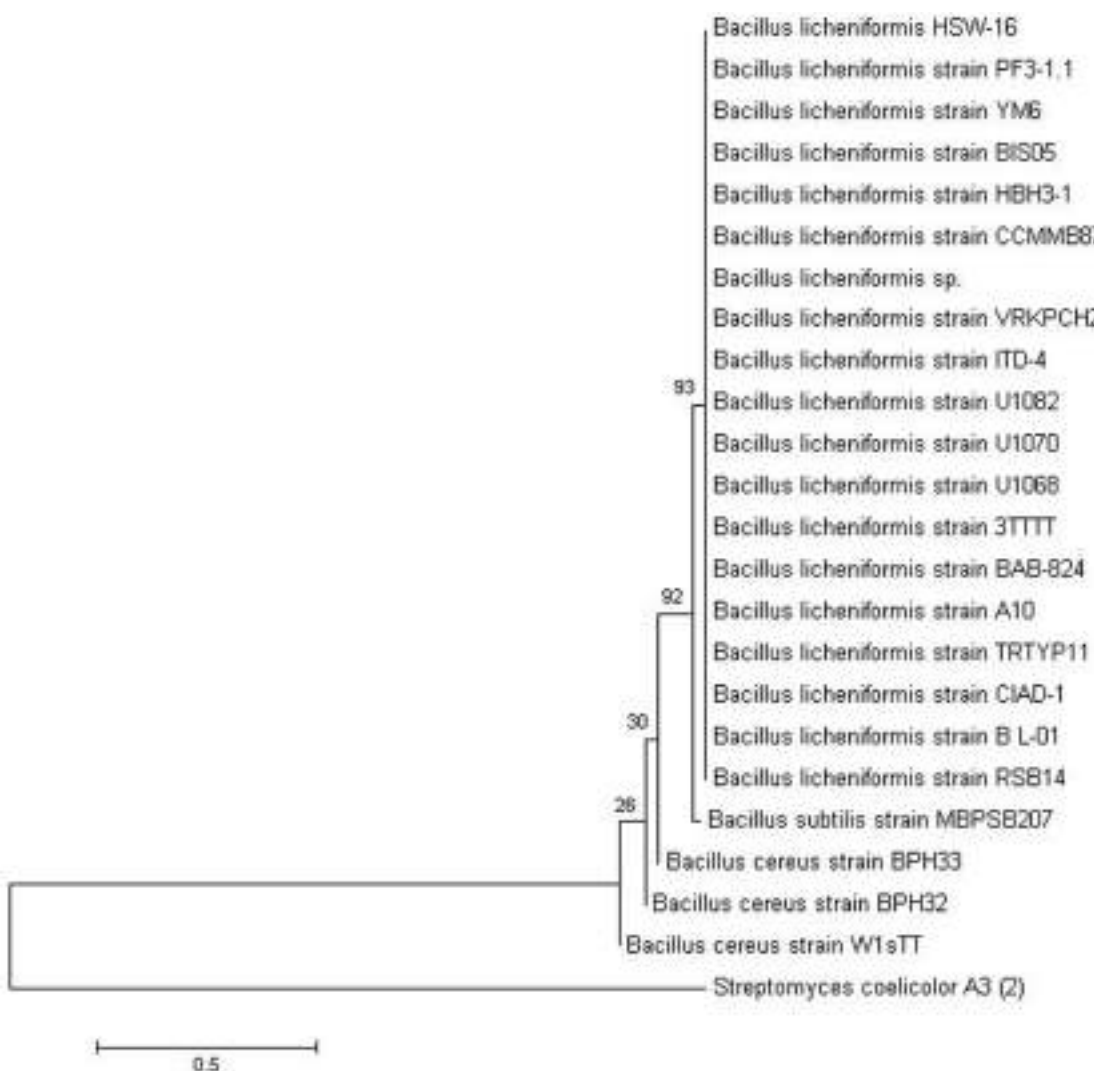


FIGURE 1 | Phylogenetic tree showing the relationship of *Bacillus licheniformis* HSW-16 to closely related bacteria. The 16S rRNA gene sequence of closely related species was obtained from NCBI GenBank database. 16S rRNA gene of *Streptomyces coelicolor* A3 was taken as an outgroup. The tree was obtained using neighbor joining method of software package Mega version 6.0 at the bootstrap value of ($n = 500$).

However, root length increased only by 11.13 and 6.18% at 175 mM and 150 mM of NaCl, respectively, in inoculated plants (**Figure 4B**). The results of fresh weight showed that HSW-16 increased fresh weight significantly at 200 and 175 mM of NaCl by 37.11 and 30.94%, respectively (**Figure 4C**). Data of dry weight of experimental plants also indicated that inoculation of HSW-16 significantly increased dry weight at 200 mM (37.5%) in comparison to their control plants treated with NaCl alone (**Figure 4D**). A remarkable increase in chlorophyll a content was recorded in HSW-16 inoculated plants which showed 159.26, 147.68, and 67.09% increase at 200, 175, and 150 mM of NaCl, respectively, over uninoculated plants. It also significantly increased the content of chlorophyll b by 26.06% than that of control plants treated with 0 mM of NaCl (**Figures 4E,F**).

Inoculation Effect on Na^+ , K^+ , and Ca^{2+} Ions Under NaCl Stress

To study the role of PGPB in ameliorating NaCl stress, plants were evaluated for fine-tuning of the ionic balance, Na^+/K^+ ratio in particular, using Atomic Absorption Spectrometry (AAS). There was a significant change in the ionic constituents of wheat seedlings grown under NaCl stress. Ionic analysis demonstrated a decrease in Na^+ content but an increase in K^+ and Ca^{2+} content in plants inoculated with test isolate HSW-16. In comparison to uninoculated control plants, inoculated plants exhibited the highest decrease in Na^+ (51.14%) and increase in K^+ content (68.42%) at 200 mM of NaCl. However, less change in Na^+ and K^+ were evident in plants grown at 150 and 175 mM (12.40%, 20.18%) of NaCl (**Figures 5A,B**). Moreover, the higher increase in Ca^{2+} (32.72%) was also observed at 200 mM of NaCl than

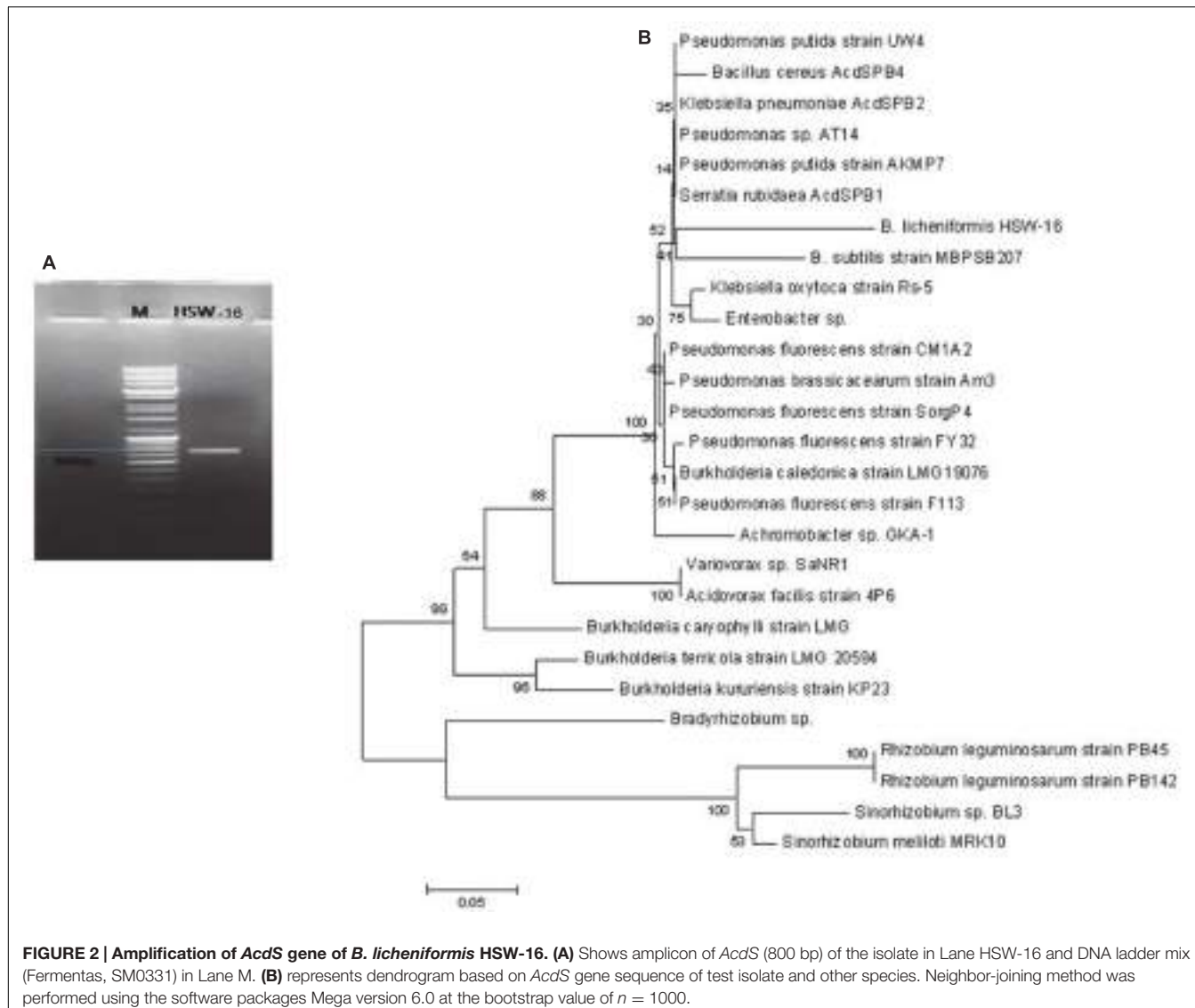


FIGURE 2 | Amplification of *AcdS* gene of *B. licheniformis* HSW-16. (A) Shows amplicon of *AcdS* (800 bp) of the isolate in Lane HSW-16 and DNA ladder mix (Fermentas, SM0331) in Lane M. (B) represents dendrogram based on *AcdS* gene sequence of test isolate and other species. Neighbor-joining method was performed using the software packages Mega version 6.0 at the bootstrap value of $n = 1000$.

the other concentrations, which was 20.51% and 15% at 175 and 150 mM of NaCl, respectively (Figure 5C).

Biochemical Analysis of Plants Treated with NaCl

The change in certain chemical components namely, proline, MDA content, TSS, IAA, and TPC known to play important protective roles during NaCl stress was assessed in wheat plants with or without bacterial inoculation. Differential levels of above components were detected in plants inoculated with or without bacterium under NaCl stress. As the NaCl concentration increased, proline content increased in the range of 36.90 to 93.70% in uninoculated plants. However, the content of proline decreased in bacterium inoculated plants subjected to NaCl stress (Figure 6A). Significant decrease in proline content (53%) was observed at 200 mM of NaCl, followed by 175 mM (41.50%) and 150 mM of NaCl, as compared to un-inoculated control (Figure 6A). Since, NaCl-induced oxidative damage to lipids is reflected by increased MDA content, the level of MDA was

estimated in plants. The amount of MDA content increased with increase in NaCl concentration in untreated plants. The increase in MDA content was 80.87% at 200 mM of NaCl as compared to the control plants. However, its concentration decreased under NaCl in plants that were inoculated with HSW-16. The maximum decrease in MDA content (50%) was observed at 200 mM of NaCl as compared to plants treated with same concentration of NaCl. Furthermore, decrease in MDA content was also observed at 150 mM (42.30%) and 175 mM of NaCl (37.56%) in bacterium inoculated plants as compared to control plants (Figure 6B).

A notable difference was found for TSS in wheat leaves stressed with different NaCl concentrations. The highest accumulation of TSS (67.51%) was observed at 150 mM of NaCl in HSW-16 inoculated plants as compared to control subjected to the same stress condition. The increase in TSS in HSW-16 inoculated plants was 52.54% and 41.90% at 175 and 200 mM of NaCl as compared to their control. However, salinity significantly reduced

TABLE 2 | Plant growth promoting traits of HSW-16.

Plant growth promoting traits	Activity
ACCD activity ($\text{nmol of } \alpha\text{-KB mg}^{-1} \text{Pr.h}^{-1}$)*	267.50 ± 19
1AA production ($\mu\text{g ml}^{-1}$)	2.89 ± 0.03
t -1\ Phosphate solubilization ($\mu\text{g ml}^{-1}$)	11.04 ± 2.44
Gibberelic acid production	—
Growth on N-free medium	+
Siderophore index	—
Ammonia production	+

*Enzyme activity was assessed after 72 h of bacterial growth.

TABLE 3 | Test of antagonistic activities of *Bacillus licheniformis* HSW-16 against bacterial and fungal pathogens.

Bacteria	Zone of inhibition (mm)
<i>Escherichia coli</i>	15.9 ± 0.35
<i>Staphylococcus aureus</i>	NZ
<i>Bacillus cereus</i>	NZ
<i>Erwinia carotovora</i>	16.6 ± 0.29
<i>Klebsiella pneumoniae</i>	14.3 ± 0.51
<i>Enterobacter</i> sp.	13.9 ± 0.43
Fungal species	
<i>Fusarium oxysporum</i>	17.1 ± 0.45
<i>Fusarium moniliforme</i>	NZ
<i>Fusarium graminearum</i>	16.8 ± 0.56
<i>Aspergillus flavus</i>	9.7 ± 0.14
<i>Candida albicans</i>	NZ
<i>Colletotrichum casici</i>	NZ
<i>Penicillium citrinum</i>	15.2 ± 0.38

±Standard deviation; NZ, no zone of inhibition

the TSS content in uninoculated plants. The highest decrease was 41.21% in control plants under 200 mM of NaCl as compared to control (Figure 6C). Similarly, inoculation of bacterium significantly improved TPC in plants under NaCl. The highest increase in protein content (48.15%) was observed at 150 mM of NaCl as compared to other concentrations (Figure 6D). HSW-16 inoculation significantly increased the protein content (38.46%) as compared to control plants under non-saline stress. Inoculation with test isolate HSW-16 also improved auxin content in wheat leaves under NaCl. The significant increase in auxin content was in the range of 38 to 49% in bacterium-inoculated plants under different concentration of NaCl. The highest increase in auxin content (48.90%) was at 175 mM of NaCl in inoculated plants as compared to respective control (Figure 6E).

EPS Quantification

The test organism was able to produce $3.09 \pm 0.07 \mu\text{g ml}^{-1}$ EPS in normal growth medium. IR spectroscopy of EPS extracts showed characteristic absorption bands indicating the presence of hydrogen-bonded compounds. Characteristic β -1,3-glucan band in crude exopolysaccharide was observed between 1000–1500 cm $^{-1}$ (1100, 1200, 1400, and 1600 cm $^{-1}$), whereas alkane was observed at 2929 cm $^{-1}$ (Supplementary Figure S2).

Confirmation of Colonization

The efficiency of colonization by HSW-16 was determined by plate counting, microscopic evaluation, and ERIC-PCR of inoculated bacteria with respect to control after 15 days of growth. After the experimental period, associated bacterium was found in a range of $1.2 \times 10^3 \text{ CFU g}^{-1}$ of the root. Colonization of bacterium was also tested by acridine orange staining, which showed a large number of fluorescent cells on the surface of plant root (Supplementary Figure S3A). No bacterial cells were observed on the root surface of uninoculated plants. Additionally, to confirm the identity of colonized bacterium, total DNA of inoculated plants was subjected to ERIC-PCR. ERIC-PCR profile obtained from total DNA of inoculated plants was identical to that of a pure culture of test isolate, which indicated that bacterium colonized plants successfully (Supplementary Figure S3B).

DISCUSSION

Some plant growth promoting bacteria can help plants combat salt stress through various means. One of the important mechanisms for ameliorating salt stress in plants is mediated by production of ACC deaminase (ACCD), which causes a decrease in the level of 'stress ethylene' produced in plants in response to stress (Glick, 2007; Saleem et al., 2007). The present study demonstrates the effectiveness of ACC deaminase bacterium *B. licheniformis* HSW-16 for improving growth of wheat plants under salt stress conditions. Inoculation of this bacterium also resulted in balancing Na^+/K^+ ratio in plants and the production of osmolytes, which protect plants from harmful effects of salinity. Thus, our report extends the understanding of plant growth promoting properties contributed by members of genus *Bacillus*. The plant growth promoting effect of *Bacillus* sp. on wheat plants under different salinity conditions has also been observed previously by Upadhyay et al. (2012). In the present study, *B. licheniformis* HSW-16 was recovered from the salt-enriched water of Sambhar salt lake located in Rajasthan, India. Isolation of salt tolerant ACC deaminase bacteria from above location has been reported in earlier studies. Based on the qualitative screening, Sahay et al. (2012) reported the isolation of a few bacterial sp. including *Bacillus* sp., *B. licheniformis*, *B. marisflavi*, *B. baekryungensis*, *B. selenatarsenatis*, *Thalassobacillus devorans*, *Halomonas salina*, *Oceanobacillus picturiae*, and *Streptomyces radiopugnans* from Sambhar salt lake which were ACCD positive.

Selection of test isolate was primarily based on high ACCD activity as well as other plant growth promoting properties. The level of ACCD activity considered for selection was based on the earlier studies which suggest that the bacteria producing $>20 \text{ nmol } \alpha\text{-KB mg}^{-1} \text{ protein h}^{-1}$ can enhance plant growth by reducing the level of stress ethylene produced in plants under stress conditions (Penrose and Glick, 2003). This was corroborated by results of *Arthrobacter protophormiae* having ACC deaminase activity of $241 \text{ nmol } \alpha\text{-KB mg}^{-1} \text{ protein h}^{-1}$, which alleviated the damages caused by NaCl stress, and resulted in higher yield (Barnawal et al., 2014).

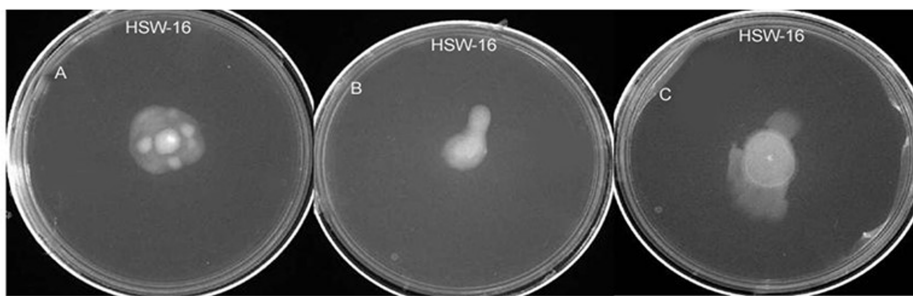


FIGURE 3 | Test of various types of motility in *B. licheniformis* HSW-16 using agar-based method. (A–C) Represent swimming, swarming, and twitching, respectively.

Furthermore, the presence of ACCD in test organism was confirmed by amplification of *AcdS*, a gene encoding ACC deaminase in bacteria. The universal primers used in this study have also been employed for successful amplification of *AcdS* gene in different environmental isolates (Jha et al., 2012; Srivastava and Kumar, 2013). The nucleotide sequence of 800 bp amplicons was confirmed by sequence analysis, which matched with the *AcdS* of other bacteria available in the database. Phylogenetic analysis suggested that the *AcdS* gene sequence of HSW-16 was similar to bacteria belonging to genus *Bacillus* as well as other bacterial genera. To the best of our knowledge, this is the first report where the presence of *AcdS* in *B. licheniformis* has been demonstrated. Phylogenetic analysis indicated similarity of *AcdS* sequences among diverse species including *Pseudomonas* sp., *Klebsiella* sp., and *Serratia* sp. This observation is supported by a recent report which illustrates that the evolution of ACCD occurred mainly through vertical transfer with occasional horizontal transfer (Nascimento et al., 2014).

In addition to ACCD activity, test isolate HSW-16 also showed other plant growth promoting properties such as the production of phytohormone (auxin) and phosphate solubilization activity which can benefit plant growth and productivity. The ability of ACCD bacteria equipped with such features to benefit host plants has been demonstrated in several studies (Sachdev et al., 2009; Karthikeyan et al., 2012). Inoculation of IAA-producing bacteria promotes root growth by increasing number and length of adventitious root as well as by altering root architecture that lead to enhanced nutrient uptake (Chakraborty et al., 2006; Yang et al., 2009; Dutta et al., 2015), which in turn promotes plant growth (Chakraborty et al., 2006; Yang et al., 2009; Dutta et al., 2015). Similarly, phosphate solubilization is an important attribute of rhizospheric microorganism that provides the bio-available phosphate for improvement of plant growth (Liu et al., 2014; Dutta et al., 2015). The presence of phosphate solubilizing bacterium in soils may be considered a positive indicator of utilizing the microbes as biofertilizers for crop production and beneficial for sustainable agriculture. The nitrogen fixation ability of associative bacteria provides the essential nitrogen content during the growth phase of the plant. The nitrogen fixation ability is evident from the amplification of *nifH* gene, that has been demonstrated in several associative as well as endophytic bacteria by using

universal primers (Desnoues et al., 2003; Jha and Kumar, 2009)

Bacterial inoculation under laboratory conditions significantly enhanced plant growth with respect to different parameters tested. A significant decrease in shoot/root lengths and fresh/dry weight was observed in uninoculated plants under salt stress, whereas inoculation with HSW-16 limited these losses significantly. It is likely that this response might be due to ACCD activity of the bacterium. Our results are in agreement with the previous report for salt tolerance in various plants induced by PGPR (Mayak et al., 2004; Saravanakumar and Samiyappan, 2007; Zahir et al., 2009). Effect of salinity stress is manifested by a decrease in K⁺ availability and its reduced transportation to growing region of plants (Grattan and Grieve, 1999). As the Na⁺ ion level increases, ionic competition results in increased Na⁺/K⁺ ratio, thus having significant negative effect on plant growth (Schachtman and Liu, 1999). Moreover, the ability of Na⁺ to bind competitively with K⁺ binding site disrupts the normal cellular function and generates metabolic toxicity (Bhandal and Malik, 1988; Ruiz-Lozano and Azcón, 2000). The altered ionic ratio of Na⁺ and K⁺ generated on accumulation of NaCl in plants can be improved by certain associative bacteria. Some PGPR help plants indirectly by strengthening their ability to combat salt stress (Nadeem et al., 2006). Therefore, plants growing under salt stress were also tested to see whether there is change in plants ability to prevent or minimize accumulation of Na⁺ in plant tissue on inoculation of HSW-16. The result of ion analysis showed that the test organism decreased Na⁺ accumulation and increase in K⁺ content in plants. These results are in agreement with by earlier studies which suggest that certain PGPR not only delay the uptake of Na⁺ but also promote the extrusion of excess Na⁺ from the shoot (Arshad et al., 2009). These PGPR up-regulate the expression of HKT1 (High affinity K⁺ transporter 1) gene which helps in Na⁺ efflux in the plant. The differential regulation of HKT1 expression in root and shoot results in reduced accumulation of Na⁺, and an increased accumulation of K⁺ under salt stress conditions (Zhang et al., 2008). Similarly, PGPR *B. subtilis* GB03 induced concomitant down- and up-regulation of HKT1 expression in roots and shoots of *Arabidopsis* seedlings, respectively (Zhang et al., 2008). Moreover, secretion of exopolysaccharides by HSW-16 also could be important for reducing Na⁺ uptake in the plant by sequestering it as suggested

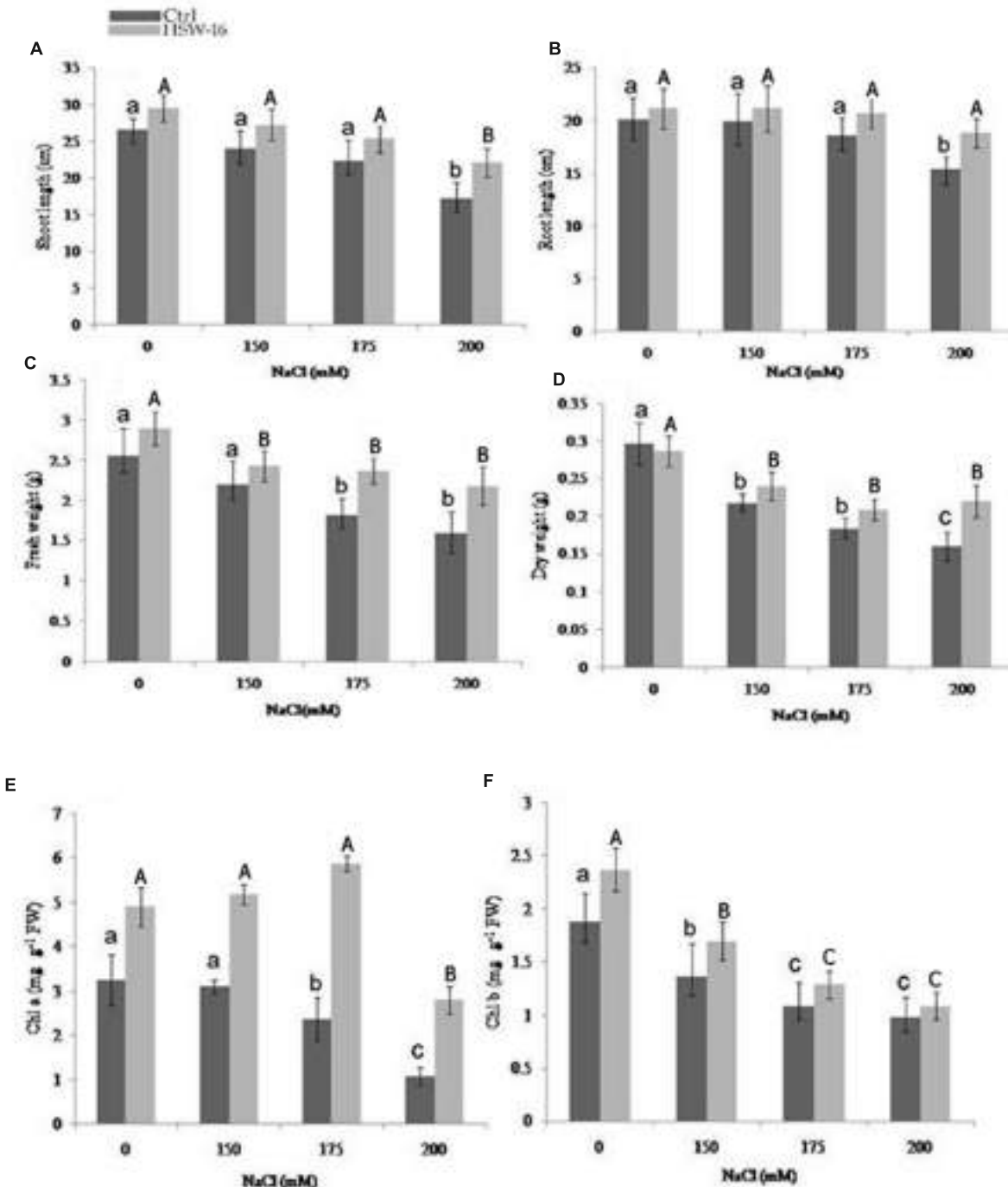


FIGURE 4 | Effect of inoculation with *B. licheniformis* HSW-16 on plant biomass and chlorophyll content under different salinity conditions (0 mM, 150 mM, 175 mM, 200 mM NaCl). (A) Shoot length, (B) root length, (C) fresh weight, (D) dry weight, (E) chlorophyll a, and (F) chlorophyll b. Small letters on the bar in each treatment indicate significant difference ($p < 0.05$) among control, whereas capital letters indicate significant difference among the bacterial treatment. Dark and light gray columns represent the control (Ctrl) and HSW-16 inoculated plants, respectively.

by earlier reports (Roberson and Firestone, 1992; Qurashi and Sabri, 2012).

Accumulation of compatible solutes (osmolytes) in response to bacterial inoculation helps to stabilize the osmotic adjustment

(Ashraf and Harris, 2004). These compatible solutes are highly soluble and are usually nontoxic at high cellular concentrations (Hasegawa et al., 2000; Ashraf and Foolad, 2007). The level of compatible solutes or osmolytes significantly increased in

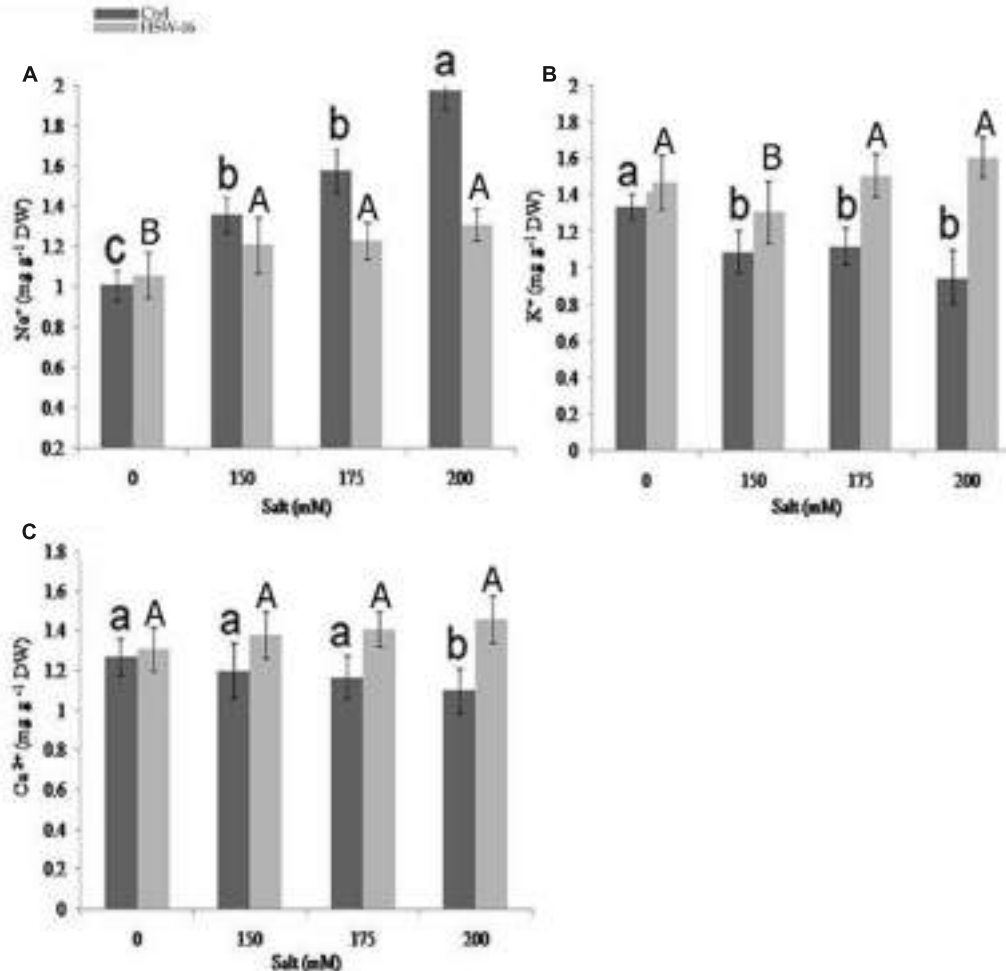


FIGURE 5 | Effect of NaCl and inoculation with *B. licheniformis* HSW-16 on ionic uptake by plants (A) Na⁺ (B) K⁺ (C) Ca²⁺. Each value is mean of five replicates. Error bar represents standard error of five replicates of mean. Small letters on the bar in each treatment indicate significant difference ($p < 0.05$) among control, whereas capital letters indicate significant difference among bacterial treatment. Dark and light gray columns represent the control (Ctrl) and HSW-16 inoculated plants, respectively.

response to salinity stress (Hasegawa et al., 2000; Chen and Murata, 2008). Increase in proline content helps to stabilize the membranes and proteins, buffers the redox potential, and acts as hydroxyl radical scavenger under salt stress (Claussen, 2005). Furthermore, among the various compatible solutes, proline accumulation is the most frequently reported modification induced by salt stress in plants (Ashraf and Foolad, 2007). In the present study, proline levels were considerably higher in uninoculated plants subjected to varying level of salt stress. However, bacterial inoculation significantly decreased the proline content indicating a lower degree of stress severity in plants under salt stress. This suggests that PGPR-inoculated plants do not face much NaCl stress, therefore, the proline accumulation is less in HSW-16 inoculated plants. In addition to proline, soluble sugars also remarkably maintain the osmotic homeostasis and constitute about 50% of the total osmotic potential in plant cells during NaCl stress (Cram, 1976). The increase in TSS content in

inoculated plants illustrates the survival of plants under saline conditions. The protein content was also higher in inoculated plants growing with or without NaCl that might have correlation with salinity tolerance. Previous report of Kandasamy et al. (2009) has shown the differential expression of protein in rice plants after inoculation with *Pseudomonas fluorescens*.

Malondialdehyde content reflects the extent of stress as well as oxidative damage caused by ROS generated by NaCl (Jain et al., 2001). Under NaCl stress, enhanced production of MDA as a consequence of decomposition of polyunsaturated fatty acids of bio-membranes has been reported (Gossett et al., 1994). In the present study, we observed that inoculation with test isolate caused a reduction in MDA content in inoculated plants as compared to uninoculated plants. Decrease in MDA content following inoculation of test organism points to cause lesser cell membrane damage and/or induce enhanced salinity tolerance to plants.

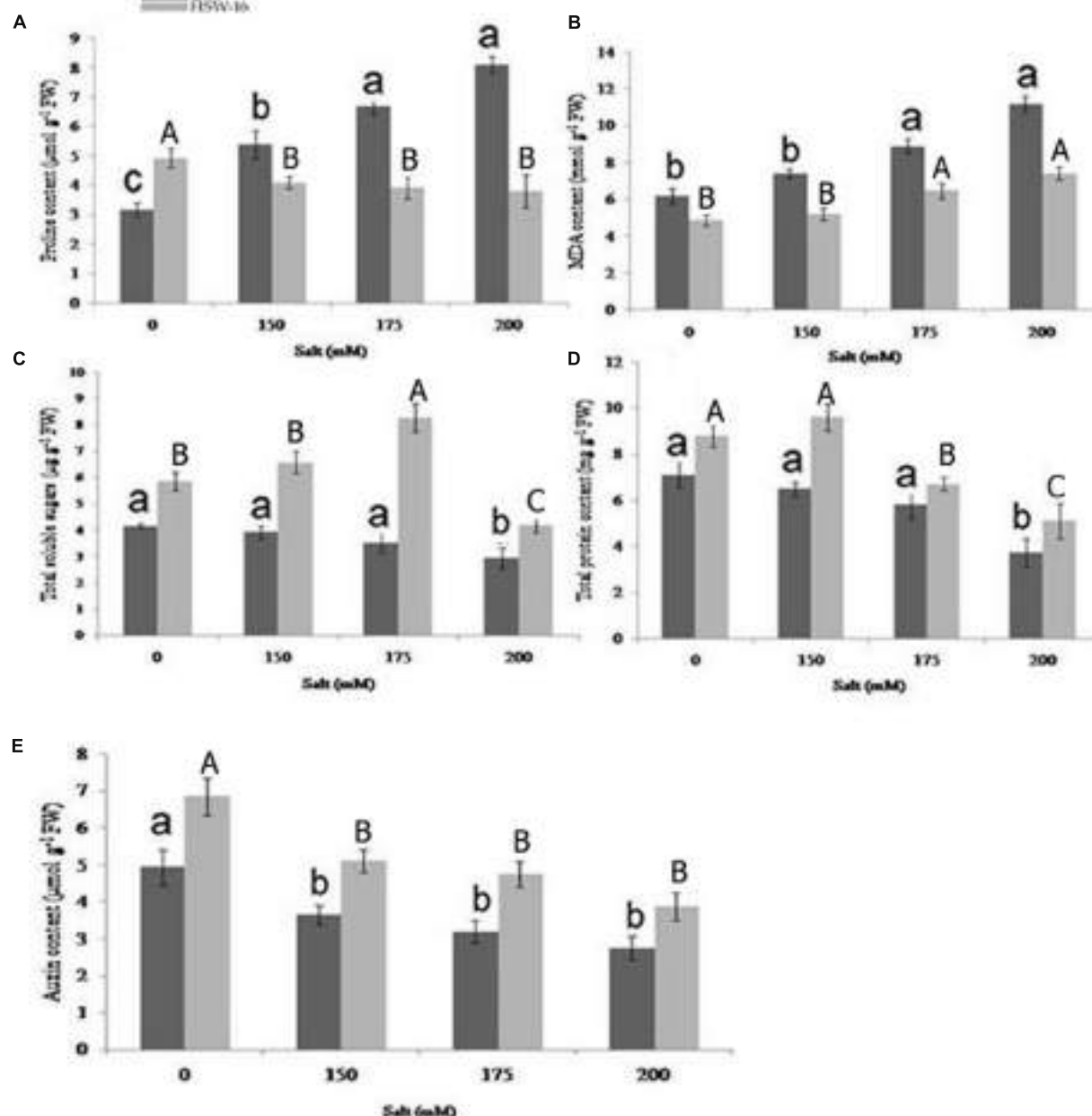


FIGURE 6 | Effect of *B. licheniformis* HSW-16 inoculation on (A) proline (B) malondialdehyde (MDA) (C) total soluble sugar (TSS) (D) total protein, and (E) auxin content under different 0 mM, 150 mM, 175 mM, 200 mM NaCl salt conditions. Values are mean of five replicates ± SD. Small letters on the bar in each treatment indicate significant difference ($p < 0.05$) among control, whereas capital letters indicate significant difference among the bacterial treatment. Dark and light gray columns represent the control and HSW-16 inoculated plants, respectively.

Maximum benefit from rhizobacterial inoculation depends on efficient colonization of bacteria in plants. Therefore, the efficiency of colonization of bacterium was tested employing multiphasic approaches. Photomicrograph of roots of plants inoculated with the bacterium and stained by acridine orange showed large number of bacterial cells adhering to the roots. It suggested that this isolate can effectively colonize plant surface

(Hobbie et al., 1977; Olsen and Bakken, 1987; Morris et al., 1997). Root colonization is the first and foremost step for plant-microbe association in which microorganisms move towards rhizosphere in response to root exudates. Thus, motility and chemotaxis play a key role in the root colonization. The test isolate HSW-16 showed all forms of motility which is required for chemotactic responses and colonization on plant surface (Van de Broek et al., 1998;

Lugtenberg et al., 2001). The role of motility by PGPR *Pseudomonas fluorescens* and *Bacillus* sp. has been demonstrated in previous studies (Misaghi et al., 1992; Bashan and Holguin, 1995; Lugtenberg and Kamilova, 2009). Moreover, recovery of bacterial colonies from inoculated plants showed that HSW-16 was efficient to colonize plants (Anith, 2009; Joshi and Bhatt, 2011). Additionally, results of ERIC-PCR confirmed the identity of recovered colonies as HSW-16 and provided evidence for successful colonization of the roots of the plant. Ability of this isolate to colonize and benefit other plants needs to be tested in detail.

CONCLUSION

The present work aimed to study the role of halotolerant ACC deaminase bacterium *B. licheniformis* HSW-16 to evaluate the plant growth under salt stress. Besides ACCD activity, the test isolate possesses other plant growth promoting properties including IAA production, and, phosphate solubilization that could mitigate salt stress-induced damages and establish ‘induced systemic tolerance’ to the plants. Inoculation of test isolate HSW-16 improved growth of the wheat plants growing under NaCl. In addition, inoculation with bacterium also improved the compatible solutes to counteract the NaCl stress. Our results provide evidence of colonization ability of HSW-16 that may be required for improvement of plant growth and regulation of ion transporters favoring amenable K⁺/Na⁺ ratio. In conclusion, this work opens up the possibility to evaluate the potential of *B. licheniformis* HSW-16 under field conditions as biofertilizer in alleviating salinity stress faced by the plants.

REFERENCES

- Abeles, F. B., Morgan, P. W., and Saltveit, M. E. (1992). *Ethylene in Plant Biology*. San Diego, CA: Academic press.
- Ames, B. N. (1964). Assay of inorganic phosphate, total phosphate and phosphatases. *Method Enzymol.* 8, 115–118. doi: 10.1016/0076-6879(66)08014-5
- Andreae, W. A., and Ysselstein, V. M. W. H. (1959). Studies on 3-indoleacetic acid metabolism. V. effect of calcium ions on 3-indoleacetic acid uptake and metabolism by pea roots. *Plant Physiol.* 35, 220–224. doi: 10.1104/pp.35.2.220
- Anith, K. N. (2009). Mature coconut as a bio-fermentor for multiplication of plant growth promoting rhizobacteria. *Curr. Sci.* 97, 1647–1653.
- Arshad, M., Nadeem, S. M., Zahir, Z. A., and Naveed, M. (2009). Rhizobacteria containing ACC-deaminase confer salt tolerance in maize grown on salt-affected fields. *Can. J. Microbiol.* 55, 1302–1309. doi: 10.1139/w09-092
- Ashraf, M., and Foolad, M. R. (2007). Roles of glycine betaine and proline in improving plant abiotic stress resistance. *Environ. Exp. Bot.* 59, 206–216. doi: 10.1016/j.envexpbot.2005.12.006
- Ashraf, M., and Harris, P. J. C. (2004). Potential biochemical indicators of salinity tolerance in plants. *Plant Sci.* 166, 3–16. doi: 10.1016/j.plantsci.2003.10.024
- Barnawal, D., Bharti, N., Maji, D., Chanotiya, C. S., and Kalra, A. (2014). ACC deaminase-containing *Arthrobacter protophormiae* induces NaCl stress tolerance through reduced ACC oxidase activity and ethylene production resulting in improved nodulation and mycorrhization in *Pisum sativum*. *J. Plant Physiol.* 171, 884–894. doi: 10.1016/j.jplph.2014.03.007
- Bashan, Y., and Holguin, G. (1995). Inter-root movement of *Azospirillum brasilense* and subsequent root colonization of crop and weed seedlings growing in soil. *Microb. Ecol.* 29, 269–281. doi: 10.1007/BF00164890
- Bates, L., Waldren, R. P., and Teare, I. D. (1973). Rapid determination of free proline for water-stress studies. *Plant Soil* 39, 205–207. doi: 10.1016/j.dental.2010.07.006
- Bhandal, I. S., and Malik, C. P. (1988). Potassium estimation, uptake and its role in the physiology and metabolism of flowering plants. *Int. Rev. Cytol.* 10, 205–224. doi: 10.1016/S0074-7696(08)61851-3
- Bradford, M. M. (1976). A rapid and sensitive method for the quantitation of microgram quantities of protein utilizing the principle of protein-dye binding. *Anal. Biochem.* 72, 248–254. doi: 10.1016/0003-2697(76)90527-3
- Cappuccino, J. G., and Sherman, N. (1992). “Biochemical activities of microorganisms,” in *Microbiology, A Laboratory Manual*, (San Francisco, CA: The Benjamin / Cummings Publishing Co).
- Chakraborty, U., Chakraborty, B., and Basnet, M. (2006). Plant growth promotion and induction of resistance in *Camellia sinensis* by *Bacillus megaterium*. *J. Basic Microbiol.* 46, 186–195. doi: 10.1002/jobm.200510050
- Chen, T. H. H., and Murata, N. (2008). Glycine betaine: an effective protectant against abiotic stress in plants. *Trends Plant Sci.* 13, 499–505. doi: 10.1016/j.tplants.2008.06.007
- Claussen, W. (2005). Proline as a measure of stress in tomato plants. *Plant Sci.* 168, 241–248. doi: 10.1016/j.plantsci.2004.07.039
- Colmer, T. D., Epstein, E., and Dvorak, J. (1995). Differential solute regulation in leaf blades of various ages in salt-sensitive wheat and a salt-tolerant wheat x *Lophopyrum elongatum* (Host) A. Love amphiploid. *Plant Physiol.* 108, 1715–1724. doi: 10.1104/pp.108.4.1715
- Connelly, M. B., Young, G. M., and Sloma, A. (2004). Extracellular proteolytic activity plays a central role in swarming motility in *Bacillus subtilis*. *J. Bacteriol.* 186, 4159–4167. doi: 10.1128/JB.186.13.4159-4167.2004

AUTHOR CONTRIBUTIONS

RPS performed the experiments and wrote a draft of the manuscript. PNJ mentored the research work and revised the manuscript.

ACKNOWLEDGMENTS

This research was financially supported by Department of Biotechnology (Grant No. BT/PR14527/AGR/21/326/2010), Govt. of India, New Delhi to PNJ. We sincerely thank Dr. Pankaj Sharma, Assistant professor, BITS Pilani, India, for thoroughly reviewing and correcting English language of the text.

SUPPLEMENTARY MATERIAL

The Supplementary Material for this article can be found online at: <http://journal.frontiersin.org/article/10.3389/fpls.2016.01890/full#supplementary-material>

FIGURE S1 | Amplification of *nifH* gene in *Bacillus licheniformis* HSW-16.

FIGURE S2 | Characterization of the EPS components of *B. licheniformis* HSW-16 by Fourier transform-infrared spectrograms (FTIR-spectroscopy).

FIGURE S3 | Efficiency of colonization of *B. licheniformis* HSW-16 was assessed 15 days after germination of bacterized wheat plants (A)

visualization of acridine orange-stained wheat plant roots showing bacterial cells using fluorescence microscopy (**B**) ERIC-PCR profile of bacterium colonized in wheat plants and confirmation of its identity using pure culture (Lane M: DNA ladder SM0311, Lane C: control DNA, Lane HSW-16: DNA of *B. licheniformis* isolated from inoculated plant).

- Cooper, J. E. (2007). Early interactions between legumes and rhizobia : disclosing complexity in a molecular dialogue. *J. Appl. Microbiol.* 103, 1355–1365. doi: 10.1111/j.1365-2672.2007.03366.x
- Cram, W. J. (1976). "Negative feedback regulation of transport in cells. The maintenance of turgor, volume and nutrient supply," in *Encyclopaedia of Plant Physiology, New Series*, Vol. 2, eds U. Luttge and M. G. Pitman (Berlin: Springer), 284–316.
- Desnoues, N., Lin, M., Guo, X., Ma, L., Carreño-Lopez, R., and Elmerich, C. (2003). Nitrogen fixation genetics and regulation in a *Pseudomonas stutzeri* strain associated with rice. *Microbiology* 149, 2251–2262. doi: 10.1099/mic.0.26270-0
- Döbereiner, J. (1995). "Isolation and identification of aerobic nitrogen fixing bacteria from soil and plants," in *Methods in Applied Soil Microbiology and Biochemistry*, eds K. Alef and P. Nannipieri (London: Academic press), 134–141.
- Duan, J., Muller, K. M., Charles, T. C., Vesely, S., and Glick, B. R. (2009). 1-Aminocyclopropane-1-carboxylate (ACC) deaminase genes in rhizobia from Southern Saskatchewan. *Microb. Ecol.* 57, 423–436. doi: 10.1007/s00248-008-9407-6
- Dubois, M., Gilles, K. A., Hamilton, J. K., Rebers, P. A., and Smith, F. (1956). Colorimetric method for determination of sugars and related substances. *Anal. Chem.* 28, 350–356. doi: 10.1021/ac60111a017
- Dutta, J., Handique, P. J., and Thakur, D. (2015). Assessment of culturable tea rhizobacteria isolated from tea estates of Assam, India for growth promotion in commercial tea cultivars. *Front. Microbiol.* 6:1252. doi: 10.3389/fmicb.2015.01252
- Duxbury, A. C., and Yentsch, C. S. (1956). Plankton pigment monographs. *J. Mar. Res.* 15, 91–101.
- Dworkin, M., and Foster, J. (1958). Experiments with some microorganisms which utilize ethane and hydrogen. *J. Bacteriol.* 75, 592–603.
- Frey-Klett, P., Chavatte, M., Clausse, M. L., Courrier, S., Le Roux, C., Raaijmakers, J., et al. (2005). Ectomycorrhizal symbiosis affects functional diversity of rhizosphere fluorescent pseudomonads. *New Phytol.* 165, 317–328. doi: 10.1111/j.1469-8137.2004.01212.x
- Fujishige, N. A., Kapadia, N. N., De Hoff, P. L., and Hirsch, A. M. (2006). Investigations of rhizobium biofilm formations. *FEMS Microbiol. Ecol.* 56, 195–206. doi: 10.1111/j.1574-6941.2005.00044.x
- Fujita, M., Fujita, Y., Noutoshi, Y., Takahashi, F., Narusaka, Y., Yamaguchi-Shinozaki, K., et al. (2006). Crosstalk between abiotic and biotic stress responses: a current view from the points of convergence in the stress signaling networks. *Curr. Opin. Plant Biol.* 9, 436–442. doi: 10.1016/j.pbi.2006.05.014
- Gamalero, E., Berta, G., Massa, N., Glick, B. R., and Lingua, G. (2008). Synergistic interactions between the ACC deaminase-producing bacterium *Pseudomonas putida* UW4 and the AM fungus *Gigaspora rosea* positively affect cucumber plant growth. *FEMS Microbiol. Ecol.* 64, 459–467. doi: 10.1111/j.1574-6941.2008.00485.x
- Gill, S. S., and Tuteja, N. (2010). Reactive oxygen species and antioxidant machinery in abiotic stress tolerance in crop plants. *Plant Physiol. Biochem.* 48, 909–930. doi: 10.1016/j.plaphy.2010.08.016
- Glick, B. R. (2007). Promotion of plant growth by bacterial ACC deaminase. *Crit. Rev. Plant Sci.* 26, 227–242. doi: 10.1080/07352680701572966
- Gordon, S. A., and Weber, R. P. (1951). Colorimetric estimation of indole acetic acid. *Plant Physiol.* 26, 192–195. doi: 10.1104/pp.26.1.192
- Gossett, D. R., Millholion, E. P., Lucas, M. C., Bands, S. W., and Marney, M. M. (1994). The effects of NaCl on antioxidant enzyme activities in callus tissue of salt tolerant and salt sensitive cotton cultivars. *Plant Cell Rep.* 13, 498–503. doi: 10.1007/BF00232944
- Grattan, S. R., and Grieve, C. M. (1999). Salinity–mineral nutrient relations in horticultural crops. *Sci. Hort.* 78, 127–157. doi: 10.1016/S0304-4238(98)00192-7
- Gupta, K. J., Shah, J. K., Brotman, Y., Jahnke, K., Willmitzer, L., and Kaiser, W. M. (2012). Inhibition of aconitase by nitric oxide leads to induction of the alternative oxidase and to a shift of metabolism towards biosynthesis of amino acids. *J. Exp. Bot.* 63, 1773–1784. doi: 10.1093/jxb/ers053
- Hasegawa, P. M., Bressan, R. A., Zhu, J. K., and Bohnert, H. J. (2000). Plant cellular and molecular responses to high salinity. *Ann. Rev. Plant Physiol. Plant Mol. Biol.* 51, 463–499. doi: 10.1146/annurev.arplant.51.1.463
- Hincha, D. K., Zuther, E., and Heyer, A. G. (2003). The preservation of liposomes by raffinose family oligosaccharides during drying is mediated by effects on fusion and lipid phase transitions. *Biochim. Biophys. Acta* 1612, 172–177. doi: 10.1016/S0005-2736(03)00116-0
- Hoagland, D. R., and Boyer, T. C. (1936). General nature of the process of salt accumulation by roots with description of experimental methods. *Plant Physiol.* 11, 471–507. doi: 10.1104/pp.11.3.471
- Hobbie, J., Daley, R., and Japer, S. (1977). Use of nucleopore filters for counting bacteria by fluorescence microscopy. *Appl. Environ. Microbiol.* 33, 1225–1228.
- Hodges, D. M., Delong, J. M., Forney, C. F., and Prange, R. K. (1999). Improving the thiobarbituric acid reactive substances assay for estimating lipid peroxidation in plant tissue containing anthocyanin and other interfering compounds. *Planta* 207, 604–611. doi: 10.1007/s004250050524
- Holbrook, A., Edge, W., and Bailey, F. (1961). Spectrophotometric method for determination of gibberellic acid. *Adv. Chem. Ser.* 28, 159–167. doi: 10.1021/ba-1961-0028.ch018
- Huang, G. T., Ma, S. L., Bai, L. P., Zhang, L., Ma, H., Jia, P., et al. (2012). Signal transduction during cold, salt and drought stresses in plants. *Mol. Biol. Rep.* 39, 969–987. doi: 10.1007/s11033-011-0823-1
- Irie, Y., Borlee, B. R., O'Connor, J. R., Hill, P. J., Harwood, C. S., Wozniak, D. J., et al. (2012). Self produced exopolysaccharide is a signal that stimulates biofilm formation in *Pseudomonas aeruginosa*. *Proc. Natl. Acad. Sci. U.S.A.* 109, 20632–20636. doi: 10.1073/pnas.1217993109
- Irigoyen, J. J., Einerich, D. W., and Sanchez-Diaz, M. (1992). Water stress induced changes in concentrations of proline and total soluble sugars in nodulated alfalfa (*Medicago sativa*) plants. *Physiol. Plant.* 84, 55–60. doi: 10.1111/j.1399-3054.1992.tb08764.x
- Jackson, M. L. (1967). *Soil Chemical Analysis*. New Delhi: Prentice hall of Indian private limited.
- Jain, M. G., Mathur, S. K., and Sarin, N. B. (2001). Ameliorative effects of proline on salt stress induced lipid peroxidation in cell lines of groundnut (*Arachis hypogea* L.). *Plant Cell Rep.* 20, 63–68.
- Jha, C. K., Annapurna, K., and Saraf, M. (2012). Isolation of Rhizobacteria from *Jatropha curcas* and characterization of produced ACC deaminase. *J. Basic Microbiol.* 52, 285–295. doi: 10.1002/jobm.201100113
- Jha, P., and Kumar, A. (2009). Characterization of novel plant growth promoting endophytic bacterium *Achromobacter xylosoxidans* from wheat plant. *Microbiol. Ecol.* 58, 179–188. doi: 10.1007/s00248-009-9485-0
- Joshi, P., and Bhatt, A. B. (2011). Diversity and function of plant growth promoting rhizobacteria associated with wheat rhizosphere in north Himalayan region. *Int. J. Environ. Sci.* 1, 1135–1143.
- Kandasamy, S., Loganathan, K., Muthuraj, R., Duraisamy, S., Seetharaman, S., Thiruvengadam, R., et al. (2009). Understanding the molecular basis of plant growth promotional effect of *Pseudomonas* fluorescences on rice through protein profiling. *Proteome Sci.* 7: 47. doi: 10.1186/1477-5956-7-47
- Karthikeyan, B., Joe, M. M., Islam, M. R., and Sa, T. (2012). ACC deaminase containing diazotrophic endophytic bacteria ameliorate salt stress in *Catharanthus roseus* through reduced ethylene levels and induction of antioxidative defense systems. *Symbiosis* 56, 77–86. doi: 10.1007/s13199-012-0162-6
- Koryo, H. W. (2006). Effect of salinity on growth, photosynthesis and solute composition of the potential cash crop halophyte *plantago*. *Environ. Exp. Bot.* 56, 136–146. doi: 10.1016/j.envexpbot.2005.02.001
- Lee, K. D., and Han, H. S. (2005). Physiological responses of soybean-inoculation of *Bradyrhizobium japonicum* with PGPR in saline soil conditions. *Res. J. Agric. Biol. Sci.* 1, 216–221.
- Liu, C., Zhao, L., and Yu, G. (2011). The dominant glutamic acid metabolic flux to produce g-amino butyric acid over proline in *Nicotiana tabacum* leaves under water stress relates to its significant role in antioxidant activity. *J. Integr. Plant Biol.* 53, 608–618. doi: 10.1111/j.1744-7909.2011.01049.x
- Liu, F. P., Liu, H. Q., Zhou, H. L., Dong, Z. G., Bai, X. H., Bai, P., et al. (2014). Isolation and characterization of phosphate-solubilizing bacteria from betel nut (*Areca catechu*) and their effects on plant growth and phosphorus mobilization in tropical soils. *Biol. Fertil. Soils* 50, 927–937. doi: 10.1007/s00374-014-0913-z
- Lugtenberg, B. J., and Kamilova, F. (2009). Plant growth promoting rhizobacteria. *Ann. Rev. Microbiol.* 63, 541–556. doi: 10.1146/annurev.micro.62.081307.162918

- Lugtenberg, B. J. J., Dekkers, L., and Bloemberg, G. V. (2001). Molecular determinants of rhizosphere colonization by *Pseudomonas*. *Ann. Rev. Phytopathol.* 39, 461–490. doi: 10.1146/annurev.phyto.39.1.461
- Mayak, S., Tirosh, T., and Glick, B. R. (2004). Plant growth-promoting bacteria confer resistance in tomato plants to salt stress. *Plant Physiol. Biochem.* 42, 565–572. doi: 10.1016/j.plaphy.2004.05.009
- Mehta, S., and Nautiyal, C. S. (2001). An efficient method for qualitative screening of phosphate-solubilizing bacteria. *Curr. Microbiol.* 43, 51–56. doi: 10.1007/s002840010259
- Misaghi, I. J., Olsen, M. W., Billotte, J. M., and Sonoda, R. M. (1992). The importance of rhizobacterial mobility in biocontrol of bacterial wilt of tomato. *Soil Biol. Biochem.* 24, 287–293. doi: 10.1016/0038-0717(92)78-90188-4
- Morgan, P. W., and Drew, M. C. (1997). Ethylene and plant responses to stress. *Physiol. Plant.* 100, 620–630. doi: 10.1034/j.1399-3054.1997.1000325.x
- Morris, C. E., Monier, J., and Jacques, M. (1997). Methods for observing microbial biofilms directly on leaf surfaces and recovering them for isolation of culturable microorganisms. *Appl. Environ. Microbiol.* 63, 1570–1576.
- Munns, R., and Tester, M. (2008). Mechanisms of salinity tolerance. *Annu. Rev. Plant Biol.* 59, 651–681. doi: 10.1146/annurev.arplant.59.032607.092911
- Nadeem, S. M., Zahir, Z. A., Naveed, M., and Arshad, M. (2007). Preliminary investigations on inducing salt tolerance in maize through inoculation with rhizobacteria containing ACC-deaminase activity. *Can. J. Microbiol.* 53, 1141–1149. doi: 10.1139/W07-081
- Nadeem, S. M., Zahir, Z. A., Naveed, M., Arshad, M., and Shahzad, S. M. (2006). Variation in growth and ion uptake of maize due to inoculation with plant growth promoting rhizobacteria under salt stress. *Soil Environ.* 25, 78–84.
- Nascimento, F. X., Rossi, M. J., Soares, C. R. F. S., McConkey, B. J., and Glick, B. R. (2014). New insights into 1-aminocyclopropane-1-carboxylate (ACC) deaminase phylogeny, evolution and ecological significance. *PLoS ONE* 9:e99168. doi: 10.1371/journal.pone.0099168
- Nicolaus, B., Lama, L., Esposito, E., Manca, M. C., Improta, R., Bellitti, M. R., et al. (1999). *Haloarcula* spp. able to biosynthesize exo- and endopolymers. *J. Ind. Microbiol. Biotechnol.* 23, 489–496. doi: 10.1038/sj.jim.2900738
- Olsen, R. A., and Bakken, L. R. (1987). Viability of soil bacteria: optimization of plate-counting technique and comparison between total counts and plate counts within different size groups. *Microb. Ecol.* 13, 59–74. doi: 10.1007/BF02014963
- Olsen, S. R., Cole, C. V., Watanabe, F. S., and Dean, L. A. (1954). *Estimation of Available Phosphorus in Soils by Extraction with Sodium Bicarbonate*. Washington, DC: Circular 939 US Department of Agriculture.
- Parida, S. K., and Das, A. B. (2005). Salt tolerance and salinity effects on plants. *Ecotoxicol. Environ. Saf.* 60, 324–349. doi: 10.1016/j.ecoenv.2004.06.010
- Penrose, D. M., and Glick, B. R. (2003). Methods for isolating and characterizing ACC deaminase-containing plant growth-promoting rhizobacteria. *Physiol. Plant.* 118, 10–15. doi: 10.1034/j.1399-3054.2003.00086.x
- Peterson, T. A., Reinsel, M. D., and Krizek, D. T. (1991). Tomato (*Lycopersicon esculentum* Mill., cv. Better Bush) plant response to root restriction. II. Root respiration and ethylene generation. *J. Exp. Bot.* 42, 1241–1249. doi: 10.1093/jxb/42.10.1233
- Pitman, M. G., and Läuchli, A. (2002). “Global impact of salinity and agricultural ecosystems,” in *Salinity: Environment – Plants – Molecules*, eds A. Läuchli and U. Lütge (Dordrecht: Kluwer Academic Publishers), 3–20.
- Poly, F., Monrozier, L. J., and Bally, R. (2001). Improvement in the RFLP procedure for studying the diversity of *nifH* genes in communities of nitrogen fixers in soil. *Res. Microbiol.* 152, 95–103. doi: 10.1016/S0923-2508(00)01172-4
- Prescott, L. M., and Harley, J. P. (2002). *Laboratory Exercises in Microbiology*, 5th Edn. Boston, MA: McGraw-Hill.
- Qurashi, W. A., and Sabri, N. A. (2012). Bacterial exopolysaccharide and biofilm formation stimulate chickpea growth and soil aggregation under salt stress. *Braz. J. Microbiol.* 43, 1183–1191. doi: 10.1590/S1517-83822012000300046
- Roberson, E. B., and Firestone, M. K. (1992). Relationship between desiccation and exopolysaccharide production in soil *Pseudomonas* sp. *Appl. Environ. Microbiol.* 58, 1284–1291.
- Ruiz-Lozano, J. M., and Azcón, R. (2000). Symbiotic efficiency and infectivity of an autochthonous arbuscular mycorrhizal *Glomus* sp. from saline soils and *Glomus deserticola* under salinity. *Mycorrhiza* 10, 137–143. doi: 10.1007/s00572000075
- Sachdev, D. P., Chaudhari, H. G., Kasure, V. M., Dahavale, D. D., and Chopade, B. A. (2009). Isolation and characterization of indole acetic acid (IAA) producing *Klebsiella pneumoniae* strains from rhizosphere of wheat (*Triticum aestivum*) and their effect on plant growth. *Ind. J. Exp. Biol.* 47, 993–1000.
- Sahay, H., Mahfooz, S., Singh, A. K., Singh, S., Kaushik, R., Saxena, A. K., et al. (2012). Exploration and characterization of agriculturally and industrially important haloalkaliphilic bacteria from environmental samples of hypersaline Sambhar lake, India. *World J. Microbiol. Biotechnol.* 28, 3207–3217. doi: 10.1007/s11274-012-1131-1
- Saleem, M., Arshad, M., Hussain, S., and Bhatti, A. S. (2007). Perspective of plant growth promoting rhizobacteria (PGPR) containing ACC deaminase in stress agriculture. *J. Ind. Microbiol. Biotechnol.* 34, 635–648. doi: 10.1007/s10295-007-0240-6
- Salkinoja-Salonen, M. S., Vuorio, R., Andersson, M. A., Kämpfer, P., Andersson, M. C., Honkanen-Buzalski, T., et al. (1999). Toxigenic strains of *Bacillus licheniformis* related to food poisoning. *Appl. Environ. Microbiol.* 65, 4637–4645.
- Saravanan Kumar, D., and Samiyappan, R. (2007). ACC deaminase from *Pseudomonas fluorescens* mediated saline resistance in groundnut (*Arachis hypogaea*) plants. *J. Appl. Microbiol.* 102, 1283–1292. doi: 10.1111/j.1365-2672.2006.03179.x
- Schachtman, D. P., and Liu, W. (1999). Piecing together the puzzle of the interaction between potassium and sodium uptake in plants. *Trends Plant Sci.* 4, 281–287. doi: 10.1016/S1360-1385(99)01428-4
- Schwyn, B., and Neilands, J. B. (1987). Universal chemical assay for the detection and determination of siderophores. *Anal. Biochem.* 160, 47–56. doi: 10.1016/0003-2697(87)90612-9
- Shabala, S., Getnet, D. A., Stuart, J. R., Meixue, Z., and John, P. B. (2014). Evaluating contribution of ionic, osmotic and oxidative stress components towards salinity tolerance in barley. *BMC Plant Biol.* 14:113. doi: 10.1186/1471-2229-14-113
- Sharma, S. S., and Dietz, K. J. (2006). The significance of amino acids and amino acid derived molecules in plant responses and adaptation to heavy metal stress. *J. Exp. Bot.* 57, 711–726. doi: 10.1093/jxb/erj073
- Shrivastava, U. P., and Kumar, A. (2013). Characterization and optimization of 1-aminocyclopropane-1-carboxylate deaminase (ACCD) activity in different rhizospheric PGPR with *Microbacterium* sp. strain ECI-12A. *Int. J. Appl. Sci. Biotechnol.* 1, 11–15. doi: 10.3126/ijasbt.v1i1.7921
- Siddikee, M. A., Tipayno, S. C., Kim, K., Chung, J. B., and Sa, T. (2011). Influence of varying degree of salinity-sodicity stress on enzyme activities and bacterial populations of coastal soils of Yellow Sea, South Korea. *J. Microbiol. Biotechnol.* 21, 341–346.
- Singh, R. P., Jha, P., and Jha, P. N. (2015). The plant growth promoting bacterium *Klebsiella* sp. SBP-8 confers induced systemic tolerance in wheat (*Triticum aestivum*) under salt stress. *J. Plant Physiol.* 184, 57–67. doi: 10.1016/j.jplph.2015.07.002
- Smirnoff, N., and Cumbers, Q. J. (1989). Hydroxyl radical scavenging activity of compatible solutes. *Phytochemistry* 28, 1057–1060. doi: 10.1016/0031-9422(89)80182-7
- Stearns, J., and Glick, B. R. (2003). Transgenic plants with altered ethylene biosynthesis or perception. *Biotechnol. Adv.* 21, 193–210. doi: 10.1016/S0734-9750(03)00024-7
- Sutherland, I. W., and Geddie, J. L. (1993). Uptake of metals by bacterial polysaccharides. *J. Appl. Bacteriol.* 74, 467–472. doi: 10.1111/j.1365-2672.1993.tb05155.x
- Tamura, K., Stecher, G., Peterson, D., Filipski, A., and Kumar, S. (2013). MEGA6: molecular evolutionary genetics analysis version 6.0. *Mol. Biol. Evol.* 30, 2725–2729. doi: 10.1093/molbev/mst197
- Upadhyay, S. K., Singh, J. S., Saxena, A. K., and Singh, D. P. (2012). Impact of PGPR inoculation on growth and antioxidant status of wheat under

- saline conditions. *Plant Biol.* 14, 605–611. doi: 10.1111/j.1438-8677.2011.00533.x
- Van de Broek, A., Lambrecht, M., and Vanderleyden, J. (1998). Bacterial chemotactic motility is important for the initiation of wheat root colonization by *Azospirillum brasilense*. *Microbiology* 144, 2599–2606. doi: 10.1099/00221287-144-9-2599
- Walkey, A. E., and Black, J. A. (1934). An examination of the Degtjareff Method for determining soil organic matter and proposed modification of the chromic acid titration method. *Soil Sci.* 37: 29. doi: 10.1097/00010694-193401000-00003
- Wang, W. X., Barak, T., Vinocur, B., Shoseyov, O., and Altman, A. (2003). “Abiotic resistance and chaperones: possible physiological role of SP1, a stable and stabilizing protein from *Populus*,” in *Plant Biotechnology 2000 and Beyond*, ed. I. K. Vasil (Dordrecht: Kluwer), 439–443.
- Yancey, P. H. (2005). Organic osmolytes as compatible, metabolic and counteracting cytoprotectants in high osmolarity and other stresses. *J. Exp. Biol.* 208, 2819–2830. doi: 10.1242/jeb.01730
- Yang, J., Kloepper, J. W., and Ryu, C. M. (2009). Rhizosphere bacteria help plants tolerate abiotic stress. *Trends Plant Sci.* 14, 1–4. doi: 10.1016/j.tplants.2008.10.004
- Zahir, Z. A., Ghani, U., Naveed, M., Nadeem, S. M., and Asghar, H. N. (2009). Comparative effectiveness of *Pseudomonas* and *Serratia* sp. containing ACC-deaminase for improving growth and yield of wheat (*Triticum aestivum* L.) under salt-stressed conditions. *Arch. Microbiol.* 191, 415–424. doi: 10.1007/s00203-009-0466-y
- Zhang, H., Kim, M. S., Sun, Y., Dowd, S. E., Shi, H., and Paré, P. W. (2008). Soil bacteria confer plant salt tolerance by tissue-specific regulation of the sodium transporter HKT1. *Mol. Plant Microbe Interact.* 21, 737–744. doi: 10.1094/MPMI-21-6-0737

Conflict of Interest Statement: The authors declare that the research was conducted in the absence of any commercial or financial relationships that could be construed as a potential conflict of interest.

Copyright © 2016 Singh and Jha. This is an open-access article distributed under the terms of the Creative Commons Attribution License (CC BY). The use, distribution or reproduction in other forums is permitted, provided the original author(s) or licensor are credited and that the original publication in this journal is cited, in accordance with accepted academic practice. No use, distribution or reproduction is permitted which does not comply with these terms.

Advantages of publishing in Frontiers



OPEN ACCESS

Articles are free to read,
for greatest visibility



COLLABORATIVE PEER-REVIEW

Designed to be rigorous
– yet also collaborative,
fair and constructive



FAST PUBLICATION

Average 85 days from
submission to publication
(across all journals)



COPYRIGHT TO AUTHORS

No limit to article
distribution and re-use



TRANSPARENT

Editors and reviewers
acknowledged by name
on published articles



SUPPORT

By our Swiss-based
editorial team



IMPACT METRICS

Advanced metrics
track your article's impact



GLOBAL SPREAD

5'100'000+ monthly
article views
and downloads



LOOP RESEARCH NETWORK

Our network
increases readership
for your article

Frontiers

EPFL Innovation Park, Building I • 1015 Lausanne • Switzerland
Tel +41 21 510 17 00 • Fax +41 21 510 17 01 • info@frontiersin.org
www.frontiersin.org

Find us on

